General Distribution

CSNI Report No. 174
Volume 3

OECD
NEA

FINAL COMPARISON REPORT FOR INTERNATIONAL STANDARD PROBLEM No 22 (SPES)

November 1990

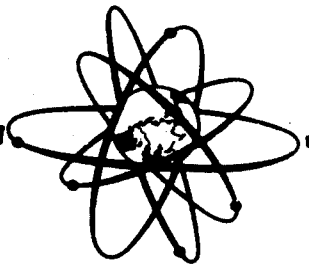

COMMITTEE ON THE SAFETY OF NUCLEAR INSTALLATIONS
OECD NUCLEAR ENERGY AGENCY
38, boulevard Suchet, 75016 Paris, France

E N E A

COMITATO NAZIONALE PER LA RICERCA E PER LO SVILUPPO
DELL'ENERGIA NUCLEARE E DELLE ENERGIE ALTERNATIVE

DIPARTIMENTO REATTORI TERMICI

OECD/CSNI ISP22

COMPARISON REPORT

VOL. III: CHAPTER 4 (4.10 TO 4.18)

G. De Toma, S. Ederli*, P Marsili**, E. Negrenti, T. Pignatelli

ENEA/TERM/MEP

* ENEA/VEL
** ENEA/DISP

NE00 1TP4B 90009
MAY 1990

ABSTRACT

OECD-CSNI International Standard Problem 22 is a "Loss of Feedwater with EFW delayed" test, performed in the SPES facility (SIET-Piacenza). It is a double blind exercise, characterized by a large participation of non-OECD countries sponsored by IAEA. The ISP22 Comparison Report is based on two fundamental elements: the comparison between the single Participants predictions and the experimental data, and the overall comparison among all calculations and test results. The conclusions drawn from these analyses highlight the major contributes to the observed discrepancies deriving from code limitations, user errors, experimental uncertainties. From a macroscopic point of view, it is concluded that most of the phenomena occurring in ISP22 experiment were generally predicted by the double blind predictions. A more accurate analysis of the single phenomena can nevertheless reveal relevant discrepancies between calculations and data. The document also contains a description of ISP22 Participants and input decks, and a collection of their comments on the differences between calculation and test results.

ABBREVIATIONS

AE	Accuracy Evaluation
AFW	Auxiliary Feedwater
BIC	Boundary and Initial Conditions
BOCH	Beginning of Core Heat up
B/U	Bottom Up
C	Code
CALC	Calculation
CF	Core Flooding
CL	Cold Leg
CONT	Continuous
C.T.	Comparison Table
DC	Downcomer
DISC	Discontinuous
DO	Dry Out
DOT	Dry Out Time
DP	Differential Pressure
DT	Delayed Trips Timing
ECCS	Emergency Core Cooling System
EFW	Emergency Feedwater
EFWS	Emergency Feedwater System
EST	Estimated
ET	Early Trips Timing
E.T. exp	Event Table experimental
EXP	Experiment
exp	experimental
FL	Flooding
G	Good
HIL	High Initial Level
HISM	High Initial Secondary Mass
HL	Hot Leg
HPIS	High Pressure Injection System
HSC	High Secondary Cooling
HSM	Heat Structures Modelling
HU	Heat Up
INTERM	Intermittent
ISP	International Standard Problem
LDP	Liquid Discharge from PRZ
LEV. OBS.	Level Obscillations
LHC	Low Heat Capacity
LHL	Low Heat Losses
LHUR	Low Heat Up Rate
LIQ	Liquid
LISM	Low Initial Secondary Mass
LOFW	Loss of Feedwater
LoLo	Low Low Level
LNC	Loss of Natural Circulation
LPIS	Low Pressure Injection System
LSIS	Low Secondary Inventory at Scram
MFW	Main Feedwater
MIX	Mixture
MSI	Main Steam Isolation
MSIV	Main Steam Isolation Valve

n. a.	Not available
NC	Natural Circulation
NEA	Nuclear Energy Agency
NOD	Nodalization
OECD	Org. for Economic Cooperation and Development
P	Poor
PC	Power Channel
PCP	Primary Coolant Pump
PCS	Primary Coolant System
PLA	Primary Leak Absence
PMD	Primary Mass Distribution
PMLM	Primary Mass Leak Modelling
PORV	Power Operated Relief Valve
PRZ	Pressurizer
PRZE	Pressurizer Emptying
PRZF	Pressurizer Full
PRZM	Pressurizer Modelling
PRZPC	Pressurizer PORV Closure
PS	Primary System
PWR	Pressurized Water Reactor
RCS	Reactor Coolant System
RFD	Reason For Discrepancy
S	Sufficient
SG	Steam Generator
SGs	Steam Generators
SGDO	Steam Generator Dry Out
SGP	Steam Generator Pressure
SL	Surge Line
SLM	Surge Line Modelling
SPR	Secondary Pressure Regulation
SPES	Simulatore PWR per Esperienze di Sicurezza
SS	Secondary Side
ST	Steam
SV	Safety Valve
SUB	Subcooled
TD	Top Down
TP	Two Phase
TPNC	Two Phase Natural Circulation
TQ	Top Quenching
U	User
UP	Upper Plenum
vs	versus
w.r.t.	with respect to

ISP22 COMPARISON REPORT

LIST OF CONTENTS

4. CALCULATIONS/EXPERIMENT COMPARISON

5. OVERALL COMPARISON

6. PARTICIPANTS COMMENTS

7. CONCLUSIONS

8. REFERENCES

ACKNOWLEDGEMENTS

The preparation of a large document such as ISP22 Draft Comparison Report is the result of a team effort during a considerable period of time. Acknowledgement is therefore here made firstly to Dr. G. Lelli, Director of ENEA Area Energetica, who made it possible the continuation of ISP22 activity in a period of difficult restructuring of ENEA connected with the reduction of nuclear activities. Acknowledgements are also made to Dr. G. Santarossa (ENEA-DISP), Dr. M. Vignolini (ENEA-TERM) and Dr. R. Caruso (OECD-NEA) for their supervision in the development of the comparison analysis. Specific acknowledgements are made to Mr. G. Napoli and Miss M.C. Maugeri (ENEA-TERM) for their fundamental contributes in the document editing. A global acknowledgement is made to SIET colleagues, for the provision of the necessary experimental data and information. Finally, acknowledgement is made to the Participants in OECD-CSNI ISP22, for their efforts in the performance of the calculations and the provision of the requested information.

4.10 KURCHATOV

4.10.1 CALCULATION DESCRIPTION

Phase 1: from LOFW to Scram (0,16 s)

Following LOFW a fast secondary level drop occurs (fig. 6, 7). Secondary pressure begins to rise (fig. 3). At 16 s the Scram signal is generated (see Events Table).

Phase 2: from Scram to PRZ PORV opening (16, 120 s)

After Scram and MSI (almost coincident) a remarkable secondary pressurization is observed (fig. 3). SGs level continue to decrease (fig. 6, 7) while primary average temperature increases significantly (see fig. 12, 42) causing PRZ level and pressure to rise accordingly (fig. 1 and 6, 7). When secondary pressure peak terminates (at about 80 s, see fig. 3) primary temperature begins to decrease slowly, but the SG dry out causes another heat up at about 100 s (fig. 12, 42).

Phase 3: from PRZ PORV opening to pumps trip (120, 176 s)

Primary pressure stabilizes at PRZ PORV set point (fig. 1) while temperature and level contine to increase slowly (fig. 6, 7, and 12, 42). Secondary pressure is at SG PORV set point. Secondary PORVs cycle with decreasing frequencies (fig. 92).

PARTICIPANT: ASMOLOV - KURCHATOV *CODE: MOCT*

EVENTS TABLE

EVENT	*CALC. TIME (s)*	*EXP. TIME (s)*
SG Low Low Level	*11.4*	*33*
Main Steam Isolation	*16.5*	*38*
Scram (power fall), t_1	*15.6*	*44*
SGs PORV opening		*82 (3)* *106 (2)* *200 (1)*
SGs Dry Out	*151* *151* *151*	*3282 (3)* *3347 (1)* *3437 (2)*
PRZ PORV opening, t_2	*120*	*4134*
PRZ full of liquid	*175*	*4222*
Pumps Trip, t_3	*176*	*4848*
Loss of Natural Circulation	*CALC. FAILURE*	*5630*
Beginning of Core Heat Up	-	*6511*
EFW actuation, t_4	-	*6532*
PRZ PORV closure	-	*6576*
PRZ emptying	-	*6811*
SG1 repressurization	-	*6878*
End of transient, t_{END}	-	*8062*

4.10.2 CALCULATION/EXPERIMENT COMPARISON

Phase 1: from LOFW to Scram

Primary pressure peak is correctly simulated (16.2 MPa). Trips timing is sensibly anticipated (LoLo level at only 11, see Comp. Table).

Phase 2: from Scram to PRZ PORV opening

Primary cooldown and depressurization after Scram is not predicted (see fig. 1 and 12, 42), probably due to the excessive secondary pressurization (fig. 3). SGs dry out occurs extremely early (see fig. 6, 7) due to the very low initial inventory (see Comp. Table). Consequently also PRZ PORV opening time results strongly underestimated.

Phase 3: from PRZ PORV opening to pumps trip

Primary pressure is at PRZ PORV set point while primary heat up continues. No further comparison is possible due to calculations failure.

PARTICIPANT: ASMOLOV - KURCHATOV CODE. MOCT

COMPARISON TABLE

PARAMETER		EXP	CALC	AE*	RFD**
1A Initial SGs mass (Kg)	1	137	30	P	NOD+?
	2	151	(est.) 30	P	(B+C+U)
	3	145	30	P	
1B Trips timing (s)	LoLo	33	11.4	P	C+U+B
	MSI	38	16.4	P	
	Scram	44	15.6	P	
1C Max primary pressure (MPa)		16.2	16.2	G	-
1D SGs mass at Scram (Kg)	1	98	16	P	1A+1B
	2	105	(est.) 16	P	(B+C+U)
	3	97	16	P	
2A Min. primary pressure (MPa)		14.5	?	P	HSM+LHL
Pressure gradients before		4.10^{-4}	?	P	(U)
and after SGs DO (MPa/s)		3.10^{-4}	?	P	
2B SGs PORV opening time (s)	1	200	15	P	HSM+?
	2	106	15	P	(C+U)
	3	82	15	P	
PC PRZ level gradient (m/s)		$-5.7.10^{-4}$	0.01	P	PTT (C+U)
2D Min. PRZ level (m)		2.3	4.87	P	PTT
2E SGs DO time, tSG1DO (s)		3347	151	P	1D+LHL (U)
tSG2DO (s)		3437	151	P	
tSG3DO (s)		3282	151	P	
2F Heat Up temperature (K/s)		0.02	0.12	P	LHL+HSM
and level (m/s) gradients		$3.6.10^{-3}$	?	-	(U)
2G Cool Insurge effect		PR. DELAY	NO	P	PRZM (U+B)
2H PRZ PORV opening time, t2 (s)		4134	120	P	2E+HSM+LHL
($dt_2 = t_2 - t_{SGDO}$)		(697)	(-31)	P	(U)
3A PRZ level at t_2 (m)		6.57	5.1	P	PRZM (C+U)
3B PRZ full time, t_{PRZF} (s)		4222	175	P	PRZM+2E
($dt_{PRZF} = t_{PRZF} - t_2$)		(88)	(55)	S	-
3C Dominant Relief Condition		LIQ	ST	P	PRZM (U)
3D Sat. Conditions before trip		NO	NO	G	-
3E Pumps Trip time, t3 (s)		4848	176	P	2E+LHL+HSM
($dt_3 = t_3 - t_2$)		(714)	(56)	P	(U)
($dt_{HU} = t_3 - t_{SGDO}$)		(1411)	(25)	P	

* ACCURACY EVALUATION : G=GOOD, S=SUFFICIENT, P=POOR

** REASON FOR DISCREPANCY : B=BIC, C=CODE, U=USER, PRZM=PRZ MODELLING HSM=HEAT STRUCTURES MODELLING, LHL=LOW HEAT LOSSES, PTT=PRIMARY TEMPERATURE TREND, NOD=NODALIZATION

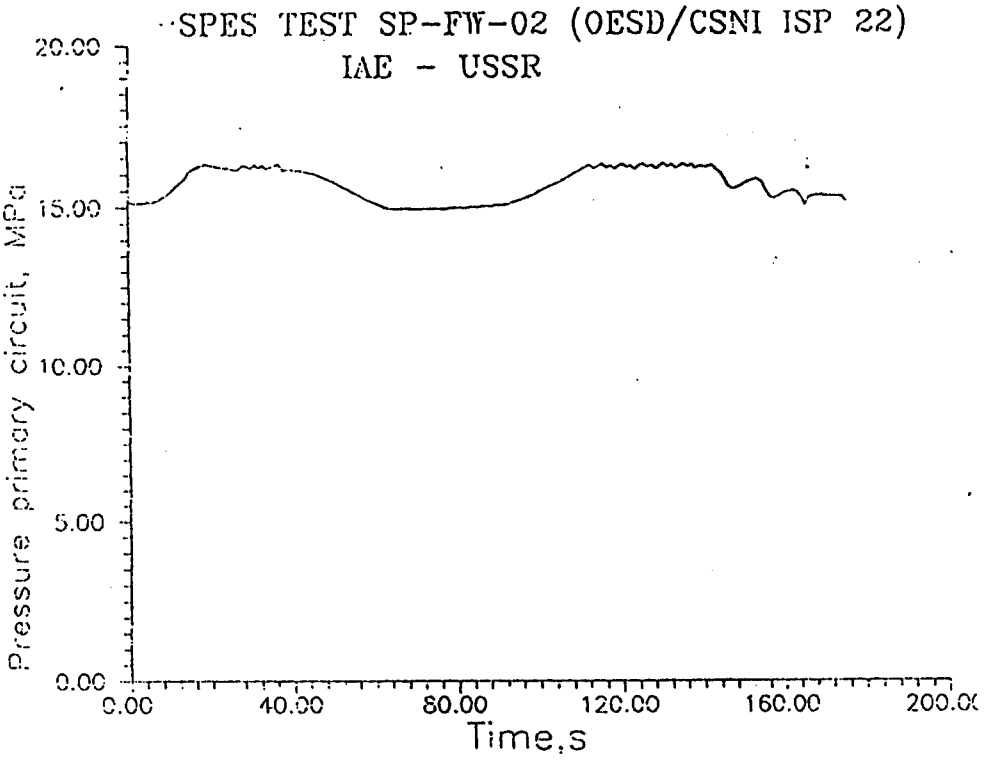

FIG. 1 PRESSURIZER PRESSURE

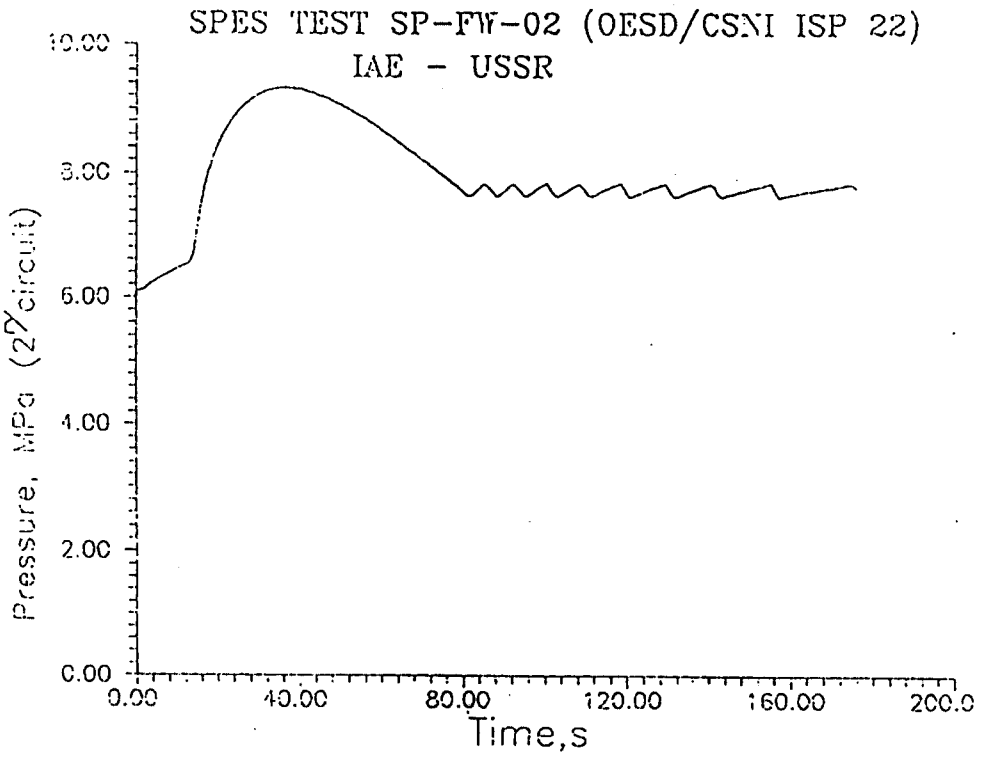

FIG. 3 SG1 STEAM DOME PRESSURE

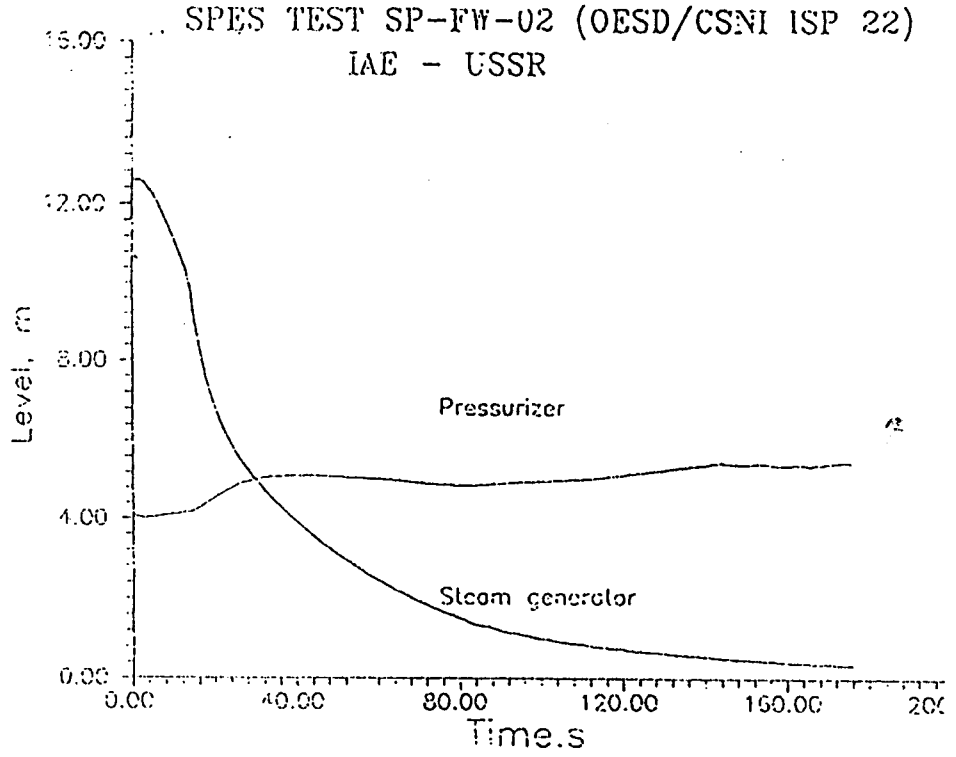

FIG. 6-7 PRESSURIZER LEVEL AND SG1 DOWNCOMER LEVEL

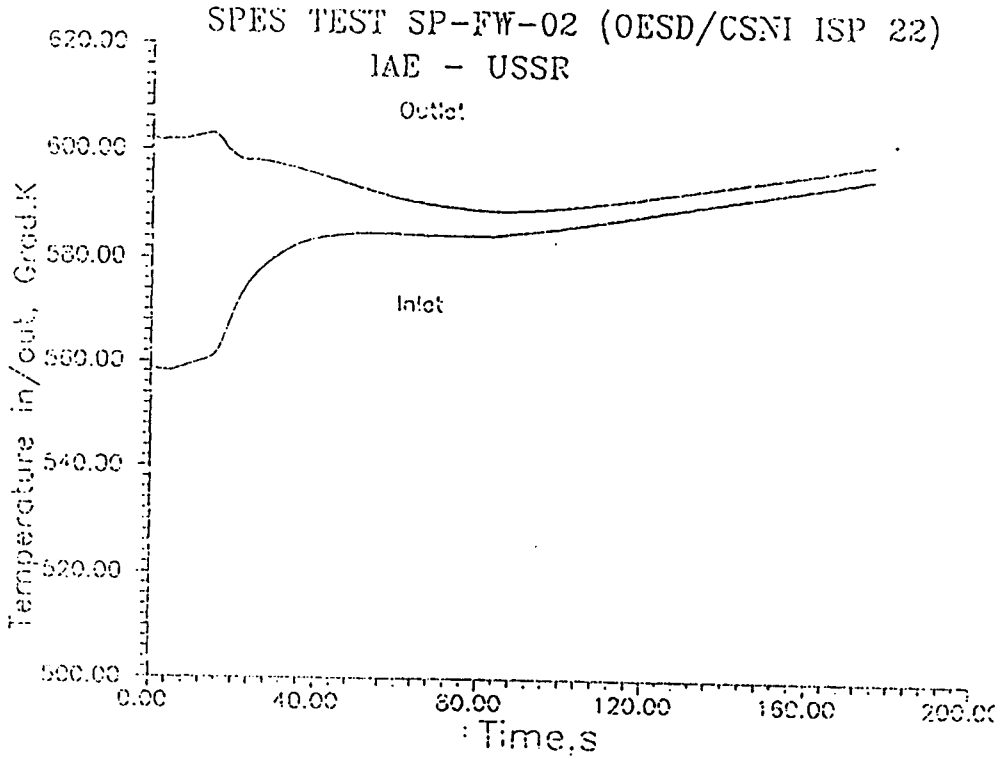

FIG. 12/42 SG1 INLET AND OUTLET TEMPERATURES

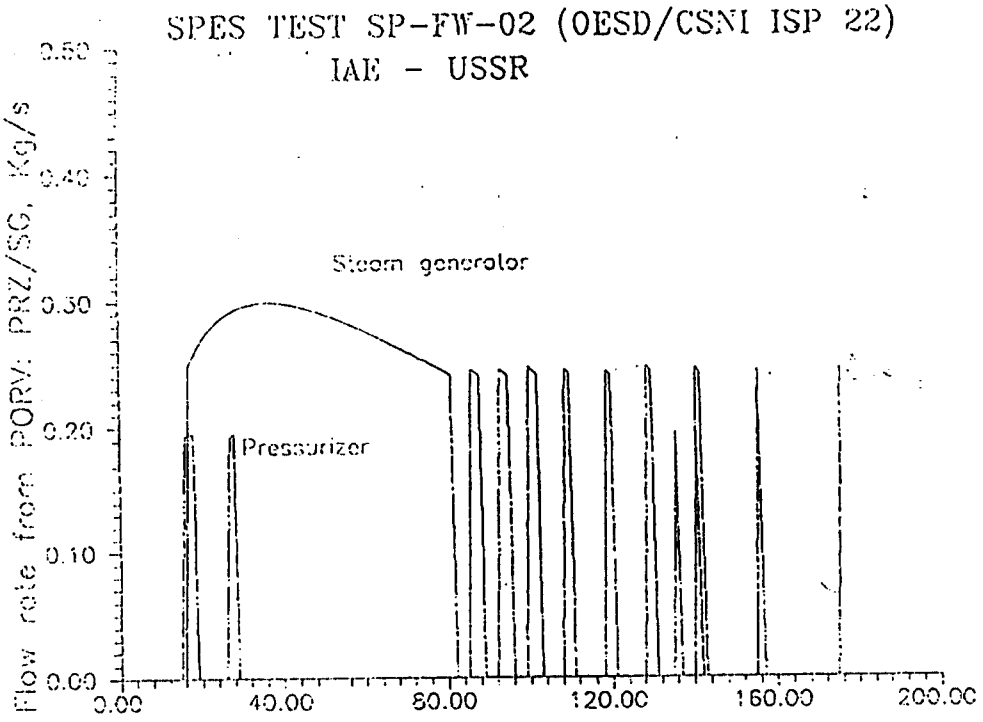

FIG. 92 PRZ PORV AND SG PORV MASS FLOWS

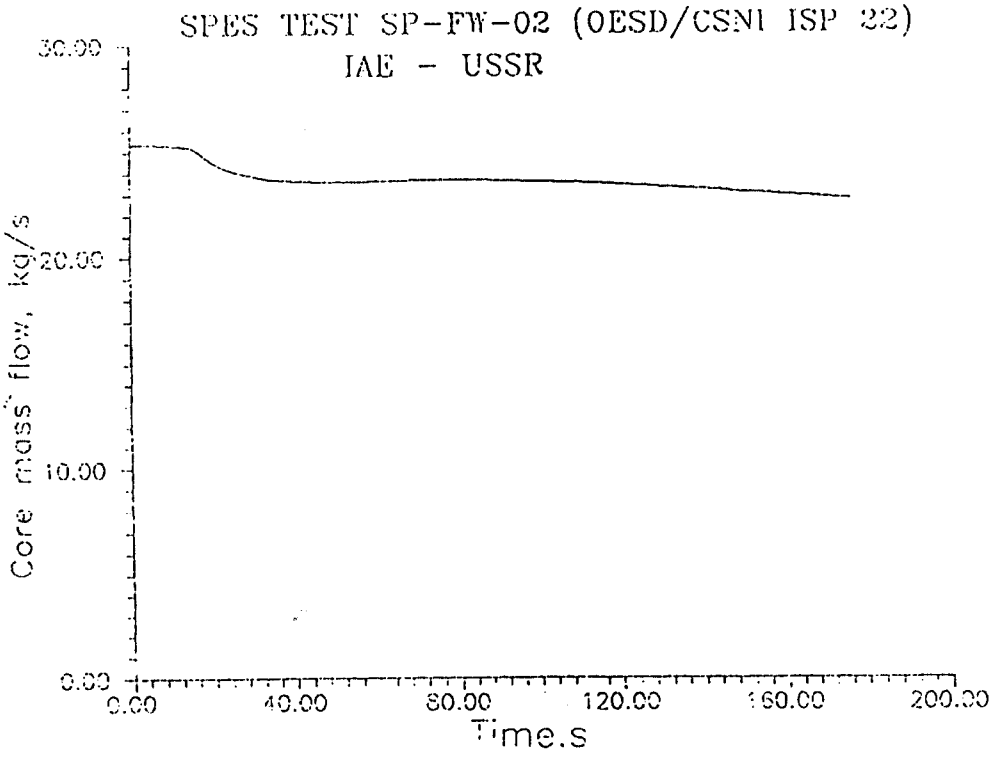

FIG. 141 CORE MASS FLOW

4.11 LJUBLJANA

4.11.1 CALCULATION DESCRIPTION

Phase 1: from LOFW to Scram (0 - 42 s)

Due to the LOFW the SGs DC level drops quickly (fig. 7b, 8b, 9b). The low-low level set point is reached at 31 s, and 5 s later the MSIV closure occurs (fig. 96b, 97b, 98b). The Scram signal is generated at 42 s causing the core power to reduce to the residual heat (fig. 81b). Primary pressure rises rapidly before reactor trip and drops immediately after it (see fig. 1b).

Phase 2: from Scram to PRZ PORV opening (42 - 3111 s)

After Scram a quick depressurization occurs in the primary side (fig. 16) as a consequence of the primary temperature decrease (fig. 12b). At about 850 s, when the SGs water inventory is strongly reduced (see figg. 86, 87 and 88), primary heat-up begins (figg. 12, 22 and 32). Consequently to primary heat-up, the primary pressure in first increases, then decreases until 2900 s. At this time a water "charging" occurs in the primary side, then the PRZ level and pressure increase up to PORV opening (fig. 1 and 6).

Phase 3: from PRZ PORV opening to pumps trip (3111 - 6738 s)

After PRZ PORV opening primary temperature continues to increase very slowly (fig. 12, 22, 32) and at 6738 s pumps trip occurs (fig. 54). SGs depressurize at decreasing rates (fig. 3, 4, 5).

Phase 4: from pumps trip to EFW actuation (6738 - 7411 s)

After pumps stop a short two phase natural circulation (TPNC) takes place in the primary side (fig. 89, 140). After NC stop, primary pressure increases quickly, over PRZ PORV set-point, up to 17.55 MPa (fig. 1).

Phase 5: from EFW actuation to the end (7411 - 11400 s)

At 7411 s, due to high rod temperature signal, EFW starts. This causes a quick repressurization in SG1 (Fig. 3). The re-established heat transfer between SG1 secondary side and primary side leads primary temperature and pressure to strongly decrease (fig. 1, 12, 42). Two phase natural circulation is reestablished in loop 1. In the other two loops the coolant flow is negligible. The DC collapsed level in SG1 (fig. 7) increases till 2.3 m at 11400 s (the ISP22 end value is 2.6 m).

PARTICIPANT: GREGORIC - LJUBLJANA *CODE: RELAP5/MOD2*

EVENTS TABLE

EVENT	*CALC. TIME (s)*	*EXP. TIME (s)*
SG Low Low Level	*30.7*	*33*
Main Steam Isolation	*35.8*	*38*
Scram (power fall), t_1	*41.8*	*44*
SGs PORV opening	*48* *48* *48*	*82 (3)* *106 (2)* *200 (1)*
SGs Dry Out	*4090* *4280 (950 ?)* *4350*	*3282 (3)* *3347 (1)* *3437 (2)*
PRZ PORV opening, t_2	*3111*	*4134*
PRZ full of liquid	*?*	*4222*
Pumps Trip, t_3	*6738*	*4848*
Loss of Natural Circulation	*7180*	*5630*
Beginning of Core Heat Up	*7375*	*6511*
EFW actuation, t_4	*7411*	*6532*
PRZ PORV closure	*7481*	*6576*
PRZ emptying	*7660 ?*	*6811*
SG1 repressurization	*7584*	*6878*
End of transient, t_{END}	*11400*	*8062*

4.11.2 CALCULATION/EXPERIMENT COMPARISON

Phase 1: from LOFW to Scram

Initial secondary inventory is largely underestimated (see C.T.). The low low level time is correctly predicted (31 s versus 33 s in the Exp.) and so the MSI and Scram times (see C.T.). The maximum primary pressure is calculated with good accuracy (see fig. 1b). Due to the wrong initial secondary inventory, the SGs masses at the Scram time are strongly underestimated (see C.T.).

Phase 2: from Scram to PRZ PORV opening

The calculated minimum primary pressure immediately after Scram, is in sufficient agreement with the experiment (fig. 1b). In the secondary side, SGs PORV opening times are underpredicted (see C.T. and fig. 3b, 4b, 5b) also if the pressurization trends are similar to the experimental ones. The SGs DC Level becomes 0 at about 4000 s versus 3300 s in the experiment), but the level trend is very strange (fig. 7, 8, 9). In the first the level drops quickly, then it remains at very small constant value and finally drops below 0 (see fig. 7, 8 and 9). We think that SGs dry-out occurs effectively at about 1000 s. The primary heat-up begins at 850 s (see figg. 12, 22 and 32) with a temperature gradient less than the experimental one (the core power is underestimated see fig. 81 a). The primary pressure (fig. 1) increases at about 1000 s, then decreases slowly till 2900 s. At this time a water charging occurs in the primary side (it' s not an ISP22 boundary condition) and PRZ level (fig. 6) increases. The calculated PRZ level becomes greater than 6.7 m (PRZ height). Due to PRZ level increasing, primary pressure increases and reaches the PRZ PORV opening set-point at 3111 s (fig. 1).

The experimental value is 4134 s. In the secondary side, SGs masses stay at constant value in time interval between 1000 and 3000 s (see fig. 86, 87 and 88, due to PORVs closure and secondary leaks trend (see fig. 137). At about 3000 s secondary leaks become greater than 0 and SGs mass and pressure decrease (see figg. 3, 4 and 5). In the experiment, secondary pressure decreases after SGs dry-out (about 3300 s).

Phase 3: from PRZ PORV opening to pumps trip

In this phase the calculated primary temperature gradient (fig. 12, 42)is strongly underestimated, due to a wrong core power (fig. 81 a) and maybe heat losse modelling. The pumps trip occurs very late (6738 s versus 4848 in the Exp.). Dominant relief condition during this phase (liquid discharge) is correctly predicted, as well as the absence of saturated points inside the primary sistem before pumps trip.

Phase 4: from pumps trip to EFW actuation

After pumps trip a two phase NC takes place in the primary side (see fig. 89). Time of loss of NC (t_{LNC}) is overestimated (7180 s versus 5630 s) but the time interval referred to trip time is underestimated (442 s versus 780 s). The calculated primary pressure shows a peak following LNC (see fig. 1). That can be related to the low quality discharge from PRZ PORV in this time interval. Core heat-up starts at 7375 s (versus 6511 in the experiment) (see fig. 52). Time interval between LNC and BOCH is underestimated (195 s versus 880 s). The low quality discharge from PRZ PORV after LNC contributes to the discrepancy. EFW actuation time is 7411 s (versus 6532 in the Exp.). The calculated phase duration dt_4 is shorter than the experimental one (673 s versus 1684 s).

Phase 5: from EFW actuation to the end

Maximum core temperature is calculated with sufficient accuracy (see fig. 52). Primary depressurization rate is initially overestimated (see fig. 1 and C.T.). Primary circulation mode is two phase natural circulation in loop 1, versus intermittent flow in the experiment. Calculated primary temperature and pressure show, in this phase, some peaks (fig. 1, 53) related to the calculated mass flow in loop 1 (fig. 89). Core reflood probably takes place from the bottom (core mass flow is always greater than 0). We can't be sure about it becouse there's a too small number of points in core surface temperature plots. SG1 repressurization time interval (see fig. 3) is underestimated (173 s vs 346 s). The calculated transient terminates at 11400 s with a SG1 DCL (fig. 7) of 2.3 m (ISP22 end value is 2.6 m). The phase duration is also overestimated (3989 s vs 1530).

PARTICIPANT: GREGORIC - LJUBLJANA CODE: RELAP5/MOD2

COMPARISON TABLE

PARAMETER		EXP	CALC	AE*	RFD**
1A Initial SGs mass (Kg)	1	137	93		
	2	151	111	P	B+C+U
	3	145	106		
1B Trips timing (s)	LoLo	33	30.7		
	MSI	38	35.8	G	-
	Scram	44	41.8		
1C Max primary pressure (MPa)		16.2	16.2	G	-
1D SGs mass at Scram (Kg)	1	98	50	P	
	2	105	68	P	1A
	3	97	62	P	
2A Min. primary pressure (MPa)		14.5	14.1	S	-
Pressure gradients before		4.10^{-4}	?	P	PRZM ? (U)
and after SGs DO (MPa/s)		3.10^{-4}	?	P	
2B SGs PORV opening time (s)	1	200	48		
	2	106	48	P	?
	3	82	48		
2C PRZ level gradient (m/s)		$-5.7.10^{-4}$	$-1.56.10^{-4}$	P	?
2D Min. PRZ level (m)		2.3	3.3	P	2C+2E
2E SGs DO time, tSG1DO (s)		3347	950(4280)		
tSG2DO (s)		3437	950(4380)	P	1D?
tSG3DO (s)		3282	950(4090)		
2F Heat Up temperature (K/s)		0.02	0.007	P	
and level (m/s) gradients		$3.6.10^{-3}$	$2.5.10^{-3}$	P	UCP? (U)
2G Cool Insurge effect		PR. DELAY	PRES.DEC?	?	?
2H PRZ PORV opening time, t2 (s)		4134	3111	P	2E+UBC(U)
($dt_2 = t_2 - t_{SGDO}$)		(697)	2161(-1239)	P	
3A PRZ level at t_2 (m)		6.57	6.4	G?	-
3B PRZ full time, t_{PRZF} (s)		4222	?	-	-
($dt_{PRZF} = t_{PRZF} - t_2$)		(88)			
3C Dominant Relief Condition		LIQ	LIQ	G	-
3D Sat. Conditions before trip		NO	NO	G	-
3E Pumps Trip time, t3 (s)		4848	6738	P	2F
($dt_3 = t_3 - t_2$)		(714)	(3627)	P	2H+2F
($dt_{HU} = t_3 - t_{SGDO}$)		(1411)	5788(2388)	P	2F

* ACCURACY EVALUATION : G=GOOD, S=SUFFICIENT, P=POOR

** REASON FOR DISCREPANCY : B=BIC, C=CODE, U=USER, PRZM=PRZ MODELLING, UCP=UNDERESTIMATE OF CORE POWER, UBC=USER BOUNDARY CONDITION, ?=NOT CLEAR HSM=HEAT STRUCTURES MODELLING

PARTICIPANT: GREGORIC - LJUBLJANA CODE: RELAP5/MOD2

COMPARISON TABLE (CONT'D)

PARAMETER	EXP	CALC	AE*	RFD**
3F RCS mass at t_3 (kg)	390	?	-	-
4A PRZ behaviour during phase 4	PART. EMPT. LEV. OBS.	PART. EMPT.	?	-
4B Primary Flow Cond.	TPNC/LNC	TPNC/LNC	G	-
4C LNC time, t_{LNC} (s)	5630	7180	P	3E
($dt_{LNC} = t_{LNC} - t_3$)	(780)	(442)	P	LDP? (C)
4D RCS mass at t_{LNC} (kg)	296	?	-	-
4E Beg. of Core Heat Up, t_{BOCH} (s)	6511	7375	S	3E
($dt_{BOCH} = t_{BOCH} - t_{LNC}$)	(880)	(195)	P	LDP (C)
4F RCS mass at tBOCH (Kg)	183	?	-	-
4G EFW act. time, t4 (s)	6532	7411	S	3E
($dt_{4B} = t_4 - t_{BOCH}$)	(21)	(36)	P	?
($dt_{4L} = t_4 - t_{LNC}$)	(900)	(231)	P	?
($dt_4 = t_4 - t_3$)	(1684)	(673)	P	LDP? (C)
4H PRZ level at t_4 (m)	4.4	4.3	G	-
5A Core Heat Up Rate (K/s)	2/5	1.8	P	?
5B Max Core Temperature (K)	770	836	S	-
5C PRZ PORV closure time, t_{PRZPC}	6576	7481	S	4G
($dt_{PRZPC} = t_{PRZPC} - t_4$)	(44)	(70)	S	-
5D RCS mass at t_{PRZPC} (Kg)	179	?	-	-
5E RCS Depress. Rate (MPa/s)	-0.016	-0.054	P	?
(Initial/Averaged on 500 s)	-0.0086	-0.008	G	-
5F Prim. Circulation Mode	INTERM	TPNC	P	C+U?
5G SG1 Press. time, t_{SG1PR} (s)	6878	7584	S	4G
($dt_{SG1PR} = t_{SG1PR} - t_4$)	(346)	(173)	P	?
5H PRZ Role	CORE FL.	CORE FL?	G?	-
5I PRZ emptying time, t_{PRZE} (s)	6811	7660?	S	4G
($dt_{PRZE} = t_{PRZE} - t_4$)	(280)	249?	S?	-
5J Core Reflood Mode	TOP-DOWN	BOTTOM/UP	P?	?
5K End of Transient time, t_{END}	8062	11400	P	4G+?

* ACCURACY EVALUATION : G=GOOD, S=SUFFICIENT, P=POOR

** REASON FOR DISCREPANCY : C=CODE, U=USER, LDP=LIQUID DISCHARGE FROM PRZ

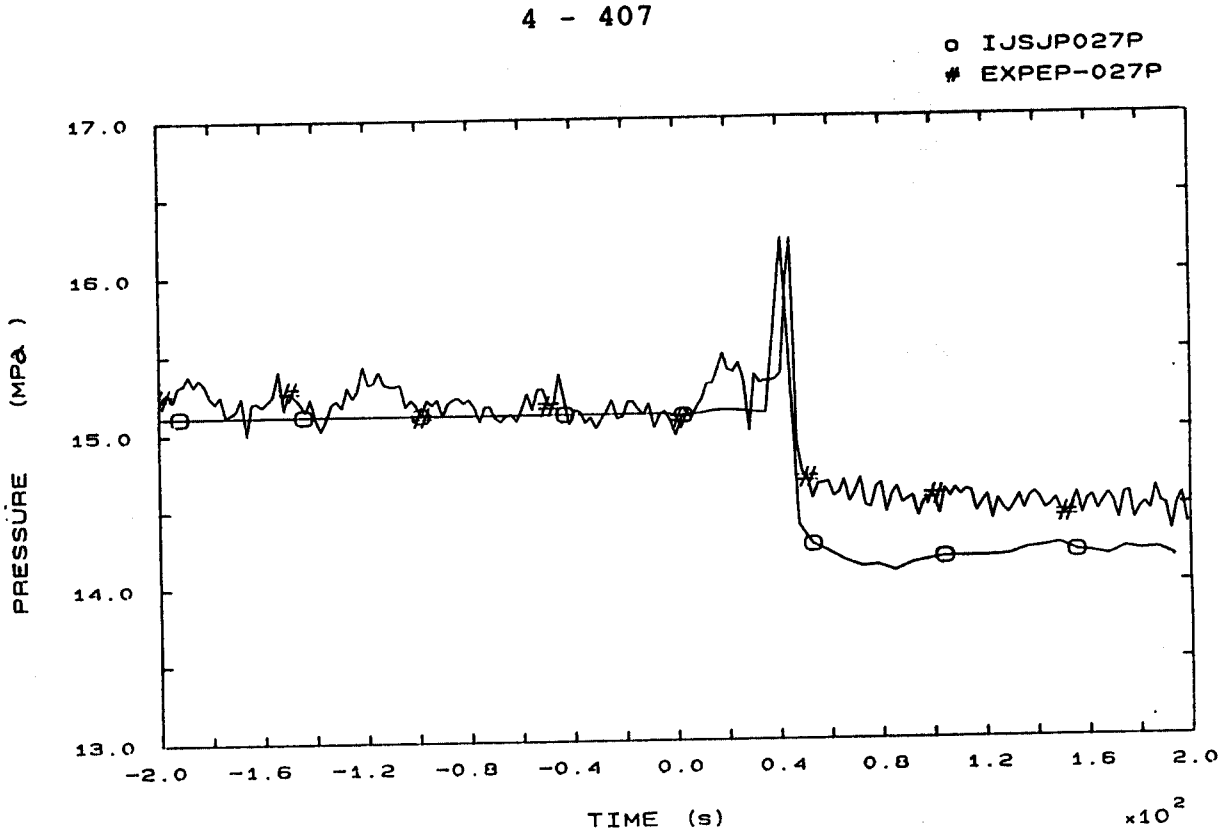

FIG. 1b PRESSURIZER PRESSURE

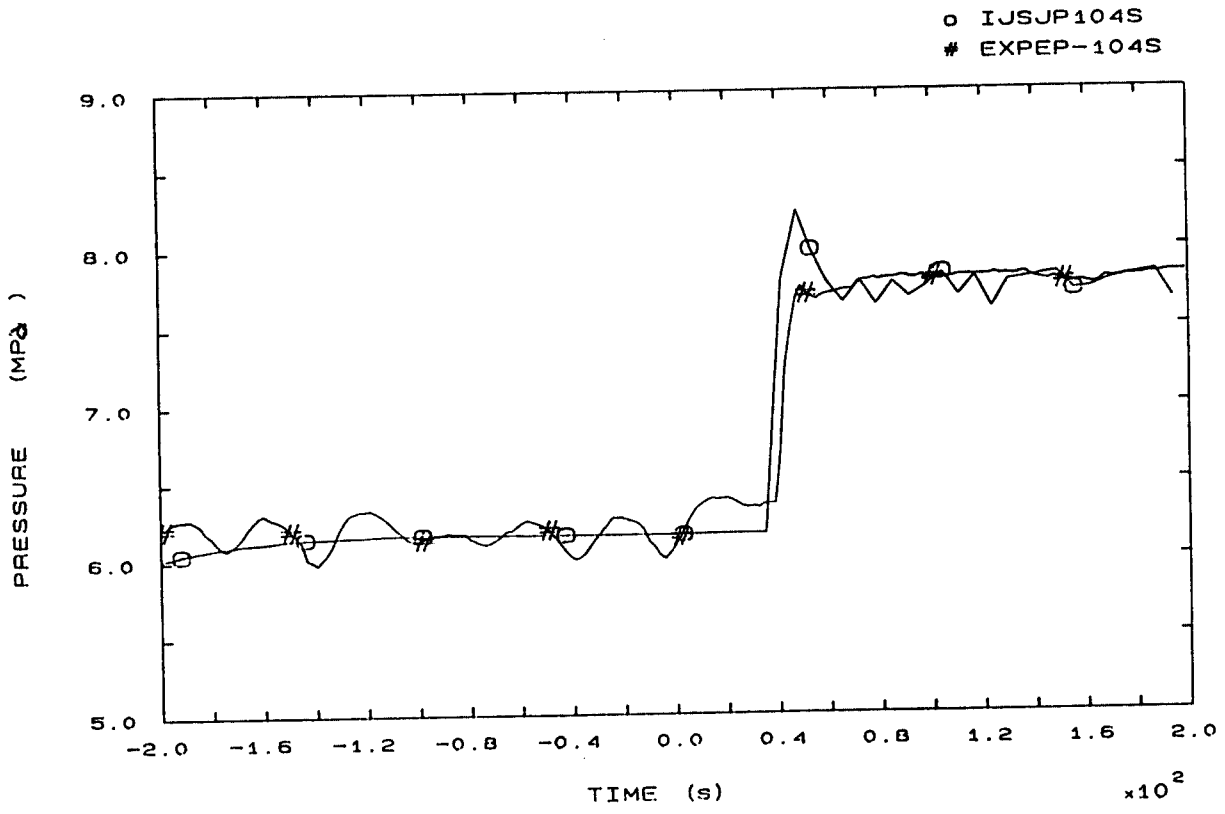

FIG. 3b SG1 STEAM DOME PRESSURE

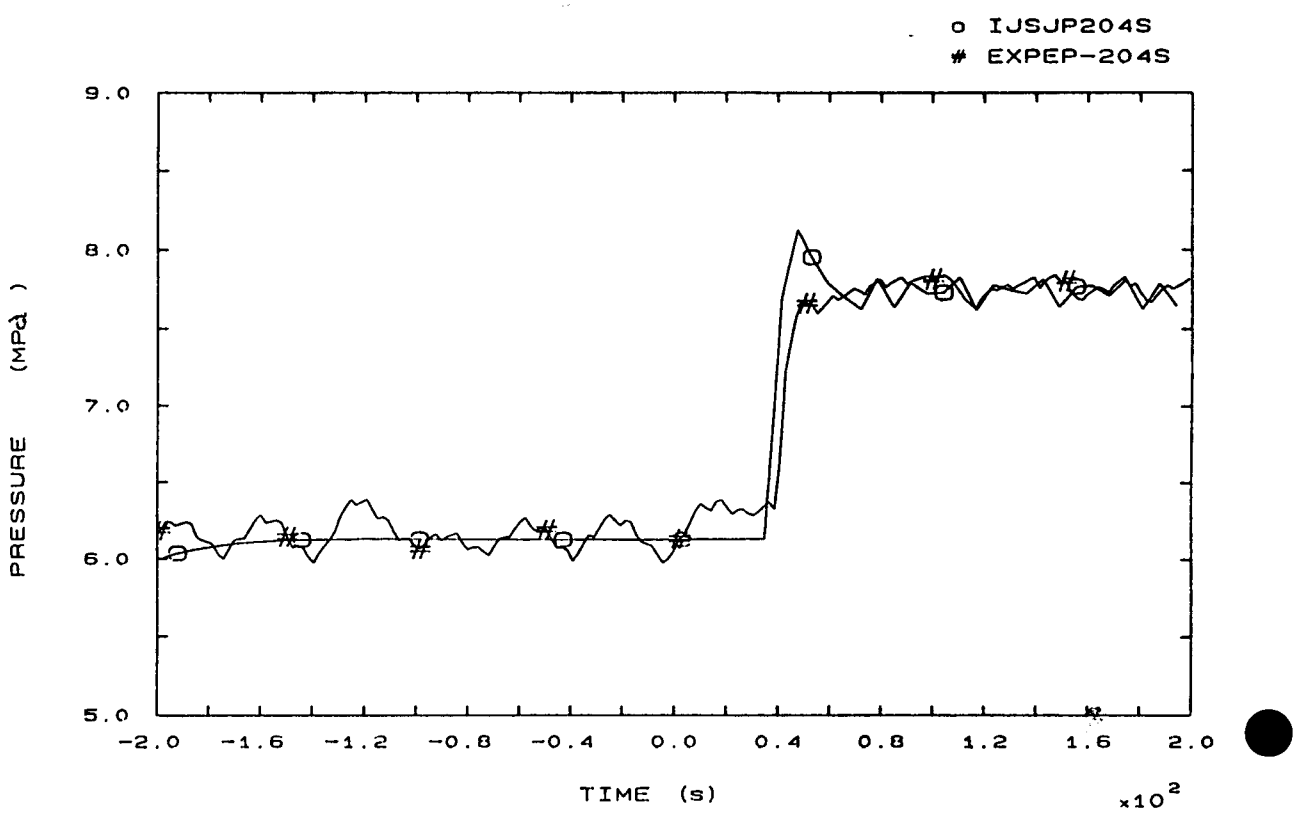

FIG. 4b SG2 STEAM DOME PRESSURE

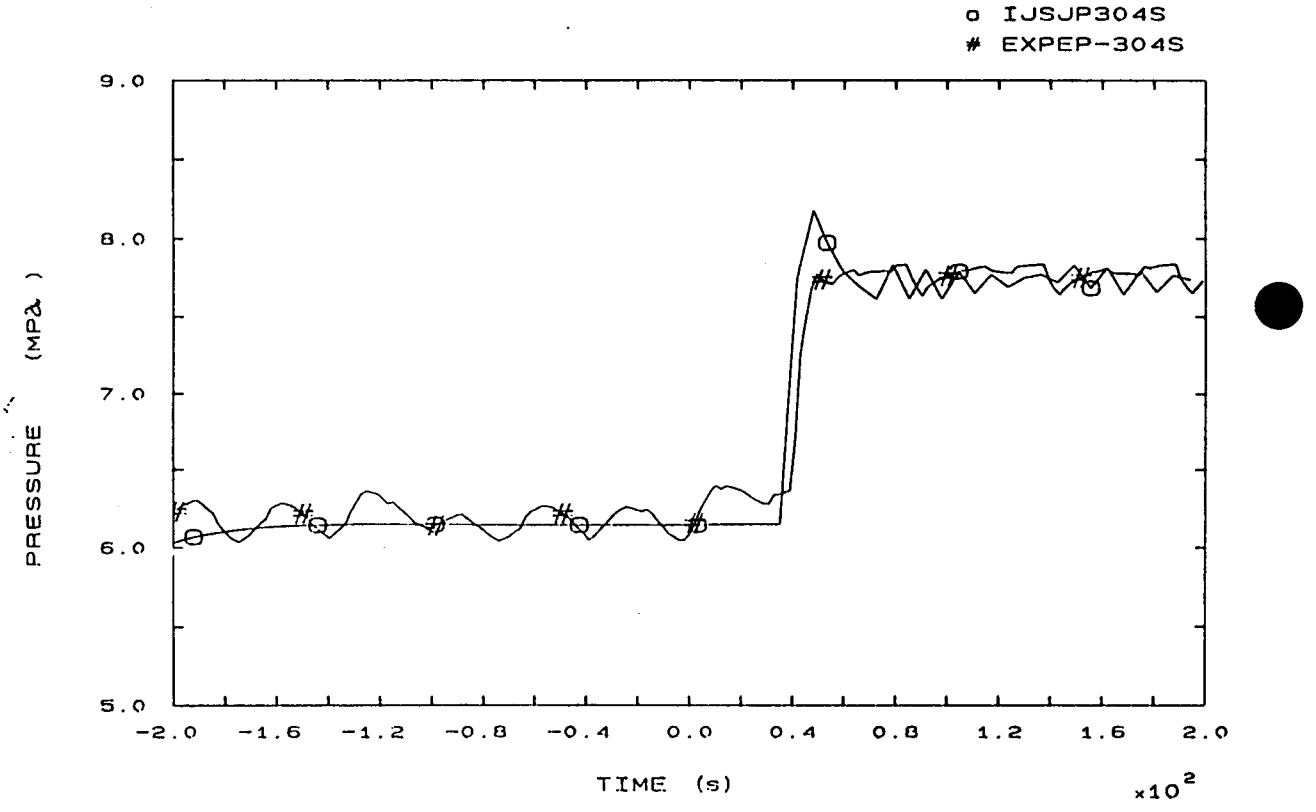

FIG. 5b SG3 STEAM DOME PRESSURE

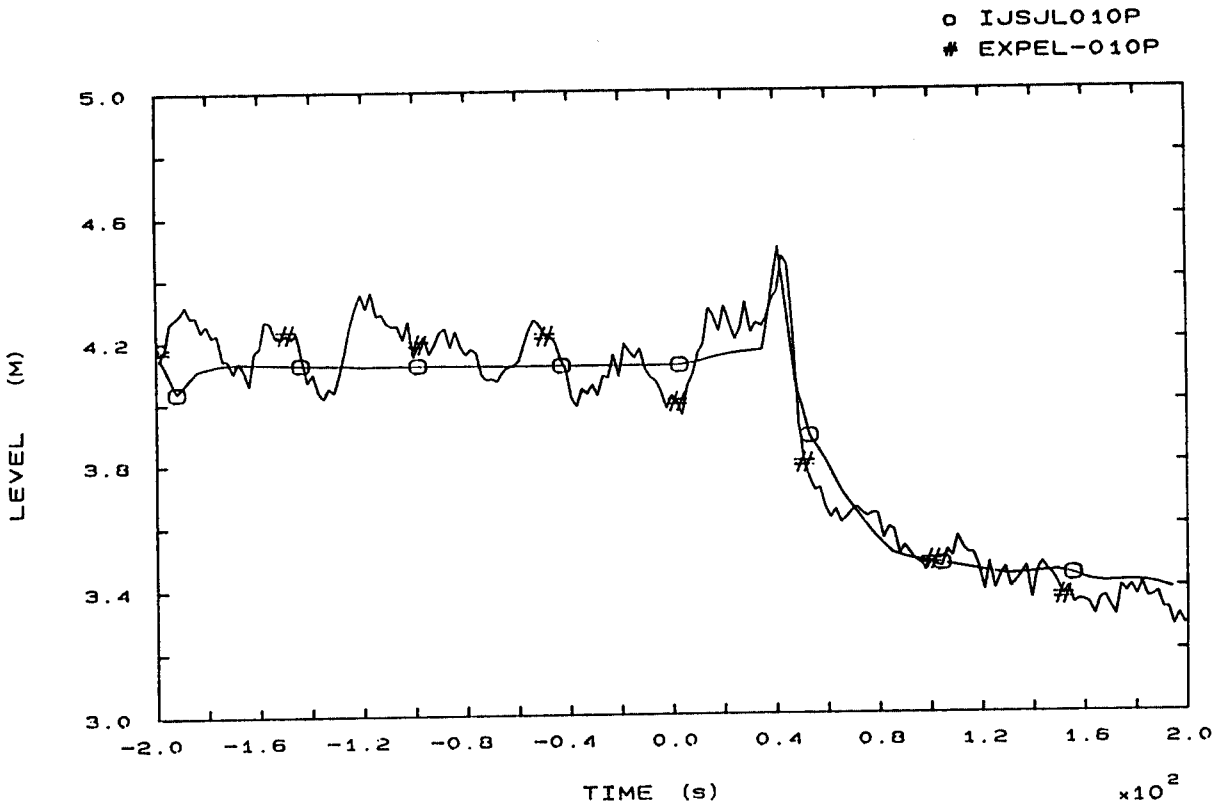

FIG. 6b PRESSURIZER LEVEL

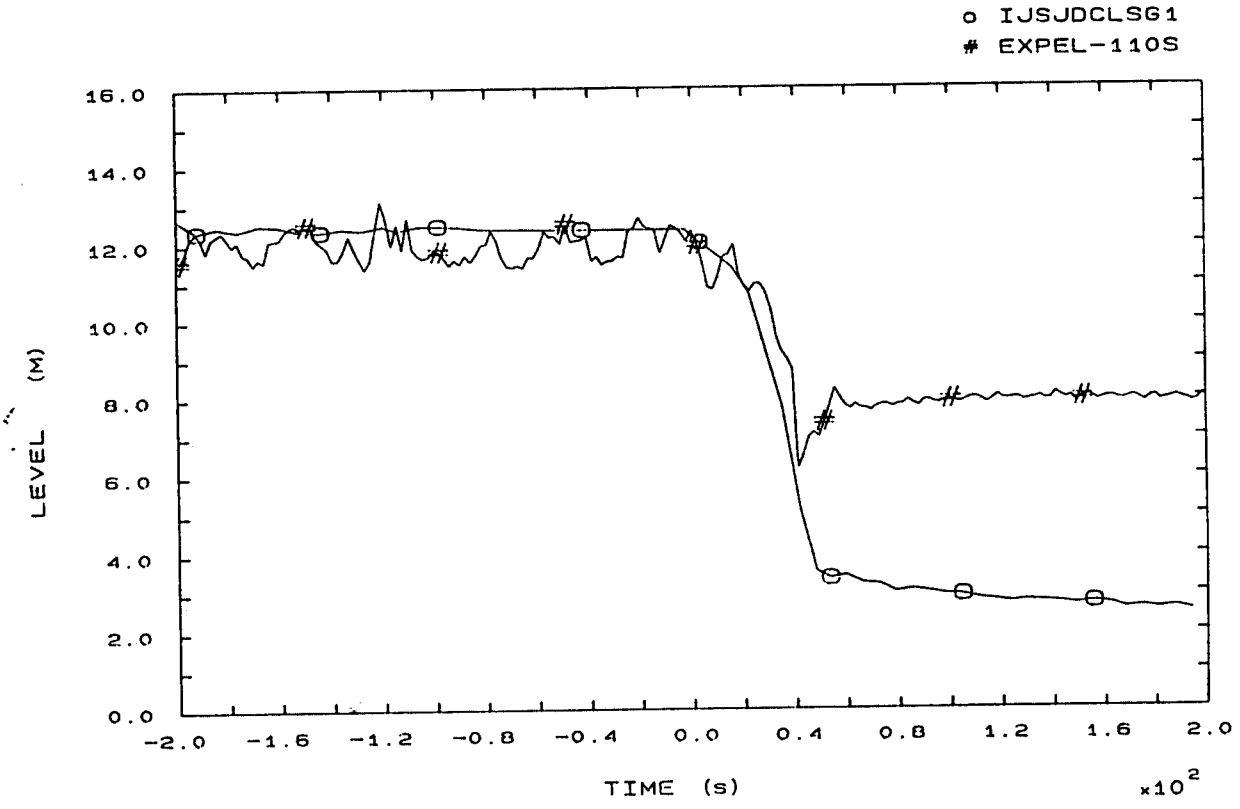

FIG. 7b SG1 DOWNCOMER LEVEL

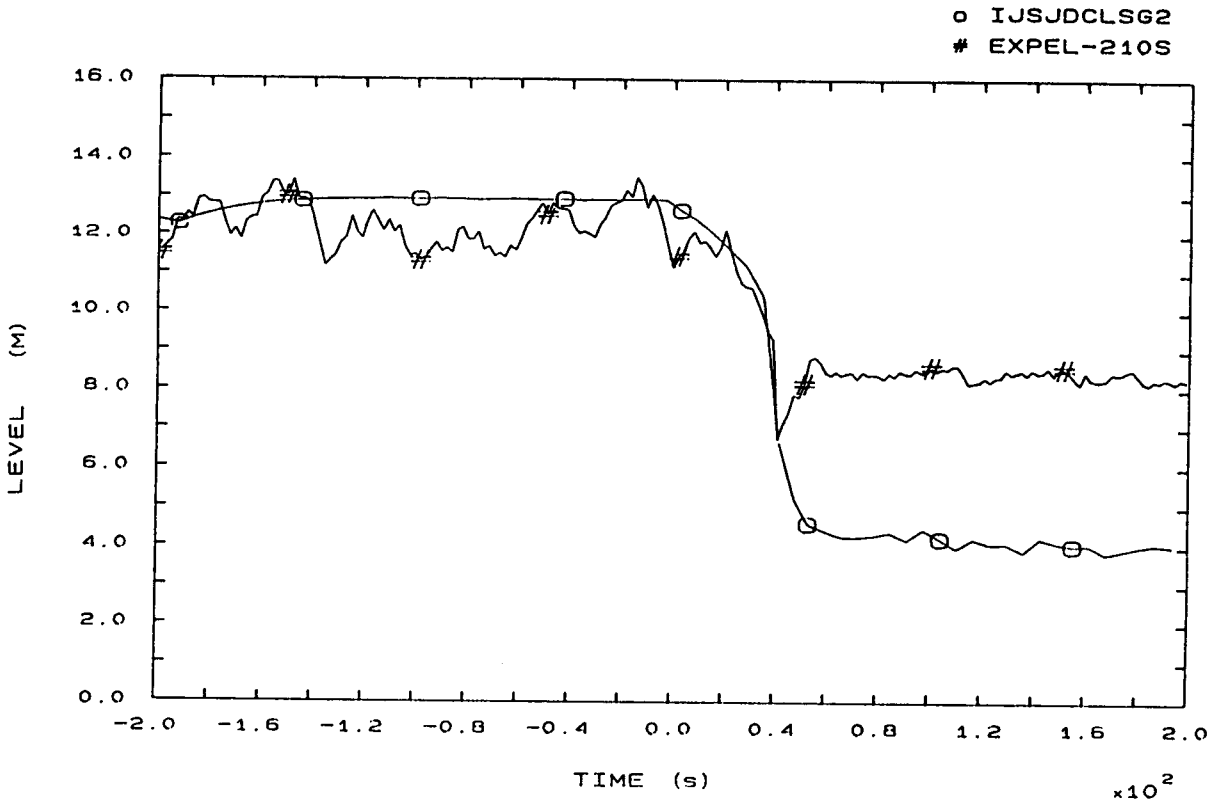

FIG. 8b SG2 DOWNCOMER LEVEL

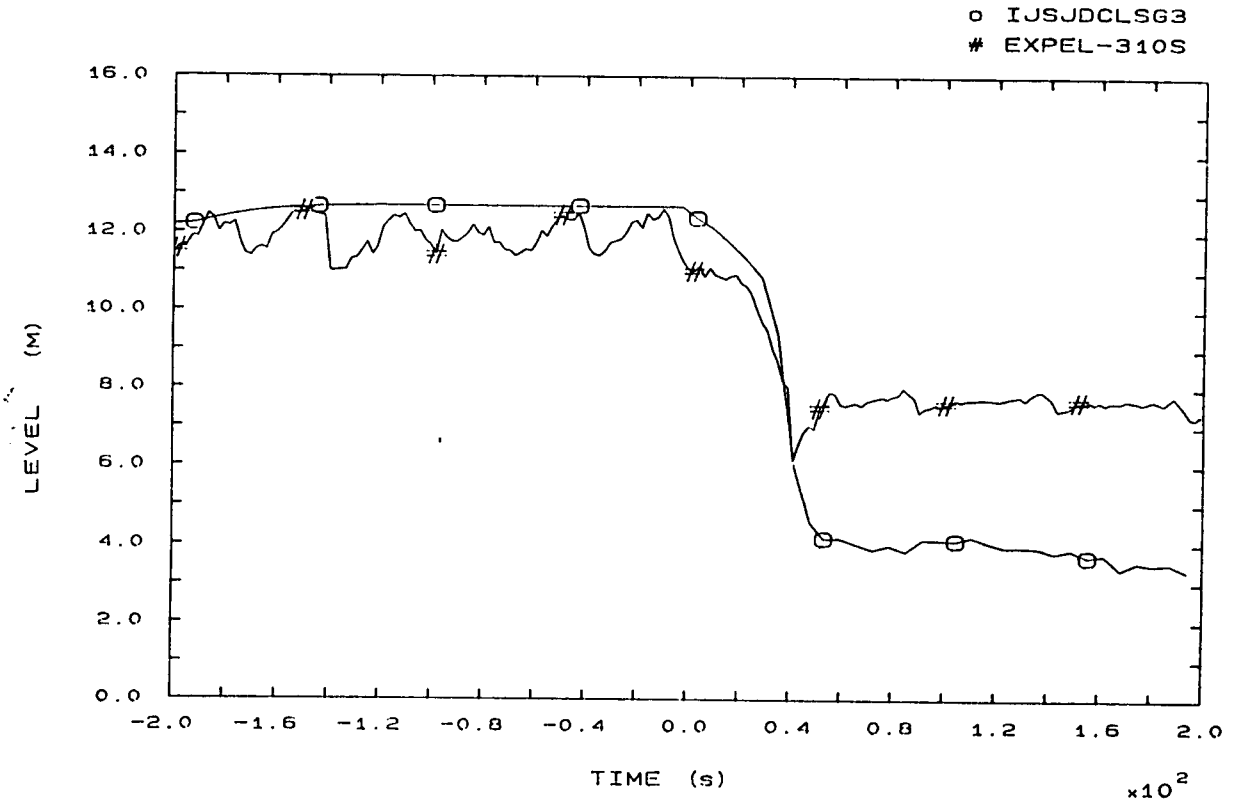

FIG. 9b SG3 DOWNCOMER LEVEL

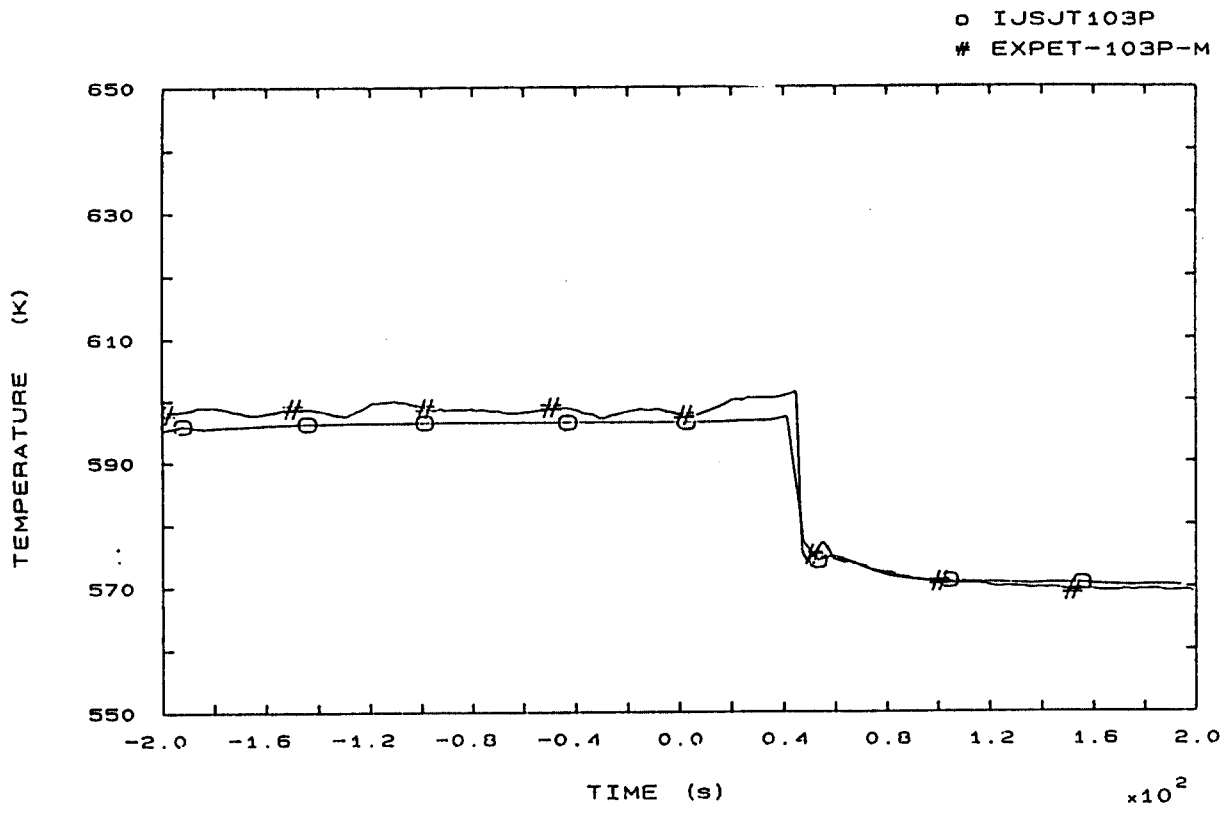

FIG. 12b LP1 HOT LEG OUTLET VESSEL TEMPERATURE

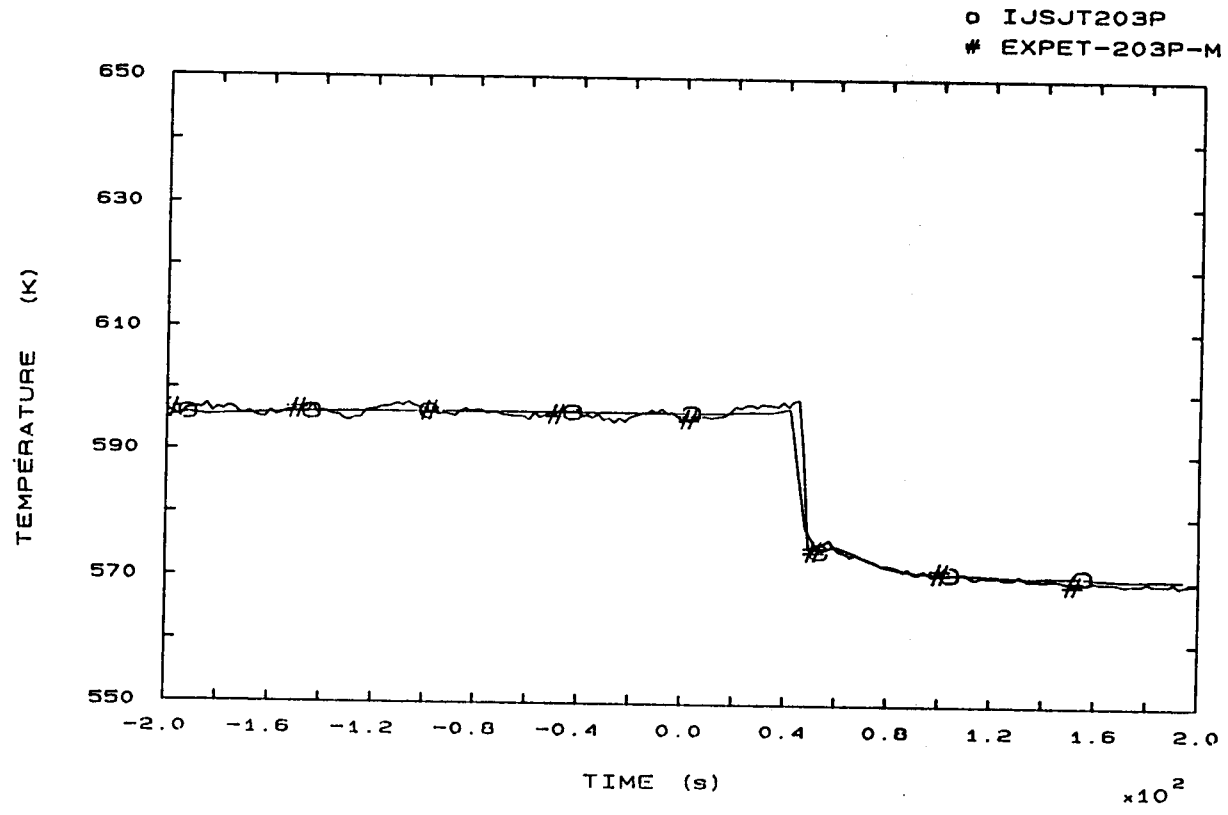

FIG. 22b LP2 HOT LEG OUTLET VESSEL TEMPERATURE

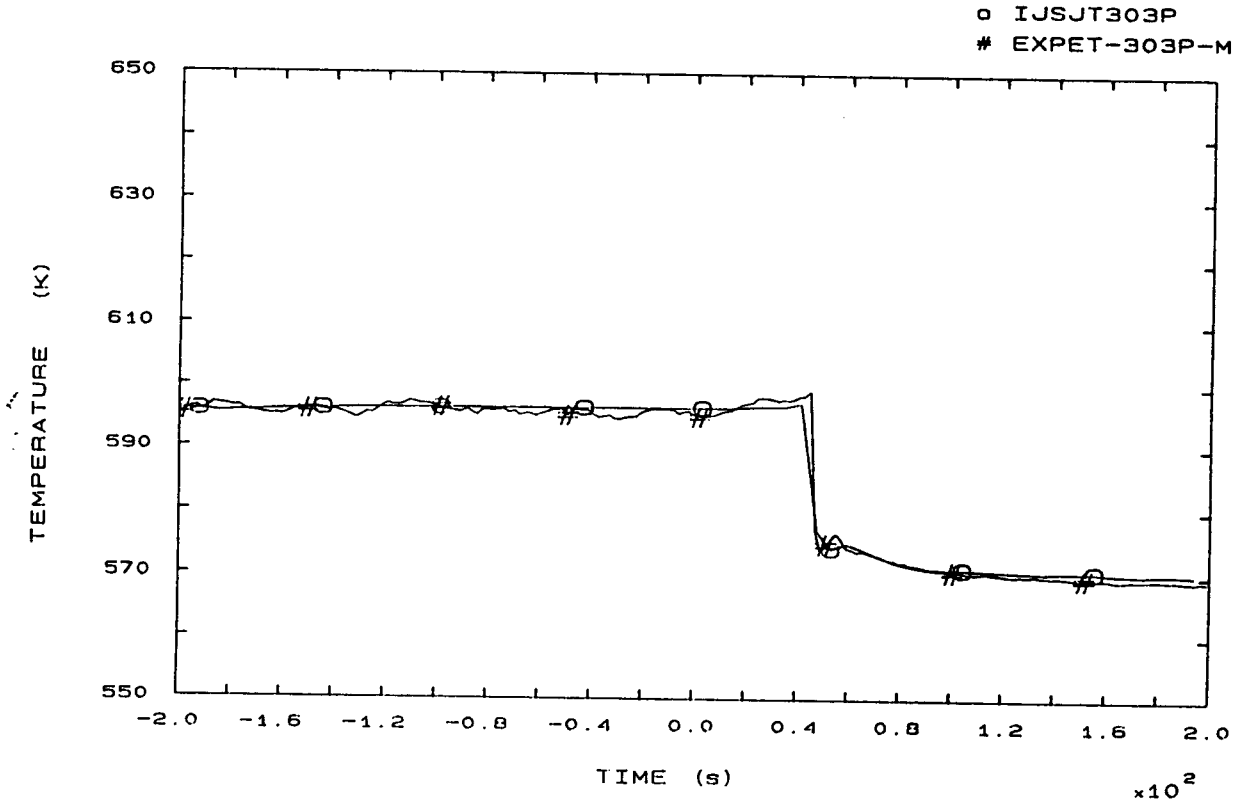

FIG. 32b LP3 HOT LEG OUTLET VESSEL TEMPERATURE

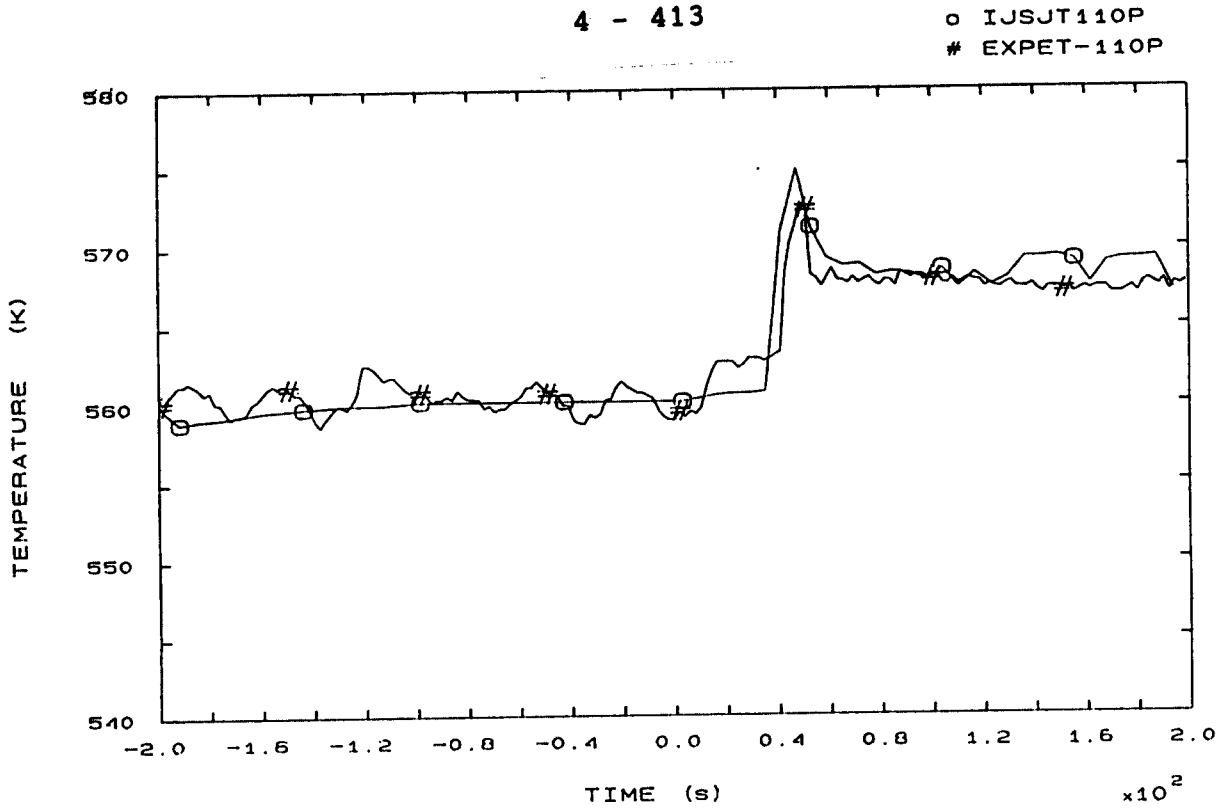

FIG. 42b SG1 OUTLET TEMPERATURE

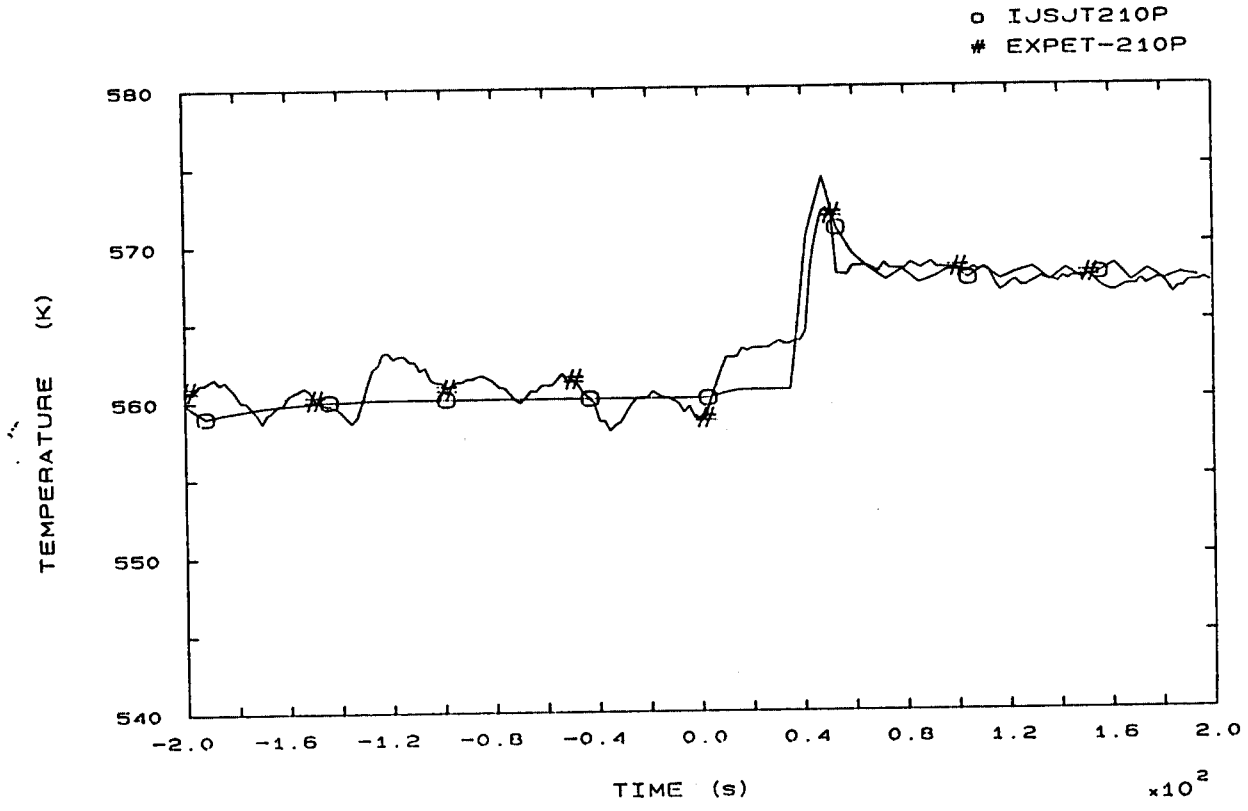

FIG. 44b SG2 OUTLET TEMPERATURE

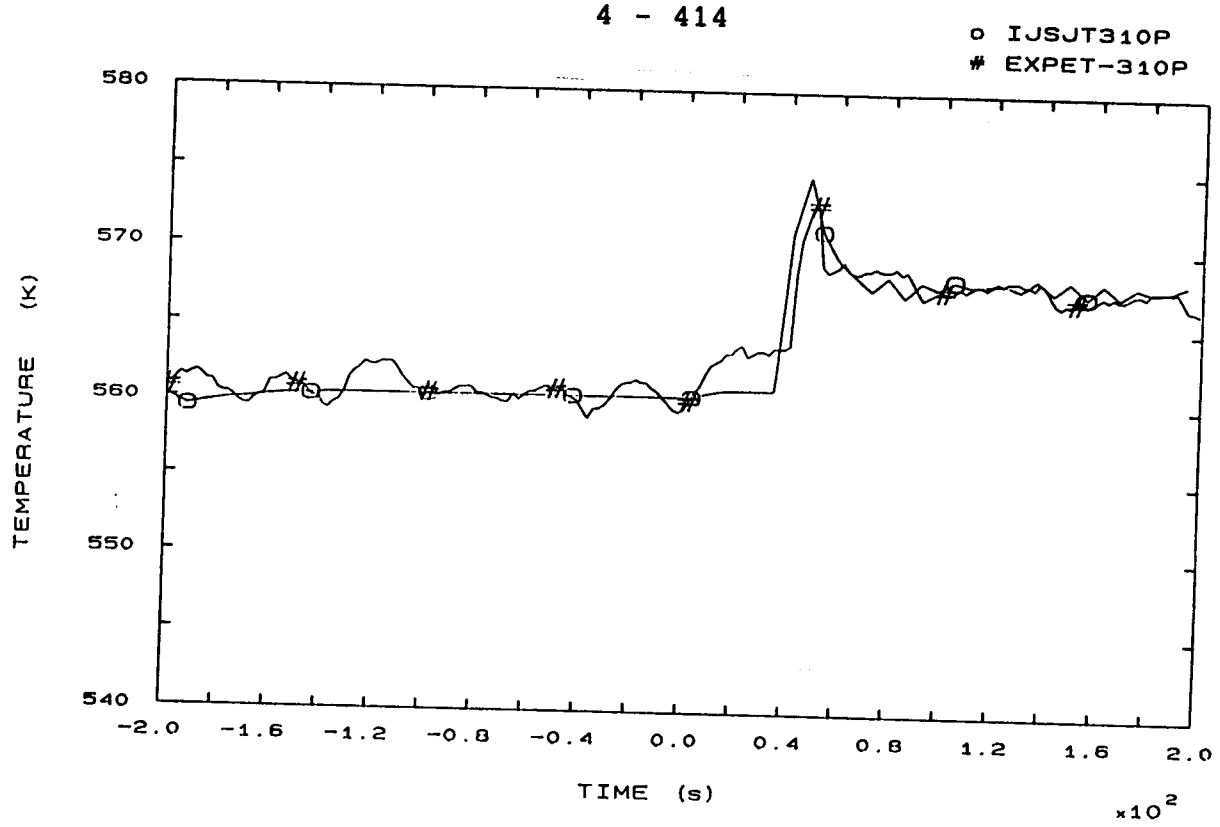

FIG. 46b SG3 OUTLET TEMPERATURE

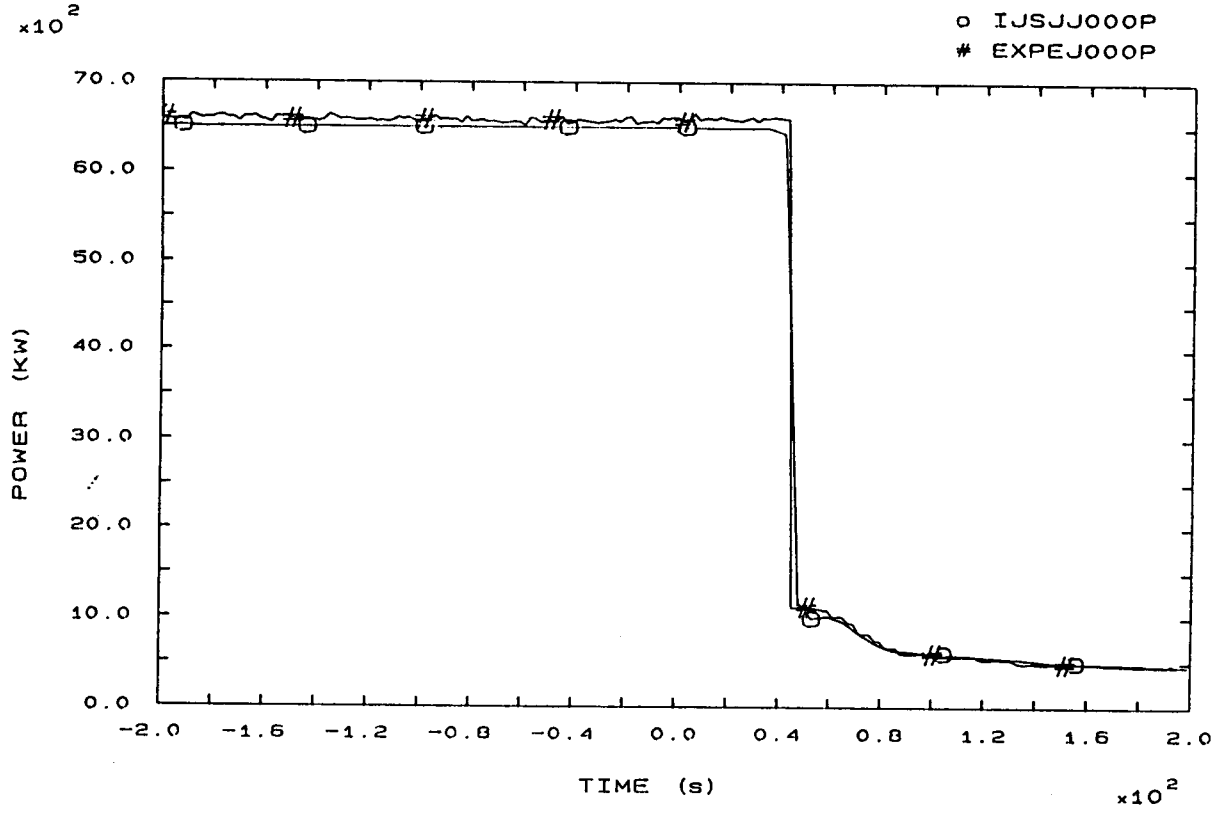

FIG. 81b HEATER RODS POWER

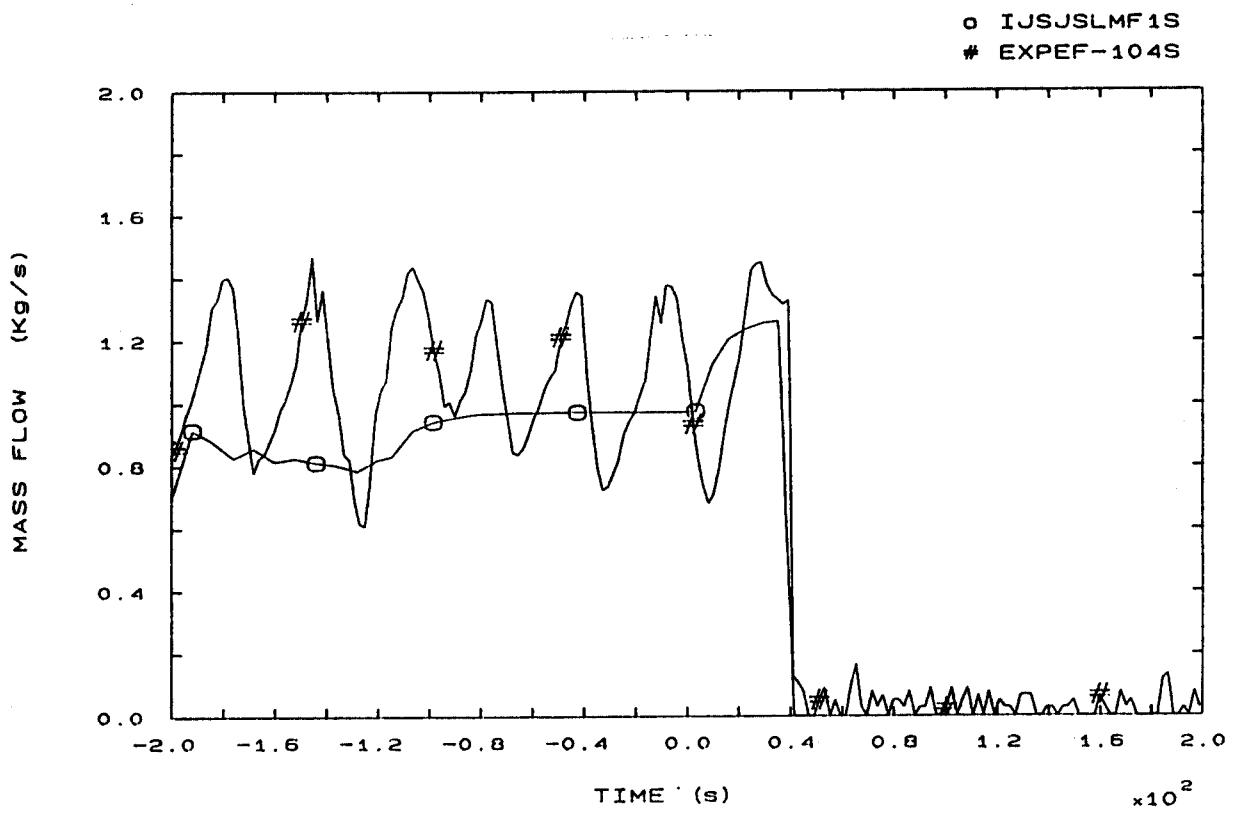

FIG. 96b STEAM LINE 1 MASS FLOW

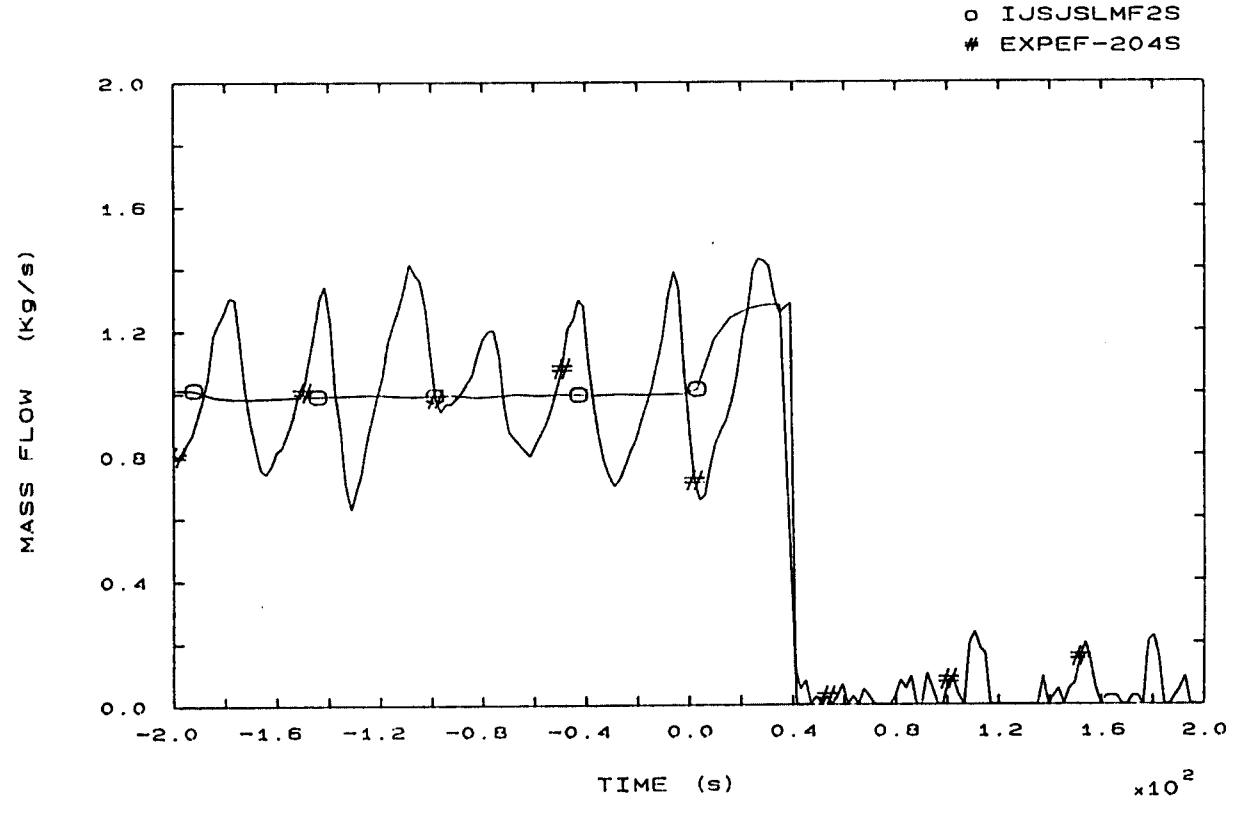

FIG. 97b STEAM LINE 2 MASS FLOW

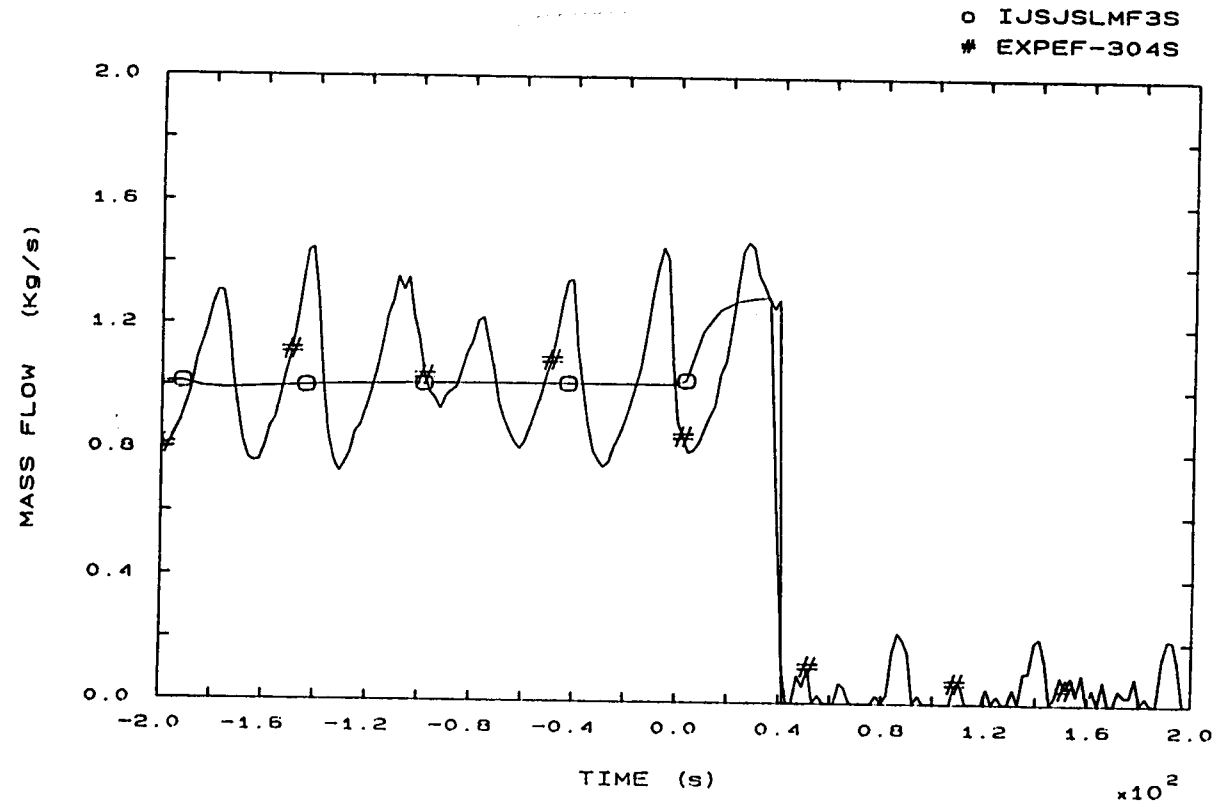

FIG. 98b STEAM LINE 3 MASS FLOW

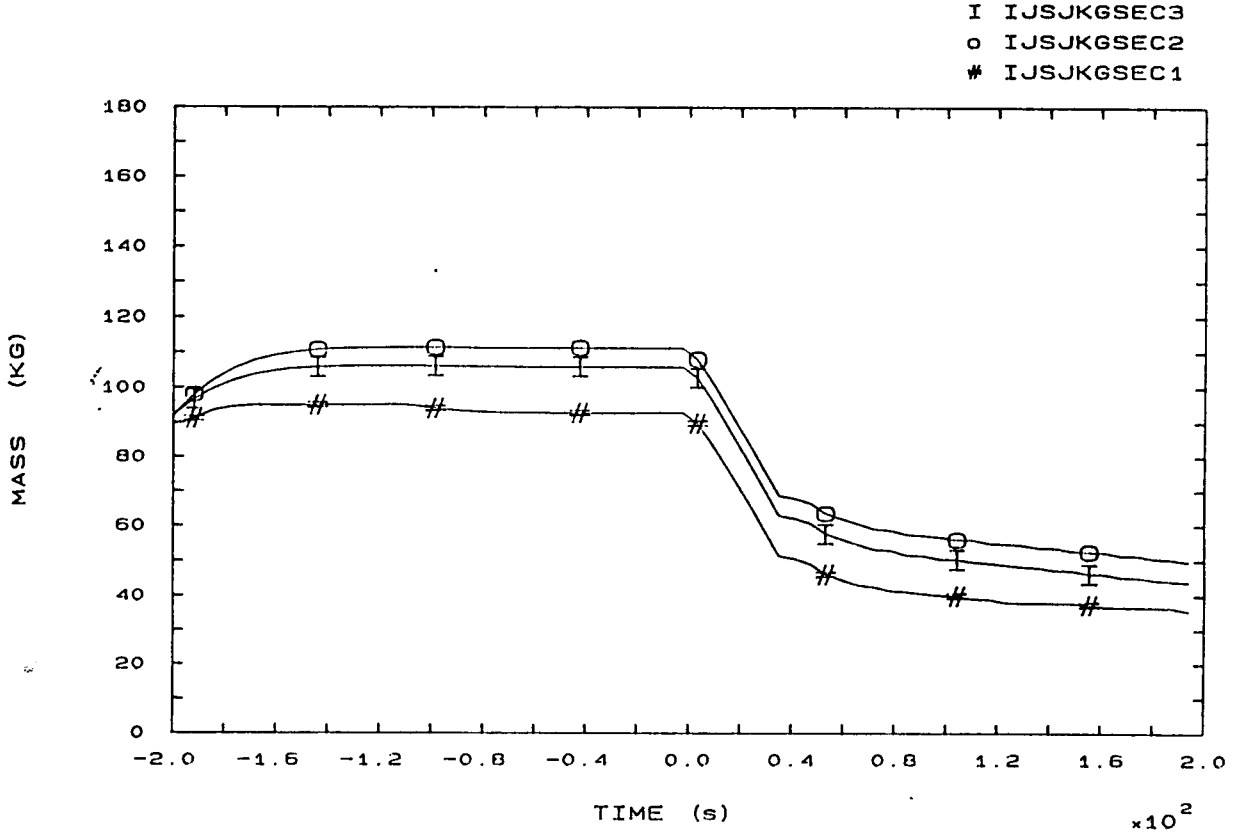

FIG. 142b SECONDARY COOLANT TOTAL MASS IN SGs

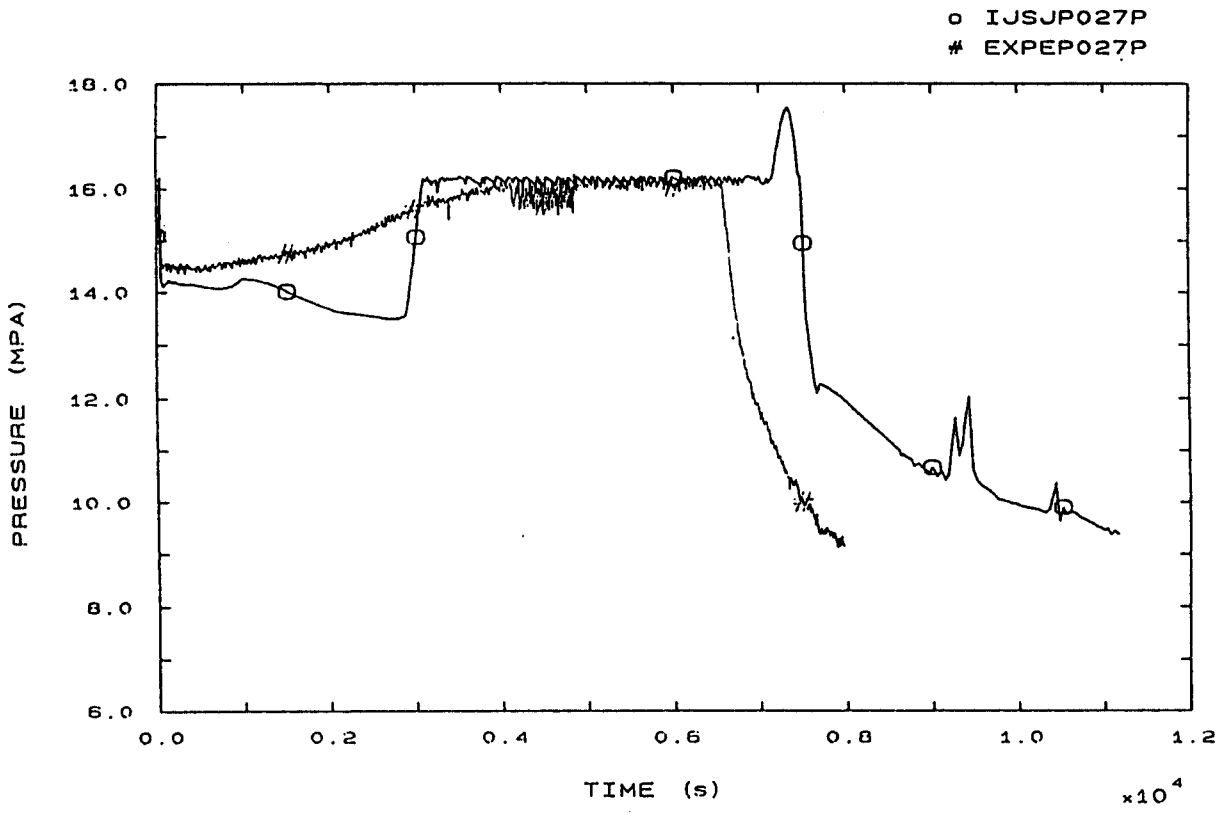

FIG. 1 PRESSURIZER PRESSURE

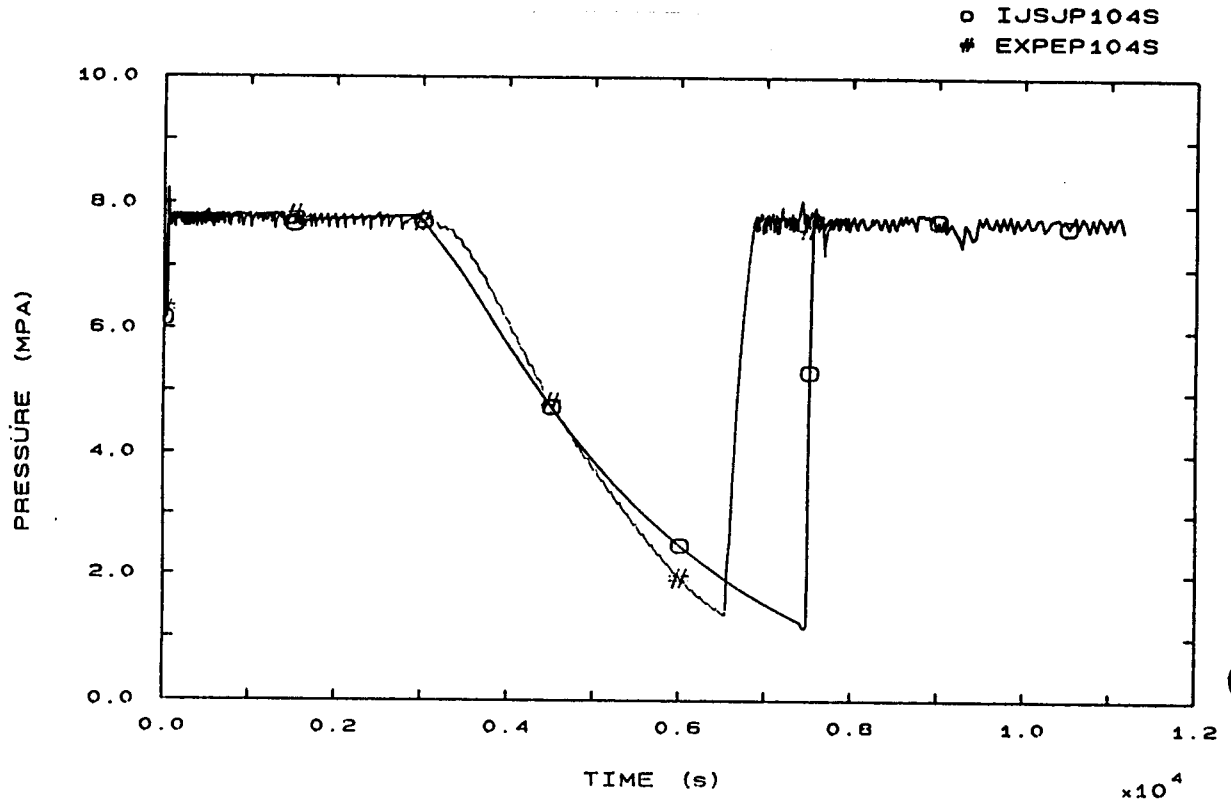

FIG. 3 SG1 STEAM DOME PRESSURE

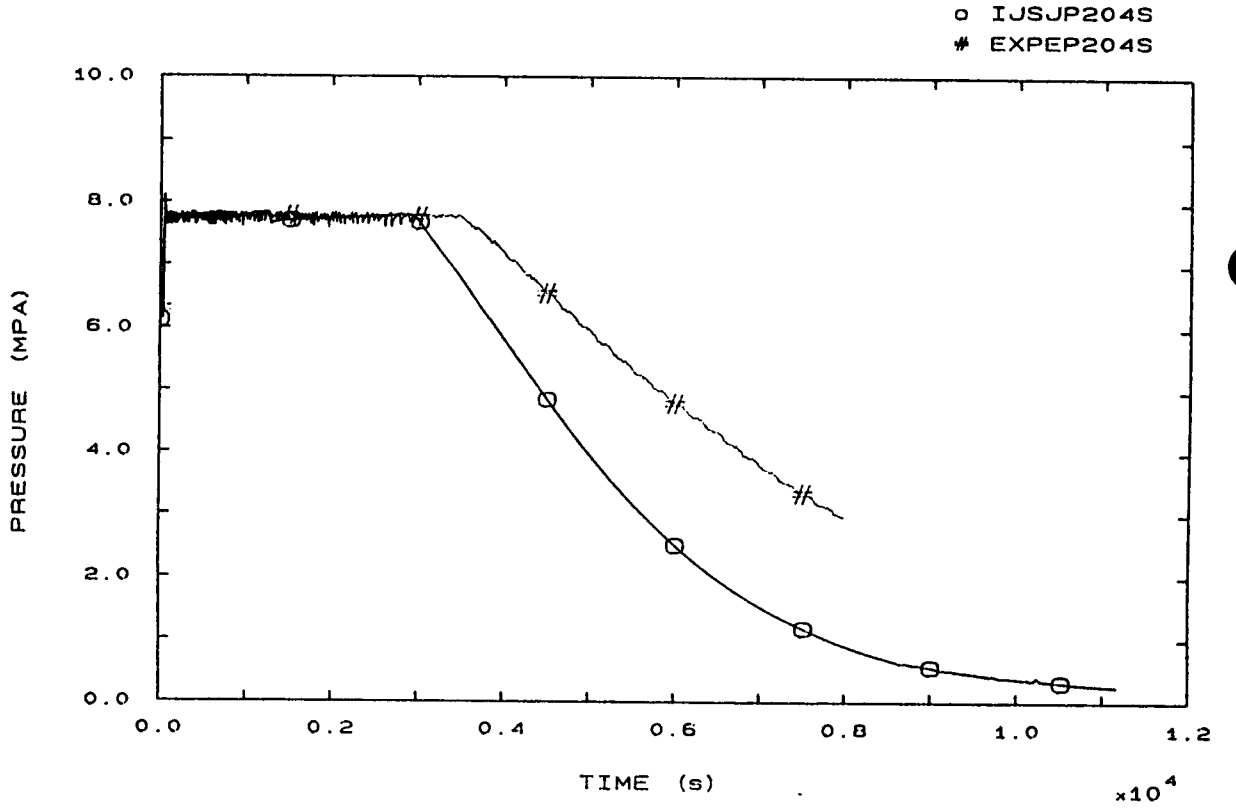

FIG. 4 SG2 STEAM DOME PRESSURE

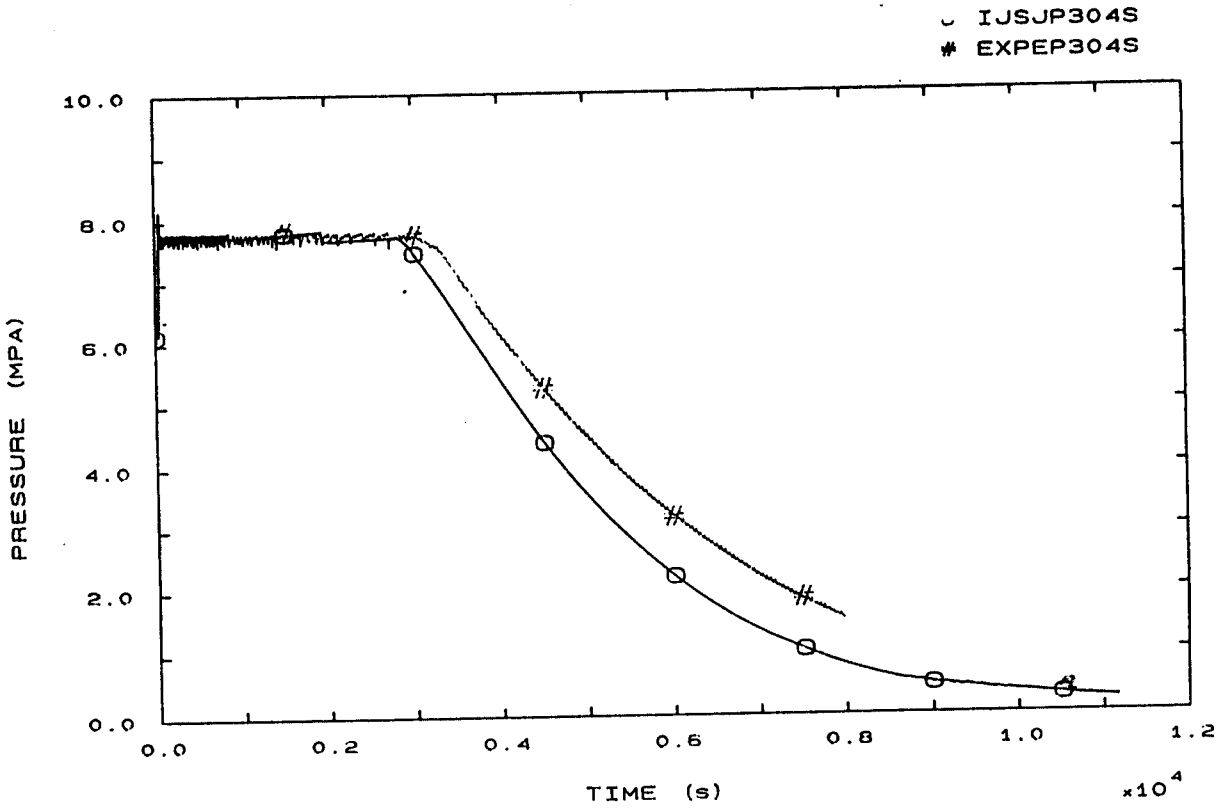

FIG. 5 SG3 STEAM DOME PRESSURE

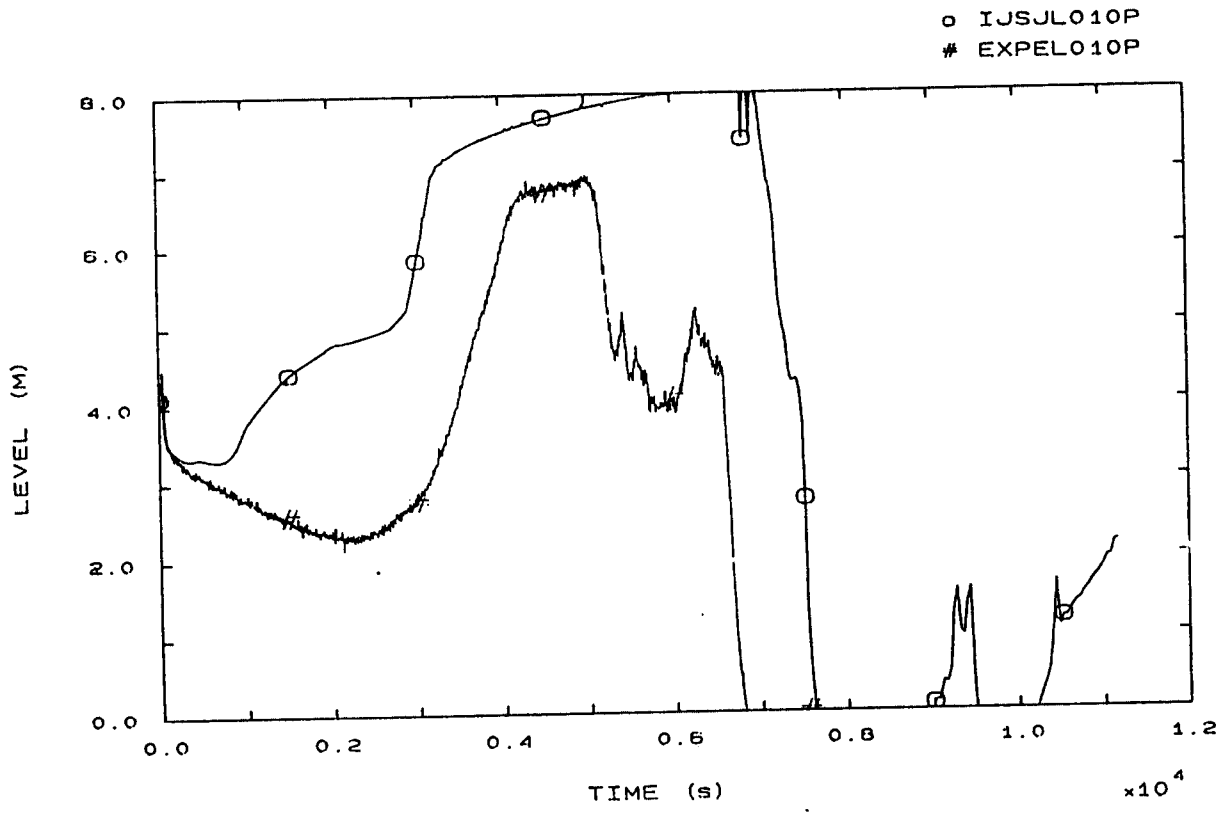

FIG. 6 PRESSURIZER LEVEL

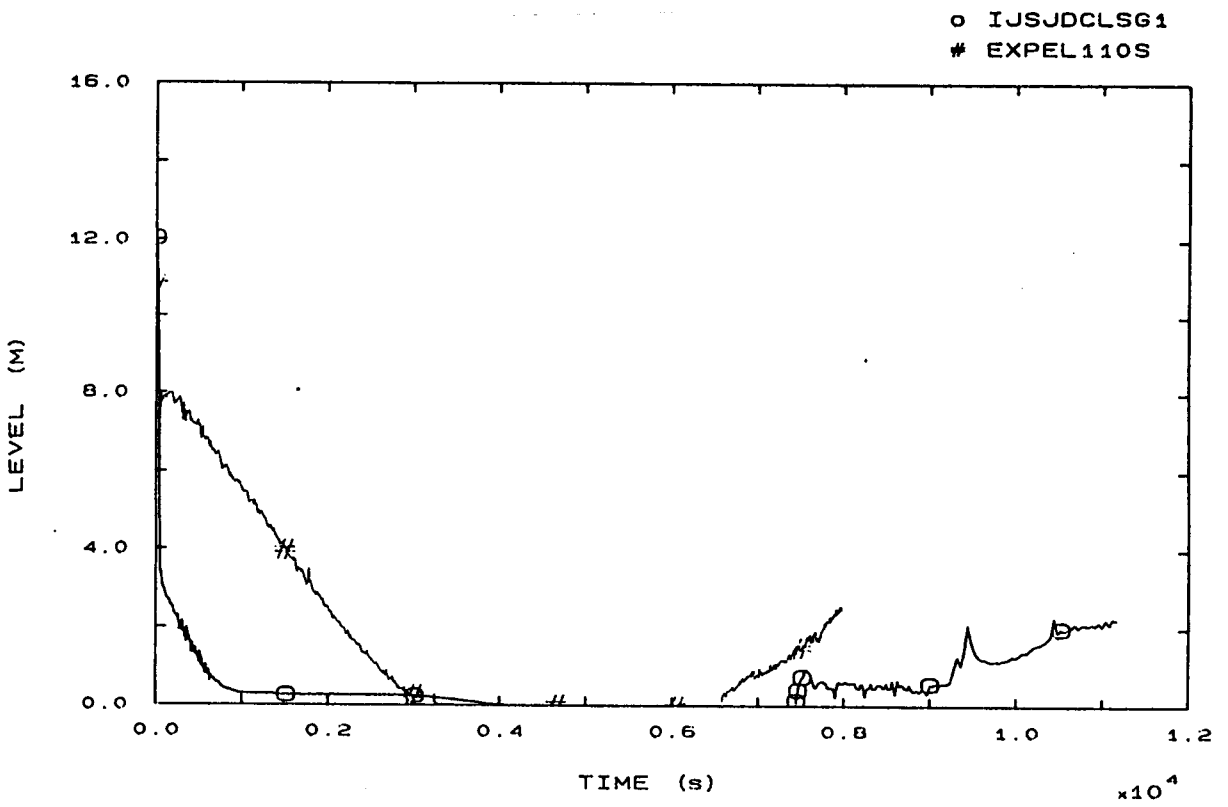

FIG. 7 SG1 DOWNCOMER LEVEL

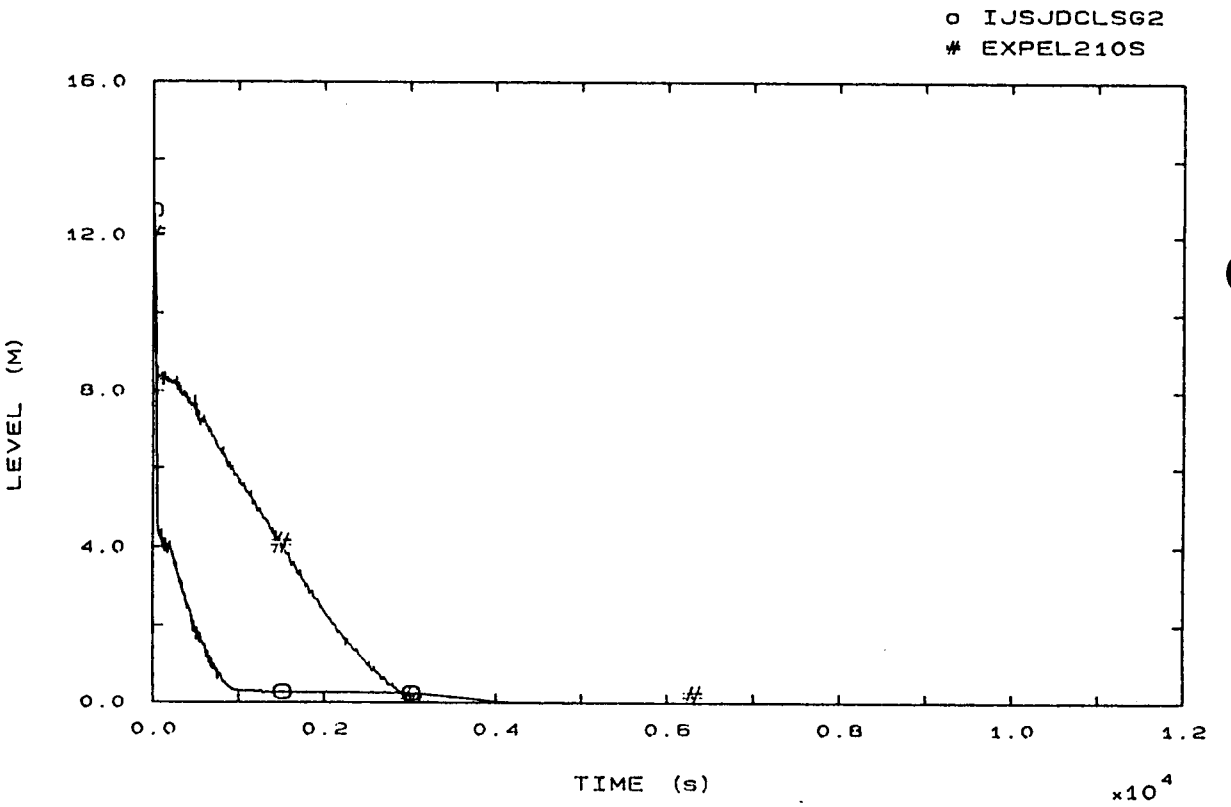

FIG. 8 SG2 DOWNCOMER LEVEL

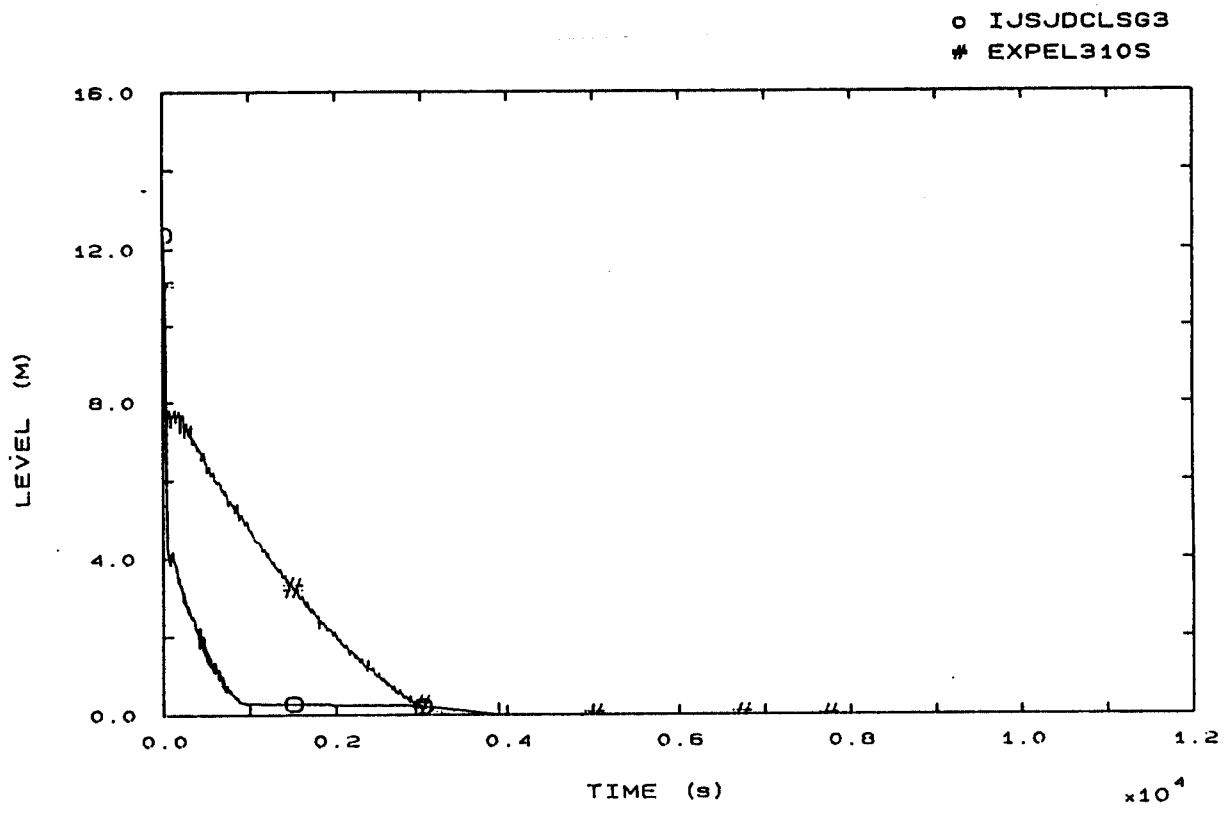

FIG. 9 SG3 DOWNCOMER LEVEL

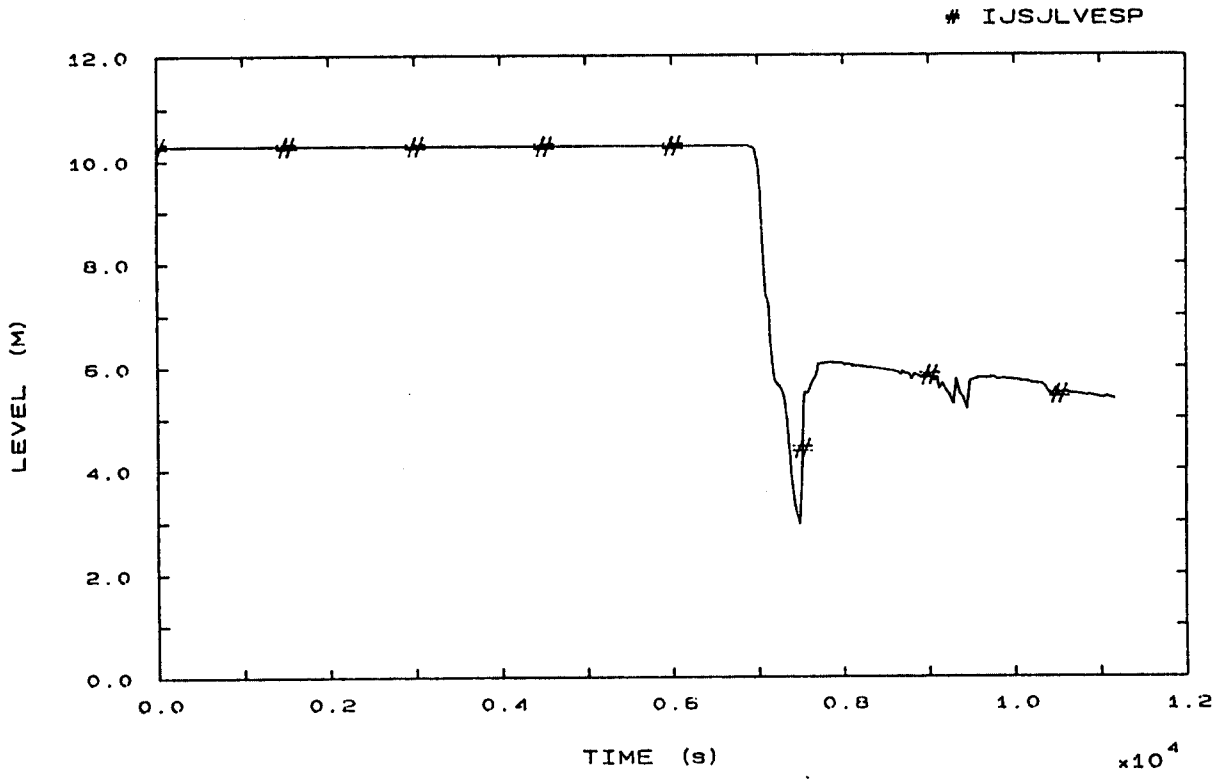

FIG. 10 VESSEL LEVEL

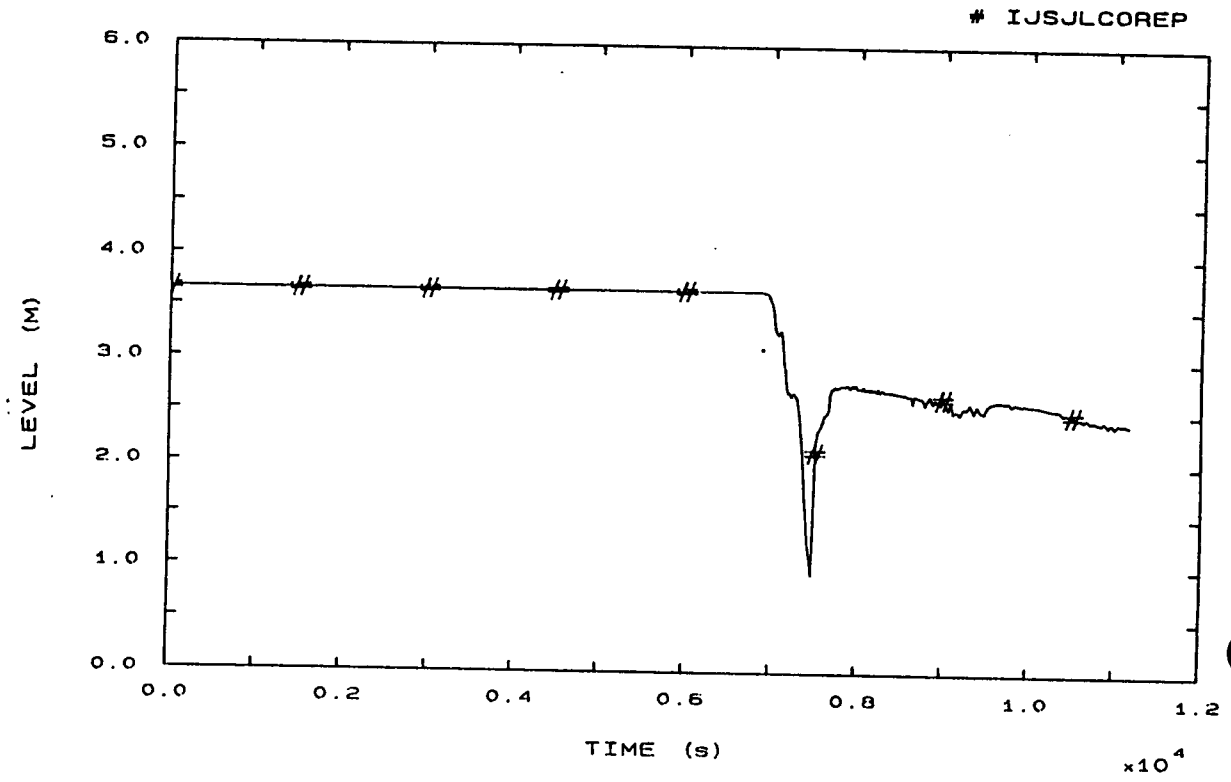

FIG. 11 CORE LEVEL

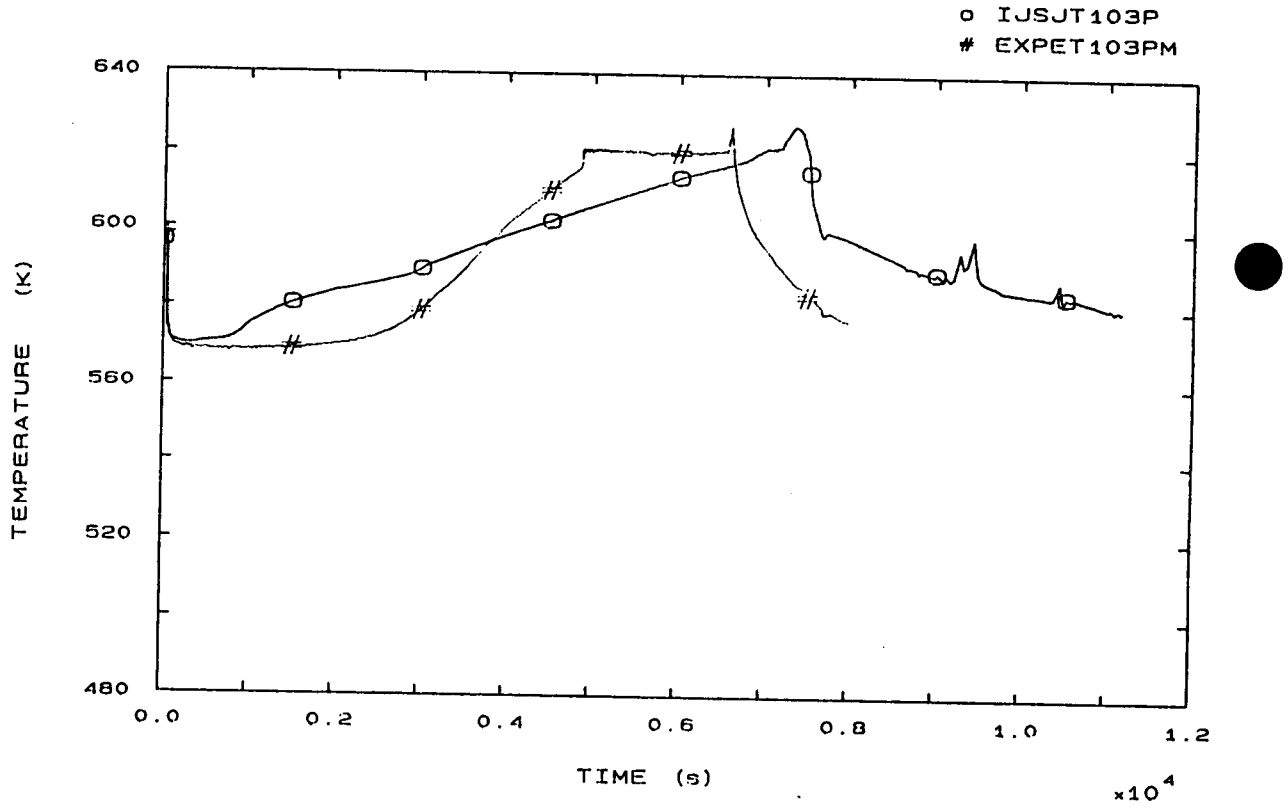

FIG. 12 LP1 HOT LEG OUTLET VESSEL TEMPERATURE

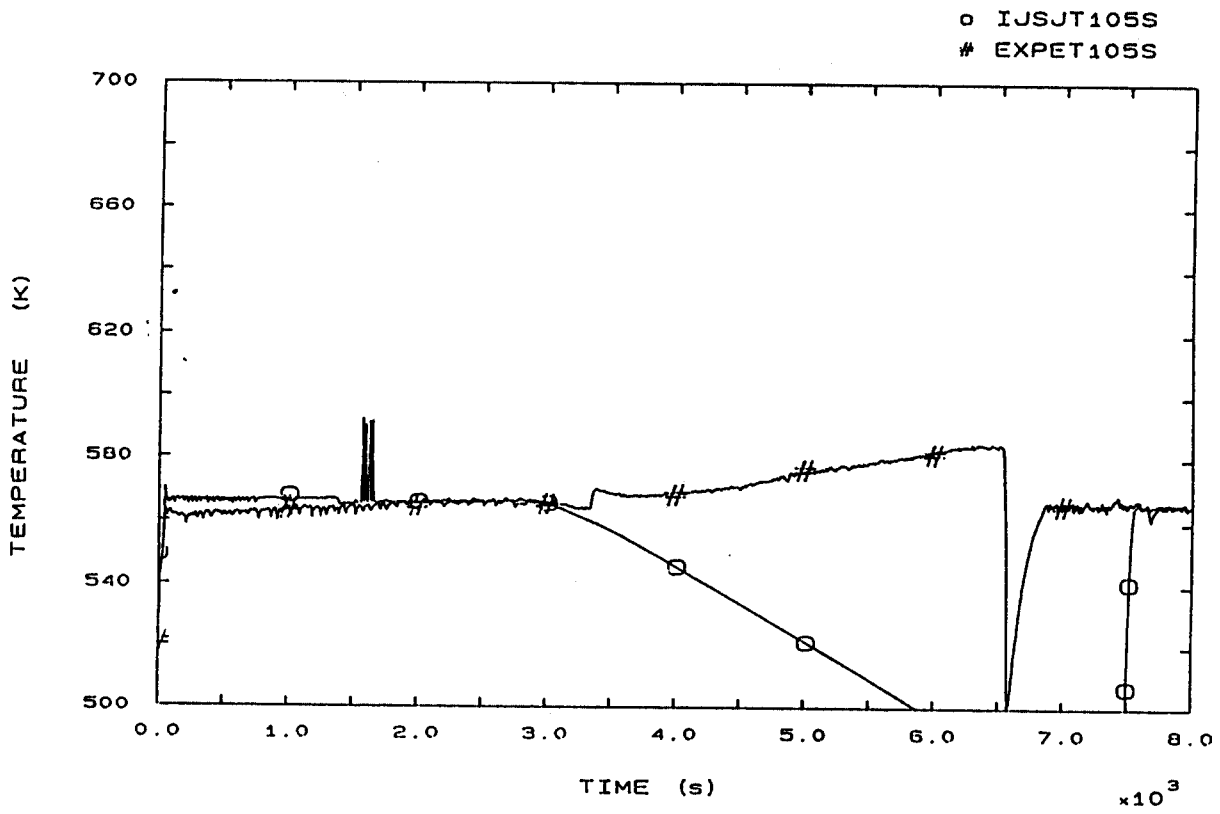

FIG. 15 FLUID TEMPERATURE SG1 RISER 185 MM A.T.S.

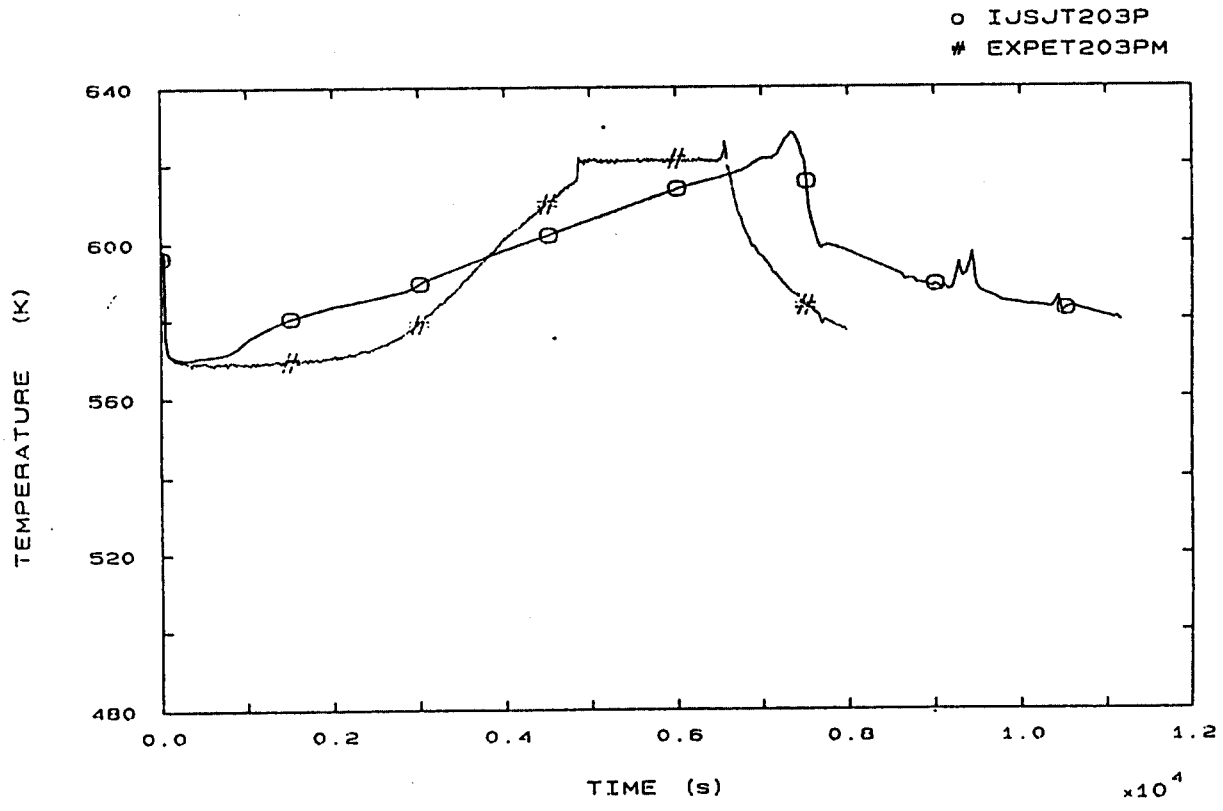

FIG. 22 LP2 HOT LEG OUTLET VESSEL TEMPERATURE

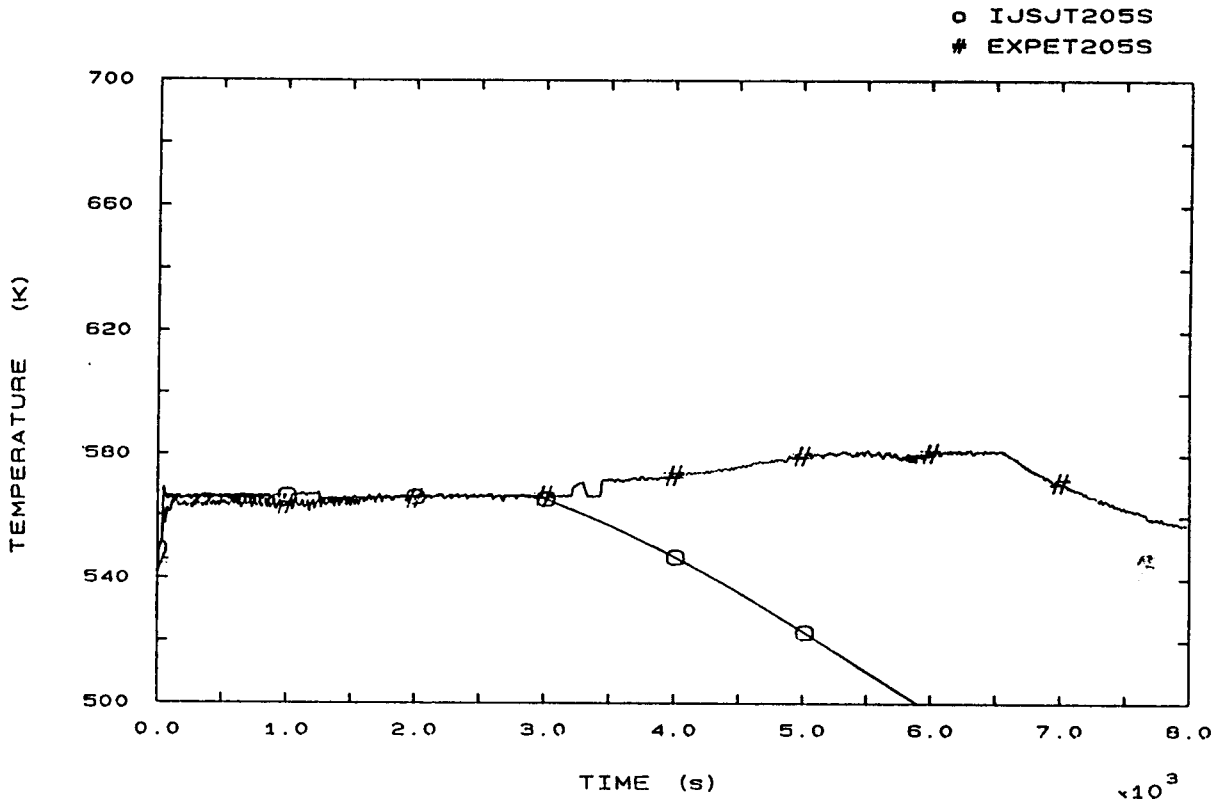

FIG. 25 FLUID TEMPERATURE SG2 RISER 185 MM A.T.S.

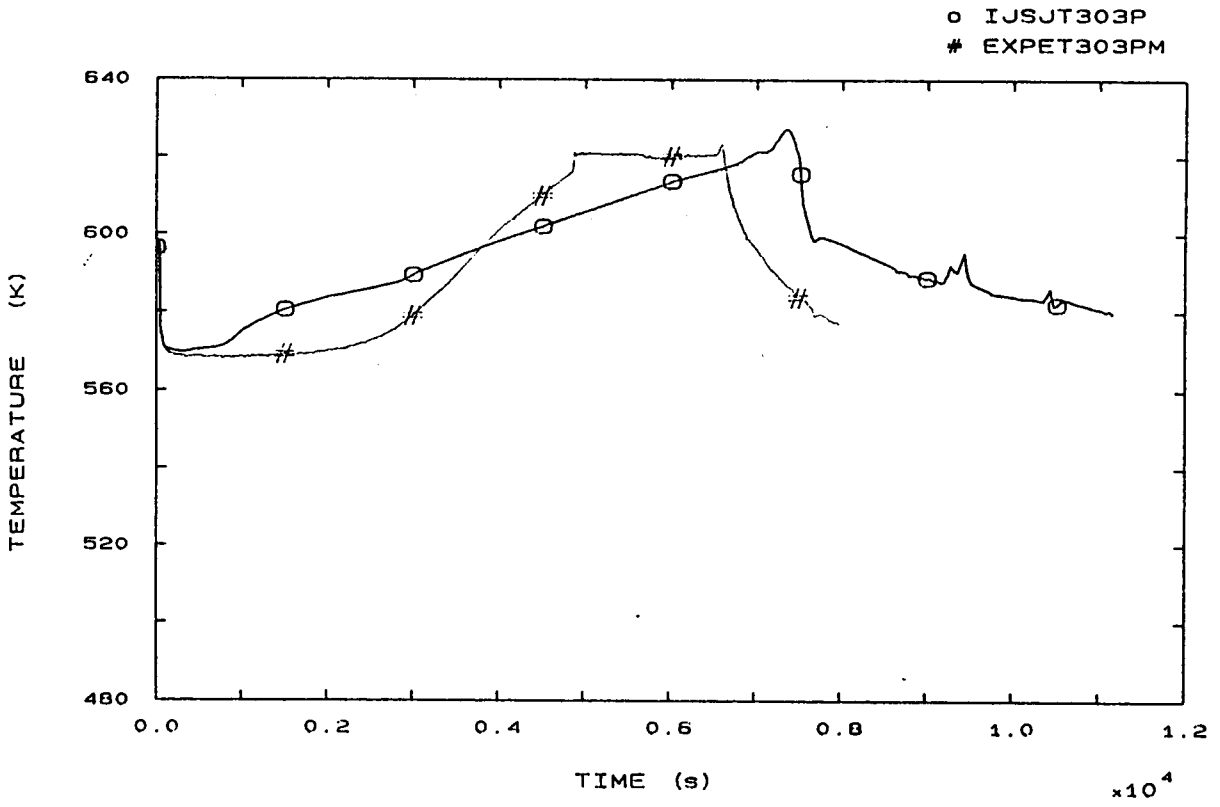

FIG. 32 LP3 HOT LEG OUTLET VESSEL TEMPERATURE

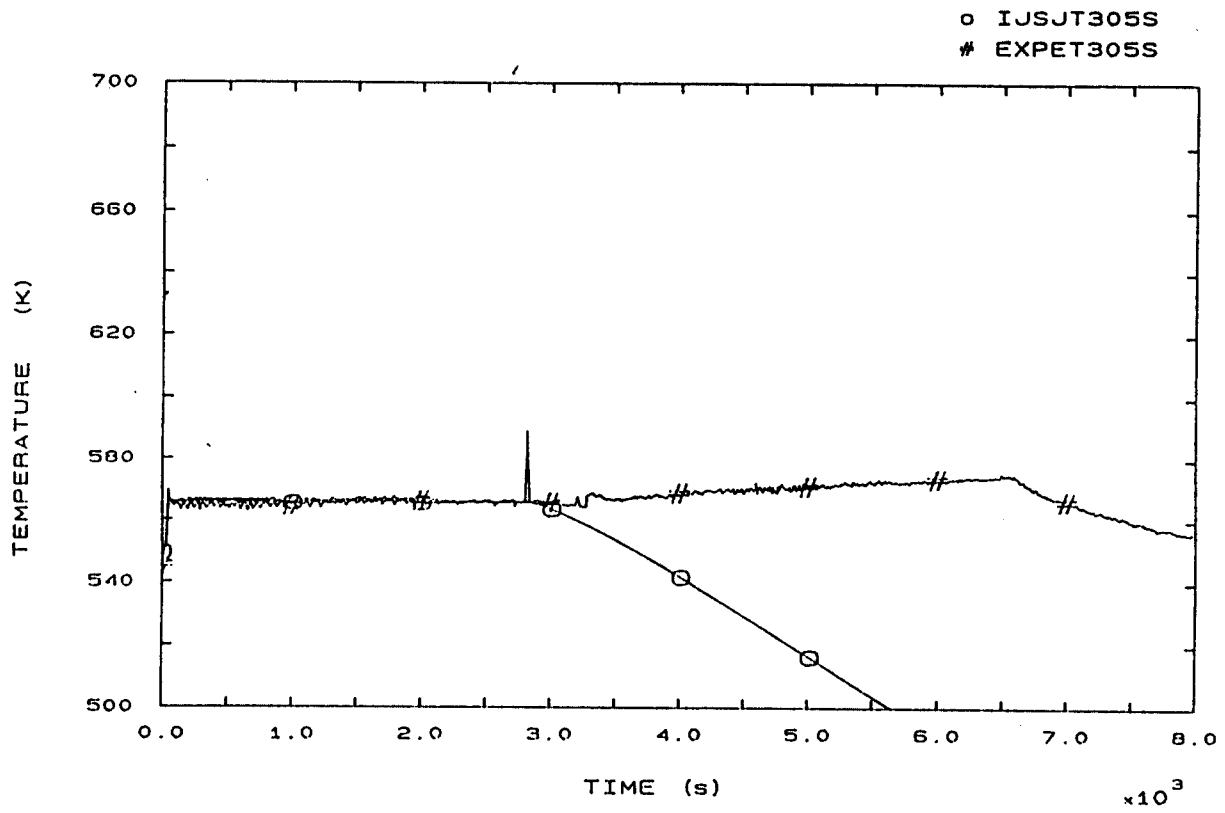

FIG. 35 FLUID TEMPERATURE SG3 RISER 185 MM A.T.S.

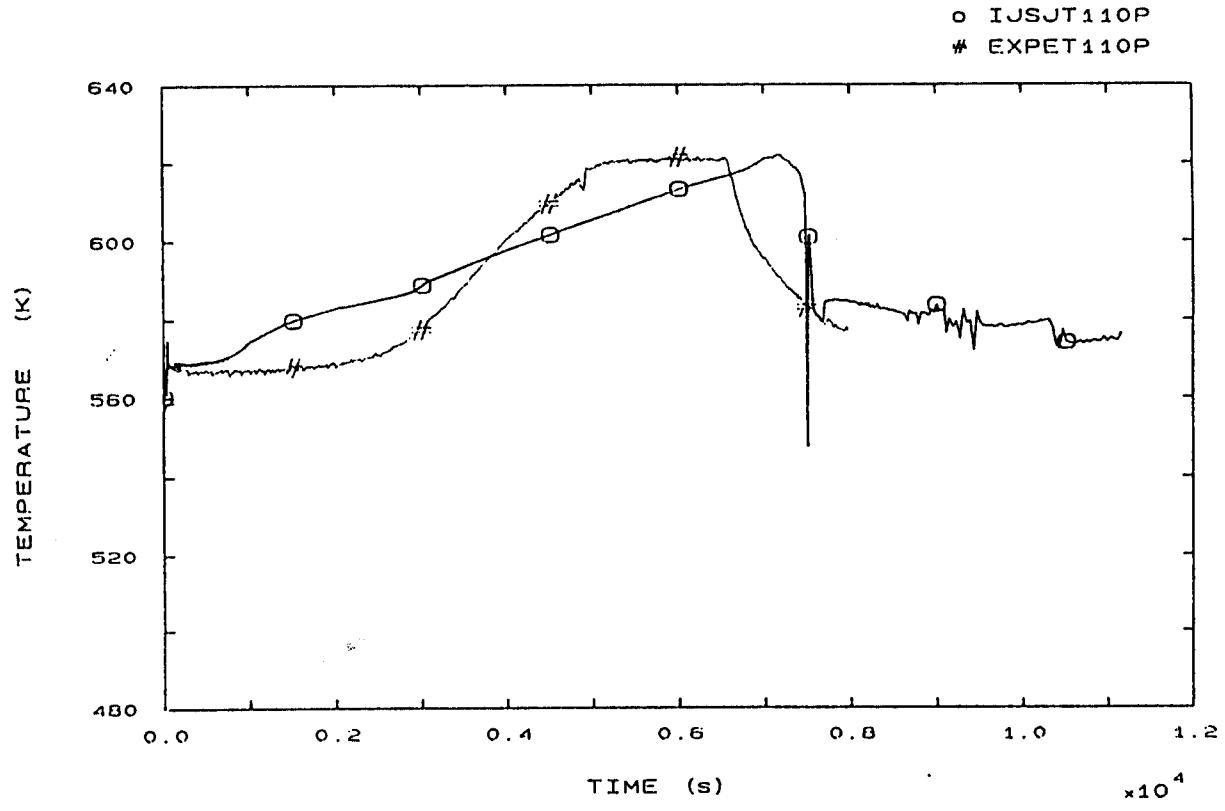

FIG. 42 SG1 OUTLET TEMPERATURE

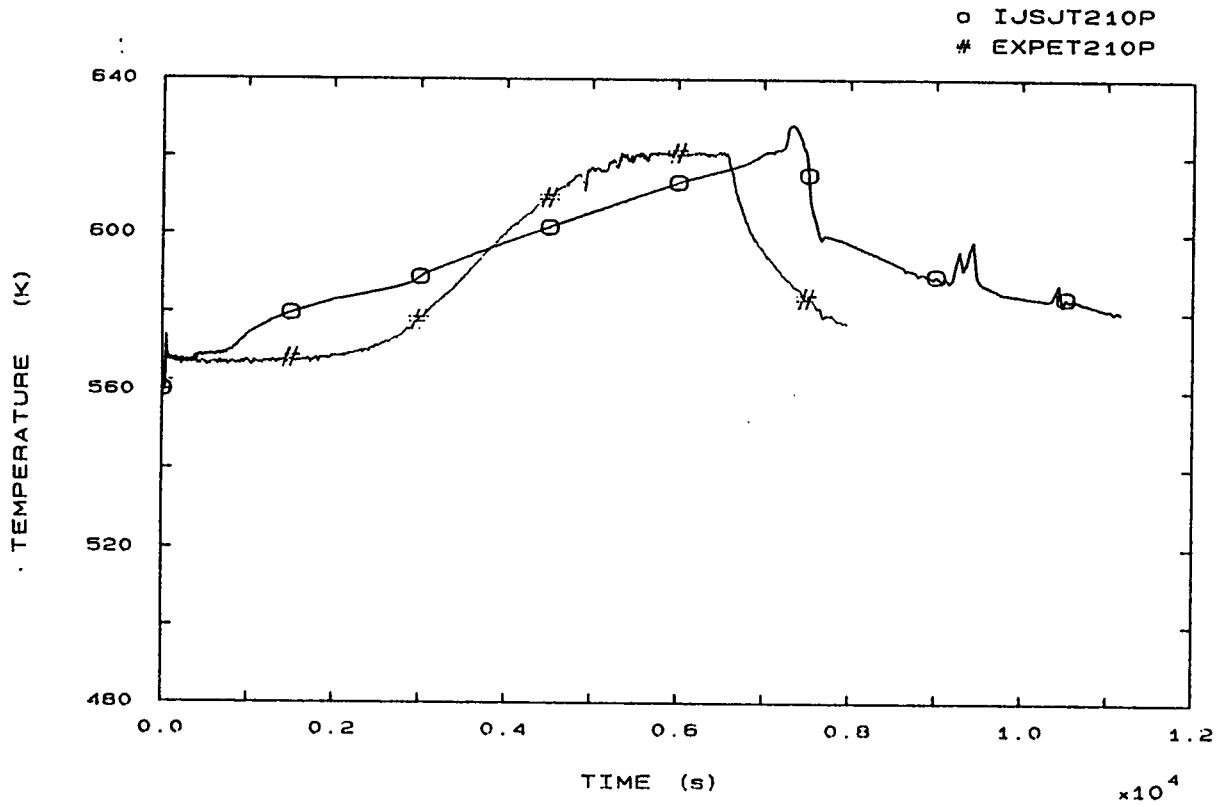

FIG. 44 SG2 OUTLET TEMPERATURE

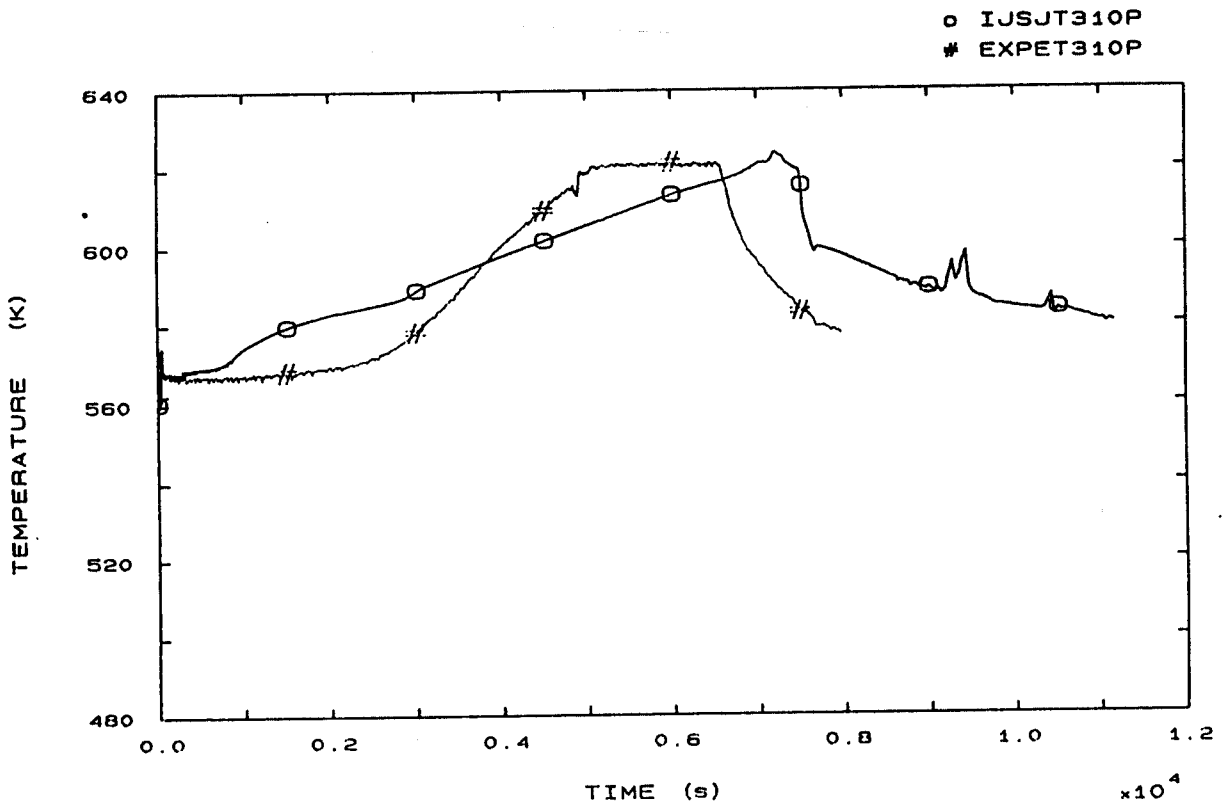

FIG. 46 SG3 OUTLET TEMPERATURE

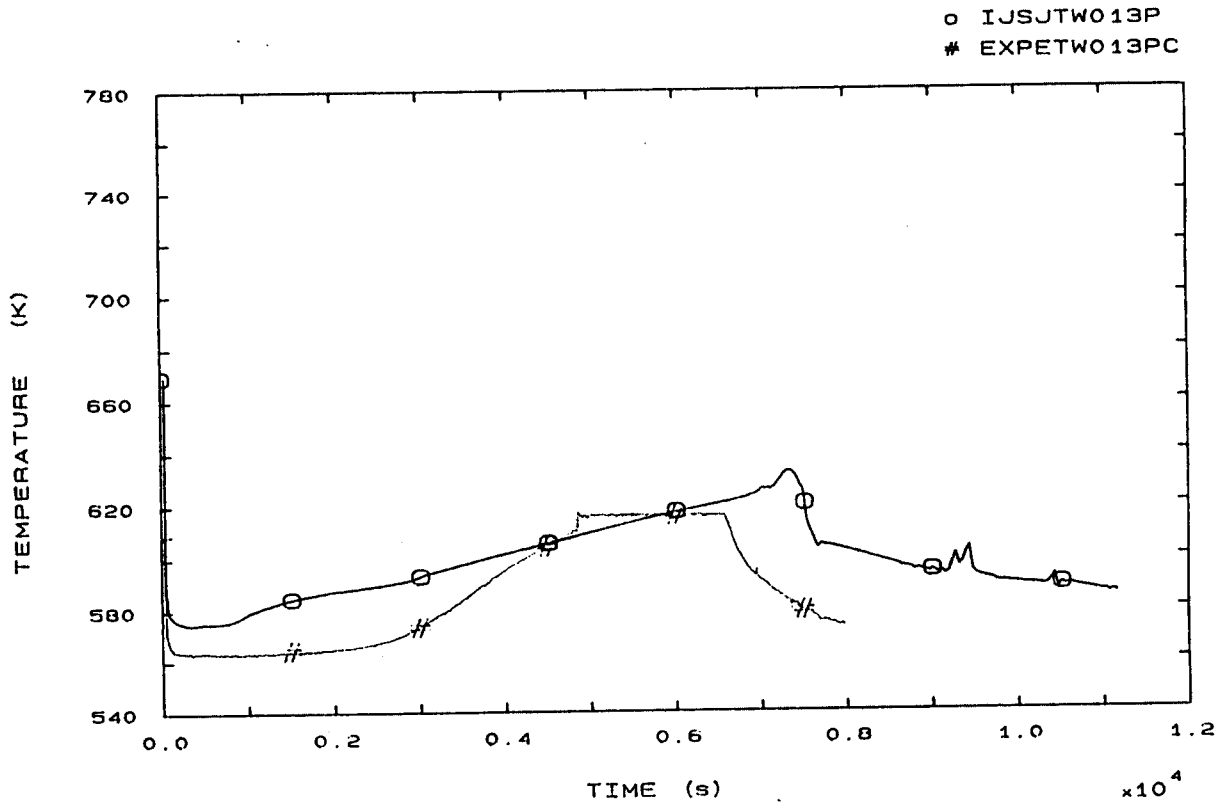

FIG. 49 CORE SURFACE TEMPERATURE AT ROD BUNDLE ELEVATION 1074 MM

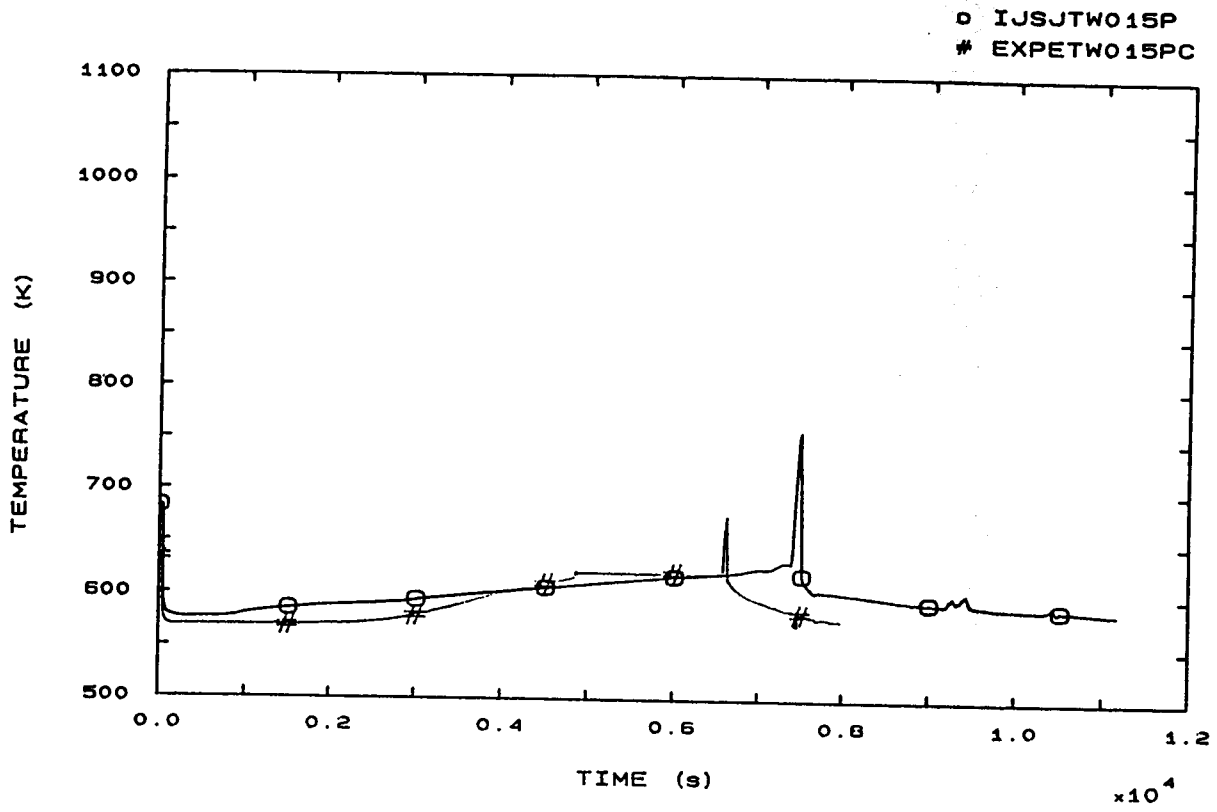

FIG. 50 SURFACE TEMPERATURE AT ROD BUNDLE ELEVATION 2294 mm

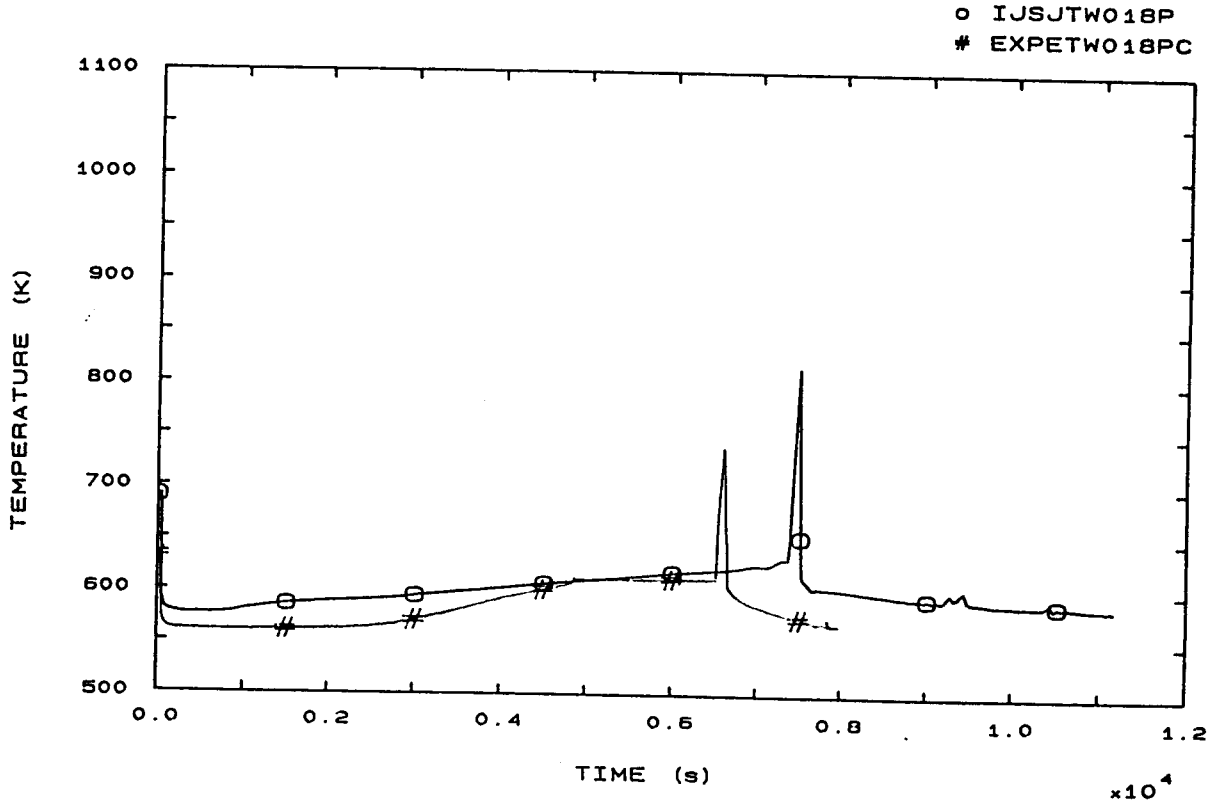

FIG. 51 SURFACE TEMPERATURE AT ROD BUNDLE ELEVATION 3294 mm

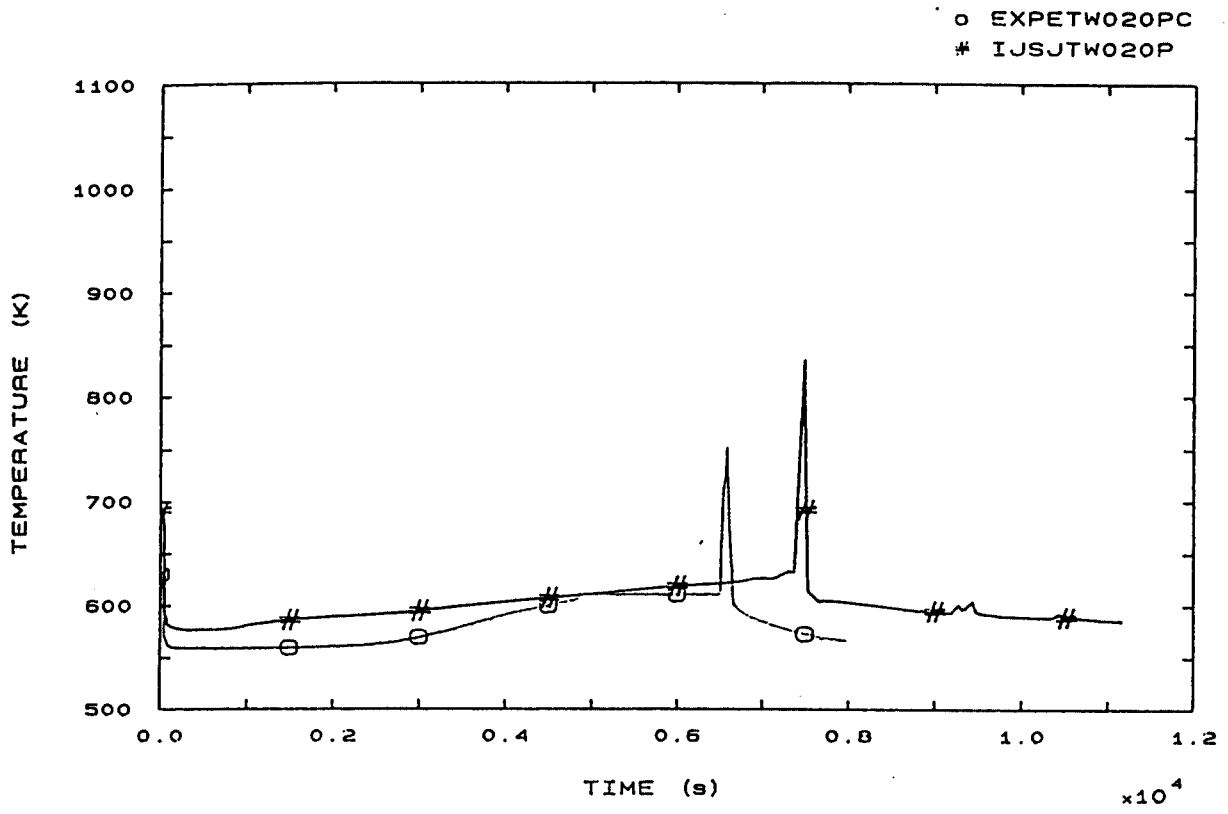

FIG. 52 SURFACE TEMPERATURE AT ROD BUNDLE ELEVATION 3640 mm

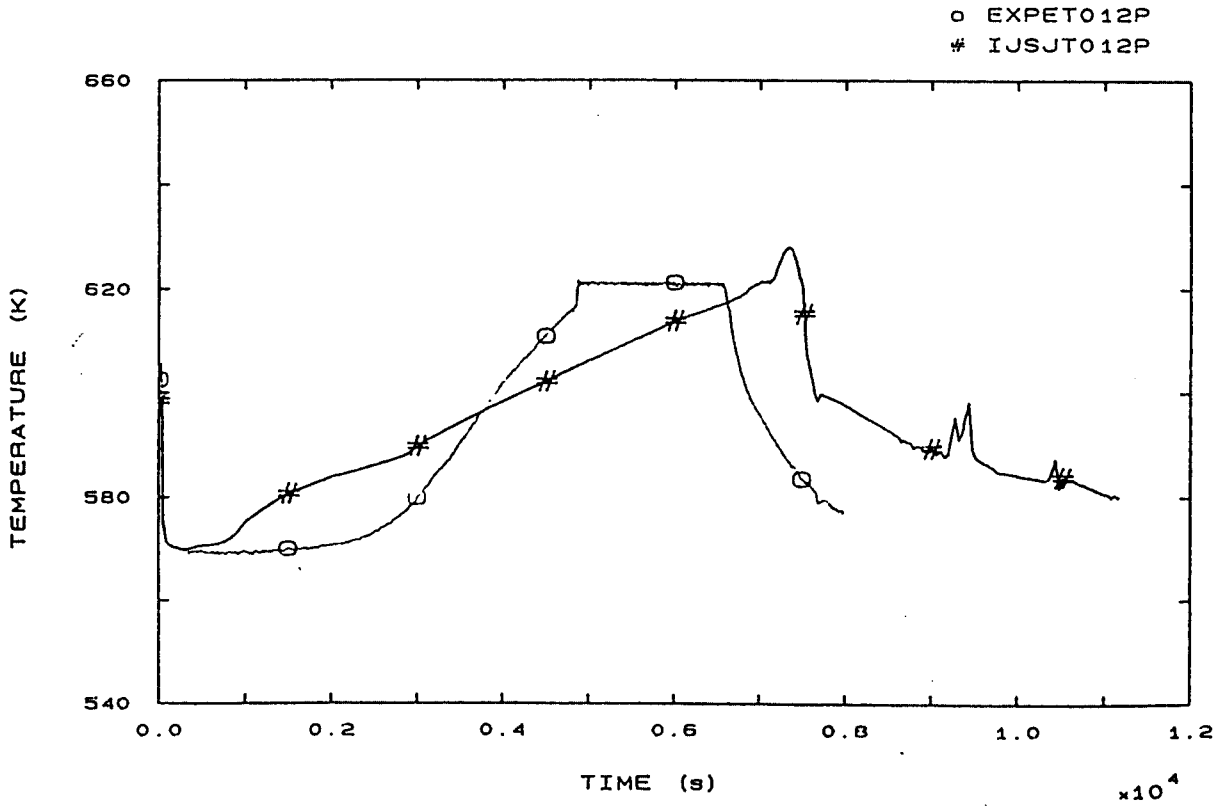

FIG. 53 CORE OUTLET TEMPERATURE

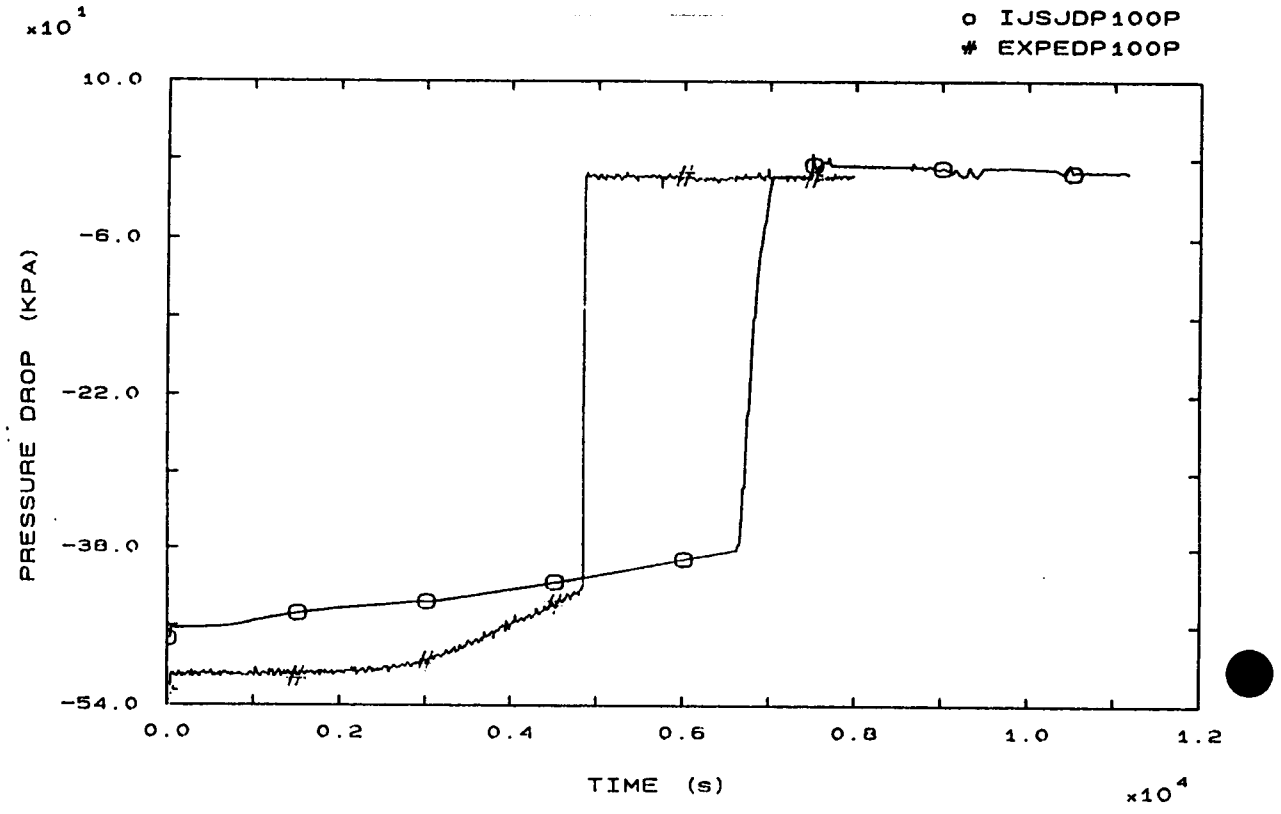

FIG. 54 PRIMARY PUMP 1 PRESSURE DROP

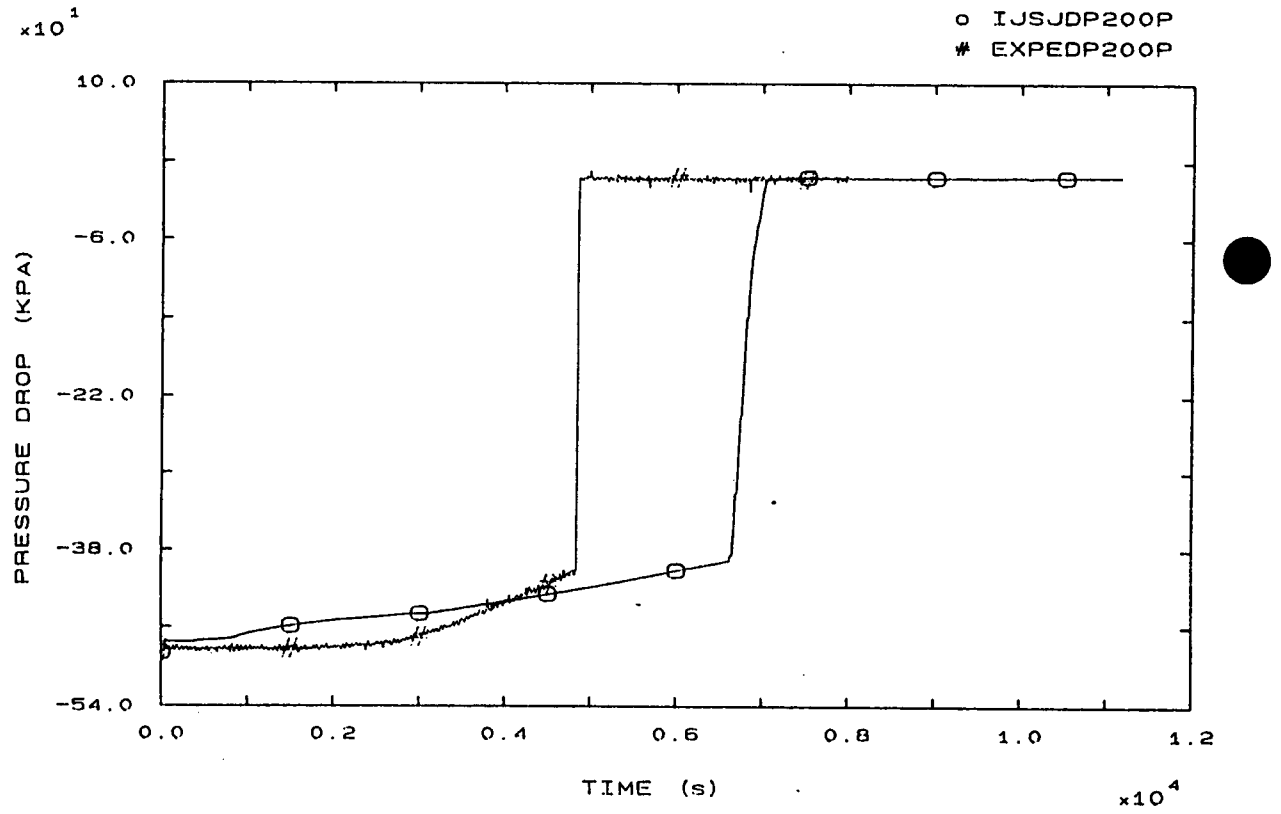

FIG. 55 PRIMARY PUMP 2 PRESSURE DROP

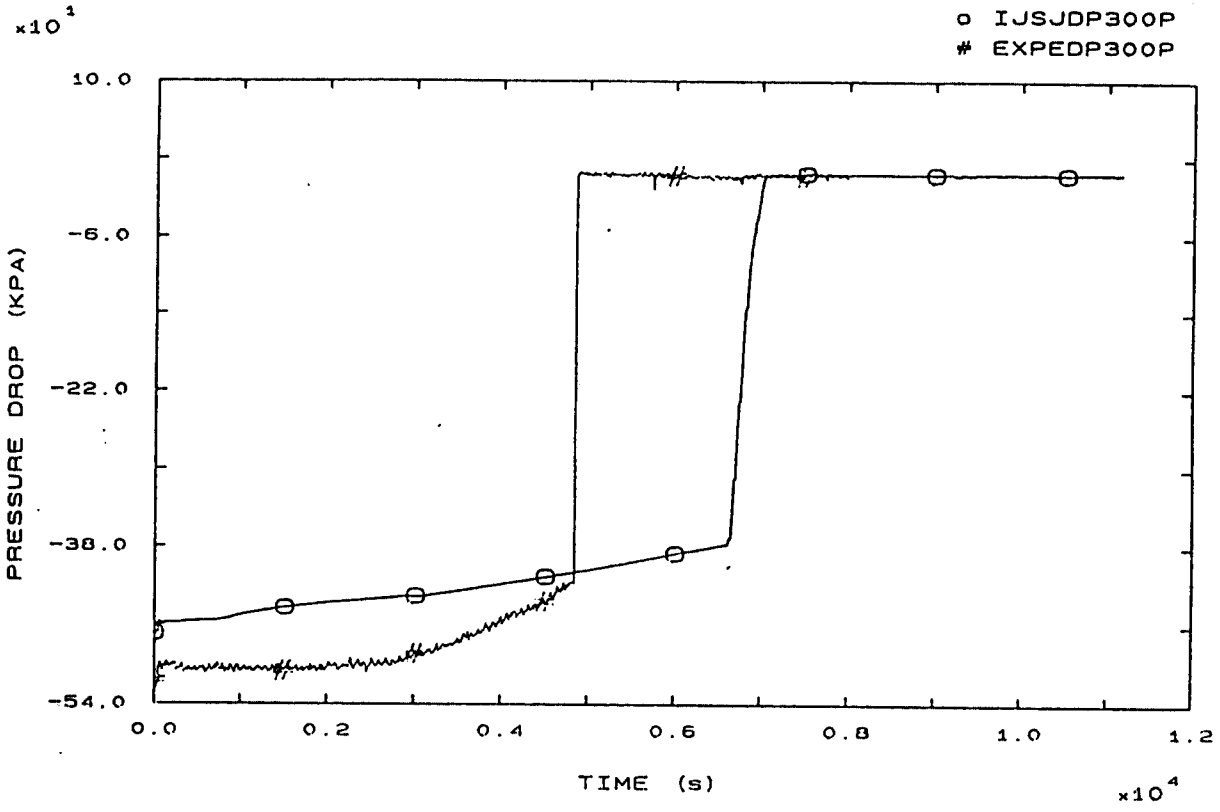

FIG. 56 PRIMARY PUMP 3 PRESSURE DROP

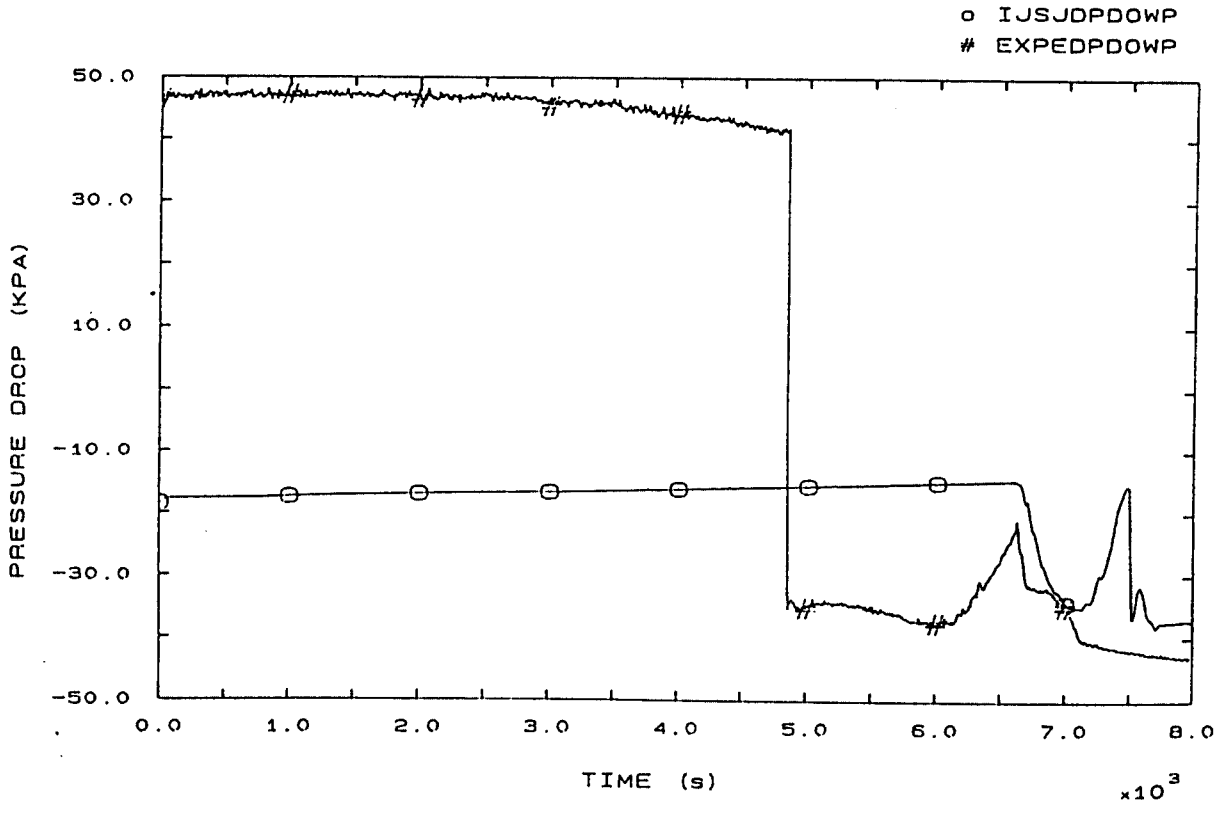

FIG. 57 VESSEL DOWNCOMER PRESSURE DROP

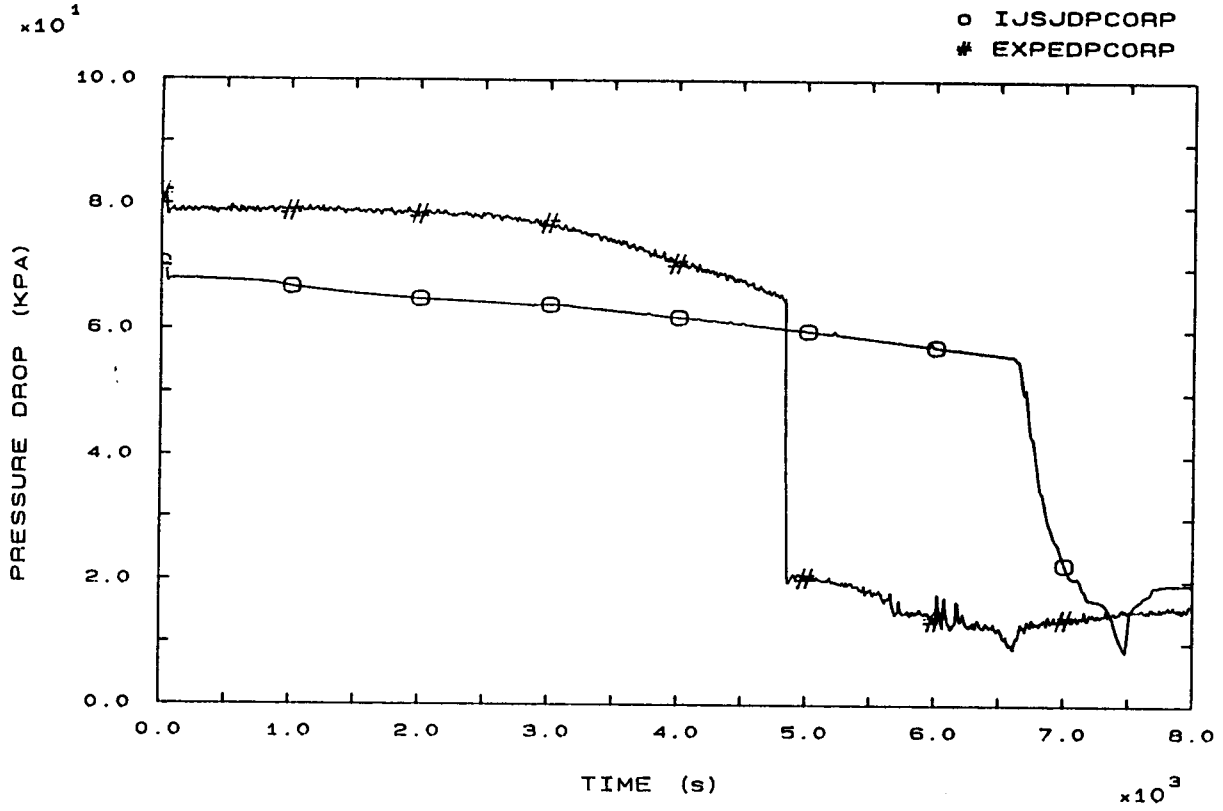

FIG. 58 CORE PRESSURE DROP

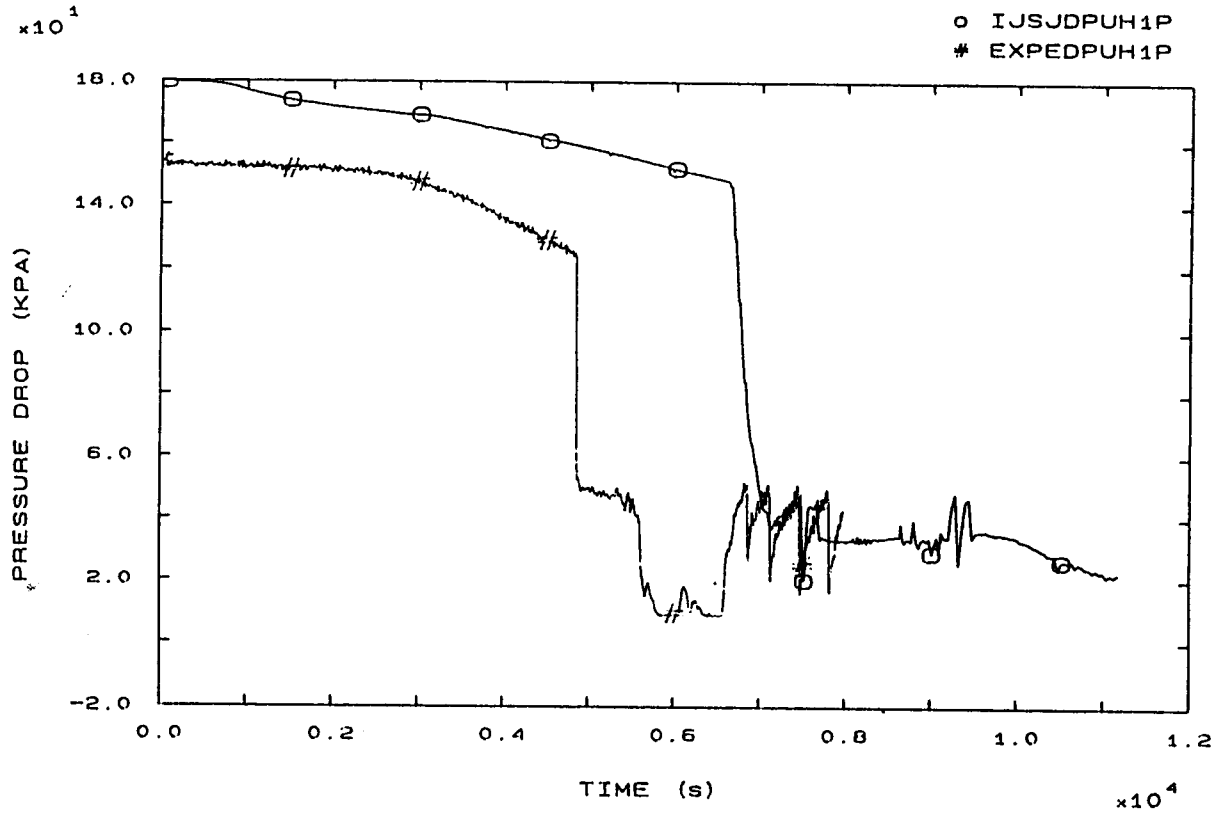

FIG. 62 SG1 INLET/U-BEND (UP-HILL) PRESSURE DROP

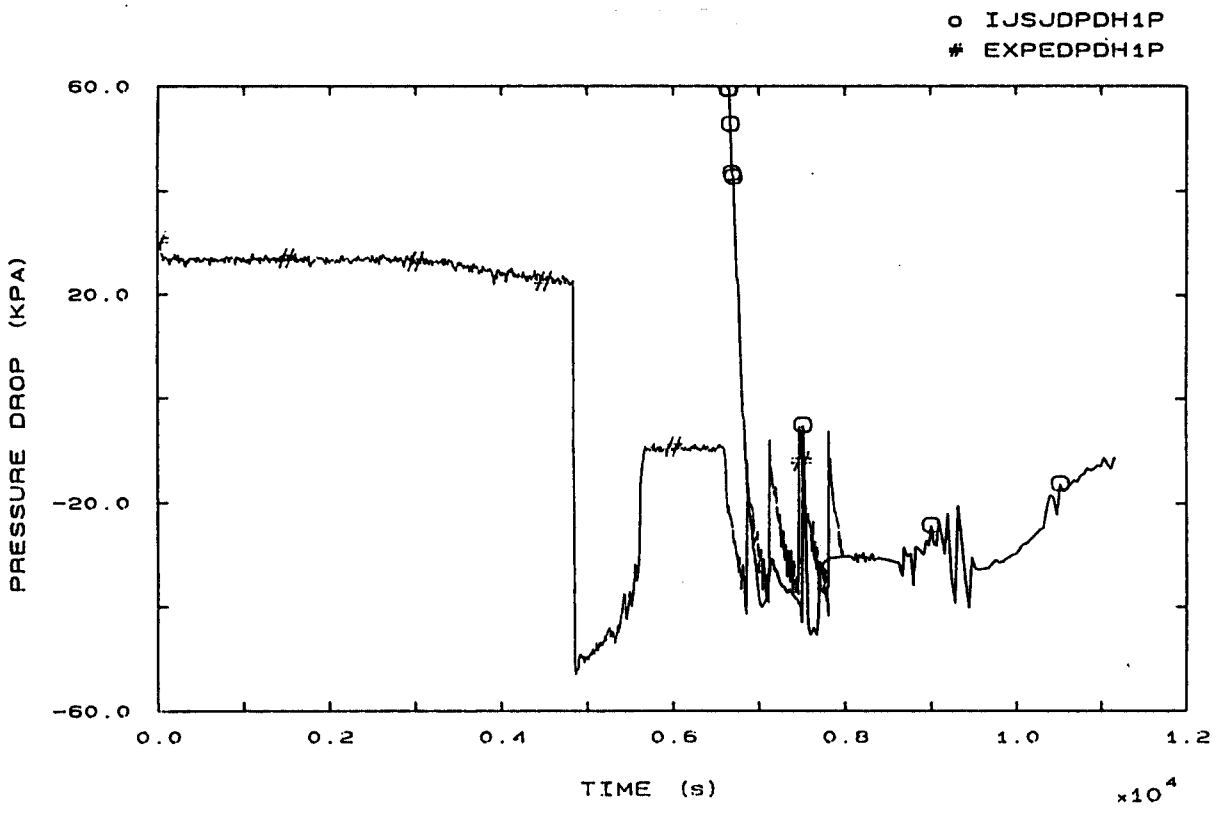

FIG. 63 SG1 U-BEND/OUTLET (DOWN-HILL) PRESSURE DROP

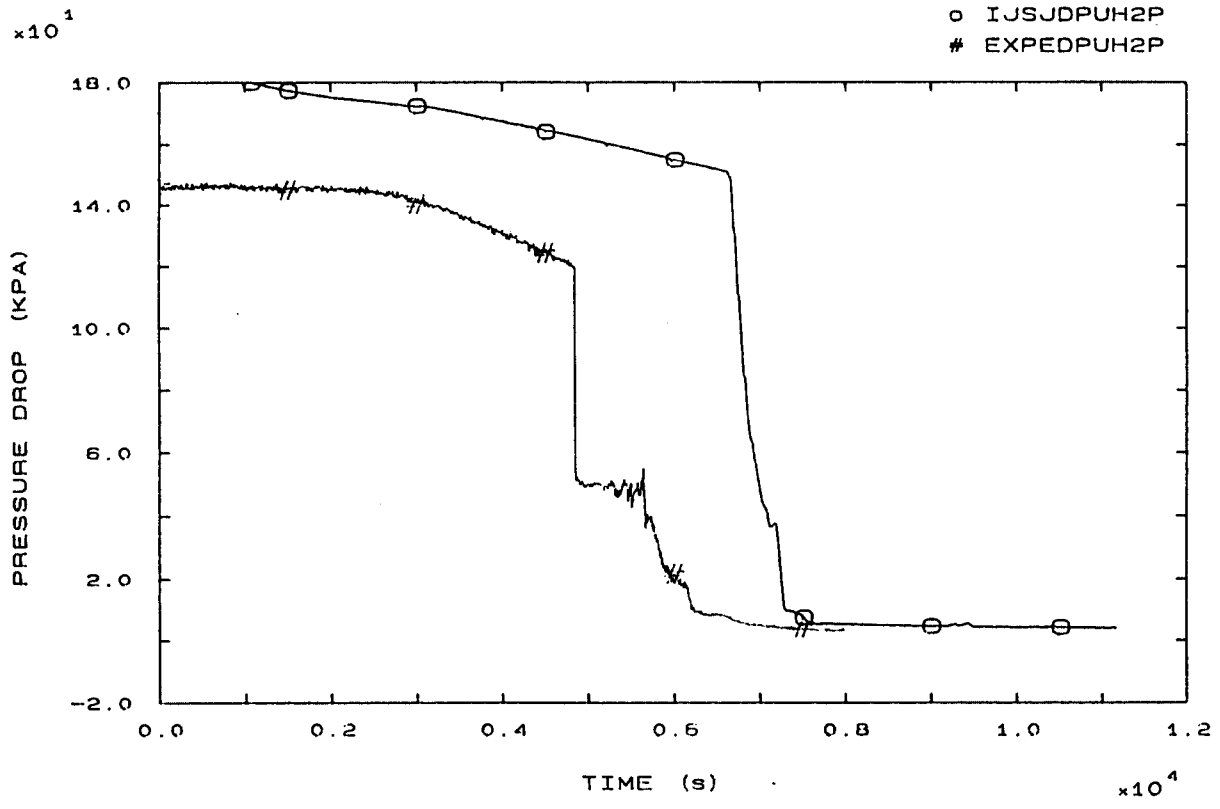

FIG. 64 SG2 INLET/U-BEND (UP-HILL) PRESSURE DROP

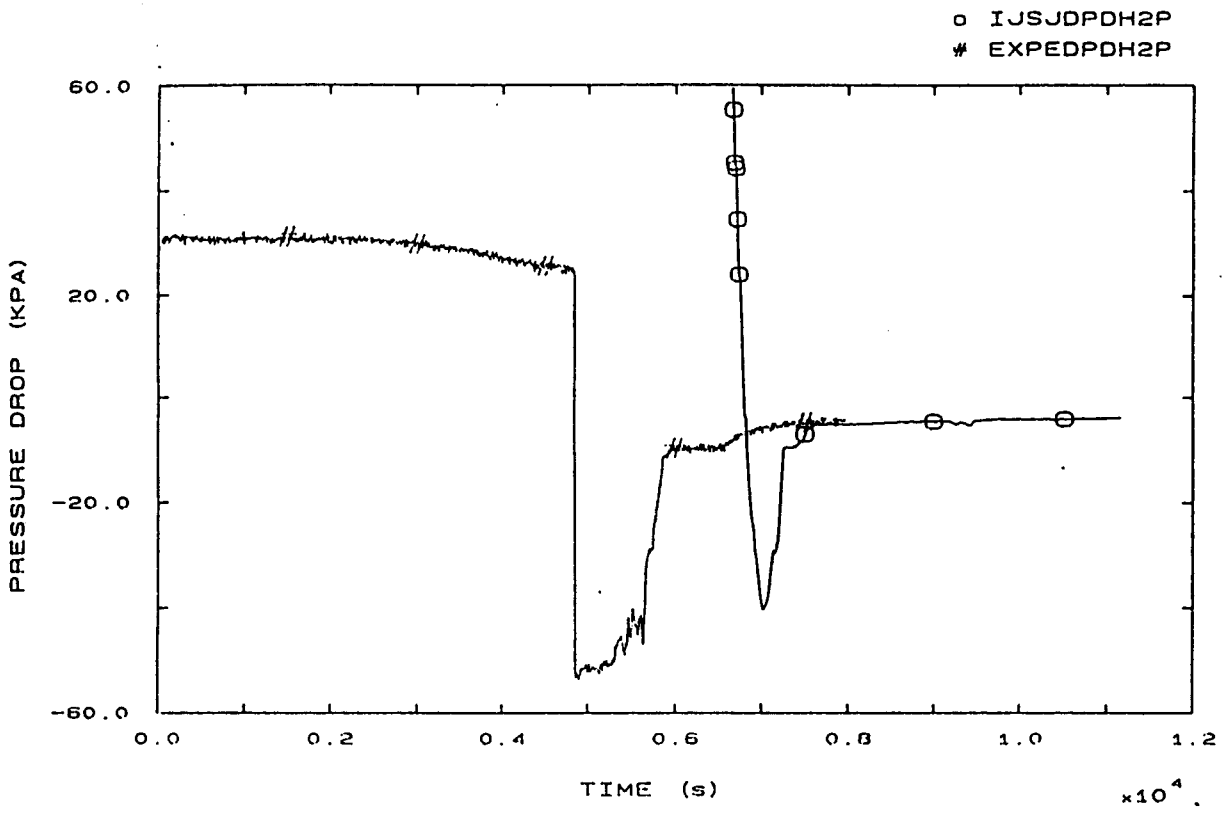

FIG. 65 SG2 U-BEND/OUTLET (DOWN-HILL) PRESSURE DROP

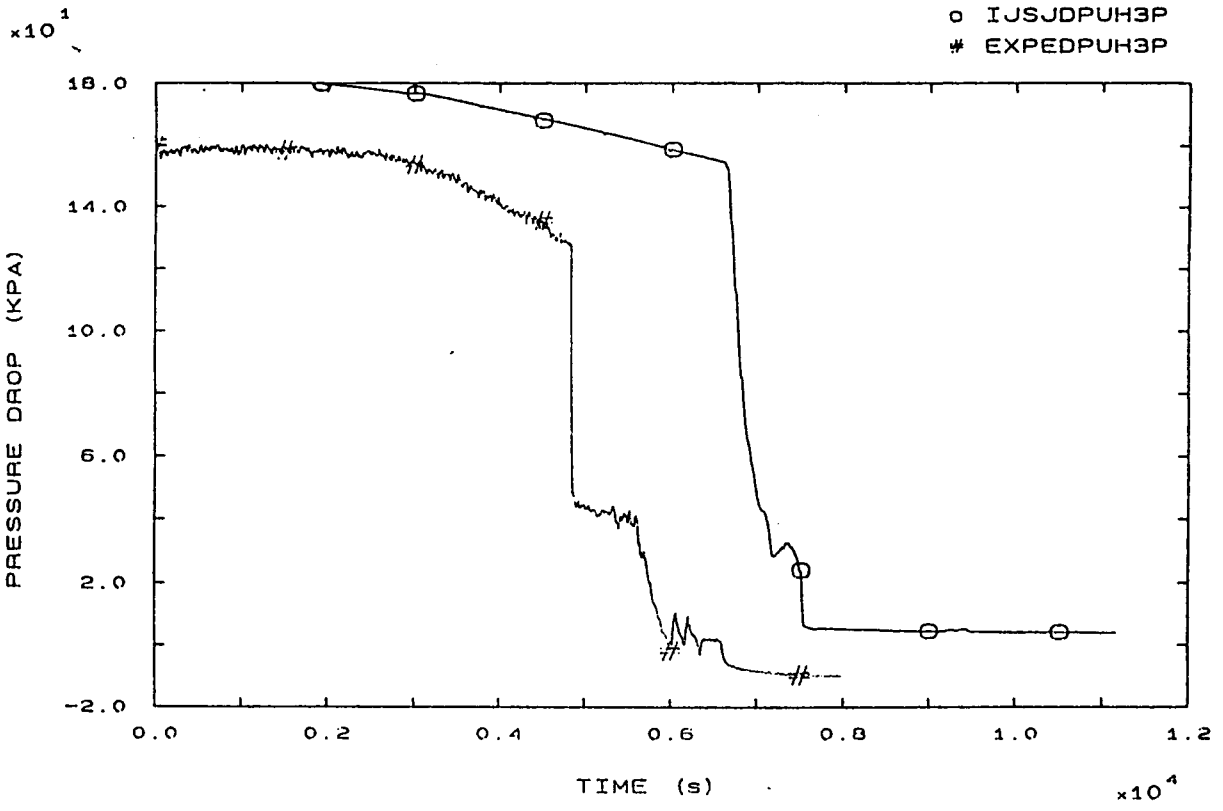

FIG. 66 SG3 INLET/U-BEND (UP-HILL) PRESSURE DROP

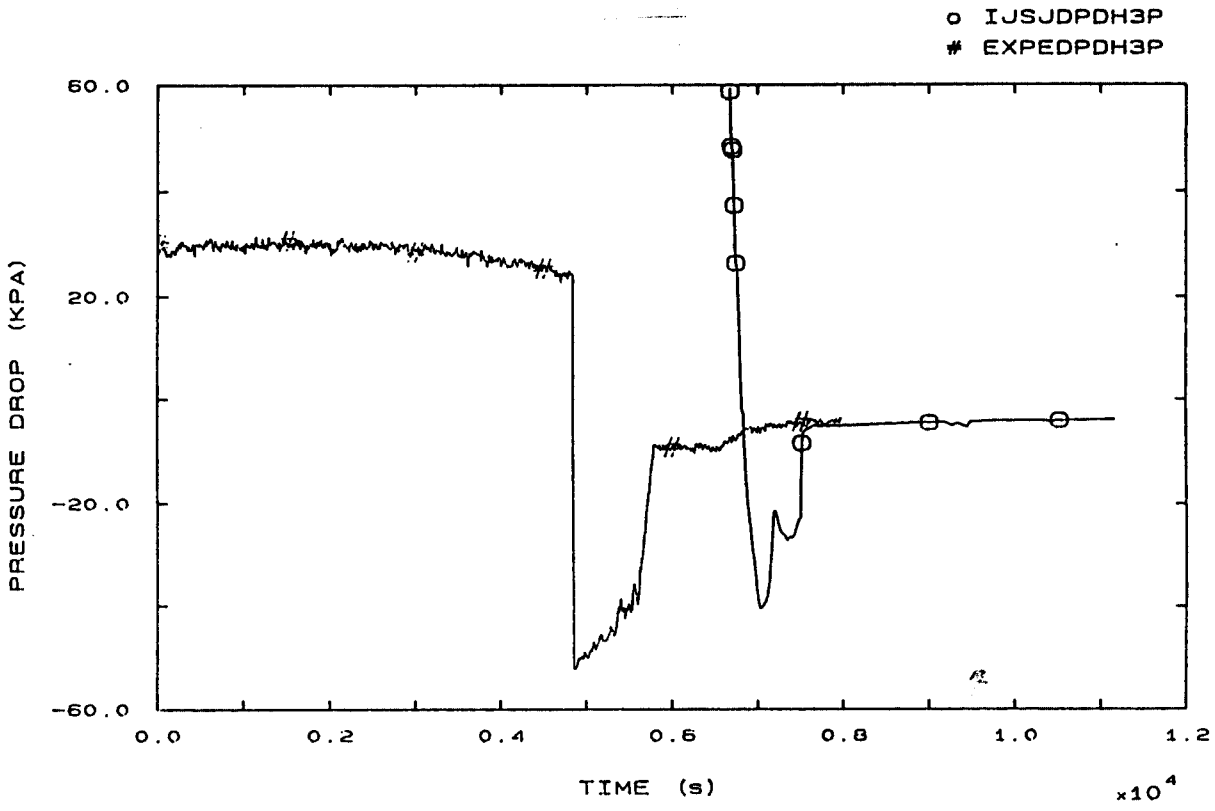

FIG. 67 SG3 U-BEND/OUTLET (DOWN-HILL) PRESSURE DROP

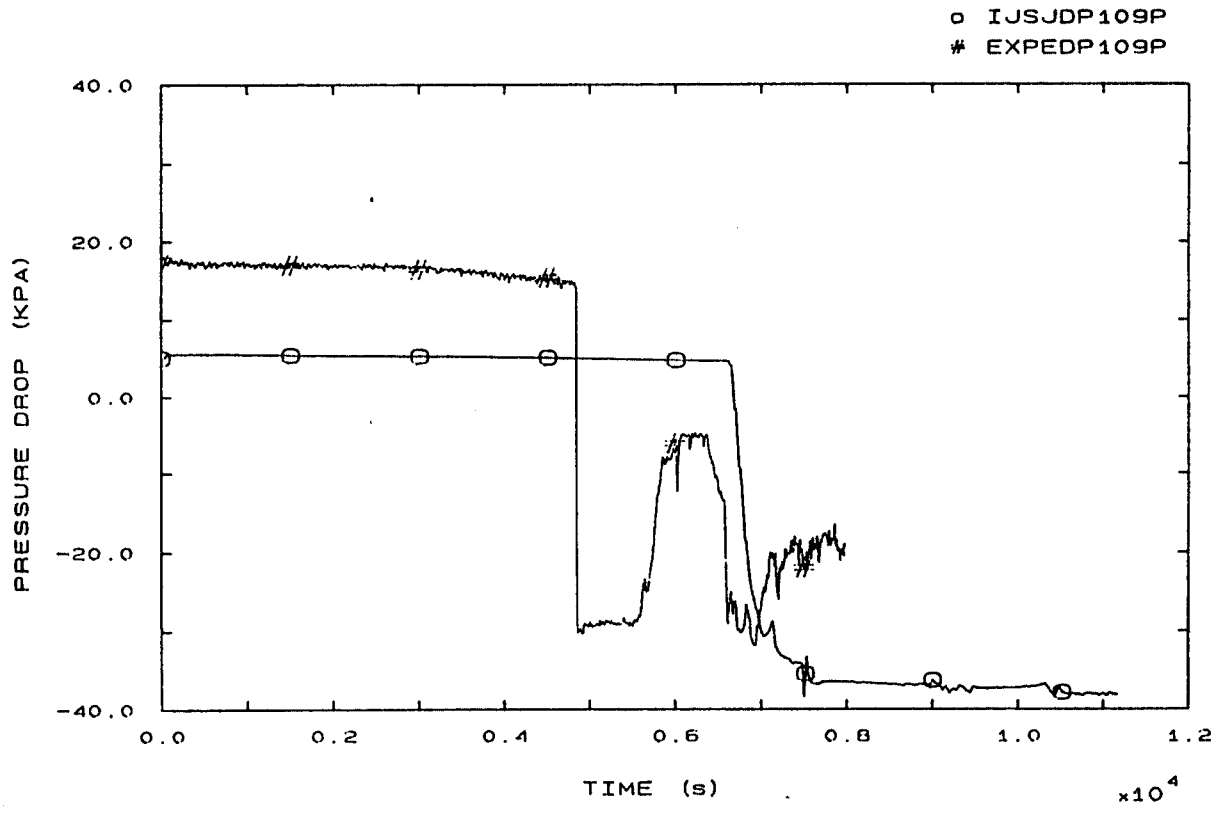

FIG. 68 SG1 OUTLET/LOOP SEAL BOTTOM PRESSURE DROP

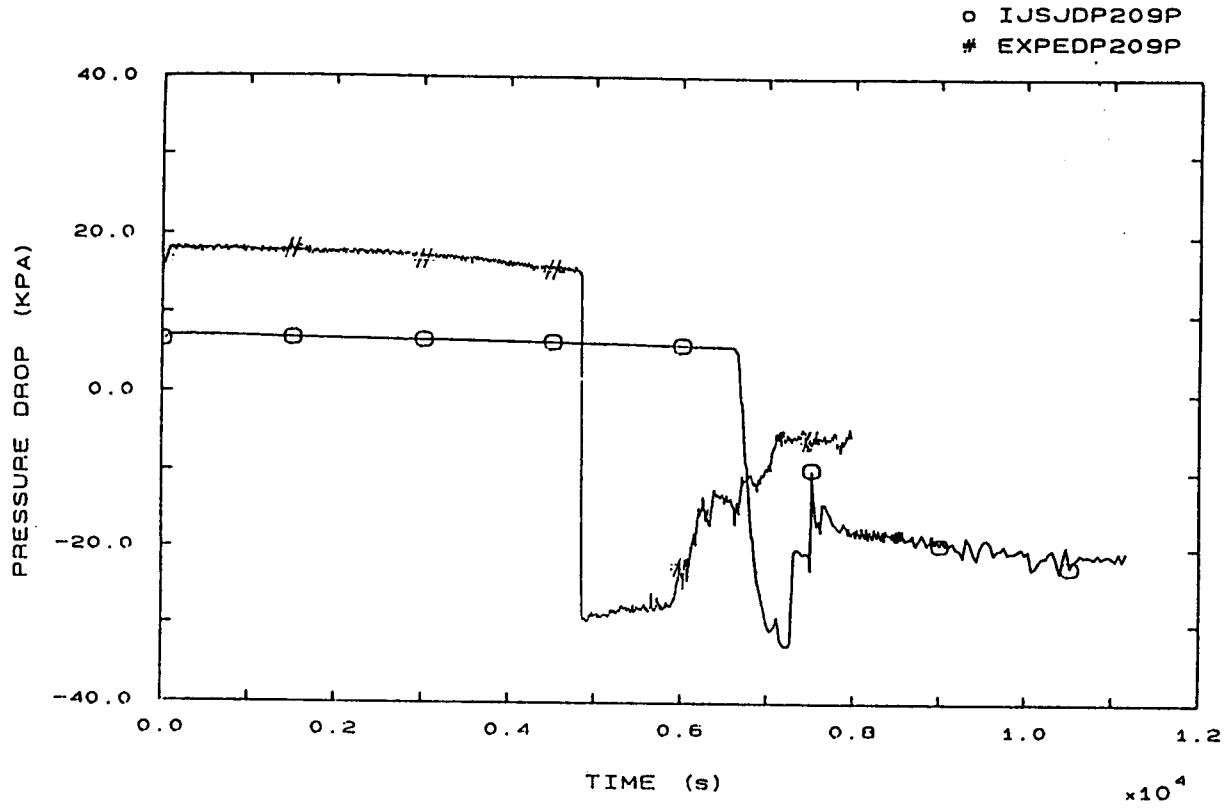

FIG. 69 SG2 OUTLET/LOOP SEAL BOTTOM PRESSURE DROP

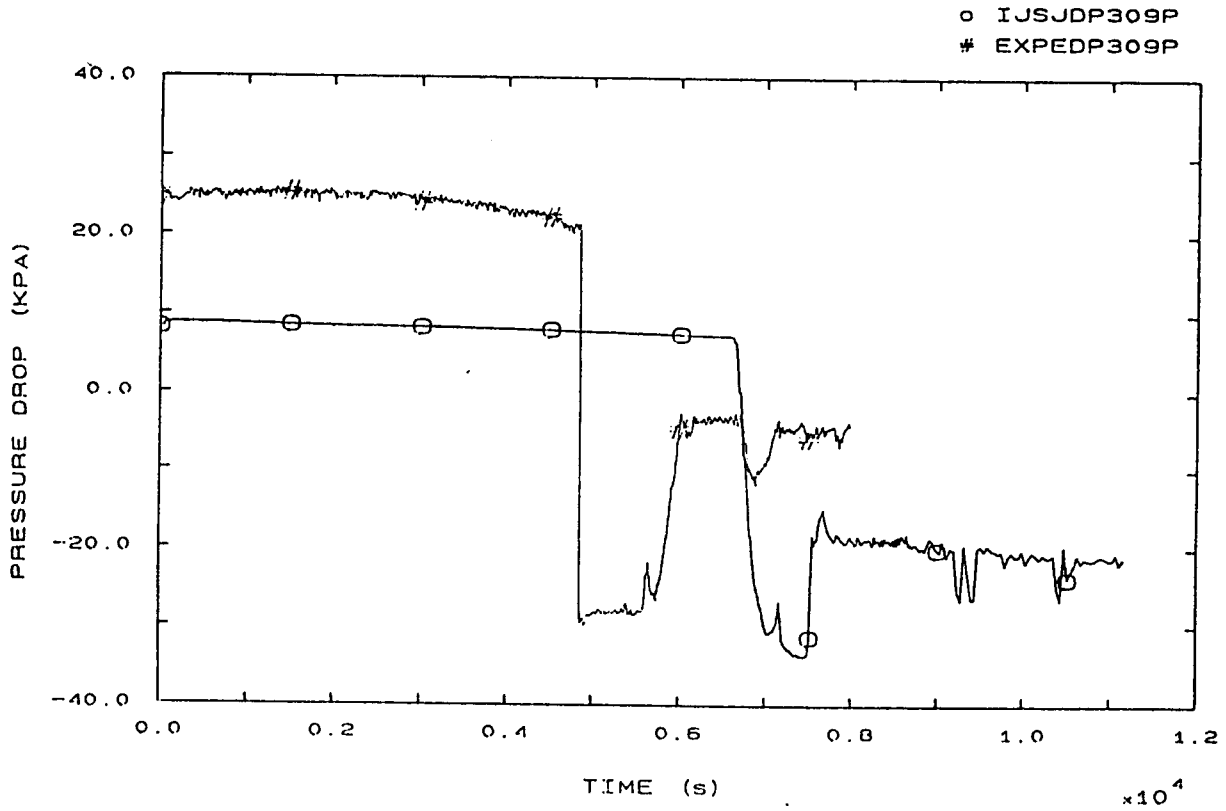

FIG. 70 SG3 OUTLET/LOOP SEAL BOTTOM PRESSURE DROP

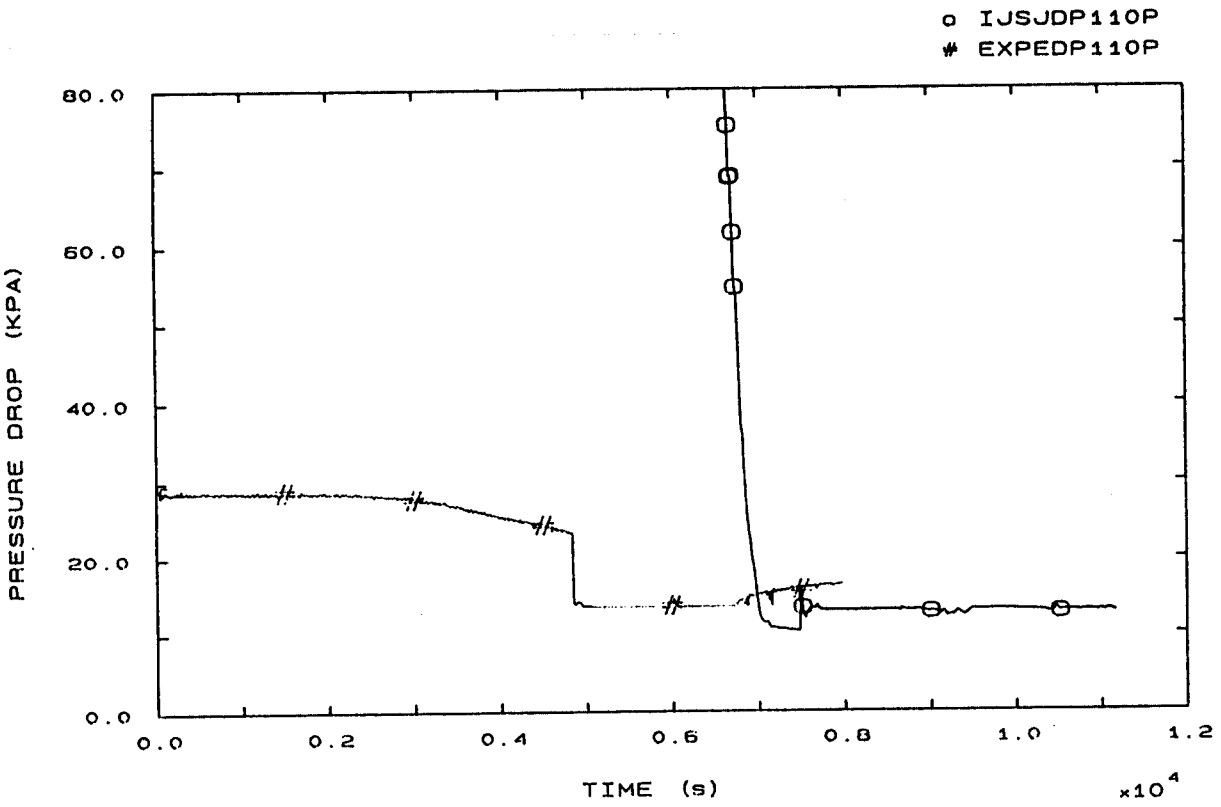

FIG. 71 LOOP SEAL BOTTOM/PUMP 1 INLET PRESSURE DROP

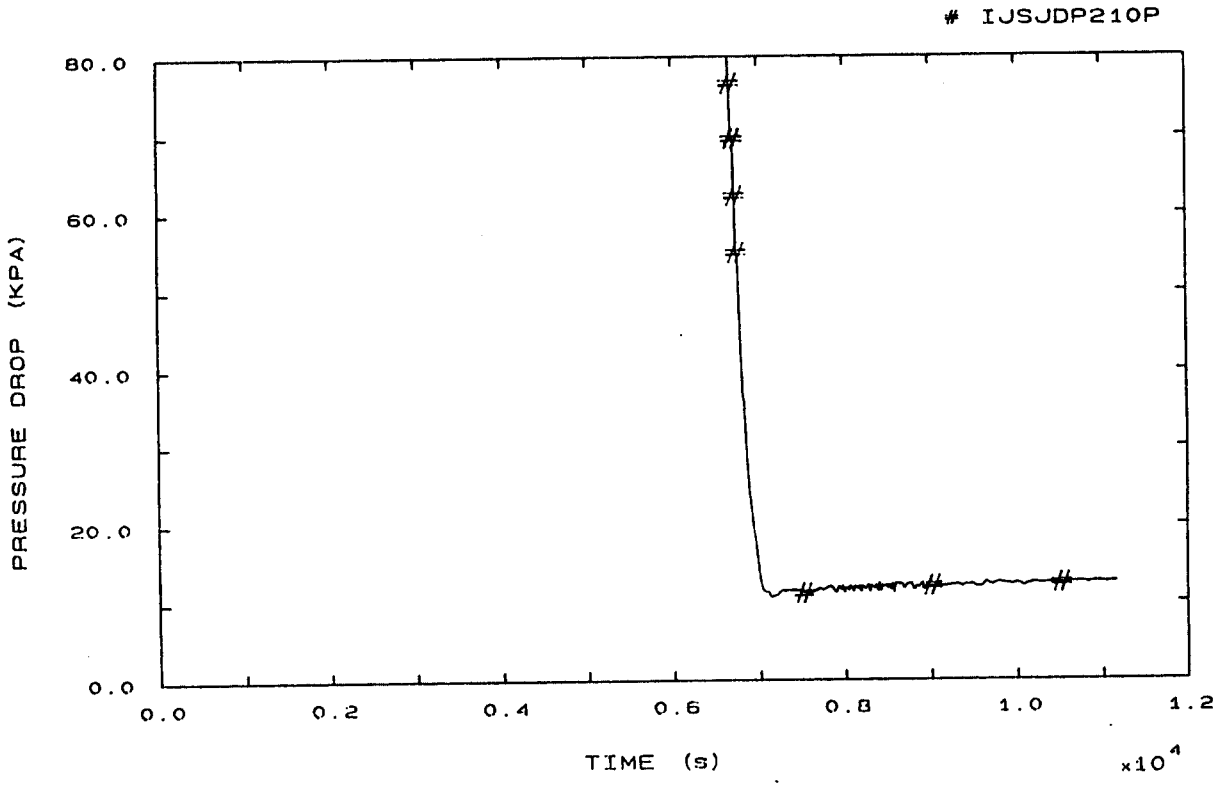

FIG. 72 LOOP SEAL BOTTOM/PUMP 2 INLET PRESSURE DROP

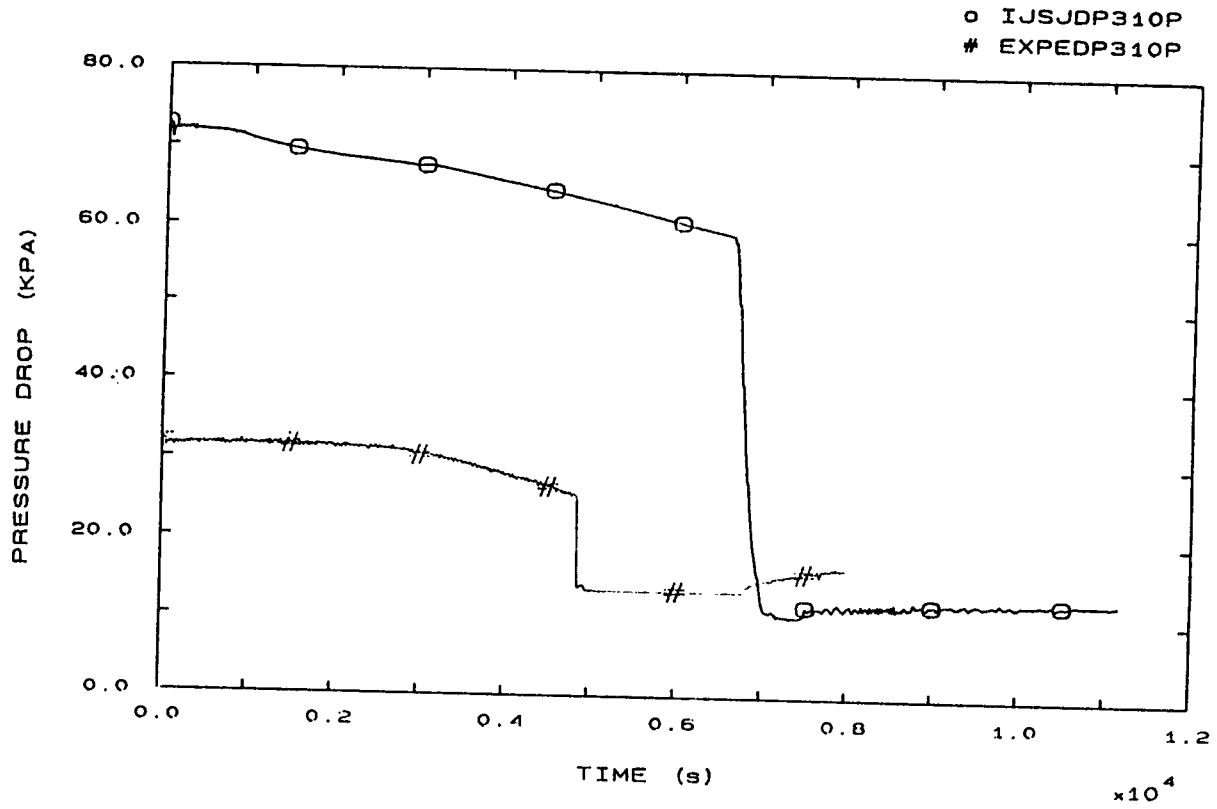

FIG. 73 LOOP SEAL BOTTOM/PUMP 3 INLET PRESSURE DROP

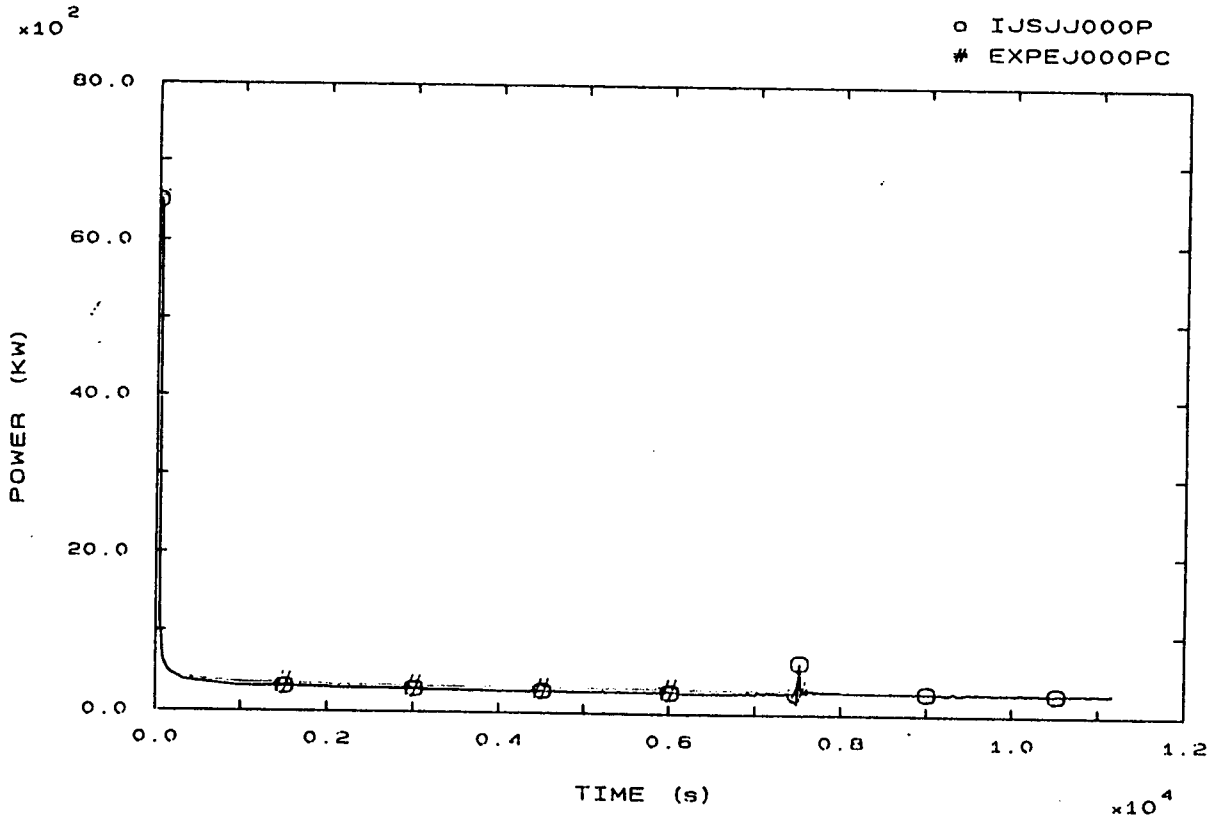

FIG. 81 HEATER RODS POWER

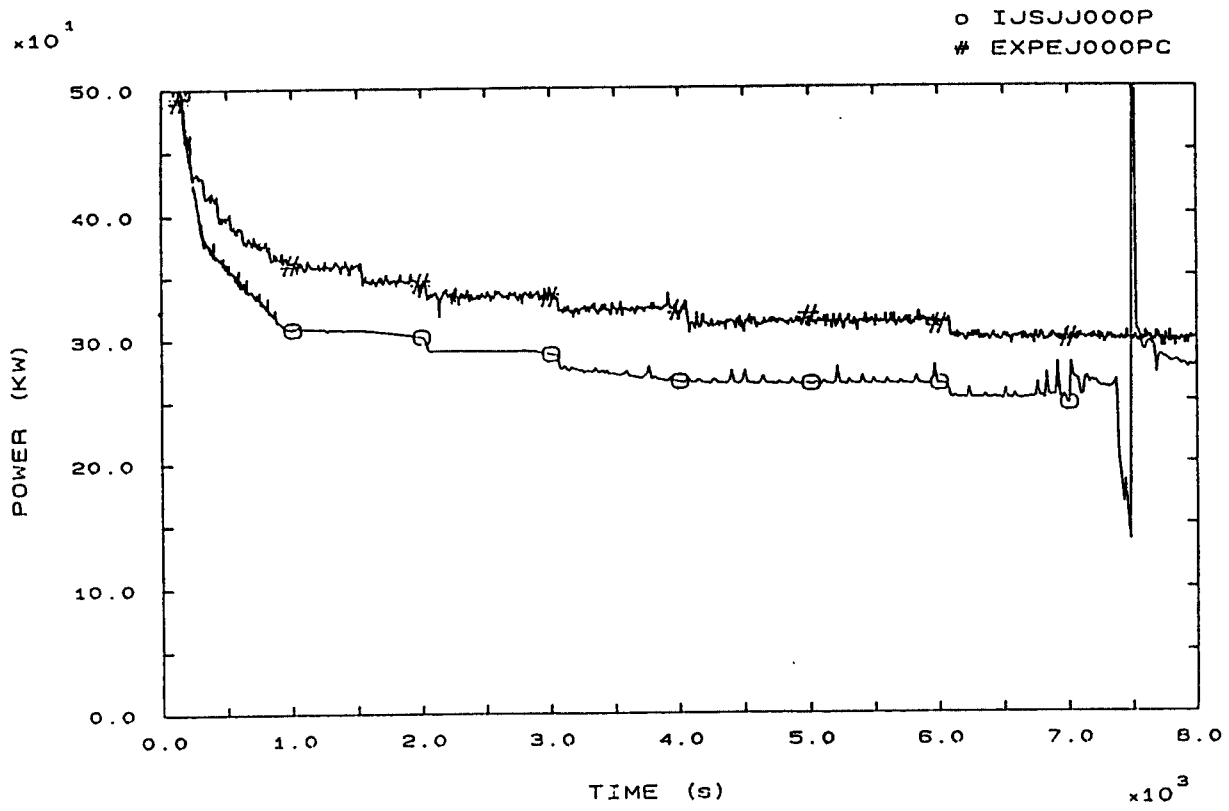

FIG. 81A HEATER RODS POWER

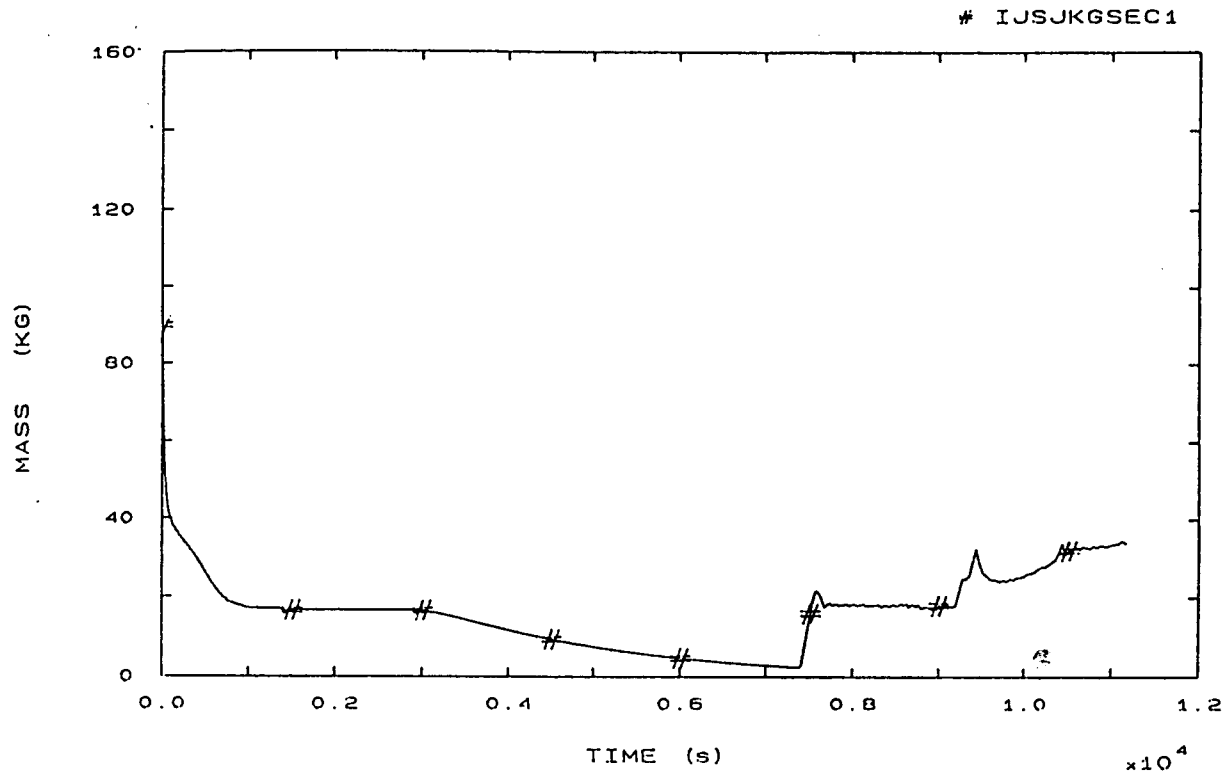

FIG. 86 SECONDARY COOLANT TOTAL MASS SG1

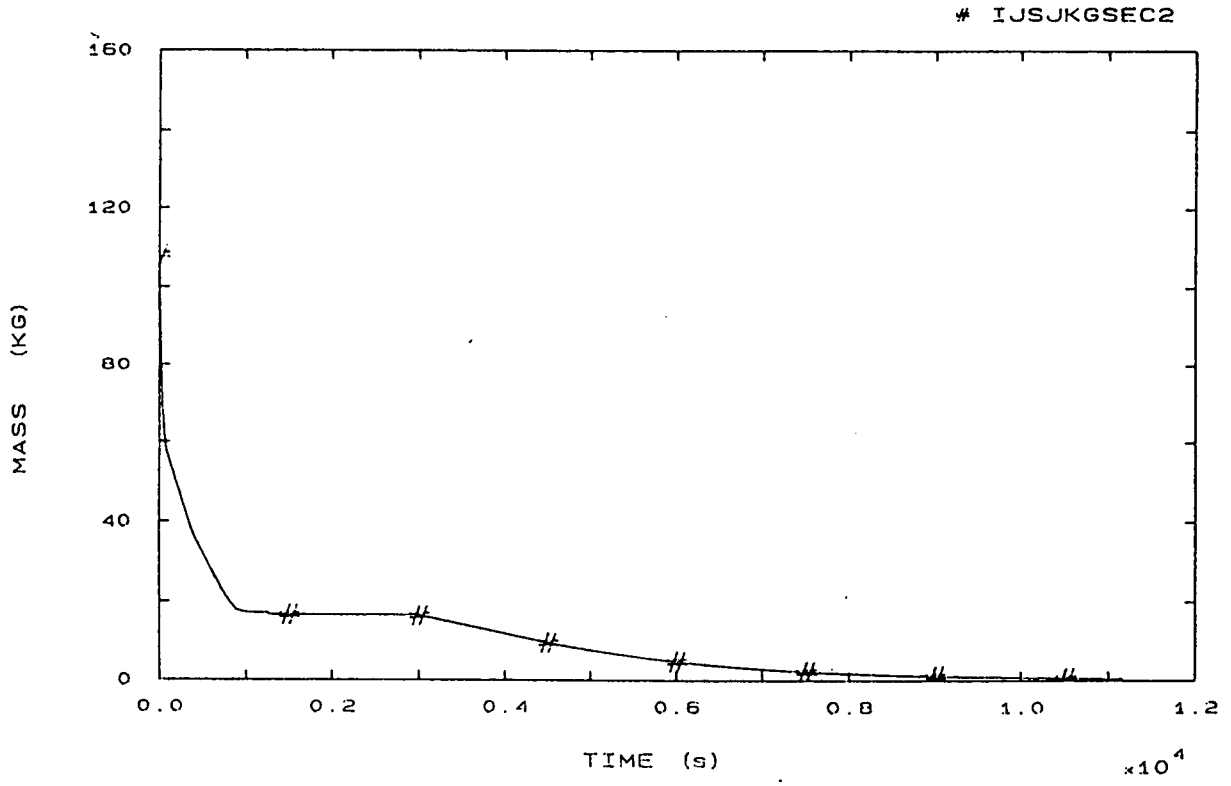

FIG. 87 SECONDARY COOLANT TOTAL MASS SG2

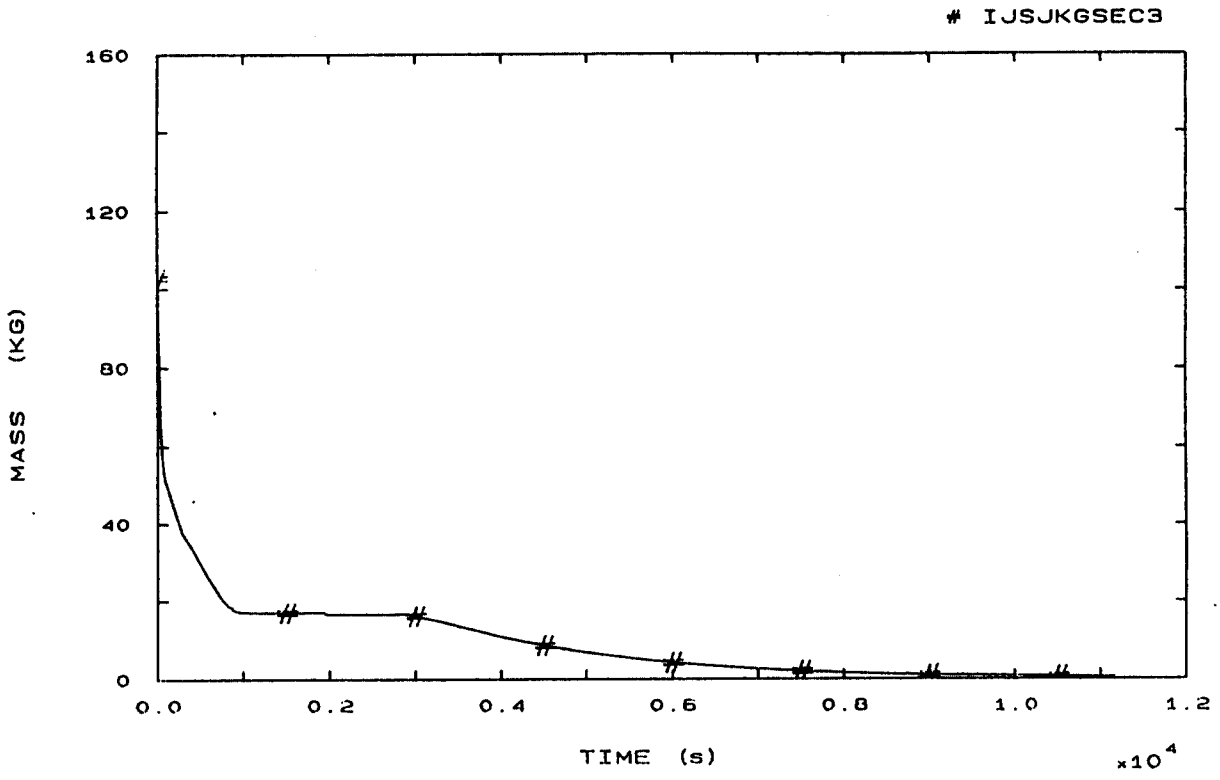

FIG. 88 SECONDARY COOLANT TOTAL MASS SG3

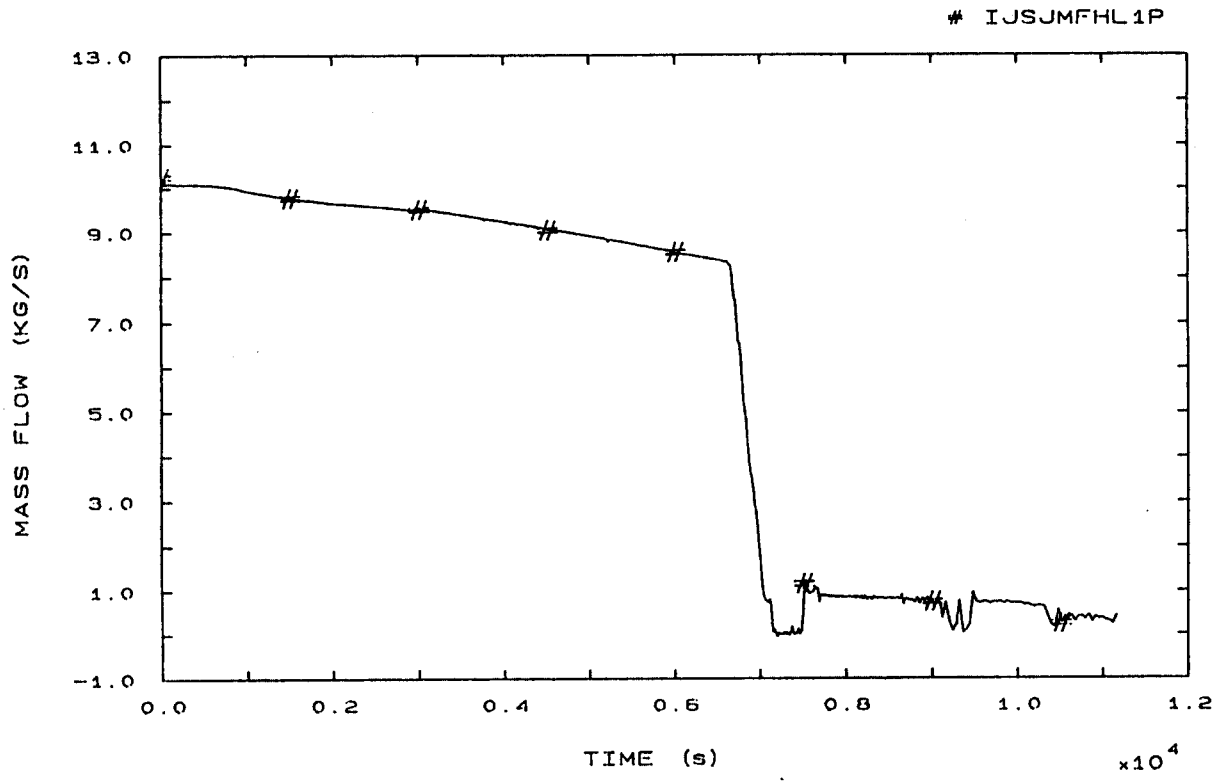

FIG. 89 HOT LEG 1 MASS FLOW

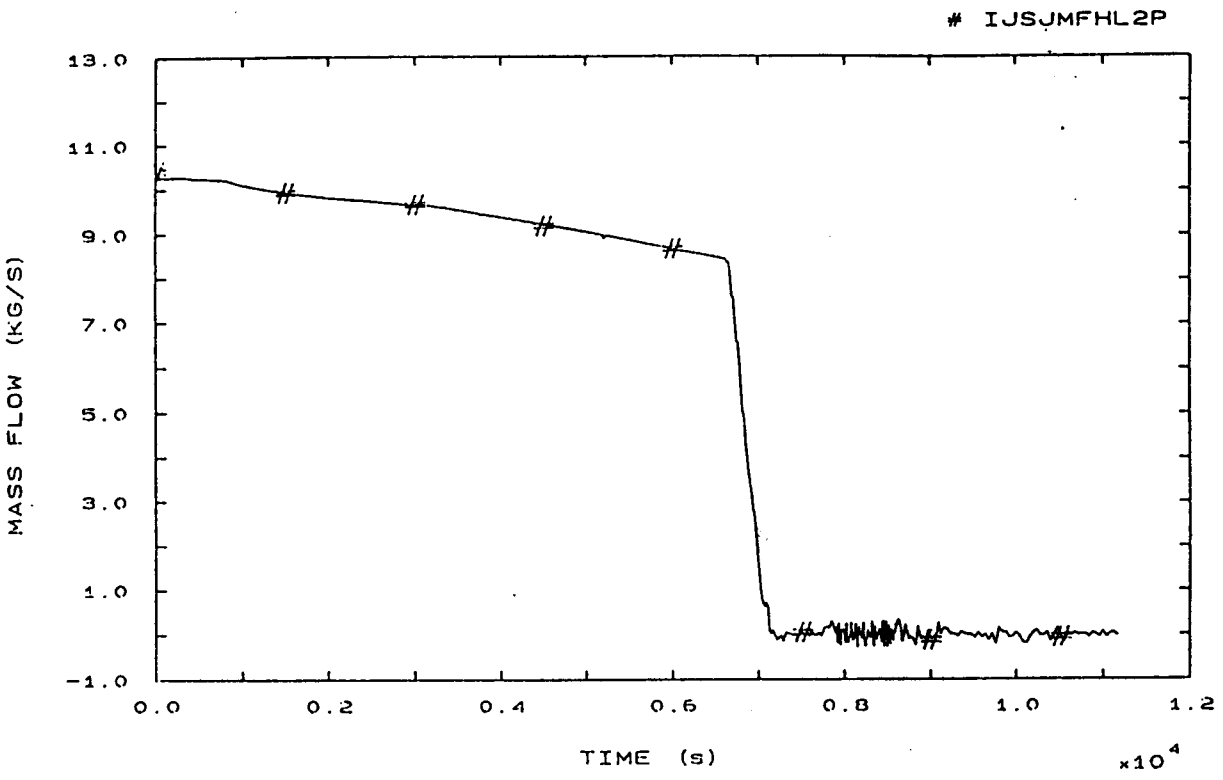

FIG. 90 HOT LEG 2 MASS FLOW

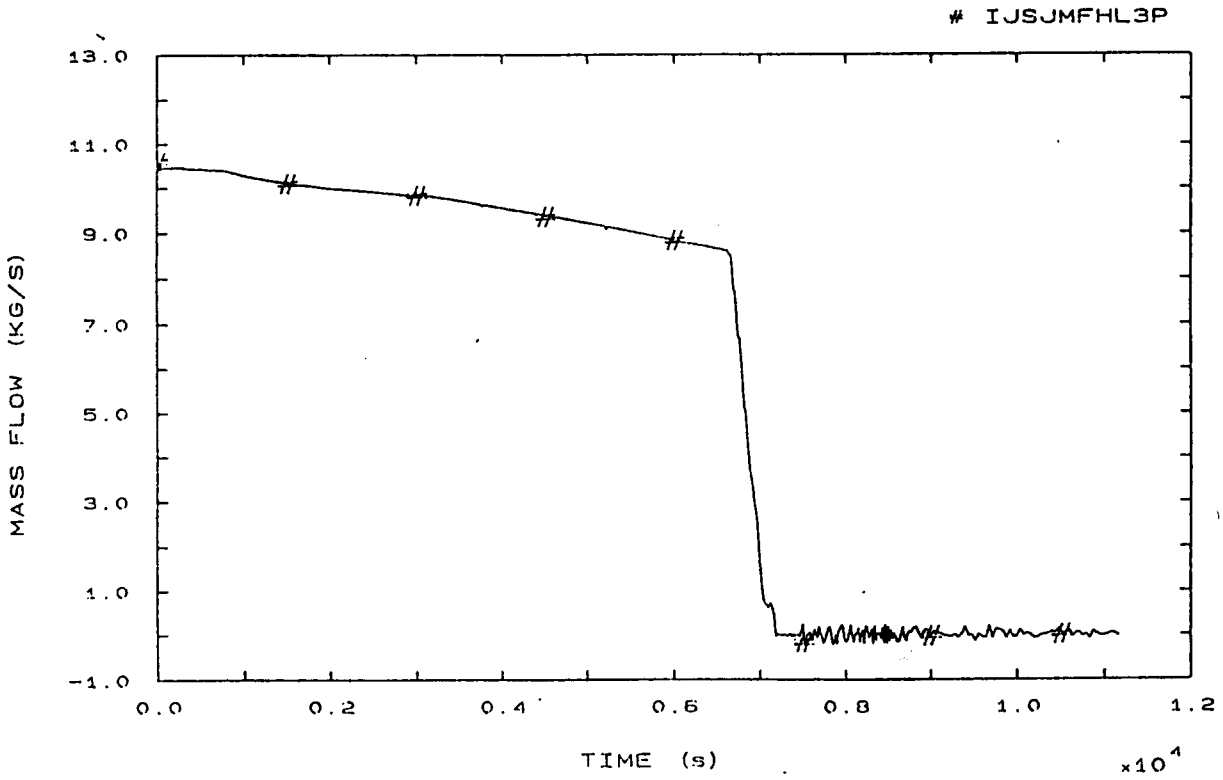

FIG. 91 HOT LEG 3 MASS FLOW

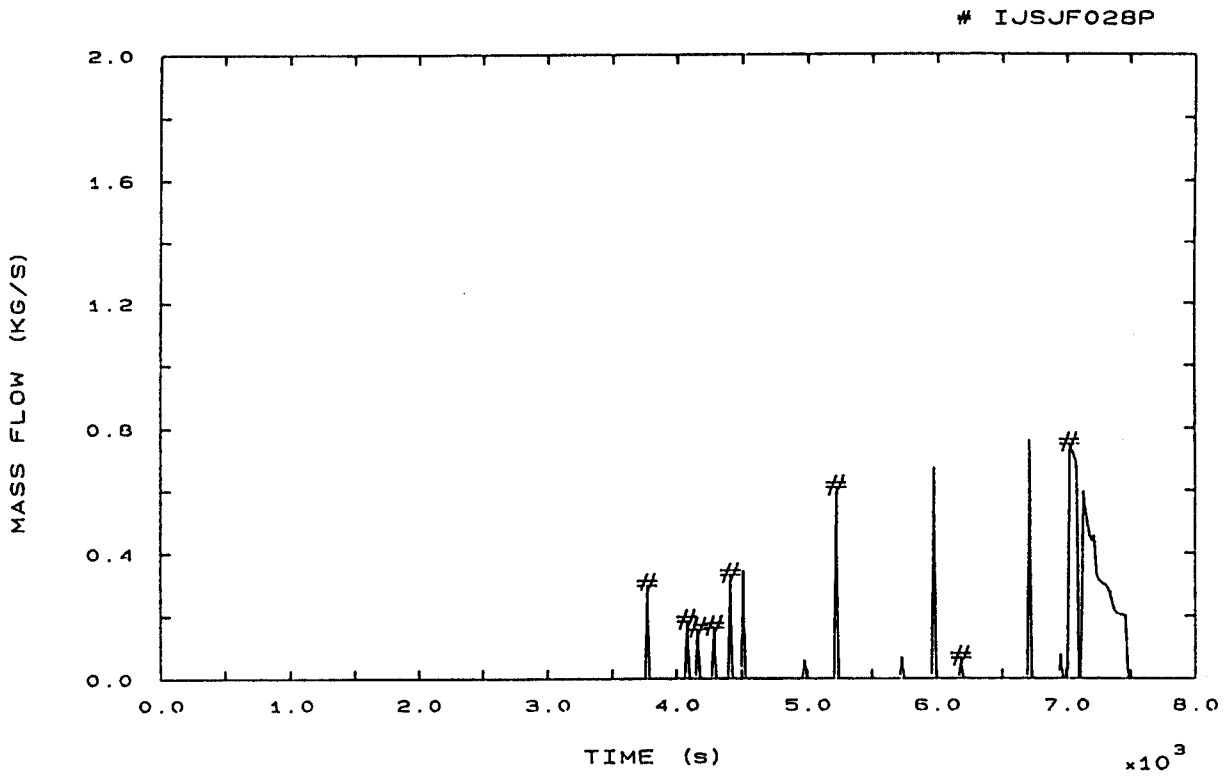

FIG. 92 PRZ PORV MASS FLOW

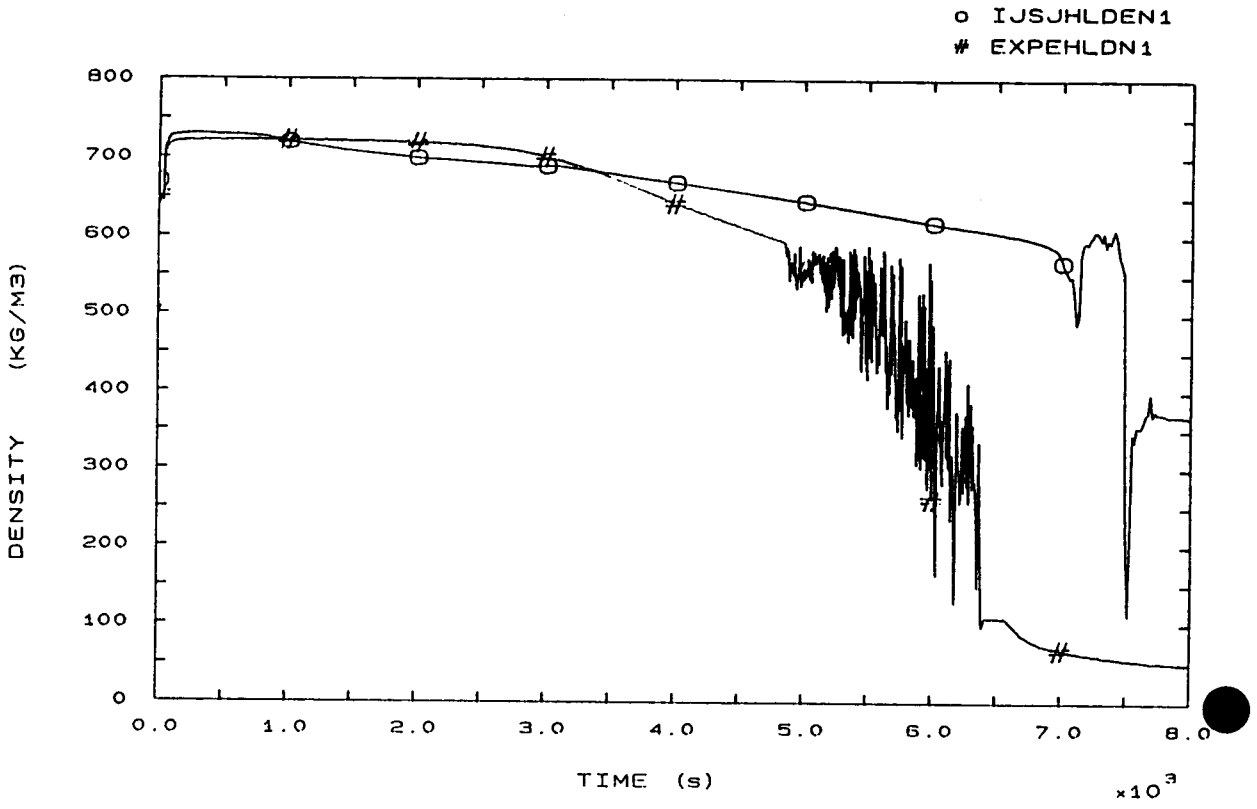

FIG. 100 HOT LEG 1 FLUID DENSITY

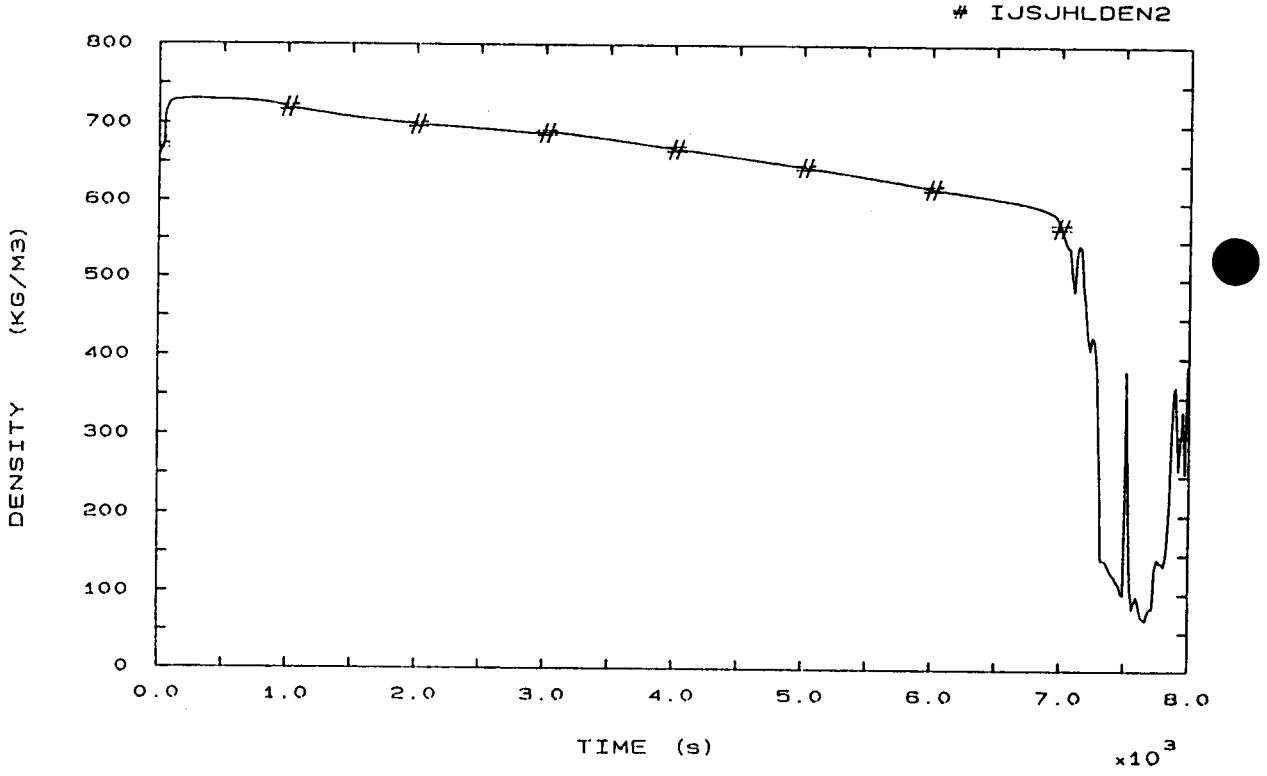

FIG. 101 HOT LEG 2 FLUID DENSITY

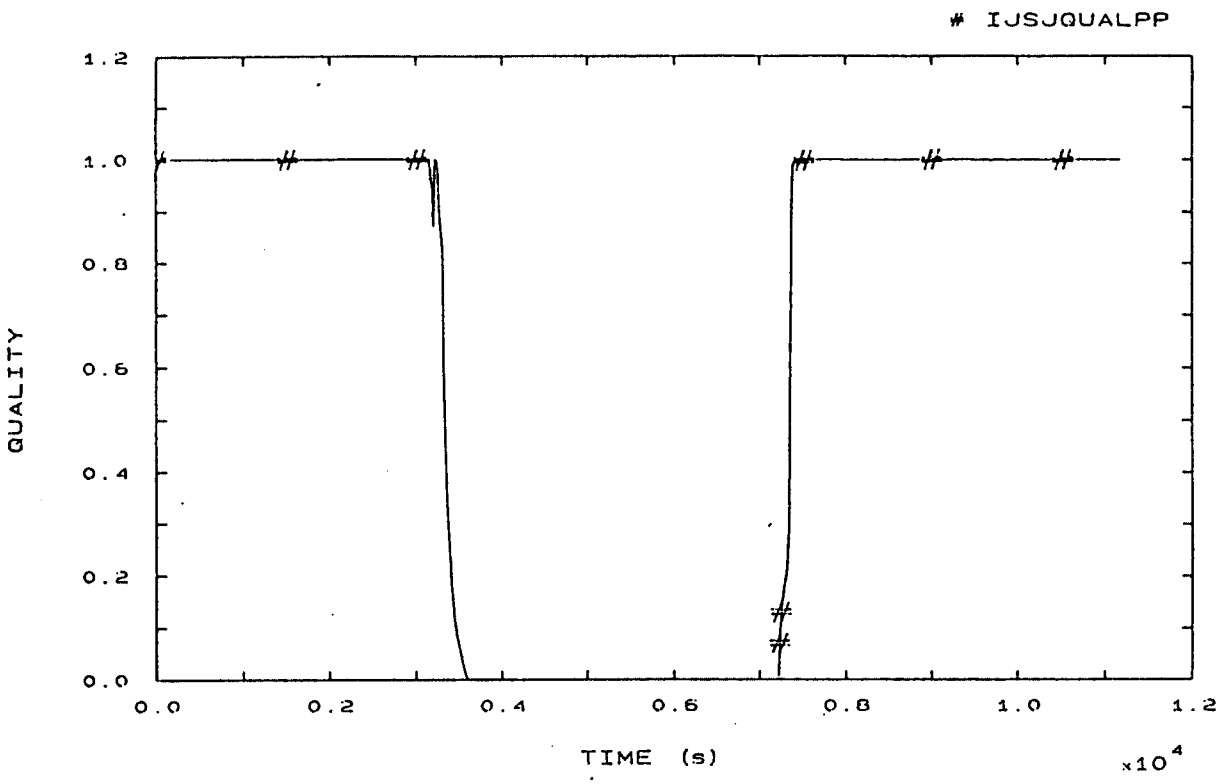

FIG. 103 PRZ PORV FLOW QUALITY

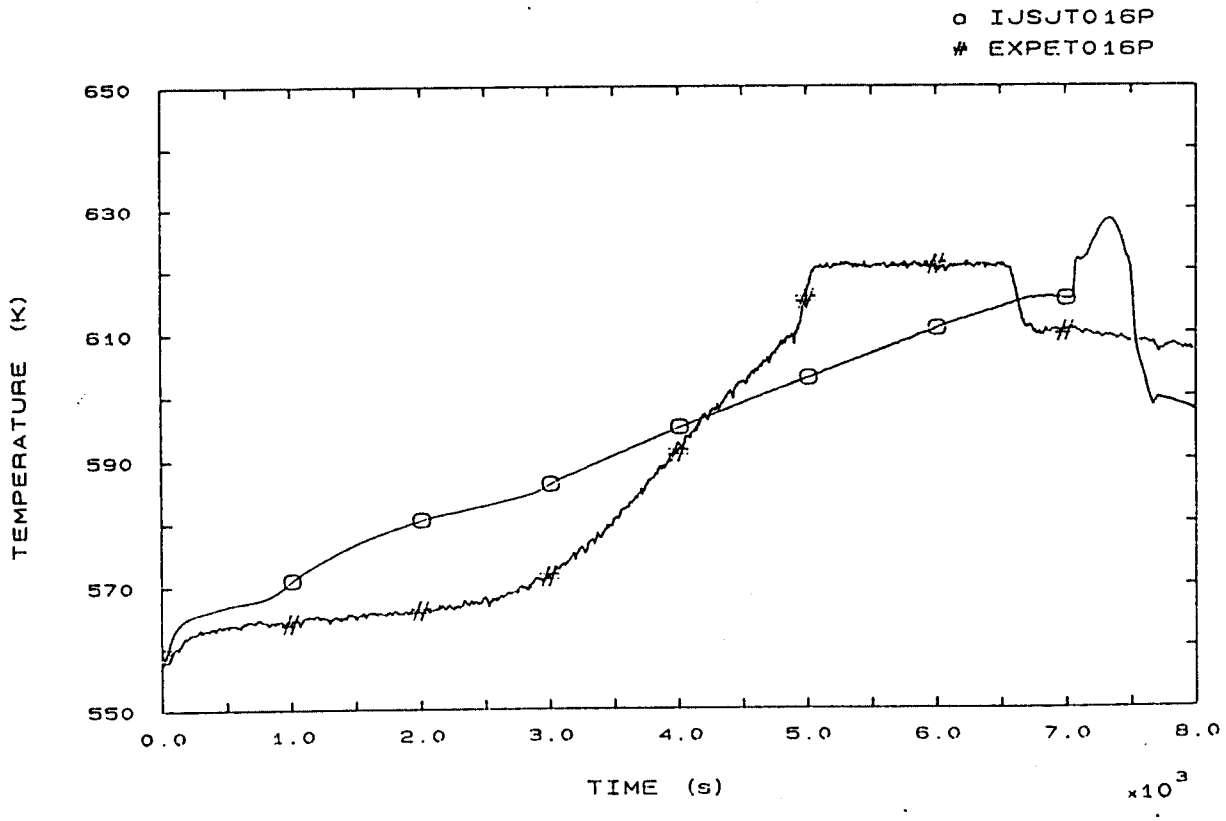

FIG. 110 FLUID TEMPERATURE VESSEL UPPER HEAD

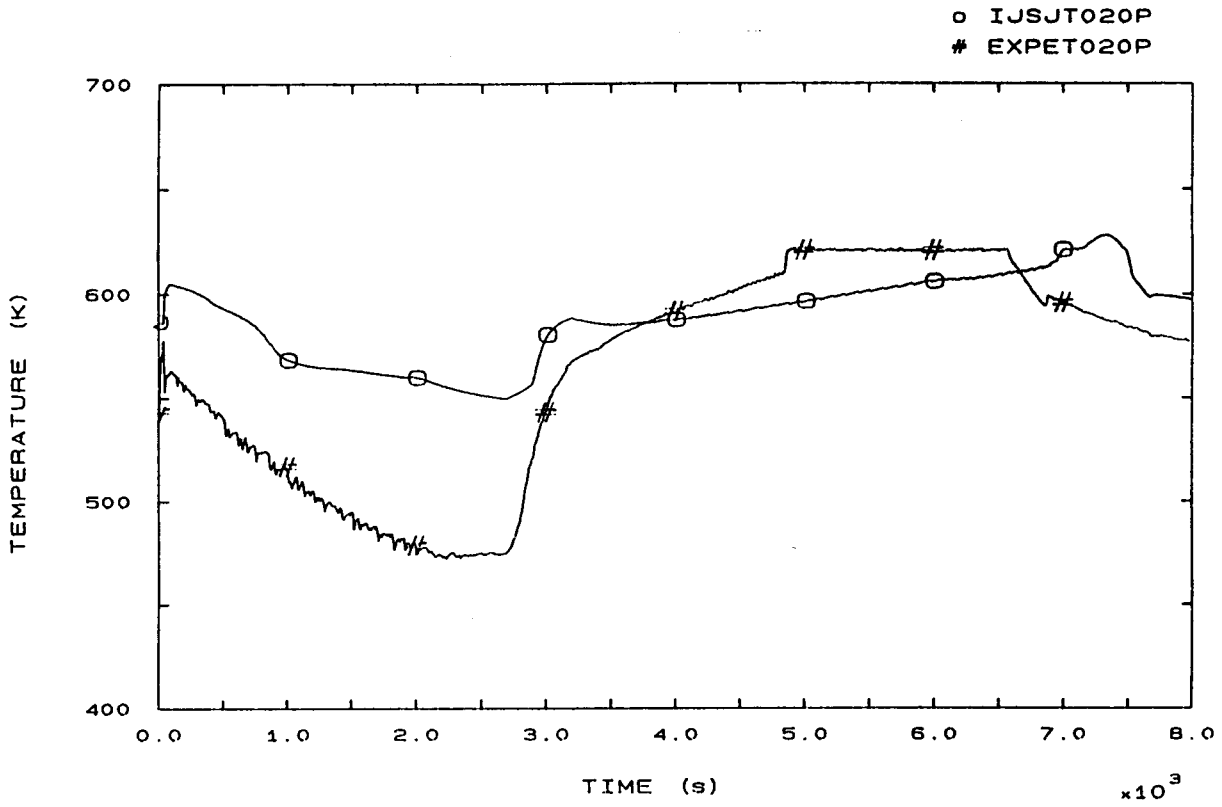

FIG. 112 FLUID TEMPERATURE SURGE LINE UPPER SIDE

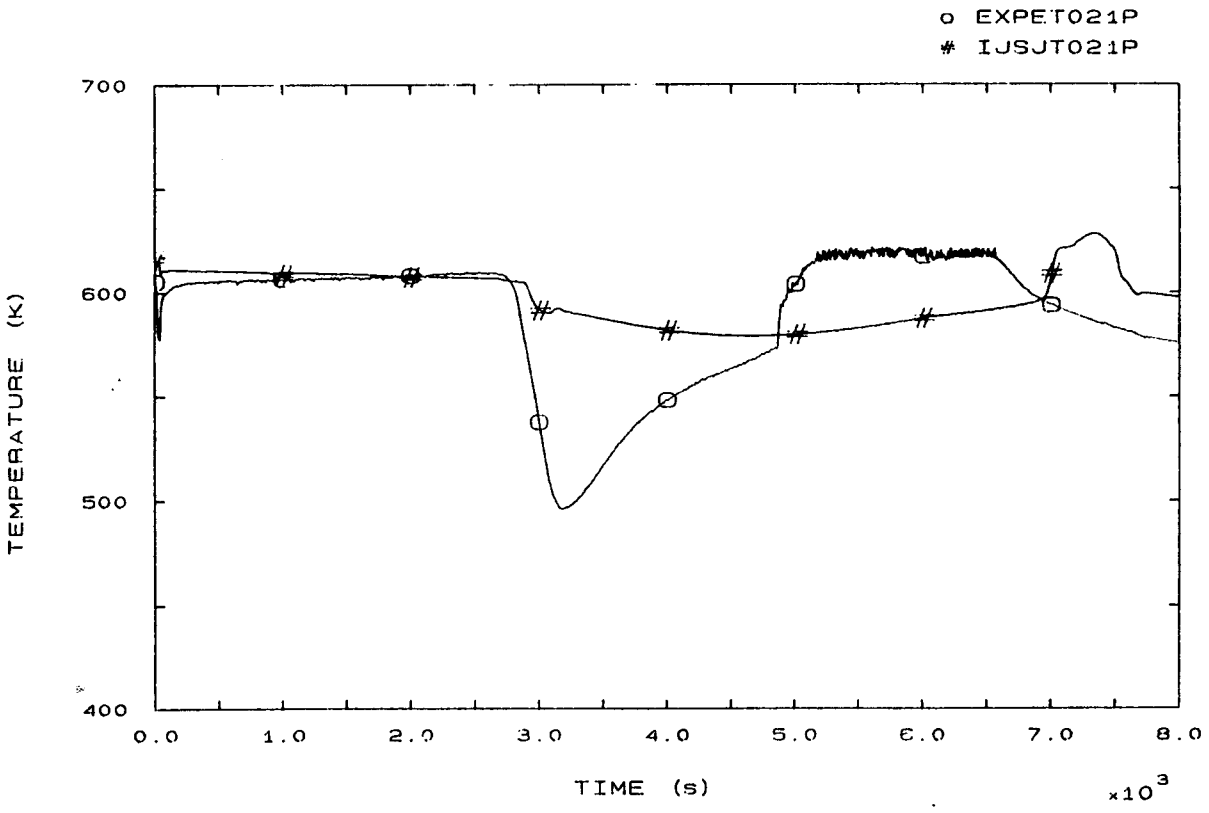

FIG. 113 PRZ FLUID TEMPERATURE

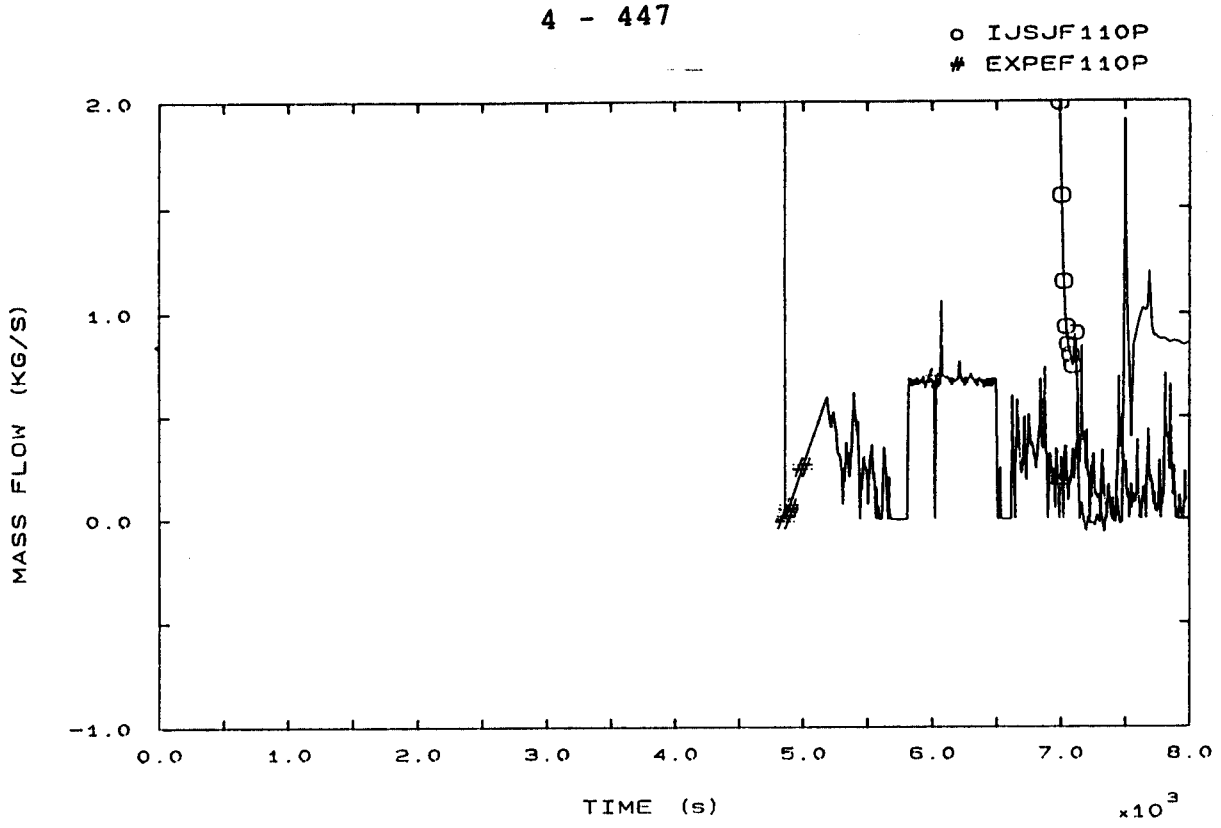

FIG. 125 LOOP SEAL 1 MASS FLOW

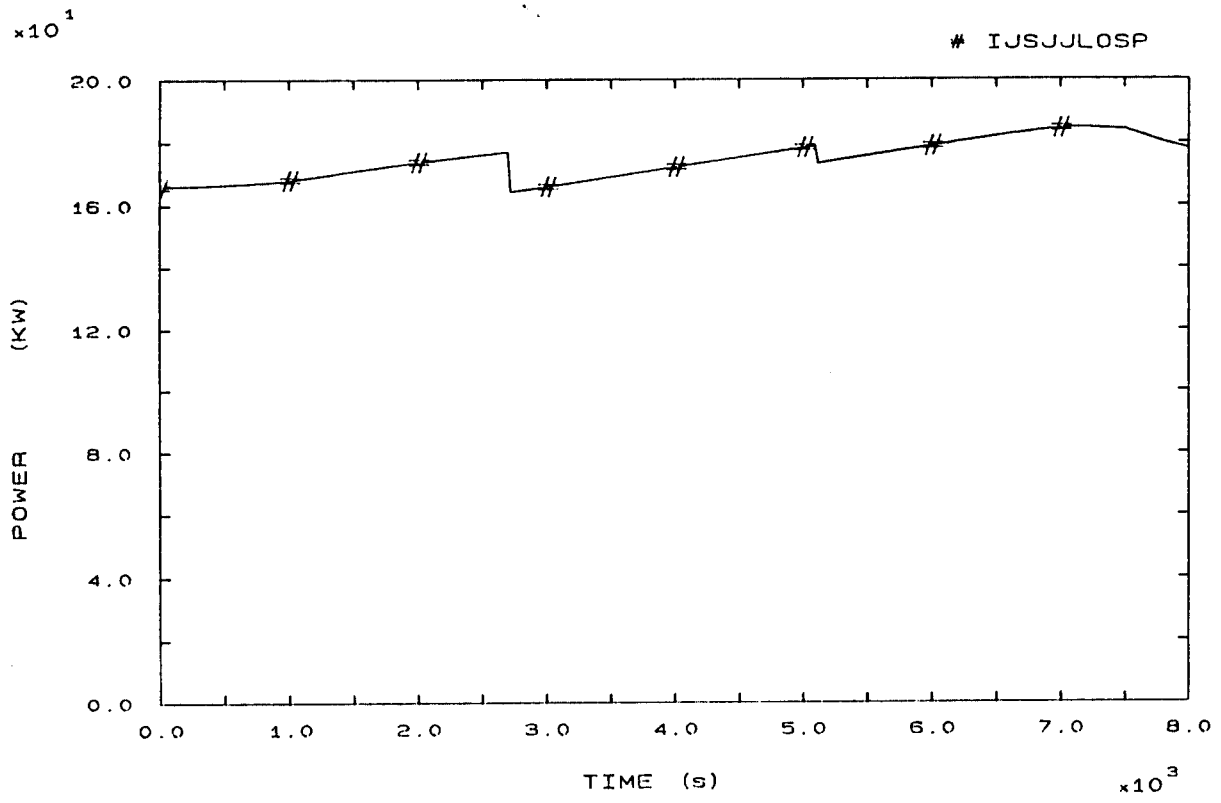

FIG. 131 PRIMARY HEAT LOSS

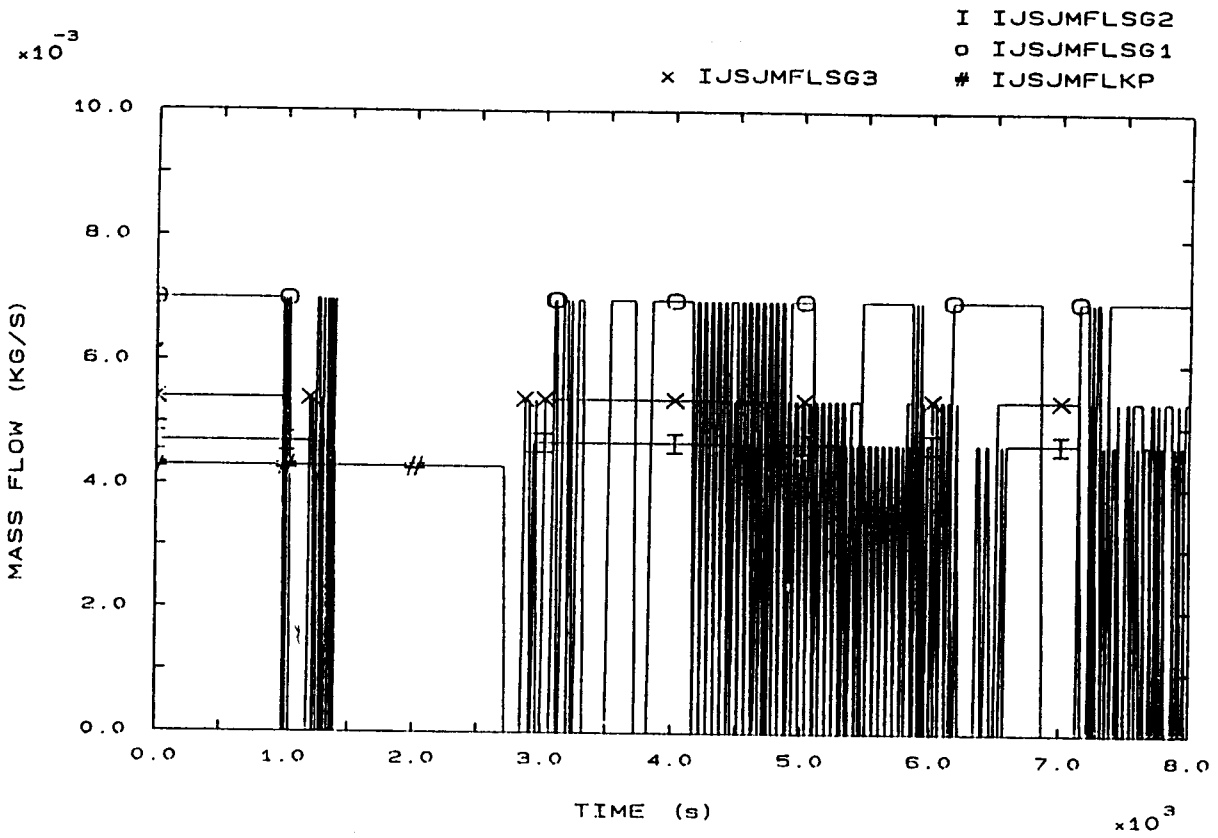

FIG. 137 PRIMARY AND SECONDARY LEAKS

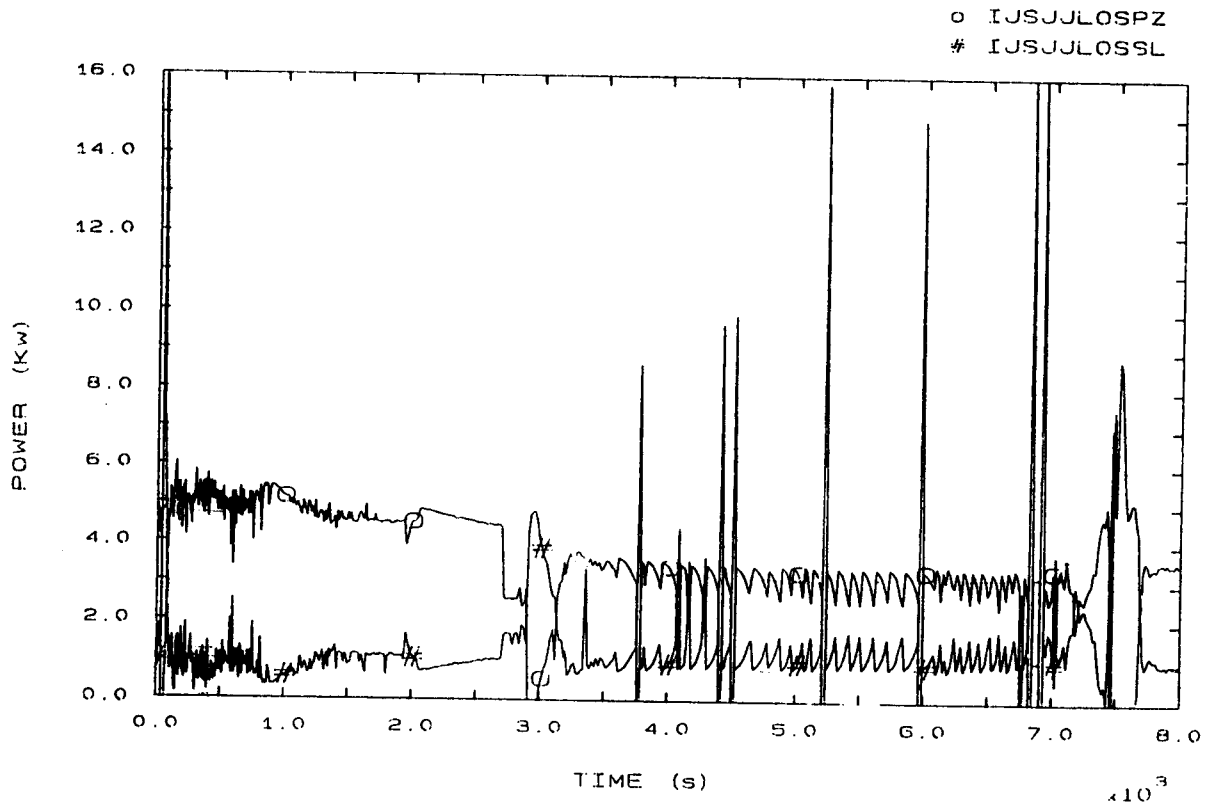

FIG. 138 PRZ AND SURGE LINE HEAT LOSSES

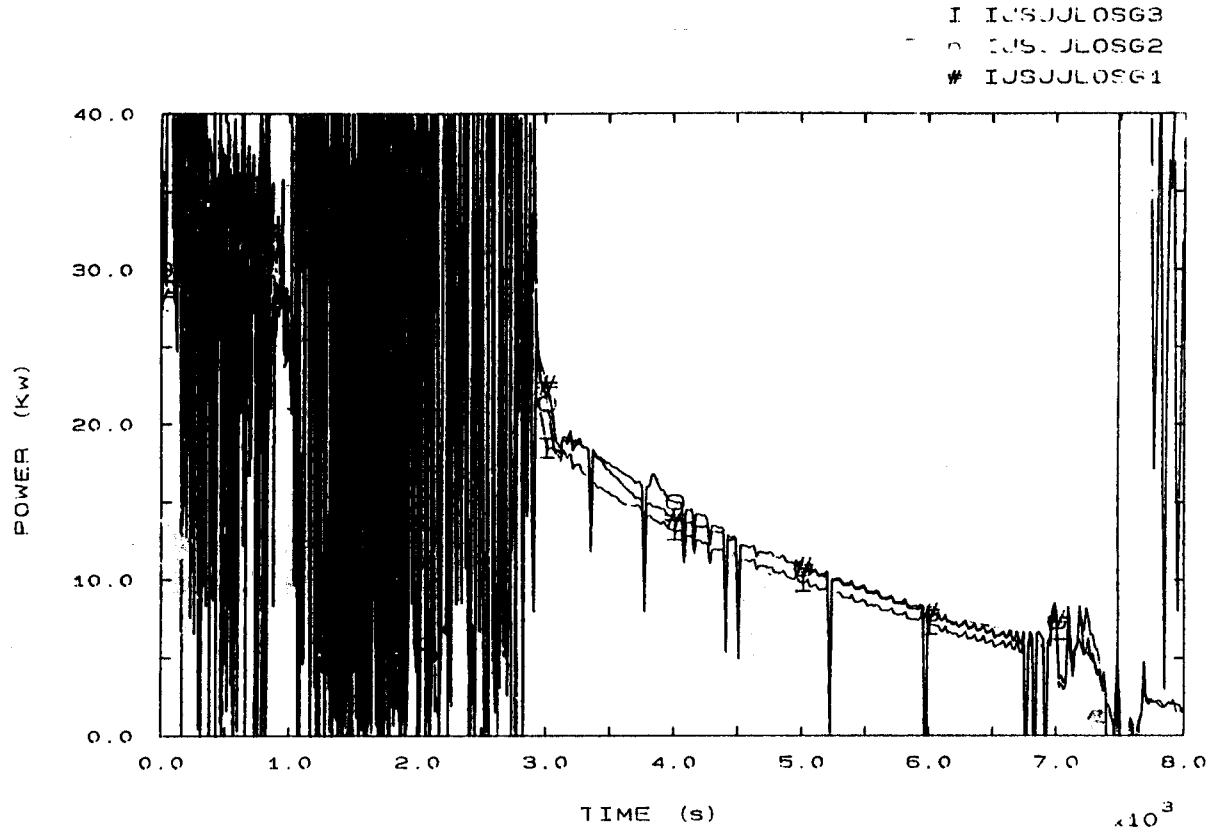

FIG. 139 SECONDARY HEAT LOSSES

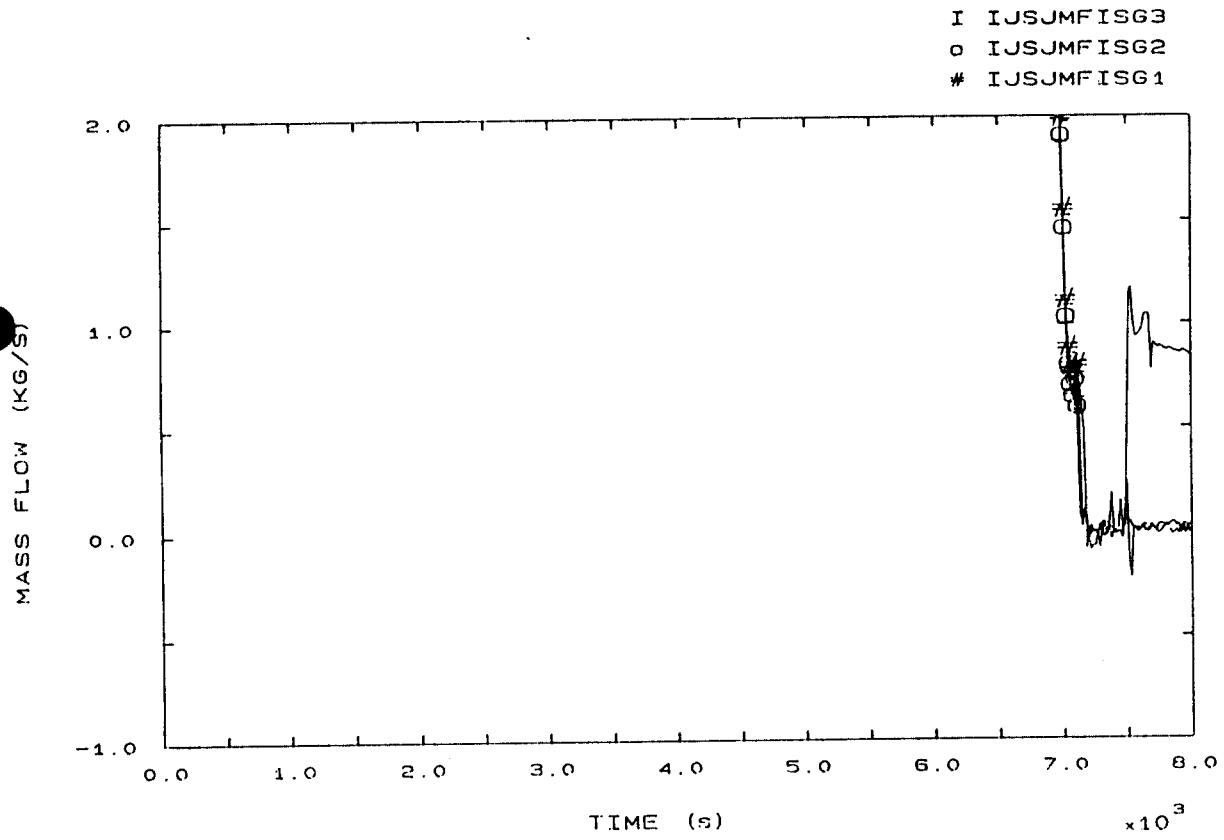

FIG. 140 SG INLET MASS FLOWS

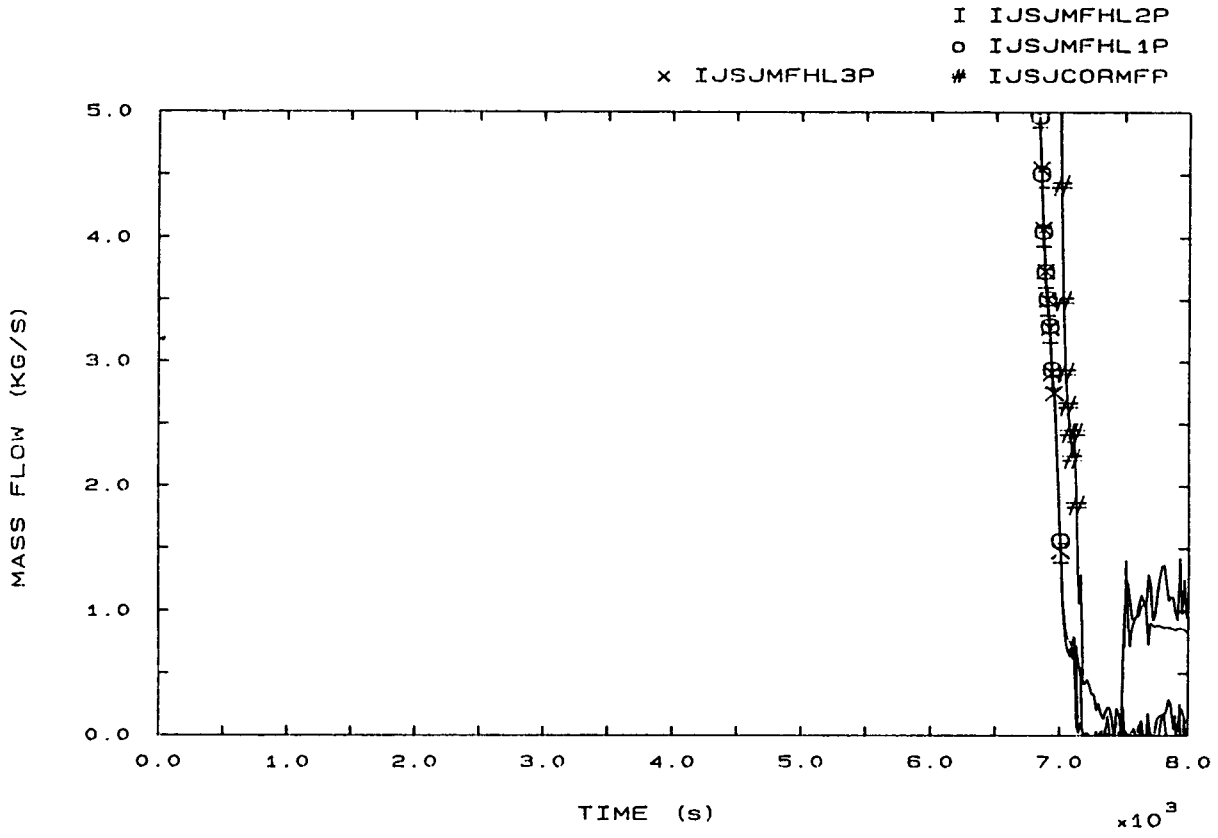

FIG. 141 BOTTOM CORE AND HOT LEG MASS FLOWS

4.12 NNC

4.12.1 CALCULATION DESCRIPTION

Phase 1: from LOFW to Scram (0 - 65 s)

At the start of the transient the main feed isolation valves begin to shut. Secondary fluid is boiled off rapidly, causing the SG inventory and level to drop (fig. 142b). The secondary pressures and temperatures rise, as a result of the absence of the subcooling caused by the feedwater (fig. 3b, 4b, 5b). The secondary temperature rise reduces the heat transferred from the SG tubes to the secondary fluid and causes the tube metal and primary fluid temperatures to rise to maintain the heat transfer from primary to secondary (fig. 12b, 42b). The SG downcomer level reaches the lolo level at 54 seconds and 5 seconds later the MSIVs start to close. This causes a rapid rise in SG pressure with the PORV setpoint being exceeded and the valves opening at about 62 seconds (fig. 3b, 4b, 5b). A maximum secondary pressure of 9.1 MPa is reached. The secondary temperature also rises causing further degradation of the primary to secondary heat transfer (fig. 12b, 42b). The primary temperature rises, causing fluid expansion and pressuriser level rise. The pressuriser PORV opens (fig. 1b) and cycles, relieving steam at a maximum flowrate of about 0.2 kg/s (fig. 92). The density reduction, due to fluid expansion, causes a slight (see fig. 89, 90, 91) pump flow reduction. The scram signal is generated at 65 seconds (fig. 81b).

Phase 2: from Scram to PRZ PORV opening (65 - 1652 s)

At scram time the heater rods power drop sharply to about 5% of its nominal value (fig. 81 b). The primary pressure falls due to the reduced heat input (fig. 1b) and the hot and cold leg temperatures both fall, to about 570 K and 568 K respectively (figg. 12b, 42b).

The secondary pressure falls to the setpoint value and the PORVs cycle to remove the decay heat less heat losses (fig. 3b, 4b, 5b). The SGs gradually dryout, and at about 1500 s the secondary pressure starts to drop due to the reduced primary heat input and the continuing secondary heat losses and steam leaks (fig. 3, 4, 5).
Following the dryout of the SG's (1500 s) and the degradation in the primary to secondary heat transfer, the primary fluid starts to heat up (fig. 12, 42). Primary fluid expands, compressing the steam in the top of the pressuriser, causing the pressurizer level and primary pressure to rise (fig. 1). During heat up the decay heat is split roughly:

15% Heat into the primary fluid
20% Heat into the primary metal
65% Heat losses

The PORV opening setpoint pressure (16.24 MPa) is reached at 1652 seconds (fig. 1).

Phase 3: from PRZ PORV opening to pumps trip (1652 -3759 s)

Following pressurizer relief valve opening, steam relief occurs (fig. 103), with the relief valve cycling. The SG pressure continues to fall due to the steam leakage (fig. 3, 4, 5). Primary system continues to heat up at the rate of 0.016 K/s (fig. 12). The pressurizer level continues to rise due to fluid expansion until 2945 s, when the pressuriser becomes water solid and liquid relief ensues with the relief valve cycling more frequently (fig. 1 and 103). Loop flows fall due to pumps degradation as the fluid density decreases (fig. 89, 90, 91). Pumps trip occurs at 3743 s in loop 1 and at 3759 s in loops 2 and 3 as the pump inlet conditions approach the saturation temperature (fig. 54, 42).

Phase 4: from pumps trip to EFW actuation (3750 - 5057 s)

The rapid coastdown of the pumps causes the loop flows to stall. The core exit fluid temperature rises quicker than before (fig. 53) and saturation is reached at about 3800 seconds. As the fluid saturates, vapour starts to form in the upper parts of the circuit.

The metal temperatures stabilize at close to the saturation temperature and heat input to the fluid increases.

Vapour formation forces increased liquid flow into the pressurizer, causing greater relief valve flow (fig. 92) and a pressure peak above the relief valve setpoint (fig. 1). As the quality of the flow in the surge line rises, the relief valve flow becomes steam and a level forms in the pressuriser. The pressuriser pressure falls back past the relief valve closing setpoint at about 4300 s (due to steam relief see fig. 103). A vessel mixture level forms in the upper plenum at about 4000 s (fig. 10) and falls to the hot leg nozzle elevation by about 4100 s. Similarly, the upper head saturates at about 4000 s and drains to the upper downcomer connection by about 4100 s. The hot legs and SG tubes saturate at about 3950 s and start to drain. The SG downsides drain down to the loop seals by 4400 s, whereas the upsides remain nearly full until about 4300 s, when they drain to the hot legs by 4400 s.

At about 4600 s the downcomer saturates due to steam flow from the upper plenum and the upper head into the downcomer. A level forms, rapidly drops to the cold leg elevation and then continues to drain from 4900 s. The cold legs which have been cooling since pump trip, due to heat losses, rapidly heat up as steam enters the cold legs from the downcomer and condenses. By 4950 s the mixture level in the upper plenum falls below the cold leg nozzle elevation and falls into the core, reaching 4.517 m above the bottom of the vessel at 5057 s. The uncovered core rods rise rapidly in temperature reaching the EFW actuation temperature at 5057 seconds (fig. 52).

Phase 5: from EFW actuation to the end (5057 - 5761 s)

Surges in primary fluid flow, caused by the pressuriser PORV cycling, lead to the core mixture level to cycle once. The core mixture level reaches its minimum of 3.097 m above the bottom of the vessel at 5151 seconds (fig. 11, 12). The maximum hot rod temperature reached is 880 K at 5173 seconds.

The cold EFW added to the loop 1 SG causes a rapid increase in heat transferred from the primary circuit to the secondary of loop 1 SG.

The primary pressure falls and the secondary pressure of loop 1 SG rises (figg. 1, 3). Primary steam and then two phase flow occurs into the loop 1 SG tubes, with vapour condensing in the tubes and no drainback occurring (the counter current flow limitation is exceeded).

The primary depressurization, which causes the pressurizer PORV to close, slows as the secondary saturation pressure is approached (fig. 1). Drain back from the pressurizer into loop 2 and then the vessel occurs between 5105 and 5223 seconds and causes the quenching of the core (fig. 52) . The vessel mixture quickly fills up to the hot leg nozzle elevation. The pressurizer drains until it empties at 5250 s, then there is steam outflow from the pressurizer, as the primary depressurizes. The primary temperature follows the saturation temperature during depressurisation.

Repressurization of the loop 1 SG, due to the heat removed from the primary of about 350 KW (average), occurs until the PORV setpoint is reached at 5391 seconds (fig. 3). Thereafter the SG 1 relief valve cycles. The loop 1 SG refills until the end of transient downcomer level is reached at 5761 seconds (fig. 86).

PARTICIPANT: BRATBY - NNC *CODE: NOTRUMP*

EVENTS TABLE

EVENT	*CALC. TIME (s)*	*EXP. TIME (s)*
SG Low Low Level	*54*	*33*
Main Steam Isolation	*59*	*38*
Scram (power fall), t_1	*65*	*44*
SGs PORV opening	*62* *62* *62*	*82 (3)* *106 (2)* *200 (1)*
SGs Dry Out	*1460 (1)* *1474 (3)* *1500 (2)*	*3282 (3)* *3347 (1)* *3437 (2)*
PRZ PORV opening, t_2	*1652*	*4134*
PRZ full of liquid	*2945*	*4222*
Pumps Trip, t_3	*3750*	*4848*
Loss of Natural Circulation	*4150*	*5630*
Beginning of Core Heat Up	*5050*	*6511*
EFW actuation, t_4	*5057*	*6532*
PRZ PORV closure	*5096*	*6576*
PRZ emptying	*5223*	*6811*
SG1 repressurization	*5391*	*6878*
End of transient, t_{END}	*5761*	*8062*

4.12.2 CALCULATION/EXPERIMENT COMPARISON

Phase 1: from LOFW to Scram

Initial SGs inventory is correctly imposed (see Comparison Table). Trips timing is delayed, due to a strong overprediction of LoLo Level time (54 s vs 33 s). This causes a sensible underprediction of SGs inventory at scram time (see Comparison Table). Maximum primary pressure is calculated with good accuracy (16.3 MPa vs 16.2), but primary pressure profile before Scram is quite different of the exp. one (fig. 1b). This is due to an overestimate of primary temperatures and secondary pressure after LOFW (fig. 3b, 12b, 42b).

Phase 2: from Scram to PRZ PORV opening

The minimum primary pressure immediately after scram is calculated with sufficient accuracy (14.2 MPa vs 14.5) and continues to be accurately calculated until about 1250 s (fig. 1). Primary temperatures are also adequately predicted during this period (fig. 12, 22, 32, 42, 44, 46) demostrating correct calculation of SG heat transfer.

Secondary PORVs opening times are strongly underestimated (see Comparison Table) and pressure profile in SG is different than in the Exp (fig. 3b, 4b, 5b). PRZ level gradient and the minimum PRZ level are well predicted (data given by the Participant in the form of graph). SGs dry out times (1500 s) are strongly underpredicted, due to underevaluation of secondary inventory at scram time. Temperature gradient following SGs dry out is correctly predicted (figg. 12, 42) while no effect on pressurization due to cool pressurizer insurge is observed in NNC calculation (fig. 1). Primary pressurization is much faster and starts earlier than in the experiment: PRZ PORV opening time is therefore strongly underestimated (1652 s vs 4134 s). Also the time interval from the latest SG dry out is extremely underestimated (150 s vs 700) due to an overestimate of pressure gradient after SGDO

(see fig. 1). This can be related to PRZ and SL modelling. In particular there is no indication of the simulation of cool insurge from SL following SGDO, which seems to be a key phenomenon for the interpretation of primary pressure trend in phase 2.

Phase 3: from PRZ PORV opening to pumps trip

PRZ level at the end of phase 2 is lower than real (3.76 m vs 6.57) and time of PRZ filling is again underestimated in the absolute sense (2945 s vs 4222) but is extremely overestimated if compared with the beginning of the phase (1300 s vs 88). This is due to the acceleration of primary pressure profile. The dominant PRZ relief condition (fig. 103) during the phase is steam discharge, due to the initial lower level value. Pumps trip time is largely underestimated even if the phase 3 duration (2100 s vs 714) is strongly overpredicted. Nevertheless primary inventory at trip time is in good agreement (380 Kg vs 390) with the evaluated experimental value.

Phase 4: from pumps trip to EFW actuation

NOTRUMP code doesn't predict a long two phase natural circulation (TPNC) period (figg. 89, 90, 91). The time of LNC with respect to pumps trip is significantly underestimated (400 s vs 780), but the primary inventory at this time is very close to the exp. value (290 Kg vs 296). Beginning of core heat up, referred to the time of LNC, is well calculated (900 s vs 880), and primary mass at this time is again well calculated (180 Kg vs 183). EFW actuation time is also underpredicted in the absolute sense, but is extremely accurate if referred to the time of LNC (907 s vs 900). Core heat up rate at bundle top (3.7 K/s) is inside the experimental range (2/5 K/s).

Phase 5: from EFW actuation to the end

Maximum core temperature (see fig. 52) is sensibly overestimated (870 K vs 770). PRZ PORV closure "absolute" time is overpredicted, but time interval from EFW actuation time is well calculated (40 s vs 44). Primary inventory at t_{PRZPC} is also correct (180 Kg vs 179).
Primary depressurization rate is well calculated, both in the first instants and in the whole period (see Comp. Table and fig. 1). NOTRUMP code succeeds in simulating some kind of primary intermittent flow (see fig. 89) but primary pressure drops data are not provided and so it is not possible to compare adequately this result with the liquid accumulation phenomena in SG1 tubes observed in the Exp. (see 2.6). Pressurization time of SG 1, if referred to EFW actuation time, is very accurately predicted (334 s vs 346).
PRZ goes empty 166 s after EFW actuation (280 s in the Exp). Core quenching is predicted by NNC to take place from the bottom, since NOTRUMP code cannot calculate a top down quench.

PARTICIPANT: BRATBY - NNC CODE: NOTRUMP

COMPARISON TABLE

PARAMETER		EXP	CALC	AE*	RFD**
1A Initial SGs mass (Kg)	1	137	137	G	-
	2	151	151	G	-
	3	145	145	G	-
1B Trips timing (s)	LoLo	33	54	P	SGM(C+B+U)
	MSI	38	59	P	Lolo
	Scram	44	65	P	LoLo
1C Max primary pressure (MPa)		16.2	16.3	G	-
1D SGs mass at Scram (Kg)	1	98	73	P	
	2	105	86	P	1B
	3	97	79	P	
2A Min. primary pressure (MPa)		14.5	14.2	S	-
Pressure gradients before		4.10^{-4}	$-9.9.10^{-5}$	S	-
and after SGs DO (MPa/s)		3.10^{-4}	$3.6.10^{-3}$	P	PRZM (U+B)
2B SGs PORV opening time (s)	1	200	62	P	SGM (U)
	2	106	62	P	?
	3	82	62	S	
2C PRZ level gradient (m/s)		$-5.7.10^{-4}$	$-5.5.10^{-4}$	G	-
2D Min. PRZ level (m)		2.3	2.9	S	-
2E SGs DO time tSG1DO (s)		3347	1460	P	
tSG2DO (s)		3437	1500	P	1D+SGM
tSG3DO (s)		3282	1474	P	
2F Heat Up temperature (K/s)		0.02	0.02	G	-
and level (m/s) gradients		$3.6.10^{-3}$	$2.3.10^{-3}$	S	-
2G Cool Insurge effect		PR. DELAY	NO	P	PRZM (U+B)
2H PRZ PORV opening time, t2 (s)		4134	1652	P	2E +
($dt_2 = t_2 - t_{SGDO}$)		(697)	(150)	P	PRZM (U+B)
3A PRZ level at t_2 (m)		6.57	3.76	P	2H
3B PRZ full time, t_{PRZF} (s)		4222	2945	P	2E
($dt_{PRZF} = t_{PRZF} - t_2$)		(88)	(1300)	P	2H
3C Dominant Relief Condition		LIQ	STEAM	P	3A
3D Sat. Conditions before trip		NO	NO	G	-
3E Pumps Trip time, t3 (s)		4848	3750	P	2E
($dt_3 = t_3 - t_2$)		(714)	(2100)	P	2H
($dt_{HU} = t_3 - t_{SGDO}$)		(1411)	(2250)	P	

* ACCURACY EVALUATION : G=GOOD, S=SUFFICIENT, P=POOR

** REASON FOR DISCREPANCY : B=BIC, C=CODE, U=USER, PRZM=PRZ MODELLING, SGM=SG MODELLING, ?=NOT CLEAR

PARTICIPANT: BRATBY - NNC CODE: NOTRUMP

COMPARISON TABLE (CONT'D)

PARAMETER	EXP	CALC	AE*	RFD**
3F RCS mass at t_3 (kg)	390	380	G	-
4A PRZ behaviour	PART. EMPT.	PART. EMPT.	G	-
during phase 4	LEV. OBS.	LEV. OBS.	G	-
4B Primary Flow Cond.	TPNC/LNC	TPNC/LNC	G	-
4C LNC time, t_{LNC} (s)	5630	4150	P	3E
($dt_{LNC} = t_{LNC} - t_3$)	(780)	(400)	P	LDP (C?)
4D RCS mass at t_{LNC} (kg)	296	290	G	4C
4E Beg. of Core Heat Up, t_{BOCH} (s)	6511	5050	P	3E
($dt_{BOCH} = t_{BOCH} - t_{LNC}$)	(880)	(900)	G	-
4F RCS mass at tBOCH (Kg)	183	180	G	-
4G EFW act. time, t4 (s)	6532	5057	P	3E
($dt_{4B} = t_4 - t_{BOCH}$)	(21)	(7)	P	
($dt_{4L} = t_4 - t_{LNC}$)	(900)	(907)	G	
($dt_4 = t_4 - t_3$)	(1684)	(1307)	S	LDP (C?)
4H PRZ level at t_4 (m)	4.4	4.3	G	-
5A Core Heat Up Rate (K/s)	2/5	3.7	G	-
5B Max Core Temperature (K)	770	870	P	C?
5C PRZ PORV closure time, t_{PRZPC}	6576	5096	P	3E
($dt_{PRZPC} = t_{PRZPC} - t_4$)	(44)	(40)	G	-
5D RCS mass at t_{PRZPC} (Kg)	179	180	G	-
5E RCS Depress. Rate (MPa/s)	-0.016	-0.018	G	-
(Initial/Averaged on 500 s)	-0.0086	-0.0089	G	-
5F Prim. Circulation Mode	INTERM	TPNC (DISC)	P	C+U?
5G SG1 Press. time, t_{SG1PR} (s)	6878	5391	P	3E
($dt_{SG1PR} = t_{SG1PR} - t_4$)	(346)	(334)	G	-
5H PRZ Role	CORE FL.	CORE FL.	G	-
5I PRZ emptying time, t_{PRZE} (s)	6811	5223	P	
($dt_{PRZE} = t_{PRZE} - t_4$)	(280)	(166)	P	
5J Core Reflood Mode	TOP-DOWN	BOTTOM-UP	P	C
5K End of Transient time, t_{END}	8062	5761	P	4G

* ACCURACY EVALUATION : G=GOOD, S=SUFFICIENT, P=POOR
** REASON FOR DISCREPANCY : C=CODE, U=USER, LDP=LIQUID DISCHARGE FROM PRZ

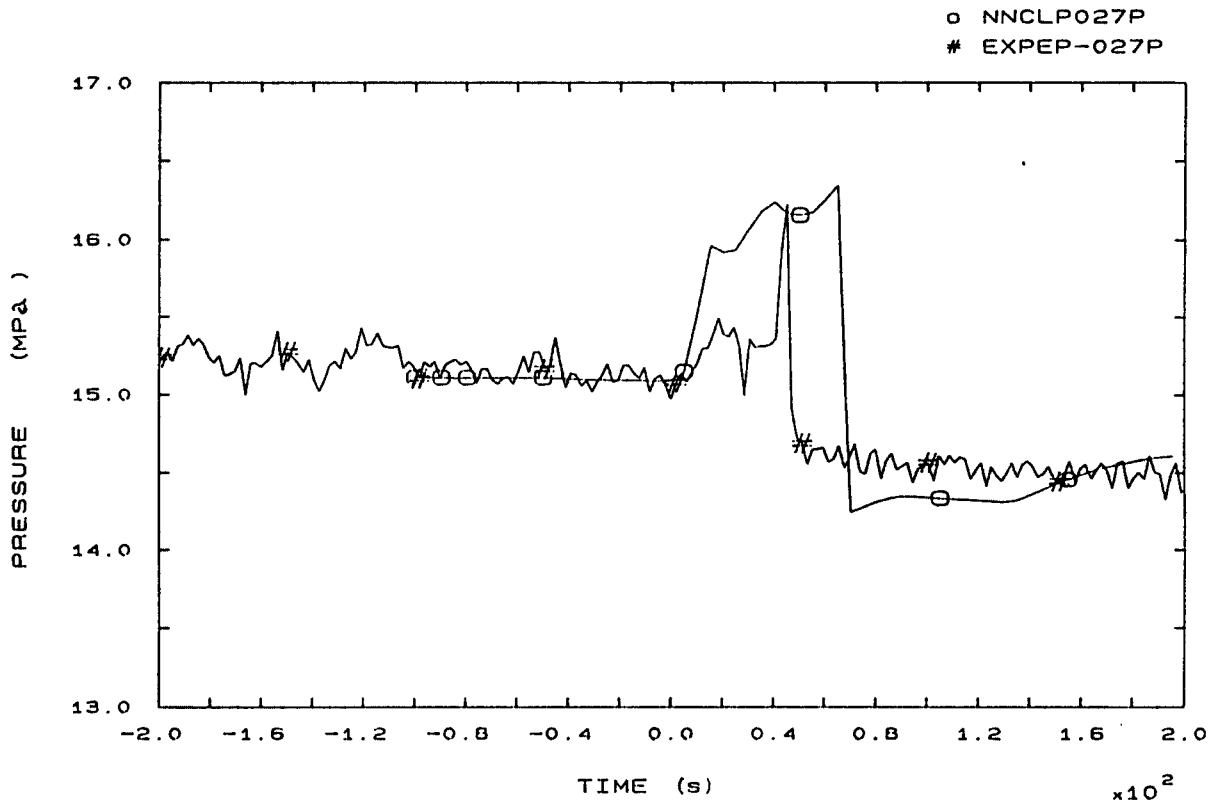

FIG. 1b PRESSURIZER PRESSURE

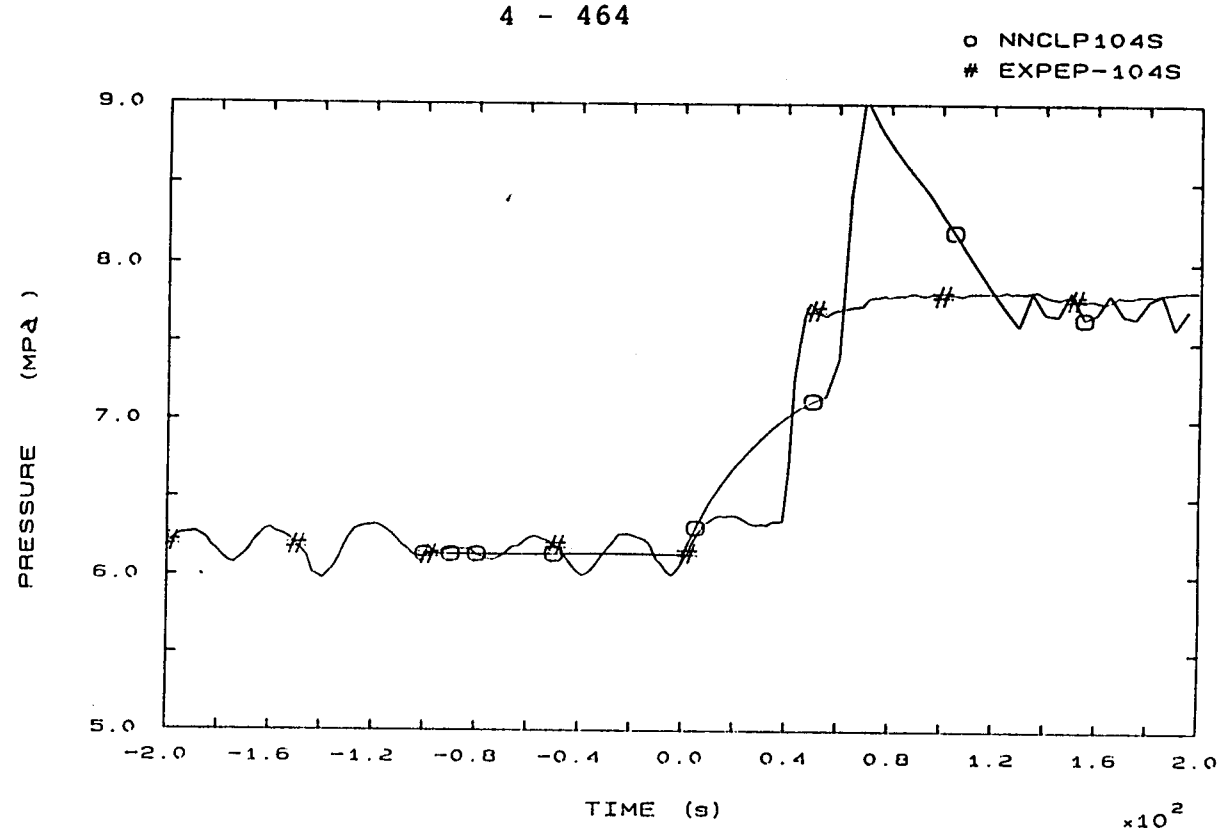

FIG. 3b SG1 STEAM DOME PRESSURE

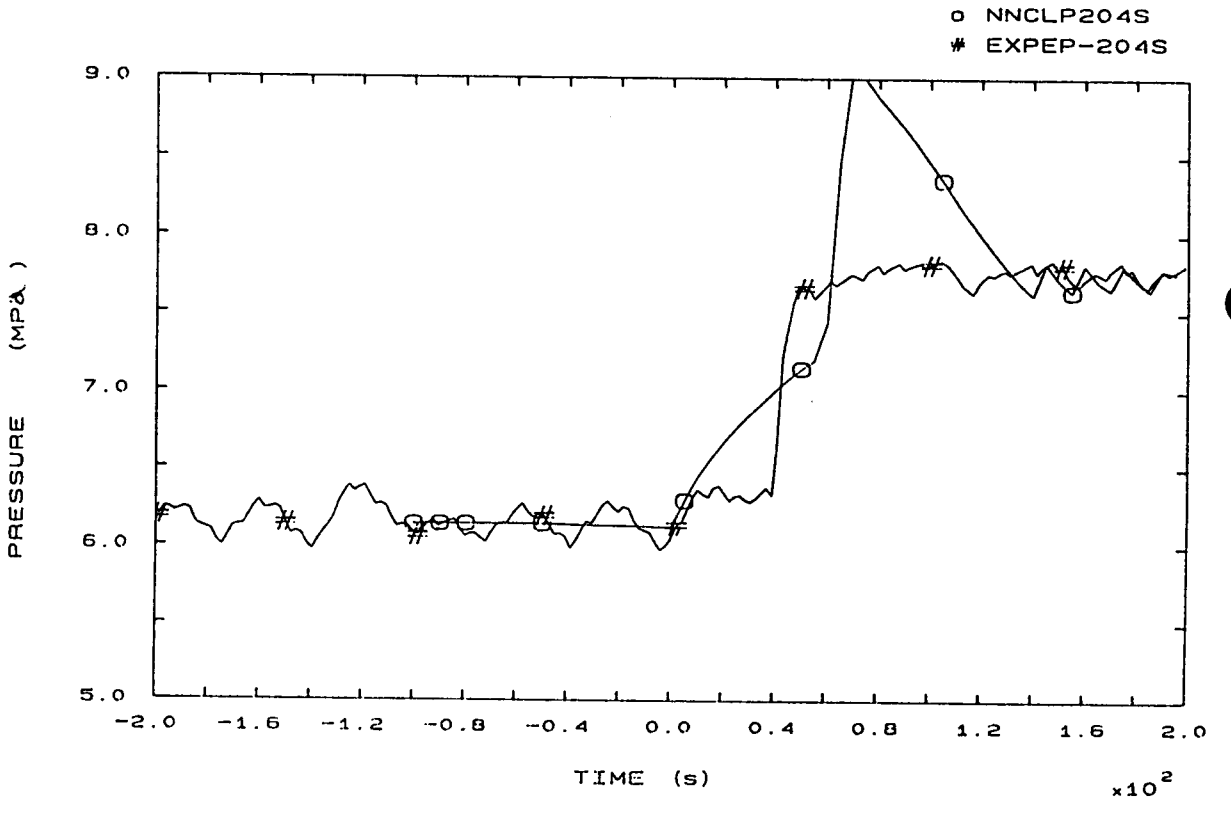

FIG. 4b SG2 STEAM DOME PRESSURE

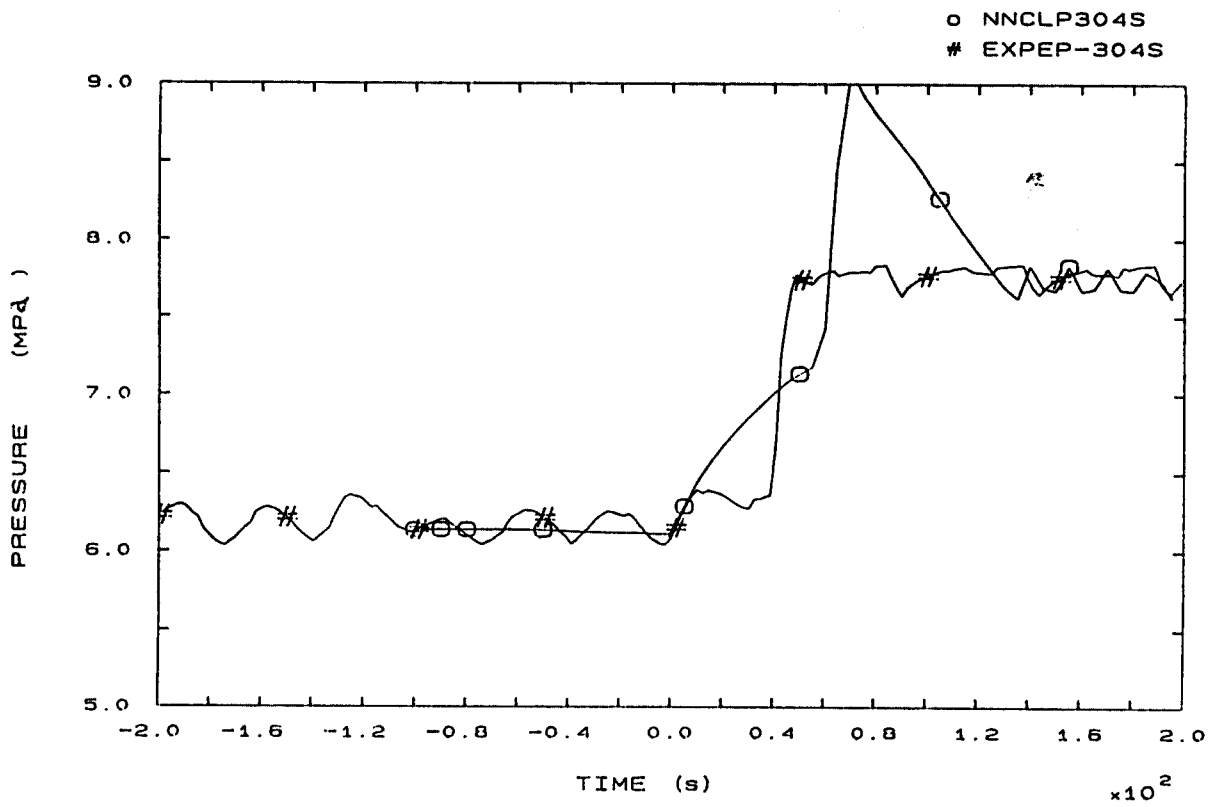

FIG. 5b SG3 STEAM DOME PRESSURE

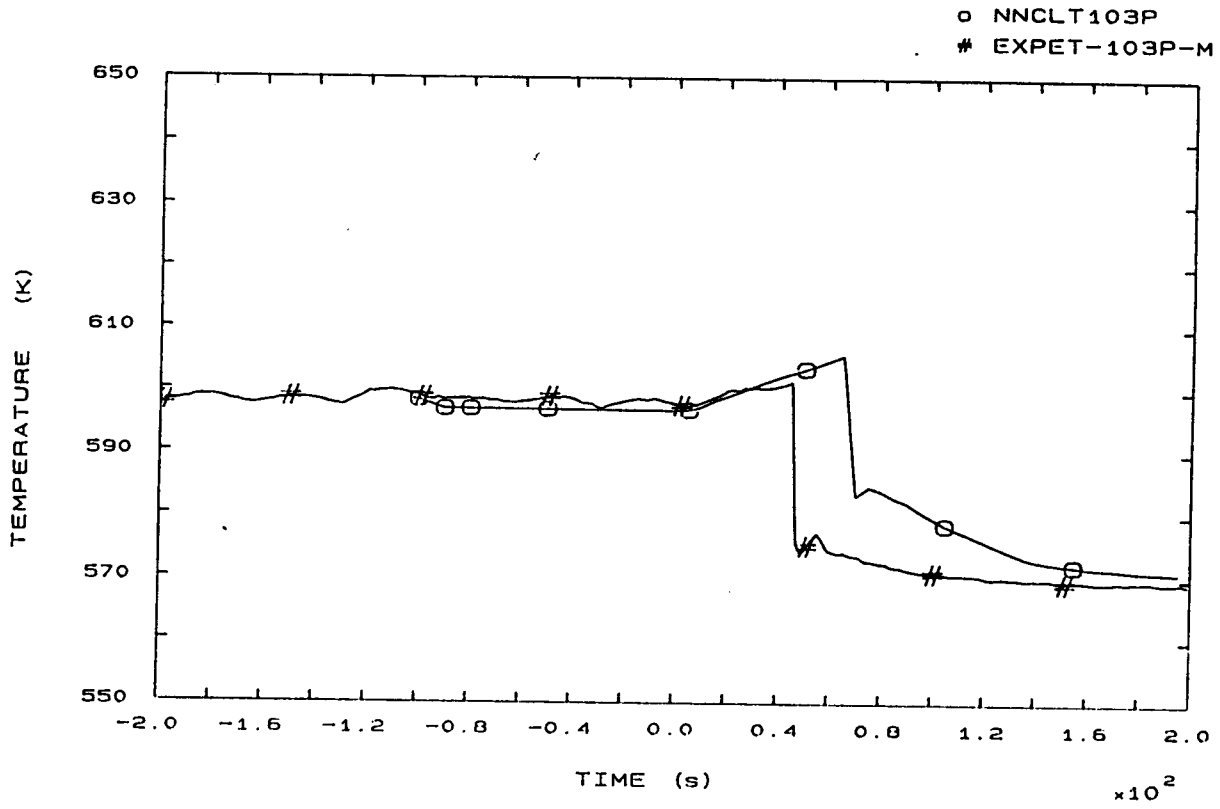

FIG. 12b LP1 HOT LEG OUTLET VESSEL TEMPERATURE

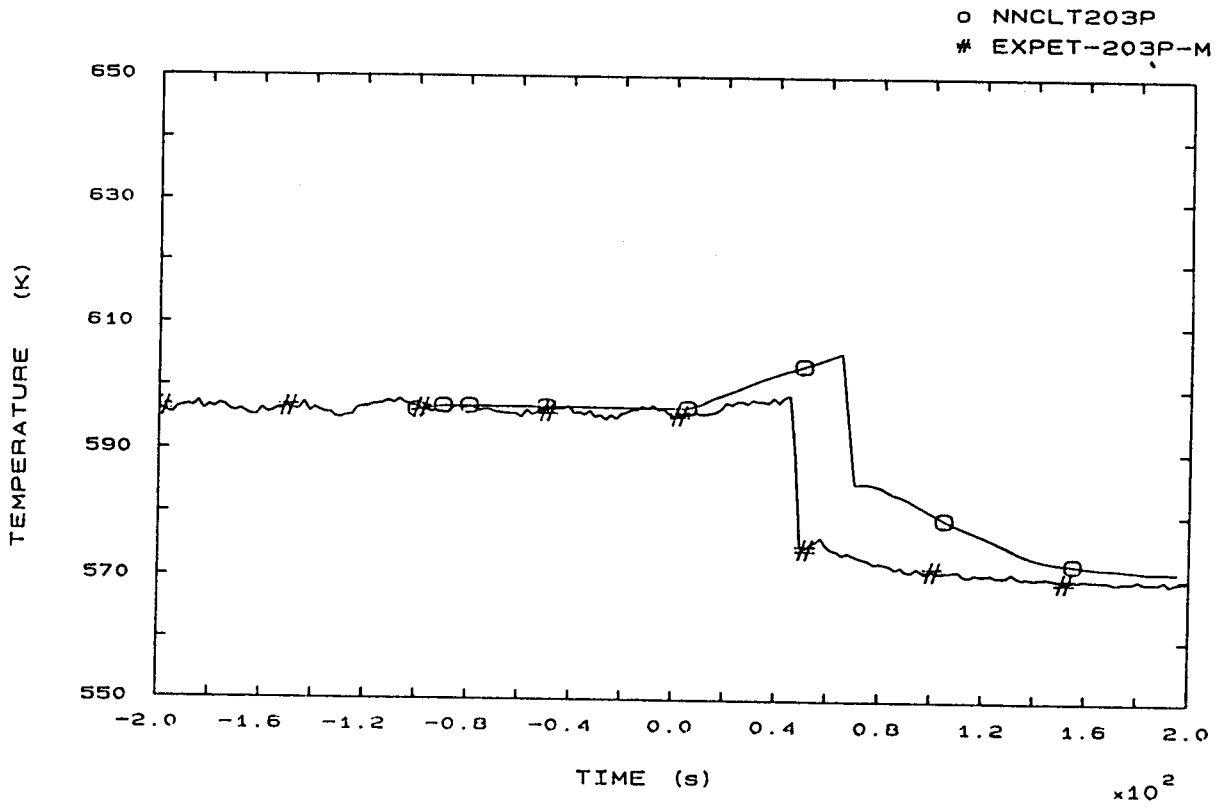

FIG. 22b LP2 HOT LEG OUTLET VESSEL TEMPERATURE

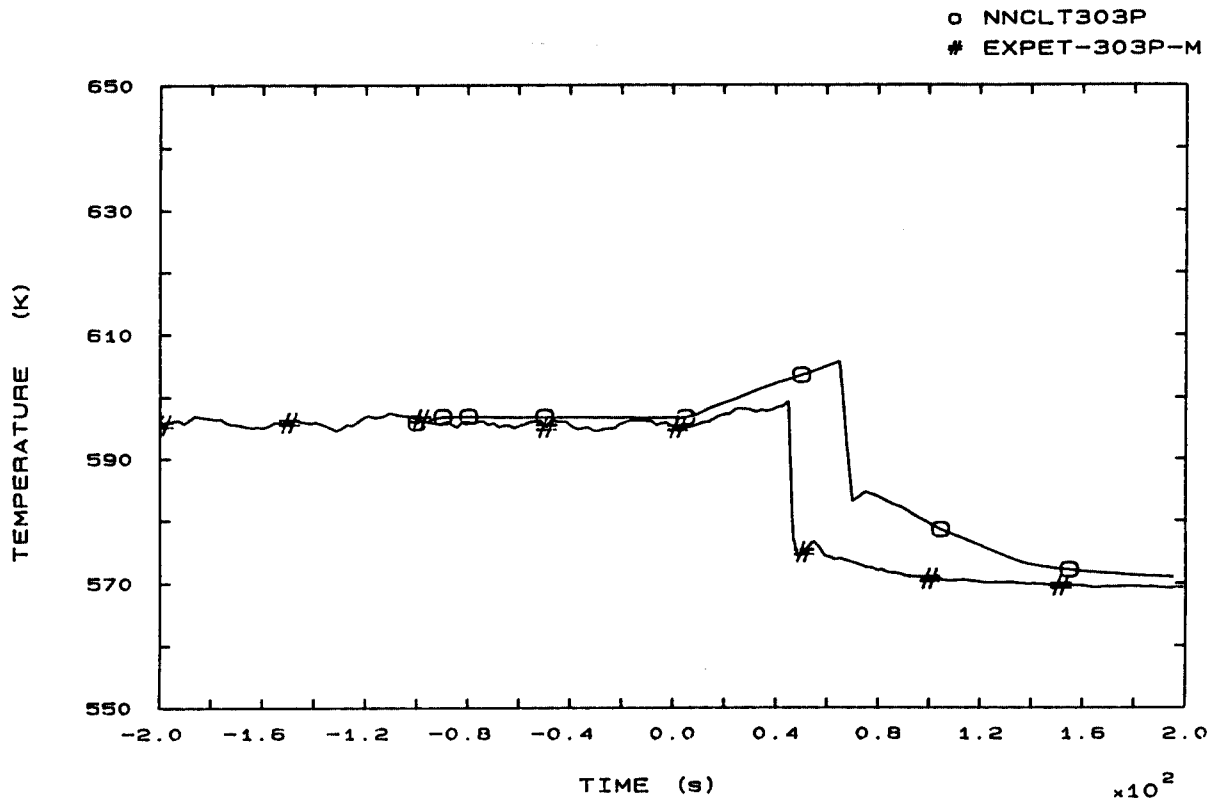

FIG. 32b LP3 HOT LEG OUTLET VESSEL TEMPERATURE

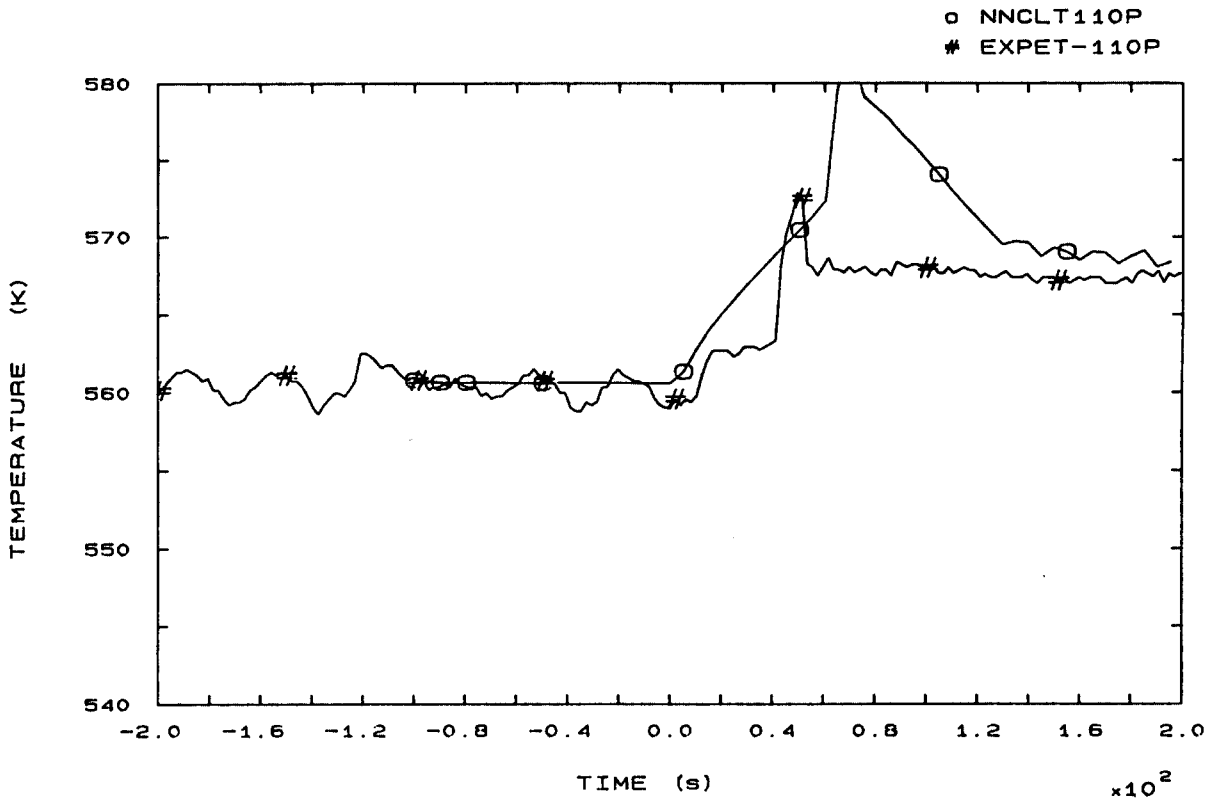

FIG. 42b SG1 OUTLET TEMPERATURE

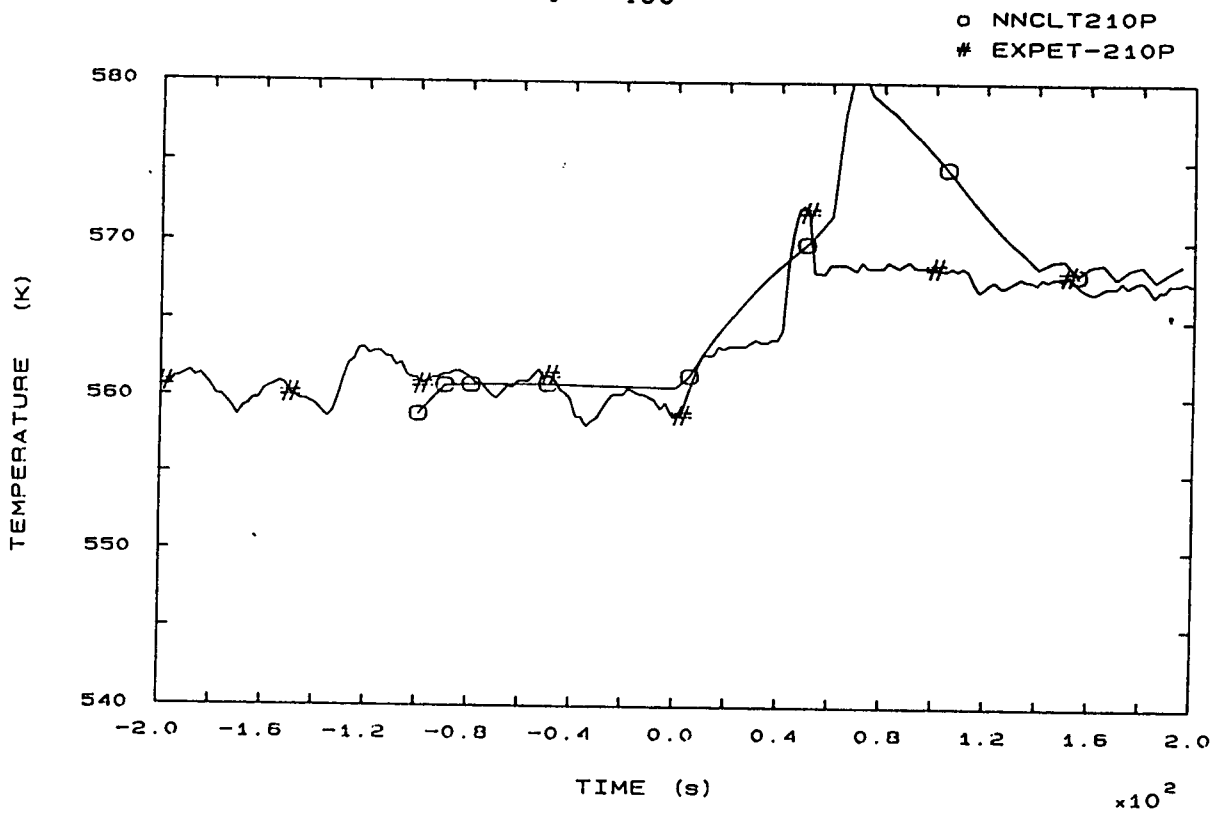

FIG. 44b SG2 OUTLET TEMPERATURE

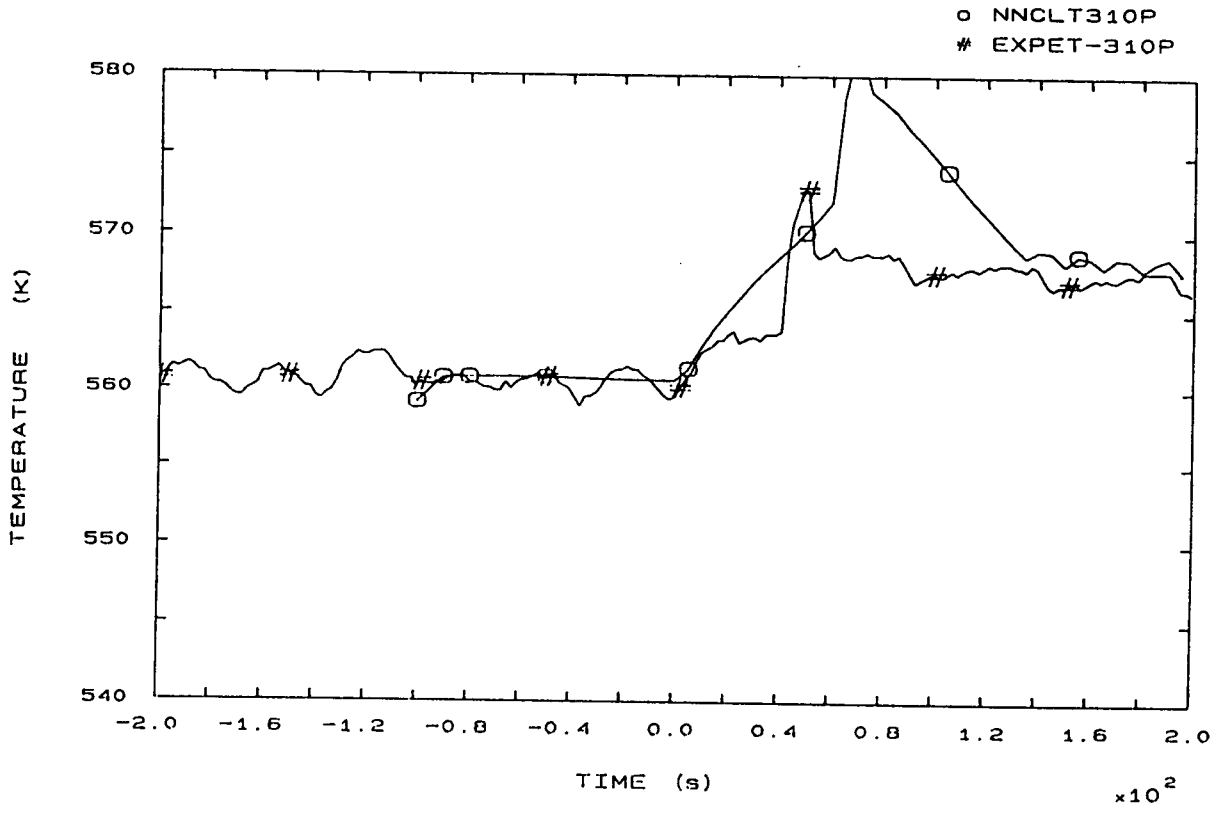

FIG. 46b SG3 OUTLET TEMPERATURE

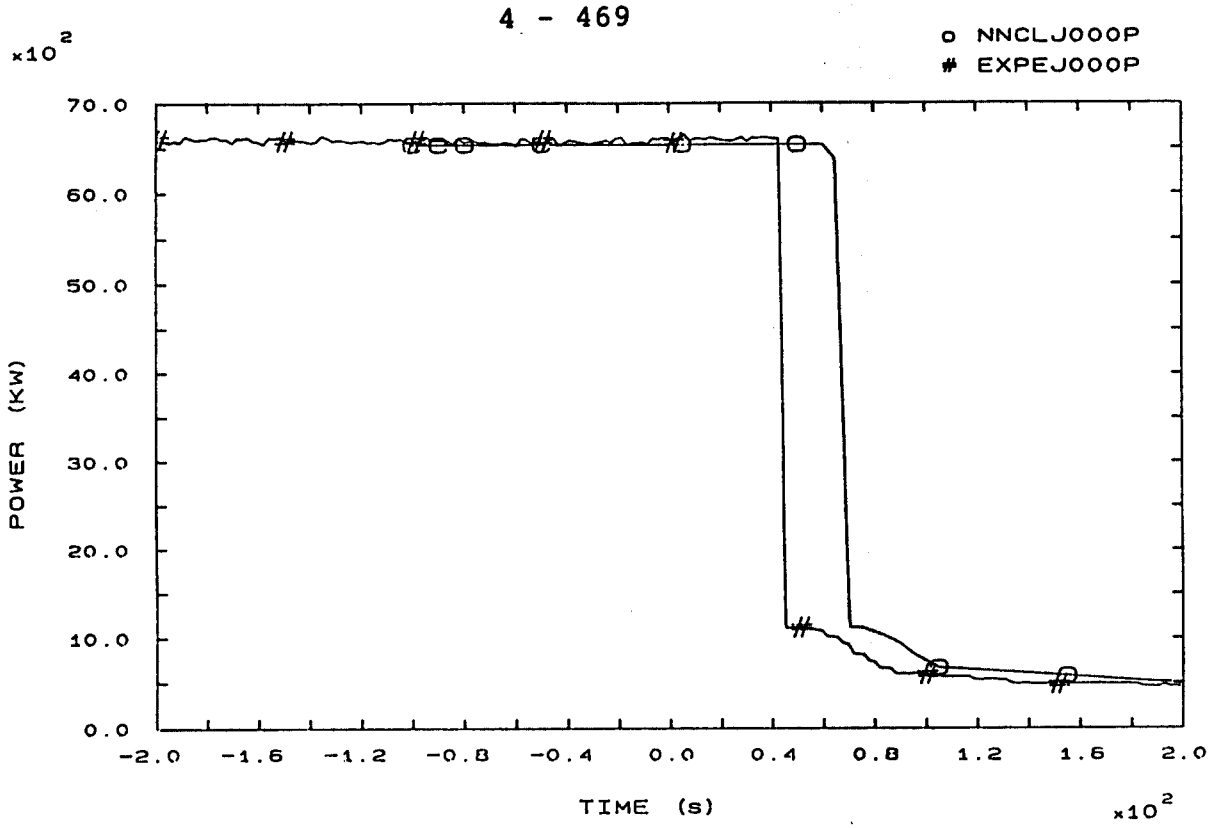

FIG. 81b HEATER RODS POWER

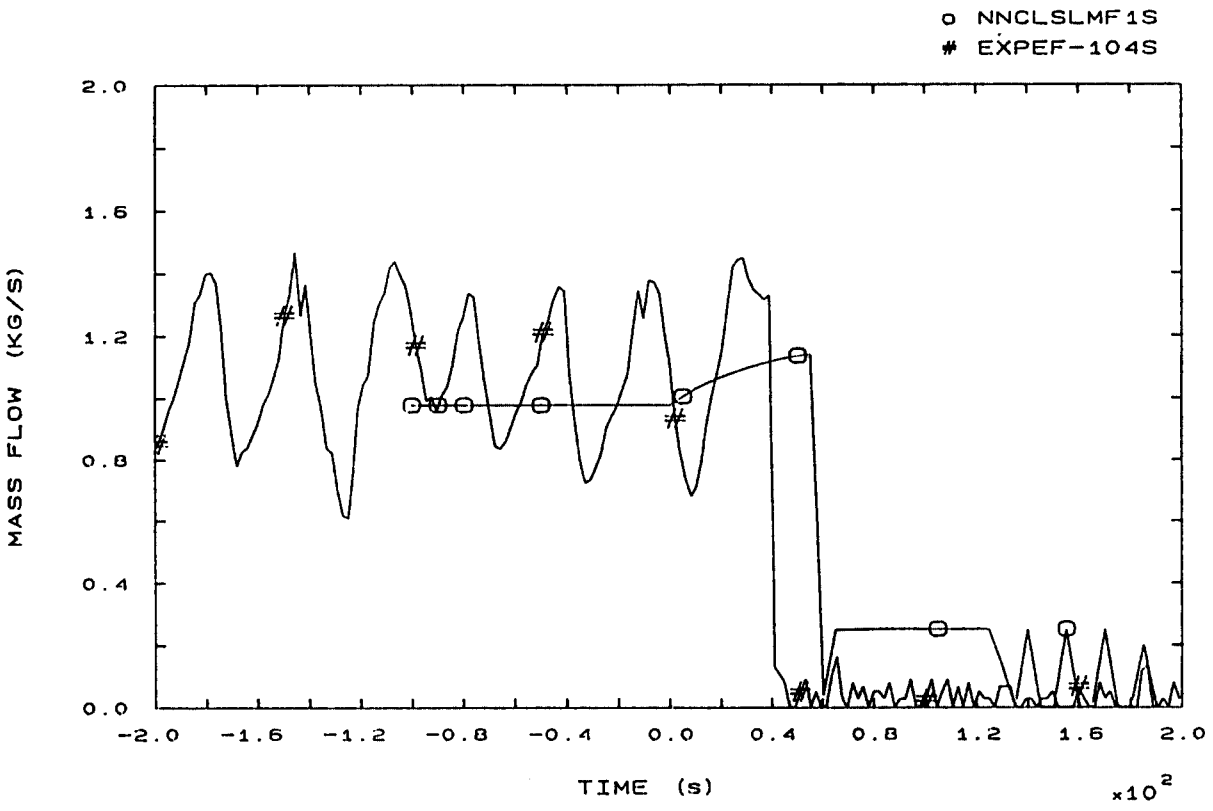

FIG. 96b STEAM LINE 1 MASS FLOW

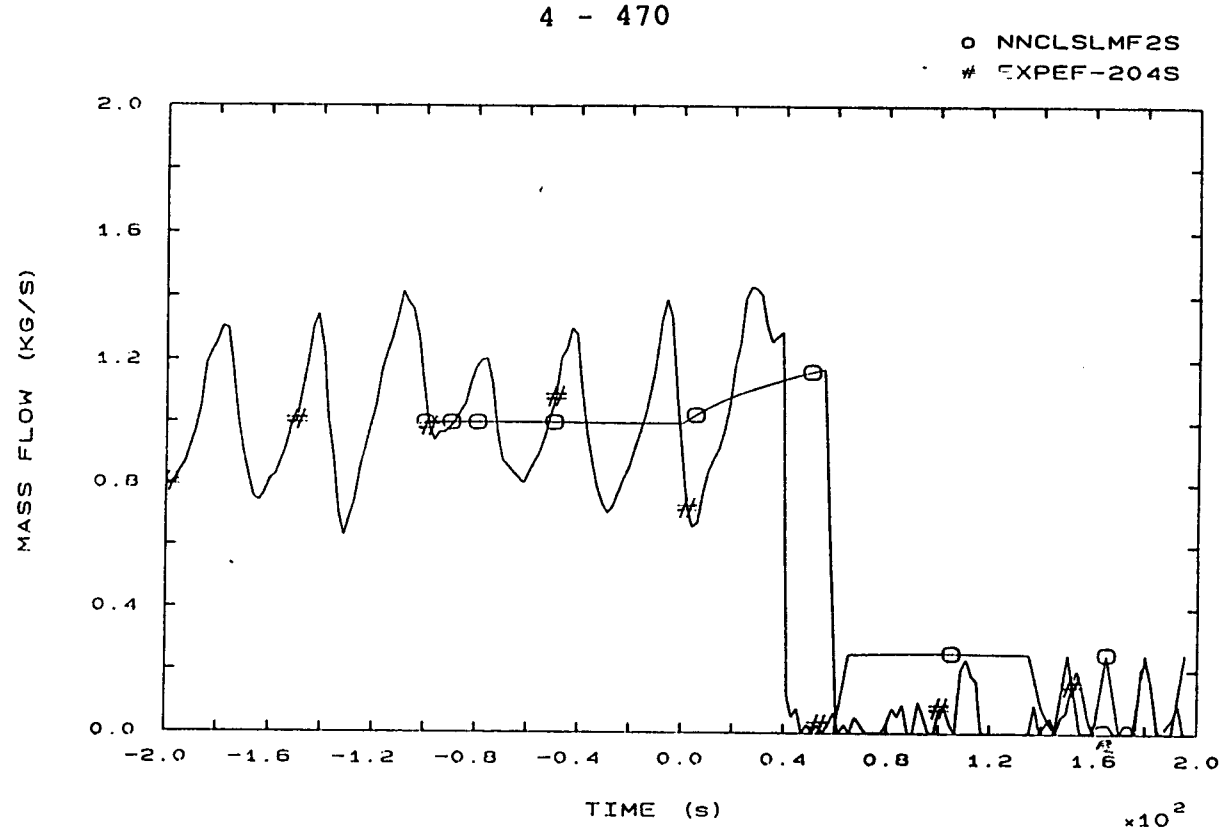

FIG. 97b STEAM LINE 2 MASS FLOW

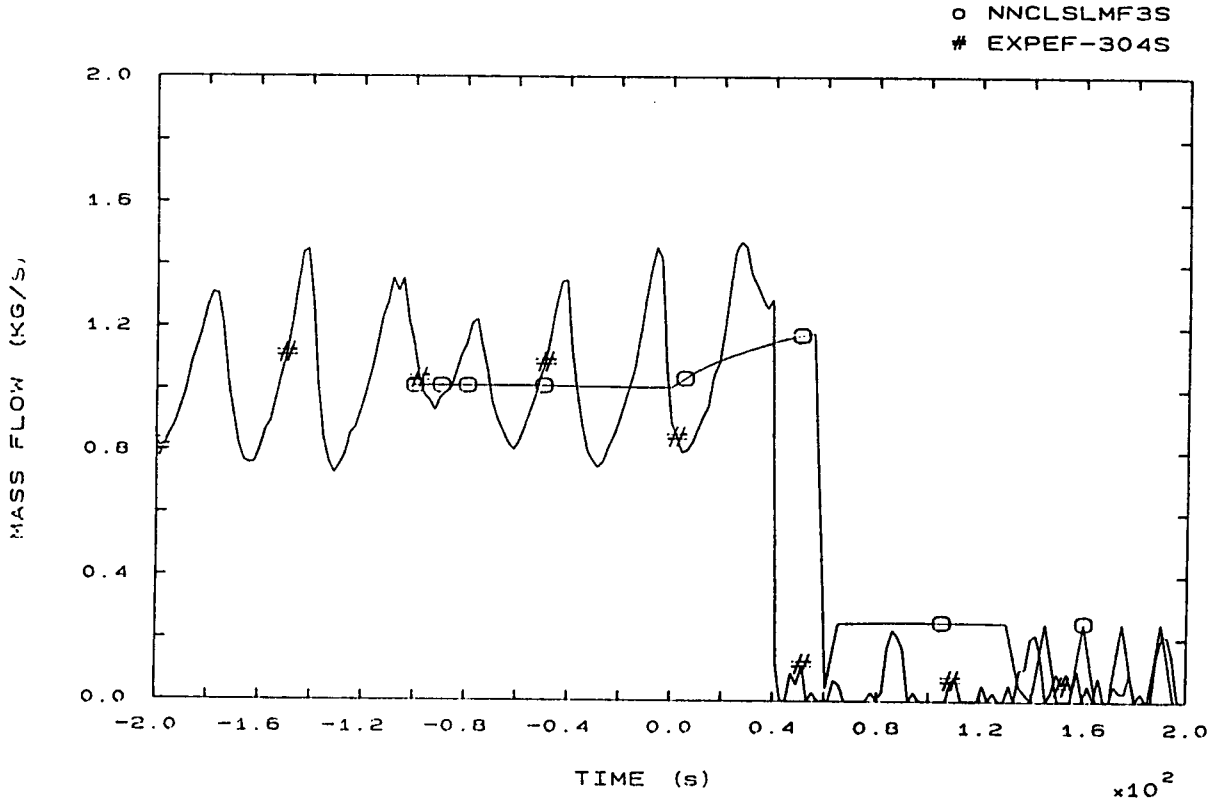

FIG. 98b STEAM LINE 3 MASS FLOW

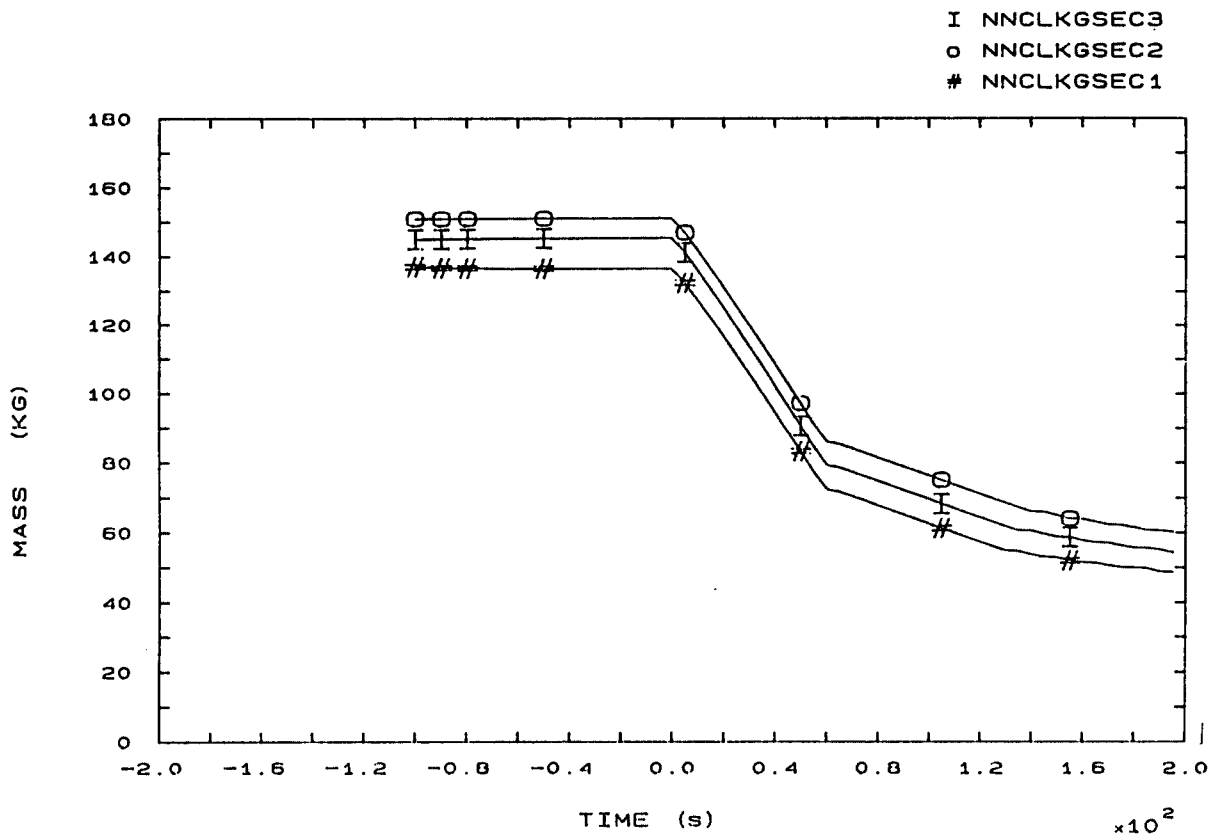

FIG. 142b SECONDARY COOLANT TOTAL MASS IN SGs

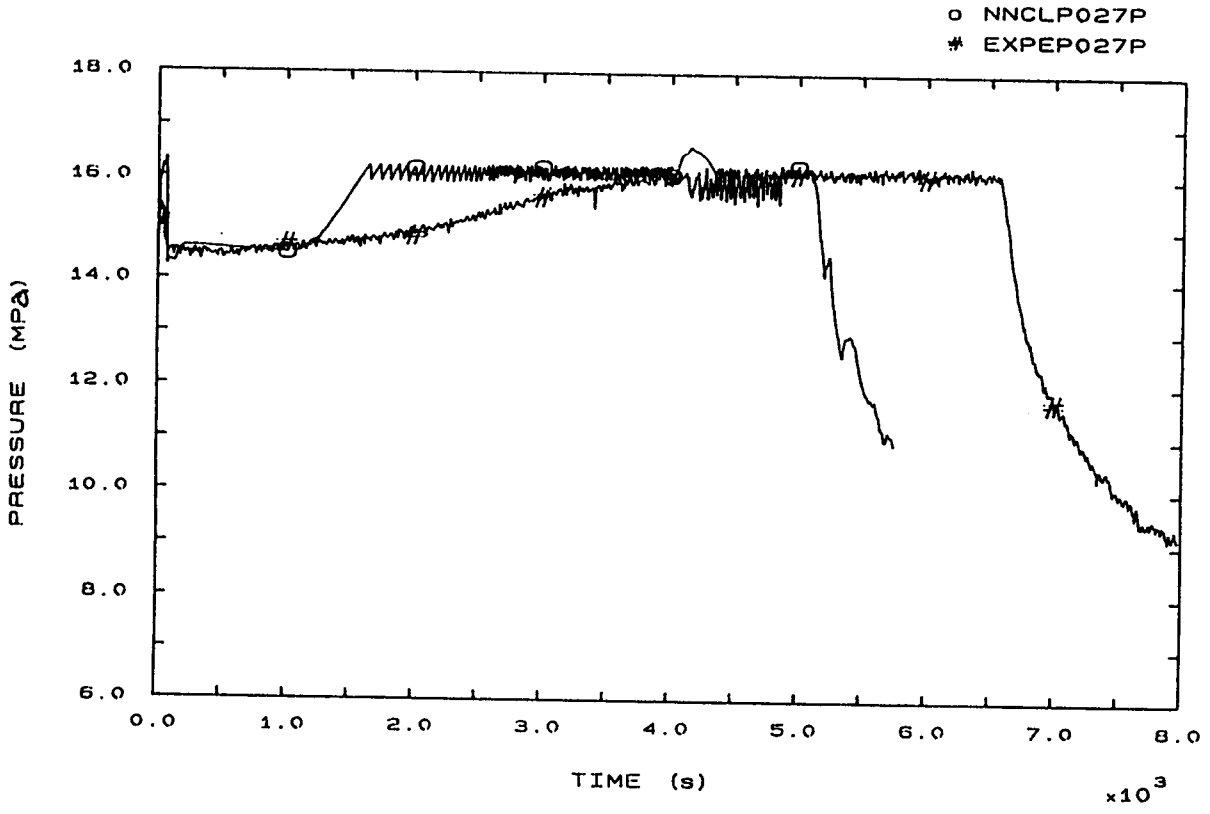

FIG. 1 PRESSURIZER PRESSURE

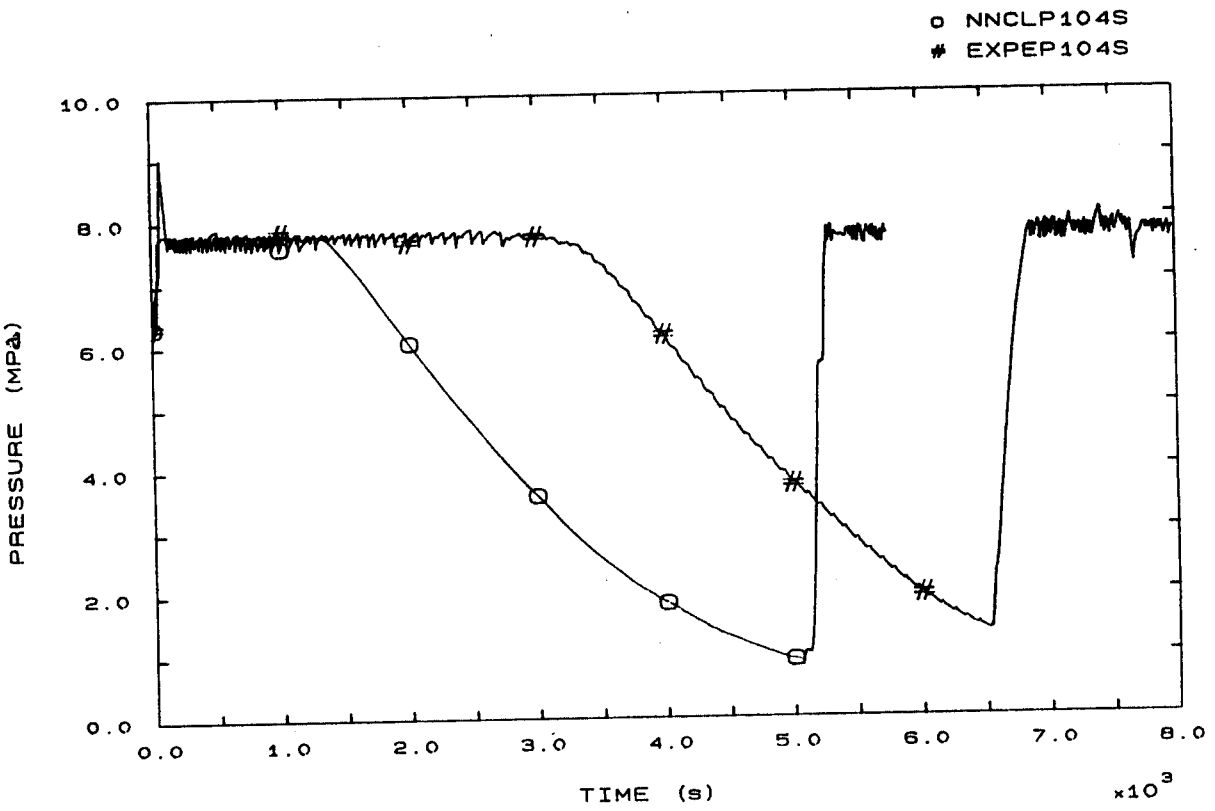

FIG. 3 SG1 STEAM DOME PRESSURE

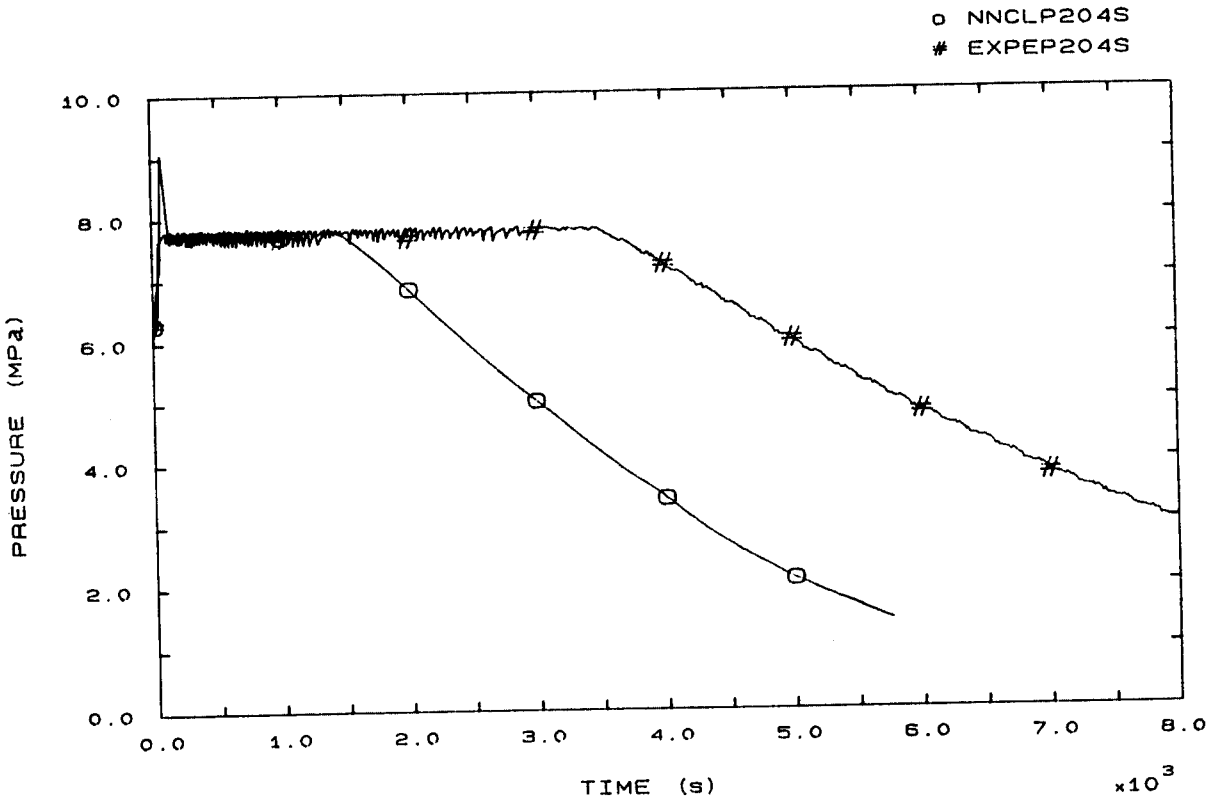

FIG. 4 SG2 STEAM DOME PRESSURE

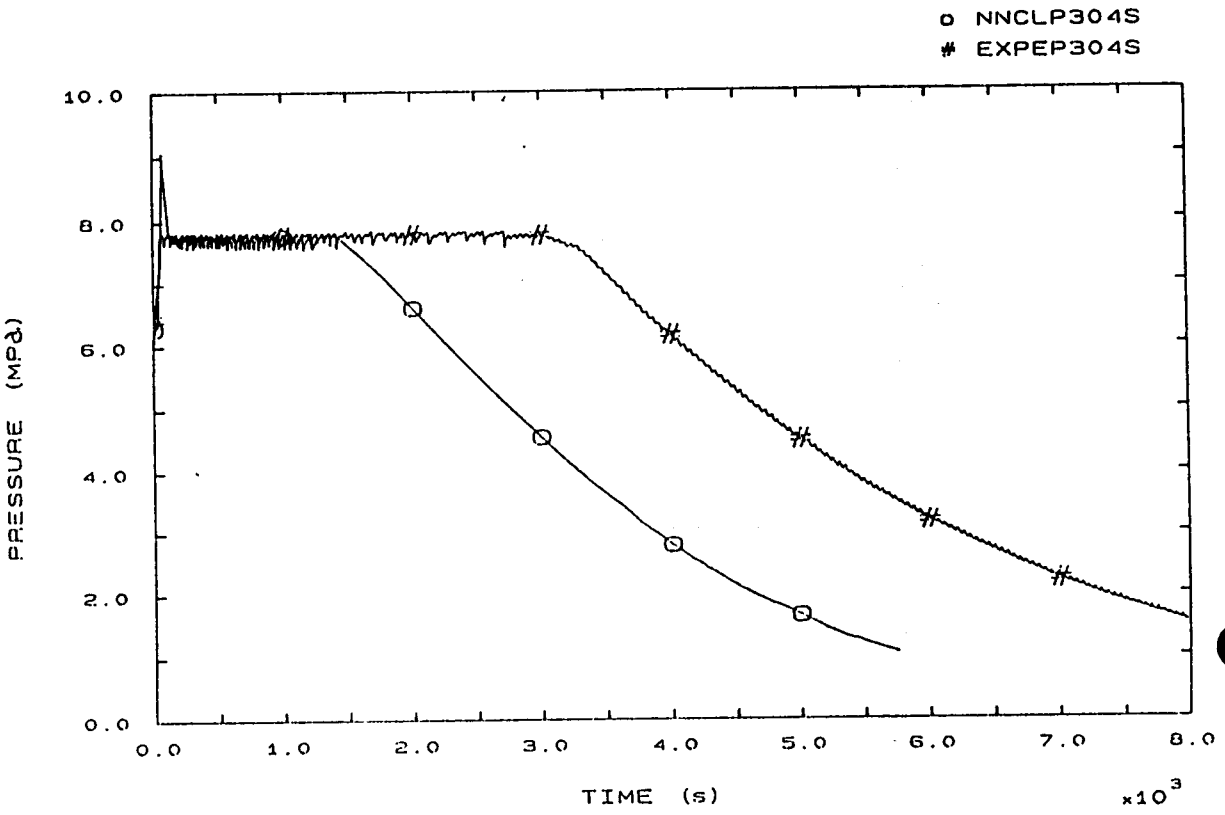

FIG. 5 SG3 STEAM DOME PRESSURE

FIG 6 PRESSURISER LEVEL

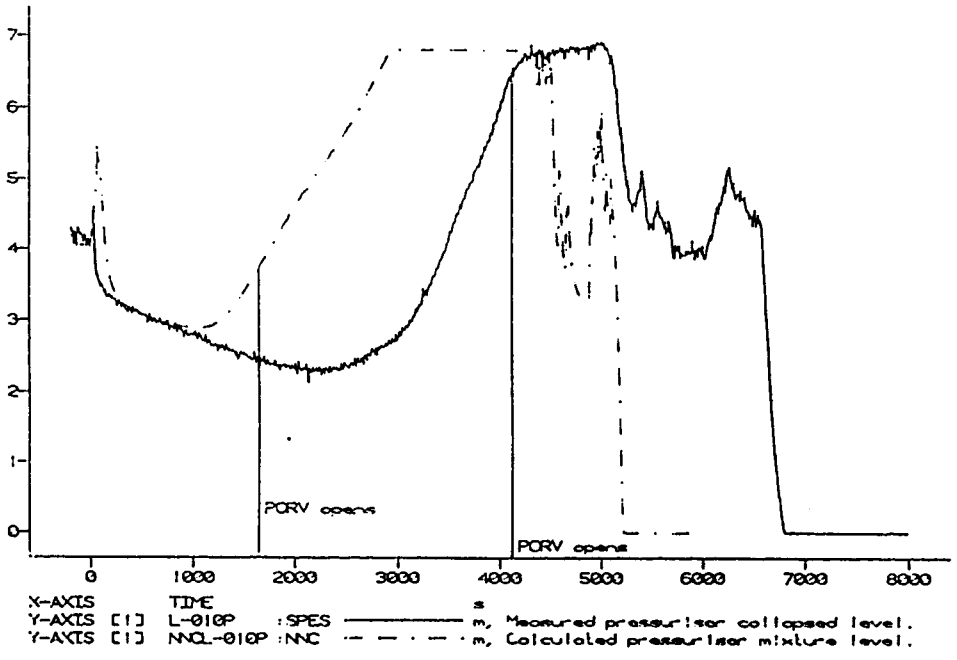

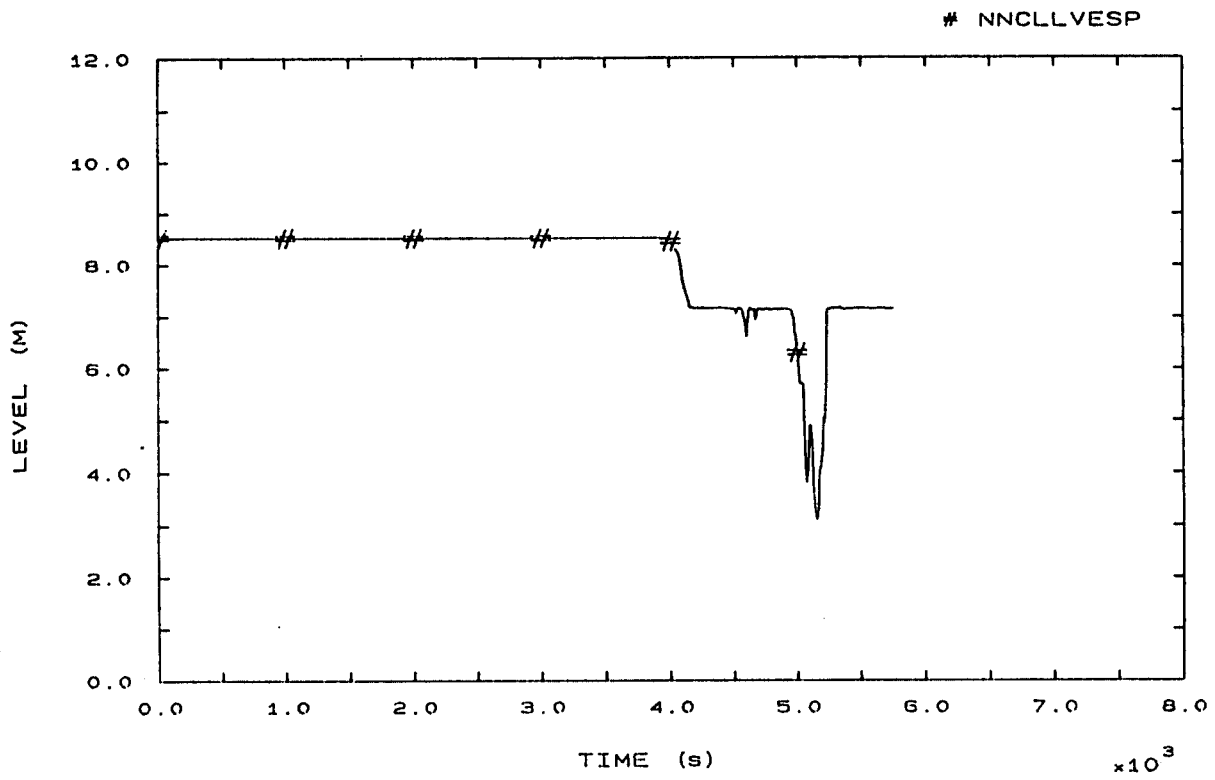

FIG. 10 VESSEL LEVEL

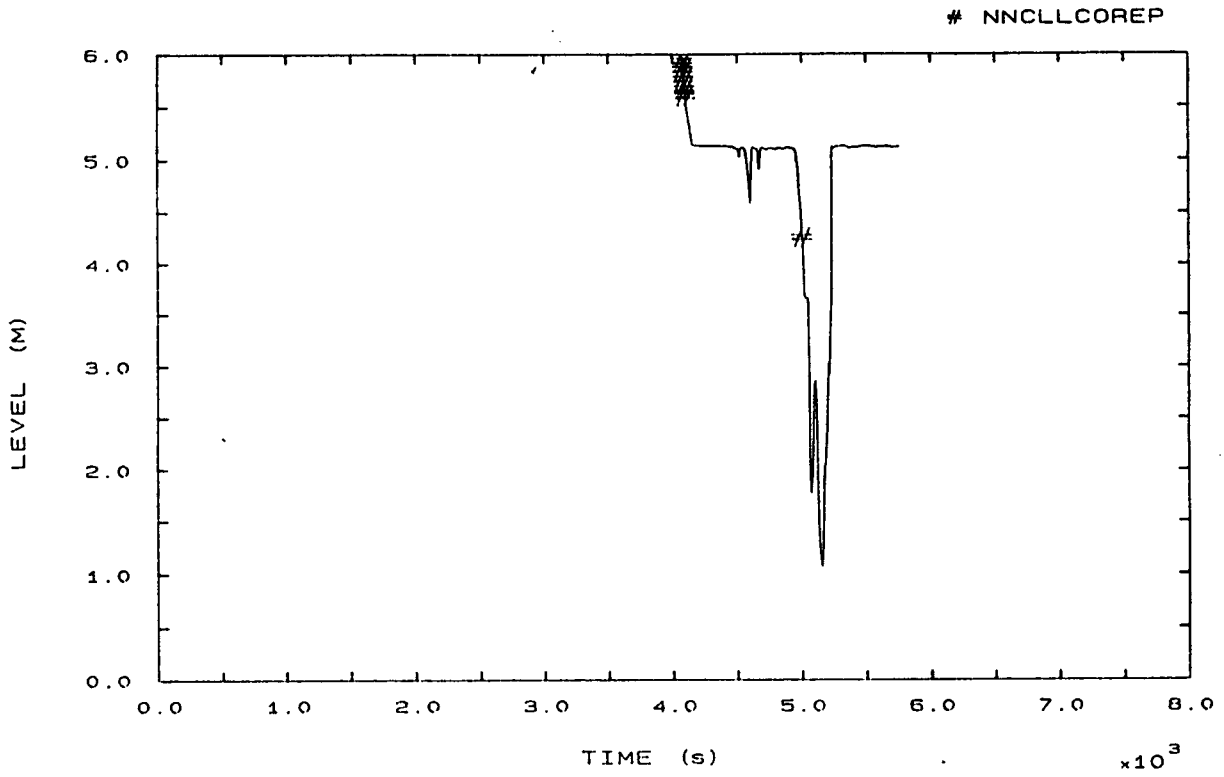

FIG. 11 CORE LEVEL

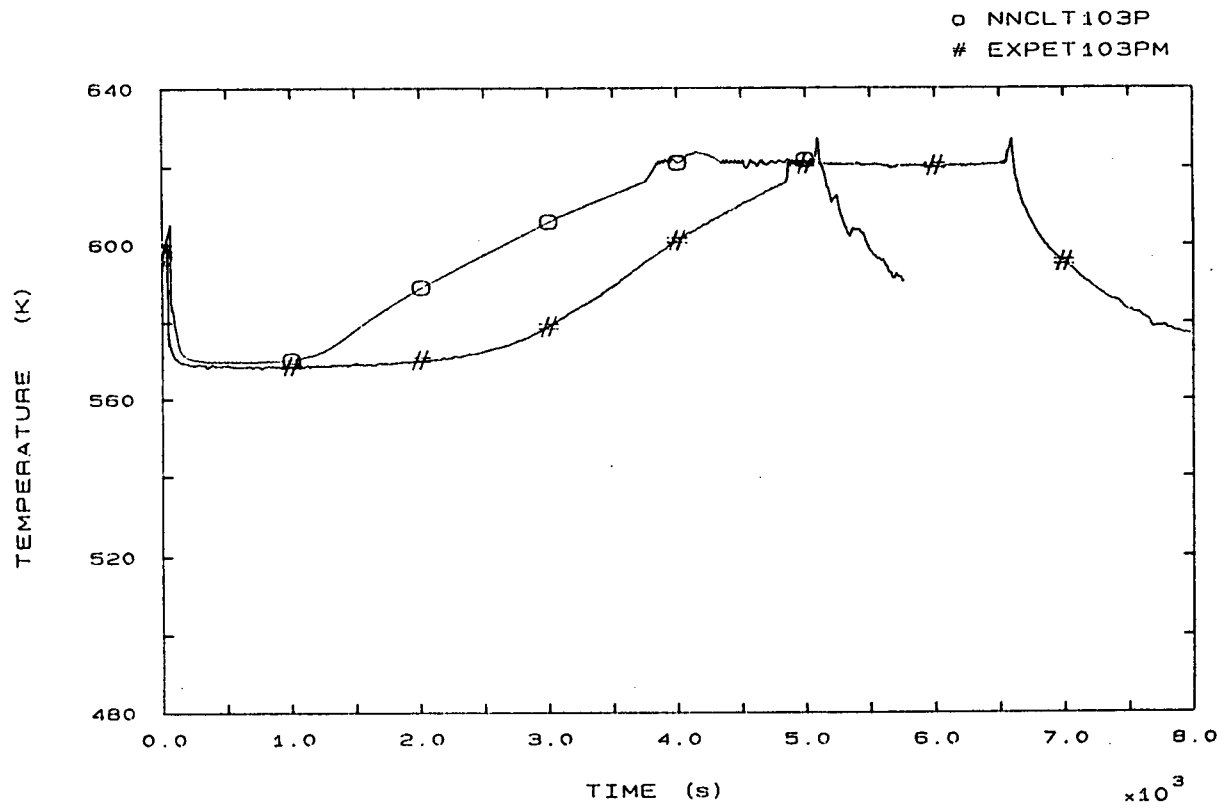

FIG. 12 LP1 HOT LEG OUTLET VESSEL TEMPERATURE

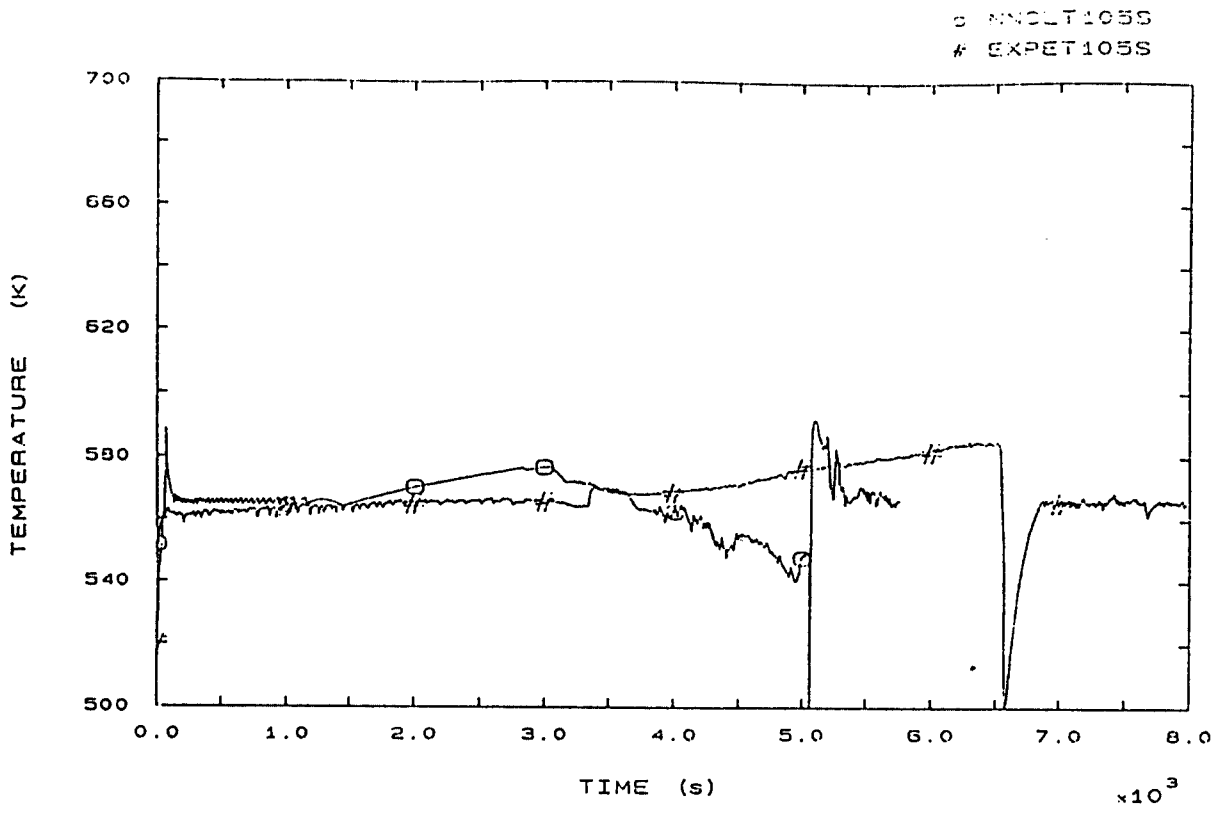

FIG. 15 FLUID TEMPERATURE SG1 RISER 185 MM A.T.S.

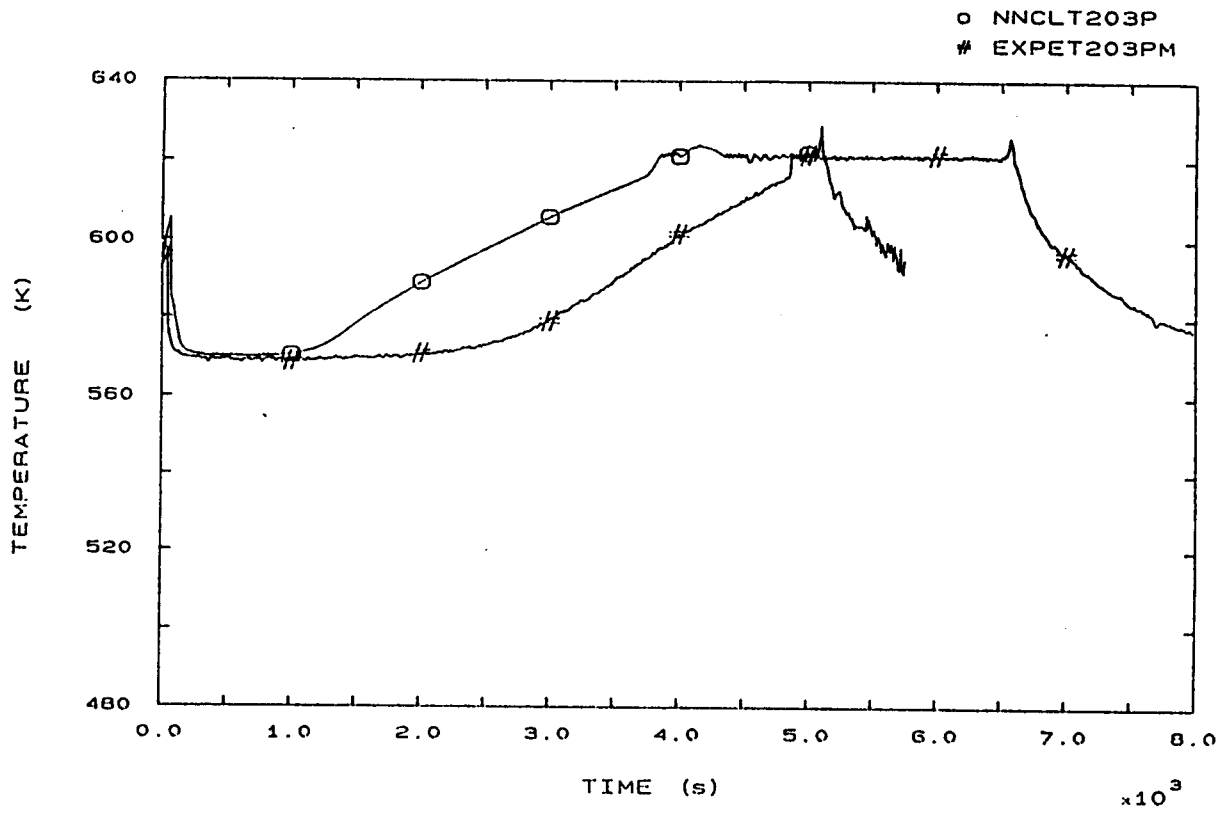

FIG. 22 LP2 HOT LEG OUTLET VESSEL TEMPERATURE

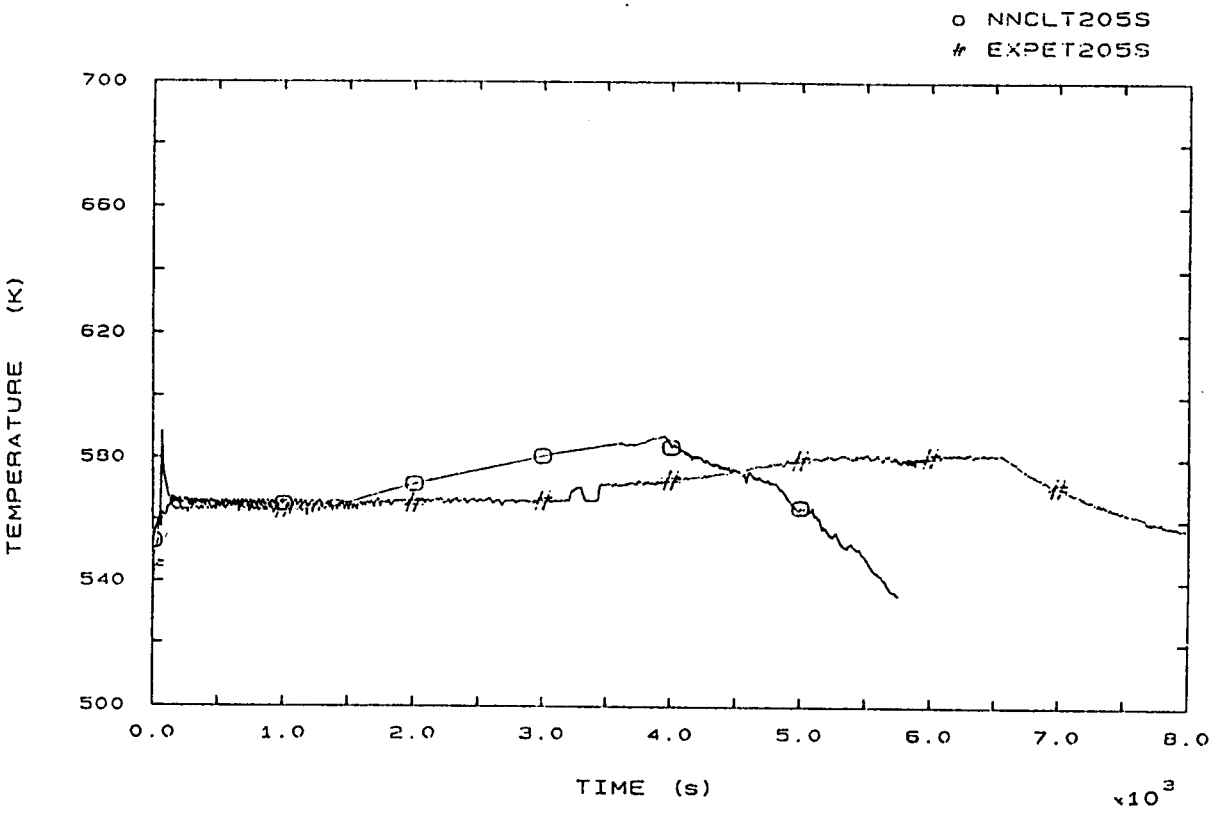

FIG. 25 FLUID TEMPERATURE SG2 RISER 185 MM A.T.S.

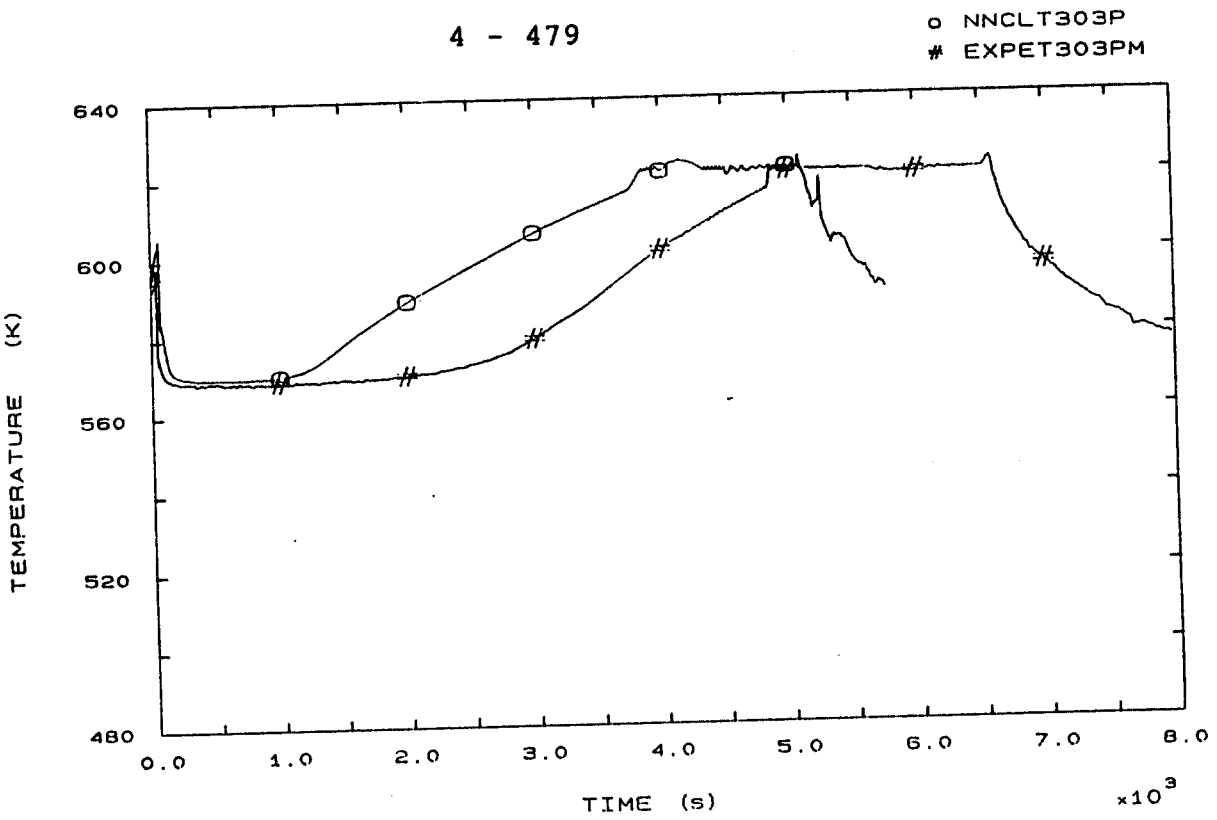

FIG. 32 LP3 HOT LEG OUTLET VESSEL TEMPERATURE

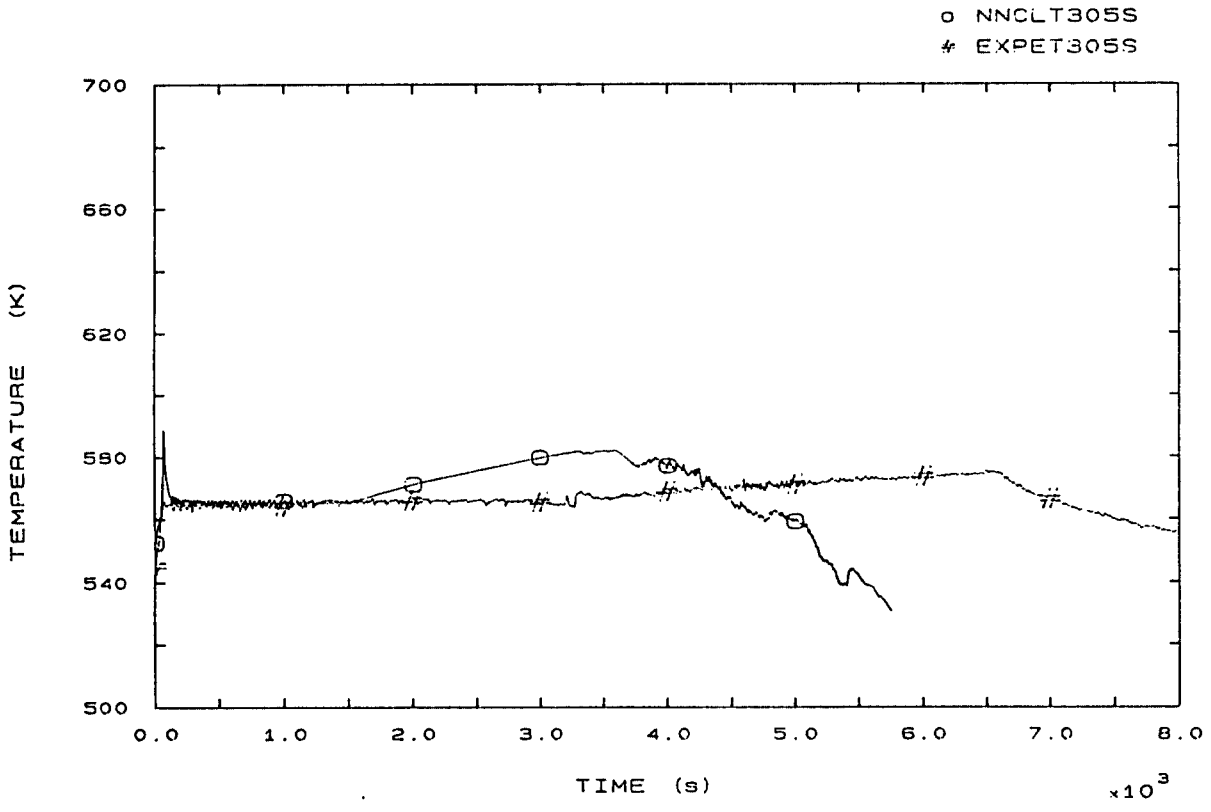

FIG. 35 FLUID TEMPERATURE SG3 RISER 185 MM A.T.S.

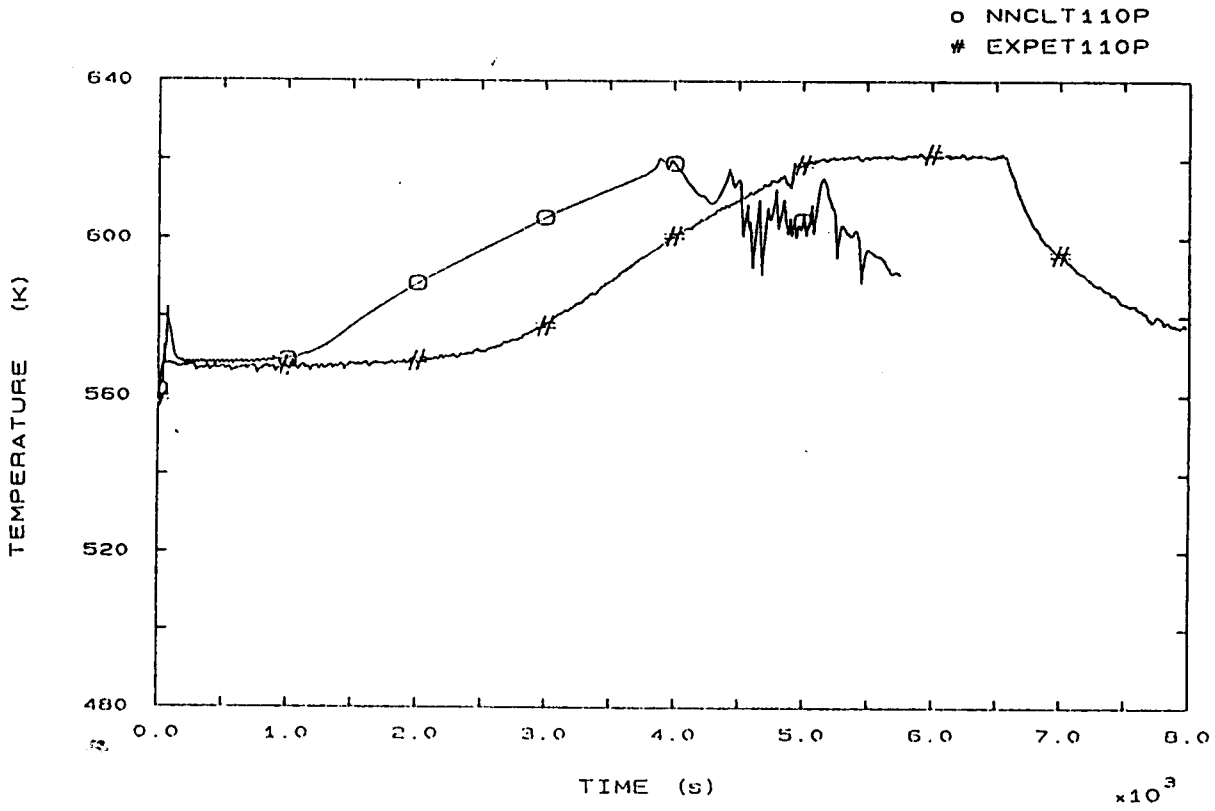

FIG. 42 SG1 OUTLET TEMPERATURE

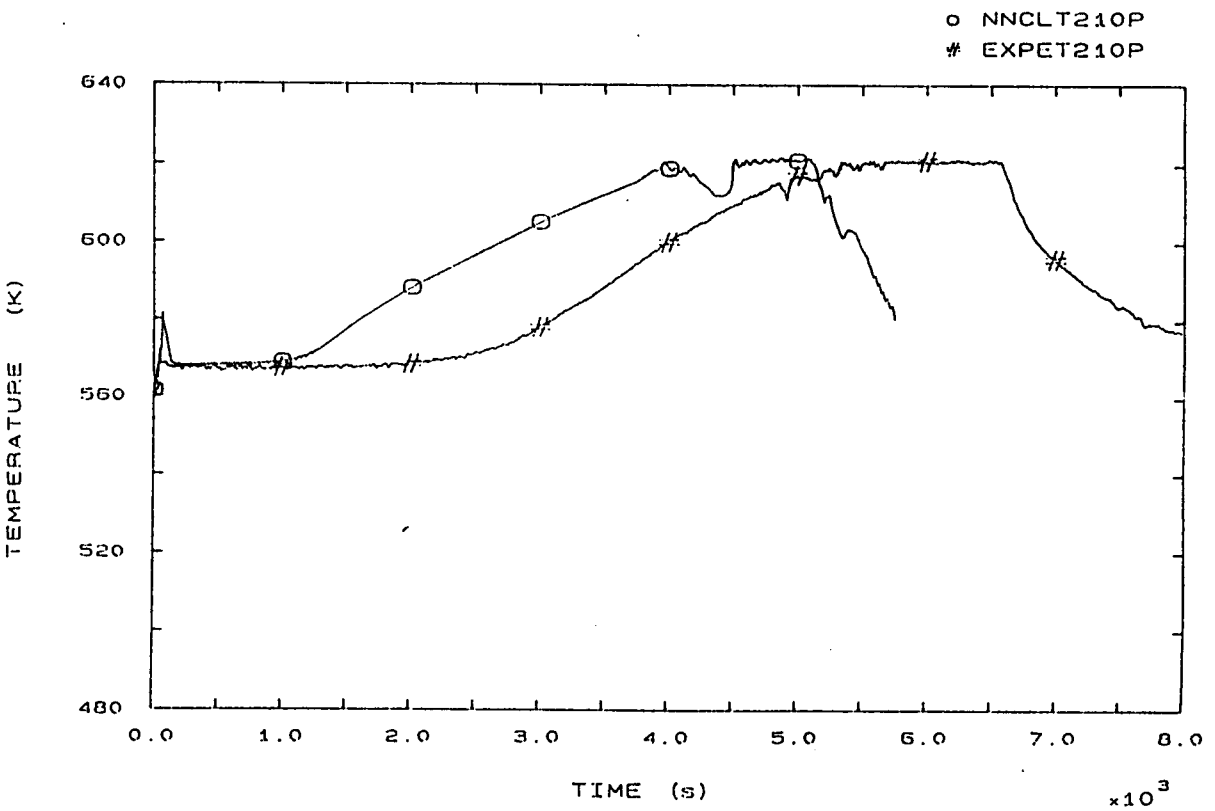

FIG. 44 SG2 OUTLET TEMPERATURE

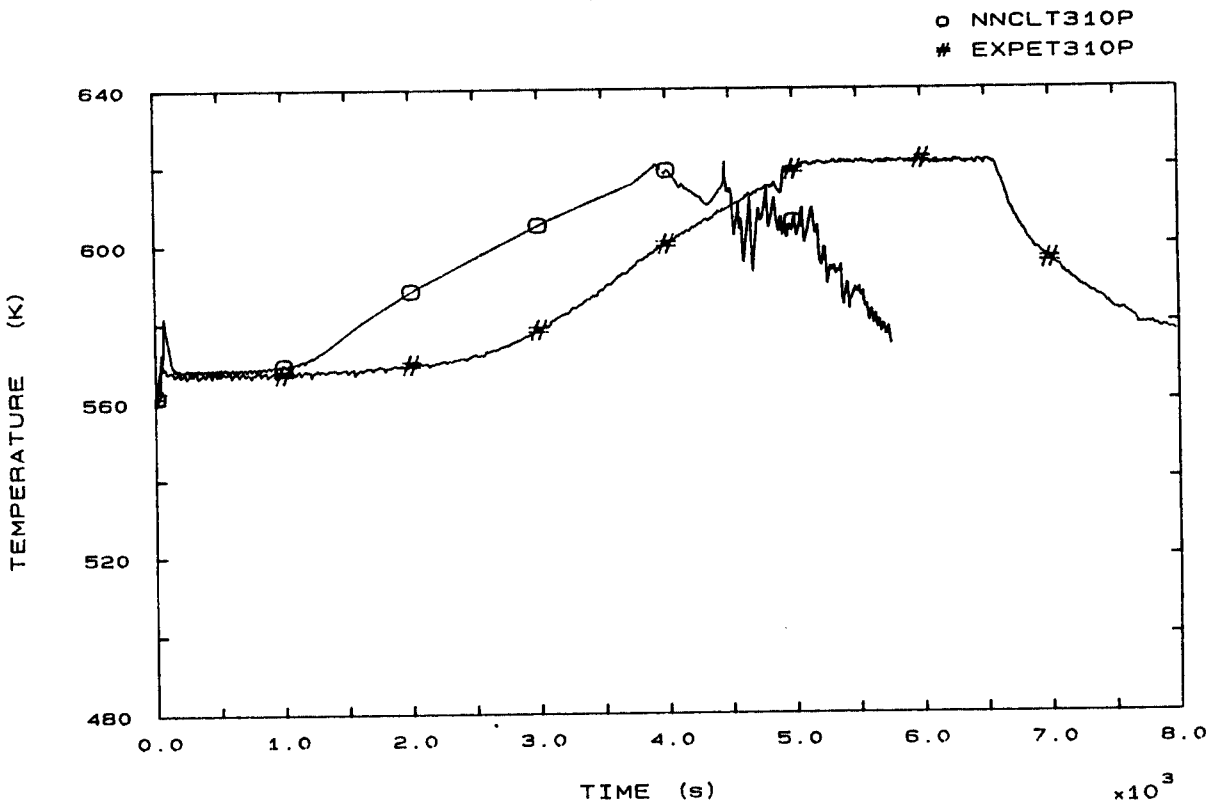

FIG. 46 SG3 OUTLET TEMPERATURE

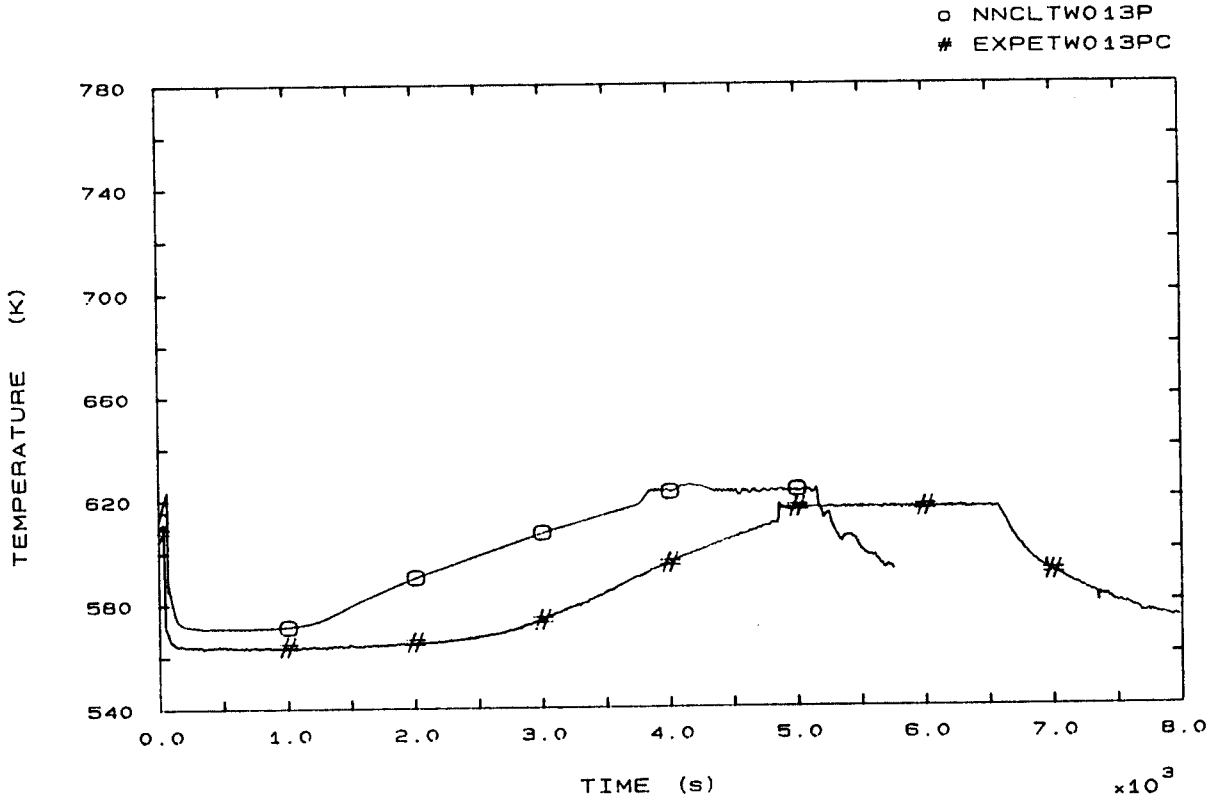

FIG. 49 CORE SURFACE TEMPERATURE AT ROD BUNDLE ELEVATION 1074 MM

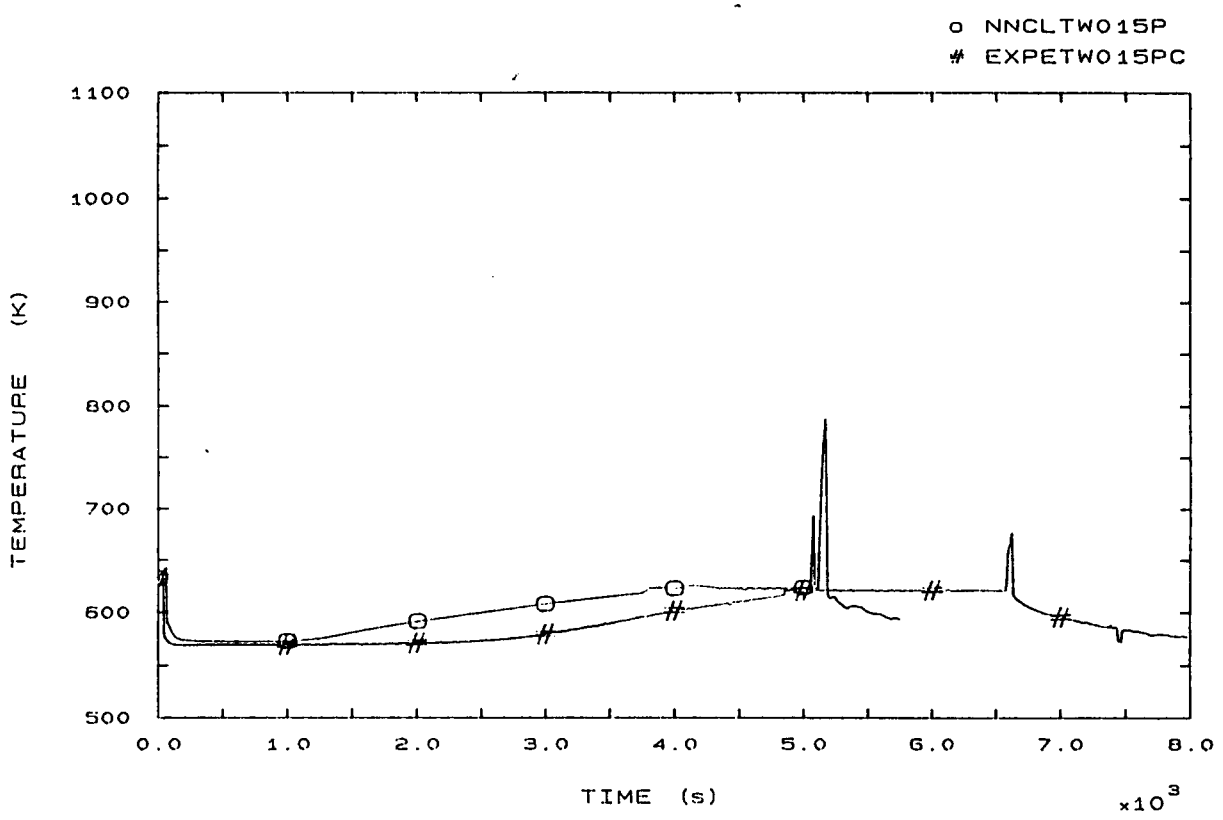

FIG. 50 SURFACE TEMPERATURE AT ROD BUNDLE ELEVATION 2294 MM

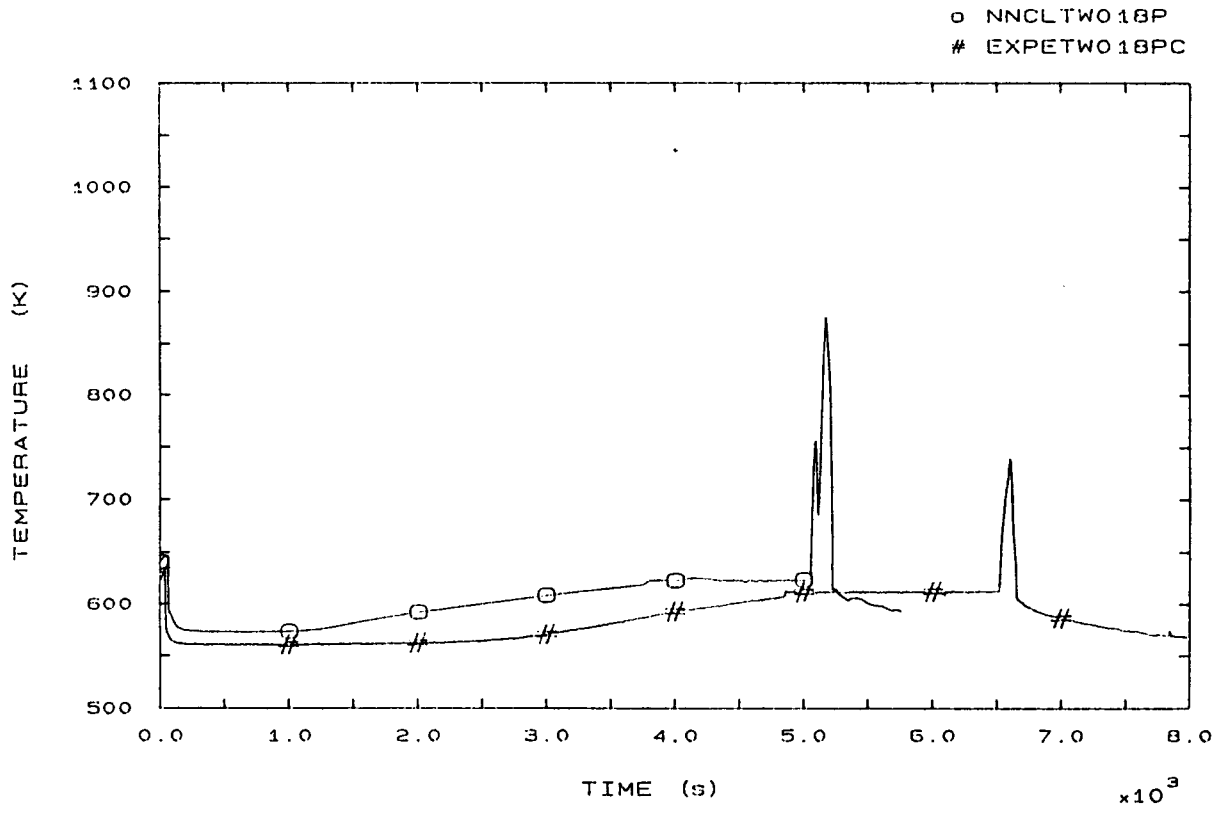

FIG. 51 SURFACE TEMPERATURE AT ROD BUNDLE ELEVATION 3294 MM

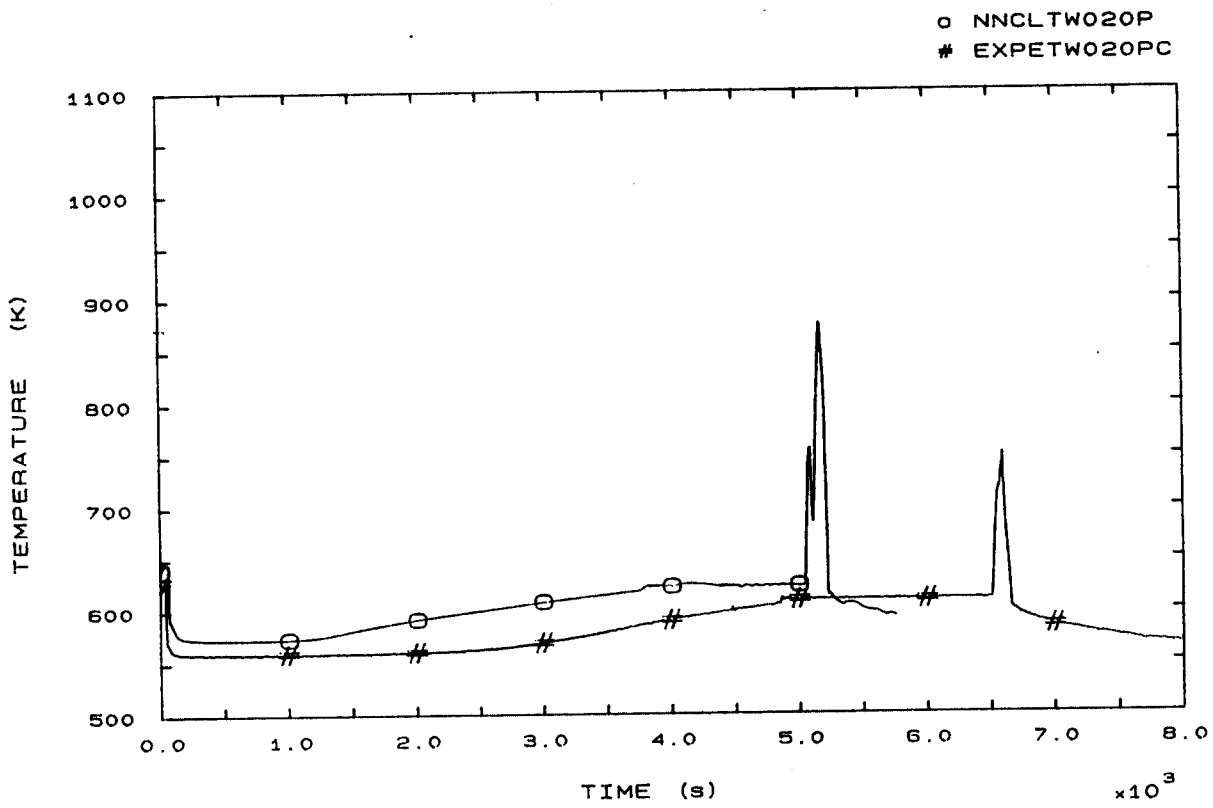

FIG. 52 SURFACE TEMPERATURE AT ROD BUNDLE ELEVATION 3640 MM

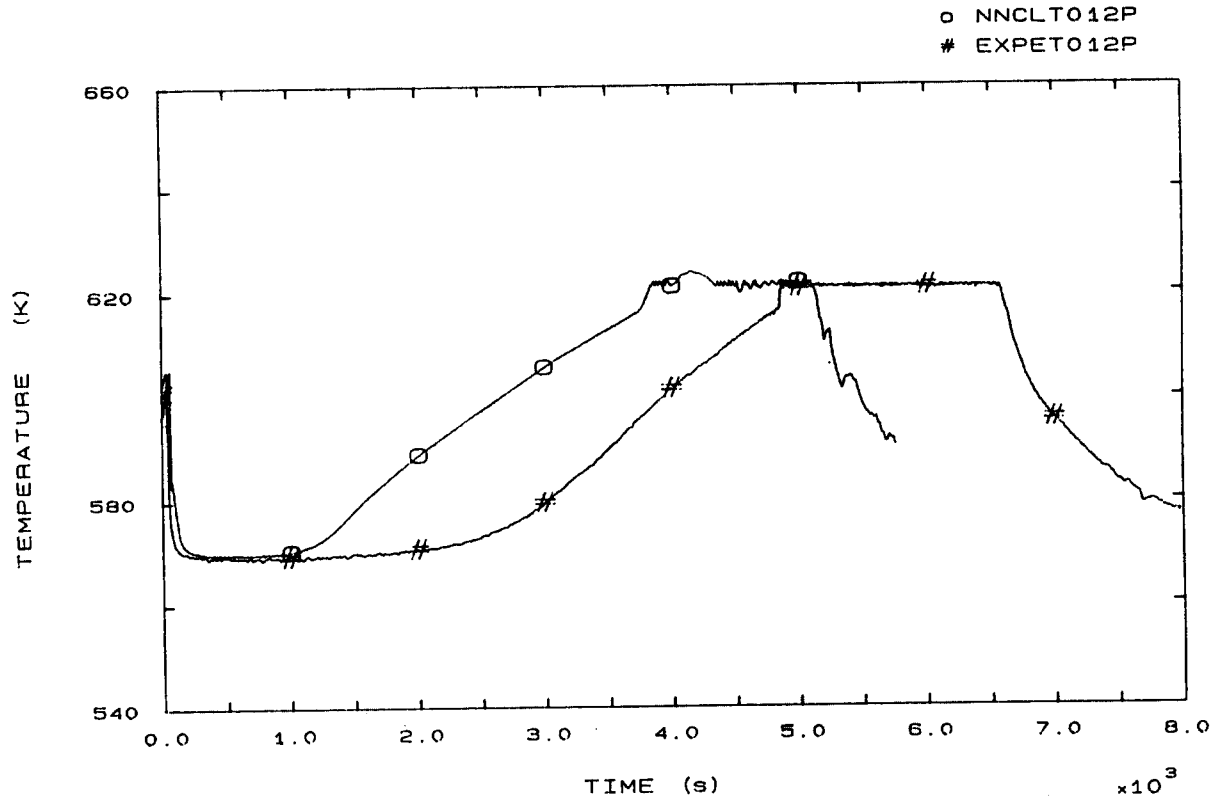

FIG. 53 CORE OUTLET TEMPERATURE

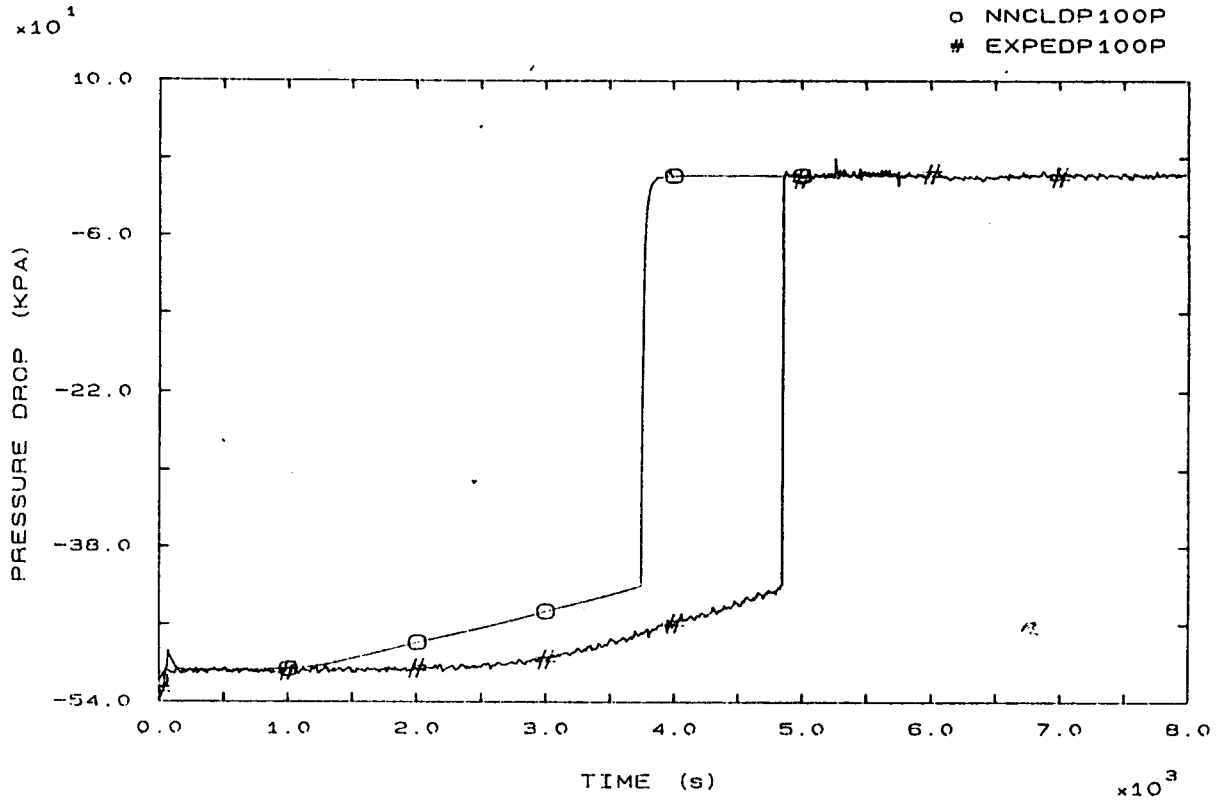

FIG. 54 PRIMARY PUMP 1 PRESSURE DROP

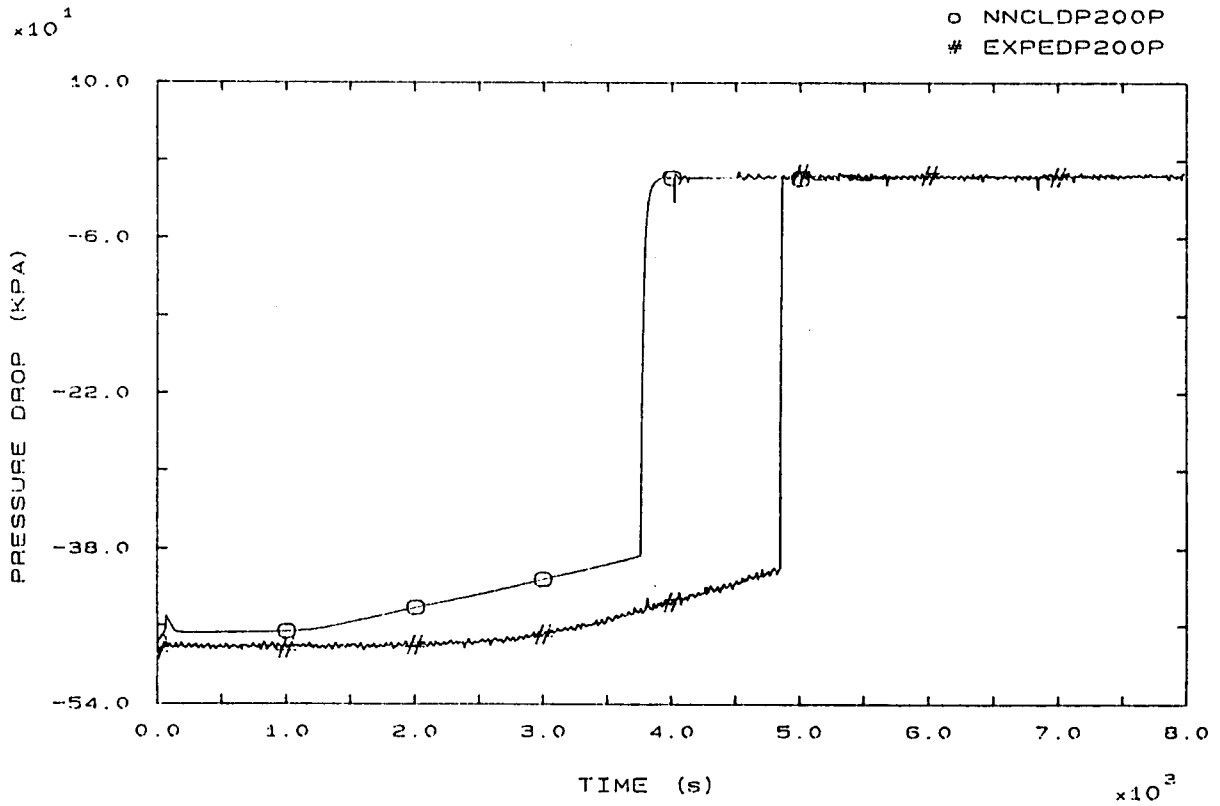

FIG. 55 PRIMARY PUMP 2 PRESSURE DROP

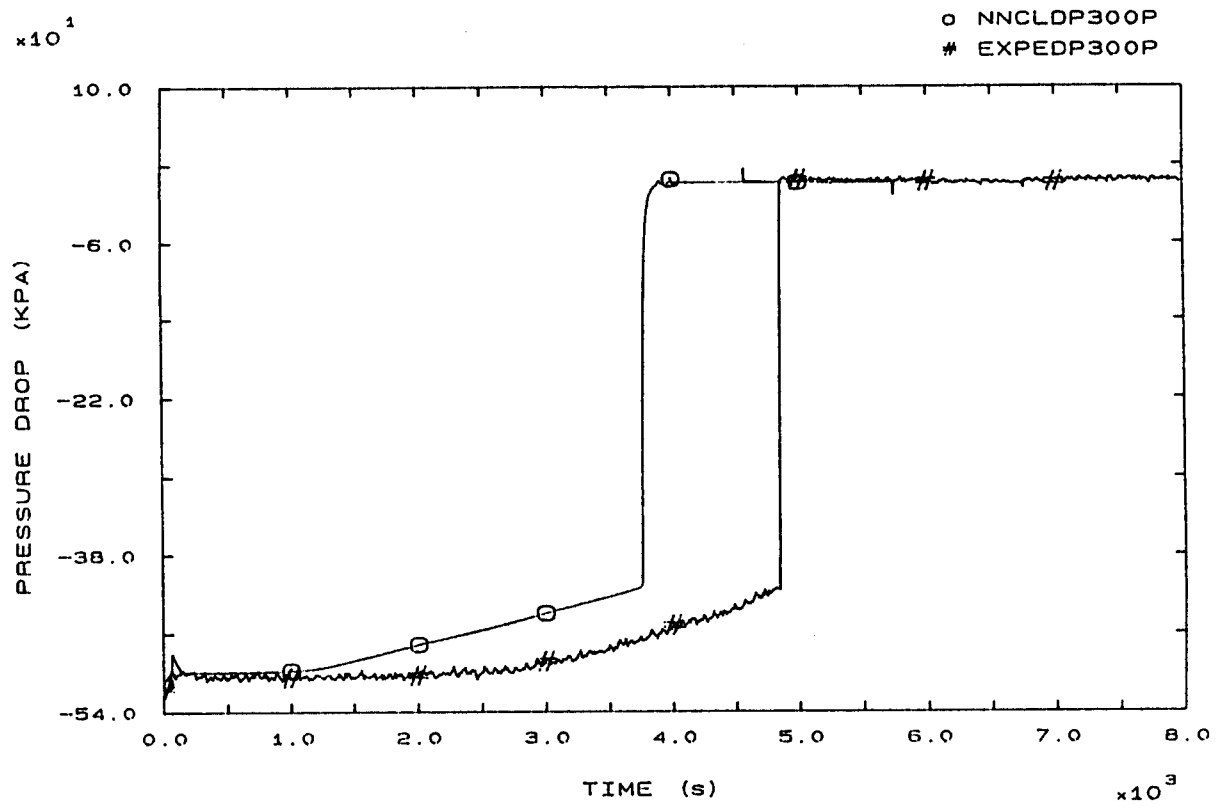

FIG. 56 PRIMARY PUMP 3 PRESSURE DROP

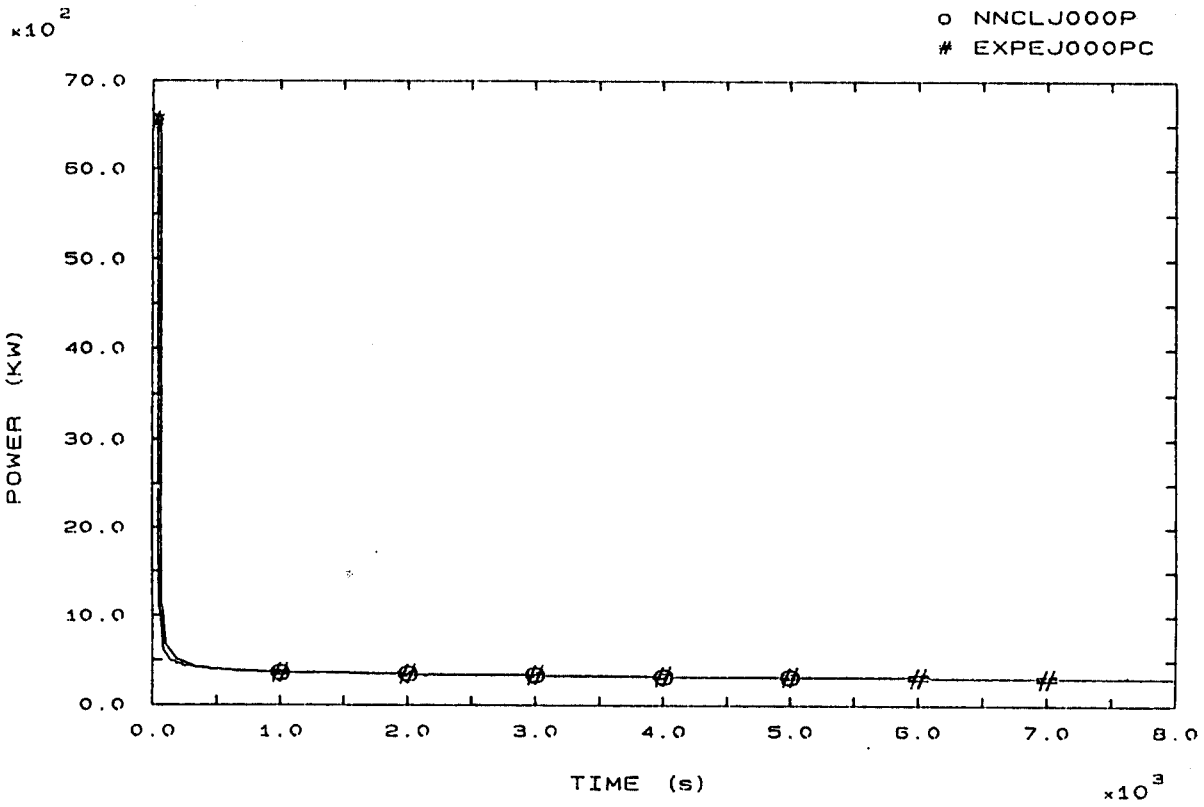

FIG. 81 HEATER RODS POWER

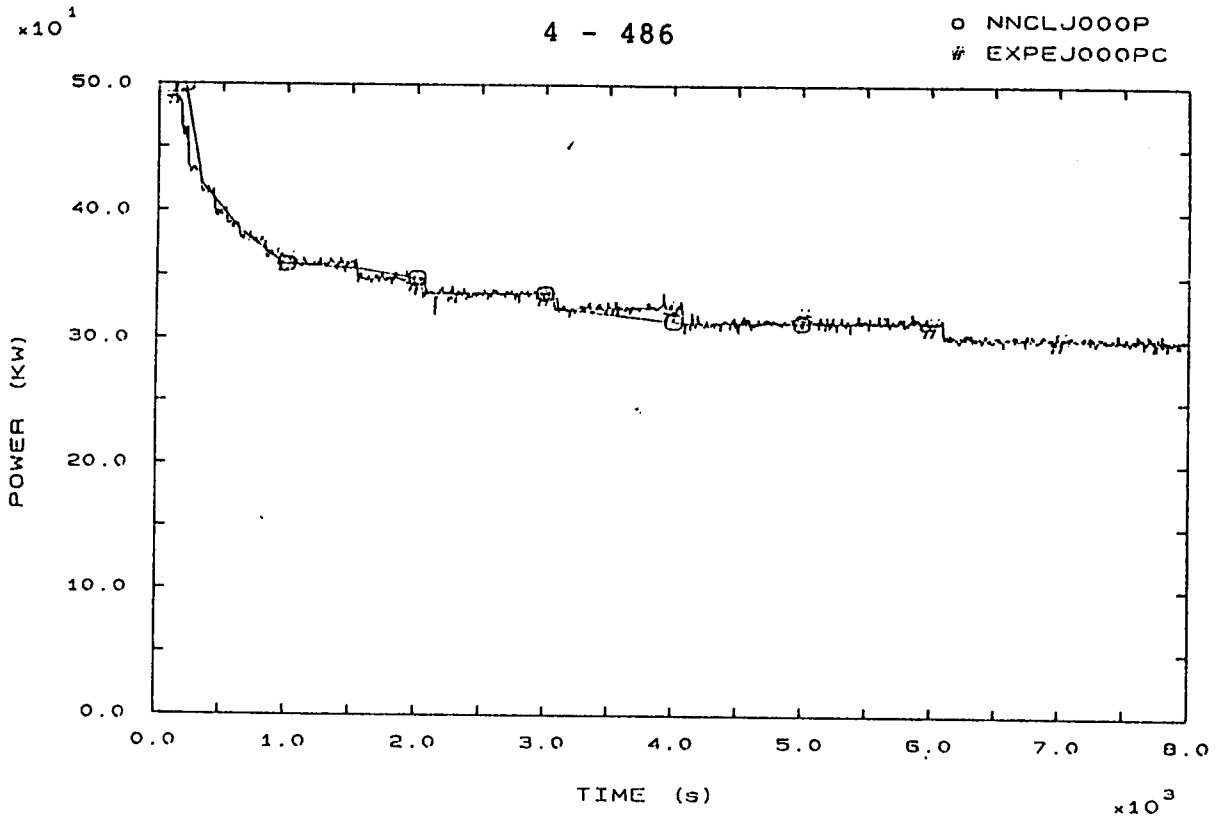

FIG. 81A HEATER RODS POWER

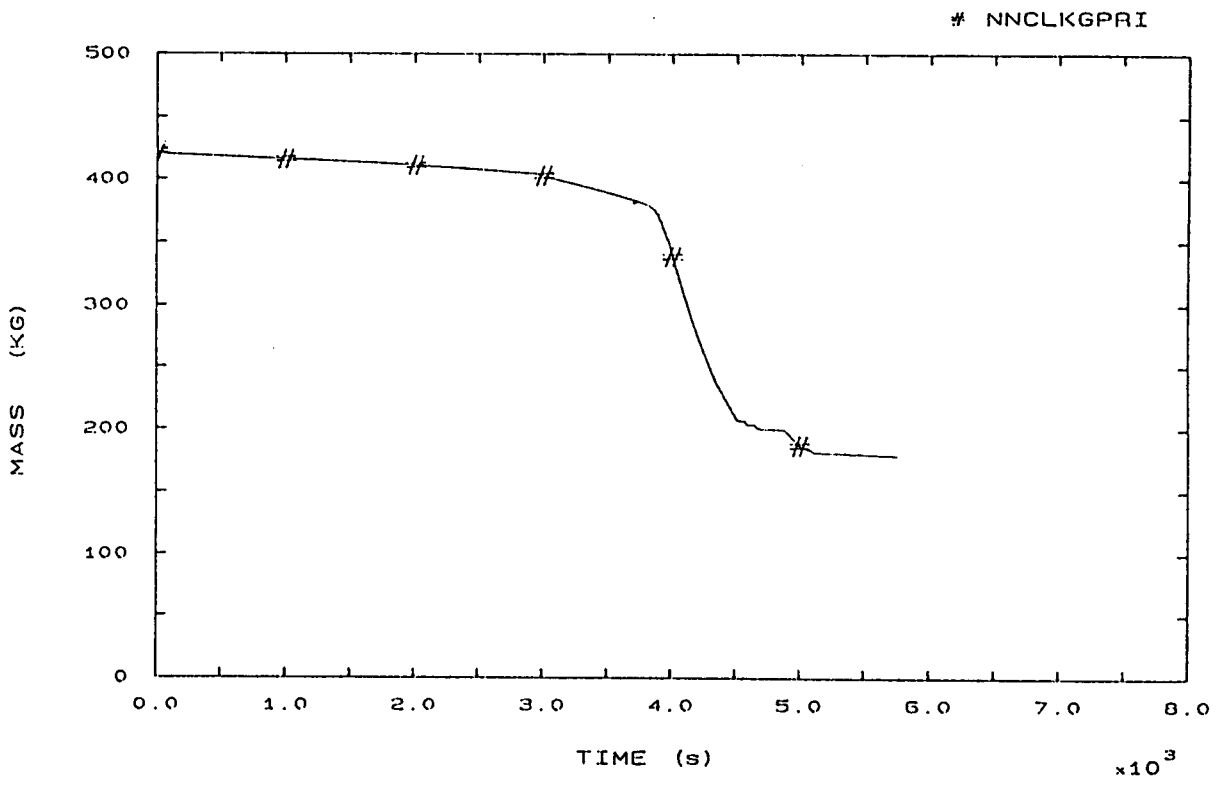

FIG. 85 PRIMARY COOLANT TOTAL MASS

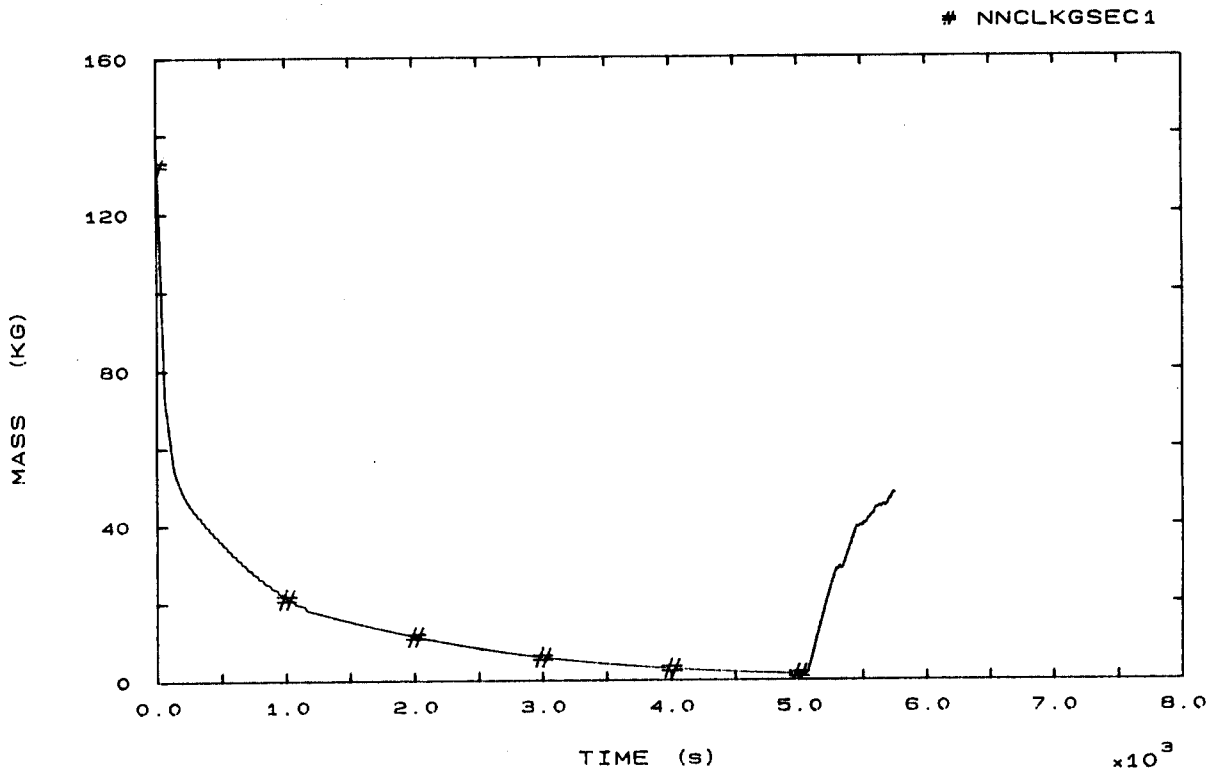

FIG. 86 SECONDARY COOLANT TOTAL MASS SG1

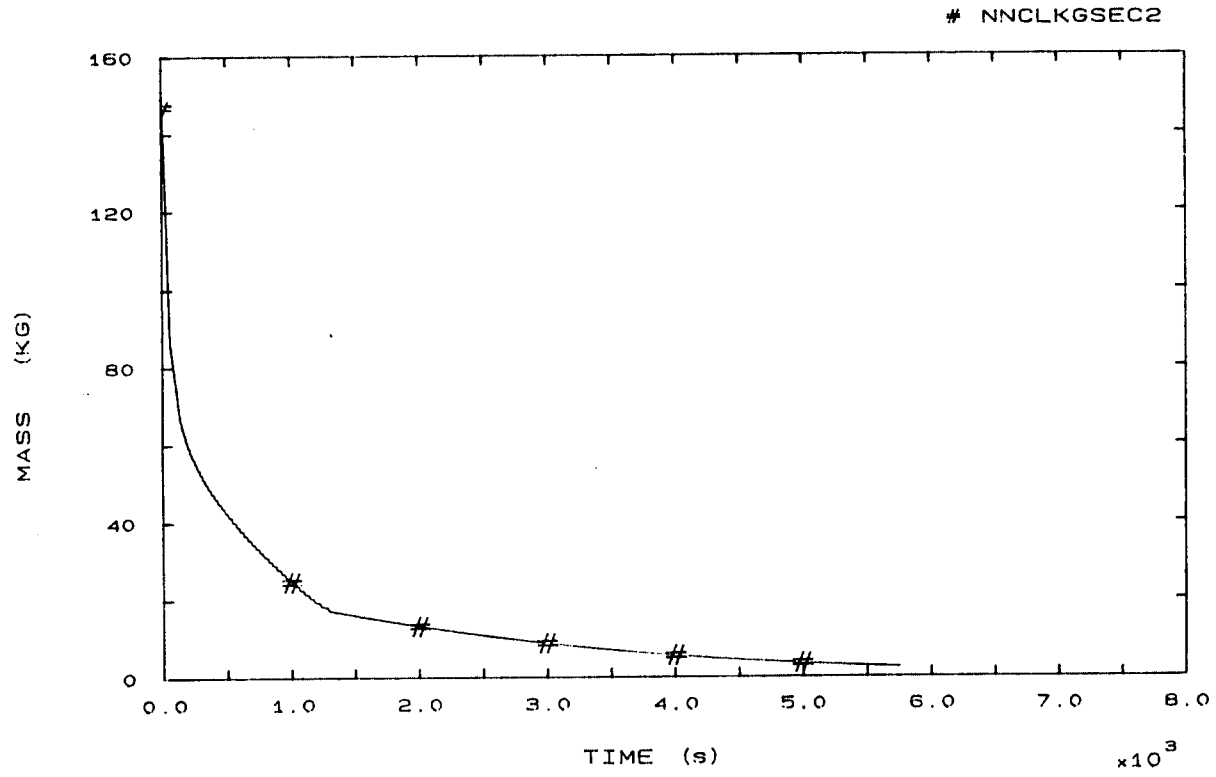

FIG. 87 SECONDARY COOLANT TOTAL MASS SG2

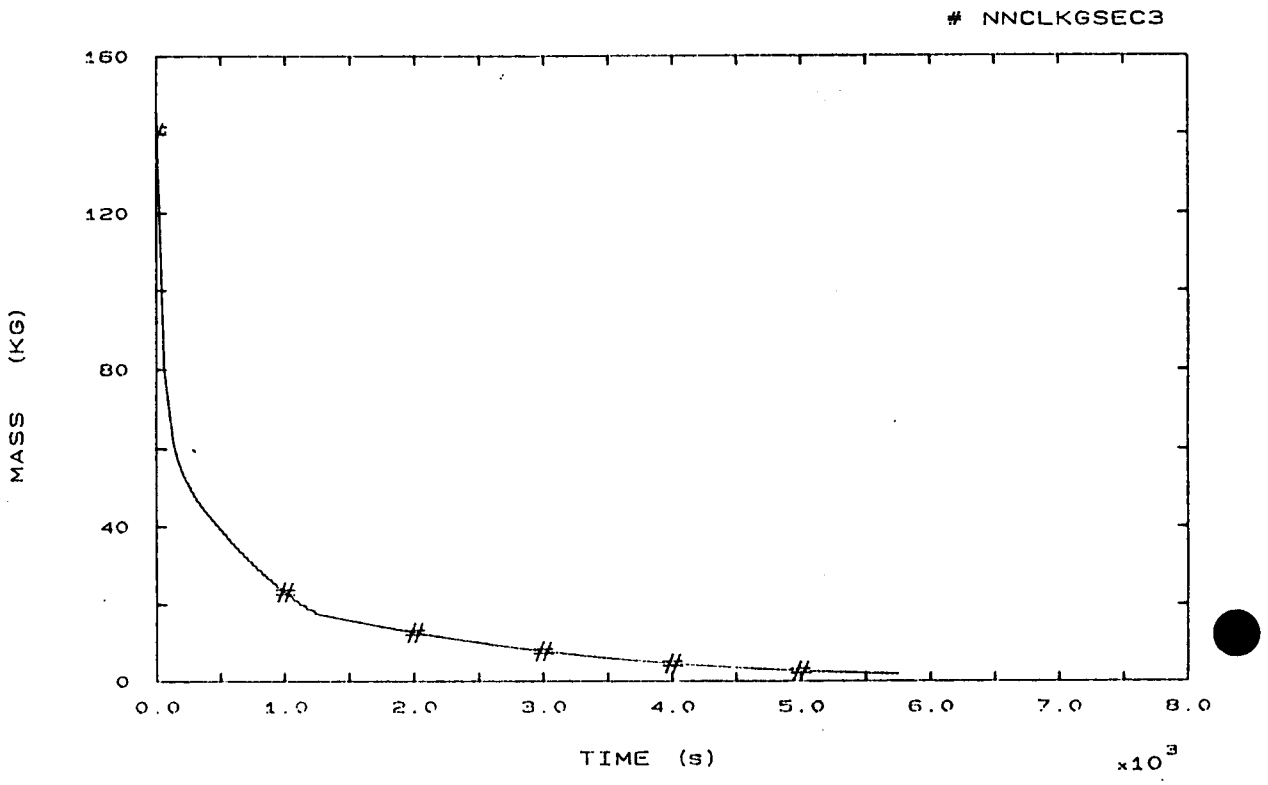

FIG. 88 SECONDARY COOLANT TOTAL MASS SG3

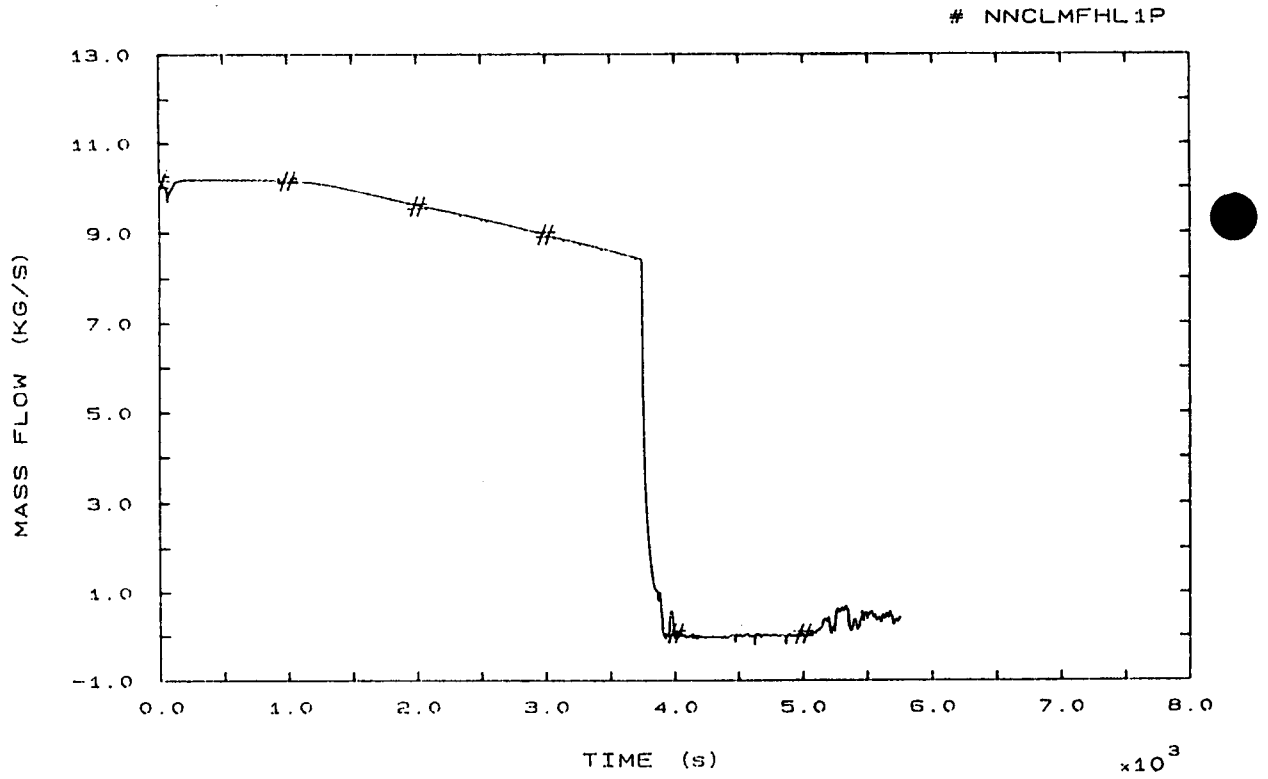

FIG. 89 HOT LEG 1 MASS FLOW

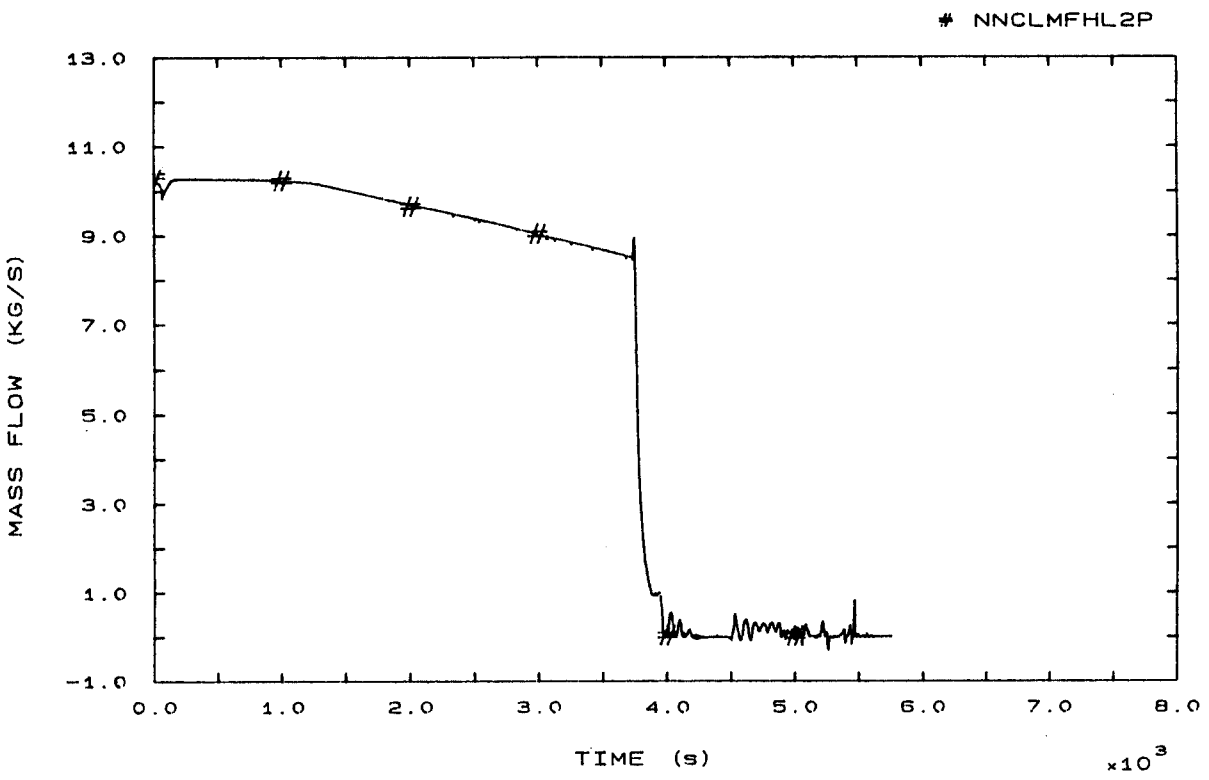

FIG. 90 HOT LEG 2 MASS FLOW

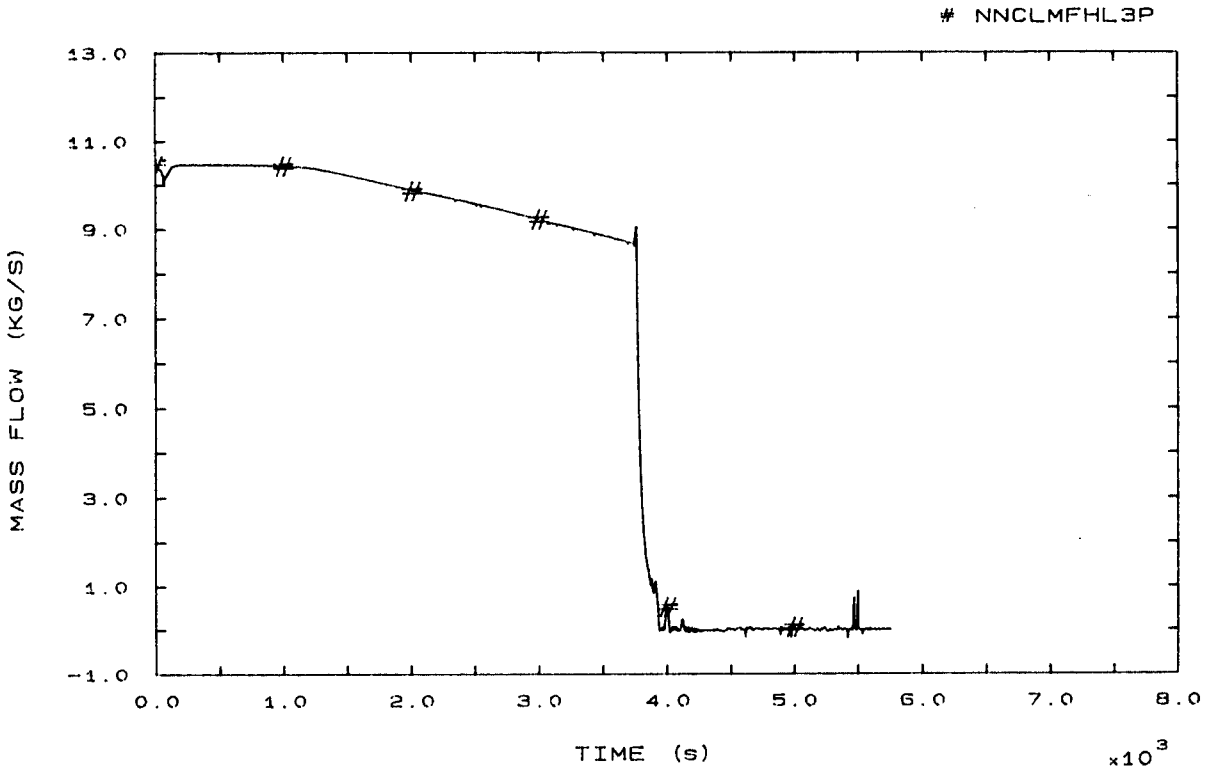

FIG. 91 HOT LEG 3 MASS FLOW

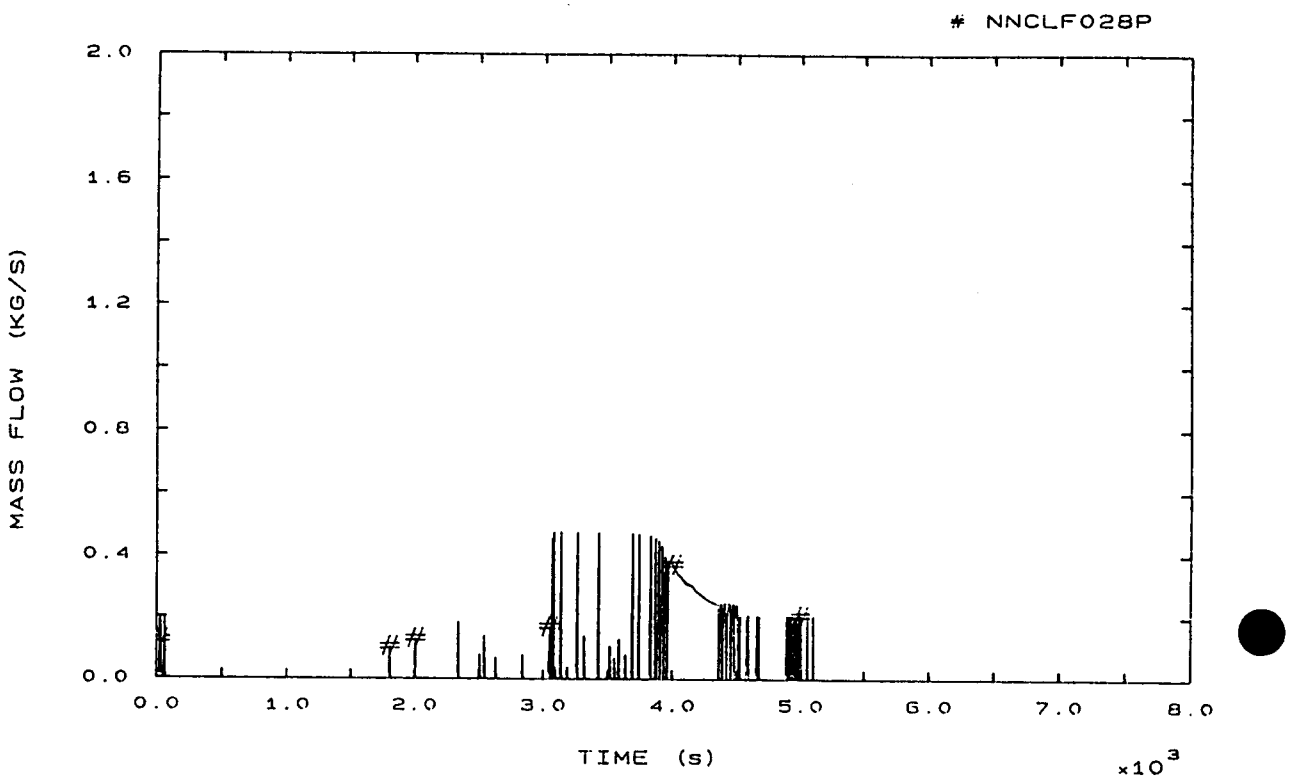

FIG. 92 PRZ PORV MASS FLOW

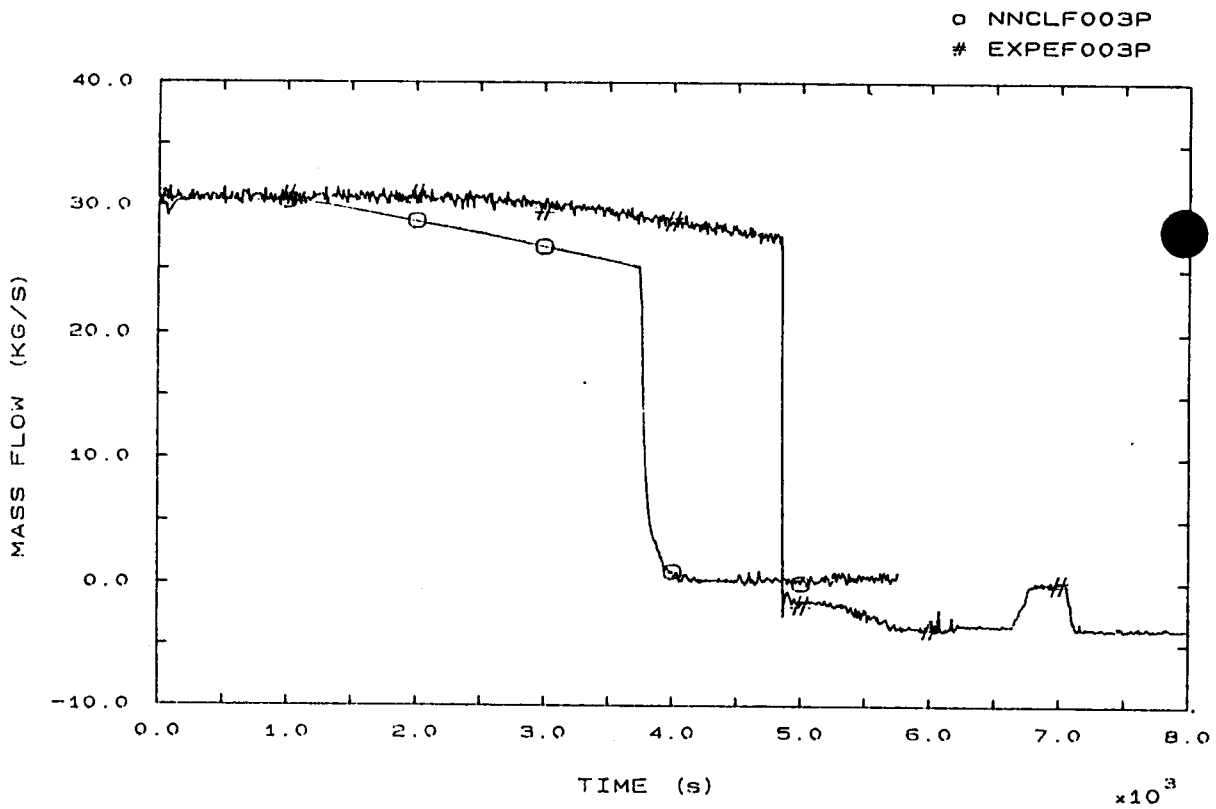

FIG. 94 VESSEL DOWNCOMER MASS FLOW

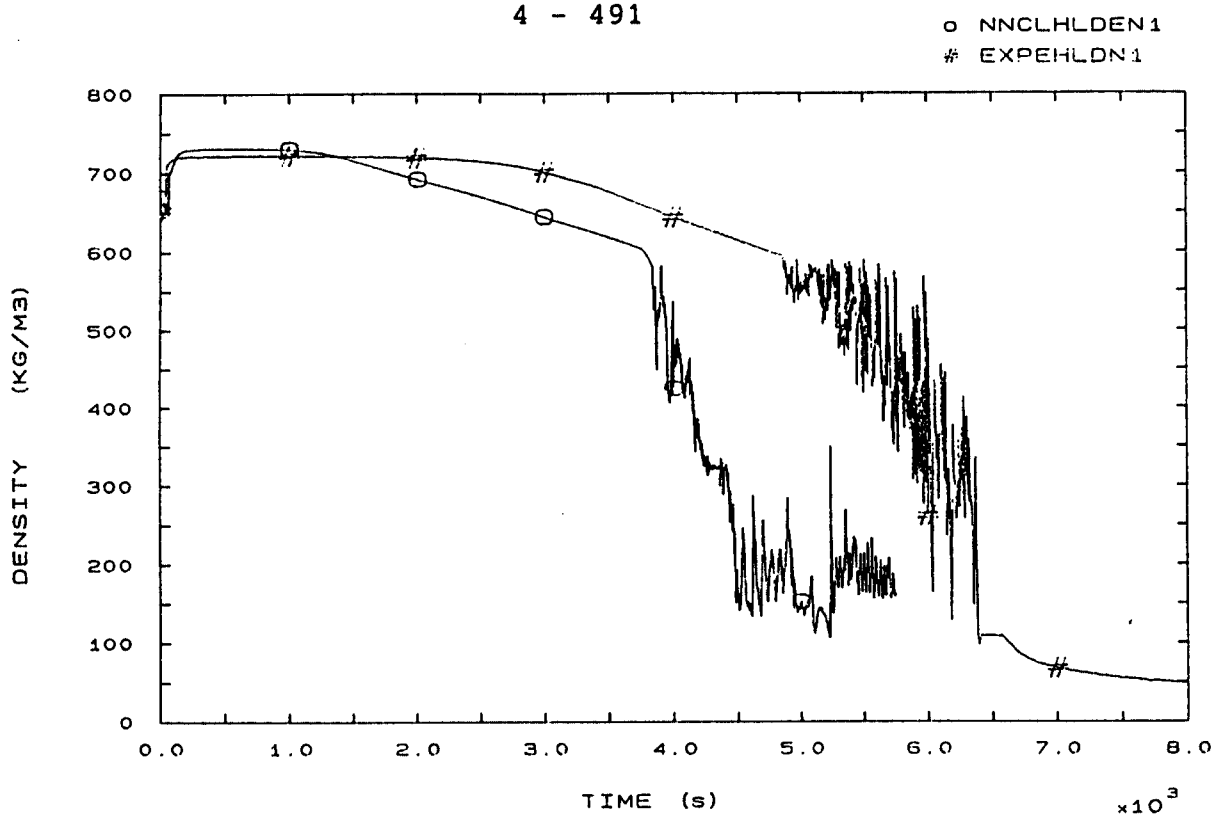

FIG. 100 HOT LEG 1 FLUID DENSITY

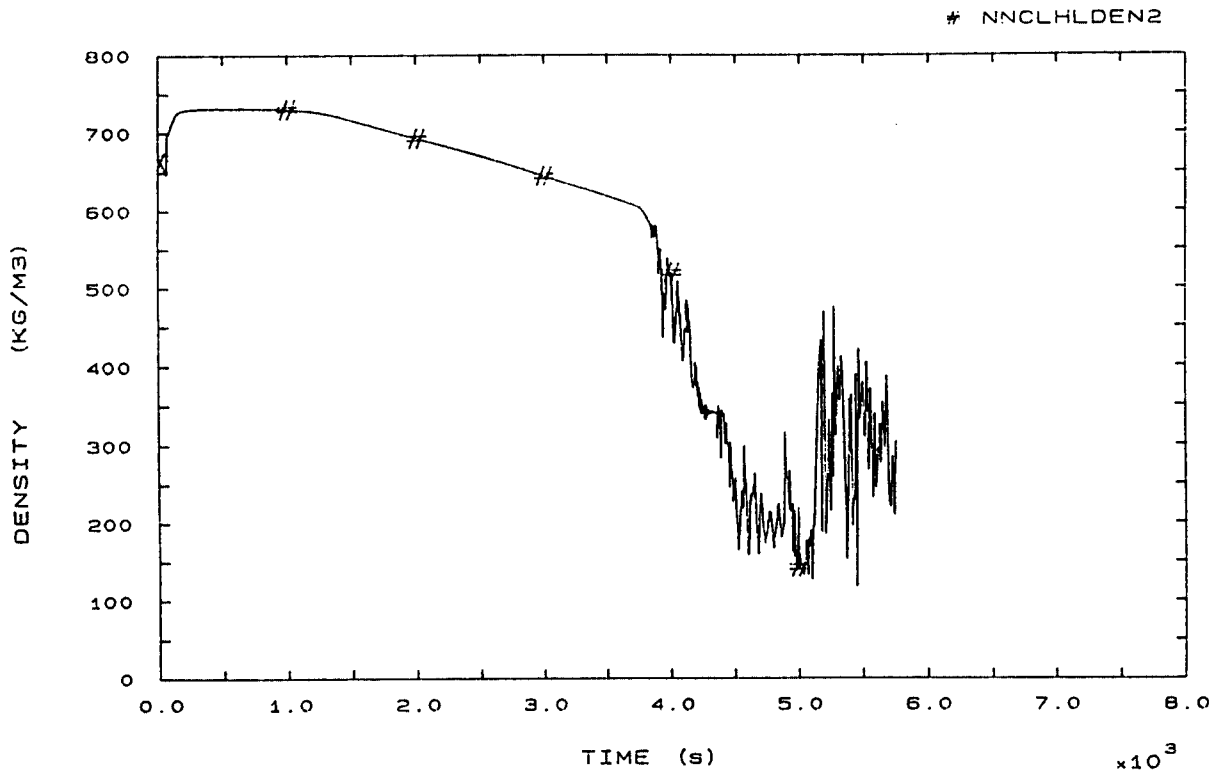

FIG. 101 HOT LEG 2 FLUID DENSITY

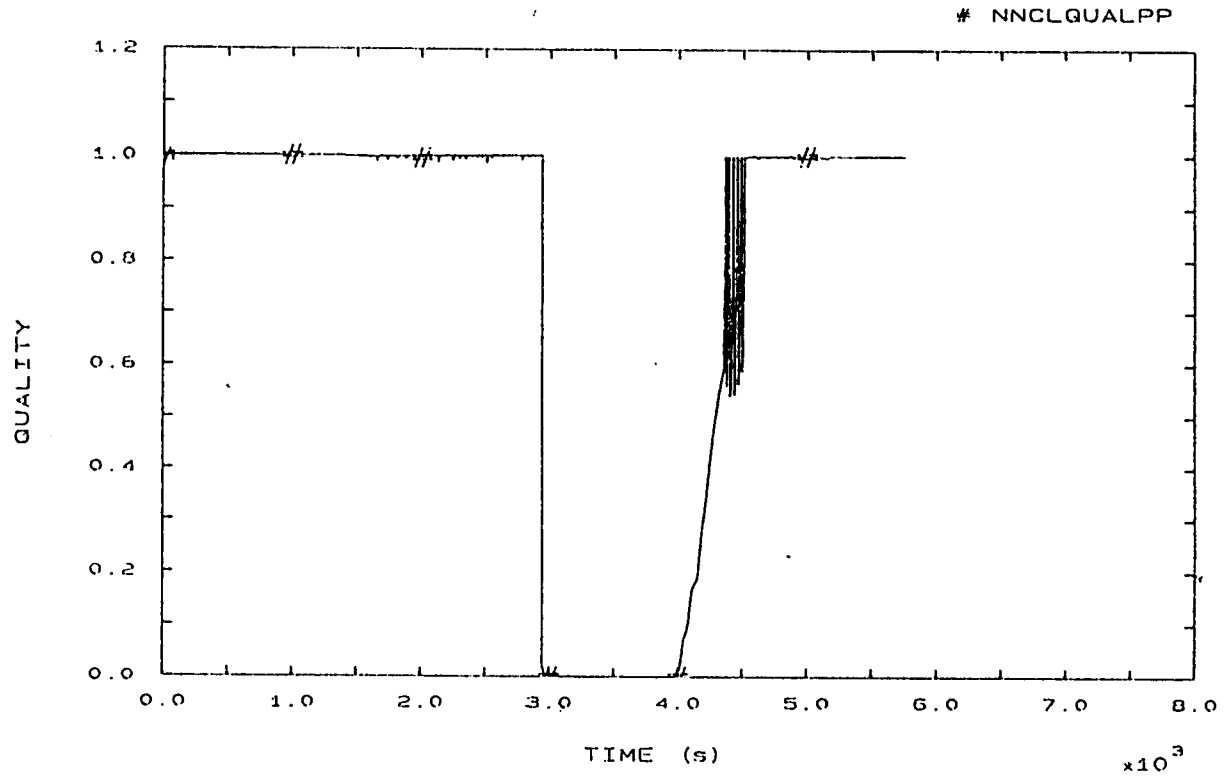

FIG. 103 PRZ PORV FLOW QUALITY

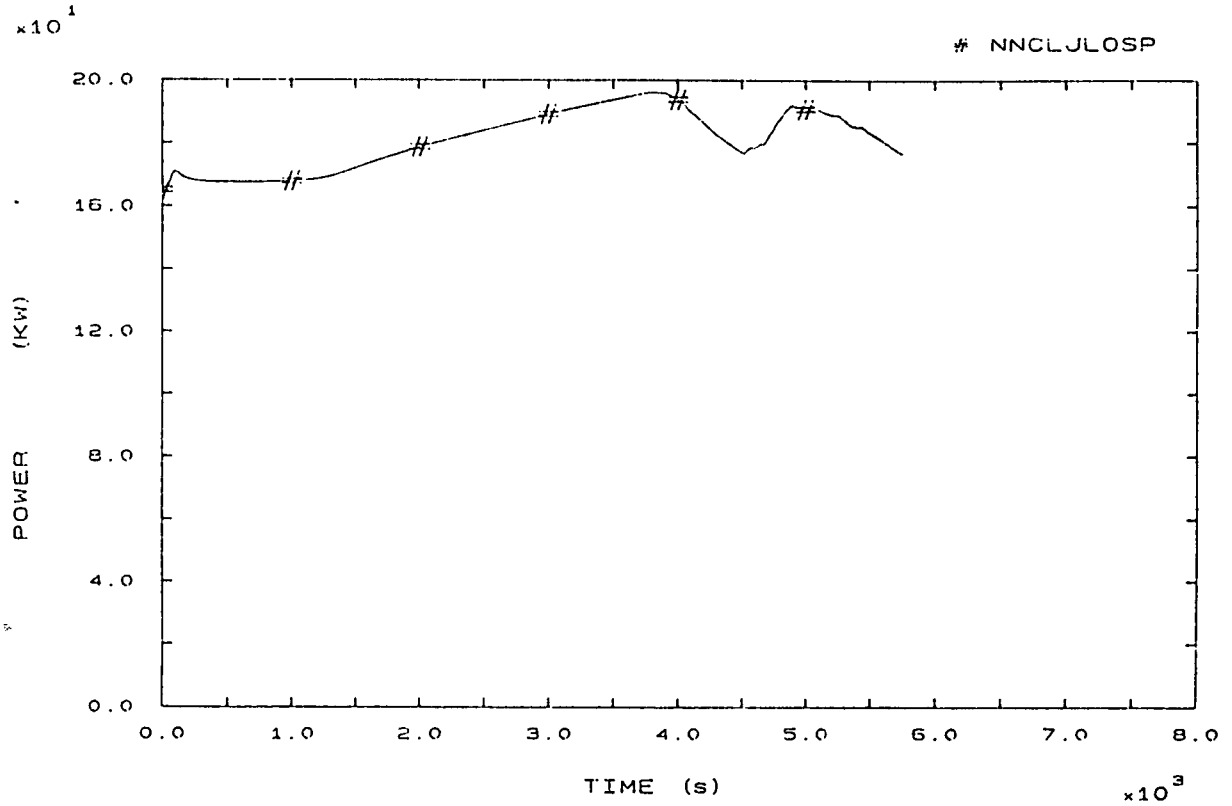

FIG. 131 PRIMARY HEAT LOSS

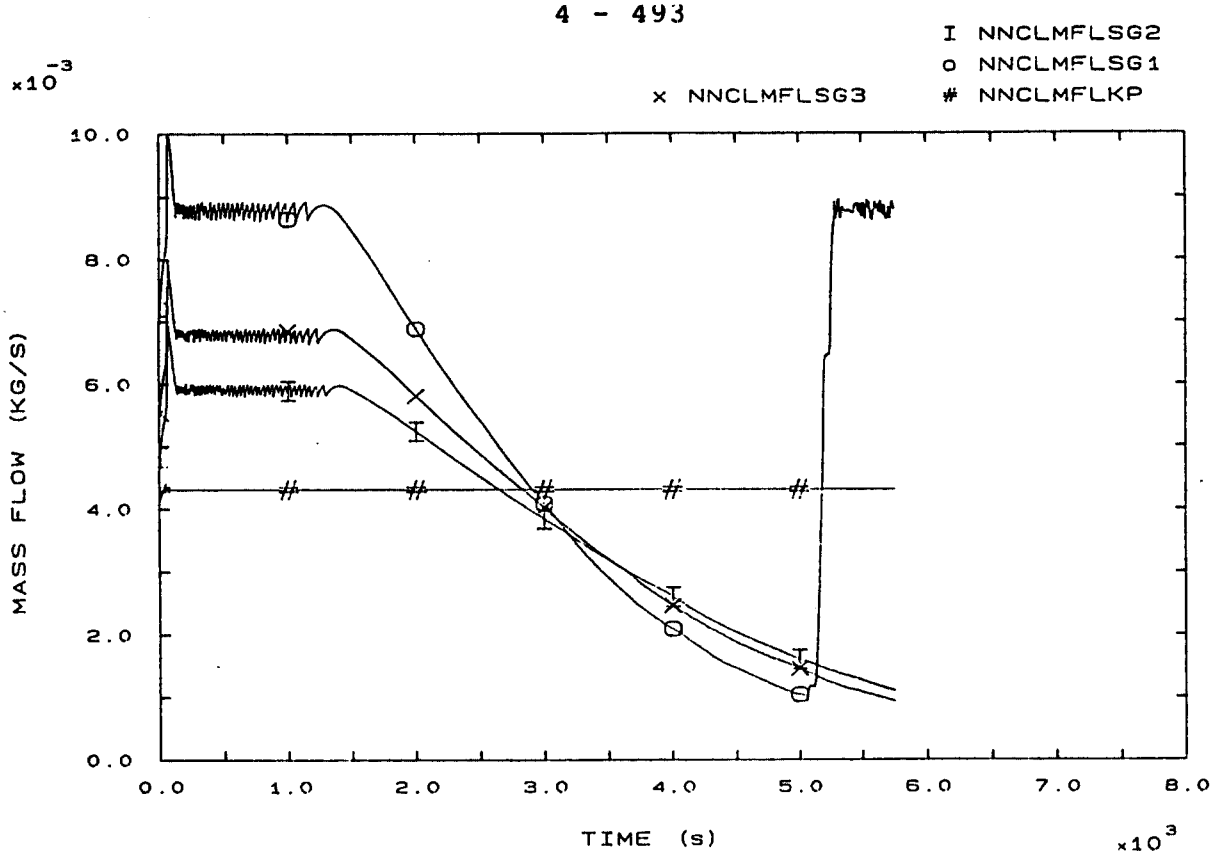

FIG. 137 PRIMARY AND SECONDARY LEAKS

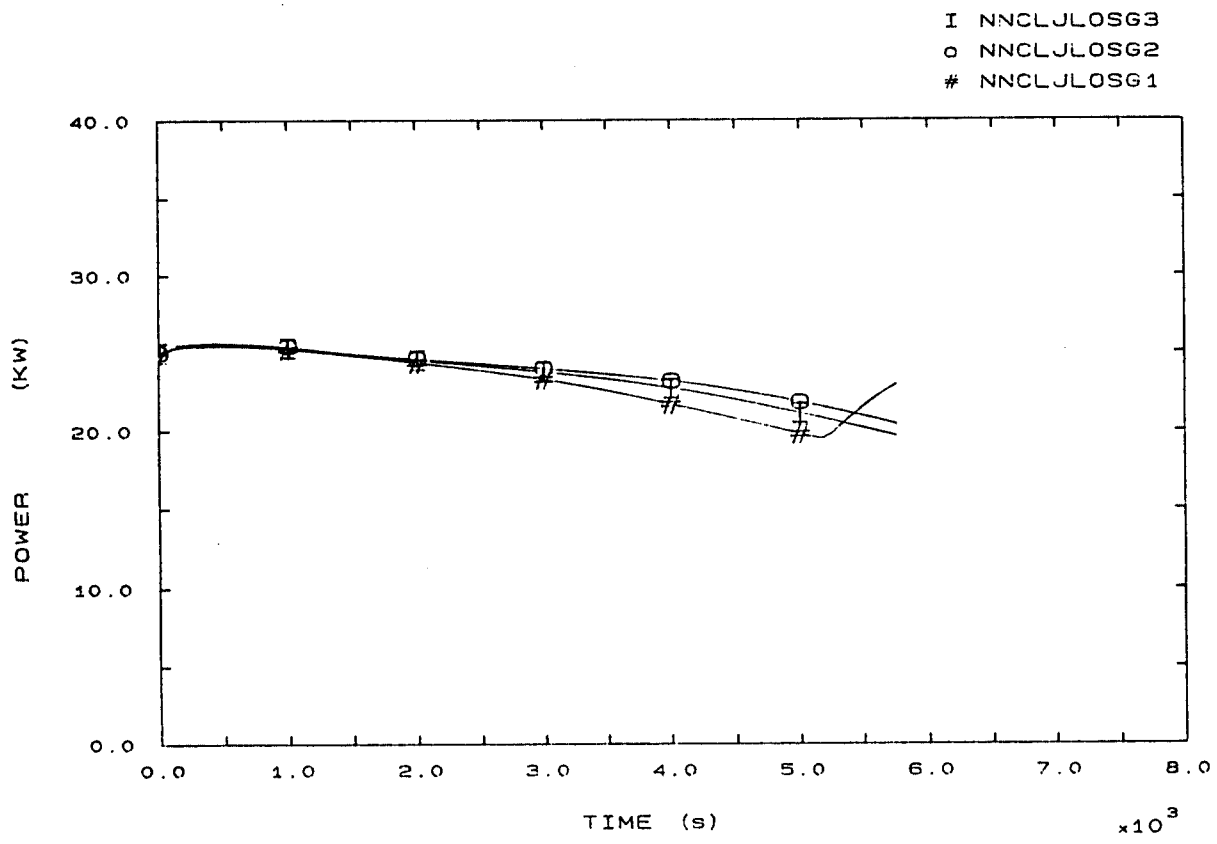

FIG. 139 SECONDARY HEAT LOSSES

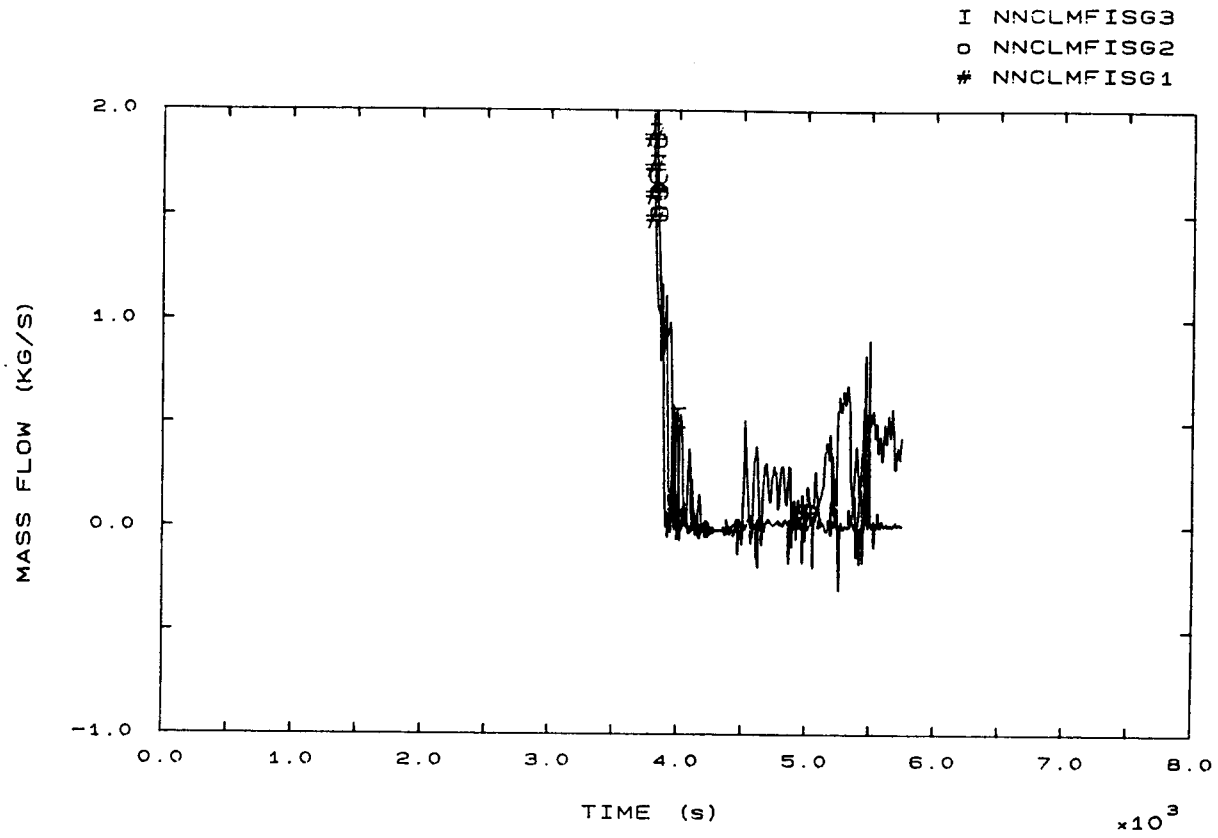

FIG. 140 SG INLET MASS FLOWS

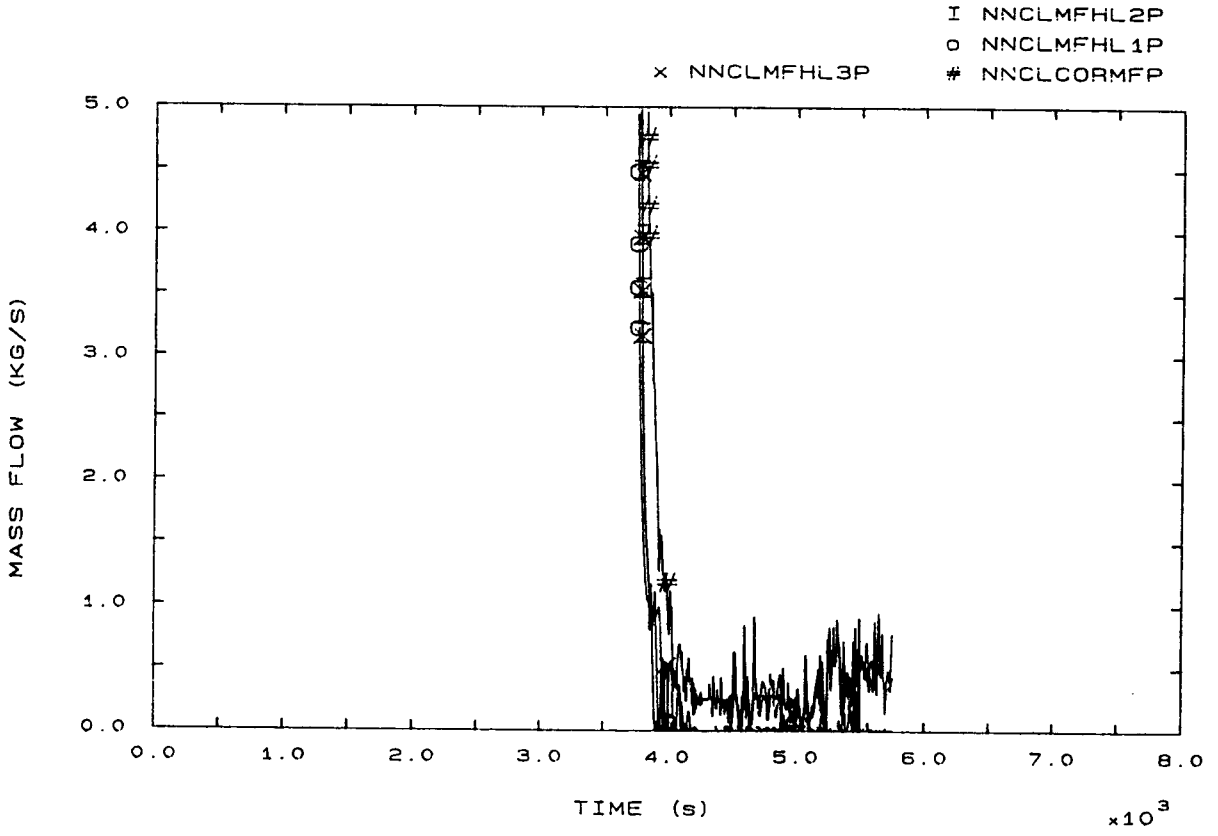

FIG. 141 BOTTOM CORE AND HOT LEG MASS FLOWS

4.13 PISA

4.13.1 CALCULATION DESCRIPTION

Phase 1: from LOFW to Scram (0 - 48 s)

Due to LOFW the DC level in SGs (fig. 7b, 8b, 9b) drops quickly and reaches the low-low level set point at 37 s (see E.T. for the MSIV closure and Scram time). Due to MSI secondary pressure increases rapidly (fig. 3b, 4b, 5b) causing SG PORV opening. Primary temperature, level and pressure (fig. 42b, 6b, 1b) increase accordingly to secondary pressurization.

Phase 2: from Scram to PRZ PORV opening (48 - 930 s)

After Scram, due to a fast decrease of primary temperature (fig. 12b), a quick depressurization occurs in primary side (fig. 1b). Following, although a PRZ level decrease is calculated (fig. 6b), the primary pressure increases due to a PRZ power unbalance (see fig. 1). The primary pressure rise causes the PRZ PORV opening at 930 s. In this phase the SGs dry-out is not yet calculated (see fig. 7).

Phase 3: from PRZ PORV opening to pumps trip (930 - 2813 s)

After about 1500 s of transient SGs dry.out occurs (fig. 7, 8, 9). Due to the consequent primary heat-up (fig. 12) the PRZ level progressively increases The pumps trip occurs at 2813 s (fig. 54). During this phase PRZ PORV continues to discharge steam (fig. 103).

Phase 4: from pumps trip to EFW actuation (2813 - 4474 s)

At time 2850 s the PRZ goes full of liquid (fig. 6). Following pumps trip a two phase natural circulation (TPNC) takes place in the primary loops and, at about 3350 s (see fig. 89), the natural circulation stops. In this phase a partial PRZ empting is calculated (fig. 6). The PRZ level drops at about 4.8 m and remains at this value (with some obscillations) until the end of the phase.

Phase 5: from EFW actuation to the end (4474 - 5130 s)

After EFW actuation (4474 s) a natural circulation flow begins in loop 1 (fig. 89). The increased heat transfer in SG1 causes a rapid drop of primary pressure (fig. 1) and this allows the PRZ to empty completely (fig. 6). The maximum core temperature is 705 K (see fig. 51) at elevation 3294 of rod bundle.
The SG downcomer level reaches the ISP22 end point at 5130 s and the calculation stops at 6000 s (see fig. 7).

PARTICIPANT: D'AURIA - PISA *CODE: RELAP5/MOD2*

EVENTS TABLE

EVENT	*CALC. TIME (s)*	*EXP. TIME (s)*
SG Low Low Level	*37*	*33*
Main Steam Isolation	*42*	*38*
Scram (power fall), t_1	*48*	*44*
SGs PORV opening	*50* *50* *50*	*82 (3)* *106 (2)* *200 (1)*
SGs Dry Out	*1550* *1520* *1580*	*3282 (3)* *3347 (1)* *3437 (2)*
PRZ PORV opening, t_2	*930*	*4134*
PRZ full of liquid	*2850*	*4222*
Pumps Trip, t_3	*2813*	*4848*
Loss of Natural Circulation	*3350*	*5630*
Beginning of Core Heat Up	*4460*	*6511*
EFW actuation, t_4	*4474*	*6532*
PRZ PORV closure	*4509*	*6576*
PRZ emptying	*4690*	*6811*
SG1 repressurization	*4700*	*6878*
End of transient, t_{END}	*5130*	*8062*

4.13.2 CALCULATION/EXPERIMENT COMPARISON

Phase 1: from LOFW to Scram

The initial SGs fluid masses are slightly underestimated (see C.T.). Nevertheless a sufficient agreement concerning the low-low level, MSI and Scram timing (see C.T.) can be noted.
The maximum primary pressure is 15.5 MPa (versus 16.2 MPa in the experiment, see fig. 1b): this means that primary pressure peak due to PRZ level rise is largely underestimated (fig. 1b, 6b). The calculated SGs fluid masses and DC levels at the scram time are lower than the experimental ones (see C.T. and fig. 7b, 8b, 9b). That's mainly due to the calculated low initial value.

Phase 2: from Scram to PRZ PORV opening

Immediately after Scram the calculated primary pressure decreases at 14.6 MPa (fig. 1b) in good agreement with the experiment (14.5 MPa). Then the primary pressure increases and the PRZ PORV opening occurs (930 s) before the SGs dry-out time, in disagreement with the experiment (fig. 1, 6). That's due to an incorrect PRZ power unbalancement (heat losses absence). The calculated PRZ level gradient in this phase is slightly greater than the experimental one (see C.T. and fig. 6). Nevertheless the calculated min. PRZ level is in good agreement with the experiment due to the early primary heat-up in the calculation. In the secondary side, the SGs PORV opening occurs at about 50 s with a strong underestimate w.r.t. the experimental values (see C.T. and fig. 3b, 4b, 5b), but the pressurization trend after MSI is correctly calculated (fig. 3b, 4b). The calculated collapsed DC level trend in SGs is correct, but the absolute value is underestimated because of the low secondary fluid masses at the scram time (fig. 7, 8, and 9).

Warm insurge effect is partally calculated (fig. 112, 113) but when it occurs (around 1500 s) PRZ pressure is already at PORV setpoint and the final consequence of the phenomanon is a momentary PORV cycling slowing down (see fig. 1).

Phase 3: from PRZ PORV opening to pumps trip

The SGs dry-out occurs, contrary to the experiment, in this phase, at about 1500 s (vs 3300 s see C.T.). The main reasons for the discrepancy are the calculated low secondary masses at the scram time. The temperature gradient during primary heat-up is 0.033 K/s in the calculation versus 0.022 K/s in the experiment (see fig. 12, 22 and 32). In this phase, due to the anticipation in SGs dry-out time, the calculated core power is higher than the experimental one. The PRZ level gradient is calculated with sufficient accuracy because the anticipated PRZ PORV opening compensates the temperature gradient effect (see fig. 6). The pumps trip occurs at 2813 s (versus 4848 in the Exp.) and at 2950 s the PRZ is full of liquid (versus 4222 in the Exp.) In the secondary side, the SGs pressure decrease after SGs dry-out (fig. 3, 4, 5). The pressure gradient isn't well calculated due to a wrong leak modelling (constant mass flow versus pressure).

Phase 4: from pumps trip to EFW actuation

After pumps stop, two phase natural circulation (TPNC) establishes in primary side till about 3350 s (fig. 89, 140) versus 5630 in the experiment. The NC duration is calculated with sufficient accuracy (537 s vs 780 s). The underestimate is due to the calculated average PRZ PORV flow quality (less than in the Exp.). The primary mass at pumps trip and LNC time are calculated with good accuracy (see C.T.). The PRZ behaviour during this phase is in good agreement with the experiment (partial emptying and level obscillations, see fig. 6).

In the calculation the EFW actuation starts at 4474 s (6532 in the Exp.). The main reason for the discrepancy is in the anticipation of SGs dry-out time. The primary mass at the beginning of core heat-up is calculated with sufficient accuracy (see C.T.).

Phase 5: from EFW actuation to the end

After EFW actuation the primary pressure decreases more rapidly in the calculation than in the experiment (see C.T. and fig. 1). The calculated core heat-up rate is in good agreement with the experiment (see C.T.). There's also a sufficient agreement calculation/experiment concerning the maximum core temperature (see C.T. and fig. 52).
The calculated primary circulation mode is two phase natural circulation (versus an intermittent flow in the experiment). The PRZ role is well predicted (supplies liquid to the core) but it's difficult to know if the calculated core reflood takes place from the top or the bottom. That's due to a small number of points in core surface temperature plots. In the secondary side, the SG1 downconer level increases more rapidly in the calculation than in the experiment (see fig. 7) and at 5130 s reaches the ISP22 end point (8062 in the Exp.).

PARTICIPANT: D'AURIA - PISA

CODE: RELAP5/MOD2

COMPARISON TABLE

PARAMETER		EXP	CALC	AE*	RFD**
1A Initial SGs mass (Kg)	1	137	133		
	2	151	138	P	(C+B+U?)
	3	145	122		
1B Trips timing (s)	LoLo	33	37		
	MSI	38	42	S	? (C+B+U)
	Scram	44	48		
1C Max primary pressure (MPa)		16.2	15.5	P	?
1D SGs mass at Scram (Kg)	1	98	64	P	
	2	105	76	P	1A+1B
	3	97	72	P	
2A Min. primary pressure (MPa)		14.5	14.6	G	-
Pressure gradients before		4.10^{-4}	$1.6.10^{-3}$	P	PRZM (U+B)
and after SGs DO (MPa/s)		3.10^{-4}	0	P	
2B SGs PORV opening time (s)	1	200	50	P	?
	2	106	50	P	
	3	82	?		
2C PRZ level gradient (m/s)		$-5.7.10^{-4}$	1.10^{-3}	P	?
2D Min. PRZ level (m)		2.3	2.5	G	2E
2E SGs DO time, tSG1DO (s)		3347	1520		
tSG2DO (s)		3437	1580	P	1D
tSG3DO (s)		3282	1550		
2F Heat Up temperature (K/s)		0.02	0.033	P	2E
and level (m/s) gradients		$3.6.10^{-3}$	$2.8.10^{-3}$	S	2E+2H
2G Cool Insurge effect		PR. DELAY	PPCS(1)	S	PRZM (U+B)
2H PRZ PORV opening time, t2 (s)		4134	930	P	
($dt_2 = t_2 - t_{SGDO}$)		(697)	(-650)	P	PRZM (U)
3A PRZ level at t_2 (m)		6.57	2.7	P	2H
3B PRZ full time, t_{PRZF} (s)		4222	2850	P	2E
($dt_{PRZF} = t_{PRZF} - t_2$)		(88)	(1920)	P	2H
3C Dominant Relief Condition		LIQ	VAP+MIX	P	3A
3D Sat. Conditions before trip		NO	NO	G	-
3E Pumps Trip time, t3 (s)		4848	2813	P	2E
($dt_3 = t_3 - t_2$)		(714)	(1883)	P	2H
($dt_{HU} = t_3 - t_{SGDO}$)		(1411)	(1233)	G	-

* ACCURACY EVALUATION : G=GOOD, S=SUFFICIENT, P=POOR

** REASON FOR DISCREPANCY : B=BIC, C=CODE, U=USER, PRZM=PRZ MODELLING,

(1) PPCS = PRZ PORV CYCLING SLOWING DOWN

PARTICIPANT: D'AURIA - PISA CODE: RELAP5/MOD2

COMPARISON TABLE (CONT'D)

PARAMETER	EXP	CALC	AE*	RFD**
3F RCS mass at t_3 (kg)	390	398	G	-
4A PRZ behaviour	PART. EMPT.	PART. EMPT.	G	-
during phase 4	LEV. OBS.	LEV. OBS	G	-
4B Primary Flow Cond.	TPNC/LNC	TPNC/LNC	G	-
4C LNC time, tLNC (s)	5630	3350	P	3E
($dt_{LNC} = t_{LNC} - t_3$)	(780)	(537)	S	-
4D RCS mass at t_{LNC} (kg)	296	304	G	-
4E Beg. of Core Heat Up, t_{BOCH} (s)	6511	4460	P	3E
($dt_{BOCH} = t_{BOCH} - t_{LNC}$)	(880)	(1100)	P	?
4F RCS mass at tBOCH (Kg)	183	194	S	-
4G EFW act. time, t4 (s)	6532	4474	P	3E
($dt_{4B} = t_4 - t_{BOCH}$)	(21)	(14)	P	?
($dt_{4L} = t_4 - t_{LNC}$)	(900)	(1124)	P	?
($dt_4 = t_4 - t_3$)	(1684)	(1661)	G	4C+4E
4H PRZ level at t_4 (m)	4.4	4.98	S	-
5A Core Heat Up Rate (K/s)	2/5	2.7	G	-
5B Max Core Temperature (K)	770	705	S	-
5C PRZ PORV closure time, t_{PRZPC}	6576	4509	P	4G
($dt_{PRZPC} = t_{PRZPC} - t_4$)	(44)	(35)	S	-
5D RCS mass at tPRZPC (Kg)	179	192	S	-
5E RCS Depress. Rate (MPa/s)	-0.016	-0.049	P	?
(Initial/Averaged on 500 s)	-0.0086	-0.0132	P	?
5F Prim. Circulation Mode	INTERM	TPNC	P	C+U?
5G SG1 Press. time, t_{SG1PR} (s)	6878	4700	P	4G
($dt_{SG1PR} = t_{SG1PR} - t_4$)	(346)	(226)	P	?
5H PRZ Role	CORE FL.	CORE FL.	G	-
5I PRZ emptying time, t_{PRZE} (s)	6811	4690	P	4G
($dt_{PRZE} = t_{PRZE} - t_4$)	(280)	(216)	S	-
5J Core Reflood Mode	TOP-DOWN	?	-	-
5K End of Transient time, t_{END}	8062	5130	P	4G

* ACCURACY EVALUATION : G=GOOD, S=SUFFICIENT, P=POOR
** REASON FOR DISCREPANCY : B=BIC, C=CODE, U=USER

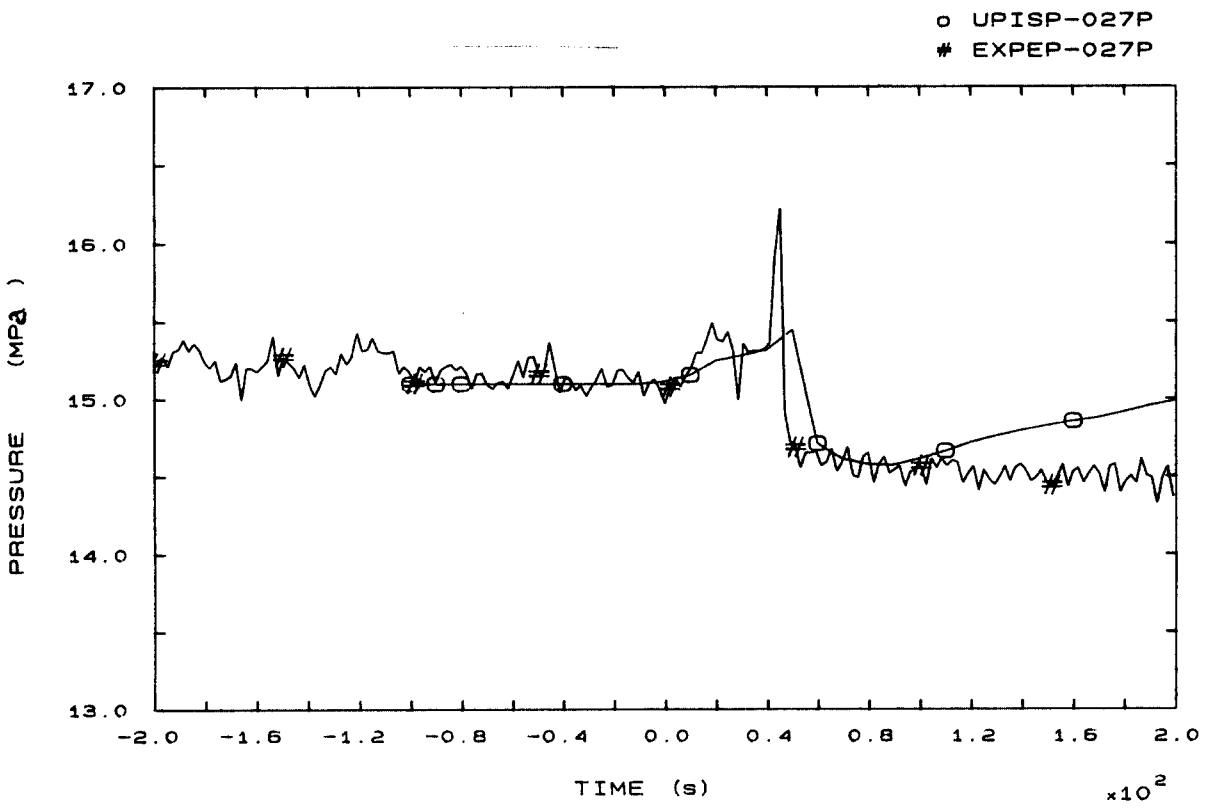

FIG. 1b PRESSURIZER PRESSURE

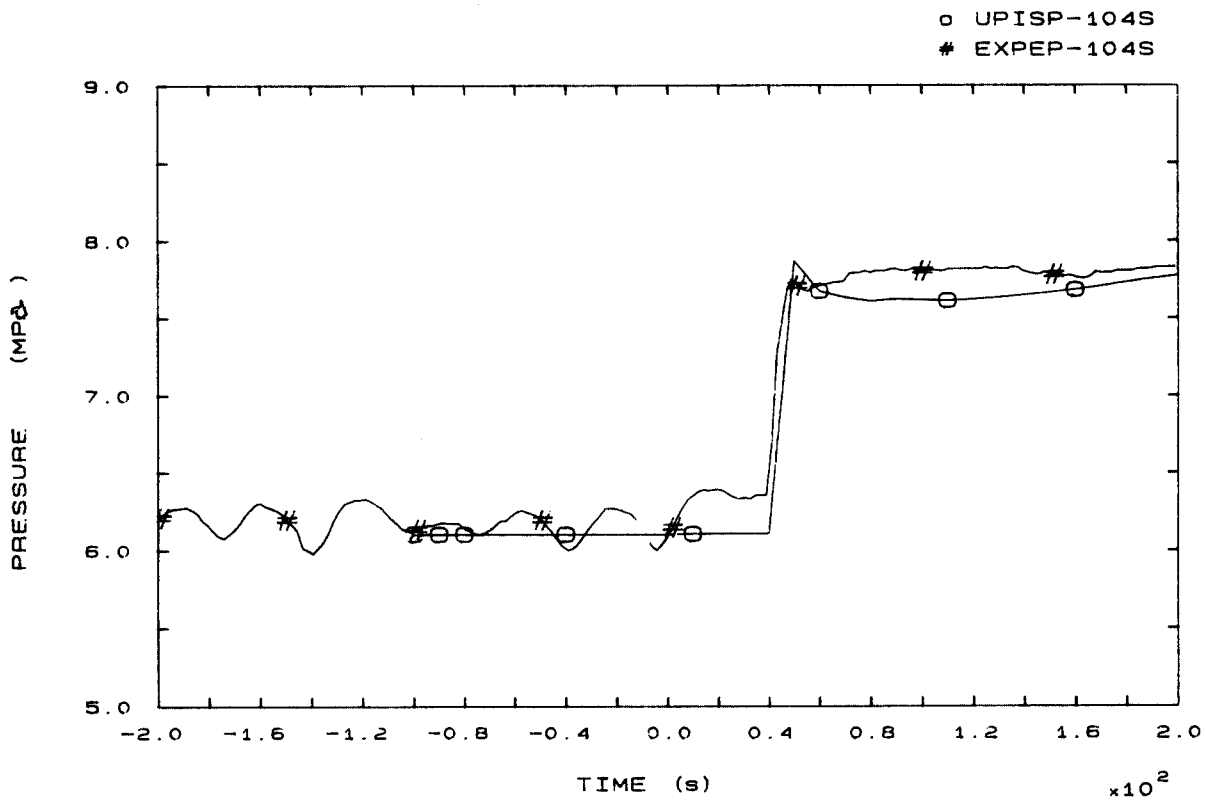

FIG. 3b SG1 STEAM DOME PRESSURE

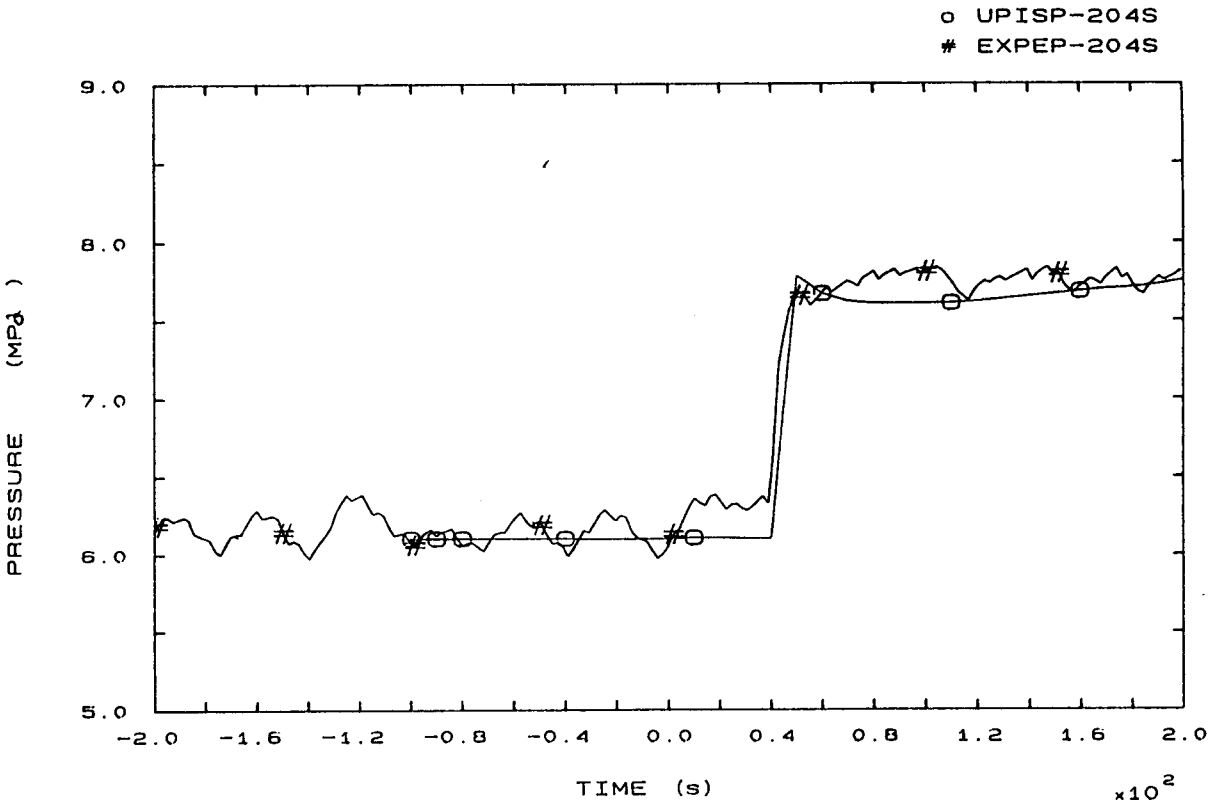

FIG. 4b SG2 STEAM DOME PRESSURE

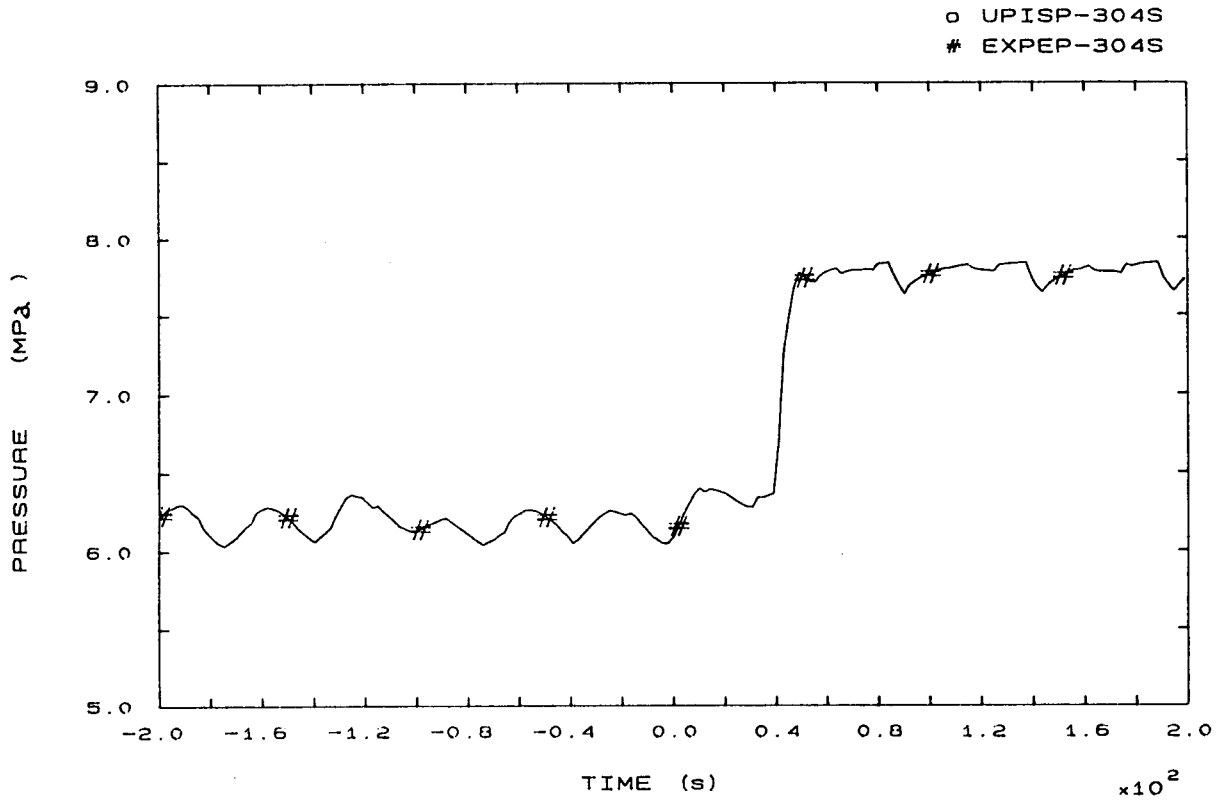

FIG. 5b SG3 STEAM DOME PRESSURE

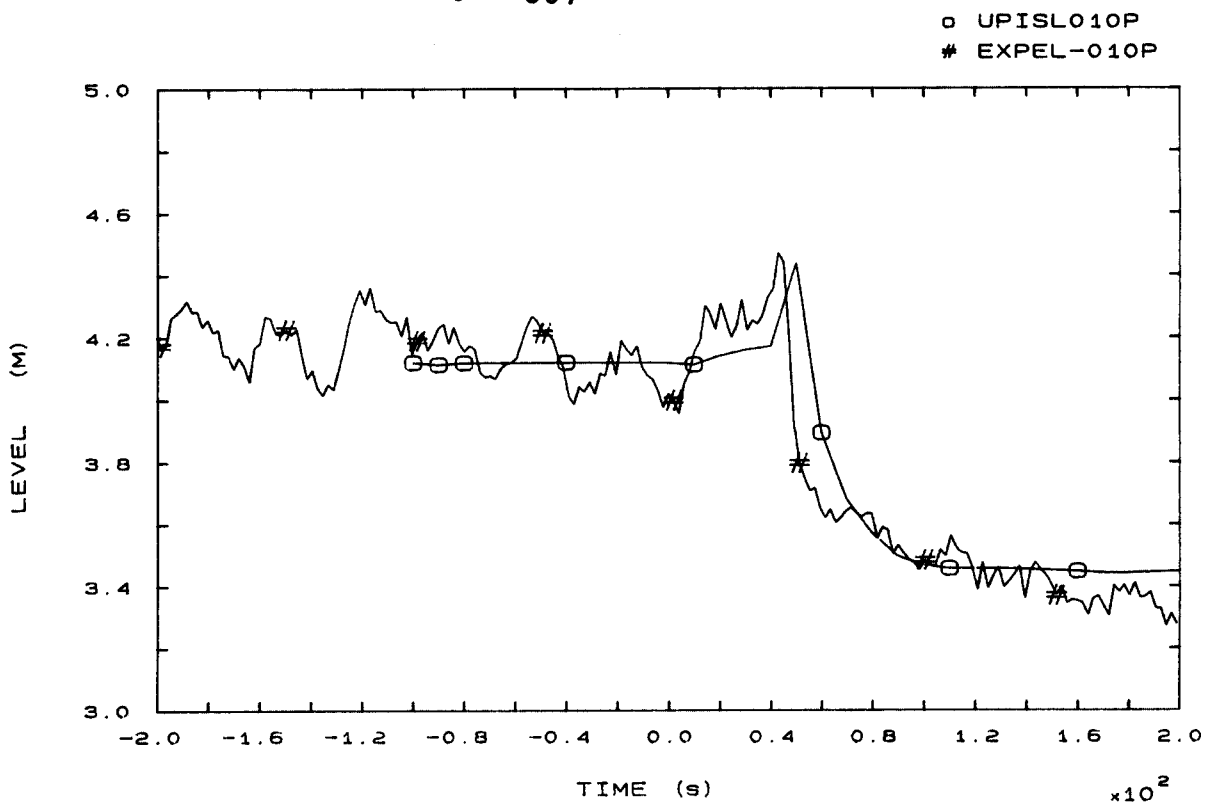

FIG. 6b PRESSURIZER LEVEL

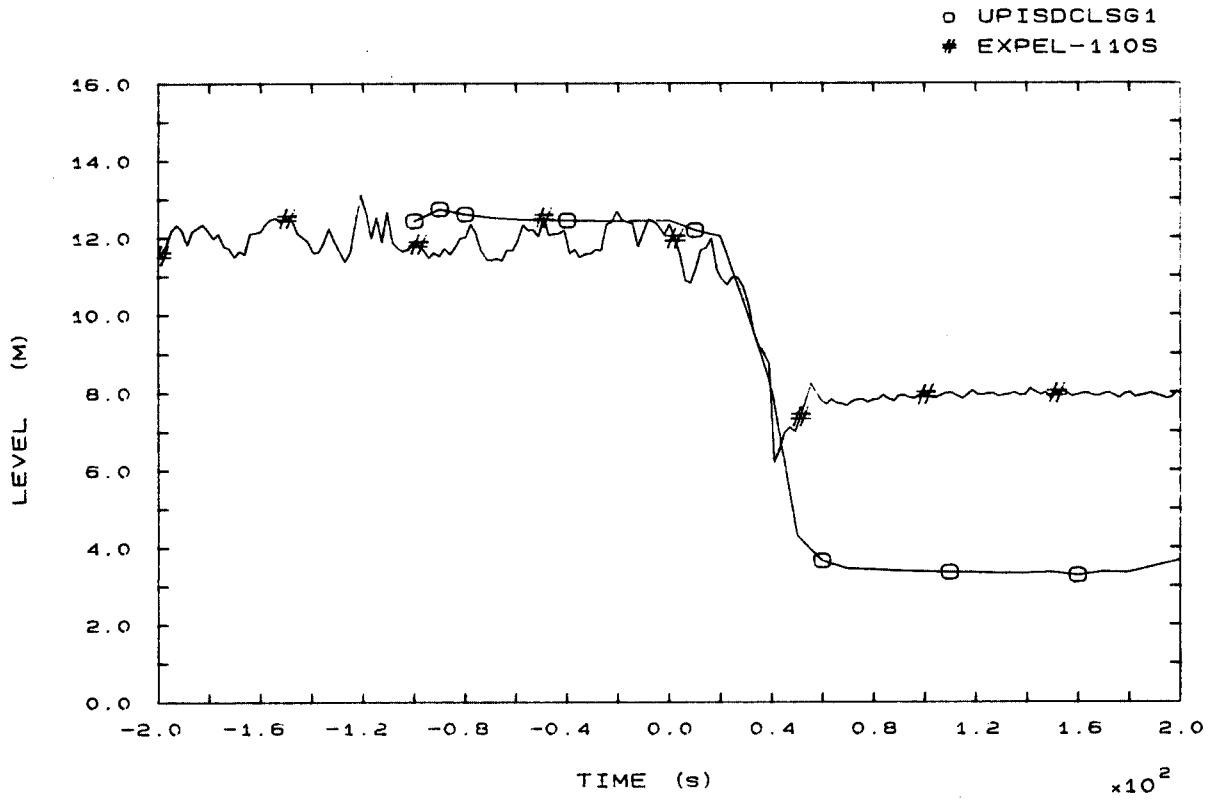

FIG. 7b SG1 DOWNCOMER LEVEL

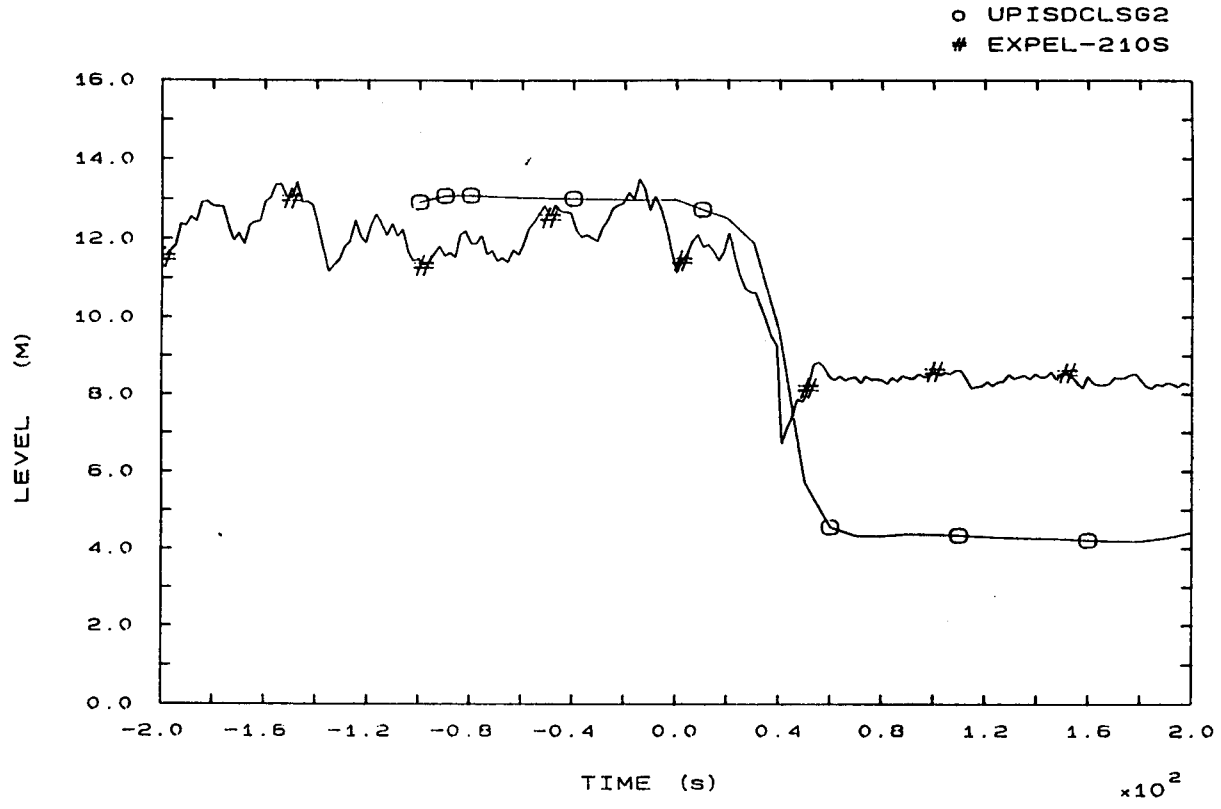

FIG. 8b SG2 DOWNCOMER LEVEL

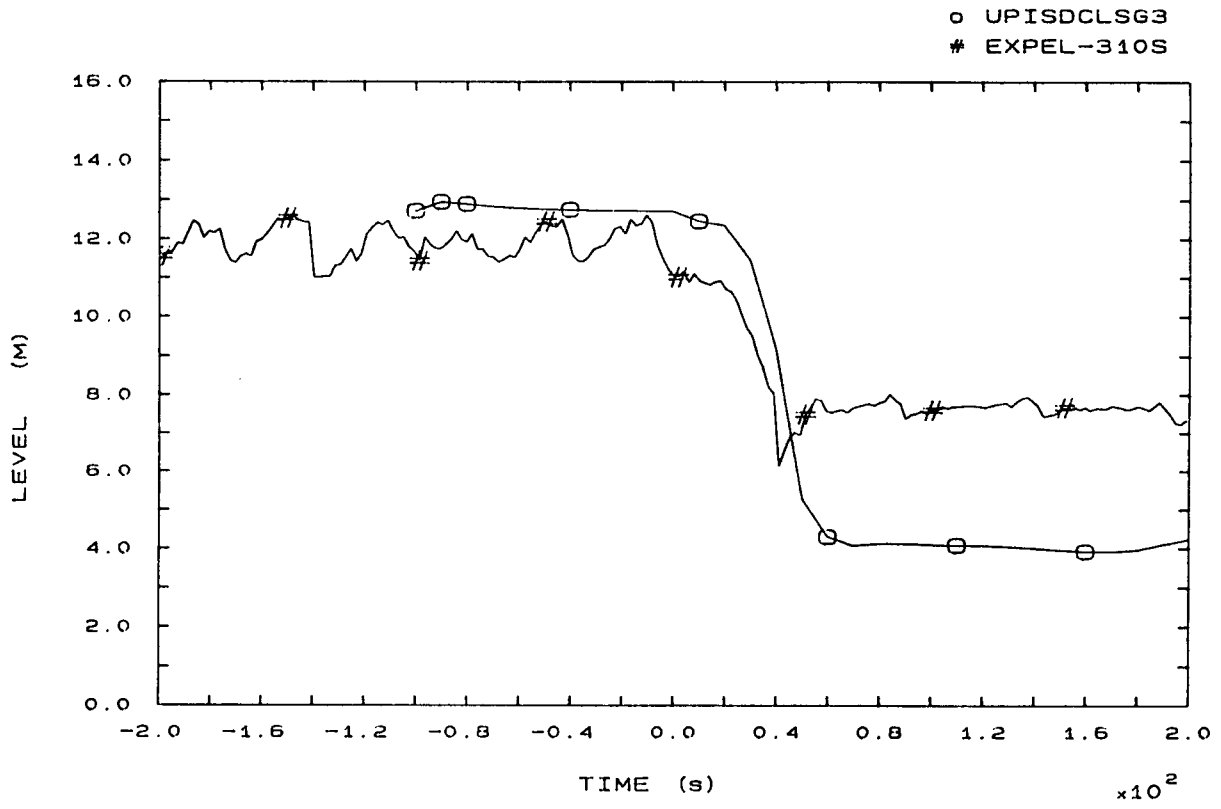

FIG. 9b SG3 DOWNCOMER LEVEL

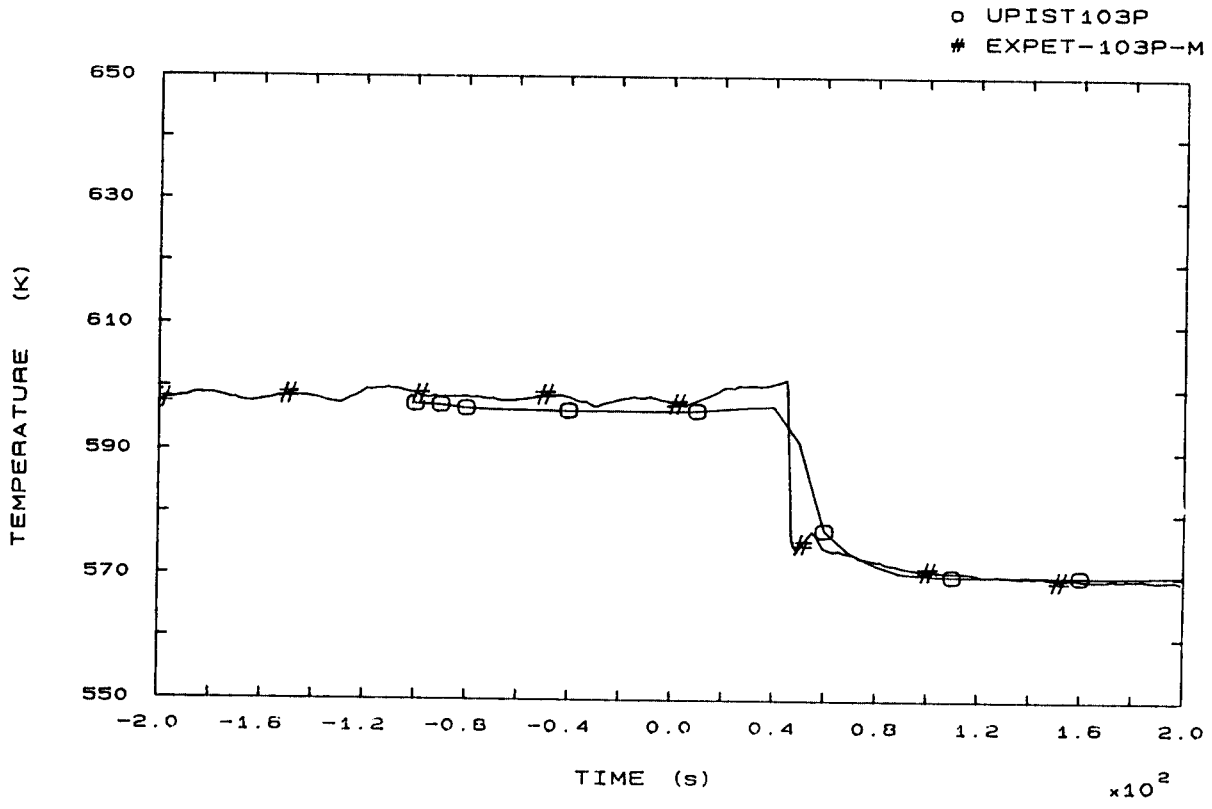

FIG. 12b LP1 HOT LEG OUTLET VESSEL TEMPERATURE

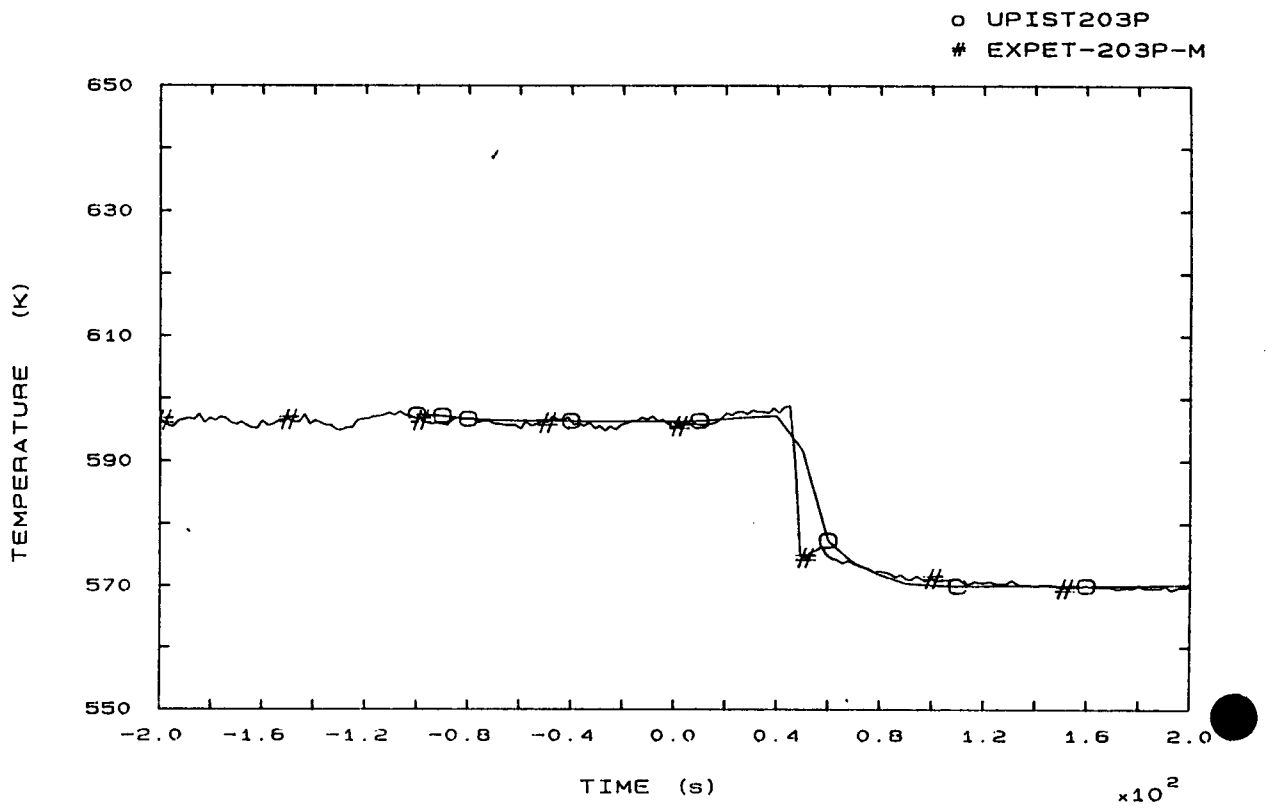

FIG. 22b LP2 HOT LEG OUTLET VESSEL TEMPERATURE

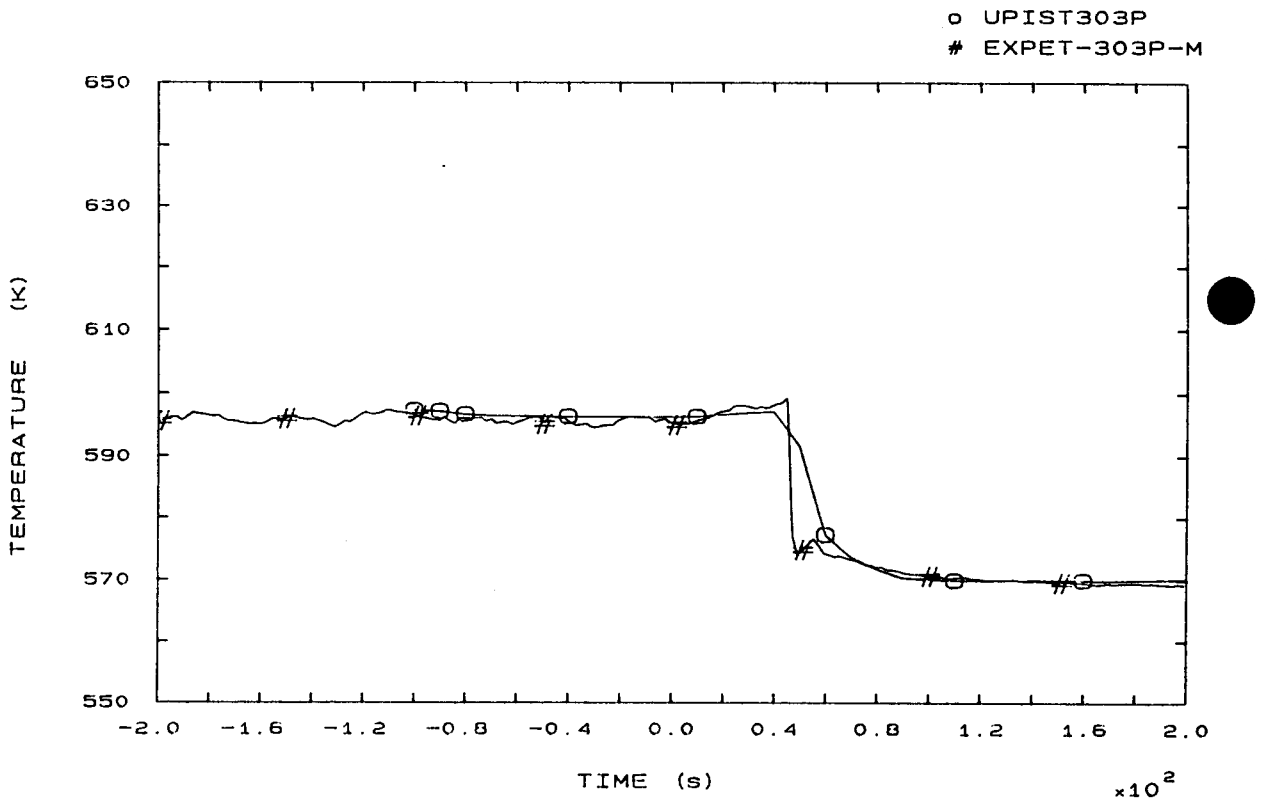

FIG. 32b LP3 HOT LEG OUTLET VESSEL TEMPERATURE

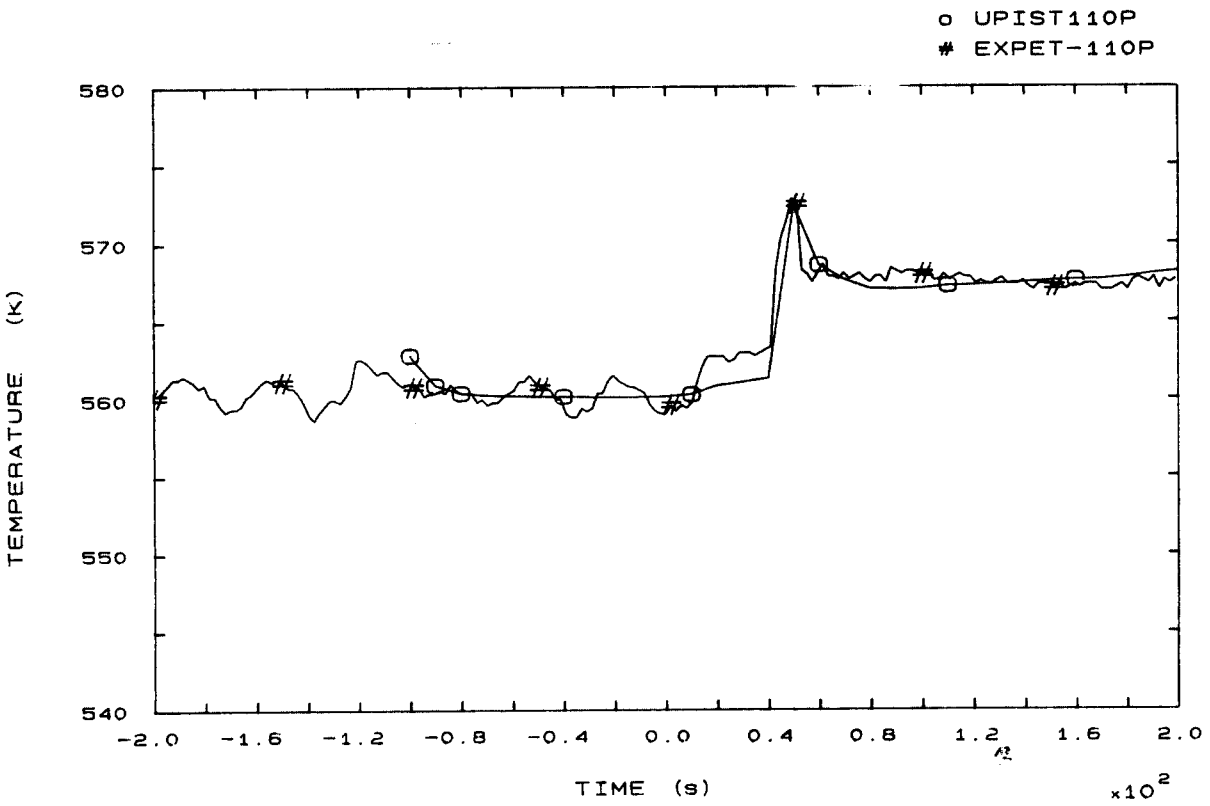

FIG. 42b SG1 OUTLET TEMPERATURE

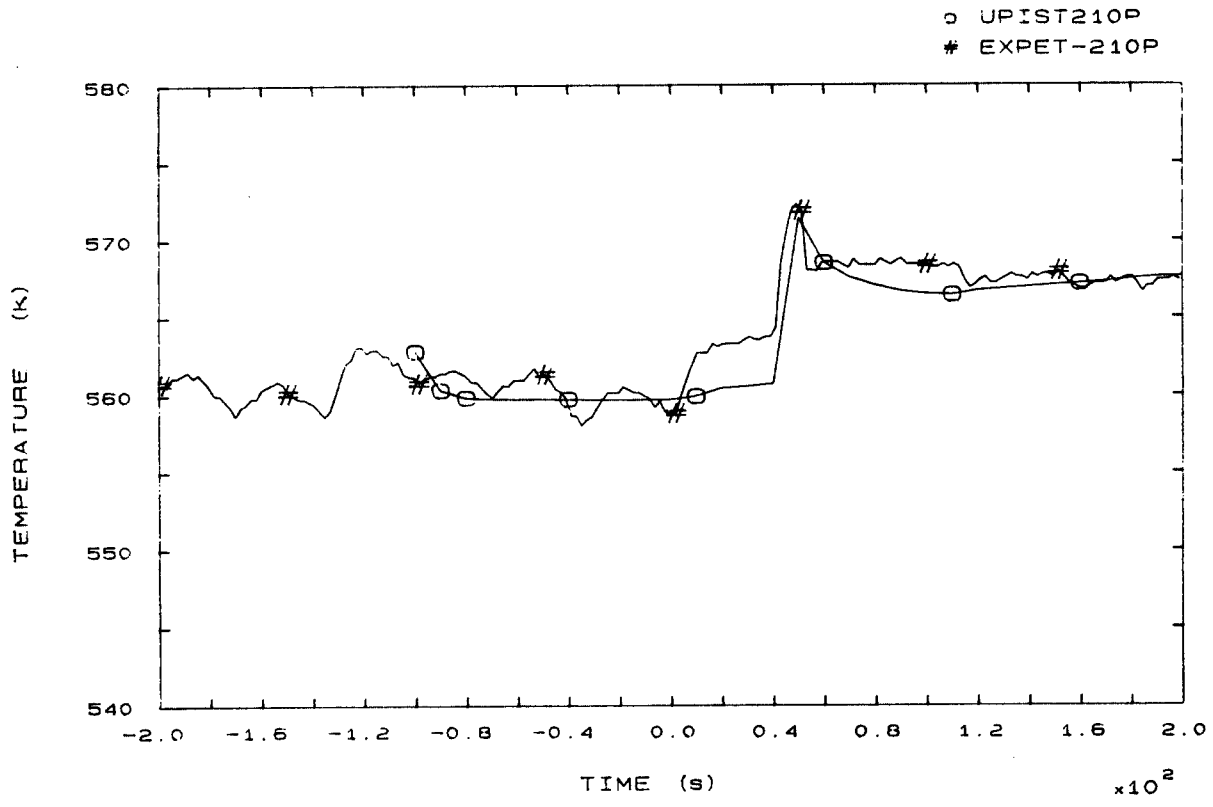

FIG. 44b SG2 OUTLET TEMPERATURE

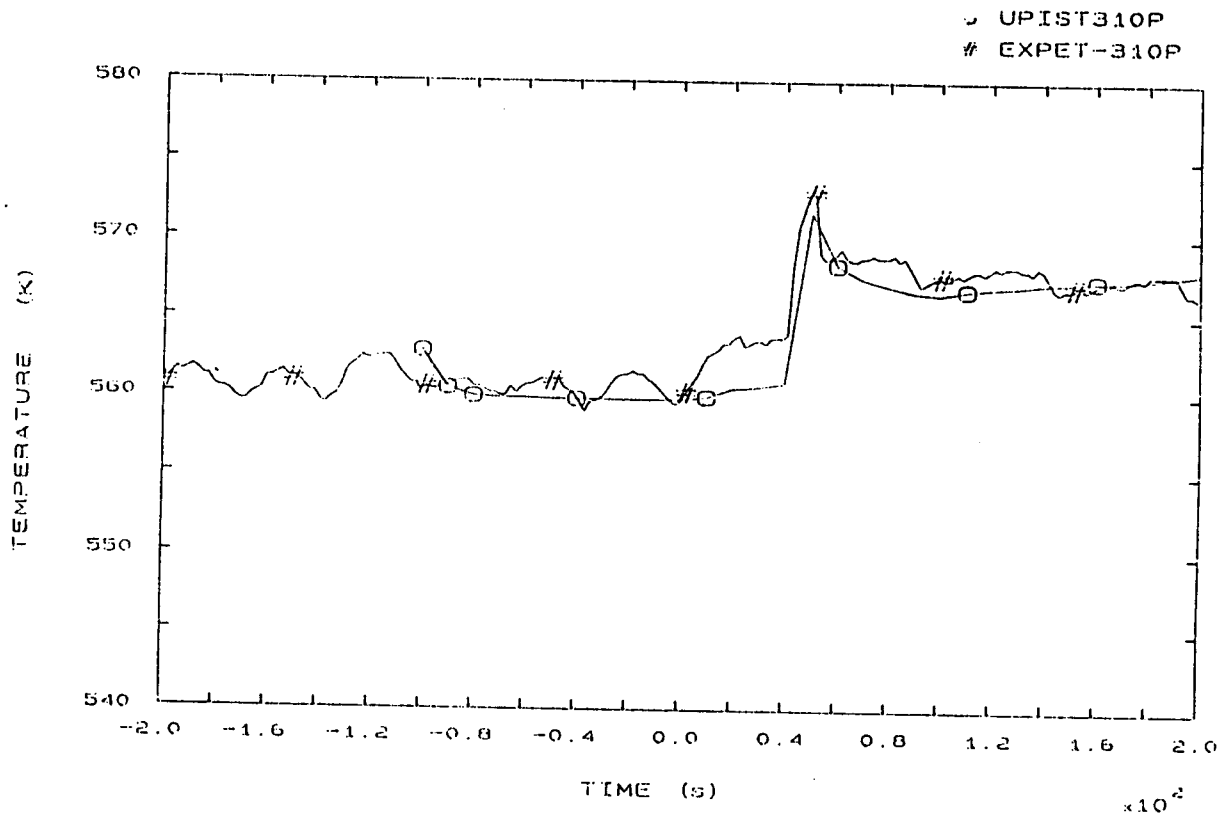

FIG. 46b SG3 OUTLET TEMPERATURE

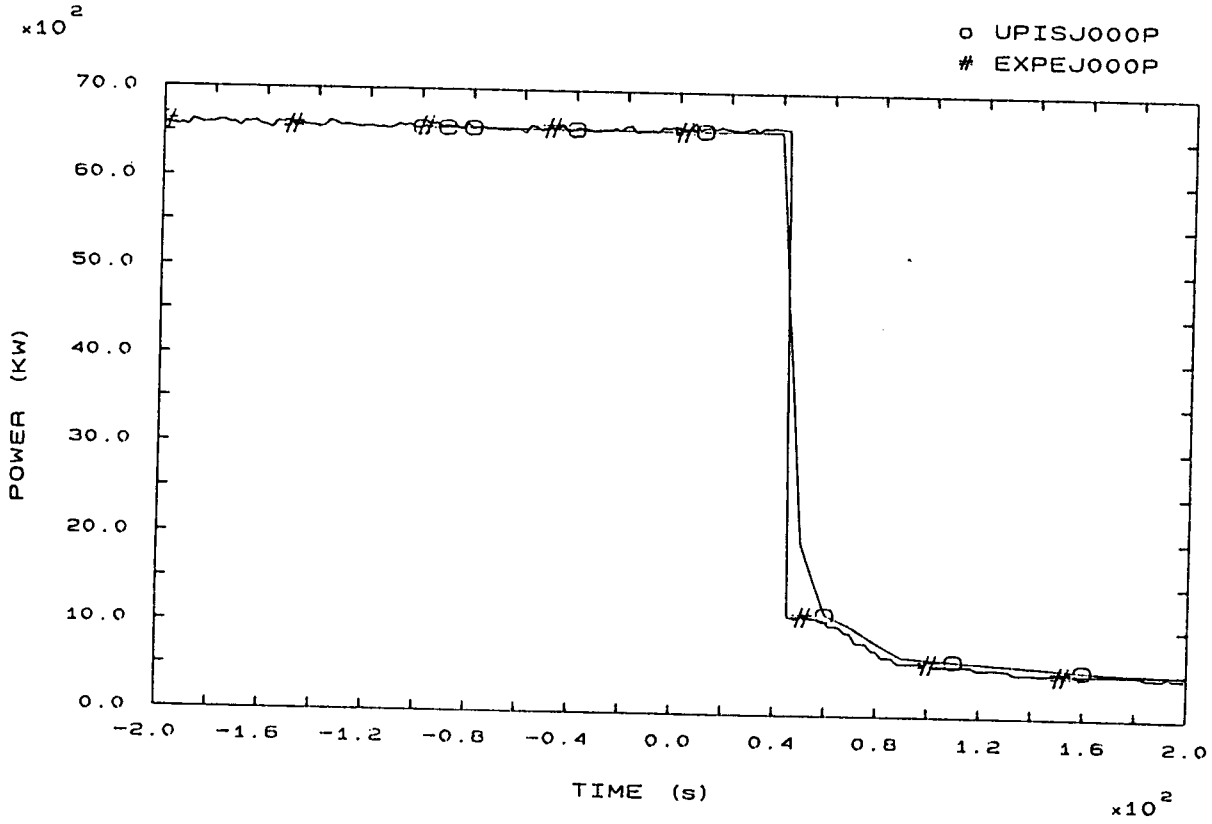

FIG. 81b HEATER RODS POWER

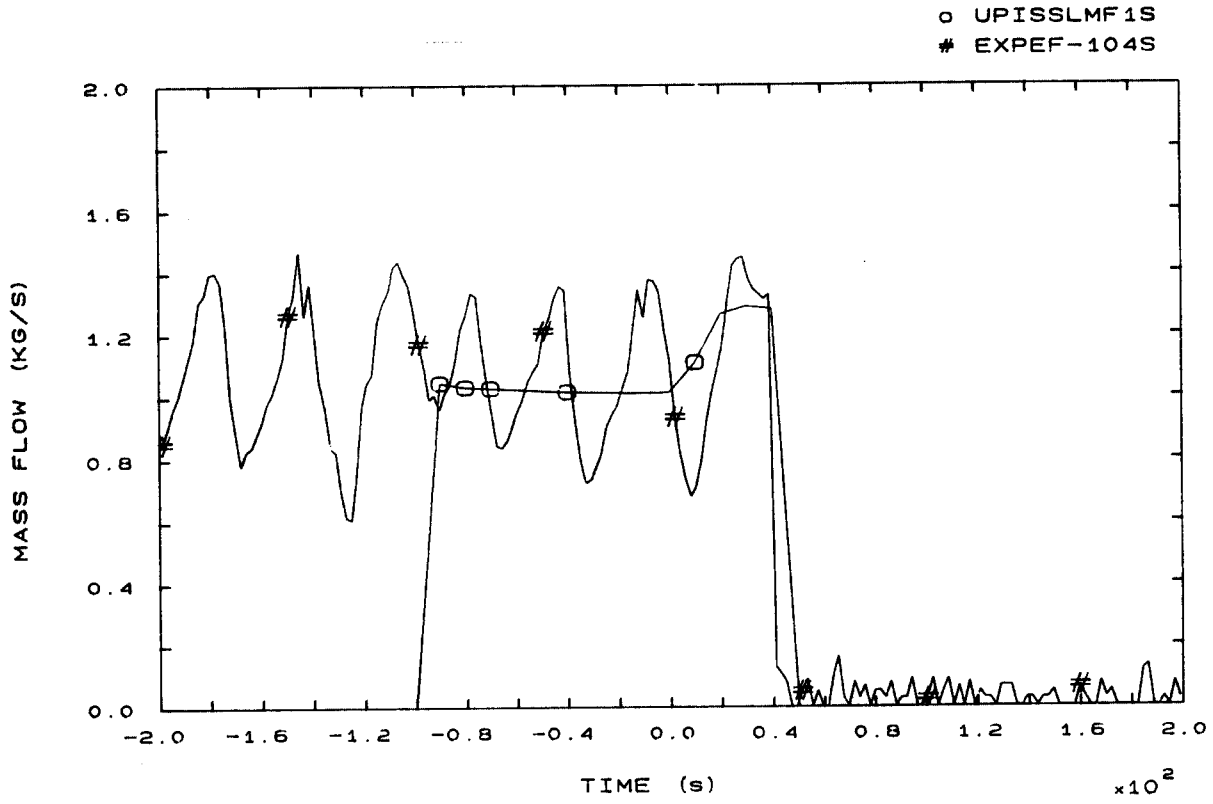

FIG. 96b STEAM LINE 1 MASS FLOW

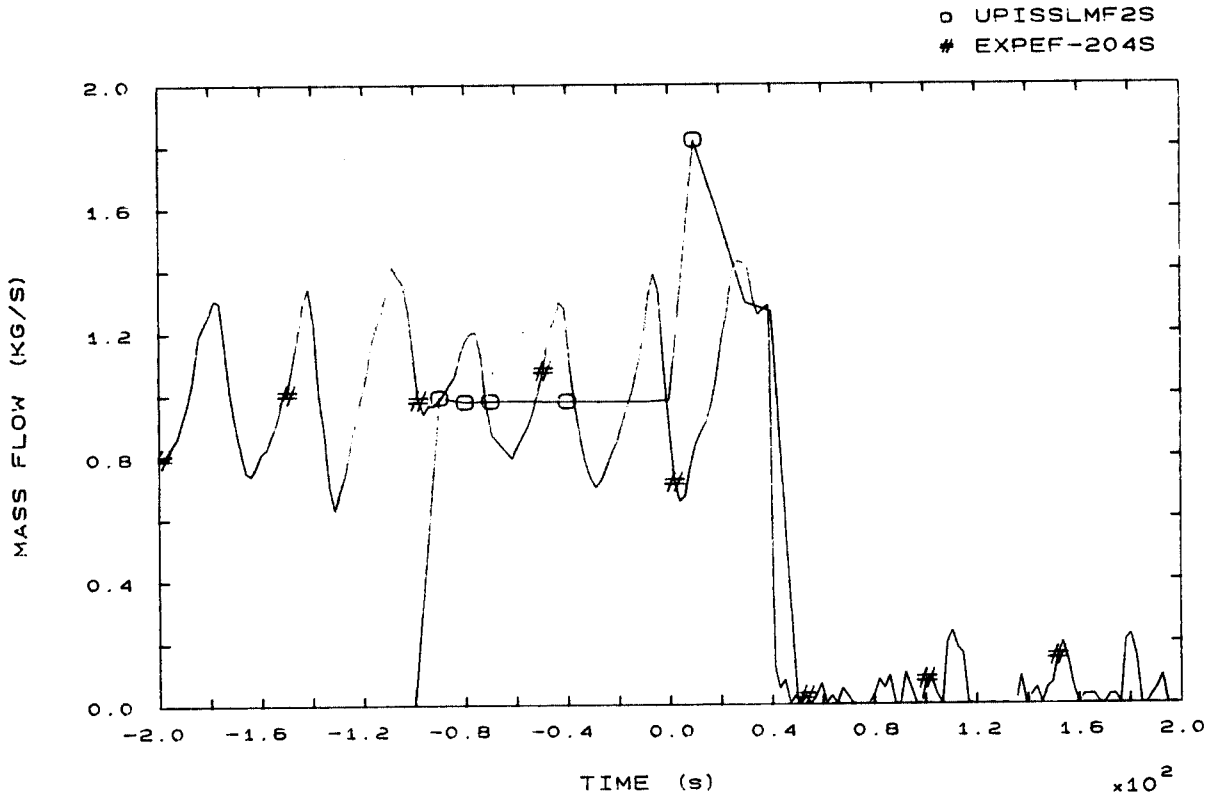

FIG. 97b STEAM LINE 2 MASS FLOW

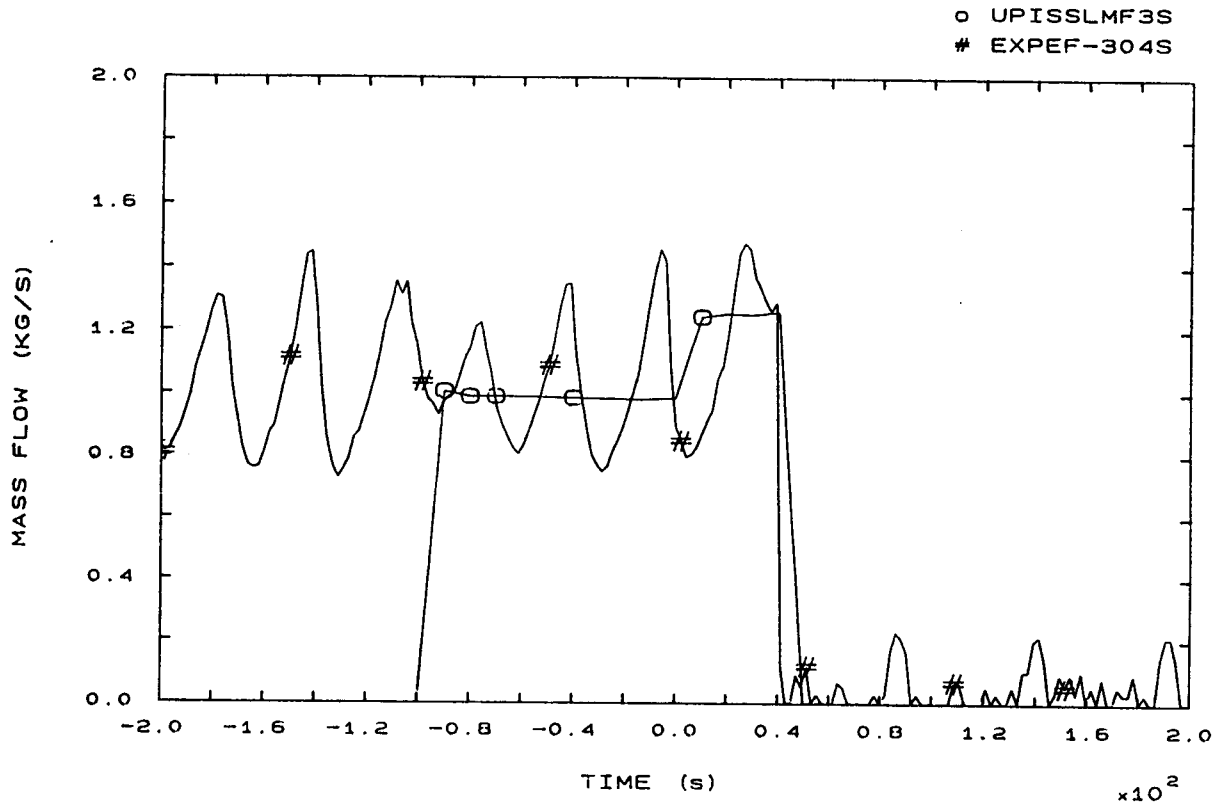

FIG. 98b STEAM LINE 3 MASS FLOW

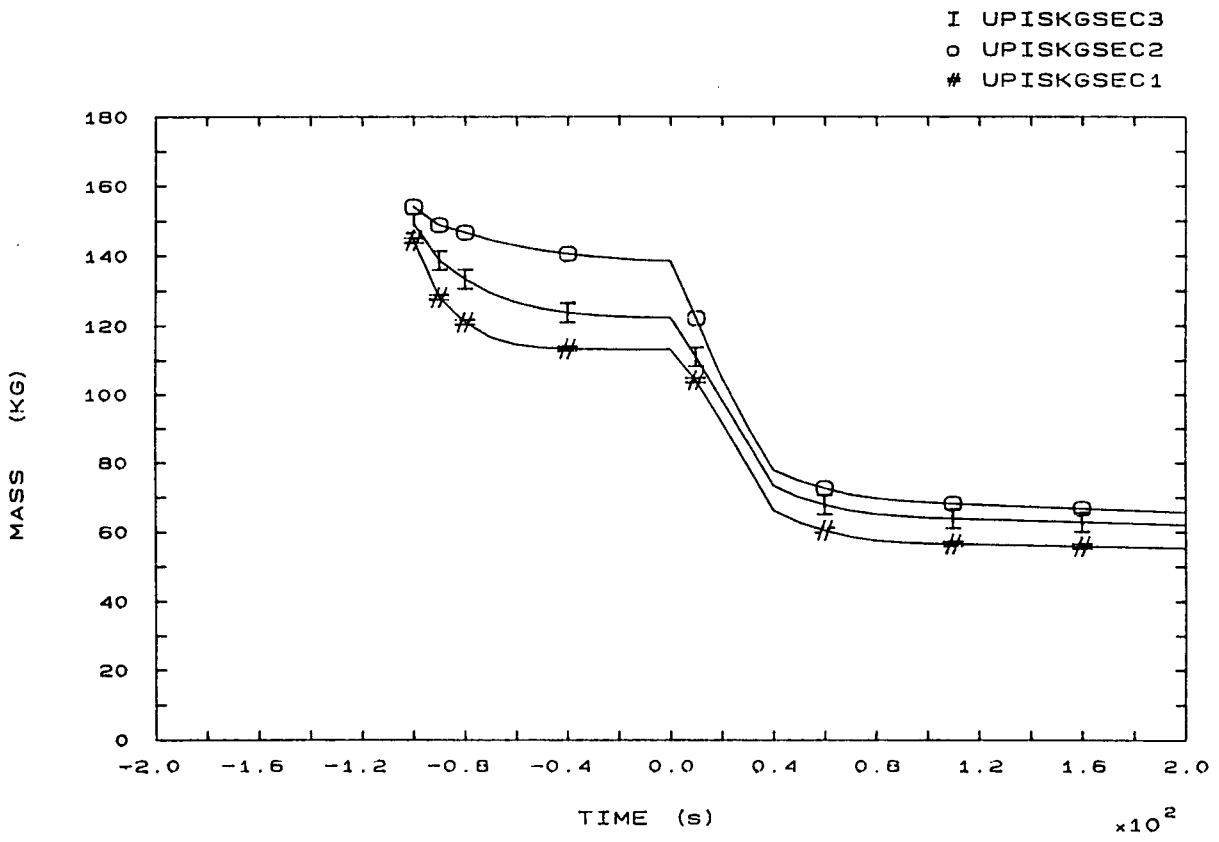

FIG. 142b SECONDARY COOLANT TOTAL MASS IN SGs

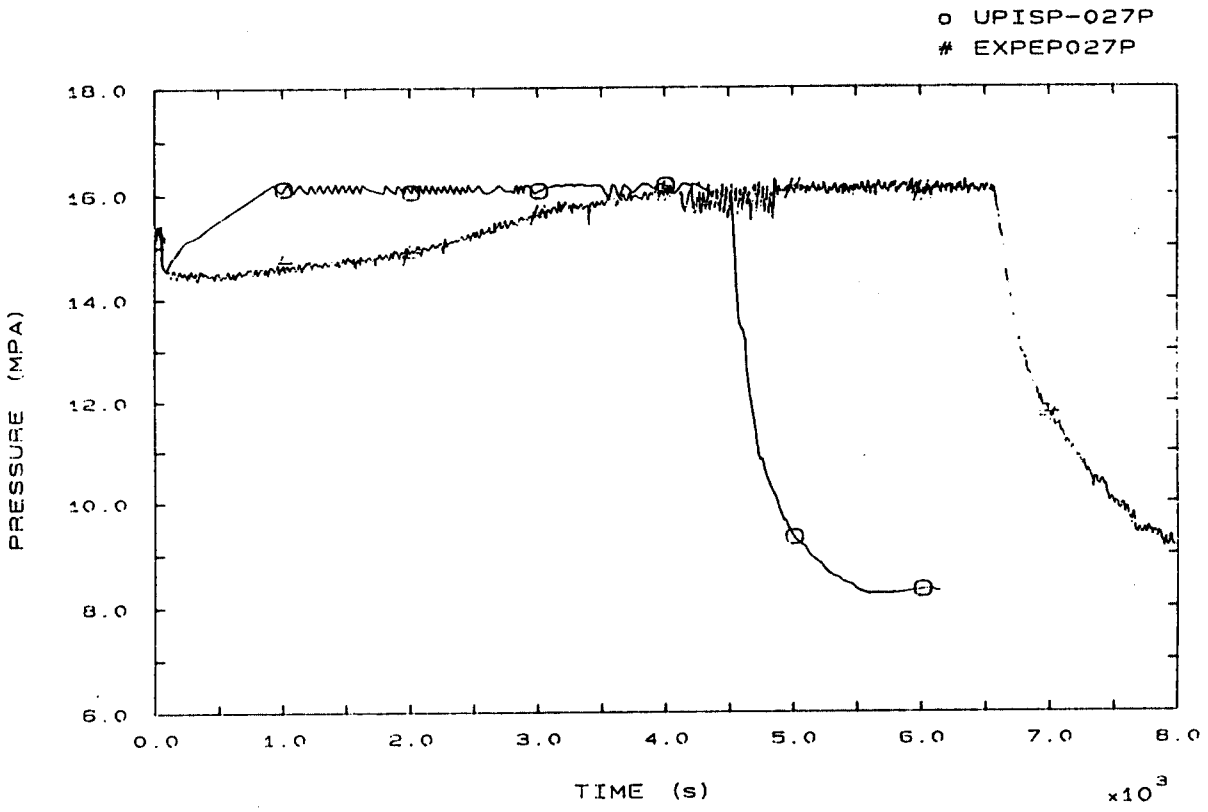

FIG. 1 PRESSURIZER PRESSURE

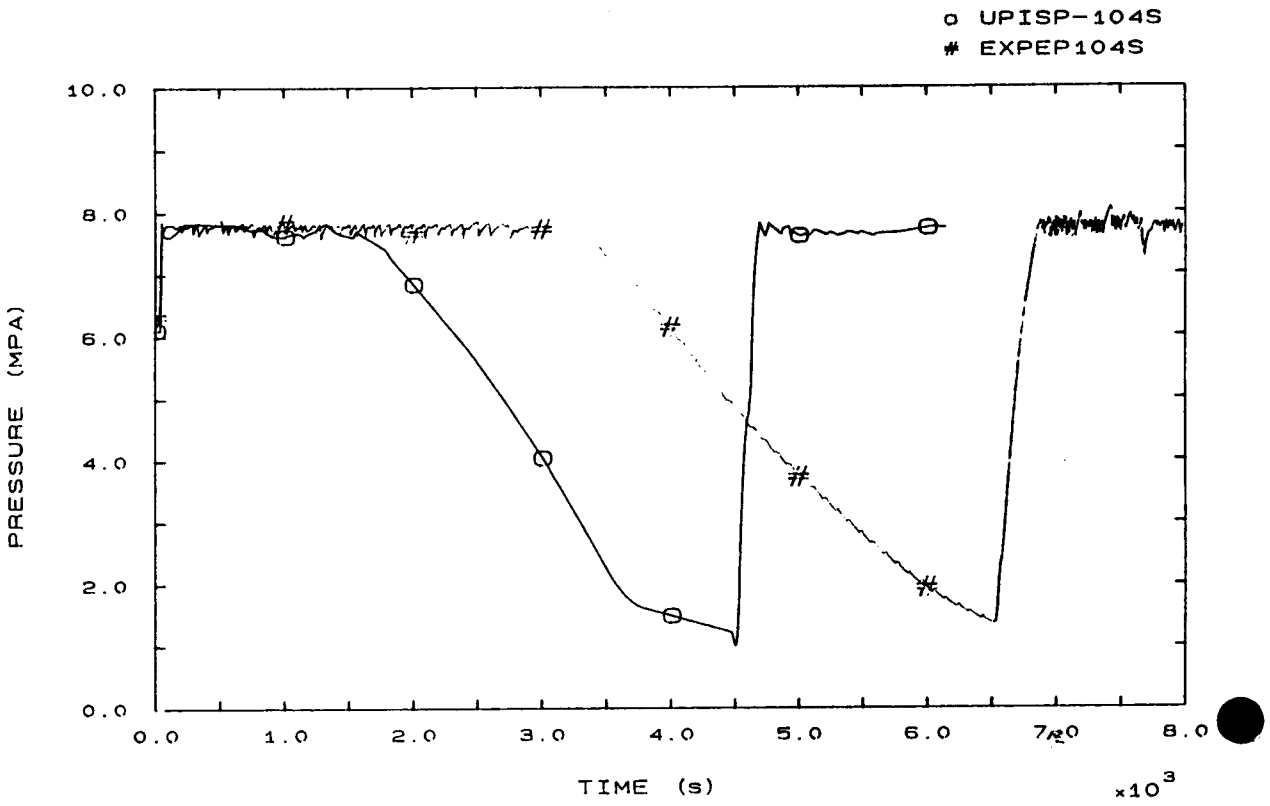

FIG. 3 SG1 STEAM DOME PRESSURE

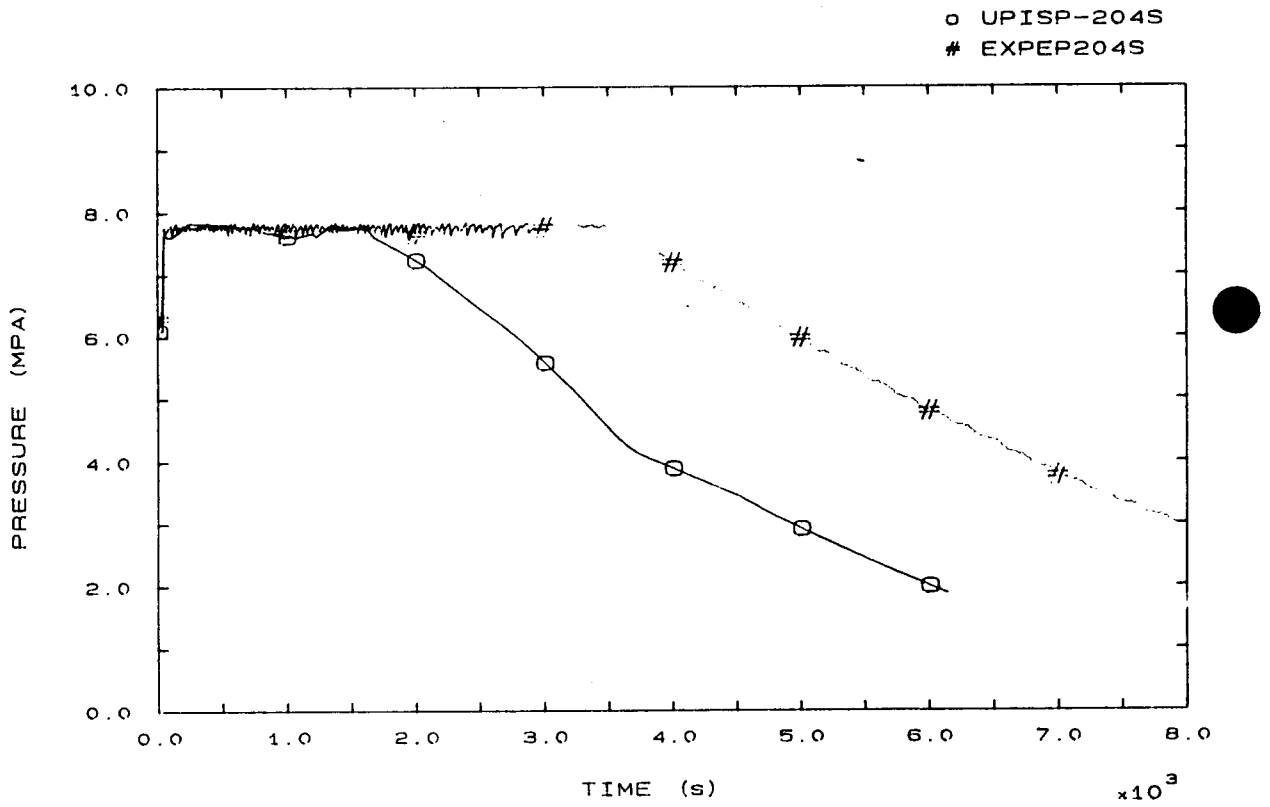

FIG. 4 SG2 STEAM DOME PRESSURE

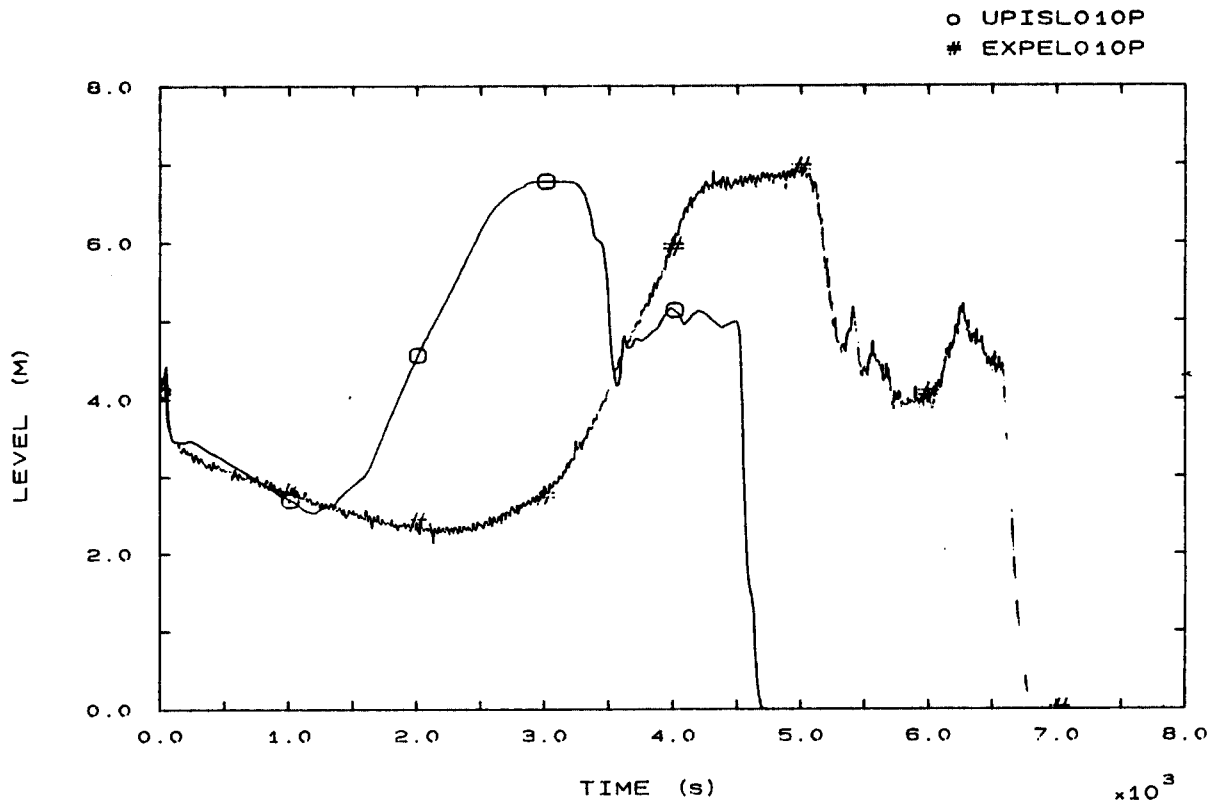

FIG. 6 PRESSURIZER LEVEL

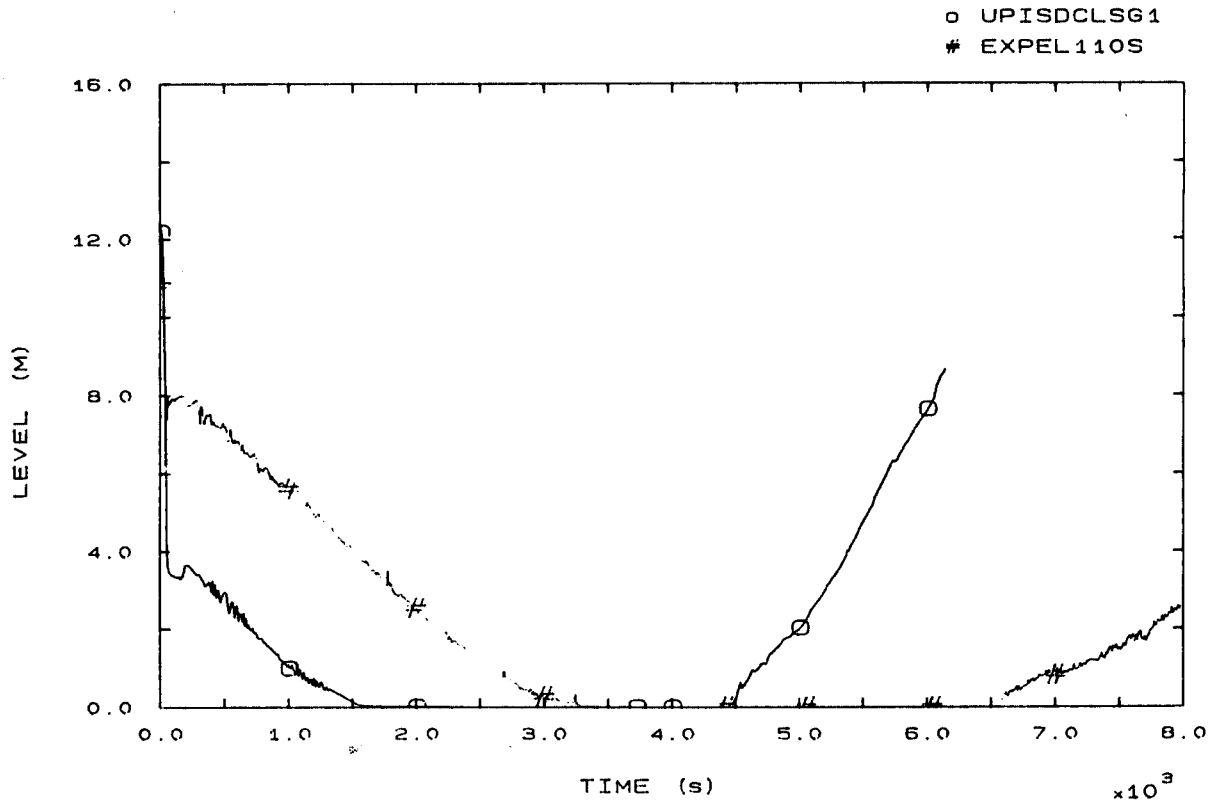

FIG. 7 SG1 DOWNCOMER LEVEL

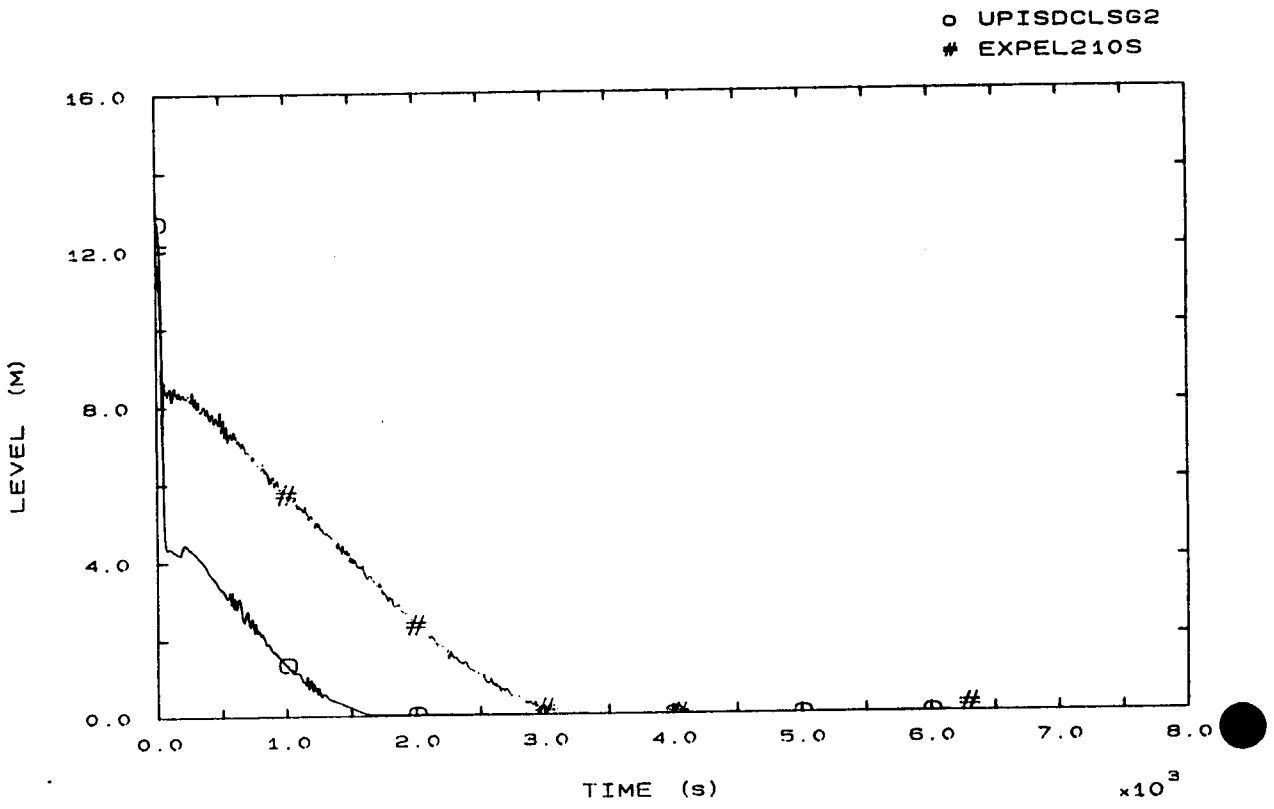

FIG. 8 SG2 DOWNCOMER LEVEL

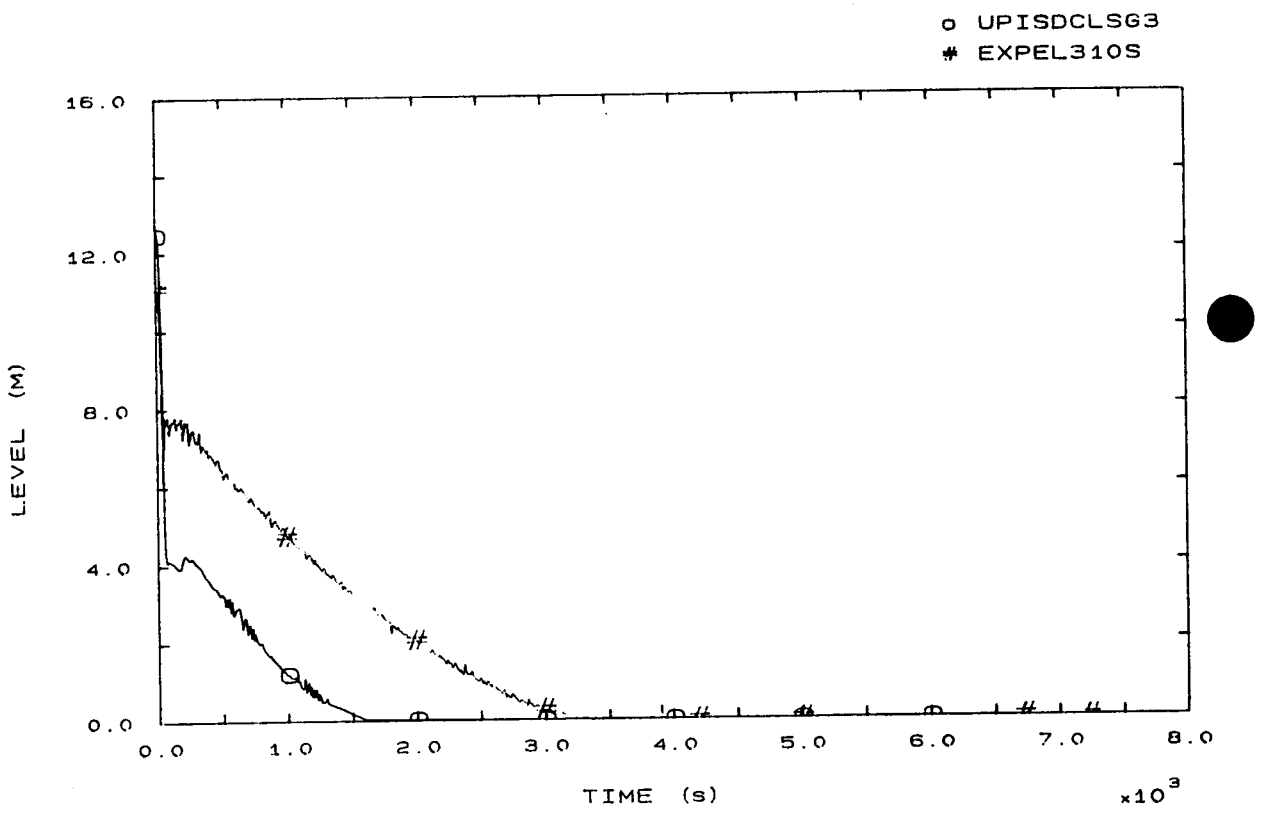

FIG. 9 SG3 DOWNCOMER LEVEL

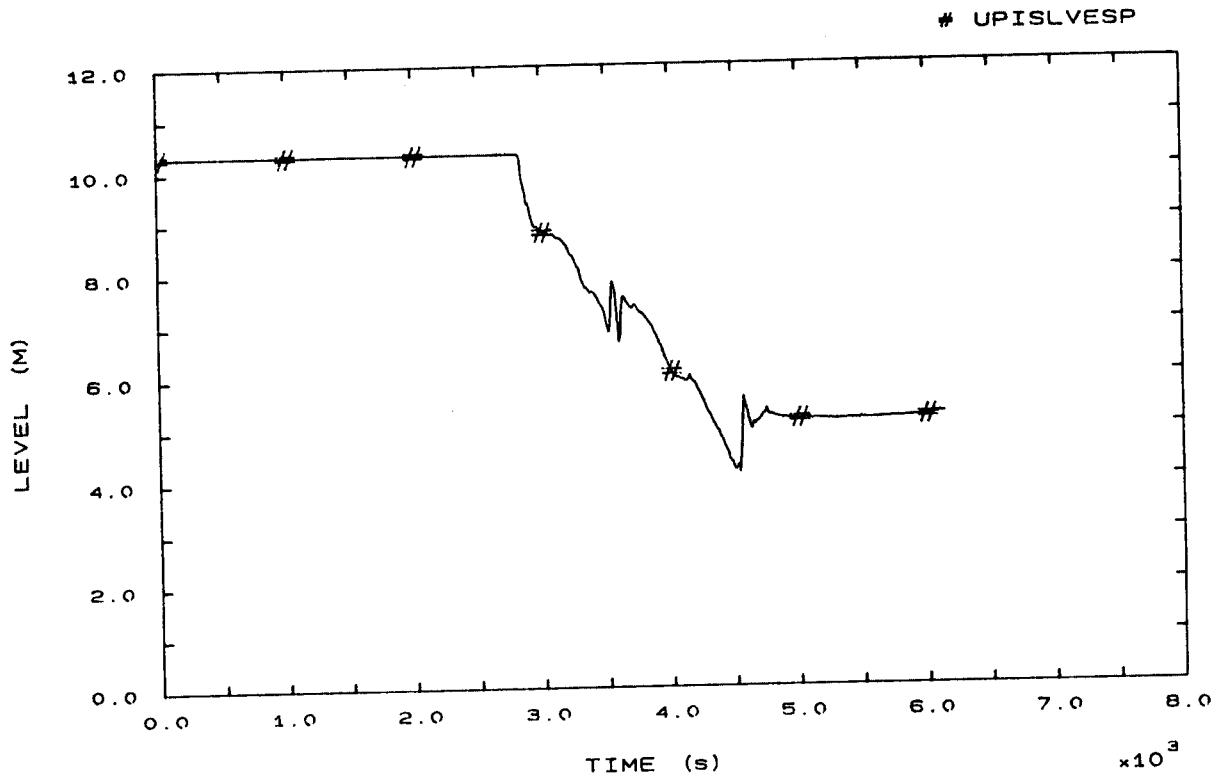

FIG. 10 VESSEL LEVEL

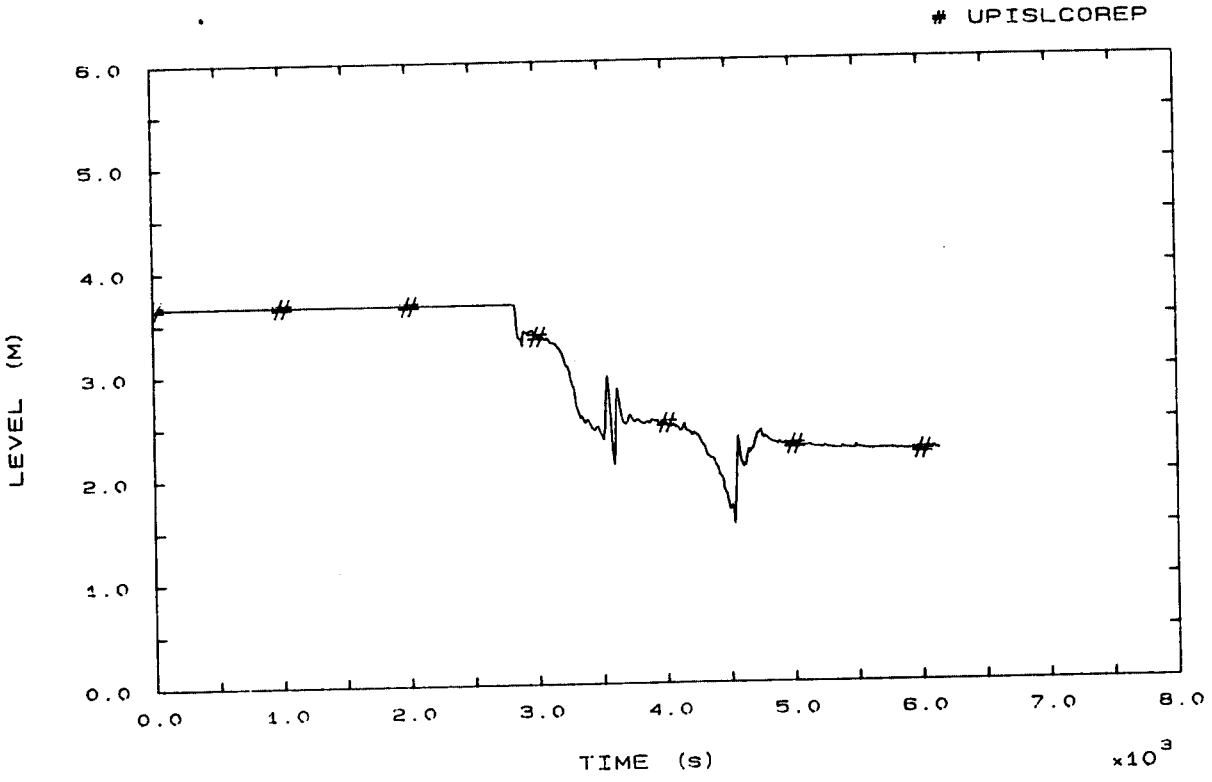

FIG. 11 CORE LEVEL

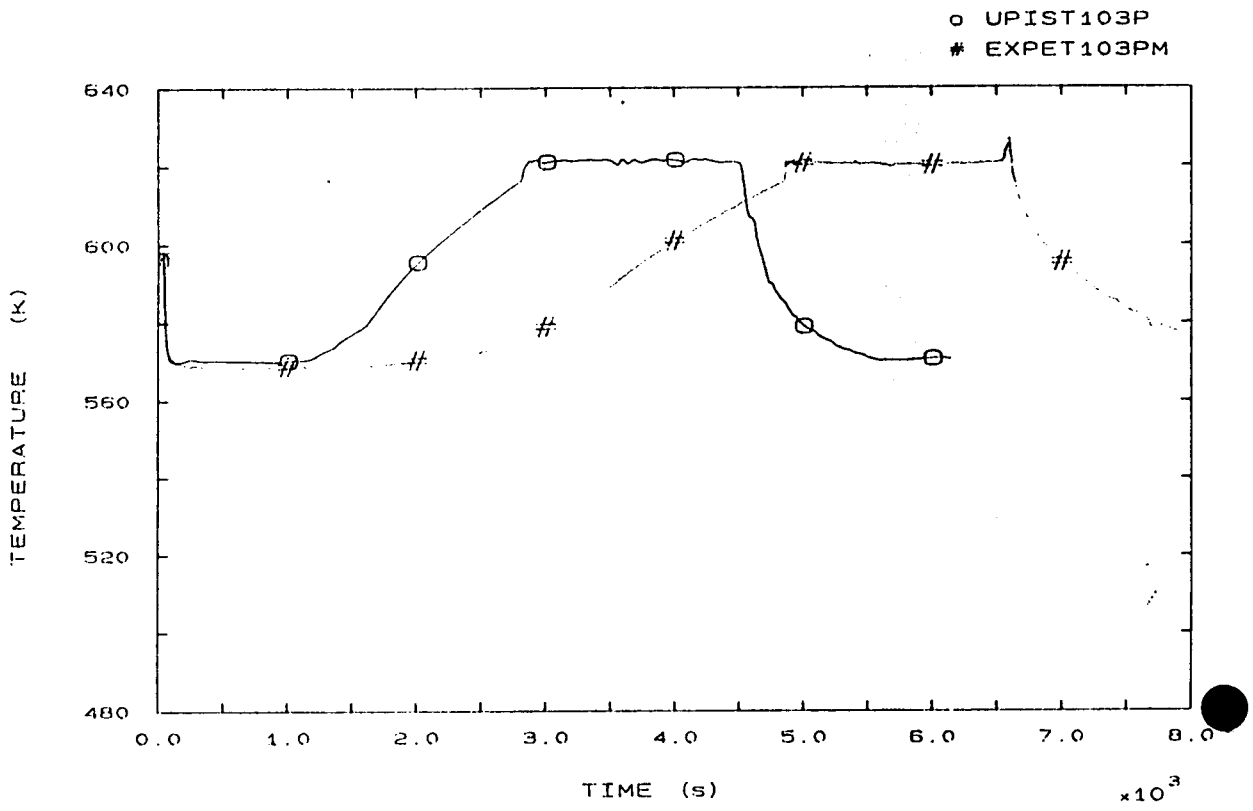

FIG. 12 LP1 HOT LEG OUTLET VESSEL TEMPERATURE

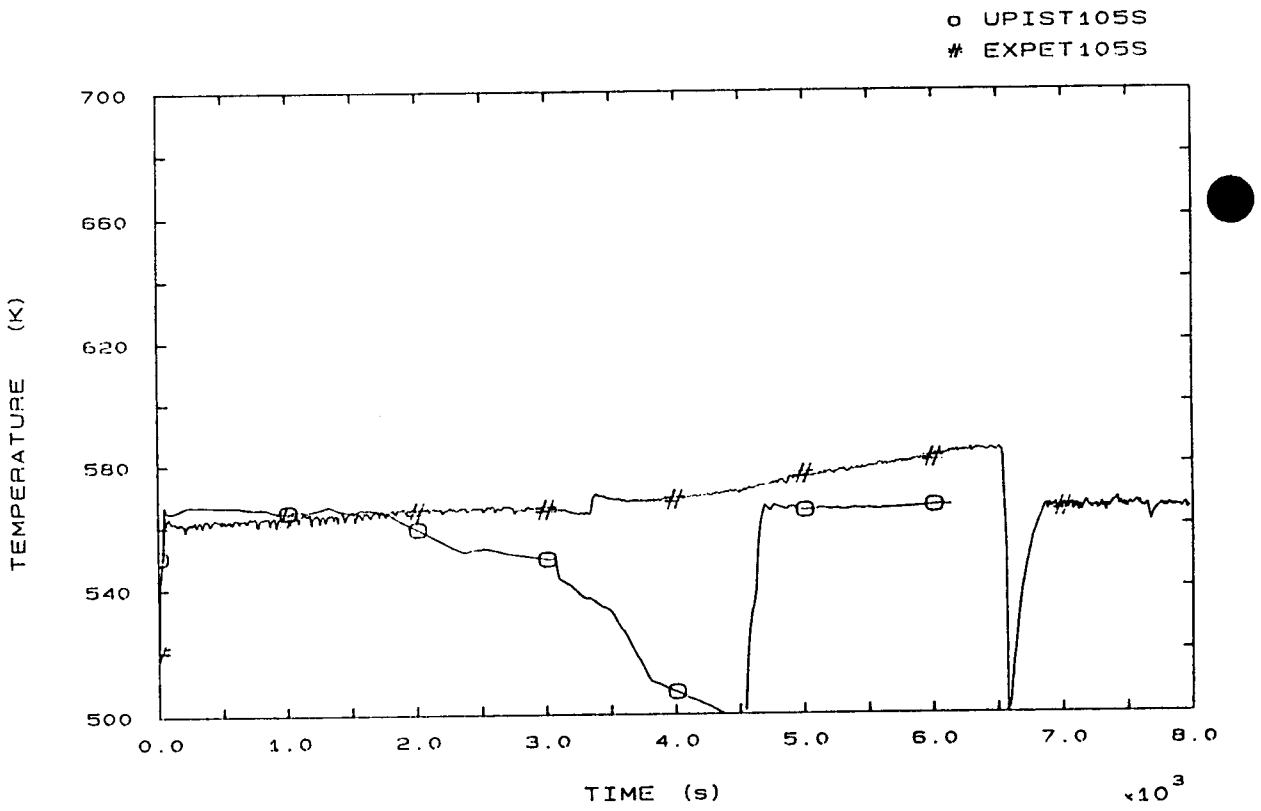

FIG. 15 FLUID TEMPERATURE SG1 RISER 185 MM A.T.S.

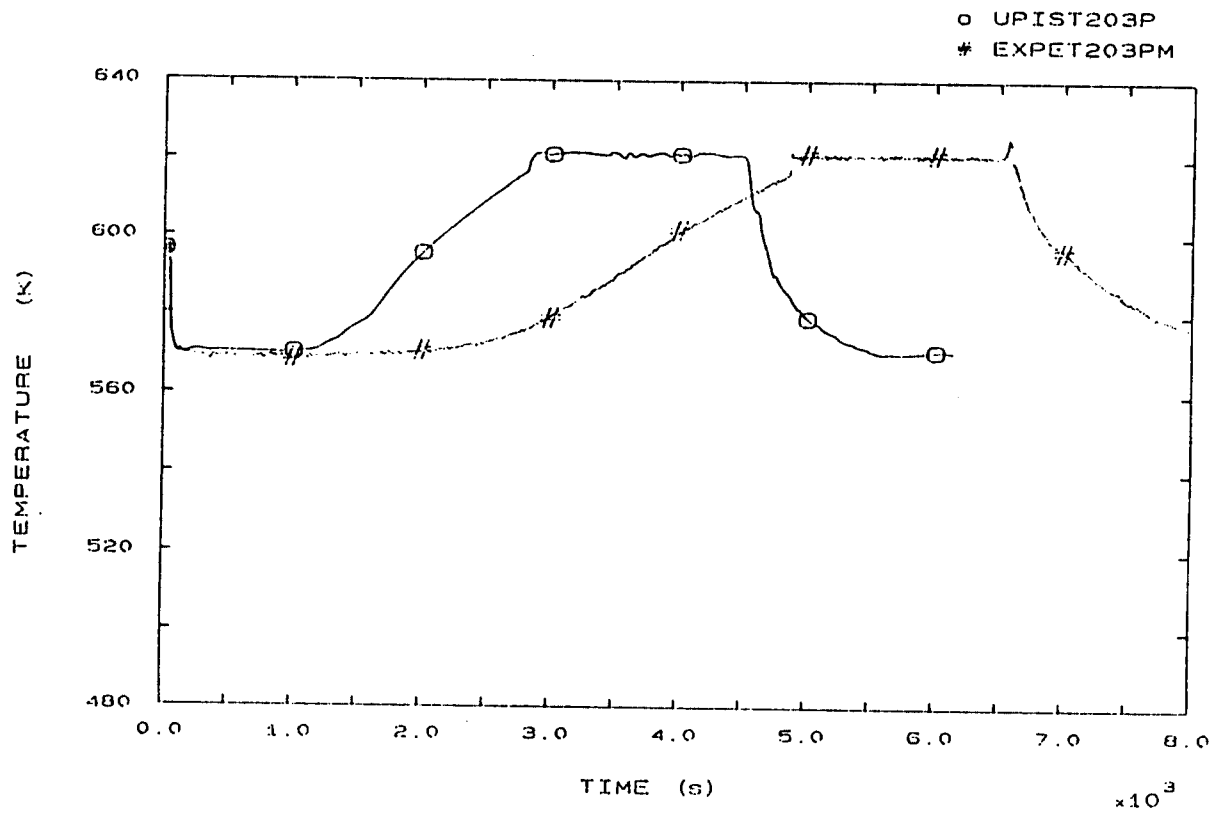

FIG. 22 LP2 HOT LEG OUTLET VESSEL TEMPERATURE

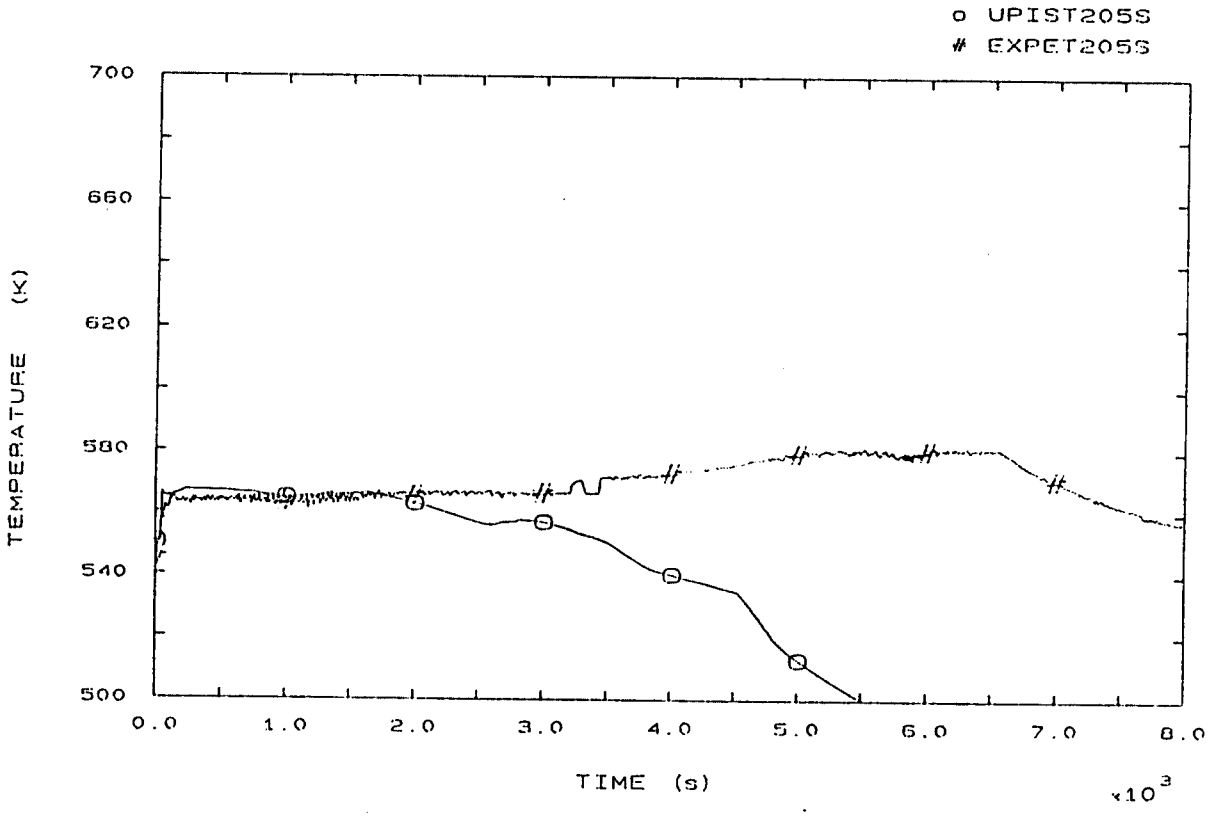

FIG. 25 FLUID TEMPERATURE SG2 RISER 185 MM A.T.S.

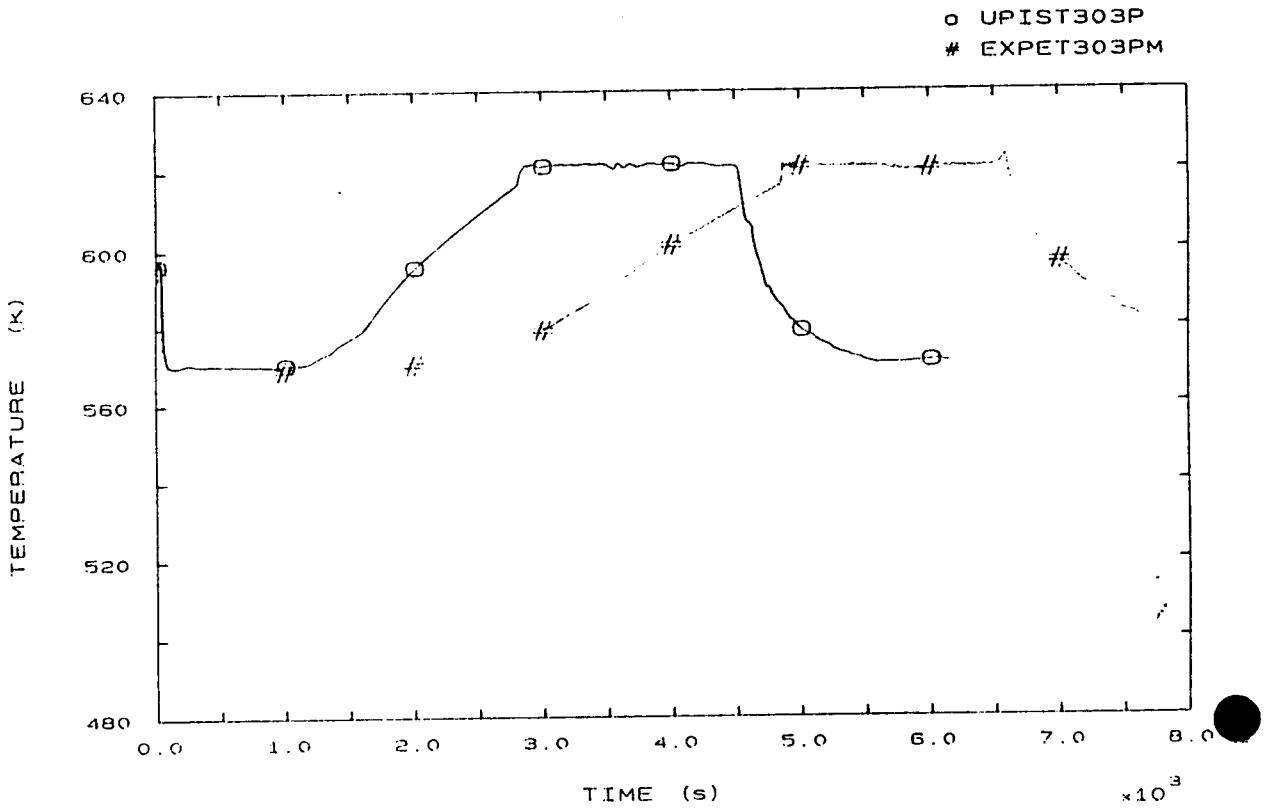

FIG. 32 LP3 HOT LEG OUTLET VESSEL TEMPERATURE

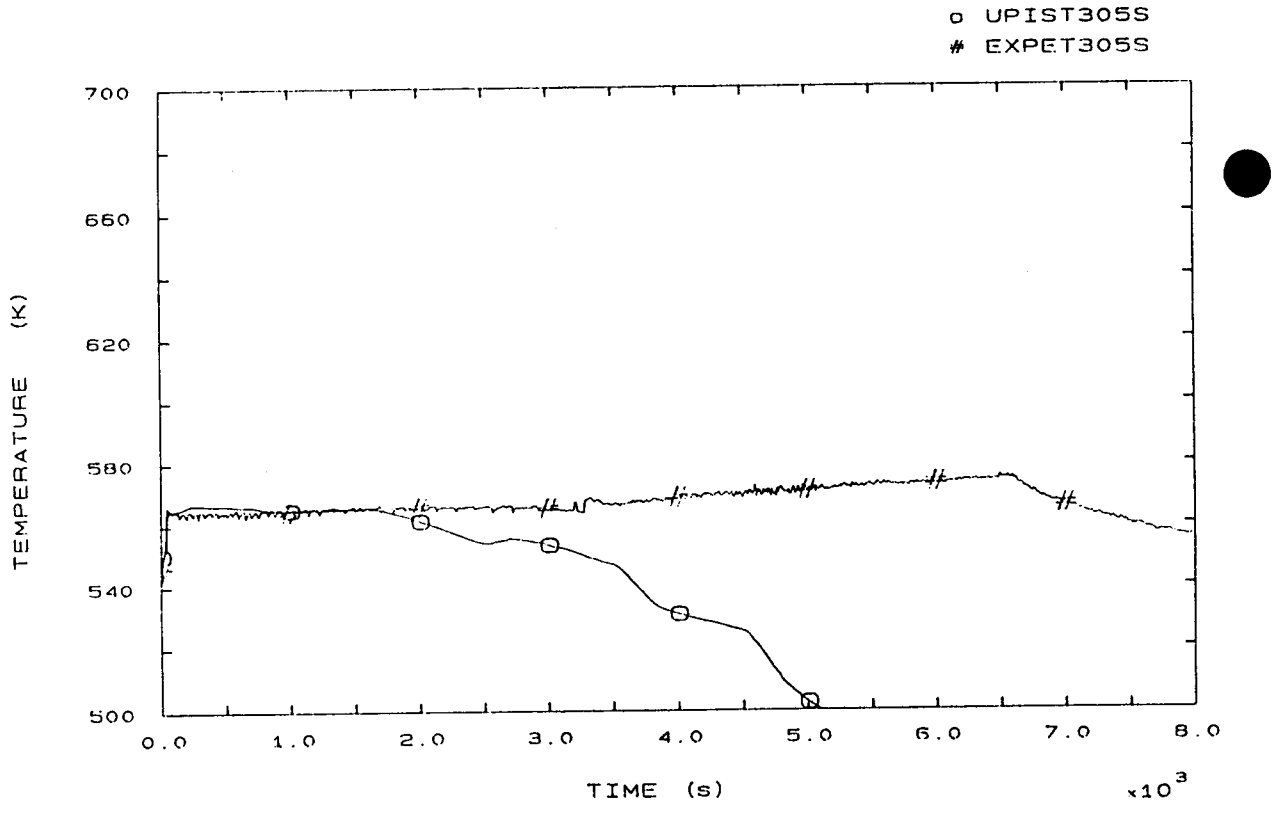

FIG. 35 FLUID TEMPERATURE SG3 RISER 185 MM A.T.S.

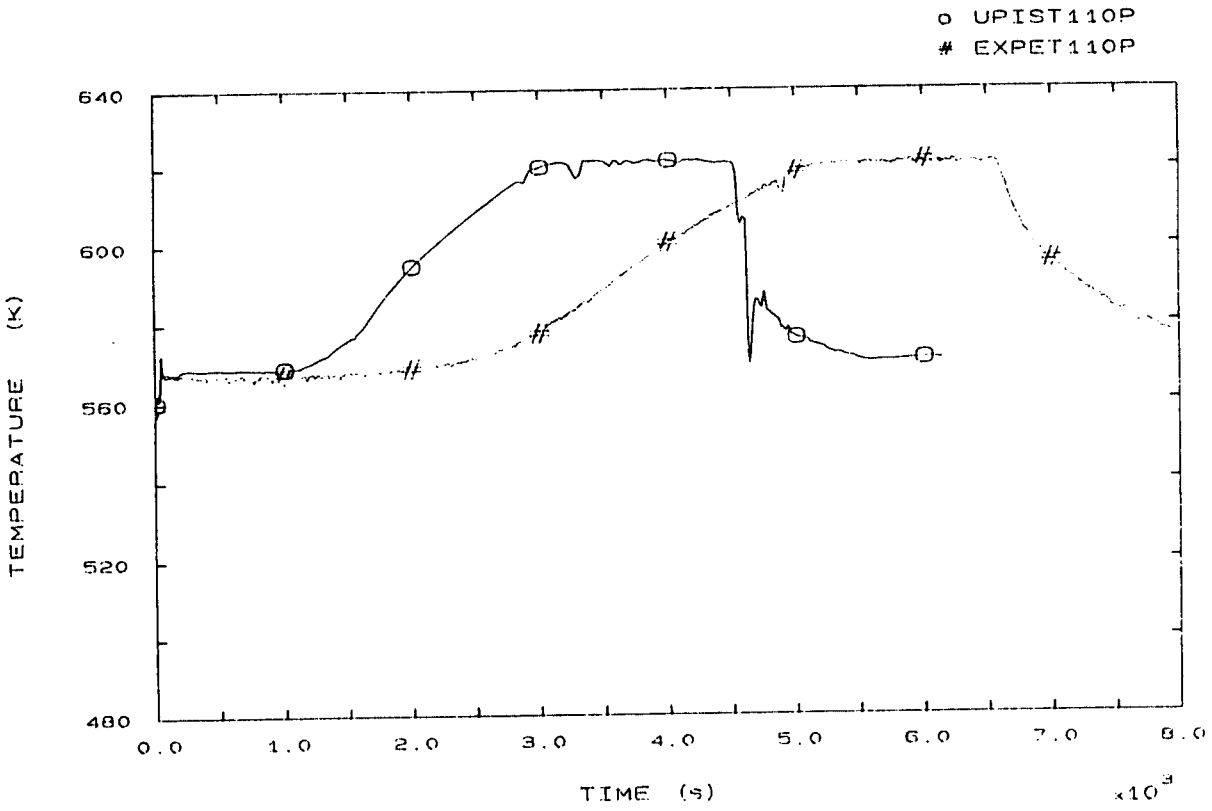

FIG. 42 SG1 OUTLET TEMPERATURE

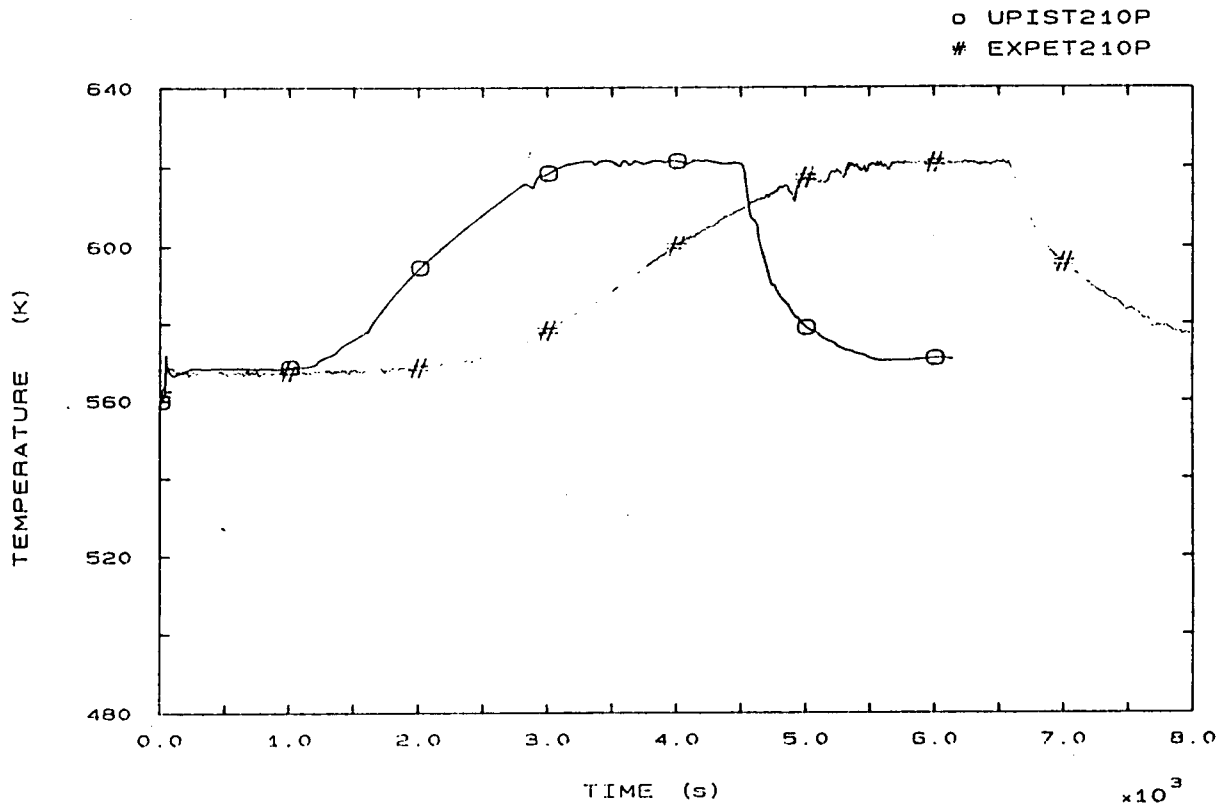

FIG. 44 SG2 OUTLET TEMPERATURE

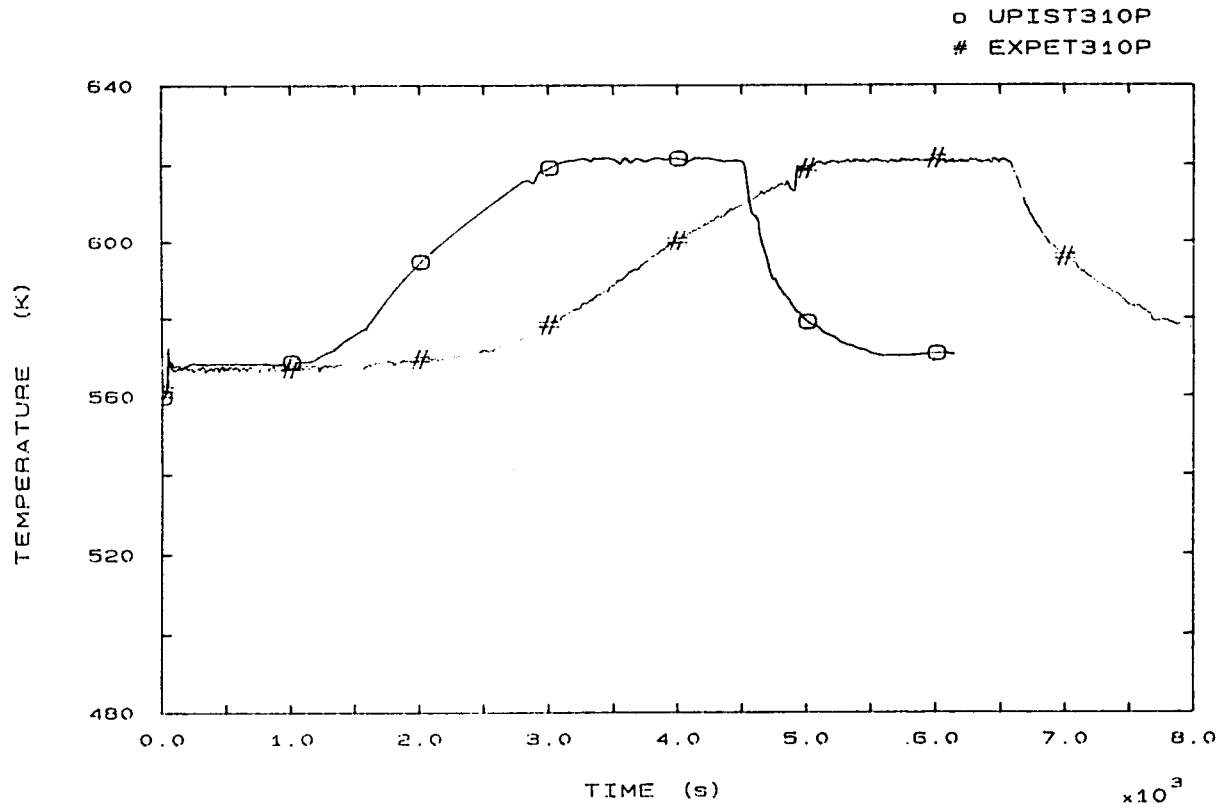

FIG. 46 SG3 OUTLET TEMPERATURE

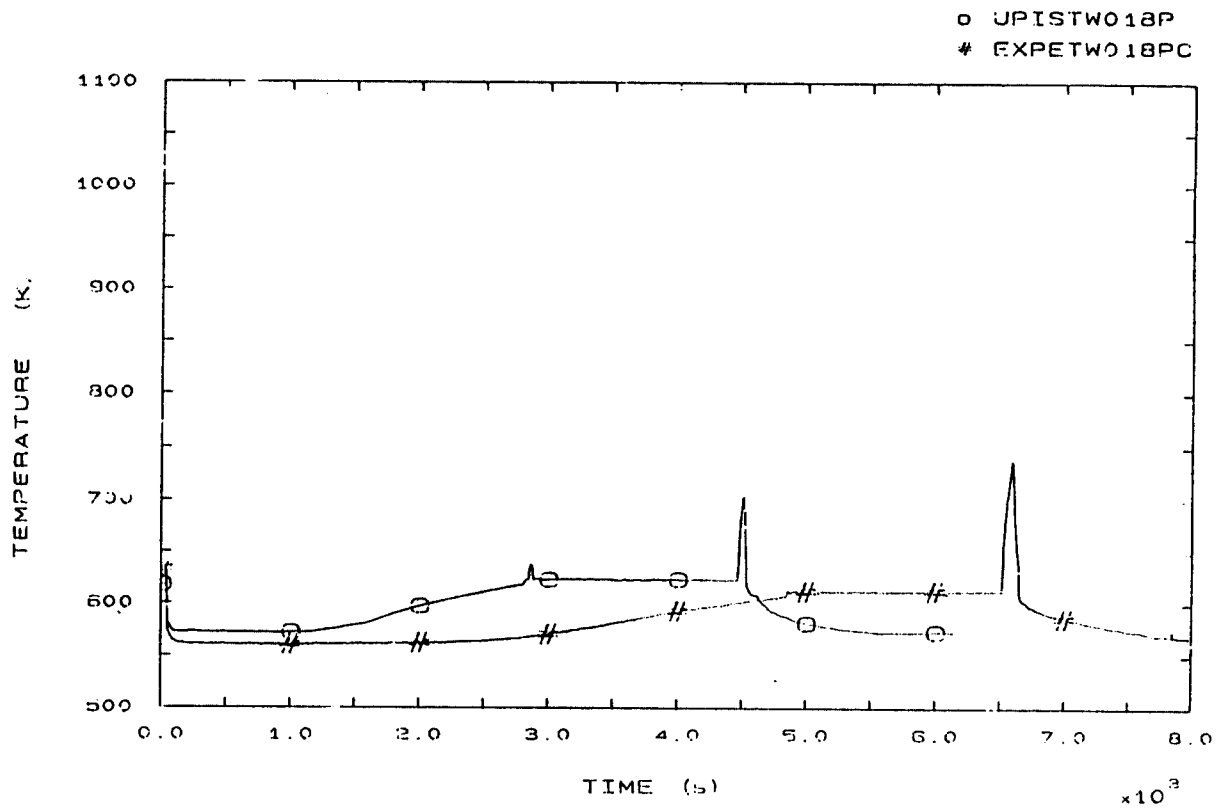

FIG. 51 SURFACE TEMPERATURE AT ROD BUNDLE ELEVATION 3294 MM

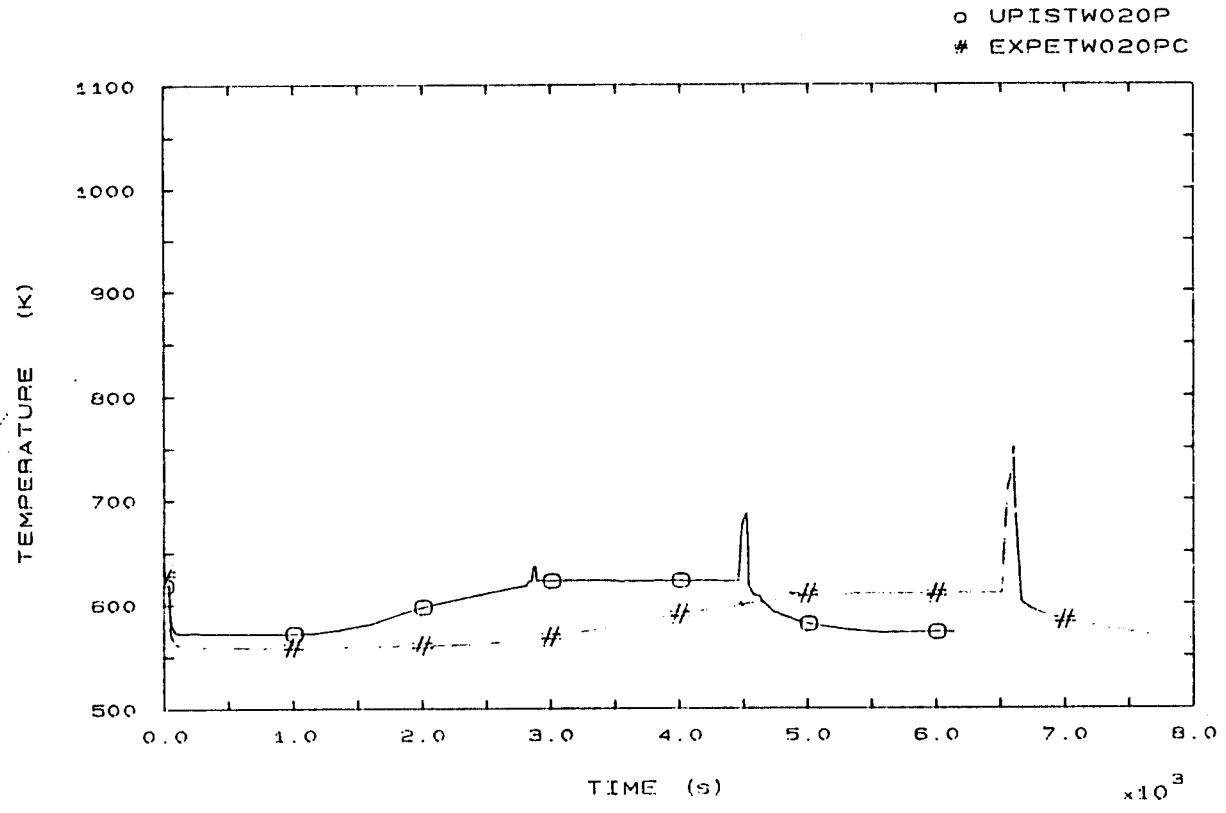

FIG. 52 SURFACE TEMPERATURE AT ROD BUNDLE ELEVATION 3640 MM

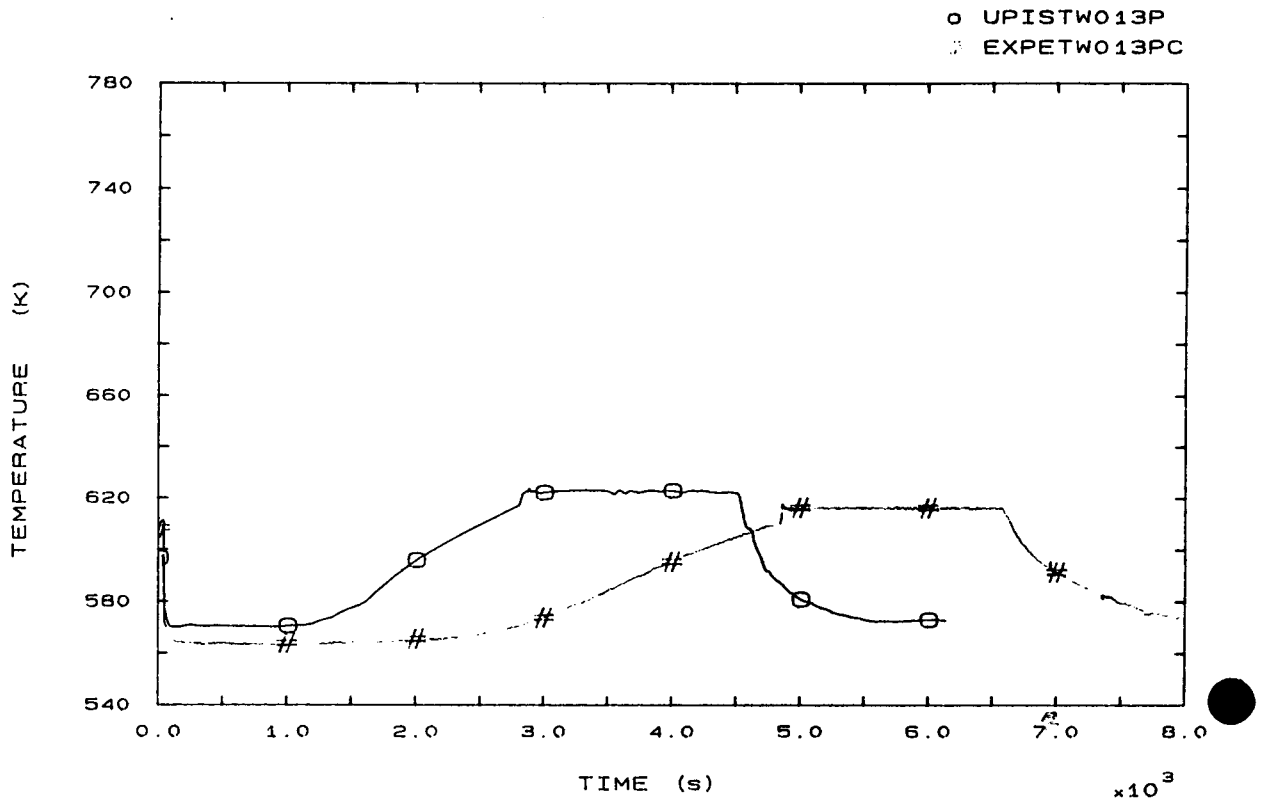

FIG. 49 CORE SURFACE TEMPERATURE AT ROD BUNDLE ELEVATION 1074 MM

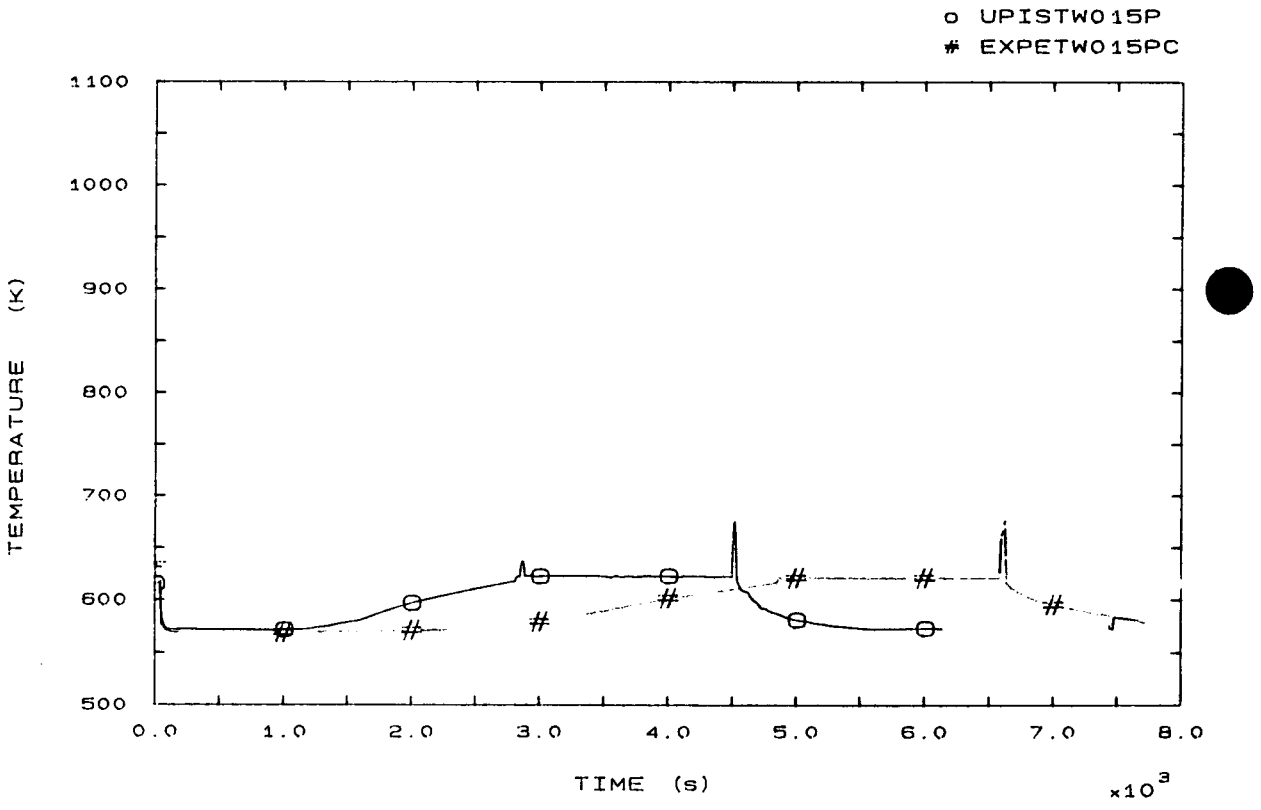

FIG. 50 SURFACE TEMPERATURE AT ROD BUNDLE ELEVATION 2294 MM

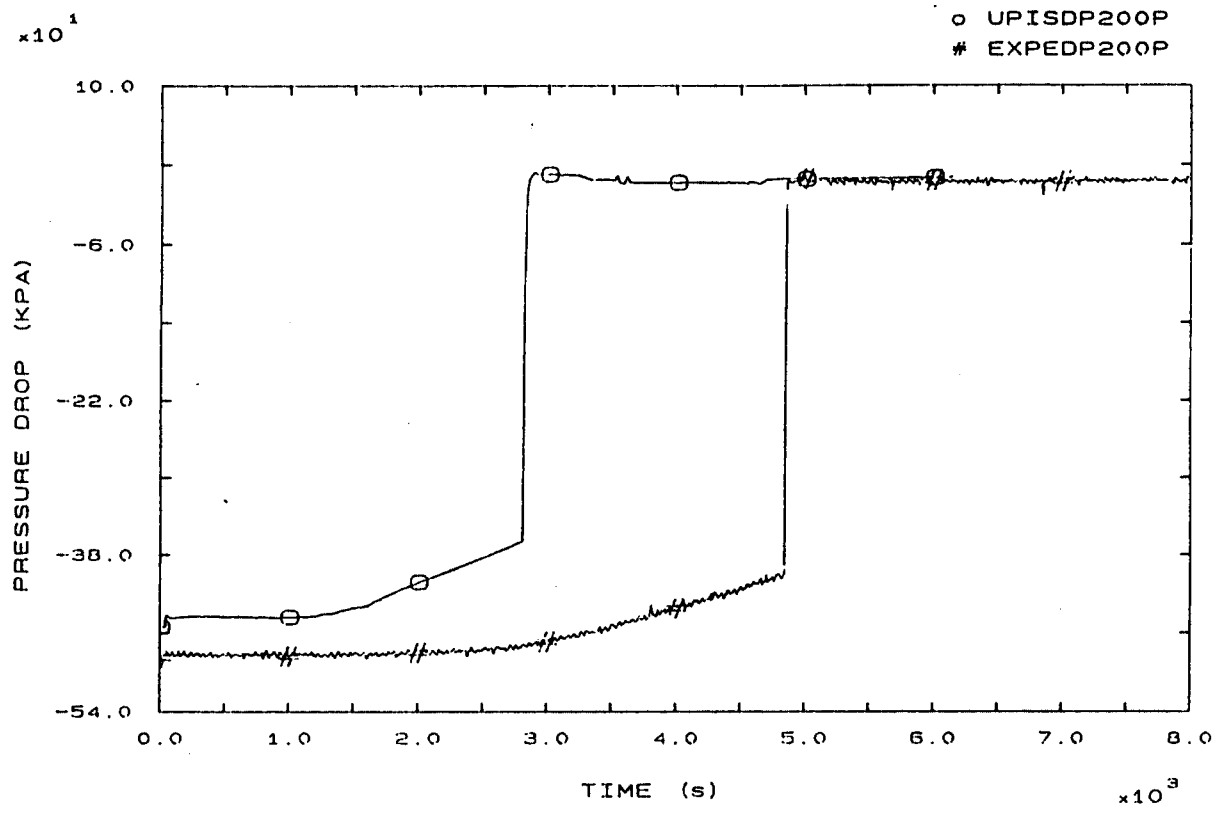

FIG. 55 PRIMARY PUMP 2 PRESSURE DROP

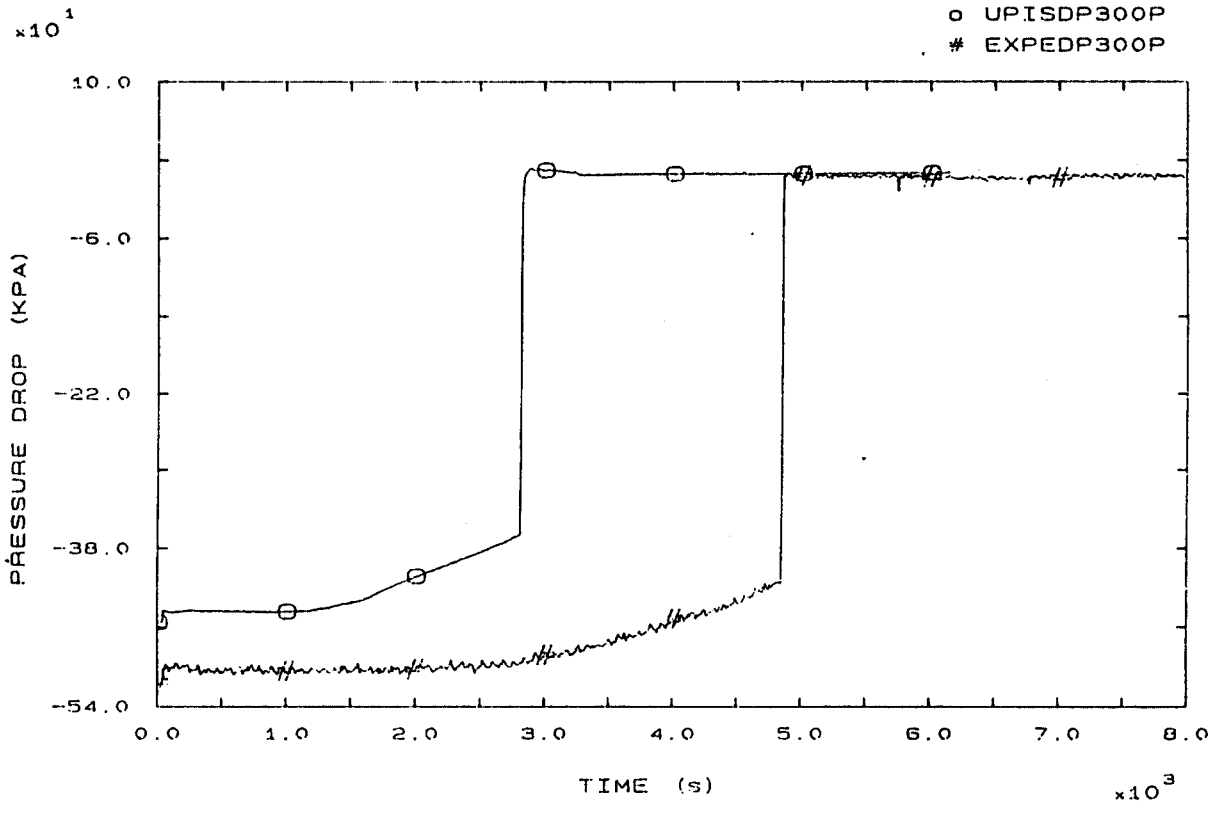

FIG. 56 PRIMARY PUMP 3 PRESSURE DROP

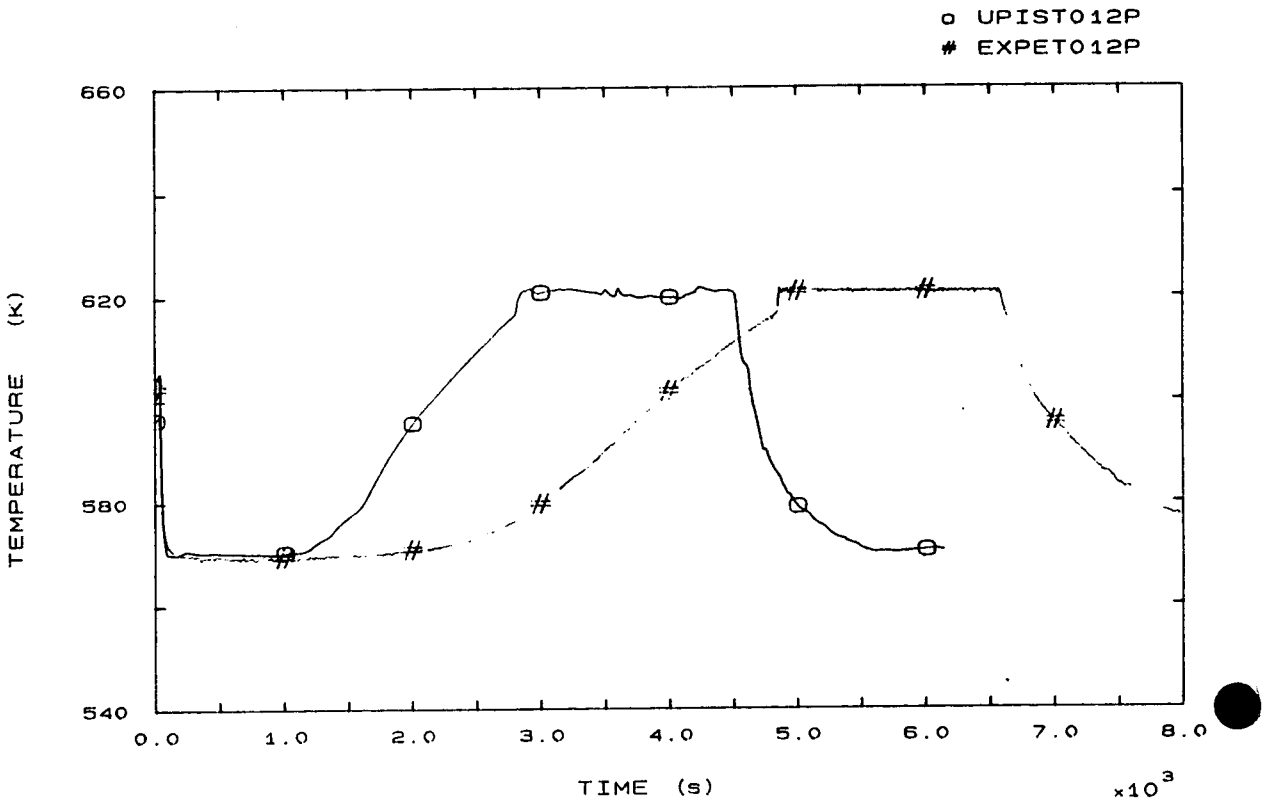

FIG. 53 CORE OUTLET TEMPERATURE

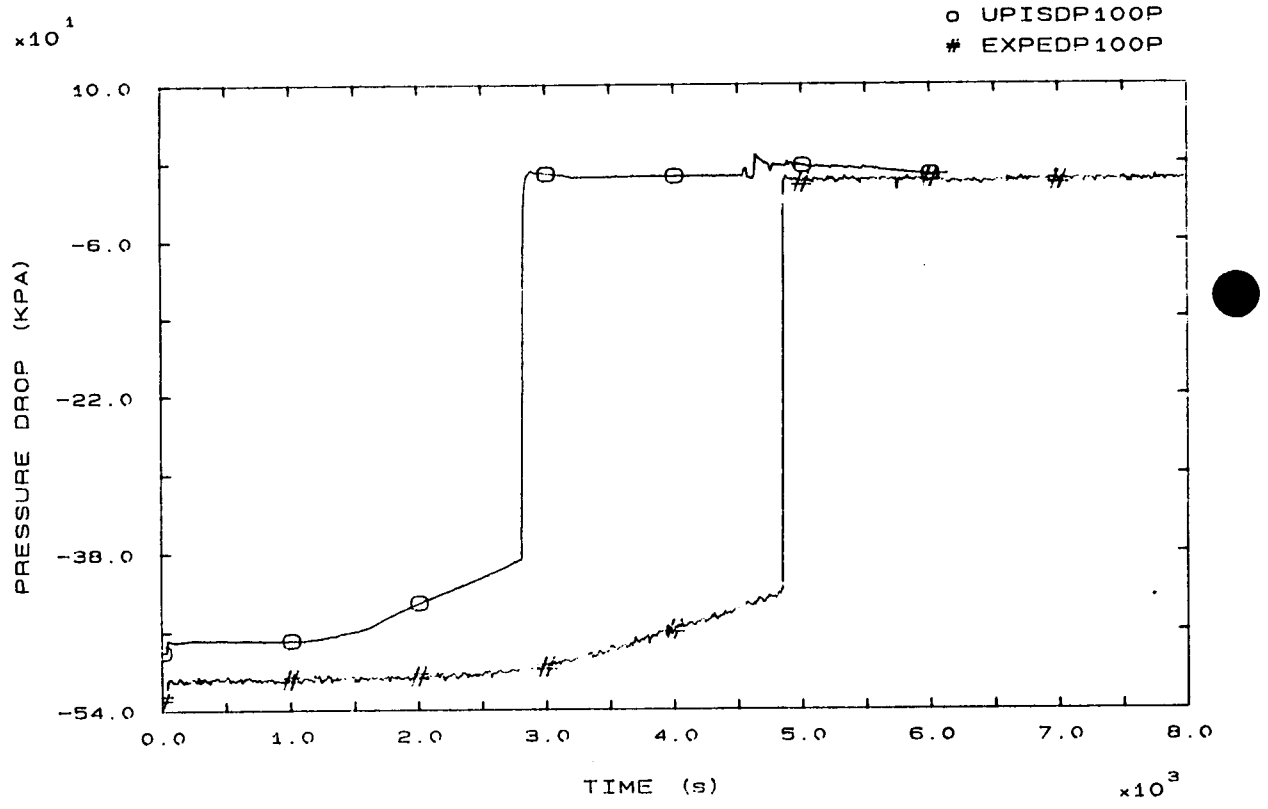

FIG. 54 PRIMARY PUMP 1 PRESSURE DROP

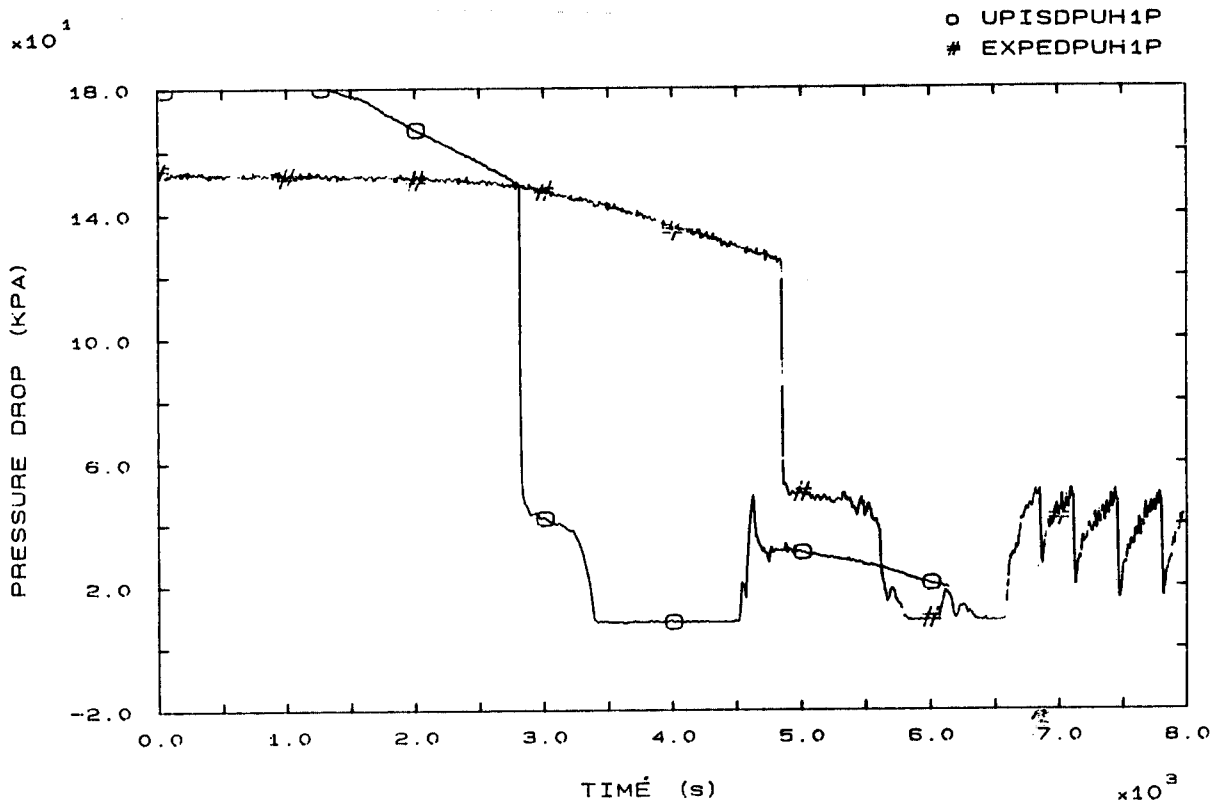

FIG. 62 SG1 INLET/U-BEND (UP-HILL) PRESSURE DROP

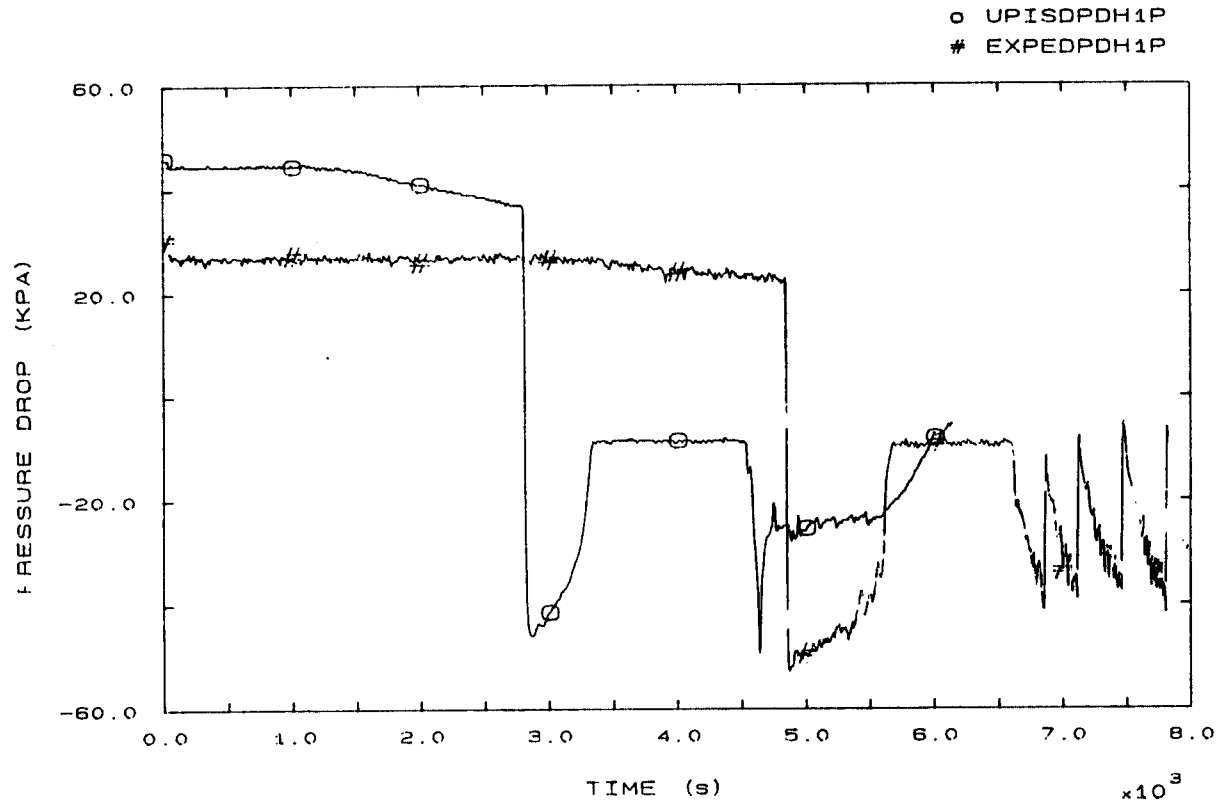

FIG. 63 SG1 U-BEND/OUTLET (DOWN-HILL) PRESSURE DROP

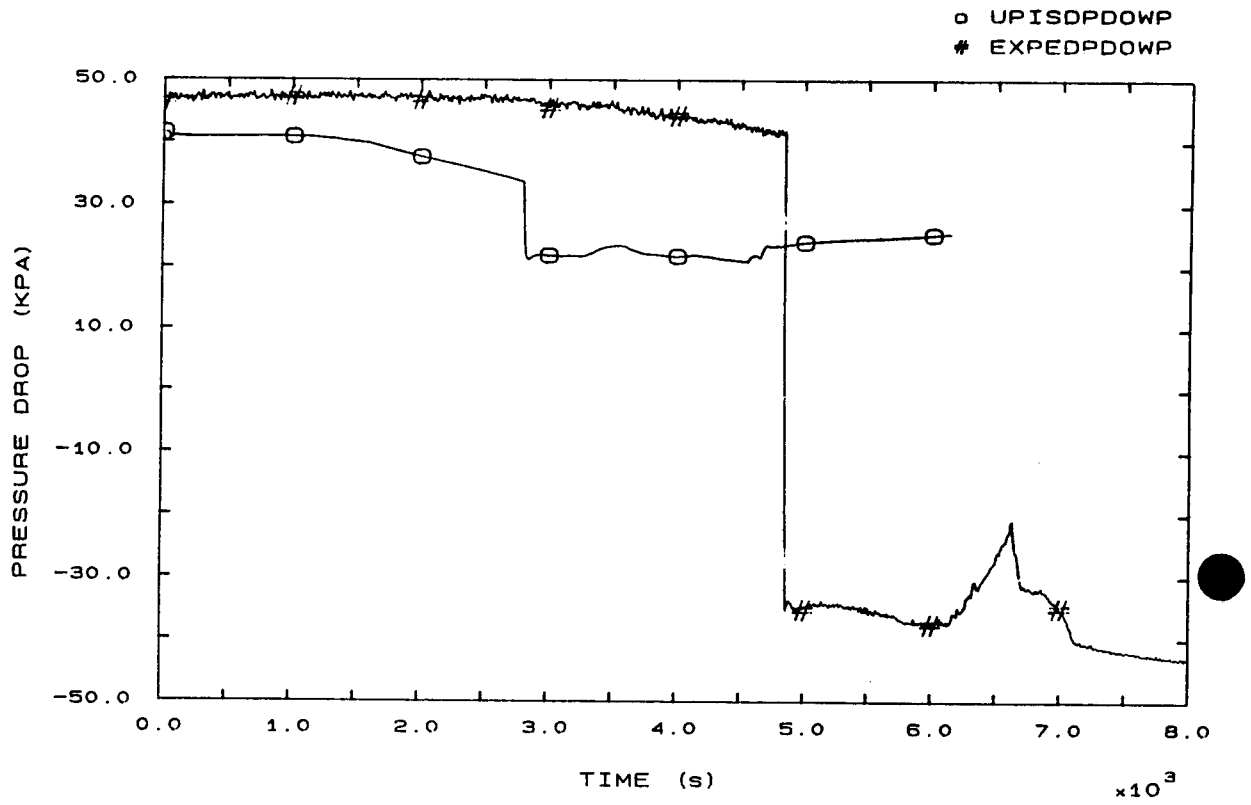

FIG. 57 VESSEL DOWNCOMER PRESSURE DROP

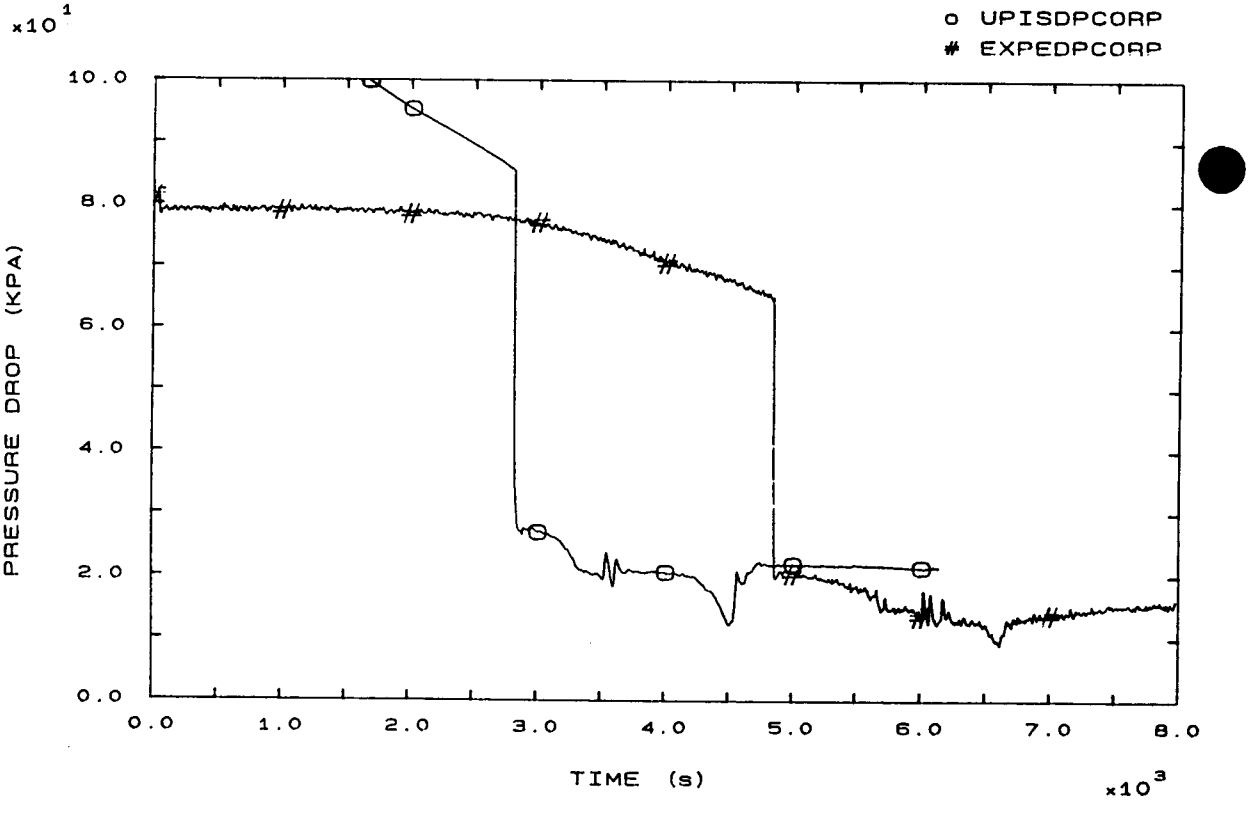

FIG. 58 CORE PRESSURE DROP

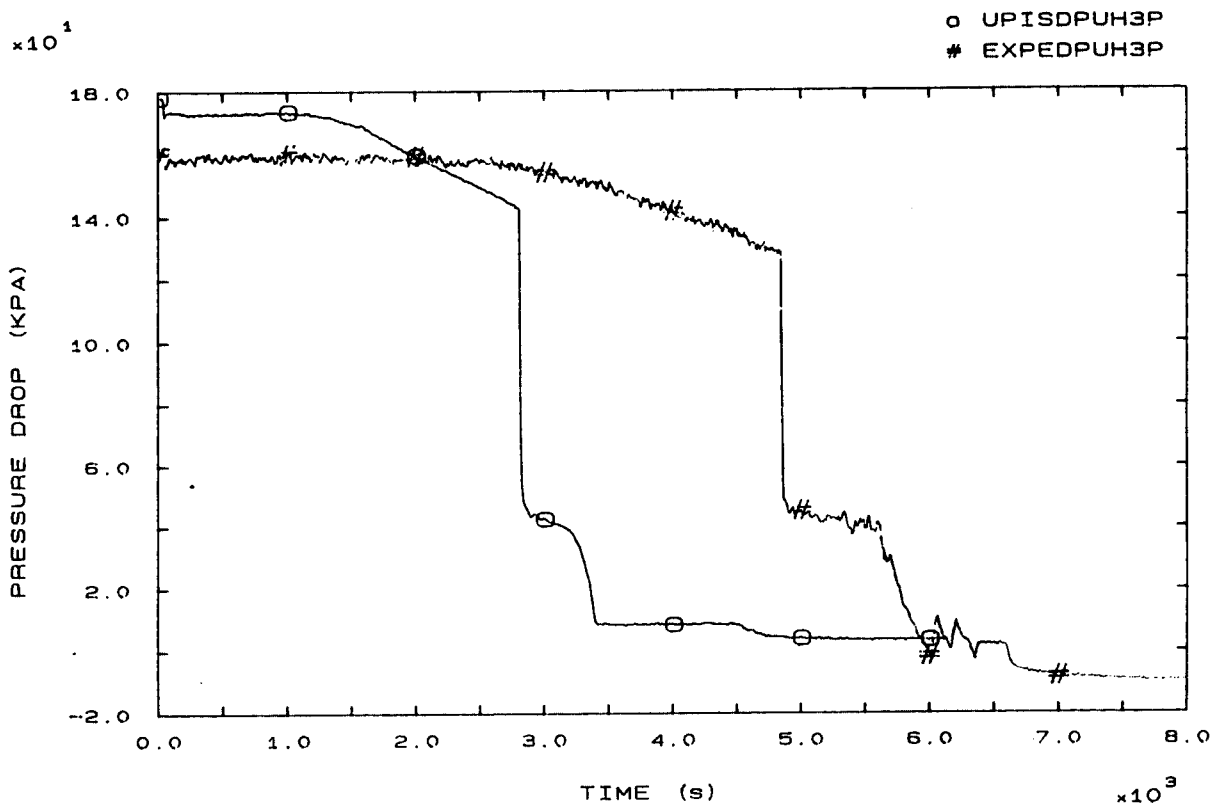

FIG. 66 SG3 INLET/U-BEND (UP-HILL) PRESSURE DROP

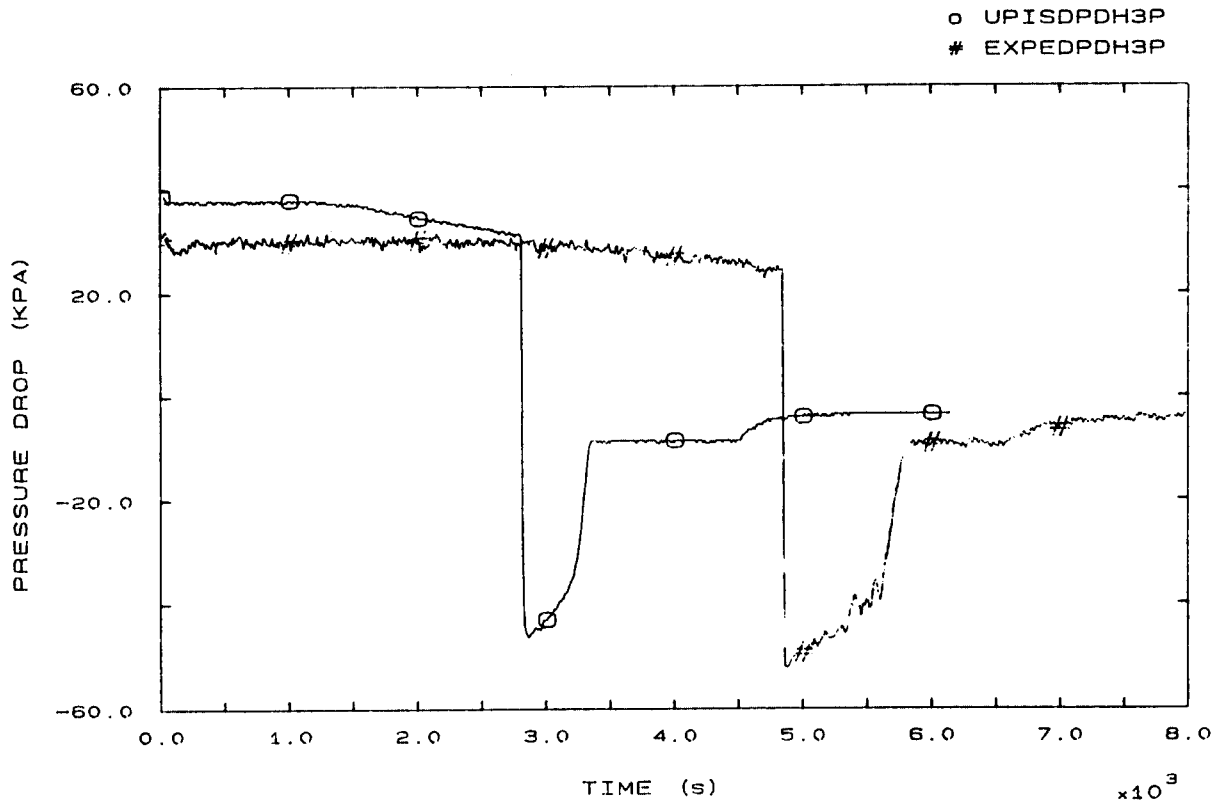

FIG. 67 SG3 U-BEND/OUTLET (DOWN-HILL) PRESSURE DROP

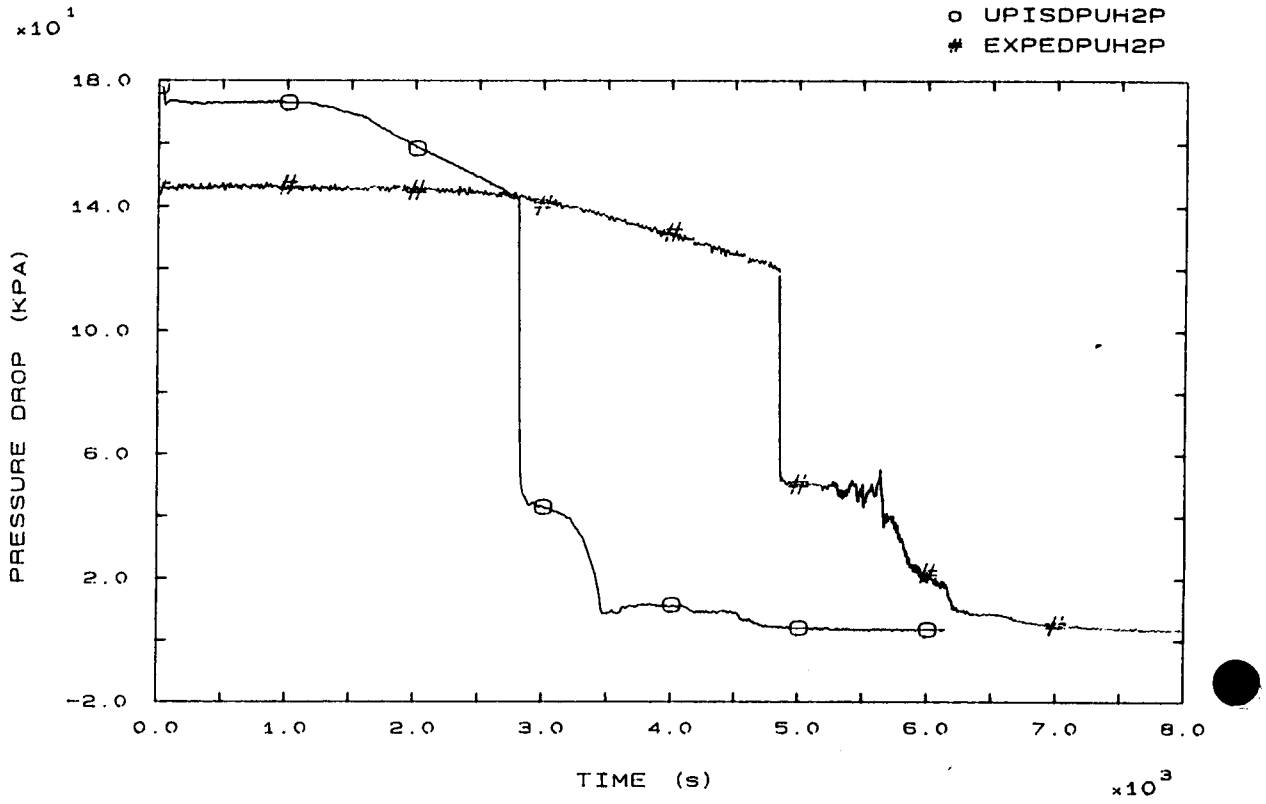

FIG. 64 SG2 INLET/U-BEND (UP-HILL) PRESSURE DROP

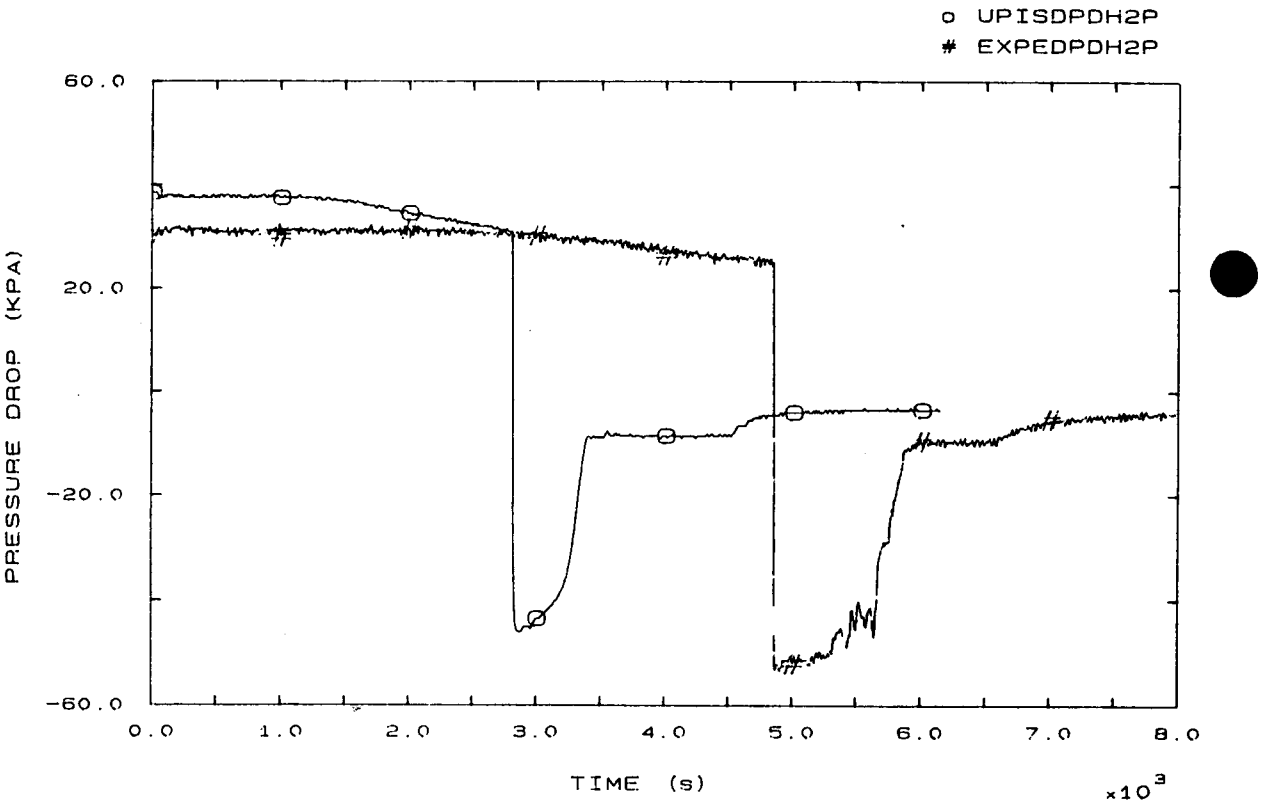

FIG. 65 SG2 U-BEND/OUTLET (DOWN-HILL) PRESSURE DROP

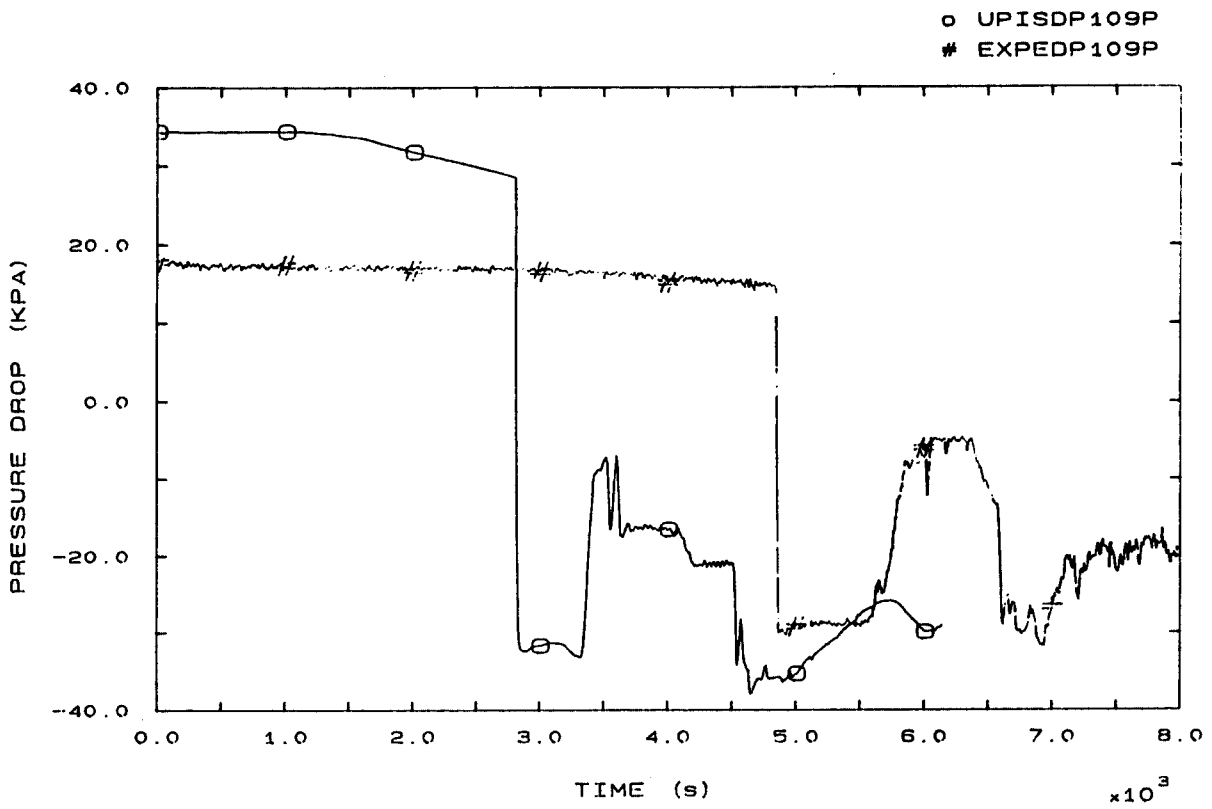

FIG. 68 SG1 OUTLET/LOOP SEAL BOTTOM PRESSURE DROP

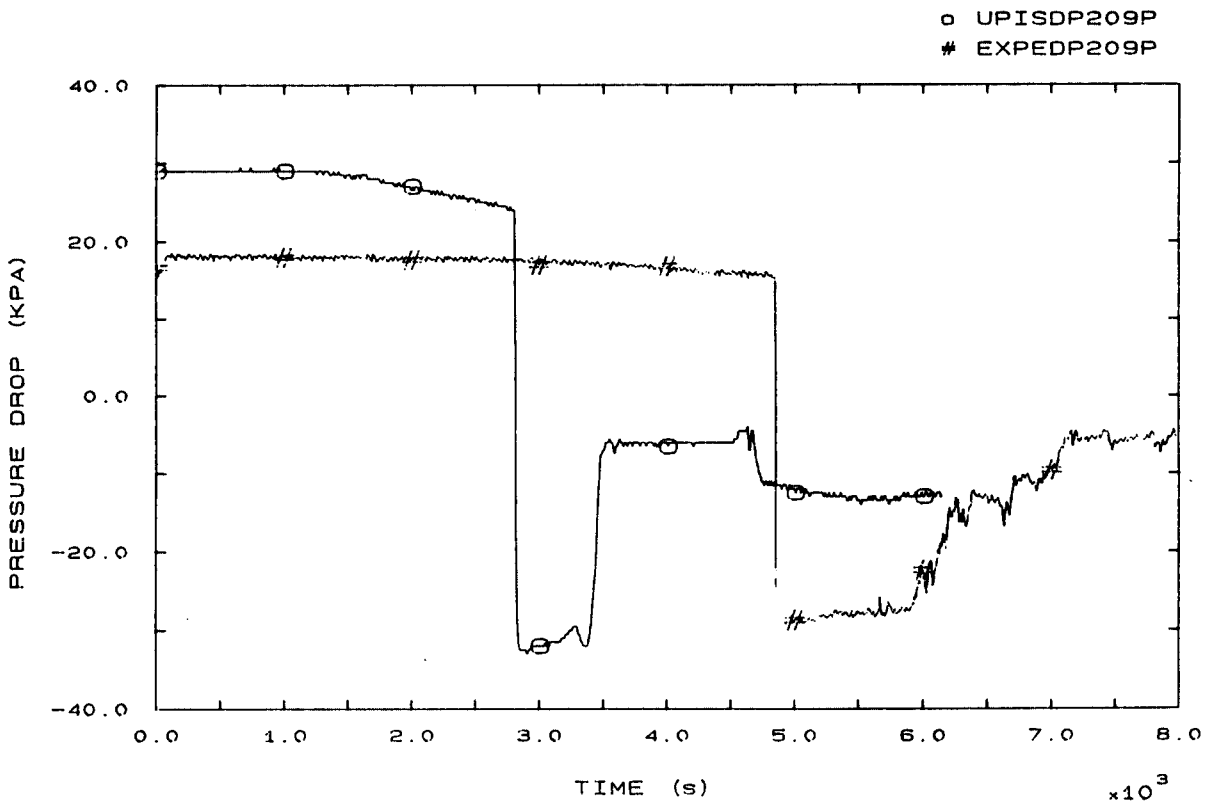

FIG. 69 SG2 OUTLET/LOOP SEAL BOTTOM PRESSURE DROP

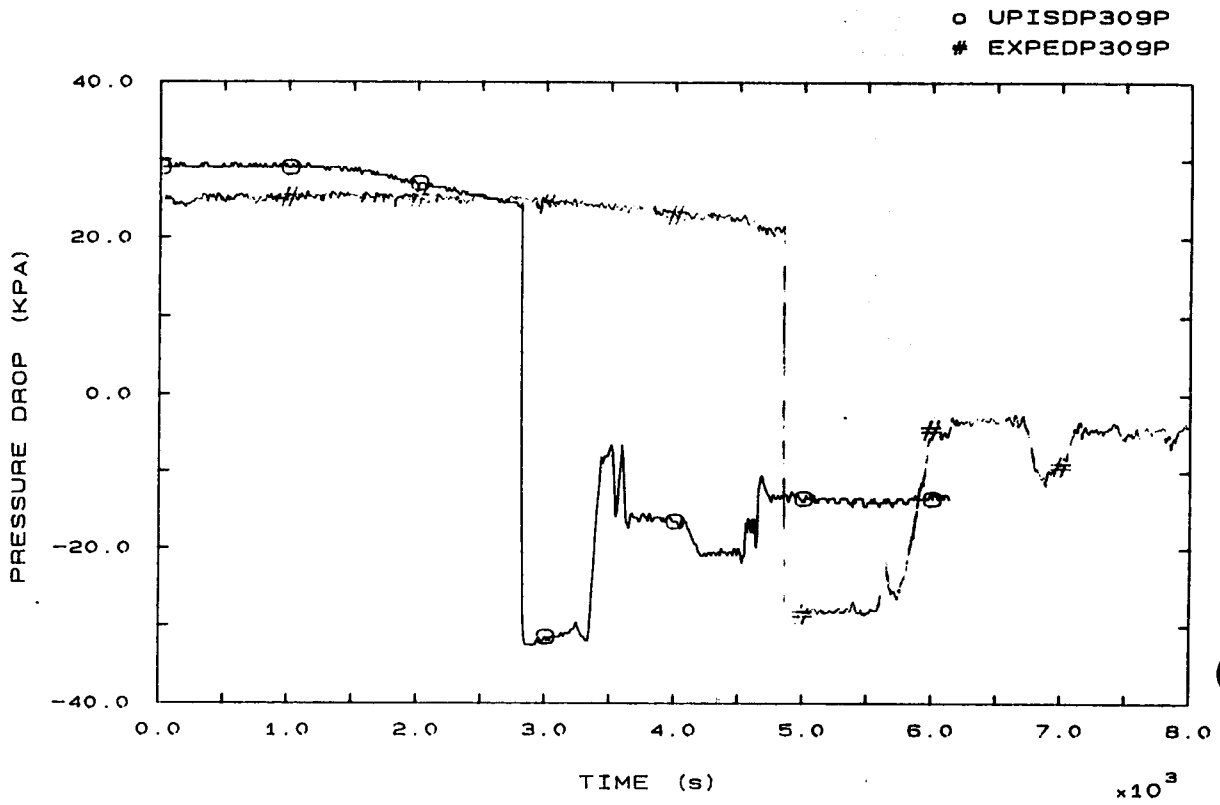

FIG. 70 SG3 OUTLET/LOOP SEAL BOTTOM PRESSURE DROP

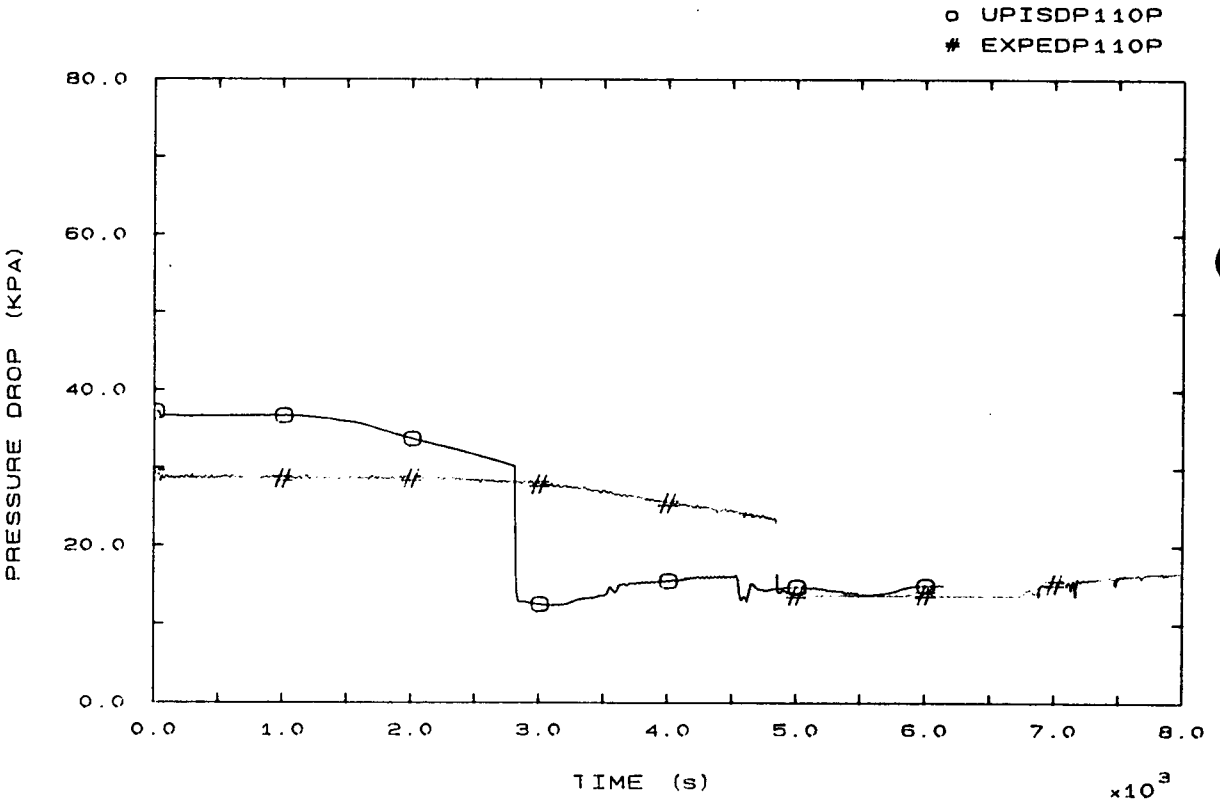

FIG. 71 LOOP SEAL BOTTOM/PUMP 1 INLET PRESSURE DROP

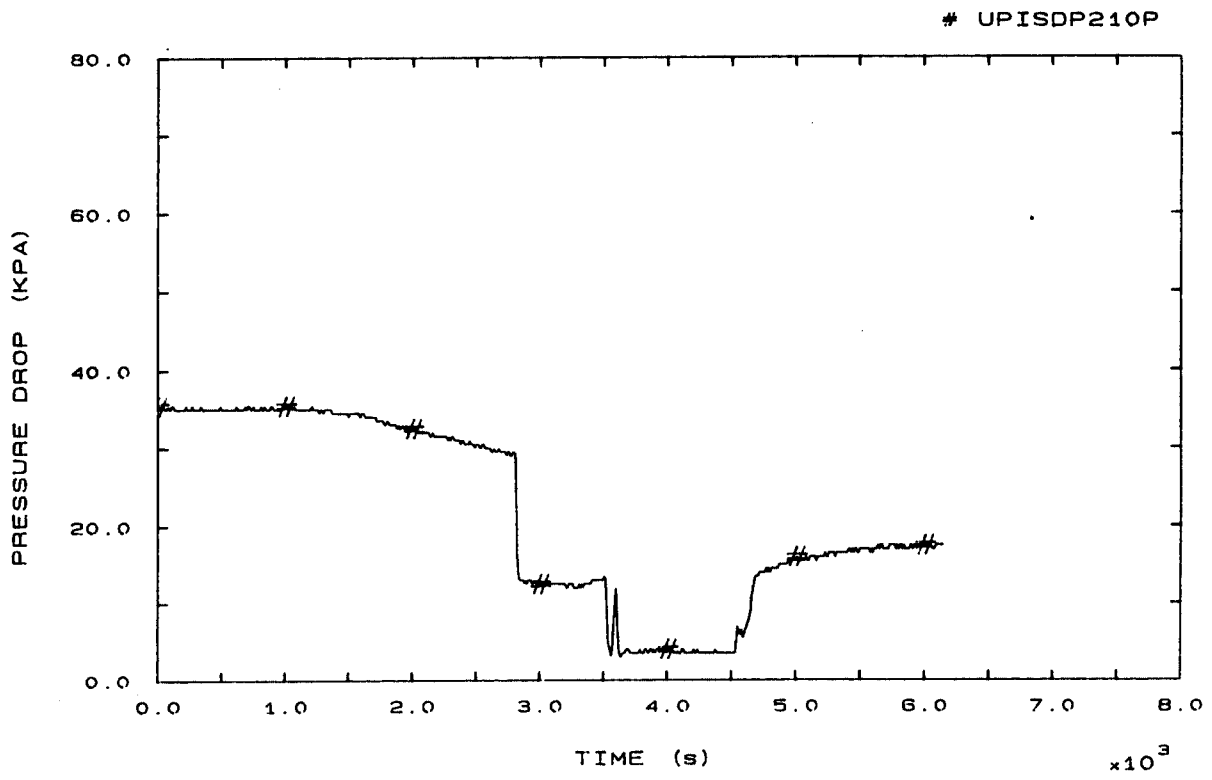

FIG. 72 LOOP SEAL BOTTOM/PUMP 2 INLET PRESSURE DROP

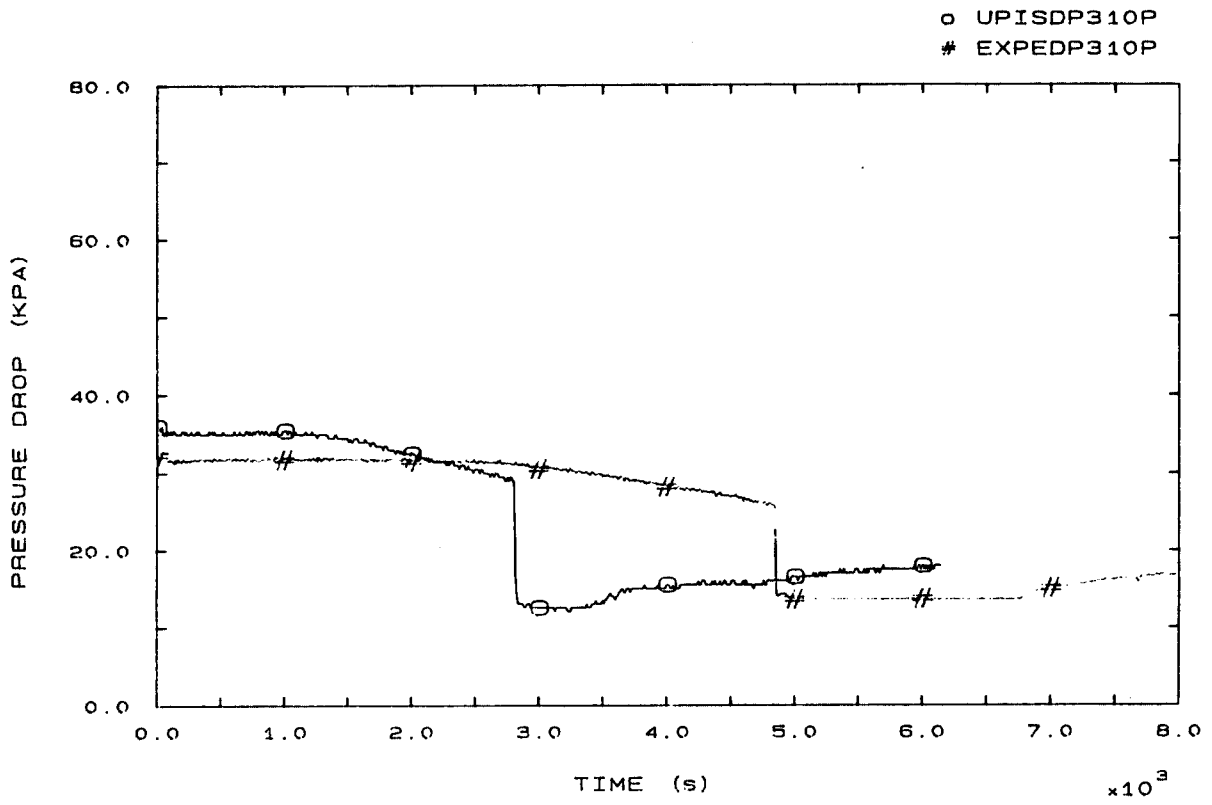

FIG. 73 LOOP SEAL BOTTOM/PUMP 3 INLET PRESSURE DROP

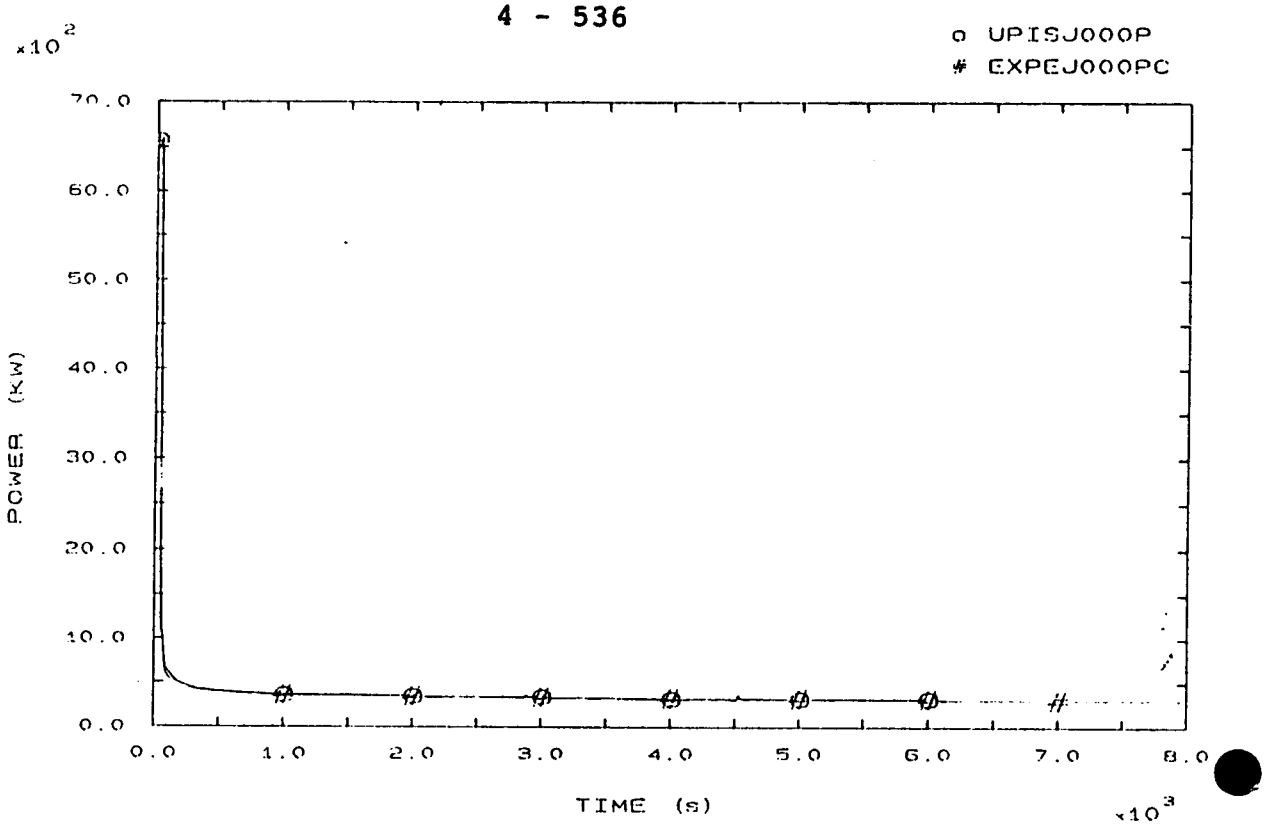

FIG. 81 HEATER RODS POWER

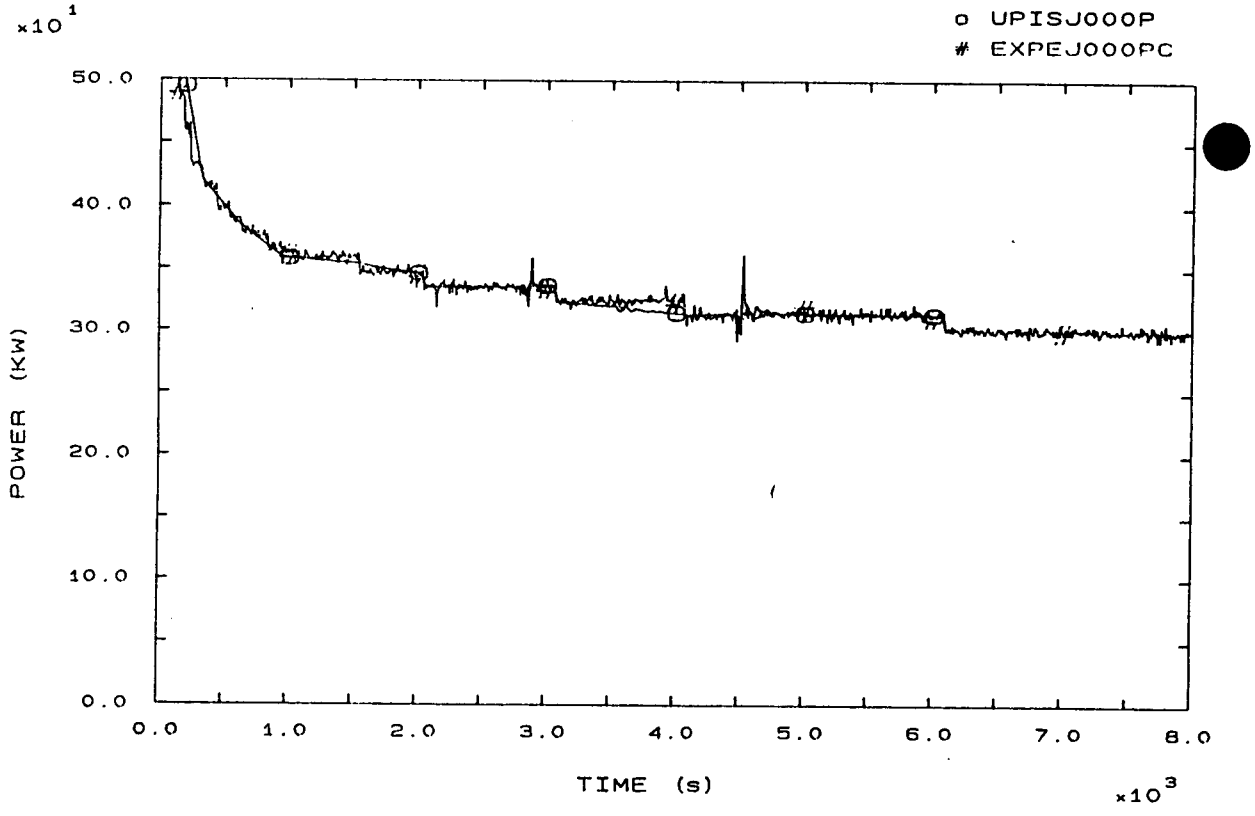

FIG. 81A HEATER RODS POWER

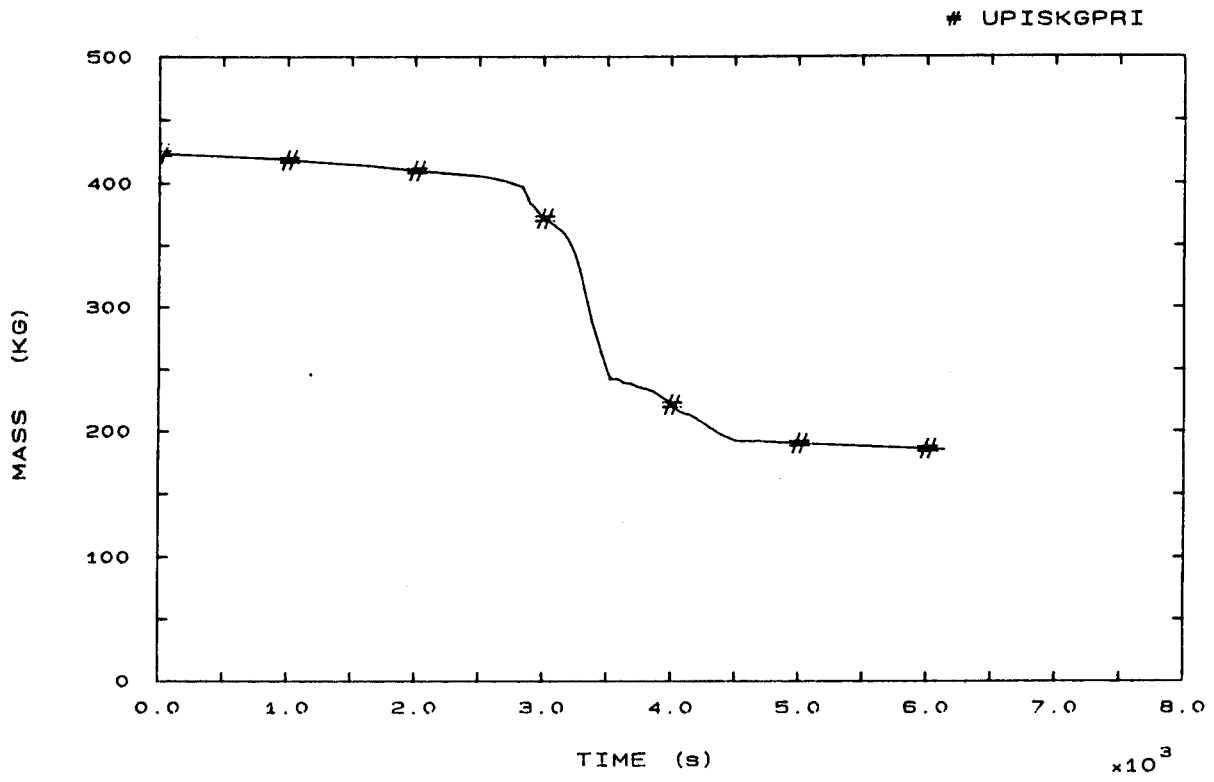

FIG. 85 PRIMARY COOLANT TOTAL MASS

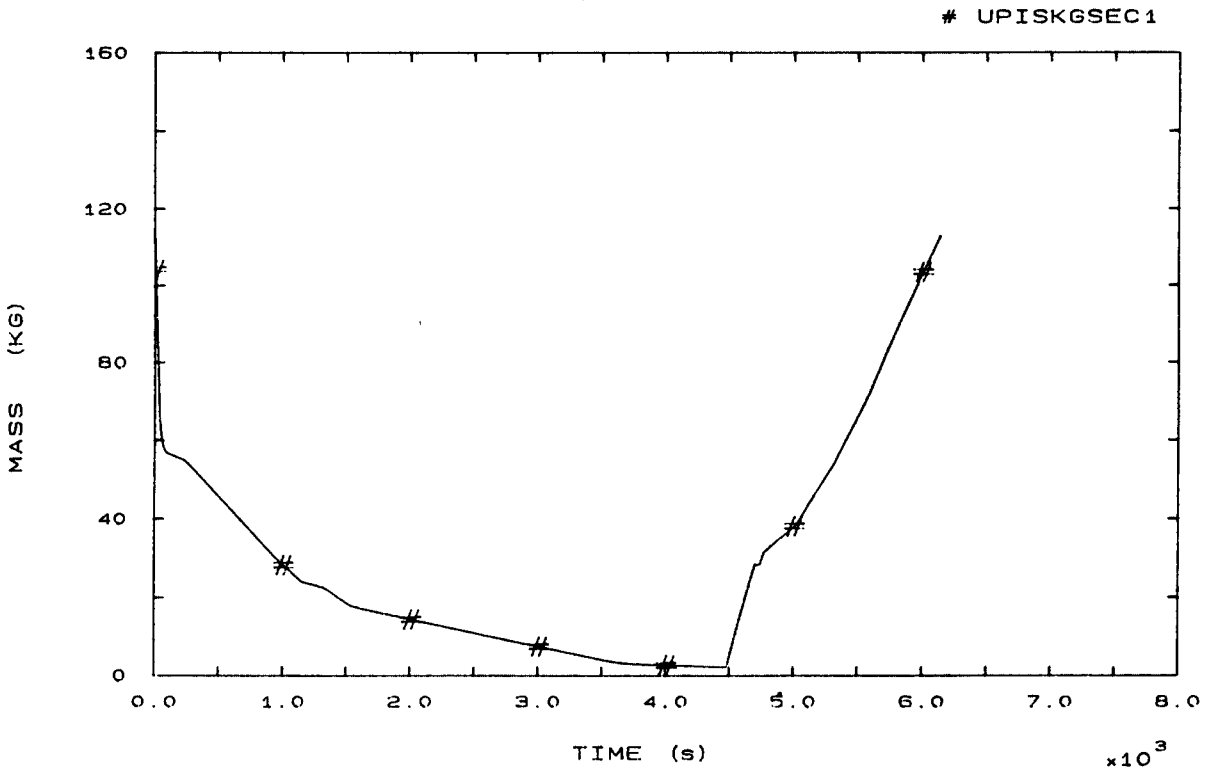

FIG. 86 SECONDARY COOLANT TOTAL MASS SG1

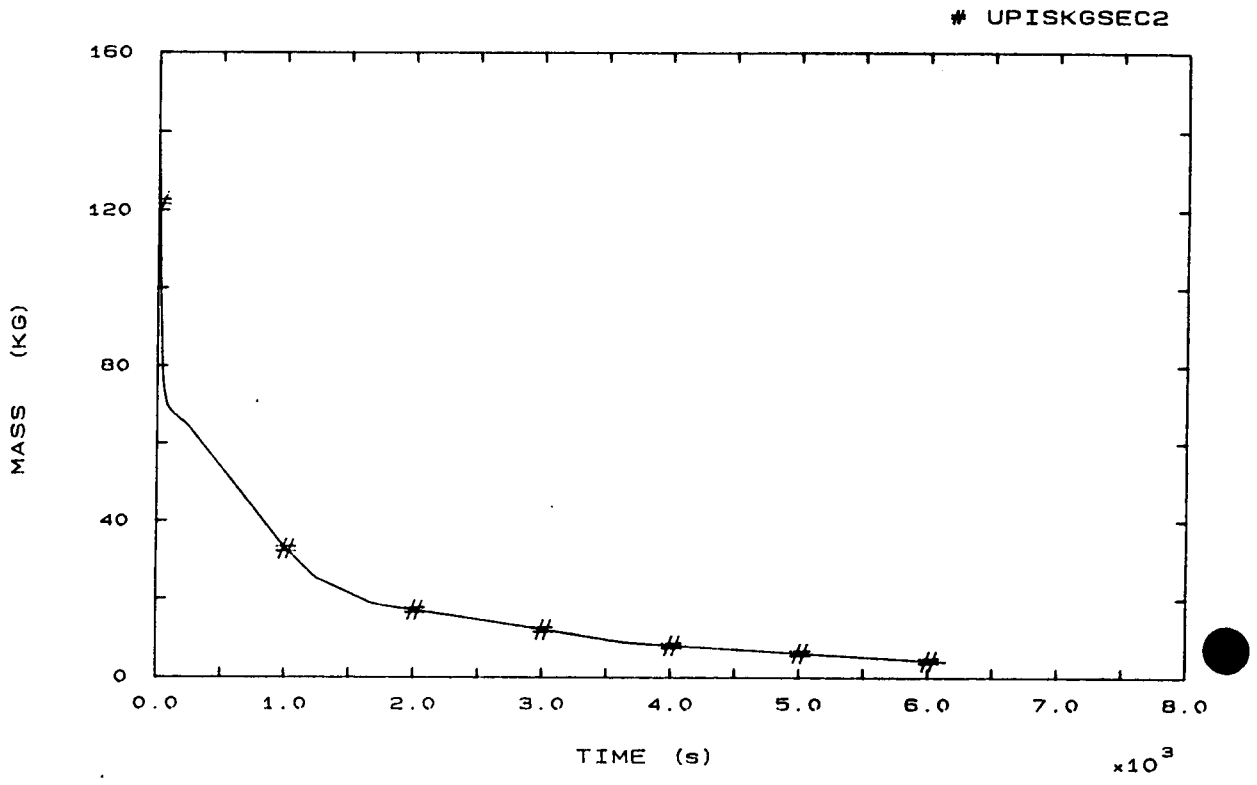

FIG. 87 SECONDARY COOLANT TOTAL MASS SG2

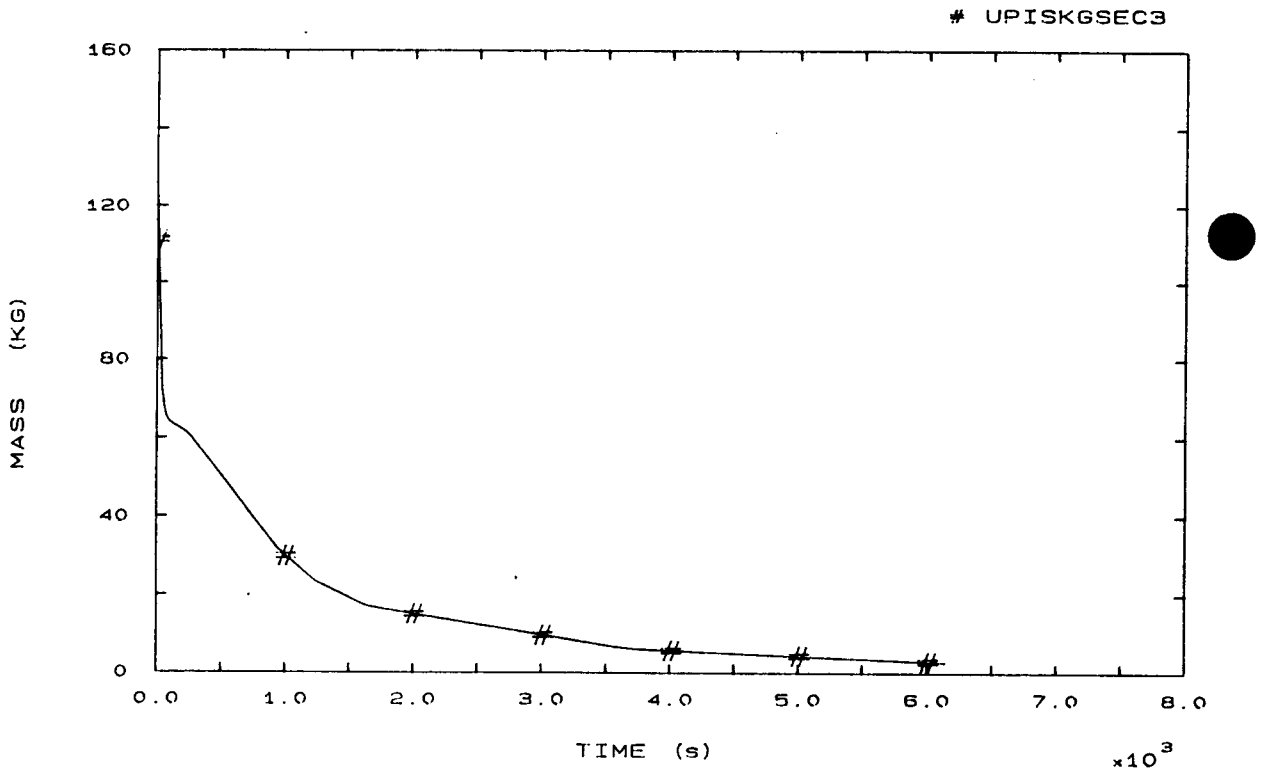

FIG. 88 SECONDARY COOLANT TOTAL MASS SG3

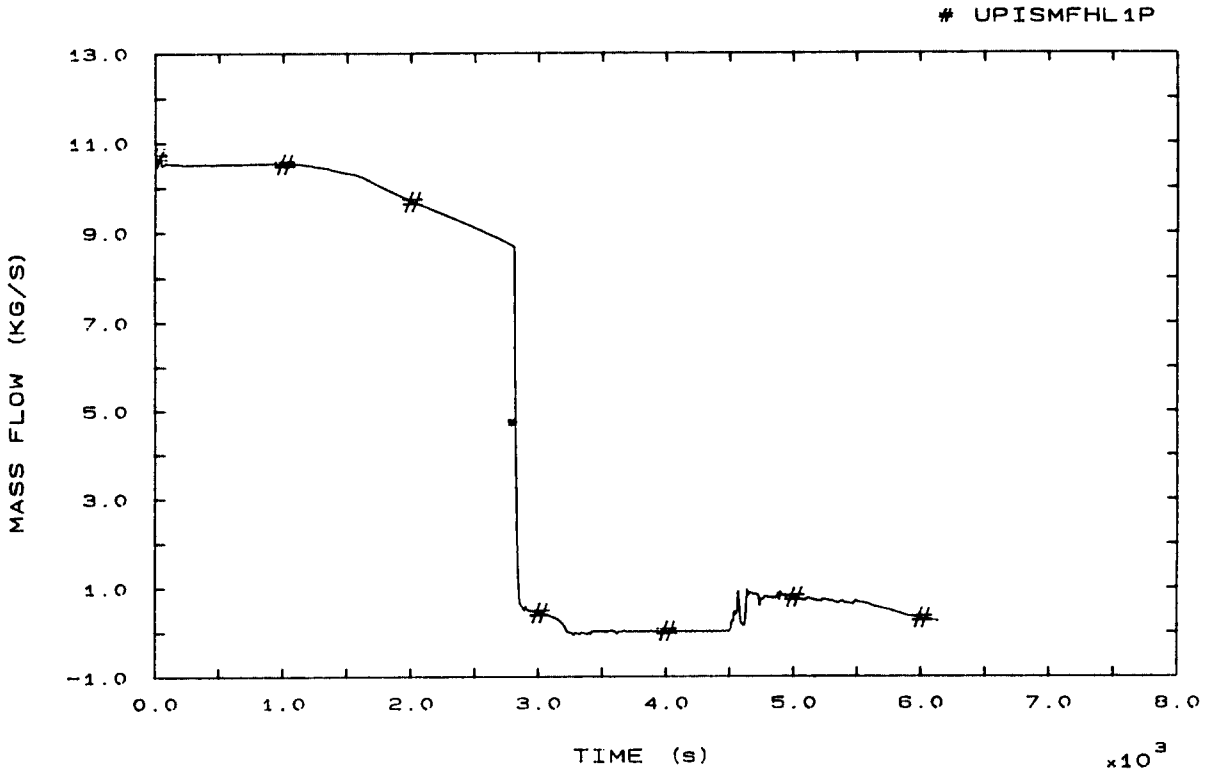

FIG. 89 HOT LEG 1 MASS FLOW

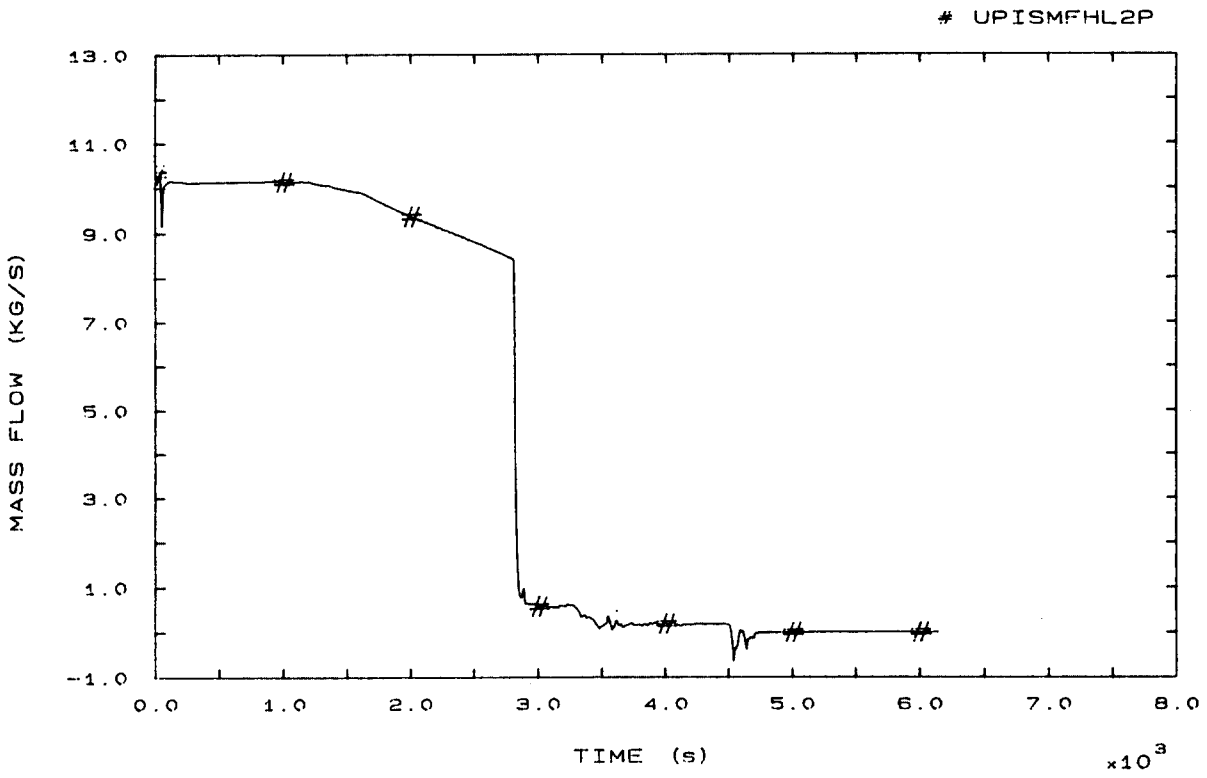

FIG. 90 HOT LEG 2 MASS FLOW

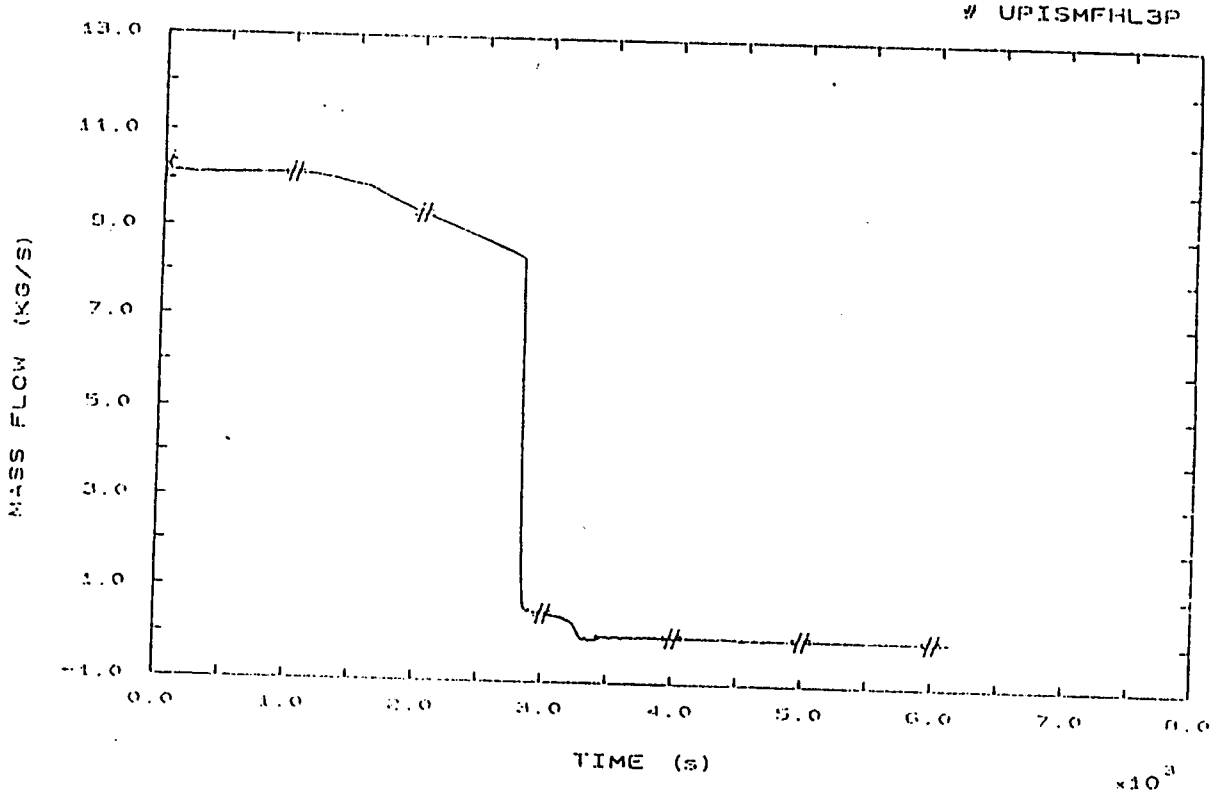

FIG. 91 HOT LEG 3 MASS FLOW

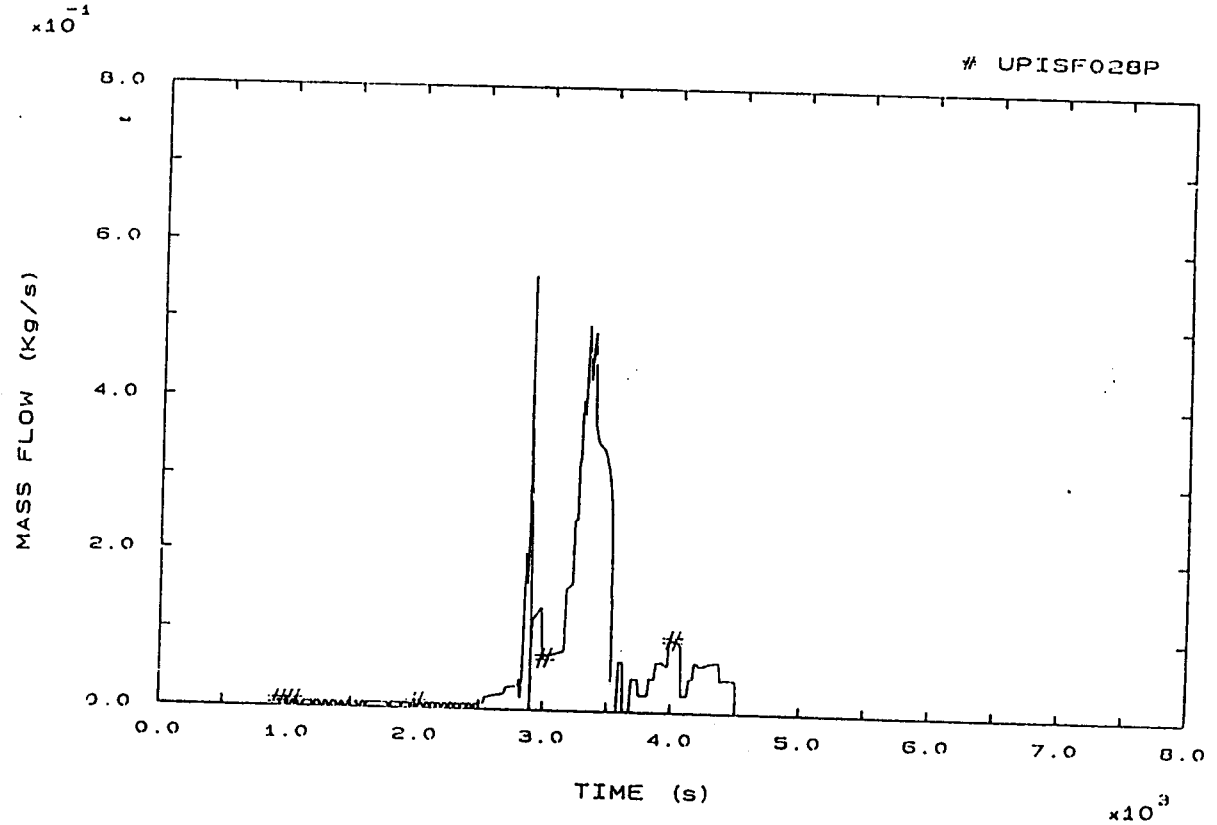

FIG. 92 PRZ PORV MASS FLOW

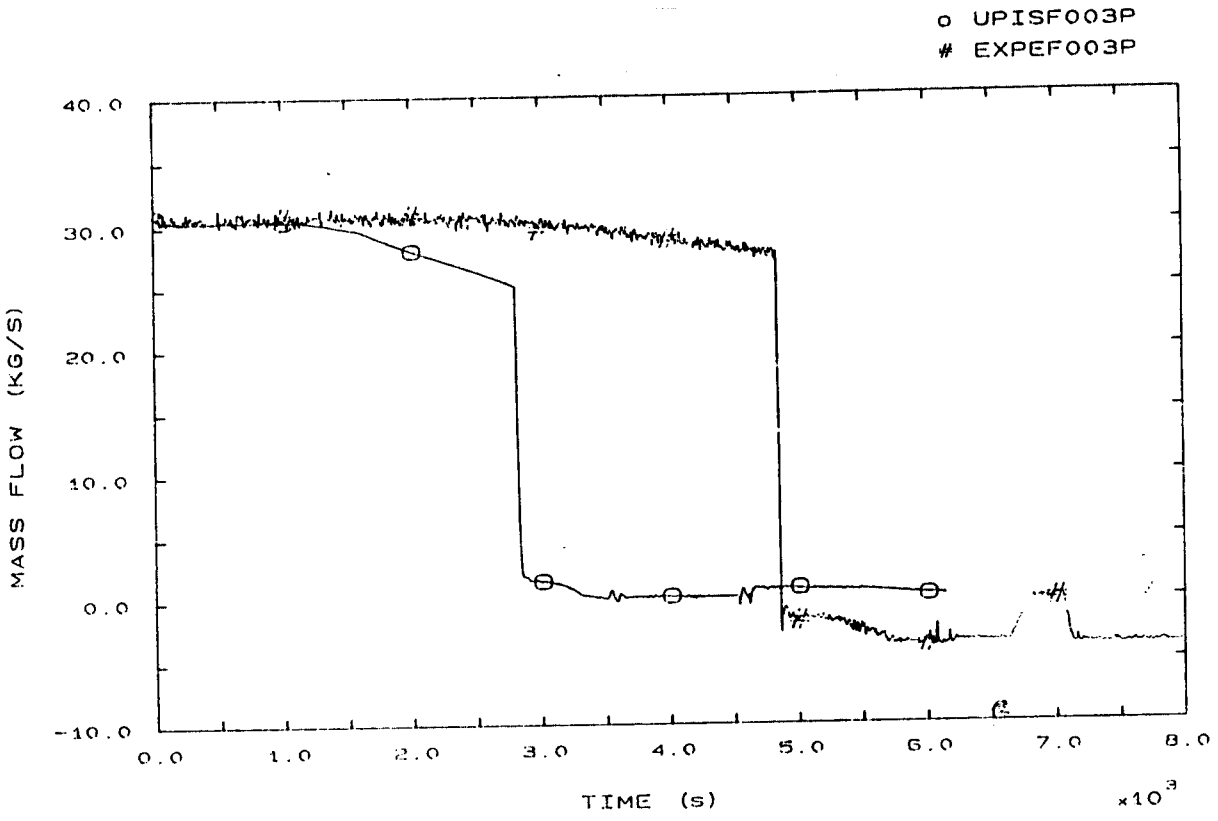

FIG. 94 VESSEL DOWNCOMER MASS FLOW

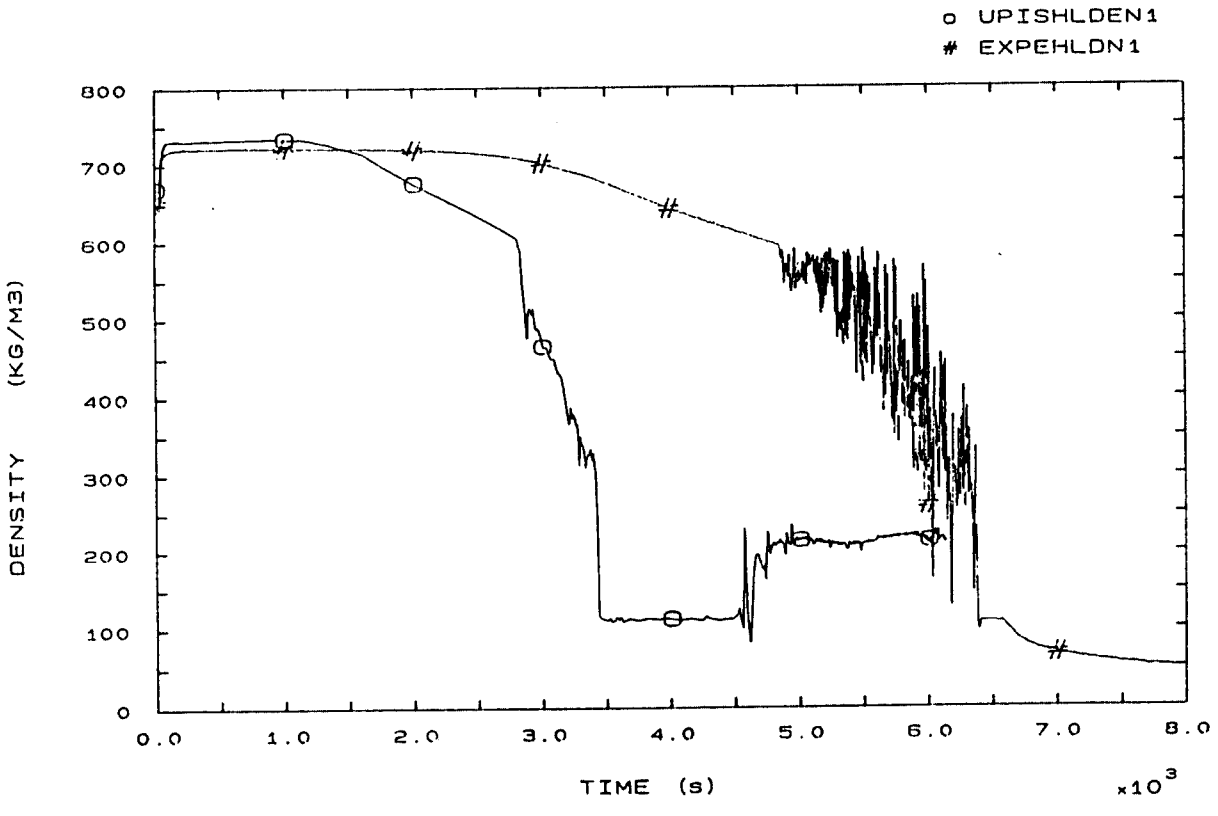

FIG. 100 HOT LEG 1 FLUID DENSITY

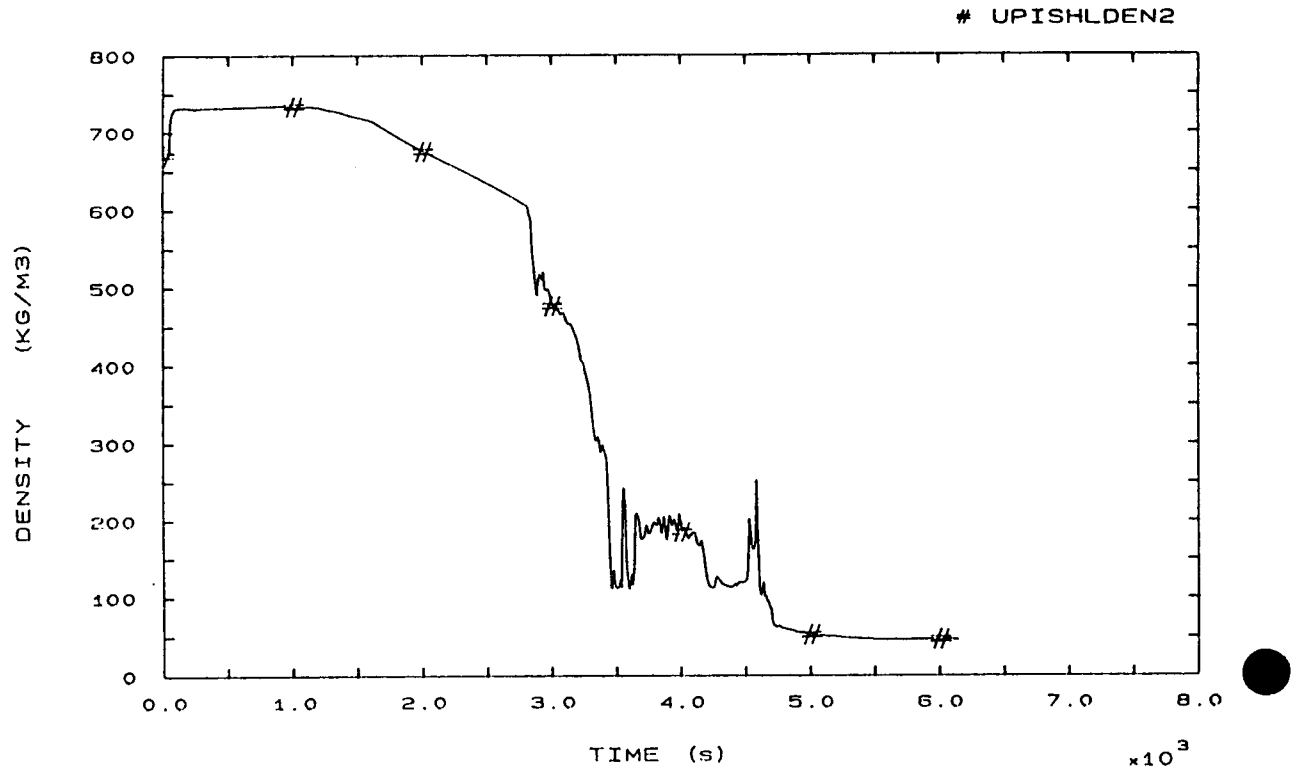

FIG. 101 HOT LEG 2 FLUID DENSITY

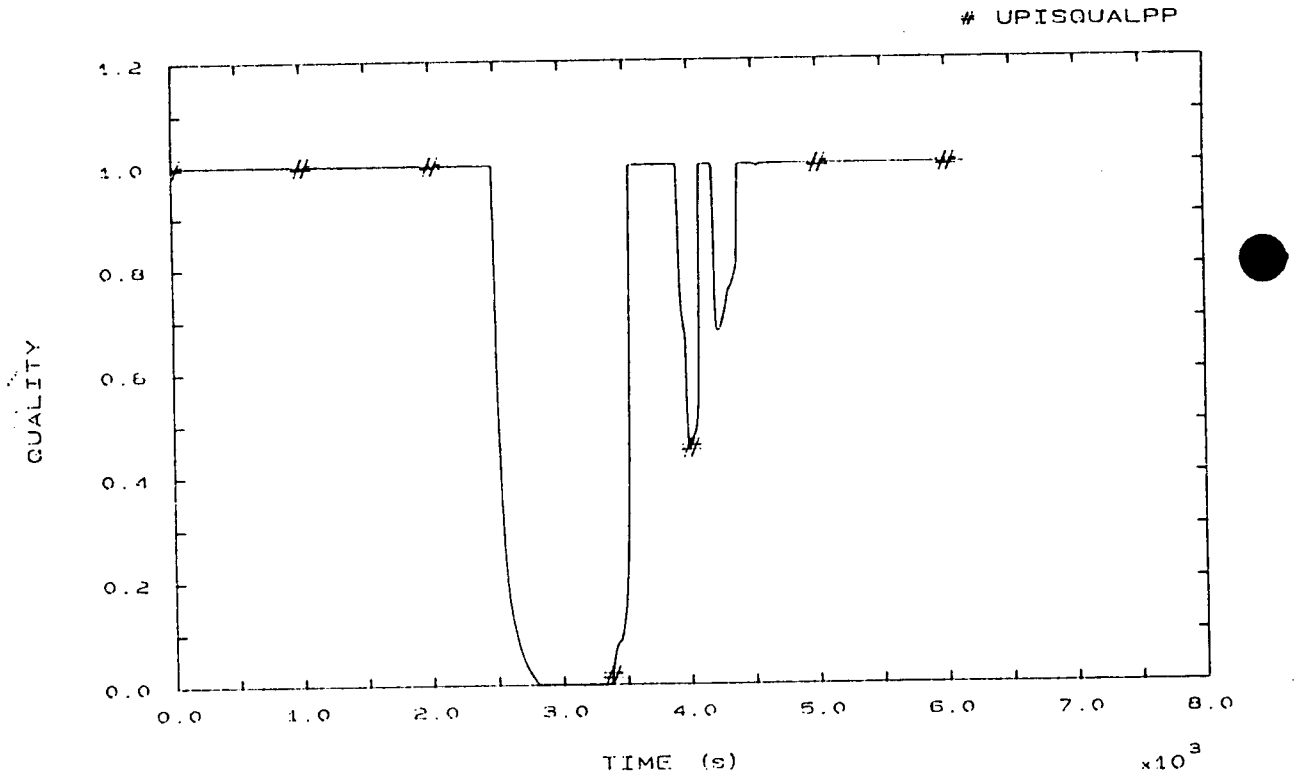

FIG. 103 PRZ PORV FLOW QUALITY

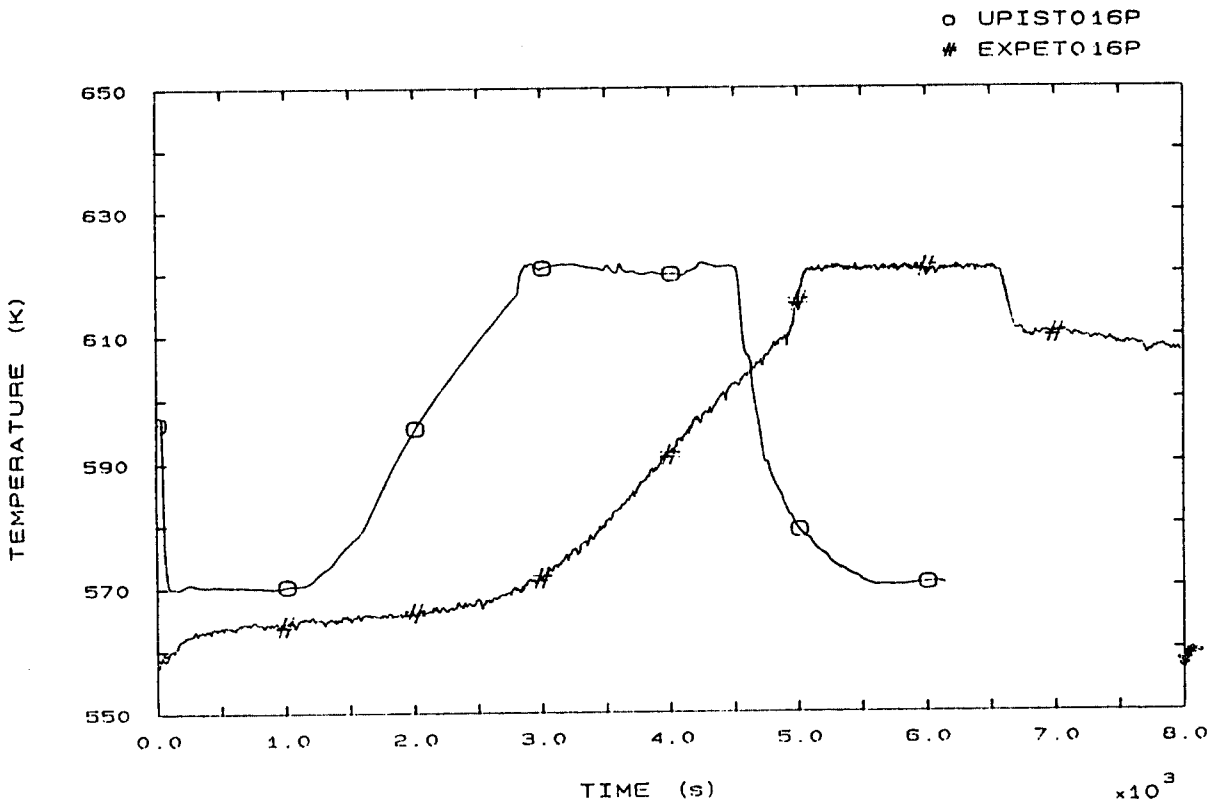

FIG. 110 FLUID TEMPERATURE VESSEL UPPER HEAD

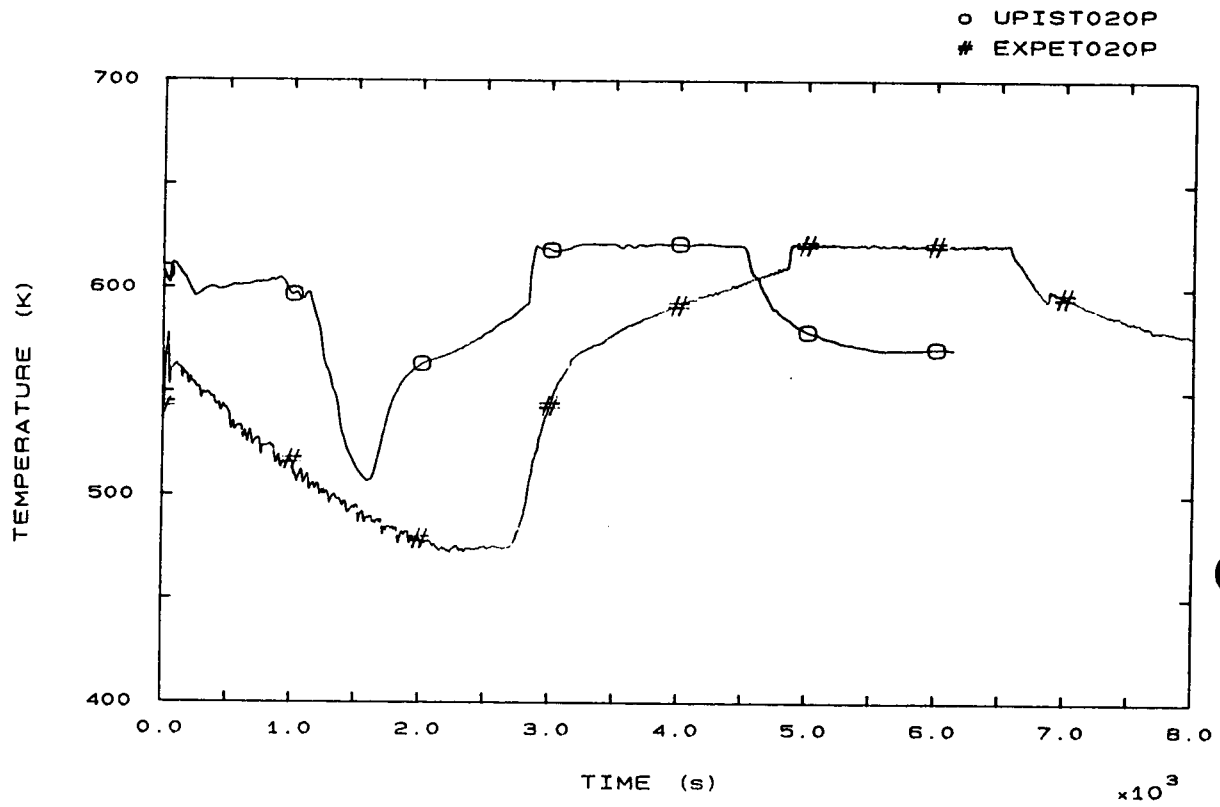

FIG. 112 FLUID TEMPERATURE SURGE LINE UPPER SIDE

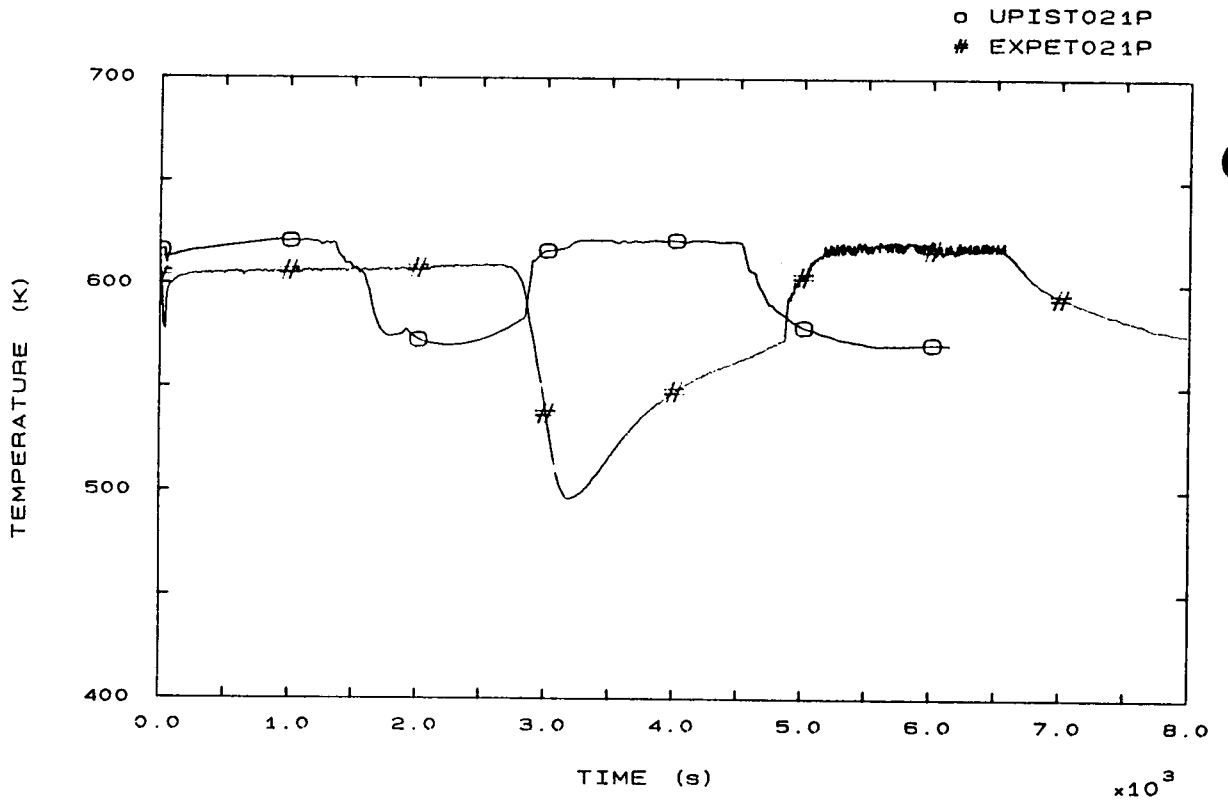

FIG. 113 PRZ FLUID TEMPERATURE

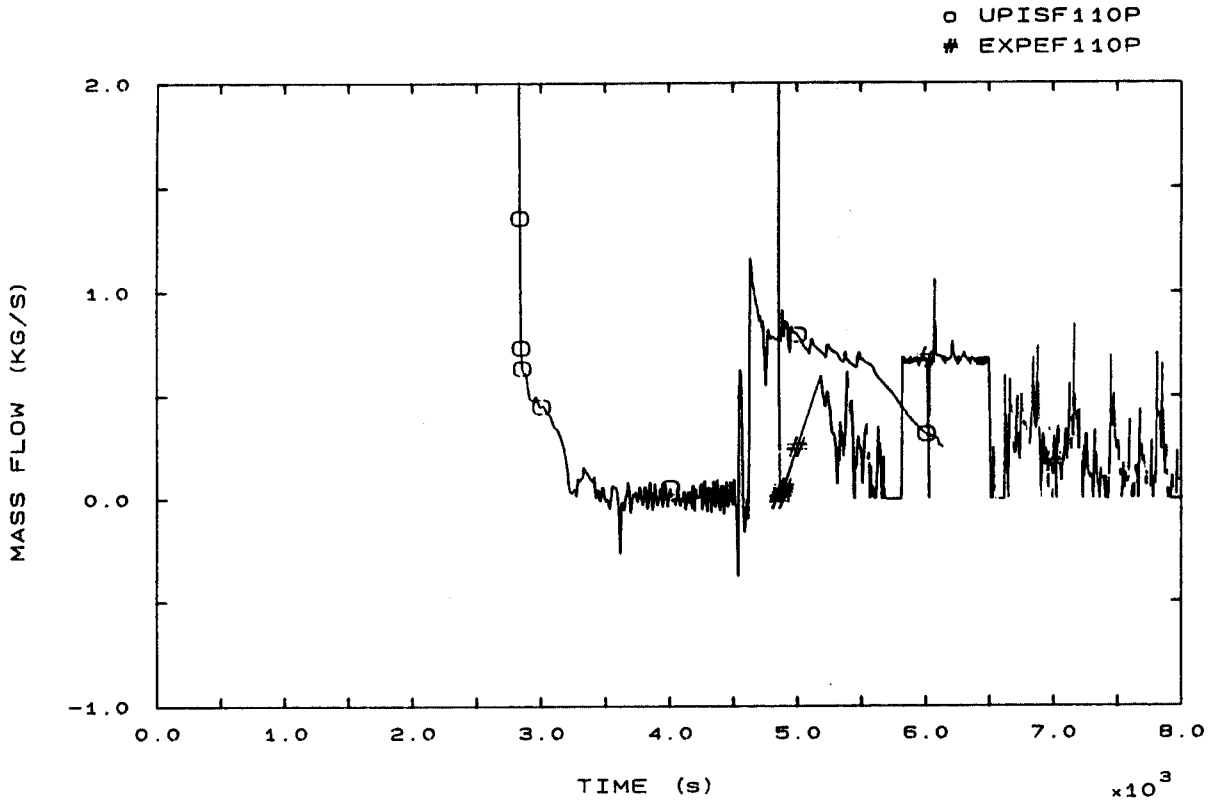

FIG. 125 LOOP SEAL 1 MASS FLOW

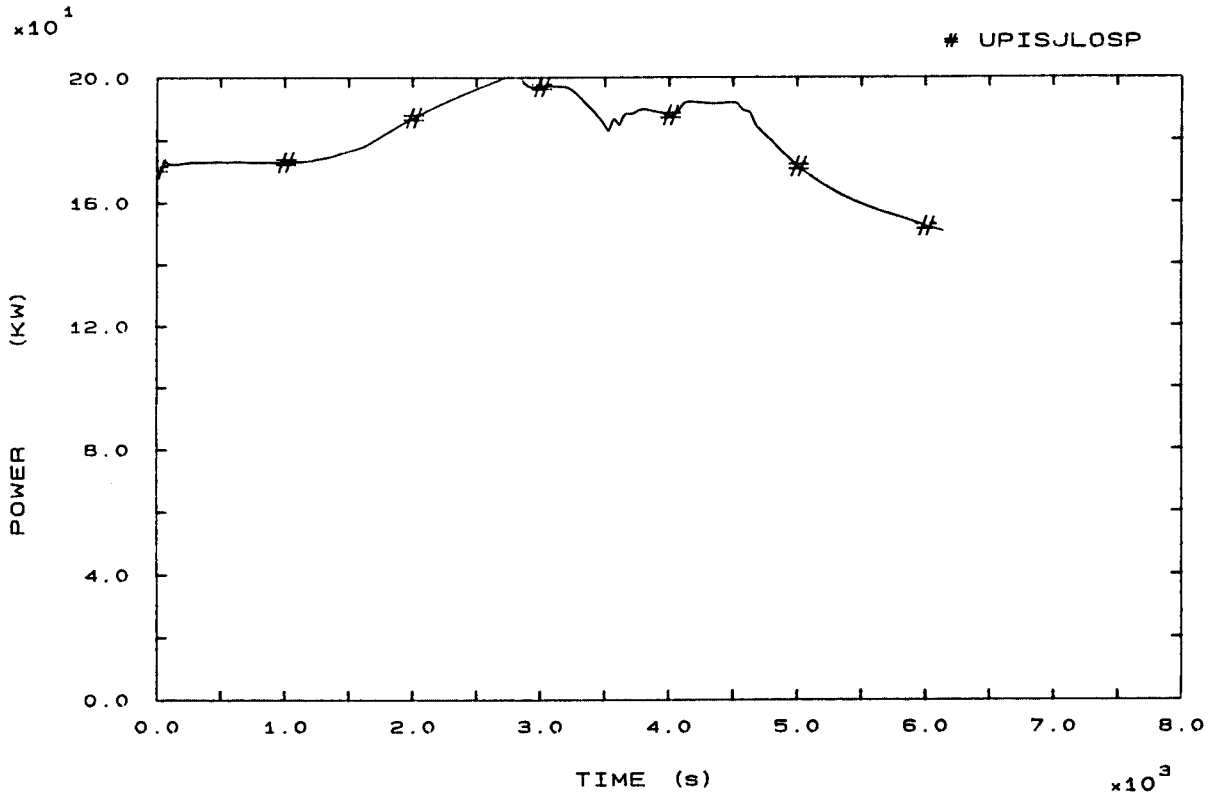

FIG. 131 PRIMARY HEAT LOSS

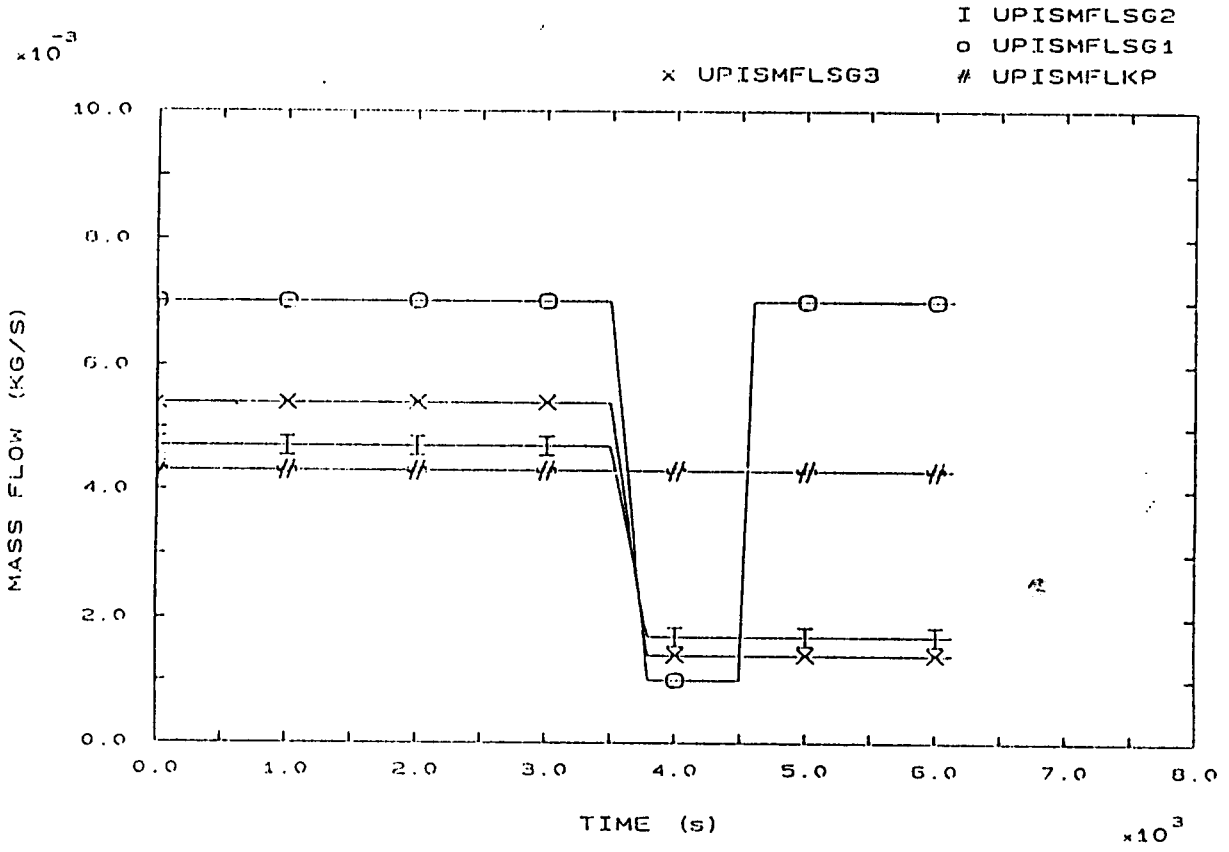

FIG. 137 PRIMARY AND SECONDARY LEAKS

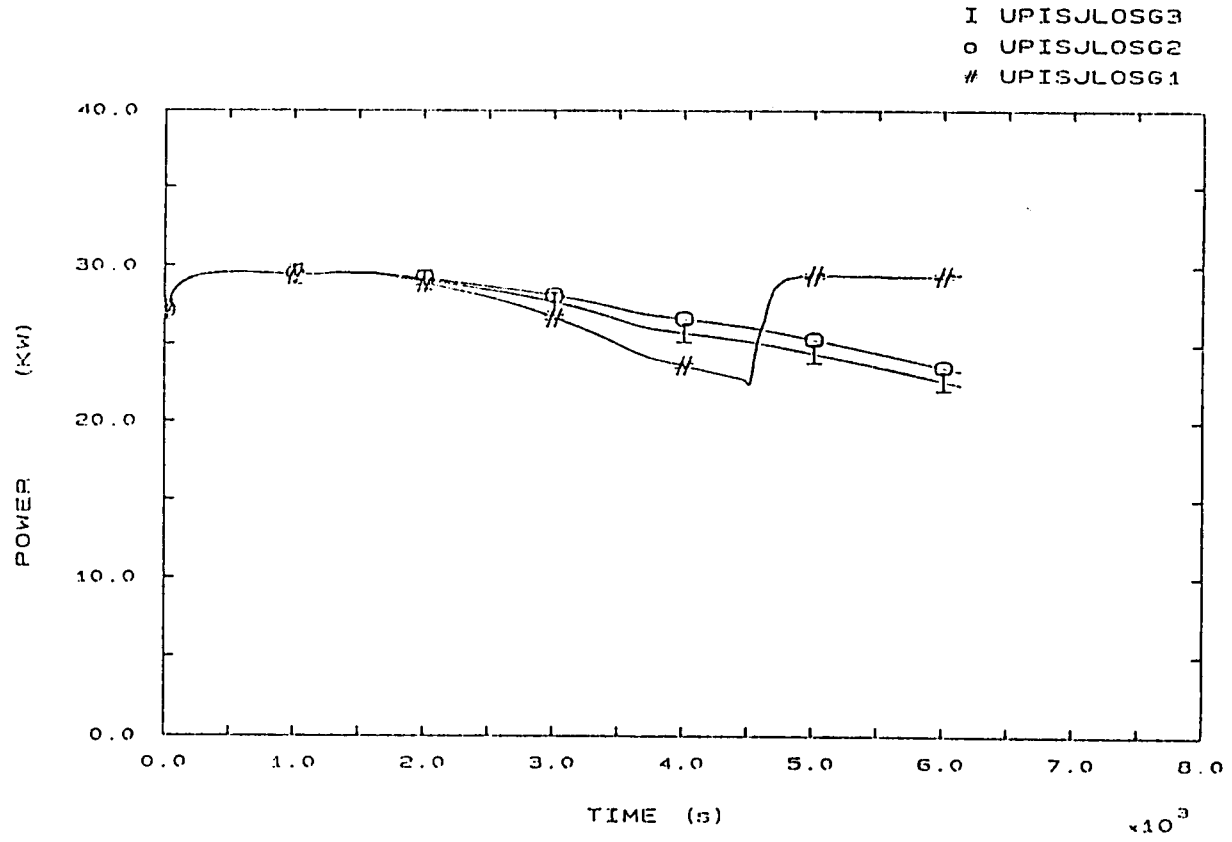

FIG. 139 SECONDARY HEAT LOSSES

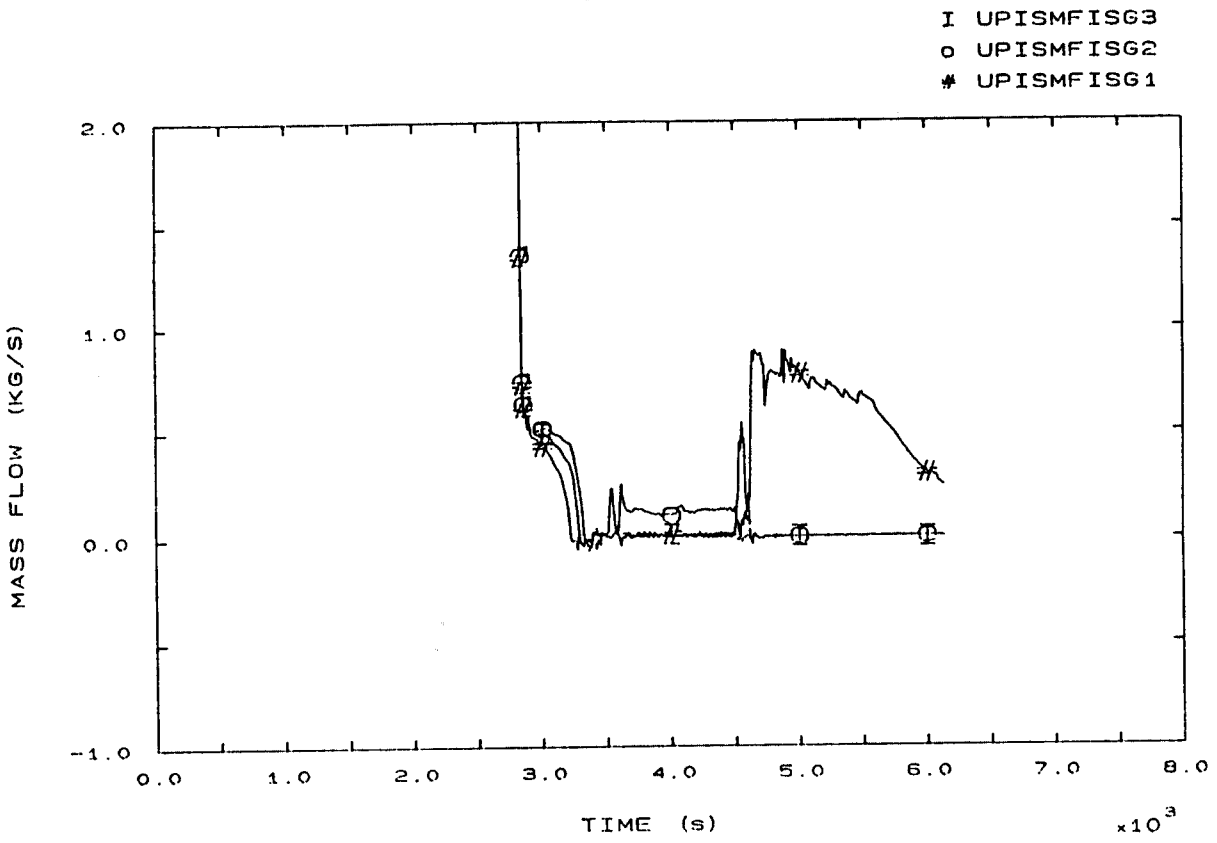

FIG. 140 SG INLET MASS FLOWS

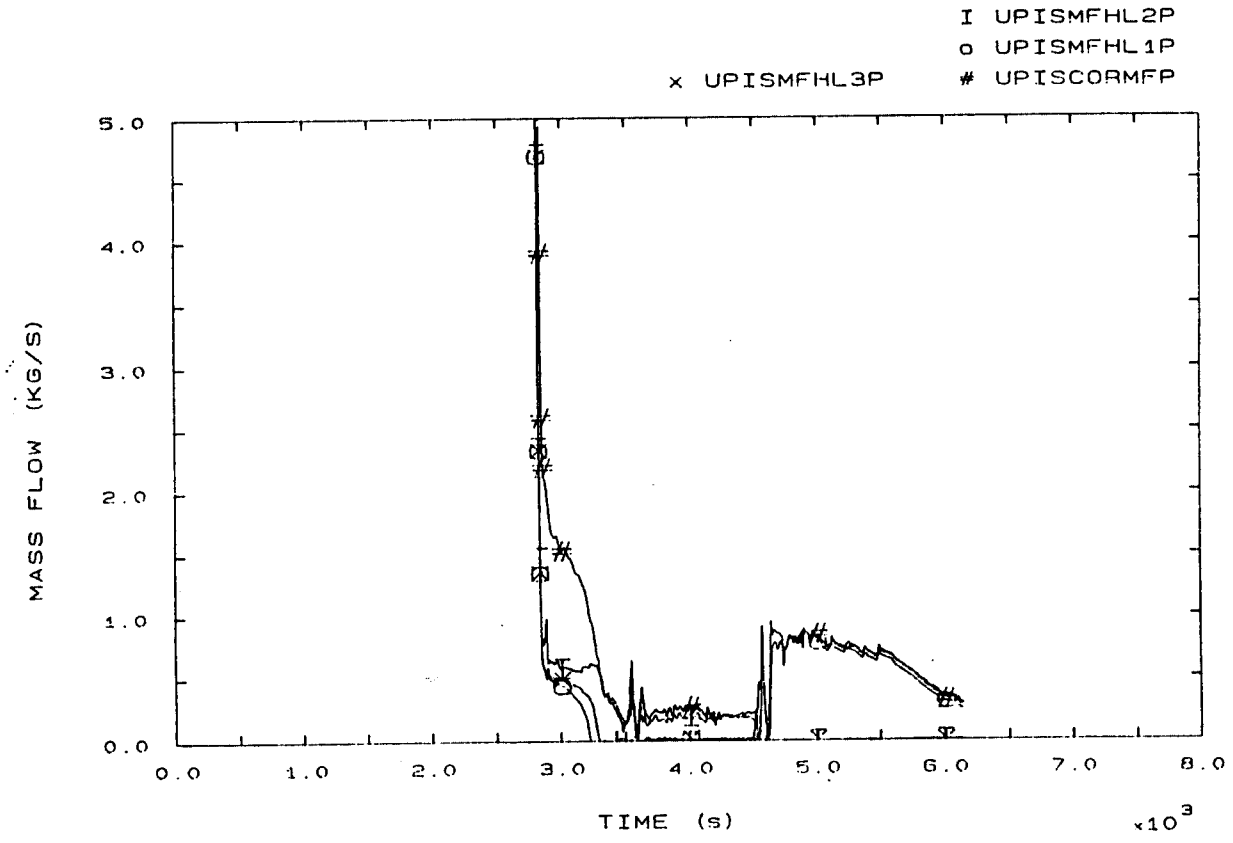

FIG. 141 BOTTOM CORE AND HOT LEG MASS FLOWS

4.14 STRATHCLYDE

4.14.1 CALCULATION DESCRIPTION

Phase 1: from LOFW to Scram (0,70 s)

A rapid loss in secondary mass inventory is observed which produces a decrease in the downcomer liquid level, reaching low-low level set point in 60 s MSIV in 65.6 s and Scram in 70.5 s (see fig. 7b, 8b, 9b).
On the primary side, a pressure peak is observed, following secondary pressure rise due to MSI (see fig. 1b, 3b). Primary pressure increases till Scram and is sufficient to open PRZ PORV.

Phase 2: from Scram to PRZ PORV opening (70, 1016 s)

On the secondary side, loss of secondary level slows down (fig. 7b) and pressure increases well above steam generator PORV set point (fig 3b, 4b, 5b). Subsequent opening and closing of S.G. valves maintain the pressure of steam generators at the set point value until dry-out, then the PORVS close and pressure decreases due to mass leakage (see figs. 3, 4, 5).
Following Scram, the primary system shows a fast decrease in primary pressure to a minimum of 14.1 MPa by 109 s (fig. 1b). Primary system then remains at a steady temperature and pressure until steam generators dry-out occurs (450 s) when the coolant temperature increases with subsequent increase in pressure and liquid level in the pressurizer (fig. 1, 6, 12).

Phase 3: from PRZ PORV opening to pumps trip (1016, 2495 s)

In the primary side the pressure is maintained at approximately the PORV set point value (fig. 1). Initially single phase vapour exits through the PORV until pressurizer fills with liquid (fig. 6),

then single phase liquid exits the primary system (fig. 103). System continues to heat up and mass flow circulating in the loops decreases as density decreases (see fig. 54, 55, 56).
In the secondary side the three steam generators continue to depressurize due to mass leakage (figs. 3, 4, 5).

Phase 4: from pumps trip to EFW actuation (2495, 3555 s)

Primary mass flow decreases rapidly as pump speed decreases (fig. 89). During this phase an over-pressurization of the primary system is predicted with the result that the PRZ PORV remains open for a large part of the time. Primary mass inventory continues to decrease. At about 2870 s LNC occurs (figs. 58, 62, 63).

Phase 5: from EFW actuation to the end (3555, 4693 s)

The core temperature increases rapidly (see fig. 50, 51, 52) to a maximum of 869 K at 3626 s. A top reflood of the core, originating from liquid being held up in the PRZ quickly reduces the rod temperatures, in conjuction with a TPNC established between the core and SG1 (fig. 62, 63). The primary pressure and temperature decrease as overcooling of the primary system takes place (fig. 1, 12, 42).
Steam generators in loops 2 and 3 continue to depressurize. Loop 1 steam generator pressurizes and the relief valve opens and maintains pressure at the set point value during refill of steam generator (fig. 3, 7).

PARTICIPANT: DEMPSTER - STRATHCLYDE *CODE: TRAC*

EVENTS TABLE

EVENT	*CALC. TIME (s)*	*EXP. TIME (s)*
SG Low Low Level	*60*	*33*
Main Steam Isolation	*66*	*38*
Scram (power fall), t_1	*70*	*44*
SGs PORV opening	*75* *75* *75*	*82 (3)* *106 (2)* *200 (1)*
SGs Dry Out	*447 (3)* *453 (2)* *466 (1)*	*3282 (3)* *3347 (1)* *3437 (2)*
PRZ PORV opening, t_2	*1016*	*4134*
PRZ full of liquid	*1307*	*4222*
Pumps Trip, t_3	*2495*	*4848*
Loss of Natural Circulation	*2870*	*5630*
Beginning of Core Heat Up	*3540*	*6511*
EFW actuation, t_4	*3555*	*6532*
PRZ PORV closure	*3582*	*6576*
PRZ emptying	*3840*	*6811*
SG1 repressurization	*3763*	*6878*
End of transient, t_{END}	*4693*	*8062*

4.14.2 CALCULATION/EXPERIMENT COMPARISON

Phase 1: from LOFW to Scram

Initial secondary inventory is underestimated, even with higher initial levels (see Comp. Table and fig. 7b, 8b, 9b). Trips timing is sensibly delayed, due to a large overestimate of low low level time (60 s vs 33) which can be partly explained by the high initial level. This causes Scram to occur at 70.5 s and, consequently, SGs to reach a very low inventory at this time (40 Kg). Primary pressure profile during this phase is calculated with sufficient accuracy (see fig. 1b).

Phase 2: from Scram to PRZ PORV opening

The minimum primary pressure immediately after Scram is slightly underestimated, also if PRZ level is accurately predicted at this time (see fig. 1b, 6b). Primary pressure gradients before and after SGs Dry Out are strongly overpredicted (see Comp. Table and fig. 1)
Such a discrepancy can be attributed to PRZ and SL modelling difficulties, particularly an insufficient simulation of cool insurge phenomenon (figs. 112, 113). SGs PORV opening times are sensibly underpredicted (see event table) but secondary pressurization trend immediately after MSI is correctly simulated (fig. 3b, 4b, 5b). SGs Dry Out time is extremely underestimated (450 s vs 3300) due to low heat losses, delayed Scram and low initial secondary inventory (see fig. 7, 8, 9). Primary temperature and level gradients during heat up are in good agreeement with the experimental values (see Comp. Table and fig. 6, 12, 22, 32). Primary pressurization during this phase is much faster than in the Exp. (fig. 1), but a pressurization slow down during warm insurge into the PRZ is observed (see fig. 1, 7, 112, 113). Time of PRZ PORV opening is consequently strongly underpredicted (1016 s vs 4134), but time interval since the latest SG dry

out is calculated with reasonable accuracy (550 s vs 697). Due to faster pressure rise during primary heat up, PRZ level at time t_2 (fig. 6) is lower than in the Exp. (5.4 m vs 6.57).

Phase 3: from PRZ PORV opening to pumps trip

PRZ goes full at 1307 s (4222 in the Exp.) due to early SGs Dry Out. Dominant relief only condition during this phase (subcooled liquid discharge) is correctly predicted, so as the absence of saturated points inside the primary system before pumps trip.
Pumps trip time (2495 s) is also strongly underpredicted (4848 s in the Exp.), but the advance w.r.t. experimental timing is reduced, due to a longer phase duration dt_3 (1480 s vs 714) that can be partly explained with the early PORV opening time and the indipendence of primary temperature profile from pressurization trend. Also heat up time interval dt_{HU} is significantly overestimated (2029 vs 1411 s), mainly due to a difference in fluid temperature at the beginning of phase 3 (figs. 12, 22 and C.T.).

Phase 4: from pumps trip to EFW actuation

PRZ behaviour during phase 4 is adequately simulated by Strathclyde calculation: both partial PRZ emptying following pumps shut off and level obscillations around a value of about 4 m are predicted (see fig. 6). Primary flow conditions are also reasonably calculated: two phase natural circulation (TPNC) is followed by a period of stagnation (fig. 62, 63, 89). Time of loss of natural circulation (t_{LNC}) is again underestimated, both in the absolute sense (2870 s vs 5630) and in the relative one, when referred to pumps trip time (375 s vs 780). Strathclyde calculation shows a primary pressure peak following LNC, which has to be related to the low quality discharge from PRZ PORV during this interval (fig. 1, 92, 103). Core heat up starts at 3540 s (vs 6511), that is 670 seconds (880 in the Exp.) after LNC time (see Comp. Table).

Core heat up rate (fig. 50, 51, 52) is calculated (3 K/s at bundle top) with good accuracy (2 to 5 K/s in SPES core). EFW actuation time t_4 (3555 s) is again strongly underestimated, but time intervals since beginning of core heat up (dt_{4B}) and loss of natural circulation time (dt_{4L}) are calculated with sufficient accuracy (see Comp. Table). EFW actuation "time advance" (w.r.t. the experimental value) is about 3000 seconds, the same amount of time "gained" by SGs dry out time. PRZ level at time t_4 is calculated with good accuracy. Phase duration dt4 is underestimated due to shorter NC and stagnation periods. This is related to low quality PRZ relief and a low value of heat losses.

Phase 5: from EFW actuation to the end

Maximum core temperature (869 K) is sensibly overpredicted (see fig. 52) also if PRZ PORV closure delay dt_{PRZPC}, primary depressurization rates and PRZ emptying time are calculated with sufficient or even extremely good accuracy (see Comp. Table and fig. 1, 6).
Primary circulation mode calculated by TRAC is of the continuous type: the intermittent SGs tubes filling/emptying observed in the Exp. is not predicted (see fig. 62, 63). Core flooding is calculated to take place from the top. PRZ emptying contributes to core flooding.
SG1 pressurization time (3763 s vs 6878 in absolute terms) is calculated with sufficient accuracy if compared with EFW actuation time: pressurization interval dt_{SG1PR} (see fig. 3) is 208 s (338 in the Exp.). The calculated transient terminates about 3400 s before the Exp.: some more time is "gained" by calculations towards the end, due to a more rapid level recovery in SG1 (see fig. 7).

PARTICIPANT: DEMPSTER - STRATHCLYDE CODE: TRAC

COMPARISON TABLE

PARAMETER		EXP	CALC	AE*	RFD**
1A Initial SGs mass (Kg)	1	137	117		
	2	151	117	P	B+C+U?
	3	145	117		
1B Trips timing (s)	LoLo	33	60		HIL (B+C+U)
	MSI	38	66	P	LoLo
	Scram	44	70		LoLo
1C Max primary pressure (MPa)		16.2	16.3	G	-
1D SGs mass at Scram (Kg)	1	98	40		
	2	105	40	P	1A+1B
	3	97	40		
2A Min. primary pressure (MPa)		14.5	14.1	G	-
Pressure gradients before		4.10^{-4}	9.6.10-4	P	PRZM (U+B)
and after SGs DO (MPa/s)		3.10^{-4}	3.3.10-3	P	PRZM (U+B)
2B SGs PORV opening time (s)	1	200	75	P	?
	2	106	75	P	?
	3	82	75	S	-
2C PRZ level gradient (m/s)		$-5.7.10^{-4}$	n.a.	-	-
2D Min. PRZ level (m)		2.3	3.2	-	-
2E SGs DO time tSG1DO (s)		3347	466	P	1D,LHL (U)
tSG2DO (s)		3437	453	P	
tSG3DO (s)		3282	447	P	
2F Heat Up temperature (K/s)		0.02	0.024	G	-
and level (m/s) gradients		$3.6.10^{-3}$	3.7.10-3	G	-
2G Cool Insurge effect		PR. DELAY	Slow down?	S	-
2H PRZ PORV opening time, t_2 (s)		4134	1016	P	2E+
($dt_2 = t_2 - t_{SGDO}$)		(697)	(550)	S	PRZM (U+B)
3A PRZ level at t_2 (m)		6.57	5.4	P	2H
3B PRZ full time, t_{PRZF} (s)		4222	1307	P	2E
($dt_{PRZF} = t_{PRZF} - t_2$)		(88)	(291)	P	3A
3C Dominant Relief Condition		LIQ	LIQ	G	-
3D Sat. Conditions before trip		NO	NO	G	-
3E Pumps Trip time, t_3 (s)		4848	2495	P	2E
($dt_3 = t_3 - t_2$)		(714)	(1480)	P	2H
($dt_{HU} = t_3 - t_{SGDO}$)		(1411)	(2029)	P	2E

* ACCURACY EVALUATION : G=GOOD, S=SUFFICIENT, P=POOR

** REASON FOR DISCREPANCY : B=BIC, C=CODE, U=USER, PRZM=PRZ MODELLING
HIL=HIGH INITIAL LEVEL, LHL = LOW HEAT LOSSES

PARTICIPANT: DEMPSTER - STRATHCLYDE CODE: TRAC

COMPARISON TABLE (CONT'D)

PARAMETER	EXP	CALC	AE*	RFD**
3F RCS mass at t_3 (kg)	390	360?	S?	(1)
4A PRZ behaviour	PART. EMPT.	PART. EMP.	G	-
during phase 4	LEV. OBS.	LEV. OBS.	G	-
4B Primary Flow Cond.	TPNC/LNC	TPNC/LNC	G	-
4C LNC time, t_{LNC} (s)	5630	2870	P	3E
($dt_{LNC} = t_{LNC} - t_3$)	(780)	(375)	P	LDP,LHL(C+U)
4D RCS mass at t_{LNC} (kg)	296	n.a.	-	-
4E Beg. of Core Heat Up, t_{BOCH} (s)	6511	3540	P	3E
($dt_{BOCH} = t_{BOCH} - t_{LNC}$)	(880)	(670)	S	-
4F RCS mass at tBOCH (Kg)	183	n.a.	-	-
4G EFW act. time, t4 (s)	6532	3555	P	3E
($dt_{4B} = t_4 - t_{BOCH}$)	(21)	(15)	S	-
($dt_{4L} = t_4 - t_{LNC}$)	(900)	(685)	S	-
($dt_4 = t_4 - t_3$)	(1684)	(1060)	P	LDP,LHL(C+U)
4H PRZ level at t_4 (m)	4.4	4.6	G	-
5A Core Heat Up Rate (K/s)	2/5	3	G	-
5B Max Core Temperature (K)	770	869	P	?
5C PRZ PORV closure time, t_{PRZPC}	6576	3582	P	3E
($dt_{PRZPC} = t_{PRZPC} - t_4$)	(44)	(27)	S	-
5D RCS mass at t_{PRZPC} (Kg)	179	n.a.	-	-
5E RCS Depress. Rate (MPa/s)	-0.016	-0.017	G	-
(Initial/Averaged on 500 s)	-0.0086	-0.01	G	-
5F Prim. Circulation Mode	INTERM	TPNC	P	(C+U)?
5G SG1 Press. time, t_{SG1PR} (s)	6878	3763	P	3E
($dt_{SG1PR} = t_{SG1PR} - t_4$)	(346)	(208)	S	-
5H PRZ Role	CORE FL.	CORE FL.	G	-
5I PRZ emptying time, t_{PRZE} (s)	6811	3840	P	3E
($dt_{PRZE} = t_{PRZE} - t_4$)	(280)	(285)	G	-
5J Core Reflood Mode	TOP-DOWN	TOP-DOWN	G	-
5K End of Transient time, t_{END}	8062	4693	P	3E

* ACCURACY EVALUATION : G=GOOD, S=SUFFICIENT, P=POOR

** REASON FOR DISCREPANCY: C=CODE, U=USER, LDP = LIQUID DISCHARGE FROM PRZ, LHL=LOW HEAT LOSSES, (1) MASS CURVE PROVIDED AS GRAPH

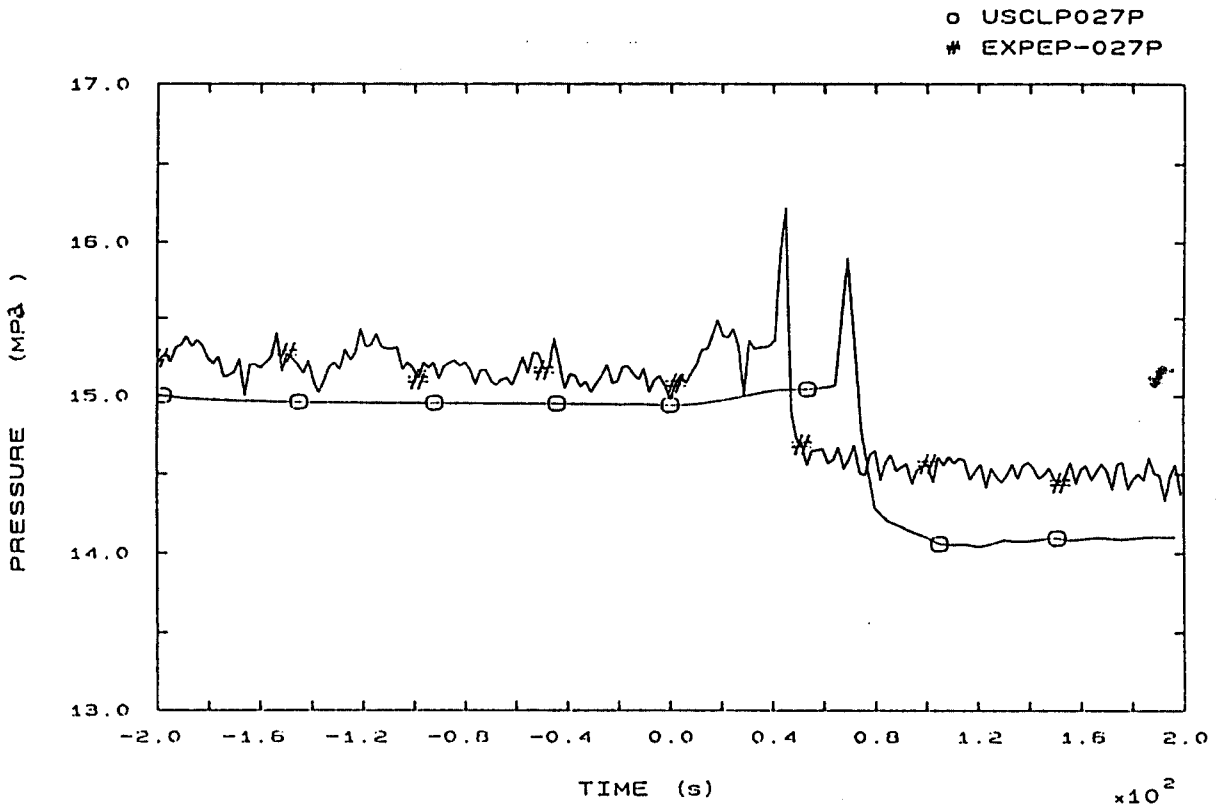

FIG. 1b PRESSURIZER PRESSURE

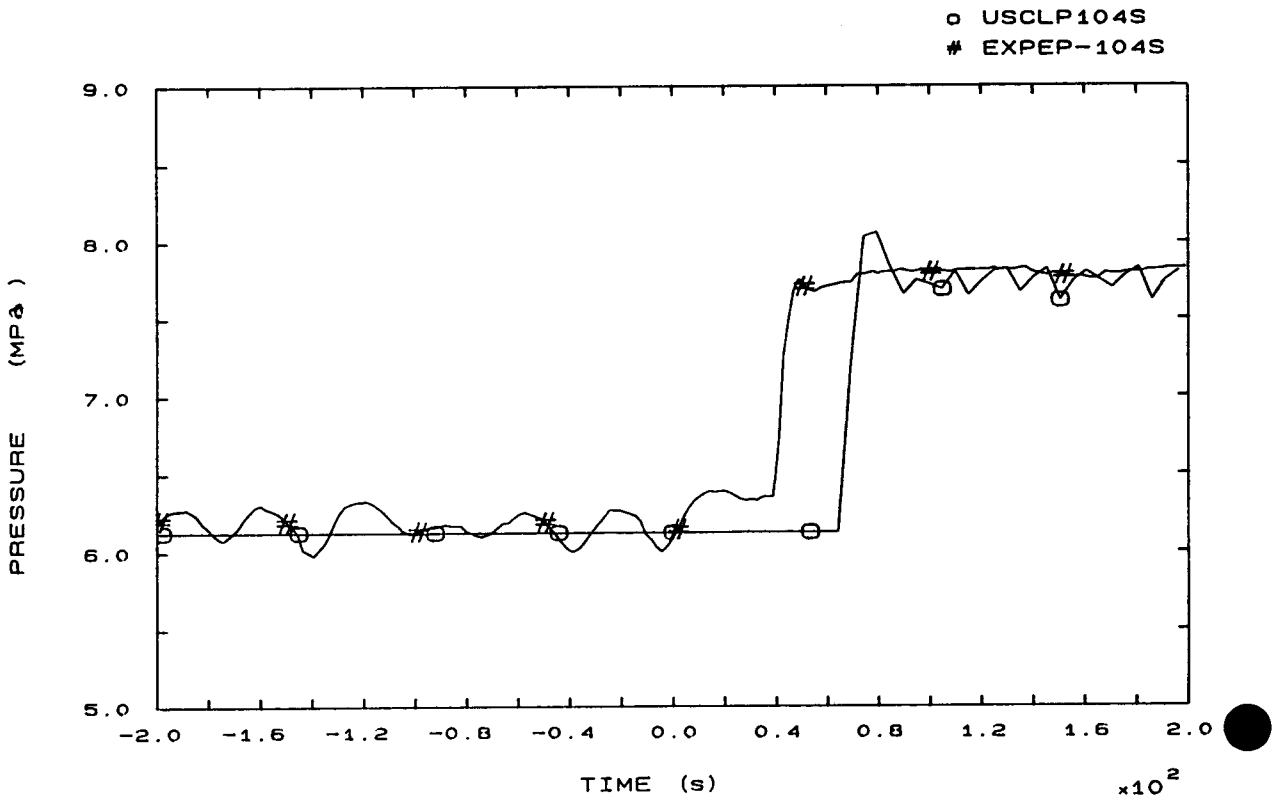

FIG. 3b SG1 STEAM DOME PRESSURE

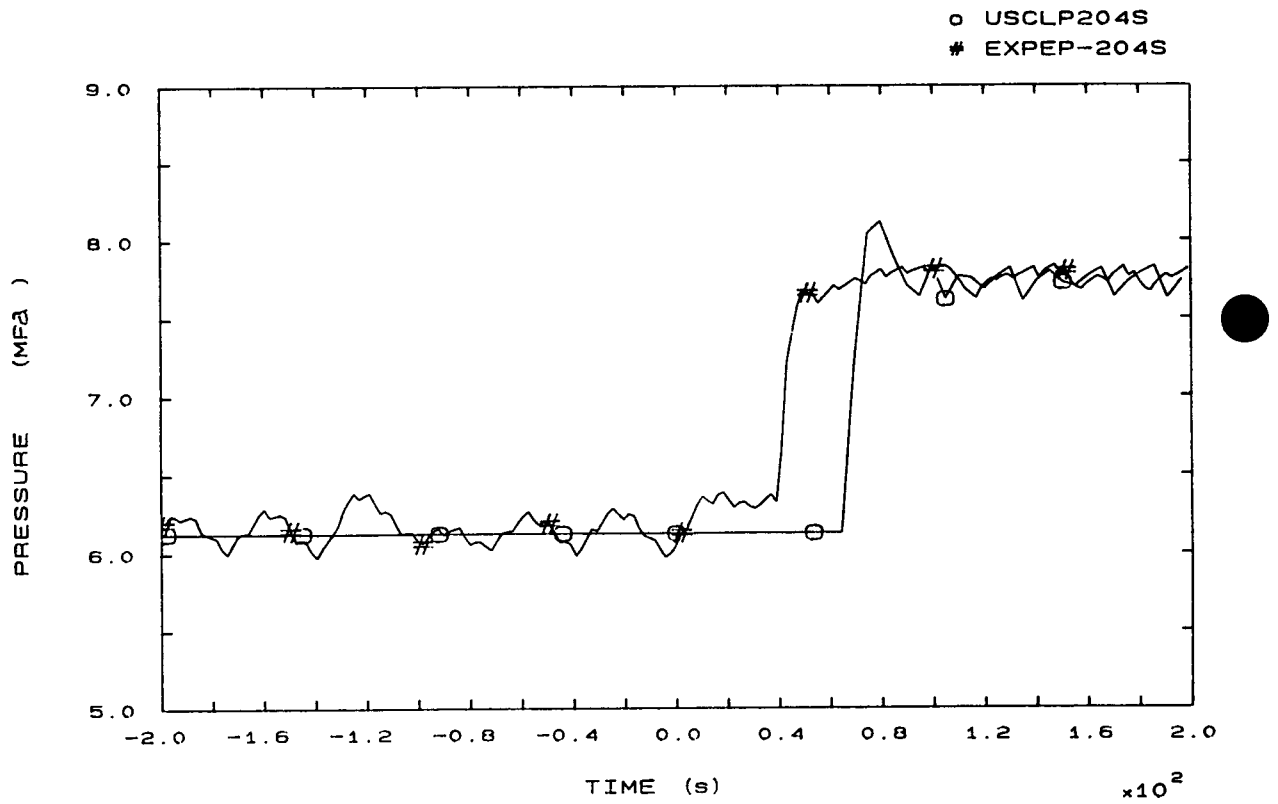

FIG. 4b SG2 STEAM DOME PRESSURE

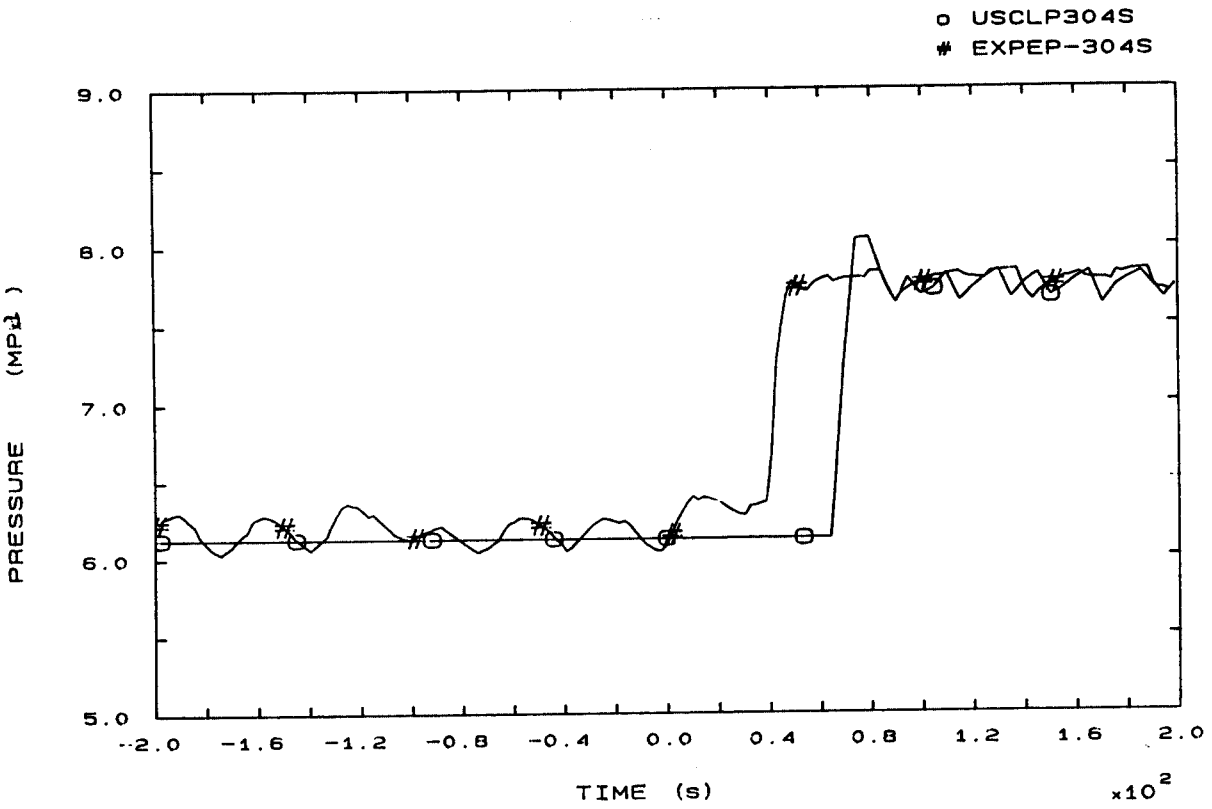

FIG. 5b SG3 STEAM DOME PRESSURE

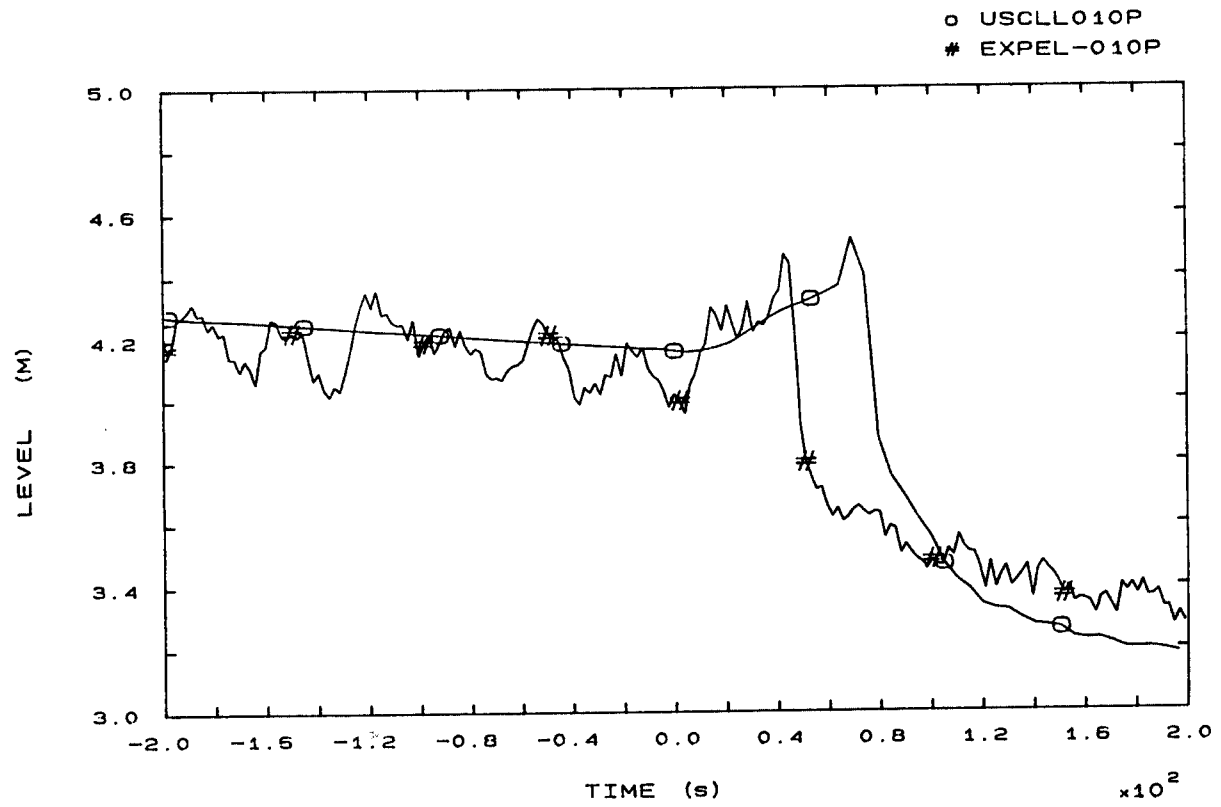

FIG. 6b PRESSURIZER LEVEL

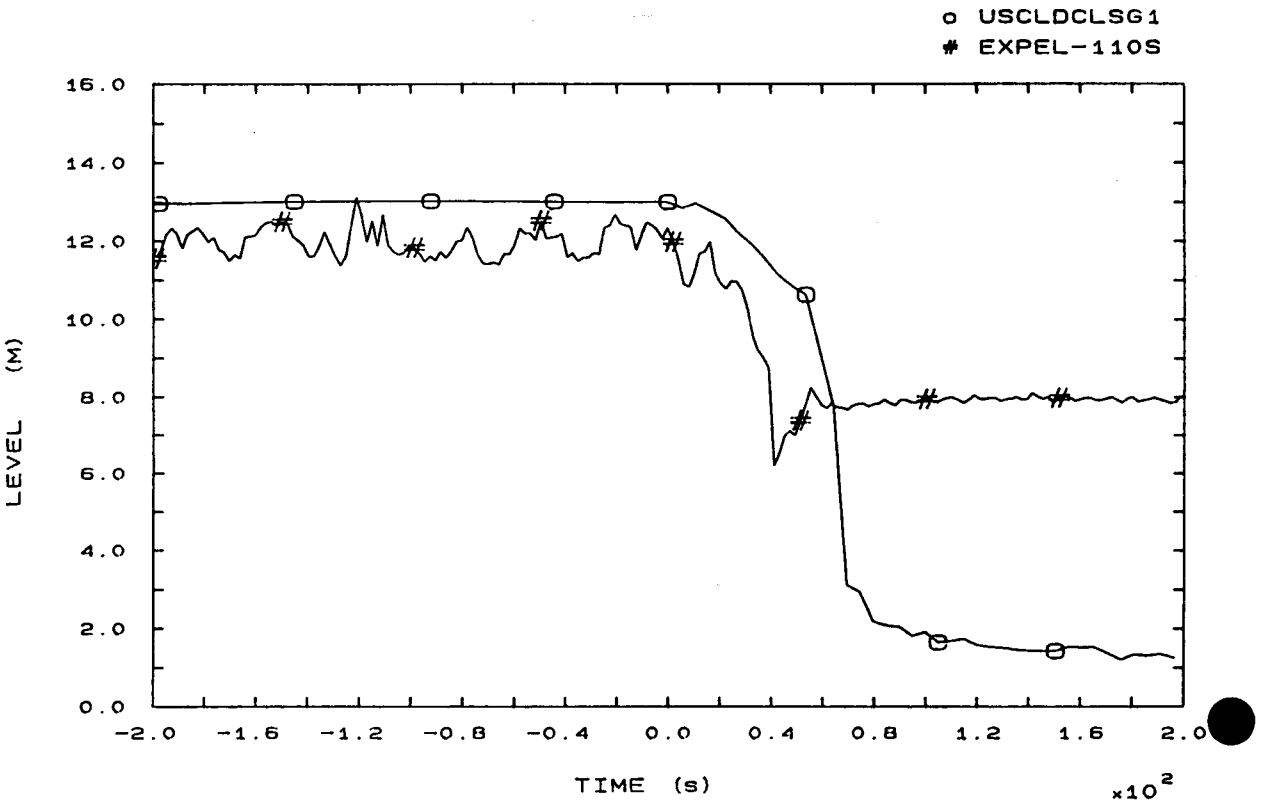

FIG. 7b SG1 DOWNCOMER LEVEL

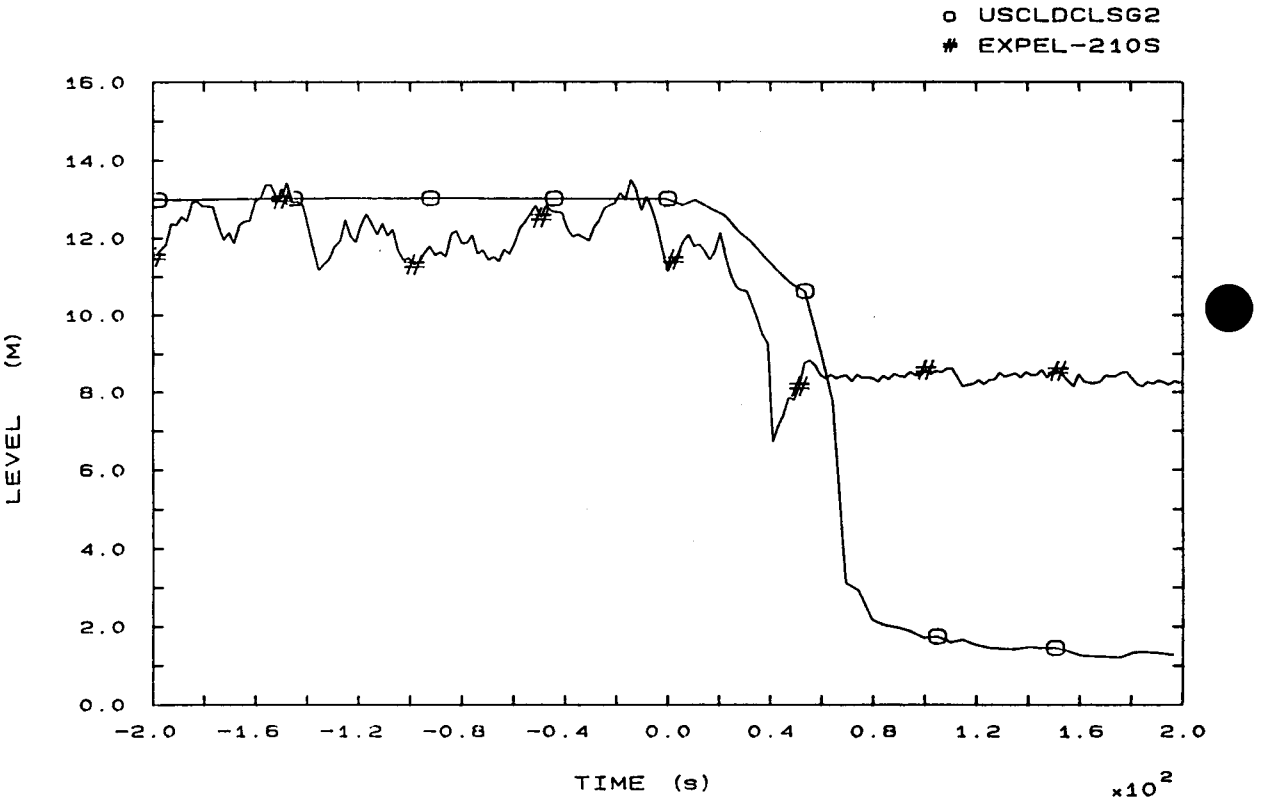

FIG. 8b SG2 DOWNCOMER LEVEL

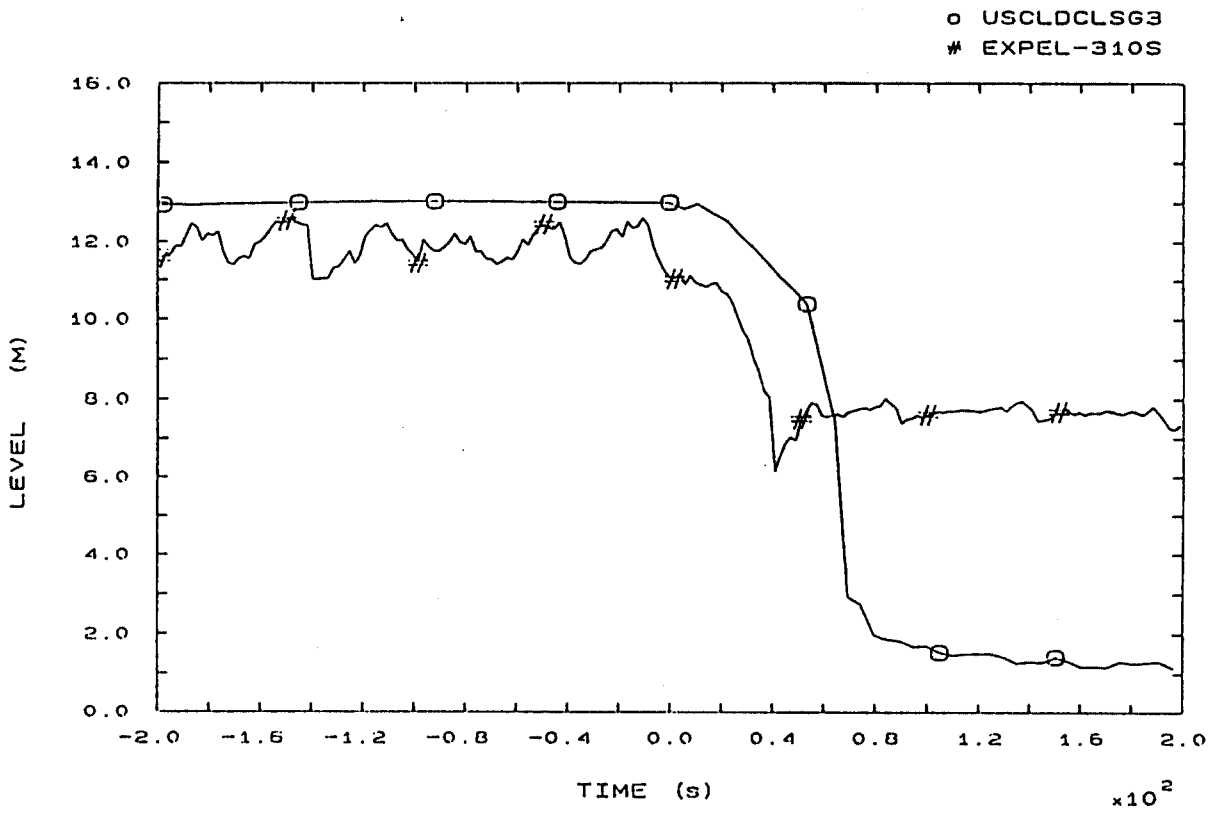

FIG. 9b SG3 DOWNCOMER LEVEL

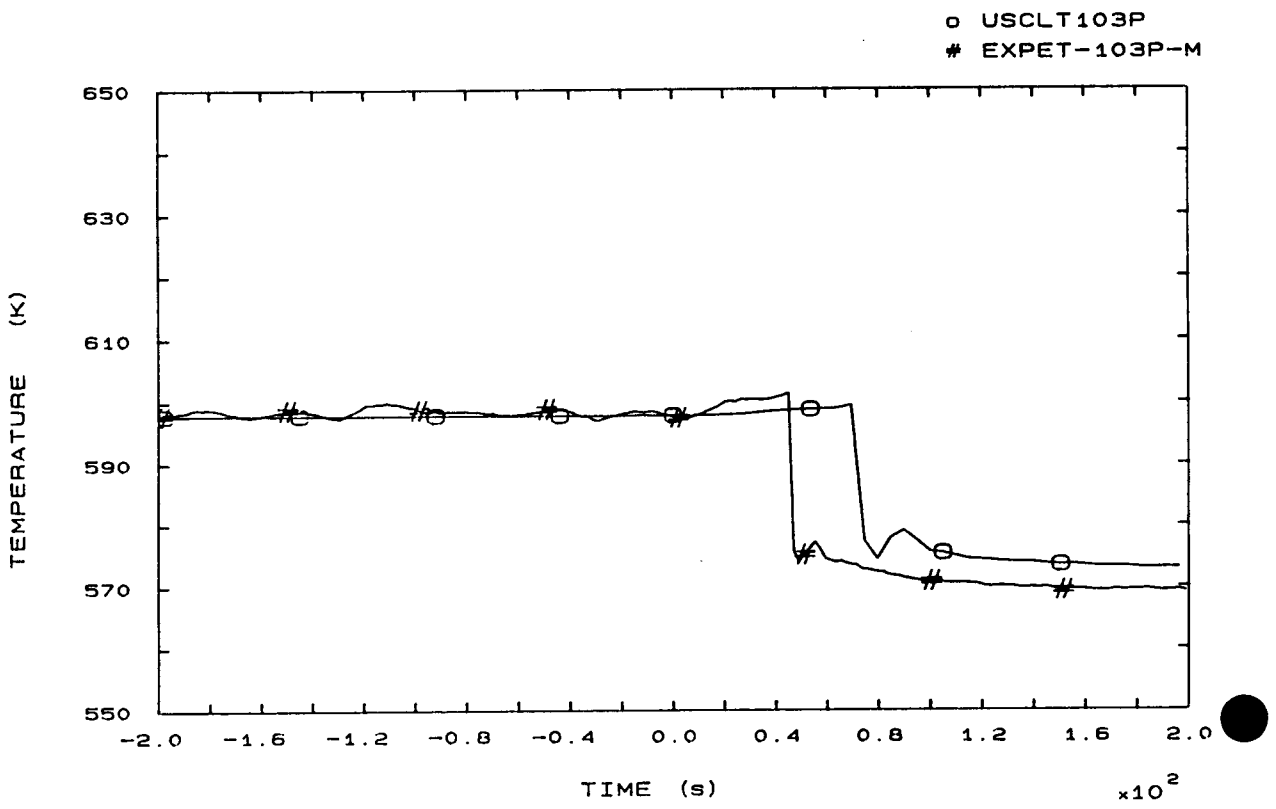

FIG. 12b LP1 HOT LEG OUTLET VESSEL TEMPERATURE

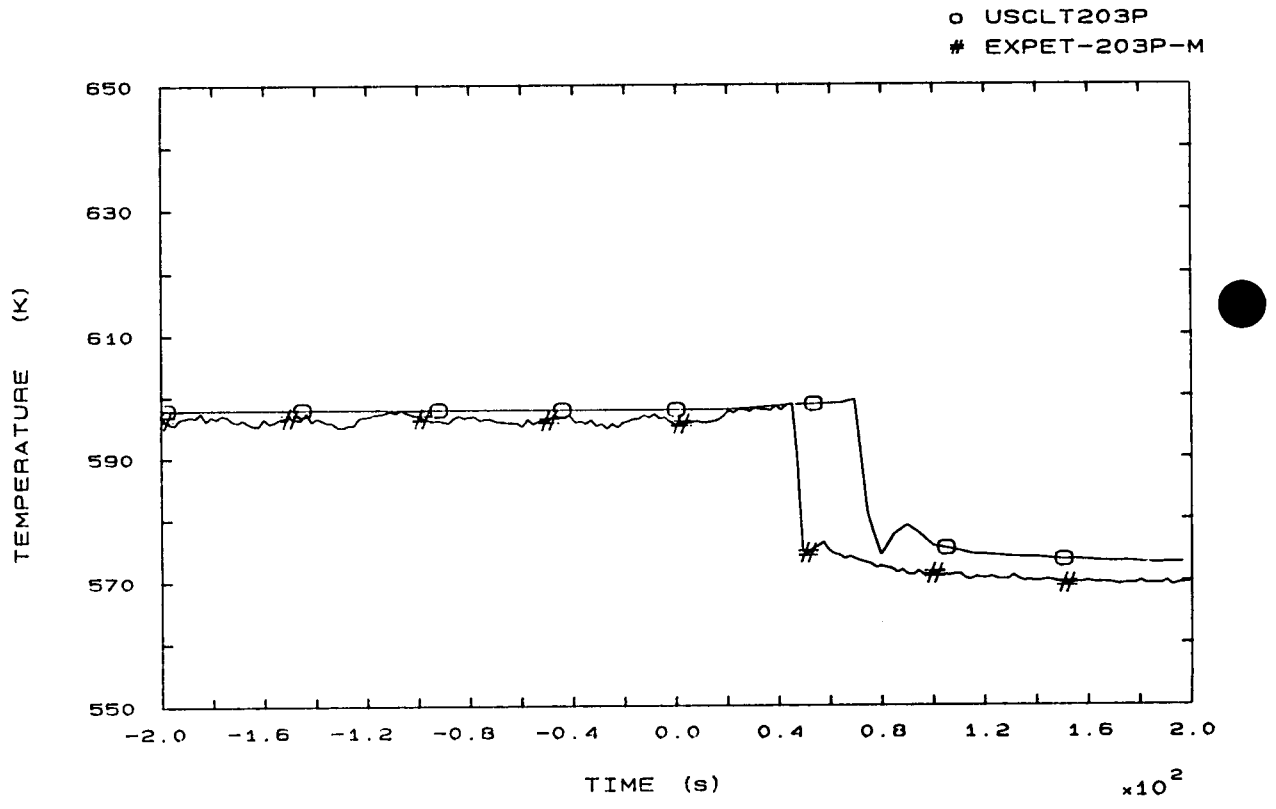

FIG. 22b LP2 HOT LEG OUTLET VESSEL TEMPERATURE

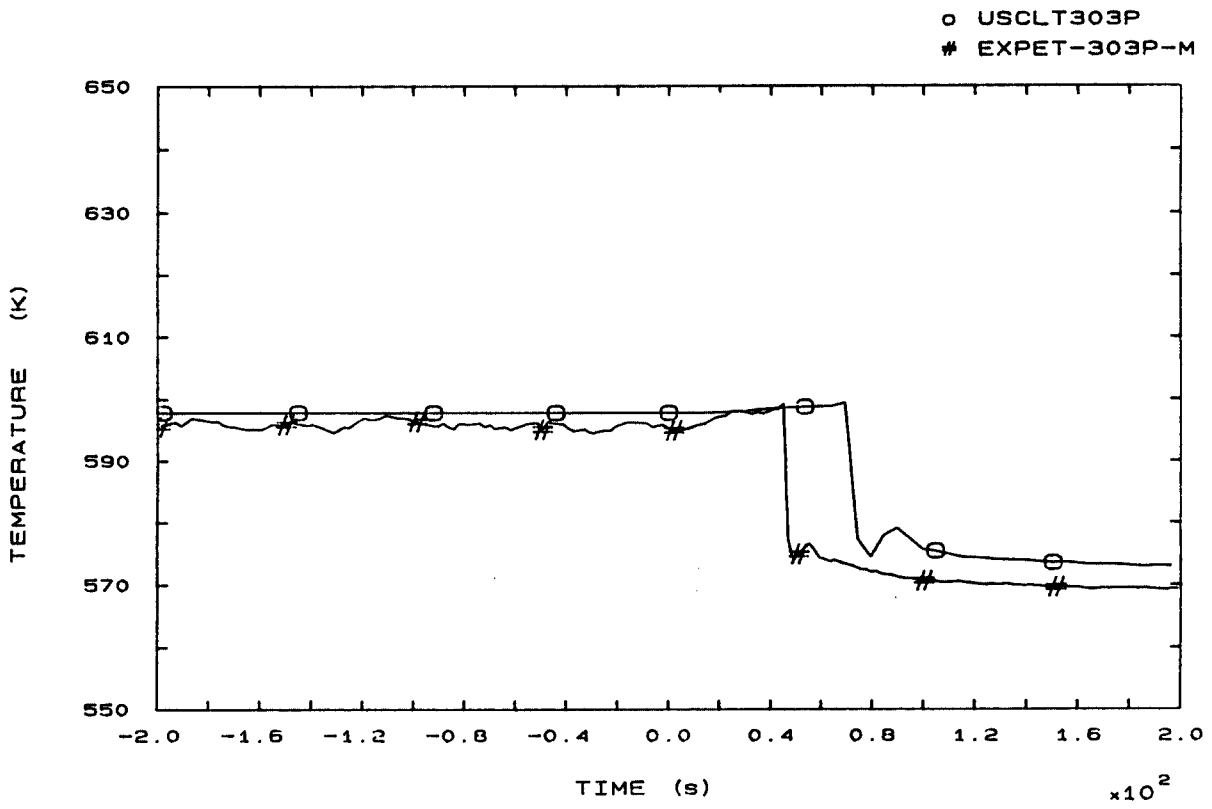

FIG. 32b LP3 HOT LEG OUTLET VESSEL TEMPERATURE

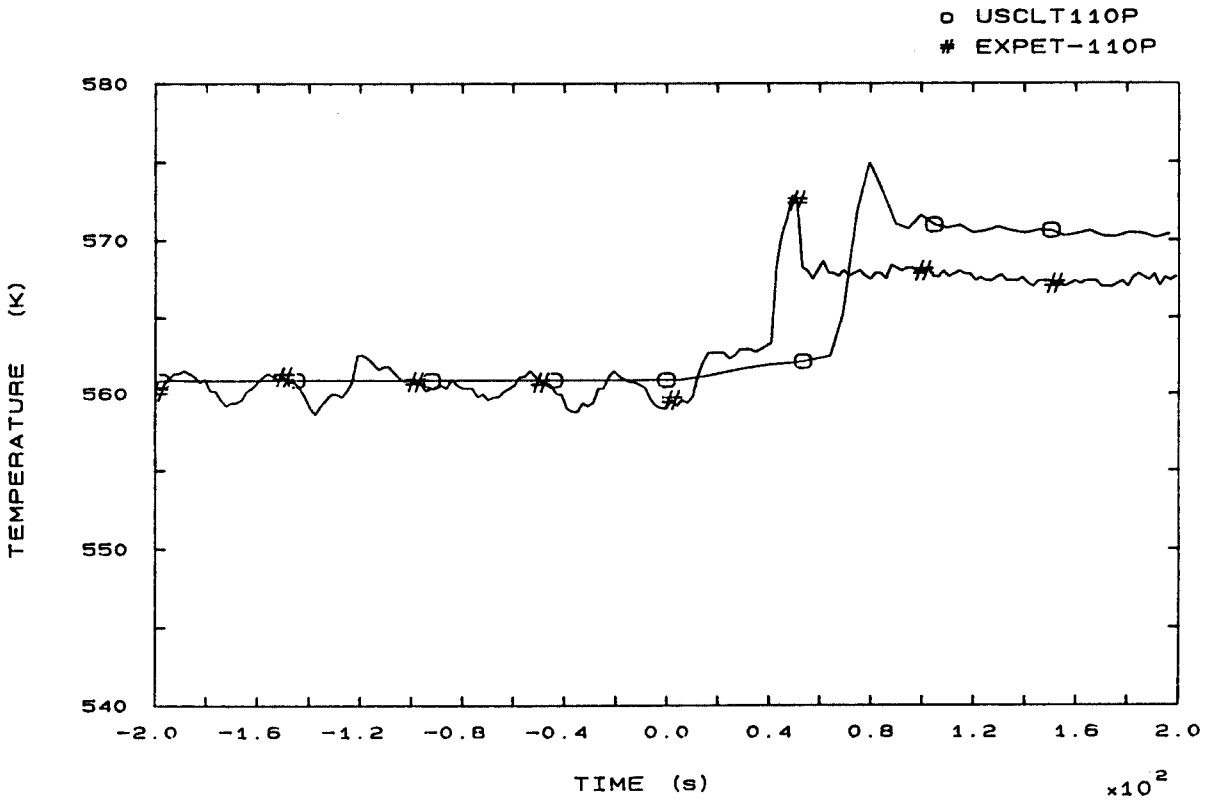

FIG. 42b SG1 OUTLET TEMPERATURE

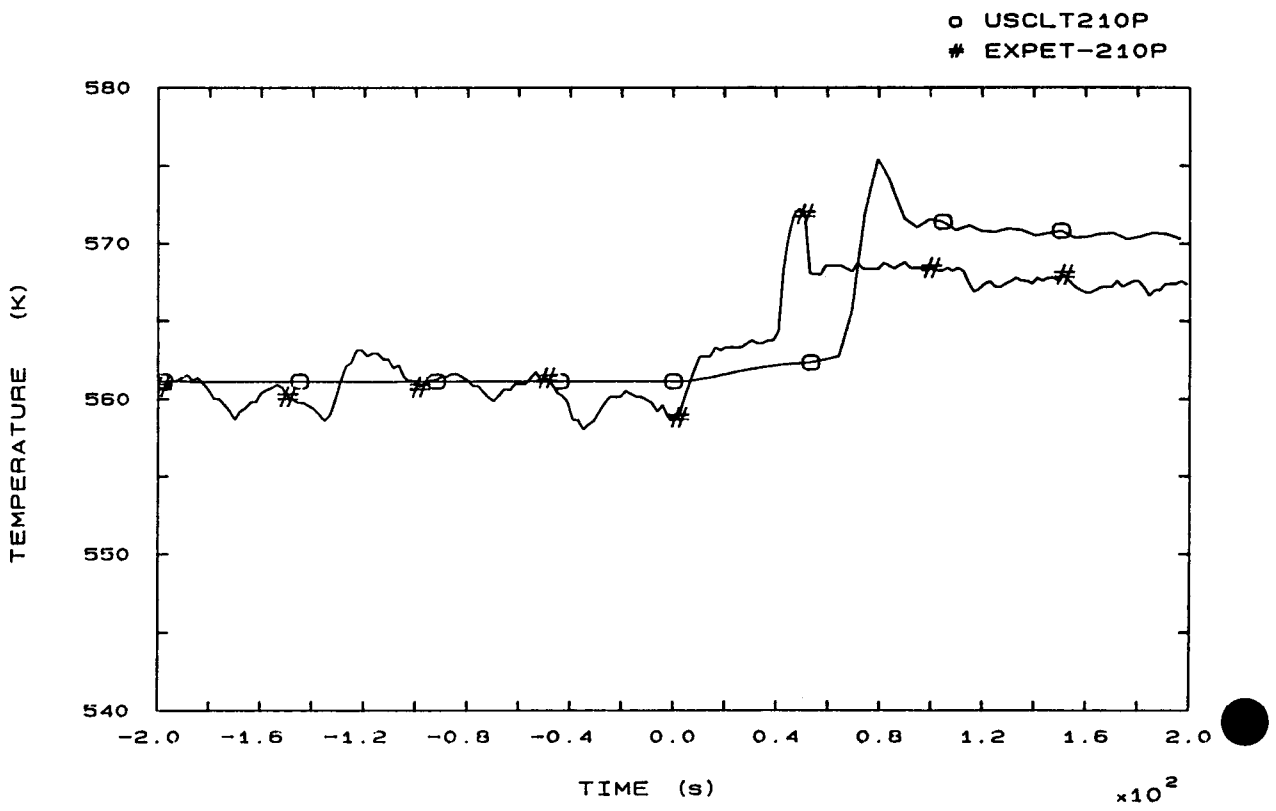

FIG. 44b SG2 OUTLET TEMPERATURE

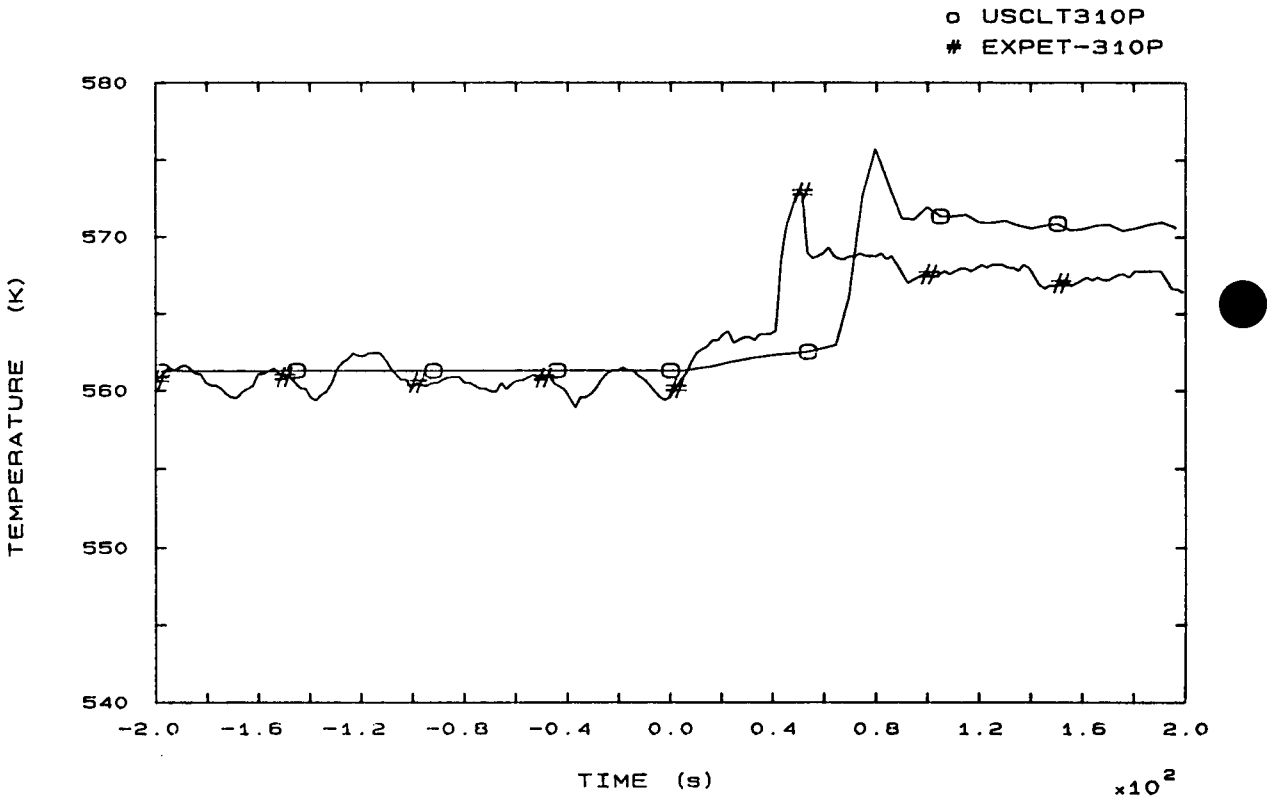

FIG. 46b SG3 OUTLET TEMPERATURE

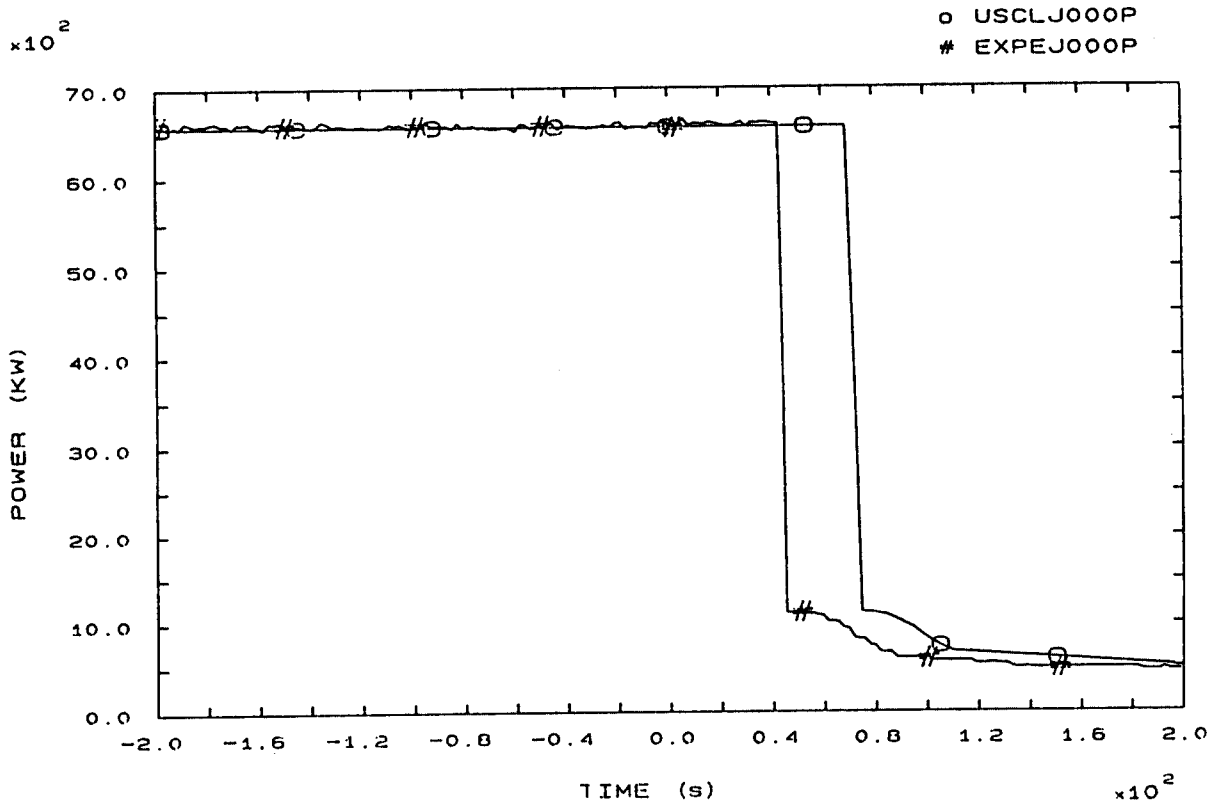

FIG. 81b HEATER RODS POWER

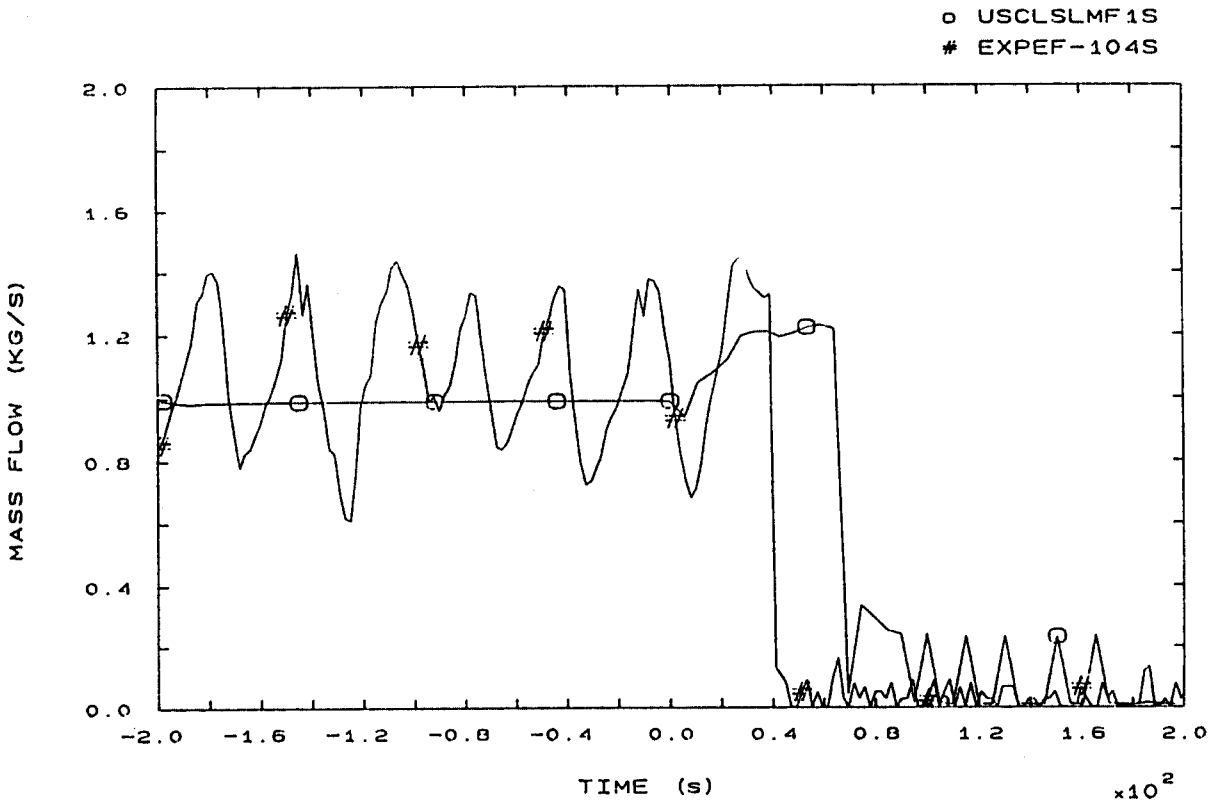

FIG. 96b STEAM LINE 1 MASS FLOW

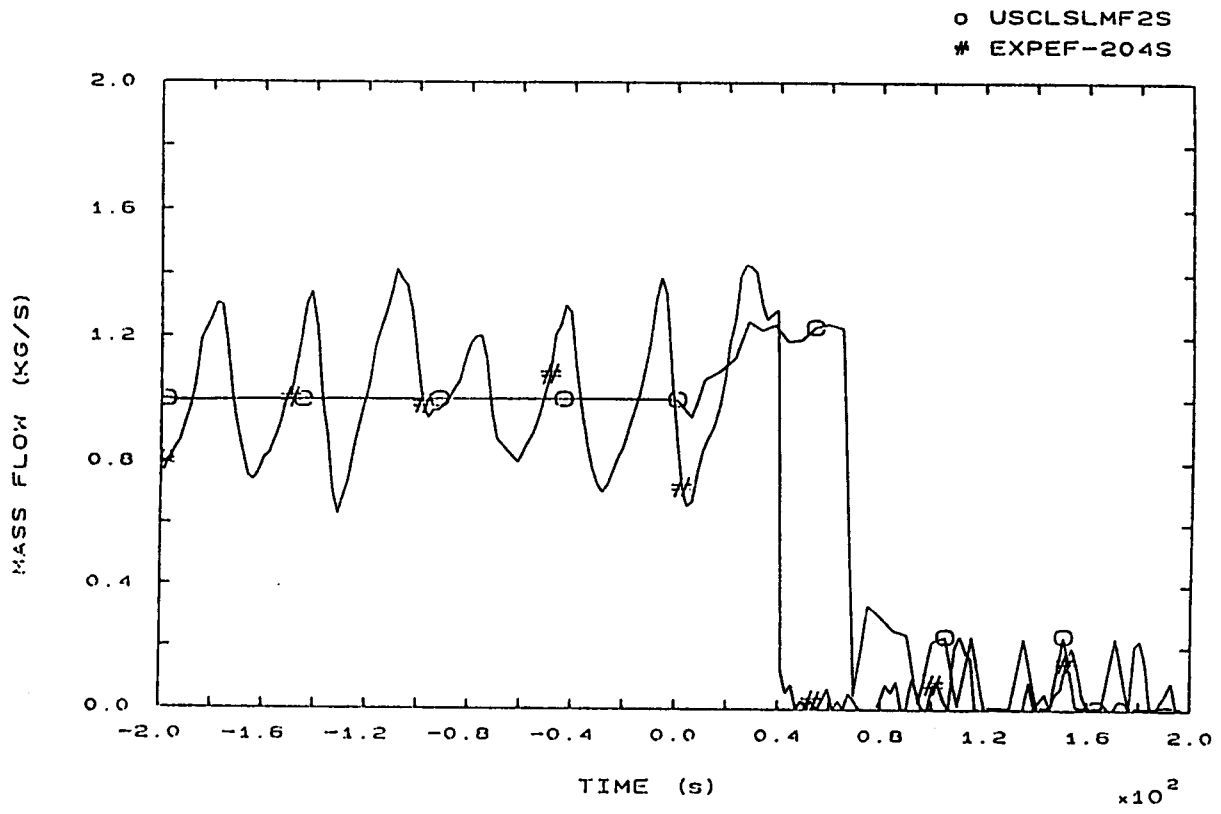

FIG. 97b STEAM LINE 2 MASS FLOW

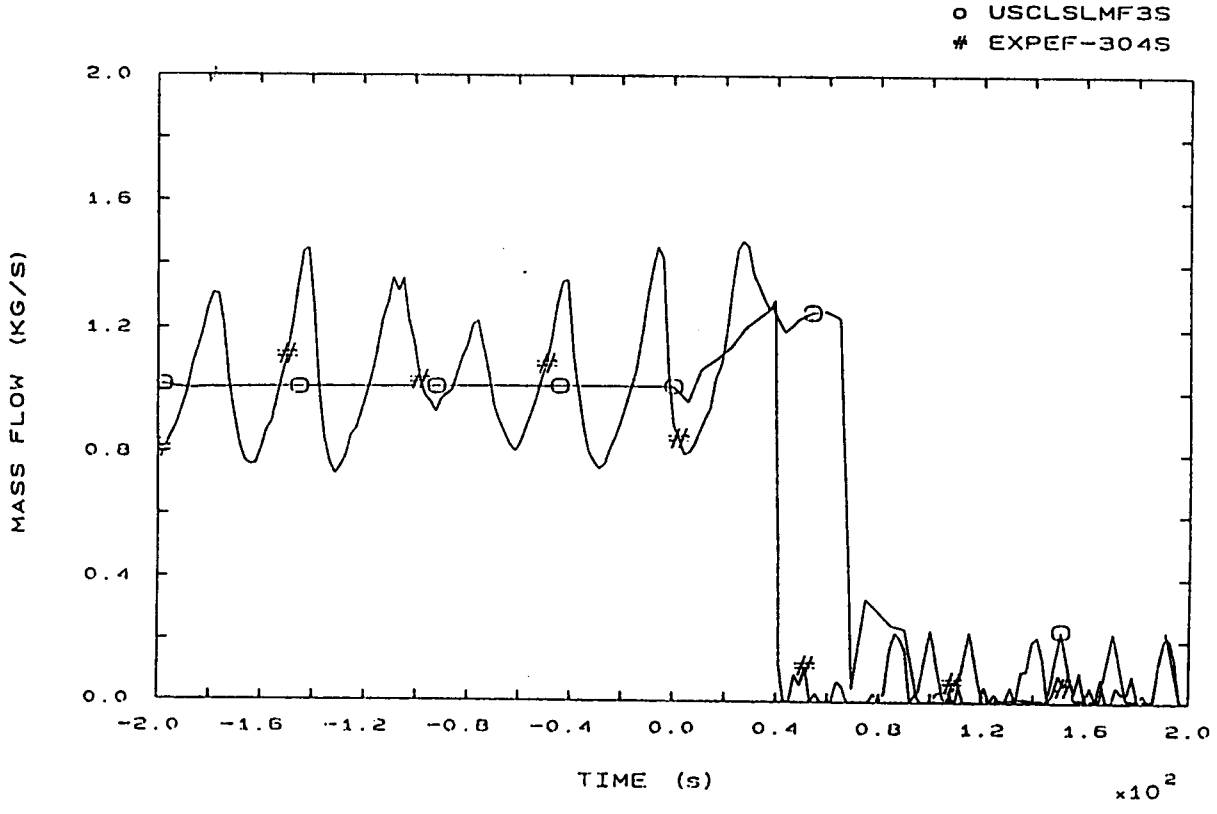

FIG. 98b STEAM LINE 3 MASS FLOW

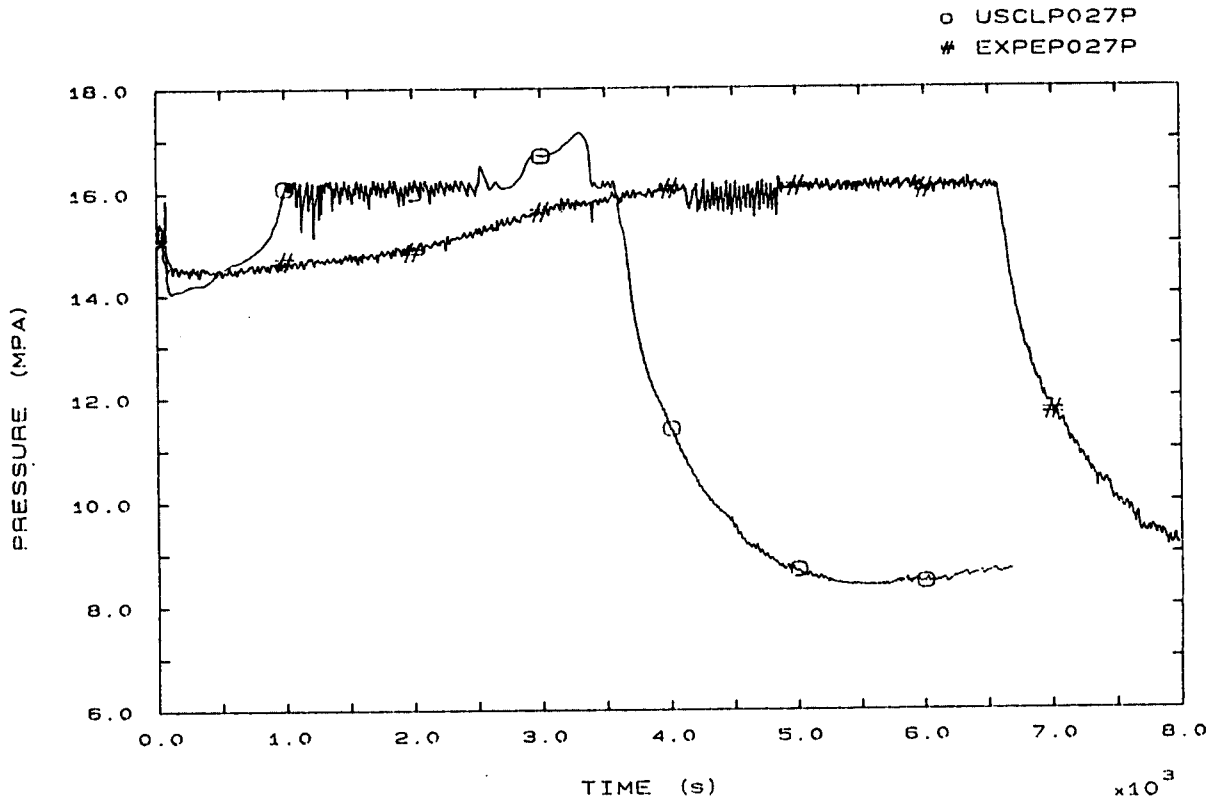

FIG. 1 PRESSURIZER PRESSURE

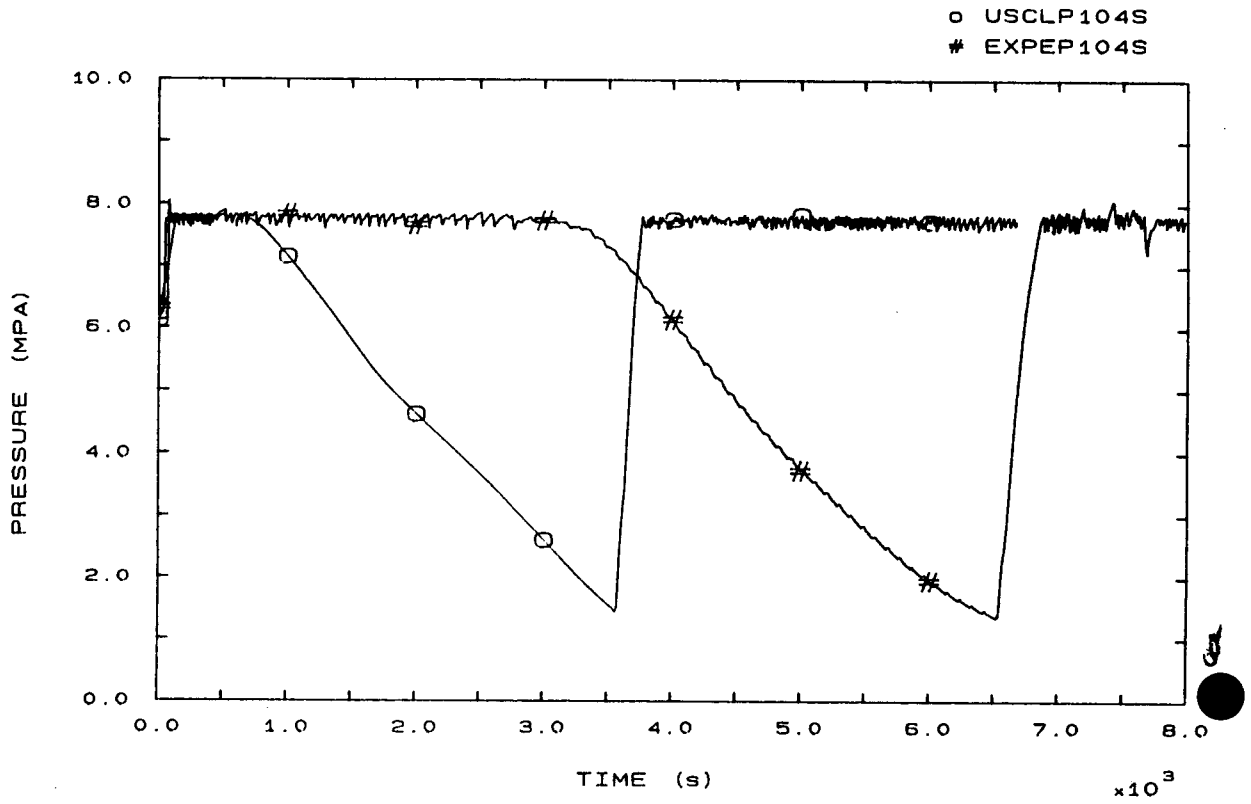

FIG. 3 SG1 STEAM DOME PRESSURE

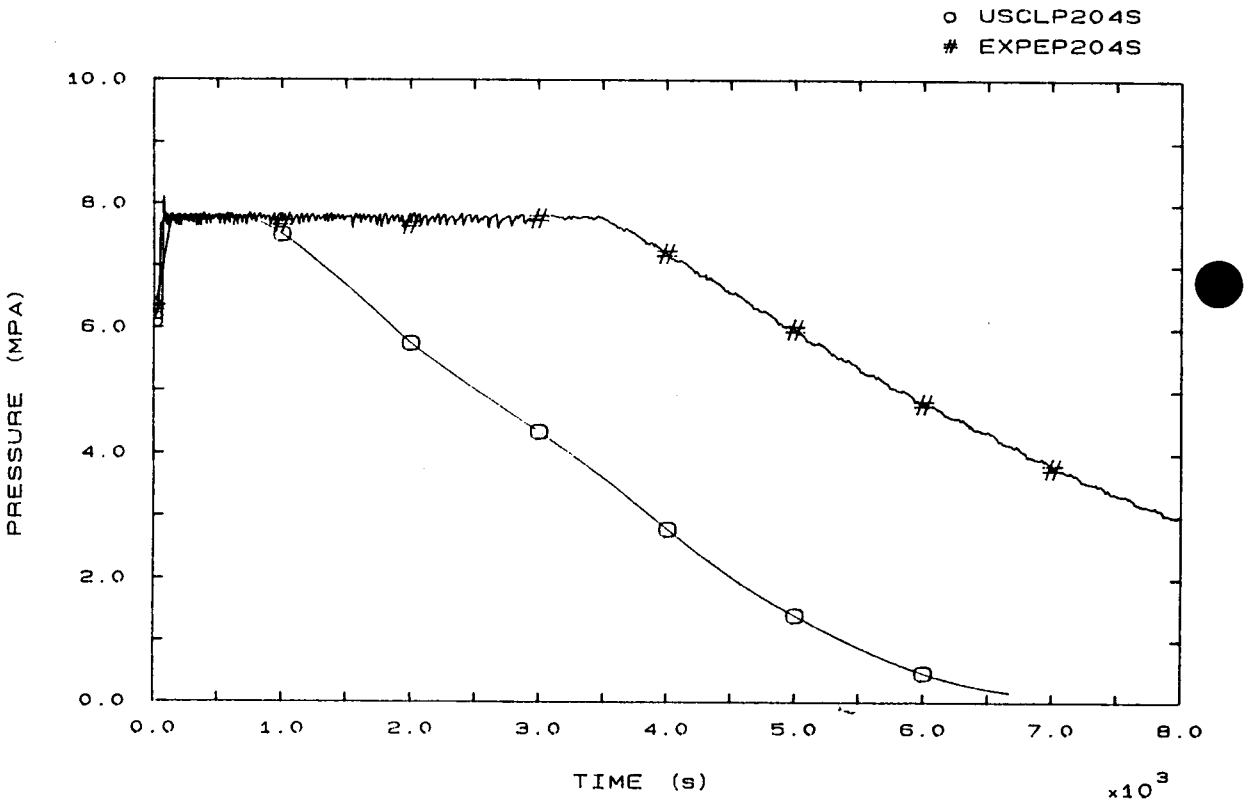

FIG. 4 SG2 STEAM DOME PRESSURE

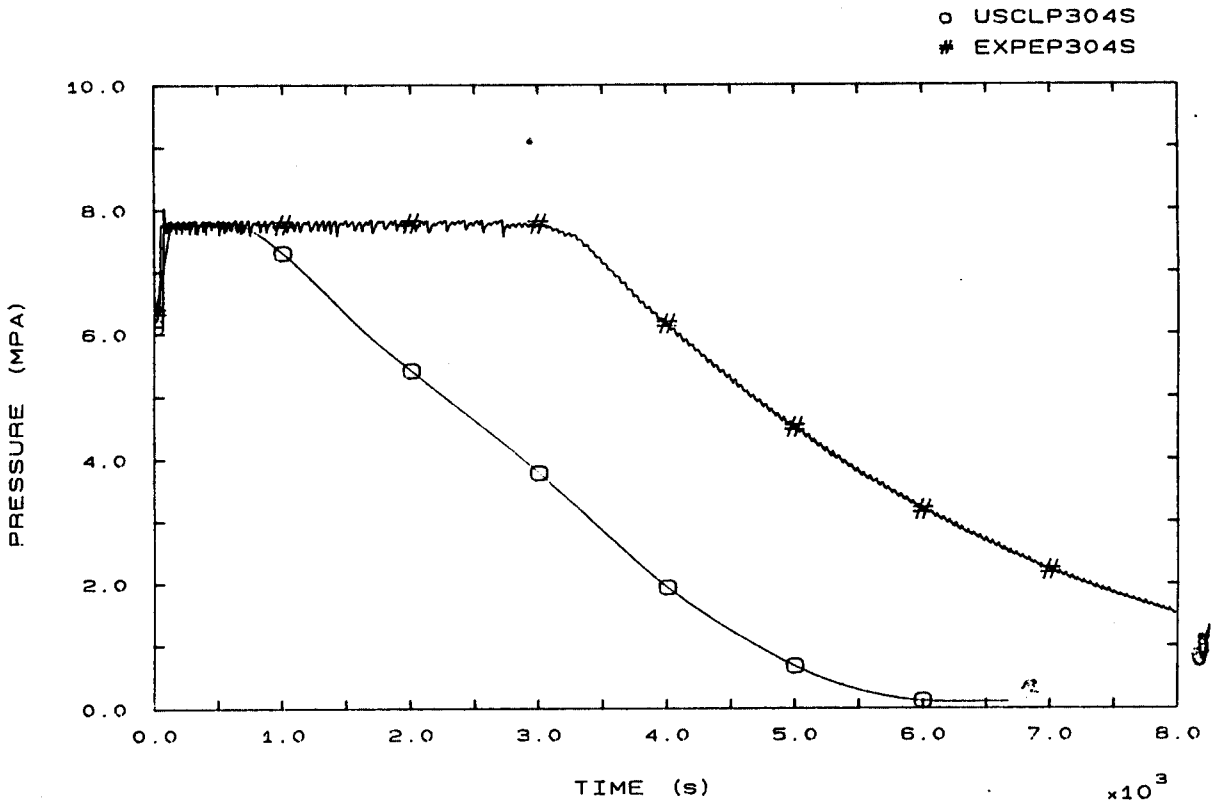

FIG. 5 SG3 STEAM DOME PRESSURE

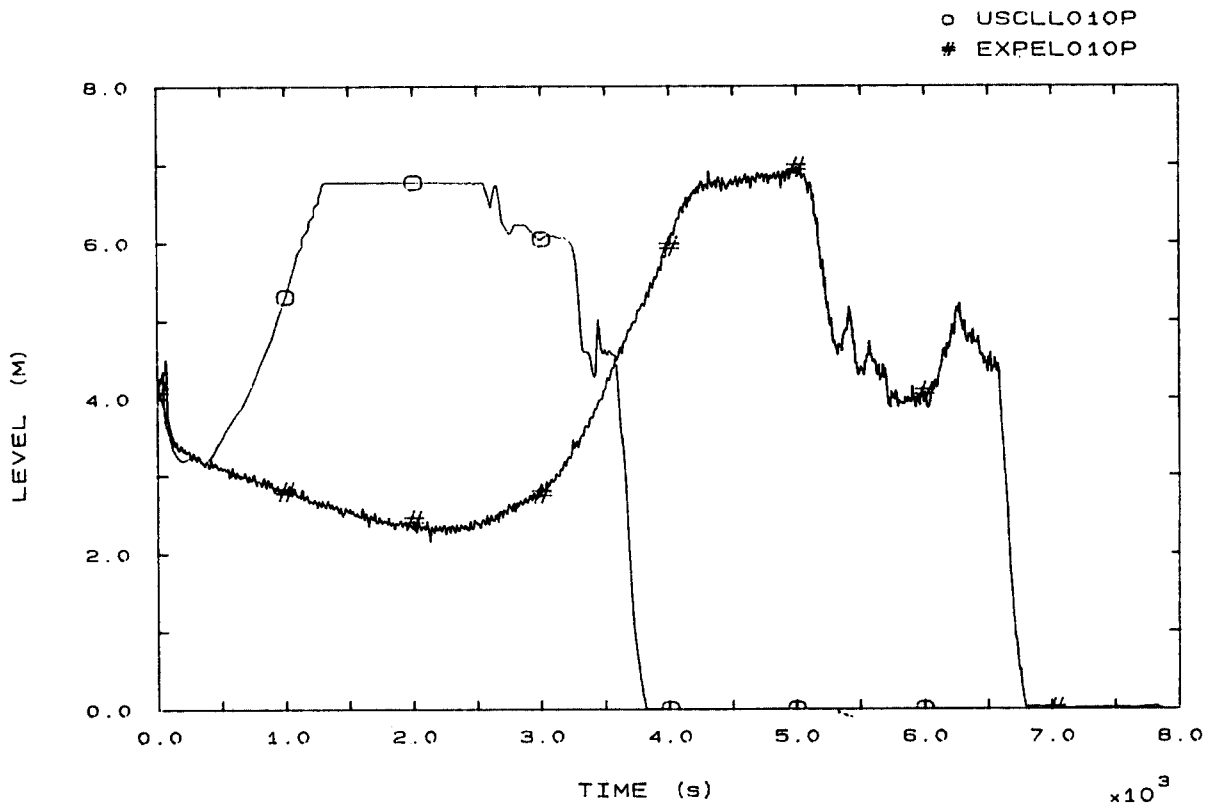

FIG. 6 PRESSURIZER LEVEL

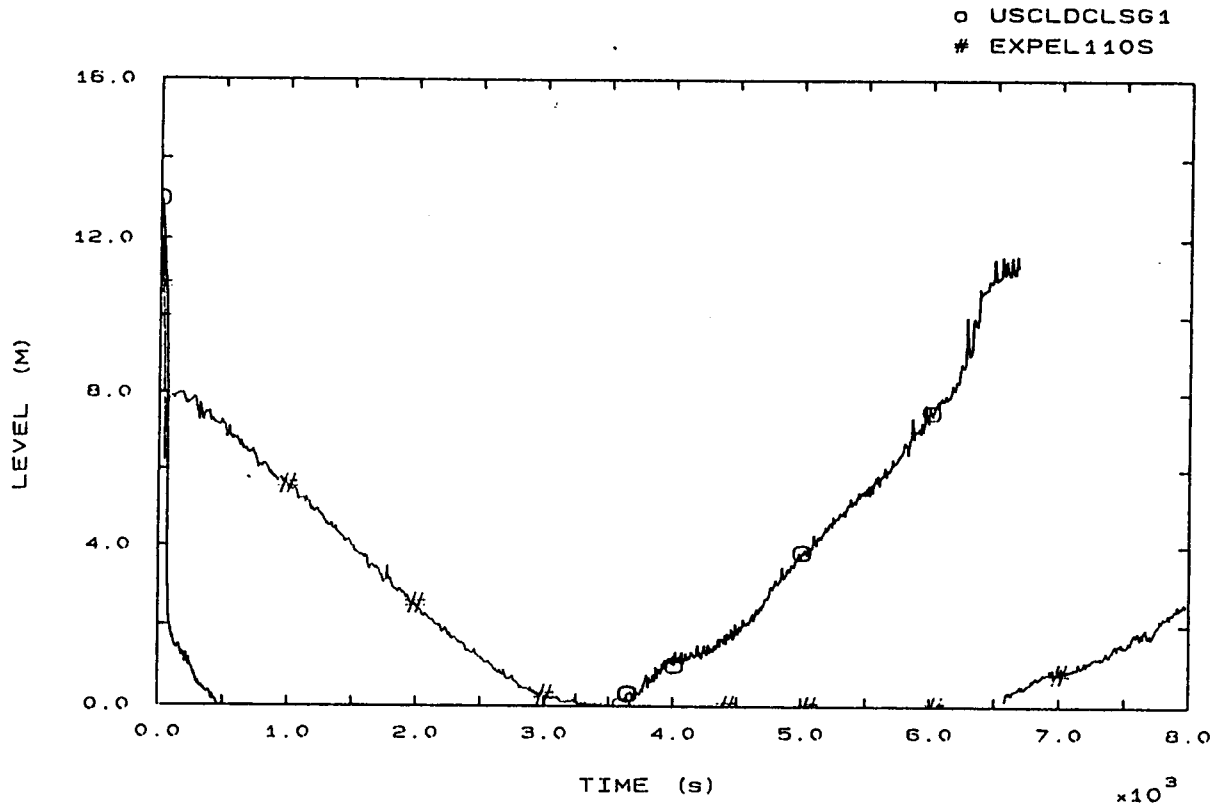

FIG. 7 SG1 DOWNCOMER LEVEL

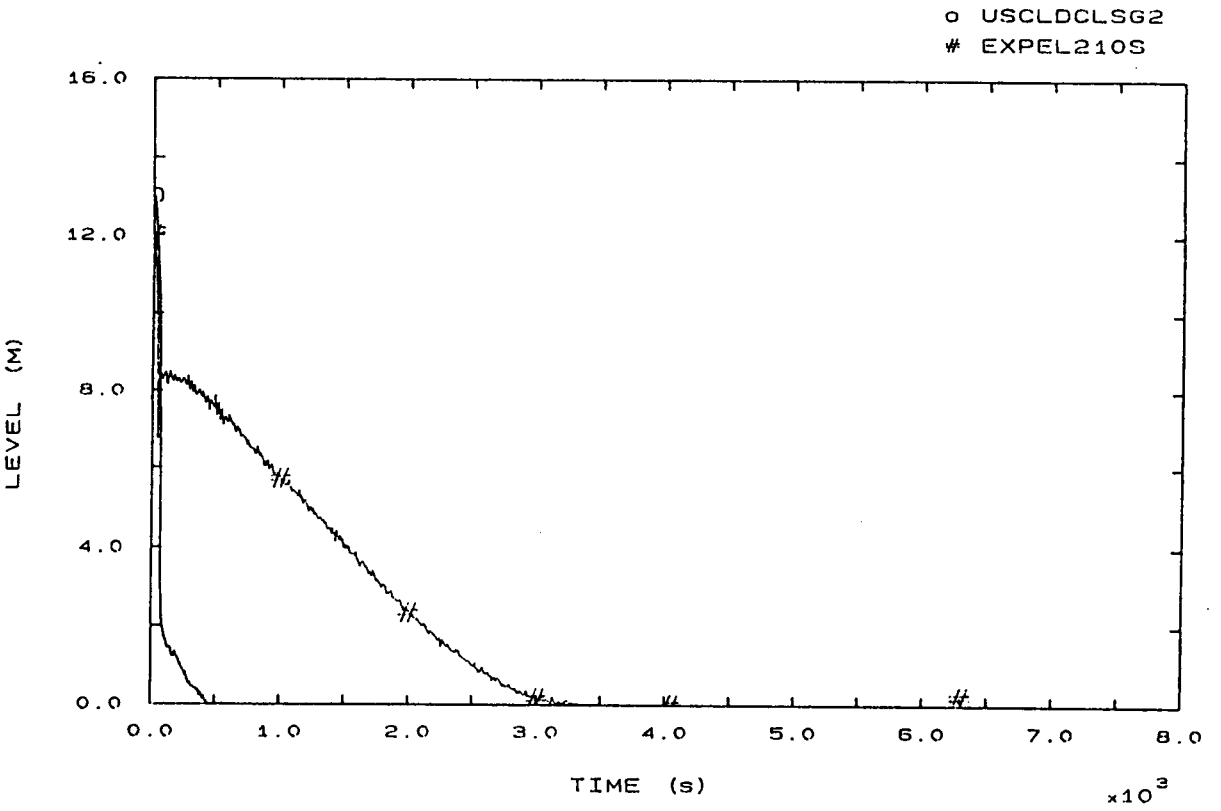

FIG. 8 SG2 DOWNCOMER LEVEL

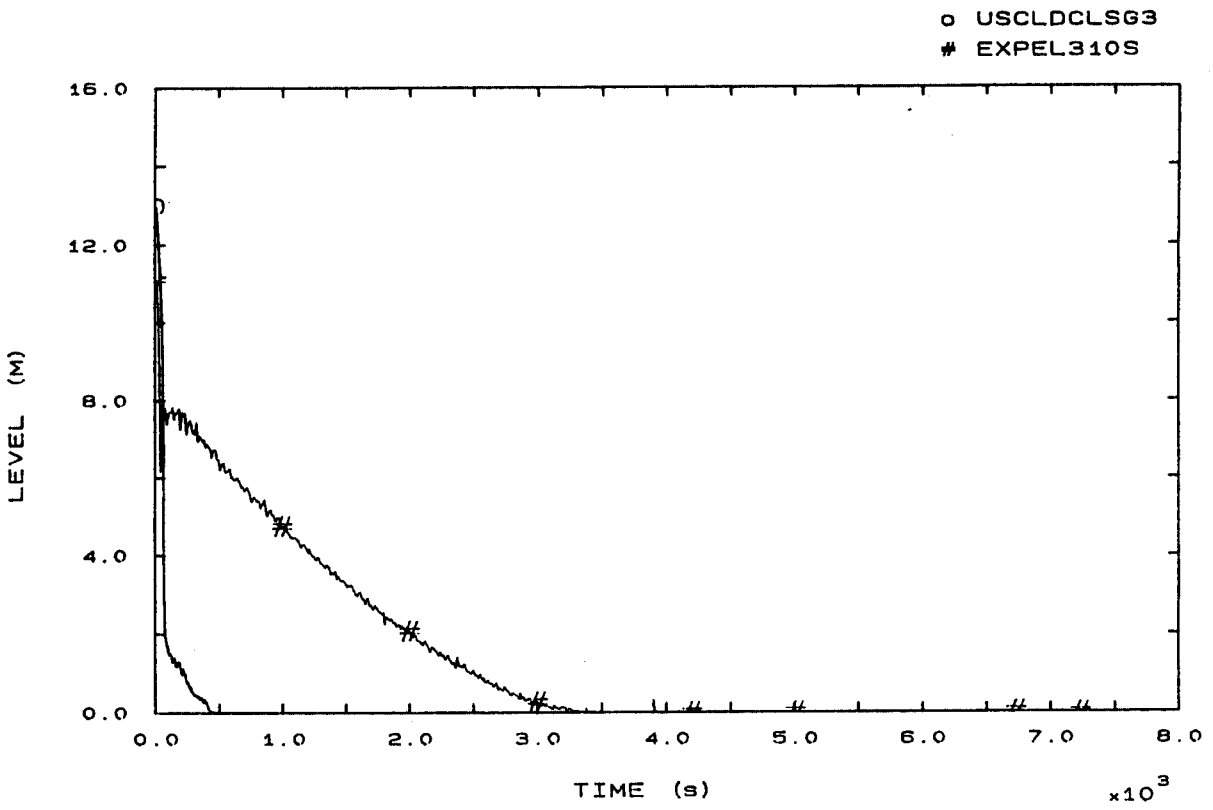

FIG. 9 SG3 DOWNCOMER LEVEL

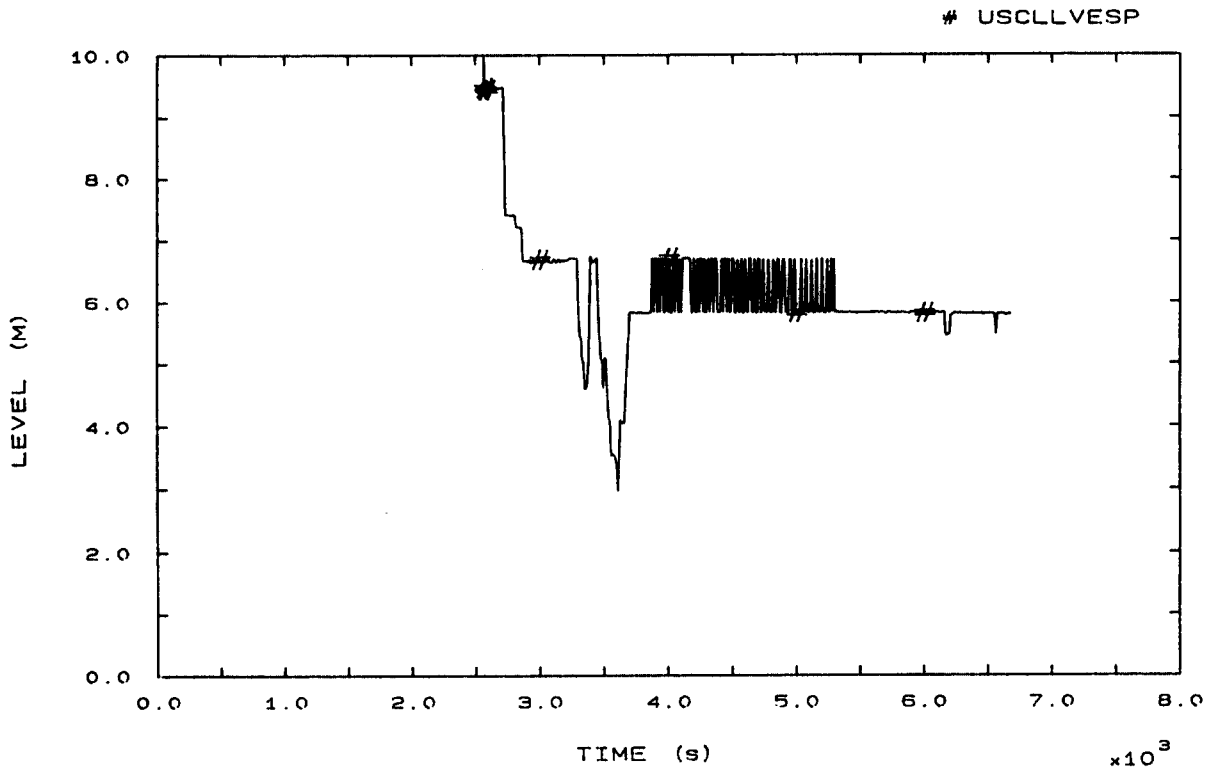

FIG. 10 VESSEL LEVEL

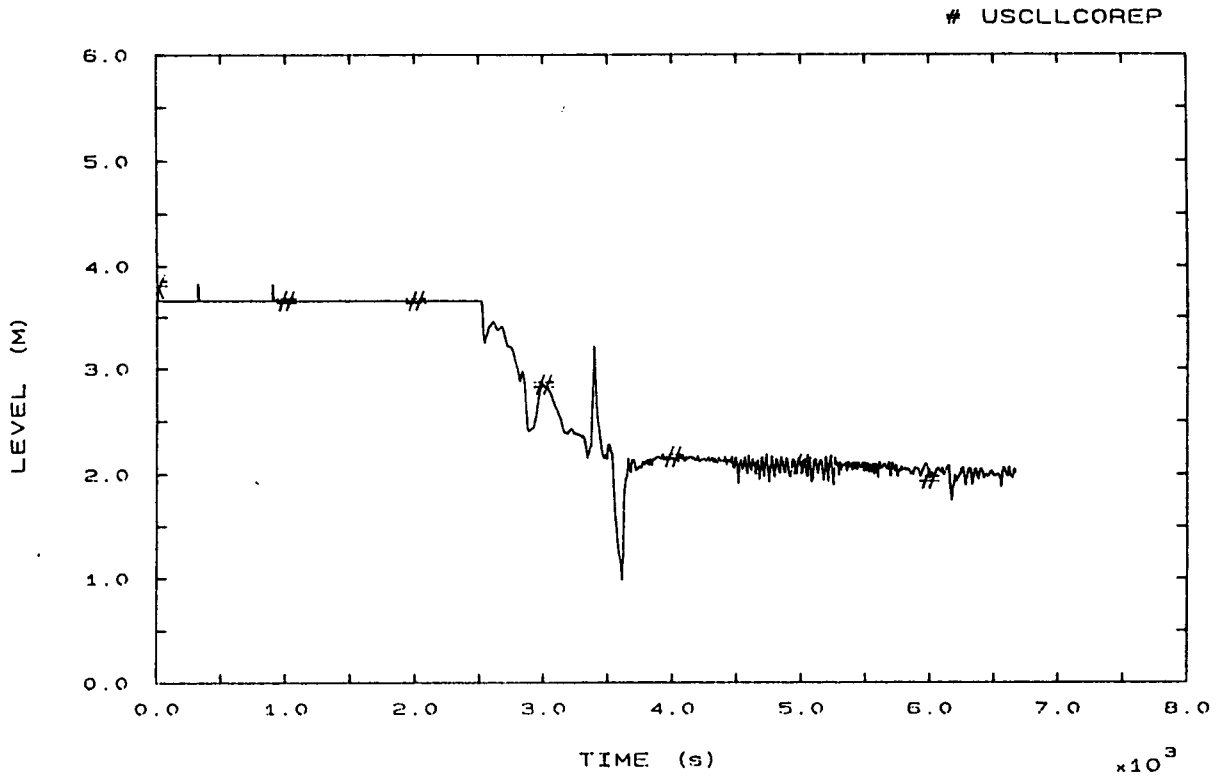

FIG. 11 CORE LEVEL

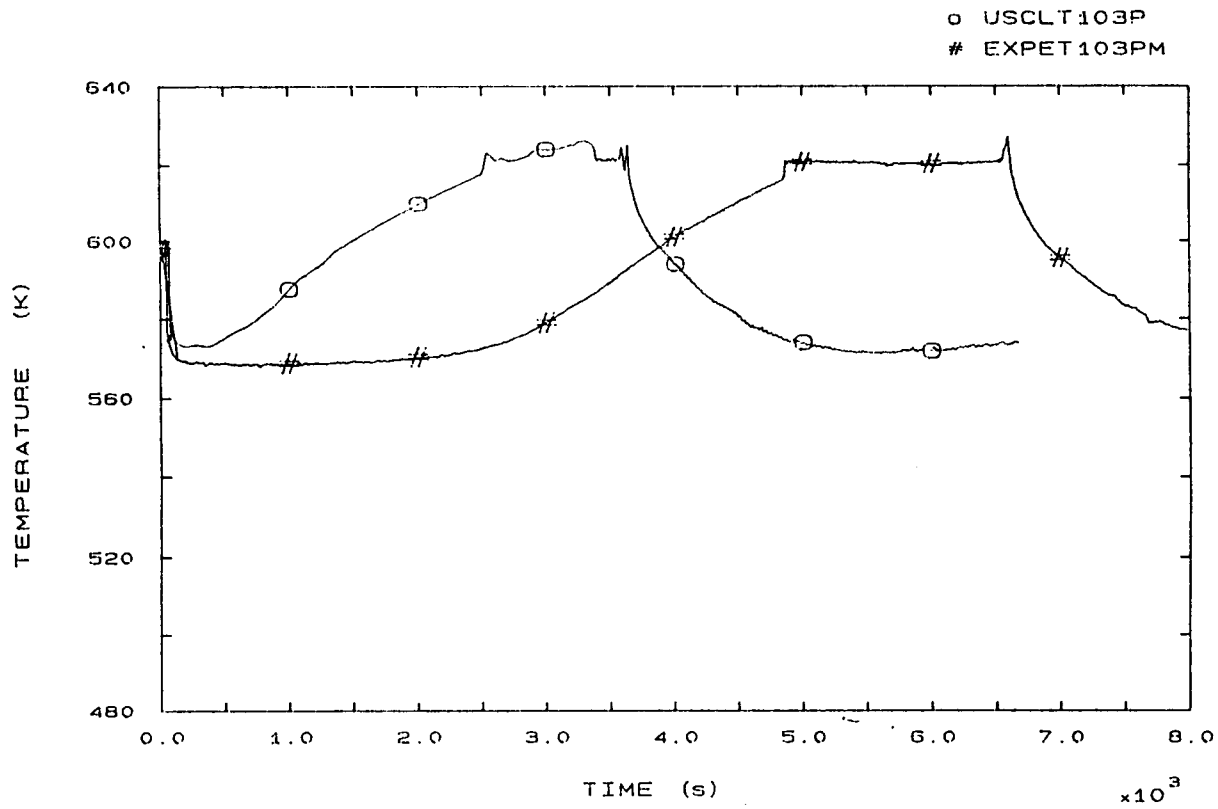

FIG. 12 LP1 HOT LEG OUTLET VESSEL TEMPERATURE

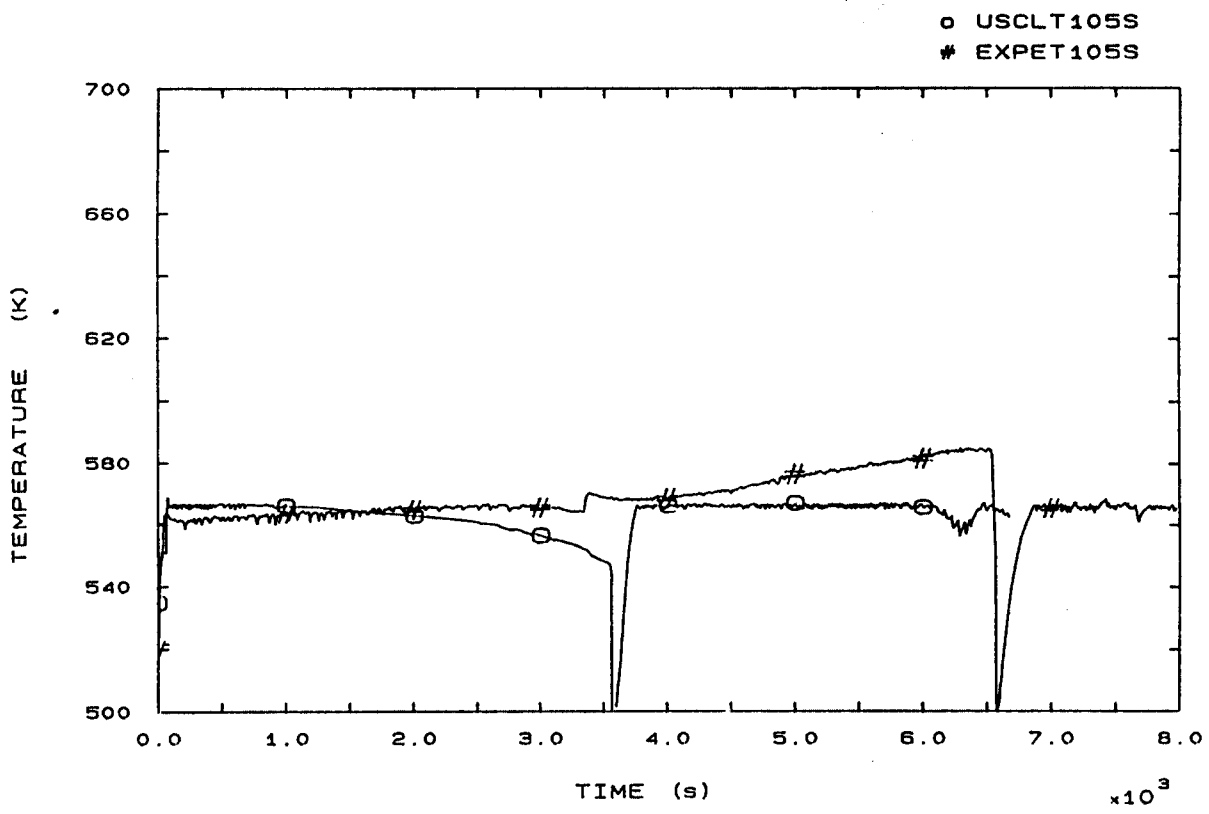

FIG. 15 FLUID TEMPERATURE SG1 RISER 185 MM A.T.S.

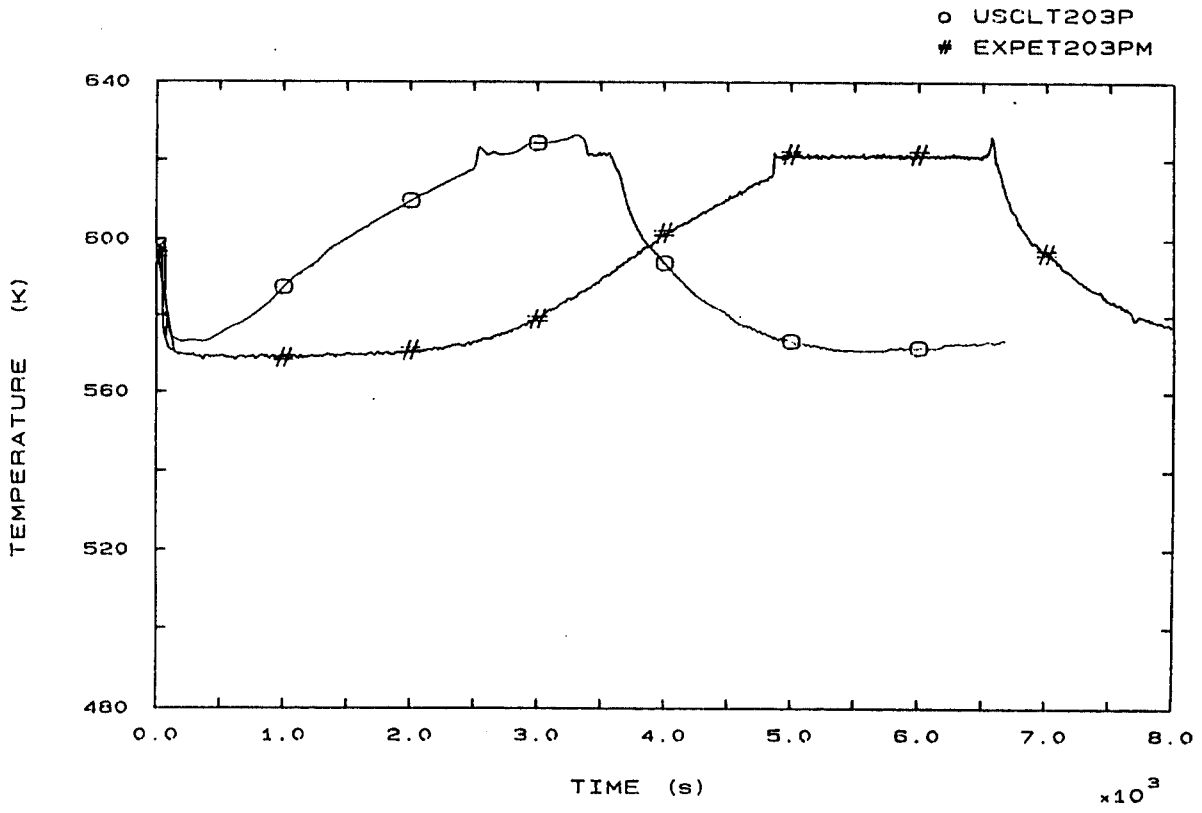

FIG. 22 LP2 HOT LEG OUTLET VESSEL TEMPERATURE

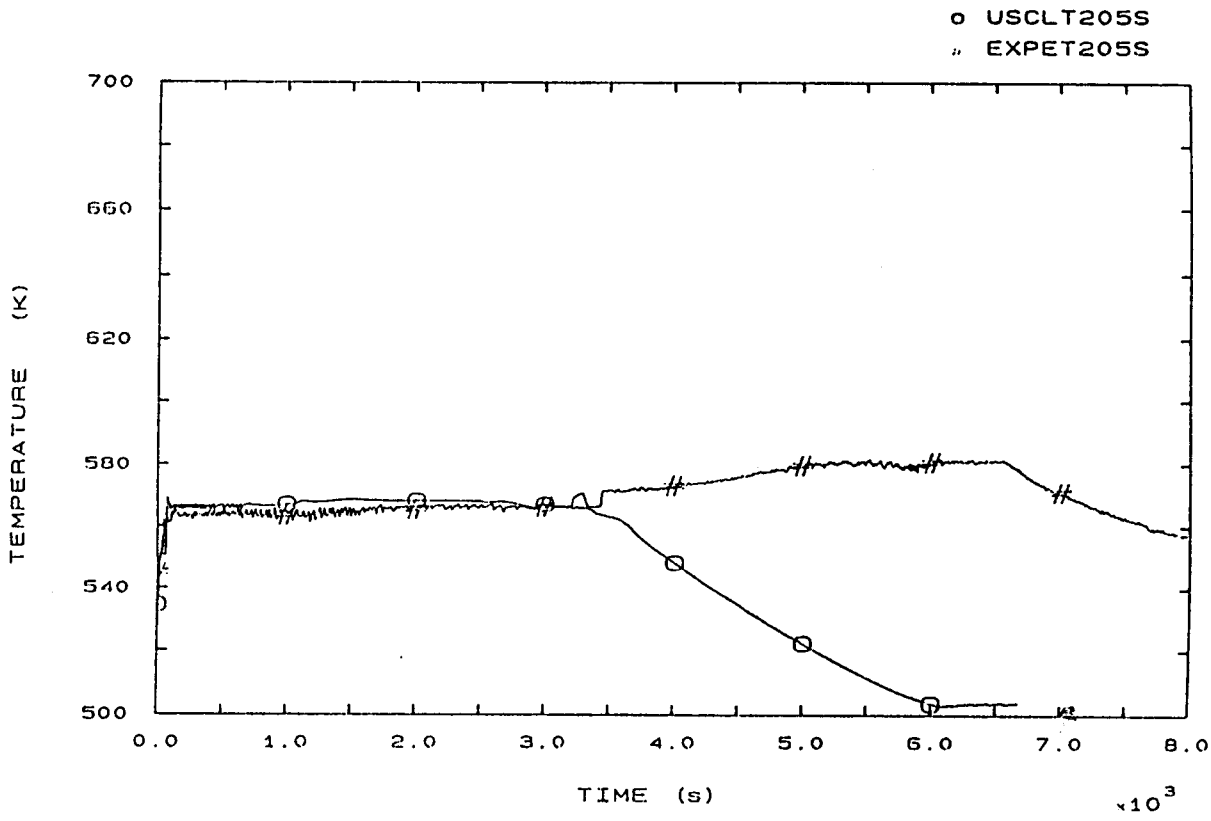

FIG. 25 FLUID TEMPERATURE SG2 RISER 185 MM.A.T.S.

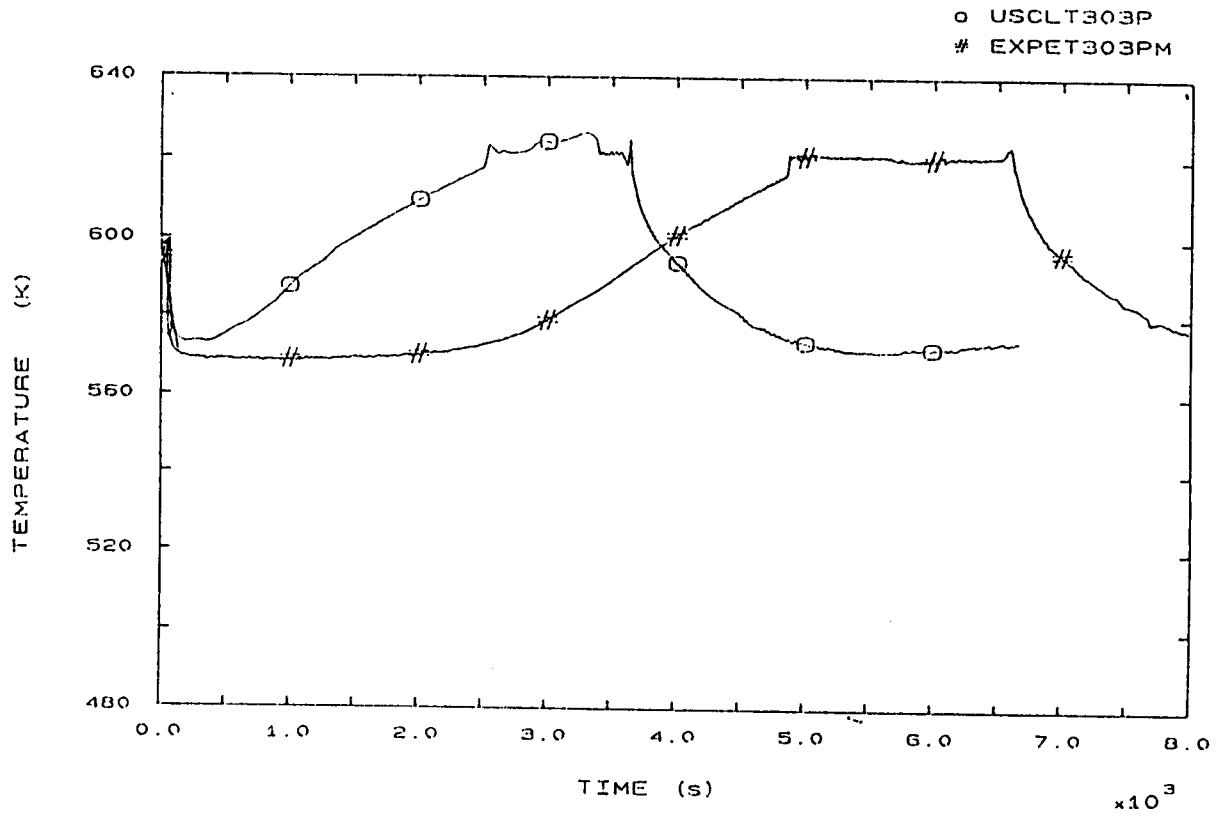

FIG. 32 LP3 HOT LEG OUTLET VESSEL TEMPERATURE

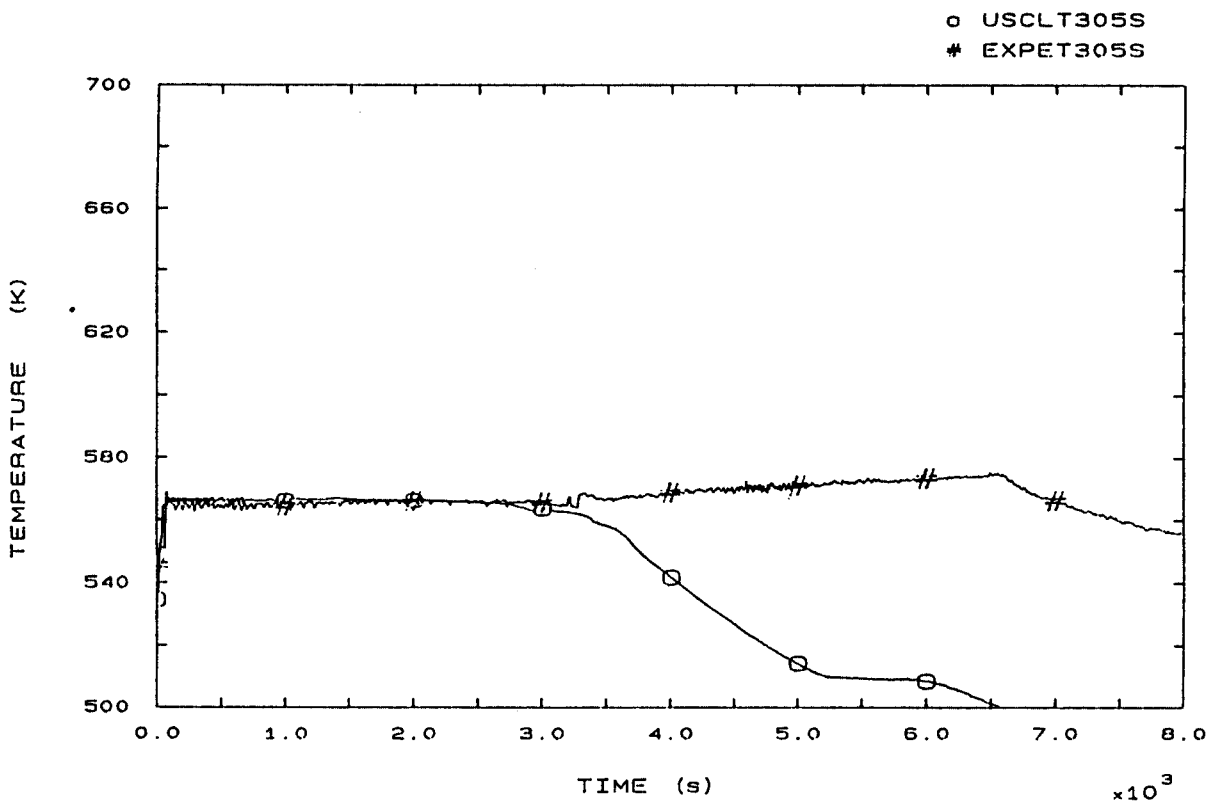

FIG. 35 FLUID TEMPERATURE SG3 RISER 185 MM A.T.S.

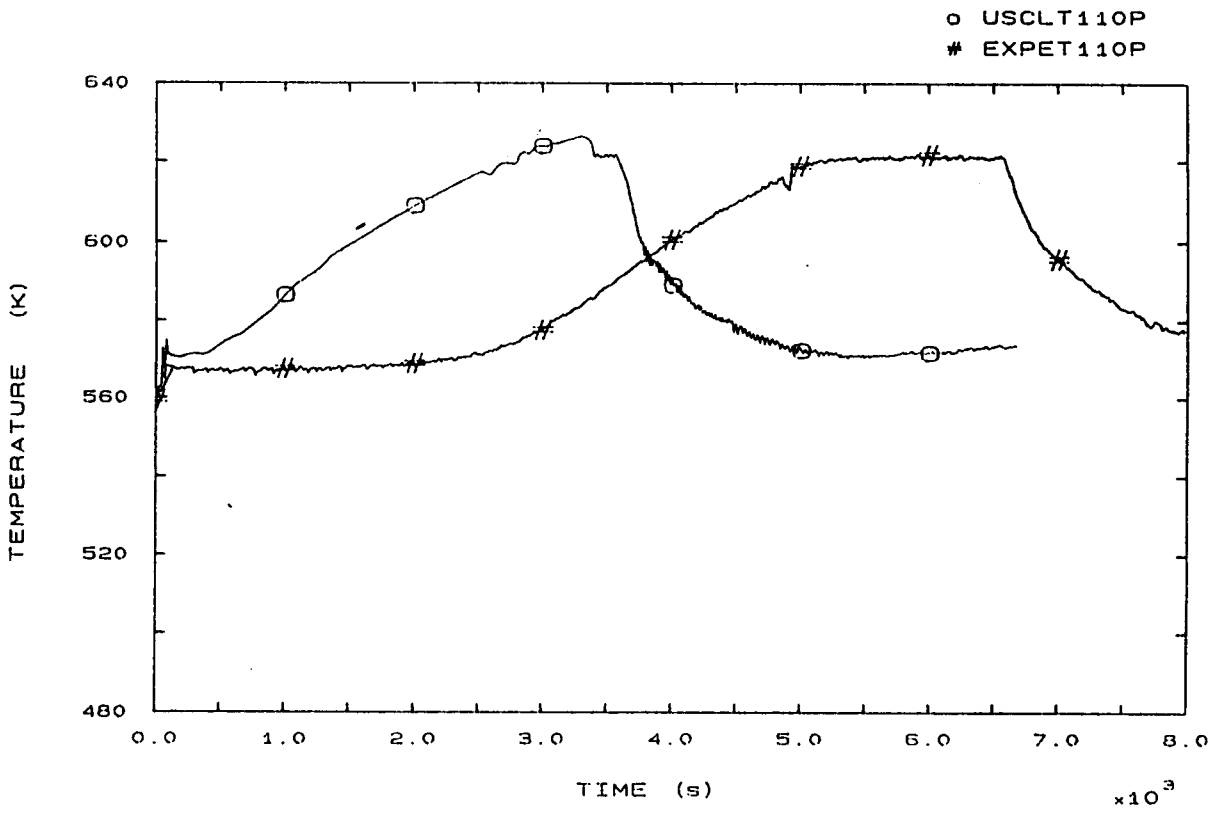

FIG. 42 SG1 OUTLET TEMPERATURE

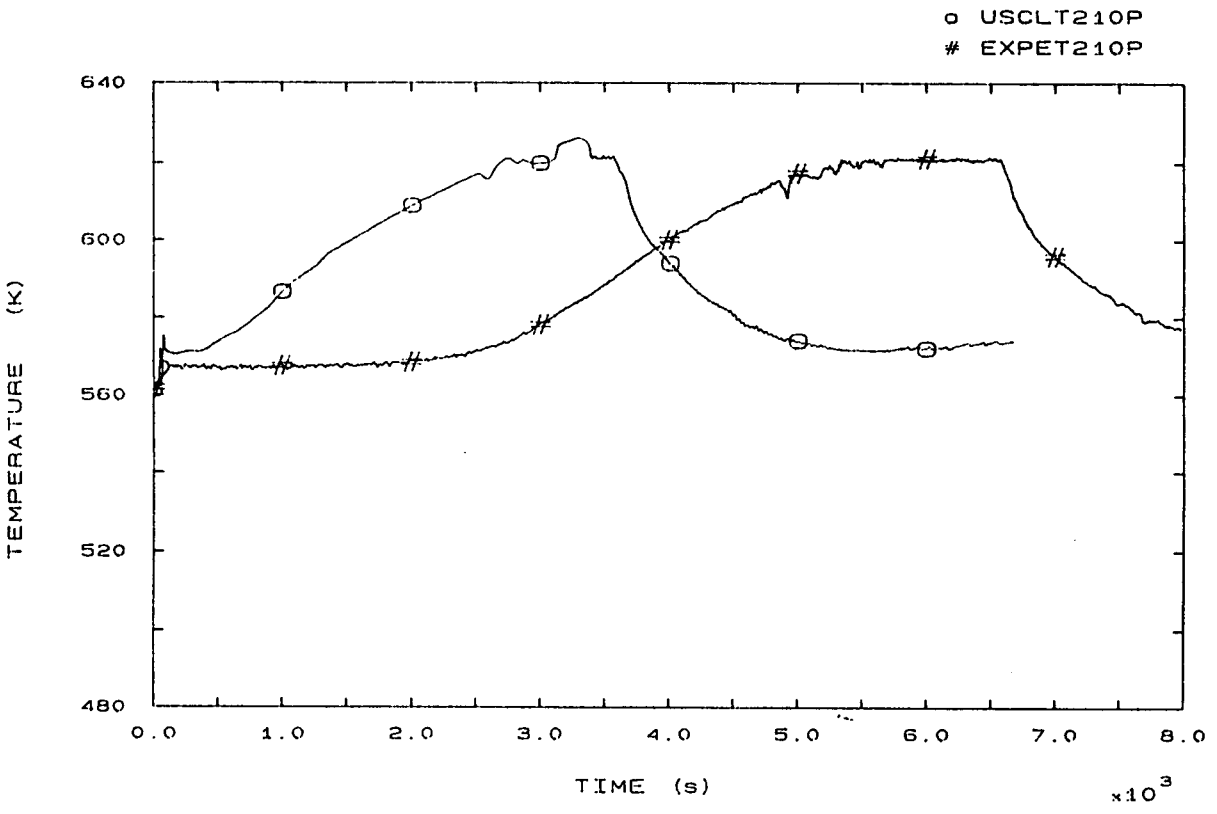

FIG. 44 SG2 OUTLET TEMPERATURE

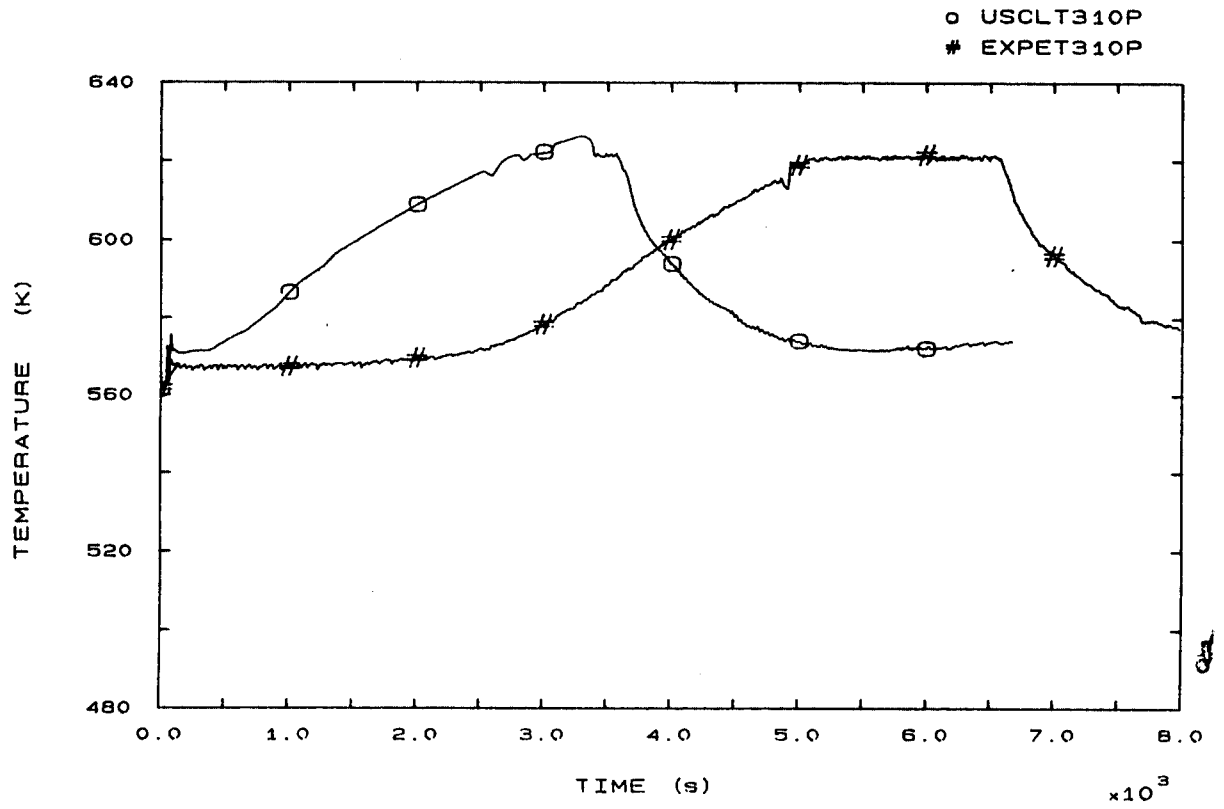

FIG. 46 SG3 OUTLET TEMPERATURE

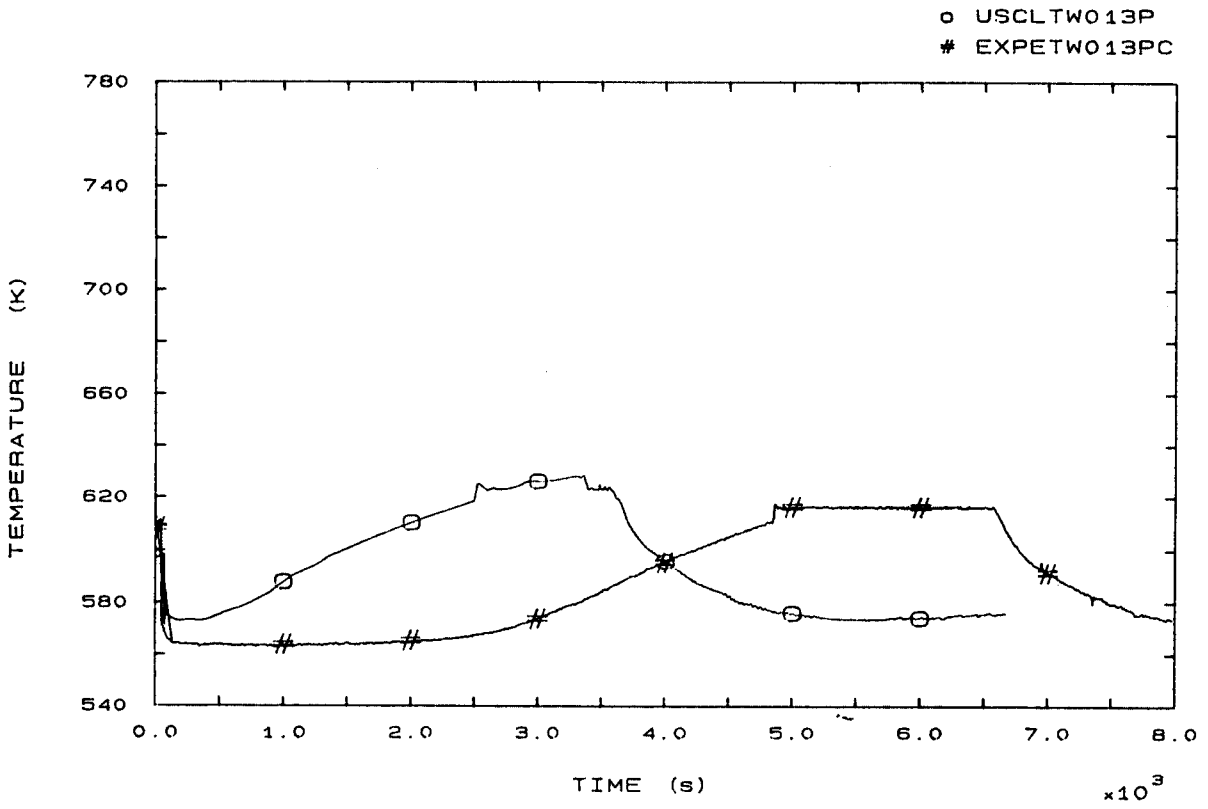

FIG. 49 CORE SURFACE TEMPERATURE AT ROD BUNDLE ELEVATION 1074 MM

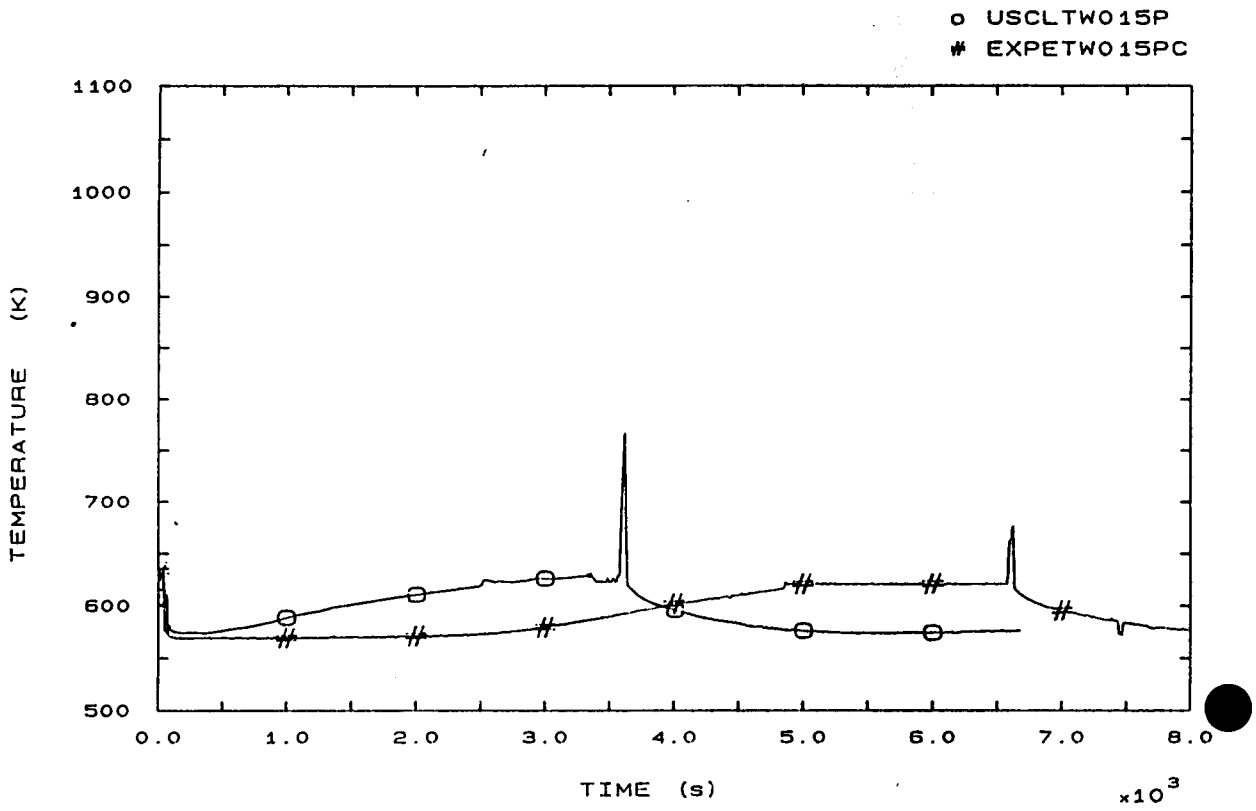

FIG. 50 SURFACE TEMPERATURE AT ROD BUNDLE ELEVATION 2294 MM

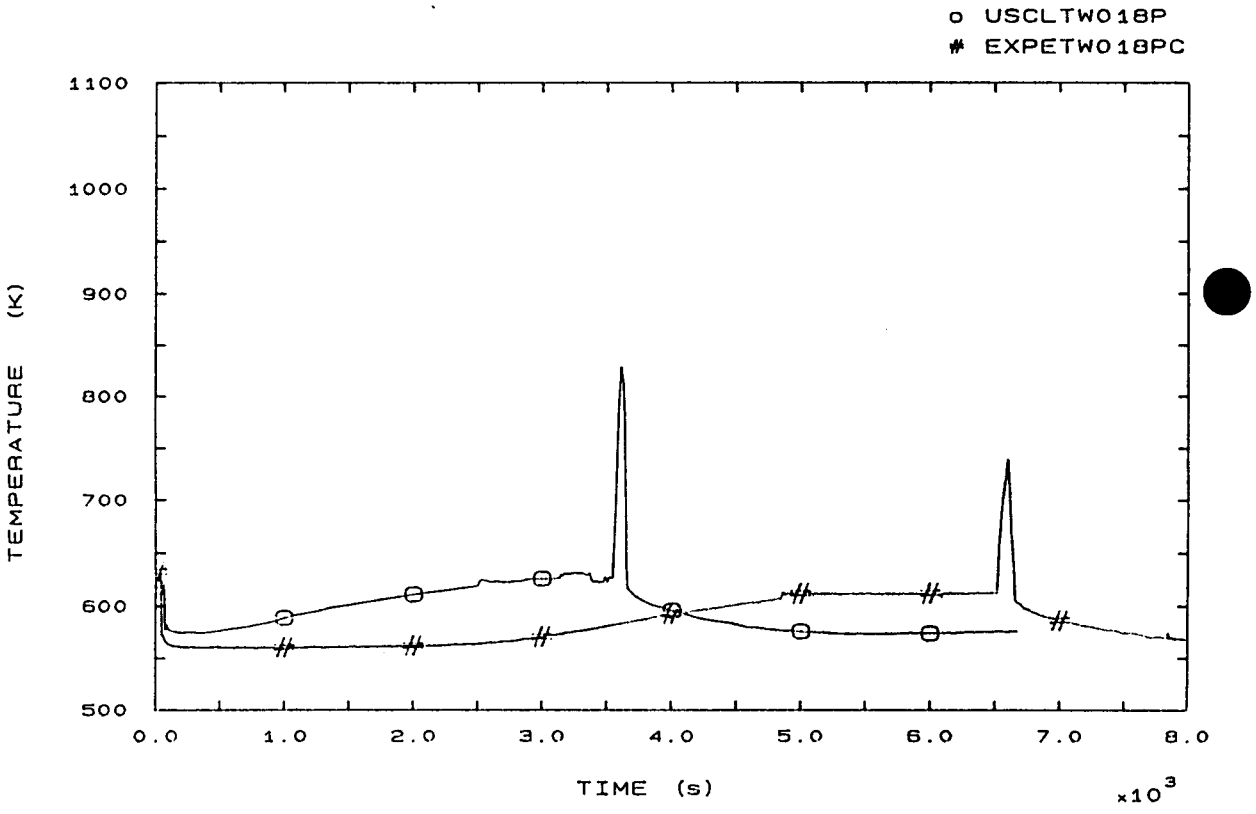

FIG. 51 SURFACE TEMPERATURE AT ROD BUNDLE ELEVATION 3294 MM

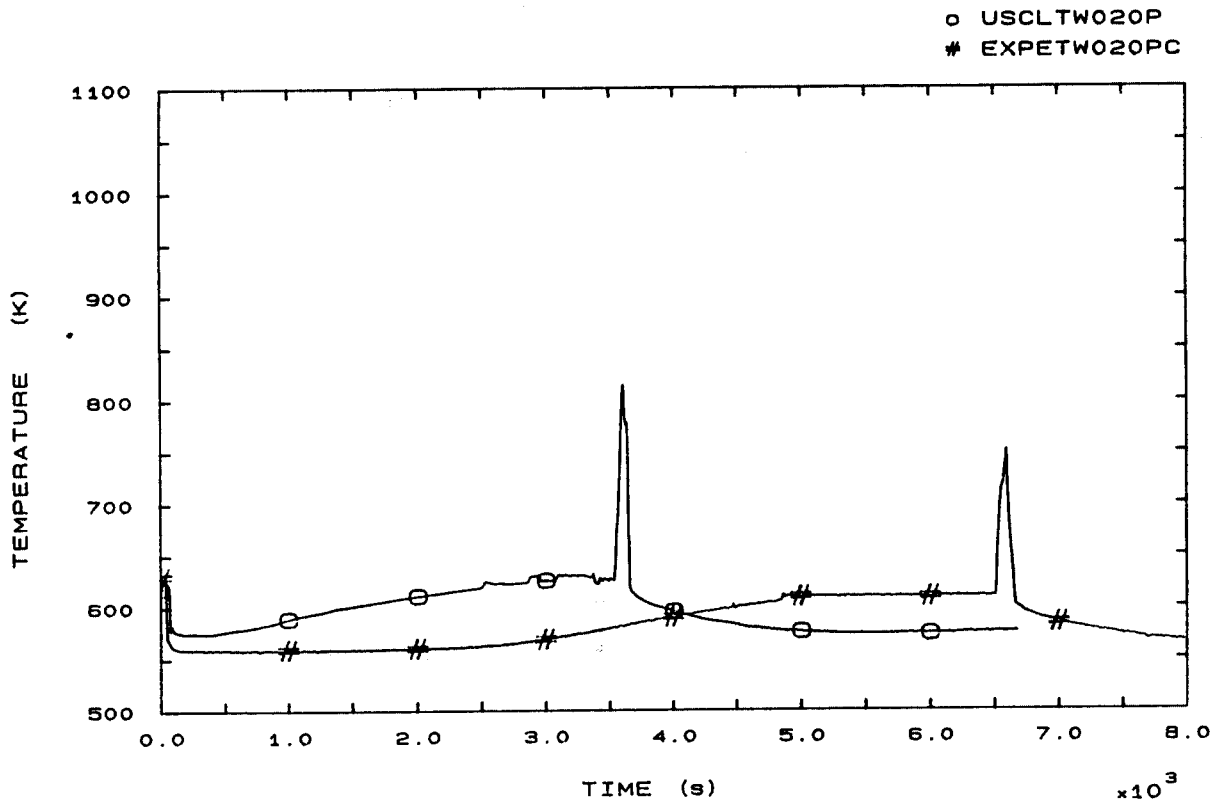

FIG. 52 SURFACE TEMPERATURE AT ROD BUNDLE ELEVATION 3640 MM

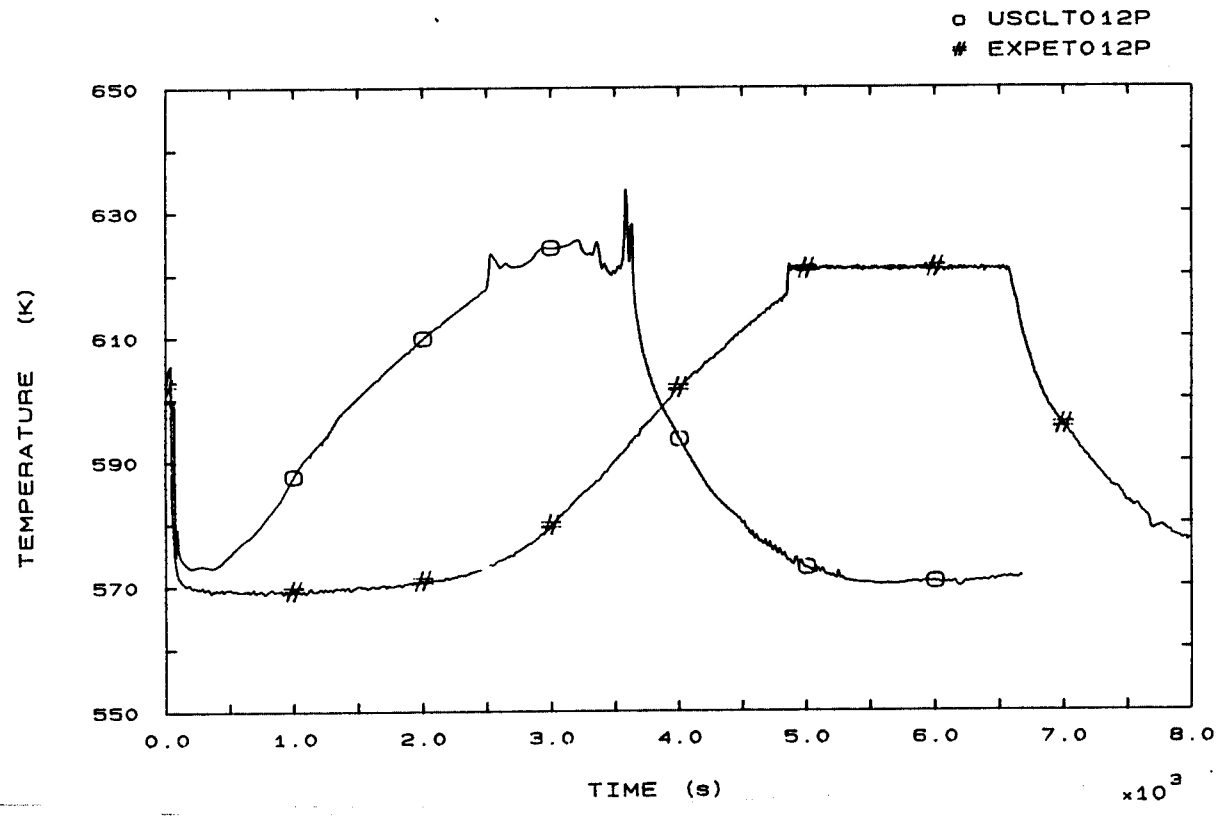

FIG. 53 CORE OUTLET TEMPERATURE

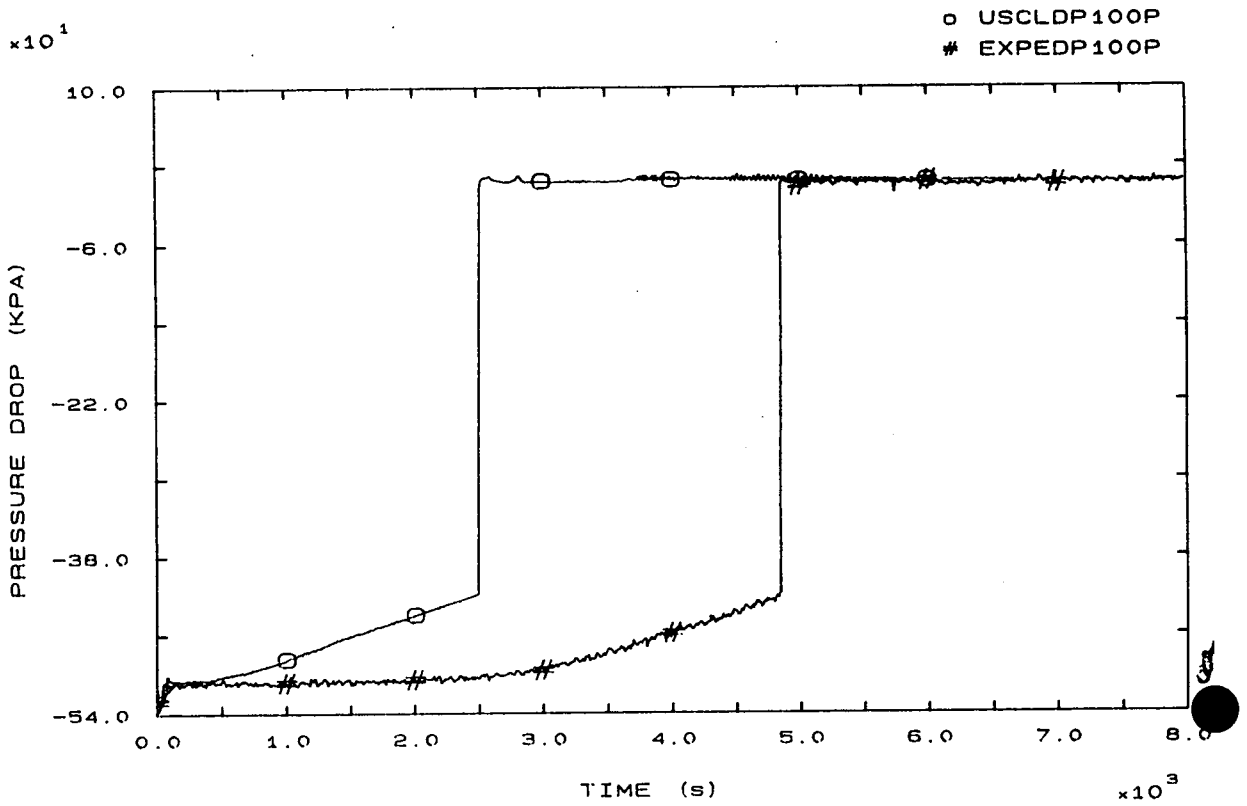

FIG. 54 PRIMARY PUMP 1 PRESSURE DROP

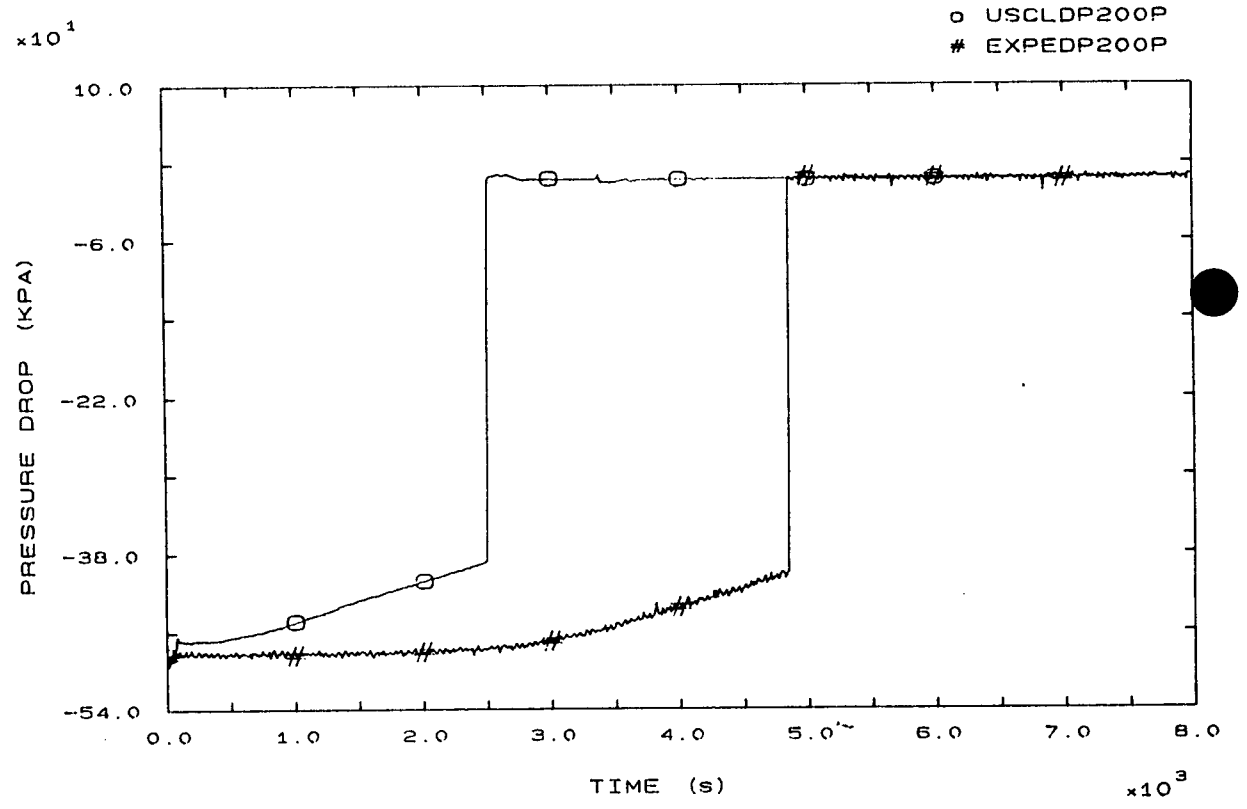

FIG. 55 PRIMARY PUMP 2 PRESSURE DROP

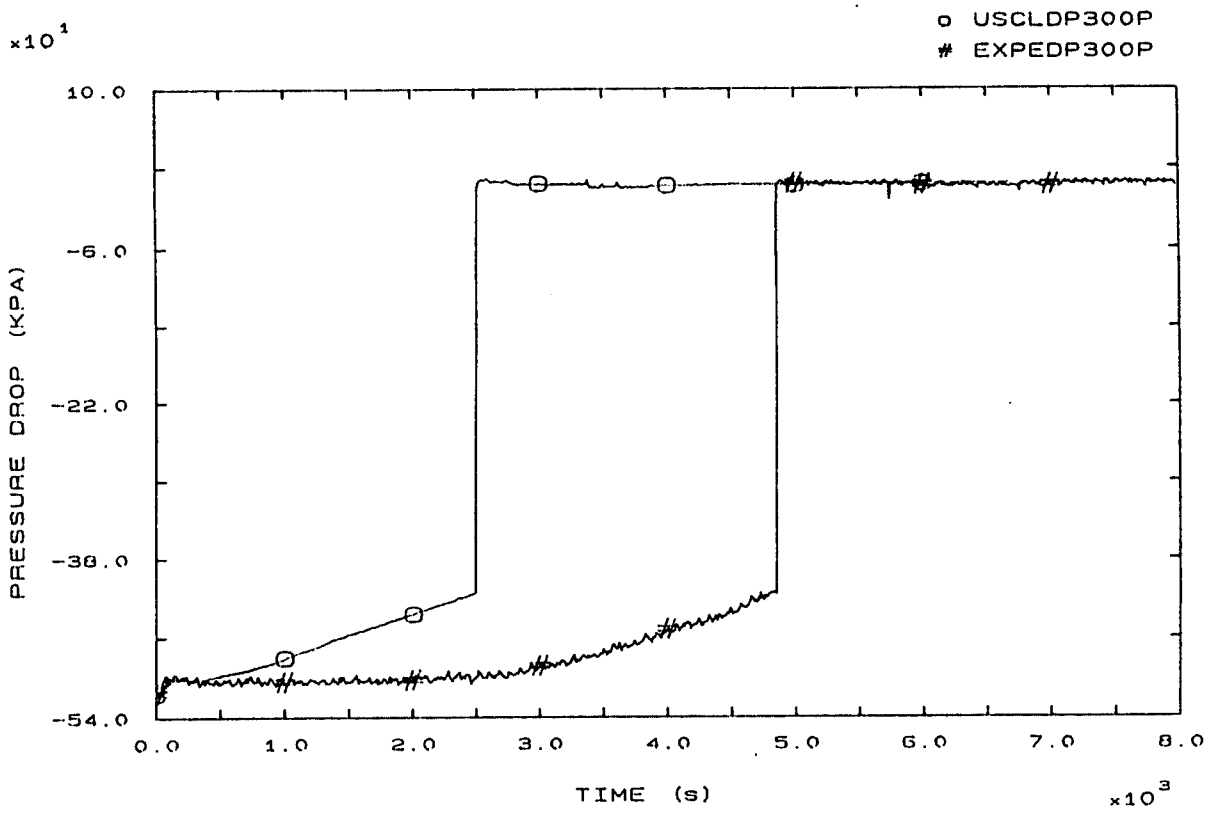

FIG. 56 PRIMARY PUMP 3 PRESSURE DROP

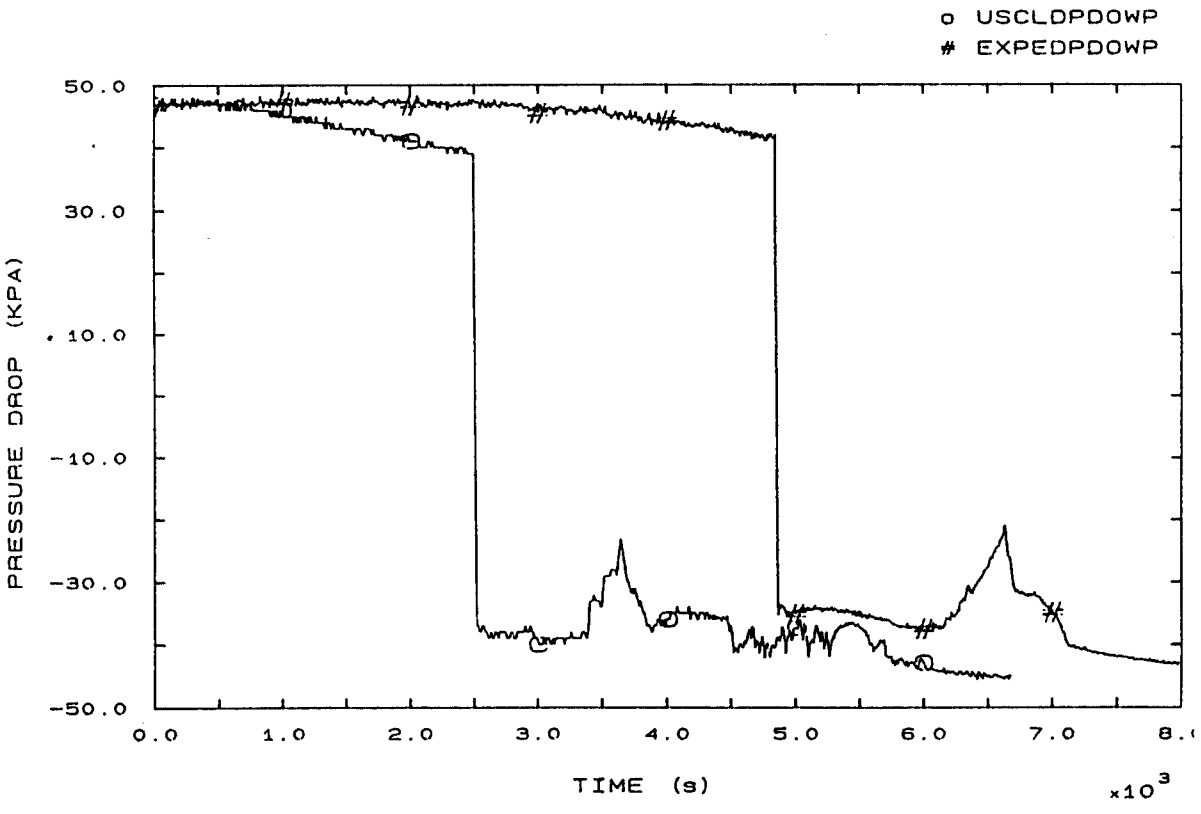

FIG. 57 VESSEL DOWNCOMER PRESSURE DROP

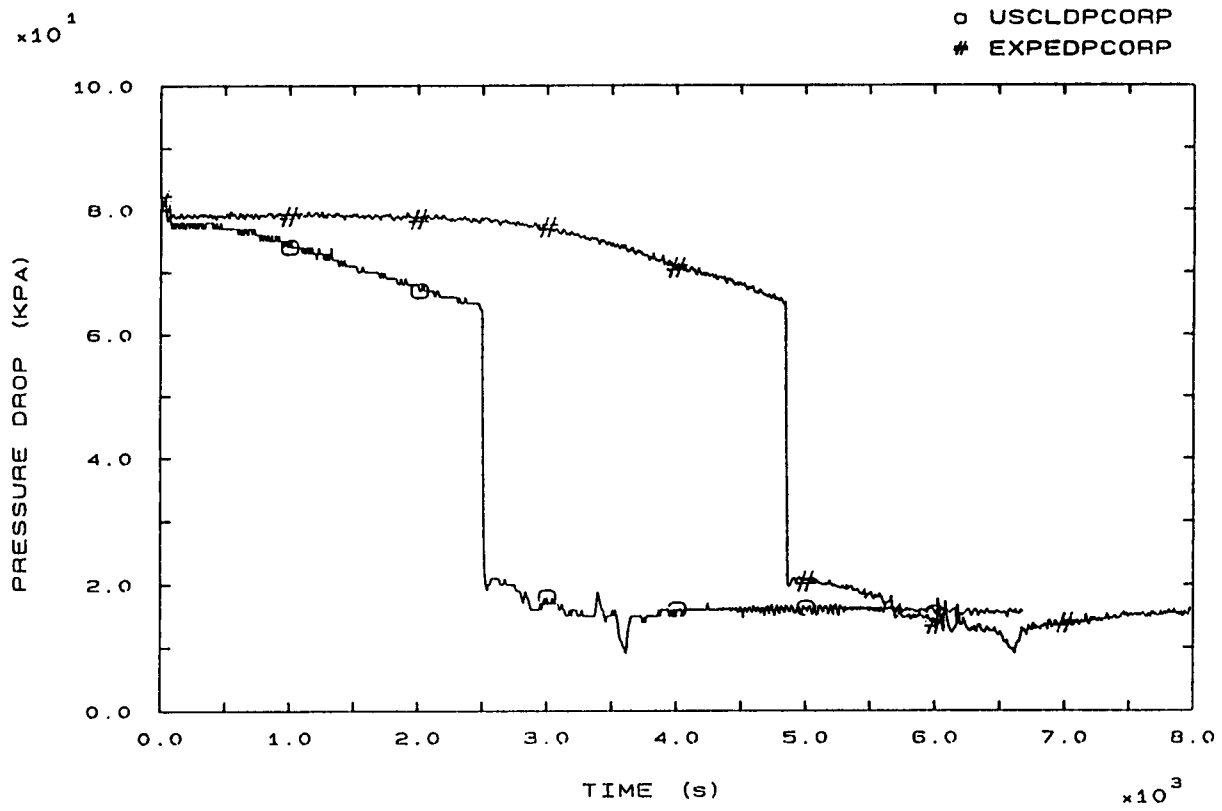

FIG. 58 CORE PRESSURE DROP

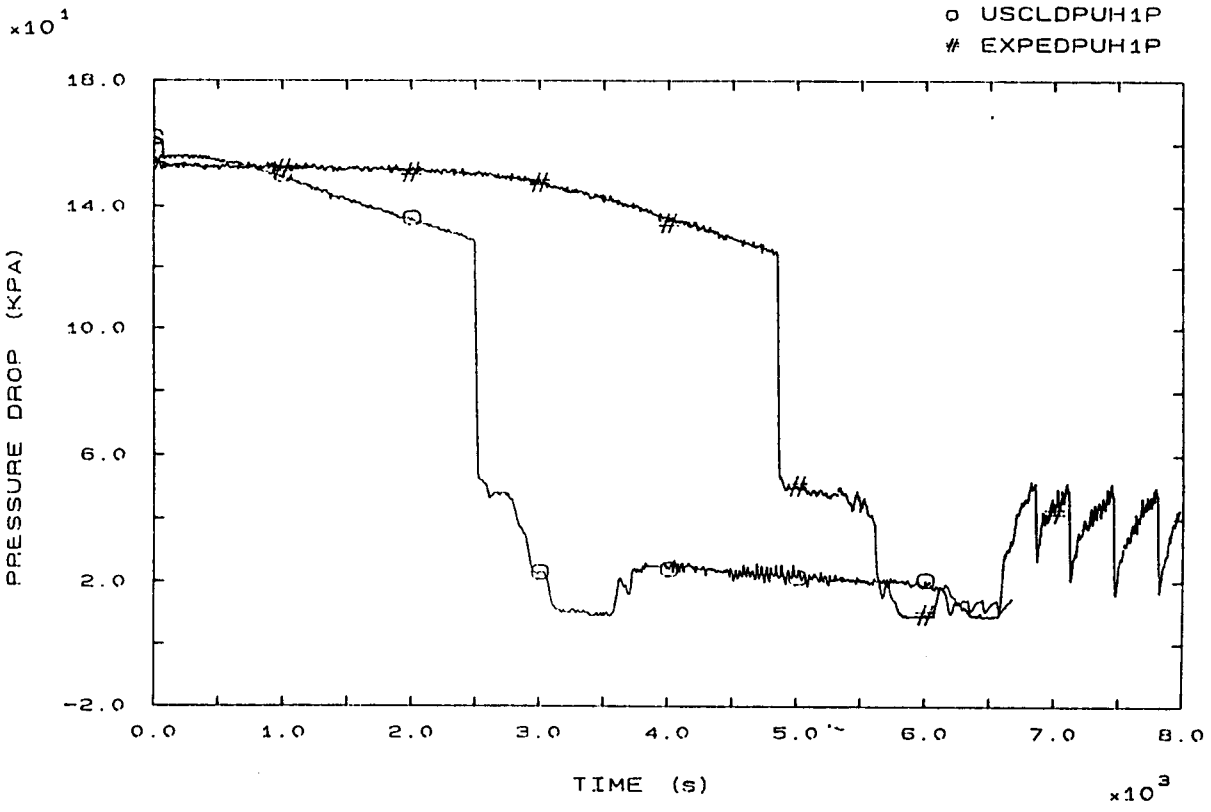

FIG. 62 SG1 INLET/U-BEND (UP-HILL) PRESSURE DROP

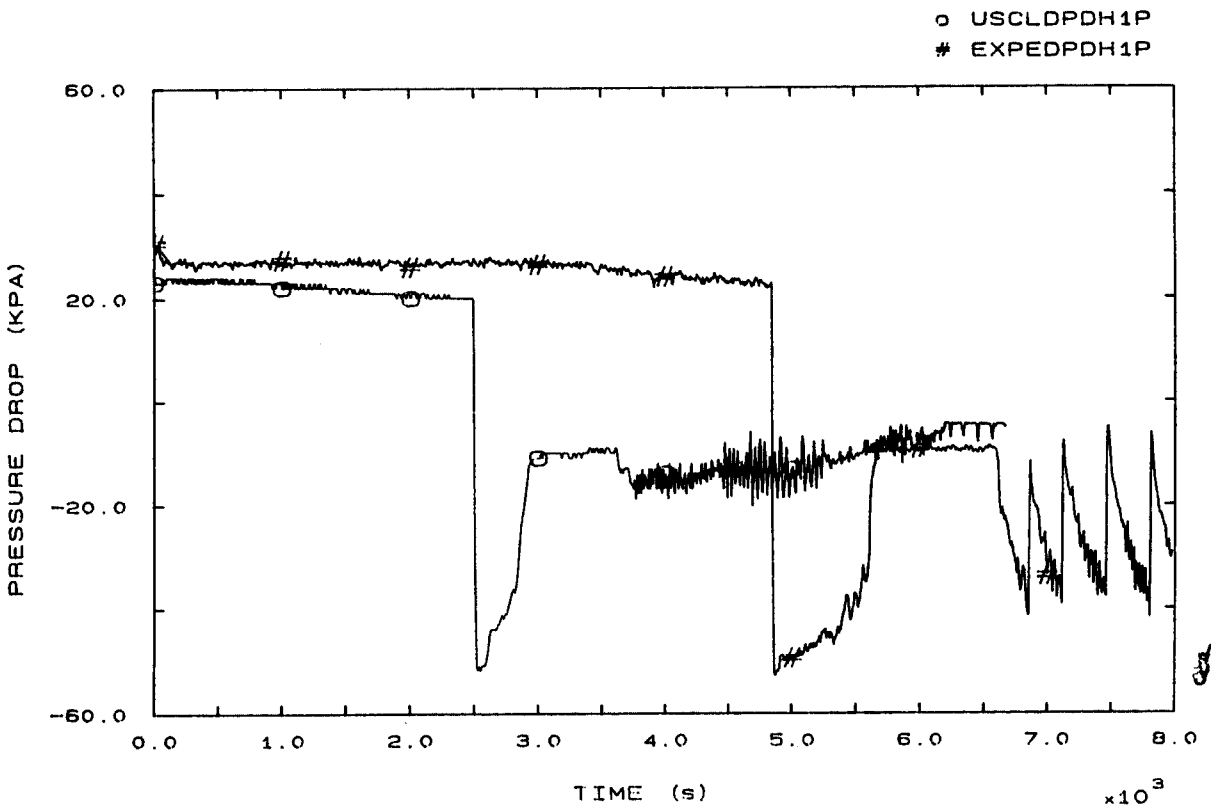

FIG. 63 SG1 U-BEND/OUTLET (DOWN-HILL) PRESSURE DROP

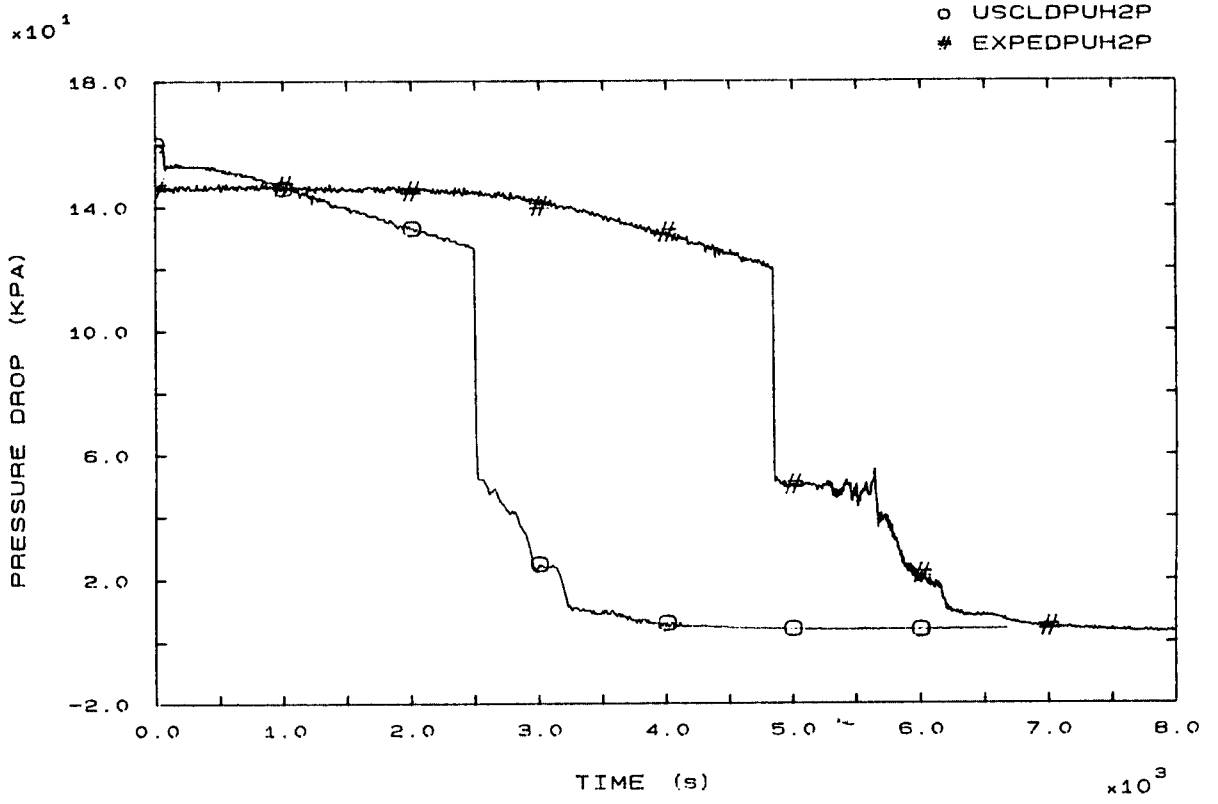

FIG. 64 SG2 INLET/U-BEND (UP-HILL) PRESSURE DROP

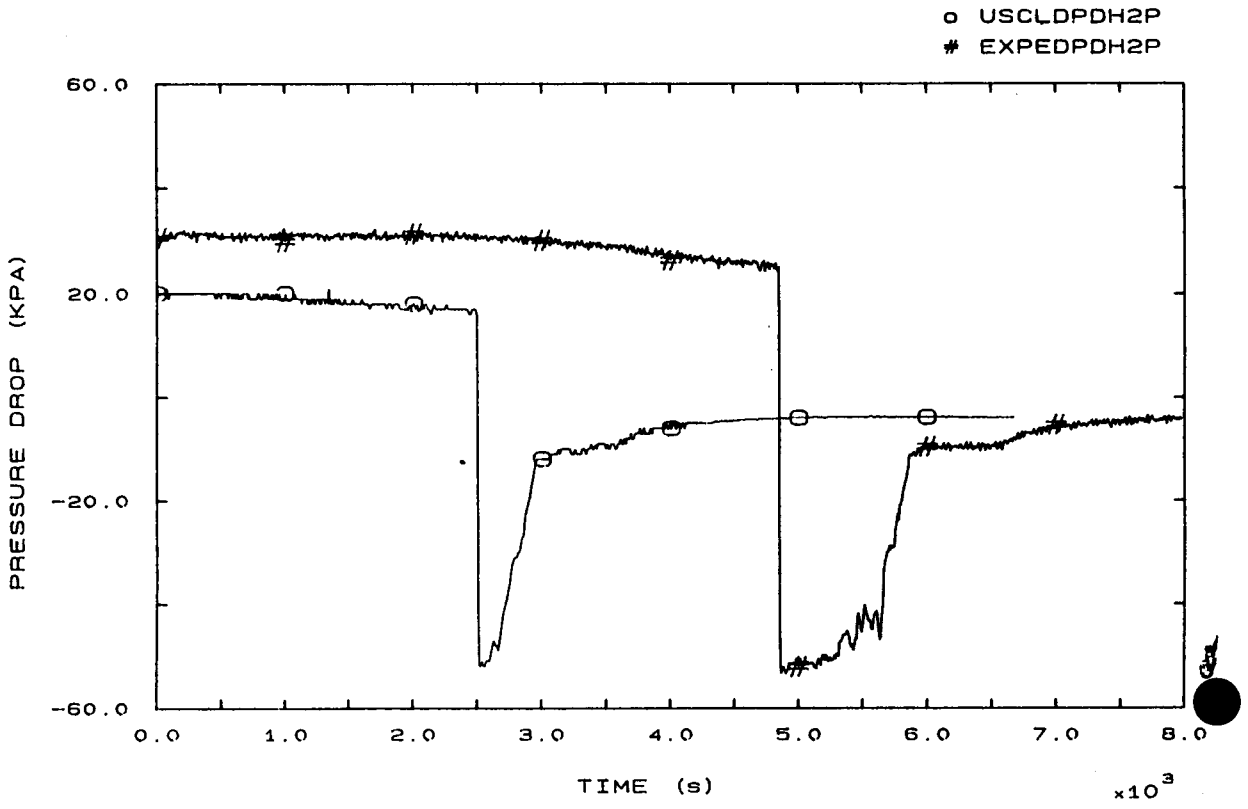

FIG. 65 SG2 U-BEND/OUTLET (DOWN-HILL) PRESSURE DROP

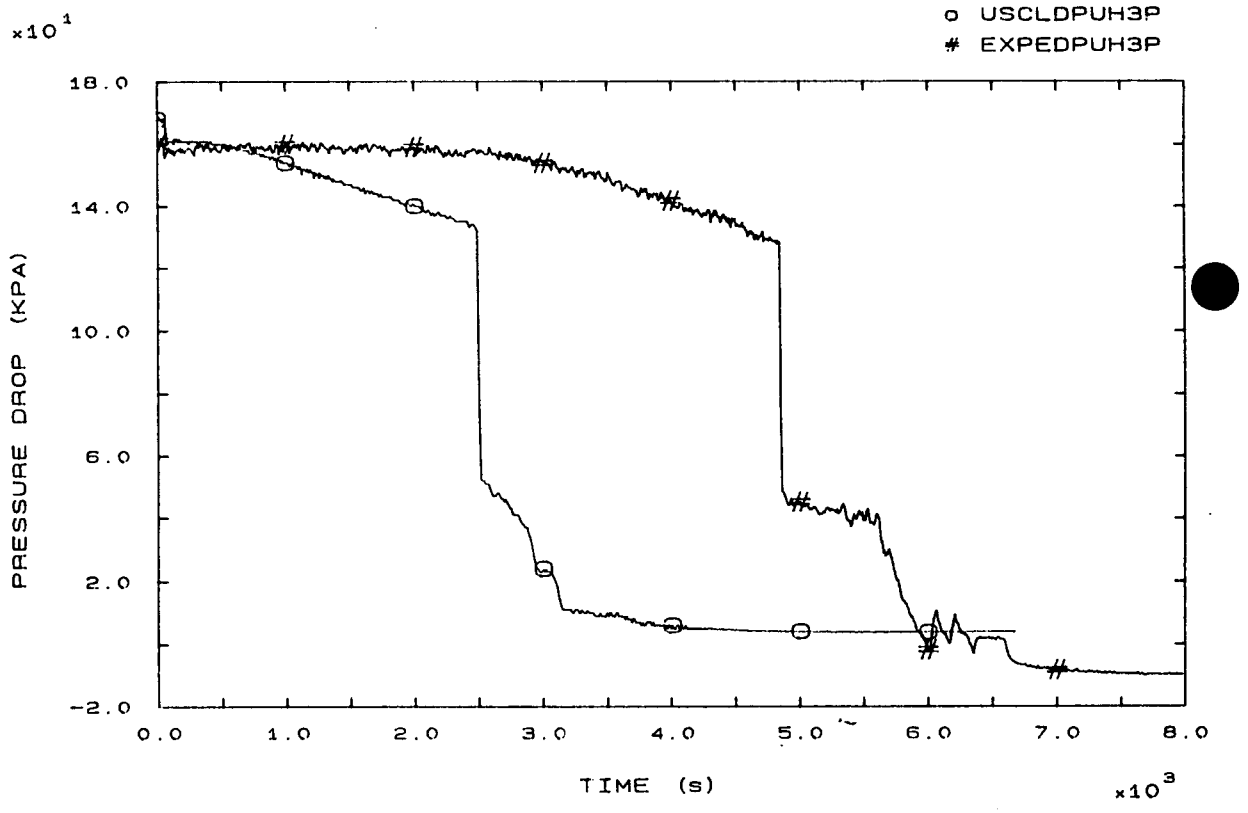

FIG. 66 SG3 INLET/U-BEND (UP-HILL) PRESSURE DROP

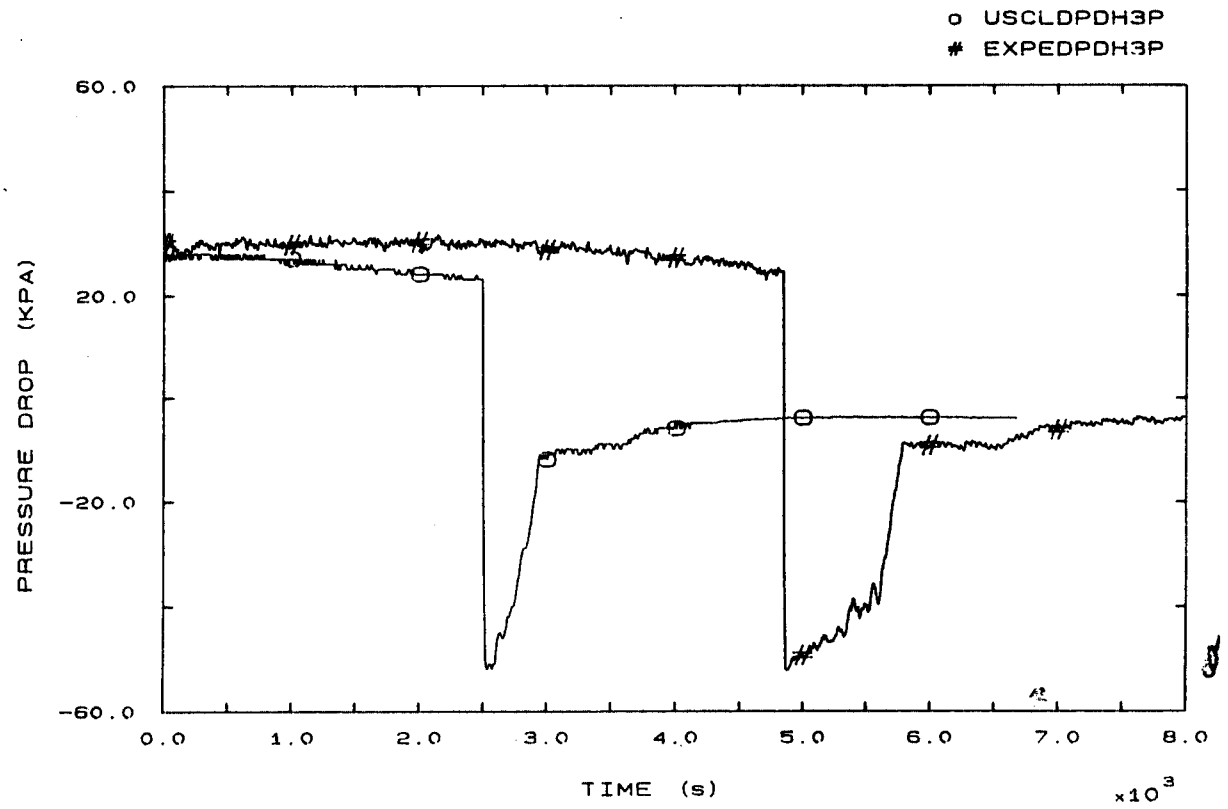

FIG. 67 SG3 U-BEND/OUTLET (DOWN-HILL) PRESSURE DROP

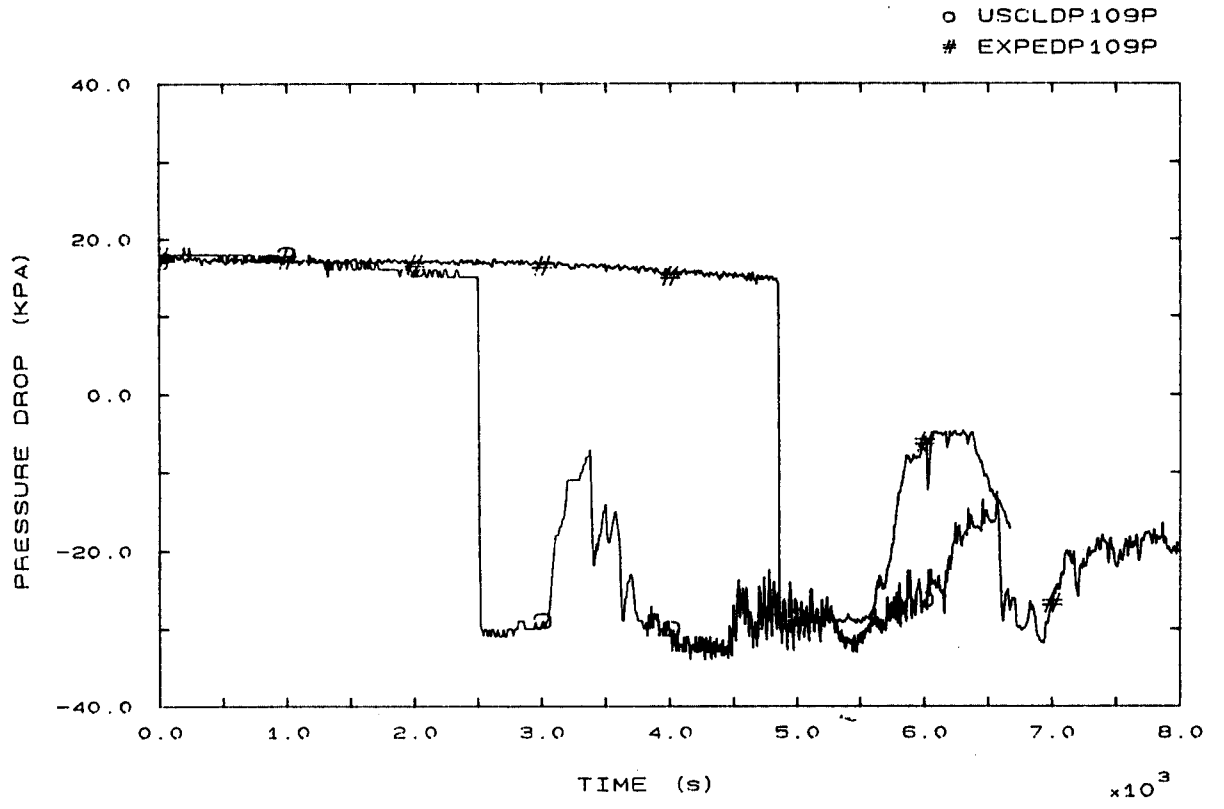

FIG. 68 SG1 OUTLET/LOOP SEAL BOTTOM PRESSURE DROP

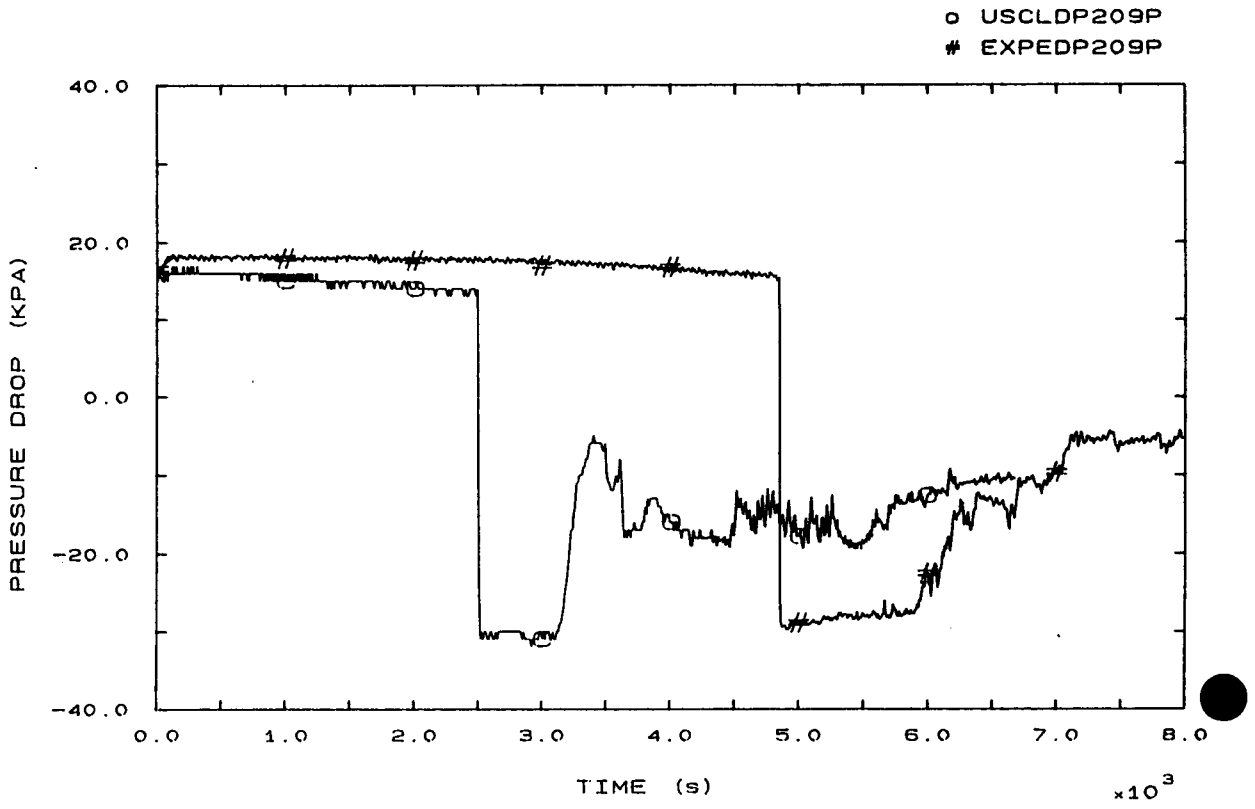

FIG. 69 SG2 OUTLET/LOOP SEAL BOTTOM PRESSURE DROP

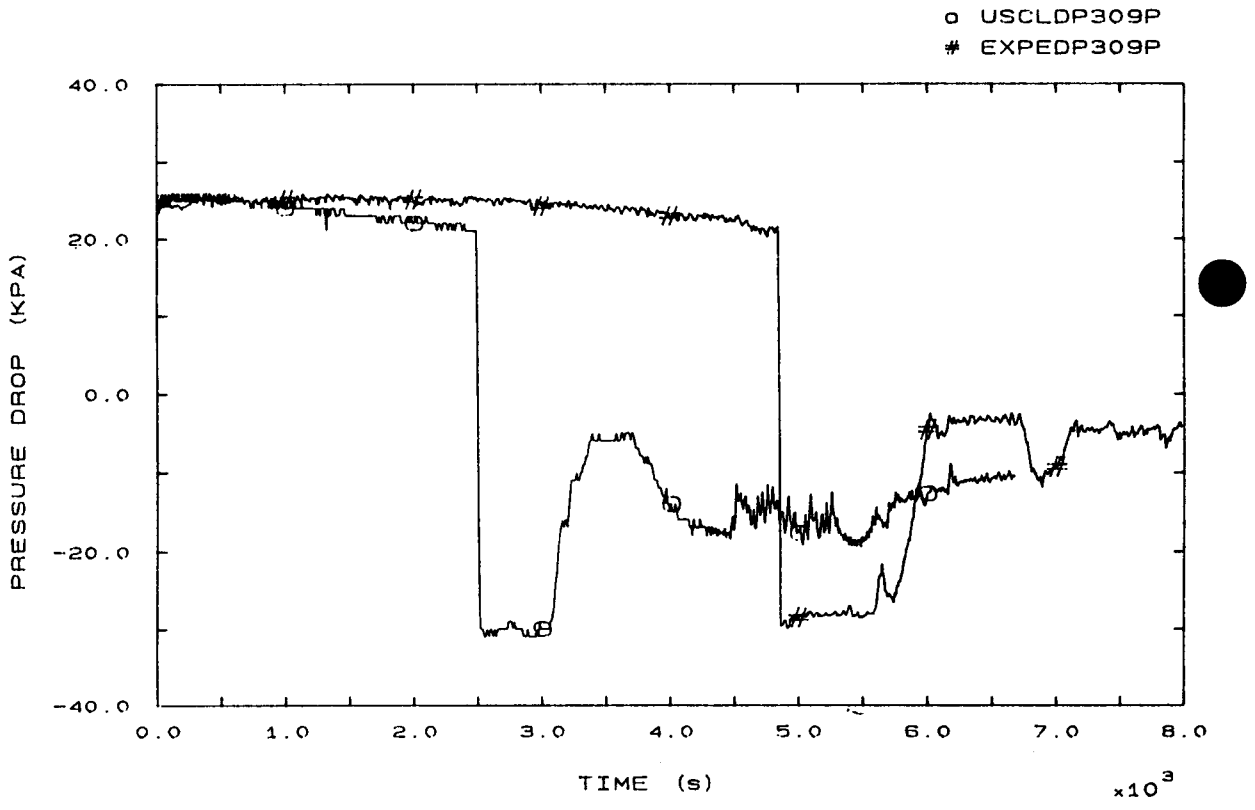

FIG. 70 SG3 OUTLET/LOOP SEAL BOTTOM PRESSURE DROP

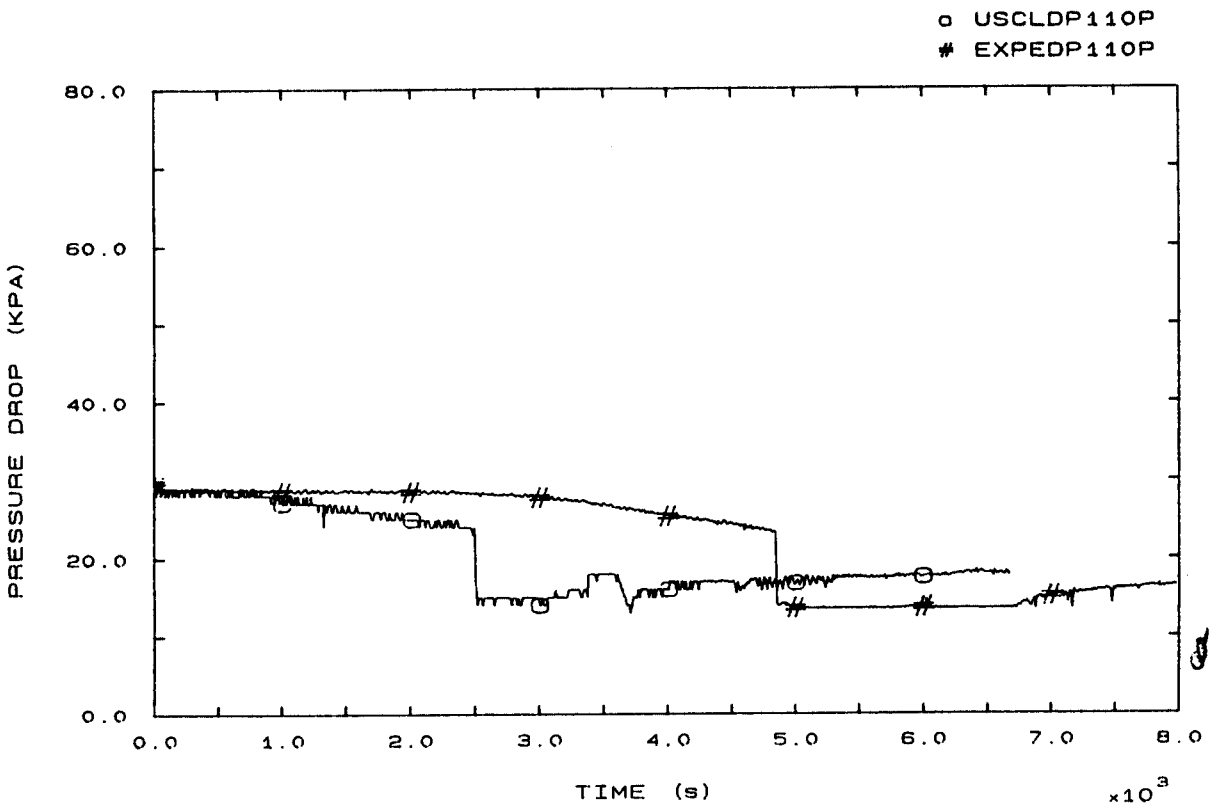

FIG. 71 LOOP SEAL BOTTOM/PUMP 1 INLET PRESSURE DROP

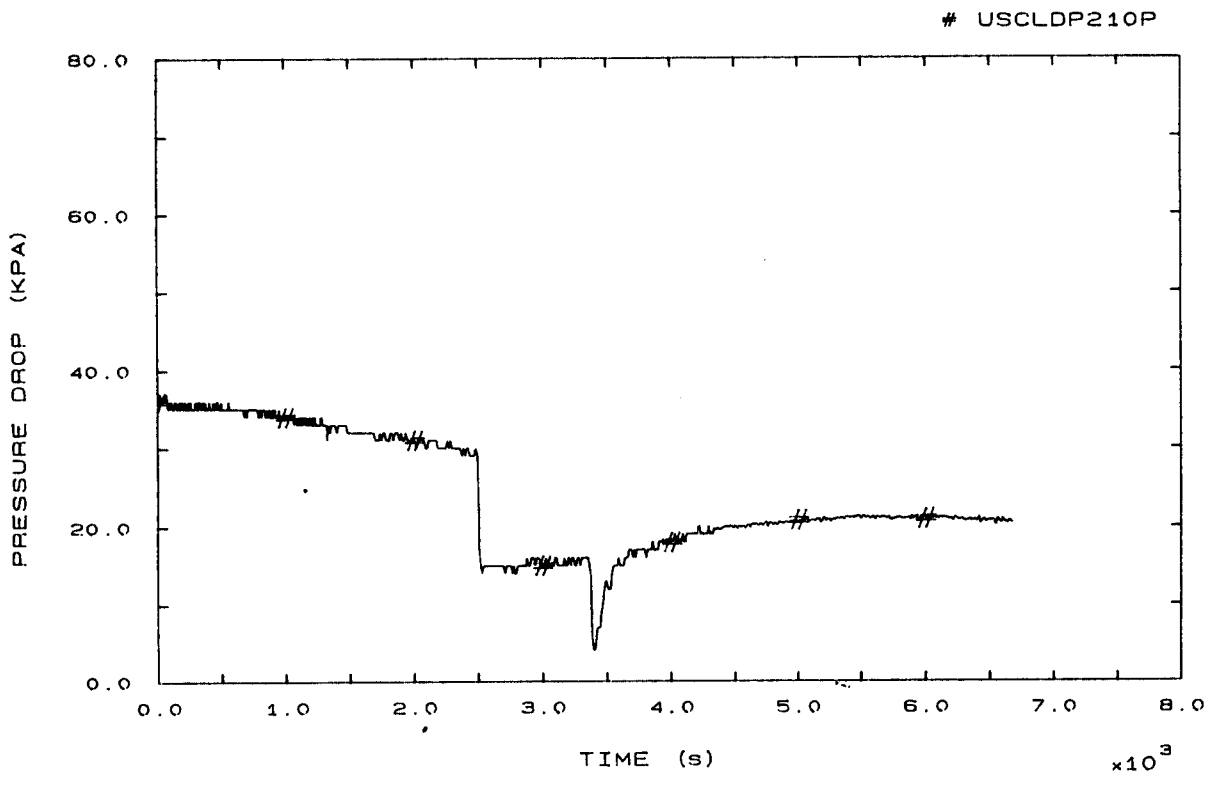

FIG. 72 LOOP SEAL BOTTOM/PUMP 2 INLET PRESSURE DROP

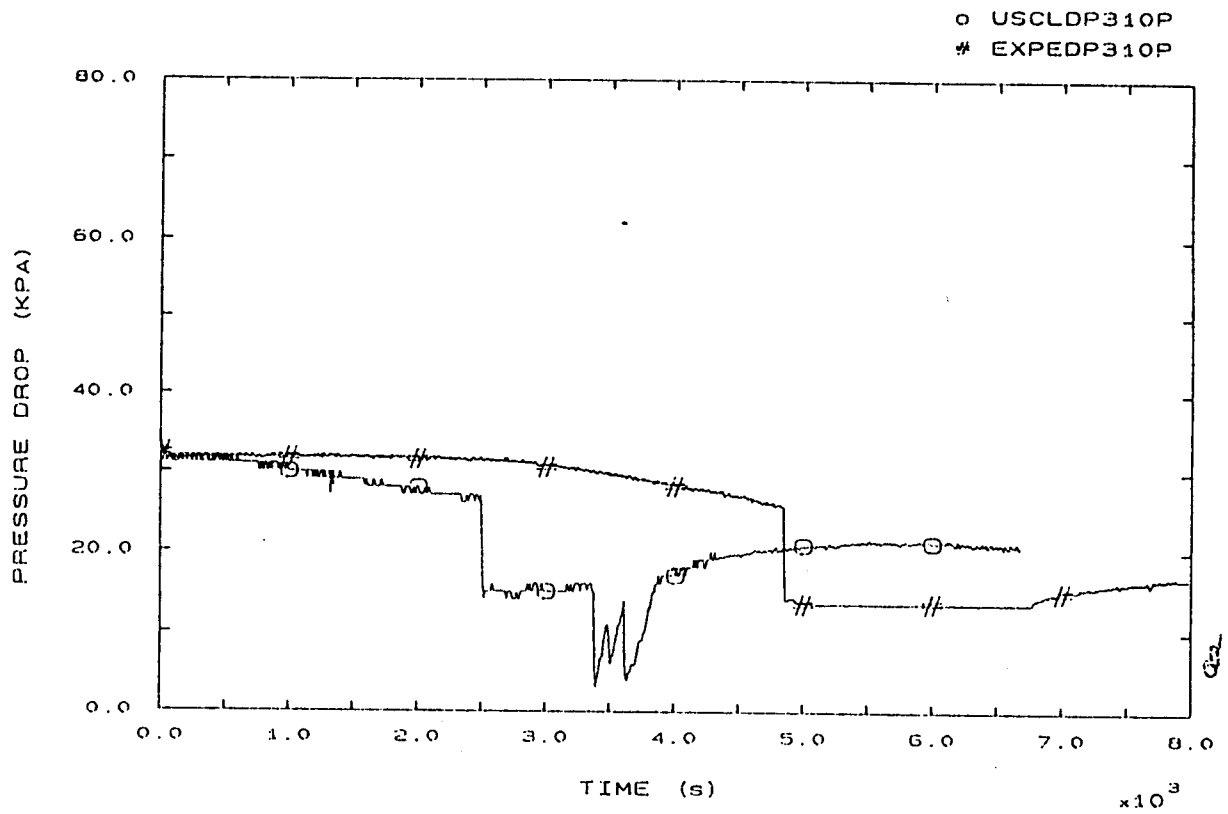

FIG. 73 LOOP SEAL BOTTOM/PUMP 3 INLET PRESSURE DROP

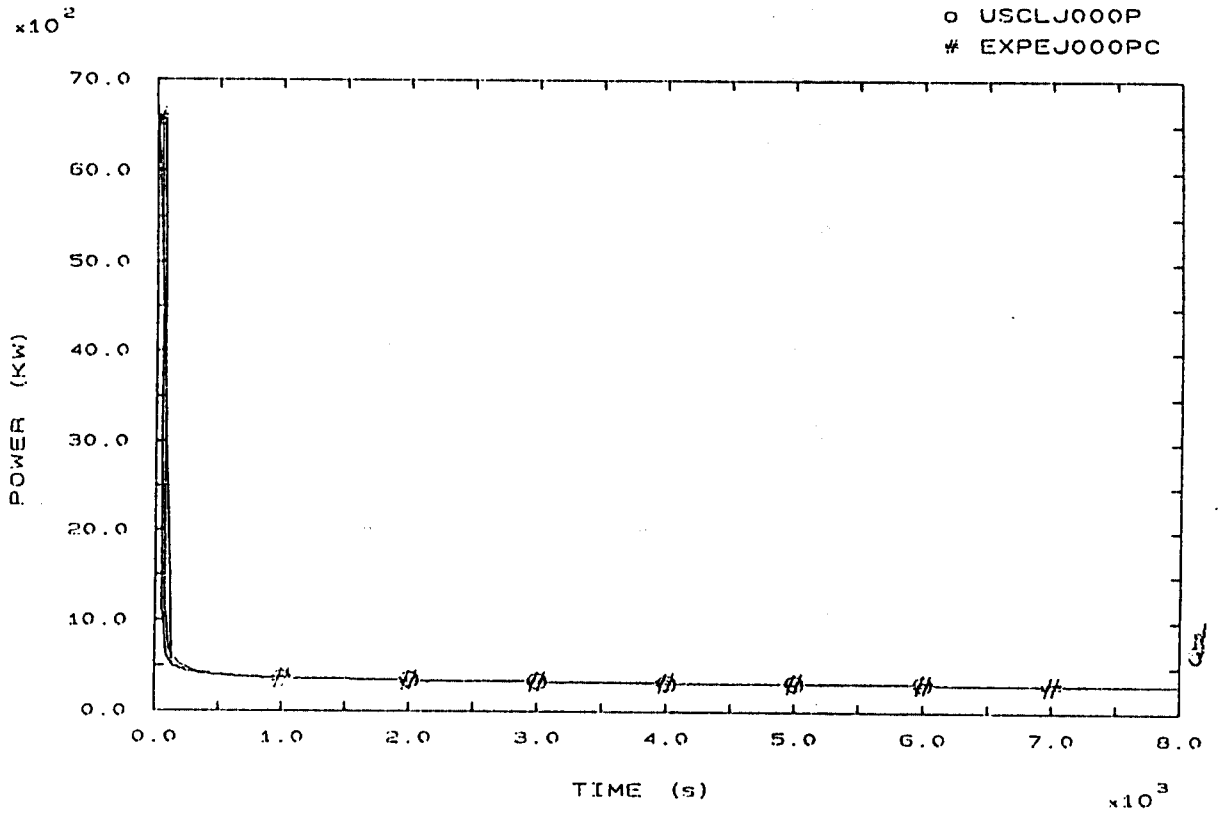

FIG. 81 HEATER RODS POWER

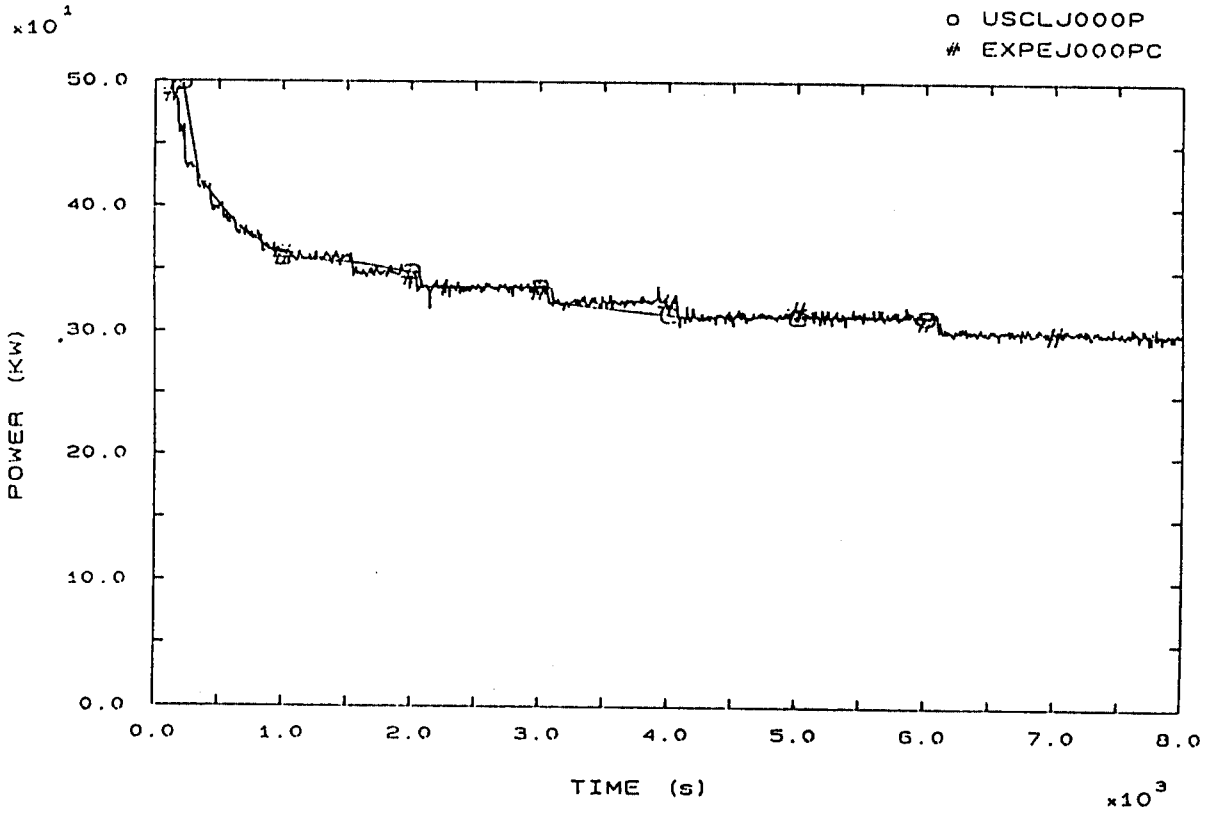

FIG. 81A HEATER RODS POWER

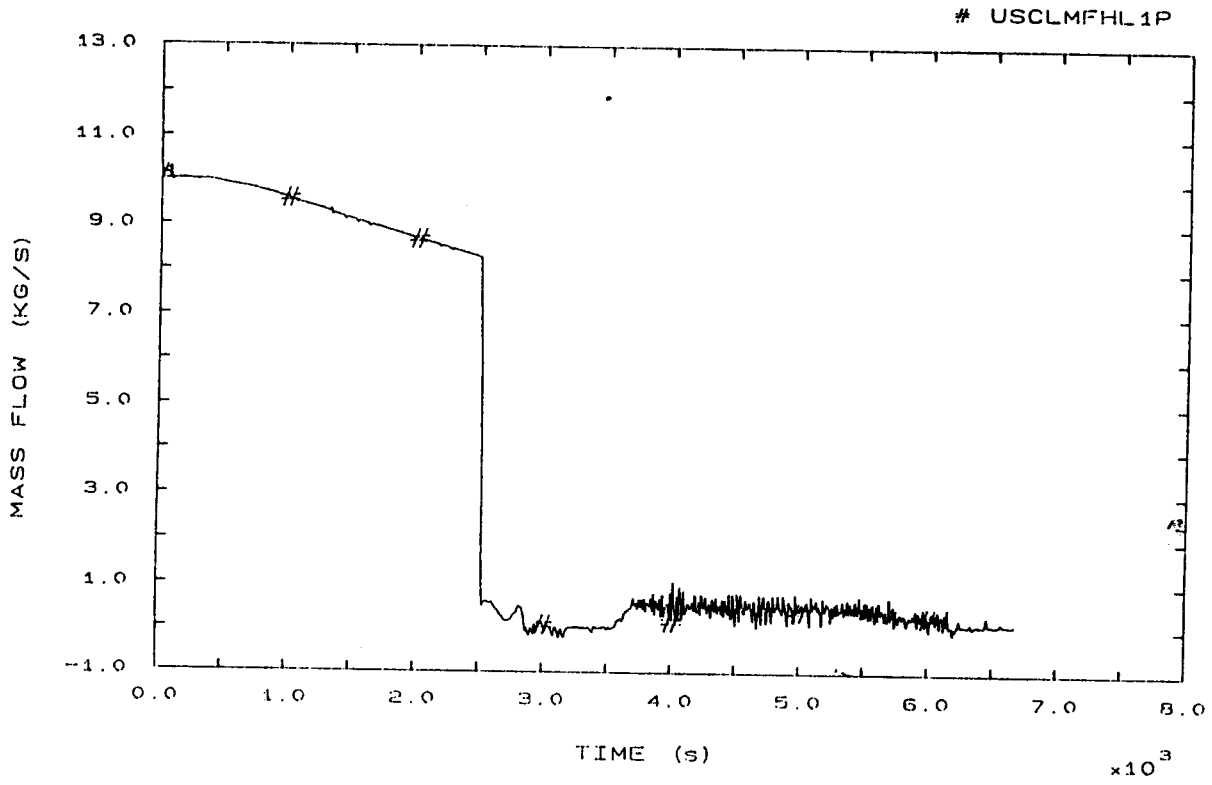

FIG. 89 HOT LEG 1 MASS FLOW

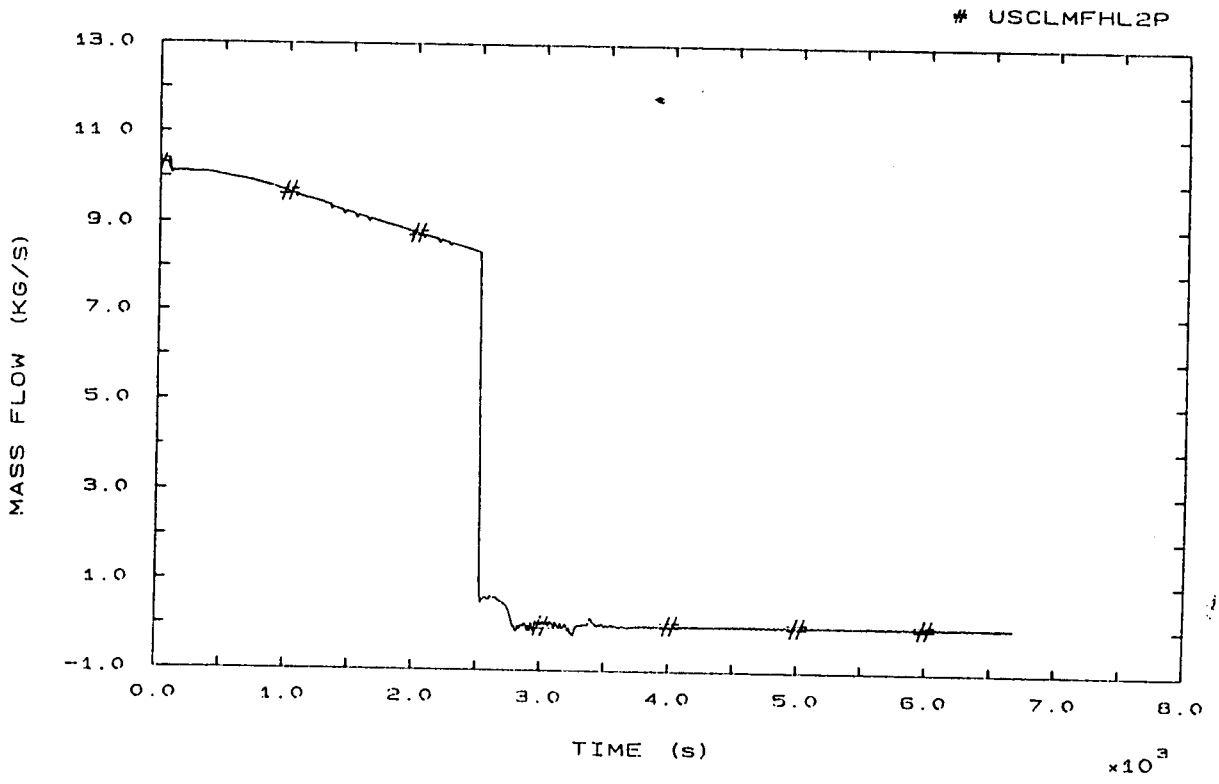

FIG. 90 HOT LEG 2 MASS FLOW

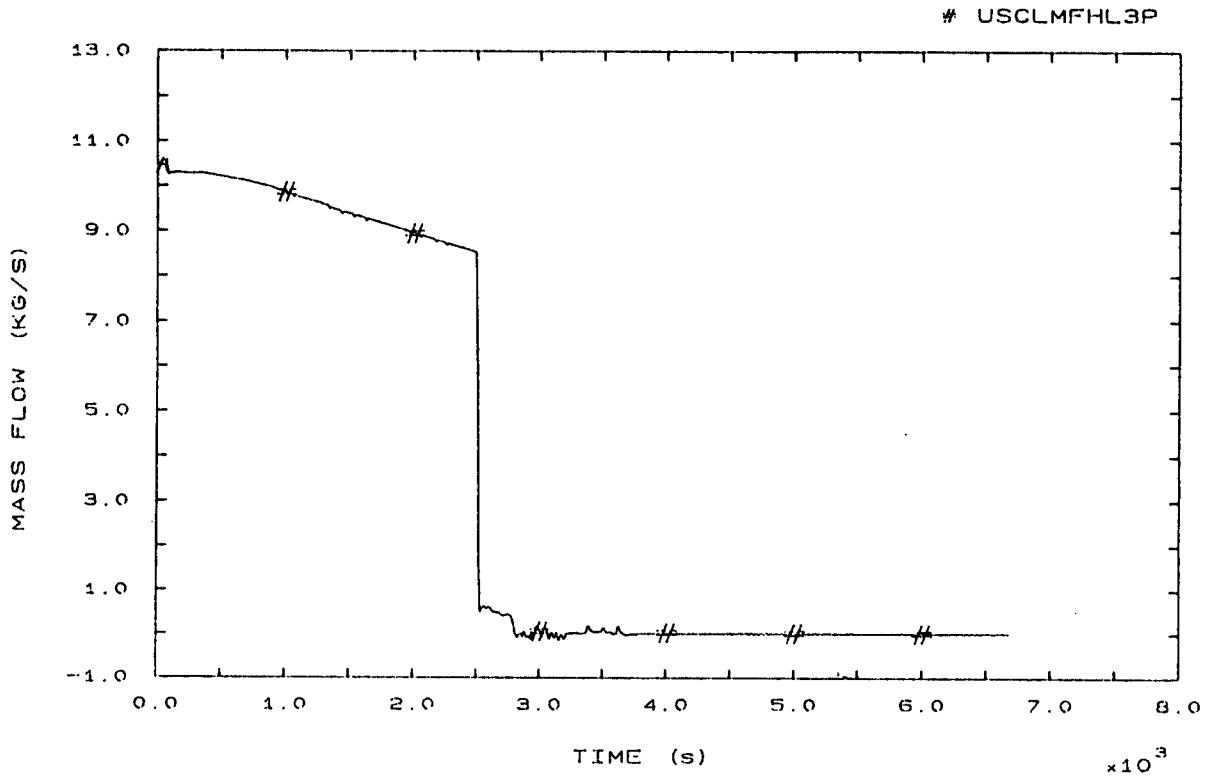

FIG. 91 HOT LEG 3 MASS FLOW

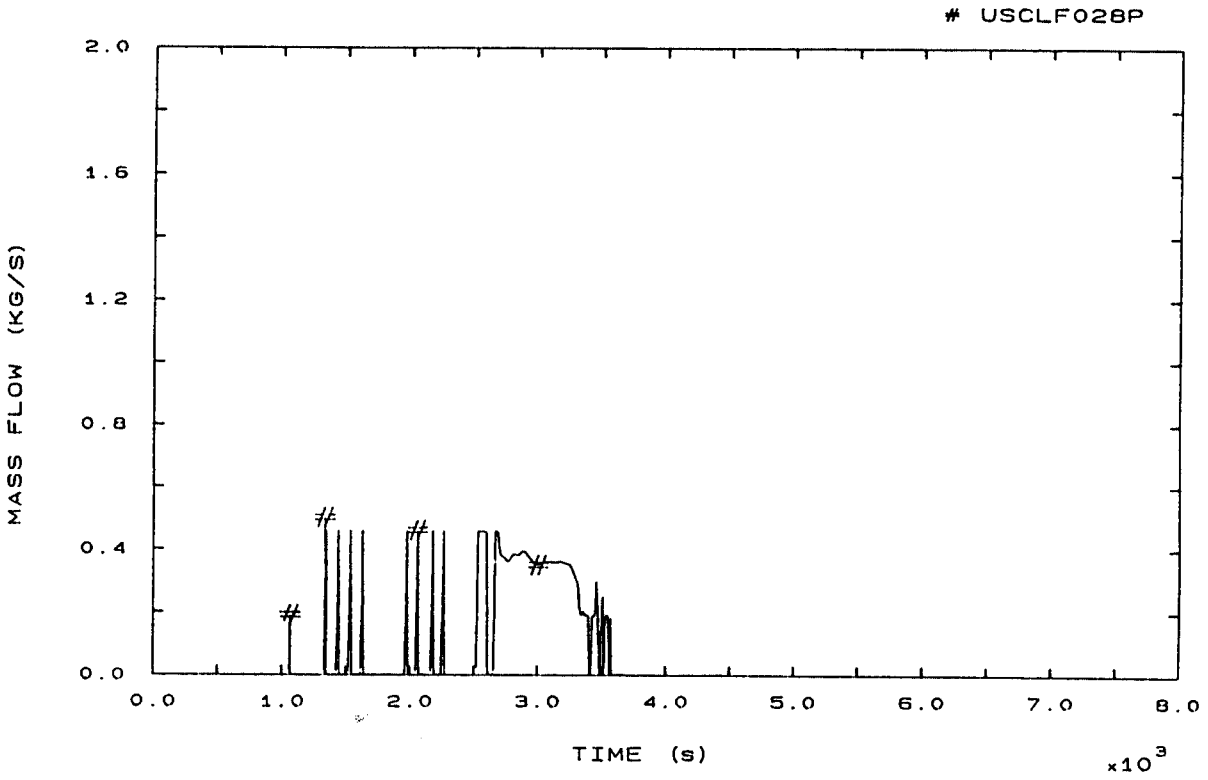

FIG. 92 PRZ PORV MASS FLOW

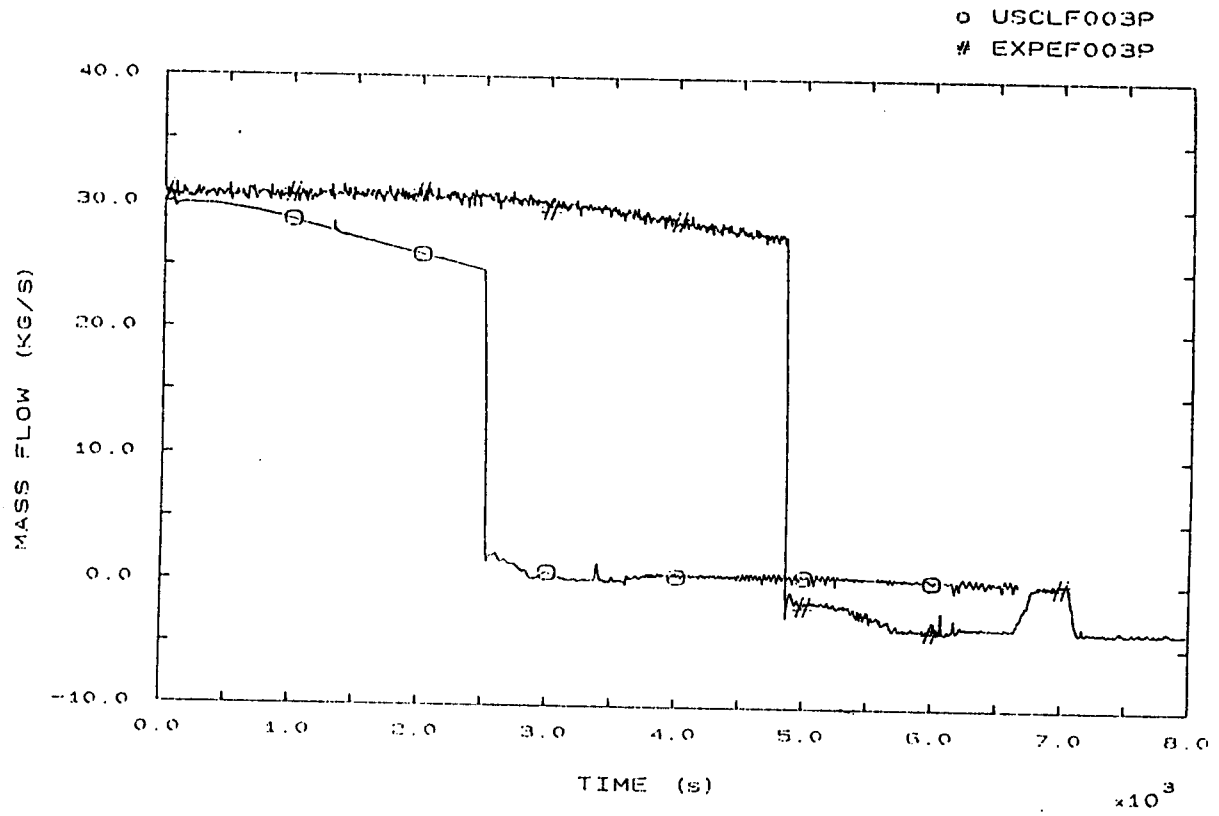

FIG. 94 VESSEL DOWNCOMER MASS FLOW

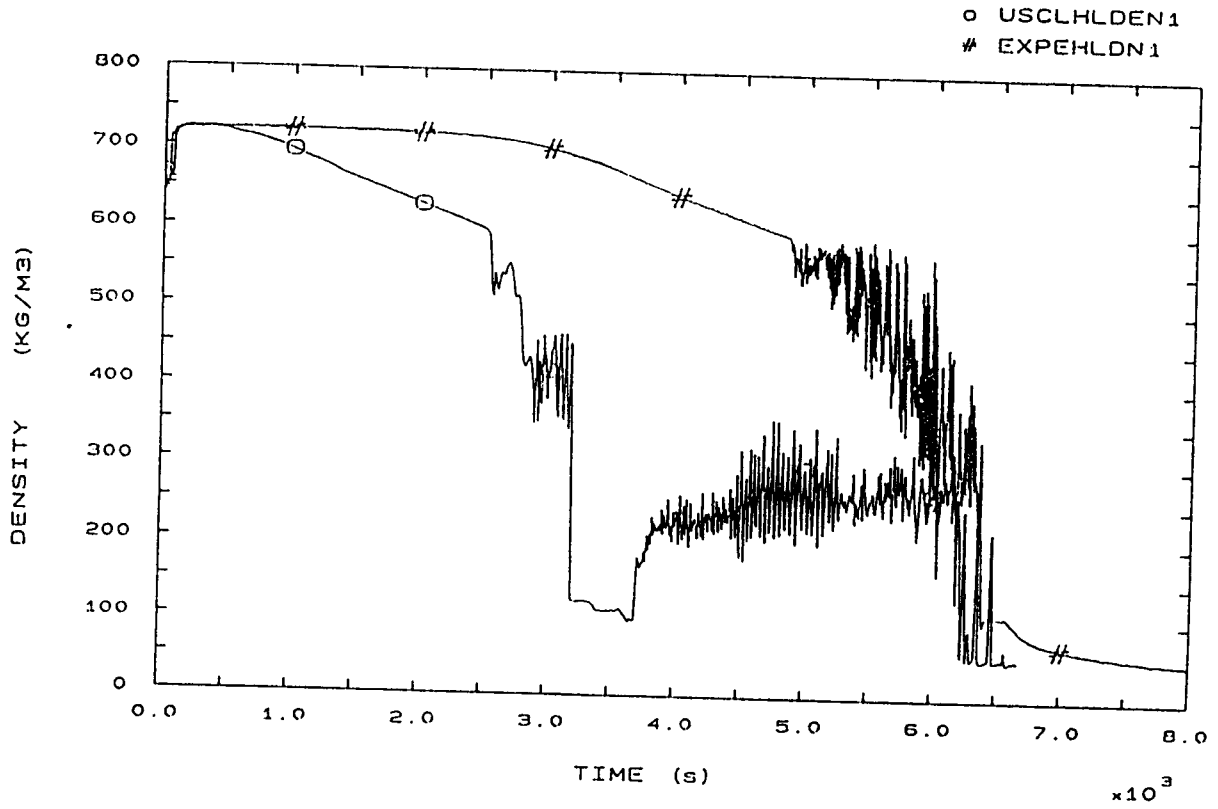

FIG. 100 HOT LEG 1 FLUID DENSITY

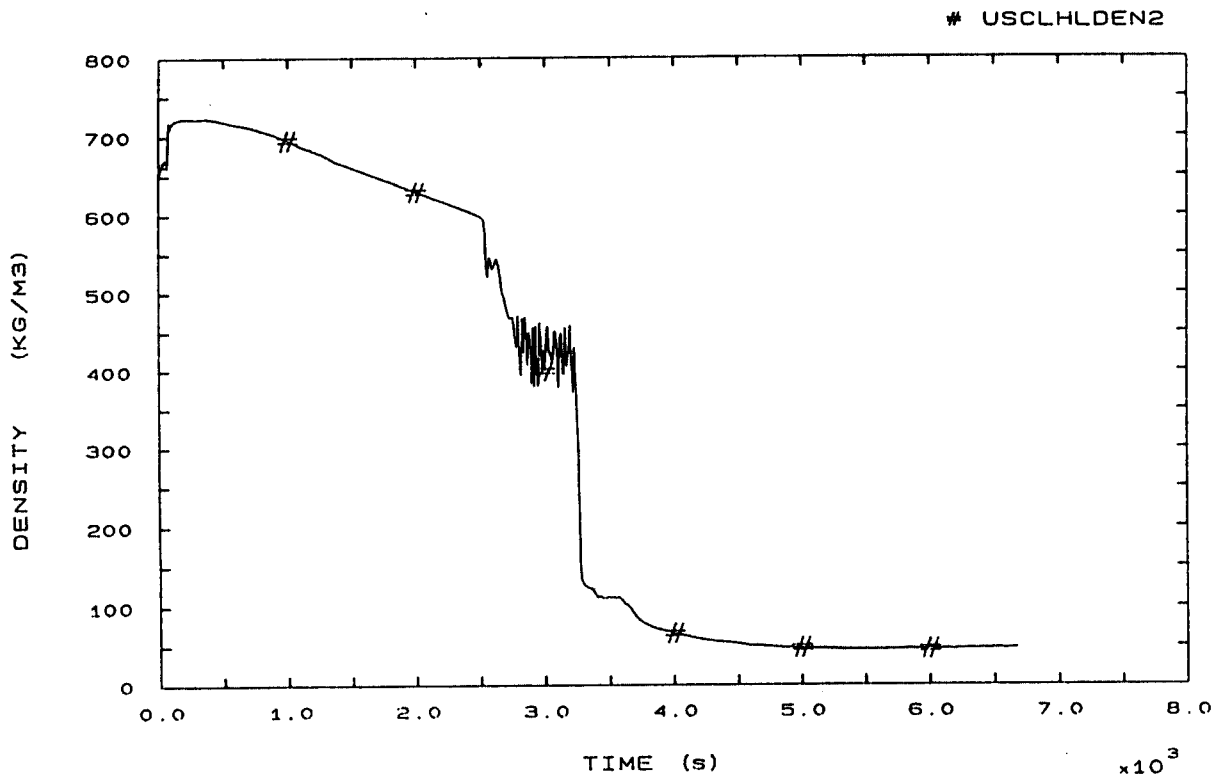

FIG. 101 HOT LEG 2 FLUID DENSITY

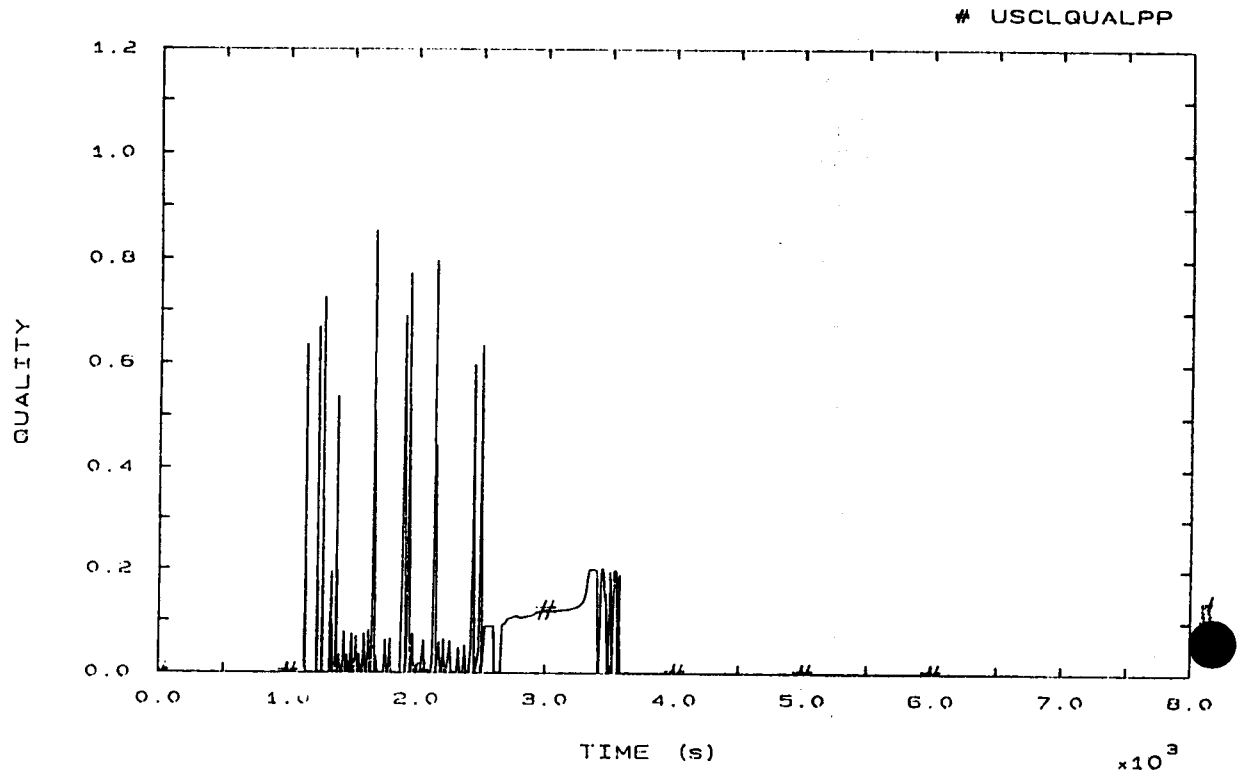

FIG. 103 PRZ PORV FLOW QUALITY

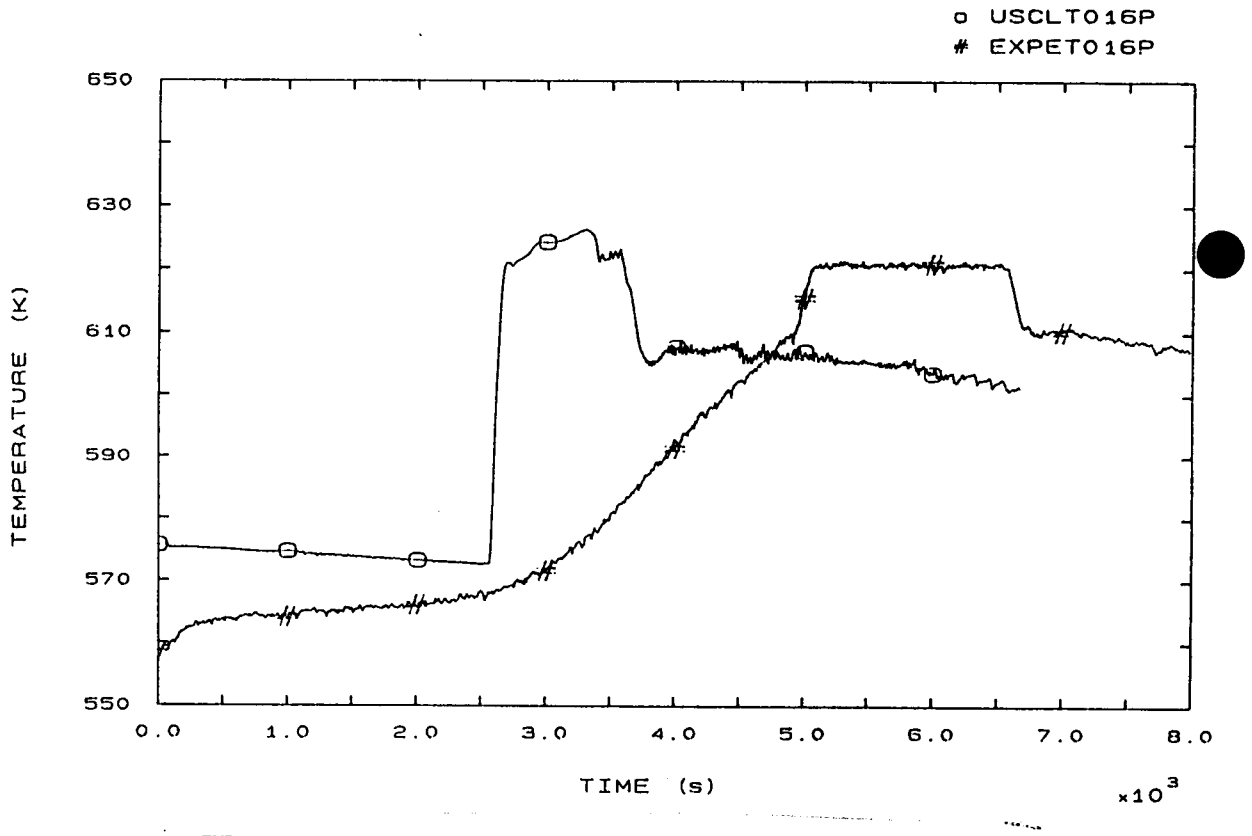

FIG. 110 FLUID TEMPERATURE VESSEL UPPER HEAD

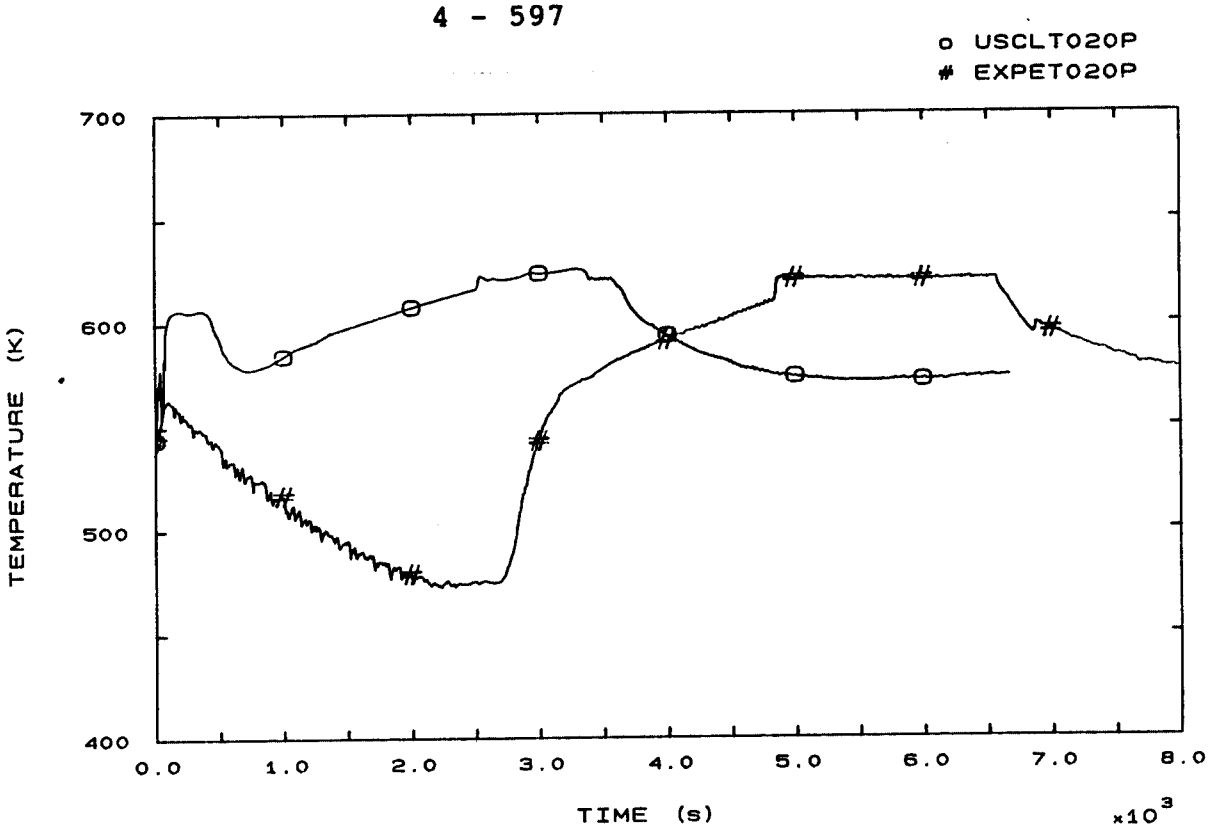

FIG. 112 FLUID TEMPERATURE SURGE LINE UPPER SIDE

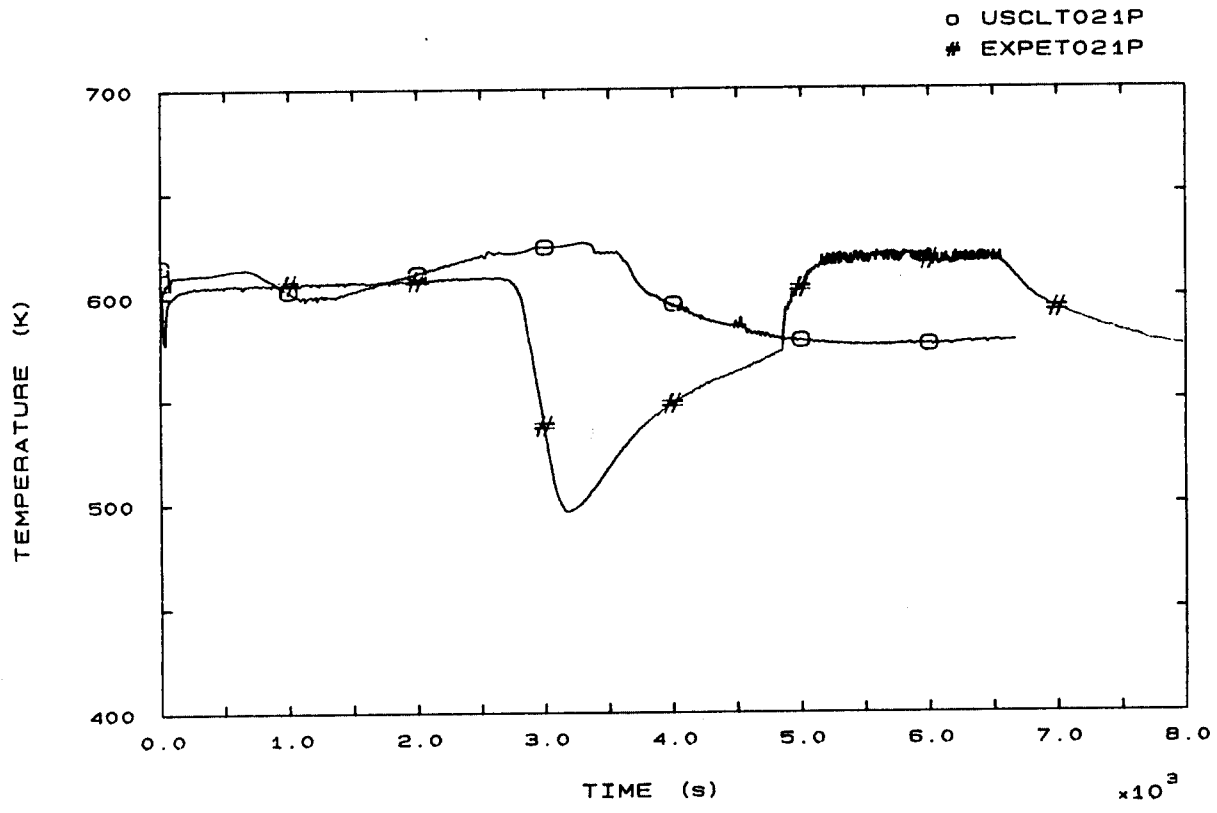

FIG. 113 PRZ FLUID TEMPERATURE

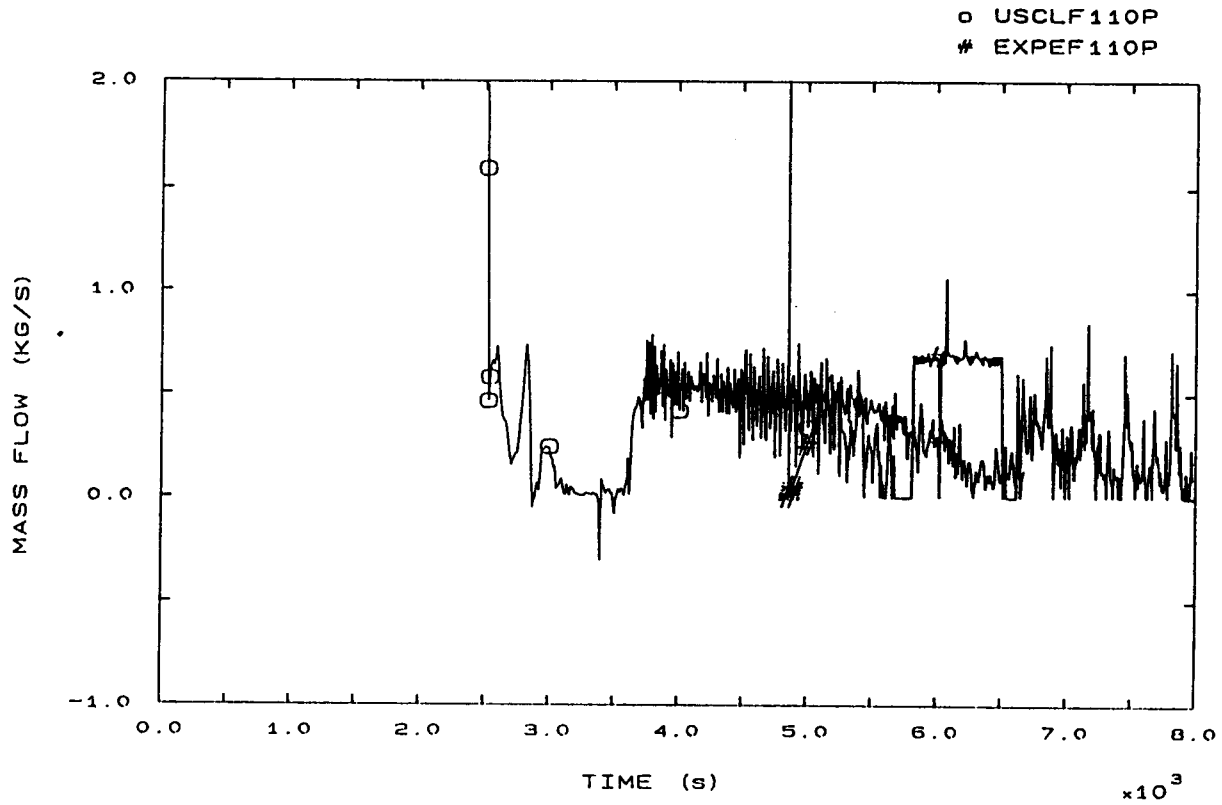

FIG. 125 LOOP SEAL 1 MASS FLOW

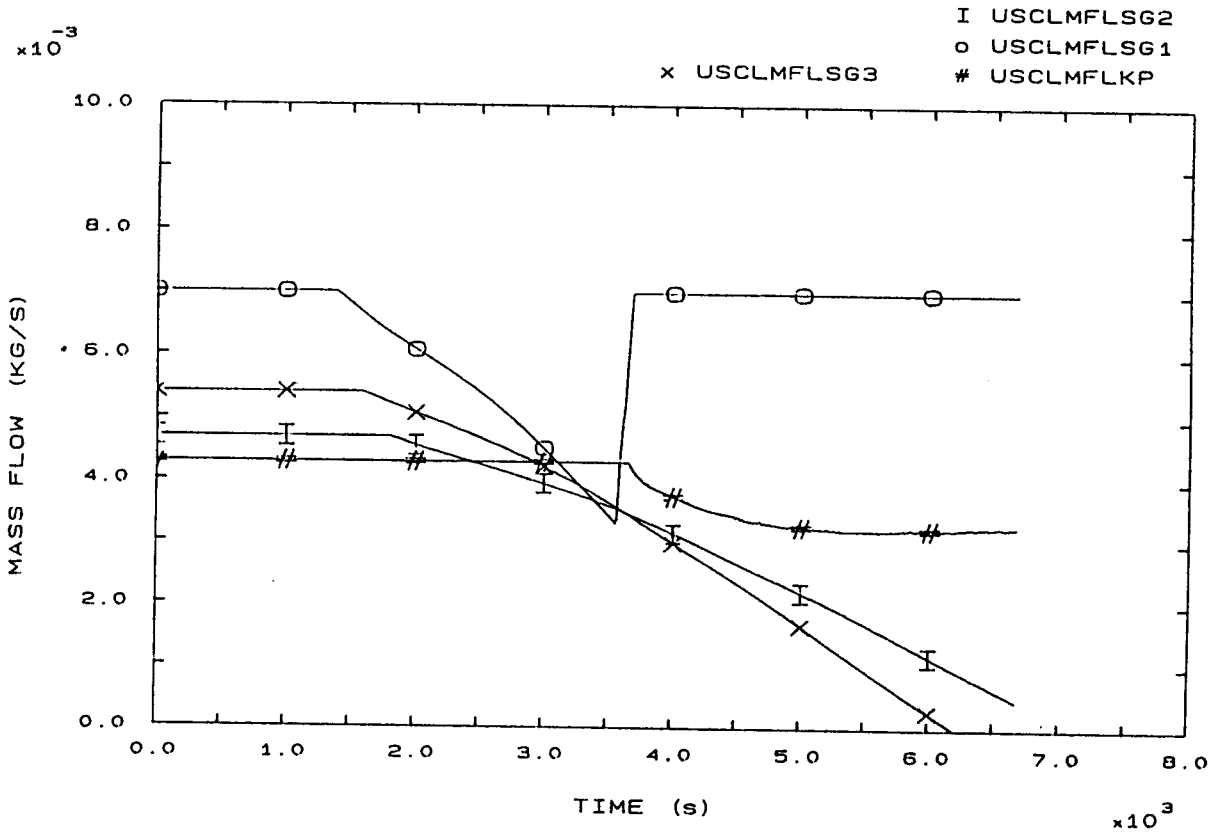

FIG. 137 PRIMARY AND SECONDARY LEAKS

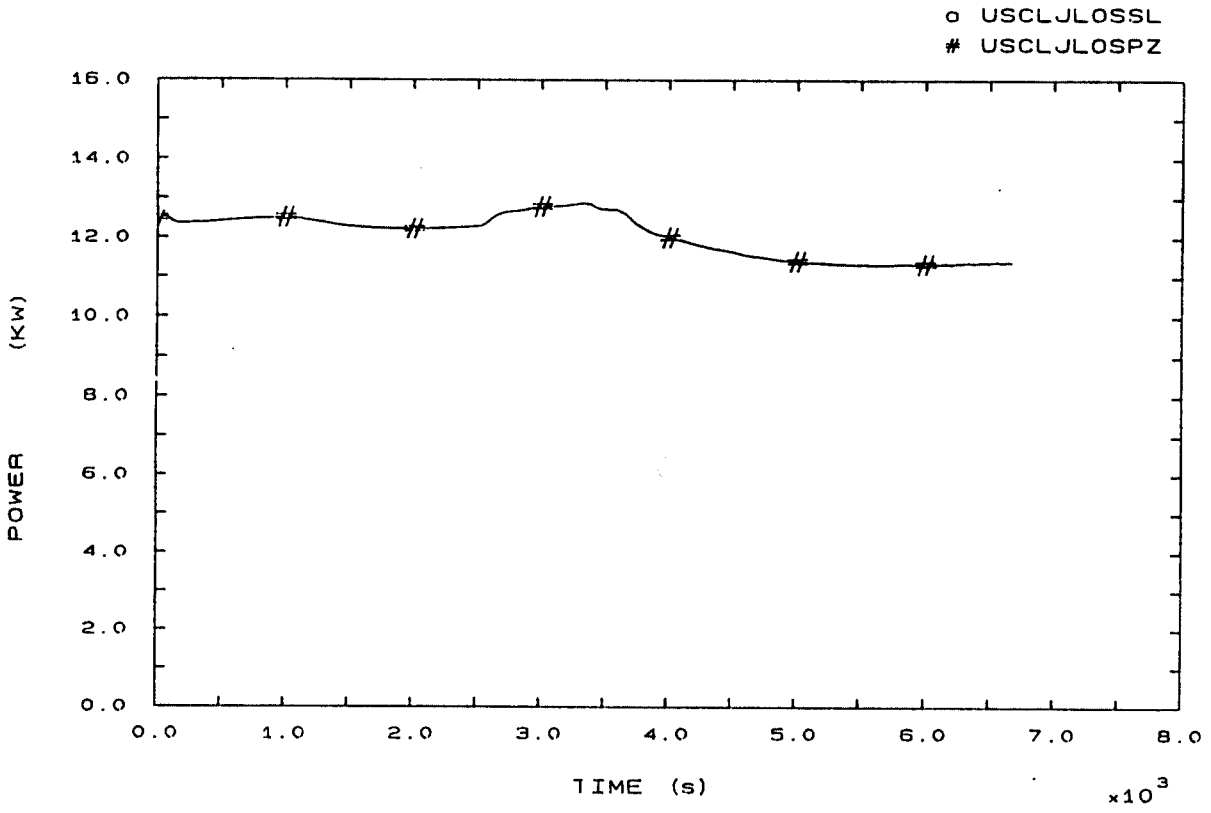

FIG. 138 PRZ AND SURGE LINE HEAT LOSSES

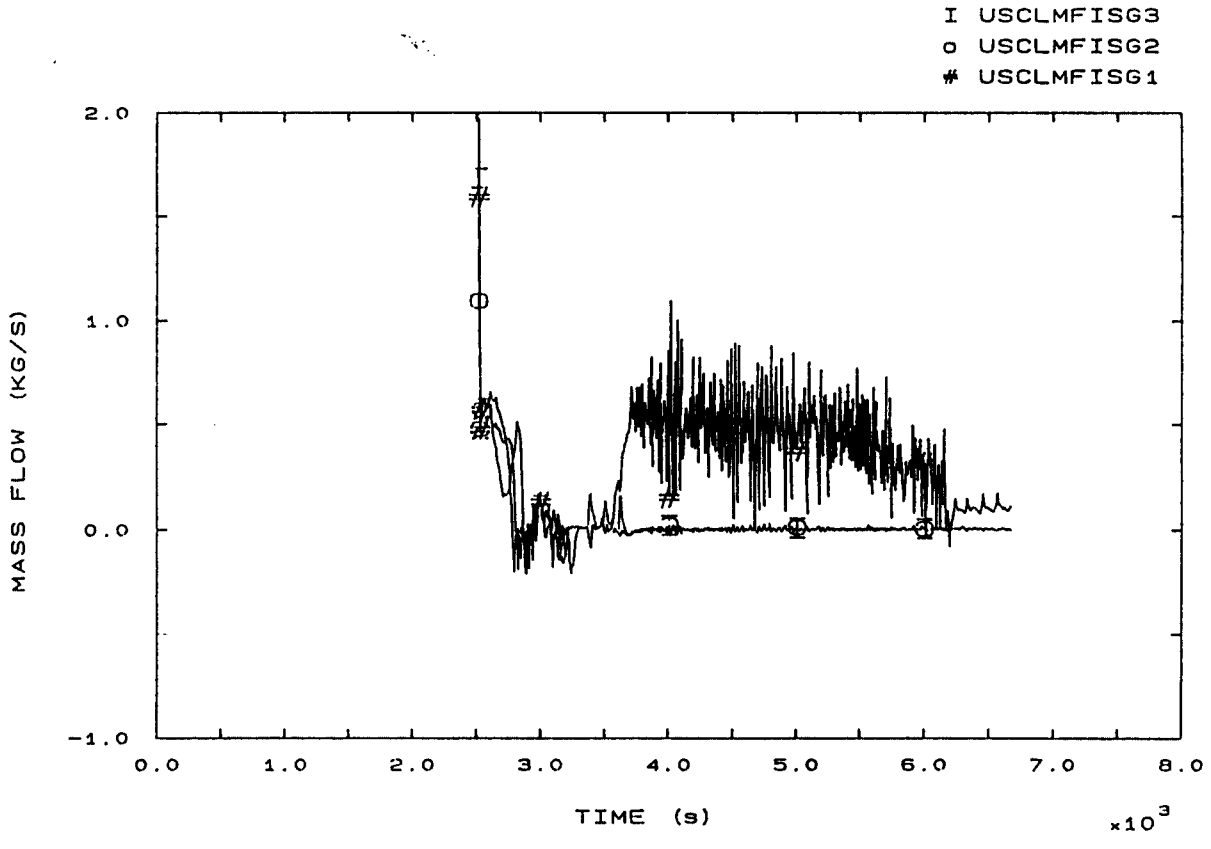

FIG. 140 SG INLET MASS FLOWS

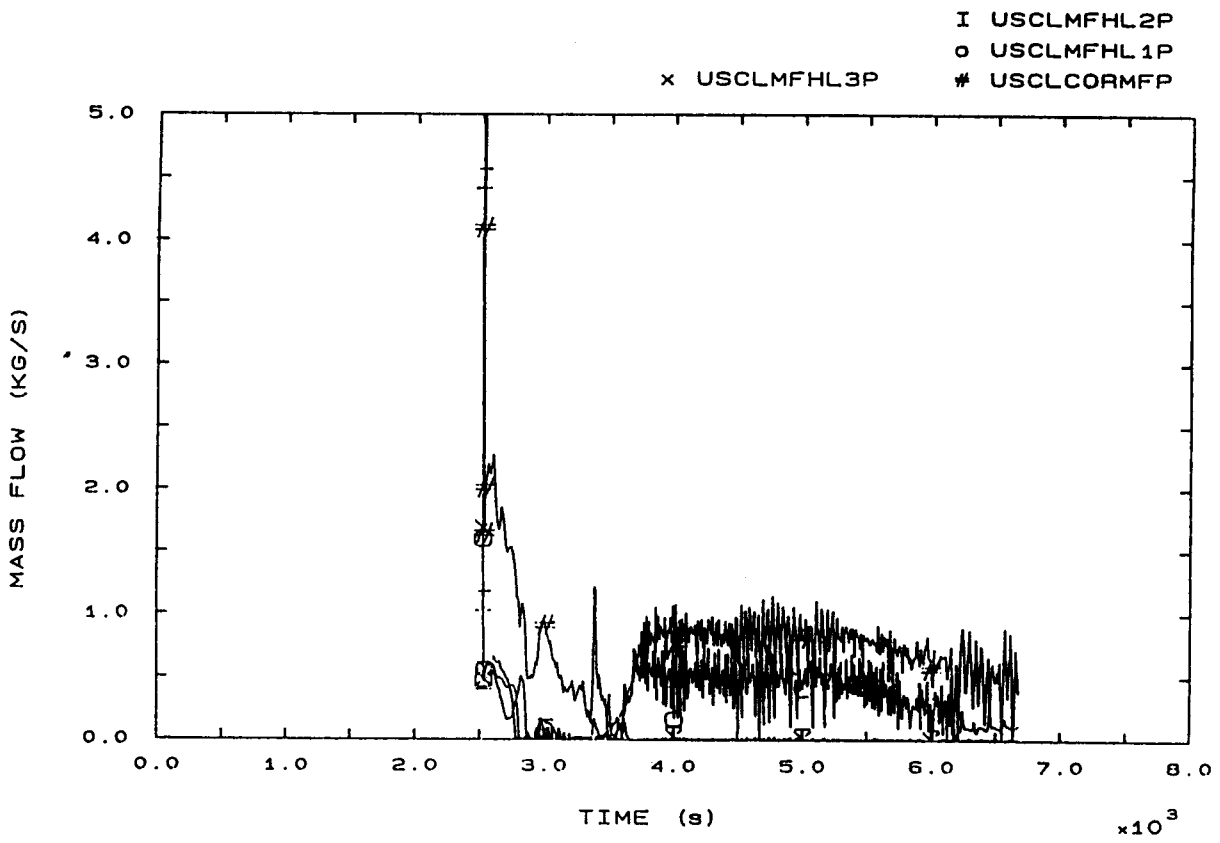

FIG. 141 BOTTOM CORE AND HOT LEG MASS FLOWS

4.15 STUDSVIK

4.15.1 CALCULATION DESCRIPTION

Phase 1: from LOFW to Scram (0,92 s)

A slight increase in pressure and steam line mass flow occurs in the SGs immediately after LOFW (fig. 3b, 96b). The SGs mass content reduces rapidly (fig. 142b) but the heat exchange essentially remains high until a first low-low level signal is obtained from SG1 at 81 s (fig.7b).
An increase of primary pressure causes the PRZ PORV to open four times from 50 s on (fig. 1b). Due to MSIV closure at 86 s the SG PORVs open at about the time of Scram (fig. 3b, 4b, 5b). PRZ level shows a peak in agreement with primary temperature increase (fig. 6b, 42b).

Phase 2: from Scram to PRZ PORV opening (92, 1273 s)

Following Scram primary pressure, temperature and level drop rapidly (fig. 1b, 6b, 12b, 42b). Secondary levels decrease very rapidly (fig. 7, 8, 9) and SGDO is completed before t = 1000 s. Primary heat up begins (fig. 12, 42) causing PRZ level (fig. 6) and pressure to rise: PRZ PORV begins to cycle at 1273 s. Steam generators begin to slowly depressurize (fig. 3, 4, 5)

Phase 3: from PRZ PORV opening to pumps trip (1273, 3718 s)

Primary pressure is maintained by PRZ PORV cycling (fig. 1). Primary heat up continues (fig. 12, 42) causing PRZ level to increase progressively (fig. 6) and pumps head to reduce because of coolant density reduction (fig. 54). SGs continue to depressurize with decreasing rates (fig. 3, 4, 5,) due to mass leaks.

Phase 4: from pumps trip to EFW actuation (3718, 4700 s)

Following pumps trip, TPNC establishes in the primary loops (fig. 89, 90, 91). Primary voiding causes core level to decrease (fig. 11) while primary temperatures reach the saturation value (fig. 12, 42). At about 4200 s loop flows stall (fig. 62, 63, 89) and a primary pressure peak is observed (fig. 1) while PRZ level starts to decrease (fig. 6) and PRZ PORV discharge high quality mixture (fig. 103). Core heat up at top of bundle starts at 4635 s (fig. 52) when core collapsed level is about 1.5. m (fig. 11).

Phase 5: from EFW actuation to the end (4700, 5785 s)

Actuation of EFW causes SG1 level recovery (fig. 7) and pressurization (fig. 3) until PORV setpoint is reached. Secondary cooling induces primary steam condensation: PRZ pressure rapidly decreases towards the secondary value, while PRZ level drops below zero (fig. 1, 6). Core heat up is terminated (fig. 52) and collapsed level is recovered (fig. 11). Primary temperatures follow the pressure trend (fig. 12, 42). A continuous two phase natural circulation (TPNC) is established in loop 1 (fig. 89).

PARTICIPANT: ERIKSSON - STUDSVIK *CODE: TRAC*

EVENTS TABLE

EVENT	*CALC. TIME (s)*	*EXP. TIME (s)*
SG Low Low Level	*81*	*33*
Main Steam Isolation	*86*	*38*
Scram (power fall), t_1	*92*	*44*
SGs PORV opening	*91* *91* *91*	*82 (3)* *106 (2)* *200 (1)*
SGs Dry Out	*783 (1)* *846 (3)* *925 (2)*	*3282 (3)* *3347 (1)* *3437 (2)*
PRZ PORV opening, t_2	*1270*	*4134*
PRZ full of liquid	*2460*	*4222*
Pumps Trip, t_3	*3718*	*4848*
Loss of Natural Circulation	*4265*	*5630*
Beginning of Core Heat Up	*4635*	*6511*
EFW actuation, t_4	*4700*	*6532*
PRZ PORV closure	*4745*	*6576*
PRZ emptying	*4798*	*6811*
SG1 repressurization	*4920*	*6878*
End of transient, t_{END}	*5785*	*8062*

4.15.2 CALCULATION/EXPERIMENT COMPARISON

Phase 1: from LOFW to Scram

SGs initial inventory is correctly imposed by assuming higher SGs initial levels (fig. 7b, 8b, 9b and Comp. Table), but trips timing is extremely delayed, due to a strong overestimate of LoLo level time (81 s vs 33) caused by a low level decrease rate after LOFW and the higher level at time 0. Maximum primary pressure is correctly calculated also if pressure trend in this phase shows several spikes which were not detected in the experiment (fig. 1b). Such a behaviour must be related to the PRZ level (fig. 6b) that follows SG outlet temperature (fig. 42b) and secondary pressure (fig. 3b). Secondary inventory at Scram time is consequently much lower than the evaluated exp. value (see Comp. Table).

Phase 2: from Scram to PRZ PORV opening

Minimum primary pressure after Scram is sensibly underestimated, also if PRZ level is higher than in the Exp (see fig. 1b and 6b).
SGs PORV opening times are well calculated for SG "2" and "3", but they contain the effect of delayed MSI. If referred to the isolation time instant, all the opening times are strongly underestimated and secondary pressures show higher values following MSI (fig. 3b, 4b, 5b). PRZ level gradient during SG emptying (fig. 6) is positive (negative in the Exp). This is related to a calculated slow primary temperature rise during this period (fig. 12, 42) and to the absence of primary leak modelling. Primary pressure gradients before and after SGs dry out are strongly overestimated (fig. 1)probably due to an incorrect modelling of PRZ. No data are provided concerning the warm insurge from SL.

SGs DO time is extremely underestimated (850 s in average w.r.t. 3300) mainly due to low SG inventories at Scram time. Both discrepancies contribute to a strong underprediction of PRZ PORV opening time (1270 s vs 4134, see fig. 1).
Primary temperature and level gradients during heat up are slightly lower than in the Exp (see fig. 6, 12, 42)

Phase 3: from PRZ PORV opening to pumps trip

PRZ full time is consequently underestimated in the absolute sense, but strongly overestimated if referred to PORV opening (1190 s vs 88). This is related to the early primary pressurization that causes PORV lift with a lower PRZ level (4.3 m vs 6.57). Pumps trip time is also underpredicted, but the absolute error (about 1100 s) is much lower than for the preceeding reference time instants.This is due to the independence of temperature profile from pressure trend. Primary inventory at pumps trip time is indeed calculated with good accuracy (399 kg vs 390). Time interval since SGDO (dt_{HU}) is overpredicted due to the lower primary temperature gradient during heat up (fig. 12).

Phase 4: from pumps trip to EFW actuation

PRZ behaviour during this phase is well predicted by Studsvik calculation: level decrease following pumps trip and an obscillations period around an intermediate level value (4m) are both simulated (fig.6). Also two-phase natural circulation (TPNC) and subsequent loss of natural circulation (LNC) are predicted reasonably (fig. 62, 63). Time of LNC is obviously underpredicted in absolute terms, but is sufficiently accurate if referred to pumps trip time (dt_{LNC} = 680 s vs 780). Primary inventory at LNC time is well calculated (295 kg vs 296), while time interval until beginning of core heat up is underestimated (230 s vs 880). Primary inventory at t_{BOCH} is nevertheless accurately calculated (185 kg vs 183, see fig. 85).

EFW actuation time t_4 is underestimated in absolute terms and w.r.t. LNC time, but is overpredicted if referred to t_{BOCH} (65 s vs 21). This can be related to a low core heat up rate (0,8 K/s vs 2 to 5 K/s in the Exp.).

Phase 5: from EFW actuation to the end

Maximum Core Temperature (fig. 52) is sensibly underestimated (668 K vs 770). PRZ PORV closure interval since EFW actuation (dt_{PRZPC}) is accurately predicted (see Comp. Table), also if primary depressurization and SG1 pressurization rates are significantly overpredicted (see Comp. Table and fig. 1, 3). These discrepancies are connected with the lower PRZ emptying period (dt_{PRZE} = 98 s vs 280, see fig. 6). The reason of these differences can be searched in an overestimate of secondary cooling in SG1. Studsvik calculation shows a rather continuous NC in loop 1 during this phase. Obscillatory behaviour observed in the Exp is not predicted (fig. 62, 63).
Core reflood is predicted to take place from the bottom. The transient terminates about 2300 s in advance w.r.t. SPES test (fig. 7). SG1 level recovery appears to be faster than in the Exp.

PARTICIPANT: ERIKSSON - STUDSVIK CODE: TRAC

COMPARISON TABLE

PARAMETER		EXP	CALC	AE*	RFD**
1A Initial SGs mass (Kg)	1	137	137		
	2	151	151	G	-
	3	145	145		
1B Trips timing (s)	LoLo	33	81	P	HIL(B+C+U)
	MSI	38	86	P	Lolo
	Scram	44	92	P	LoLo
1C Max primary pressure (MPa)		16.2	16.2	G	-
1D SGs mass at Scram (Kg)	1	98	46		
	2	105	57	P	1B
	3	97	51		
2A Min. primary pressure (MPa)		14.5	13.9	P	
Pressure gradients before		4.10^{-4}	1.4.10-3	P	PRZM (B+U)
and after SGs DO (MPa/s)		3.10^{-4}	2.7.10-3	P	
2B SGs PORV opening time (s)	1	200	91	P	
	2	106	91	S	SECM ?
	3	82	91	S	
2C PRZ level gradient (m/s)		$-5.7.10^{-4}$	2.10^{-4}	P	PLA (U)
2D Min. PRZ level (m)		2.3	3.7	P	2C, 2E
2E SGs DO time tSG1DO (s)		3347	783		
tSG2DO (s)		3437	925	P	1D+HSM (U)
tSG3DO (s)		3282	846		
2F Heat Up temperature (K/s)		0.02	0.014	S	HSM (U)
and level (m/s) gradients		$3.6.10^{-3}$	2.10-3	S	HSM (U)
2G Cool Insurge effect		PR. DELAY	?	?	?
2H PRZ PORV opening time, t2 (s)		4134	1270	P	2E
$(dt_2 = t_2 - t_{SGDO})$		(697)	(345)	P	PRZM (U+B)
3A PRZ level at t_2 (m)		6.57	4.3	P	2H
3B PRZ full time, t_{PRZF} (s)		4222	2460	P	2E
$(dt_{PRZF} = t_{PRZF} - t_2)$		(88)	(1190)	P	2H
3C Dominant Relief Condition		LIQ	VAP/MIX/LIQ	P	3B
3D Sat. Conditions before trip		NO	NO	G	-
3E Pumps Trip time, t3 (s)		4848	3718	P	2E+2F
$(dt_3 = t_3 - t_2)$		(714)	(2448)	P	2H+2F
$(dt_{HU} = t_3 - t_{SGDO})$		(1411)	(2793)	P	2F

* ACCURACY EVALUATION : G=GOOD, S=SUFFICIENT, P=POOR

** REASON FOR DISCREPANCY : B=BIC, C=CODE, U=USER, PRZM=PRZ MODELLING, PLA=PRIMARY LEAK ABSENCE, SECM=SECONDARY MODELLING, LHL=LOW HEAT LOSSES, HIL=HIGH INITIAL LEVEL

PARTICIPANT: ERIKSSON - STUDSVIK CODE: TRAC

COMPARISON TABLE (CONT'D)

PARAMETER	EXP	CALC	AE*	RFD**
3F RCS mass at t_3 (kg)	390	399	G	-
4A PRZ behaviour	PART. EMPT.	PART. EMP.	G	-
during phase 4	LEV. OBS.	LEV. OBS.	G	-
4B Primary Flow Cond.	TPNC/LNC	TPNC/LNC	G	-
4C LNC time, tLNC (s)	5630	4265	P	3E
($dt_{LNC} = t_{LNC} - t_3$)	(780)	(547)	S	LDP (C)
4D RCS mass at t_{LNC} (kg)	296	295	G	-
4E Beg. of Core Heat Up, t_{BOCH} (s)	6511	4635	P	4C+
($dt_{BOCH} = t_{BOCH} - t_{LNC}$)	(880)	(230)	P	LDP (C)
4F RCS mass at tBOCH (Kg)	183	185	G	-
4G EFW act. time, t4 (s)	6532	4700	P	3E+LDP(C)
($dt_{4B} = t_4 - t_{BOCH}$)	(21)	(65)	P	LHUR (5A)
($dt_{4L} = t_4 - t_{LNC}$)	(900)	(300)	P	LDP (C)
($dt_4 = t_4 - t_3$)	(1684)	(982)	P	LDP (C)
4H PRZ level at t_4 (m)	4.4	3.9	G	-
5A Core Heat Up Rate (K/s)	2/5	0.8	P	HSM? (U)
5B Max Core Temperature (K)	770	668	P	5E,HSM?(U)
5C PRZ PORV closure time, t_{PRZPC}	6576	4745	P	4G
($dt_{PRZPC} = t_{PRZPC} - t_4$)	(44)	(45)	G	-
5D RCS mass at tPRZPC (Kg)	179	178	G	-
5E RCS Depress. Rate (MPa/s)	-0.016	-0.036	P	HSC
(Initial/Averaged on 500 s)	-0.0086	-0.013	S	-
5F Prim. Circulation Mode	INTERM	CONT.	P	C+U
5G SG1 Press. time, t_{SG1PR} (s)	6878	4920	P	HSC
($dt_{SG1PR} = t_{SG1PR} - t_4$)	(346)	(220)	S	-
5H PRZ Role	CORE FL.	?	-	-
5I PRZ emptying time, t_{PRZE} (s)	6811	4798	P	5C
($dt_{PRZE} = t_{PRZE} - t_4$)	(280)	(98)	P	5E
5J Core Reflood Mode	TOP-DOWN	BOTTOM-UP	P	(C+U)?
5K End of Transient time, t_{END}	8062	5785	P	4G

* ACCURACY EVALUATION : G=GOOD, S=SUFFICIENT, P=POOR

** REASON FOR DISCREPANCY : C=CODE, U=USER, LHUR=LOW HEAT UP RATE, HSM=HEAT STRUCTURES MODELLING, HSC=HIGH SECONDARY COOLING, LDP=LIQUID DISCHARGE FROM PRZ

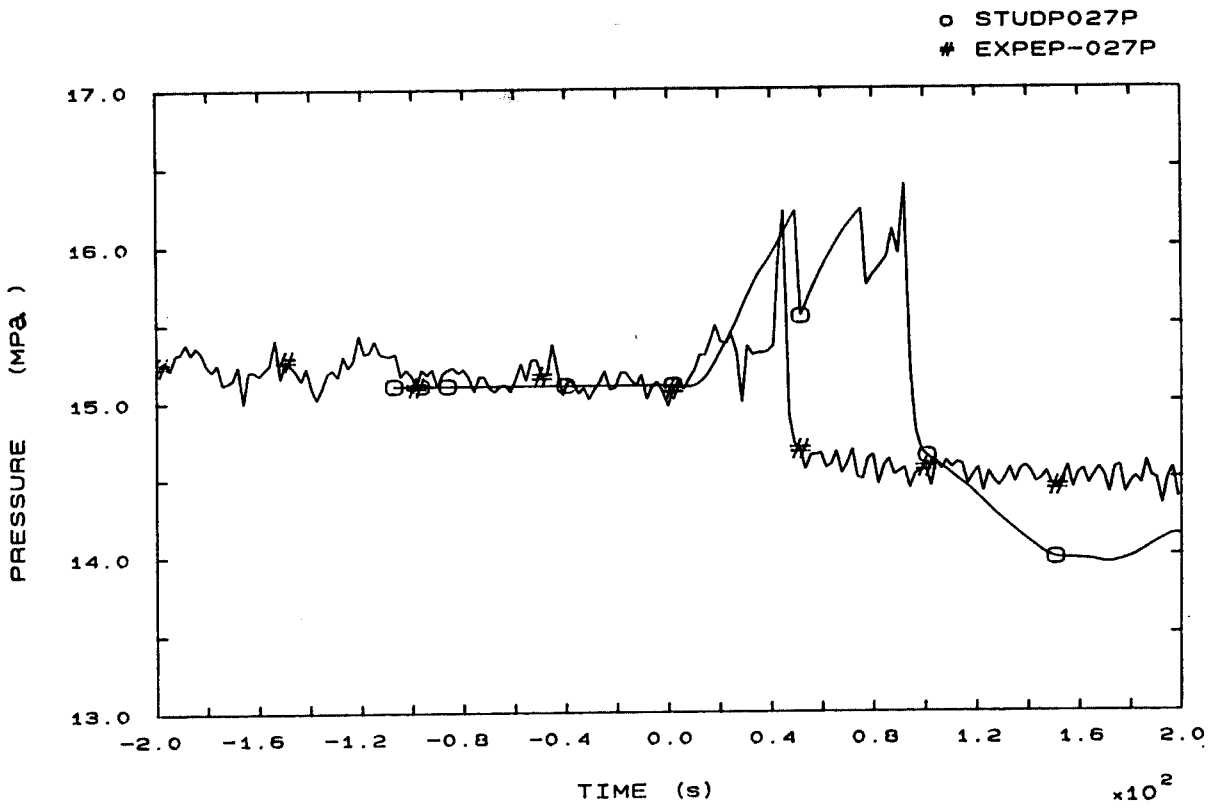

FIG. 1b PRESSURIZER PRESSURE

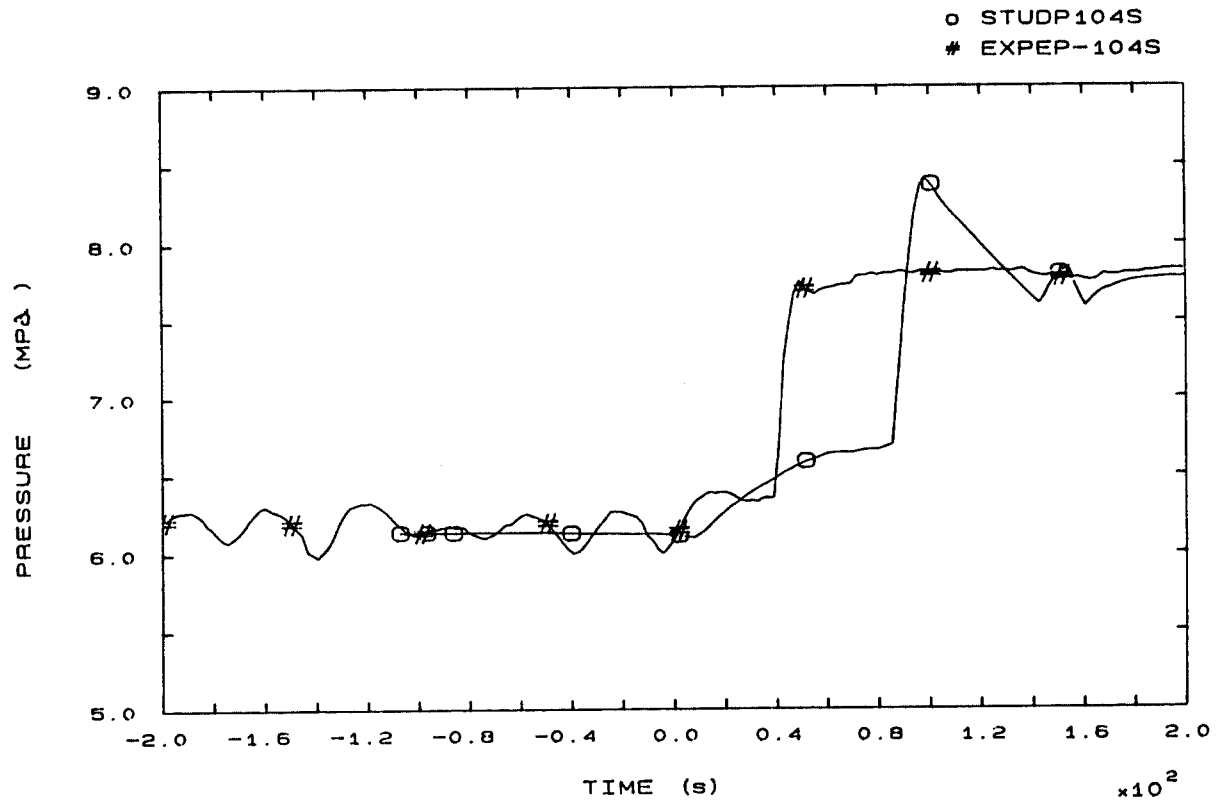

FIG. 3b SG1 STEAM DOME PRESSURE

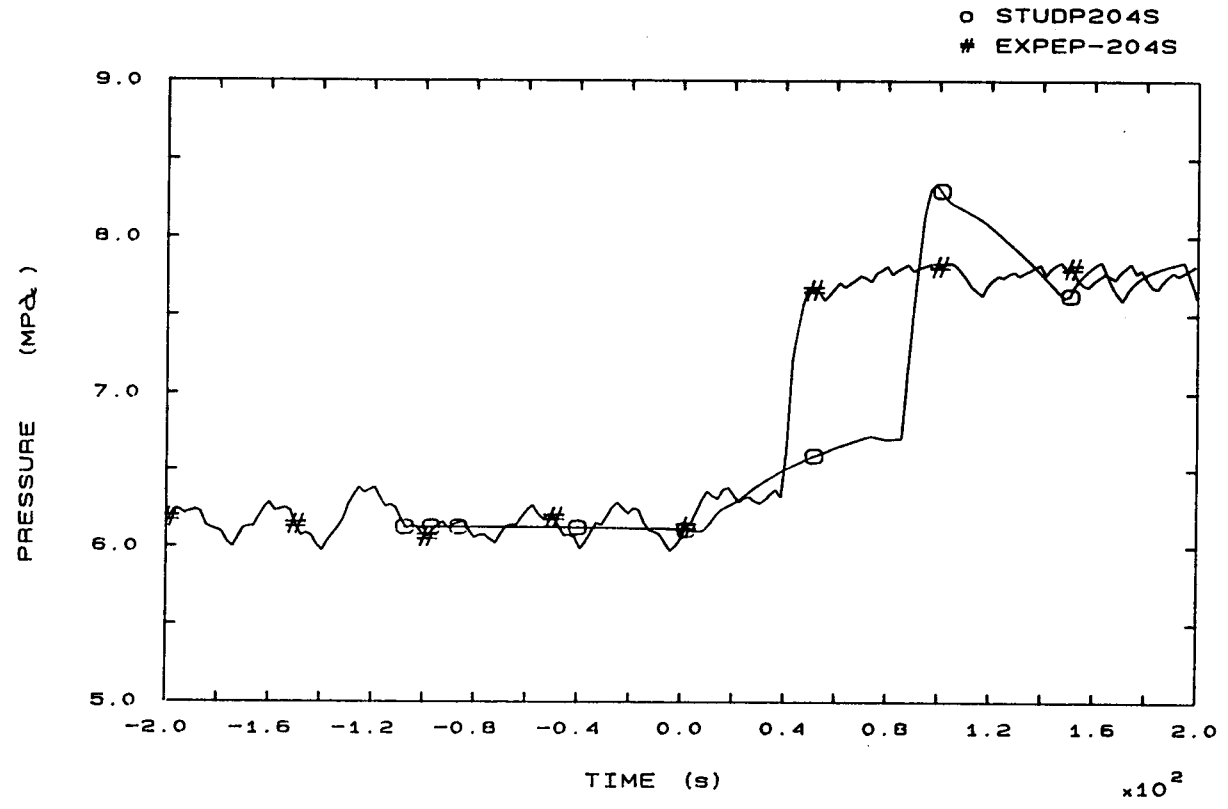

FIG. 4b SG2 STEAM DOME PRESSURE

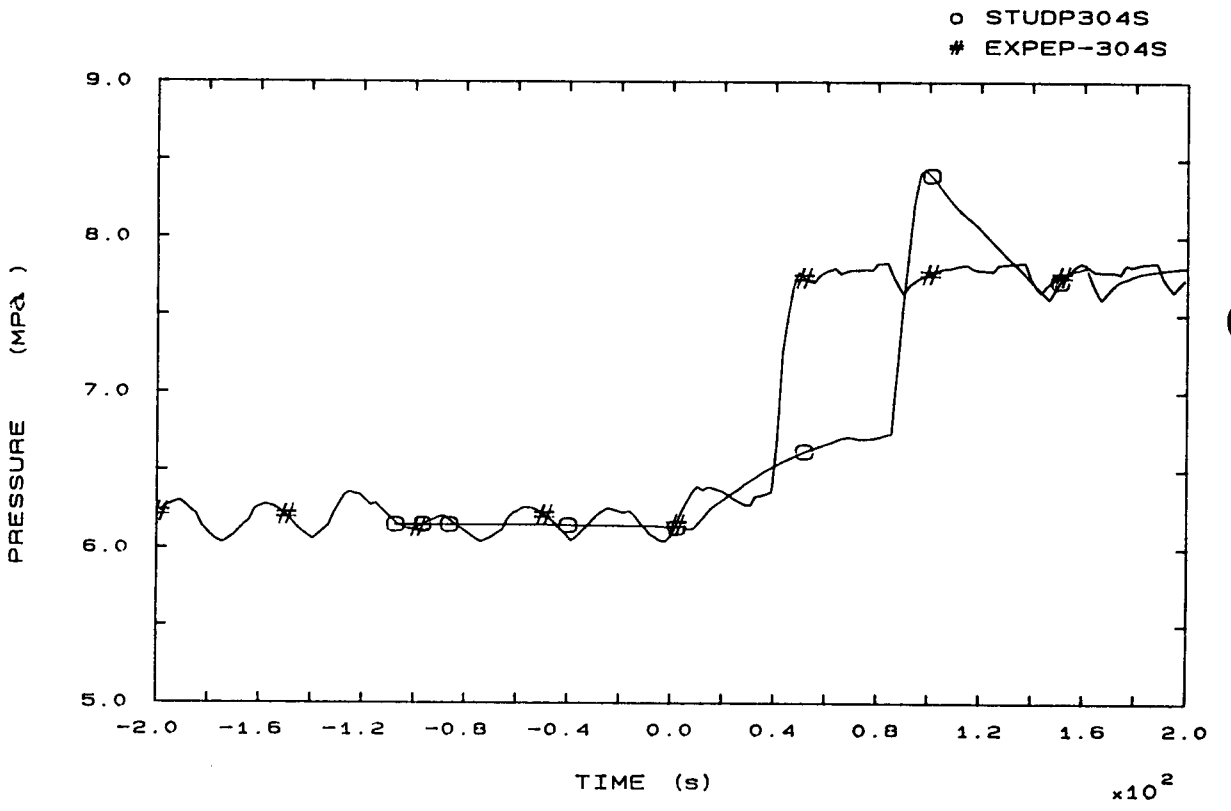

FIG. 5b SG3 STEAM DOME PRESSURE

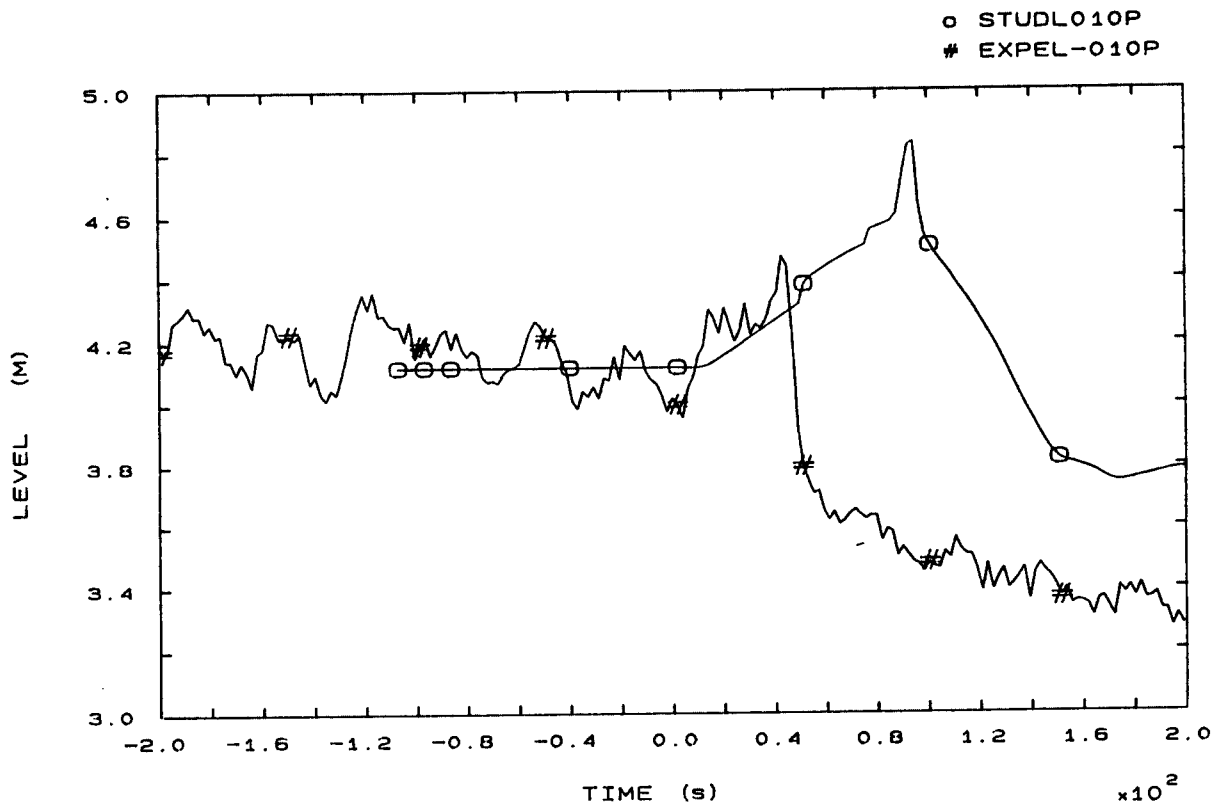

FIG. 6b PRESSURIZER LEVEL

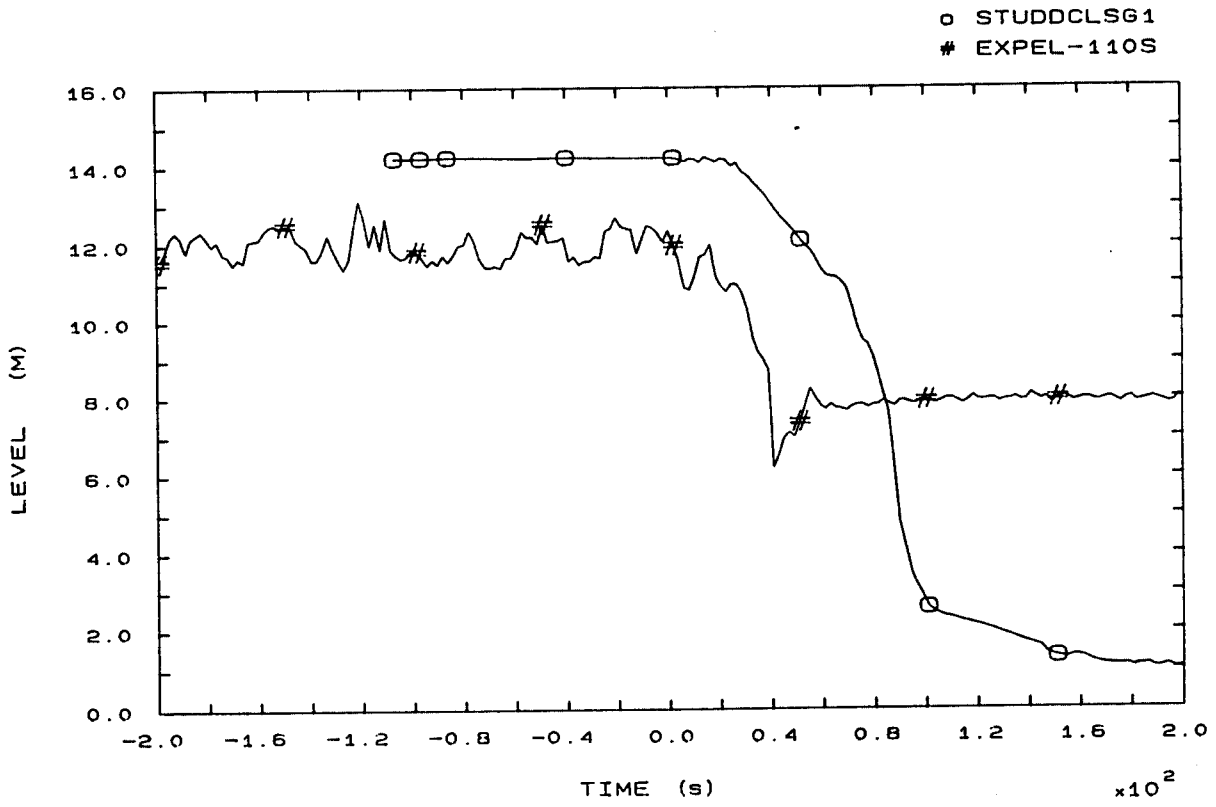

FIG. 7b SG1 DOWNCOMER LEVEL

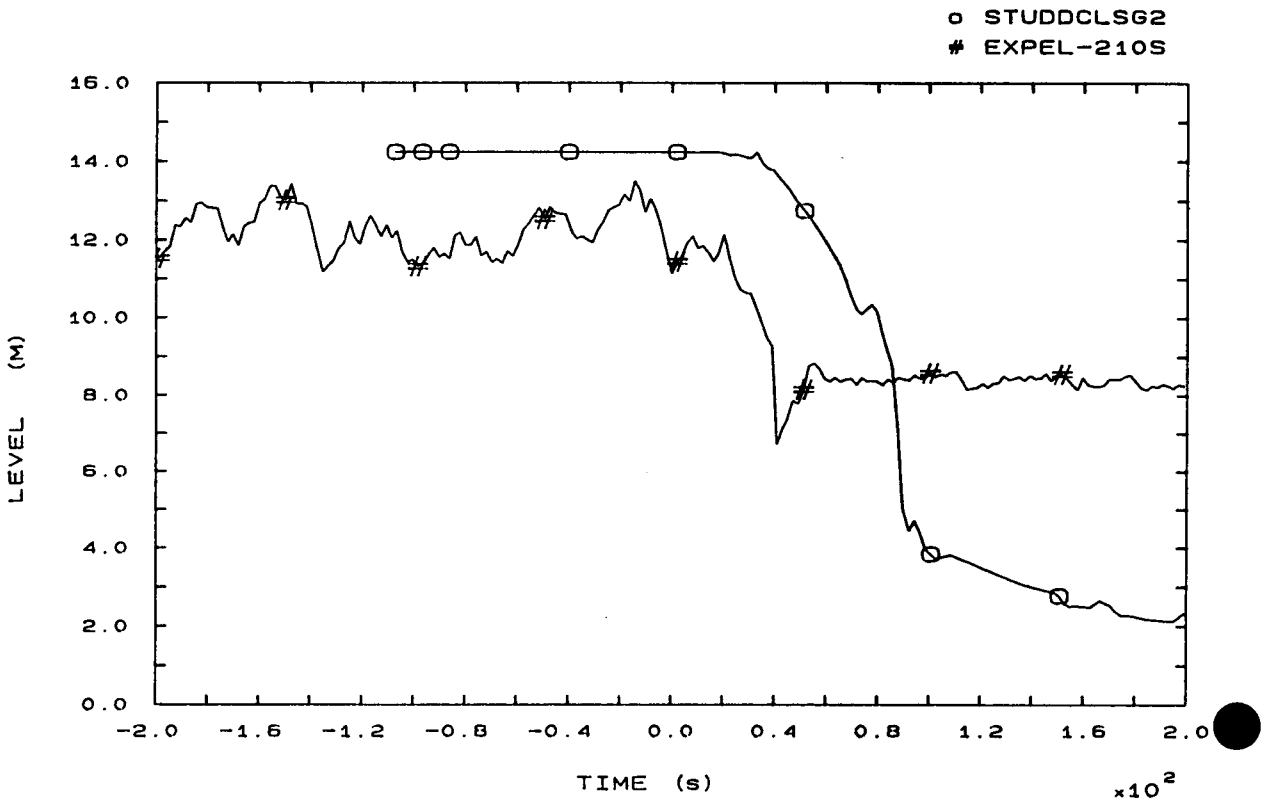

FIG. 8b SG2 DOWNCOMER LEVEL

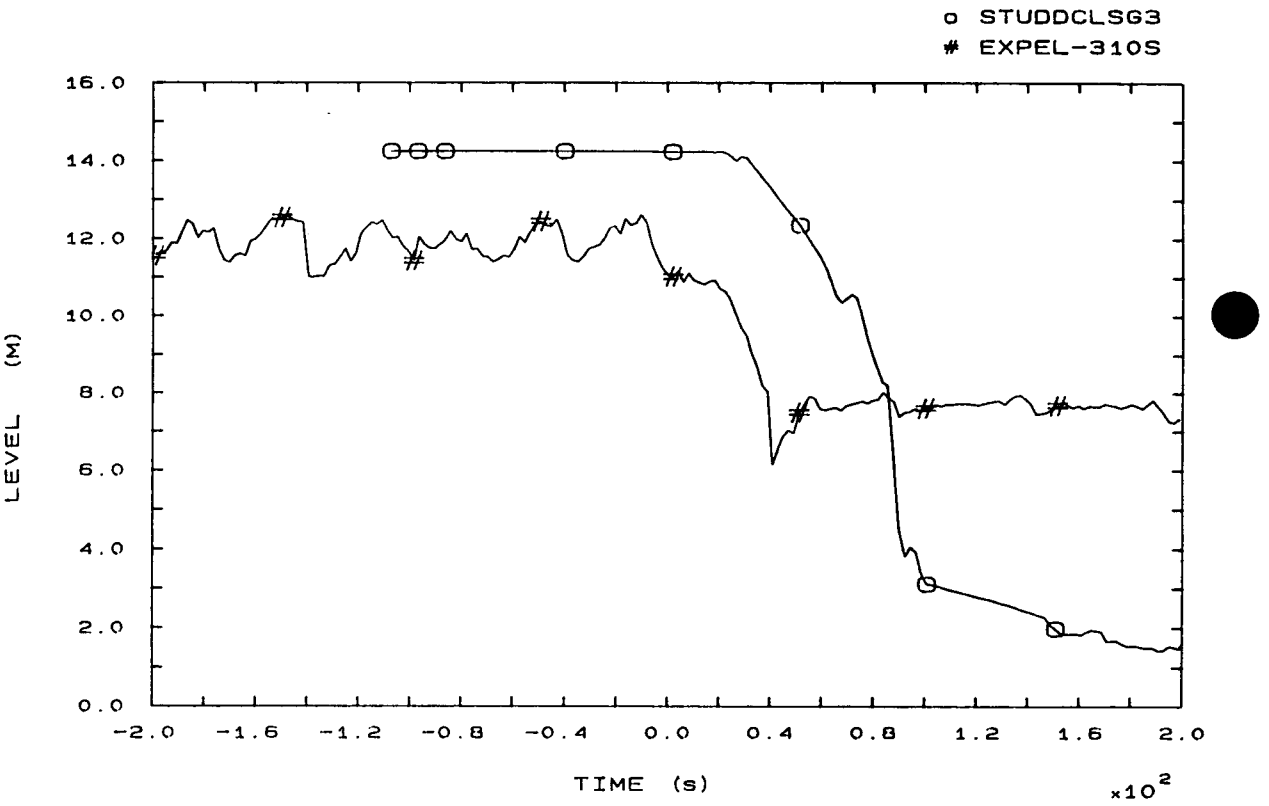

FIG. 9b SG3 DOWNCOMER LEVEL

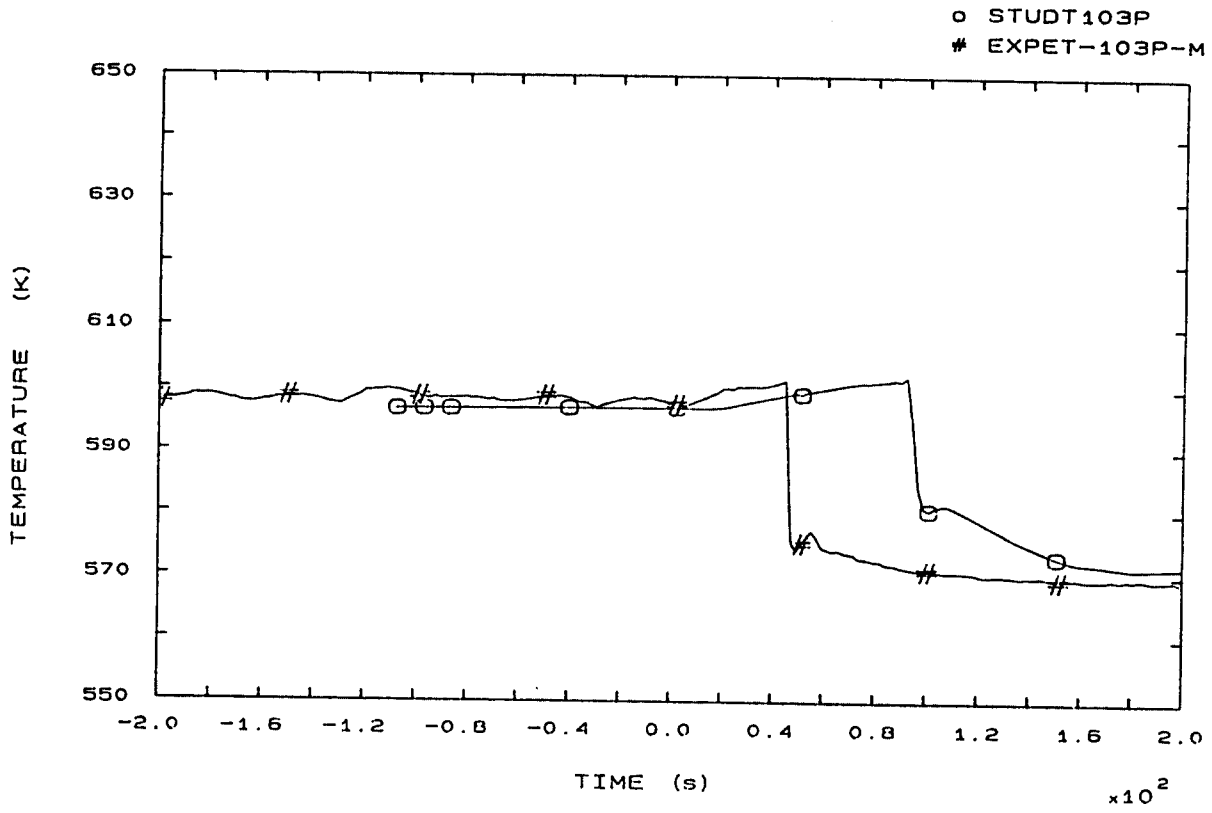

FIG. 12b LP1 HOT LEG OUTLET VESSEL TEMPERATURE

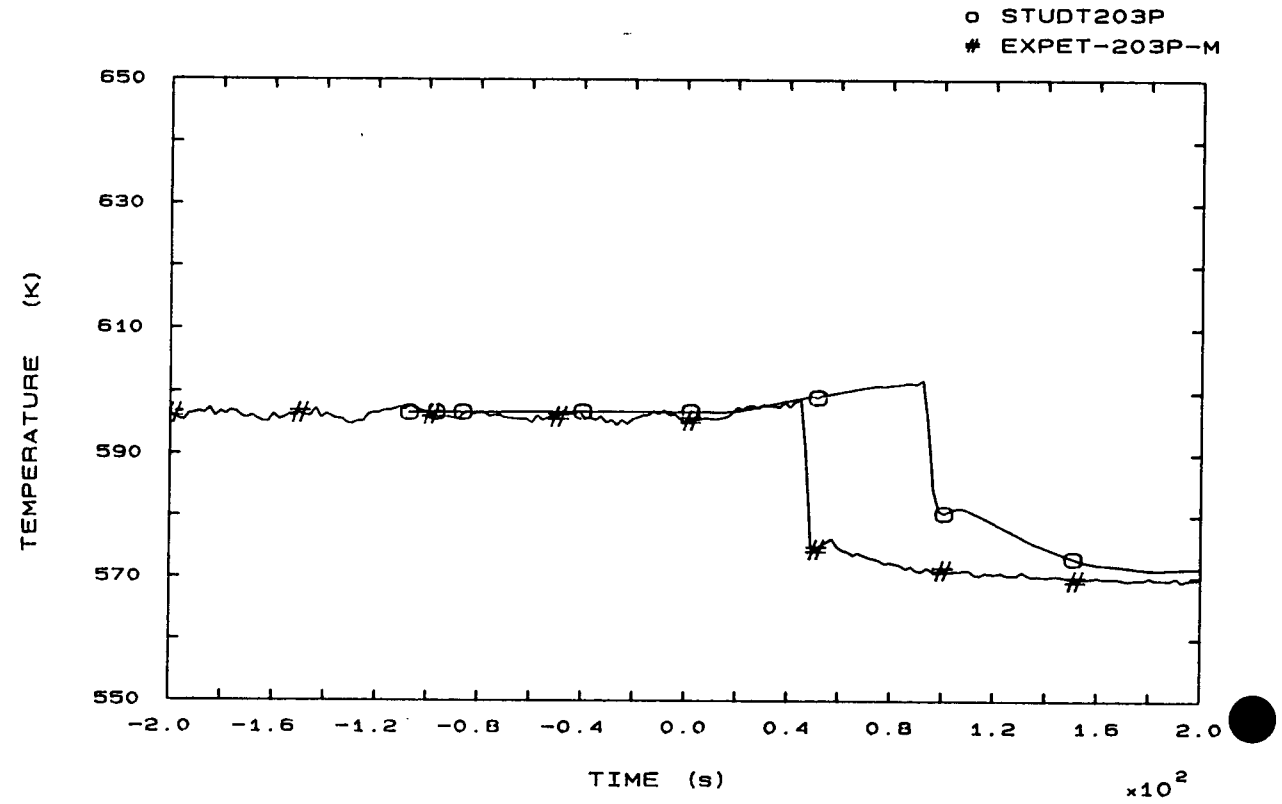

FIG. 22b LP2 HOT LEG OUTLET VESSEL TEMPERATURE

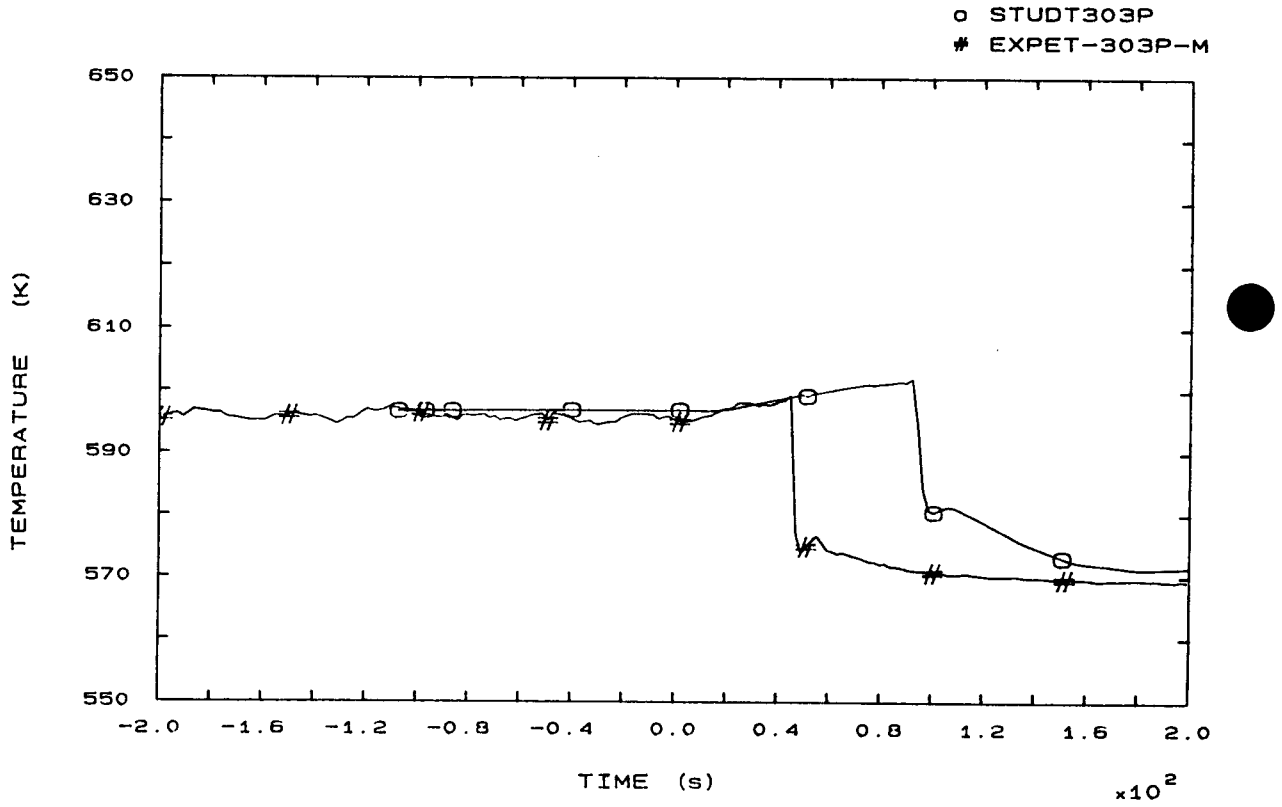

FIG. 32b LP3 HOT LEG OUTLET VESSEL TEMPERATURE

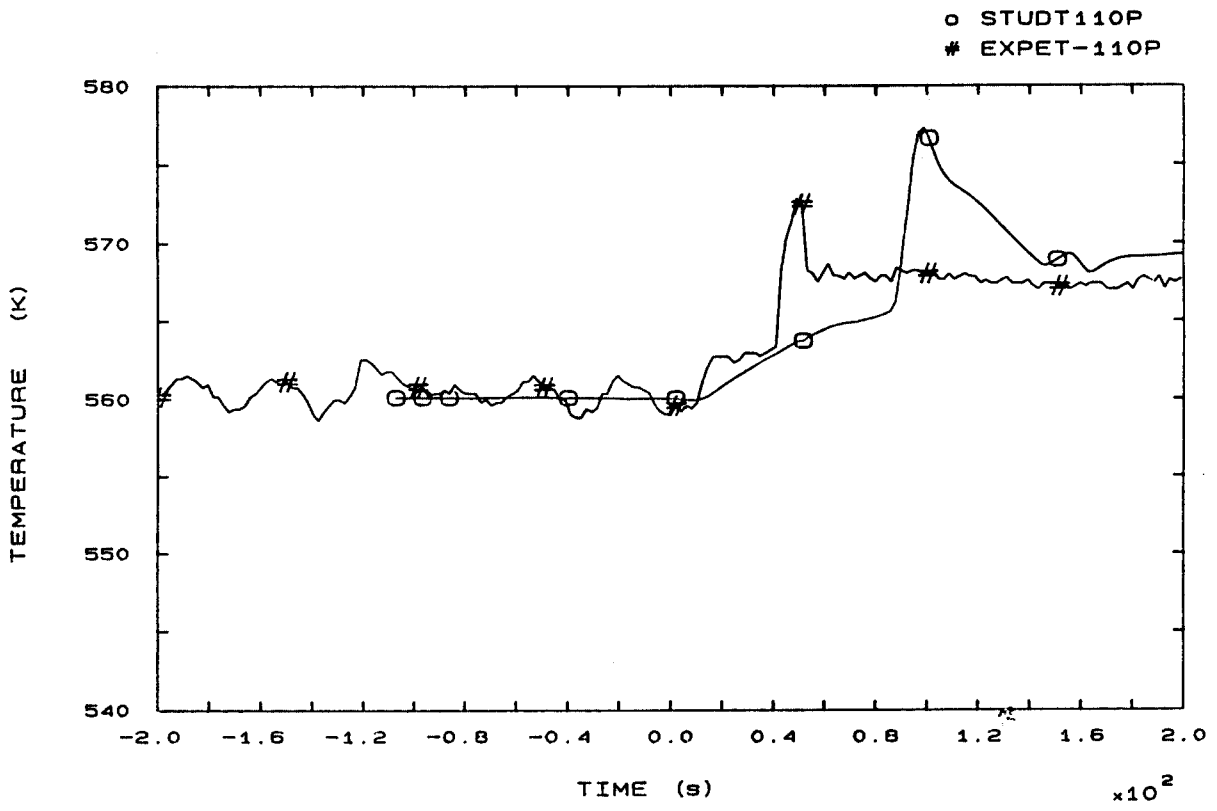

FIG. 42b SG1 OUTLET TEMPERATURE

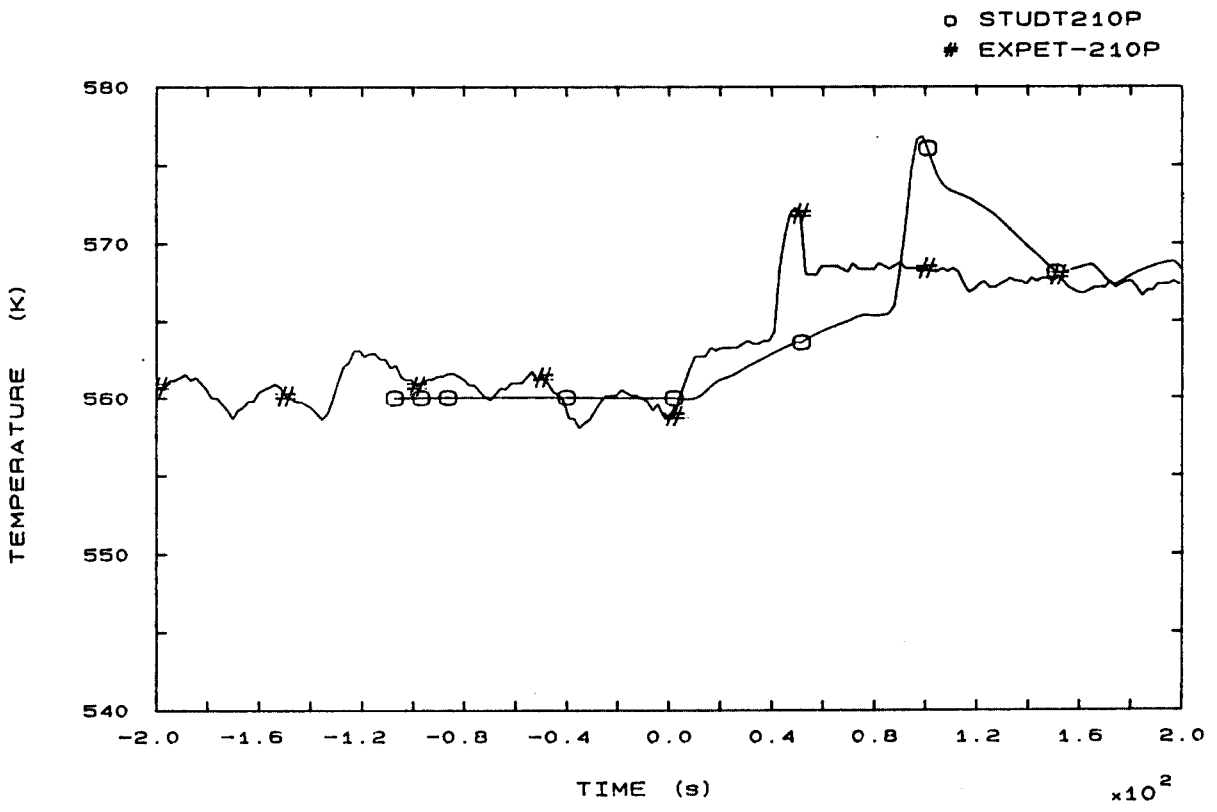

FIG. 44b SG2 OUTLET TEMPERATURE

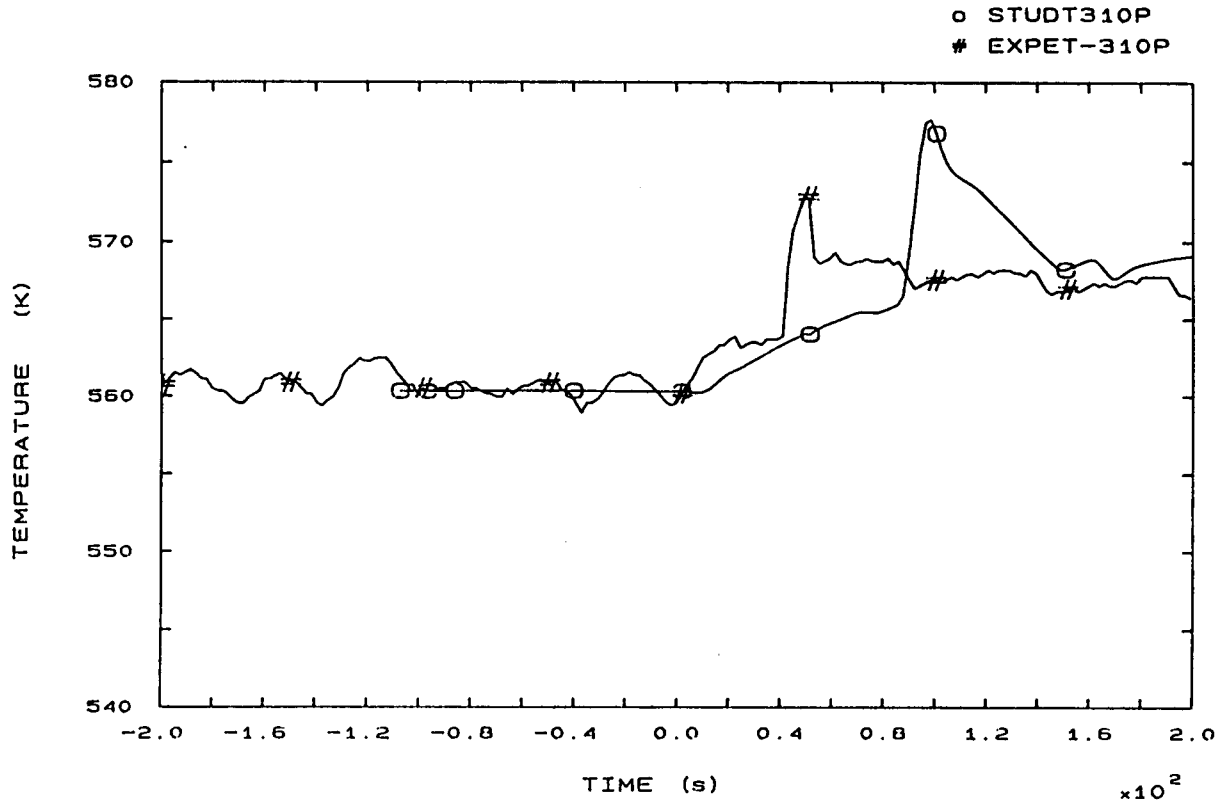

FIG. 46b SG3 OUTLET TEMPERATURE

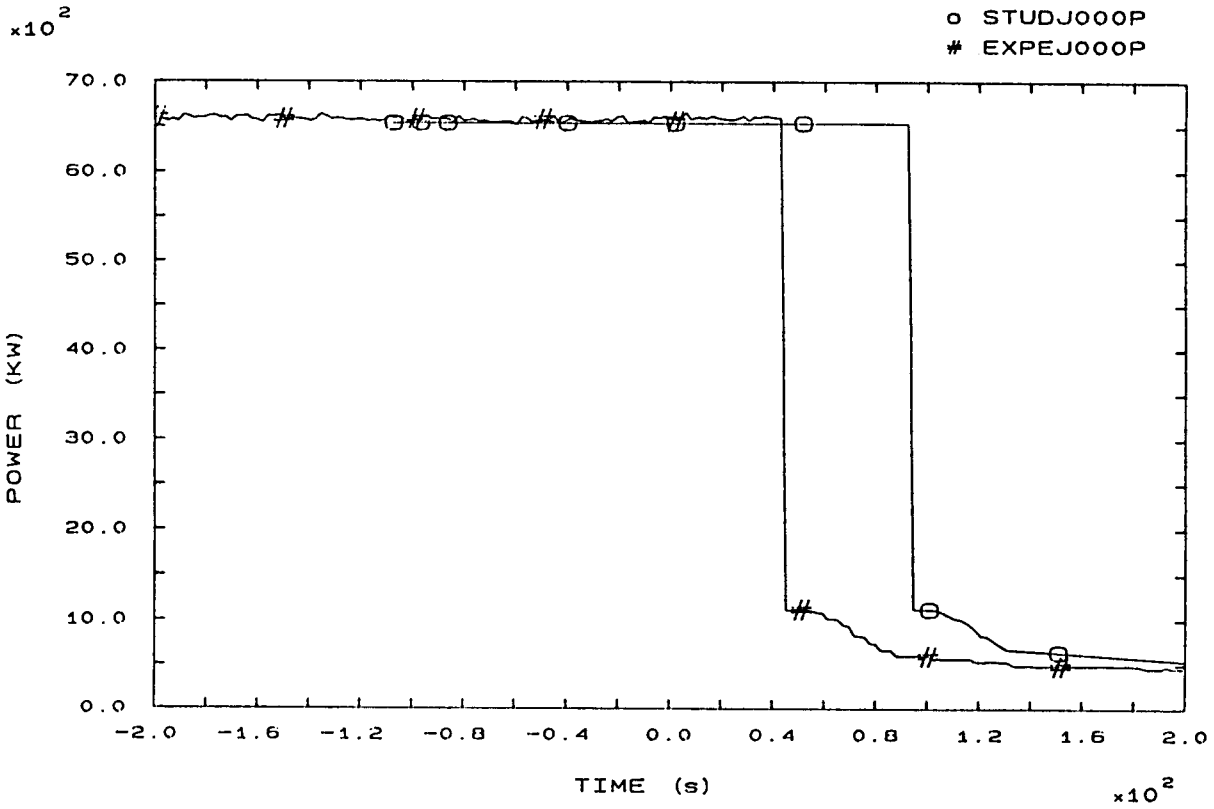

FIG. 81b HEATER RODS POWER

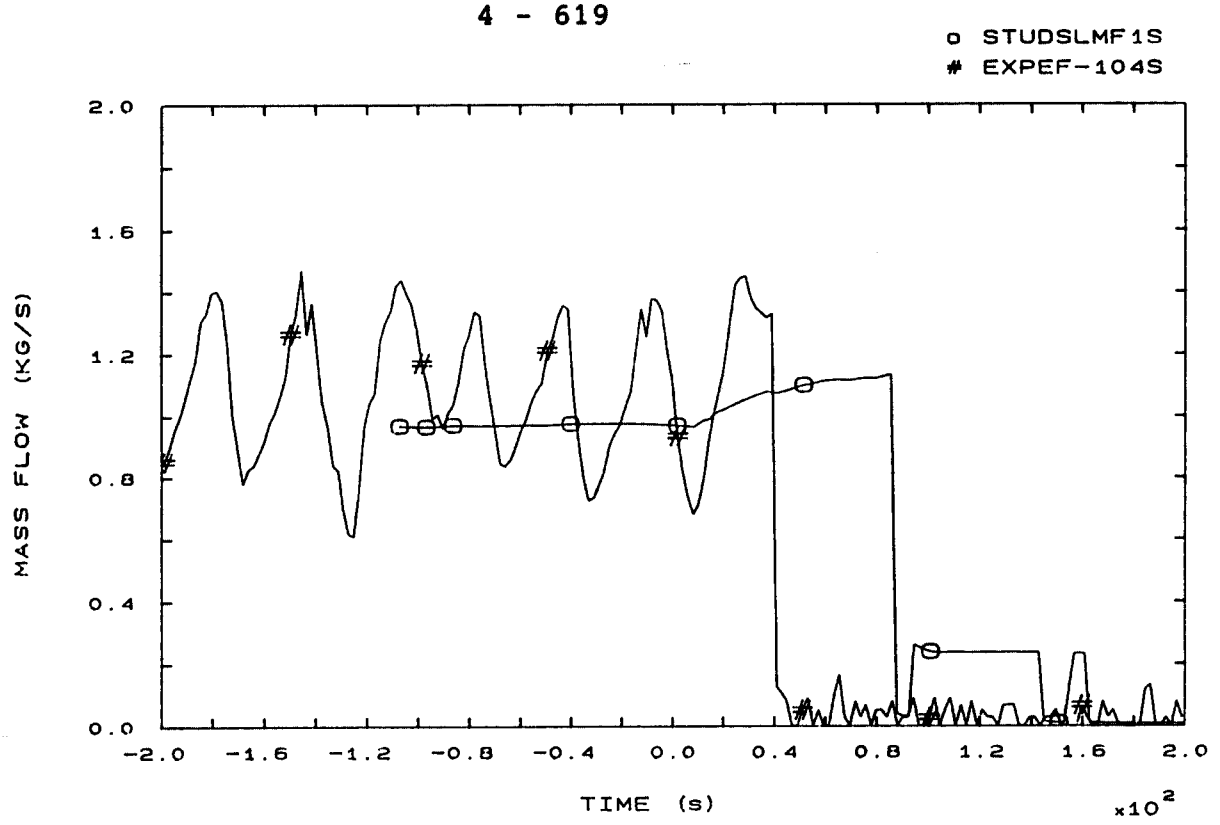

FIG. 96b STEAM LINE 1 MASS FLOW

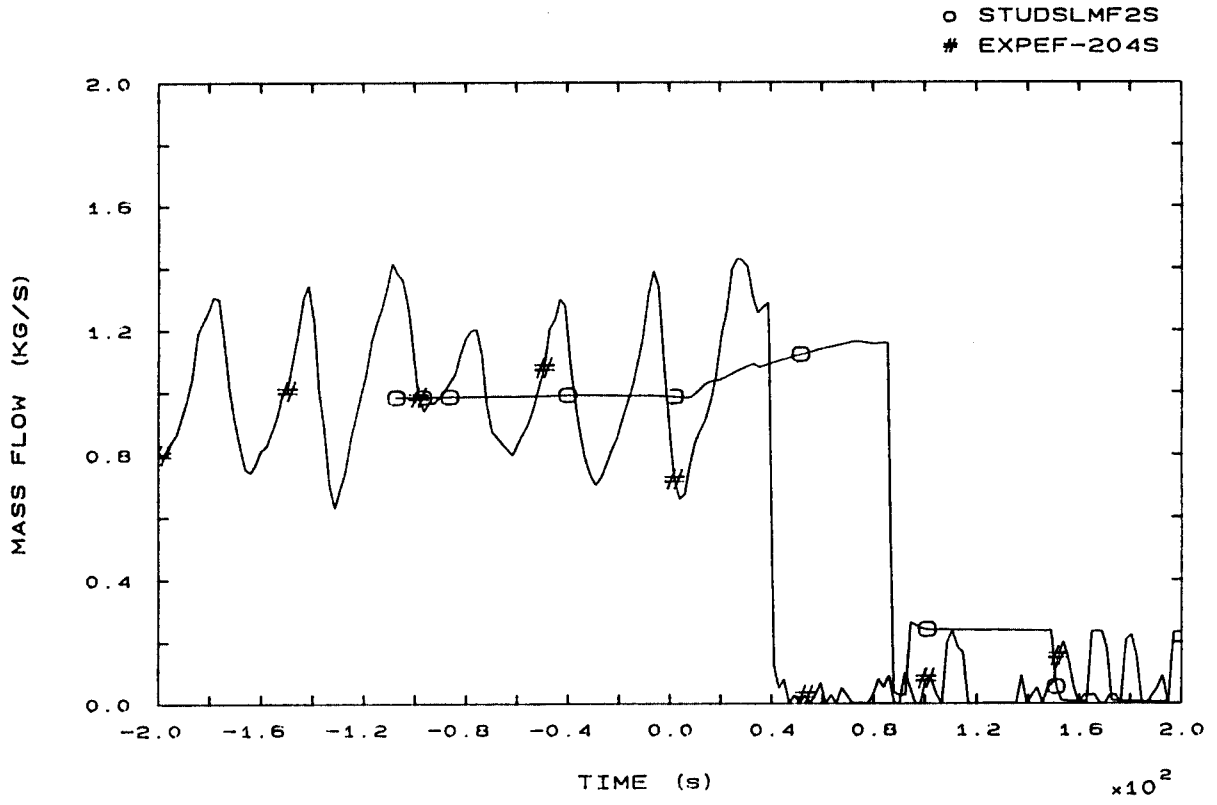

FIG. 97b STEAM LINE 2 MASS FLOW

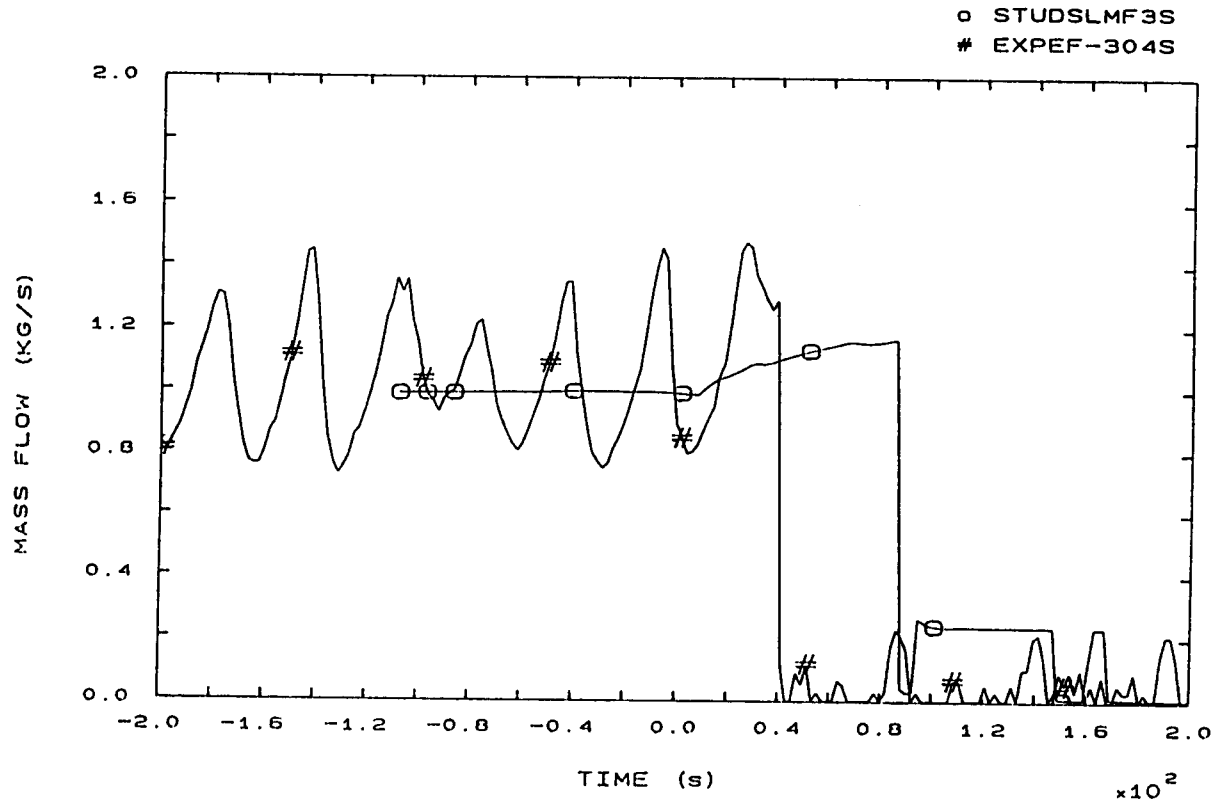

FIG. 98b STEAM LINE 3 MASS FLOW

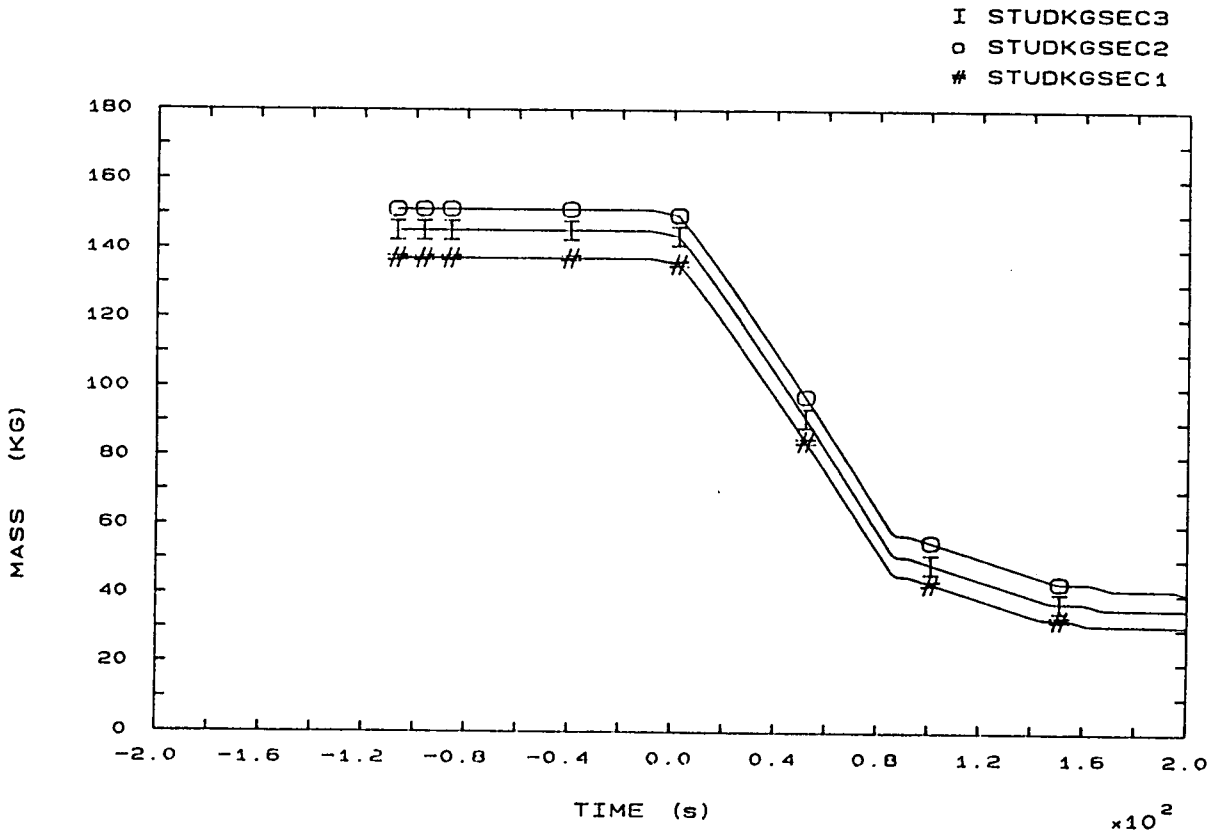

FIG. 142b SECONDARY COOLANT TOTAL MASS IN SGs

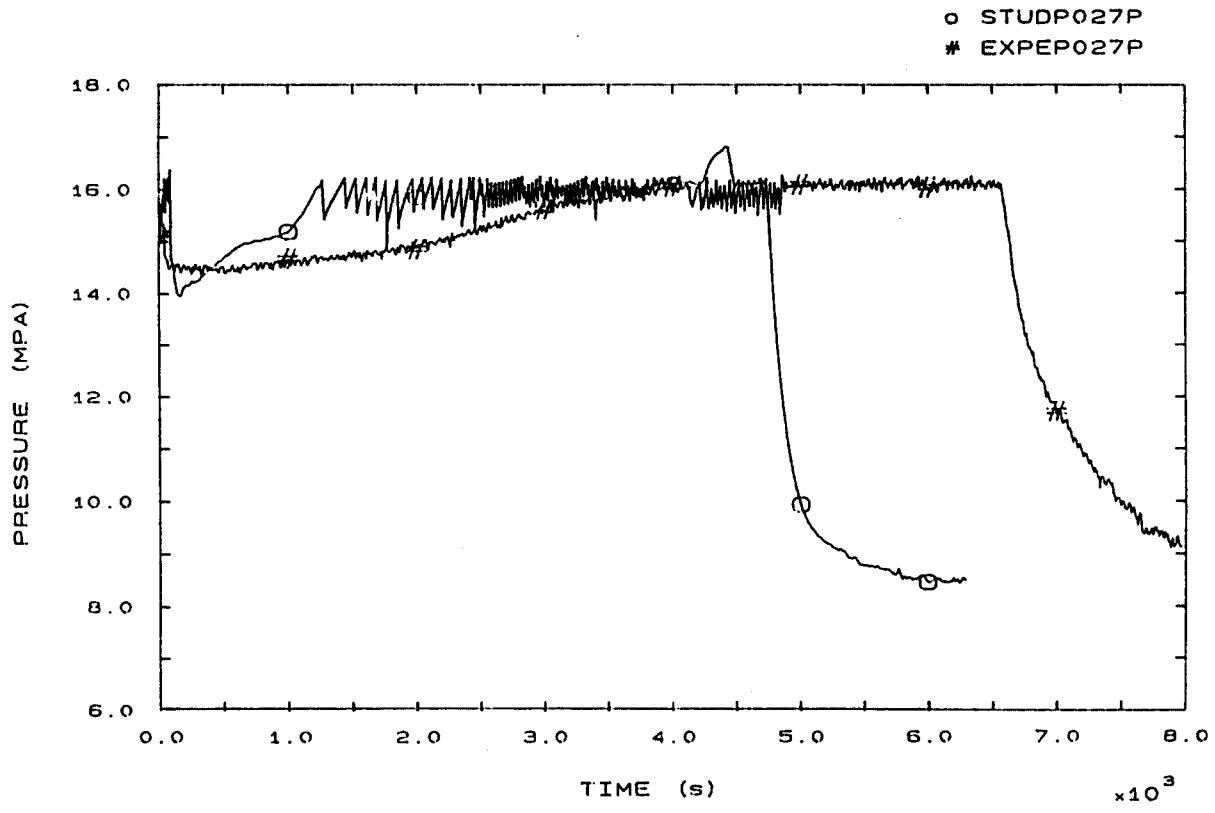

FIG. 1 PRESSURIZER PRESSURE

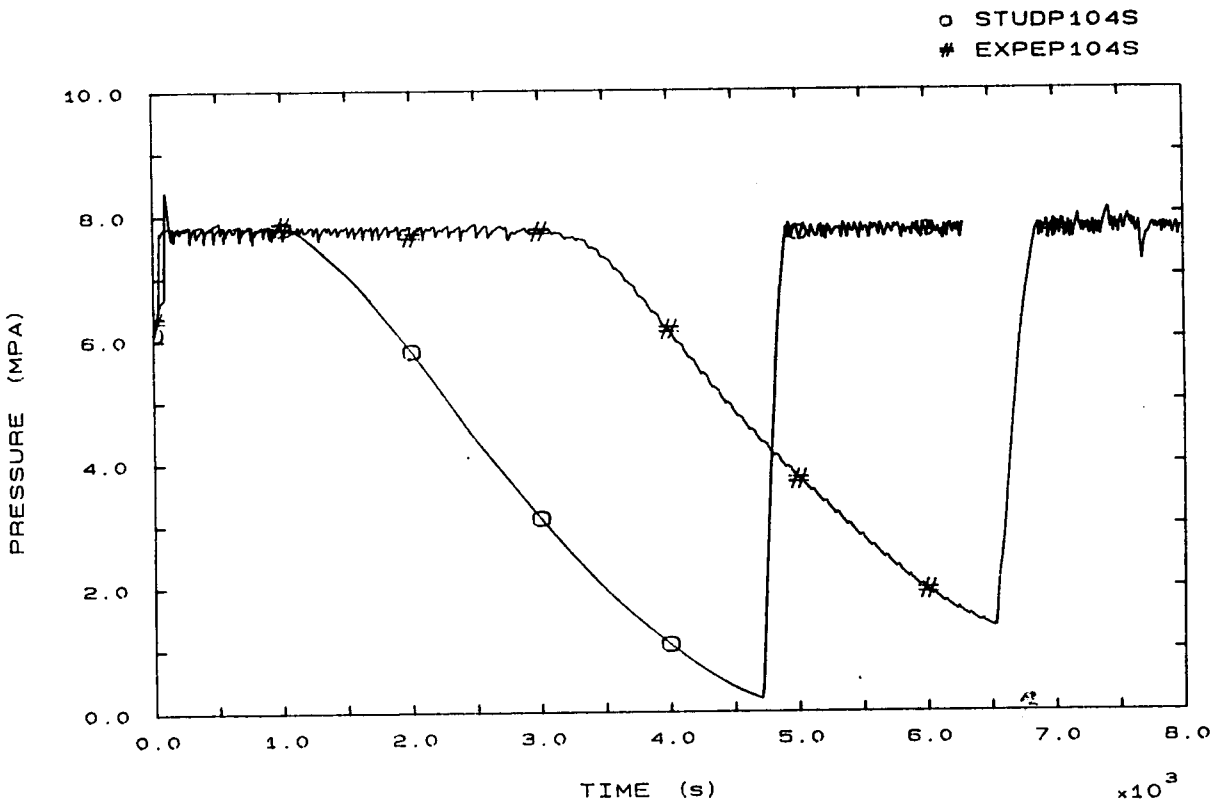

FIG. 3 SG1 STEAM DOME PRESSURE

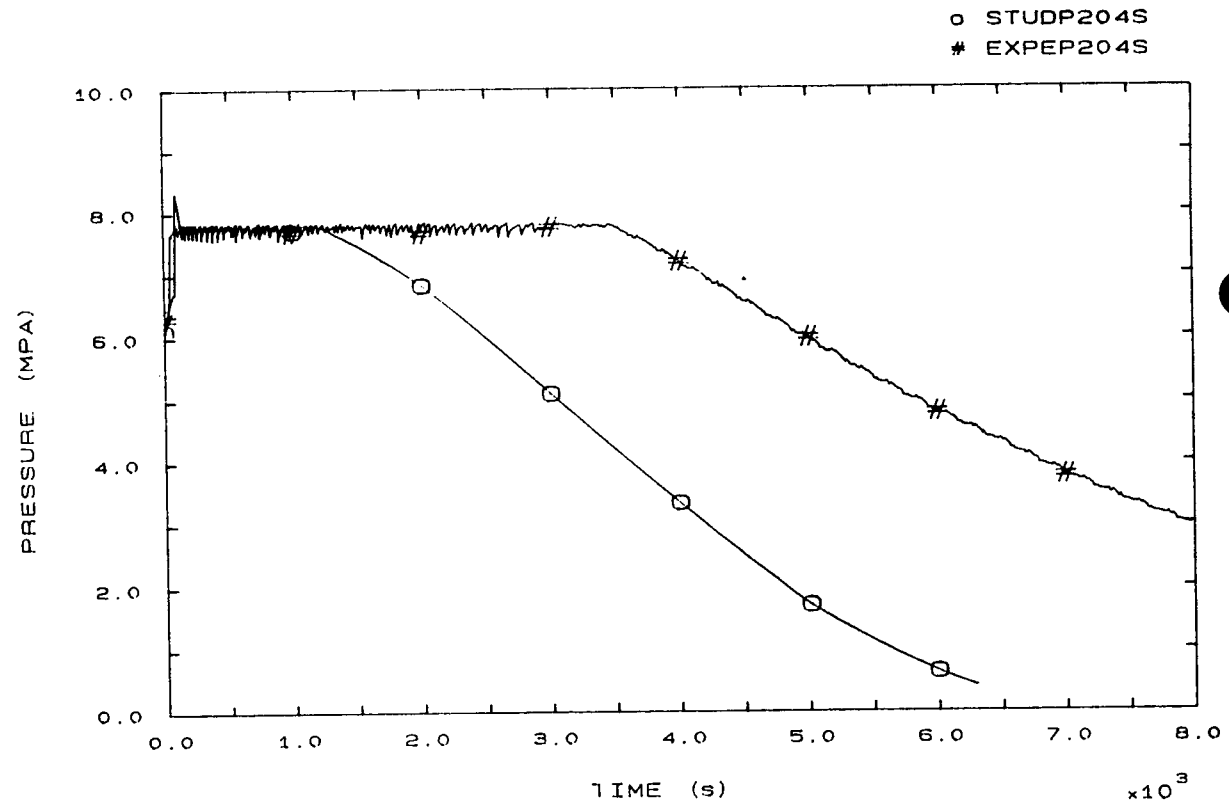

FIG. 4 SG2 STEAM DOME PRESSURE

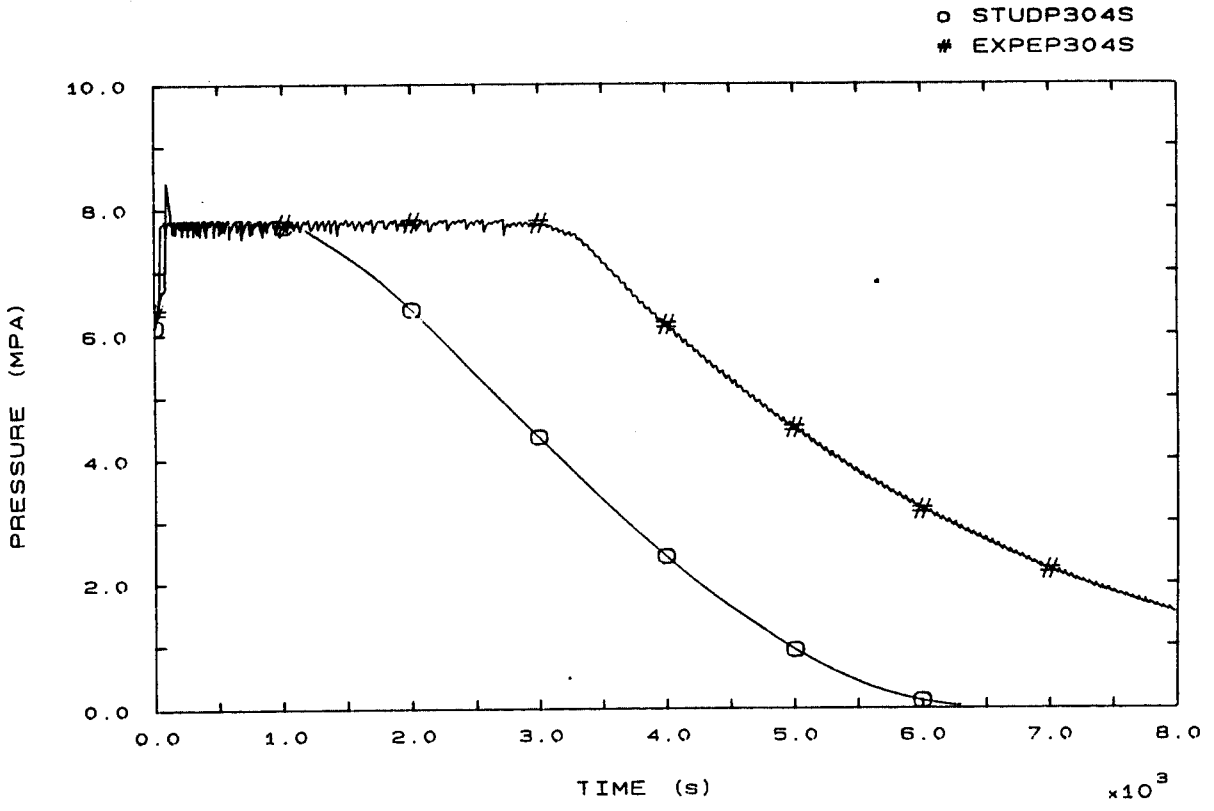

FIG. 5 SG3 STEAM DOME PRESSURE

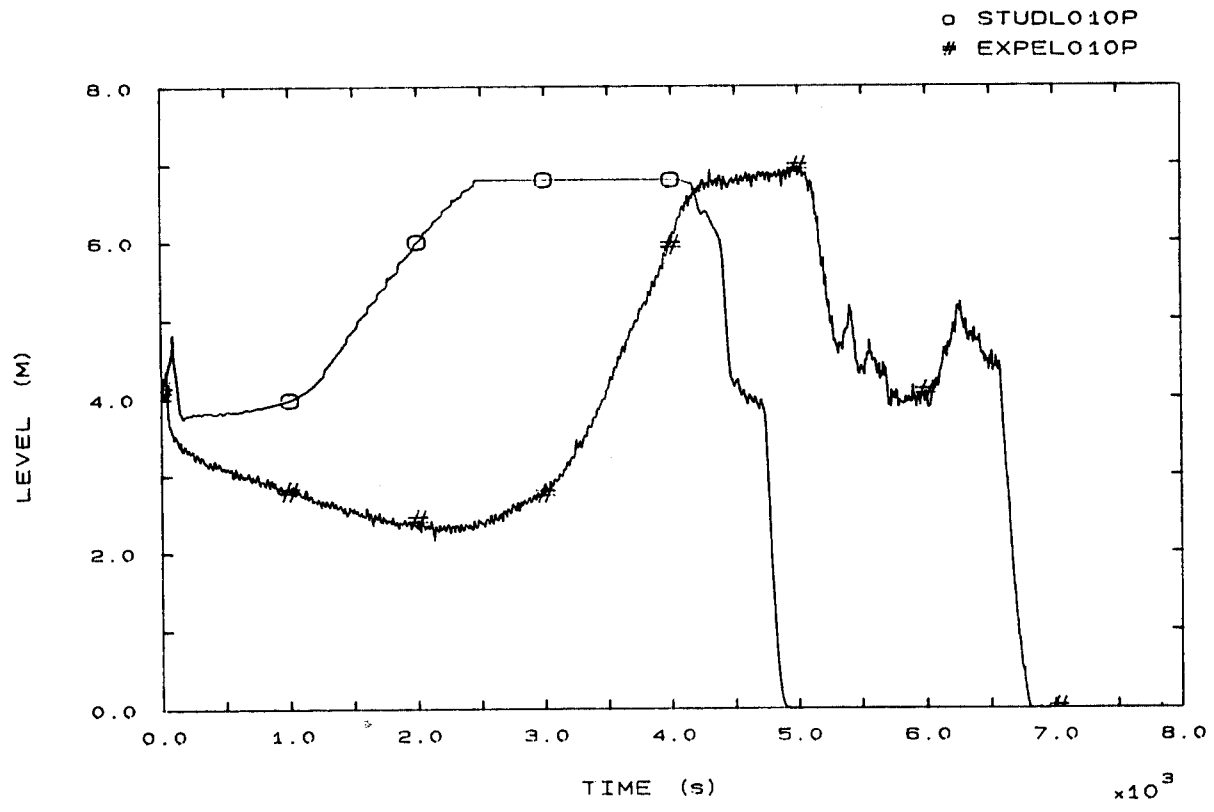

FIG. 6 PRESSURIZER LEVEL

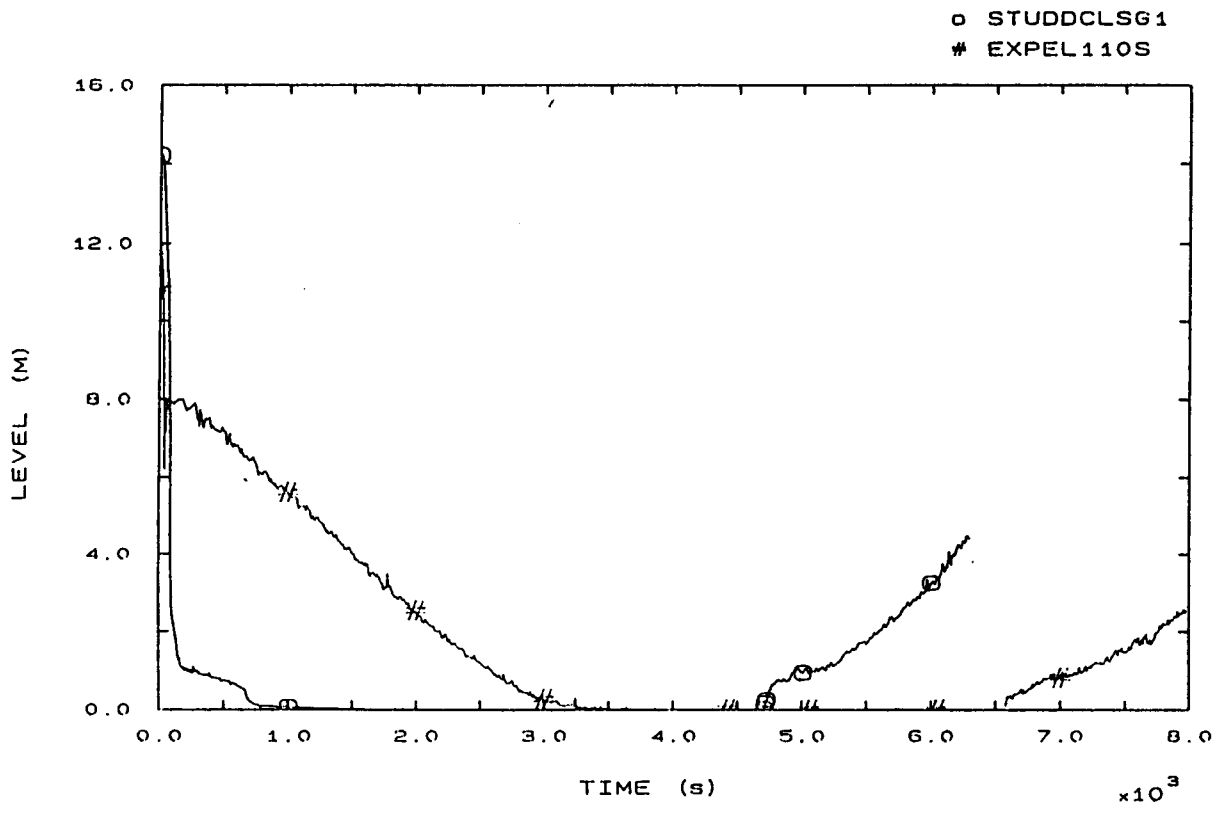

FIG. 7 SG1 DOWNCOMER LEVEL

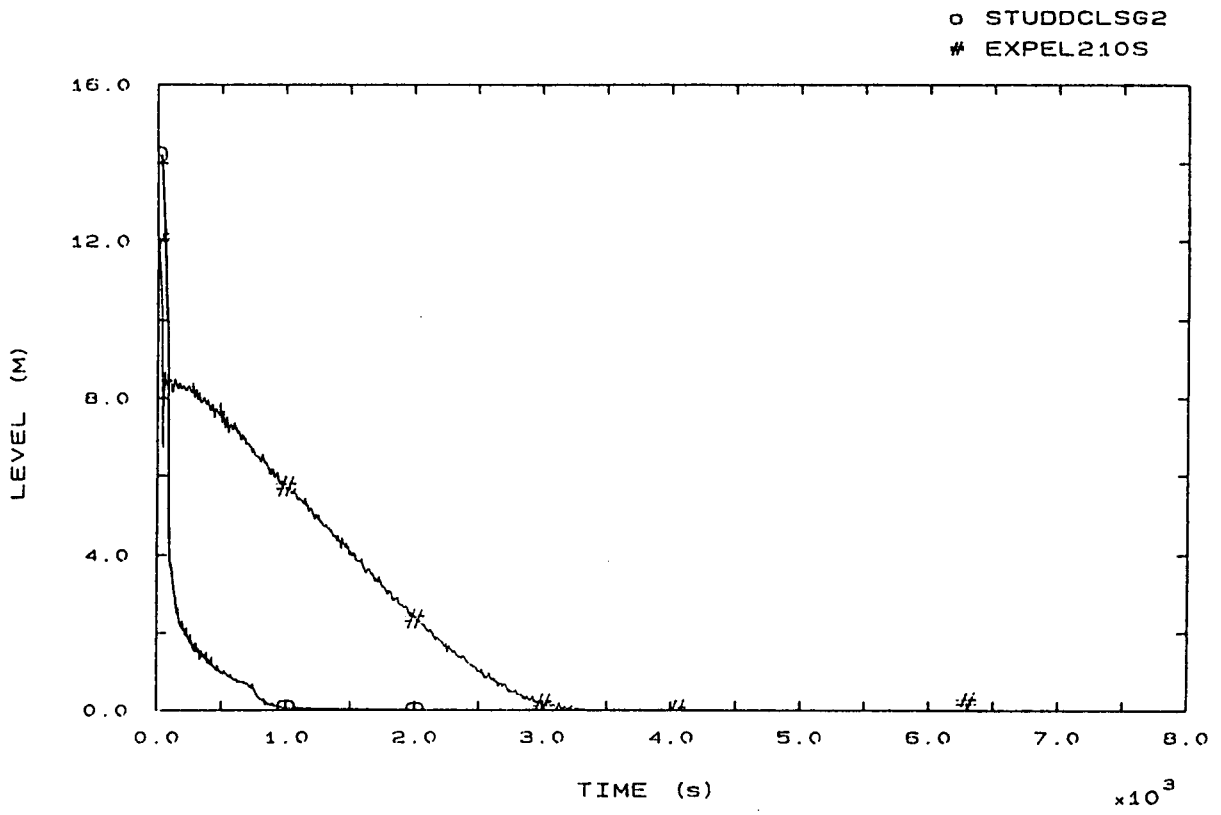

FIG. 8 SG2 DOWNCOMER LEVEL

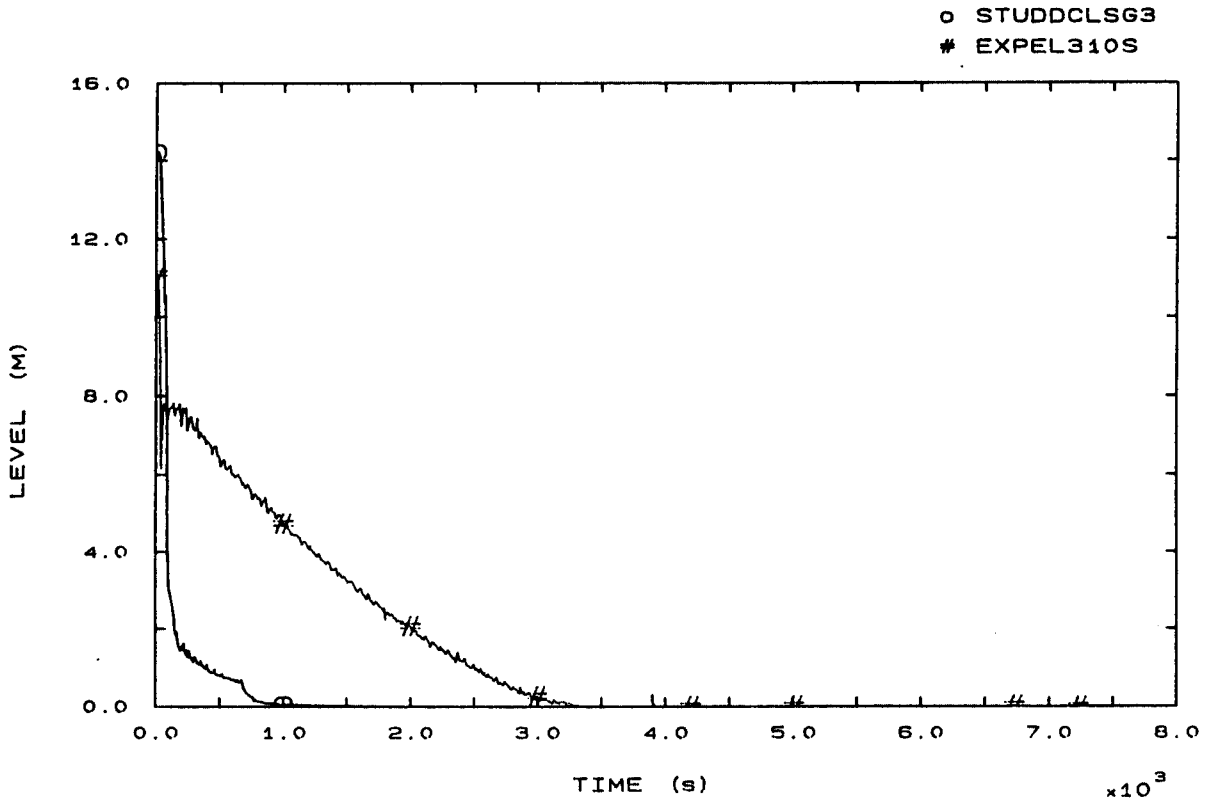

FIG. 9 SG3 DOWNCOMER LEVEL

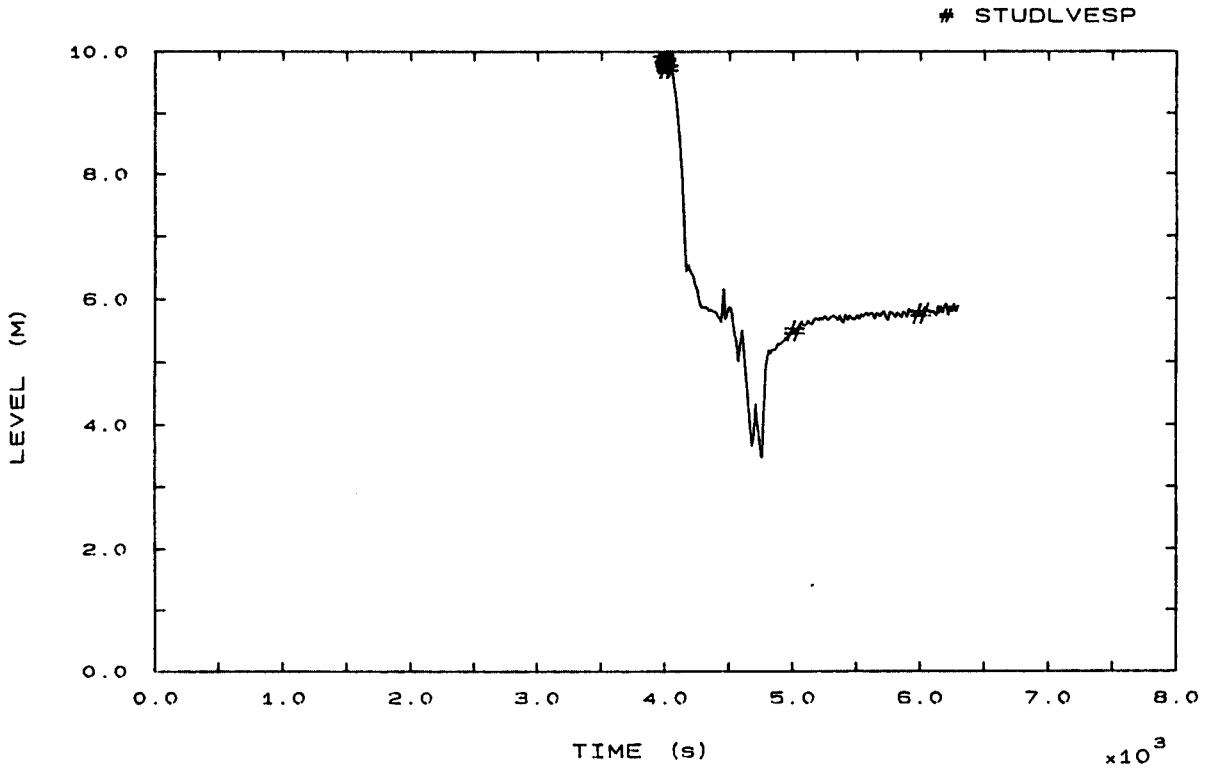

FIG. 10 VESSEL LEVEL

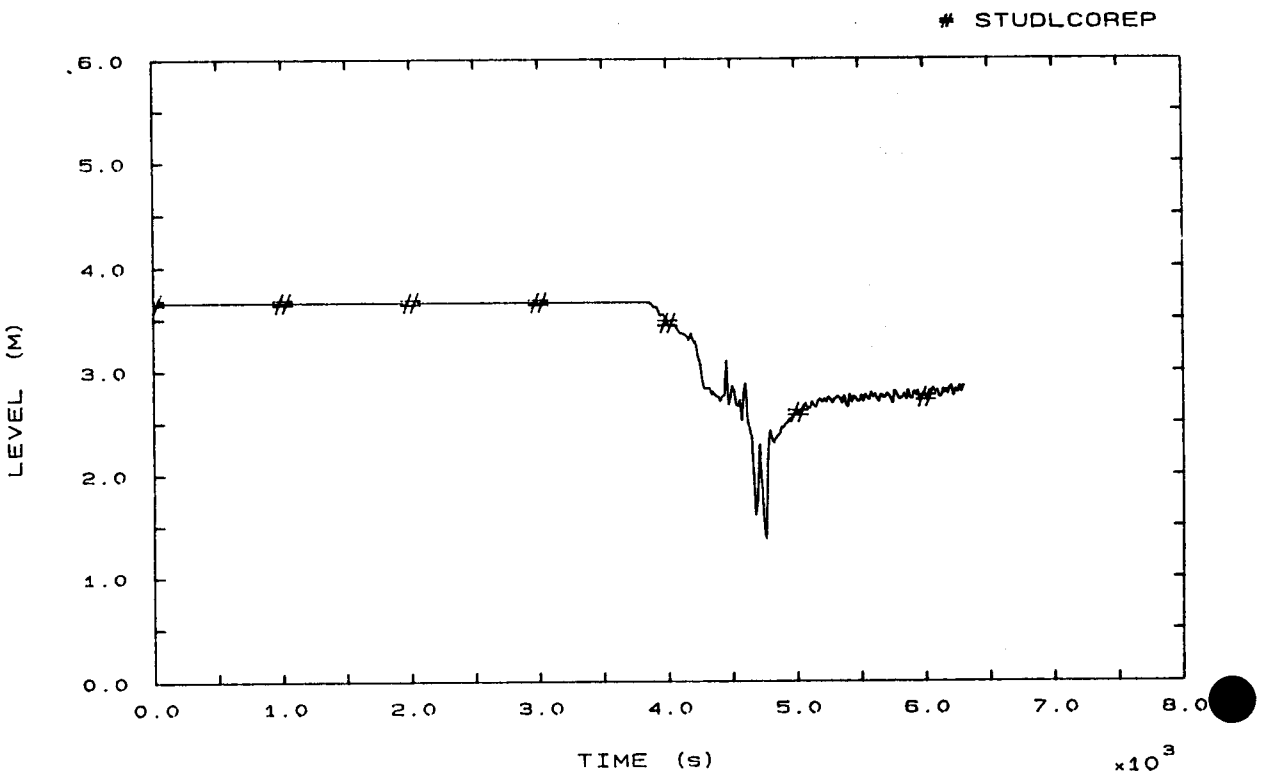

FIG. 11 CORE LEVEL

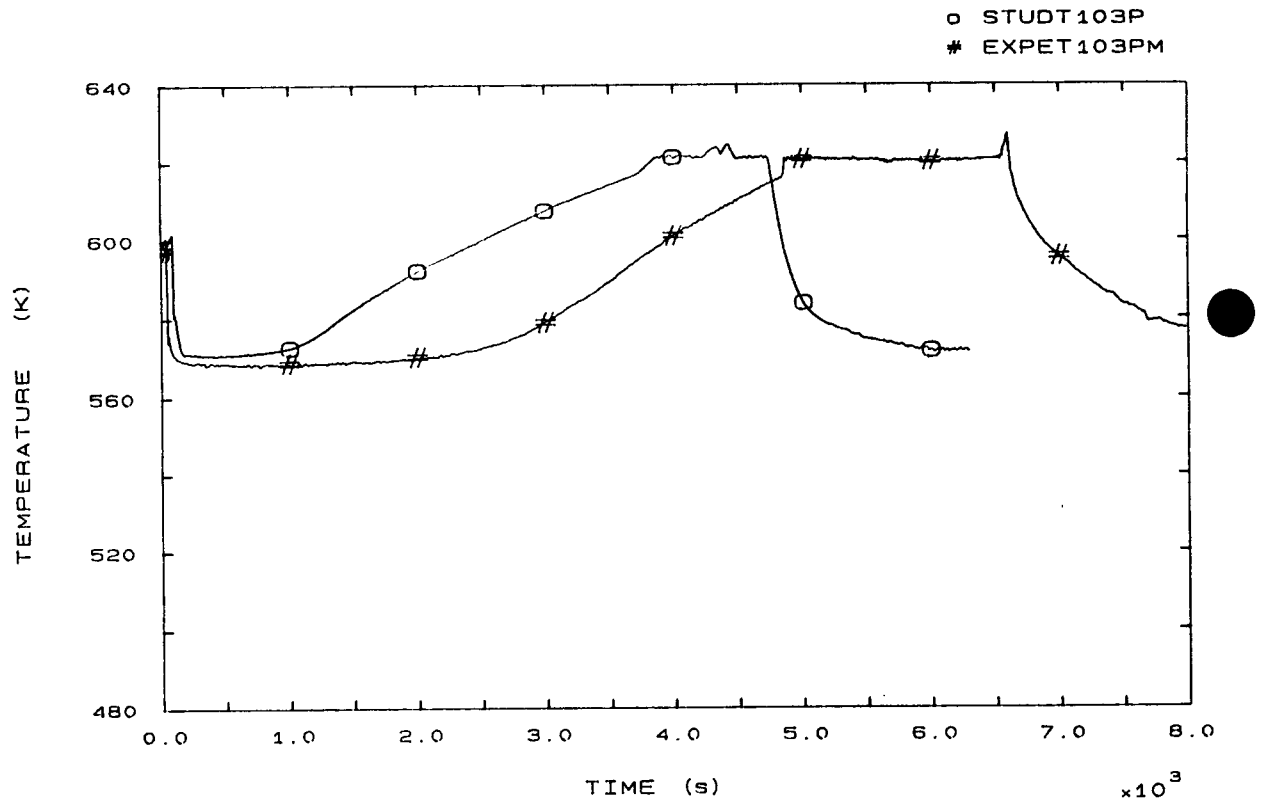

FIG. 12 LP1 HOT LEG OUTLET VESSEL TEMPERATURE

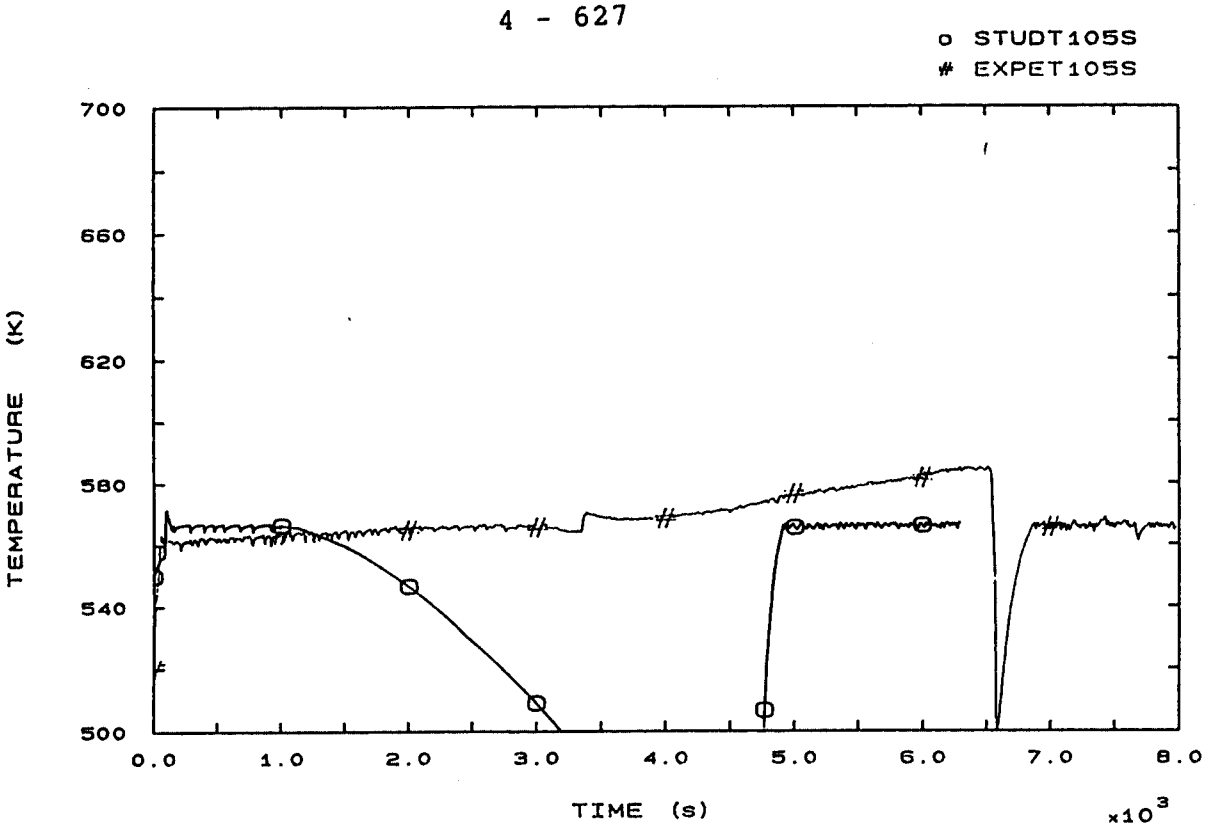

FIG. 15 FLUID TEMPERATURE SG1 RISER 185 MM A.T.S.

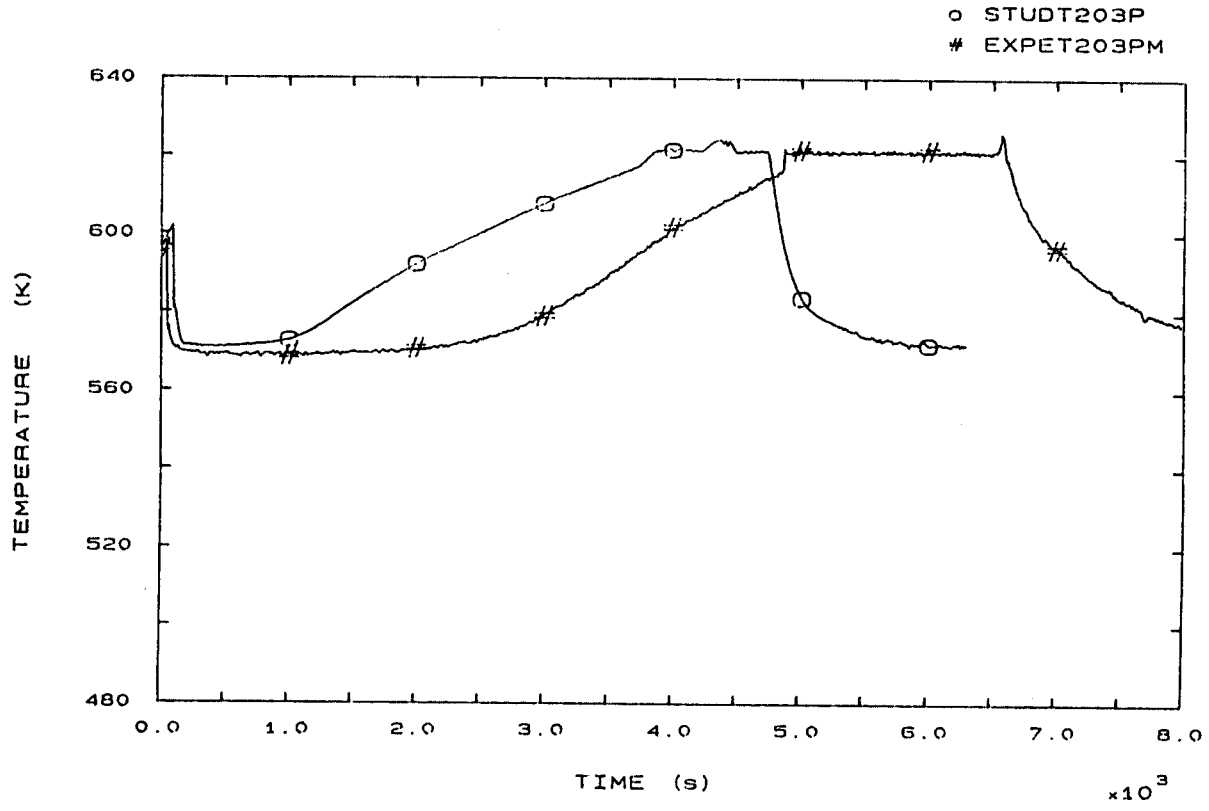

FIG. 22 LP2 HOT LEG OUTLET VESSEL TEMPERATURE

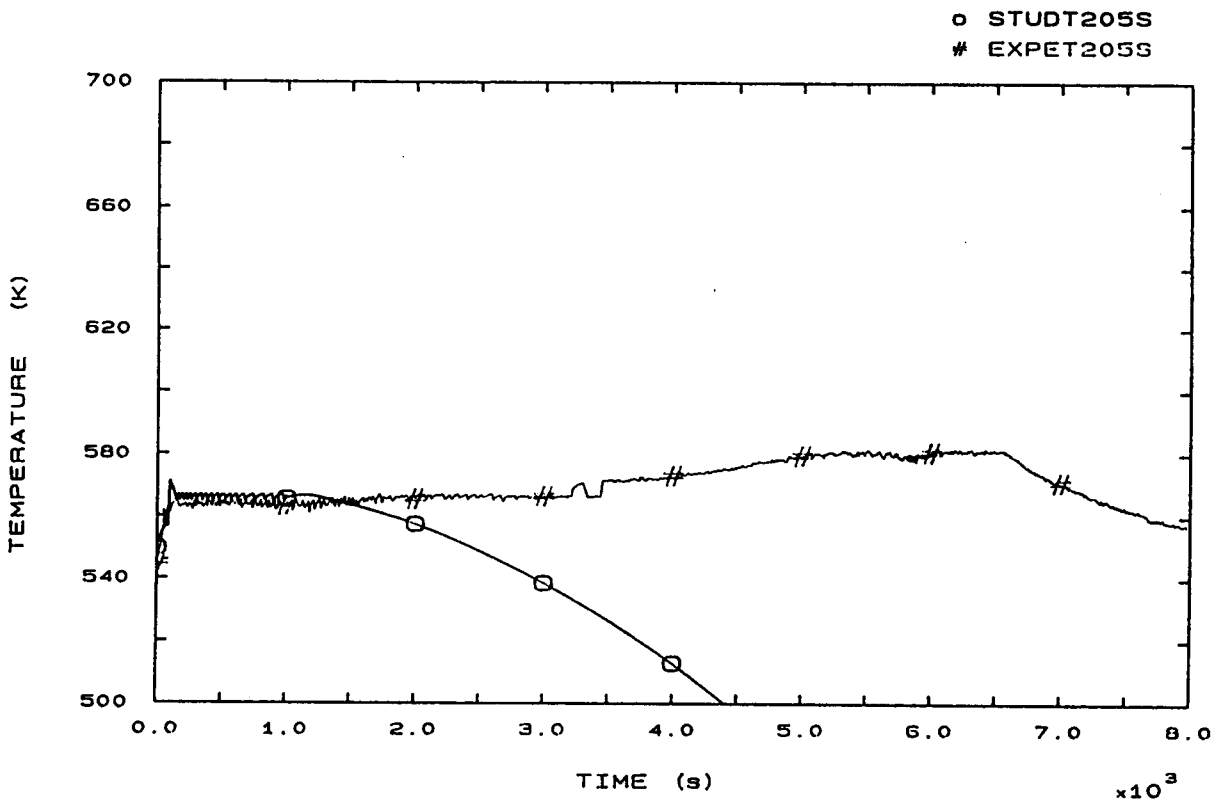

FIG. 25 FLUID TEMPERATURE SG2 RISER 185 MM A.T.S.

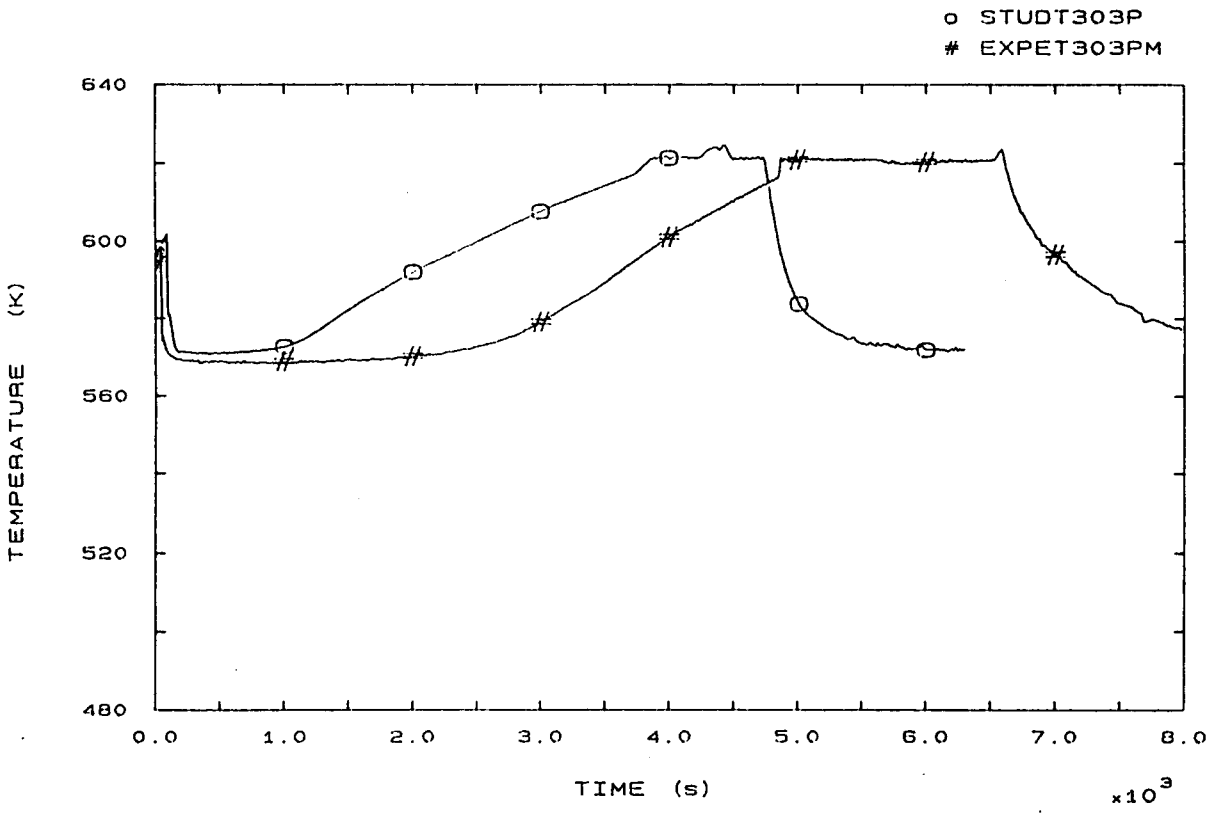

FIG. 32 LP3 HOT LEG OUTLET VESSEL TEMPERATURE

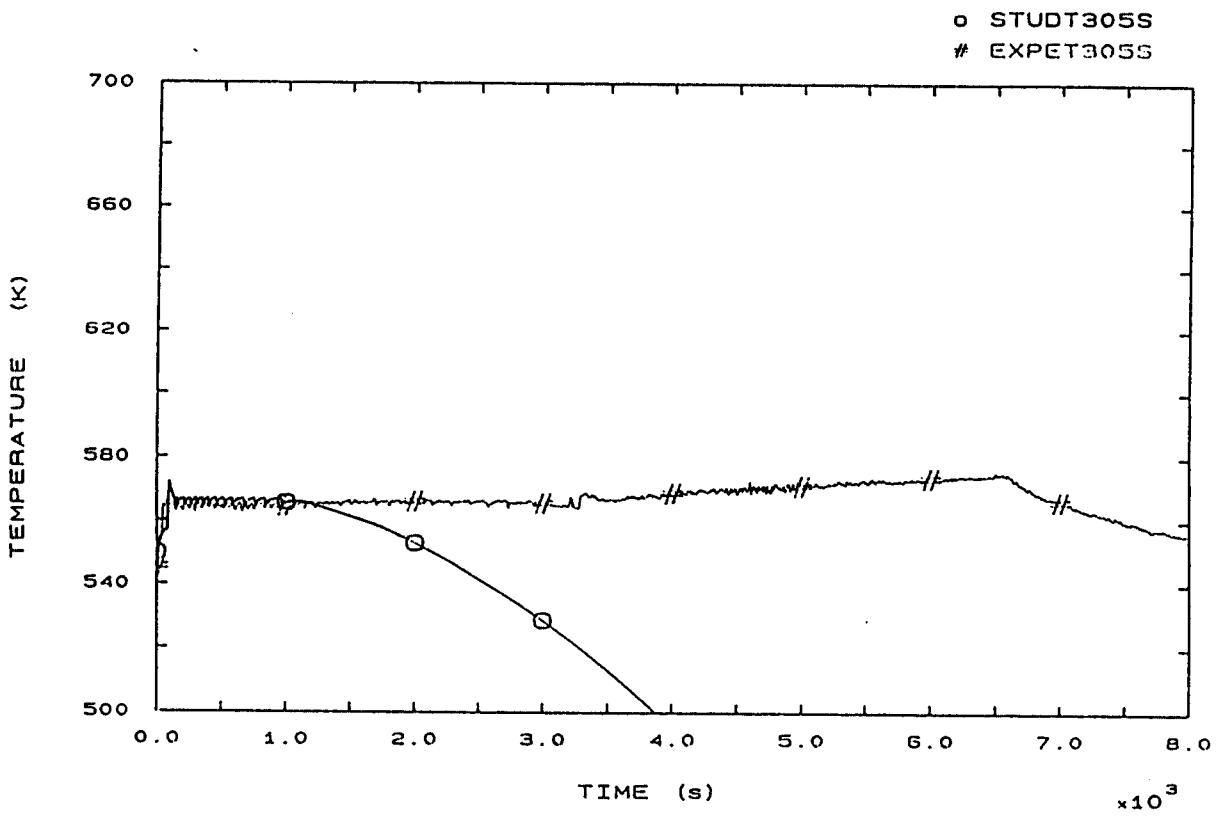

FIG. 35 FLUID TEMPERATURE SG3 RISER 185 MM A.T.S.

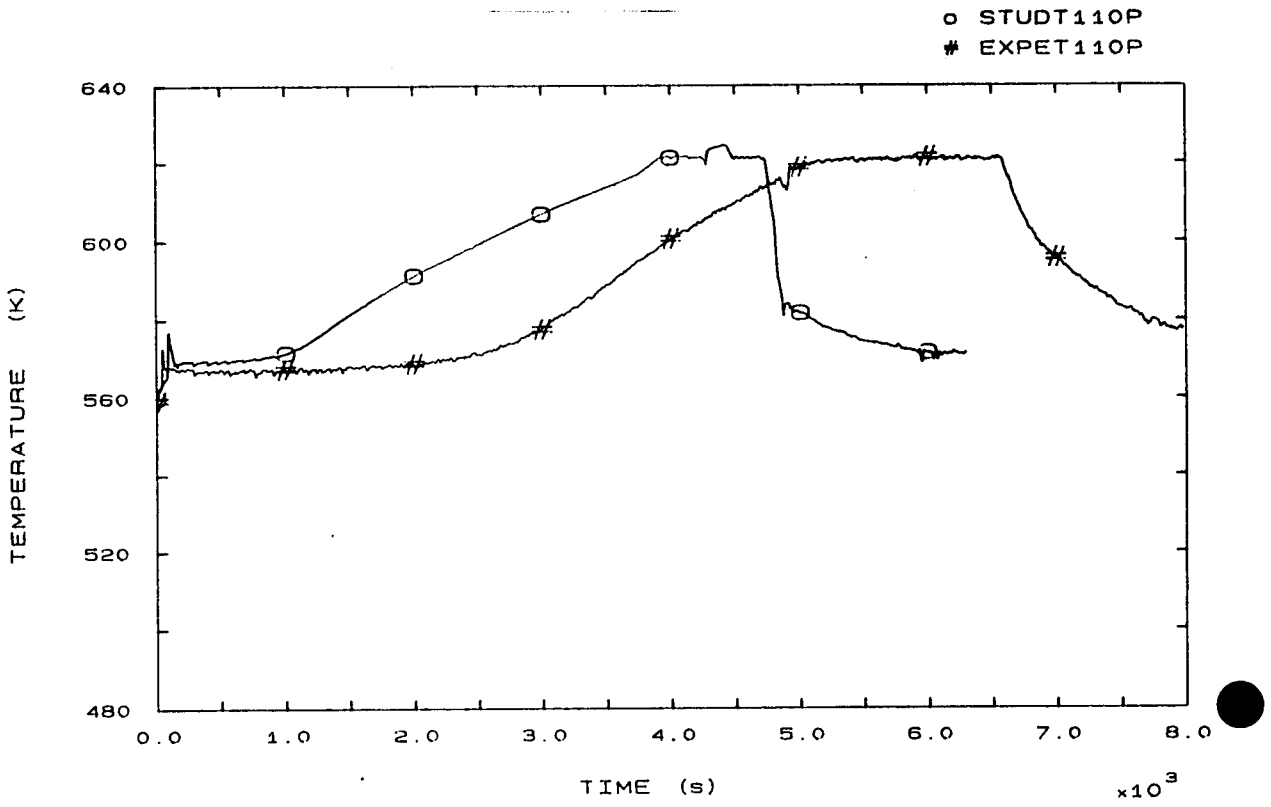

FIG. 42 SG1 OUTLET TEMPERATURE

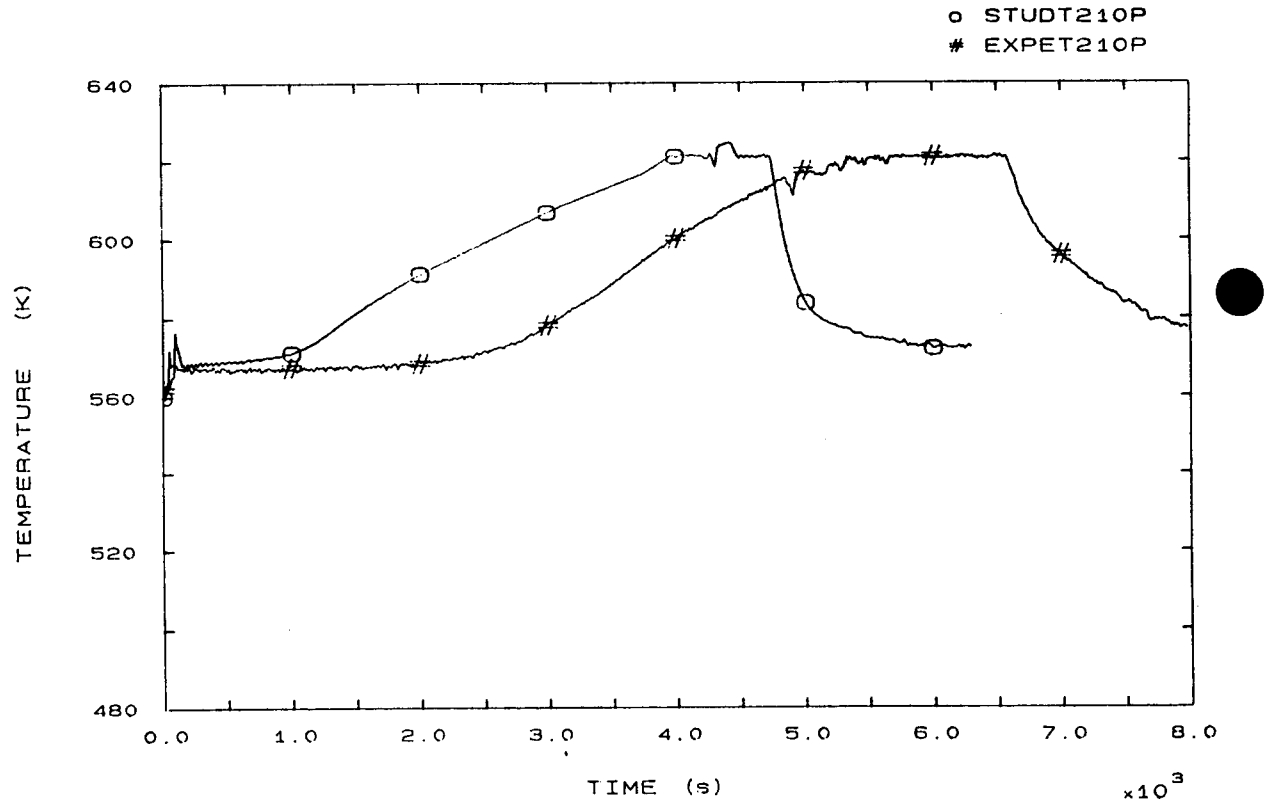

FIG. 44 SG2 OUTLET TEMPERATURE

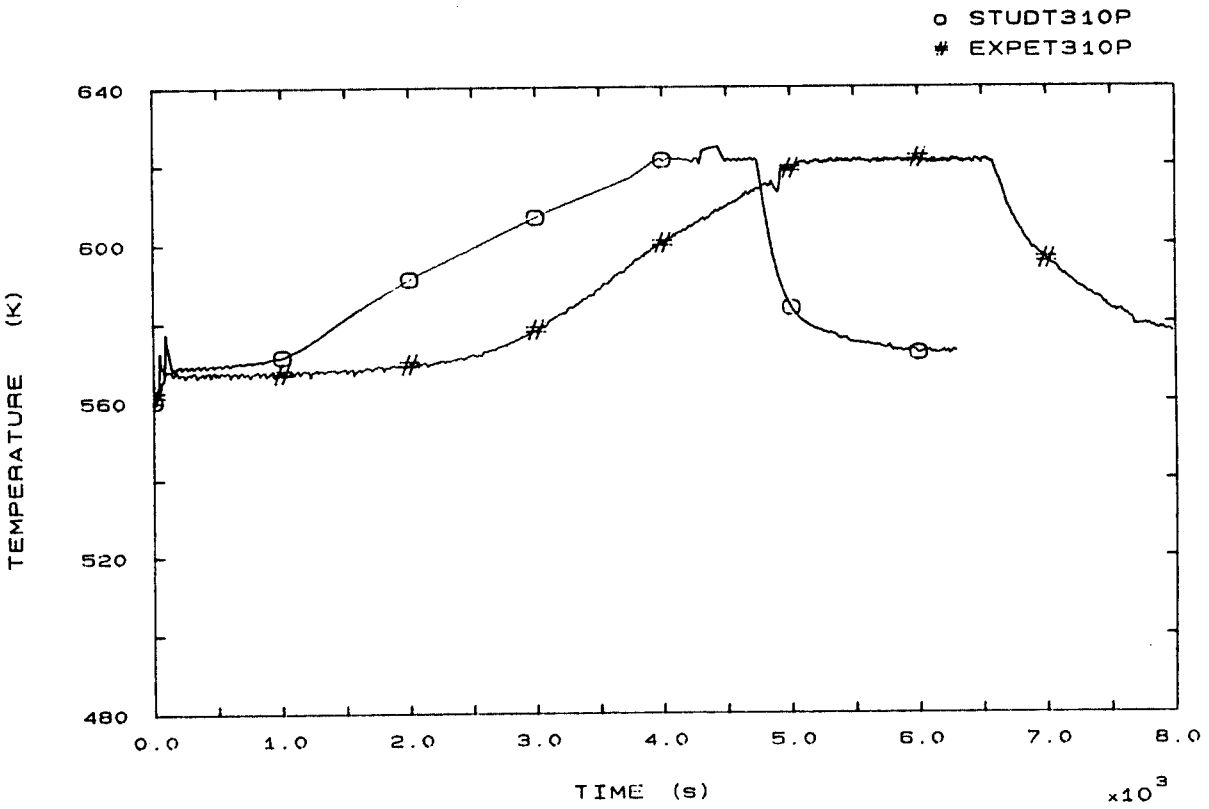

FIG. 46 SG3 OUTLET TEMPERATURE

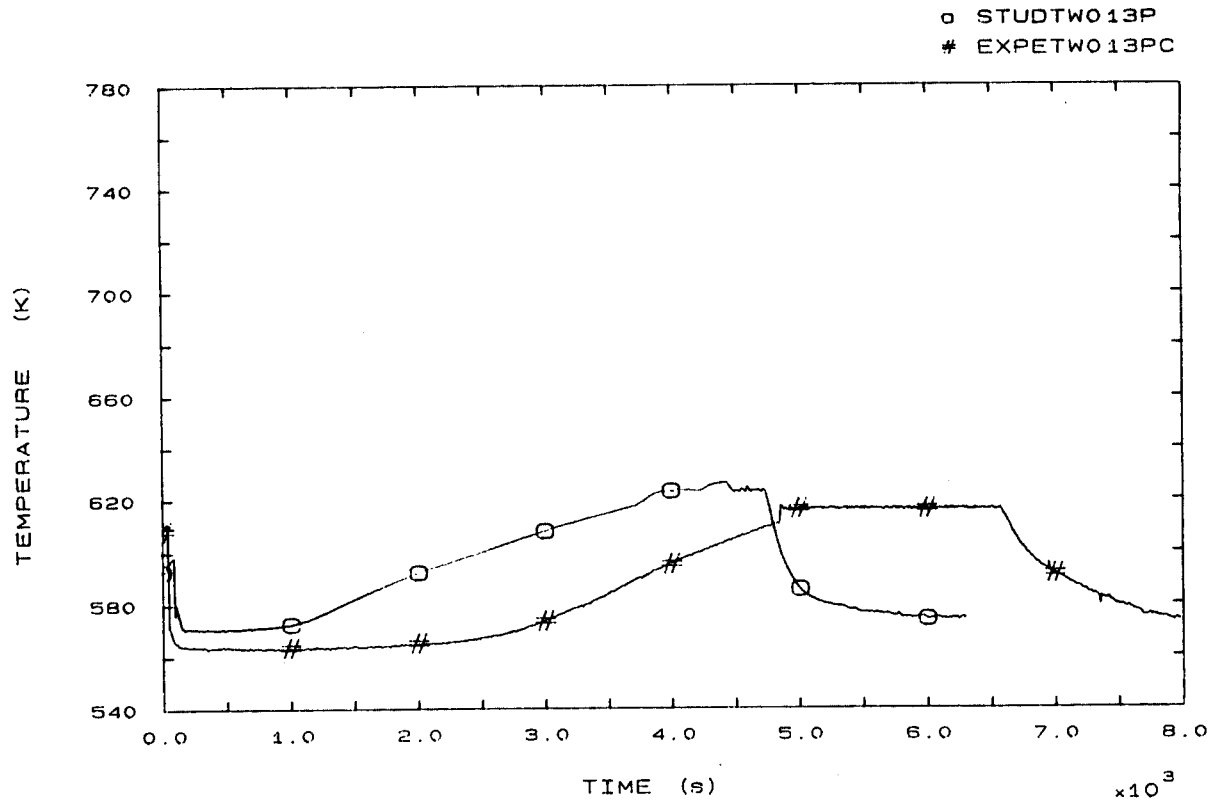

FIG. 49 CORE SURFACE TEMPERATURE AT ROD BUNDLE ELEVATION 1074 MM

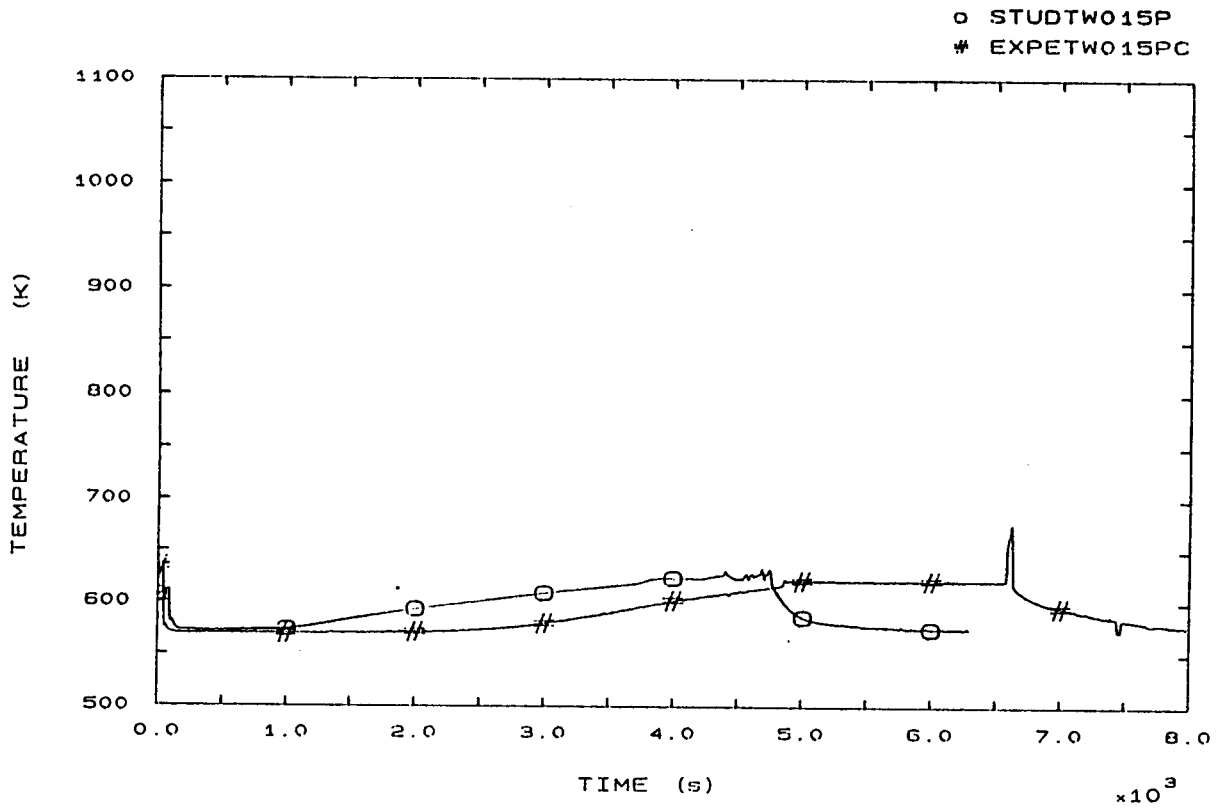

FIG. 50 SURFACE TEMPERATURE AT ROD BUNDLE ELEVATION 2294 MM

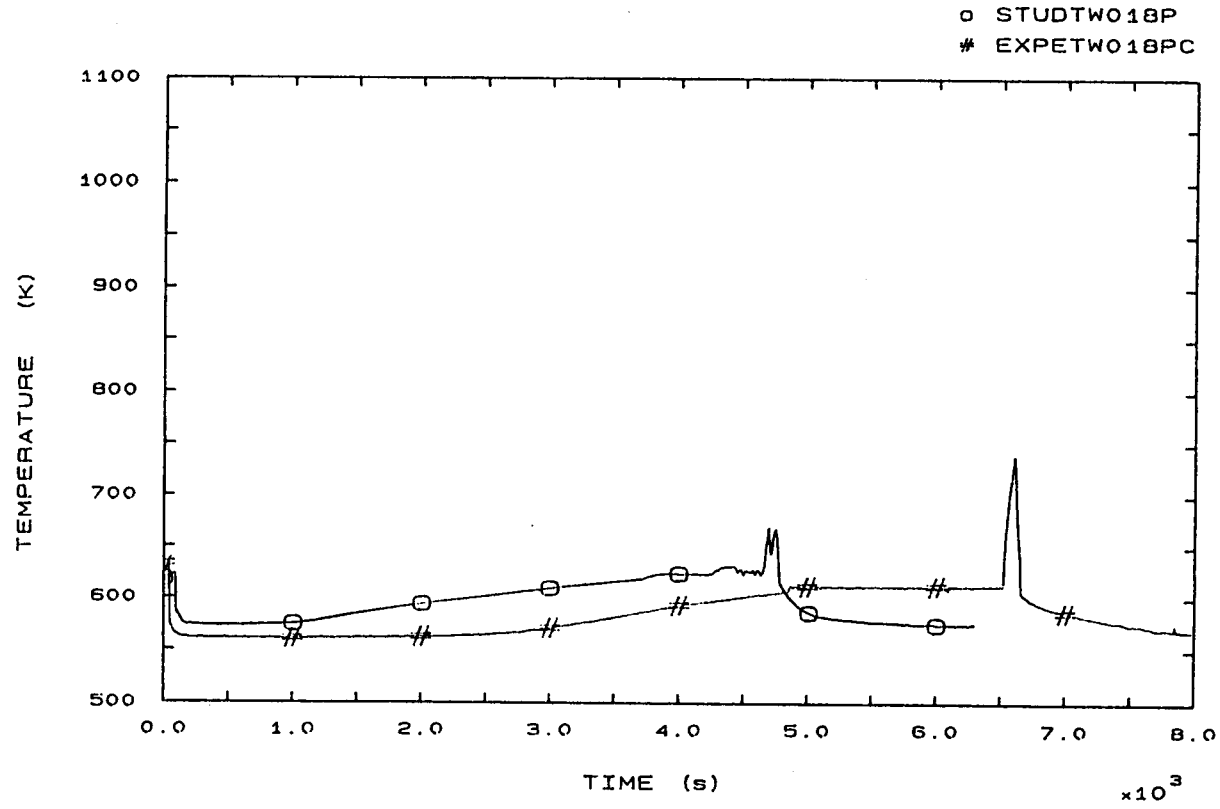

FIG. 51 SURFACE TEMPERATURE AT ROD BUNDLE ELEVATION 3294 MM

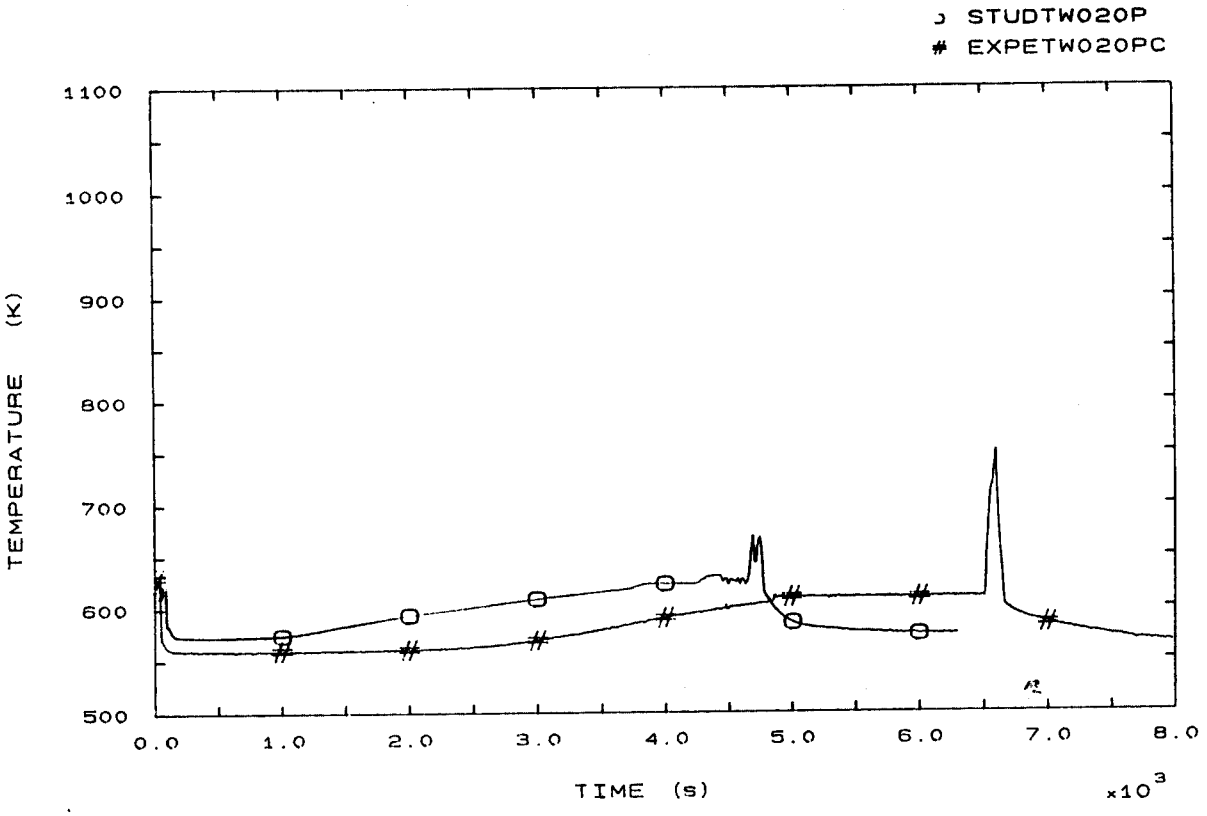

FIG. 52 SURFACE TEMPERATURE AT ROD BUNDLE ELEVATION 3640 MM

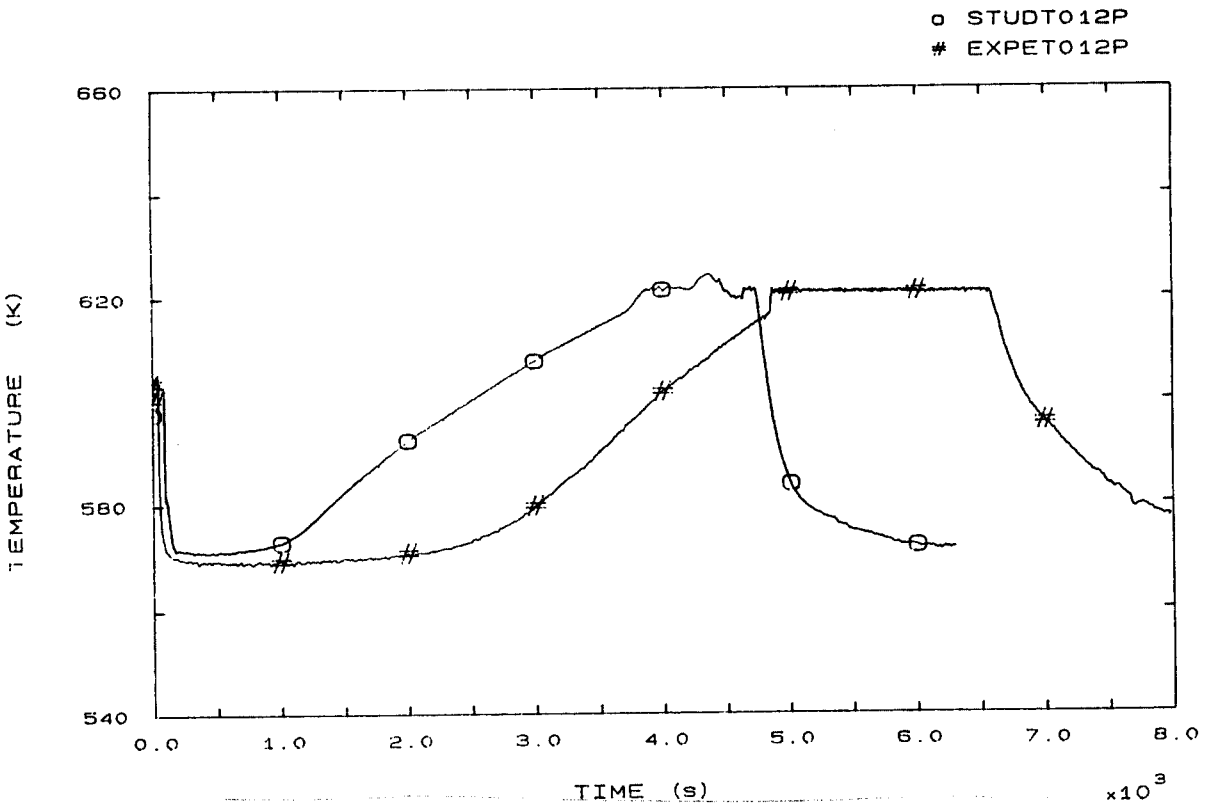

FIG. 53 CORE OUTLET TEMPERATURE

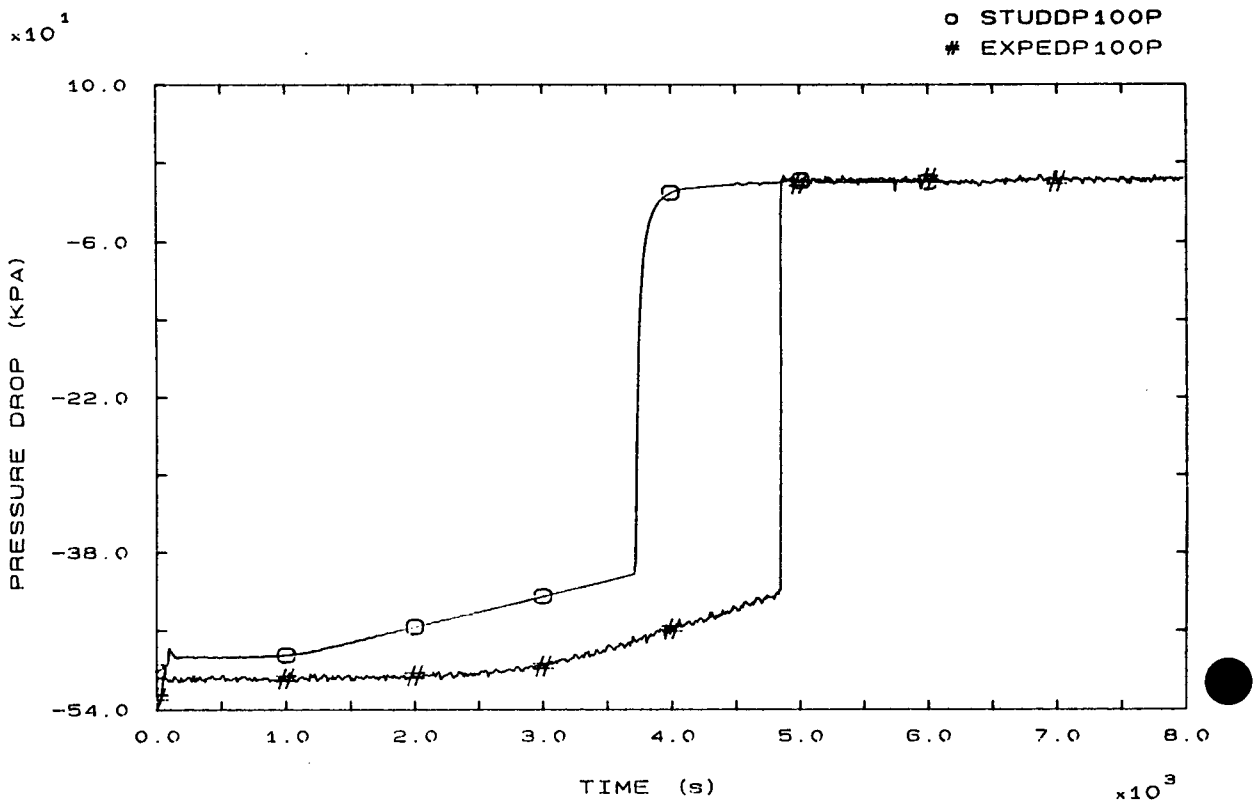

FIG. 54 PRIMARY PUMP 1 PRESSURE DROP

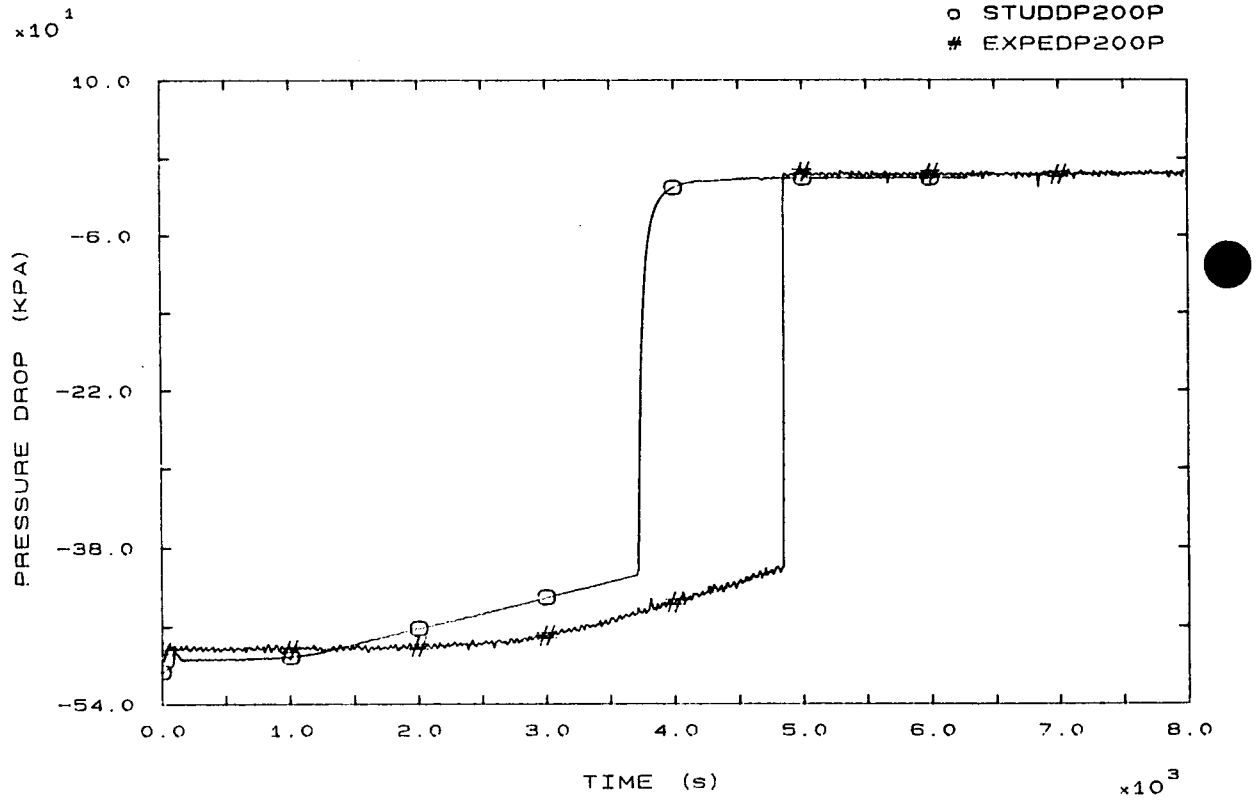

FIG. 55 PRIMARY PUMP 2 PRESSURE DROP

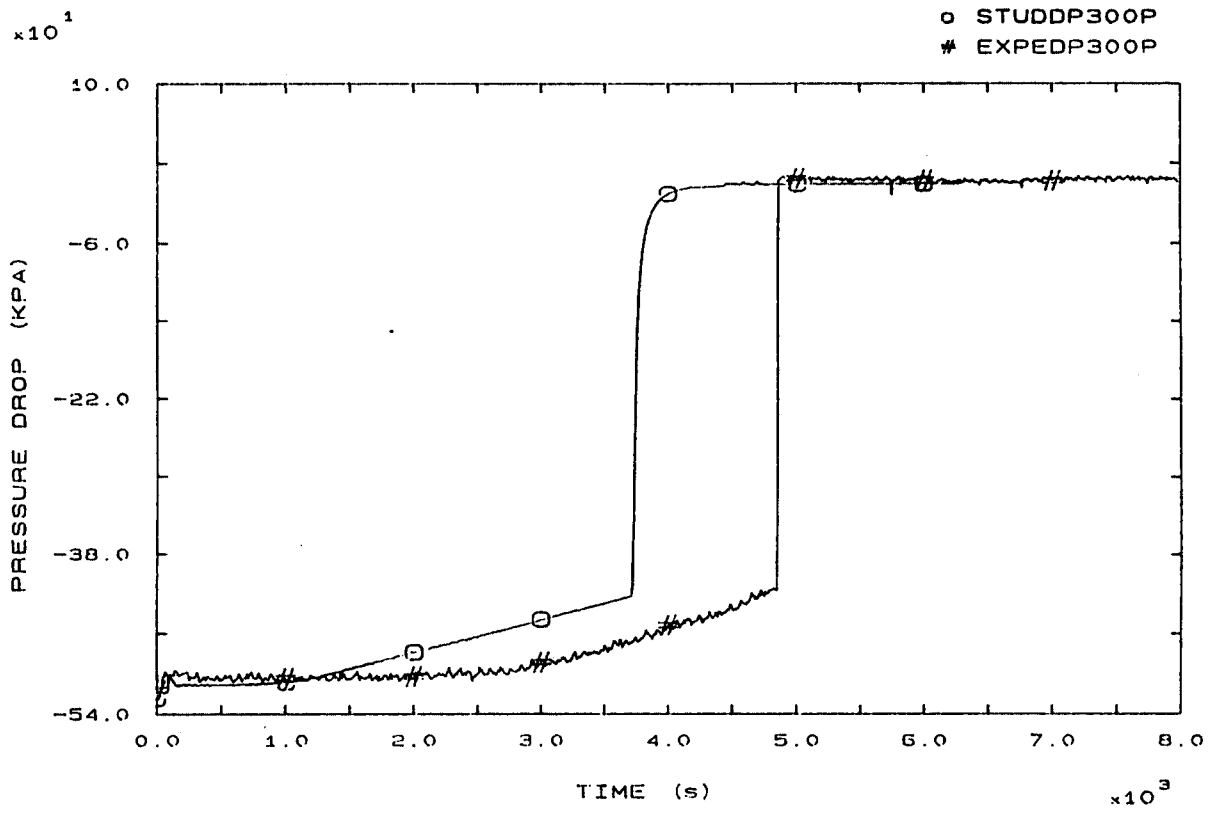

FIG. 56 PRIMARY PUMP 3 PRESSURE DROP

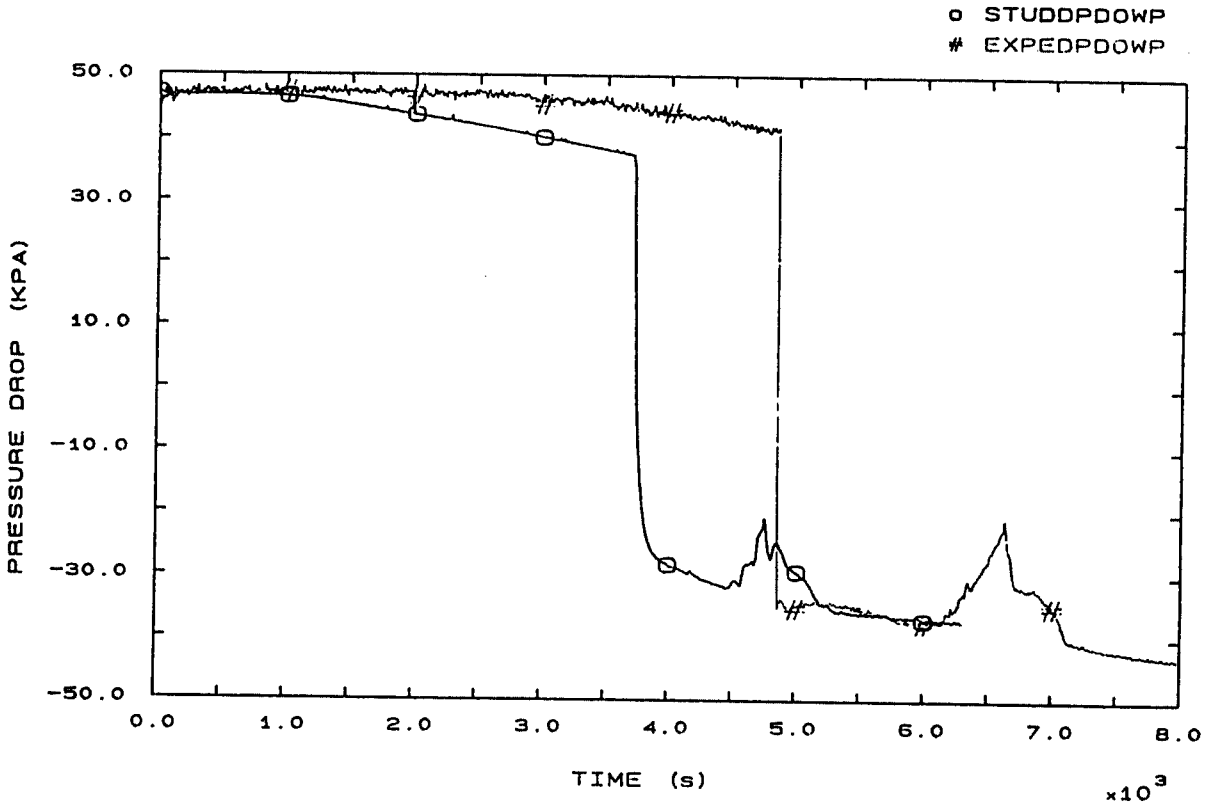

FIG. 57 VESSEL DOWNCOMER PRESSURE DROP

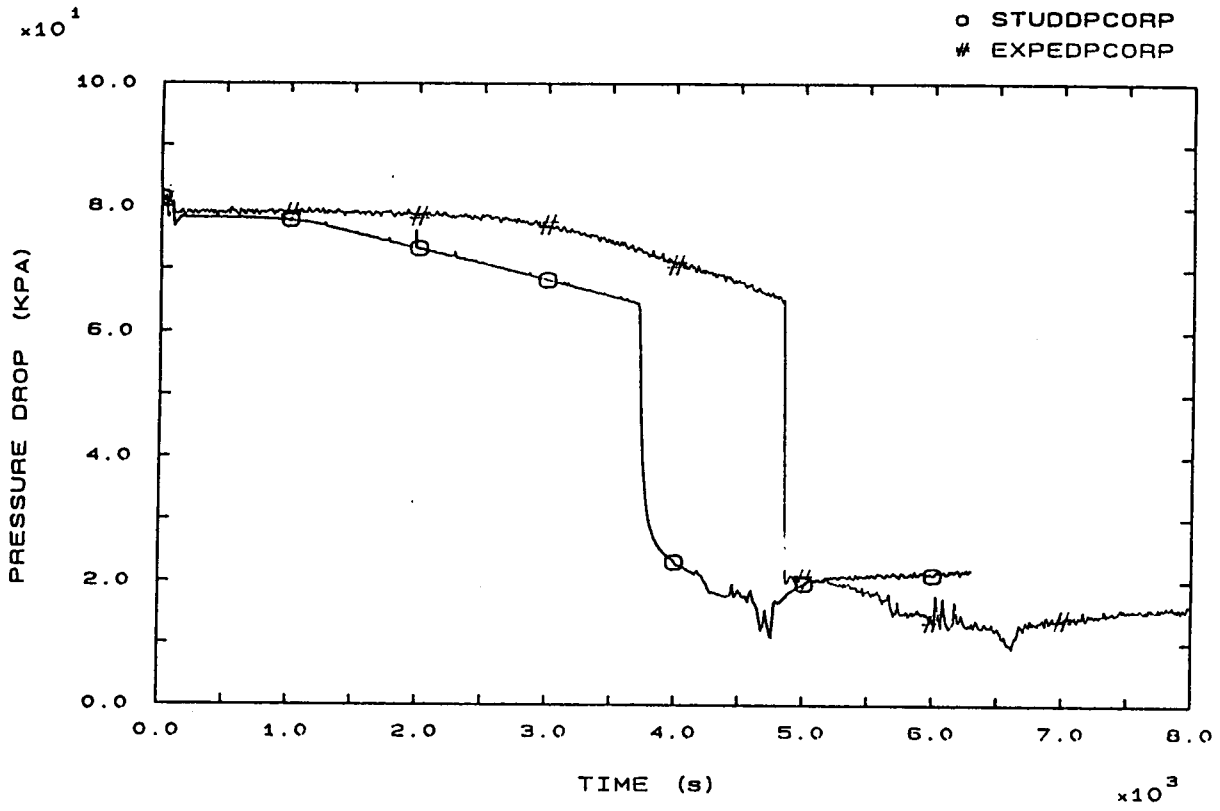

FIG. 58 CORE PRESSURE DROP

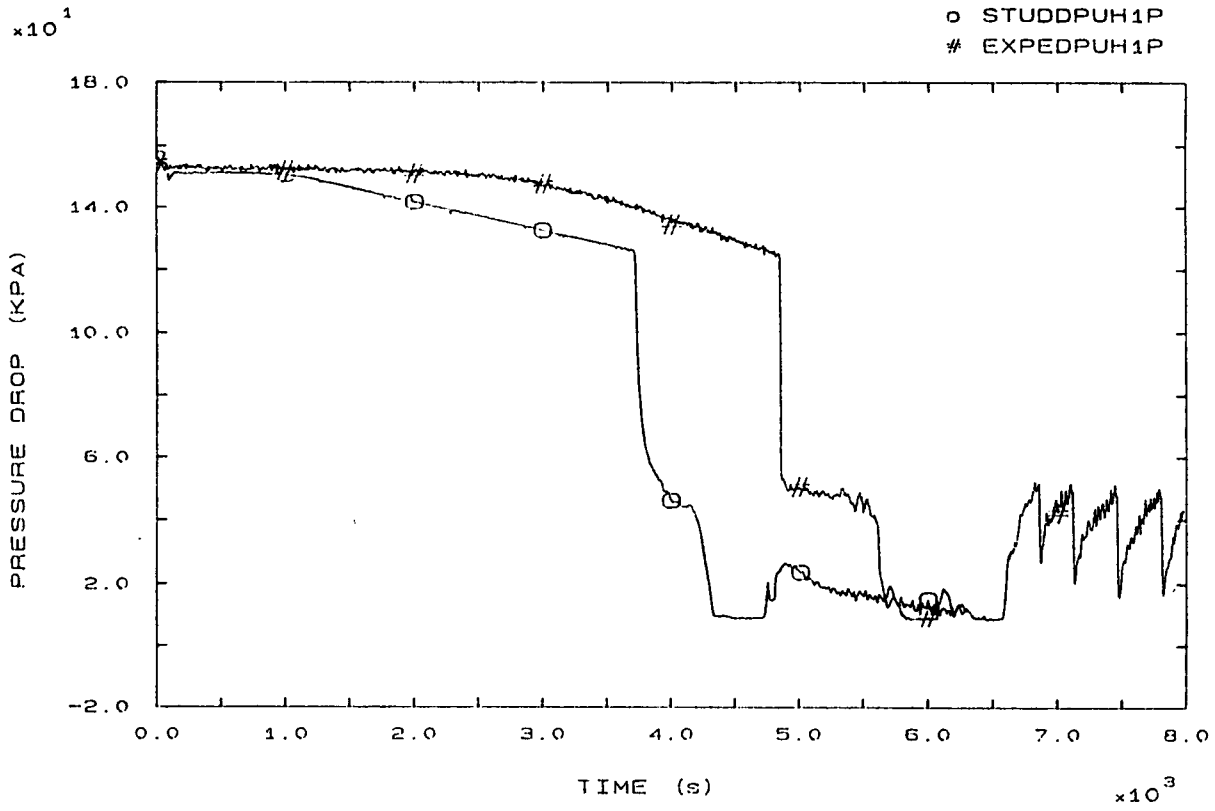

FIG. 62 SG1 INLET/U-BEND (UP-HILL) PRESSURE DROP

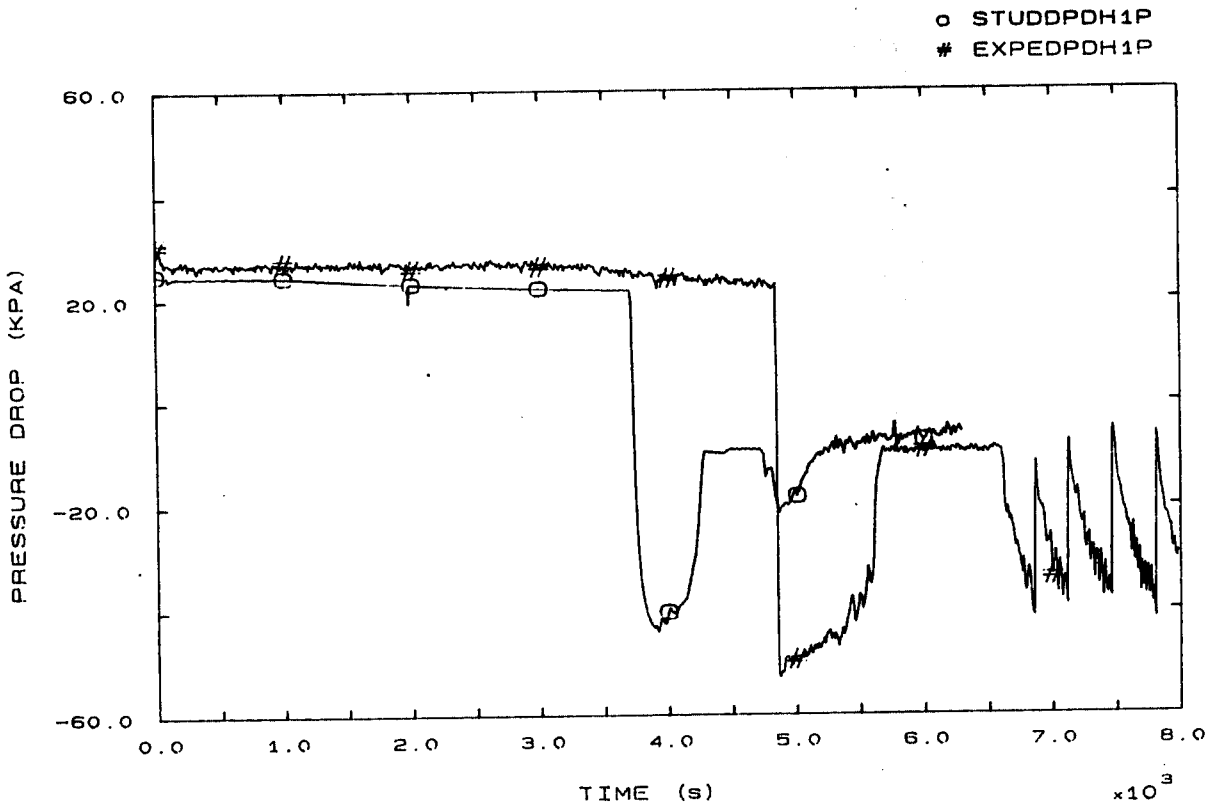

FIG. 63 SG1 U-BEND/OUTLET (DOWN-HILL) PRESSURE DROP

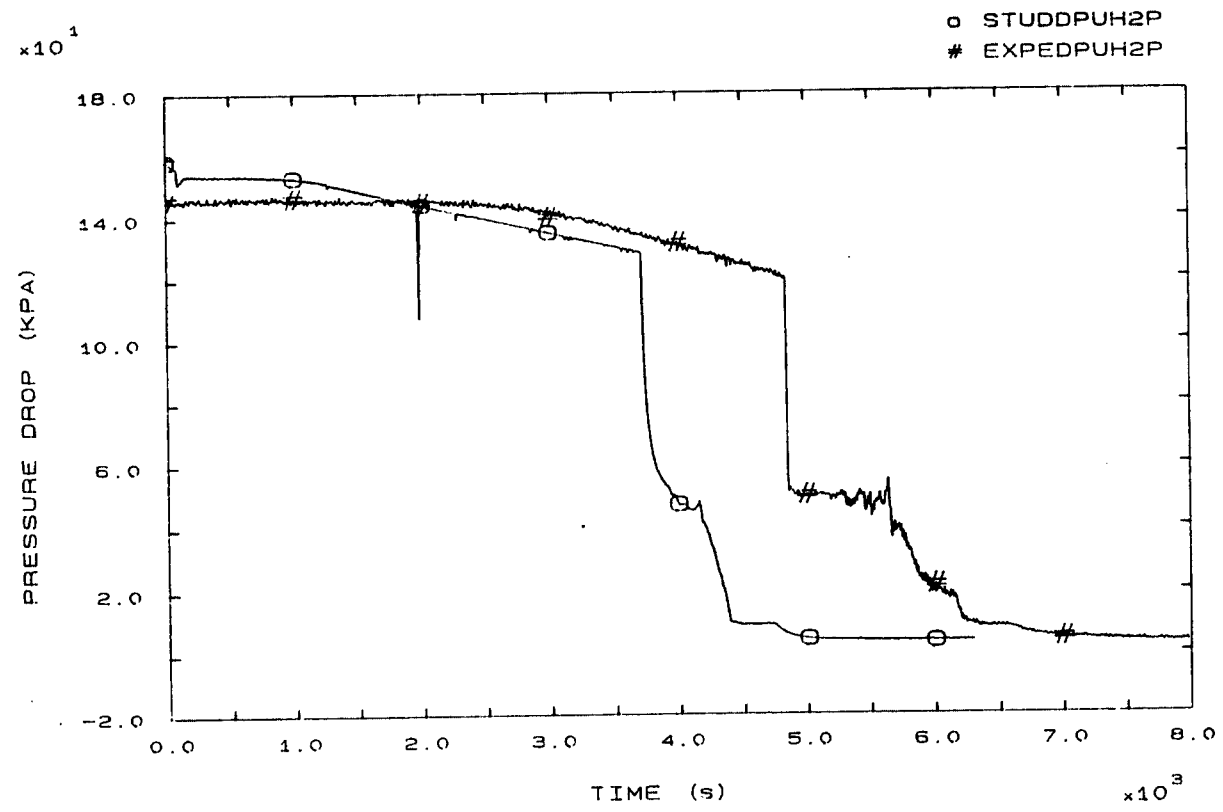

FIG. 64 SG2 INLET/U-BEND (UP-HILL) PRESSURE DROP

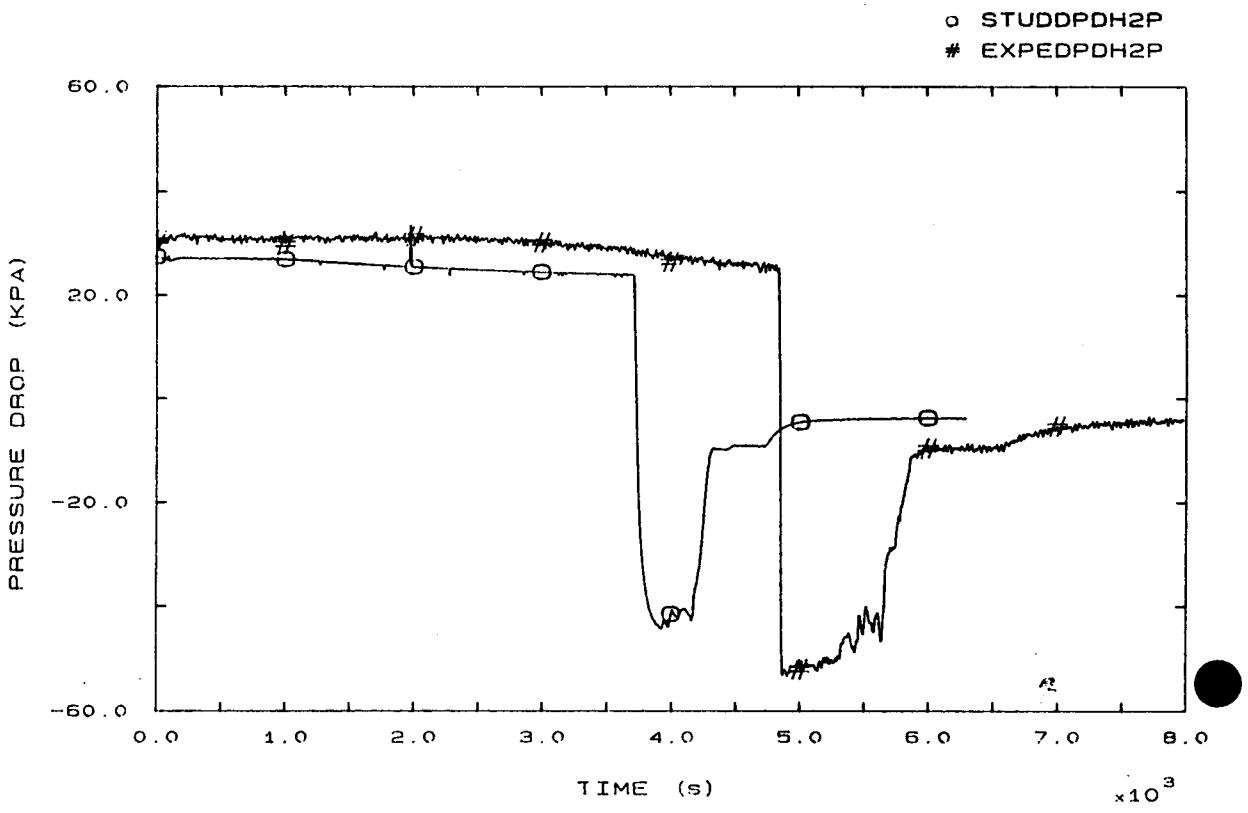

FIG. 65 SG2 U-BEND/OUTLET (DOWN-HILL) PRESSURE DROP

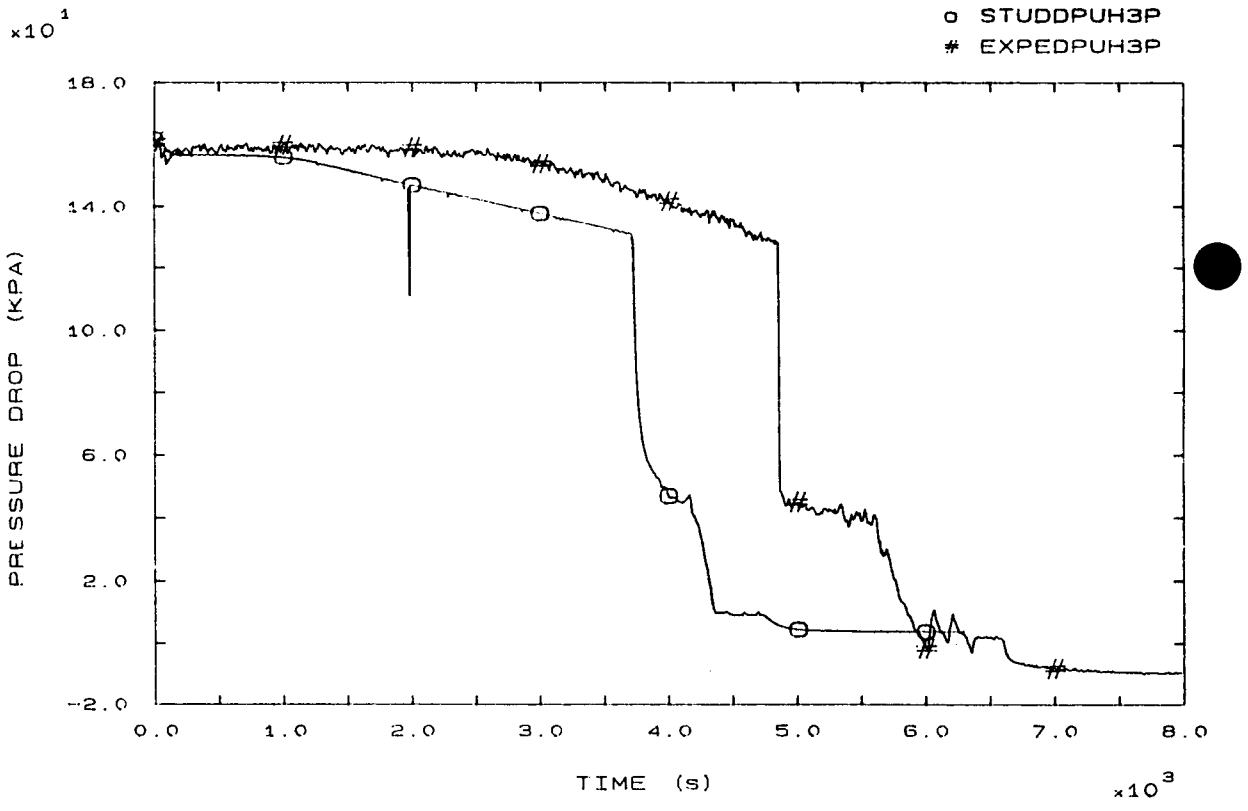

FIG. 66 SG3 INLET/U-BEND (UP-HILL) PRESSURE DROP

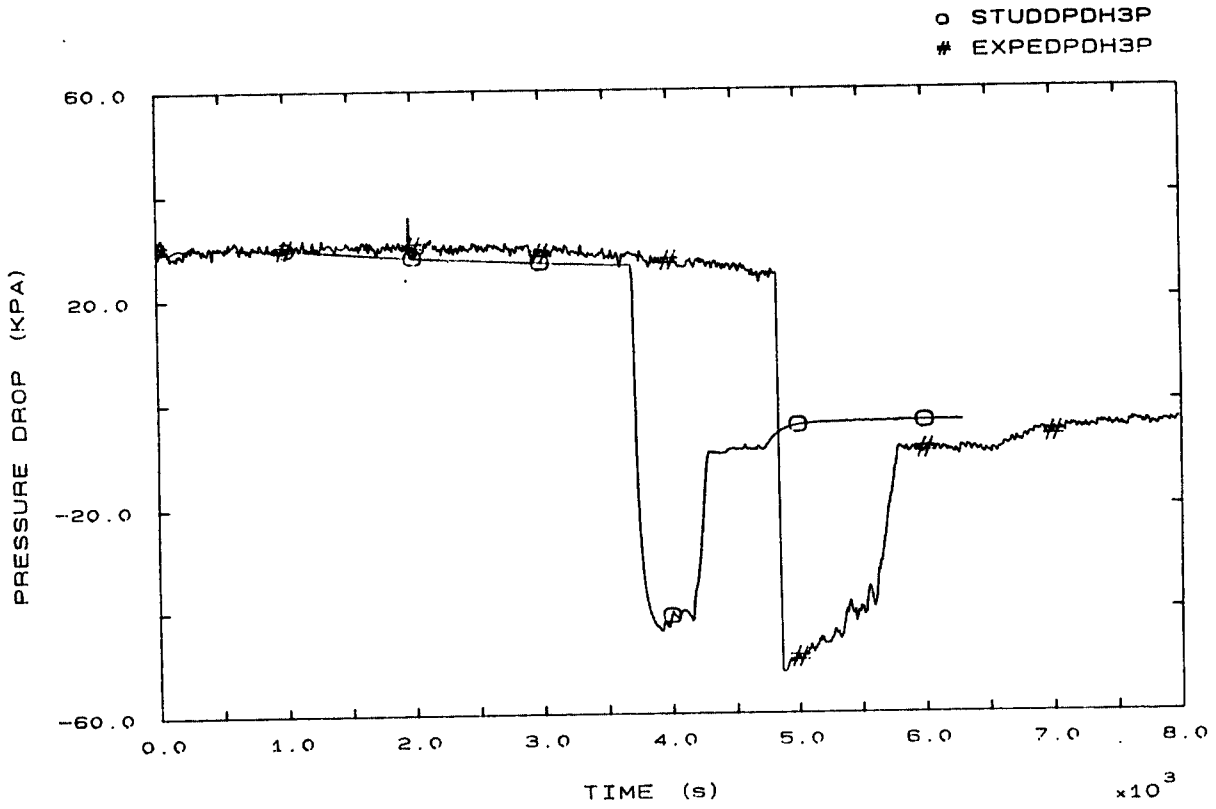

FIG. 67 SG3 U-BEND/OUTLET (DOWN-HILL) PRESSURE DROP

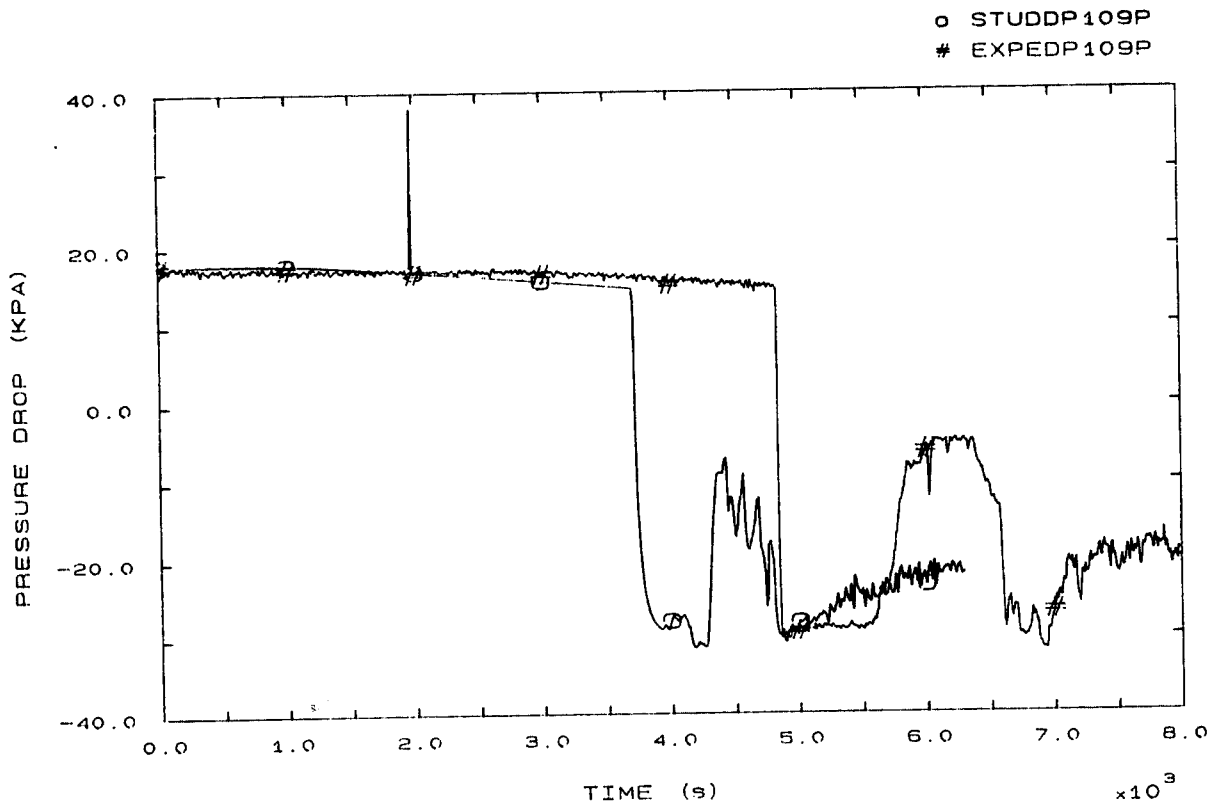

FIG. 68 SG1 OUTLET/LOOP SEAL BOTTOM PRESSURE DROP

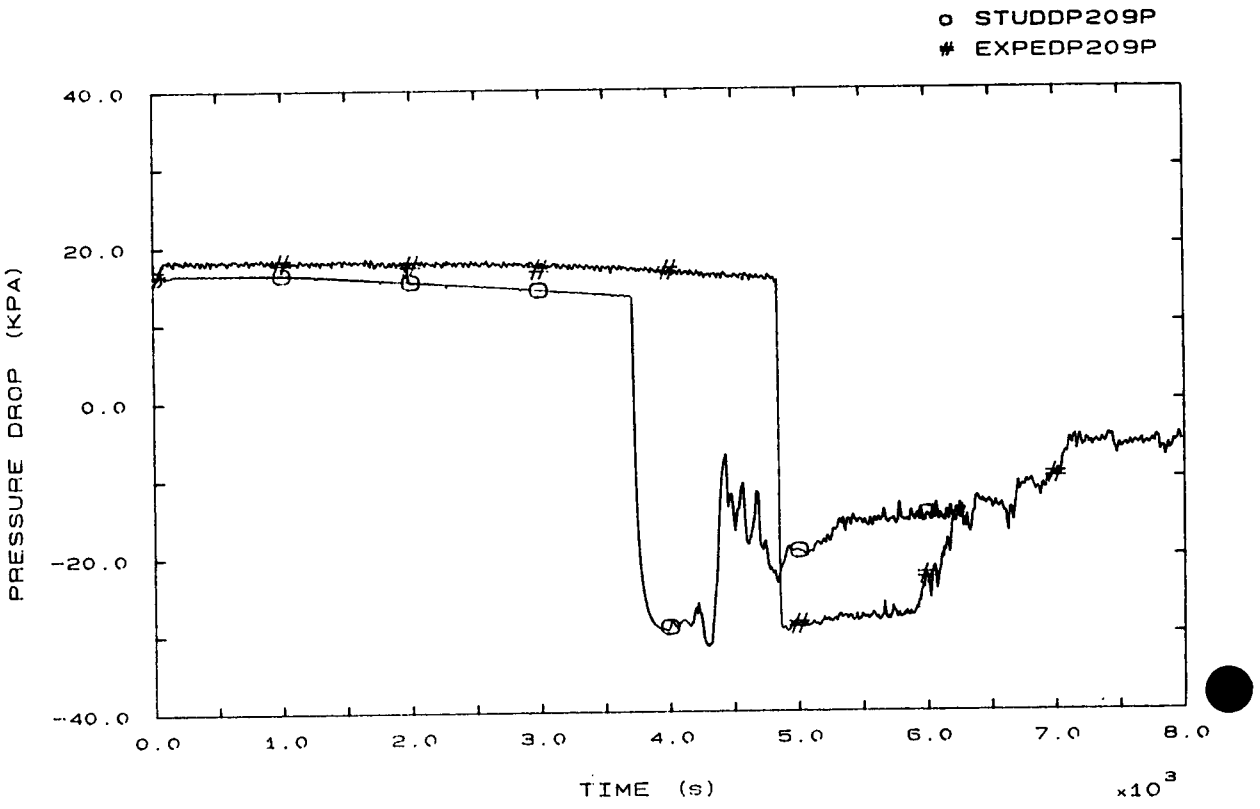

FIG. 69 SG2 OUTLET/LOOP SEAL BOTTOM PRESSURE DROP

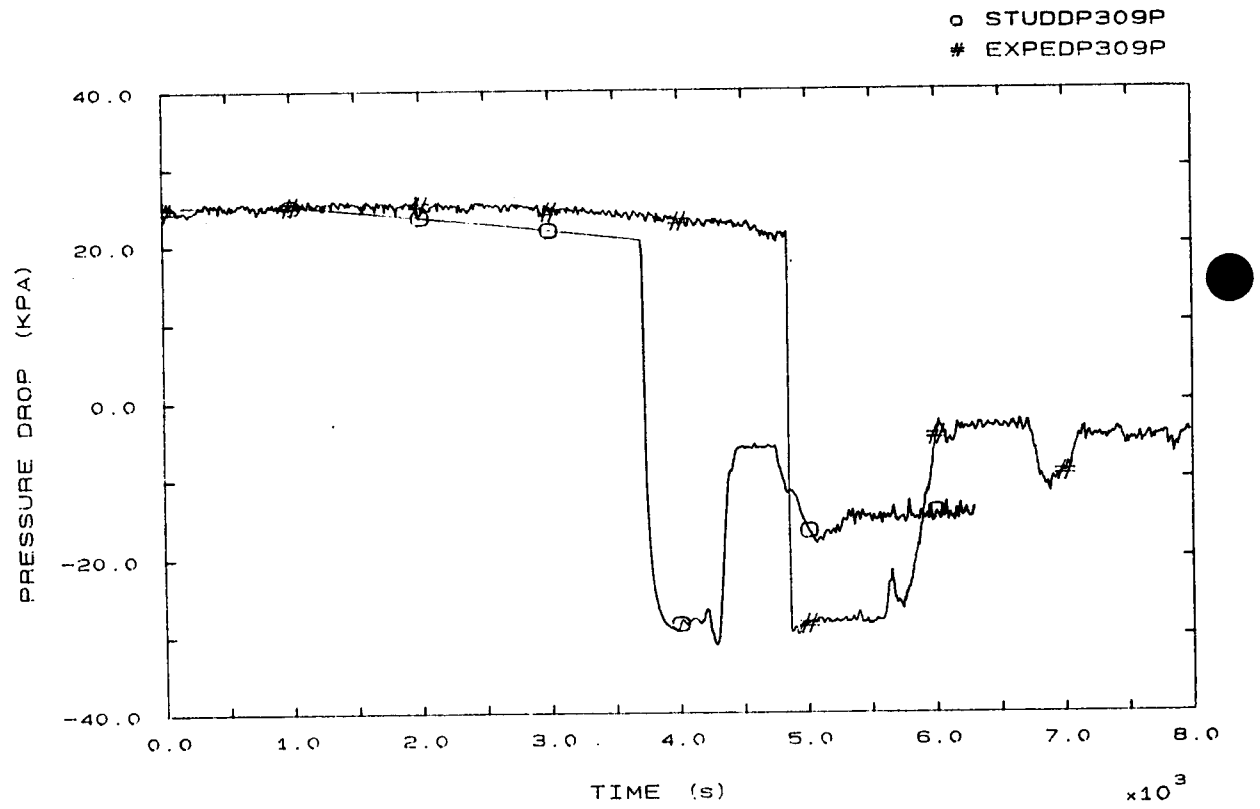

FIG. 70 SG3 OUTLET/LOOP SEAL BOTTOM PRESSURE DROP

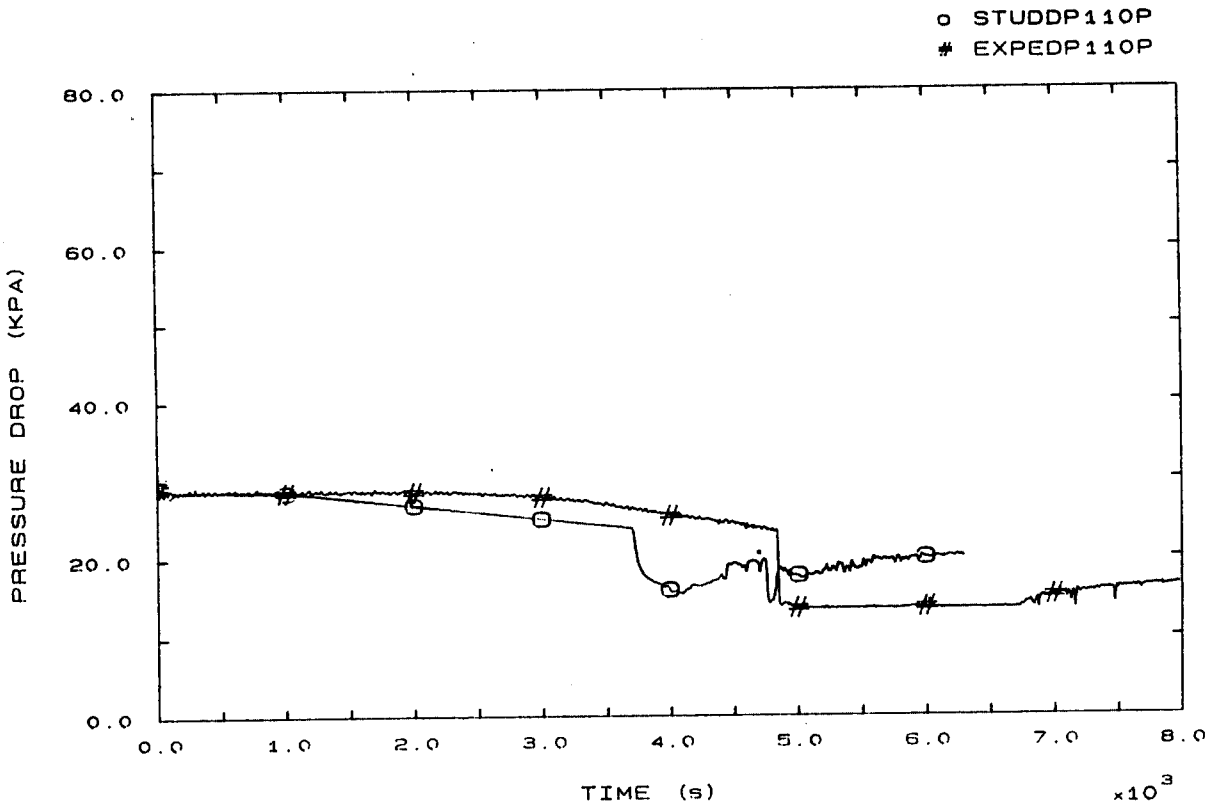

FIG. 71 LOOP SEAL BOTTOM/PUMP 1 INLET PRESSURE DROP

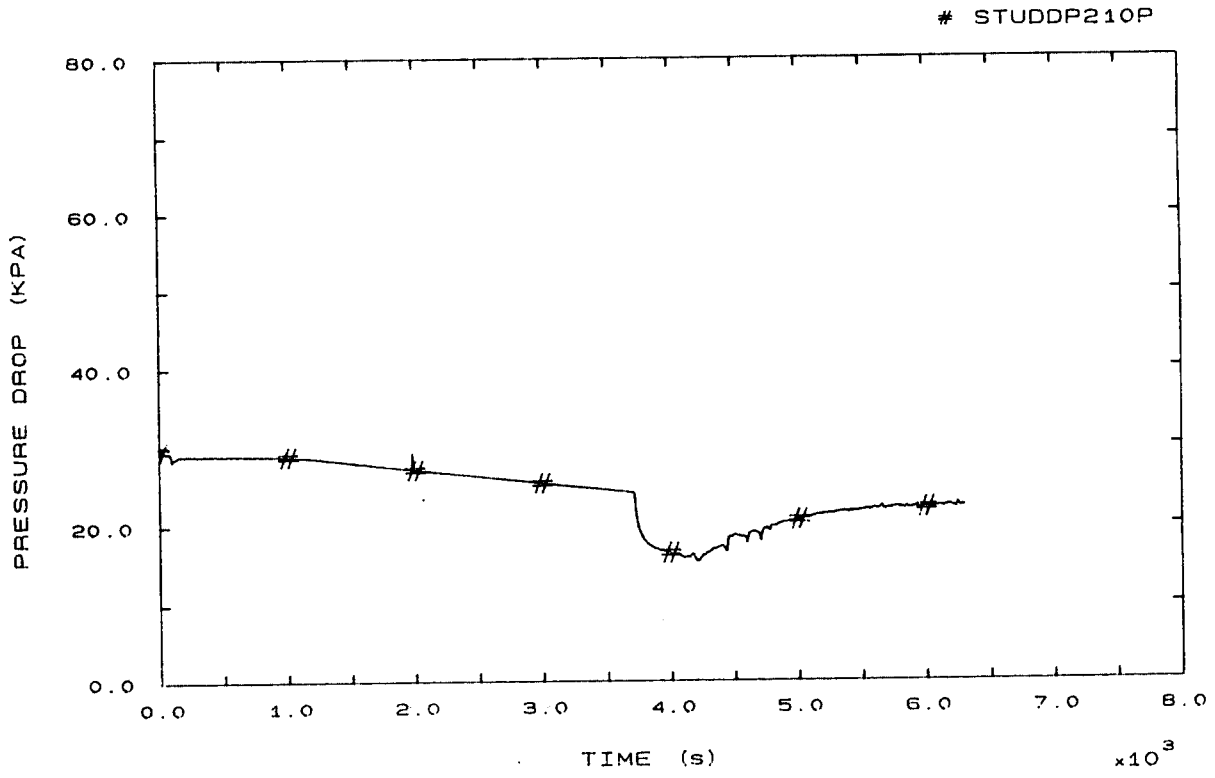

FIG. 72 LOOP SEAL BOTTOM/PUMP 2 INLET PRESSURE DROP

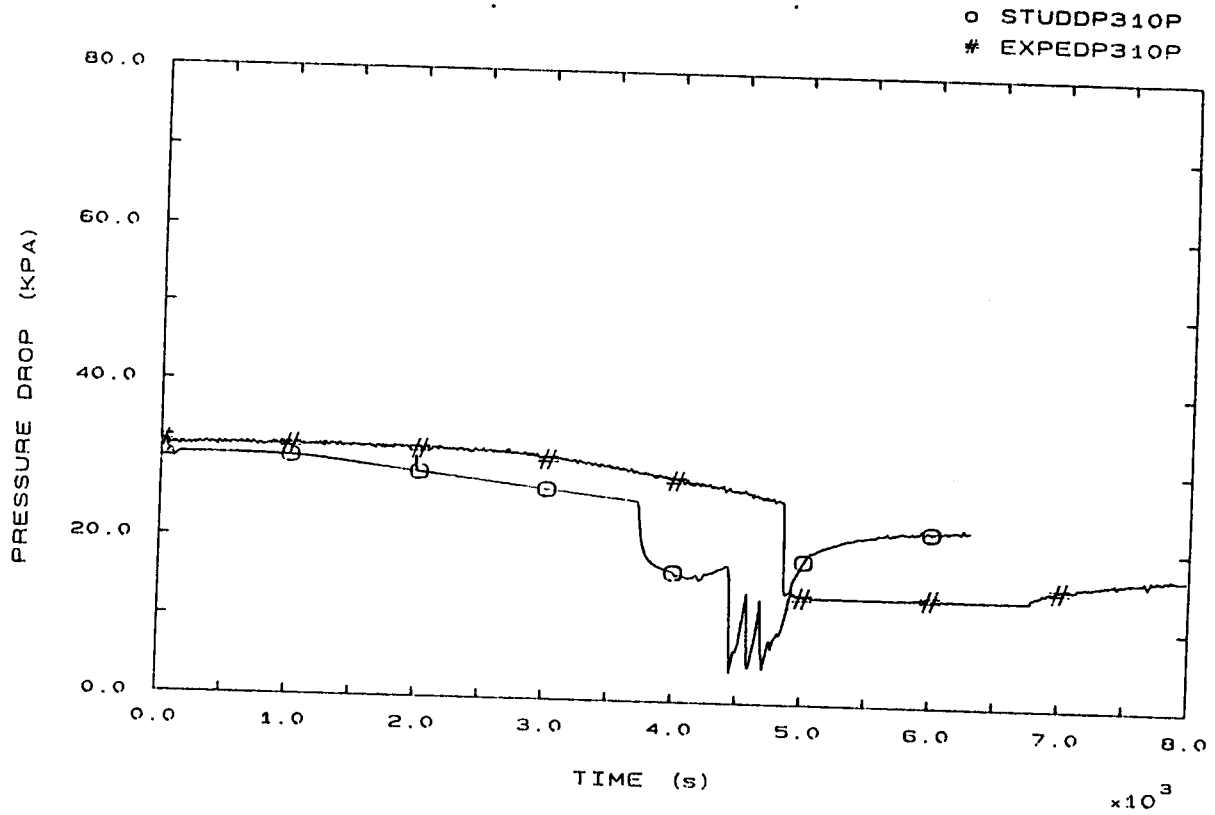

FIG. 73 LOOP SEAL BOTTOM/PUMP 3 INLET PRESSURE DROP

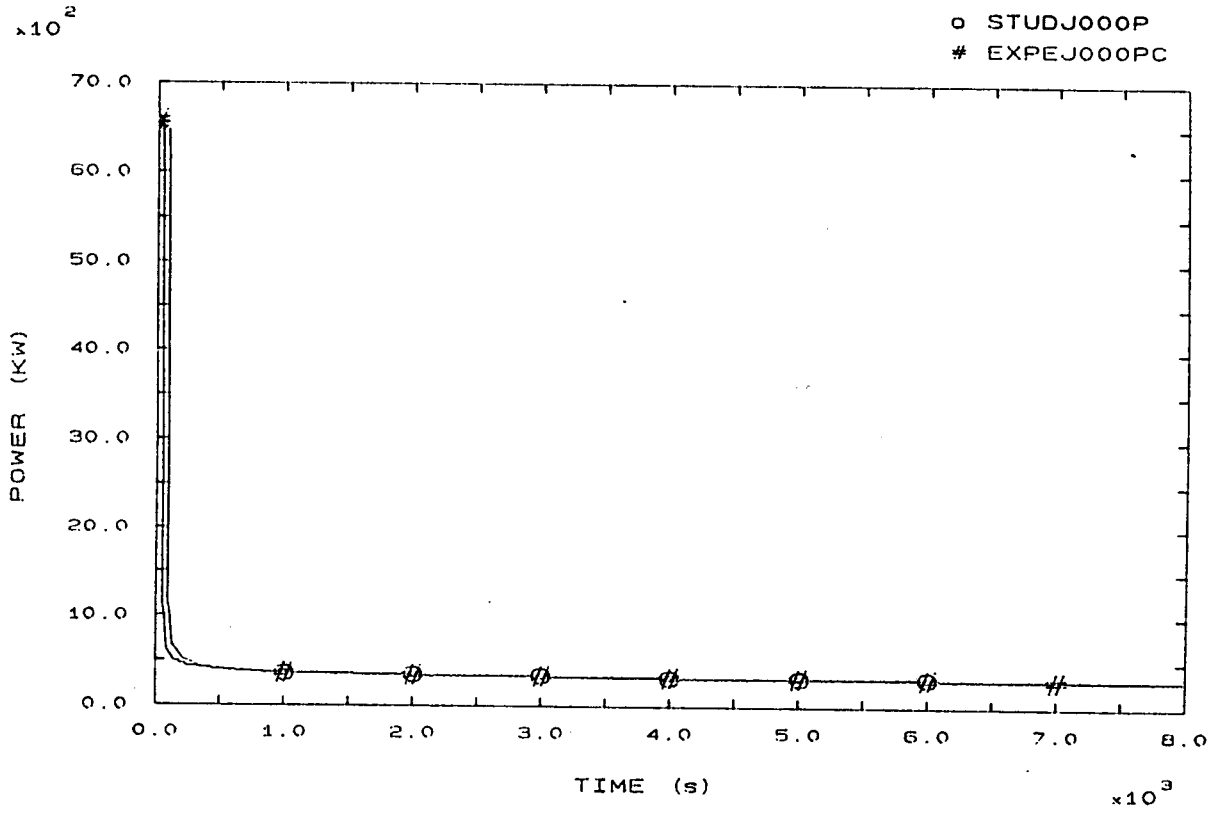

FIG. 81 HEATER RODS POWER

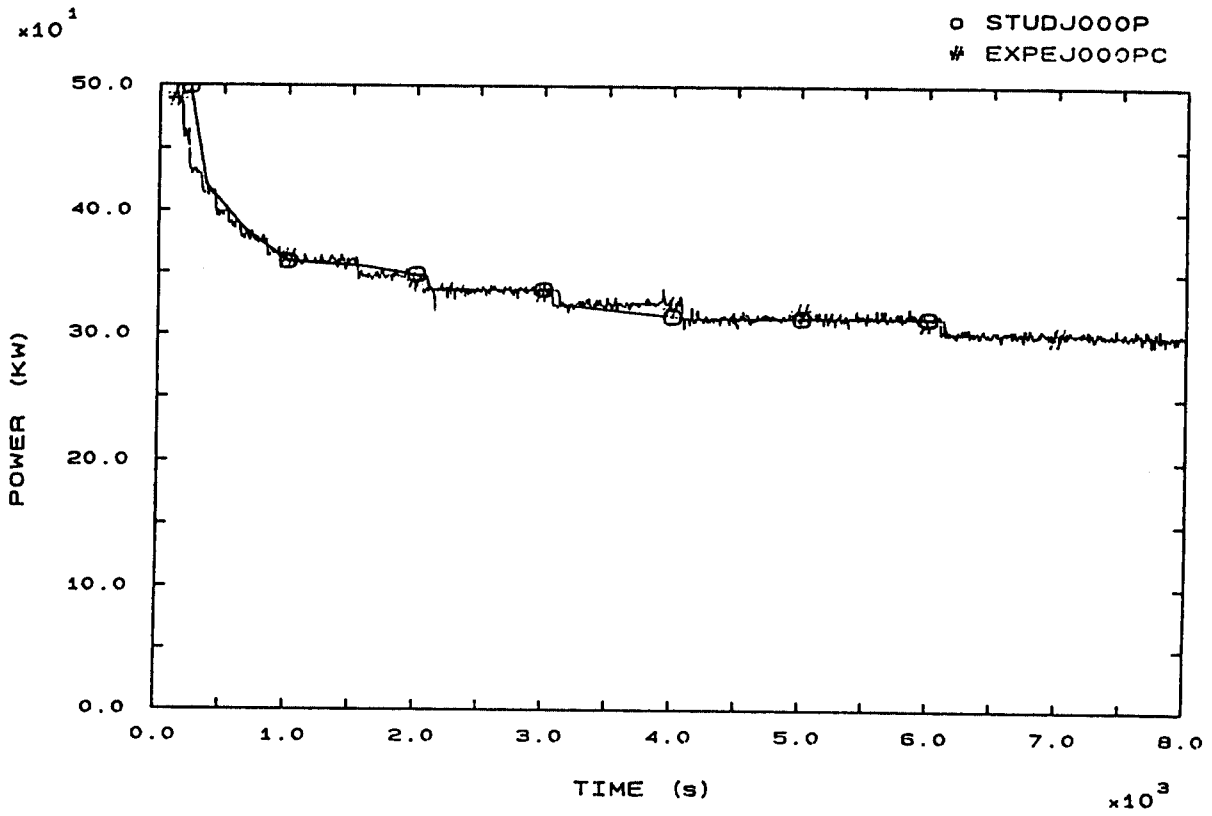

FIG. 81A HEATER RODS POWER

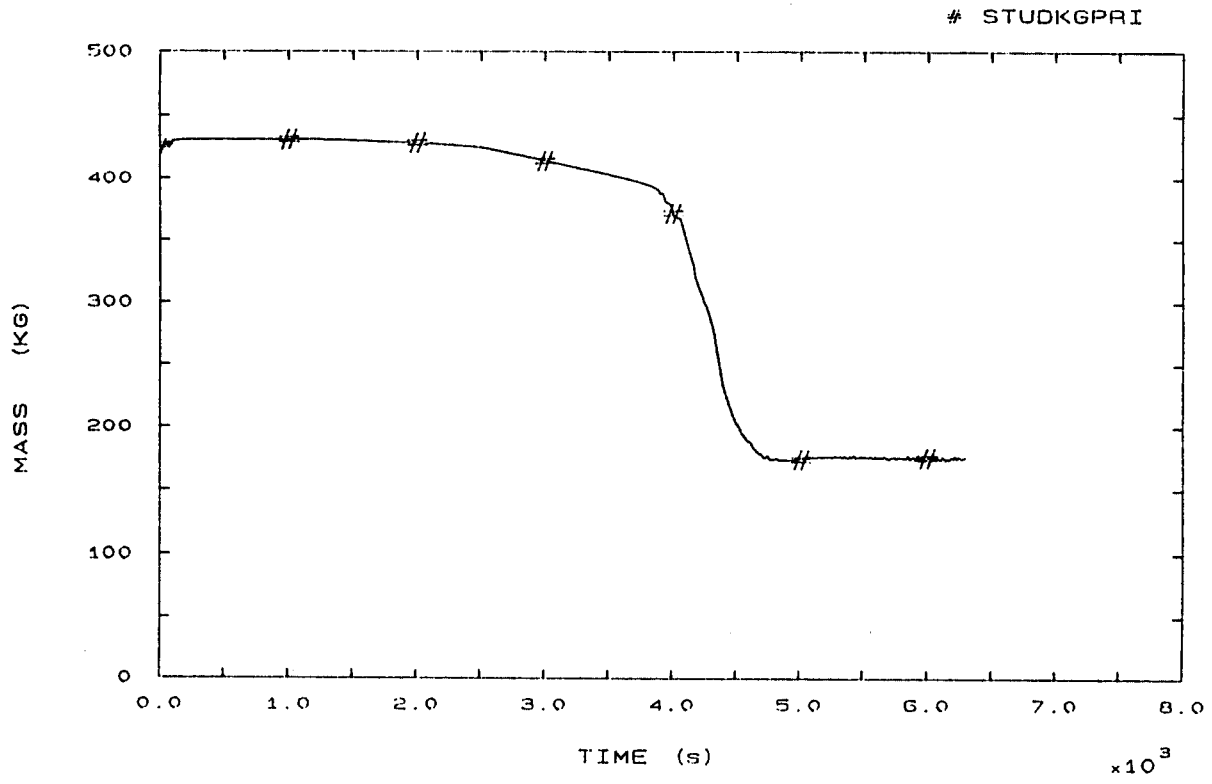

FIG. 85 PRIMARY COOLANT TOTAL MASS

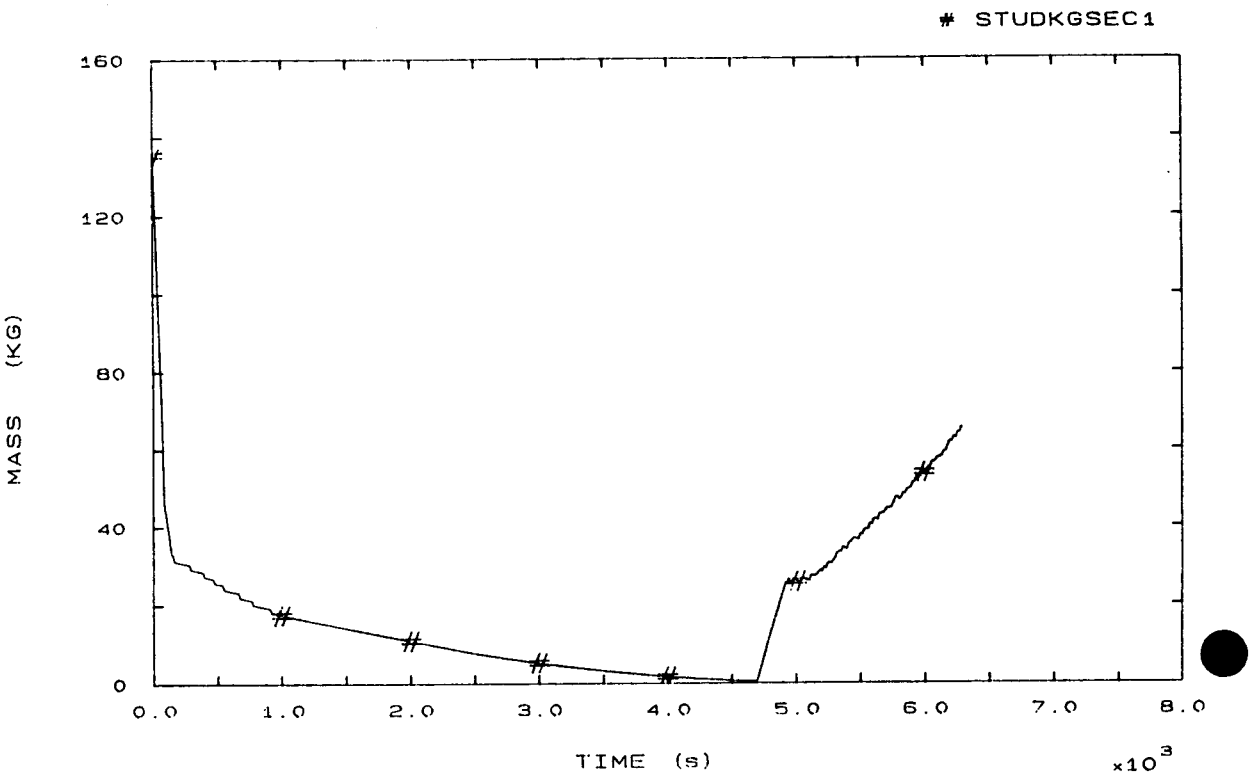

FIG. 86 SECONDARY COOLANT TOTAL MASS SG1

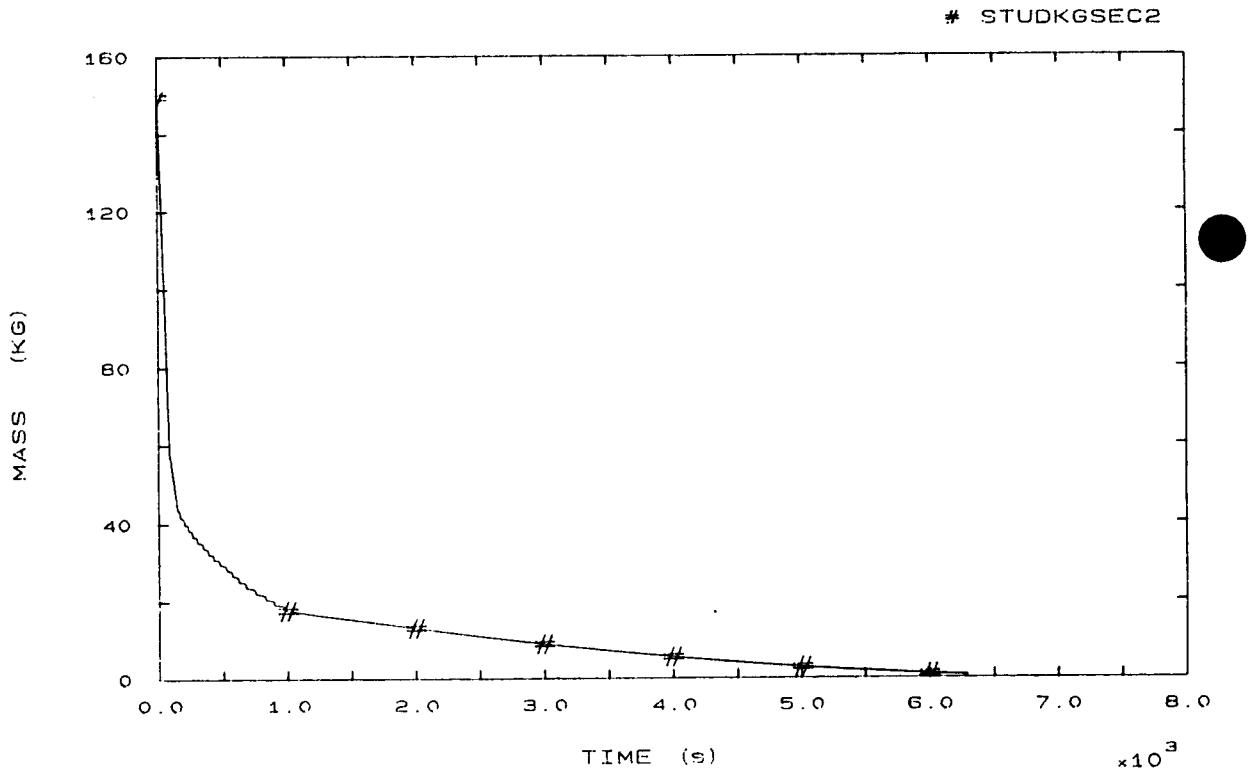

FIG. 87 SECONDARY COOLANT TOTAL MASS SG2

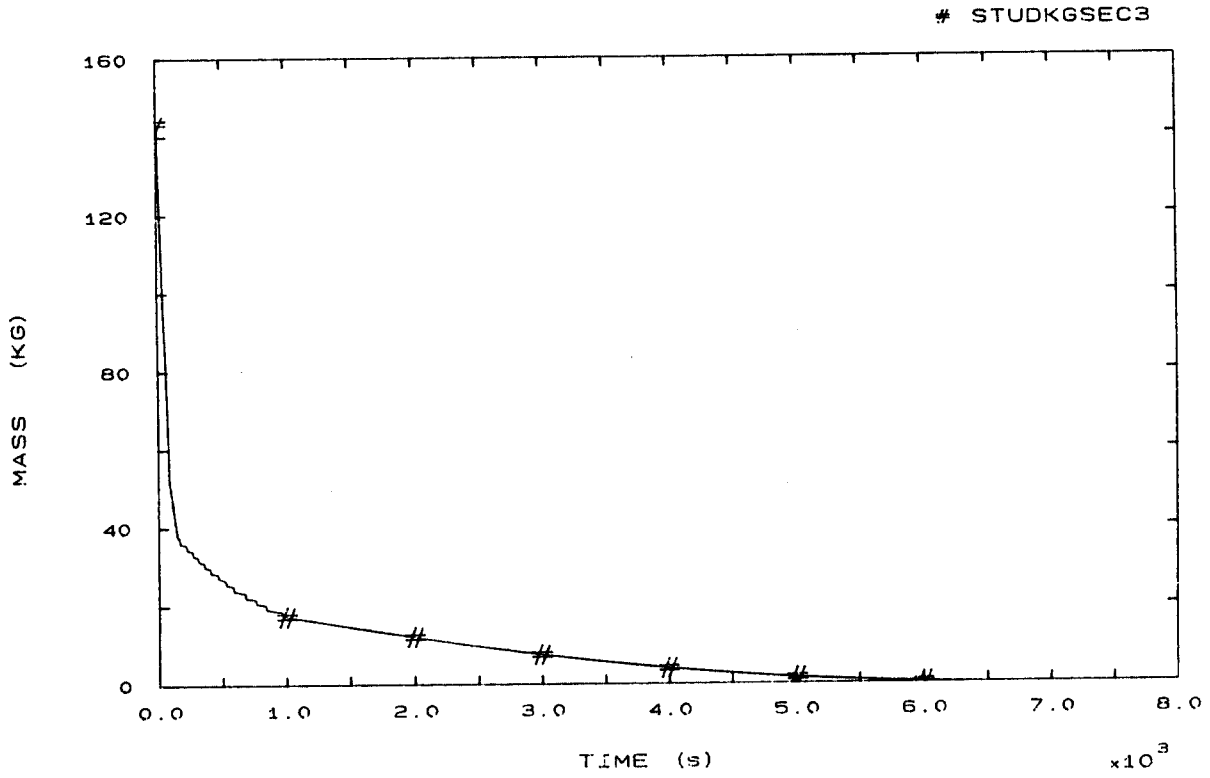

FIG. 88 SECONDARY COOLANT TOTAL MASS SG3

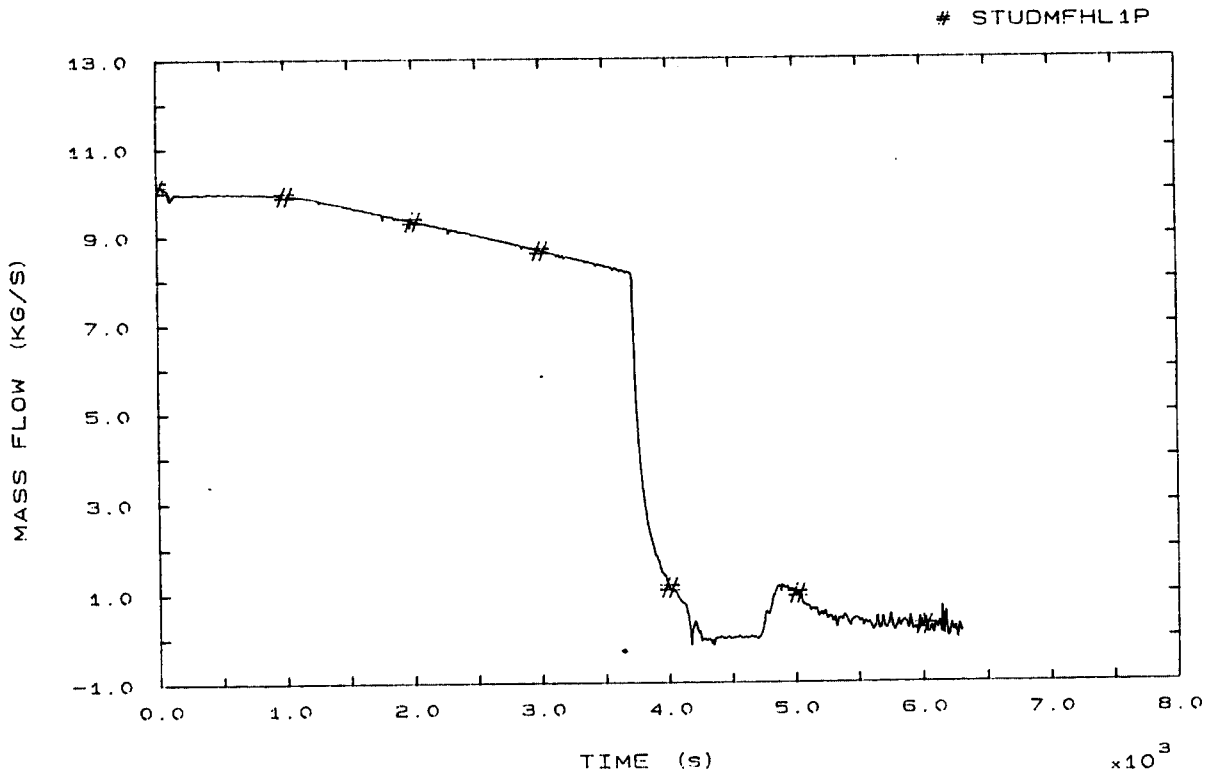

FIG. 89 HOT LEG 1 MASS FLOW

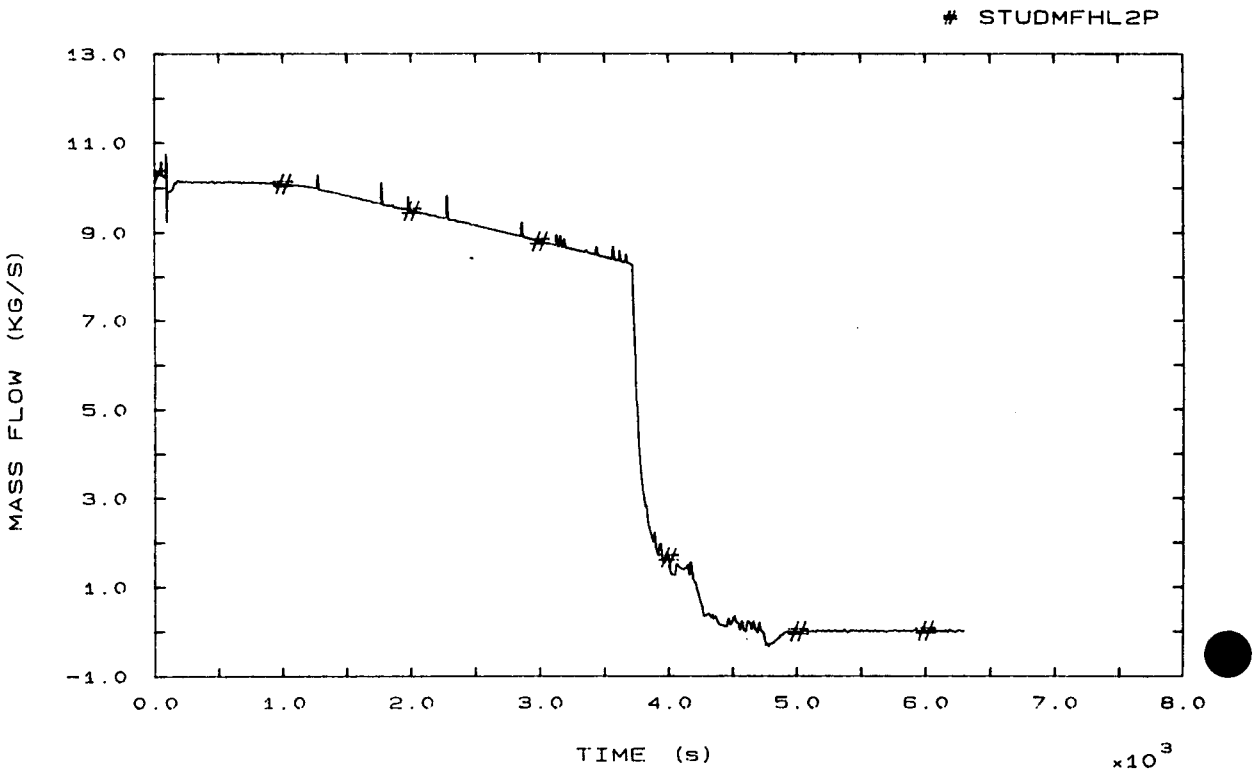

FIG. 90 HOT LEG 2 MASS FLOW

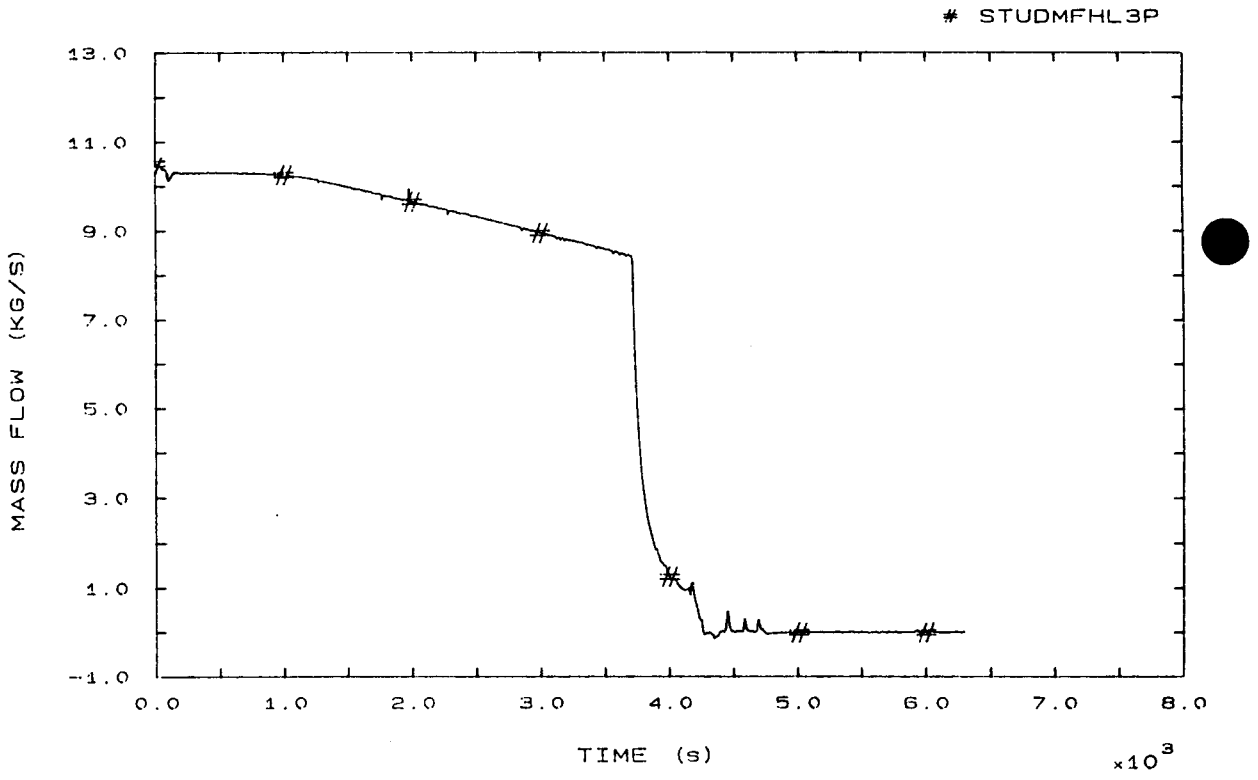

FIG. 91 HOT LEG 3 MASS FLOW

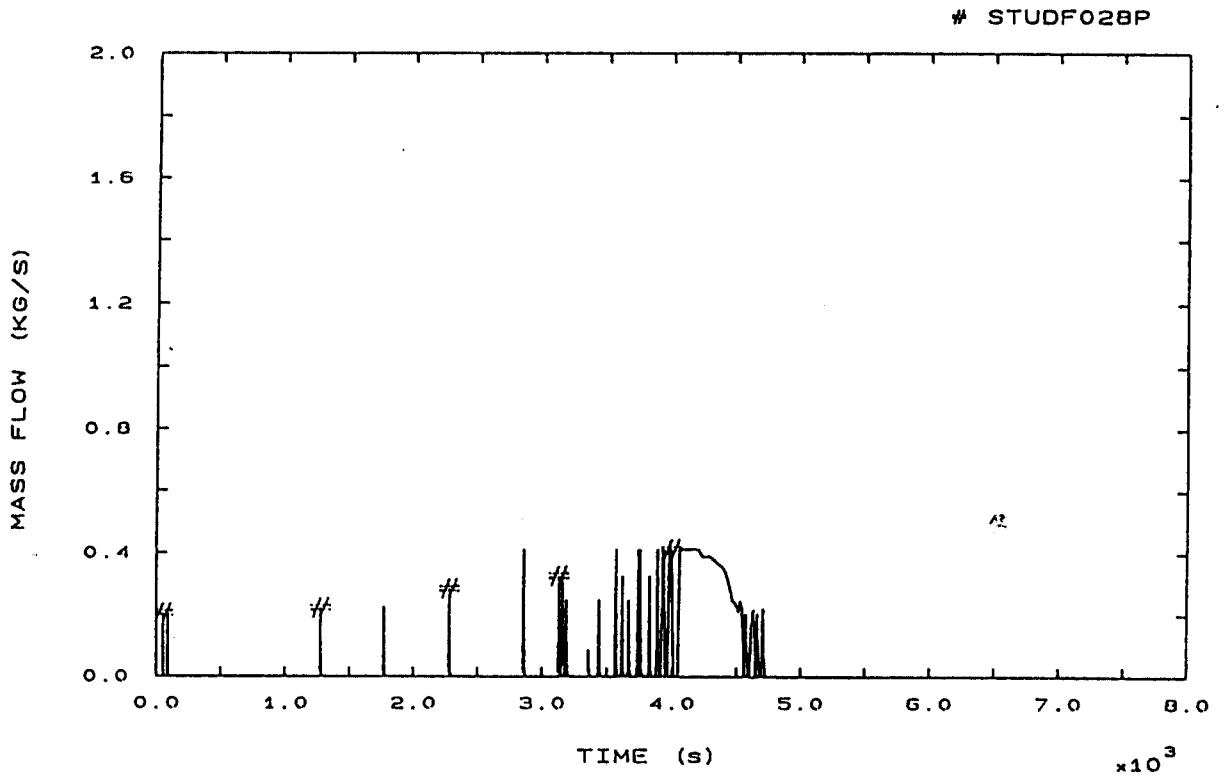

FIG. 92 PRZ PORV MASS FLOW

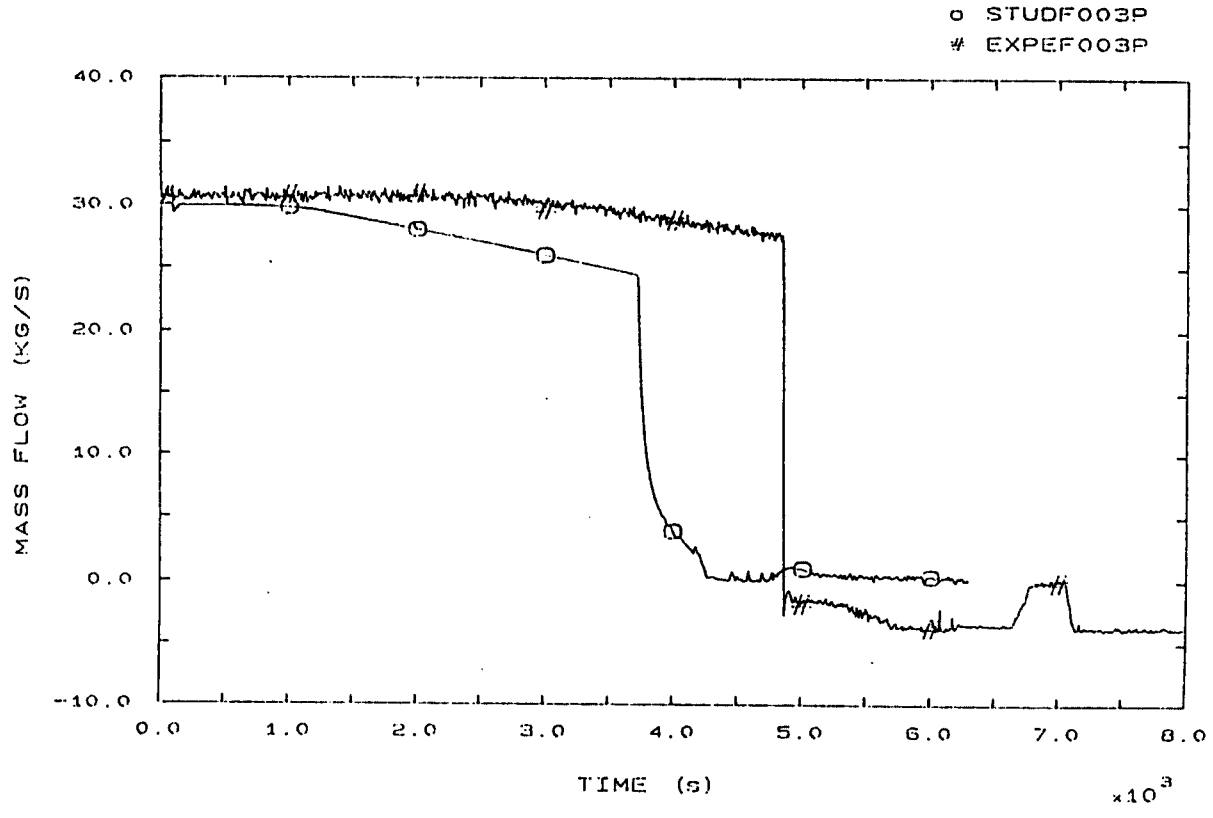

FIG. 94 VESSEL DOWNCOMER MASS FLOW

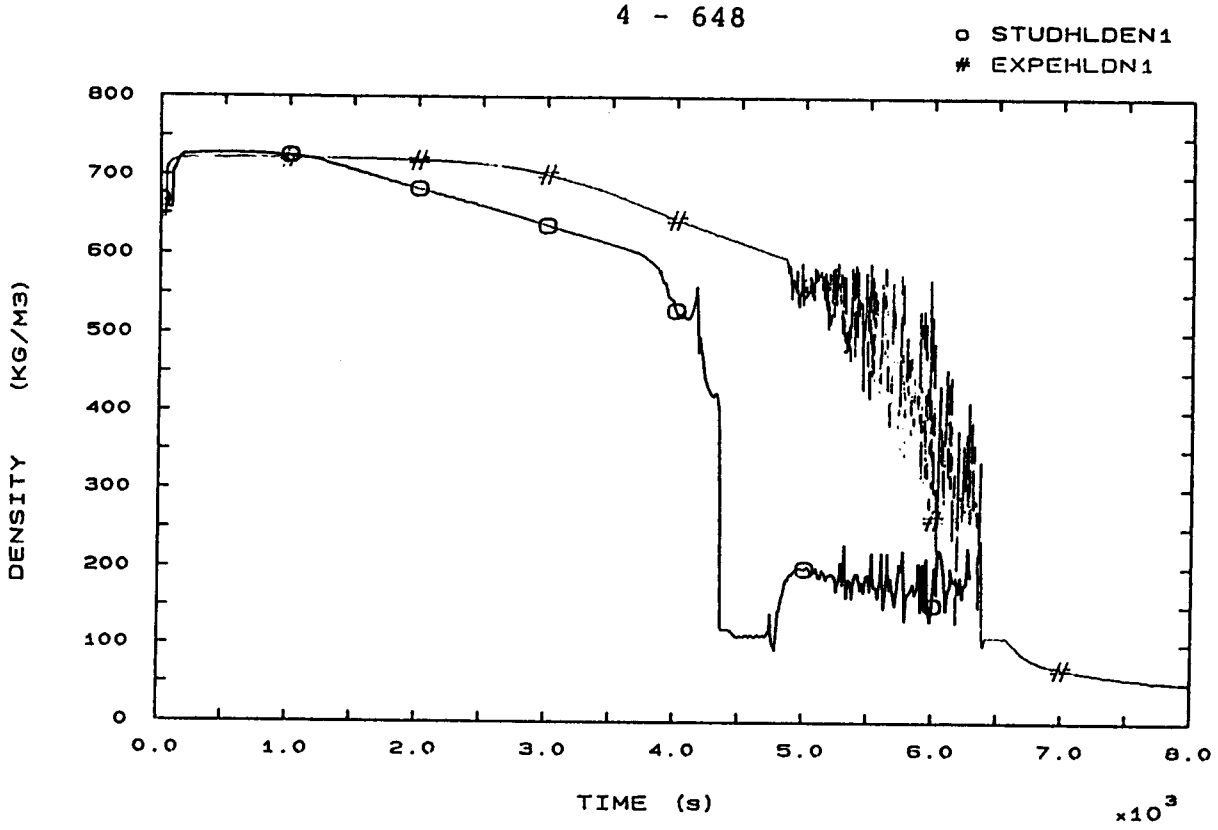

FIG. 100 HOT LEG 1 FLUID DENSITY

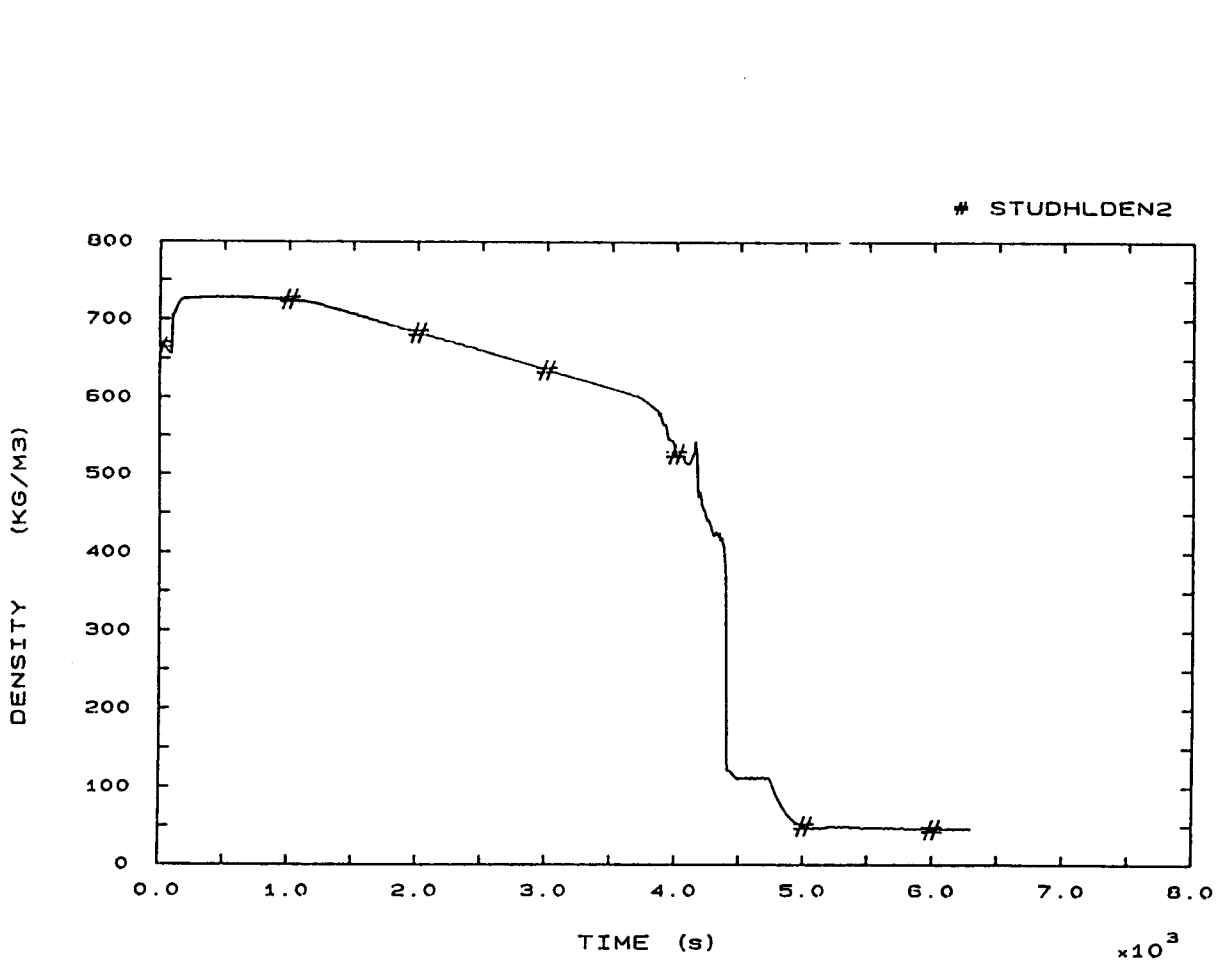

FIG. 101 HOT LEG 2 FLUID DENSITY

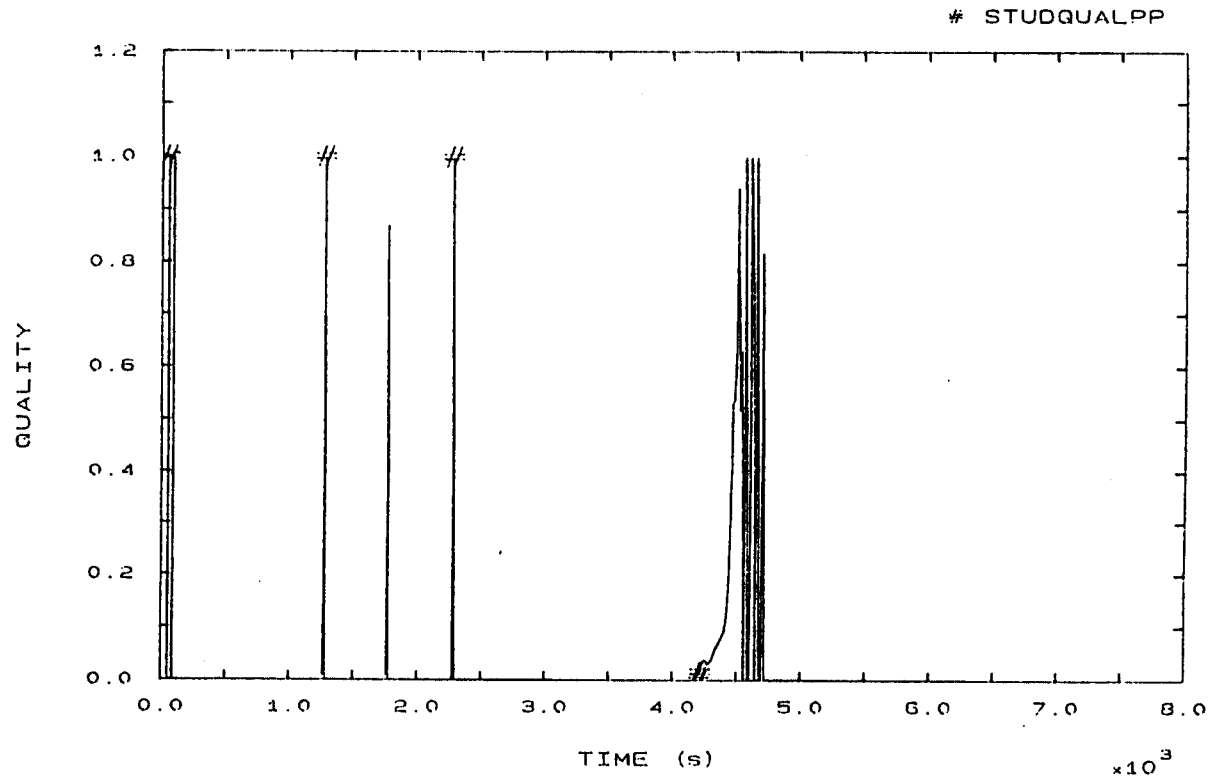

FIG. 103 PRZ PORV FLOW QUALITY

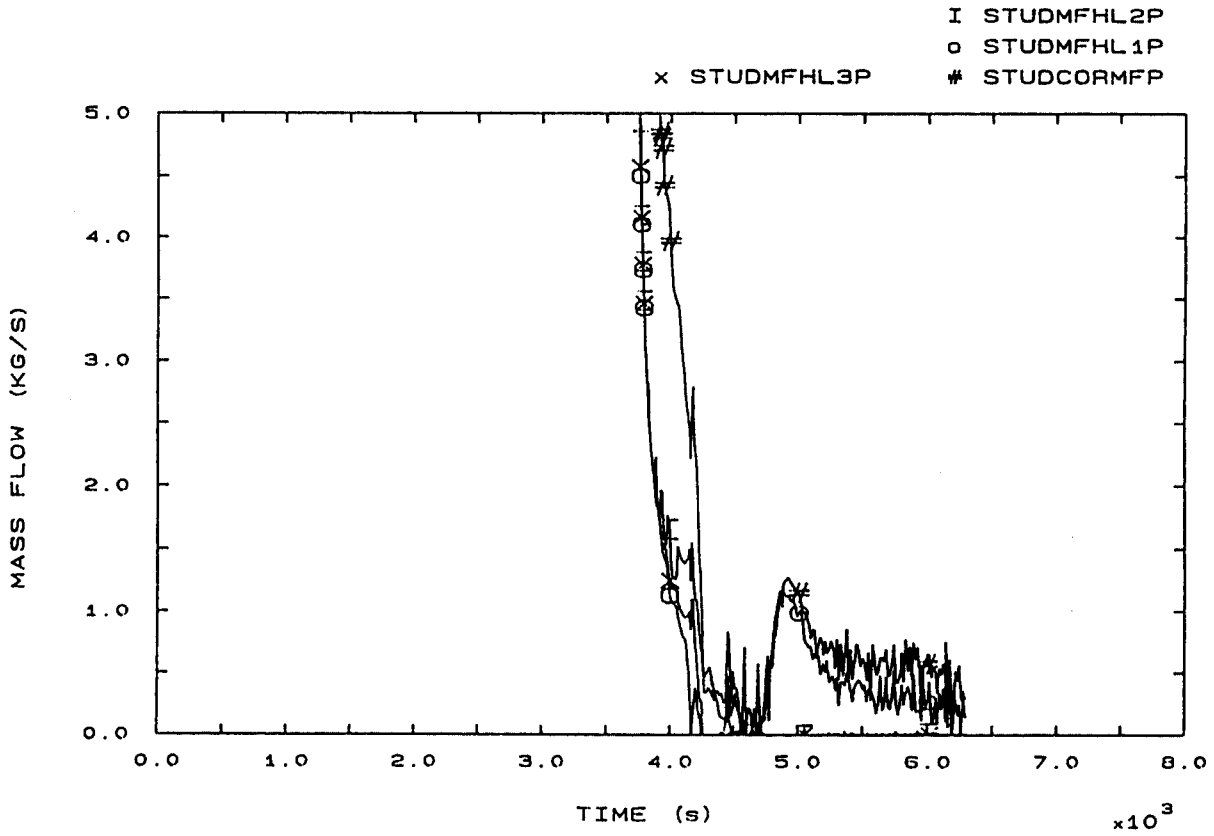

FIG. 141 BOTTOM CORE AND HOT LEG MASS FLOWS

4.16 SWCR

4.16.1 CALCULATION DESCRIPTION

Phase 1: from LOFW to Scram (0,53 s)

Following LOFW a rapid SG level decrease occurs (fig. 7b, 8b, 9b). Low Low level signal is generated at 42 s. Main steam isolation takes place 5 s later and causes secondary pressure to rise consistently above PORV set point (fig. 3b, 4b, 5b). Primary temperature (fig. 12, 42) follows secondary pressure, causing primary level and pressure to rise accordingly (fig. 1b, 6b). Scram occurs at 53 s (fig. 81b) followed by a rapid temperature and pressure fall (fig. 1b, 12b, 42b).

Phase 2: from Scram to the end of calculation (53-1000 s)

SGs go empty very rapidly (fig. 7, 8, 9): extrapolated Dry Out time is about 1100 s. During secondary boil-off primary temperature stabilizes (fig. 12, 42), then rises in proximity of SGs dry out. In this period primary pressure and PRZ level slowly decrease (fig. 1, 6). Secondary pressure is maintained by PORVs cycling (fig. 3, 4, 5).

PARTICIPANT: CHEN - SWCR *CODE: RELAP5/MOD1*

EVENTS TABLE

EVENT	*CALC. TIME (s)*	*EXP. TIME (s)*
SG Low Low Level	*42*	*33*
Main Steam Isolation	*47*	*38*
Scram (power fall), t_1	*53*	*44*
SGs PORV opening	*52*	*82 (3)*
	52	*106 (2)*
	52	*200 (1)*
SGs Dry Out (extrap.)	*1100*	*3282 (3)*
	1100	*3347 (1)*
	1100	*3437 (2)*
PRZ PORV opening, t_2	*CALC. FAILURE*	*4134*
PRZ full of liquid		*4222*
Pumps Trip, t_3		*4848*
Loss of Natural Circulation		*5630*
Beginning of Core Heat Up		*6511*
EFW actuation, t_4		*6532*
PRZ PORV closure		*6576*
PRZ emptying		*6811*
SG1 repressurization		*6878*
End of transient, t_{END}		*8062*

4.16.2 CALCULATION/EXPERIMENT COMPARISON

Phase 1: from LOFW to Scram

Initial steam generator inventory is underestimated for SG2 and SG3, but is overpredicted for SG1 (see Comp. Table).
Trips timing is slightly delayed: lo lo level set point is reached at 42 s w.r.t. 33 s in the Exp. This may be explained by the higher initial levels (fig. 7b, 8b, 9b). Secondary inventory at scram time is therefore slightly underpredicted (see Comp. Table and fig. 142b). Maximum primary pressure is correctly calculated (fig. 1b). Secondary pressure rises following LOFW and MSI are both overpredicted (fig. 3b, 4b, 5b) probably due to secondary heat structures modelling.

Phase 2: from Scram to PRZ PORV opening

Secondary PORVs opening is calculated to occur much earlier than in the Exp. (52 s), practically in coincidence with scram and only 5 seconds after MSI (see fig. 3b, 4b, 5b and C.T.). Minimum primary pressure after Scram is slightly underpredicted (14.1 MPa vs 14.5). PRZ level gradient during an approximately constant temperature time interval (270-400 s) is in good agreement with the exp. value (see Comp. Table and fig. 6, 12). Minimum PRZ level during phase 2 is overpredicted (2.8 m vs 2.3) due to the short duration of thermal equilibrium period. Time of SGs dry out (extrapolated on the grounds of provided calculated data) is about 1100 s, extremely underpredicted w.r.t. 3300 s in the Exp. This is partially due to the low secondary inventory at scram time but mainly caused by the faster level decrease (see fig. 7,8,9) due to low primary and secondary heat losses (see fig. 131, 139). Primary pressure gradient during secondary emptying is wrongly calculated (fig. 1): this may be related do difficulties in modelling the PRZ.

PARTICIPANT: CHEN - SWCR CODE: RELAP5/MOD1

COMPARISON TABLE

PARAMETER		EXP	CALC	AE*	RFD**
1A Initial SGs mass (Kg)	1	137	145		
	2	151	141	S	B+C+U?
	3	145	136		
1B Trips timing (s)	LoLo	33	42		HIL(B+C+U)
	MSI	38	47	S	LoLo
	Scram	44	53		LoLo
1C Max primary pressure (MPa)		16.2	16.1	G	-
1D SGs mass at Scram (Kg)	1	98	95	G	
	2	105	91	S	1A+1B
	3	97	86	S	
2A Min. primary pressure (MPa)		14.5	14.1	S	-
Pressure gradients before		4.10^{-4}	-6.10^{-4}	P	PRZM(B+U)
and after SGs DO (MPa/s)		3.10^{-4}	n.a.	-	-
2B SGs PORV opening time (s)	1	200	52		
	2	106	52	P	HSM? (U)
	3	82	52		
2C PRZ level gradient (m/s)		$-5.7.10^{-4}$	-7.10^{-4}	G	-
2D Min. PRZ level (m)		2.3	2.8	S	-
2E SGs DO time, tSG1DO (s)		3347	1100		1D +
tSG2DO (s)		3437	1100	P	LHL (U)
tSG3DO (s)		3282	1100		
2F Heat Up temperature (K/s)		0.02	CALC. FAILURE		
and level (m/s) gradients		$3.6.10^{-3}$			
2G Cool Insurge effect		PR. DELAY			
2H PRZ PORV opening time, t2 (s)		4134			
$(dt_2 = t_2 - t_{SGDO})$		(697)			
3A PRZ level at t_2 (m)		6.57			
3B PRZ full time, t_{PRZF} (s)		4222			
$(dt_{PRZF} = t_{PRZF} - t_2)$		(88)			
3C Dominant Relief Condition		LIQ			
3D Sat. Conditions before trip		NO			
3E Pumps Trip time, t3 (s)		4848			
$(dt_3 = t_3 - t_2)$		(714)			
$(dt_{HU} = t_3 - t_{SGDO})$		(1411)			

* ACCURACY EVALUATION : G=GOOD, S=SUFFICIENT, P=POOR

** REASON FOR DISCREPANCY : B=BIC, C=CODE, U=USER, PRZM=PRZ MODELLING, HIL= HIGH INITIAL LEVEL, LHL=LOW HEAT LOSSES, HSM=HEAT STRUCTURES MODELLING

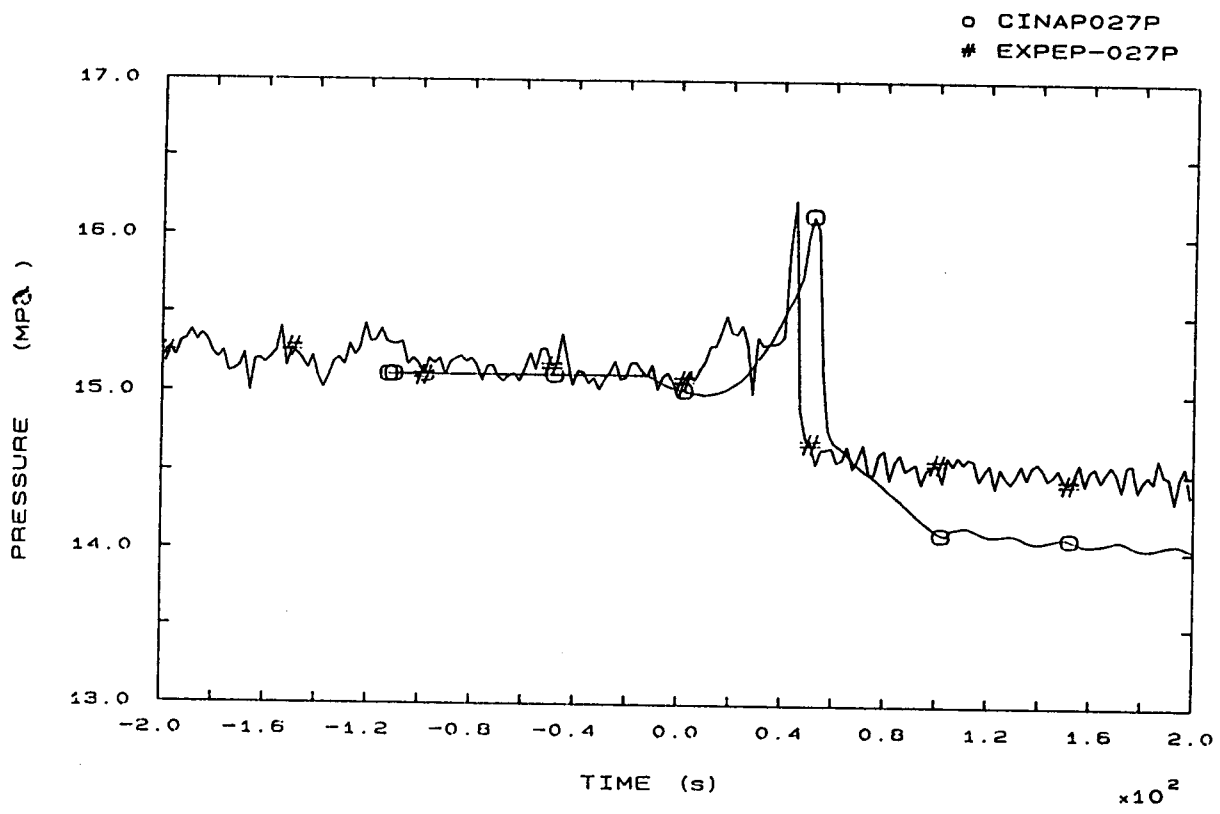

FIG. 1b PRESSURIZER PRESSURE

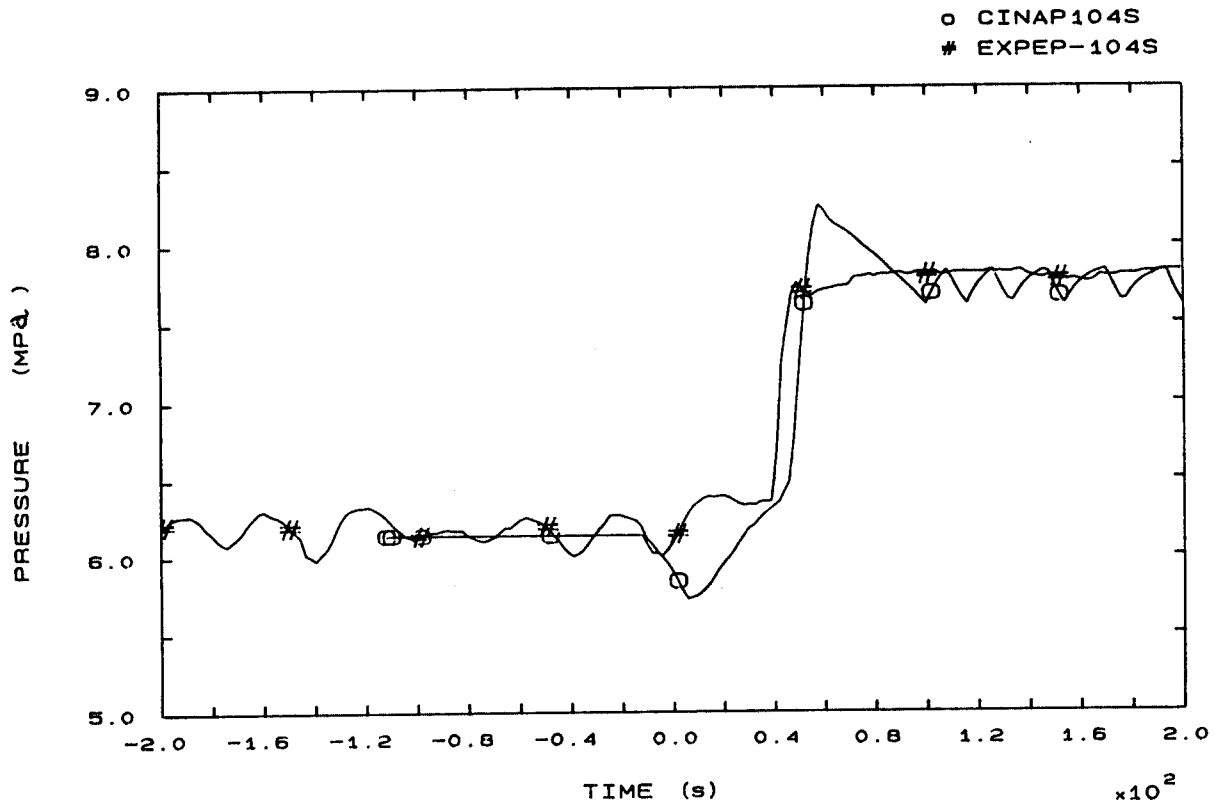

FIG. 3b SG1 STEAM DOME PRESSURE

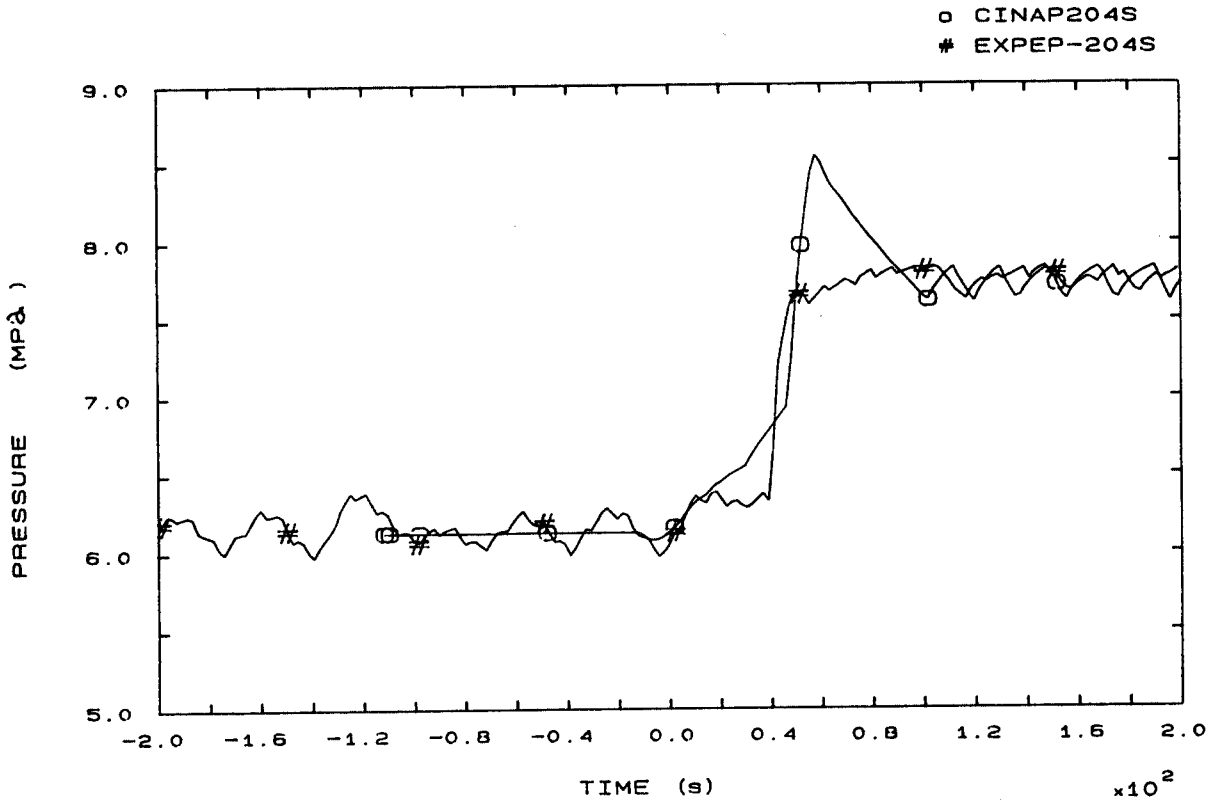

FIG. 4b SG2 STEAM DOME PRESSURE

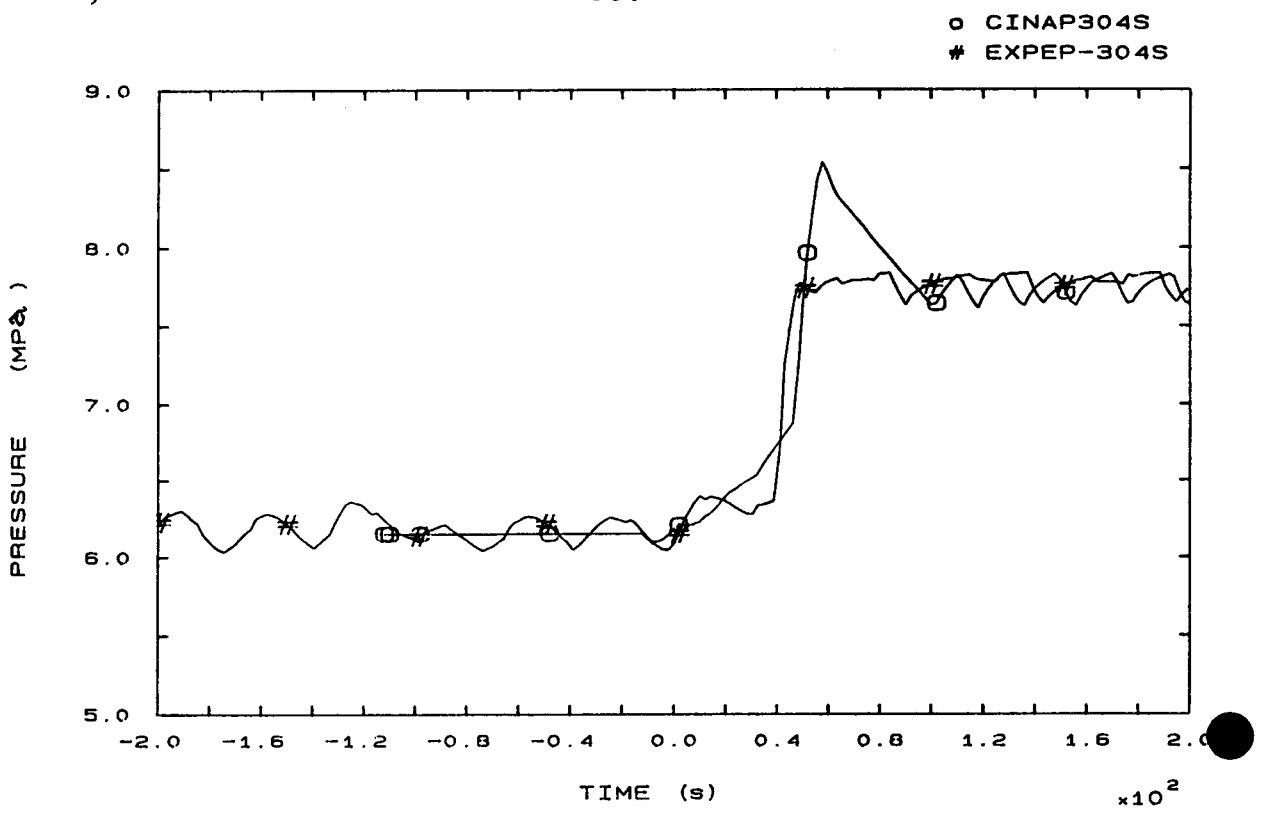

FIG. 5b SG3 STEAM DOME PRESSURE

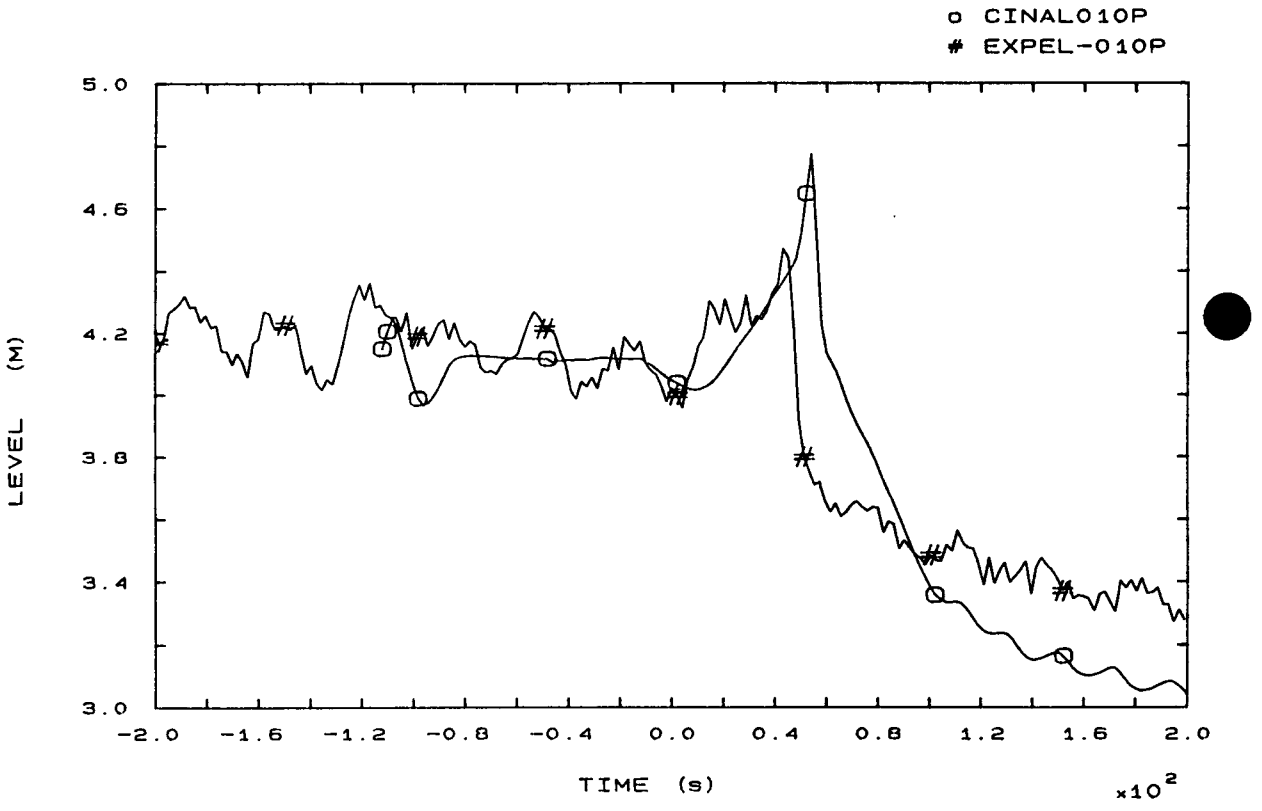

FIG. 6b PRESSURIZER LEVEL

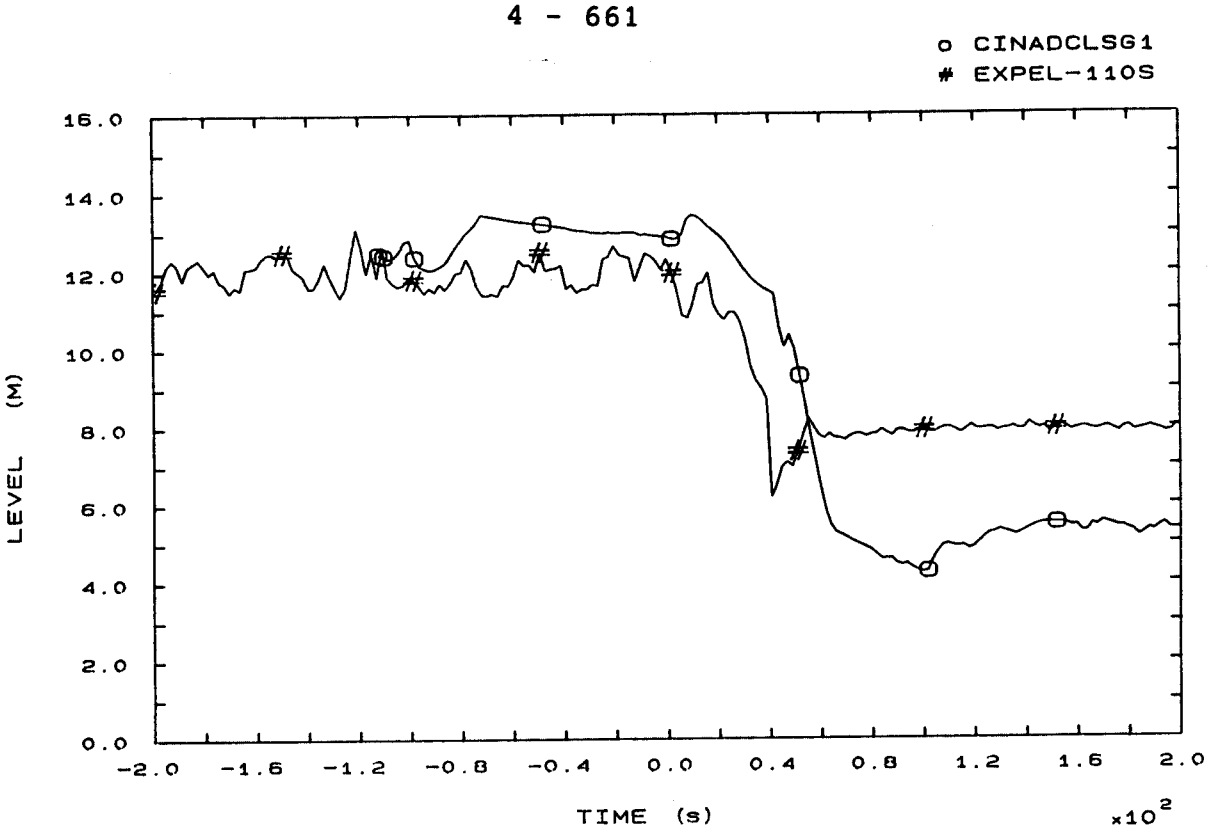

FIG. 7b SG1 DOWNCOMER LEVEL

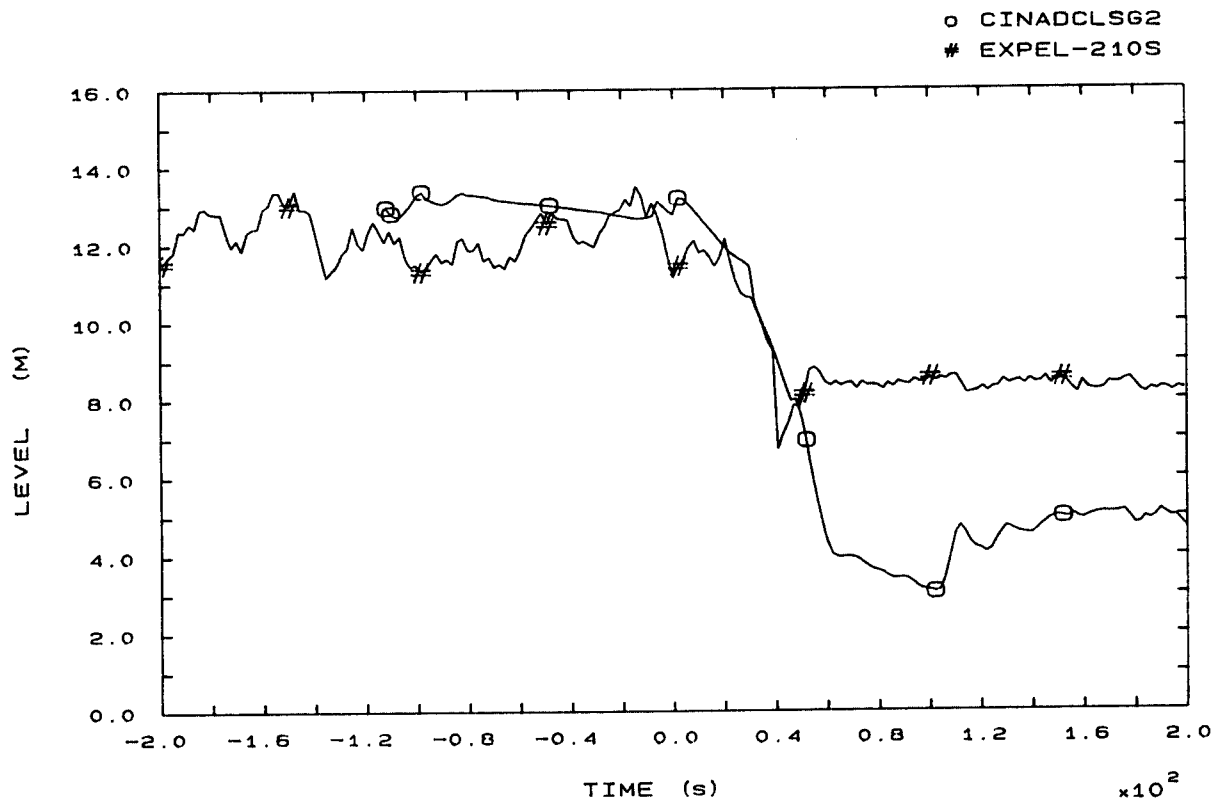

FIG. 8b SG2 DOWNCOMER LEVEL

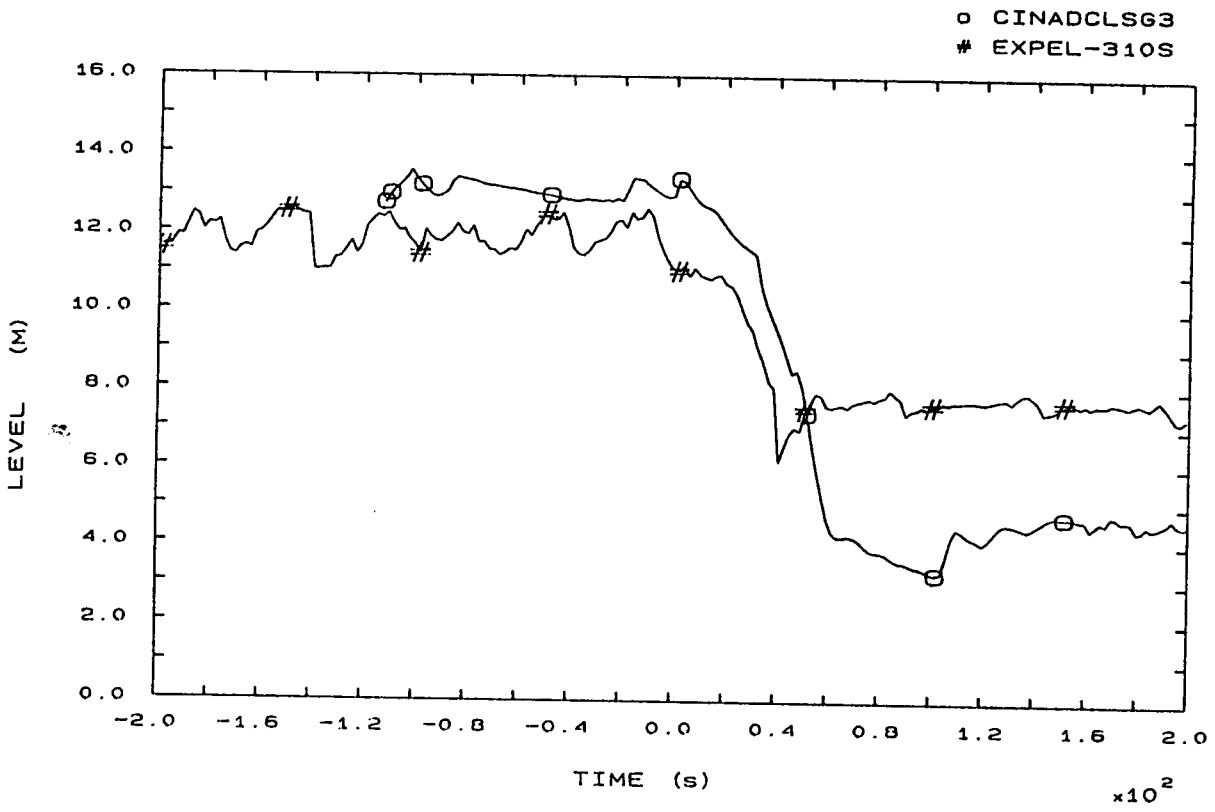

FIG. 9b SG3 DOWNCOMER LEVEL

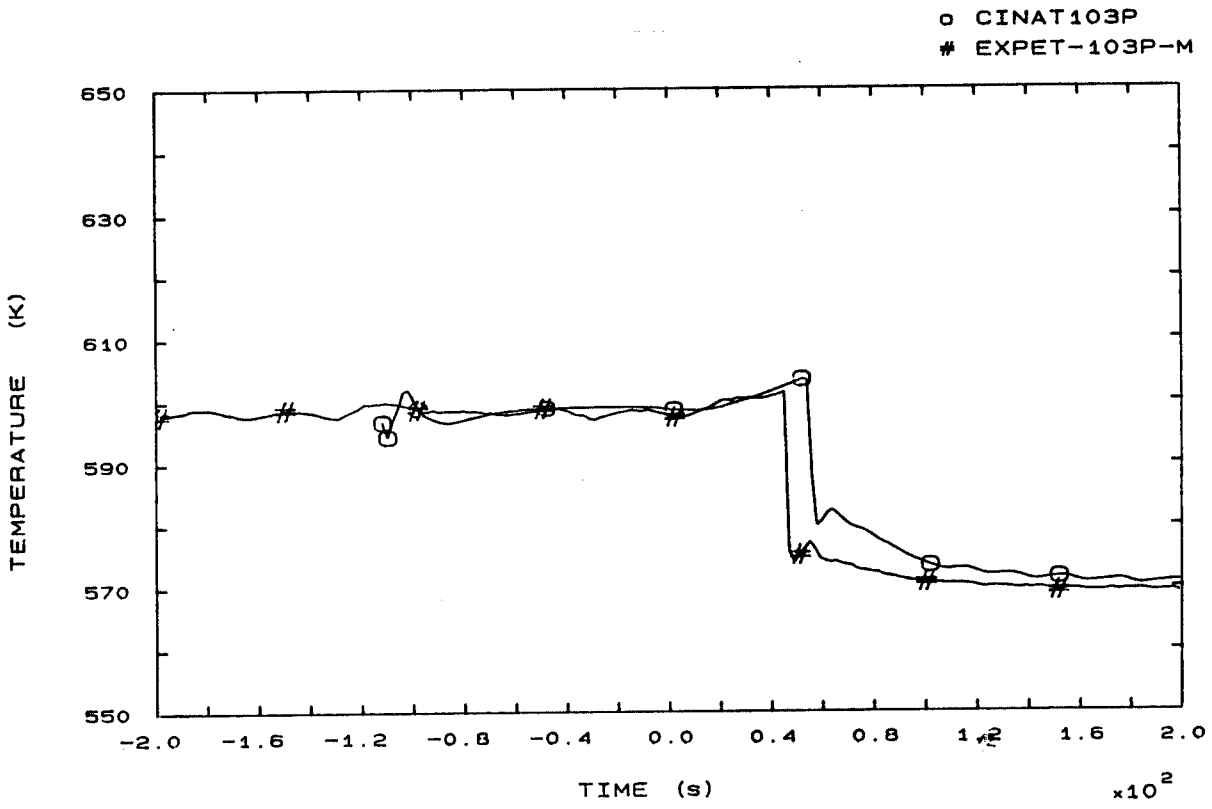

FIG. 12b LP1 HOT LEG OUTLET VESSEL TEMPERATURE

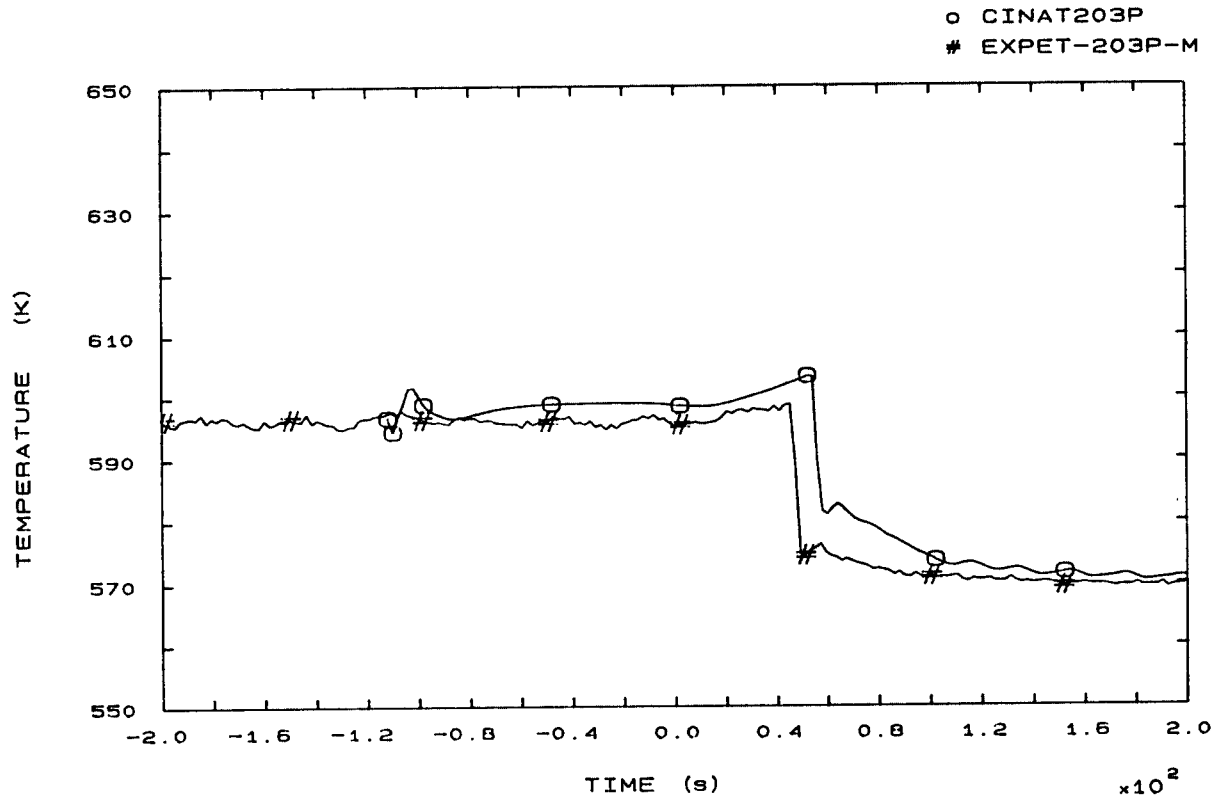

FIG. 22b LP2 HOT LEG OUTLET VESSEL TEMPERATURE

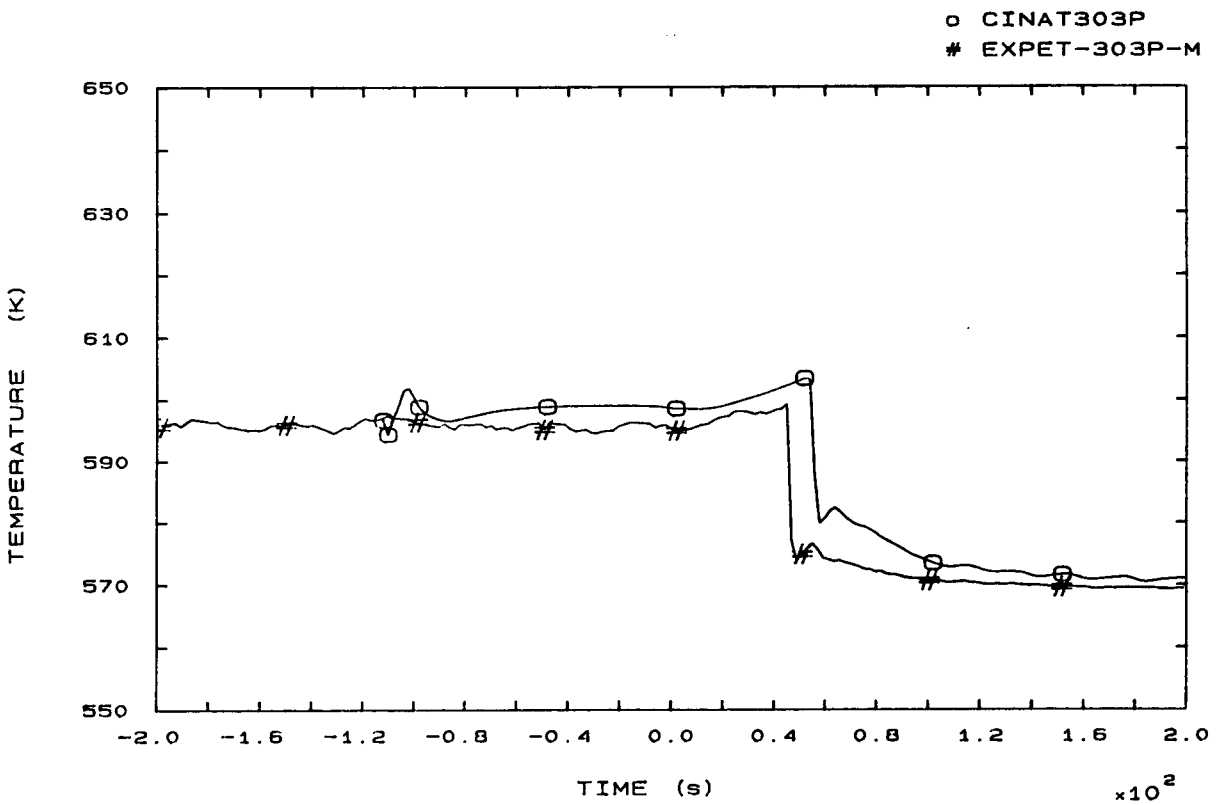

FIG. 32b LP3 HOT LEG OUTLET VESSEL TEMPERATURE

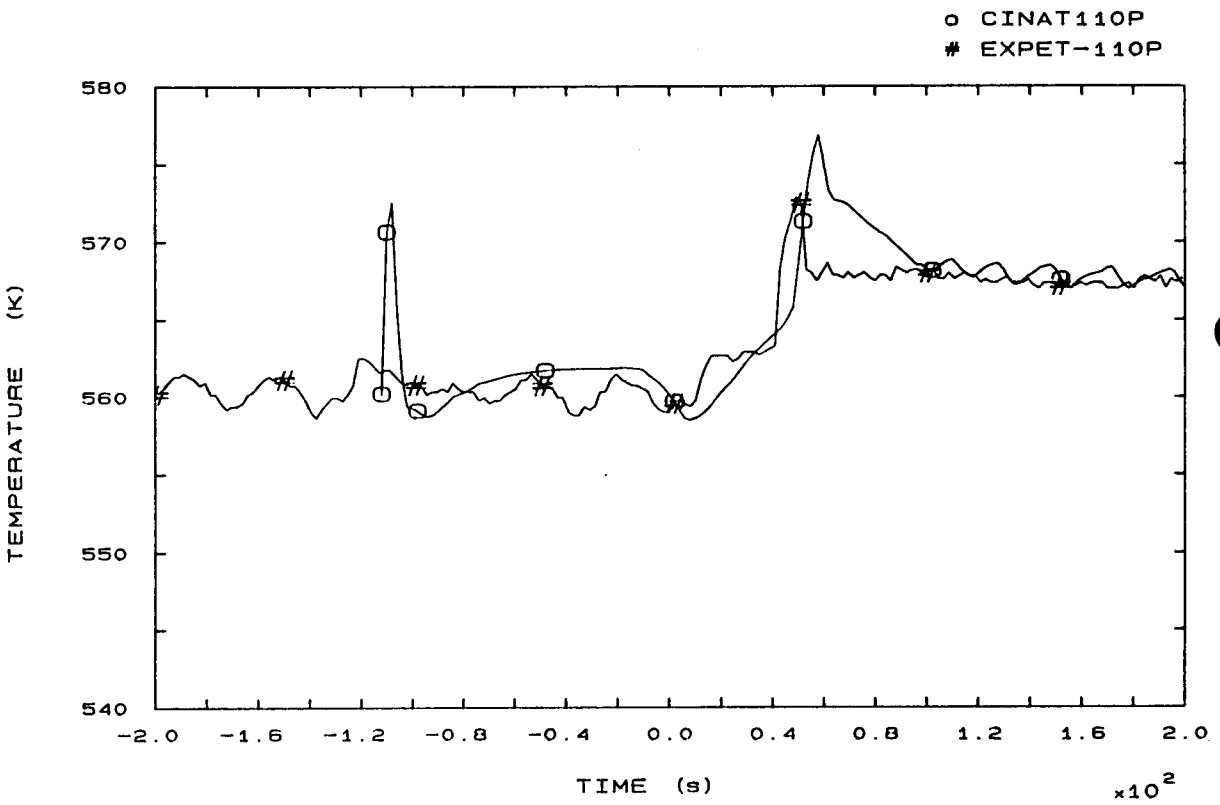

FIG. 42b SG1 OUTLET TEMPERATURE

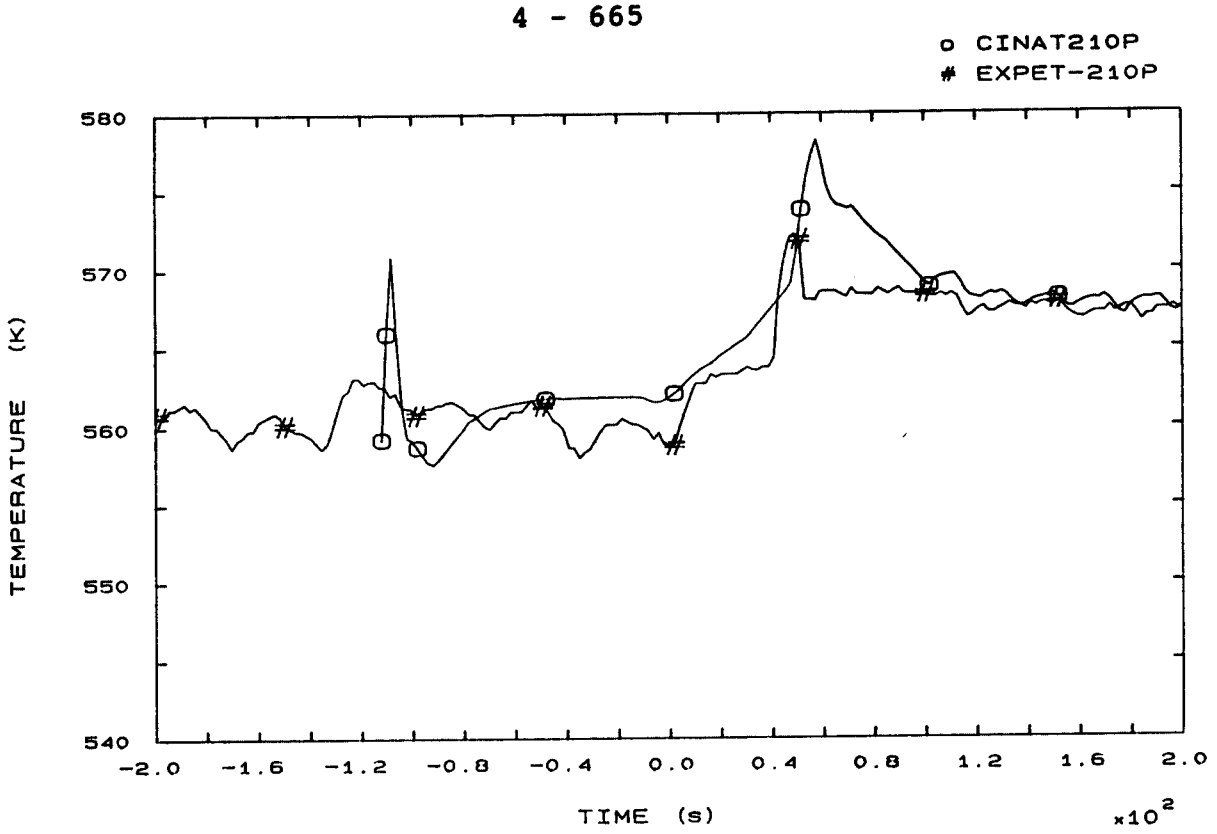

FIG. 44b SG2 OUTLET TEMPERATURE

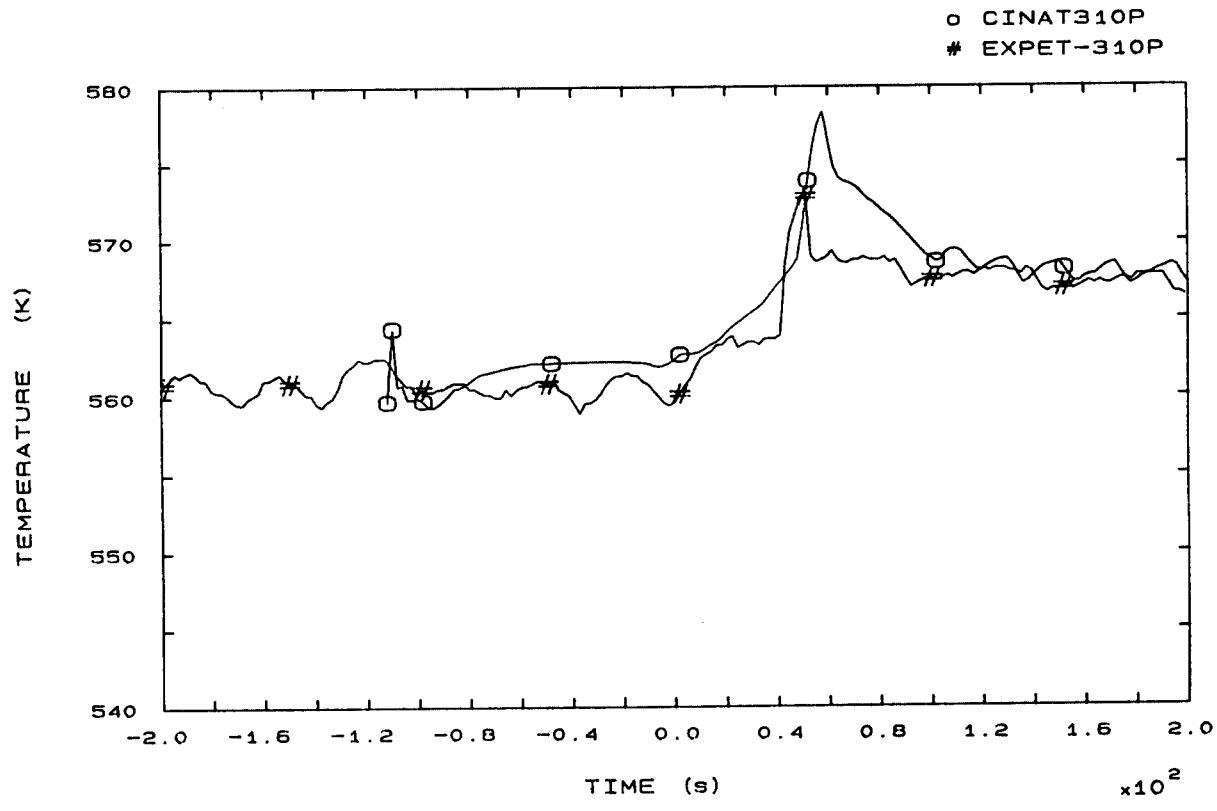

FIG. 46b SG3 OUTLET TEMPERATURE

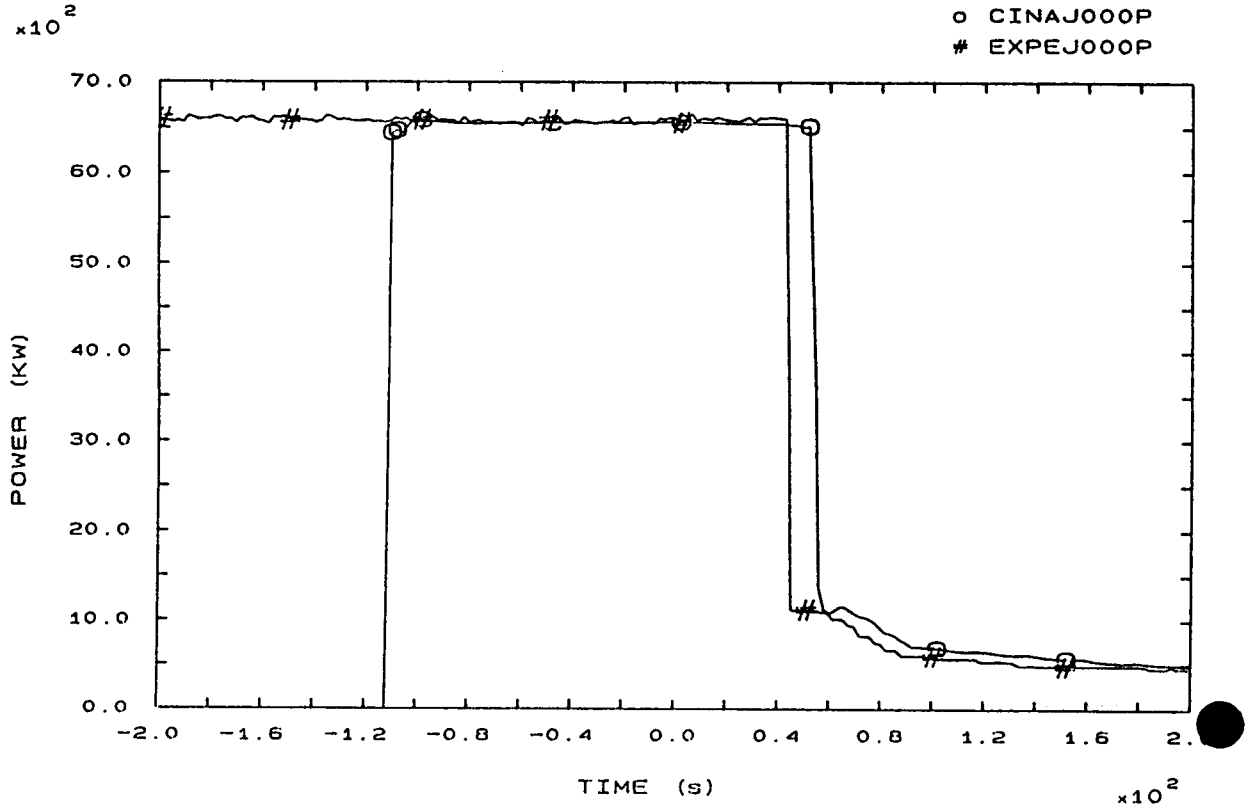

FIG. 81b HEATER RODS POWER

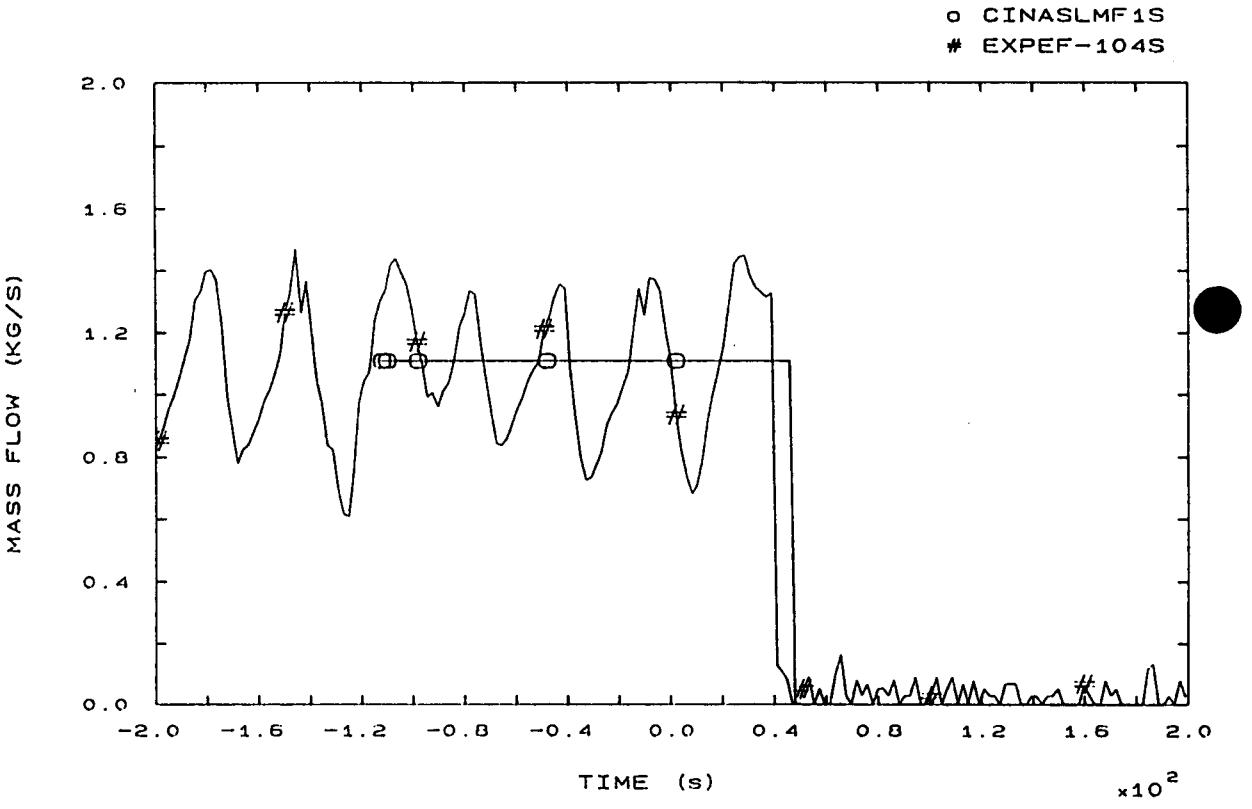

FIG. 96b STEAM LINE 1 MASS FLOW

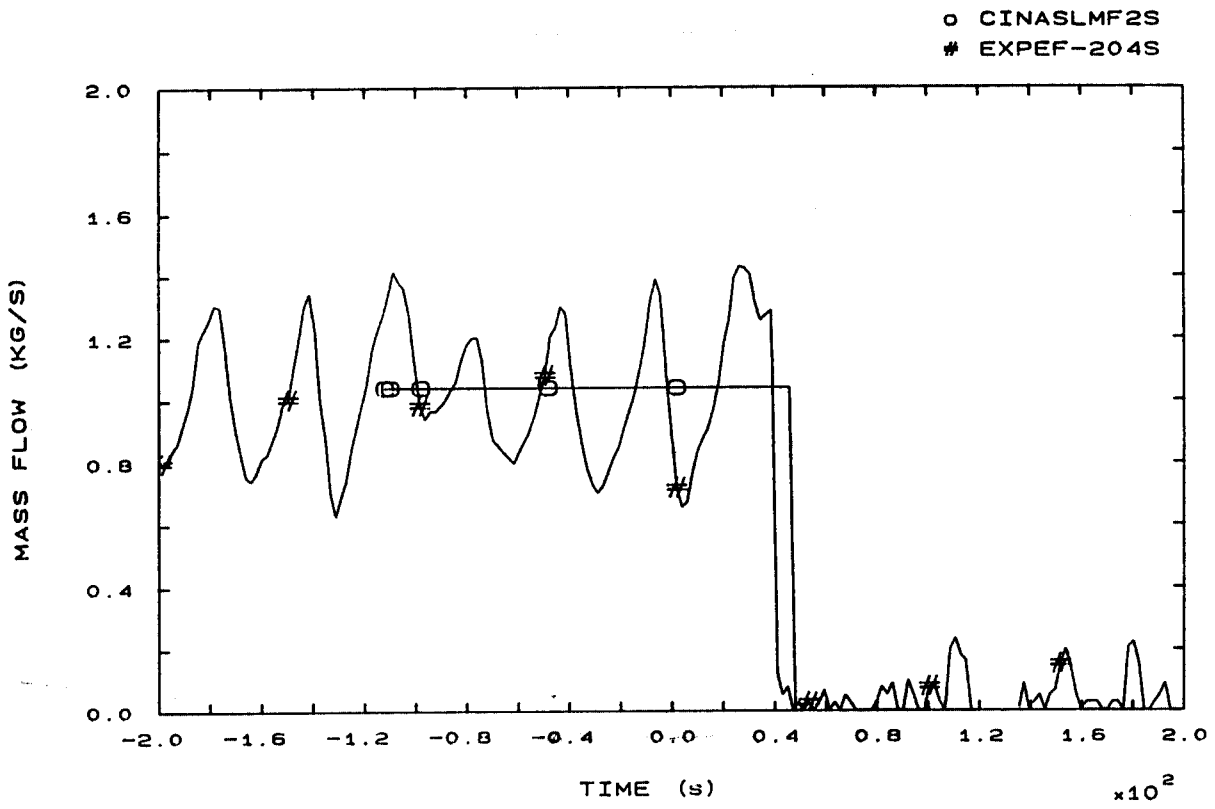

FIG. 97b STEAM LINE 2 MASS FLOW

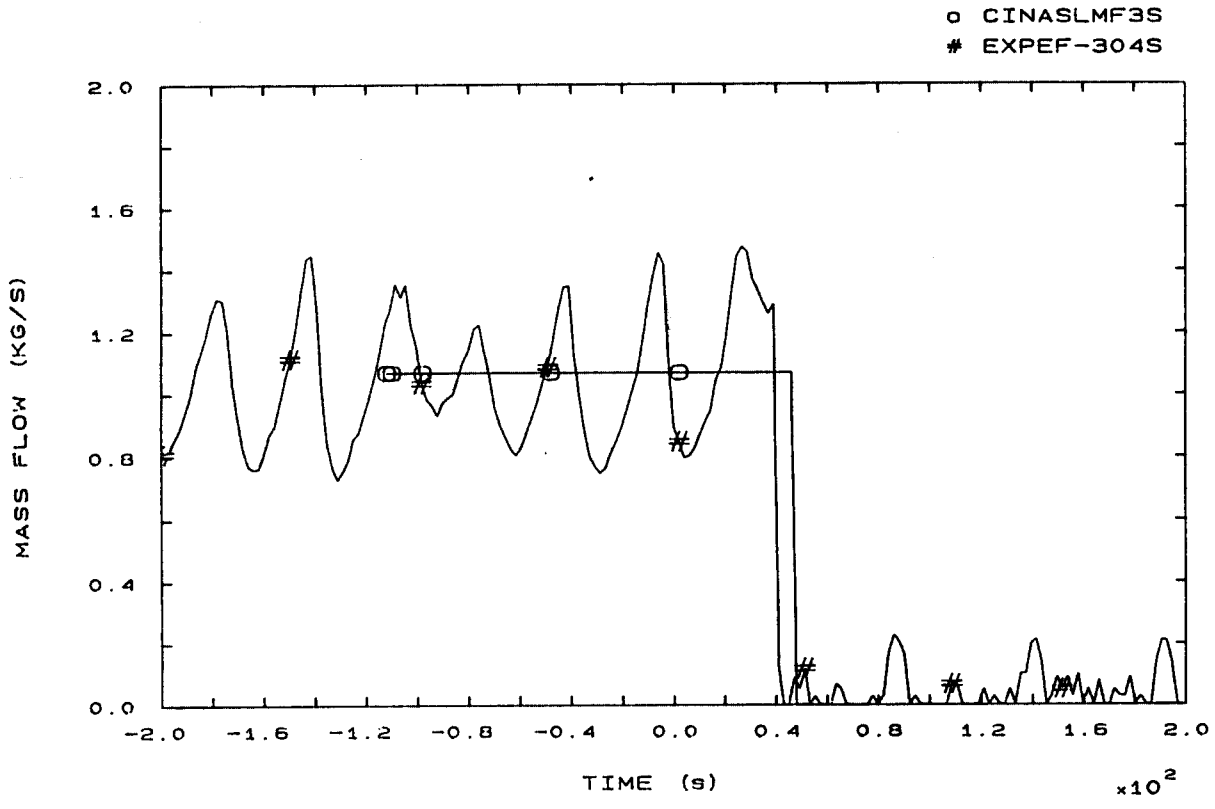

FIG. 98b STEAM LINE 3 MASS FLOW

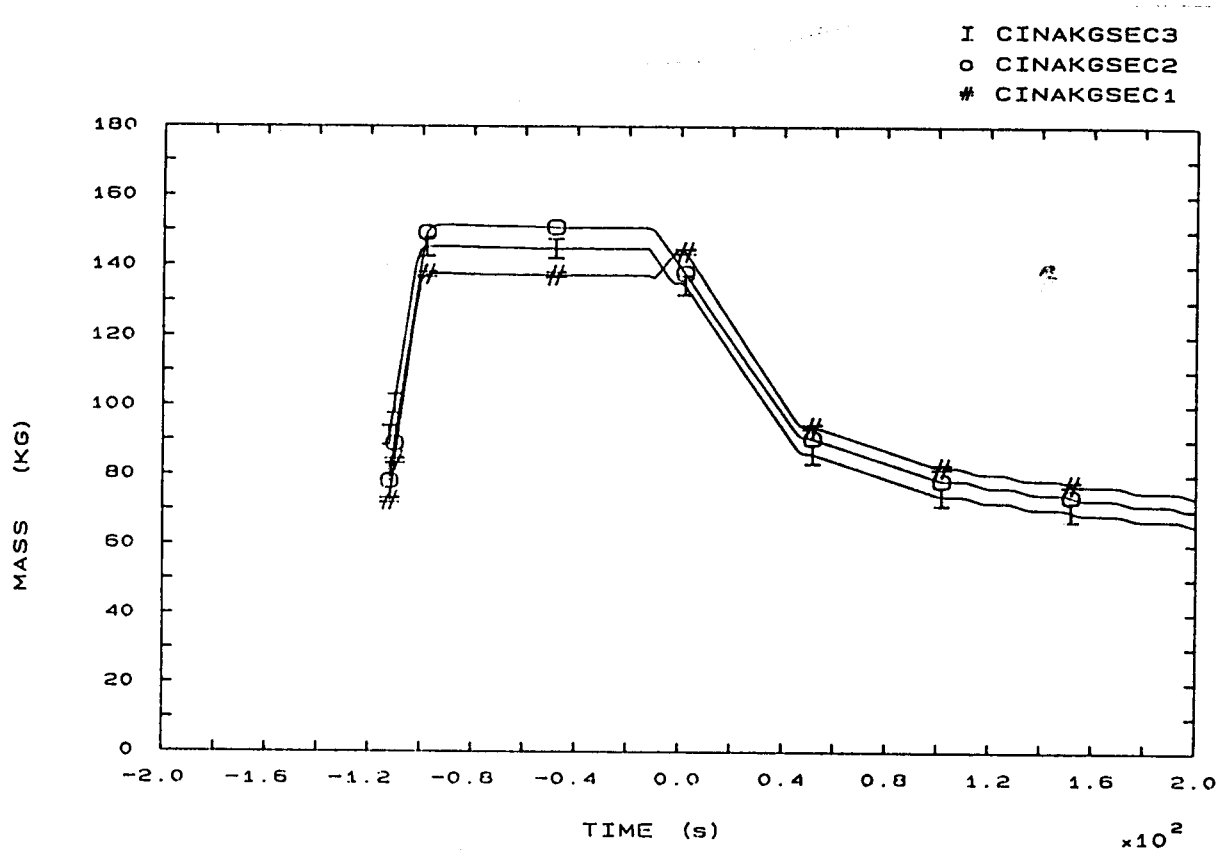

FIG. 142b SECONDARY COOLANT TOTAL MASS IN SGs

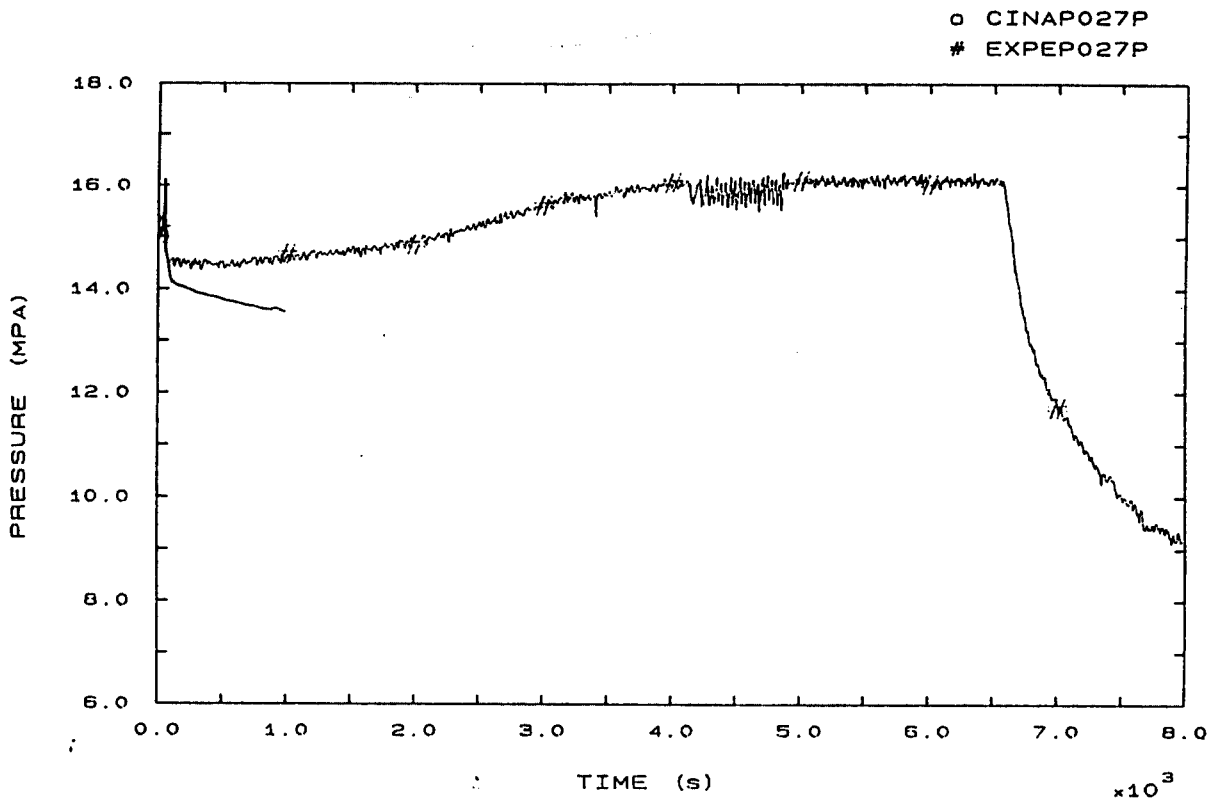

FIG. 1 PRESSURIZER PRESSURE

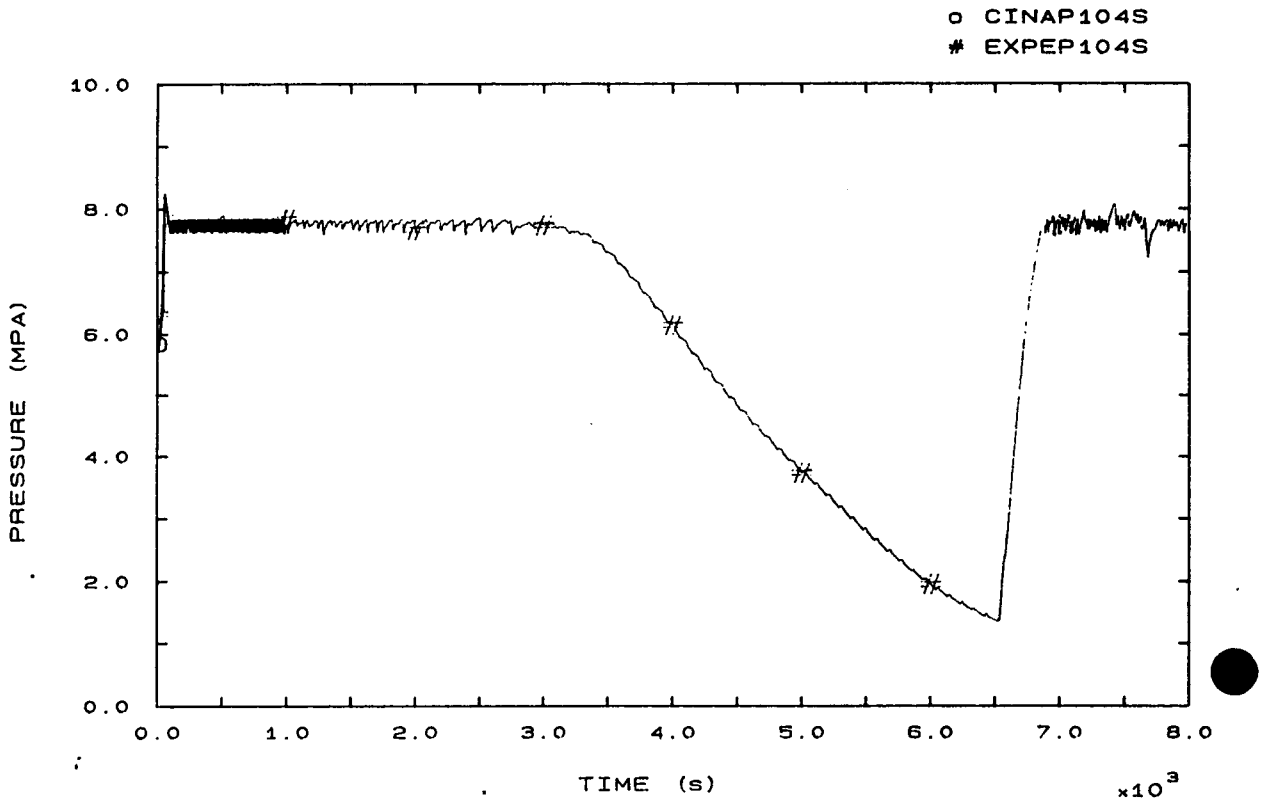

FIG. 3 SG1 STEAM DOME PRESSURE

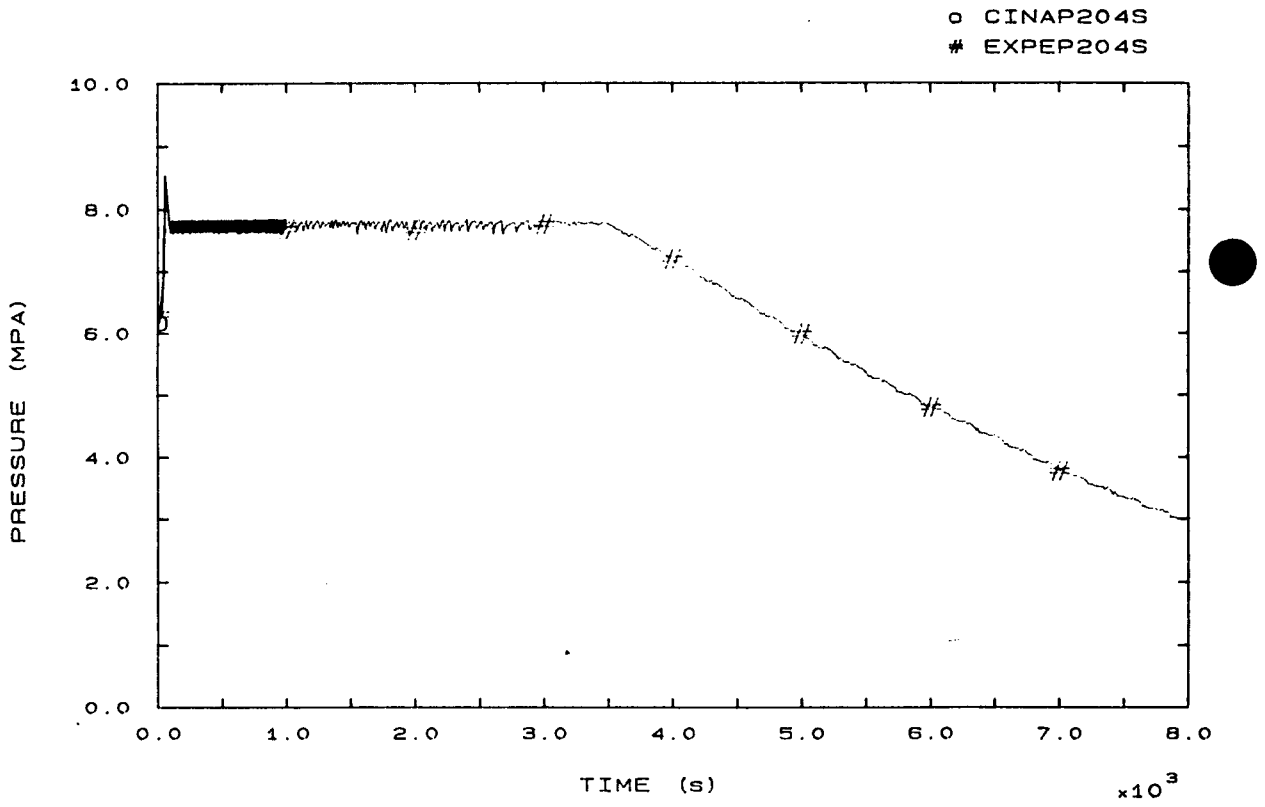

FIG. 4 SG2 STEAM DOME PRESSURE

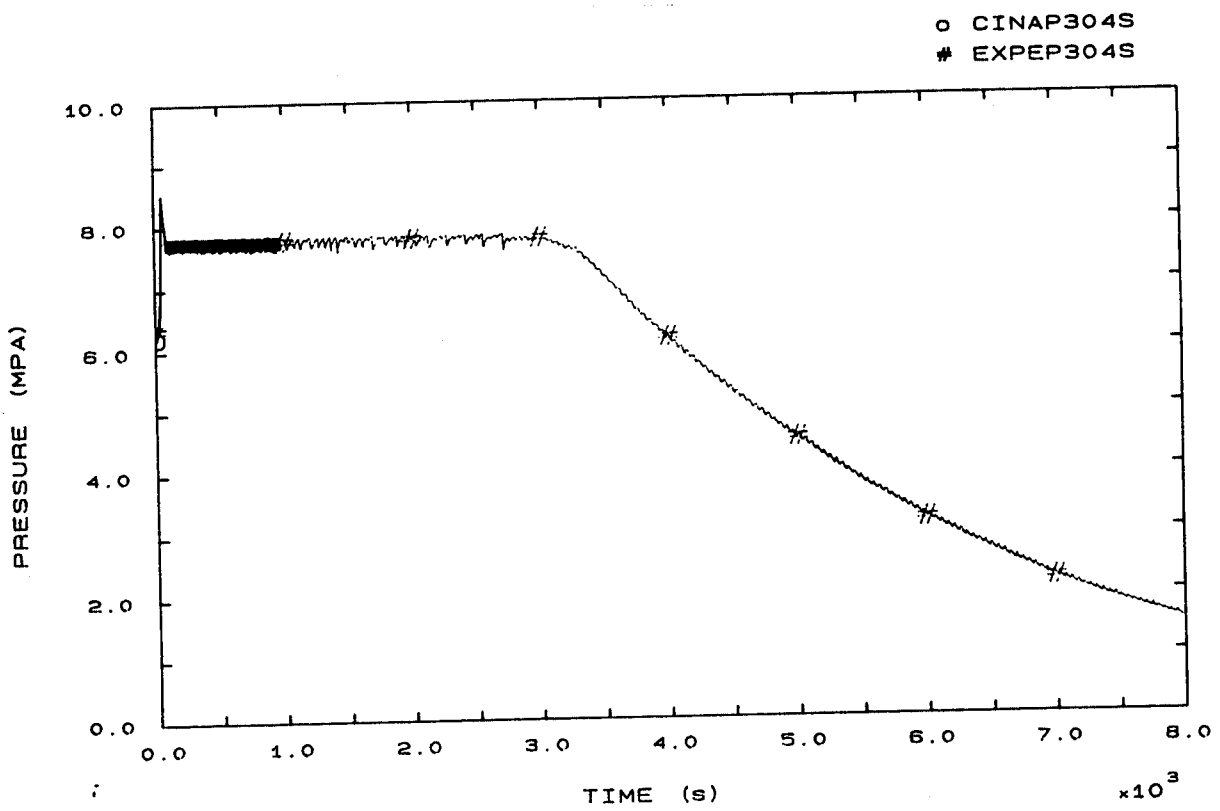

FIG. 5 SG3 STEAM DOME PRESSURE

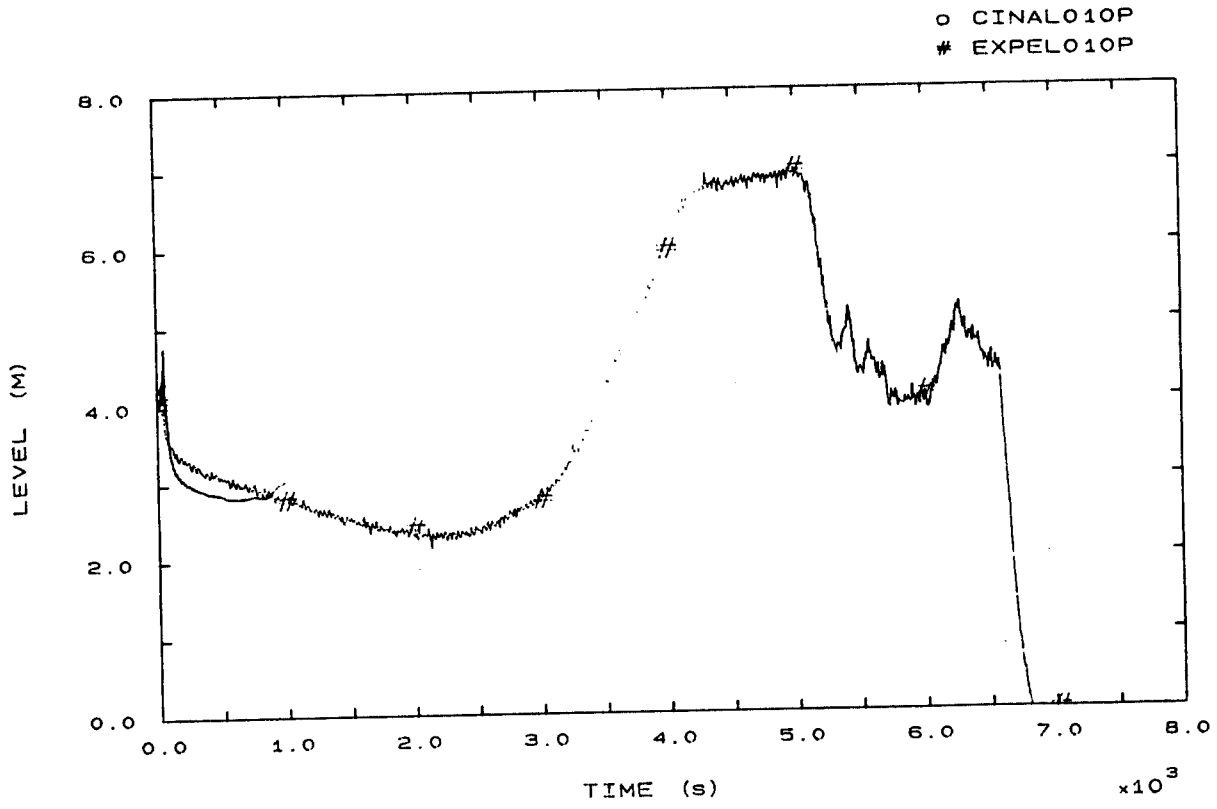

FIG. 6 PRESSURIZER LEVEL

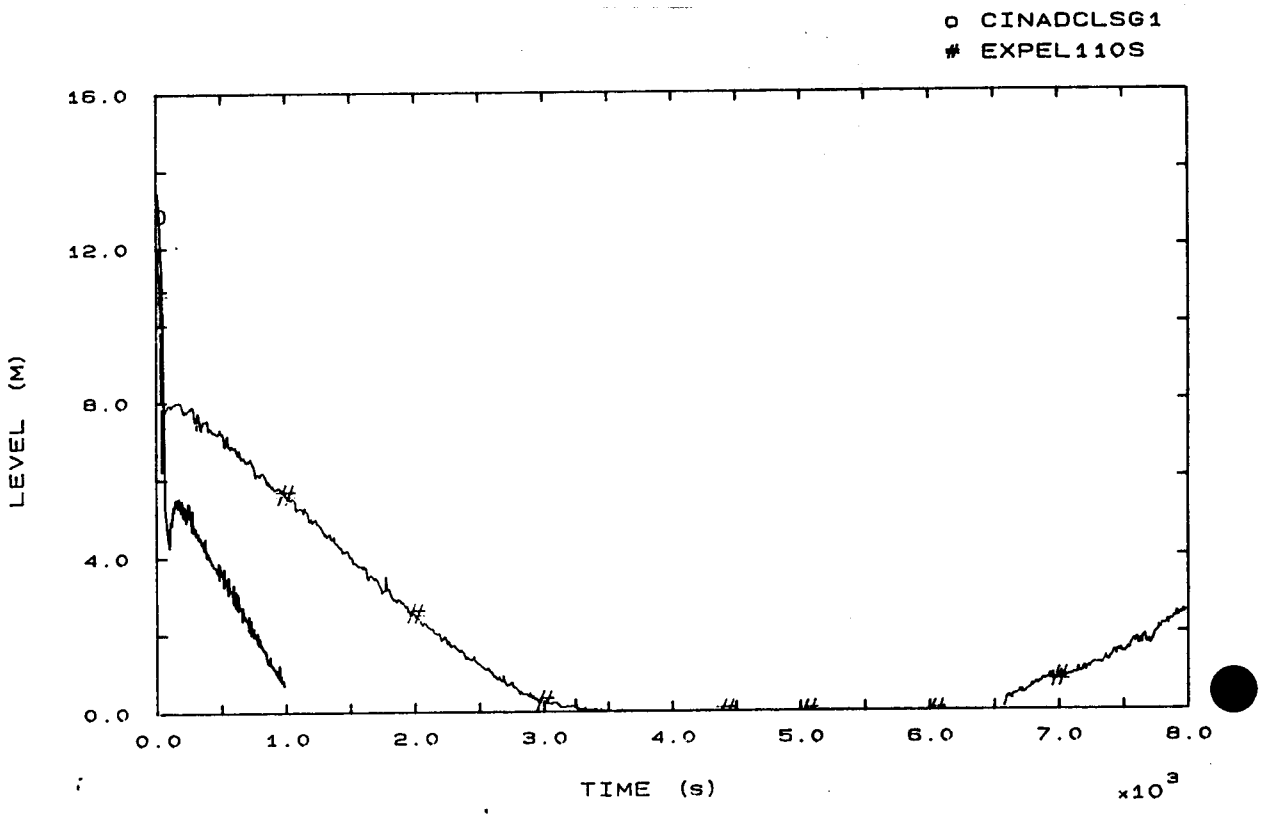

FIG. 7 SG1 DOWNCOMER LEVEL

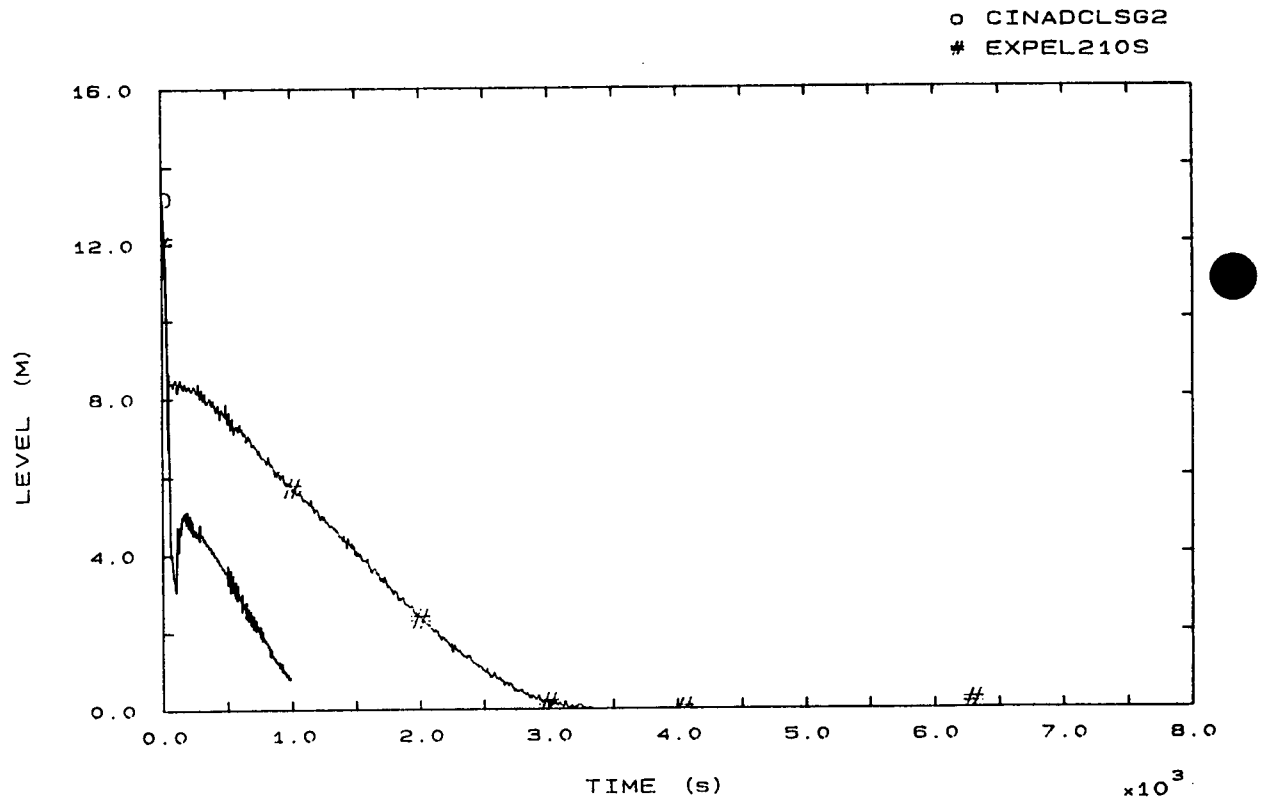

FIG. 8 SG2 DOWNCOMER LEVEL

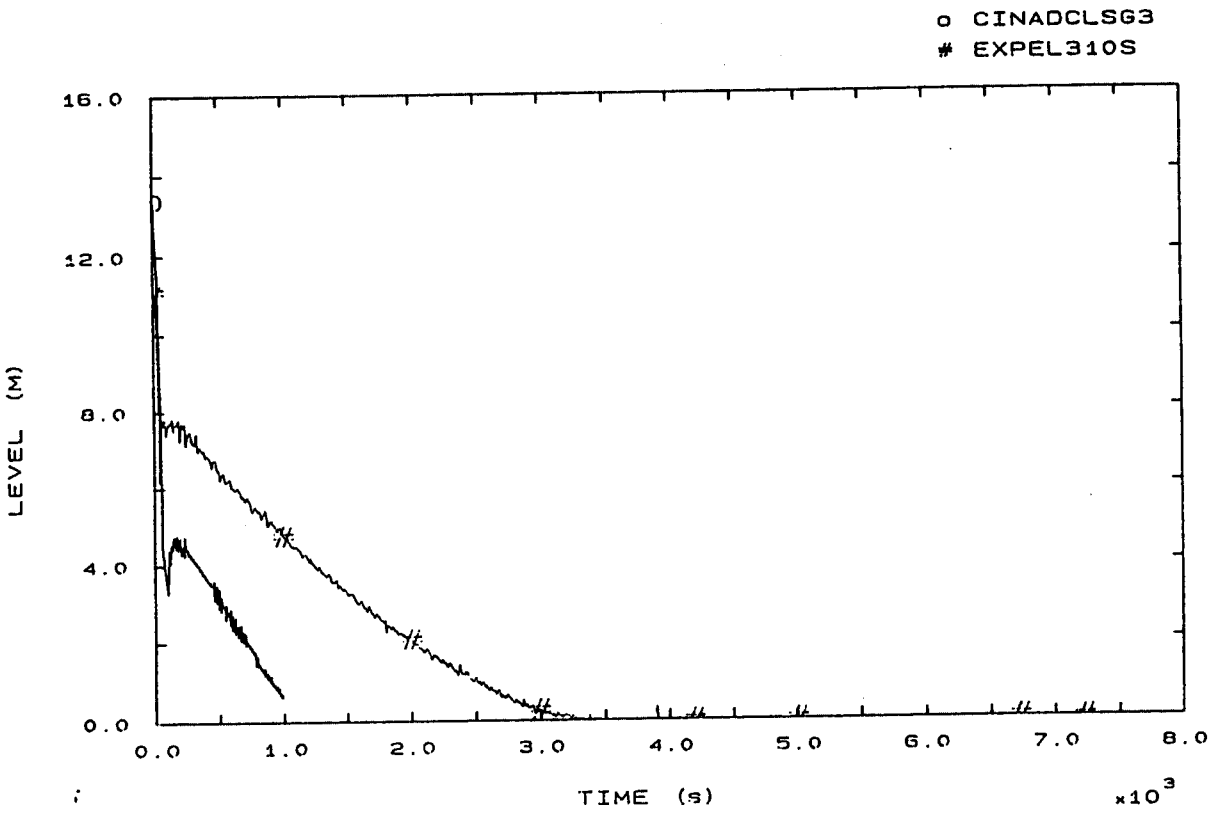

FIG. 9 SG3 DOWNCOMER LEVEL

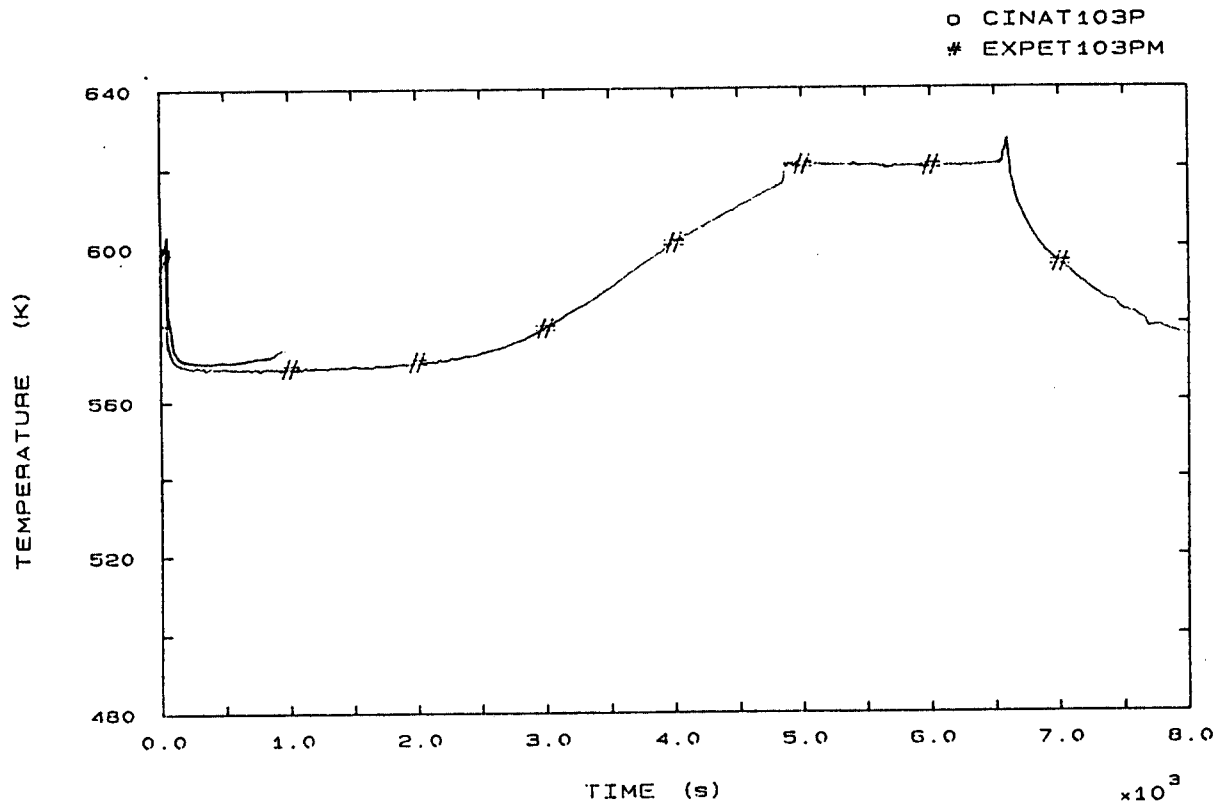

FIG. 12 LP1 HOT LEG OUTLET VESSEL TEMPERATURE

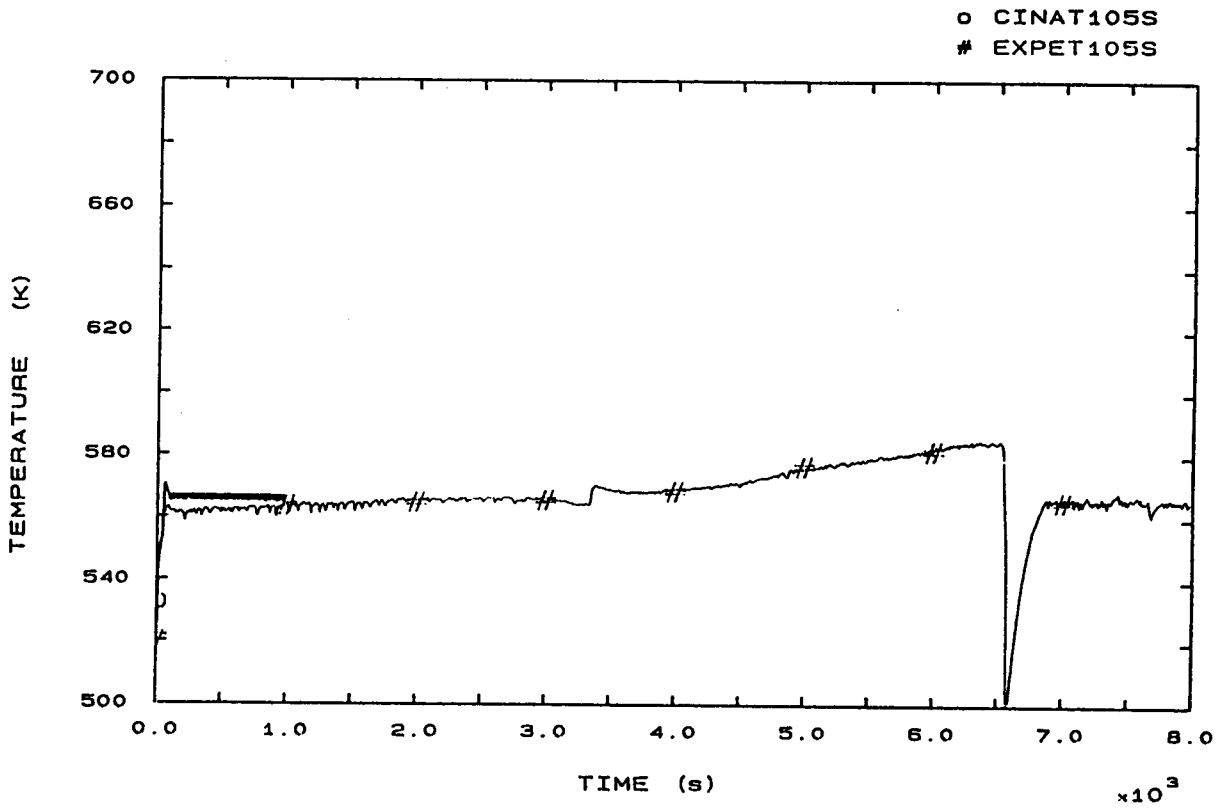

FIG. 15 FLUID TEMPERATURE SG1 RISER 185 MM A.T.S.

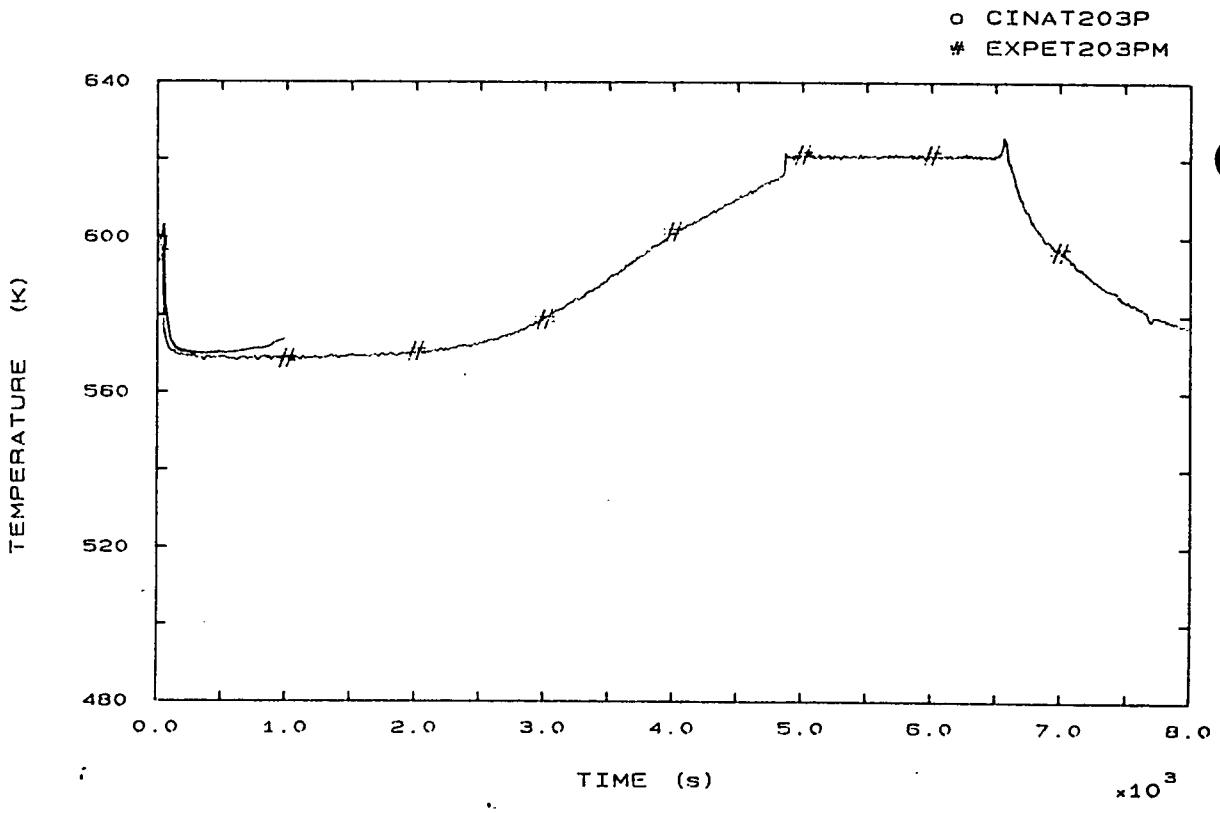

FIG. 22 LP2 HOT LEG OUTLET VESSEL TEMPERATURE

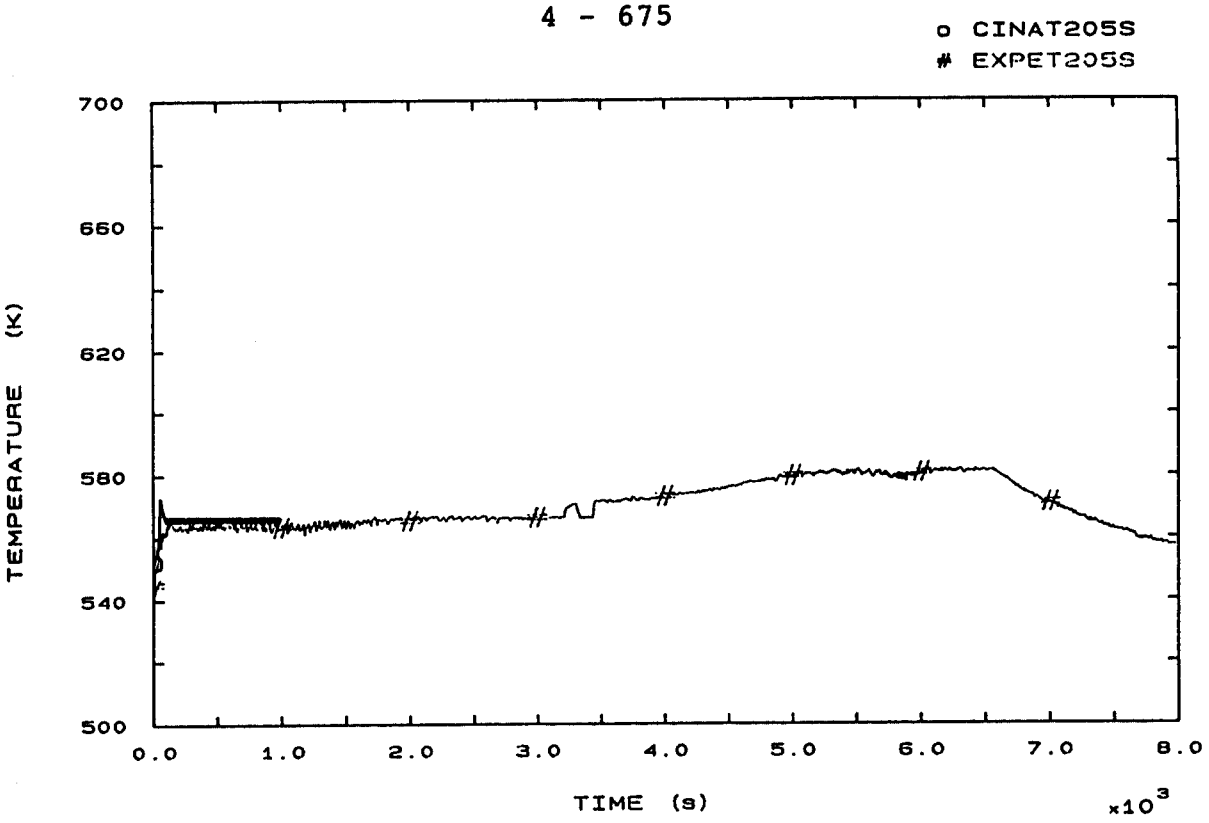

FIG. 25 FLUID TEMPERATURE SG2 RISER 185 MM A.T.S.

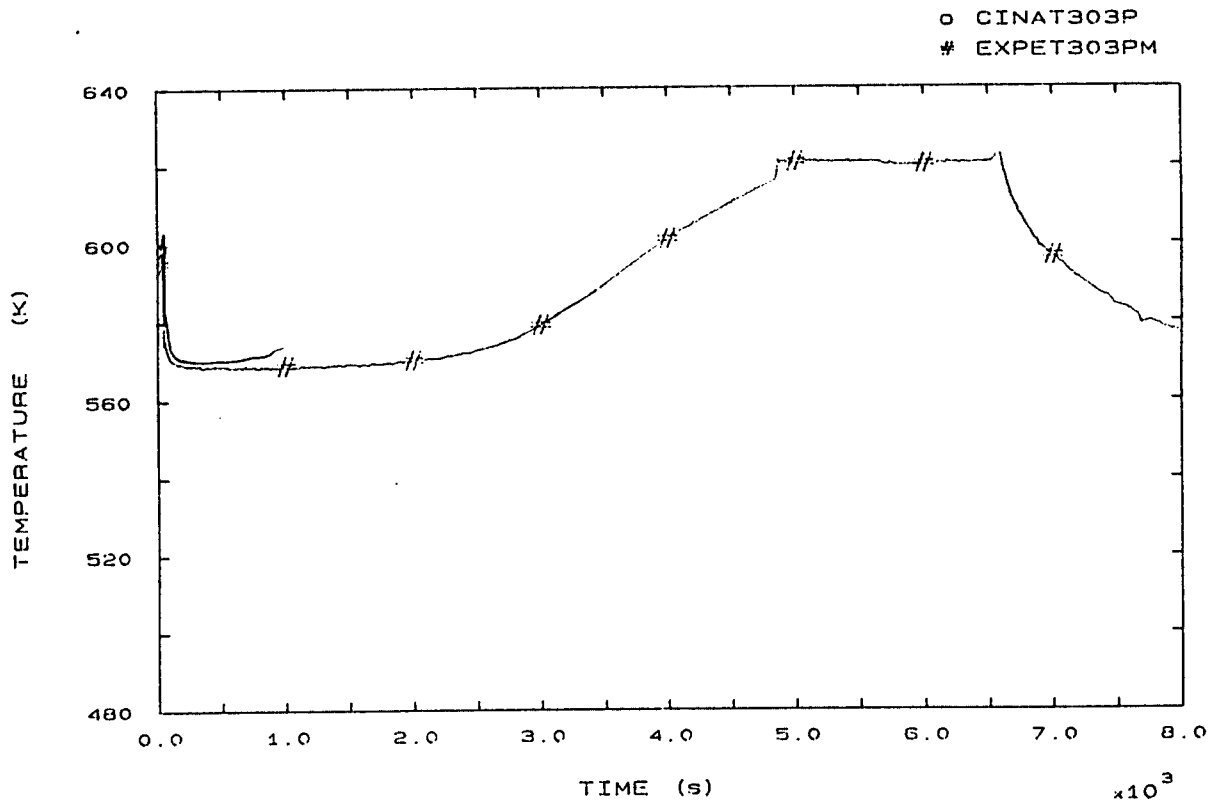

FIG. 32 LP3 HOT LEG OUTLET VESSEL TEMPERATURE

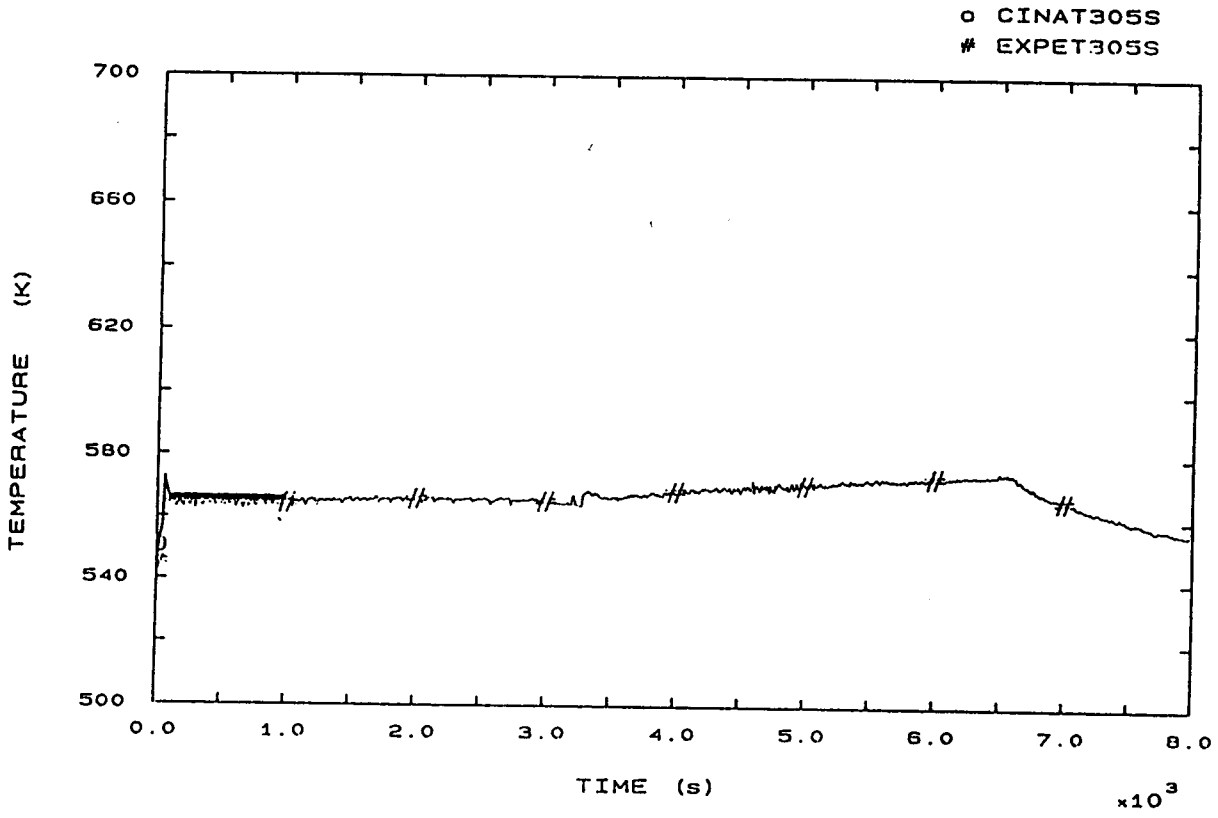

FIG. 35 FLUID TEMPERATURE SG3 RISER 185 MM A.T.S.

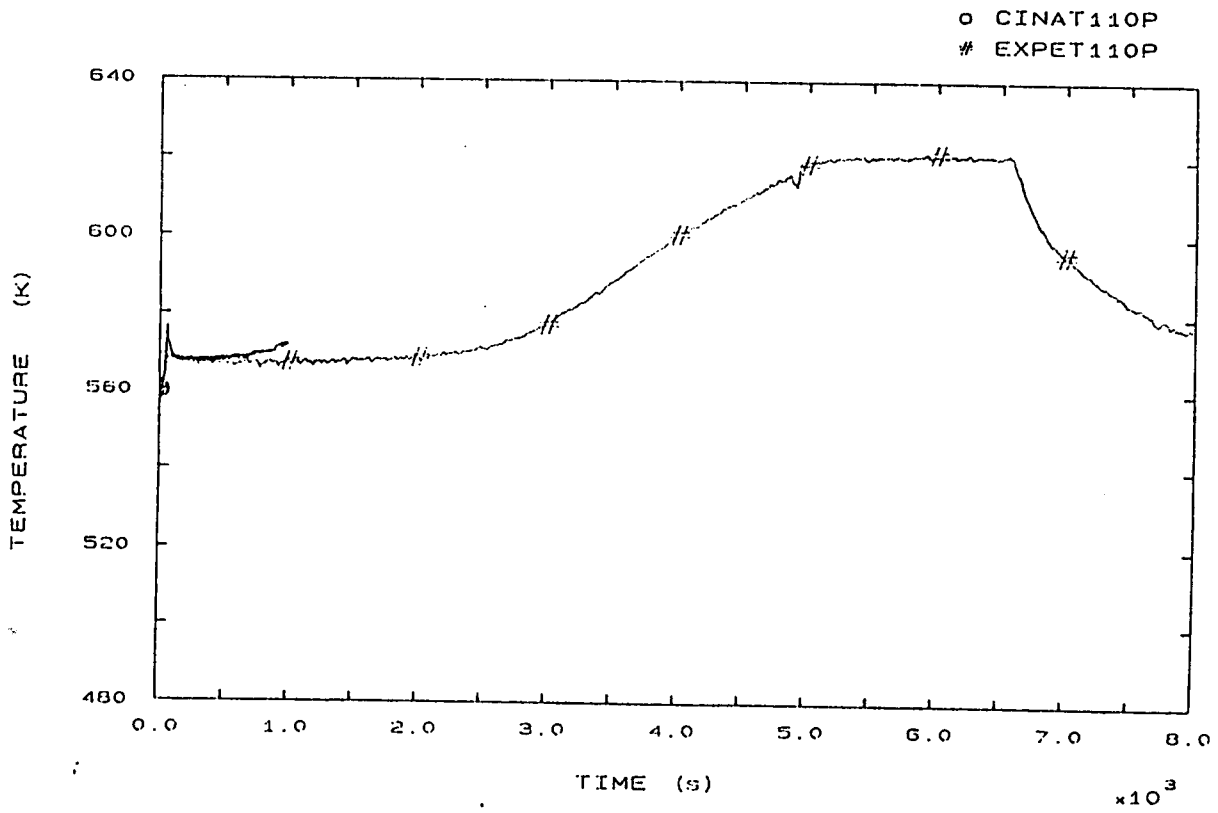

FIG. 42 SG1 OUTLET TEMPERATURE

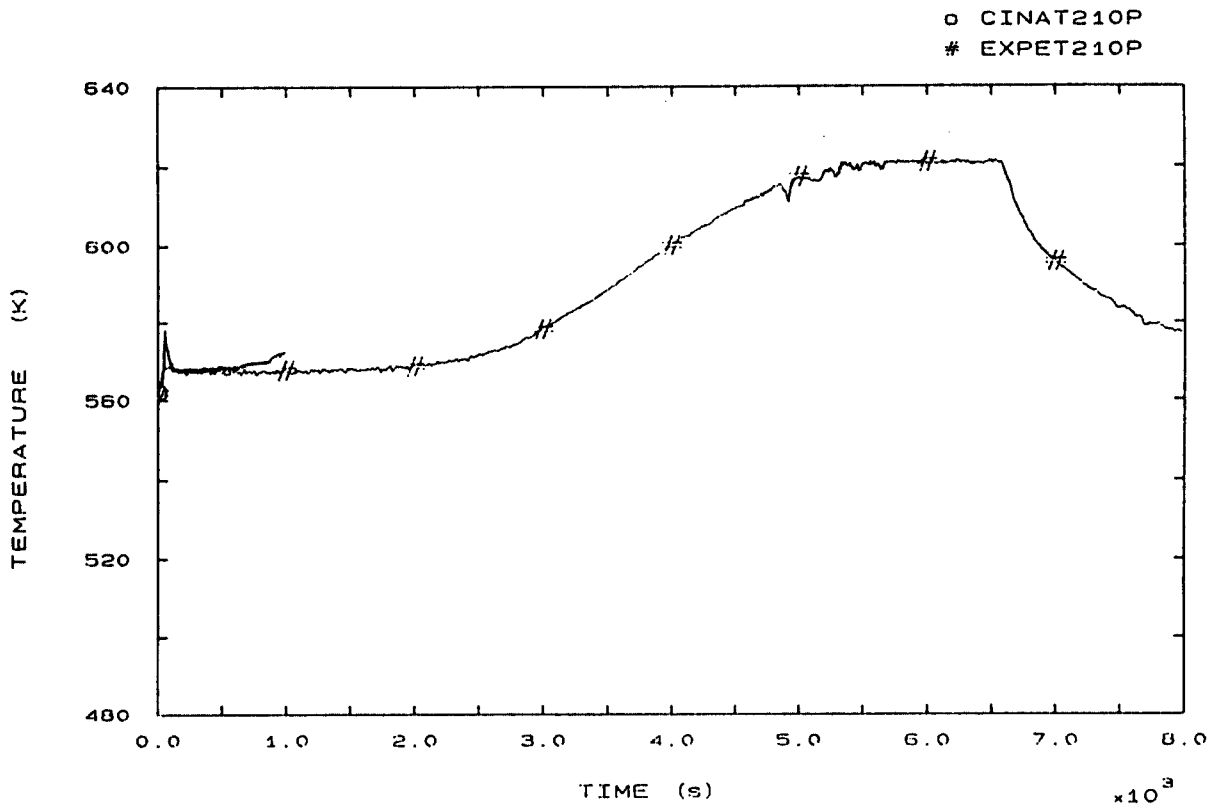

FIG. 44 SG2 OUTLET TEMPERATURE

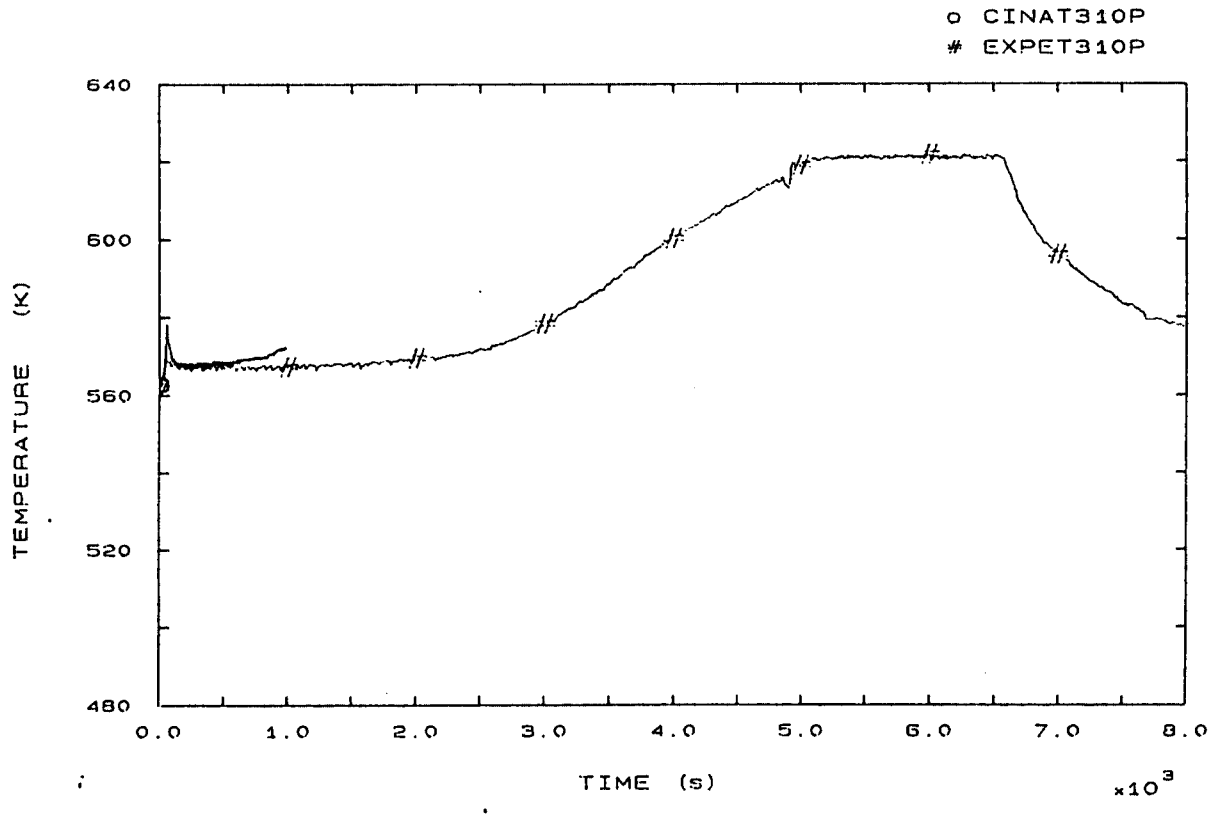

FIG. 46 SG3 OUTLET TEMPERATURE

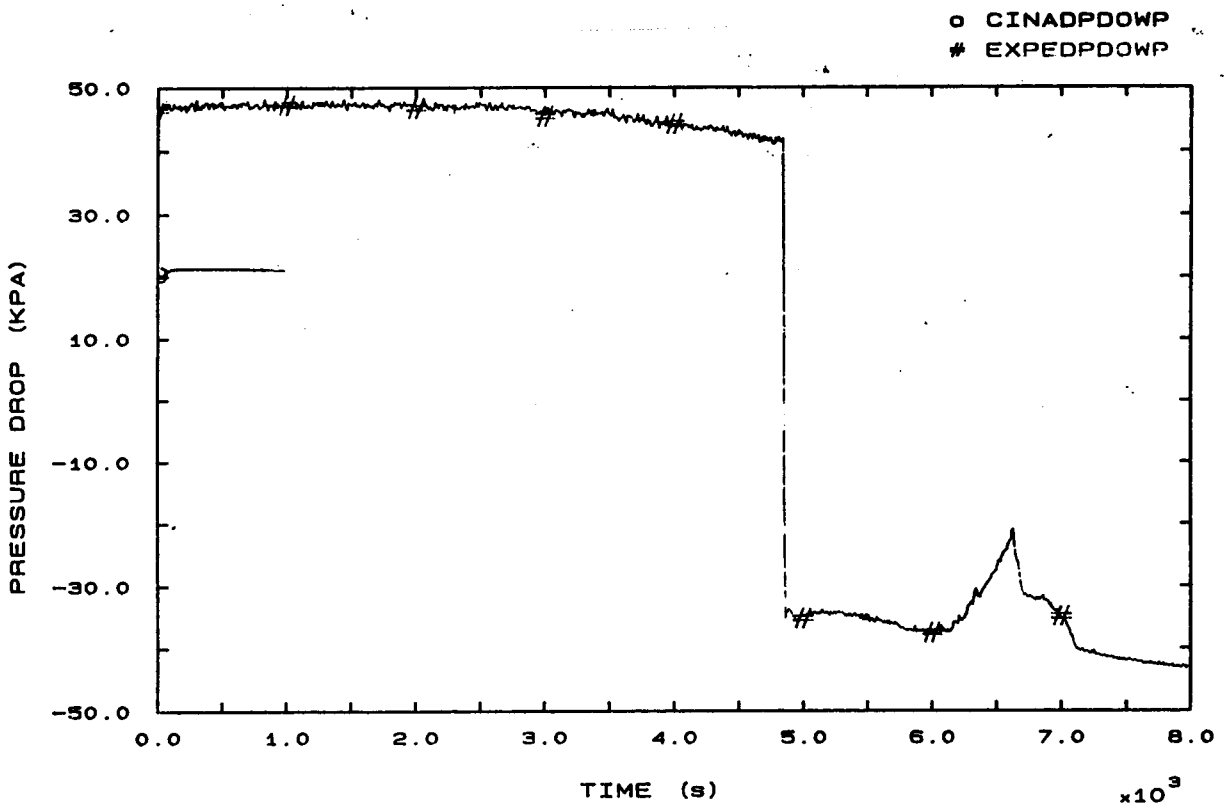

FIG. 57 VESSEL DOWNCOMER PRESSURE DROP

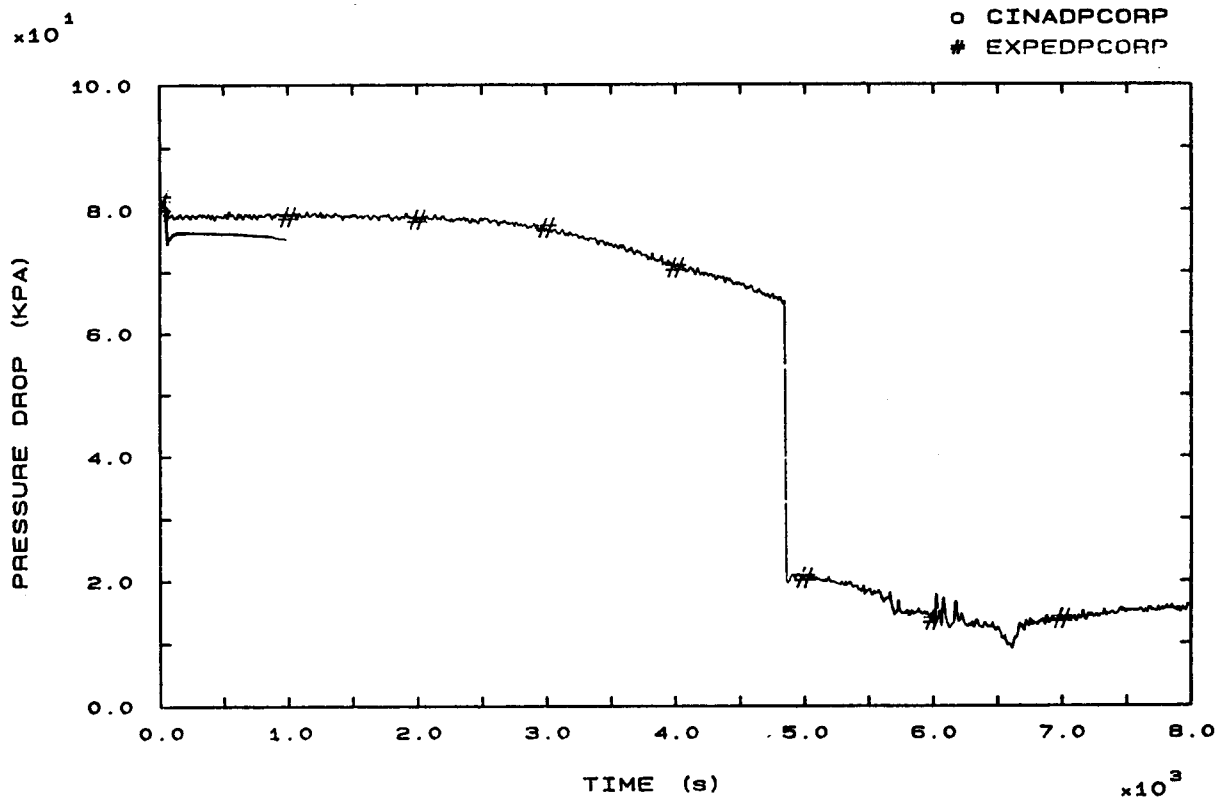

FIG. 58 CORE PRESSURE DROP

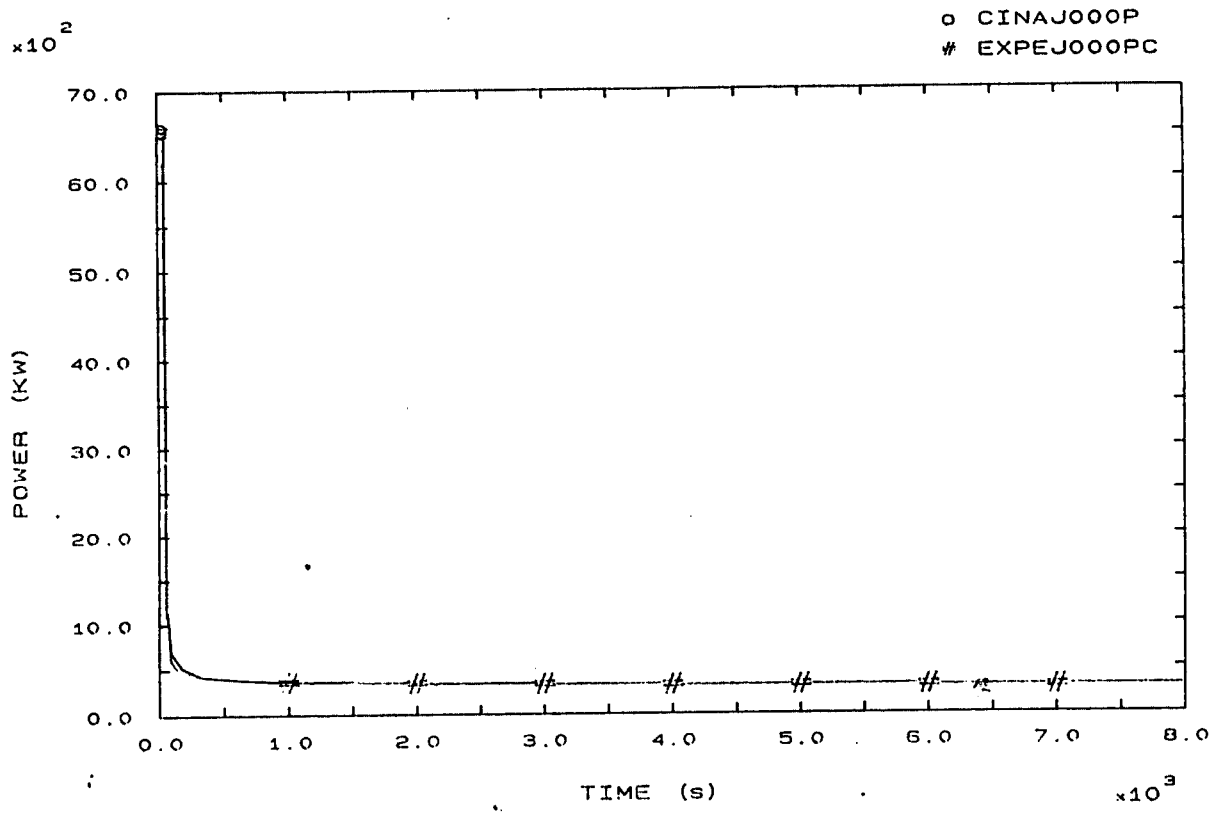

FIG. 81 HEATER RODS POWER

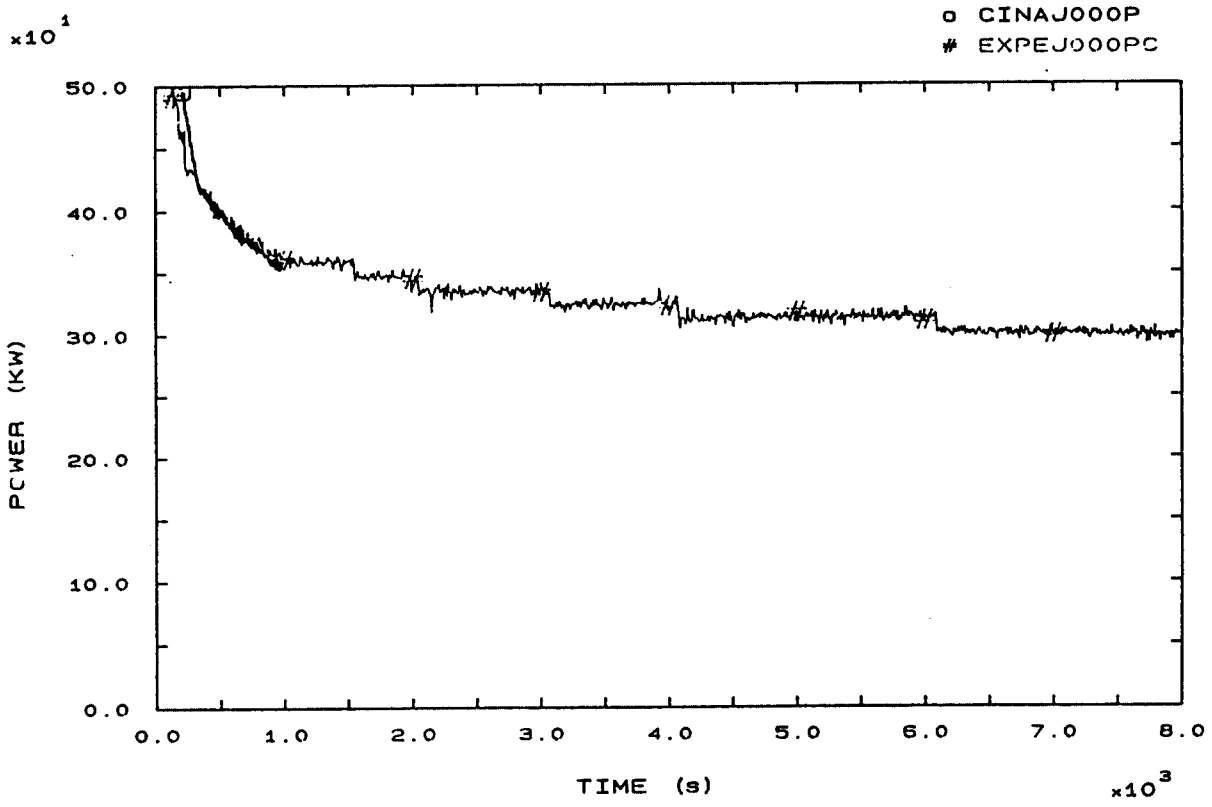

FIG. 81A HEATER RODS POWER

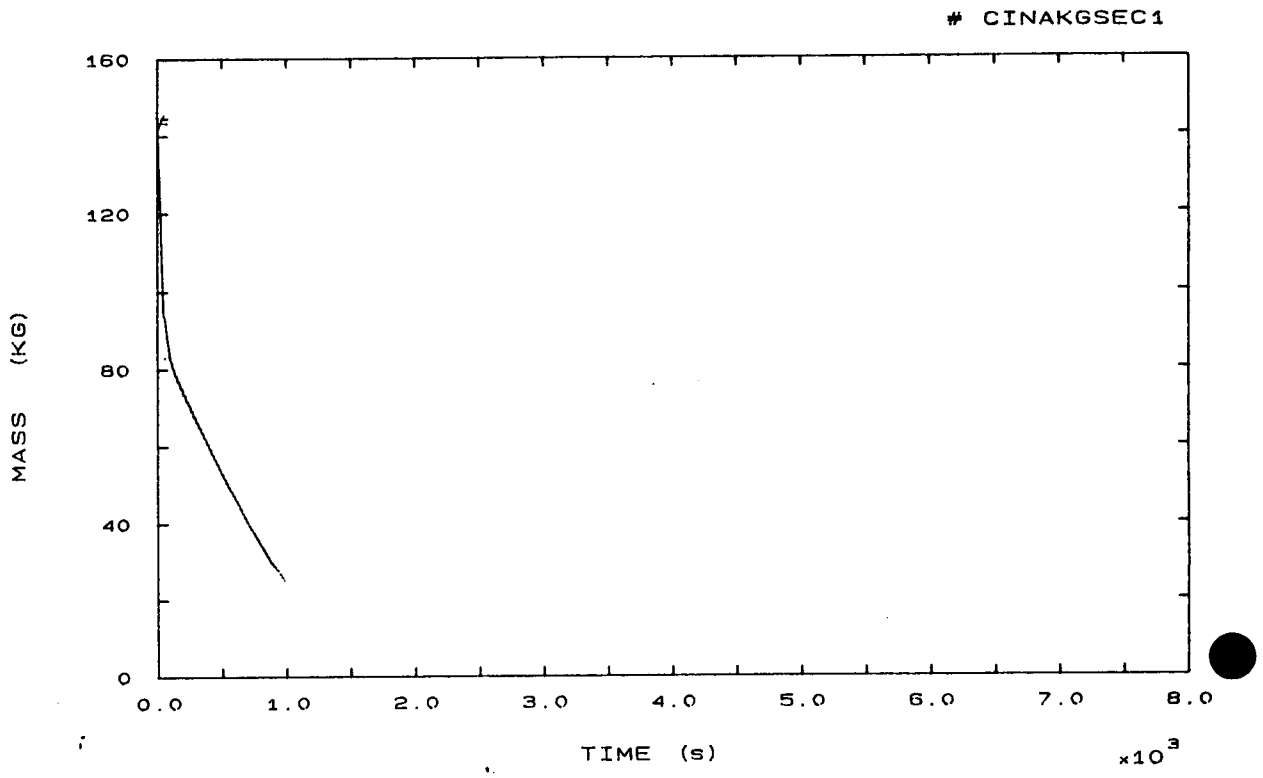

FIG. 86 SECONDARY COOLANT TOTAL MASS SG1

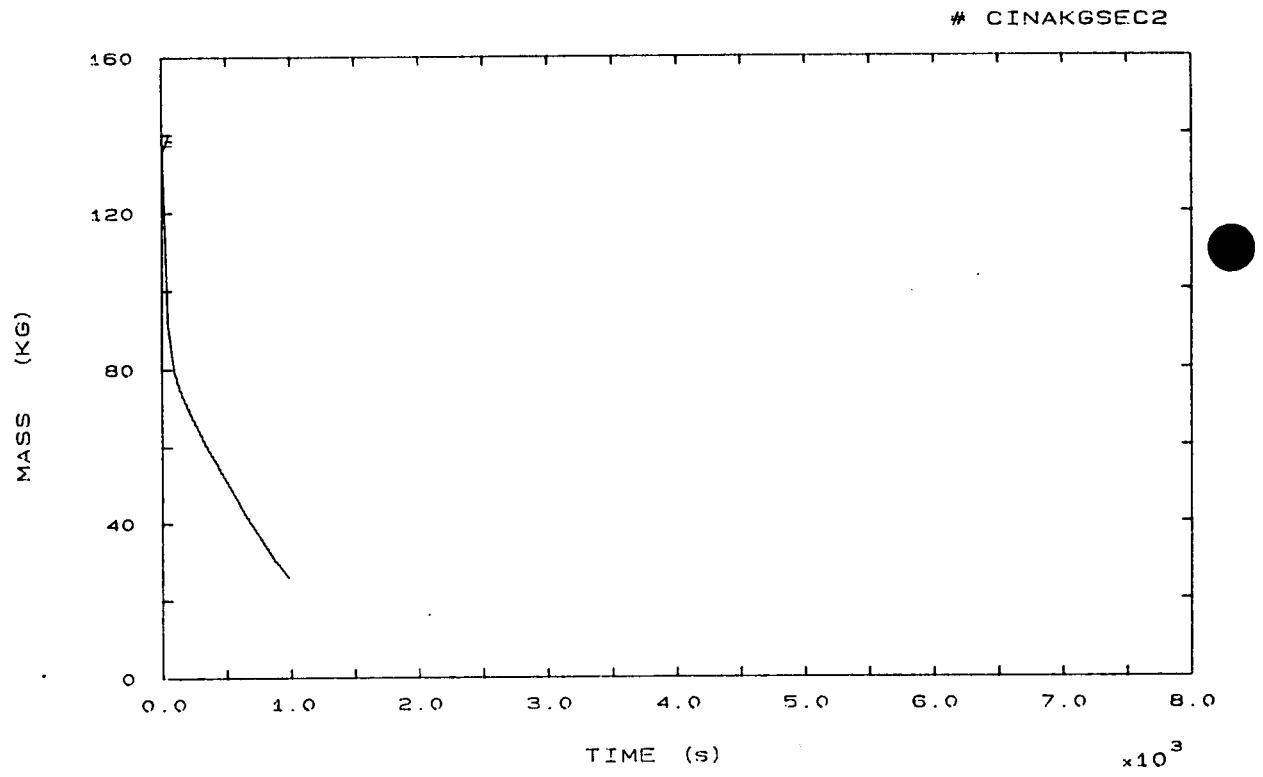

FIG. 87 SECONDARY COOLANT TOTAL MASS SG2

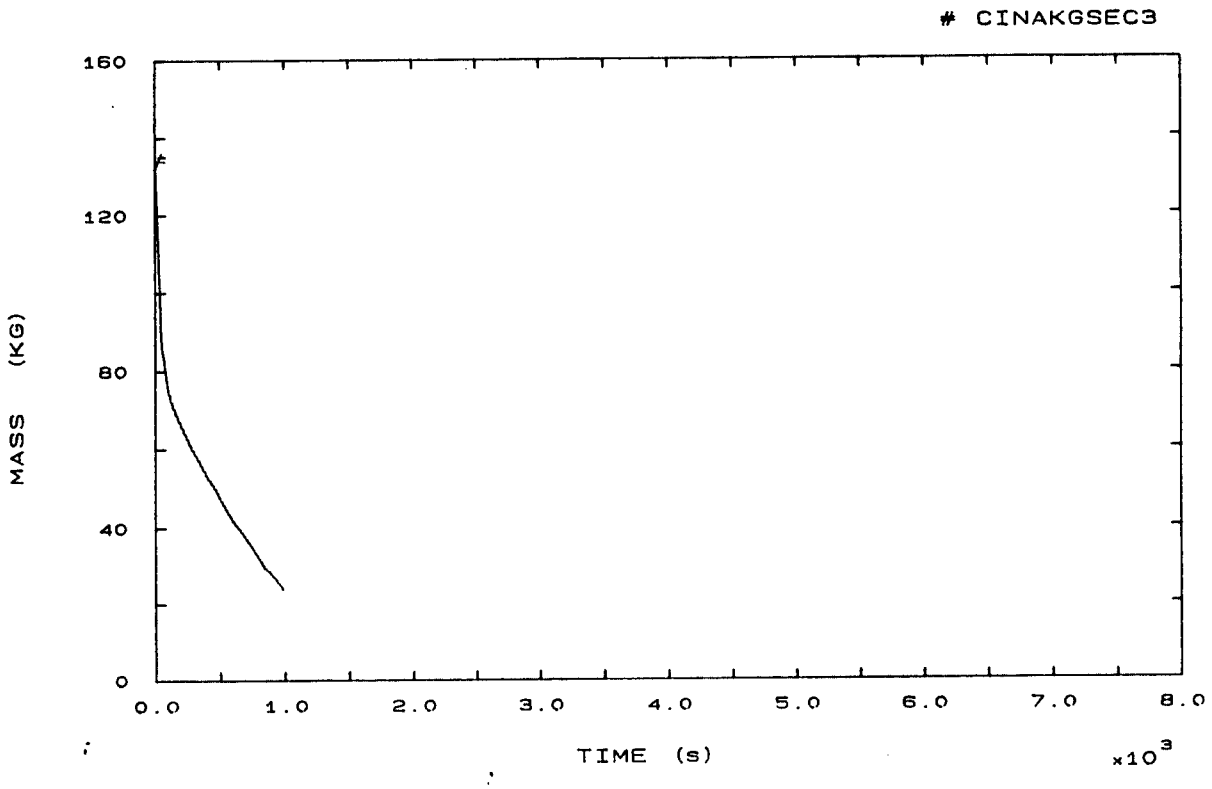

FIG. 88 SECONDARY COOLANT TOTAL MASS SG3

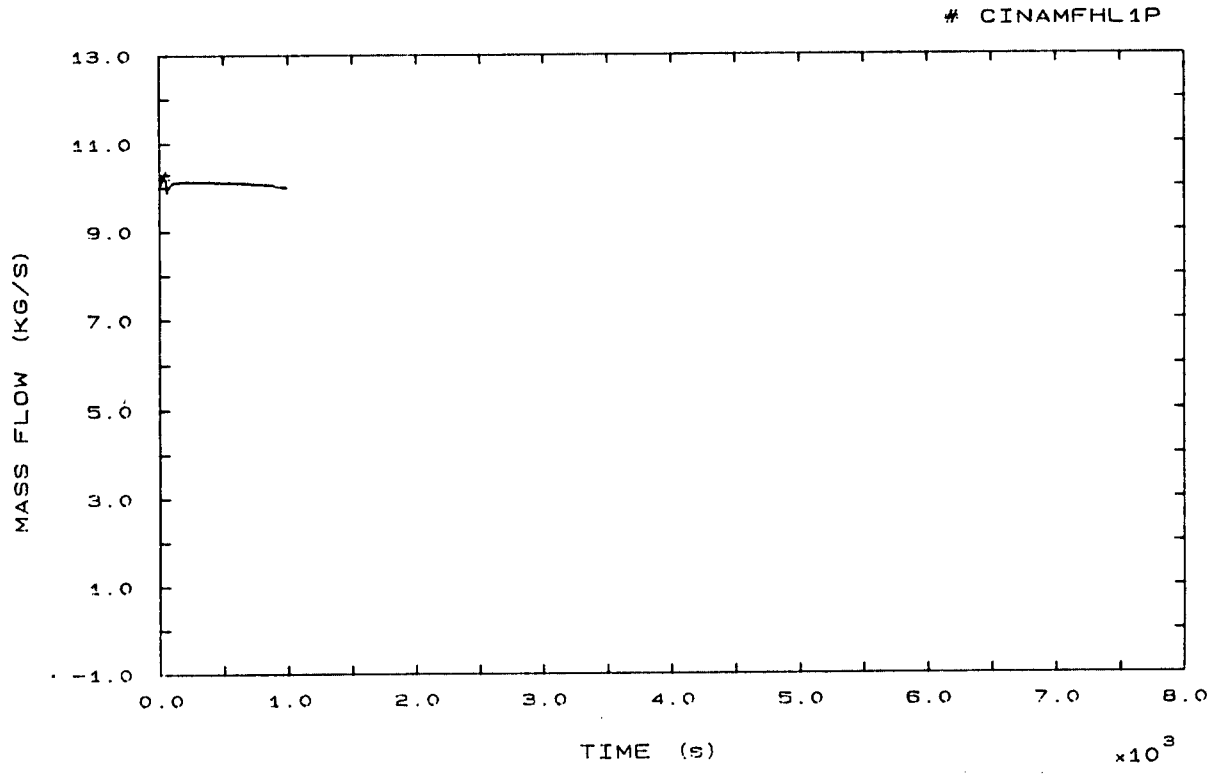

FIG. 89 HOT LEG 1 MASS FLOW

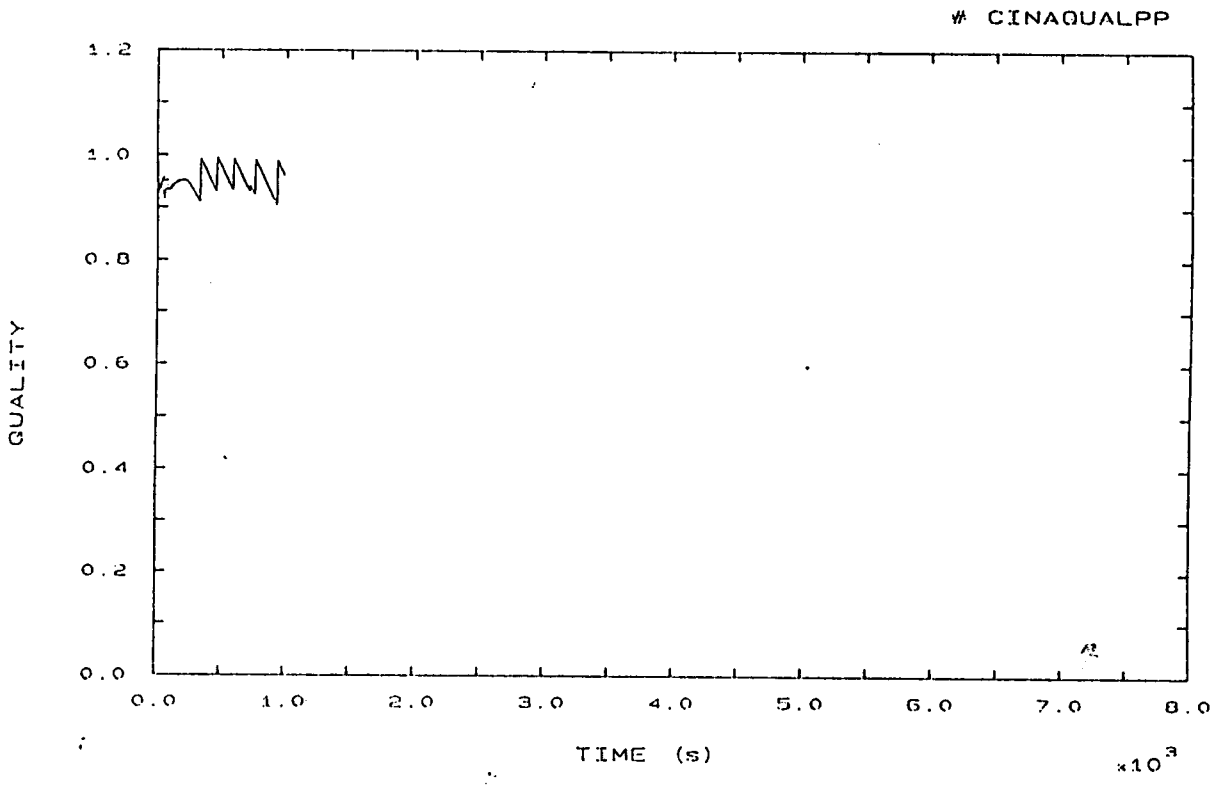

FIG. 103 PRZ PORV FLOW QUALITY

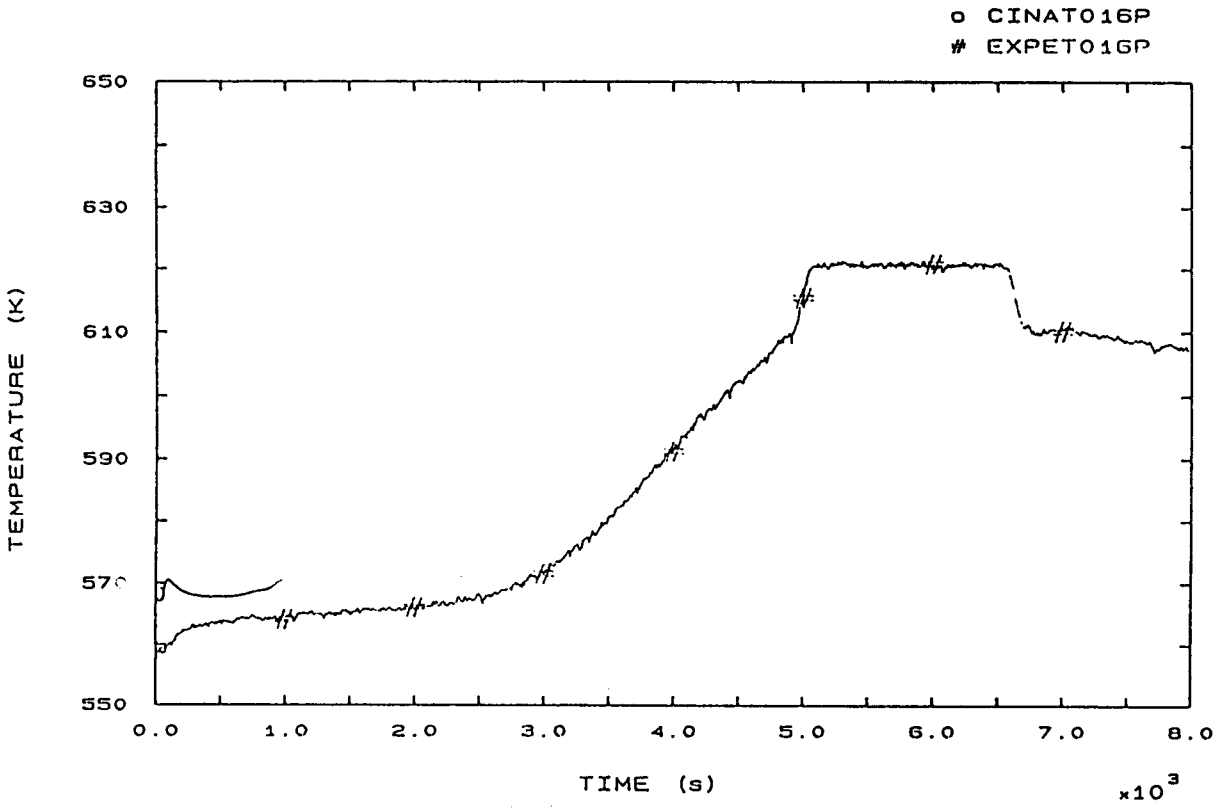

FIG. 110 FLUID TEMPERATURE VESSEL UPPER HEAD

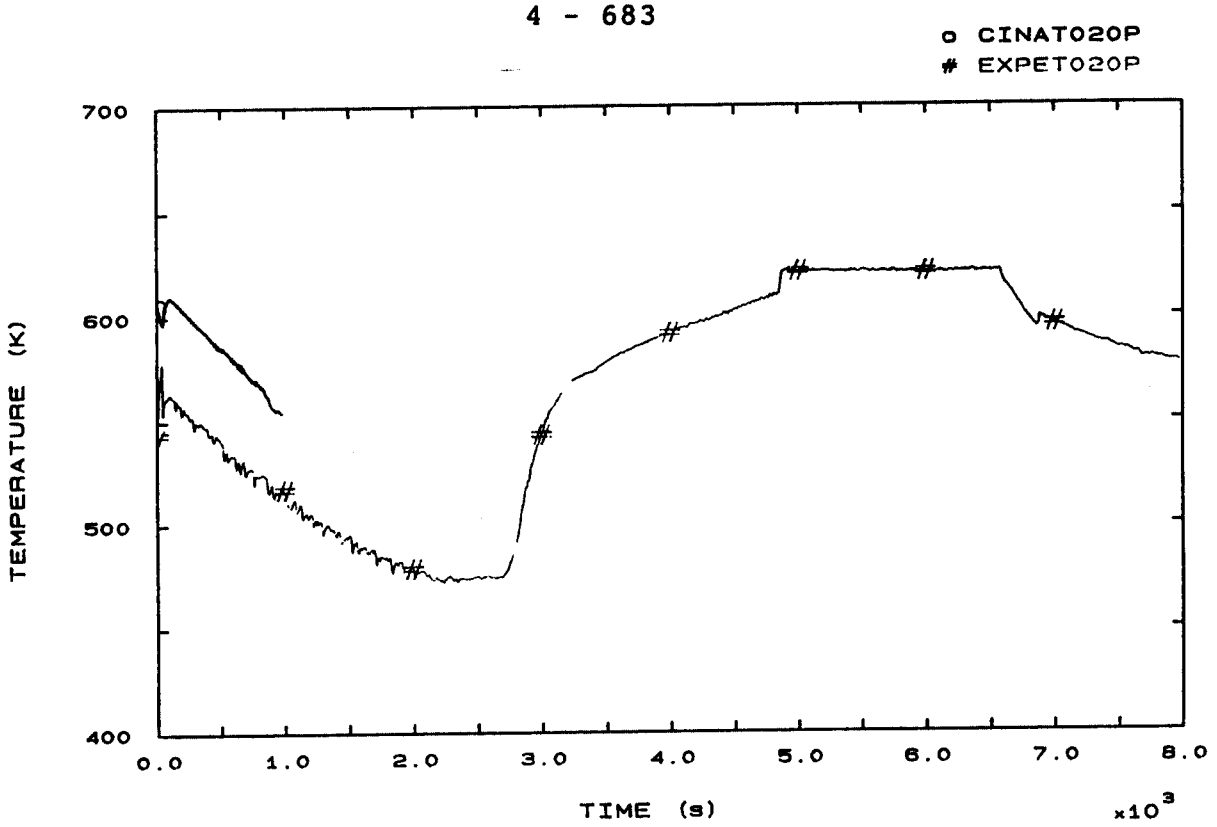

FIG. 112 FLUID TEMPERATURE SURGE LINE UPPER SIDE

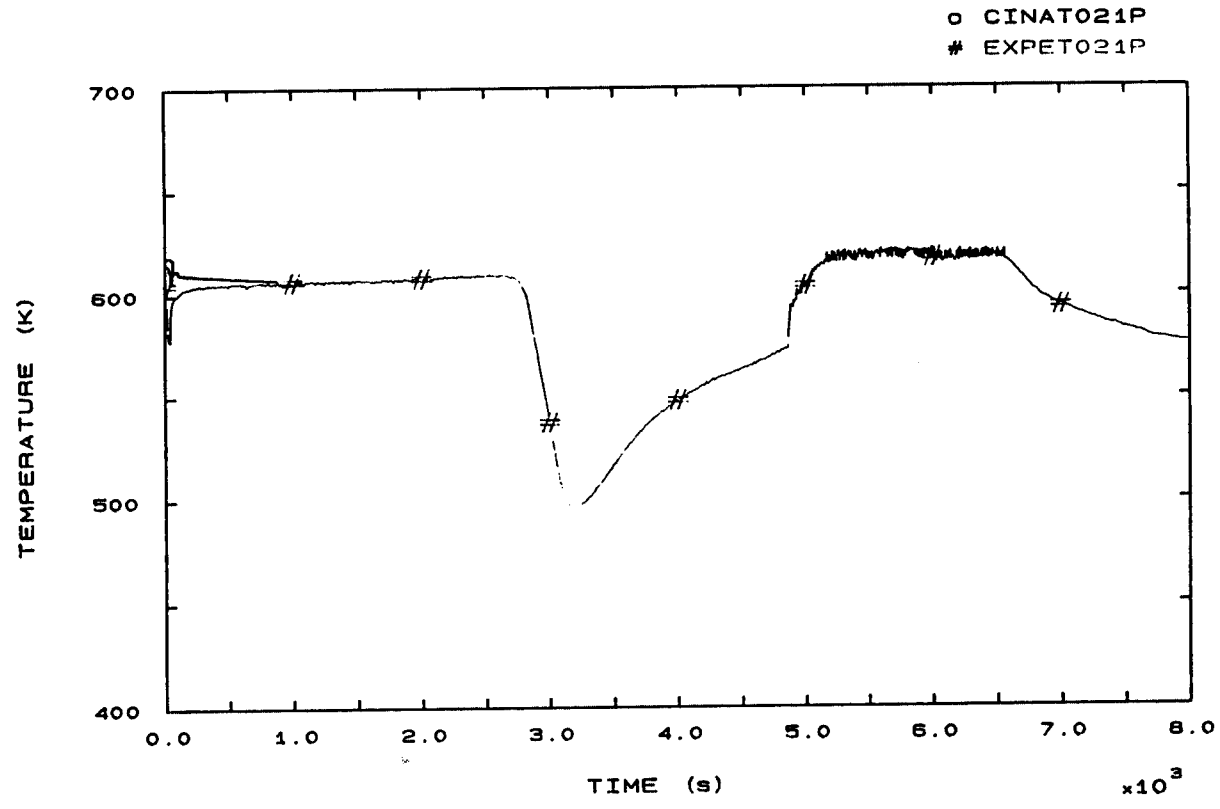

FIG. 113 PRZ FLUID TEMPERATURE

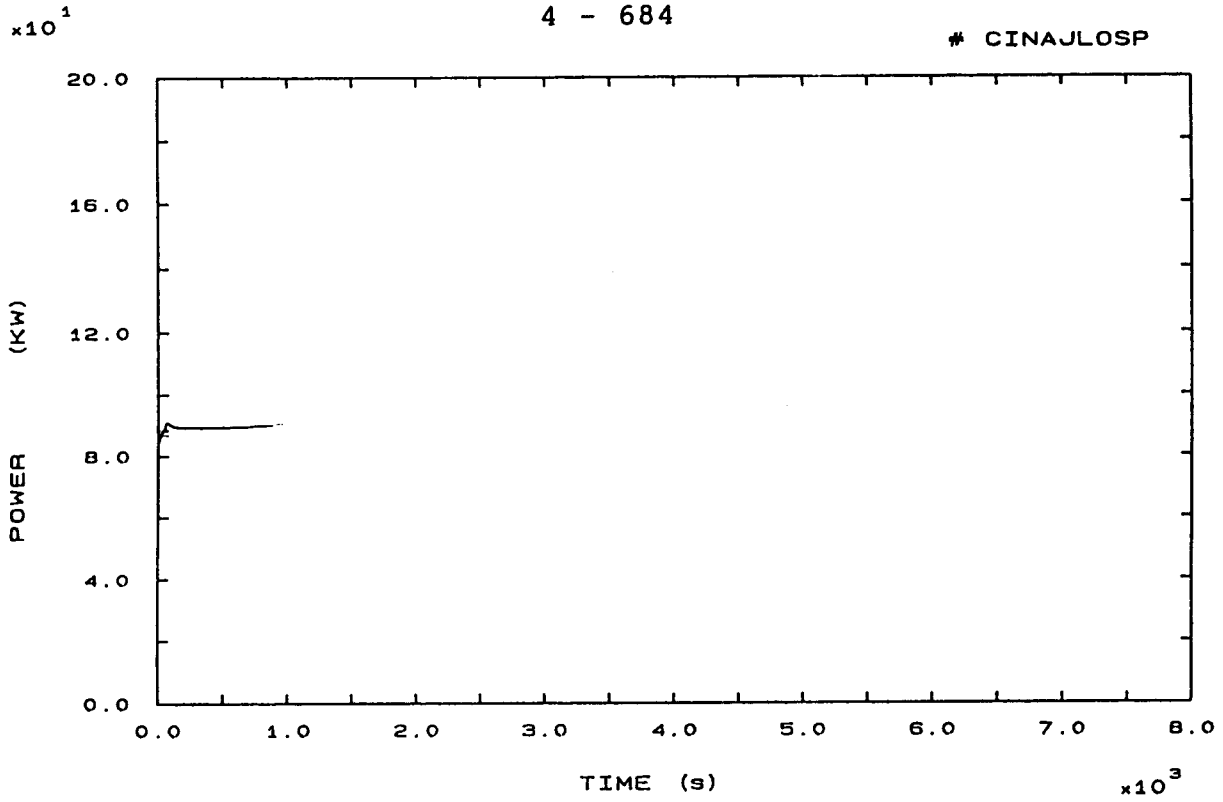

FIG. 131 PRIMARY HEAT LOSS

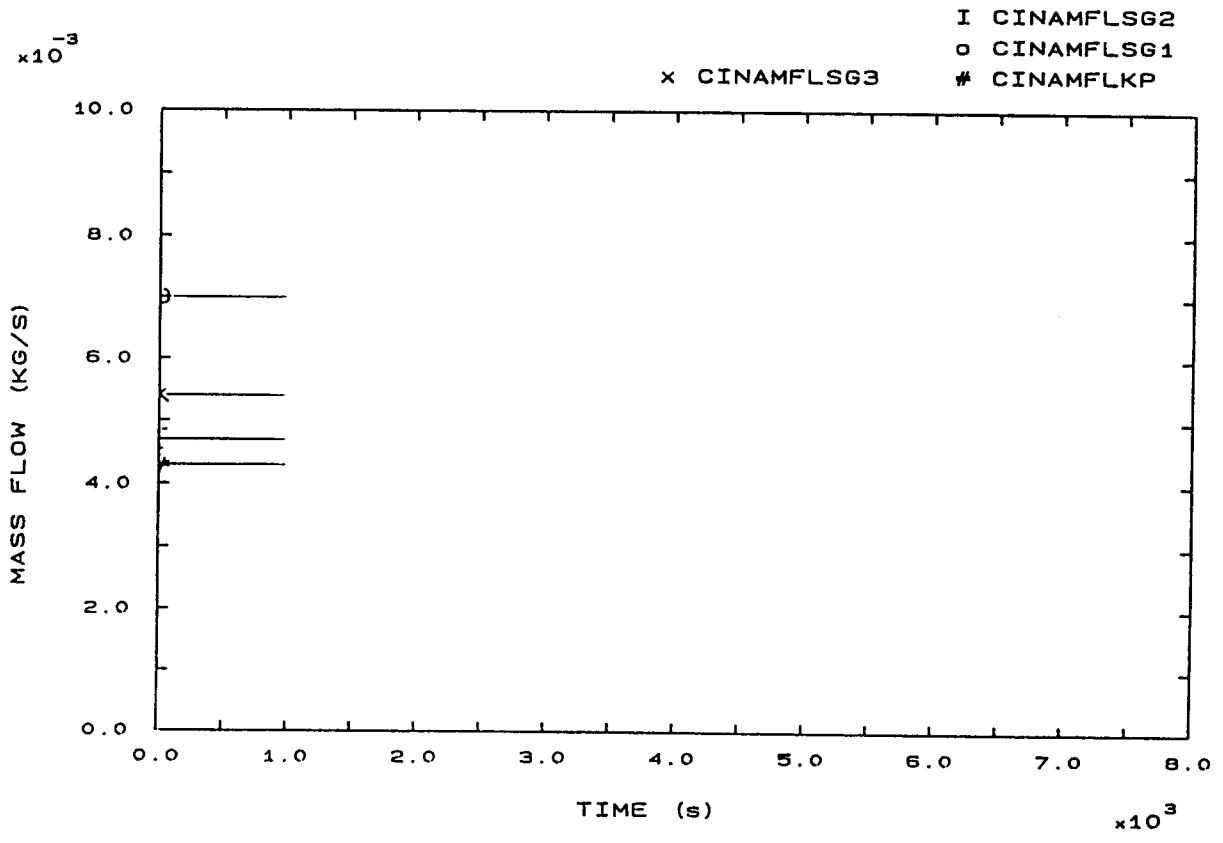

FIG. 137 PRIMARY AND SECONDARY LEAKS

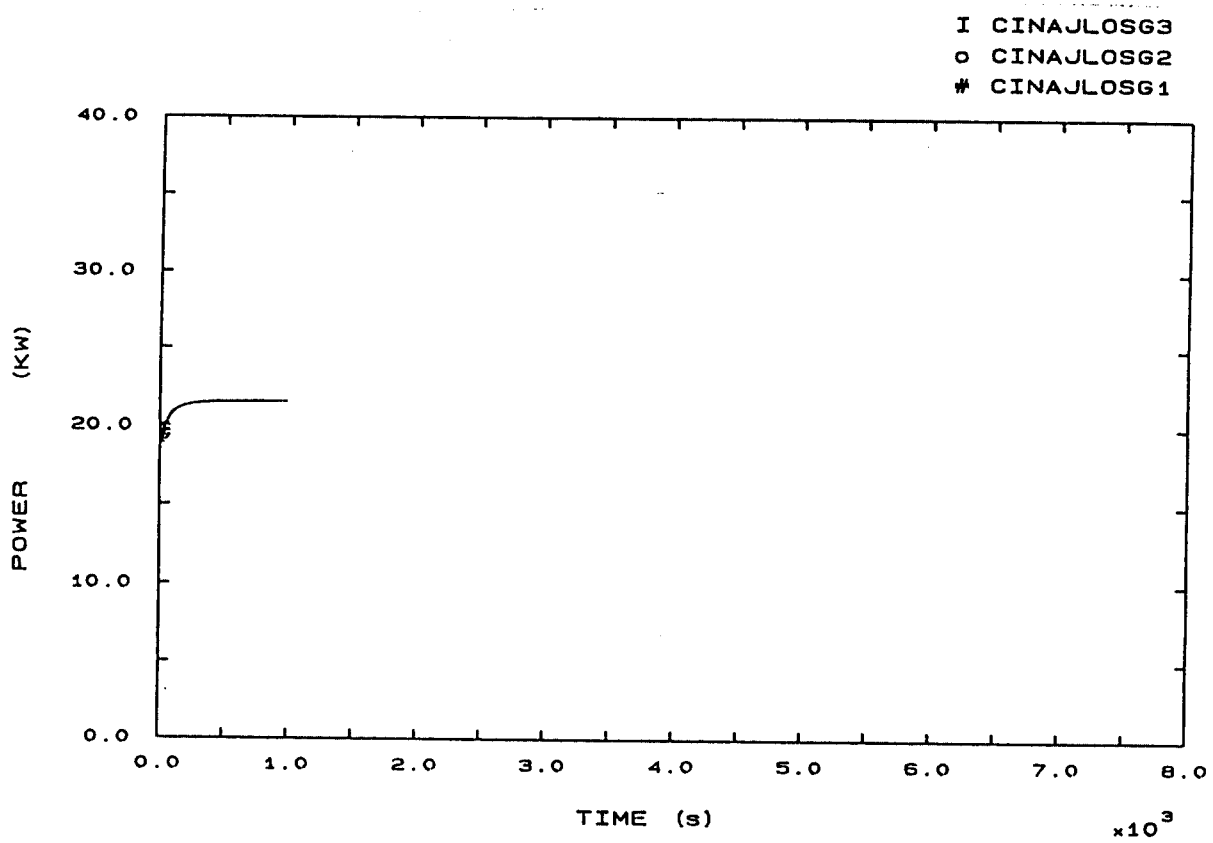

FIG. 139 SECONDARY HEAT LOSSES

4.17 UKAEA

4.17.1 CALCULATION DESCRIPTION

Phase 1: from LOFW to Scram (0- 61 s)

The loss of MFW causes the secondary inventory to decrease (see fig. 7b, 8b, 9b, 142b). When the downcomer level is at the low-low set point value (t = 50 s) the closure of MSIV and scram are actuated (with 5 s and 11 s delay respectively). Following the SGs isolation, secondary pressure and temperature increase (fig. 3b, 4b, 5b); the heat transfer to the SGs decreases determining a pressure and temperature increase in the primary system (fig. 1b, 42b, 44b, 46b). Primary pressure reaches 16,29 MPa, being limited by the PRZ PORV opening and the scram.

Phase 2: from Scram to PRZ PORV opening (61 - 1595 s)

After scram primary pressure decreases rapidly to 14.15 MPa (minimum value) (fig. 1b).
Secondary system pressure is first limited by SG-PORV opening, then, due to Scram, it decreases to the SG-PORV closure value (fig. 3b, 4b, 5b). After SGs-PORV closure the secondary pressure start increasing again and, at t=161 s, the PORVs in all three SGs start cycling and secondary mass decreases progressively (fig. 142b). The progressive secondary mass depletion reduces the SG heat transfer surface, and when the secondary system reaches the dry out condition (at about 1300 s) a rapid increase of primary pressure caused by heat up determines the PRZ-PORV opening (fig. 1, 7, 8, 9, 12, 22, 32).

Phase 3: from PRZ PORV opening to pumps trip (1595 - 2316 s)

The PRZ becomes full of liquid at t = 1890 s (fig. 6), while the PCS inventory decreases (fig. 85). The PCS temperature increases reducing the fluid subcooling, and at t = 2316 s the PCP trip is actuated according to the operating conditions (fig. 54, 55, 56). Following dry out, SGs depressurize due to secondary leaks (fig. 3, 4, 5, 137).

Phase 4: from pumps trip to EFW actuation (2316 - 3143 s)

After PCP trip the PCS becomes soon saturated, and when pumps coast down is terminated natural circulation estabilishes in the primary loops (fig. 89, 90, 91). At t = 2650 s the natural circulation is interrupted and a fast increase of the vapour generation rate takes place inside the core (fig. 11). The primary pressure increases rapidly well above the PRZ-PORV opening value (fig. 1) because at that time the PRZ-PORV flow quality is very low (fig. 103).
The PRZ-level decreases during the PCS pressure rise period (fig. 6) because of the unbalance between the PRZ-PORV mass release and the fluid rising from the surge line into the PRZ. When the PRZ-PORV quality flow increases the PRZ mass loss is balanced by the insurge so that the PRZ collapsed liquid level stops decreasing. At the same time a liquid drainage interests the SG U-tubes (fig. 62, 67). The PCS mass depletion continues, the higher parts of PCS go empty and the core starts uncovering. Consequently dry out conditions are established in the PC and the clad temperature starts to increase (fig. 50, 51, 52,). At t = 3143 s the EFW starts injecting into the secondary side of SG1.

Phase 5: from EFW actuation to the end (3143 - 4551 s)

The vaporization of EFW injected into SG1 causes a quite immediate repressurization of SG1 secondary side (fig. 3) while the recovery of SG1 downcomer level begins (fig. 7). The heat transfer coefficient between primary and secondary increases by determining the condensation of the steam in the U-tubes and a rapid PCS depressurization (fig. 1).
Due to PCS pressure decrease the PRZ-PORV closes at t = 3160 s and the liquid in the PRZ (43 kg) falls down to the PC (fig. 6, 11). The core heat up is then interrupted and the level starts recovering (fig. 51, 52,). The PRZ goes empty at t = 3354 s. The peak clad temperature is 713 K. The core reflooding starts from the bottom and two phase natural circulation establishes in the PCS (fig. 62, 63). At t = 4551 s the calculated SG1 level reaches the "end of transient" value (fig. 7).

PARTICIPANT: ALLEN - UKAEA *CODE: TRAC*

EVENTS TABLE

EVENT	*CALC. TIME (s)*	*EXP. TIME (s)*
SG Low Low Level	*50*	*33*
Main Steam Isolation	*55*	*38*
Scram (power fall), t_1	*61*	*44*
SGs PORV opening	*64* *64* *64*	*82 (3)* *106 (2)* *200 (1)*
SGs Dry Out	*1226 (1)* *1277 (3)* *1302 (2)*	*3282 (3)* *3347 (1)* *3437 (2)*
PRZ PORV opening, t_2	*1595*	*4134*
PRZ full of liquid	*1890*	*4222*
Pumps Trip, t_3	*2316*	*4848*
Loss of Natural Circulation	*2650*	*5630*
Beginning of Core Heat Up	*3130-3140*	*6511*
EFW actuation, t_4	*3143*	*6532*
PRZ PORV closure	*3160*	*6576*
PRZ emptying	*3354*	*6811*
SG1 repressurization	*3160*	*6878*
End of transient, t_{END}	*4551*	*8062*

4.17.2 CALCULATION EXPERIMENT COMPARISON

Phase 1: from LOFW to Scram

The comparison between experimental data and code calculation shows a good agrement as far as it concerns the phenomena occurred during this phase. In fact in both cases after the loss of feed water the SG downcomer level (fig. 7b, 8b, 9b) decreases to the low low set point value by determining the closure of MSIV (after 5 sec.) and Scram (after 11 sec.). The calculated SG levels show however an unrealistic "plateau" shightly below 11 m (fig. 7b, 8b, 9b). The calculated primary and secondary pressures are in good agreement with the experimental data (fig. 1b, 3b, 4b, 5b). In the period between the MSIV closure and Scram the code calculated a brief opening of the SG PORV while during the test this occurs later (see C.T.). The comparison of the events timing does not show the same good agreement. In particular, as it is shown in the C.T., the time calculated by the code for SG - DC low low level, MSIV closure and PC scram is delayed 17 s with respect to the experimental data.
The reason of this discrepancy is related to the deficiency of the code to calculate the mass distribution in the secondary side of SG: for a given value of SG-DC level the code tends to calculate a mass inventory that is lower than the experimental one. In order to impose an initial inventory close to the exp value the analysit can adopt a higher initial level, but in this case trip time is delayed and secondary mass at Scram is low all the same (see C.T.).

Phase 2: from Scram to PRZ PORV opening

The second phase of the experiment was qualitatively well simulated by TRAC. The major phenomena observed during the test were simulated, but again the timing and the value of the main calculated parameters don't agree with the experimental data.

Considering the primary pressure (fig. 1) it is evident the good simulation of the pressure decrease following scram, but later on the value is underestimated untill SGDO. This is due to an imperfect modelling of PRZ power balance.
In the opposite, the pressure rise following the SGs dry out is overpredicted and the PRZ PORV opening set point is reached much earlier with respect to the experiment. At the time of SGs dry out (about 1300 s) the calculated power generation is about 25 KW higher then the test data (fig. 81). That can partially explain the higher pressurization rate calculated by the code. Another important reason can be the limited simulation of the warm insurge from SL into the PRZ, which in the causes steam production stop (fig. 112, 113). The timing discrepancy concerning SGDO is due to the large difference between the calculated and the experimental secondary mass inventory at the time of Scram (see C.T.). Secondary pressure results (fig. 3, 4, 5) are shifted, but the trend is almost the same as in the test. At PRZ PORV opening time the calculated PRZ collapsed level is about 1 m. lower than the experimental one (see C.T. and fig. 1, 6).

Phase 3: from PRZ PORV opening to pumps trip

The PRZ goes full much earlier than in the Exp (1890 s vs 4222) due to the early SGDO (see C.T.), but the time interval since PRZ PORV opening (dt_{PRZF}) is overestimated (295 s vs 88) due to the even more accelerated pressure profile (see fig. 1, 7). The dominant relief condition during this phase is correctly predicted as essentially liquid (see fig. 103). Pumps trip absolute time is again sensibly underestimated (due too early SGDO and faster heat up) but time intervals since PORV opening time (dt_3) and SGDO (dt_{HU}) are calculated with good and sufficient accuracy respectively (see C.T.). No saturation conditions in PCS before pumps trip are calculated.

Phase 4: from pumps trip to EFW actuation

At the time of pumps trip the calculated RCS mass is slightly overestimated (401 Kg vs 390 Kg) . The two phase natural circulation time period is strongly underestimated by the code (334 sec. vs 780 s. fig. 89, 90, 91): this is probably due to differences in RCS mass distribution and PRZ PORV discharge quality after pumps trip. In fact at the time of loss of natural circulation the net RCS mass (the total mass minus PRZ mass) calculated by the code is equal to that evaluated from the experimental data.

A primary over pressure is predicted by the code when stagnant flow conditions are estabilished in the primary loops (fig. 1). At the same time the PRZ level decrease (initiated 50 sec. earlier) is temporarily interrupted because the surge line is fed with "cold" water coming from the SG2 - U tubes. The calculated pressurization (above PRZ PORV set point) terminates when the PRZ PORV flow quality approaches to 1, and at the same time the PRZ level stops decrease again (fig. 6). In this way the PRZ level behaviour observed during the test is qualitatively well reproduced. The calculated stagnation interval dt_{BOCH} *(*t_{BOCH} *-* t_{LNC}*) is shorter than the test value (480 s vs 880 s) showing the calculation a faster RCS emptying. Primary inventory at* t_{BOCH} *is accurately calculated (see C.T.). Max core Temperature is adequately predicted. The calculated duration of this phase (*dt_4*) is a half of the experimental result (827 sec. vs 1684).*

Phase 5: from EFW actuation to the end

During this phase the code calculated quite well such phenomena as RCS depressurization (fig. 1), PC recovery (fig. 51, 52), PRZ emptying (fig. 6) and secondary pressurization in SG1 (fig. 7). The peak clad temperature was underestimated (713 K vs 770 K) probably due to the shorter PRZ delay to go empty (211 s vs 280 s, see C.T.) after EFW initiation. The natural circulation mode estabilished after PC recovery was evaluated to be different from the real one. In fact

while the code calculation shows a positive flow in loop1 (fig. 62, 63, 89) the test data showed intermittent flow in loop1 (fig. 62, 63). PRZ role was correctly predicted. Core reflood mode could not be clearly identified.

PARTICIPANT: ALLEN - UKAEA CODE: TRAC

COMPARISON TABLE

PARAMETER		EXP	CALC	AE*	RFD**
1A Initial SGs mass (Kg)	1	137	107	P	
	2	151	108	P	B+C+U?
	3	145	113	P	
1B Trips timing (s)	LoLo	33	50	P	HIL(B+C+U)
	MSI	38	55	P	LoLo
	Scram	44	61	P	LoLo
1C Max primary pressure (MPa)		16.2	16.29	G	
1D SGs mass at Scram (Kg)	1	98	51	P	1A+1B
	2	105	62	P	
	3	97	54	P	
2A Min. primary pressure (MPa)		14.5	14.15	S	-
Pressure gradients before		4.10^{-4}	$-1.4.10^{-4}$	P	PRZM (U+B)
and after SGs DO (MPa/s)		3.10^{-4}	$3.9.10^{-3}$	P	PRZM (U+B)
2B SGs PORV opening time (s)	1	200	64	P	HSM (U)
	2	106	64	P	HSM (U)
	3	82	64	P	HSM (U)
2C PRZ level gradient (m/s)		$-5.7.10^{-4}$	$-3.4.10^{-4}$	S	-
2D Min. PRZ level (m)		2.3	3.41	P	2C+2E
2E SGs DO time, tSG1DO (s)		3347	1226	P	1D
tSG2DO (s)		3437	1302	P	
tSG3DO (s)		3282	1277	P	
2F Heat Up temperature (K/s)		0.02	0.035	P	HSM (U)+2E
and level (m/s) gradients		$3.6.10^{-3}$	$4.2E^{-3}$	S	
2G Cool Insurge effect		PR. DELAY	NO	P	PRZM (U+B)
2H PRZ PORV opening time, t2 (s)		4134	1595	P	2E+2F
$(dt_2 = t_2 - t_{SGDO})$		(697)	(293)	P	+PRZM(U+B)
3A PRZ level at t_2 (m)		6.57	5.3	P	2H
3B PRZ full time, t_{PRZF} (s)		4222	1890	P	2E
$(dt_{PRZF} = t_{PRZF} - t_2)$		(88)	(295)	P	2H
3C Dominant Relief Condition		LIQ	LIQ	G	-
3D Sat. Conditions before trip		NO	NO	G	-
3E Pumps Trip time, t3 (s)		4848	2316	P	2E+2F
$(dt_3 = t_3 - t_2)$		(714)	(721)	G	2H+3E(t_3)
$(dt_{HU} = t_3 - t_{SGDO})$		(1411)	(1014)	S	2F

* ACCURACY EVALUATION : G=GOOD, S=SUFFICIENT, P=POOR

** REASON FOR DISCREPANCY : B=BIC, C=CODE, U=USER, PRZM=PRZ MODELLING, HSM=HEAT STRUCTURES MODELLING, HIL=HIGH INITIAL LEVEL

PARTICIPANT: ALLEN - UKAEA CODE: TRAC

COMPARISON TABLE (CONT'D)

PARAMETER	EXP	CALC	AE*	RFD**
3F RCS mass at t_3 (kg)	390	401	S	-
4A PRZ behaviour during phase 4	PART. LEV. EMPT. OBS.	PART. LEV. EMPT. OBS.	G	-
4B Primary Flow Cond.	TPNC/LNC	TPNC/LNC	G	-
4C LNC time, t_{LNC} (s)	5630	2650	P	3E+LDP(C)
($dt_{LNC} = t_{LNC} - t_3$)	(780)	(334)	P	LDP(C)
4D RCS mass at t_{LNC} (kg)	296	310	G	-
4E Beg. of Core Heat Up, t_{BOCH} (s)	6511	3130	P	4C+LDP(C)
($dt_{BOCH} = t_{BOCH} - t_{LNC}$)	(880)	(480)	P	LDP(C)
4F RCS mass at tBOCH (Kg)	183	184	G	-
4G EFW act. time, t4 (s)	6532	3142	P	4E+LDP(C)
($dt_{4B} = t_4 - t_{BOCH}$)	(21)	(12)	P	?
($dt_{4L} = t_4 - t_{LNC}$)	(900)	(493)	P	LDP(C)
($dt_4 = t_4 - t_3$)	(1684)	(827)	P	LDP(C)
4H PRZ level at t_4 (m)	4.4	4.52	G	-
5A Core Heat Up Rate (K/s)	2/5	1.47	P	CHC? (U)
5B Max Core Temperature (K)	770	713	S	-
5C PRZ PORV closure time, t_{PRZPC}	6576	3172	P	4G
($dt_{PRZPC} = t_{PRZPC} - t_4$)	(44)	(29)	S	-
5D RCS mass at t_{PRZPC} (Kg)	179	179	G	-
5E RCS Depress. Rate (MPa/s)	-0.016	-0.029	P	HSM? (U)
(Initial/Averaged on 500 s)	-0.0086	-0.01	G	
5F Prim. Circulation Mode	INTERM	TPNC	P	PMD?(C?)
5G SG1 Press. time, t_{SG1PR} (s)	6878	3160	P	4G+HSM(U)
($dt_{SG1PR} = t_{SG1PR} - t_4$)	(346)	(17)	P	
5H PRZ Role	CORE FL.	CORE FL.	G	-
5I PRZ emptying time, t_{PRZE} (s)	6811	3354	P	4G
($dt_{PRZE} = t_{PRZE} - t_4$)	(280)	(211)		
5J Core Reflood Mode	TOP-DOWN	?		?
5K End of Transient time, t_{END}	8062	4551	P	4G

* ACCURACY EVALUATION : G=GOOD, S=SUFFICIENT, P=POOR
** REASON FOR DISCREPANCY : C=CODE, U=USER, LDP=LIQUID DISCHARGE FROM PRESSURIZER, PMD=PRIMARY MASS DISTRIBUTION, CHC=CORE HEAT CAPACITY

4.17.3 SENSITIVITY CASE

Since TRAC code takes no account of fluid condition in determining the mass exchange between main and side pipes (the average density in the main pipe is passed to the side pipe), a sensitivity calculation was performed, with the flow area at the junction between hot leg and surge line increased by a factor of 100. In such a way it's possible to enphasize the phase gravity separation and the preferential passage of steam towards the surge line. Actually pressurizer level behaviour after pumps trip is strongly influenced by the flow quality in surge line, which is in turn strongly influenced by the void distribution in the hot leg cross section during two phase natural circulation period and, later, in stagnation conditions (with horizontal stratification).

In fig. 3S primary coolant mass is plotted. In the increased junction area case (indicated by AEAS) primary mass decrease rate after loss of TPNC is lower than in the base case, denoting a higher quality in the volume upstream PRZ PORV (that is a lower PRZ collapsed level). The increased volume discharge capability of the valve can be seen also in primary pressure behaviour (fig. 2S): the primary pressure peak following the stagnation (observed in the base case) doesn't occurs any more in the sensitivity case.

The delayed primary emptying of the sensitivity case involves a delayed core level drop (fig. 5S) and therefore delayed core dry out (fig. 6S).

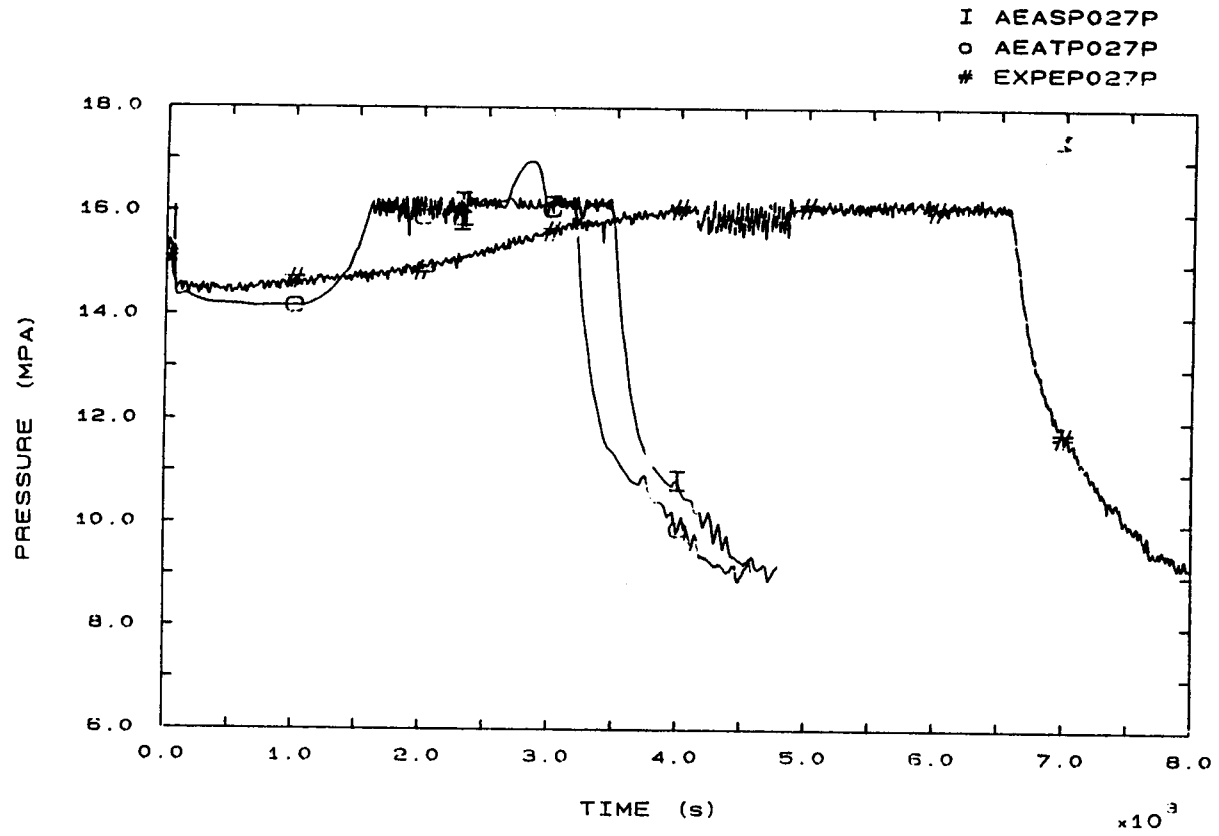

FIG. 2S PRESSURIZER PRESSURE

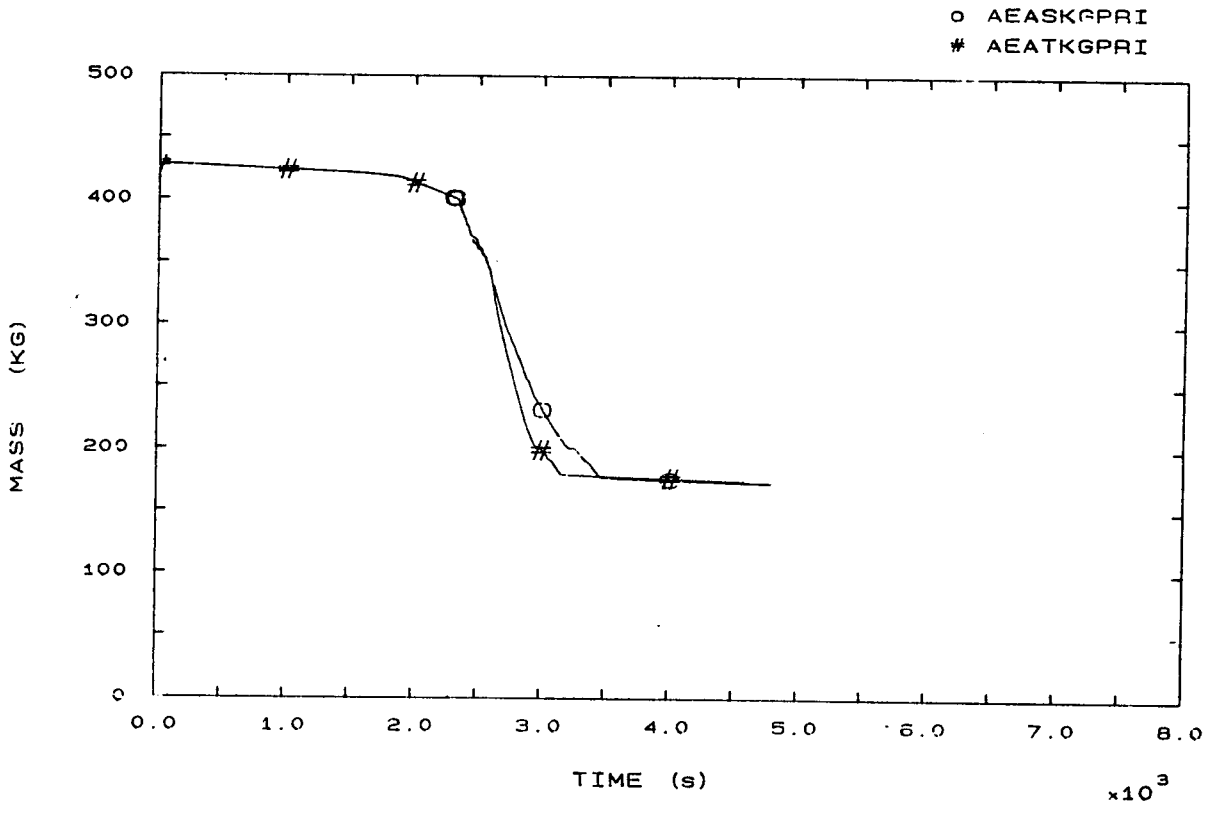

FIG. 3S PRIMARY COOLANT TOTAL MASS

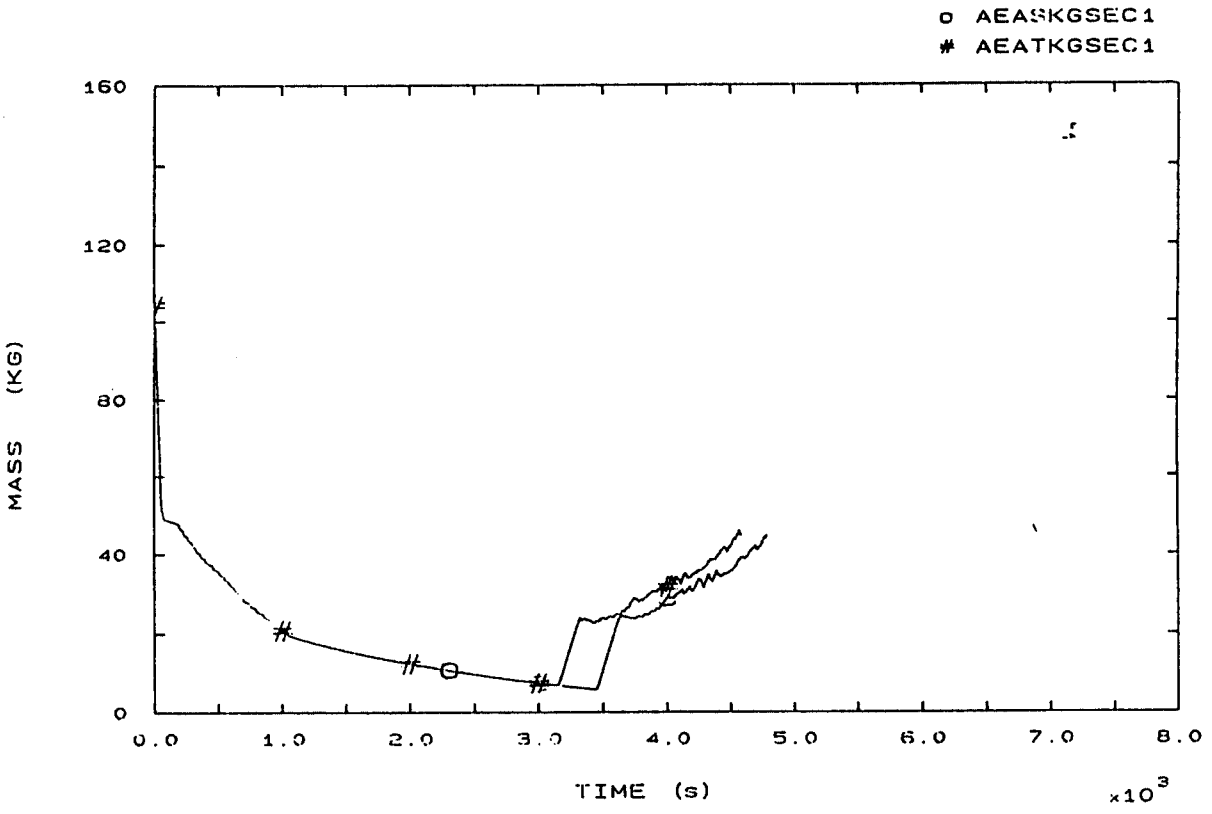

FIG 4S SECONDARY COOLANT TOTAL MASS SG1

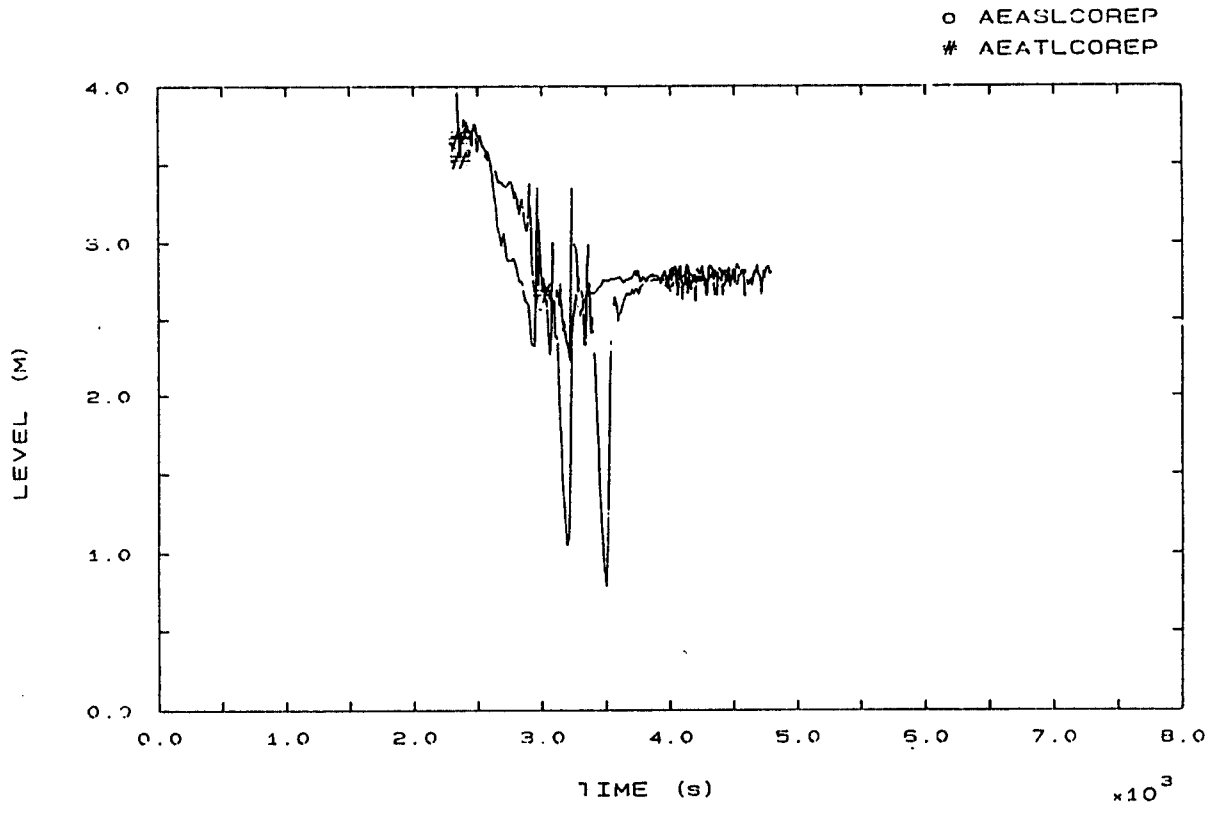

FIG. 5S CORE LEVEL

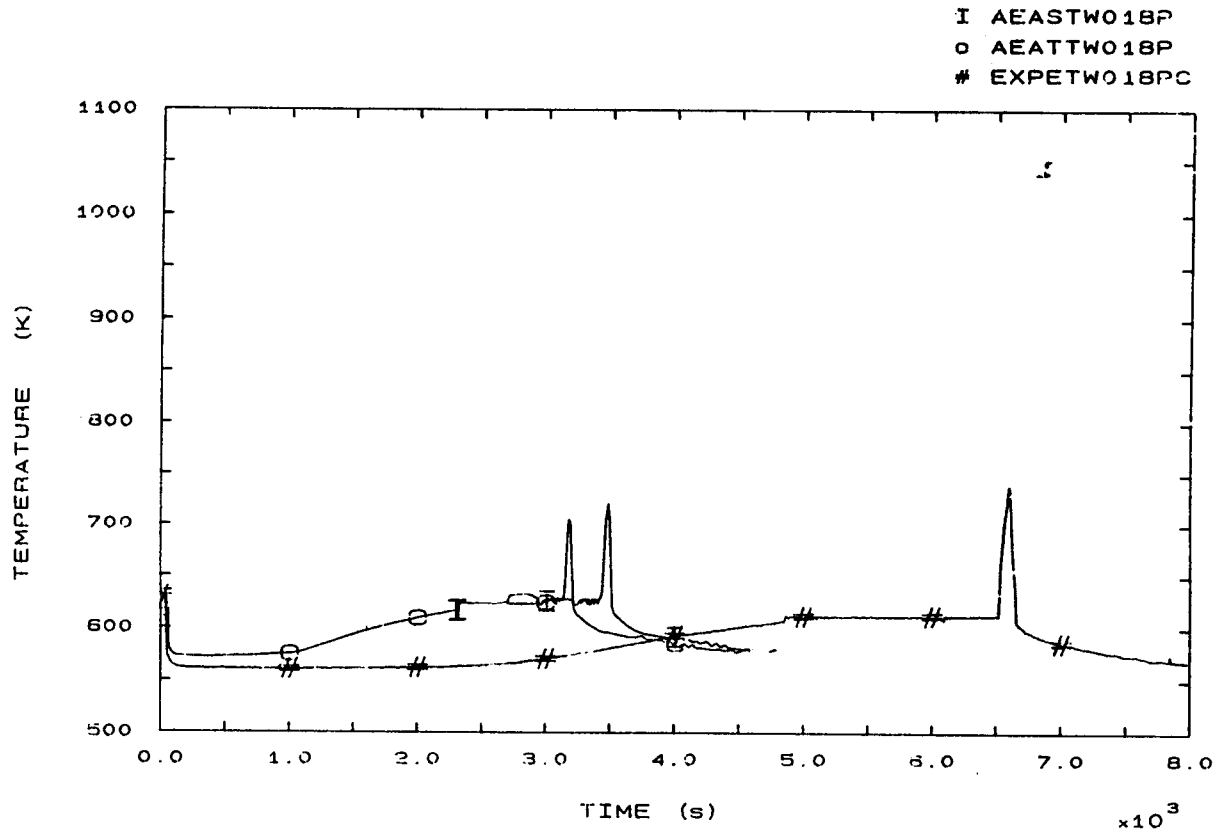

FIG. 6S SURFACE TEMPERATURE AT ROD BUNDLE ELEVATION 3294 MM

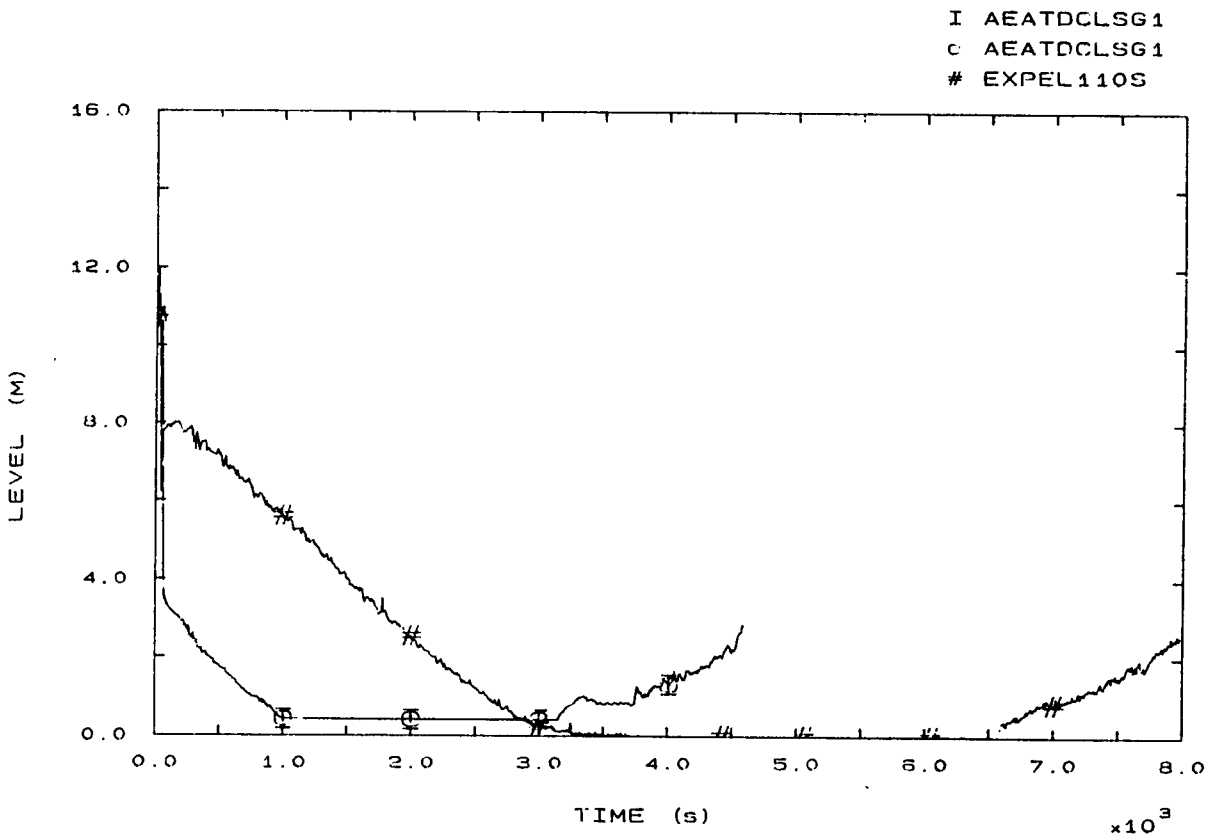

FIG. 7S SG1 DOWNCOMER LEVEL

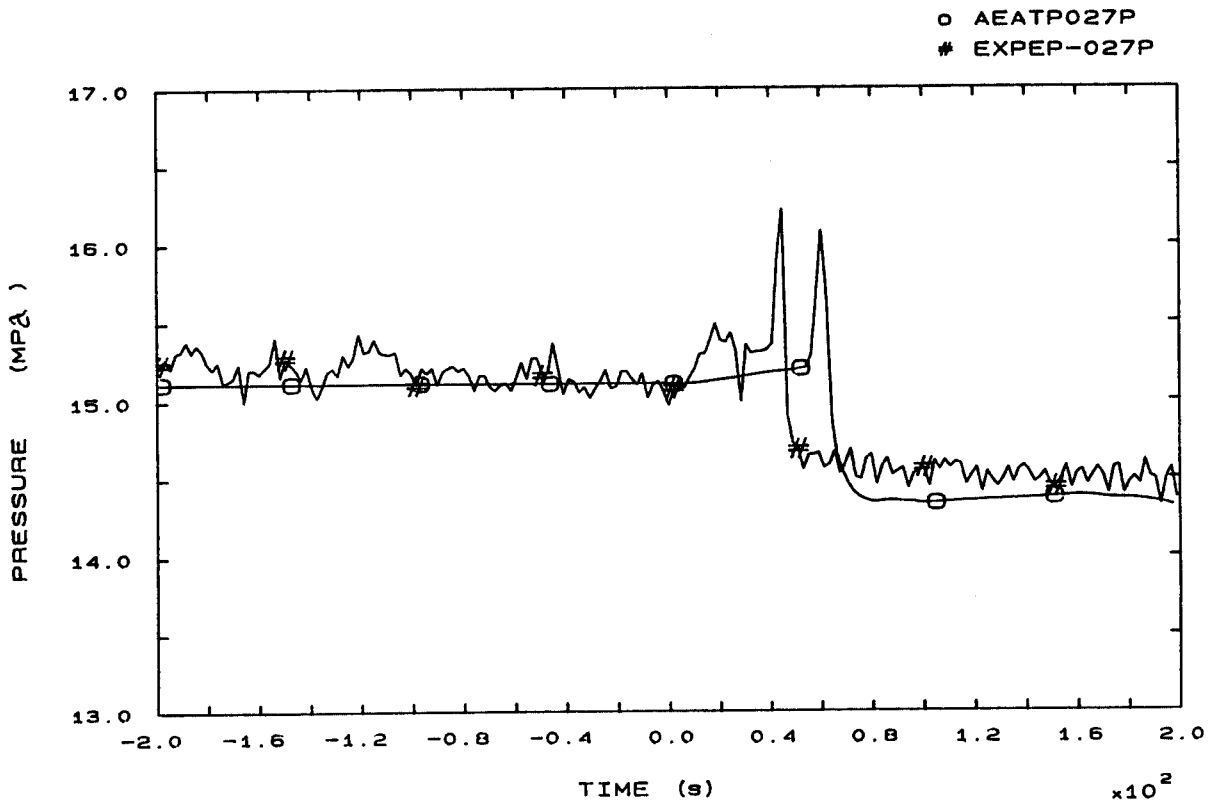

FIG. 1b PRESSURIZER PRESSURE

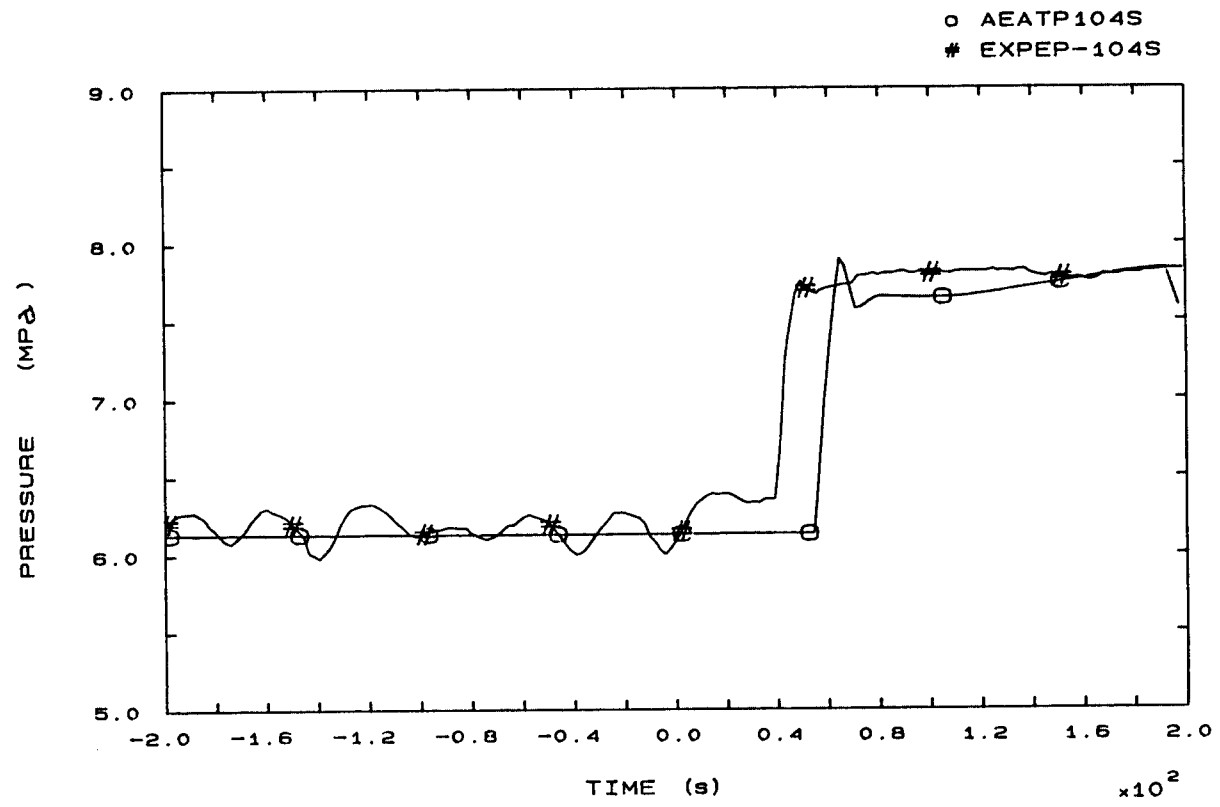

FIG. 3b SG1 STEAM DOME PRESSURE

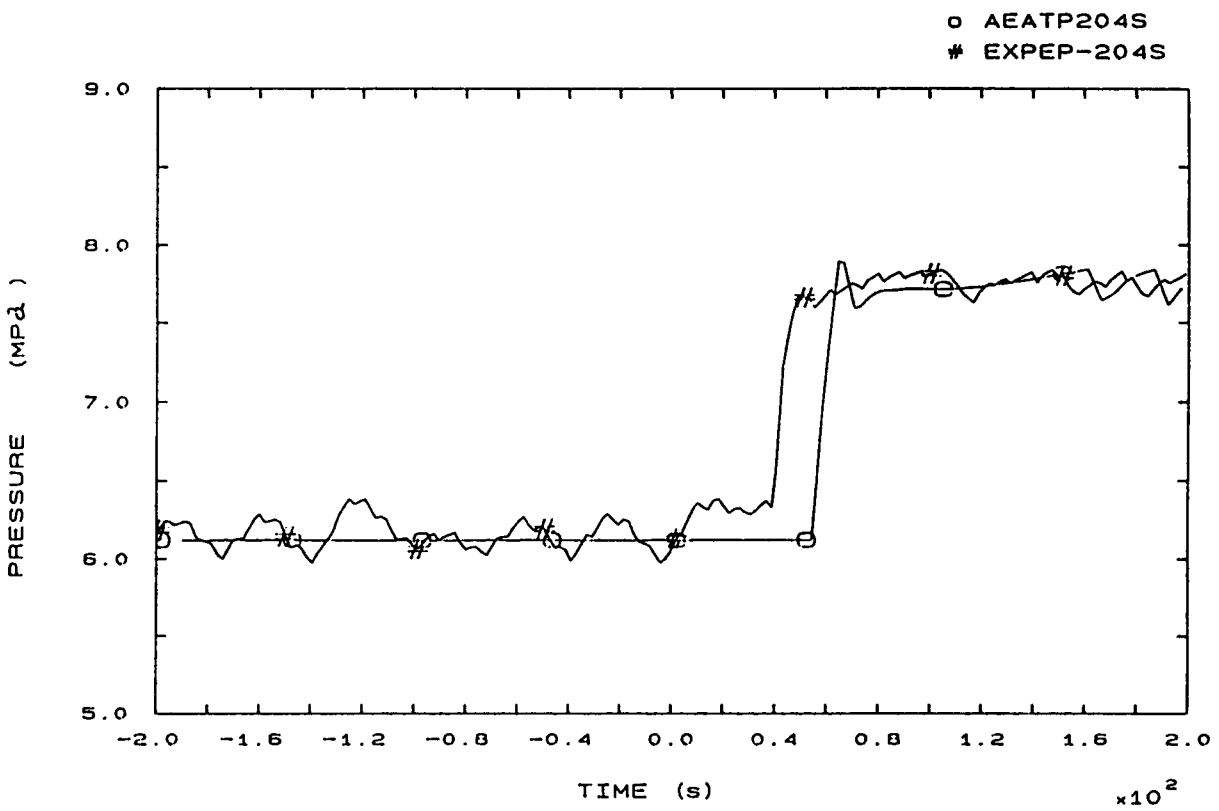

FIG. 4b SG2 STEAM DOME PRESSURE

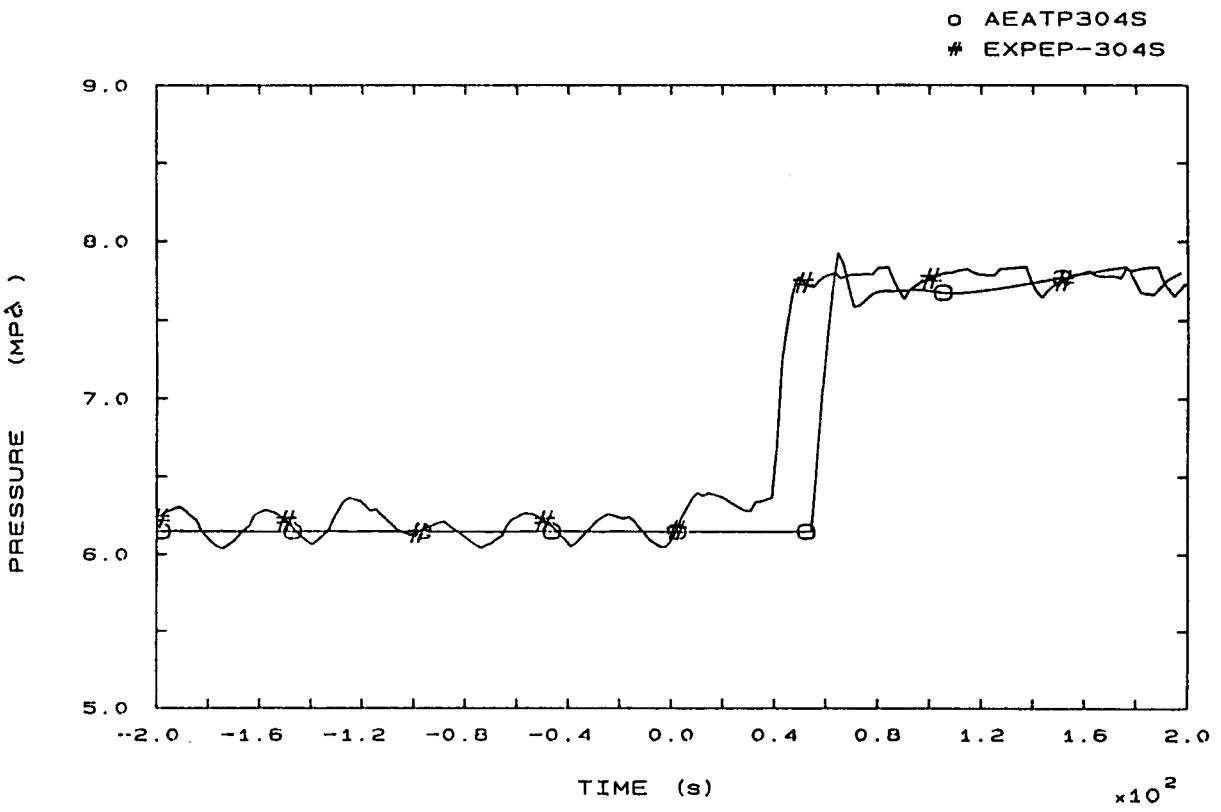

FIG. 5b SG3 STEAM DOME PRESSURE

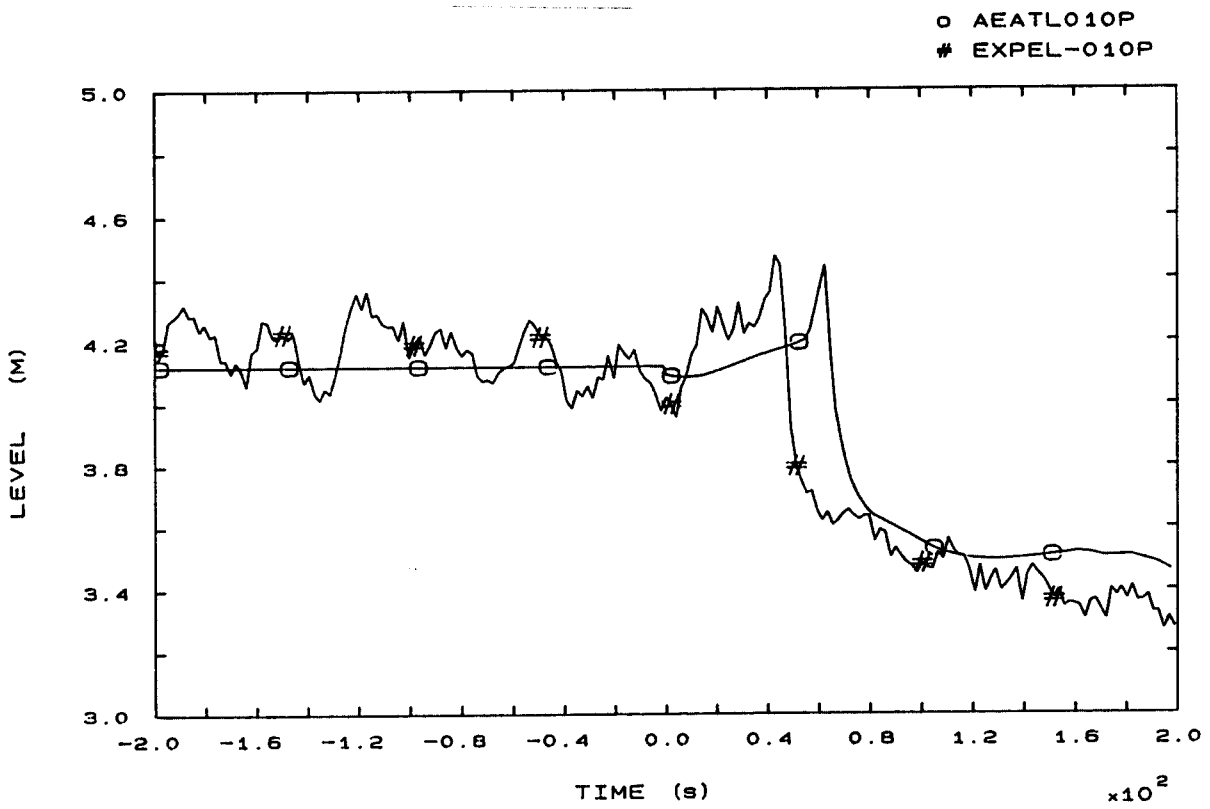

FIG. 6b PRESSURIZER LEVEL

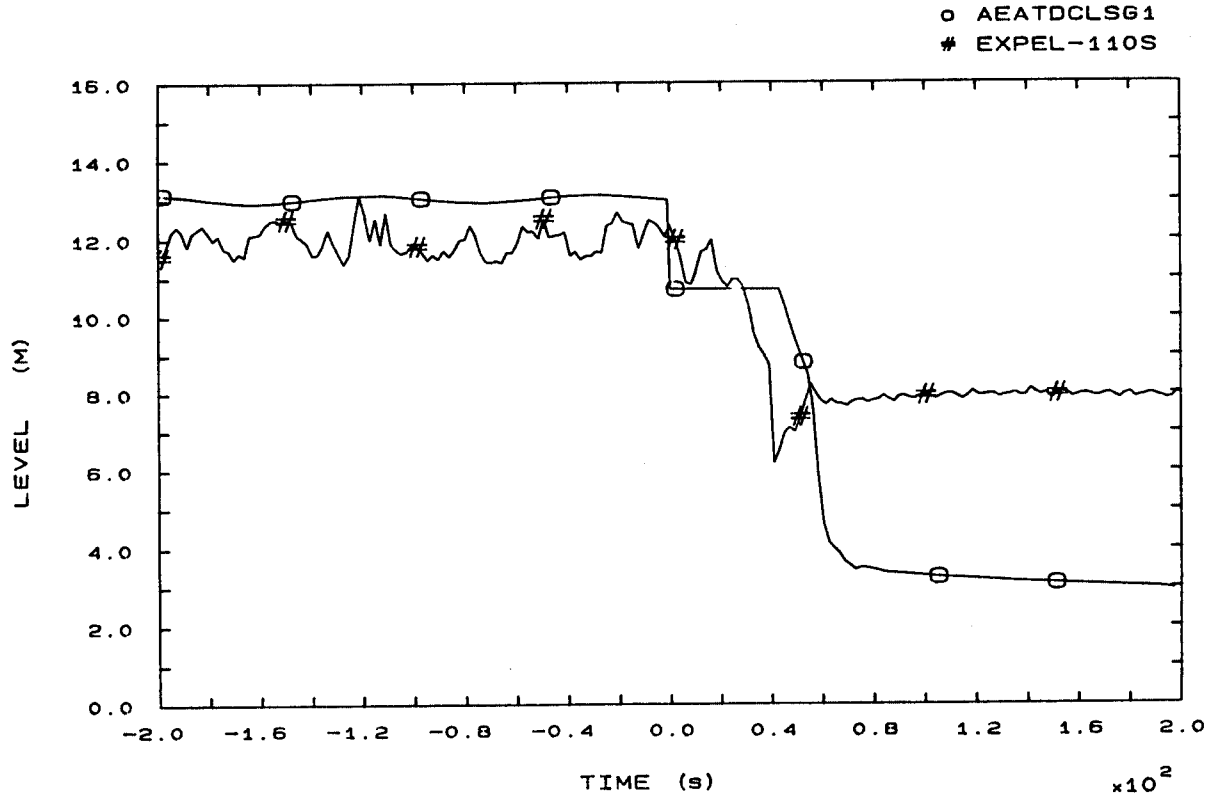

FIG. 7b SG1 DOWNCOMER LEVEL

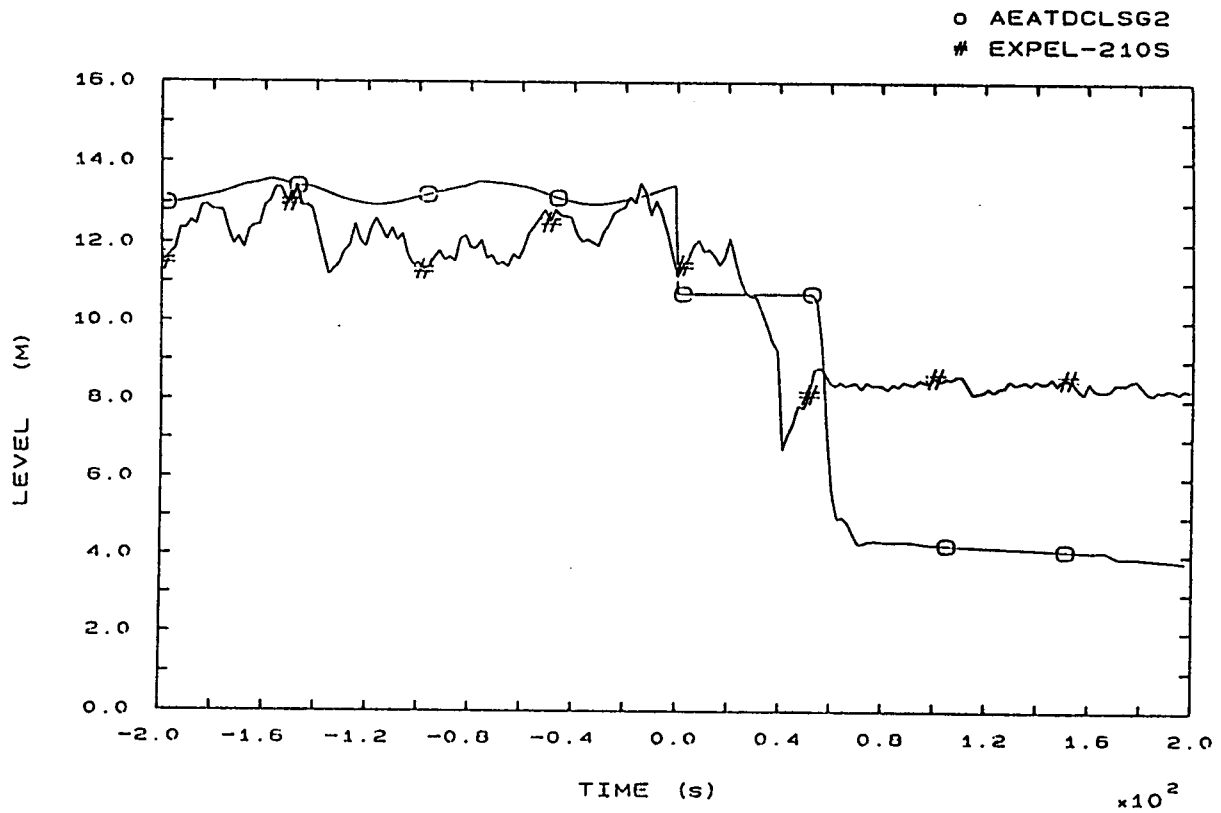

FIG. 8b SG2 DOWNCOMER LEVEL

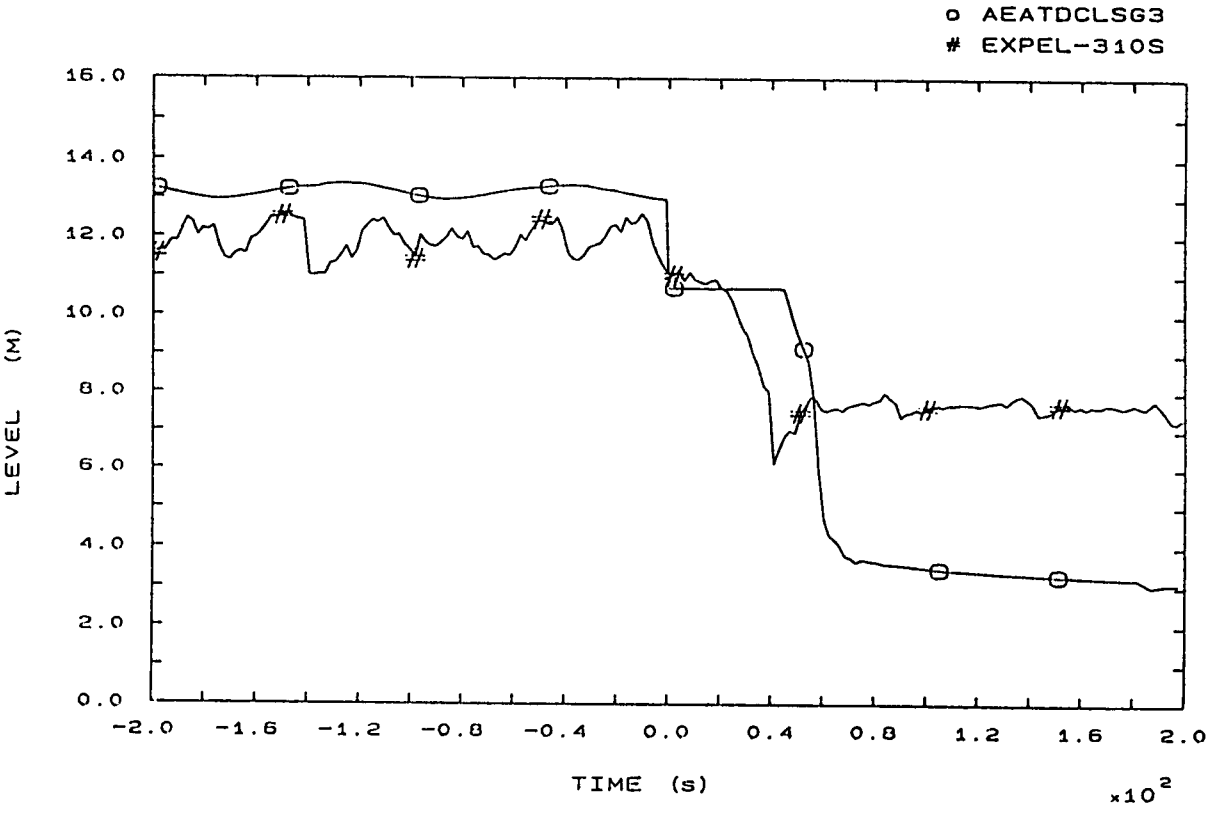

FIG. 9b SG3 DOWNCOMER LEVEL

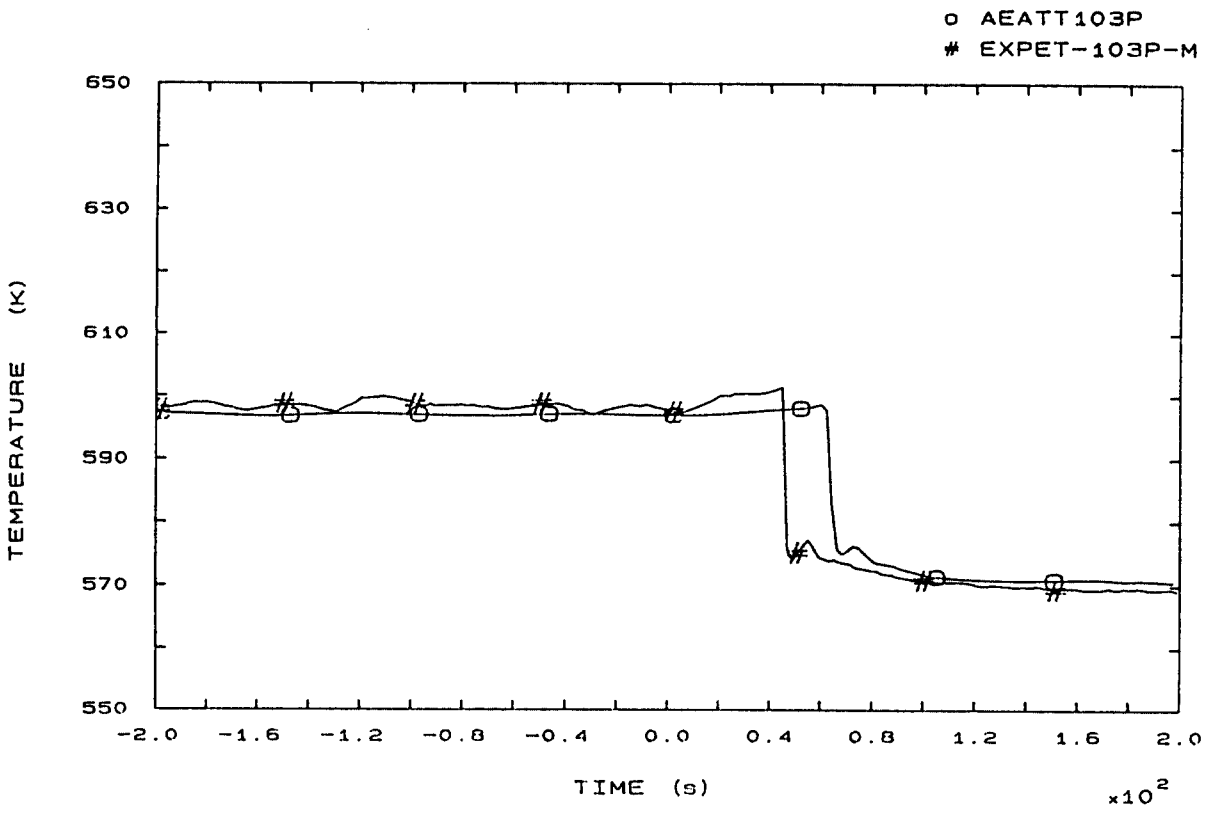

FIG. 12b LP1 HOT LEG OUTLET VESSEL TEMPERATURE

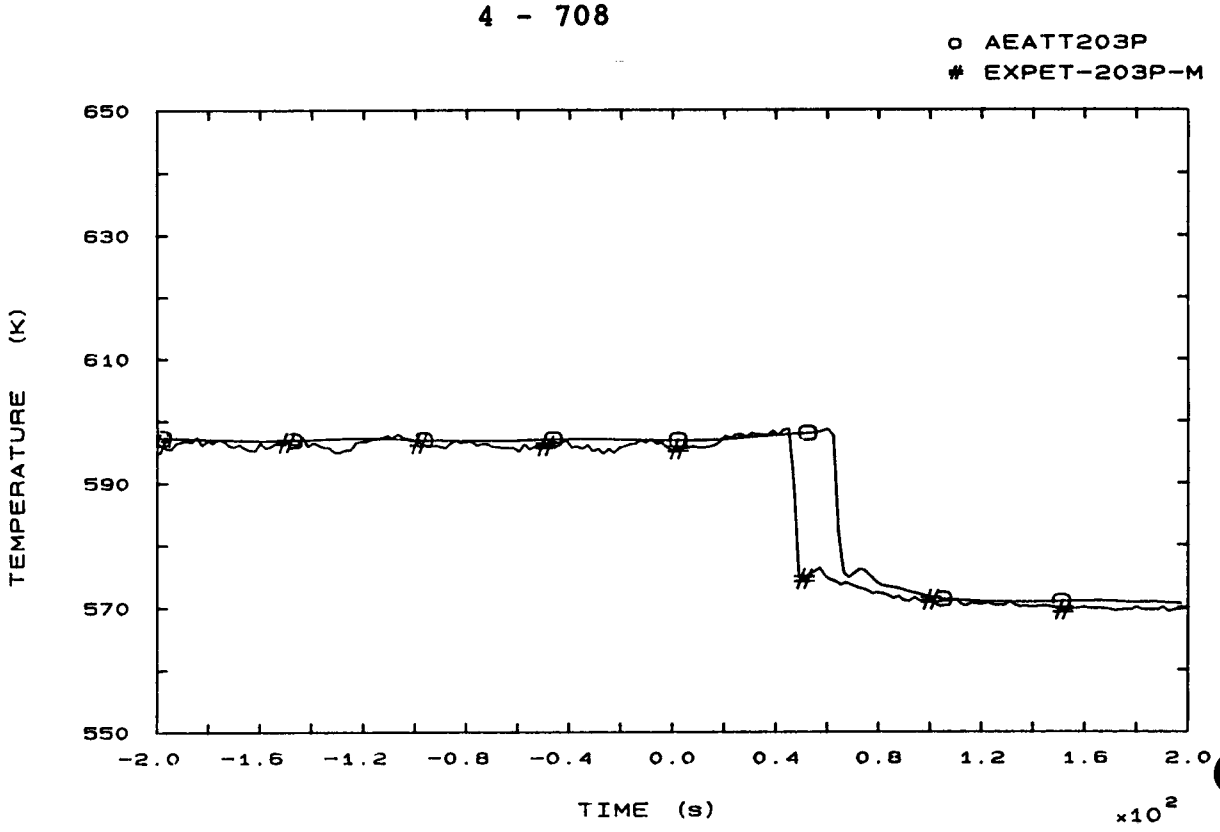

FIG. 22b LP2 HOT LEG OUTLET VESSEL TEMPERATURE

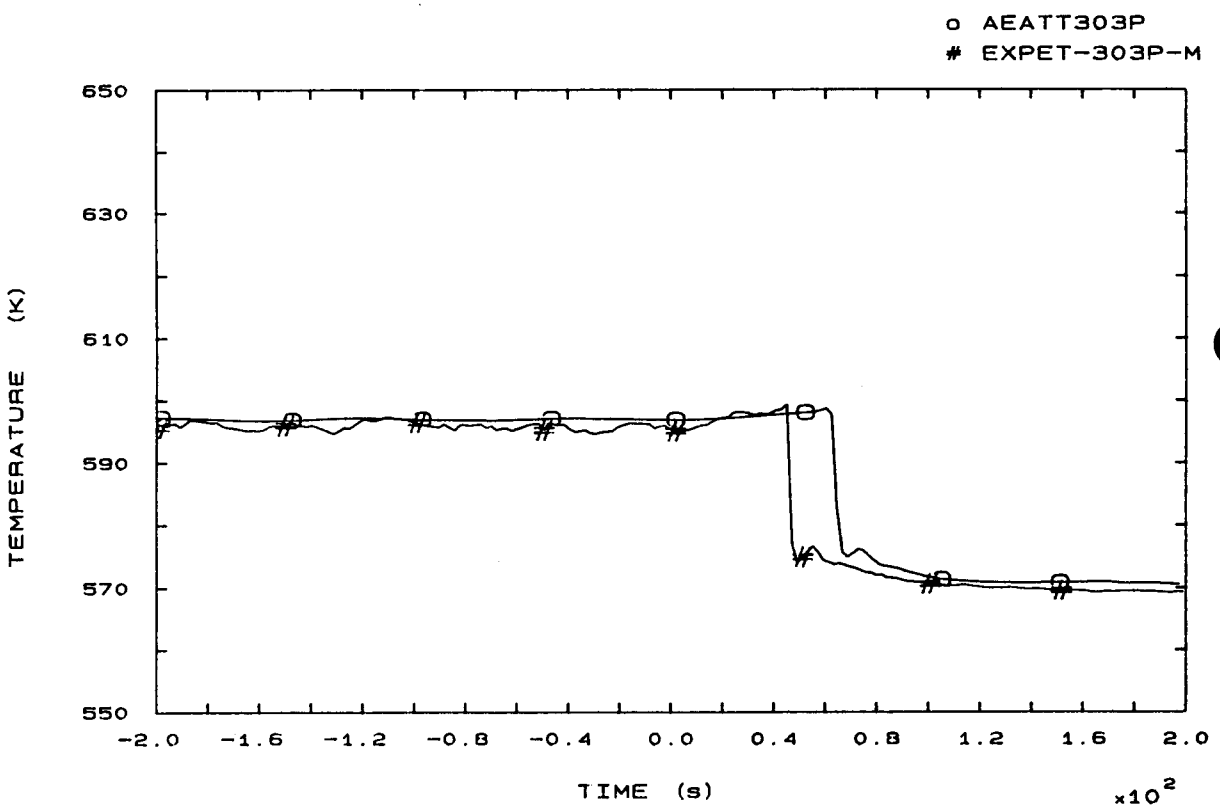

FIG. 32b LP3 HOT LEG OUTLET VESSEL TEMPERATURE

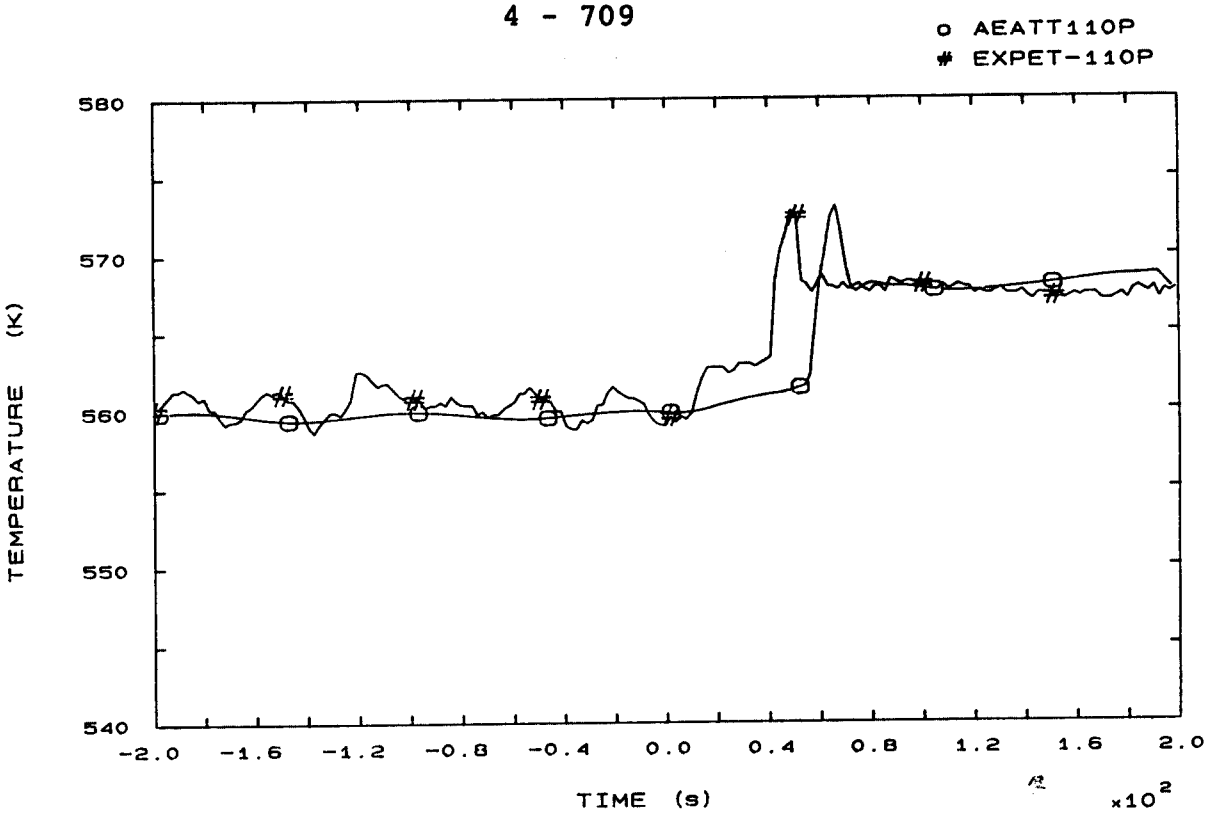

FIG. 42b SG1 OUTLET TEMPERATURE

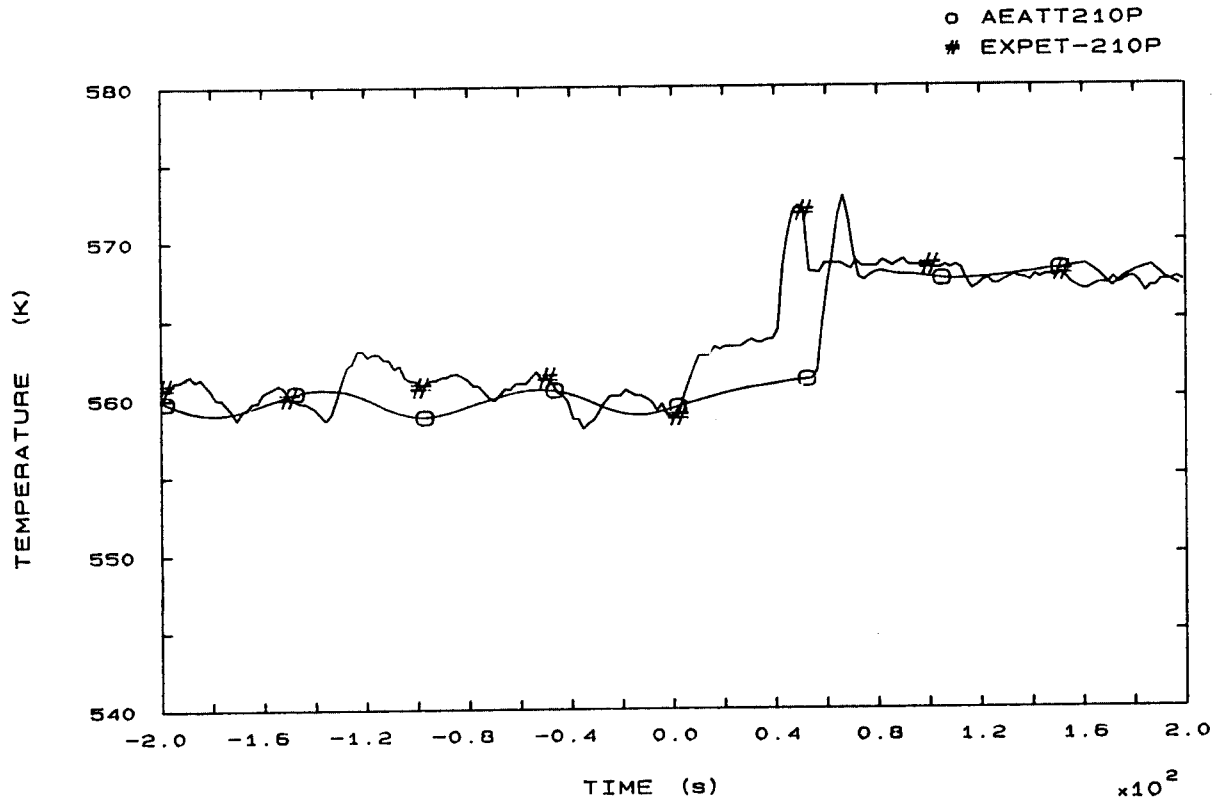

FIG. 44b SG2 OUTLET TEMPERATURE

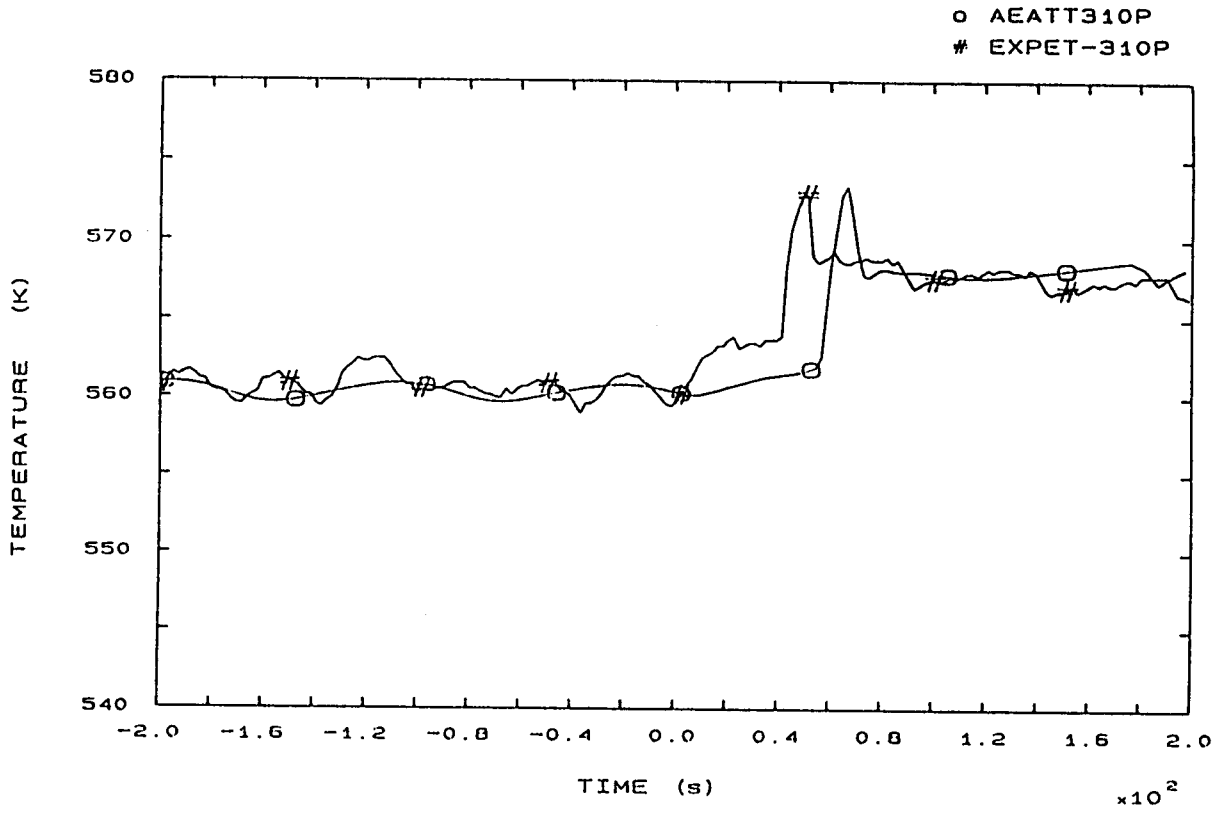

FIG. 46b SG3 OUTLET TEMPERATURE

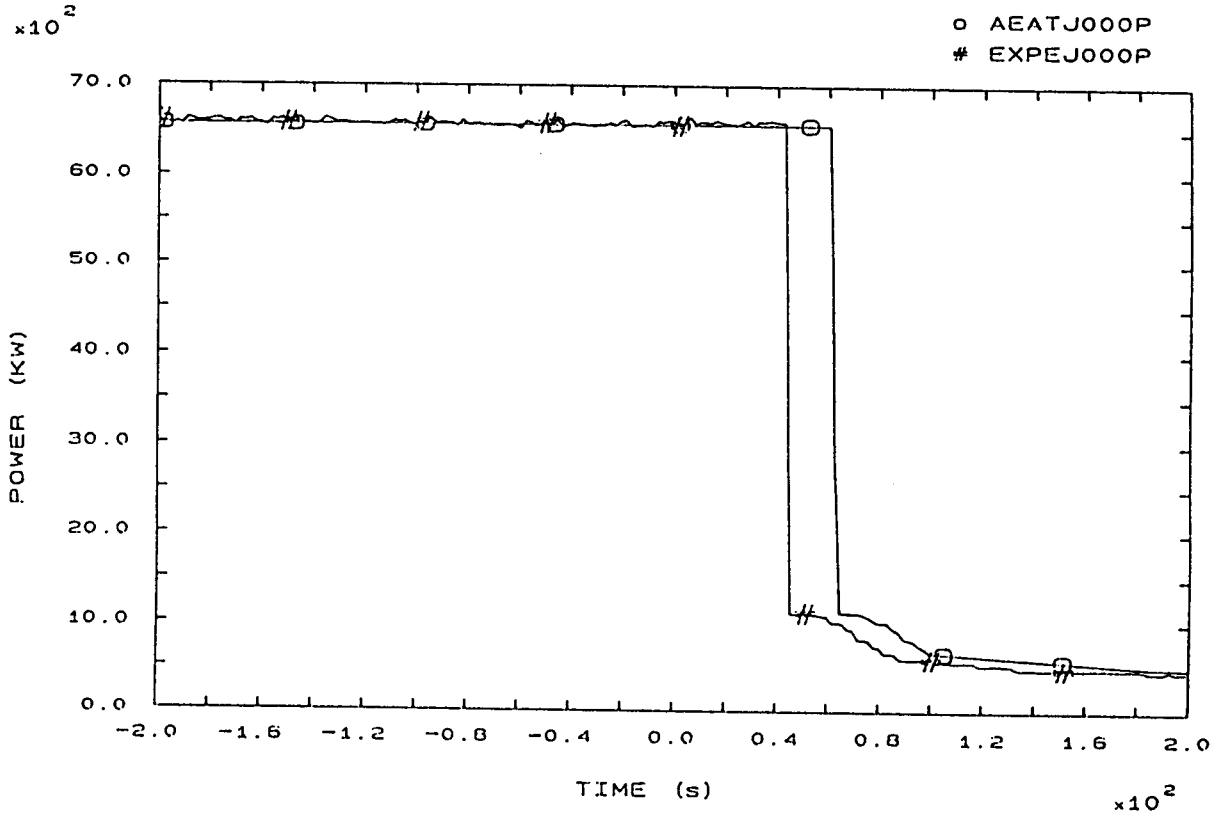

FIG. 81b HEATER RODS POWER

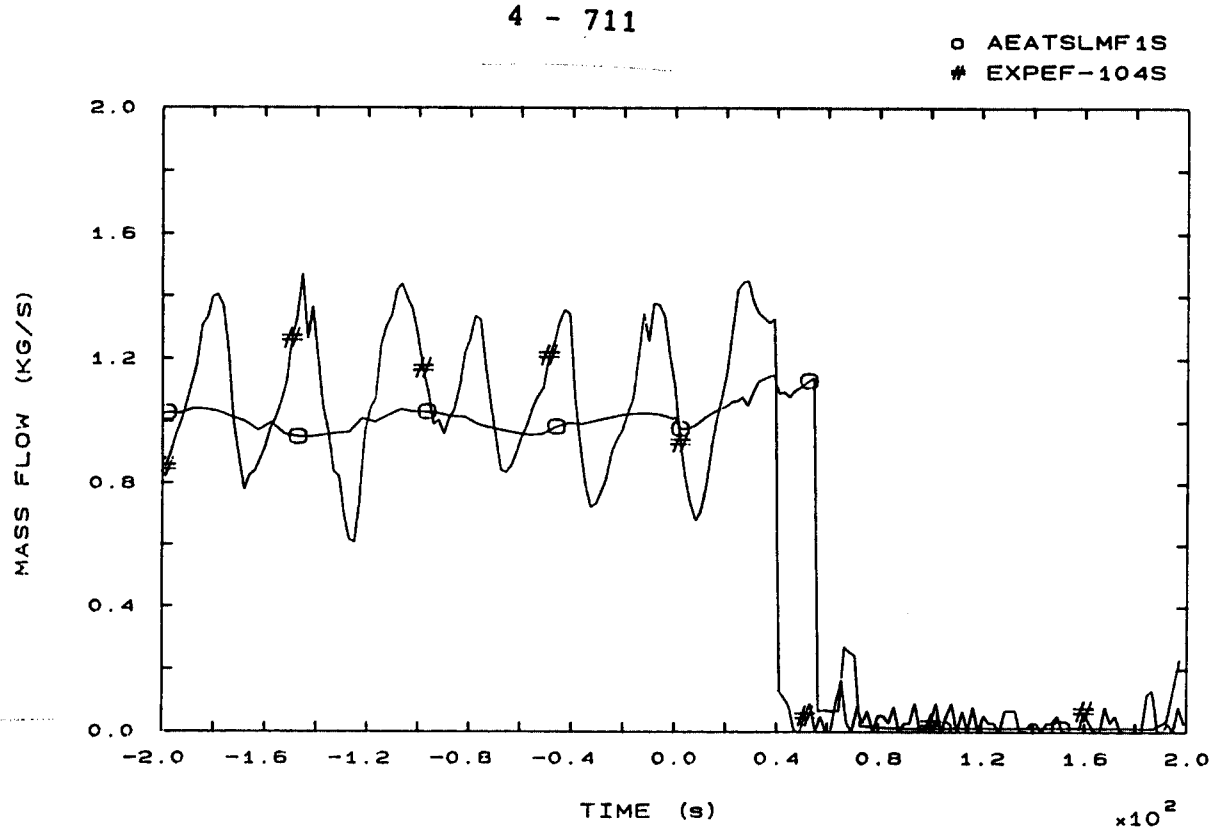

FIG. 96b STEAM LINE 1 MASS FLOW

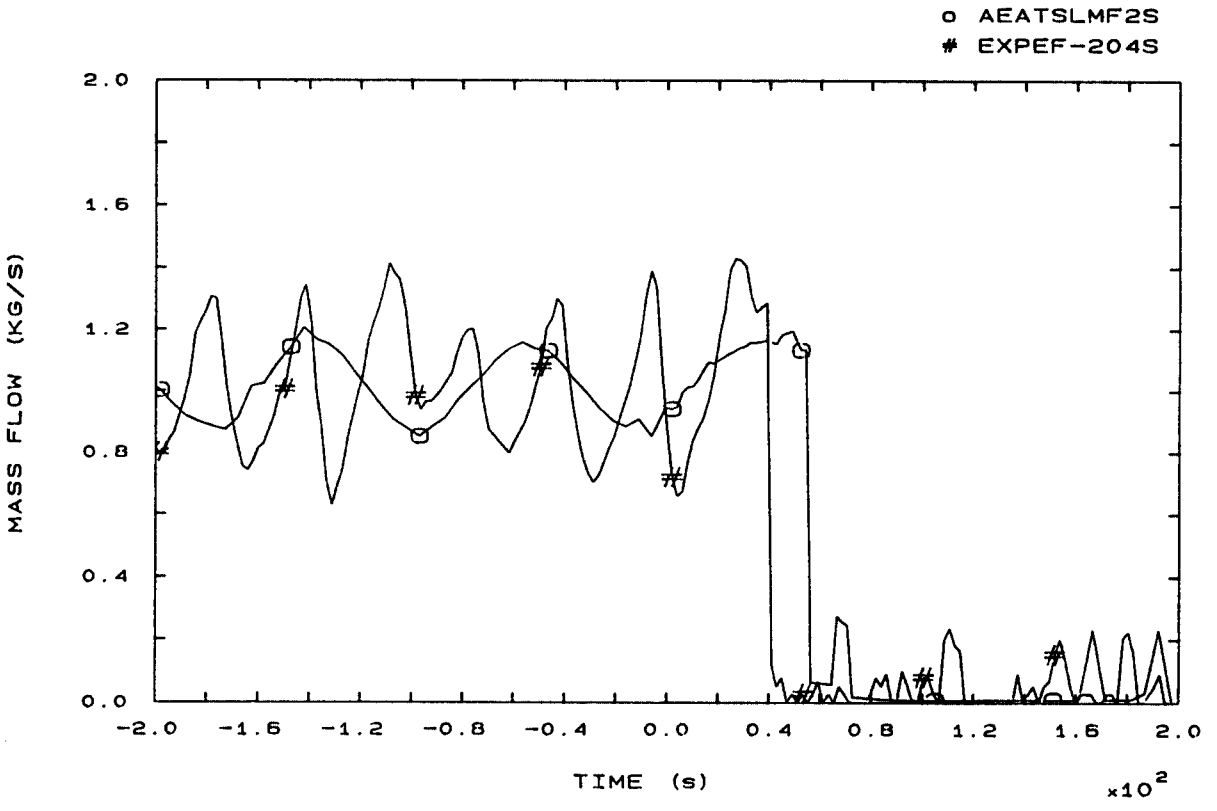

FIG. 97b STEAM LINE 2 MASS FLOW

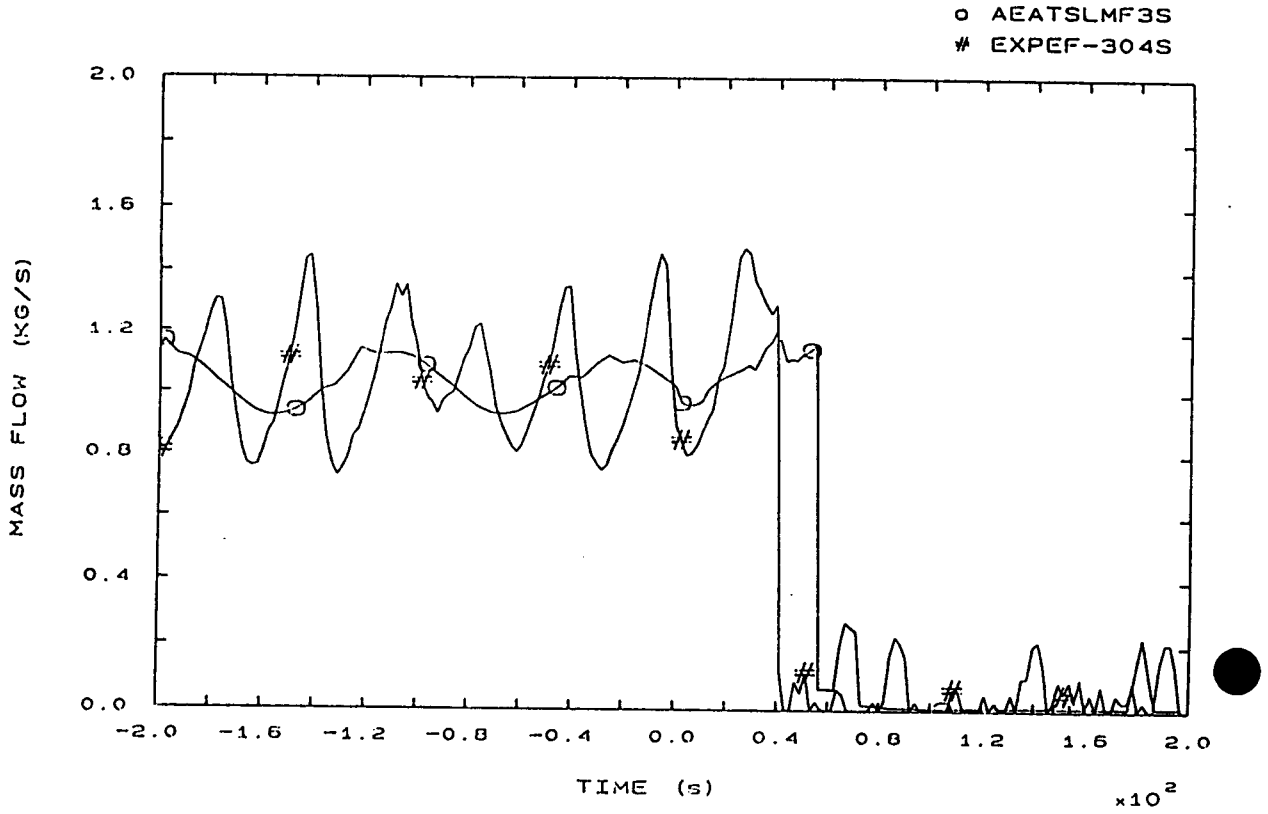

FIG. 98b STEAM LINE 3 MASS FLOW

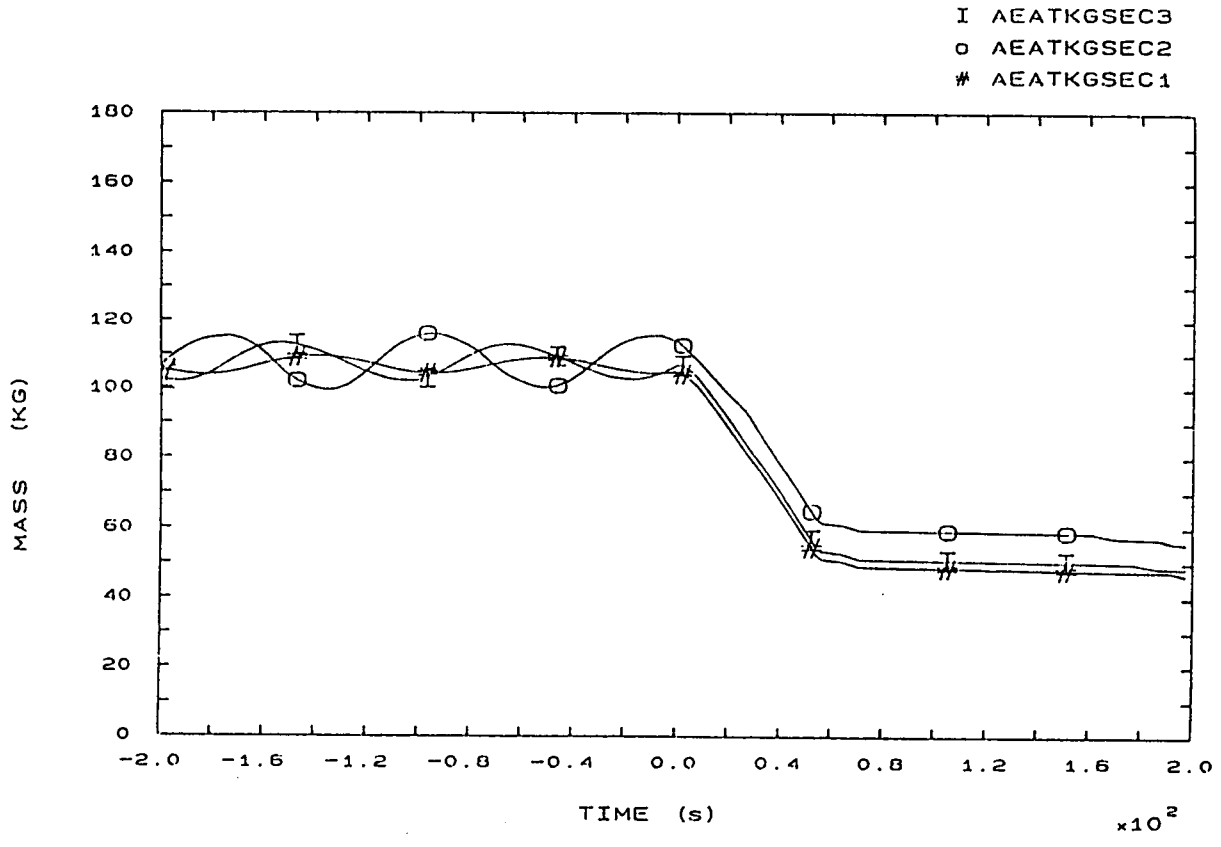

FIG. 142b SECONDARY COOLANT TOTAL MASS IN SGs

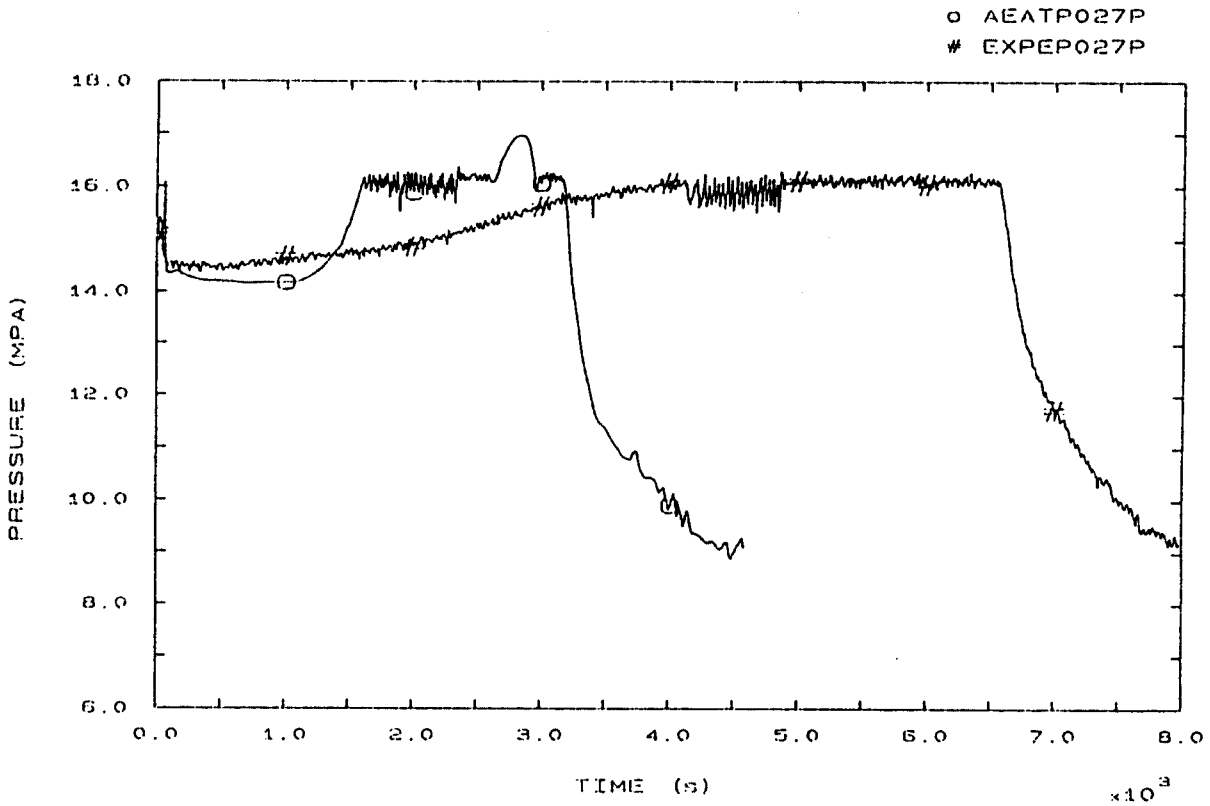

FIG. 1 PRESSURIZER PRESSURE

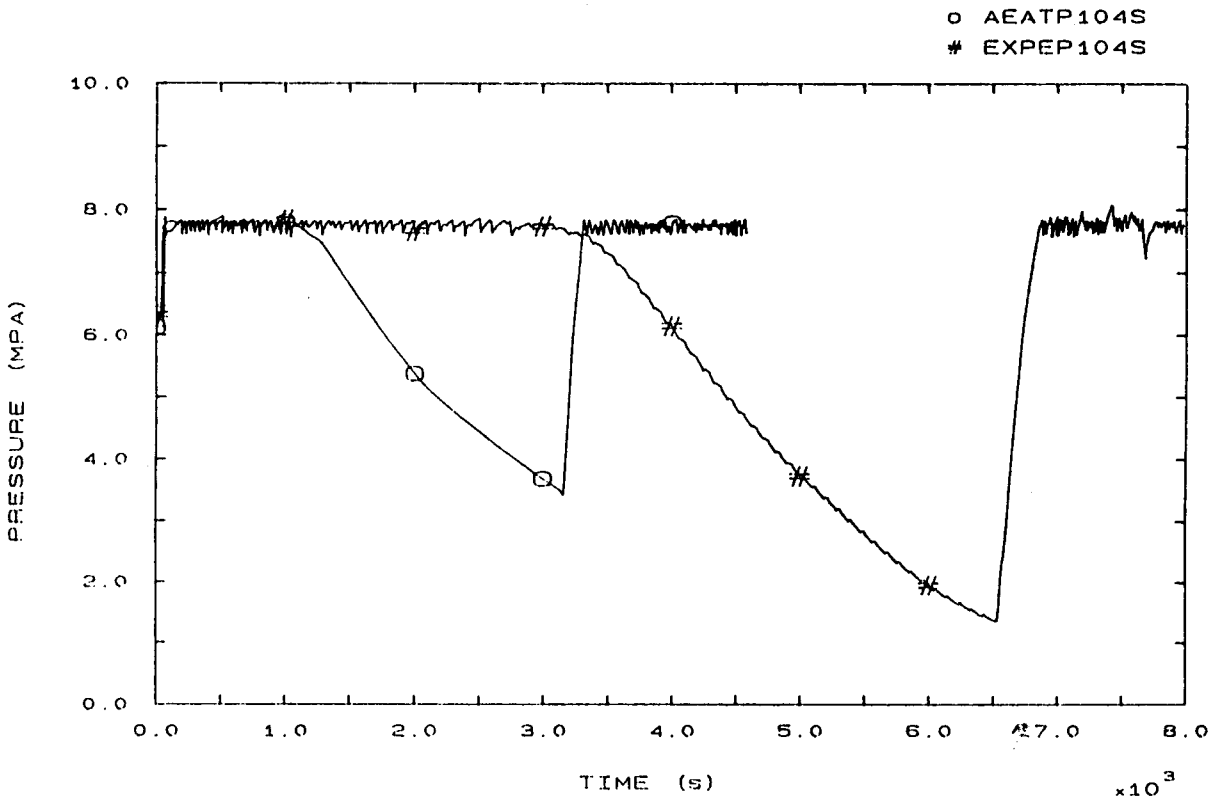

FIG. 3 SG1 STEAM DOME PRESSURE

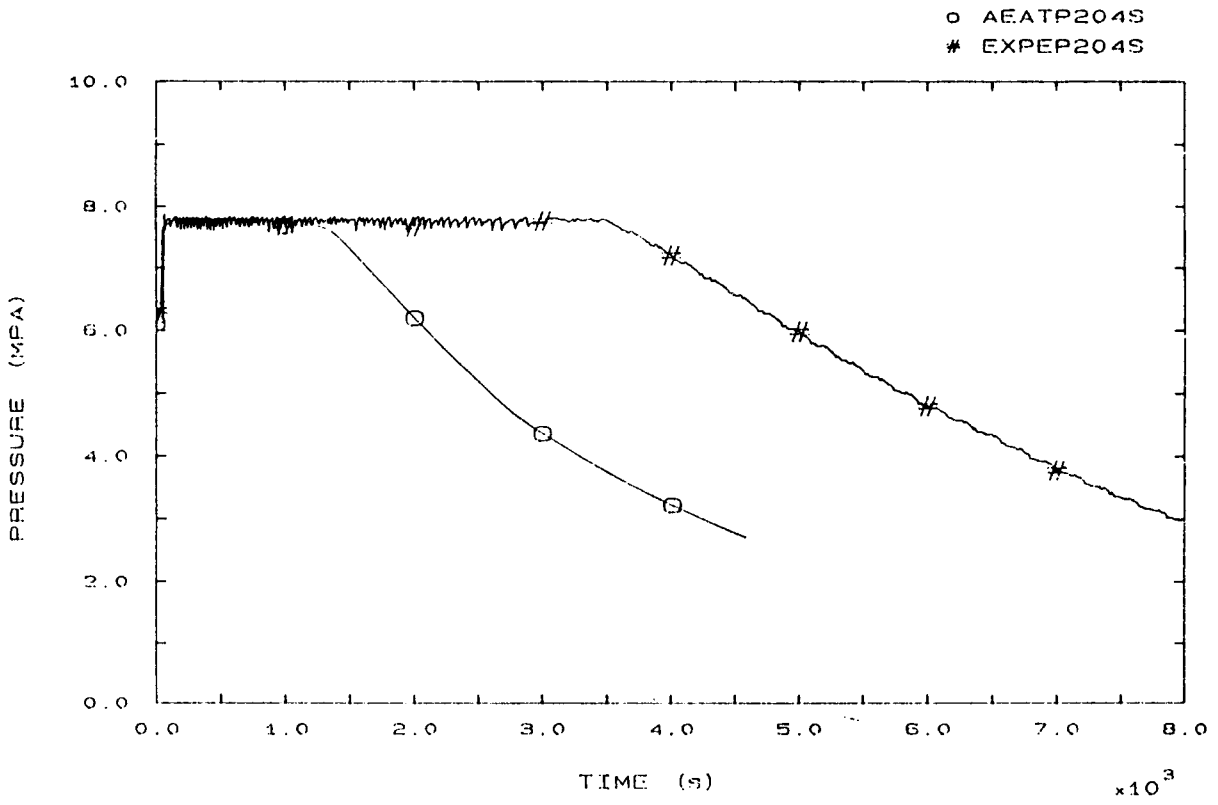

FIG. 4 SG2 STEAM DOME PRESSURE

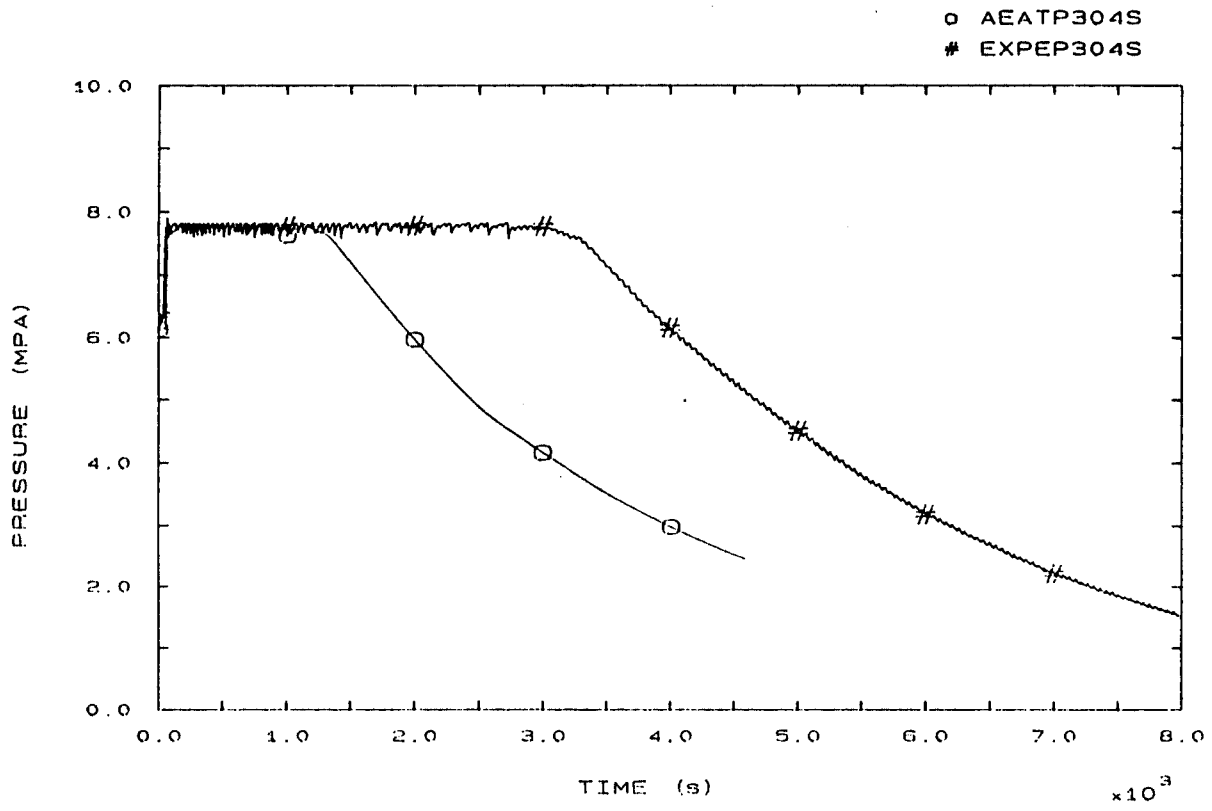

FIG. 5 SG3 STEAM DOME PRESSURE

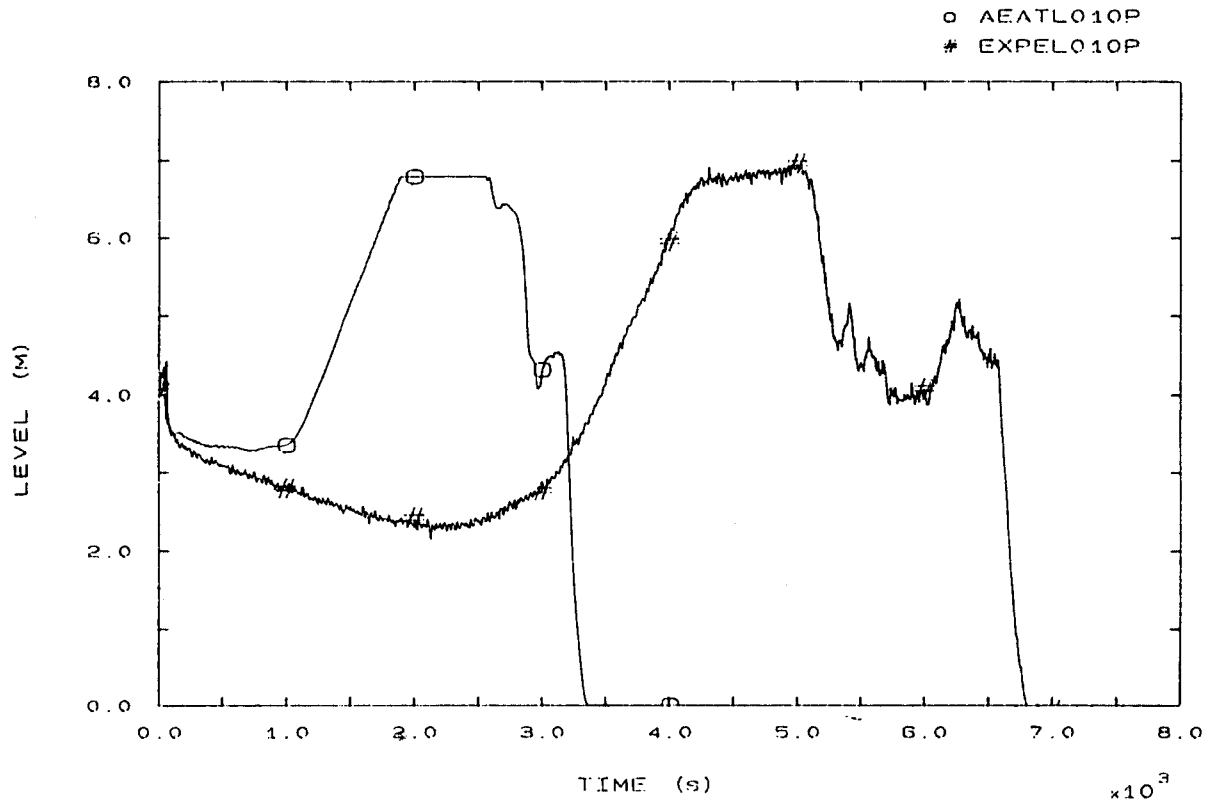

FIG. 6 PRESSURIZER LEVEL

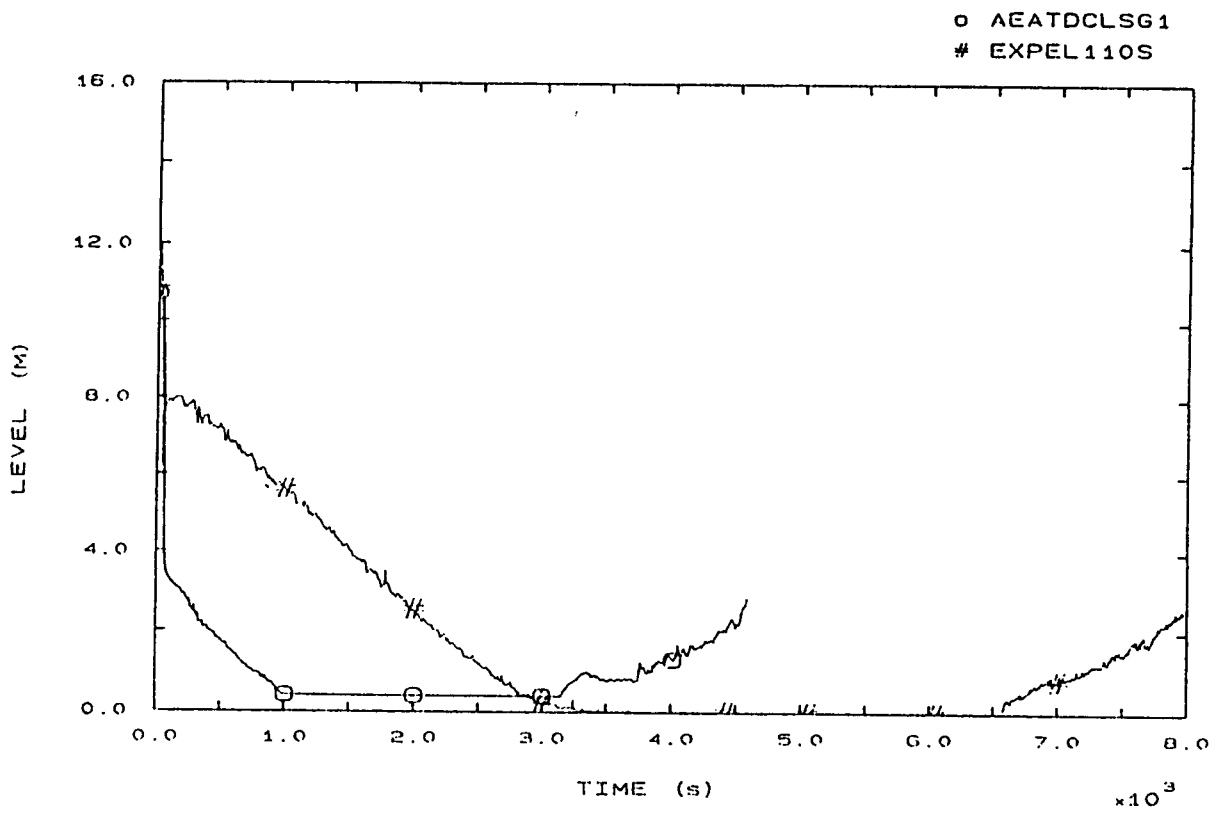

FIG. 7 SG1 DOWNCOMER LEVEL

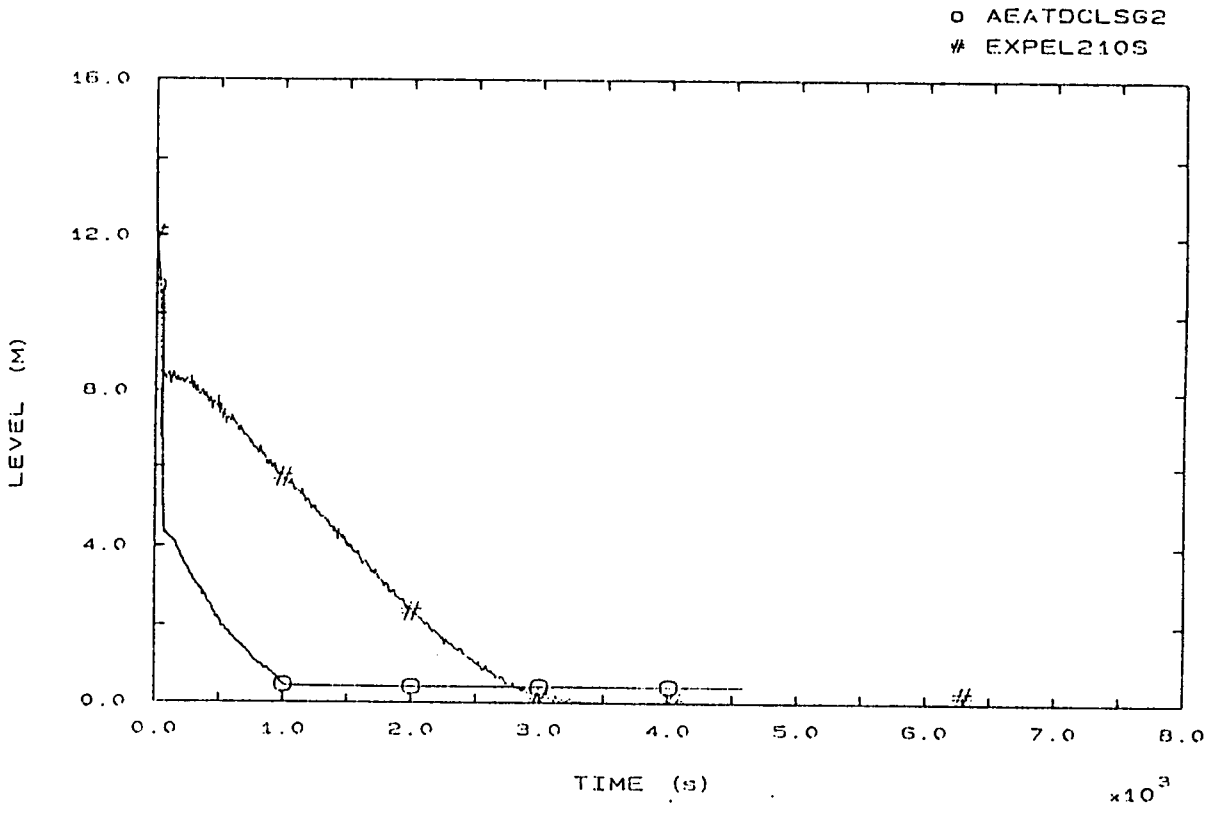

FIG. 8 SG2 DOWNCOMER LEVEL

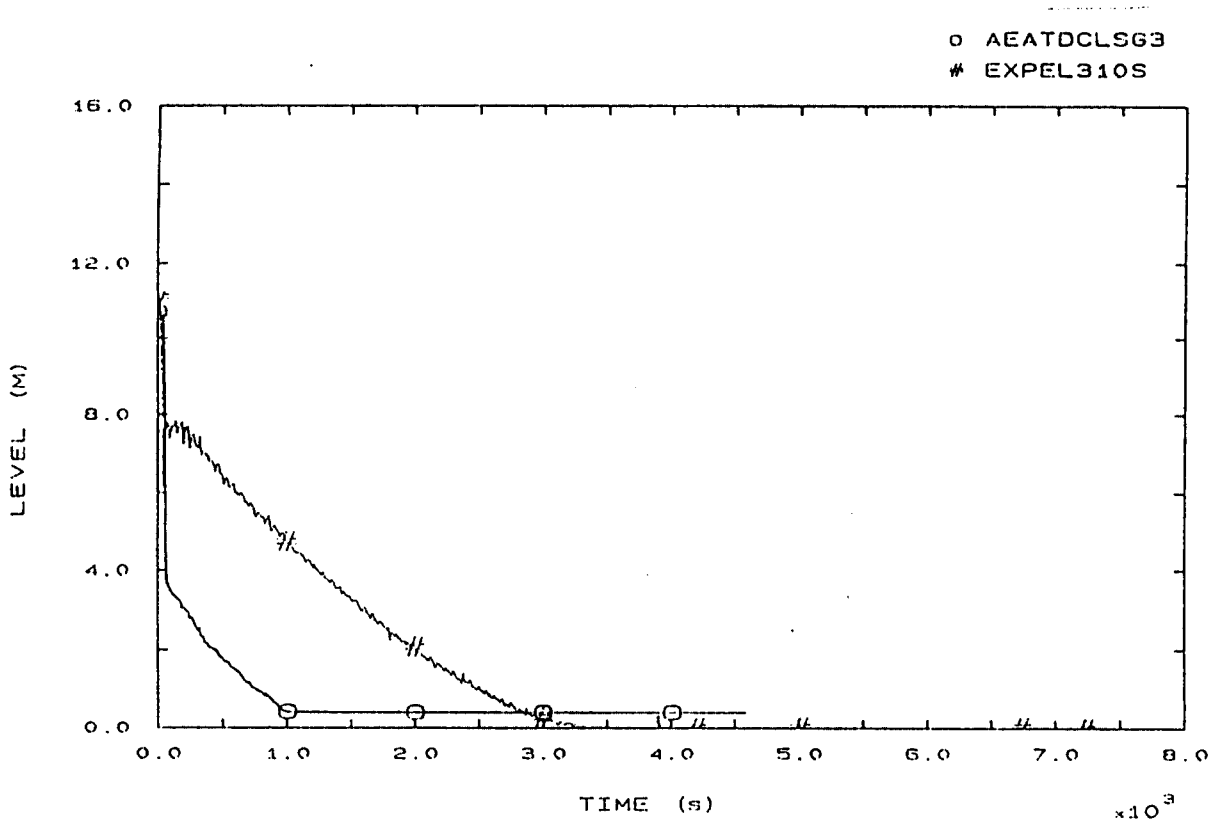

FIG. 9 SG3 DOWNCOMER LEVEL

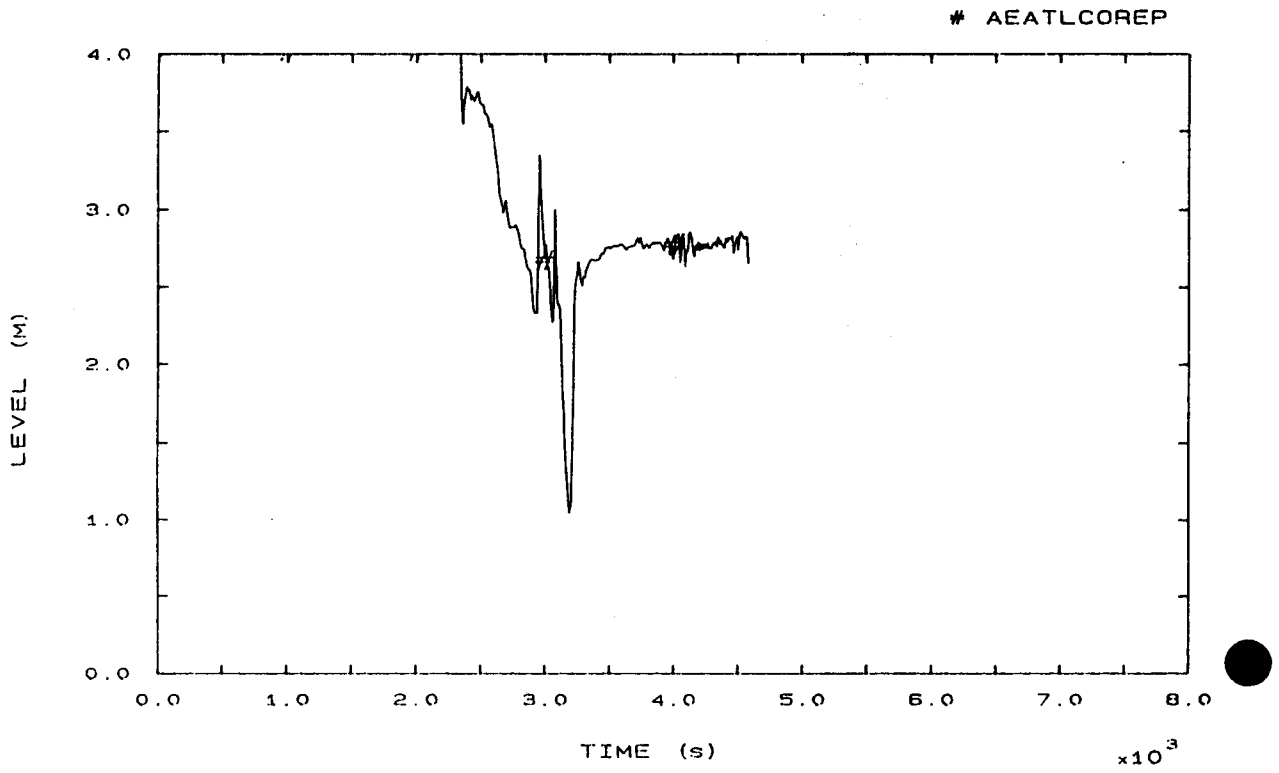

FIG. 11 CORE LEVEL

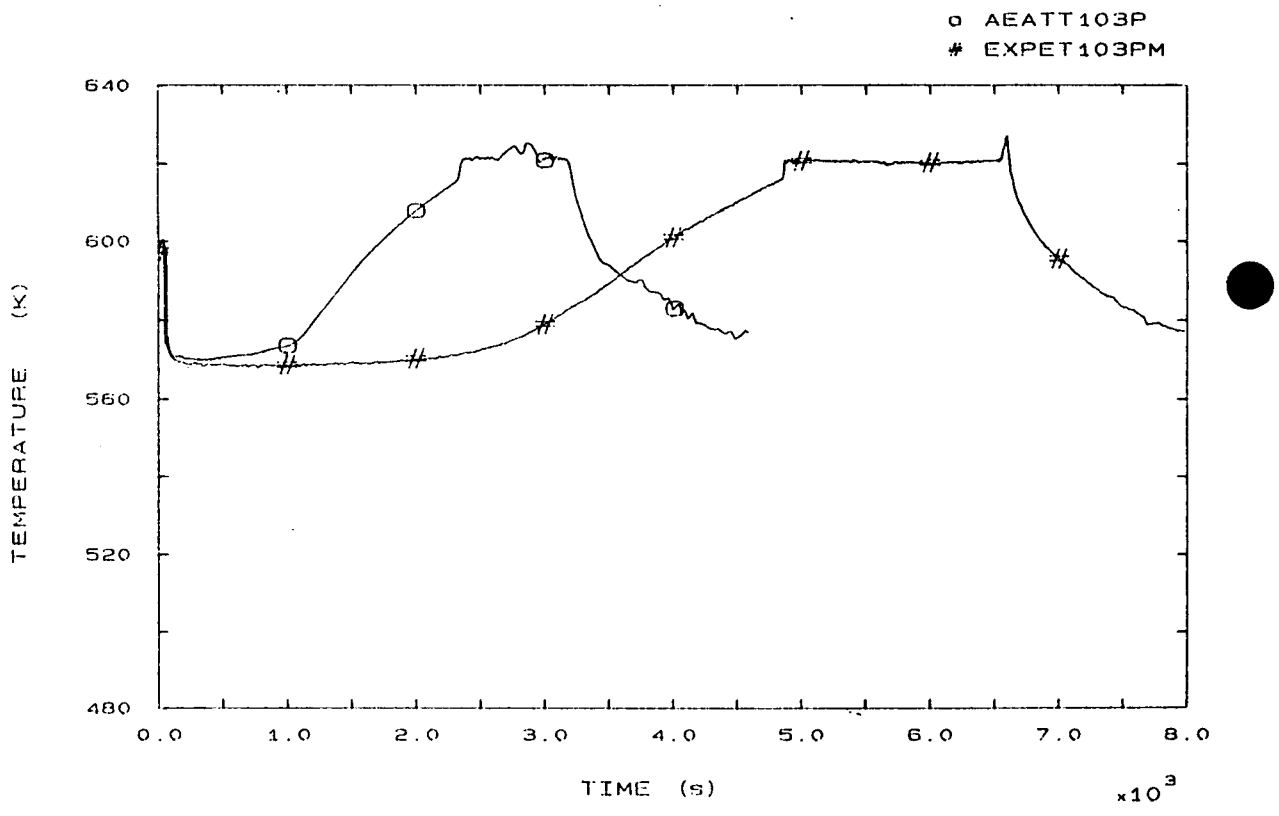

FIG. 12 LP1 HOT LEG OUTLET VESSEL TEMPERATURE

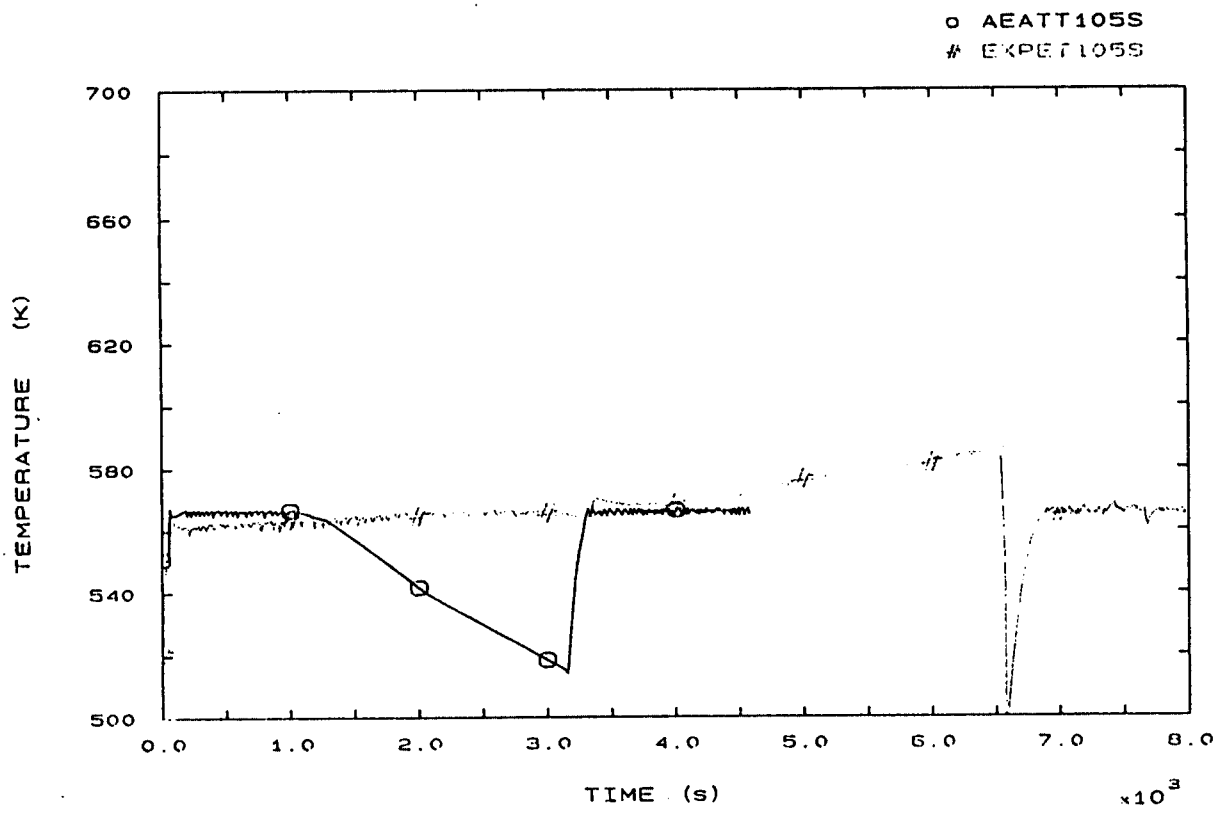

FIG. 15 FLUID TEMPERATURE SG1 RISER 185 MM A.T.S.

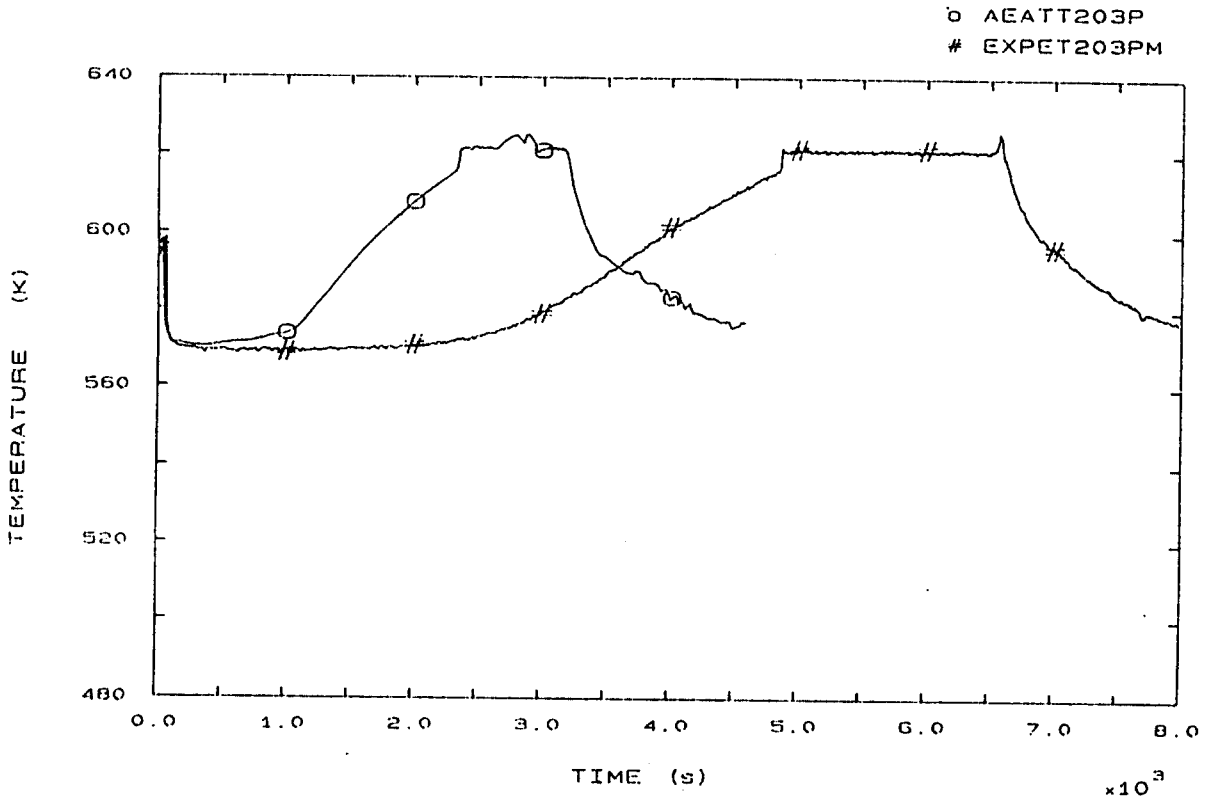

FIG. 22 LP2 HOT LEG OUTLET VESSEL TEMPERATURE

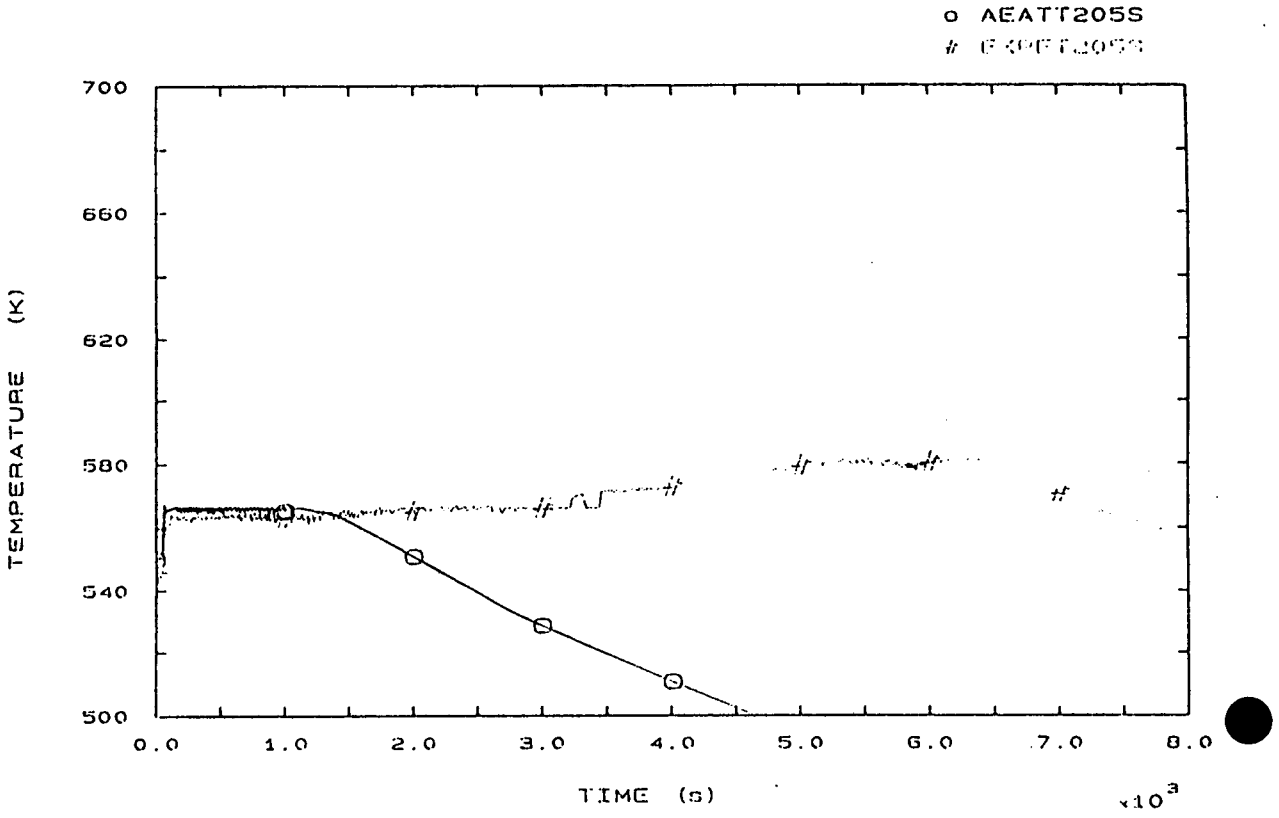

FIG. 25 FLUID TEMPERATURE SG2 RISER 185 MM A.T.S.

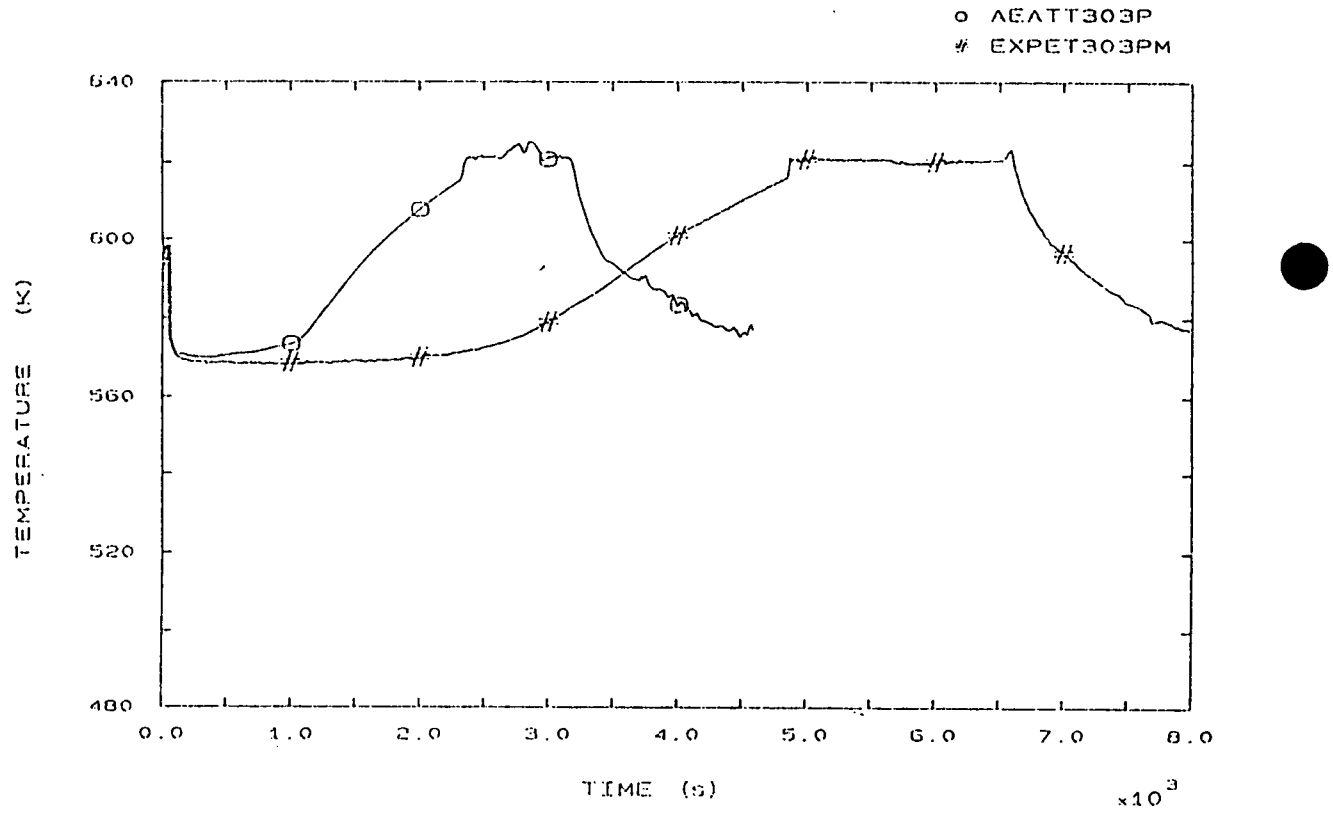

FIG. 32 LP3 HOT LEG OUTLET VESSEL TEMPERATURE

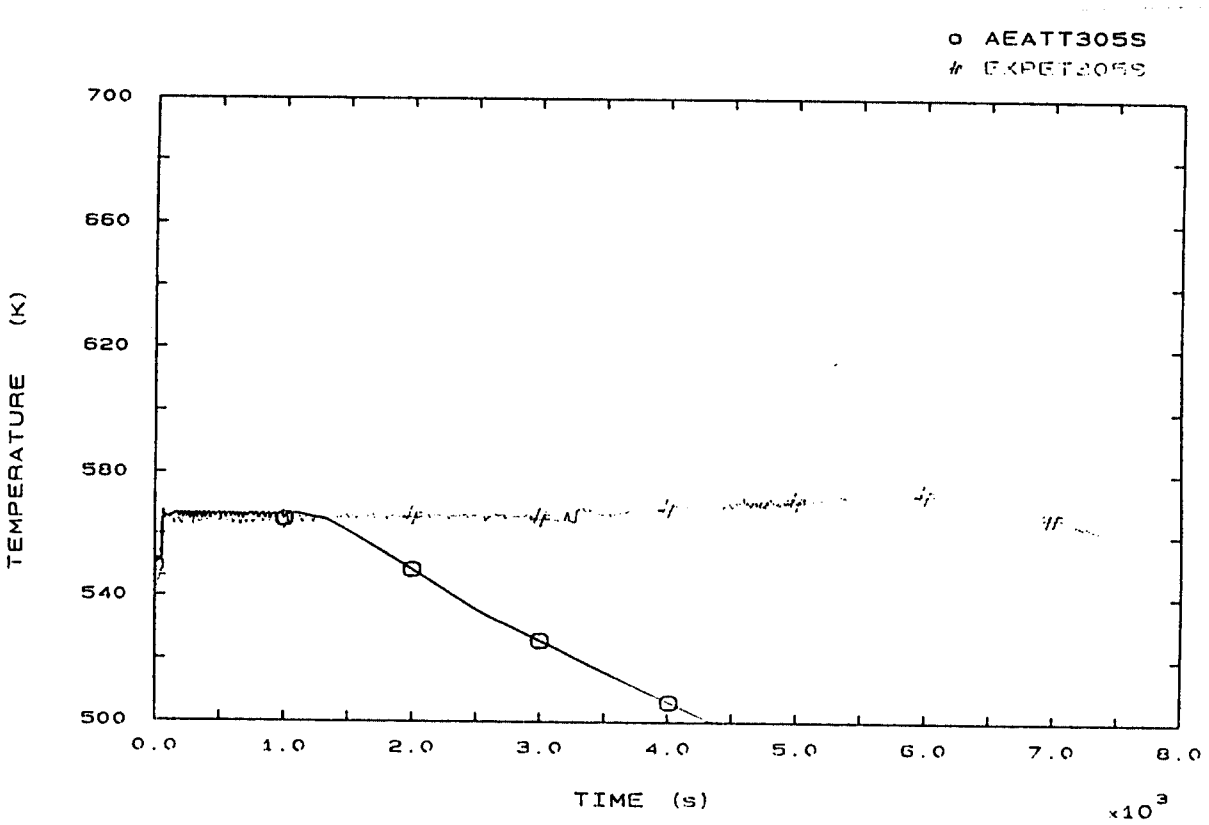

FIG. 35 FLUID TEMPERATURE SG3 RISER 185 MM A.T.S.

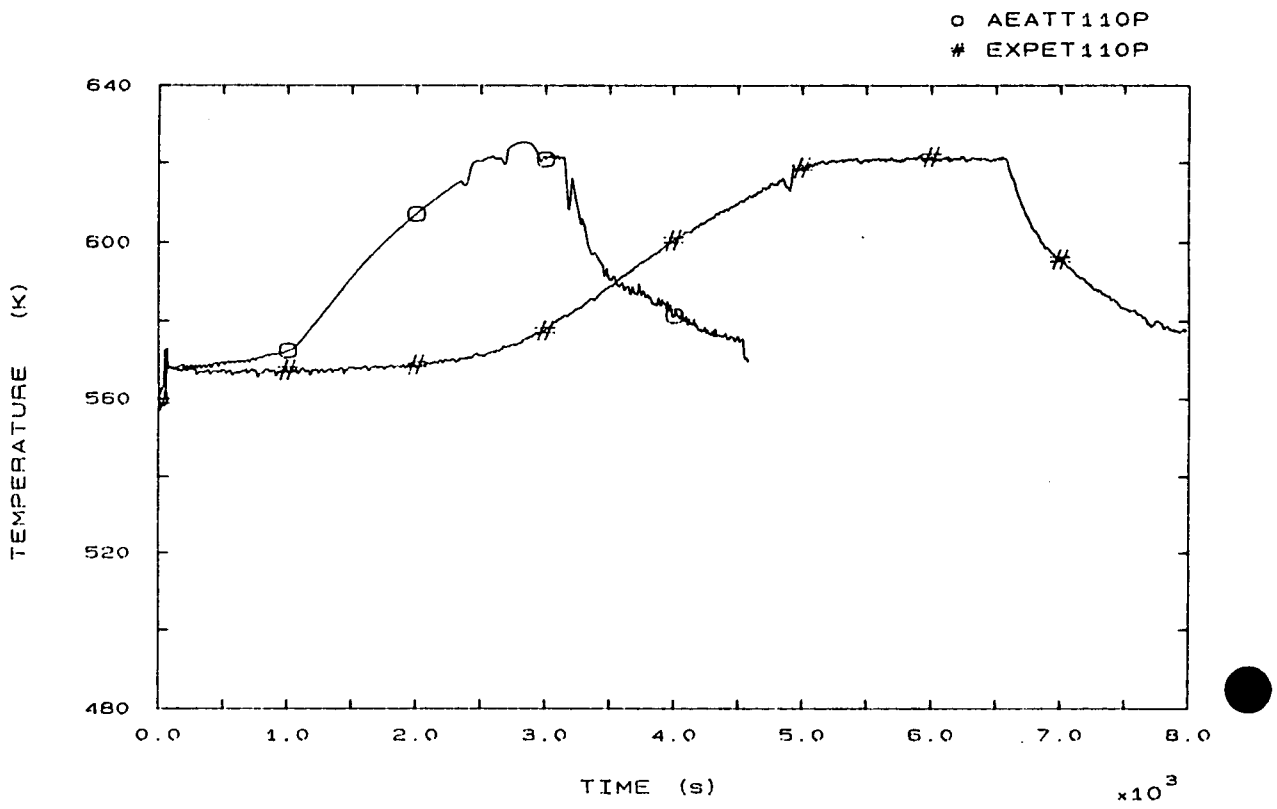

FIG. 42 SG1 OUTLET TEMPERATURE

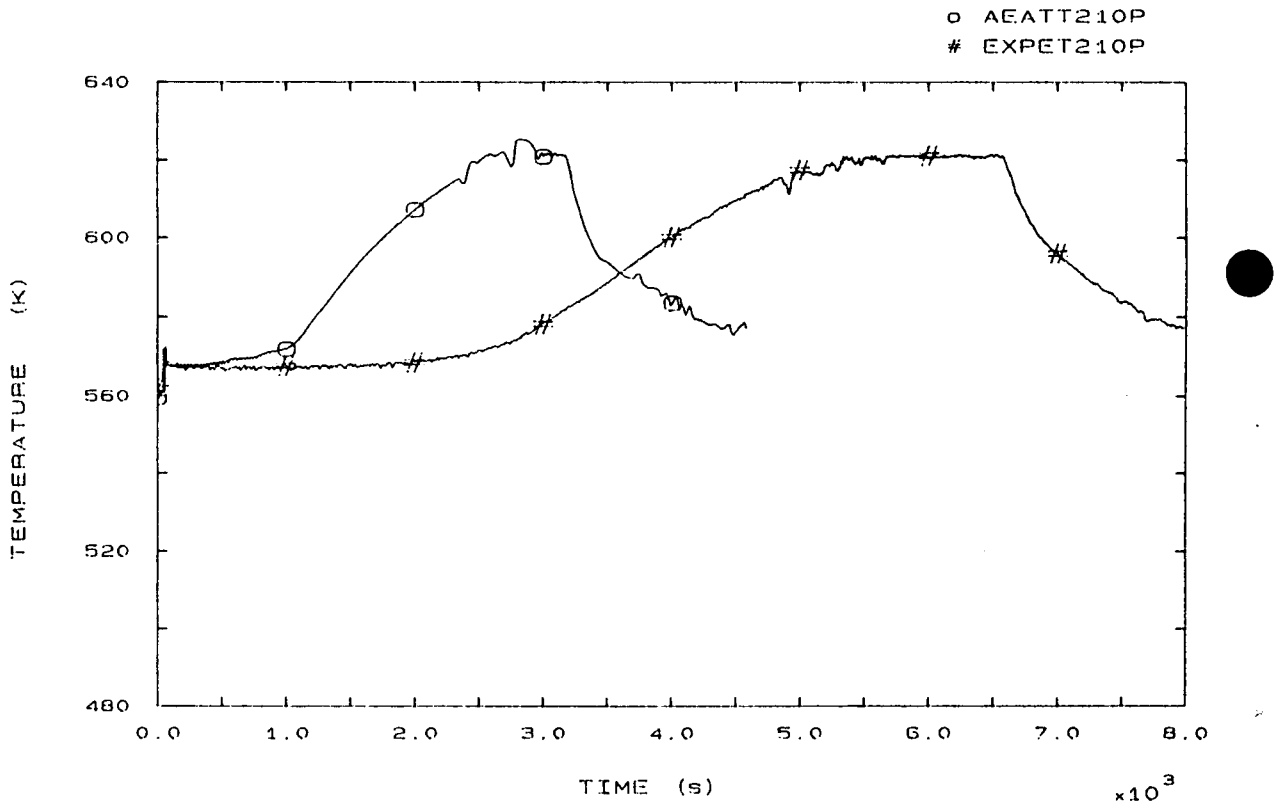

FIG. 44 SG2 OUTLET TEMPERATURE

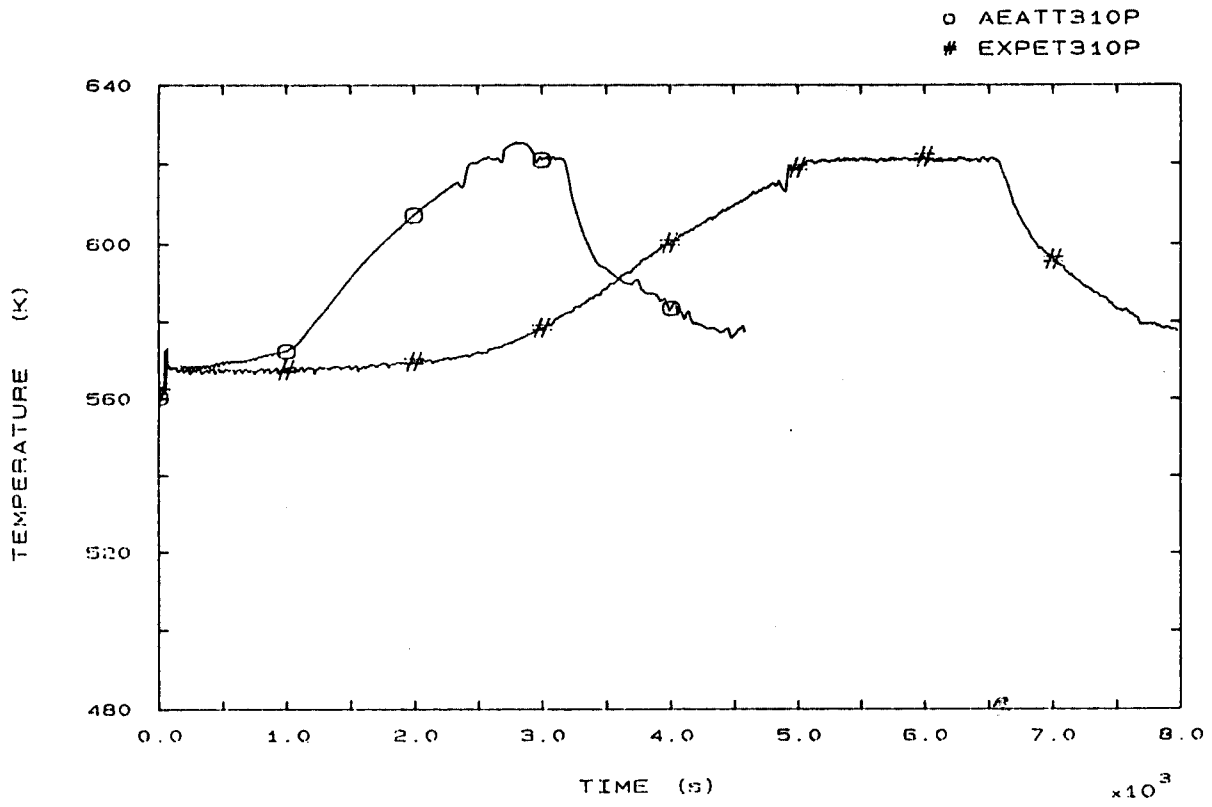

FIG. 46 SG3 OUTLET TEMPERATURE

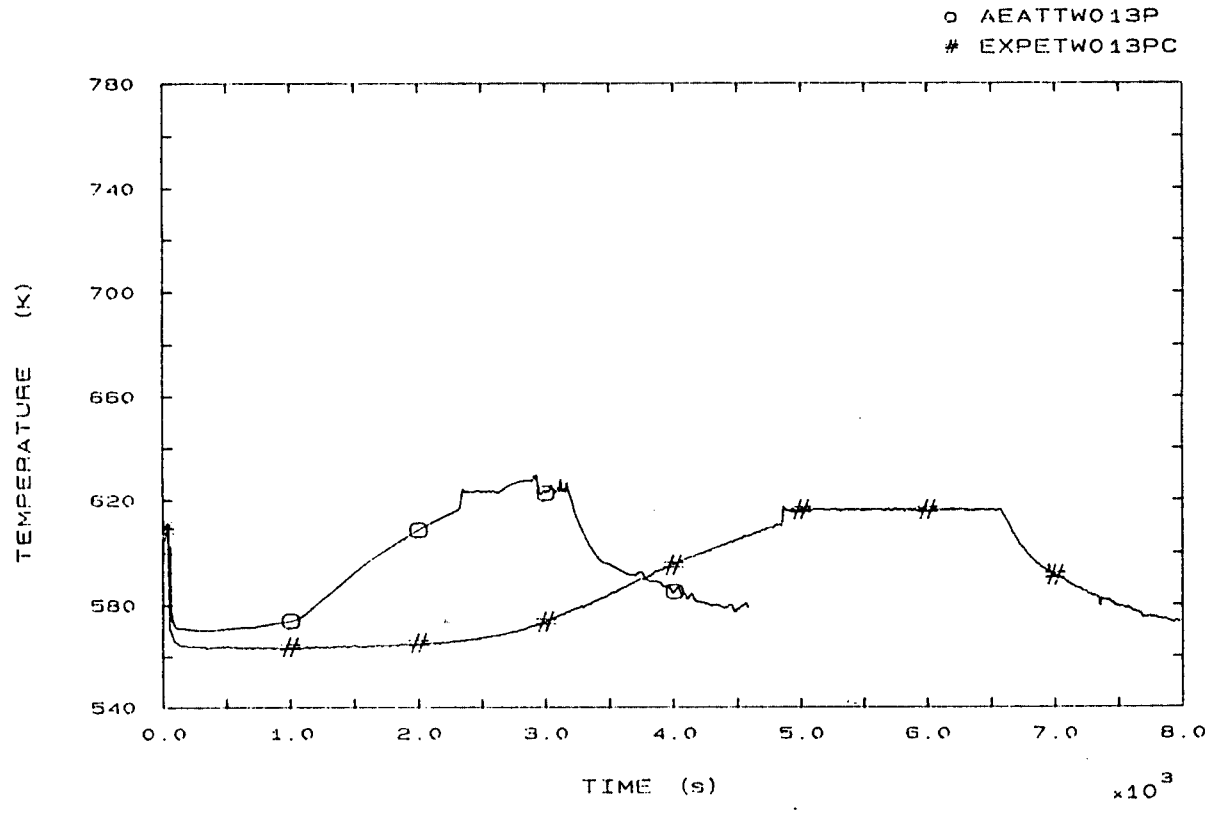

FIG. 49 CORE SURFACE TEMPERATURE AT ROD BUNDLE ELEVATION 1074 MM

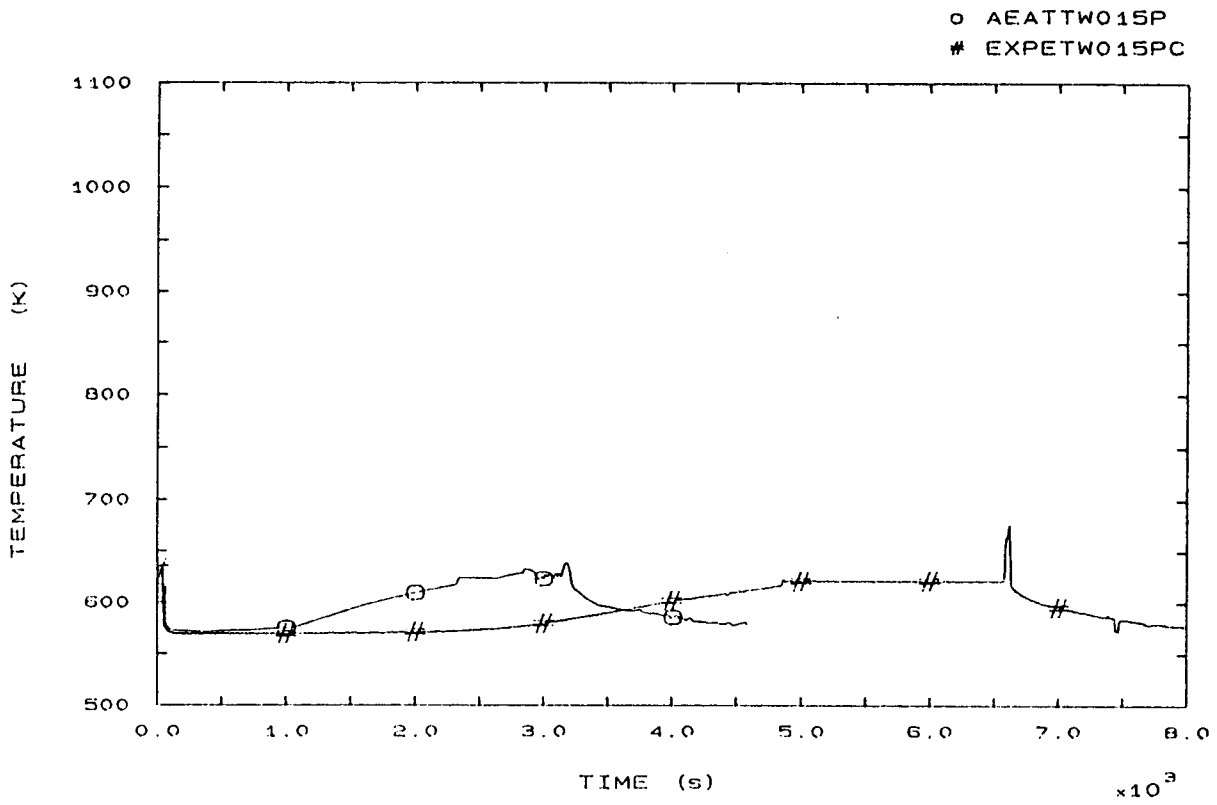

FIG. 50 SURFACE TEMPERATURE AT ROD BUNDLE ELEVATION 2294 MM

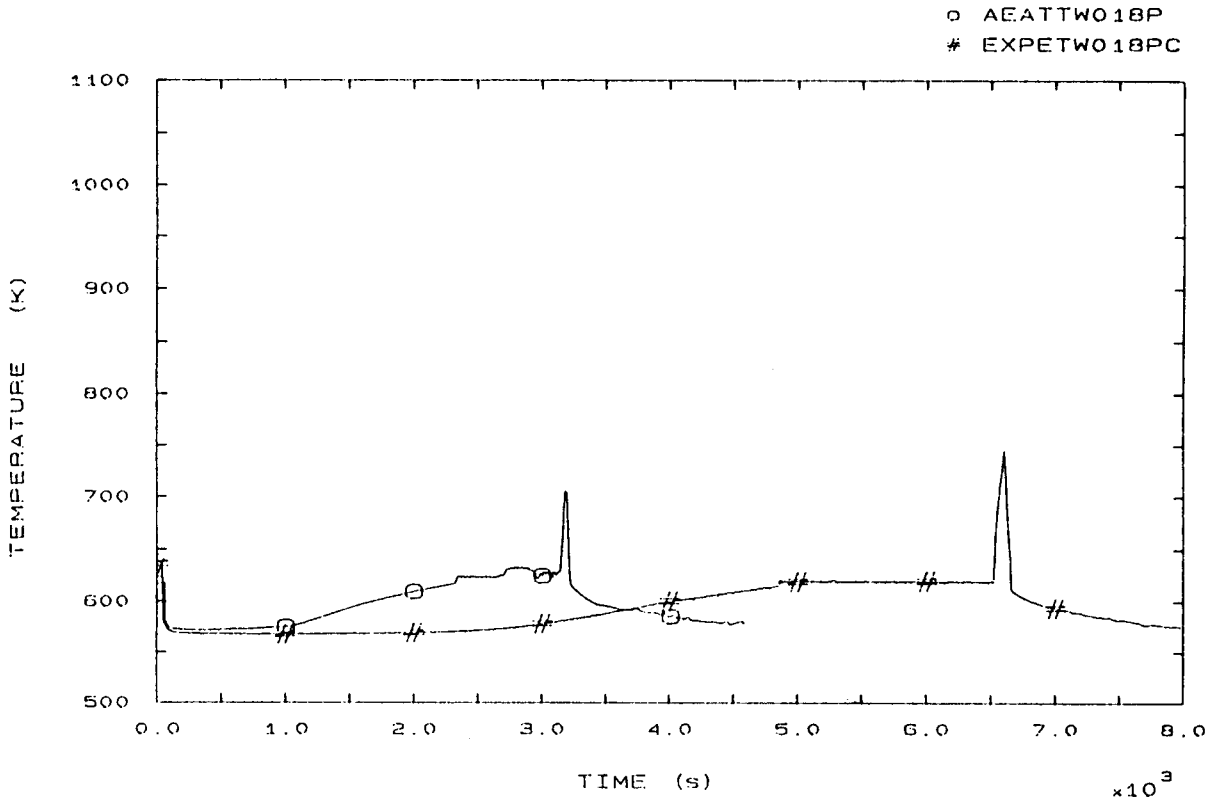

FIG. 51 SURFACE TEMPERATURE AT ROD BUNDLE ELEVATION 3294 MM

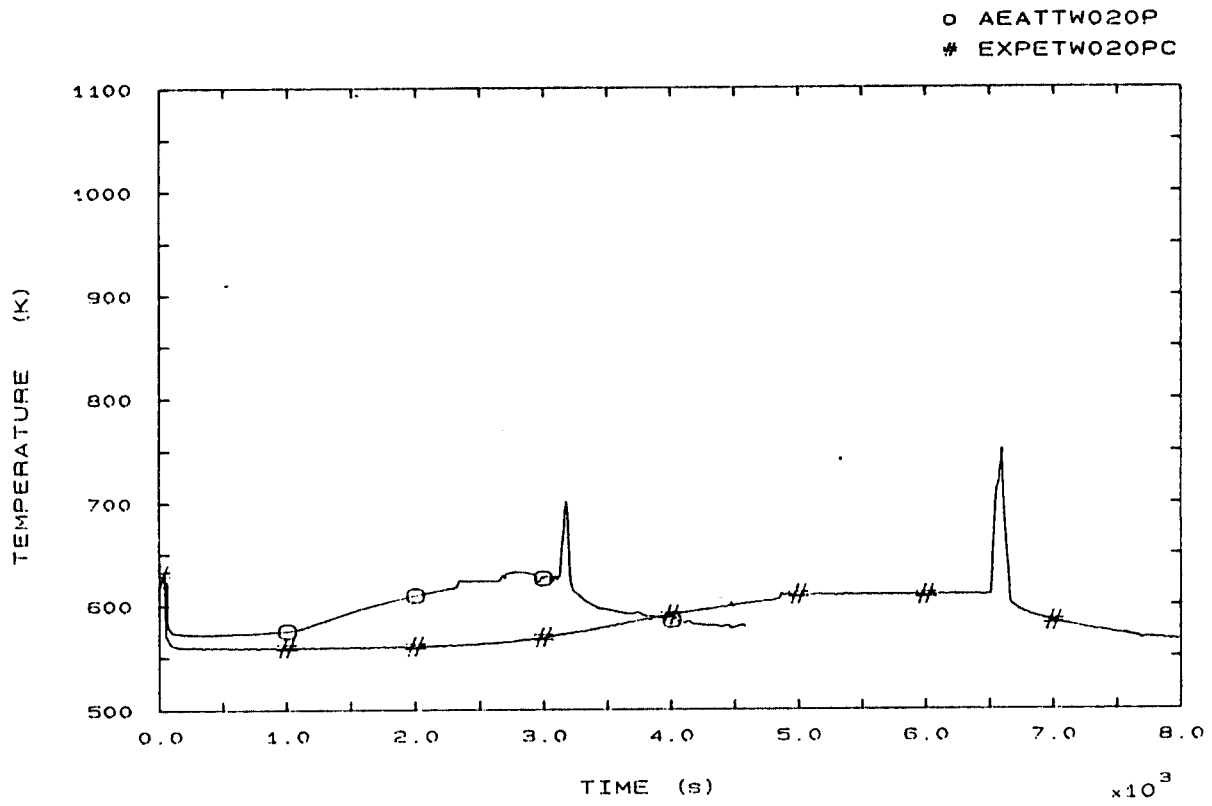

FIG. 52 SURFACE TEMPERATURE AT ROD BUNDLE ELEVATION 3640 MM

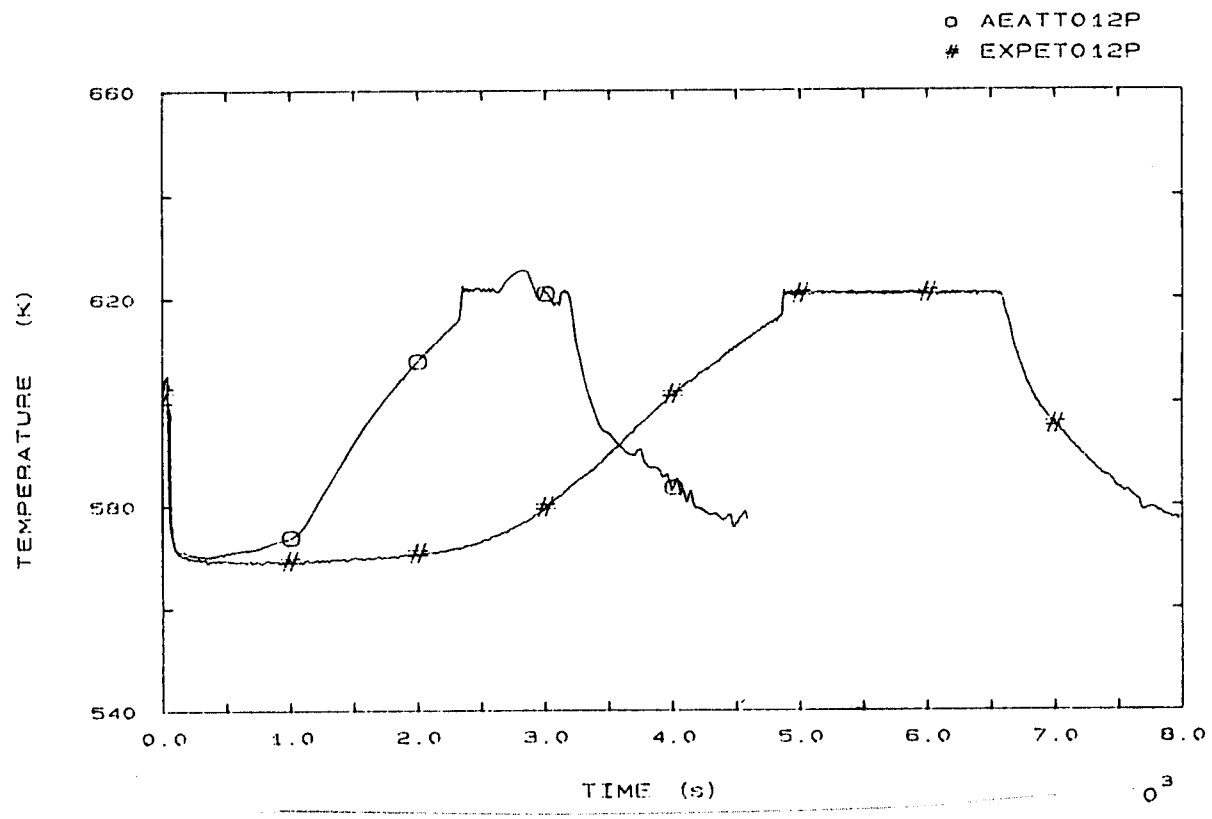

FIG. 53 CORE OUTLET TEMPERATURE

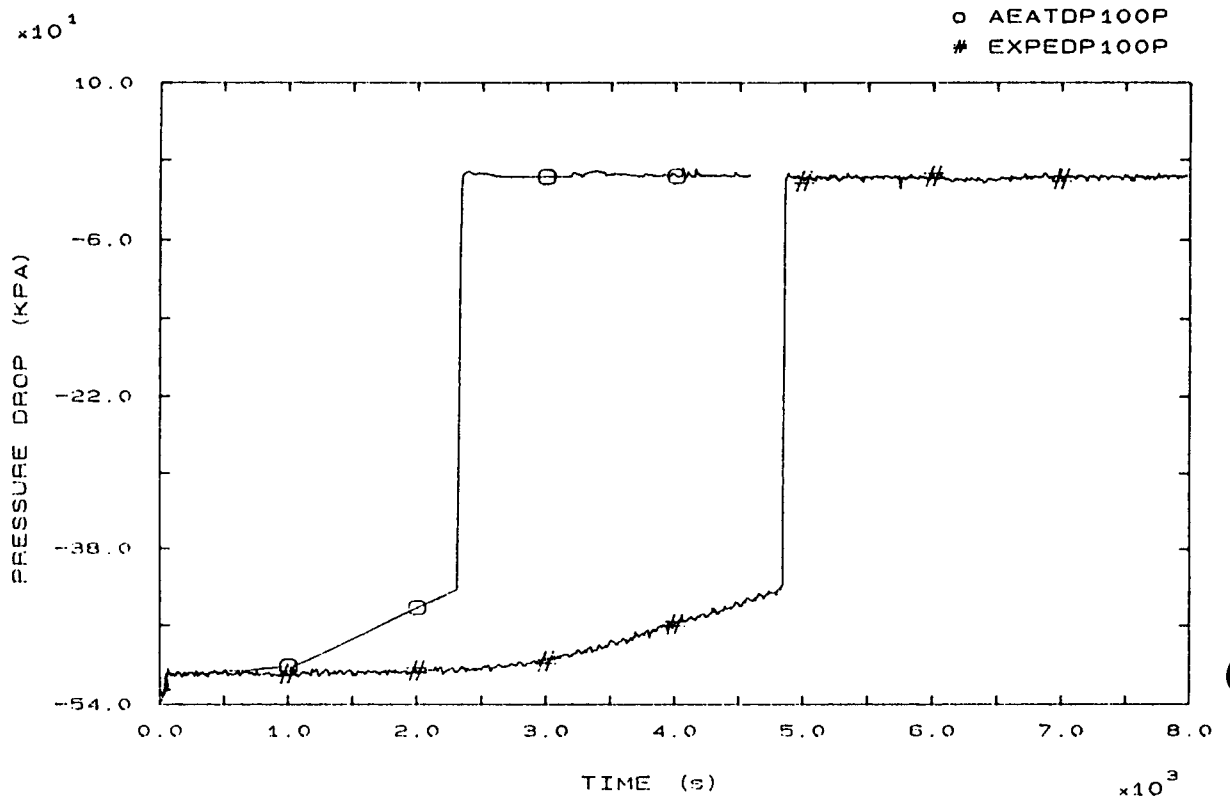

FIG. 54 PRIMARY PUMP 1 PRESSURE DROP

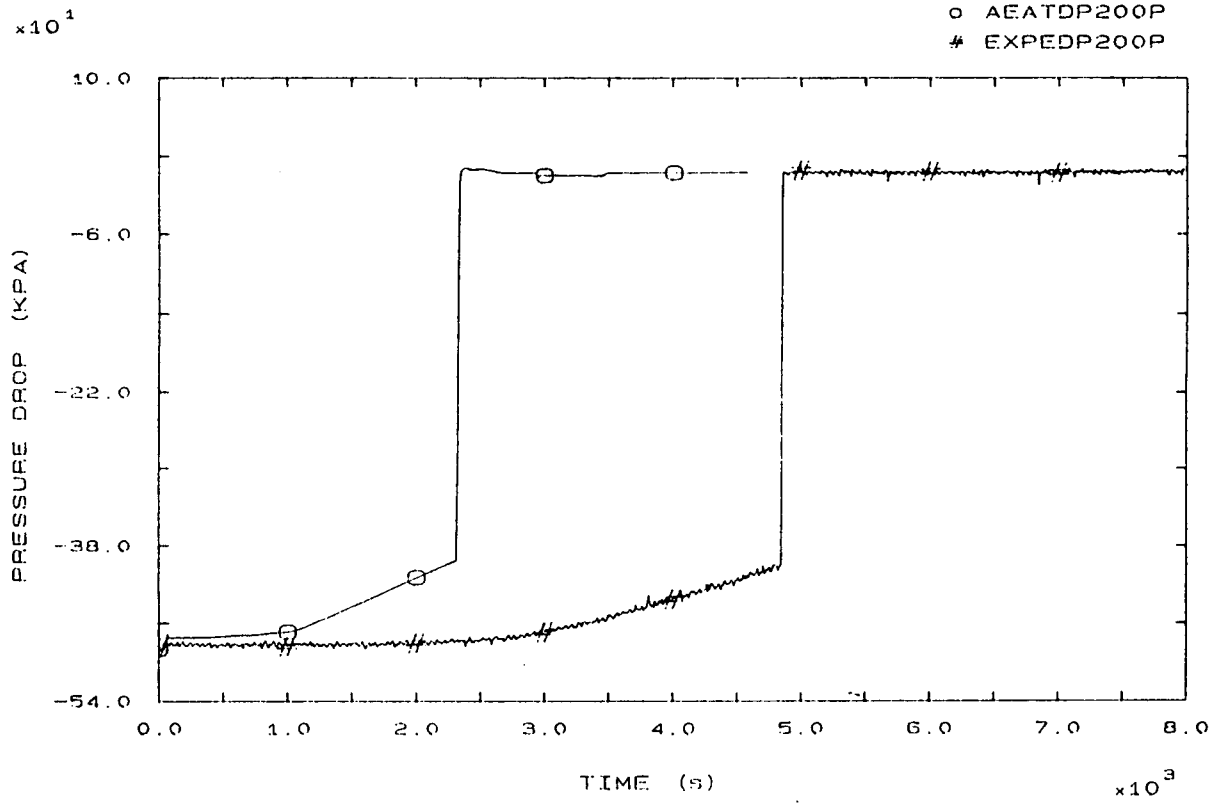

FIG. 55 PRIMARY PUMP 2 PRESSURE DROP

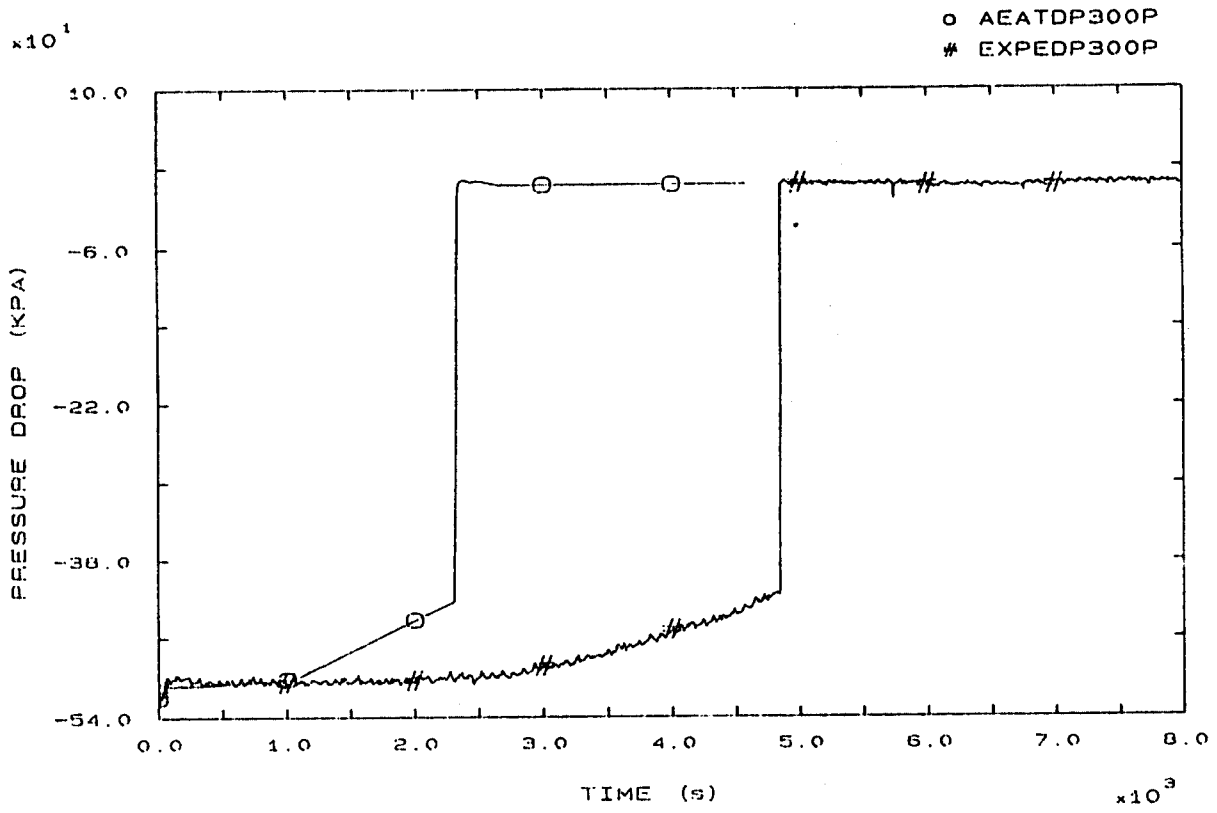

FIG. 56 PRIMARY PUMP 3 PRESSURE DROP

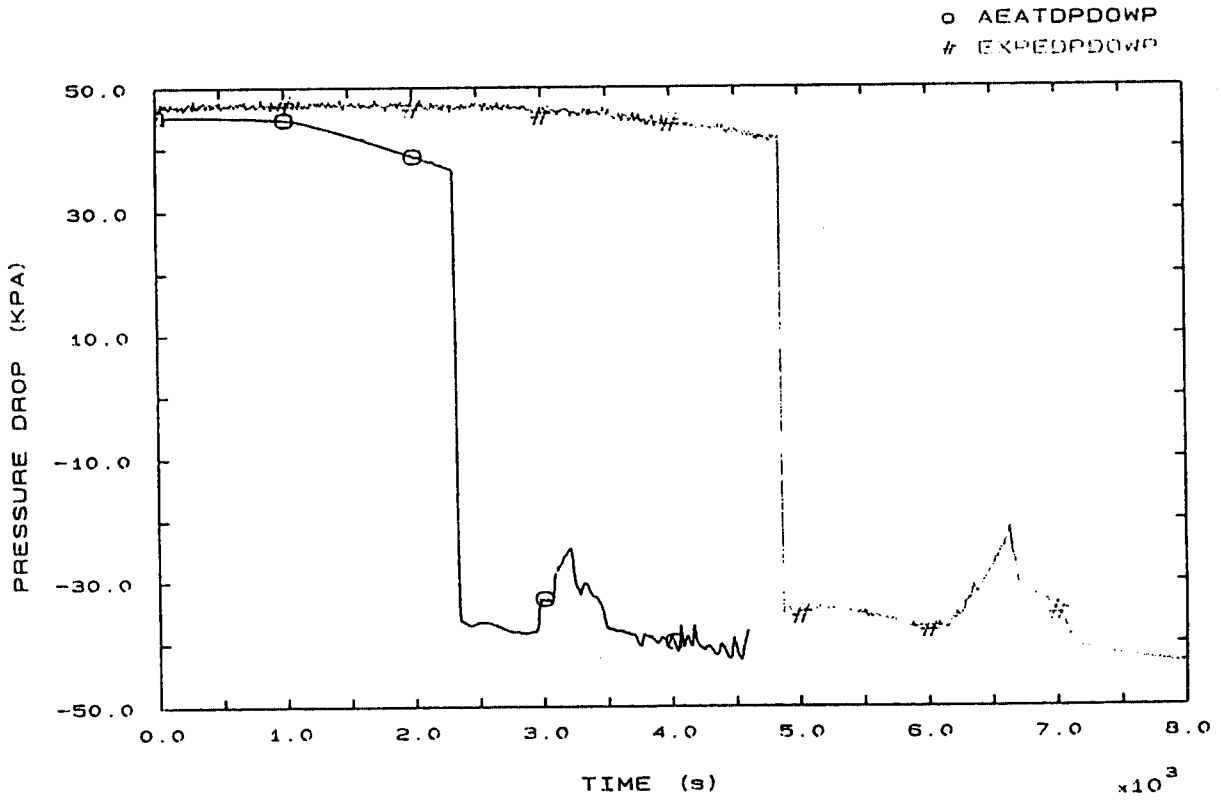

FIG. 57 VESSEL DOWNCOMER PRESSURE DROP

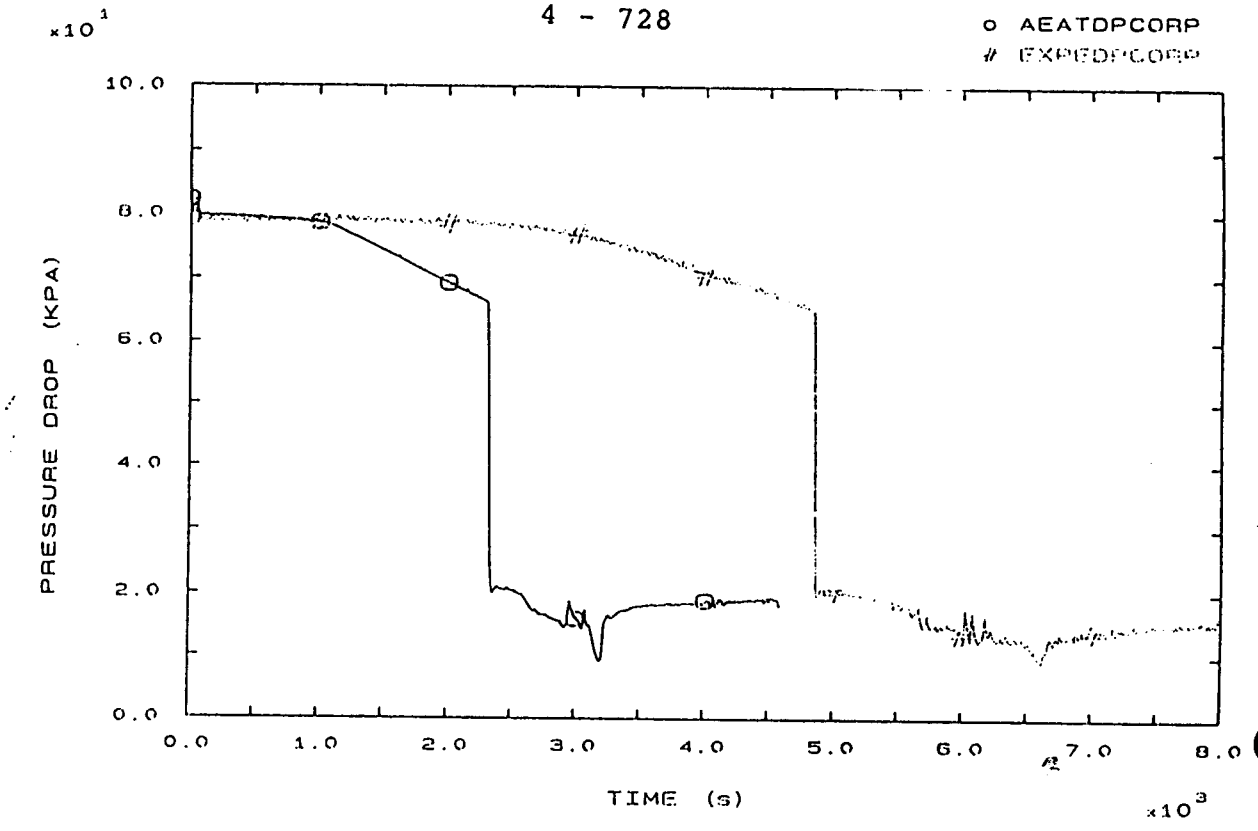

FIG. 58 CORE PRESSURE DROP

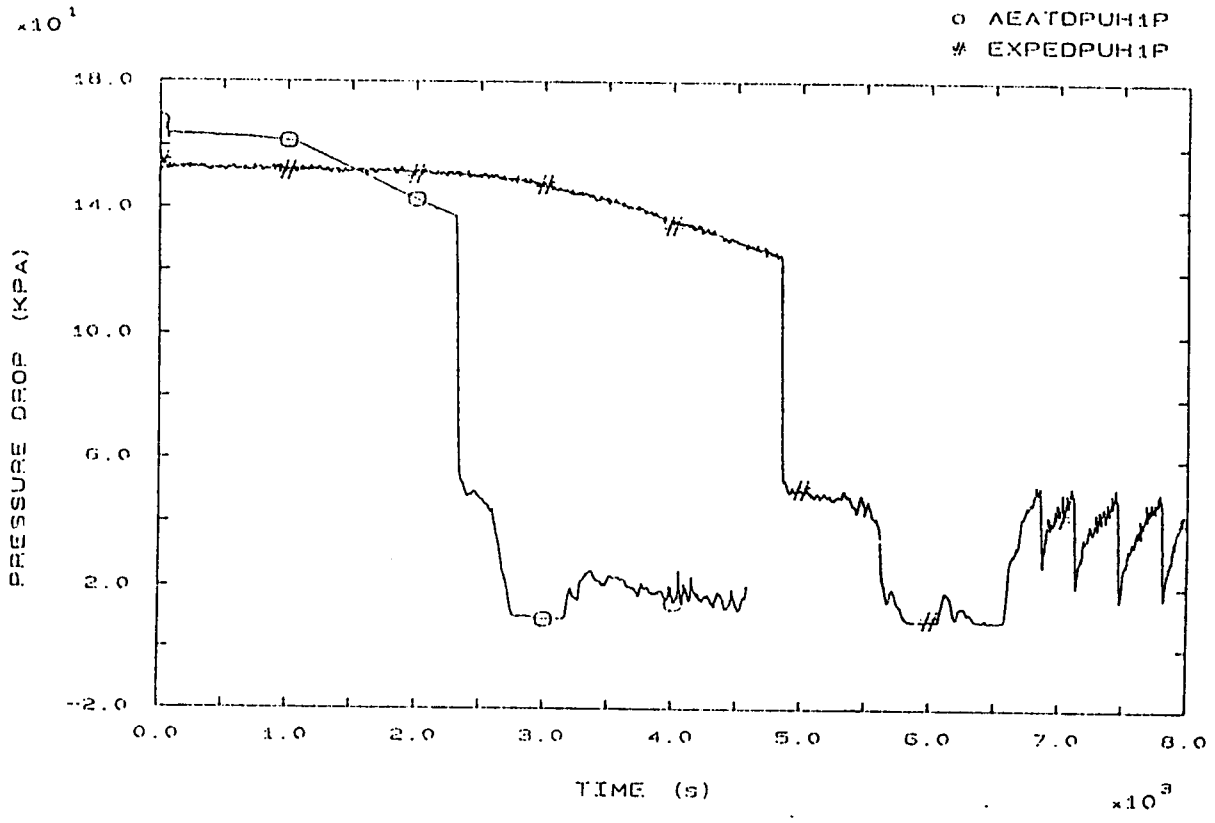

FIG. 62 SG1 INLET/U-BEND (UP-HILL) PRESSURE DROP

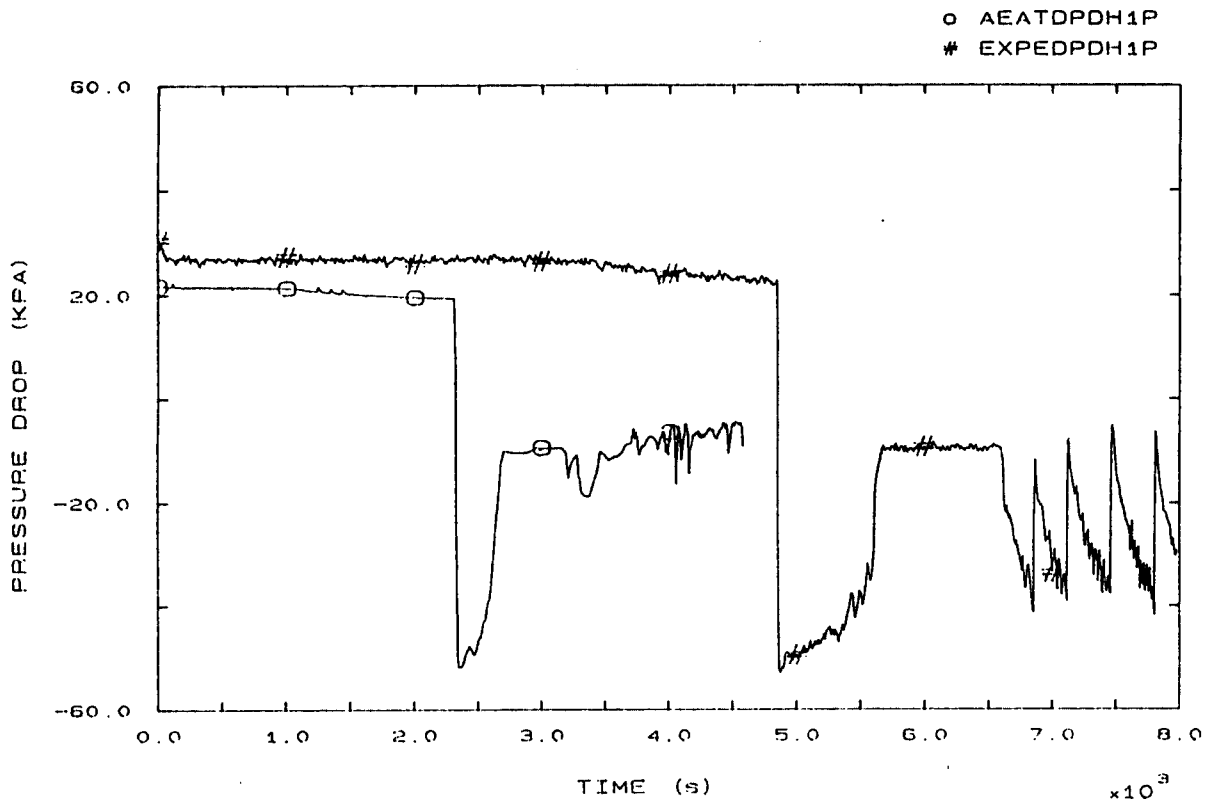

FIG. 63 SG1 U-BEND/OUTLET (DOWN-HILL) PRESSURE DROP

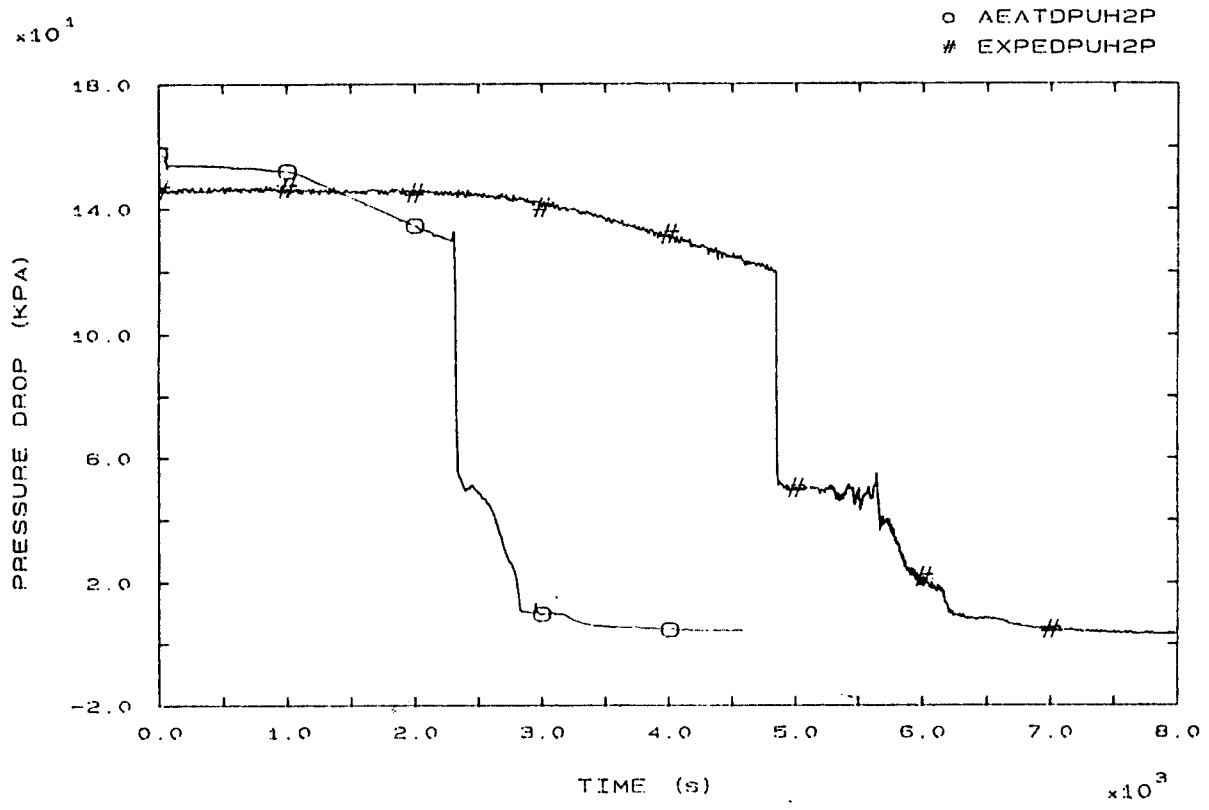

FIG. 64 SG2 INLET/U-BEND (UP-HILL) PRESSURE DROP

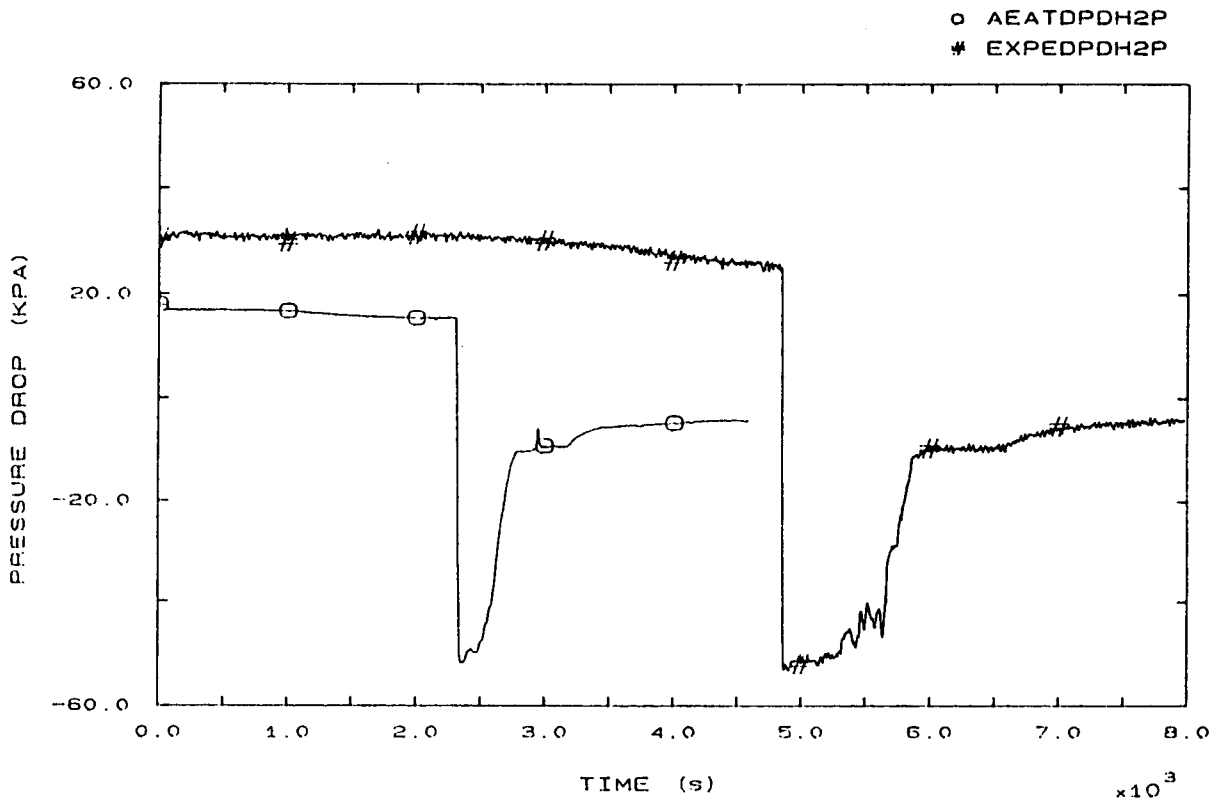

FIG. 65 SG2 U-BEND/OUTLET (DOWN-HILL) PRESSURE DROP

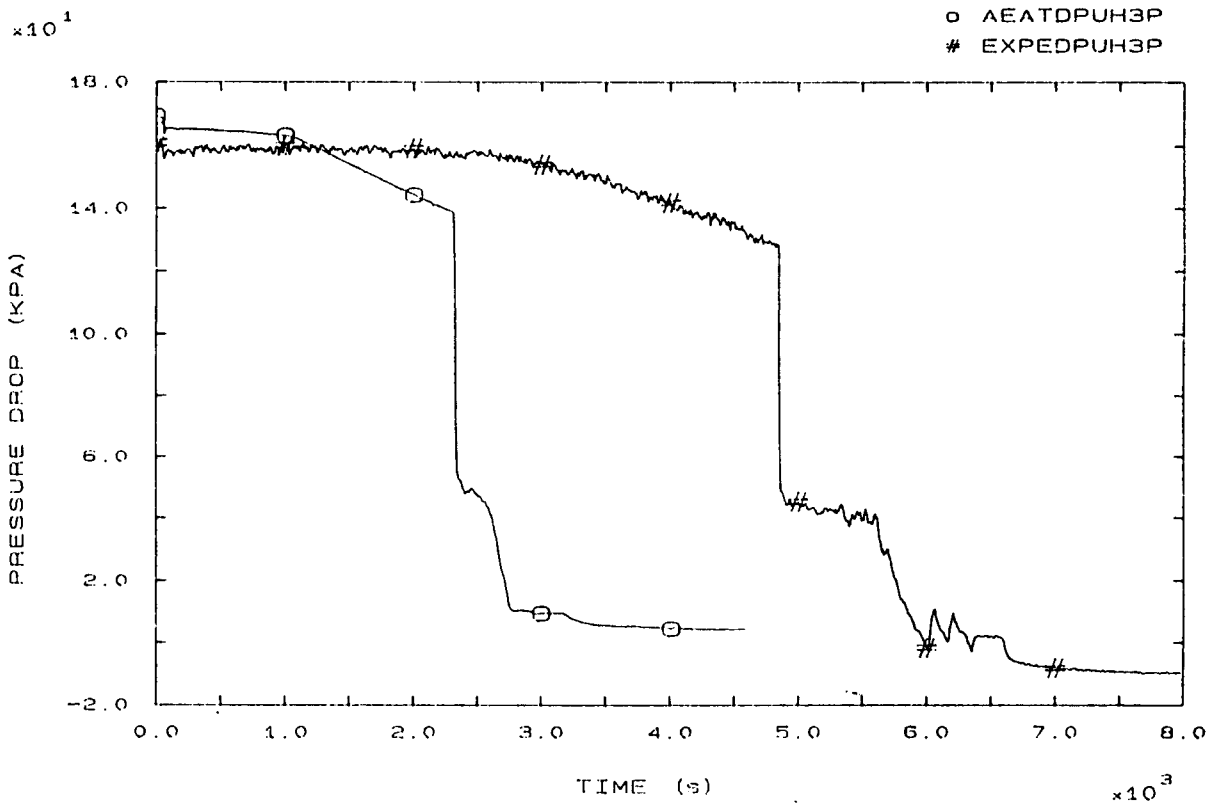

FIG. 66 SG3 INLET/U-BEND (UP-HILL) PRESSURE DROP

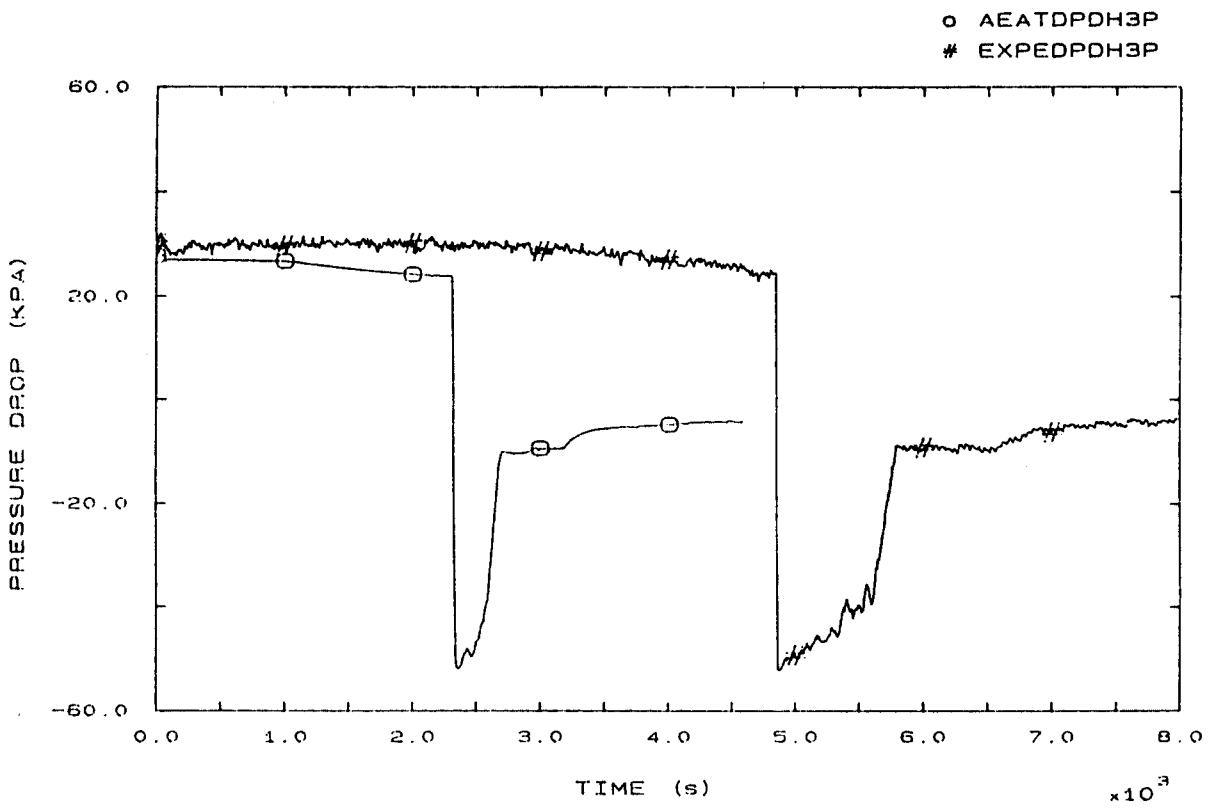

FIG. 67 SG3 U-BEND/OUTLET (DOWN-HILL) PRESSURE DROP

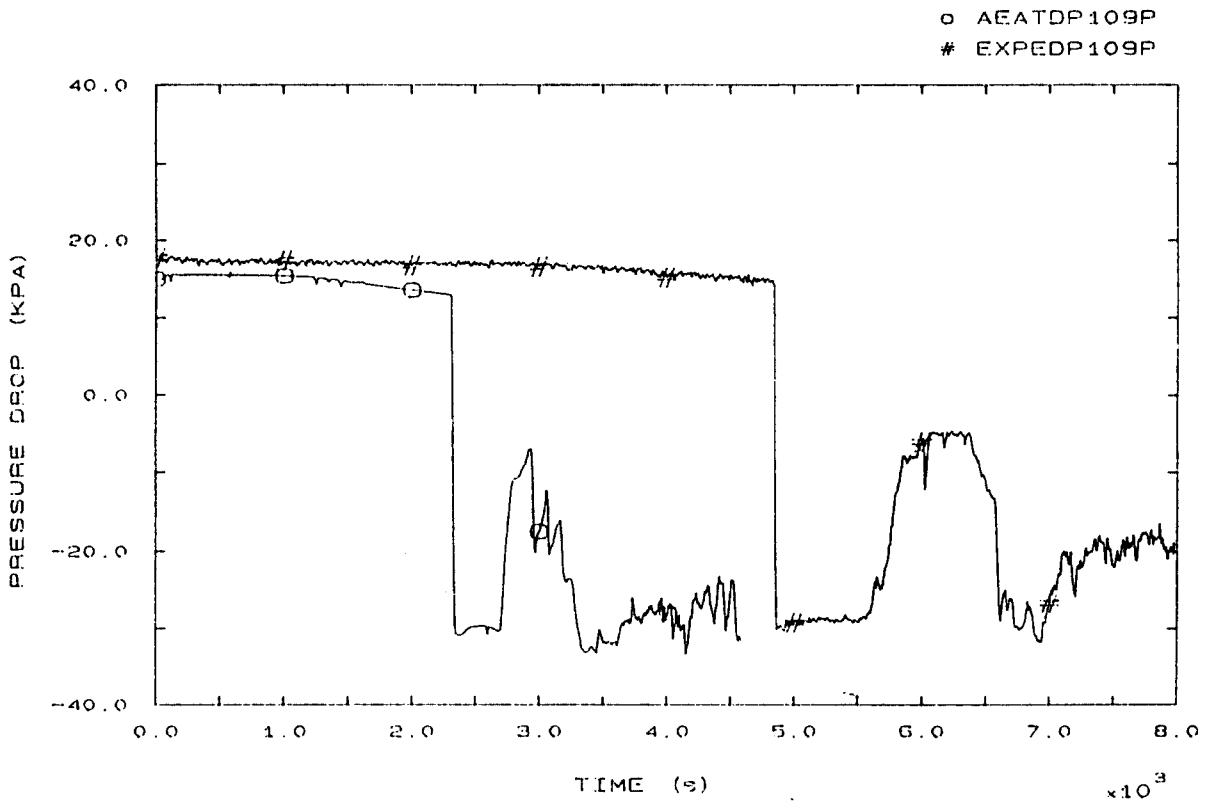

FIG. 68 SG1 OUTLET/LOOP SEAL BOTTOM PRESSURE DROP

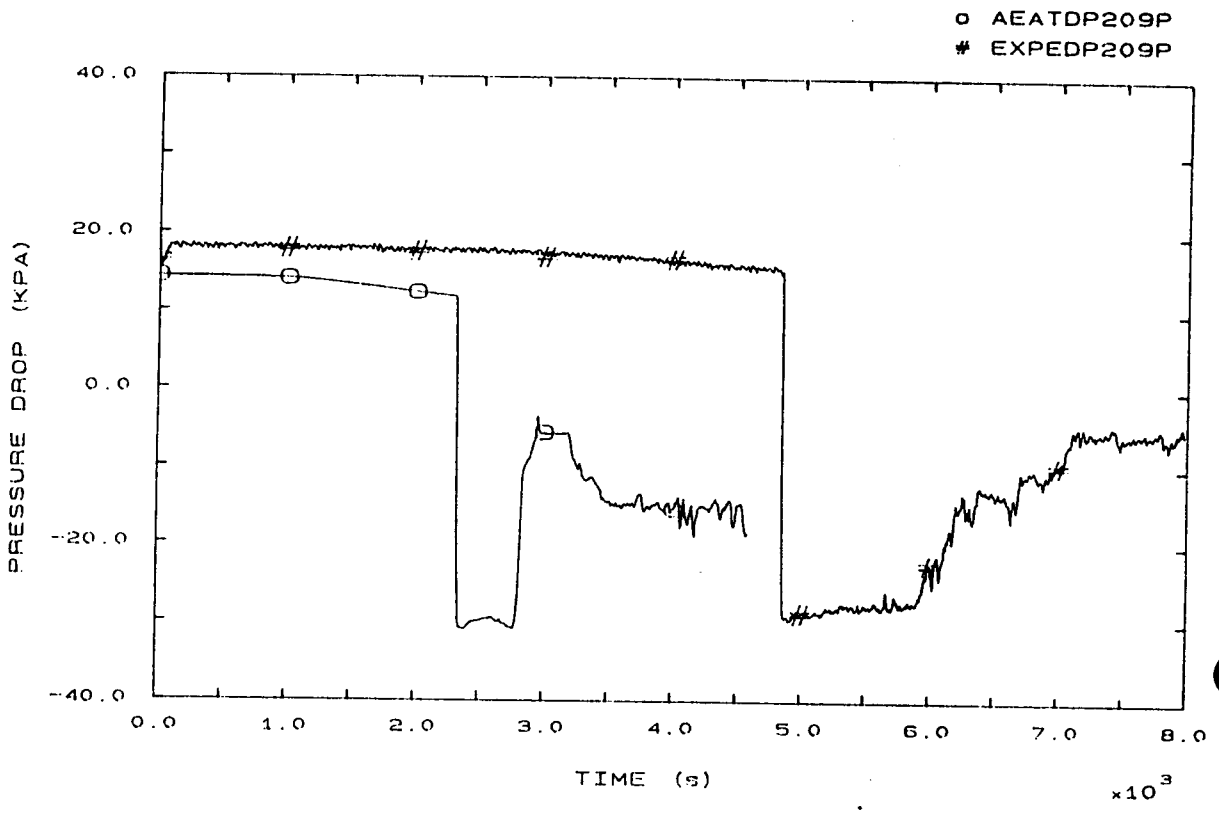

FIG. 69 SG2 OUTLET/LOOP SEAL BOTTOM PRESSURE DROP

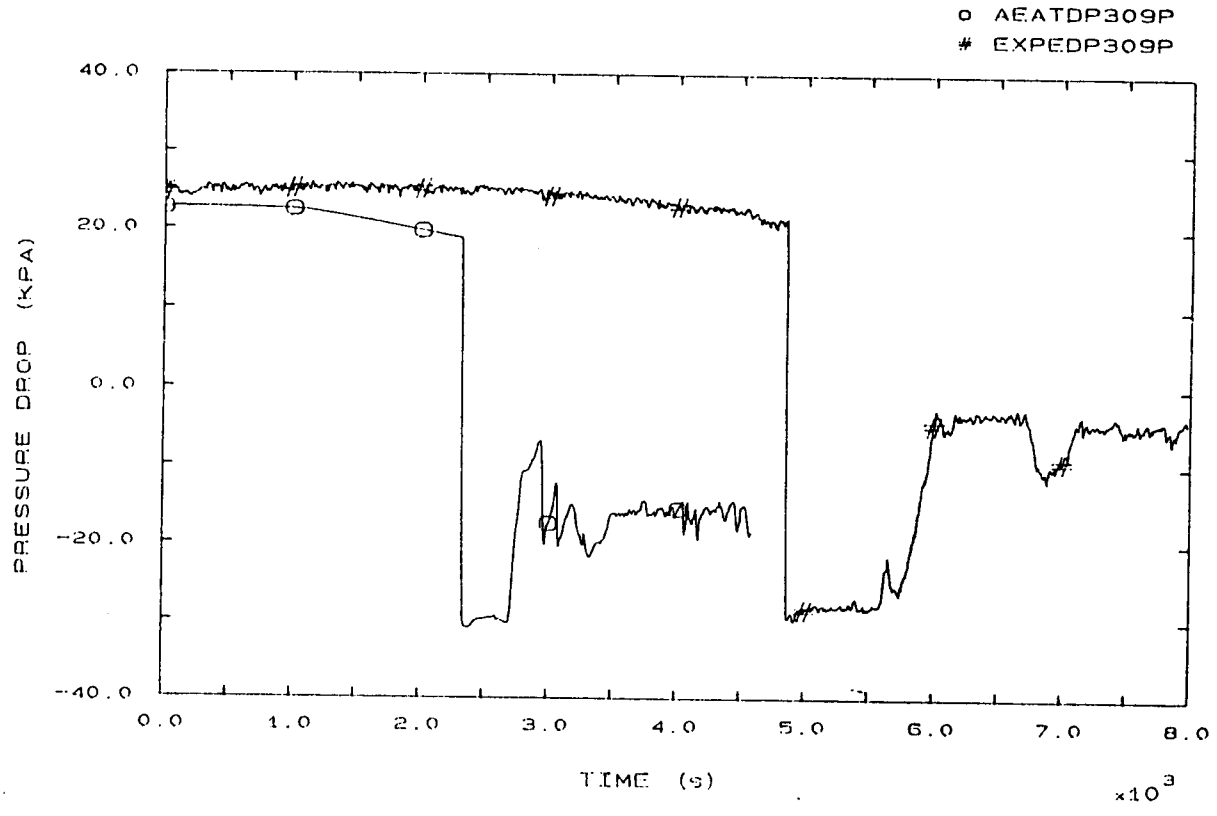

FIG. 70 SG3 OUTLET/LOOP SEAL BOTTOM PRESSURE DROP

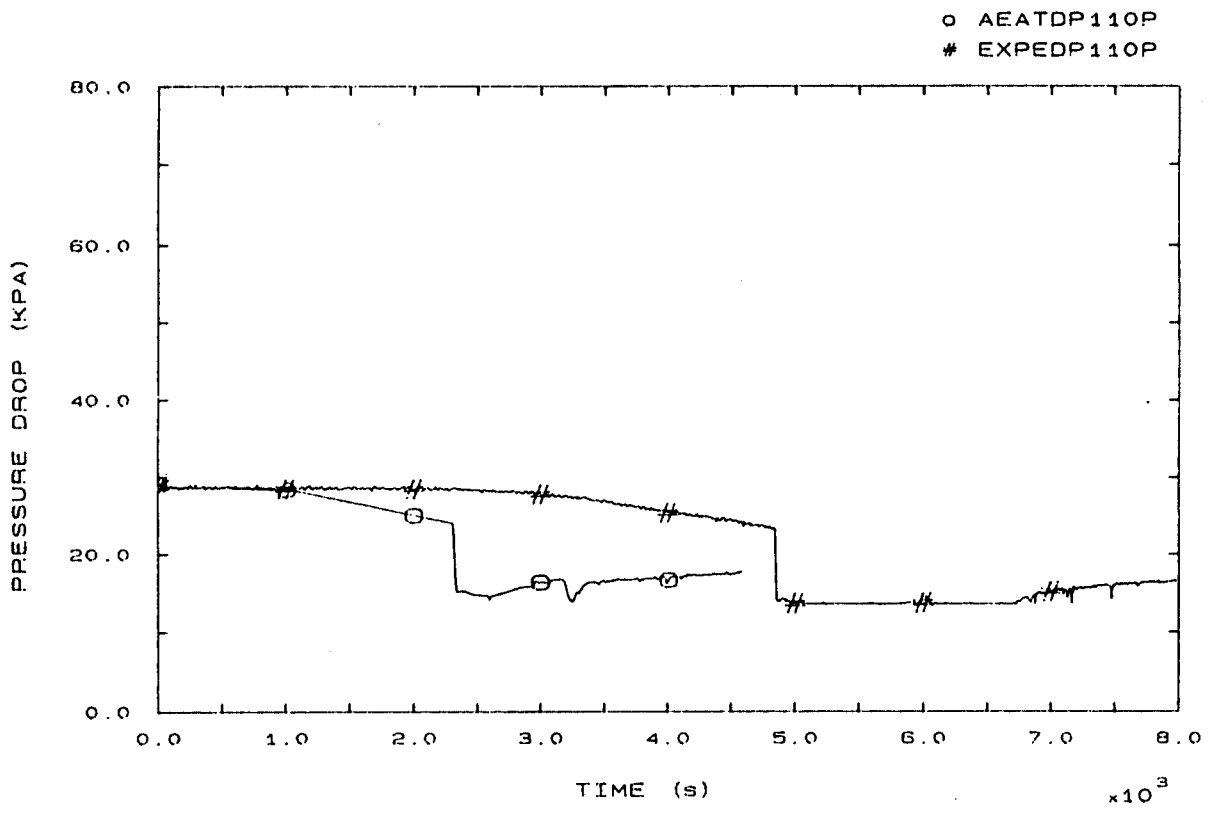

FIG. 71 LOOP SEAL BOTTOM/PUMP 1 INLET PRESSURE DROP

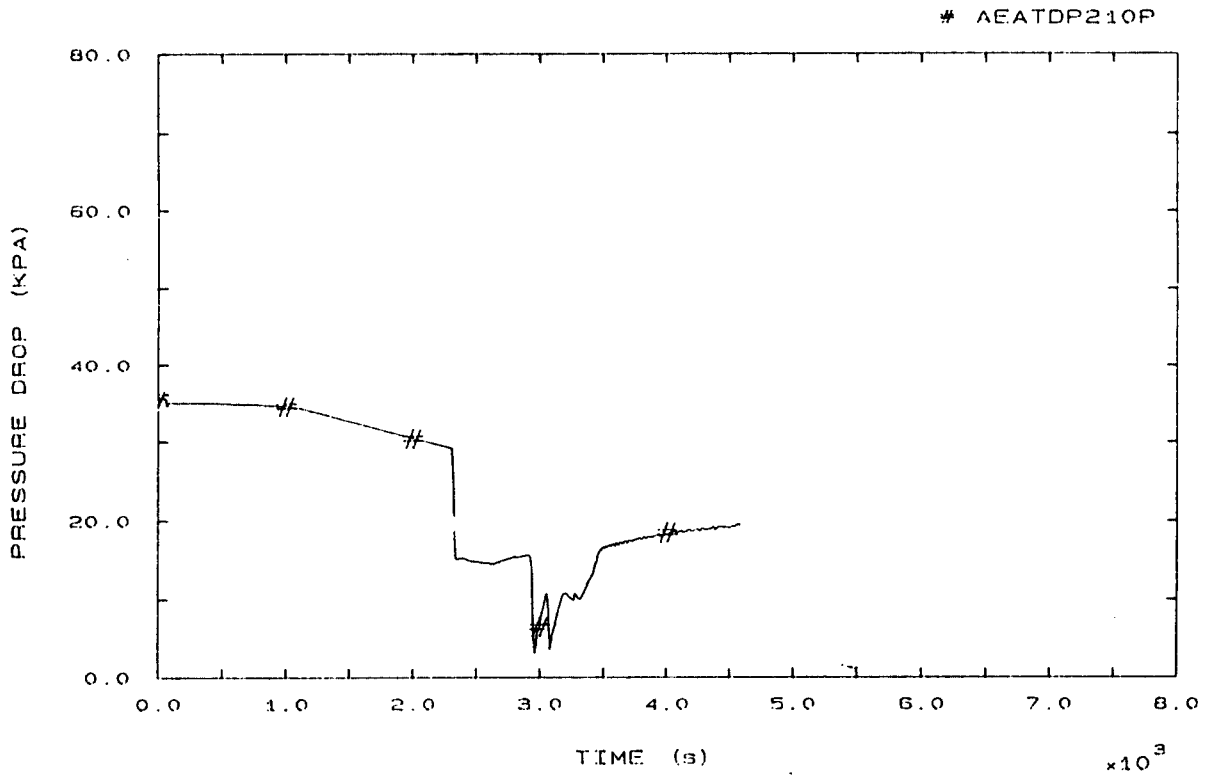

FIG. 72 LOOP SEAL BOTTOM/PUMP 2 INLET PRESSURE DROP

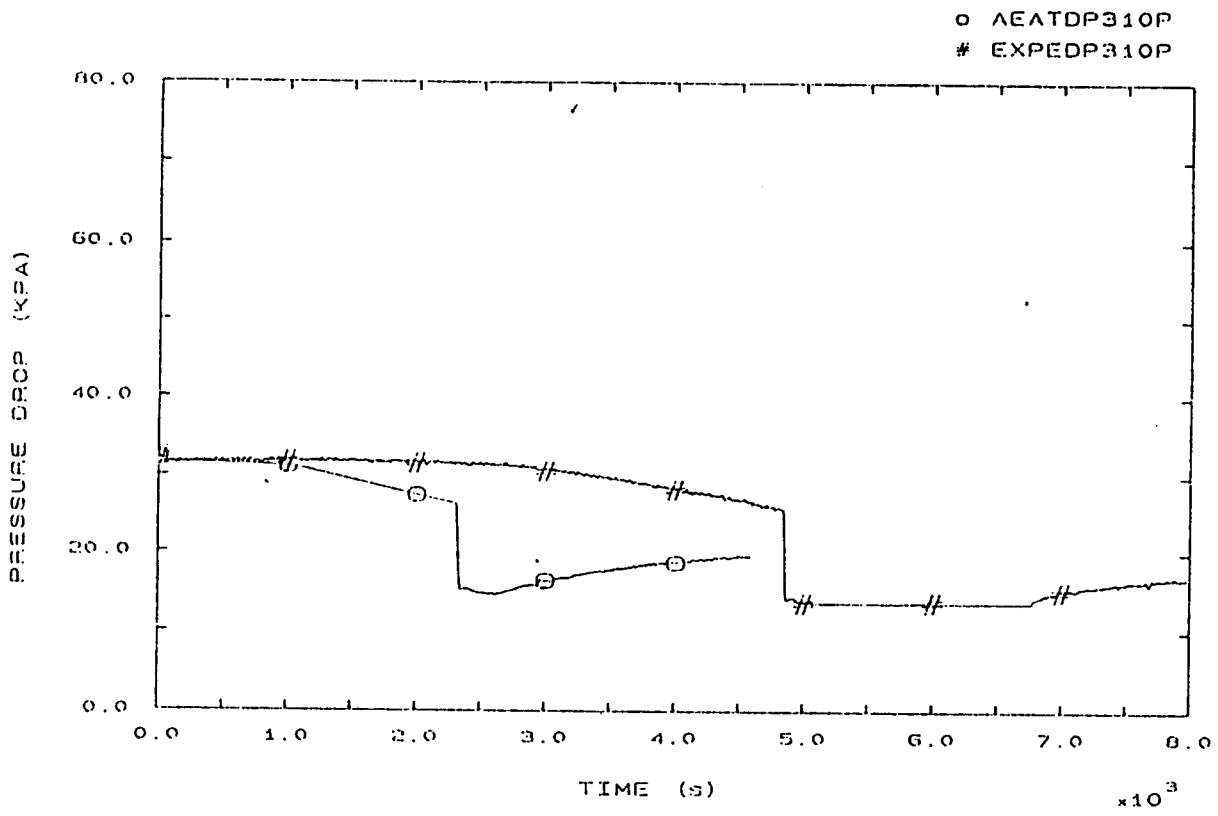

FIG. 73 LOOP SEAL BOTTOM/PUMP 3 INLET PRESSURE DROP

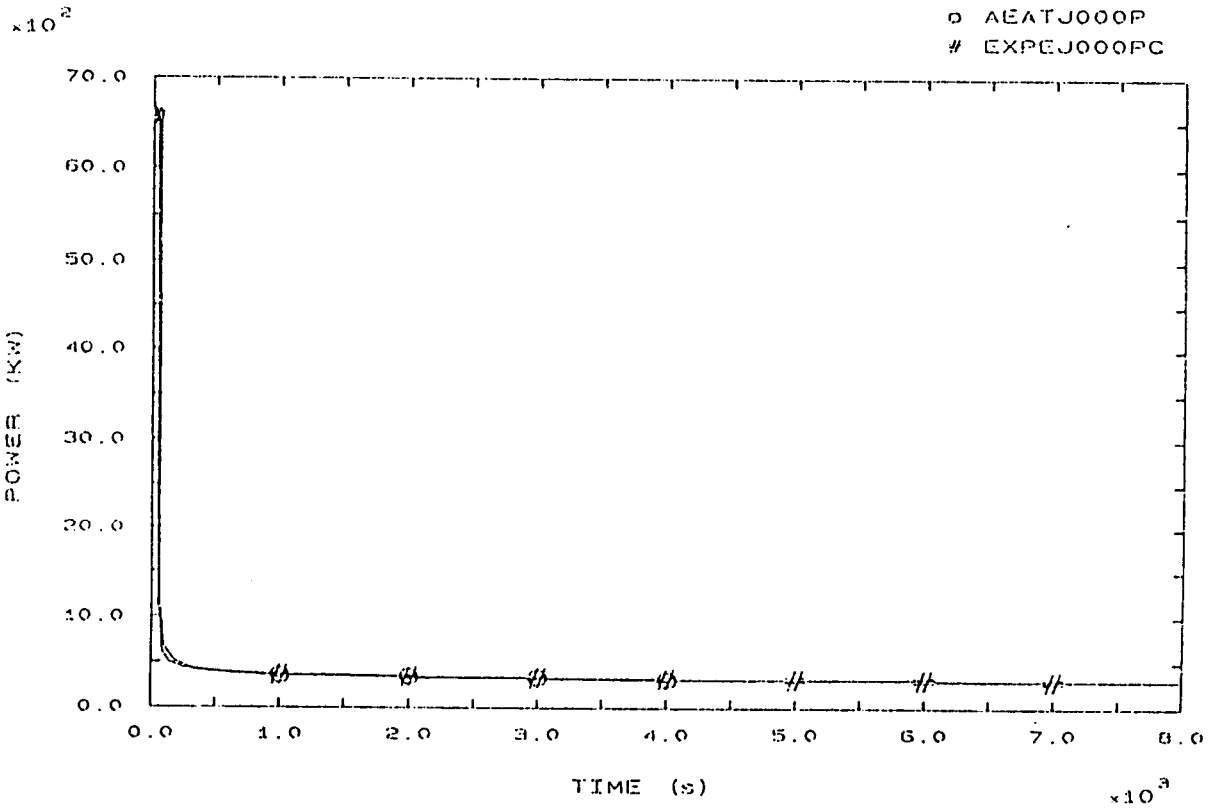

FIG. 81 HEATER RODS POWER

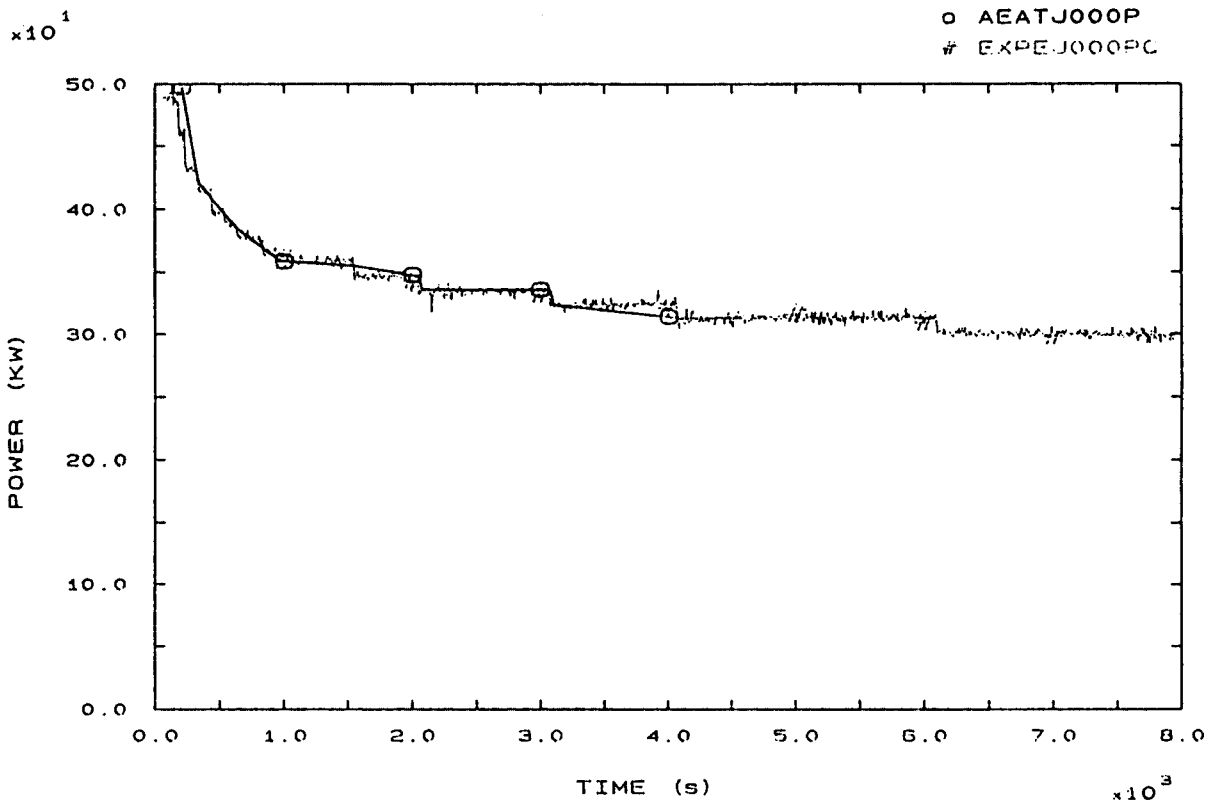

FIG. 81A HEATER RODS POWER

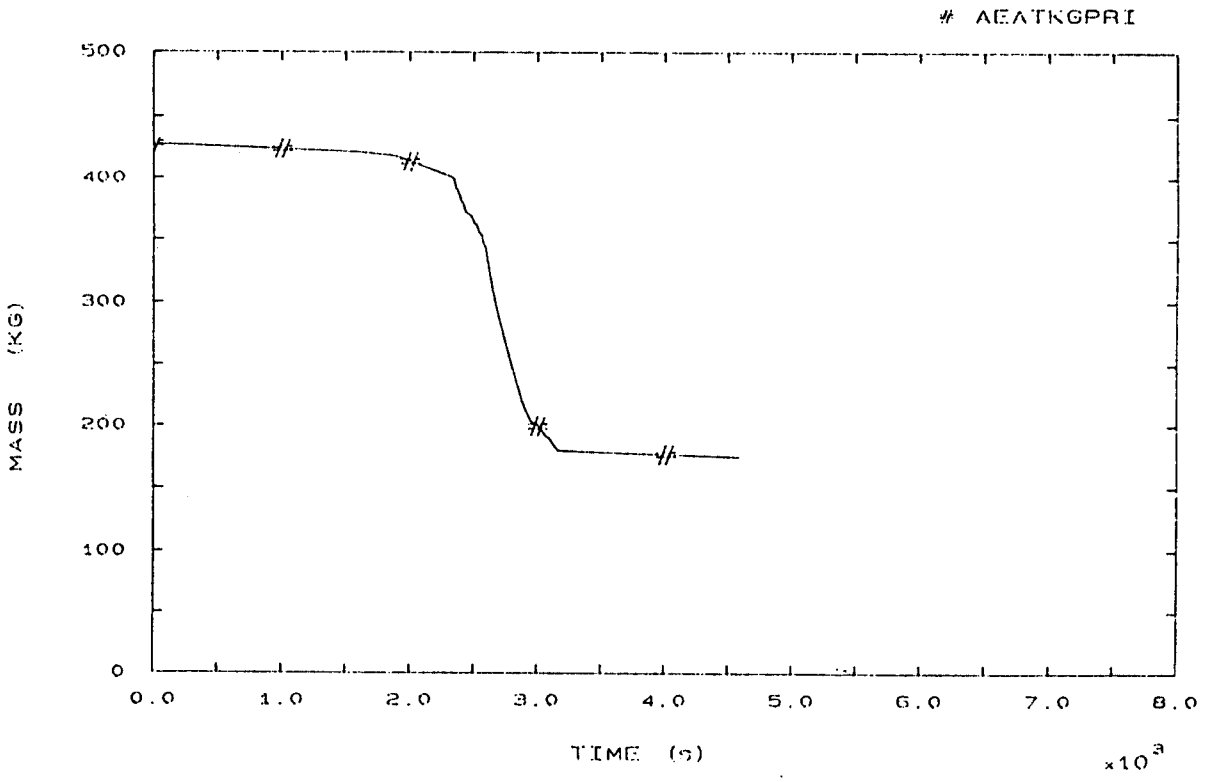

FIG. 85 PRIMARY COOLANT TOTAL MASS

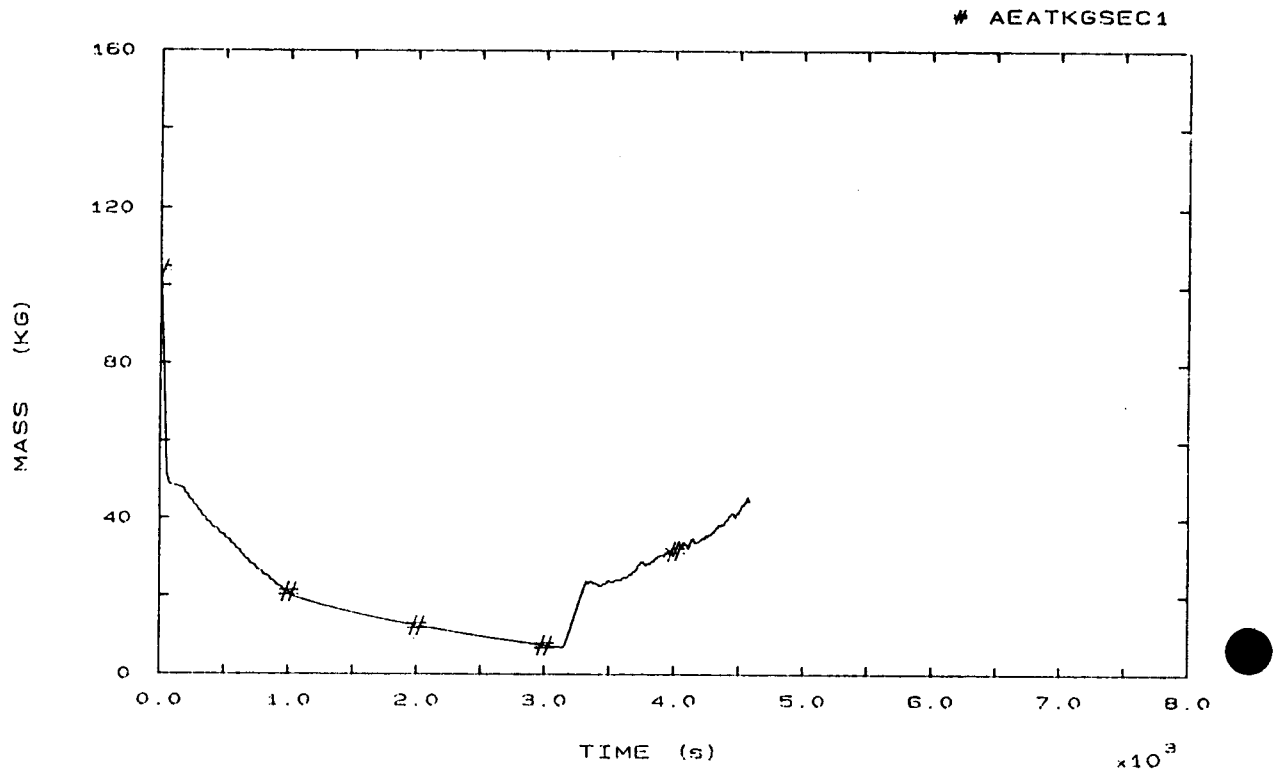

FIG. 86 SECONDARY COOLANT TOTAL MASS SG1

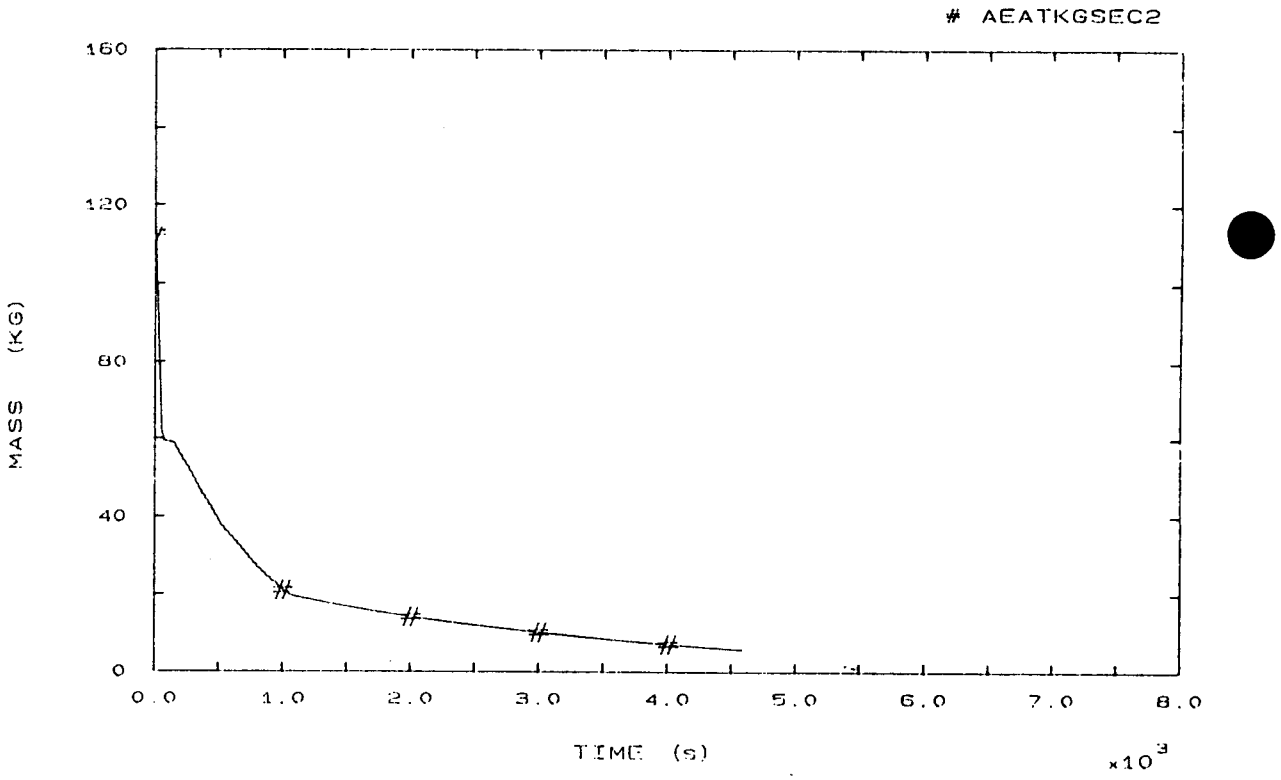

FIG. 87 SECONDARY COOLANT TOTAL MASS SG2

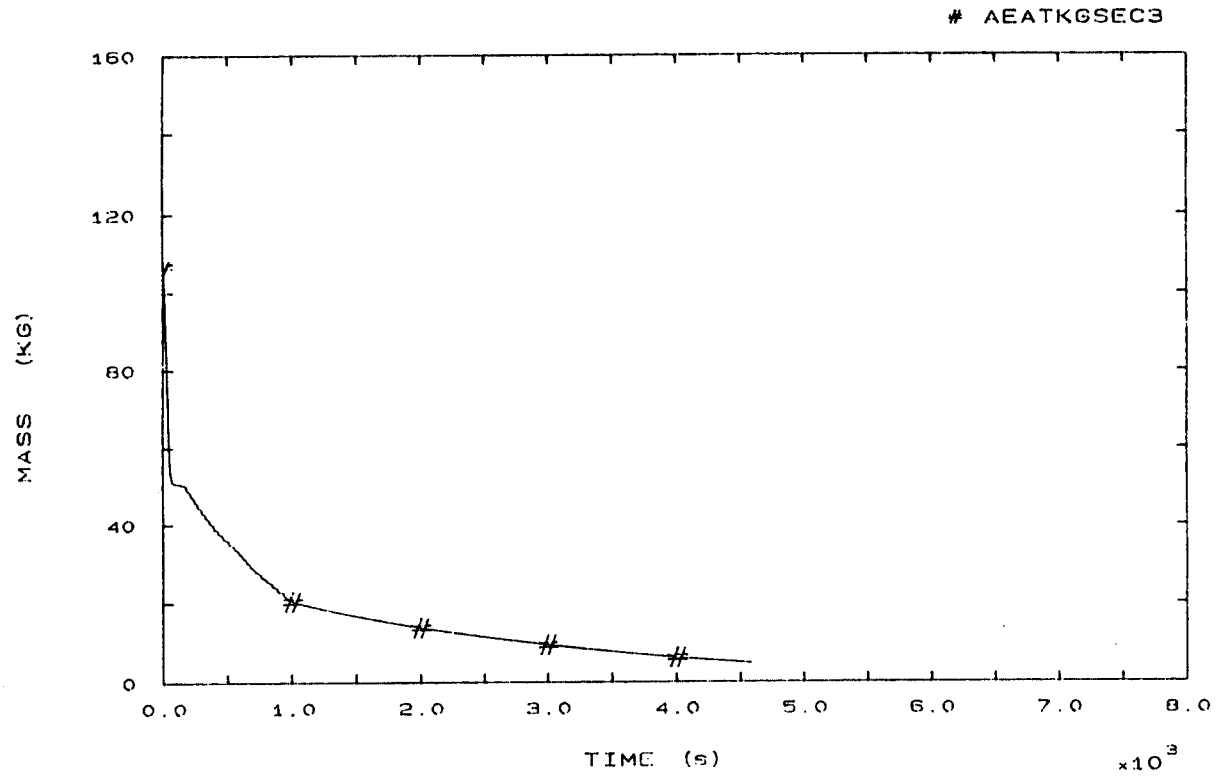

FIG. 88 SECONDARY COOLANT TOTAL MASS SG3

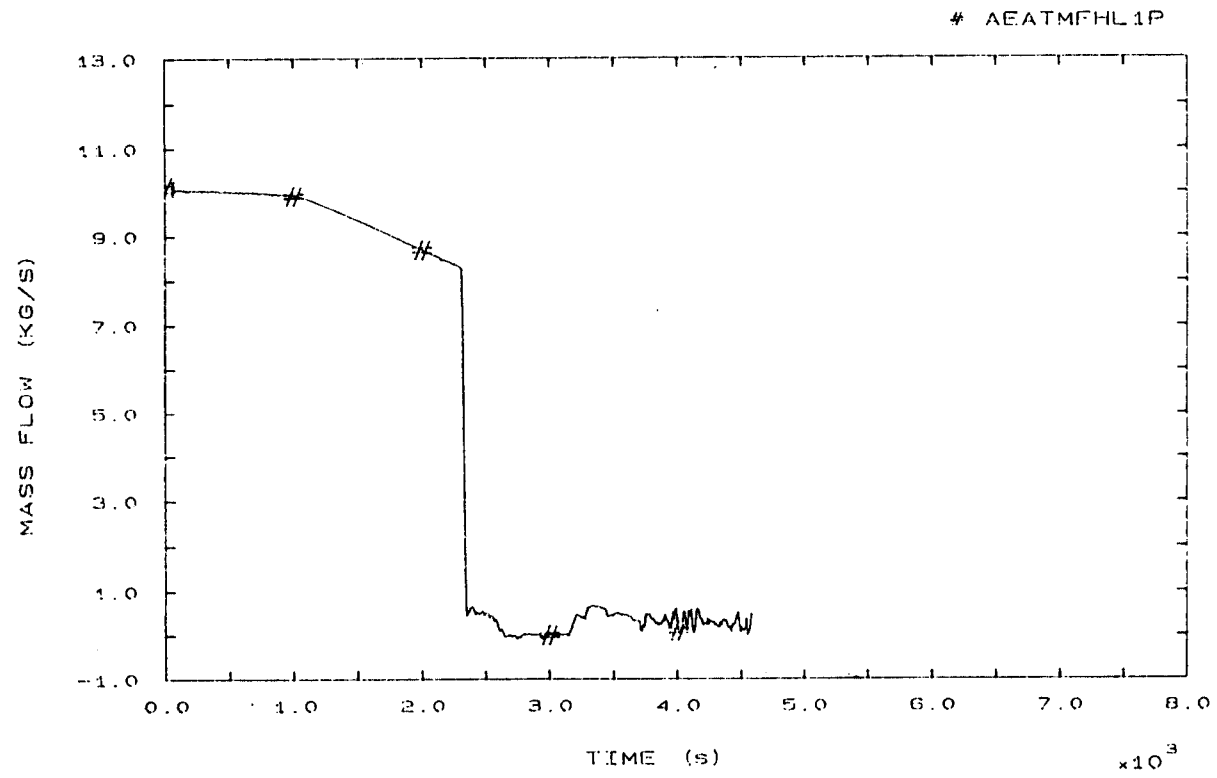

FIG. 89 HOT LEG 1 MASS FLOW

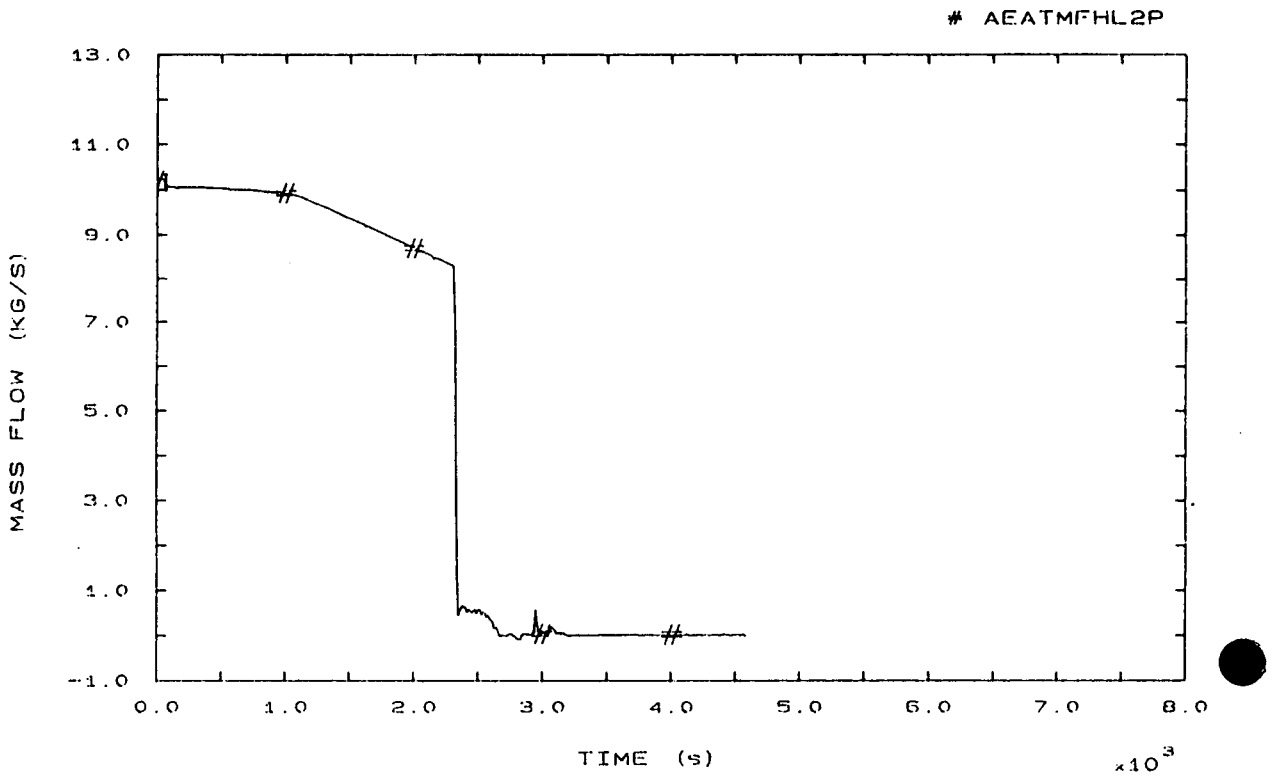

FIG. 90 HOT LEG 2 MASS FLOW

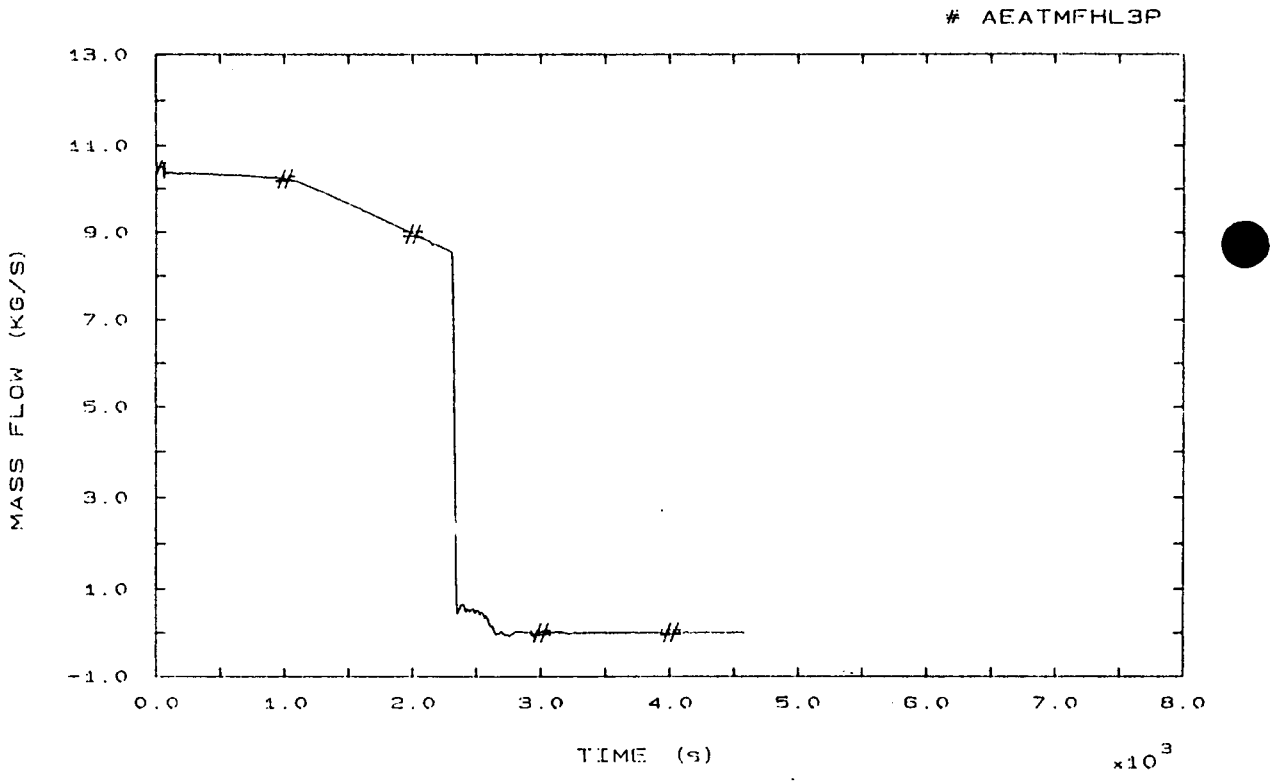

FIG. 91 HOT LEG 3 MASS FLOW

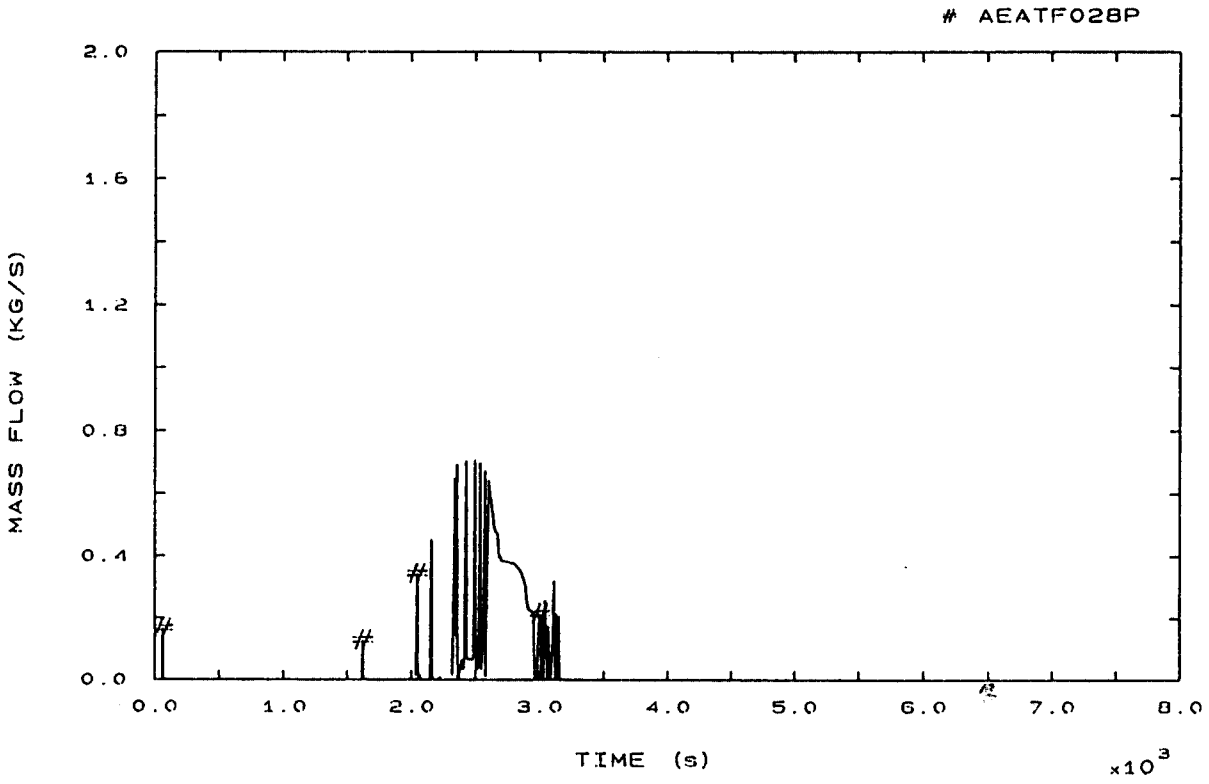

FIG. 92 PRZ PORV MASS FLOW

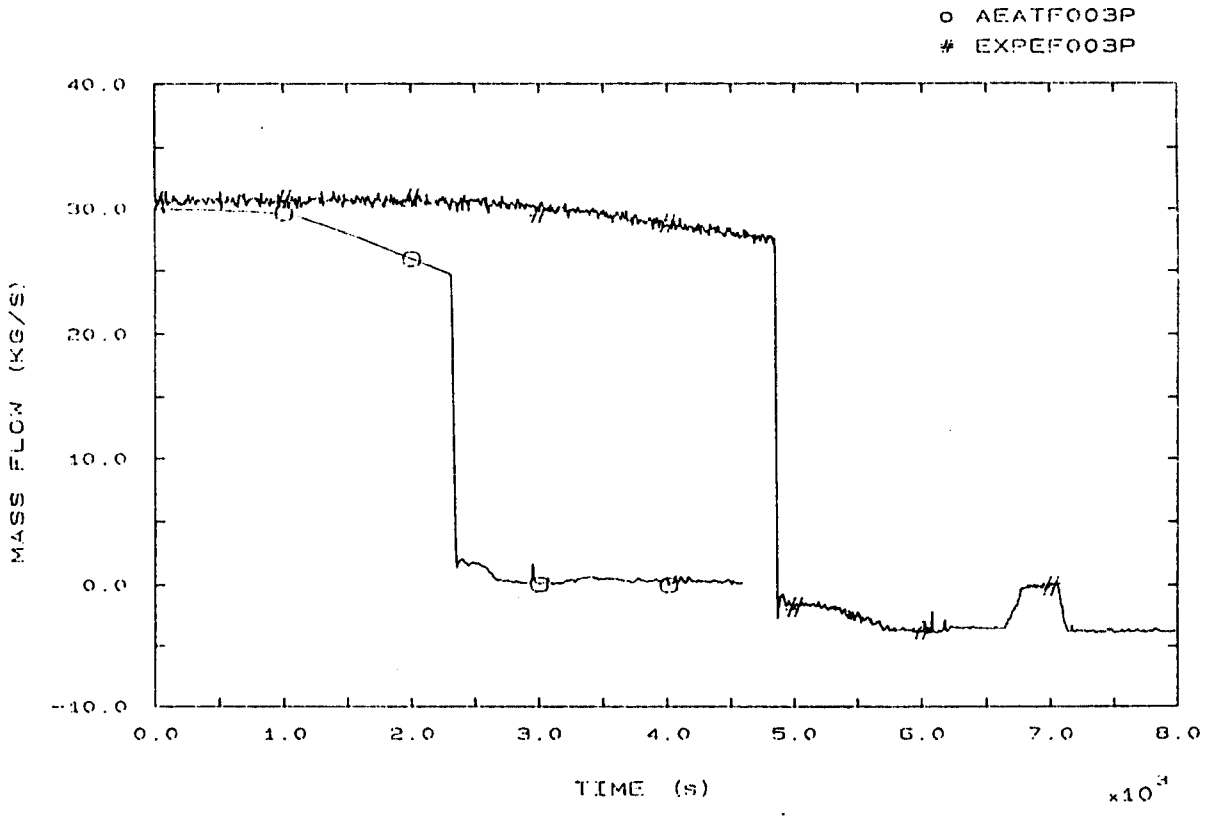

FIG. 94 VESSEL DOWNCOMER MASS FLOW

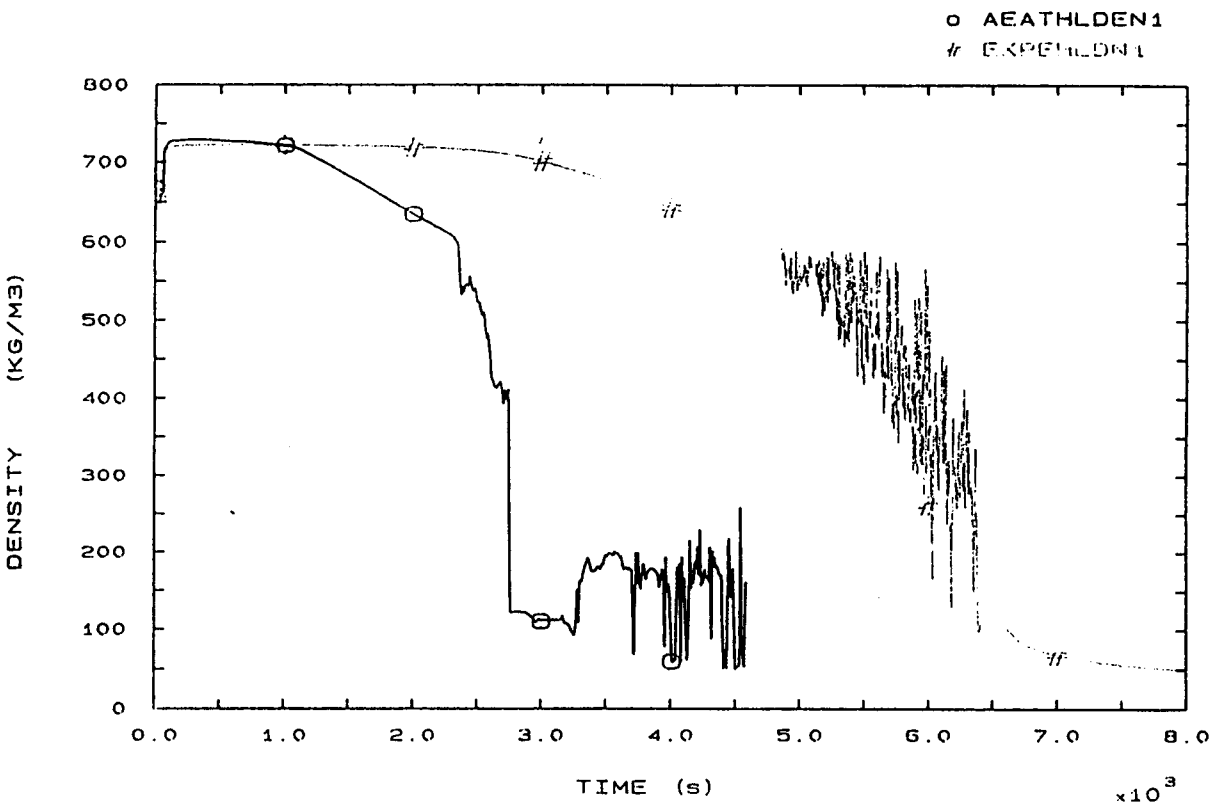

FIG. 100 HOT LEG 1 FLUID DENSITY

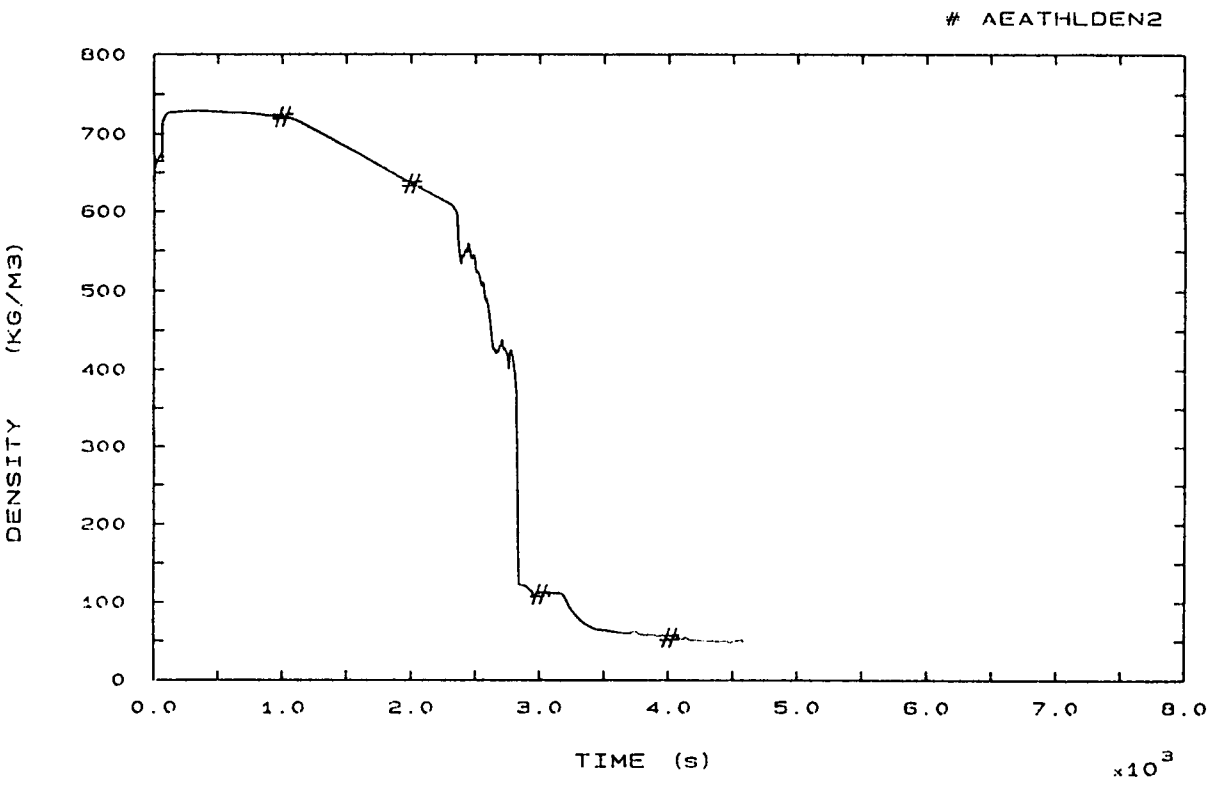

FIG. 101 HOT LEG 2 FLUID DENSITY

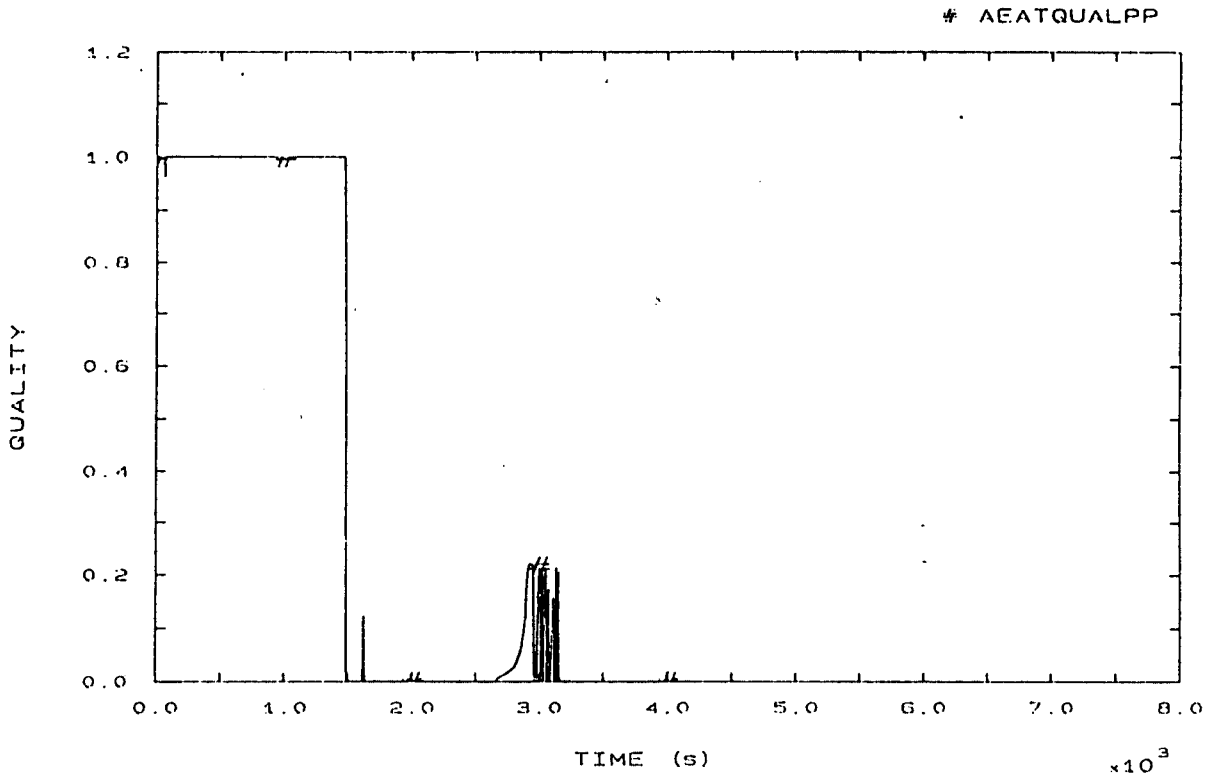

FIG. 103 PRZ PORV FLOW QUALITY

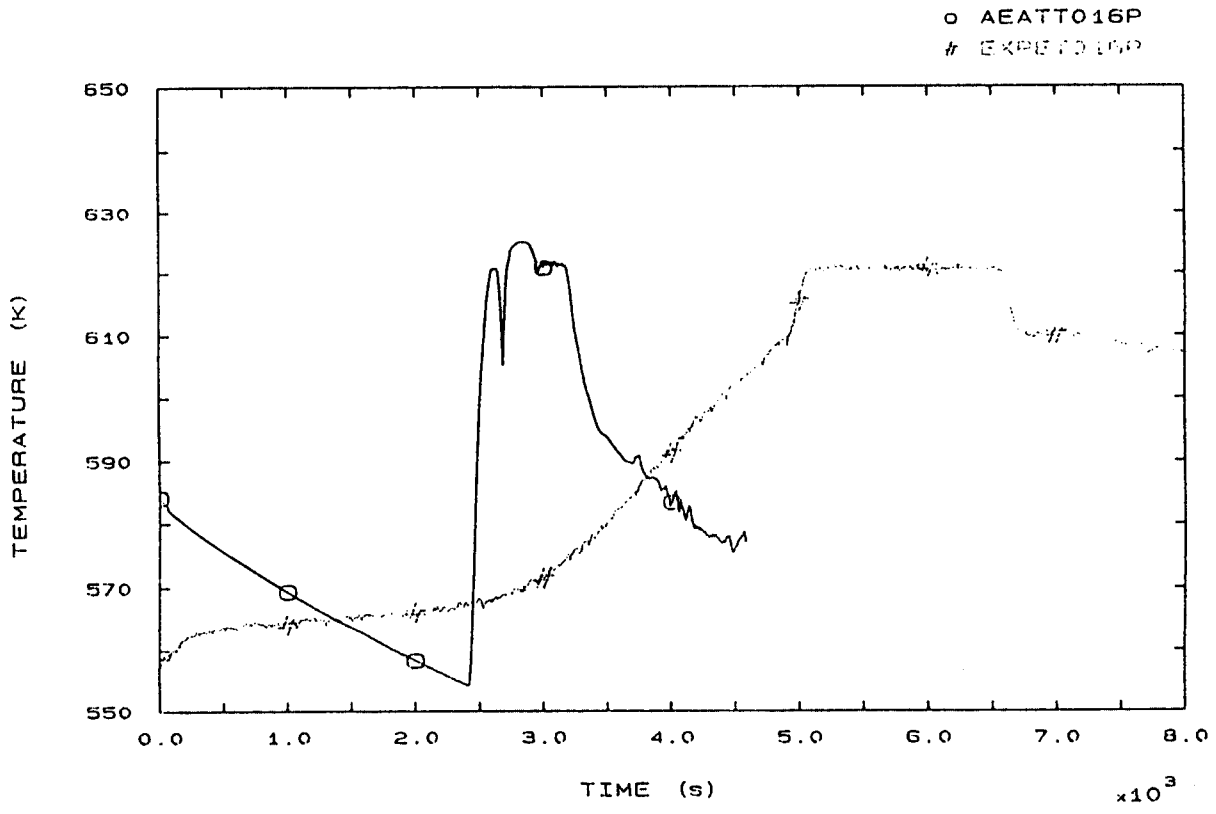

FIG. 110 FLUID TEMPERATURE VESSEL UPPER HEAD

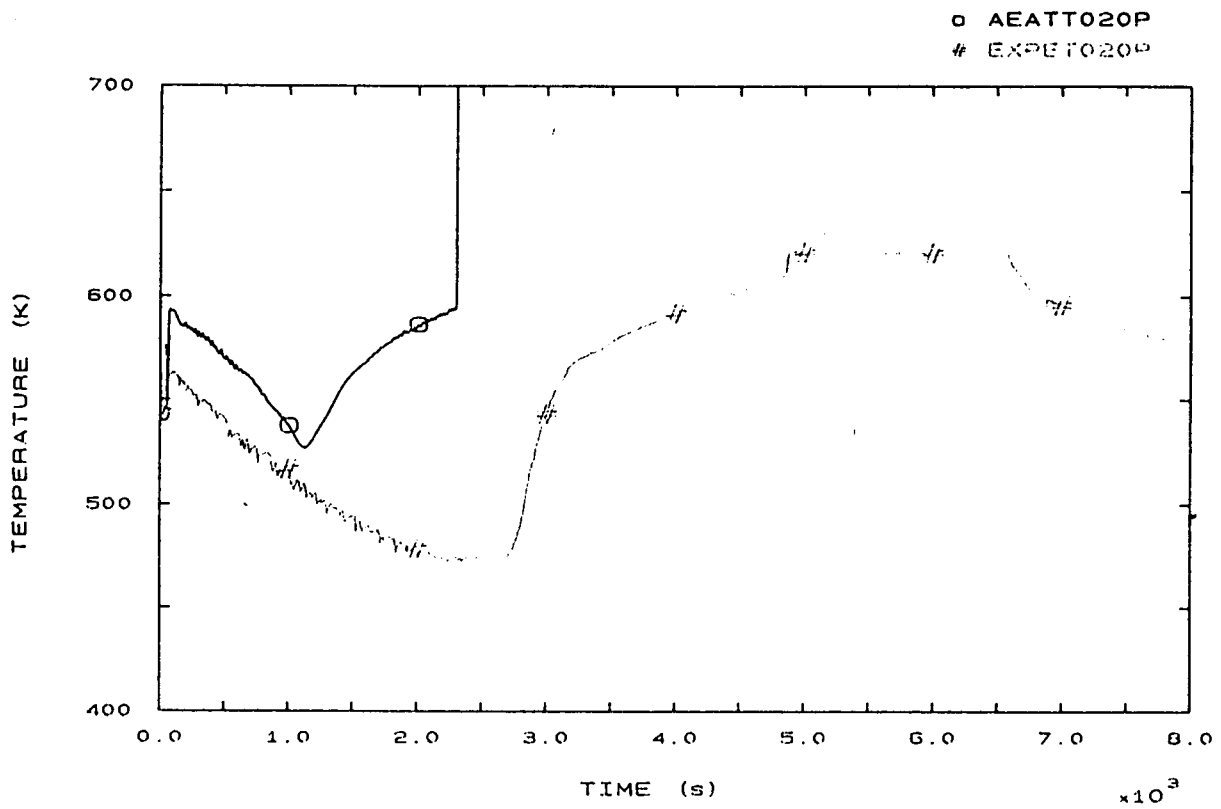

FIG. 112 FLUID TEMPERATURE SURGE LINE UPPER SIDE

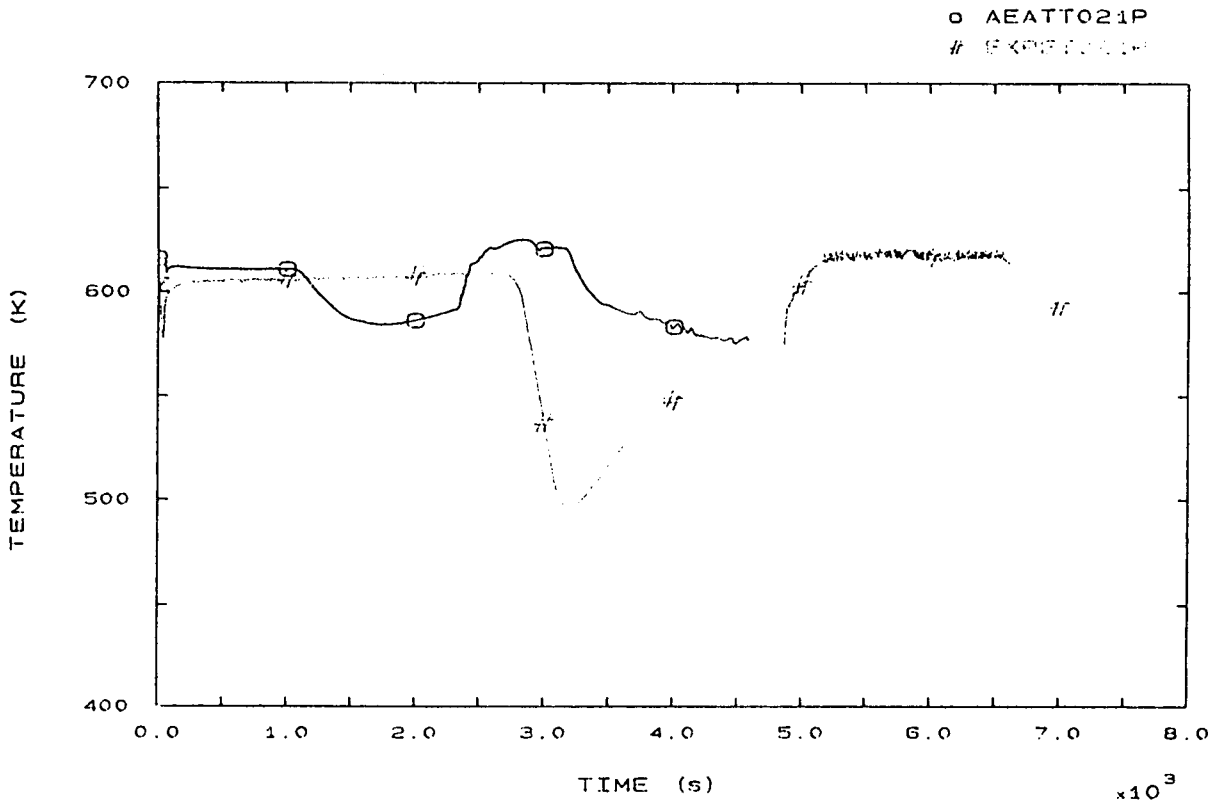

FIG. 113 PRZ FLUID TEMPERATURE

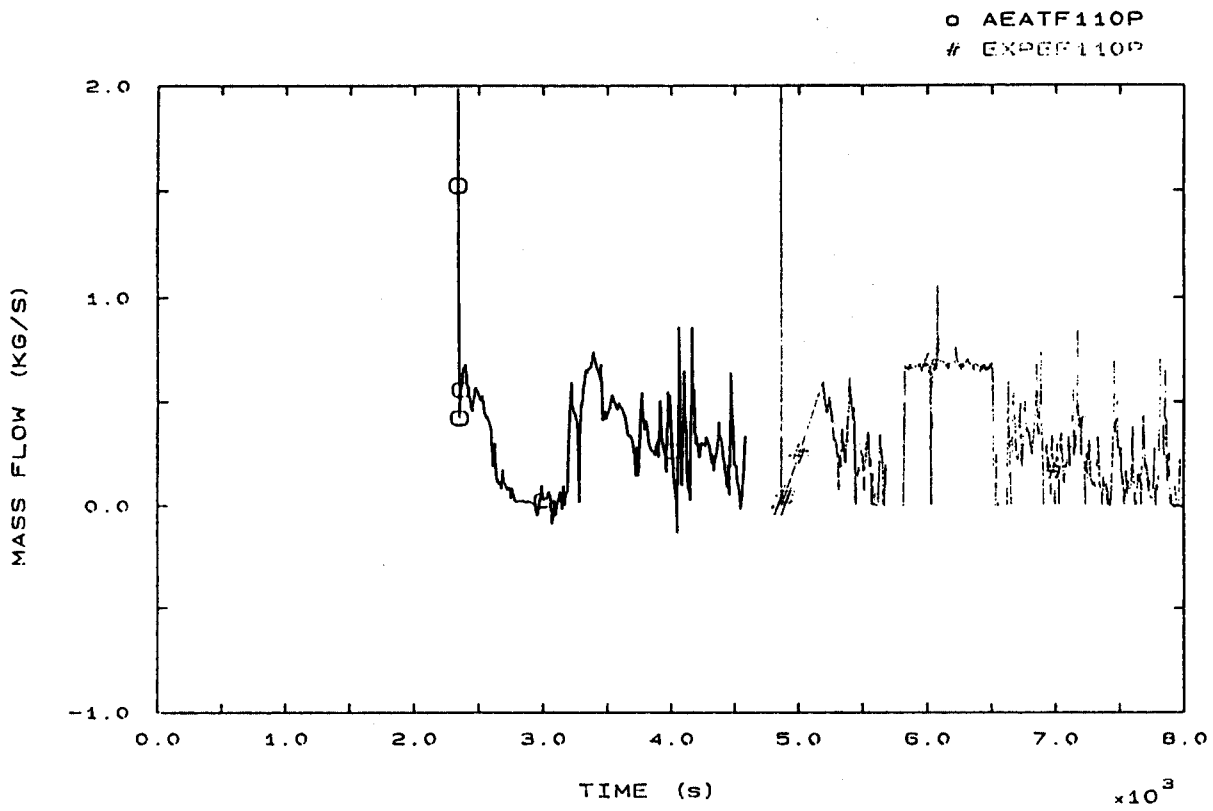

FIG. 125 LOOP SEAL 1 MASS FLOW

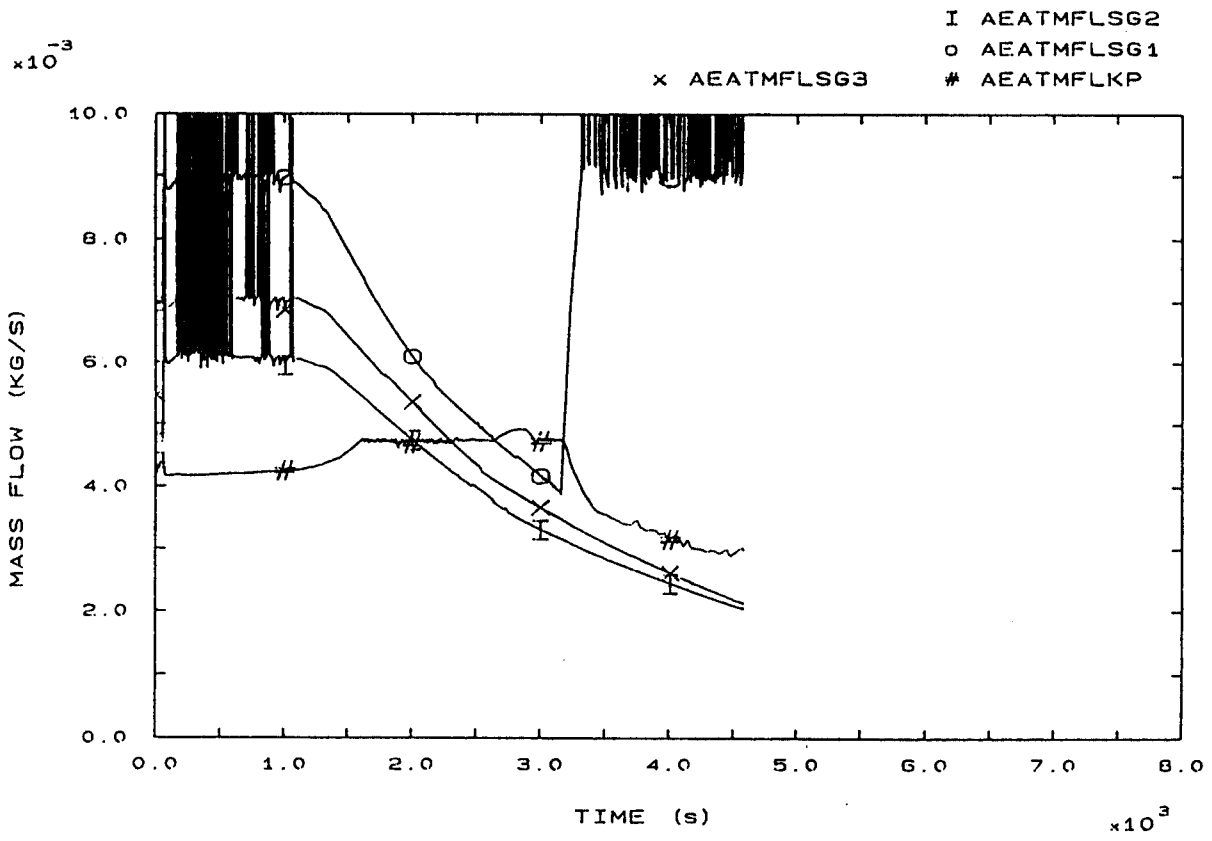

FIG. 137 PRIMARY AND SECONDARY LEAKS

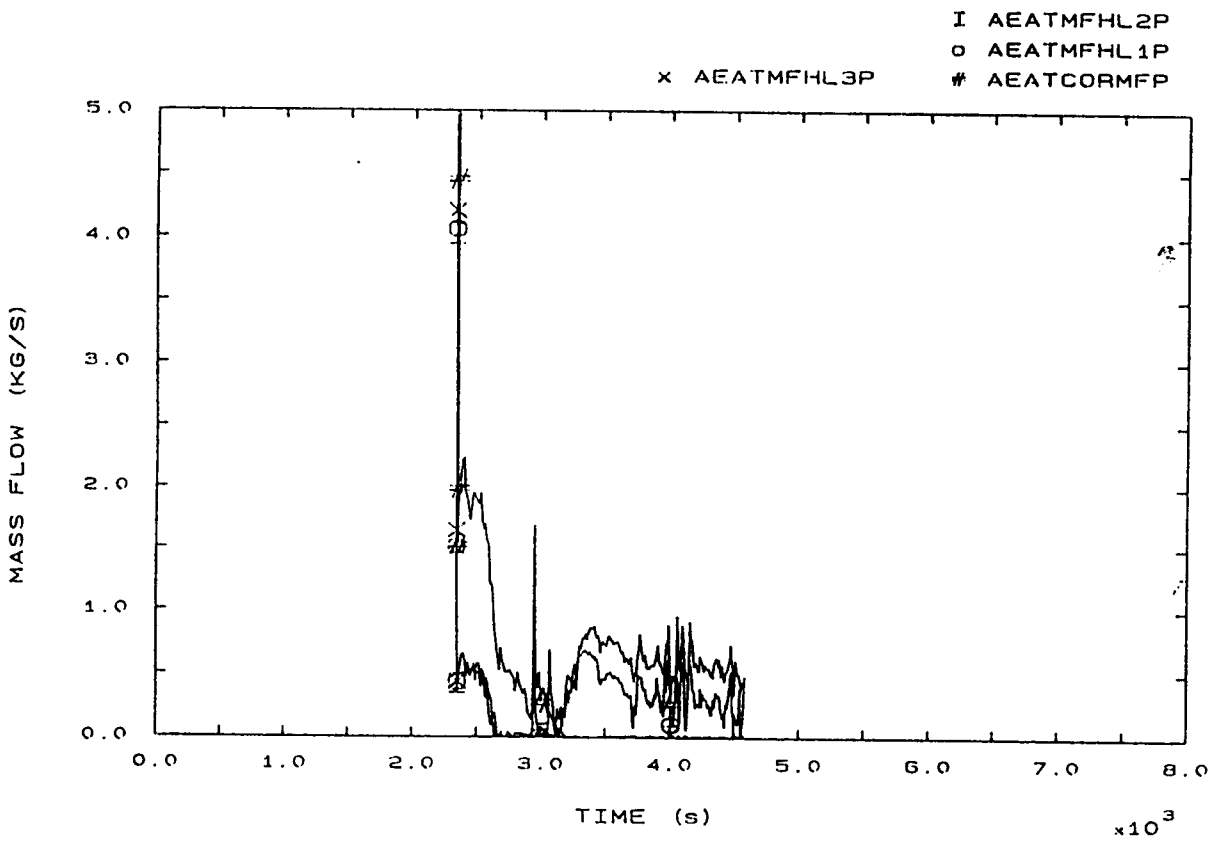

FIG. 141 BOTTOM CORE AND HOT LEG MASS FLOWS

4.18 VTT

4.18.1 CALCULATION DESCRIPTION

Phase 1: from LOFW to Scram (0,50 s)

The scram from low low level in SG2 (fig. 8b) is actuated at 40 s, causing MSI to occur at 49 s (fig. 96b) and effective power reduction beginning at 51 s (fig. 81). Just after that, the maximum primary pressure is 16.07 MPa at 55 s (fig. 1b). Secondary isolation causes SGs pressure to rise (fig. 3b, 4b, 5b). Primary CL temperature rises accordingly (fig. 42b) by inducing PRZ level to increase (fig. 6b).

Phase 2: from Scram to PRZ PORV opening (50, 1512 s)

After Scram the primary pressure drops to a minimum value of 14.8 MPa (fig. 1b). The primary temperature keeps approximately constant during the time interval 135 to 1000 s (fig. 12), and during this time the PRZ level drops slowly from 3.92 m to 3.48 m (fig. 6)due to mass leak. Steam generators dry-out takes place at 1200 s for SG1, at 1135 s for SG2 and at 995 s for SG3 (fig. 7, 8, 9). The primary system heat up takes place during the interval 1005 s to 1512 s (fig. 12): during this time period the primary hot leg temperature (T103P) increases from 571.9 K to 595.6 K, while PRZ level increases from 3.48 m to 5.85 m (fig. 6), causing primary pressure to rise up to PRZ PORV setpoint (see fig. 1).

Phase 3: from PRZ PORV opening to pumps trip (1512, 1767 s)

PRZ PORV opens for the first time at 1512 s when the PRZ collapsed level is 5.83 m and PORV void fraction is still 1 (see fig. 6, 103). PRZ becomes full at 1670 s (fig. 6). During PRZ relief valve opening the upstream void fraction is unity between 1512 and 1670 and approximately zero (liquid discharge) between 1670 and 2035 (fig.

103). During this period the primary loop subcooling drops from 46 K to 3.9 K. Steam generators, following dry out, continue to depressurize with decreasing rates (fig. 3, 4, 5).

Phase 4: from pumps trip to EFW actuation (1767, 2287 s)

The pumps are tripped at 1767 s (fig. 54, 55, 56). After pumps trip the PRZ keeps full until 2035 s (fig 6). After that the PORV void fraction increases from 0.0 to 1.0 between 2035 and 2130 s (fig. 103) while PRZ level decreases progressively (fig. 103). Following pumps trip, natural circulation conditions are established, with core flow rate decreasing from 2.6 to 2.0 Kg/s (fig. 94), but gradually this flow estinguishes and LNC occurs at 2065 s. The driving force for natural circulation are enthalpy rise in the core and heat losses. The cooling effect of secondary steam has a minor importance. After about 190 s of stagnation, core heat up begins ar 2255 s (fig. 51, 52).

Phase 5: from EFW actuation to the end (2287, 3580 s)

The EFW is actuated at 2287 s from core cladding temperature 658 K. After that the core temperature still increases, reaching a maximum of 662 K at 2290 s (fig. 52). After EFW actuation the natural circulation through the core starts again (fig. 89, 94). The condensation is so efficient that primary pressure and level drop significantly (fig.1, 6). The PRZ PORV is closed finally at 2293 s (fig. 1), when PRZ level is 4.88 m, then level drops rapidly to 0.0 m (2590 s). The core reflood takes place mainly from the bottom. On the secondary side, level recovery and pressurization are observed in SG 1 (fig. 3, 7).

PARTICIPANT: MIETTINEN - VTT *CODE: SMABRE*

EVENTS TABLE

EVENT	*CALC. TIME (s)*	*EXP. TIME (s)*
SG Low Low Level	*42*	*33*
Main Steam Isolation	*49*	*38*
Scram (power fall), t_1	*50*	*44*
SGs PORV opening	*60* *60* *60*	*82 (3)* *106 (2)* *200 (1)*
SGs Dry Out	*995 (3)* *1135 (2)* *1200 (1)*	*3282 (3)* *3347 (1)* *3437 (2)*
PRZ PORV opening, t_2	*1512*	*4134*
PRZ full of liquid	*1670*	*4222*
Pumps Trip, t_3	*1767*	*4848*
Loss of Natural Circulation	*2065*	*5630*
Beginning of Core Heat Up	*2255*	*6511*
EFW actuation, t_4	*2287*	*6532*
PRZ PORV closure	*2293*	*6576*
PRZ emptying	*2590*	*6811*
SG1 repressurization	*2438*	*6878*
End of transient, t_{END}	*3580*	*8062*

4.18.2 CALCULATION/EXPERIMENT COMPARISON

Phase 1: from LOFW to Scram

Initial SGs inventory is underestimated (see Comp. Table) also if initial SG DC levels are slightly higher than in the test (fig. 7b, 8b, 9b). Trips timing is delayed, due to late LoLo Level trip (42 s vs 33, see fig. 7b, 8b, 9b). This can be explained with the higher level values. Both discrepancies contribute to a significant underevaluation of secondary inventory at Scram time (see Comp. Table). Maximum primary pressure is well predicted (16.1 MPa vs 16.2) even if, due to the short time interval between MSI and Scram (only 1 s), PRZ PORV doesn' t lift in this phase (see fig. 1b).

Phase 2: from Scram to PRZ PORV opening

Minimum primary pressure immediately following scram (fig. 1b) is calculated with sufficient accuracy (14.8 MPa vs 14.5). SGs PORV opening time is underestimated (see Comp. Table) also if secondary prezzurization on trend after MSI is well predicted (fig. 3b, 4b, 5b). PRZ level gradient during constant primary temperature period (fig. 6) is well predicted, but minimum PRZ level during the phase is overpredicted (3.48 m vs 2.3) due to a higher value immediately after Scram and the reduced SG emptying duration.
Dry Out time is extremely underestimated (about 1200 s vs 3400) due to the underevalutation of secondary inventory at Scram time (see C.T.) and to an overestimate of SG level gradient caused by low heat losses (fig. 7, 8, 9, 131, 139). Primary temperature and level gradients during heat up are largely overestimated (see Comp. Table and fig. 6, 12). This can be related to an incorrect heat losses and primary heat capacities simulation. No cool insurge relevant effect is observed in SMABRE prediction also if a limited surge line cooldown during SGs

emptying is calculated (see fig. 112, 113). Due to early SGs dry out and subsequent faster primary pressurization (fig. 1), time of PRZ PORV opening (t_2) is strongly underpredicted (1512 s vs 4134), also in terms of time interval from latest SG dry out (312 s vs 697). PRZ conditions at time t_2 are partially predicted: PRZ level is slightly lower than in the experiment (5.83 m vs 6.57), while the estimated void fraction is accordingly higher.

Phase 3: from PRZ PORV opening to pumps trip

The "absolute" time of PRZ filling is consequently largely underestimated (1670 s vs 4222), while time interval from PRZ PORV opening is overpredicted (fig. 1, 6 and C.T.), due to the lower level value at time t_2. Relief condition during phase 3 varies from steam (until filling) to liquid (fig. 6, 103). The primary system remains subcooled during the phase. Pumps trip is calculated at time 1767 s (vs 4848), that is 255 s (vs 714) after the PRZ PORV opening. Time interval since SGDO (dt_{HU}) is underpredicted due to the faster temperature trend during primary heat up (fig. 12, 42).

Phase 4: from pumps trip to EFW actuation

Primary mass at pumps trip time is slightly underestimated (366 Kg vs 390). This is due to a lower value of initial primary inventory and cannot explain the shorter LNC time interval from trip time (298 s vs 780). This seems due to an excessive discharge of liquid from PRZ PORV.

Primary inventory at time of LNC is instead well calculated (289 Kg vs 296). PRZ behaviour during this phase is simulated by SMABRE in terms of partial emptying (after t = 2000 s), while the obscillations period observed in the Exp is not calculated (fig. 6). This can be related to the short duration of the phase (520 s vs 1684).

Both periods of two-phase natural circulation and flow stagnation are predicted by VTT calculation but the duration of such phenomena is

largely underestimated (see C.T.). Time when core heat up begins (t_{BOCH}) is strongly underpredicted, even if related to the time of LNC (190 s vs 880). Primary mass at this time is obviously overestimated (205 Kg vs 183). Emergency Feed Water actuation is predicted 222 s after time of LNC (900 s in the Exp). PRZ level at time of EFW actuation is very close to the exp value (4.8 vs 4.4). Average core heat up rate at top of bundle (fig. 52) is at the lower limit of the exp range (2 K/s).

Phase 5: From EFW actuation to the end

The maximum core temperature (fig. 52) is sensibly underpredicted (662 K vs 770), so as PRZ PORV closure time interval from EFW actuation (6 s instead of 44). The reason of this fast response of core cooling to EFW can be related to the overestimate of primary mass inventory at time of PRZ PORV closure (196 Kg vs 179).
Primary depressurization rate is initially very close to the exp. value (see fig. 1), while later on it becomes slightly higher (see Comp. Table). VTT calculation predicts TPNC due to condensation in primary system and preminent bottom-up core reflood. SG1 pressurization period (fig. 3) is only 151 s (338 in the Exp), while PRZ emptying period (fig. 6) is calculated with good accuracy (300 s vs 280). SG 1 level recovery occurs in a particular way: level immediately rises to about 1 m, then remains at this value for about 700 s, and finally starts increasing again at a rate sensibly higher than the exp. one (see fig. 7).

PARTICIPANT: MIETTINEN - VTT CODE: SMABRE

COMPARISON TABLE

PARAMETER		EXP	CALC	AE*	RFD**
1A Initial SGs mass (Kg)	1	137	127		
	2	151	123	P	C+B+U ?
	3	145	113		
1B Trips timing (s)	LoLo	33	42	P	HIL?(C+B+U)
	MSI	38	49	P	LoLo
	Scram	44	50	P	LoLo
1C Max primary pressure (MPa)		16.2	16.1	G	-
1D SGs mass at Scram (Kg)	1	98	77		
	2	105	72	P	1A+1B
	3	97	61		
2A Min. primary pressure (MPa)		14.5	14.8	S	-
Pressure gradients before		4.10^{-4}	<0	P	PRZM (U+B)
and after SGs DO (MPa/s)		3.10^{-4}	?	P	PRZM (U+B)
2B SGs PORV opening time (s)	1	200	60	P	
	2	106	60	P	?
	3	82	60	S	
2C PRZ level gradient (m/s)		$-5.7.10^{-4}$	$-5.9.10^{-4}$	G	-
2D Min. PRZ level (m)		2.3	3.48	P	2E
2E SGs DO time, tSG1DO (s)		3347	1200	P	1D+
tSG2DO (s)		3437	1135	P	LHL (U)
tSG3DO (s)		3282	995	P	
2F Heat Up temperature (K/s)		0.02	0.06	P	LHL
and level (m/s) gradients		$3.6.10^{-3}$	7.10^{-3}	P	+LHC (U)
2G Cool Insurge effect		PR. DELAY	NO	P	PRZM (U+B)
2H PRZ PORV opening time, t2 (s)		4134	1512	P	2E+LHL(U)
($dt_2 = t_2 - t_{SGDO}$)		(697)	(312)	P	PRZM(U+B)+2F
3A PRZ level at t_2 (m)		6.57	5.83	S	2A+2F
3B PRZ full time, t_{PRZF} (s)		4222	1670	P	2E+2F
($dt_{PRZF} = t_{PRZF} - t_2$)		(88)	(158)	P	3A
3C Dominant Relief Condition		SUB	ST/MIX	S	3A
3D Sat. Conditions before trip		NO	NO	G	-
3E Pumps Trip time, t3 (s)		4848	1767	P	2E+2F
($dt_3 = t_3 - t_2$)		(714)	(255)	P	2H,3E
($dt_{HU} = t_3 - t_{SGDO}$)		(1411)	(567)	P	2F

* ACCURACY EVALUATION : G=GOOD, S=SUFFICIENT, P=POOR

** REASON FOR DISCREPANCY : C=CODE, U=USER, PRZM=PRESSURIZER MODELLING
LHL=LOW HEAT LOSSES, HIL=HIGH INITIAL LEVEL, LHC=LOW HEAT CAPACITIES

PARTICIPANT: MIETTINEN - VTT CODE: SMABRE

COMPARISON TABLE (CONT'D)

PARAMETER	EXP	CALC	AE*	RFD**
3F RCS mass at t3 (kg)	390	366	S	LII(U)
4A PRZ behaviour during phase 4	PART. EMPT. LEV. OBS.	PART. EMPT.	S	-
4B Primary Flow Cond.	TPNC/LNC	TPNC/LNC	G	-
4C LNC time, t_{LNC} (s)	5630	2065	P	3E,(C?)
($dt_{LNC} = t_{LNC} - t_3$)	(780)	(298)	P	LDP+3F
4D RCS mass at t_{LNC} (kg)	296	289	G	-
4E Beg. of Core Heat Up, t_{BOCH} (s)	6511	2255	P	4C
($dt_{BOCH} = t_{BOCH} - t_{LNC}$)	(880)	(190)	P	LHL(U),LDP(C?)
4F RCS mass at tBOCH (Kg)	183	203	P	4E+PMD(C?)
4G EFW act. time, t4 (s)	6532	2287	P	3E+4C+4E
($dt_{4B} = t_4 - t_{BOCH}$)	(21)	(32)	S	-
($dt_{4L} = t_4 - t_{LNC}$)	(900)	(222)	P	LHL(U)
($dt_4 = t_4 - t_3$)	(1684)	(520)	P	LHL(U)
4H PRZ level at t_4 (m)	4.4	4.8	G	-
5A Core Heat Up Rate (K/s)	2/5	2	S	-
5B Max Core Temperature (K)	770	662	P	SSNOD(U)
5C PRZ PORV closure time, t_{PRZPC}	6576	2293	P	4G
($dt_{PRZPC} = t_{PRZPC} - t_4$)	(44)	(6)	P	SSNOD(U)
5D RCS mass at t_{PRZPC} (Kg)	179	196	S	-
5E RCS Depress. Rate (MPa/s)	-0.016	-0.0.15	G	-
(Initial/Averaged on 500 s)	-0.0086	-0.0133	S	SSNOD(U)
5F Prim. Circulation Mode	INTERM	TPNC	P	C+U ?
5G SG1 Press. time, t_{SG1PR} (s)	6878	2438	P	4G
($dt_{SG1PR} = t_{SG1PR} - t_4$)	(346)	(151)	P	SECM(U)
5H PRZ Role	CORE FL.	?	P	-?
5I PRZ emptying time, t_{PRZE} (s)	6811	2590	P	4G
($dt_{PRZE} = t_{PRZE} - t_4$)	(280)	(303)	G	-
5J Core Reflood Mode	TOP-DOWN	BOTTOM/UP	P	5H
5K End of Transient time, t_{END}	8062	3580	P	4G

* ACCURACY EVALUATION : G=GOOD, S=SUFFICIENT, P=POOR

** REASON FOR DISCREPANCY : C=CODE, U=USER, LDP=LIQUID DISCHARGE FROM PRZ, PMD=PRIMARY MASS DISTRIBUTION, SSNOD=SECONDARY SIDE NODALIZATION, SECM=SECONDARY MODELLING, LII=LOW INITIAL INVENTORY

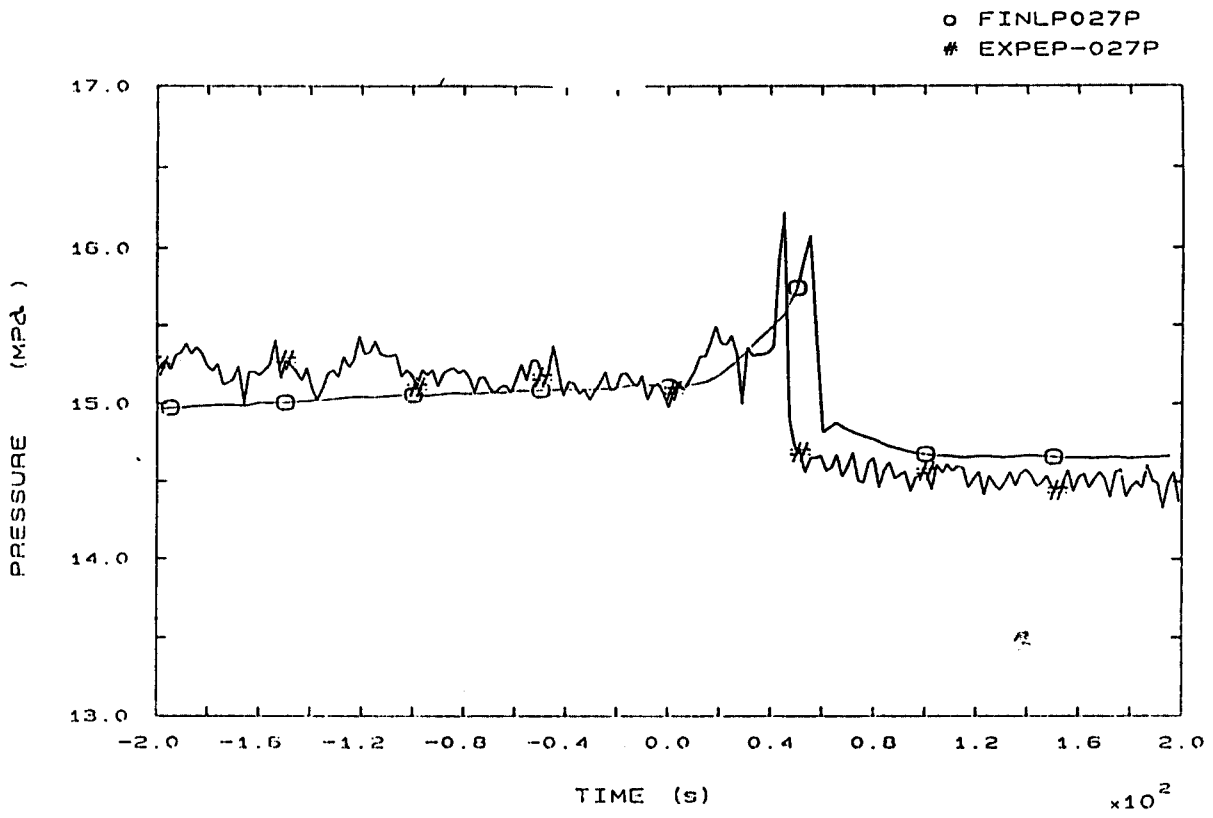

FIG. 1b PRESSURIZER PRESSURE

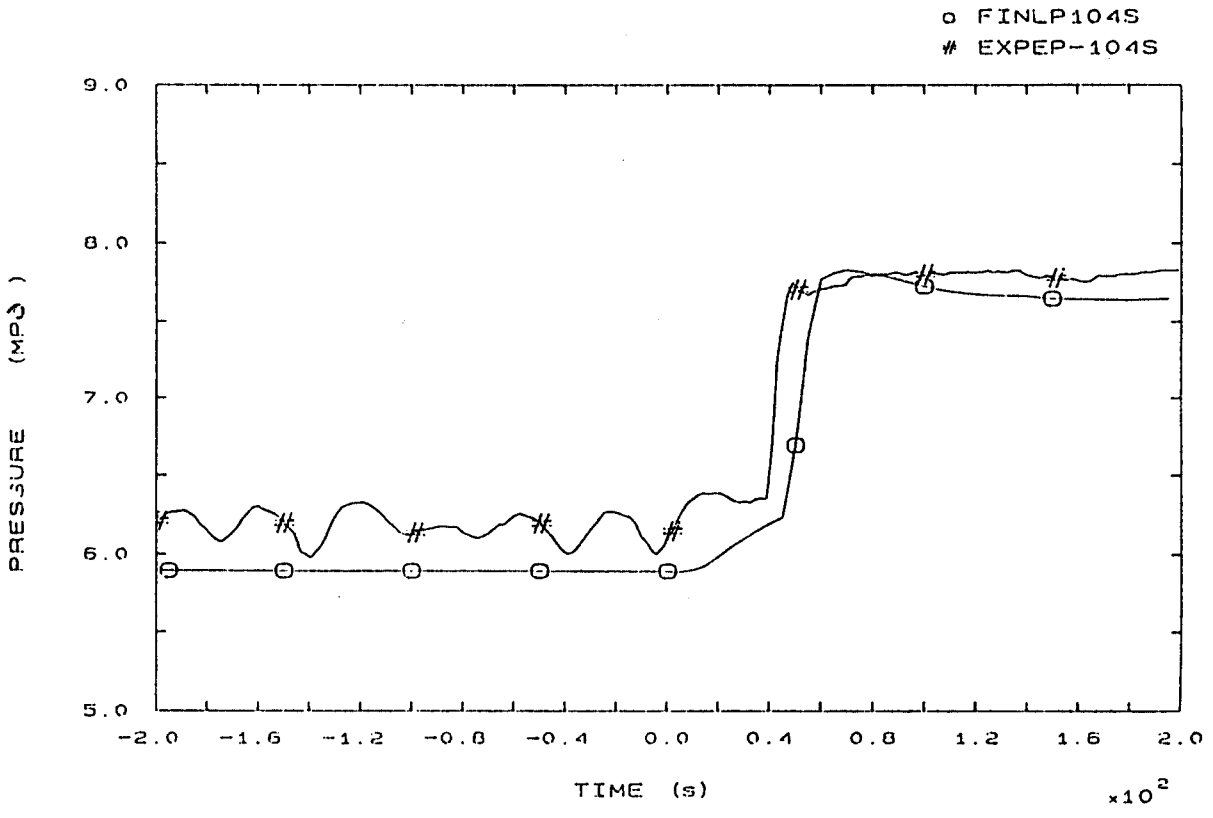

FIG. 3b SG1 STEAM DOME PRESSURE

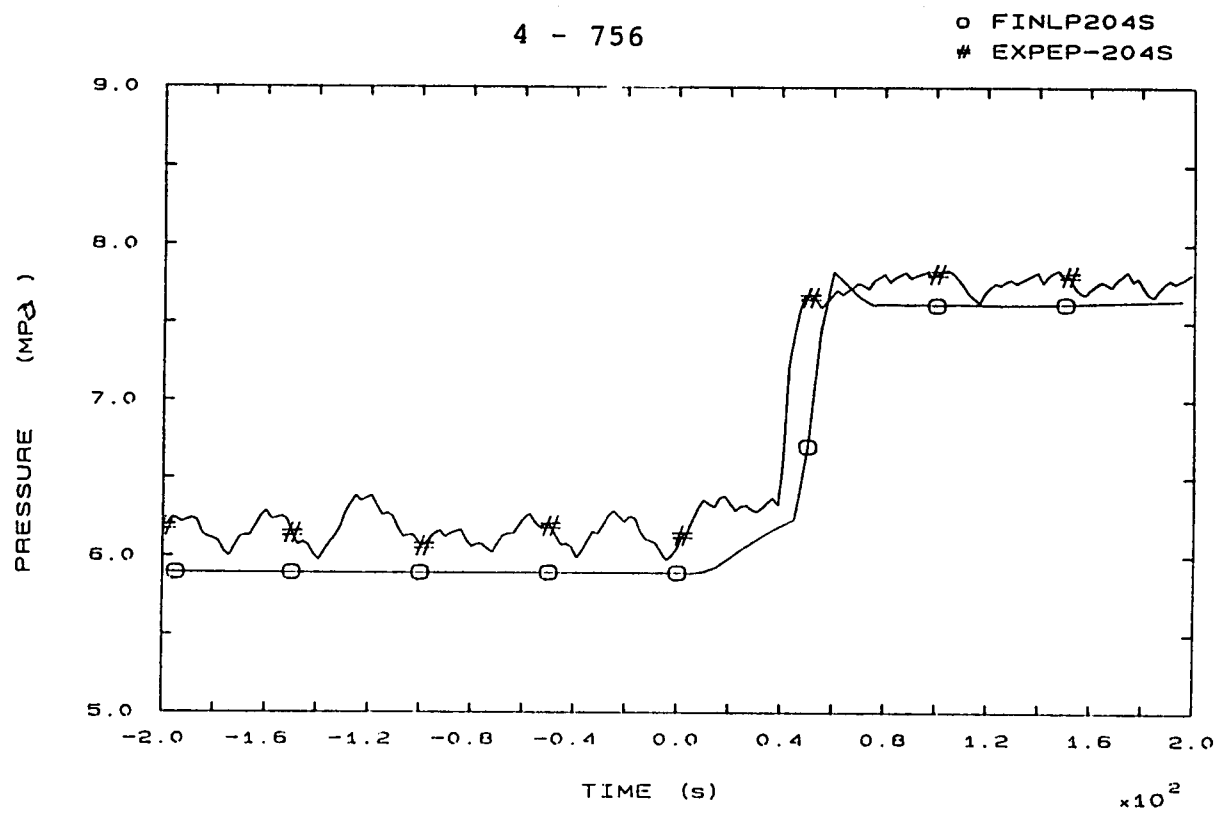

FIG. 4b SG2 STEAM DOME PRESSURE

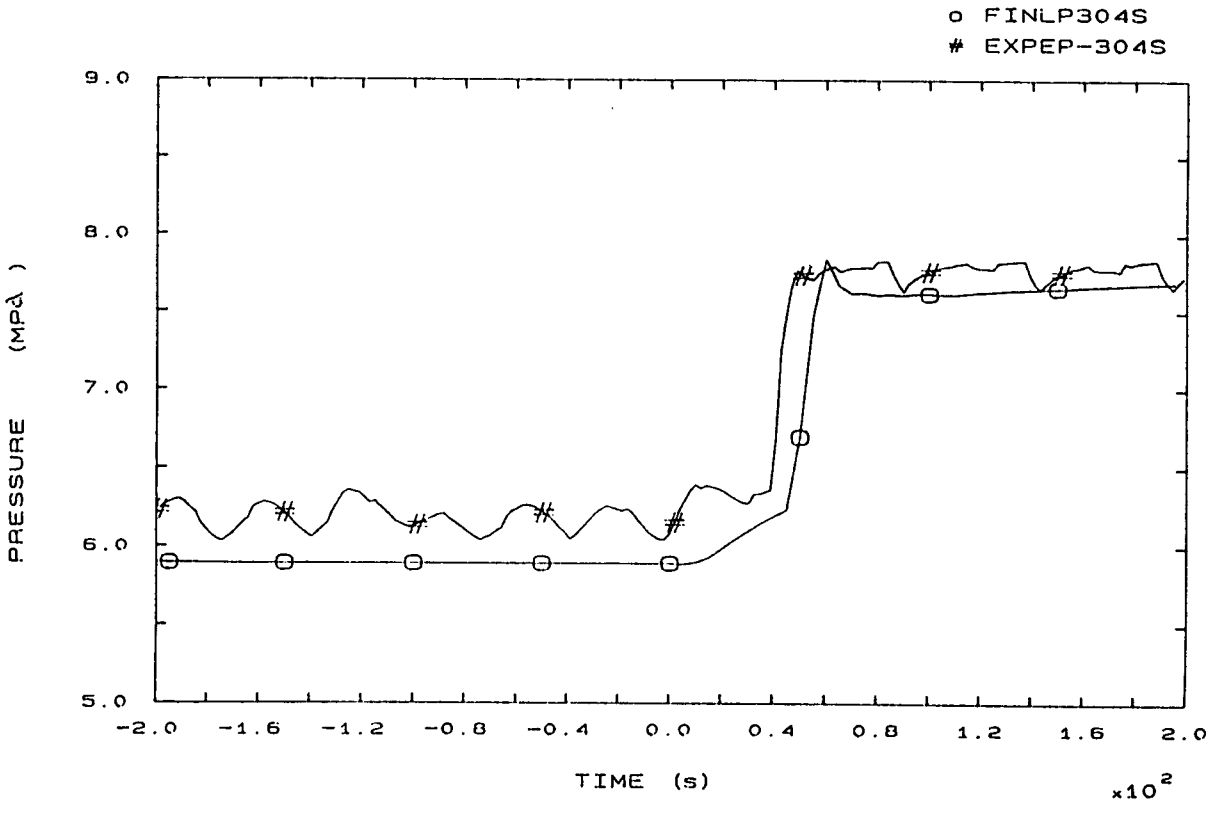

FIG. 5b SG3 STEAM DOME PRESSURE

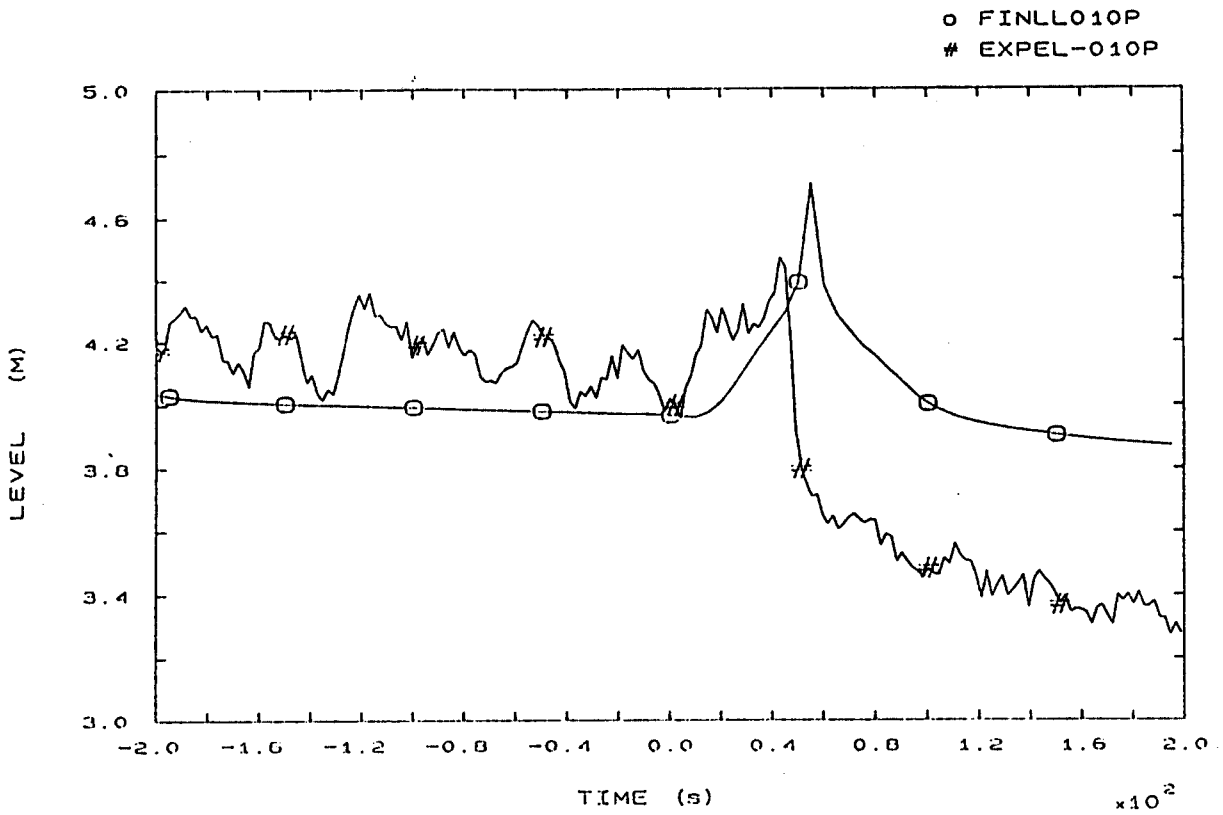

FIG. 6b PRESSURIZER LEVEL

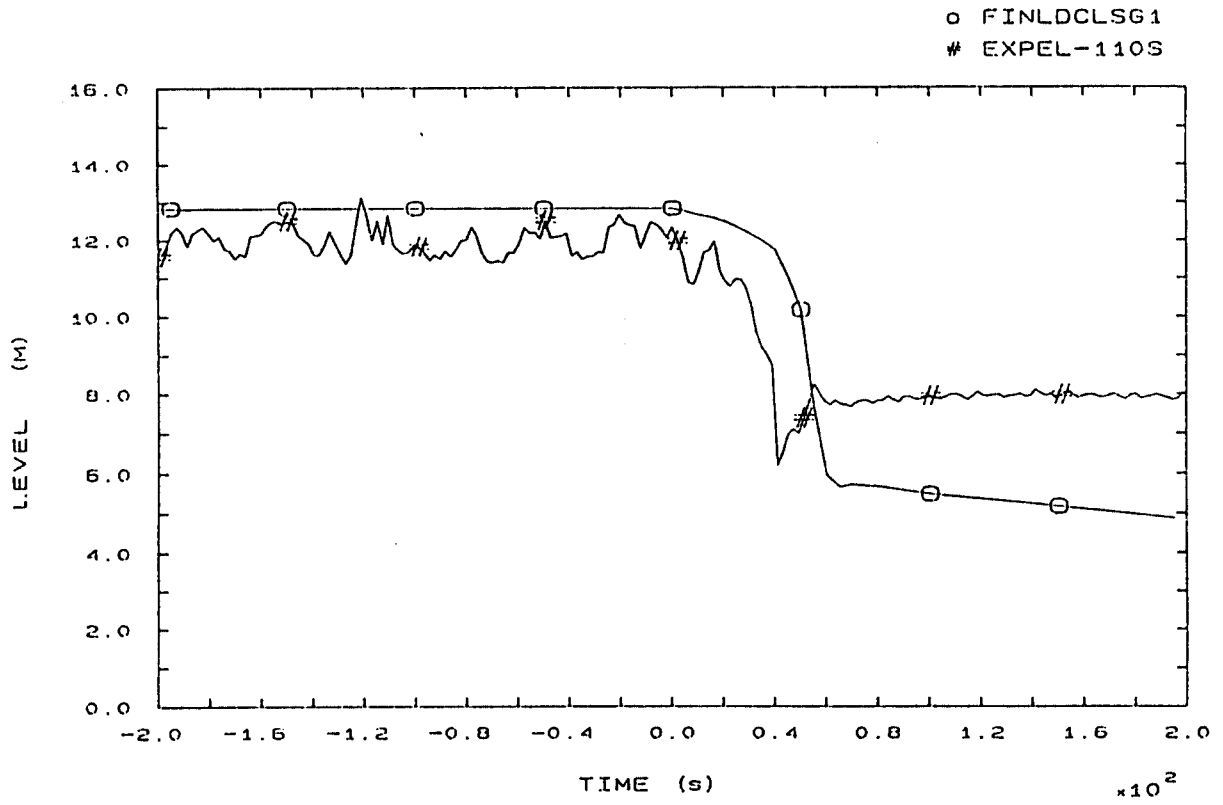

FIG. 7b SG1 DOWNCOMER LEVEL

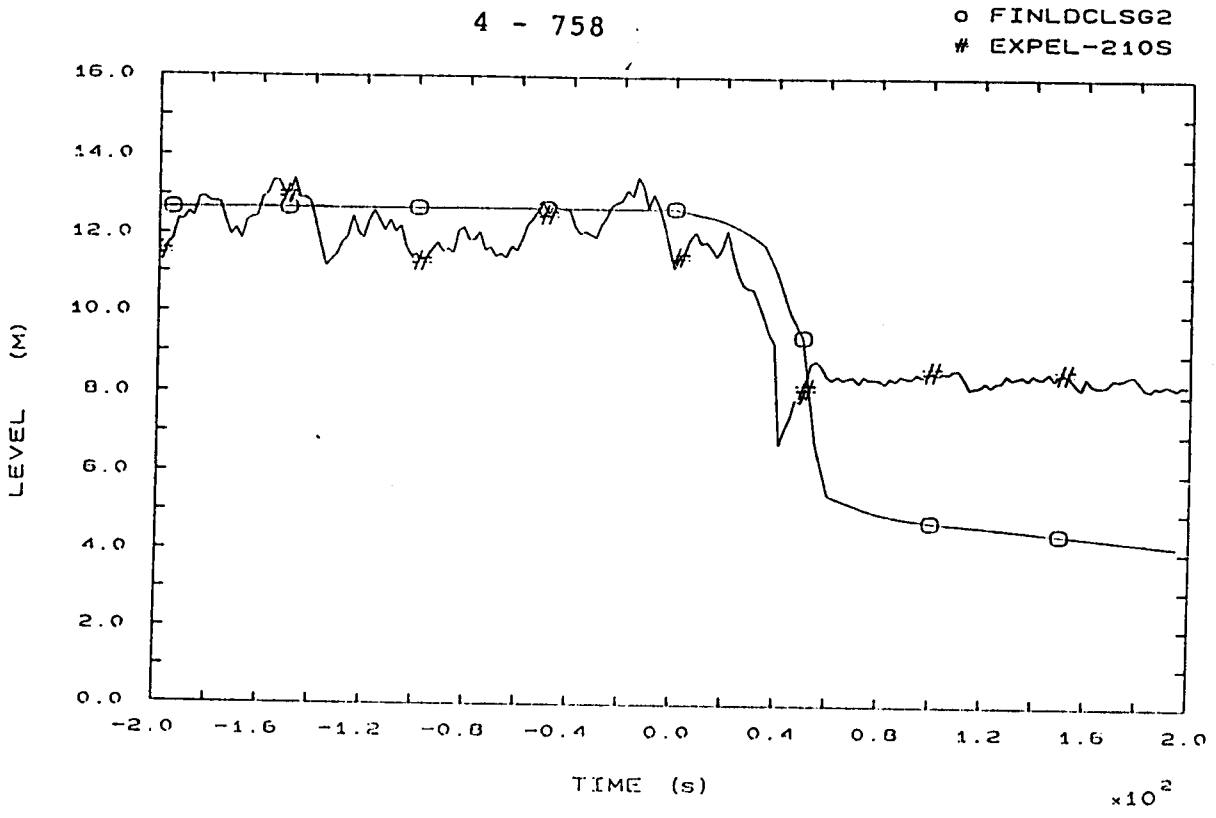

FIG. 8b SG2 DOWNCOMER LEVEL

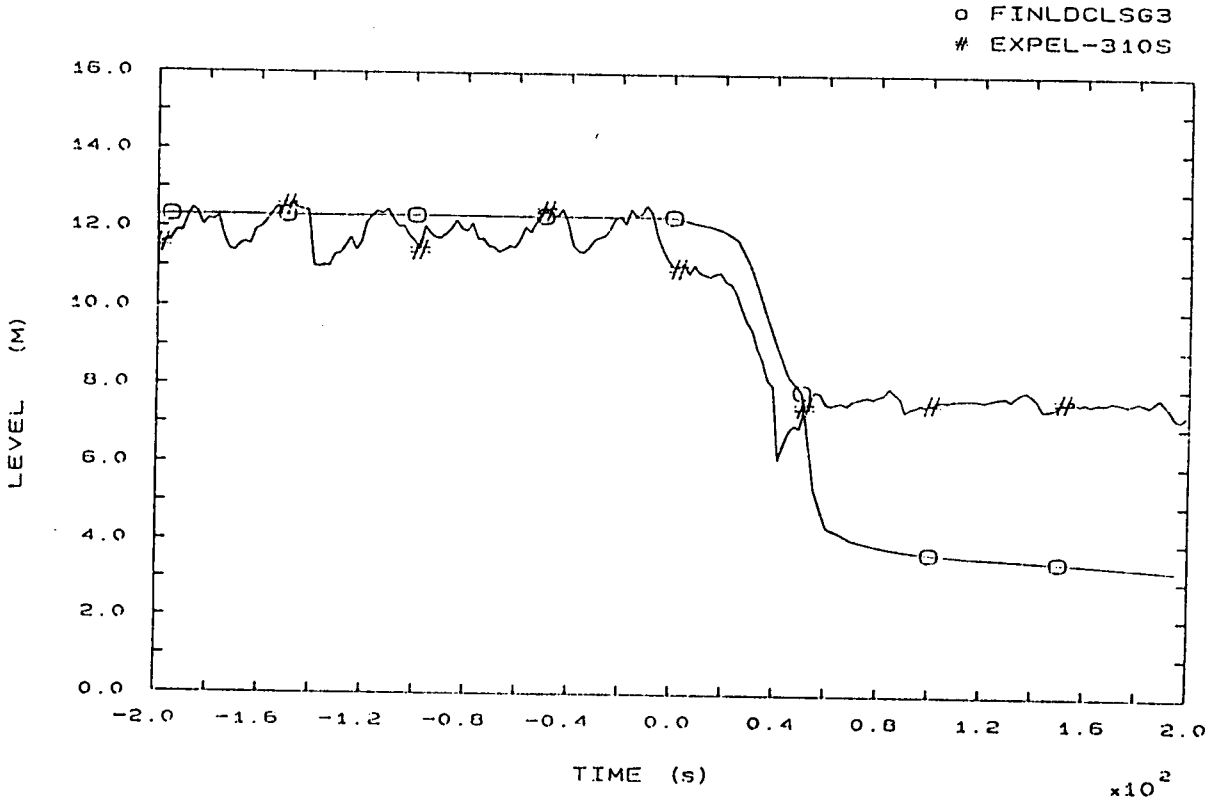

FIG. 9b SG3 DOWNCOMER LEVEL

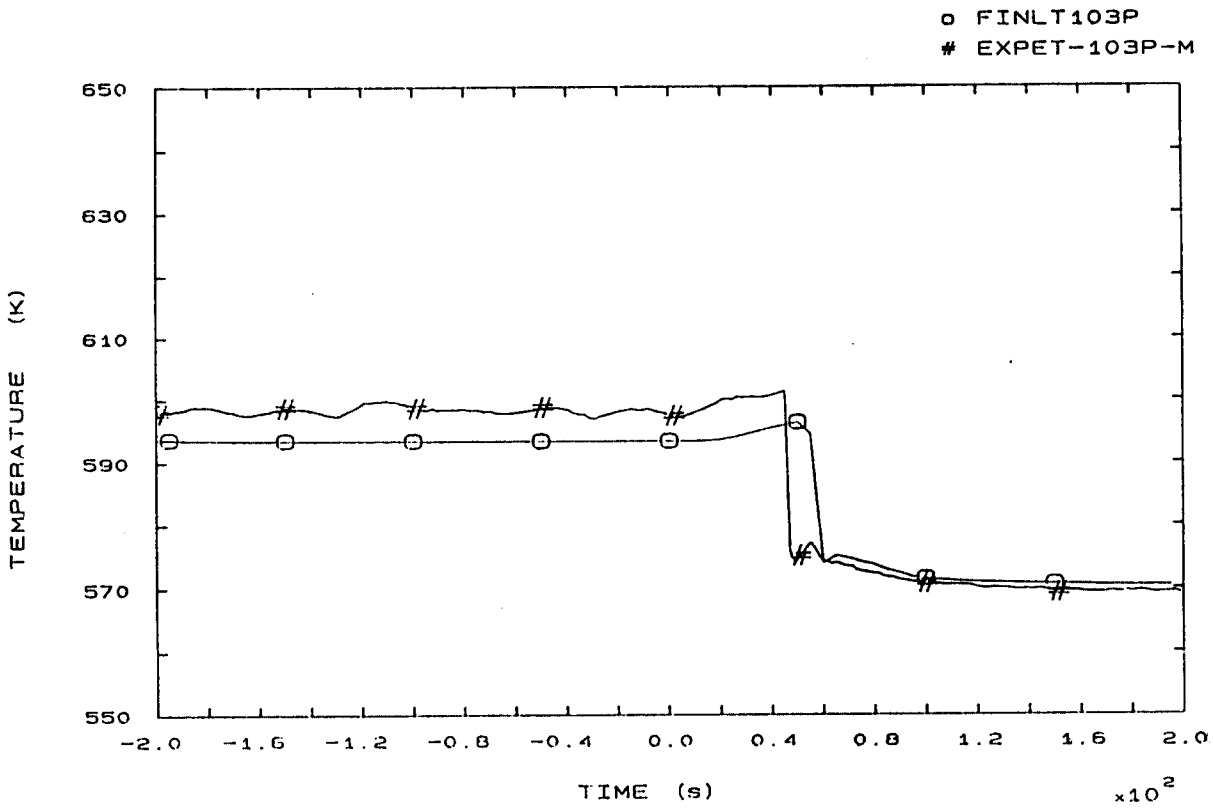

FIG. 12b LP1 HOT LEG OUTLET VESSEL TEMPERATURE

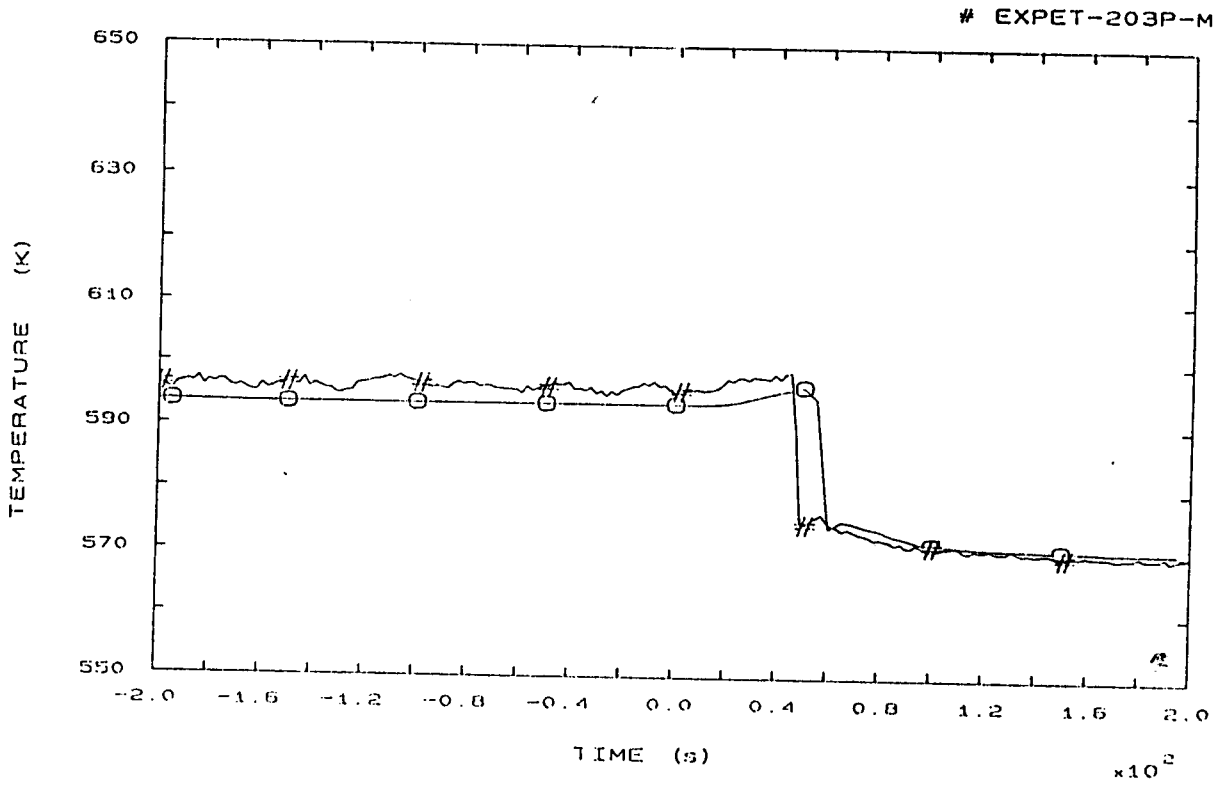

FIG. 22b LP2 HOT LEG OUTLET VESSEL TEMPERATURE

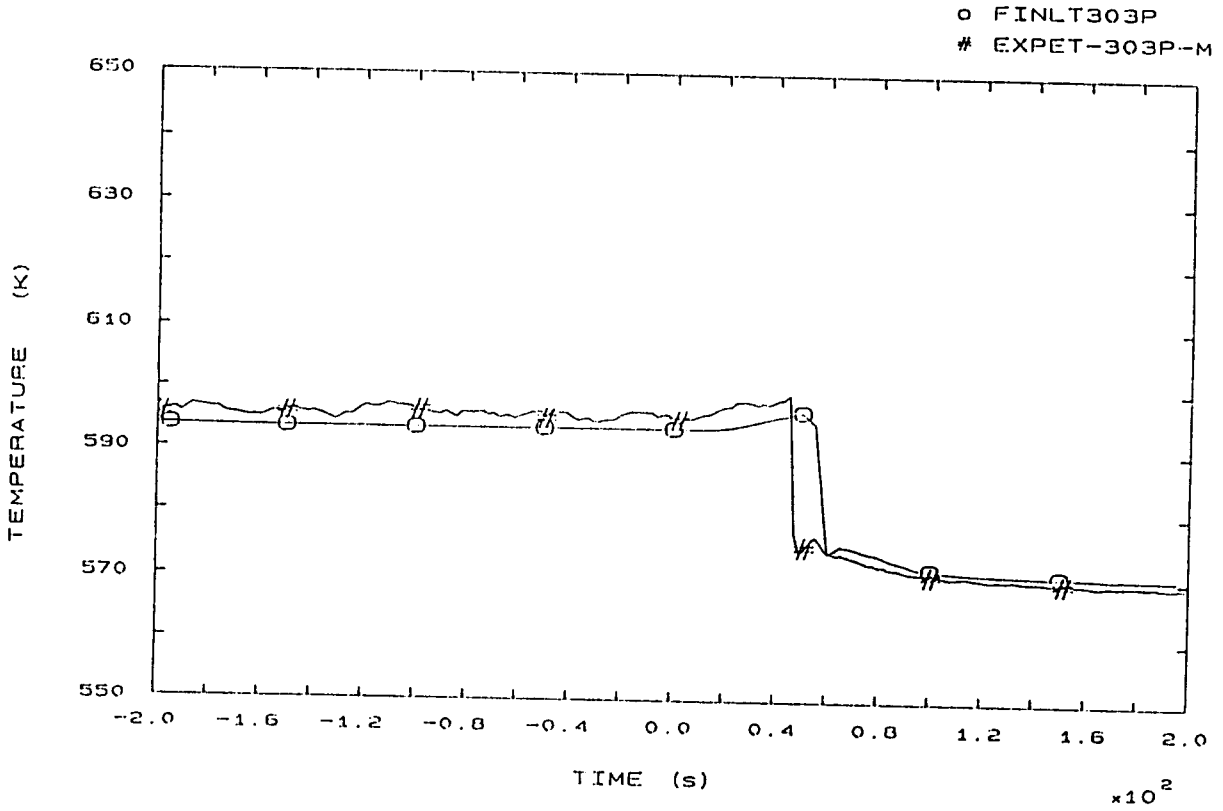

FIG. 32b LP3 HOT LEG OUTLET VESSEL TEMPERATURE

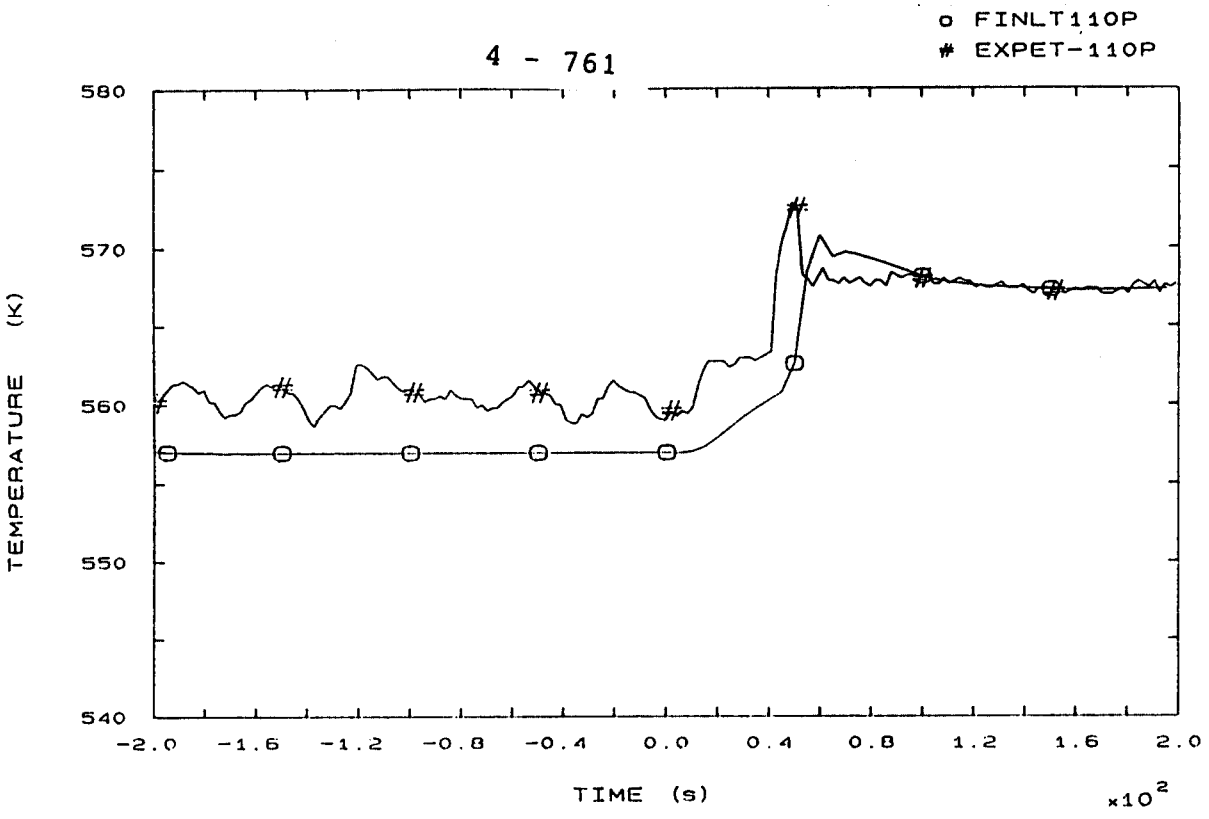

FIG. 42b SG1 OUTLET TEMPERATURE

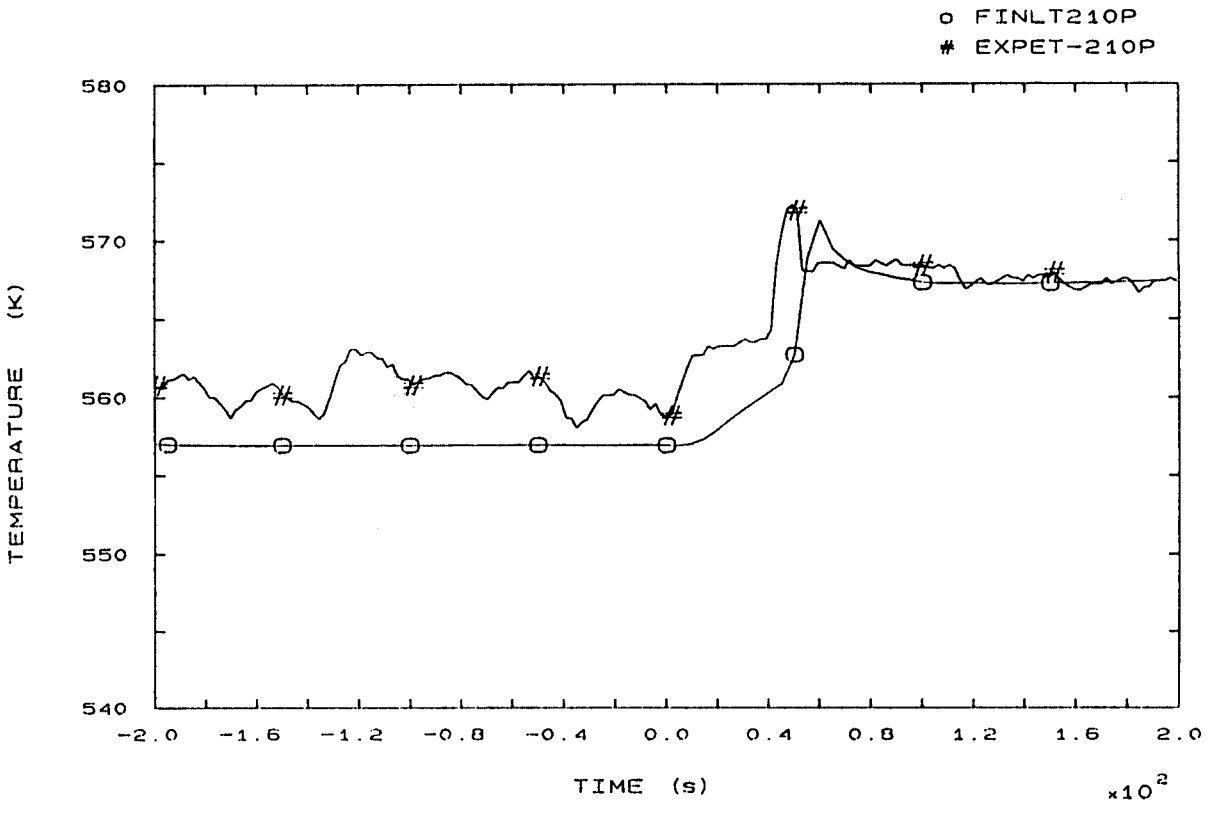

FIG. 44b SG2 OUTLET TEMPERATURE

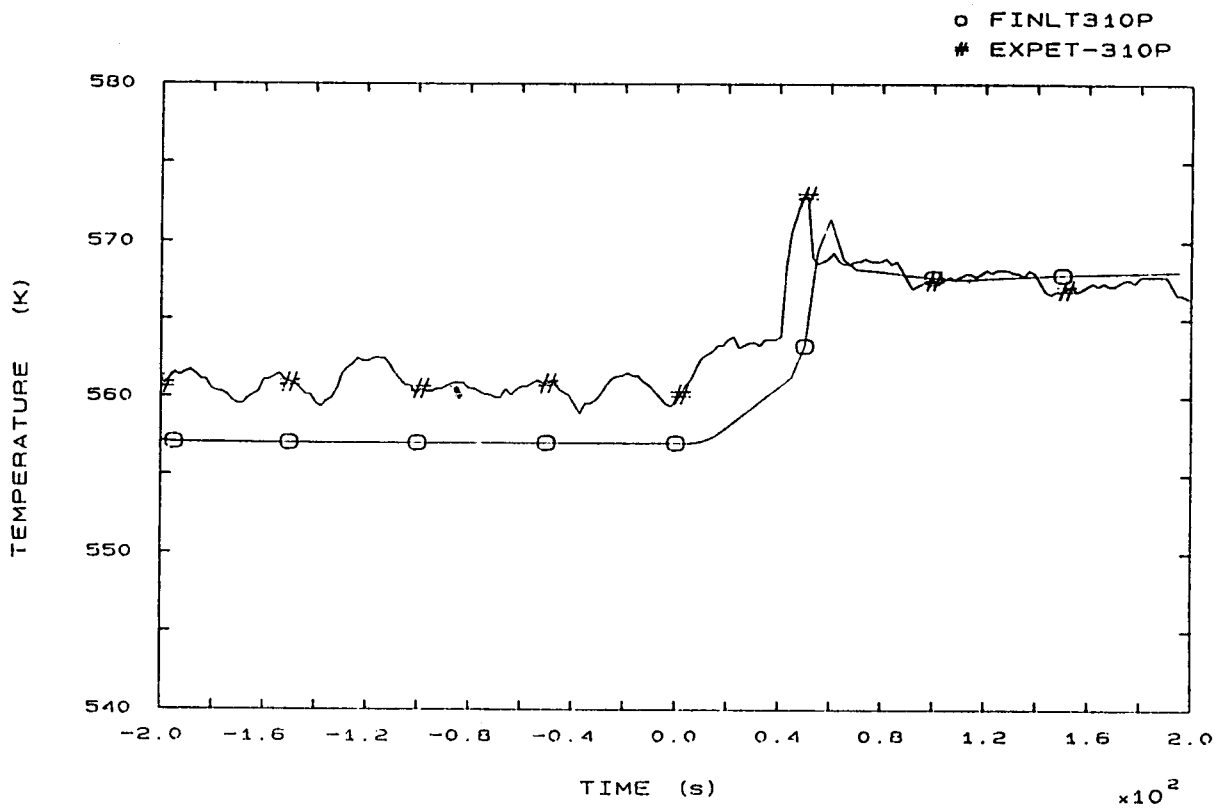

FIG. 46b SG3 OUTLET TEMPERATURE

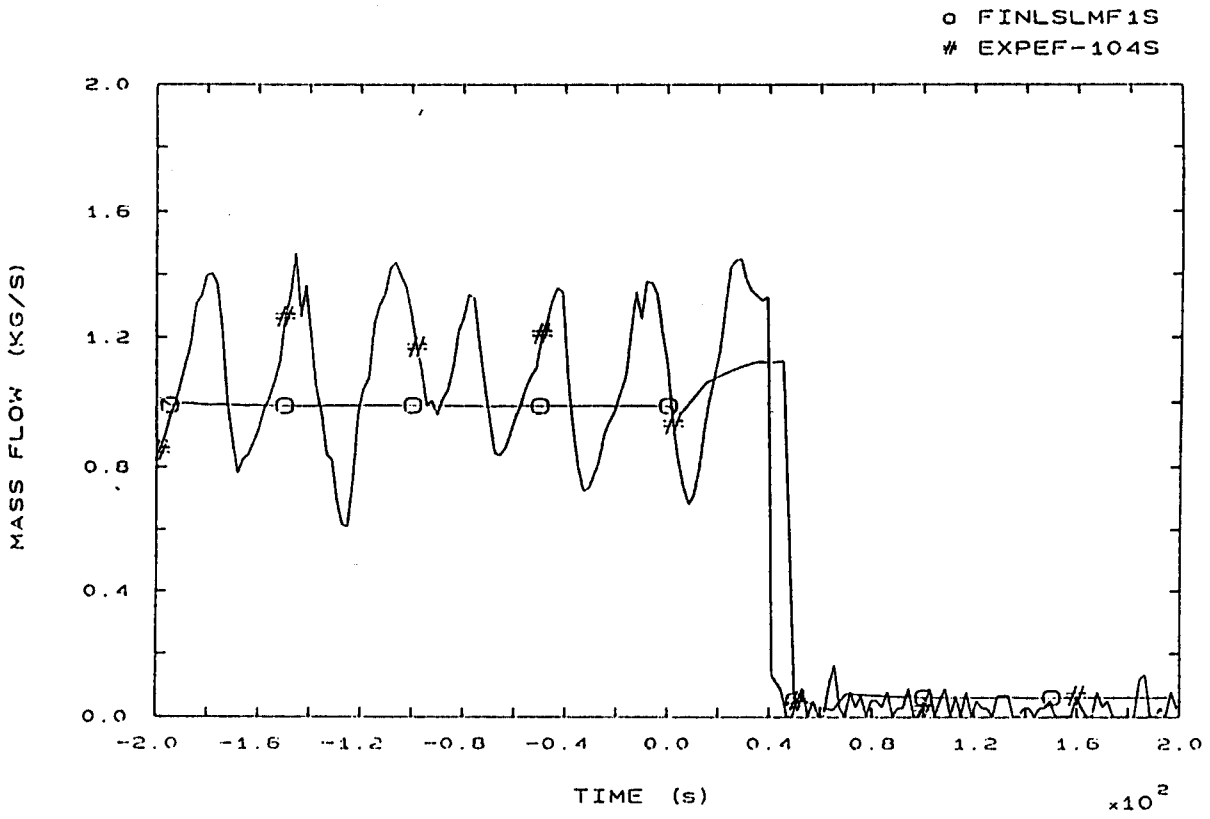

FIG. 96b STEAM LINE 1 MASS FLOW

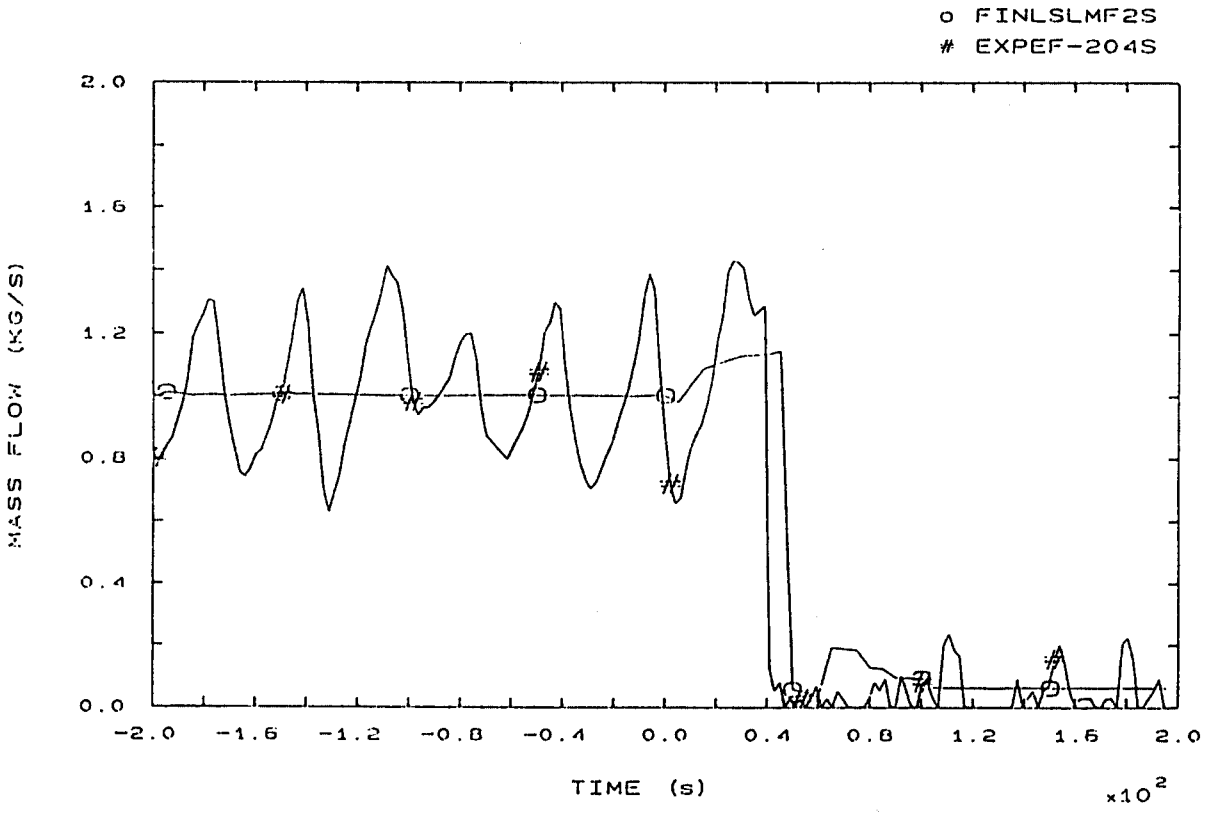

FIG. 97b STEAM LINE 2 MASS FLOW

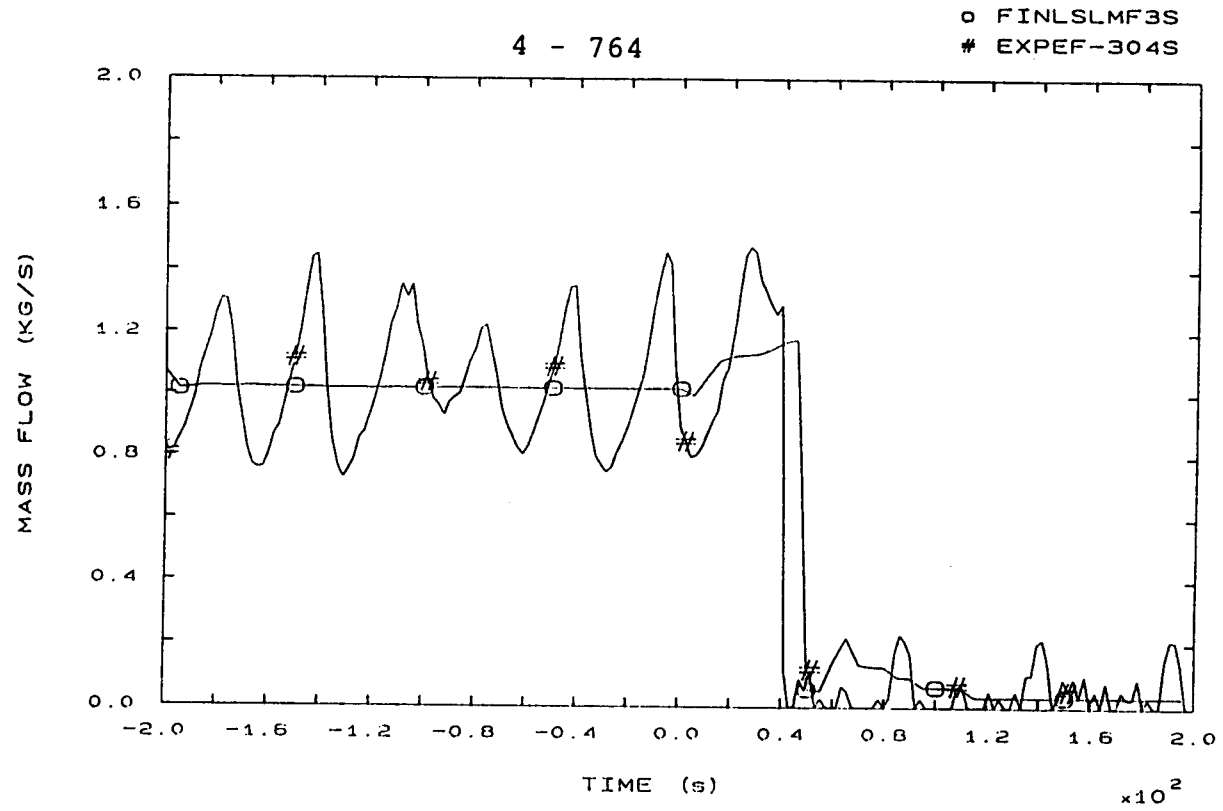

FIG. 98b STEAM LINE 3 MASS FLOW

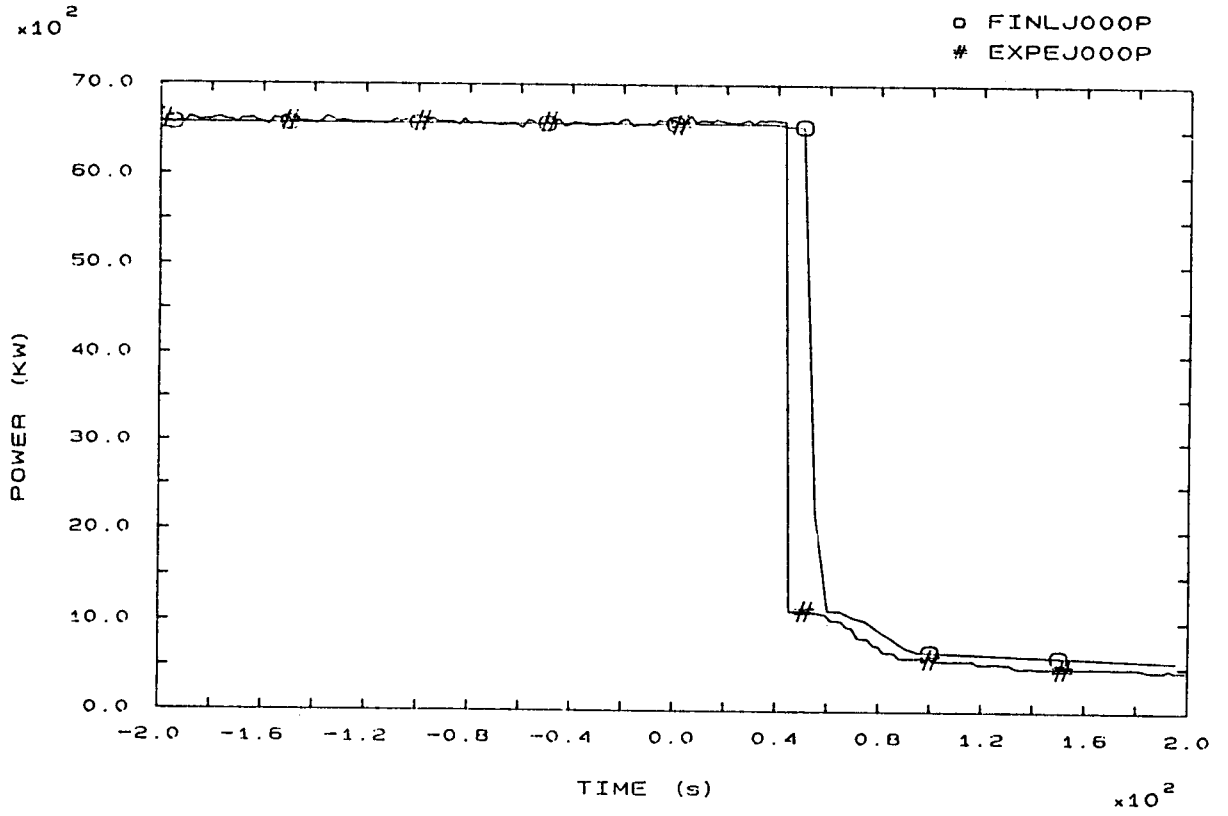

FIG. 81b HEATER RODS POWER

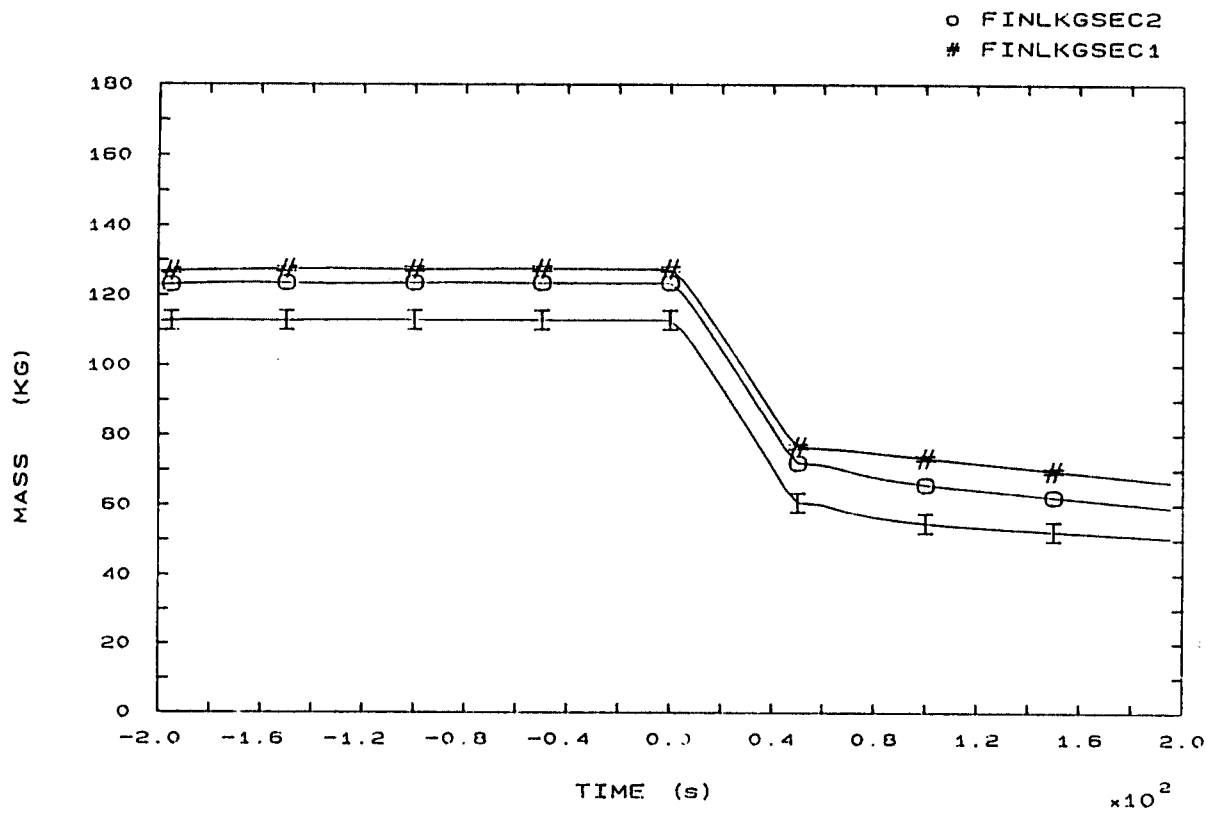

FIG. 142b SECONDARY COOLANT TOTAL MASS IN SGs

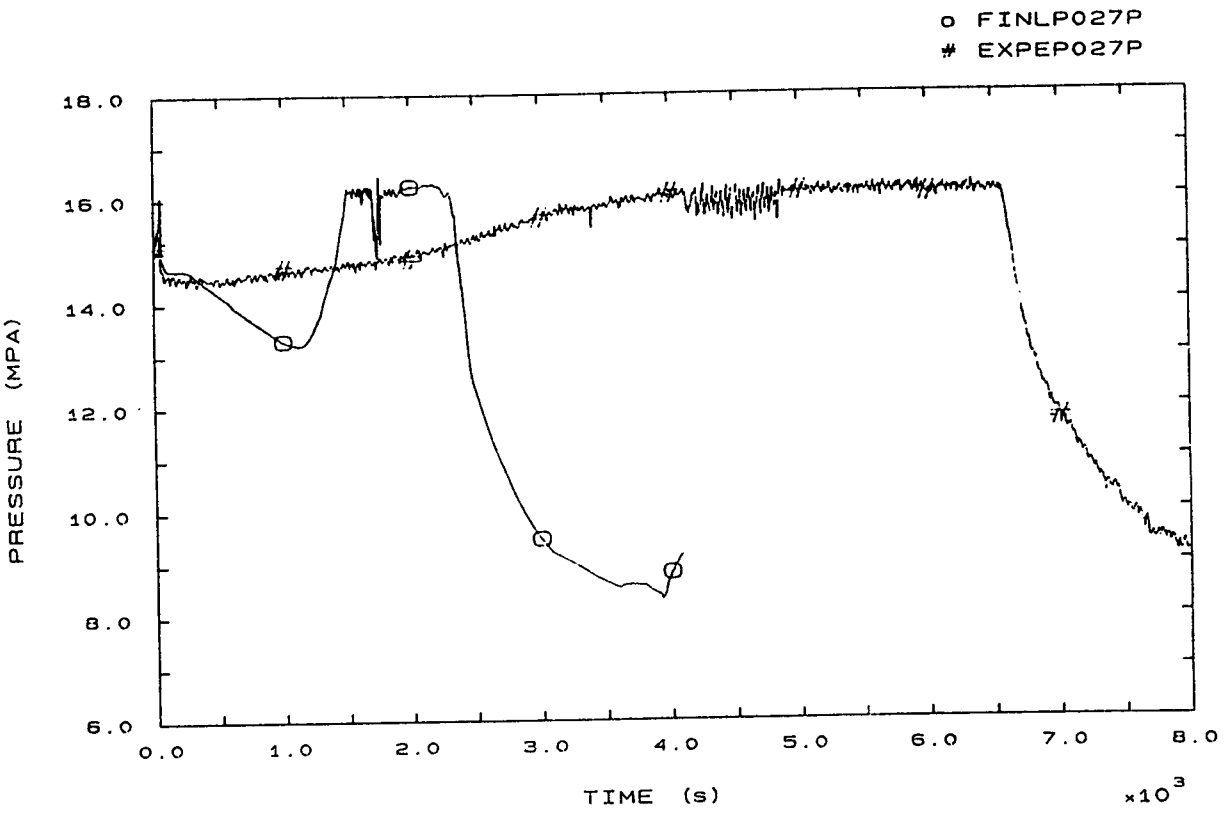

FIG. 1 PRESSURIZER PRESSURE

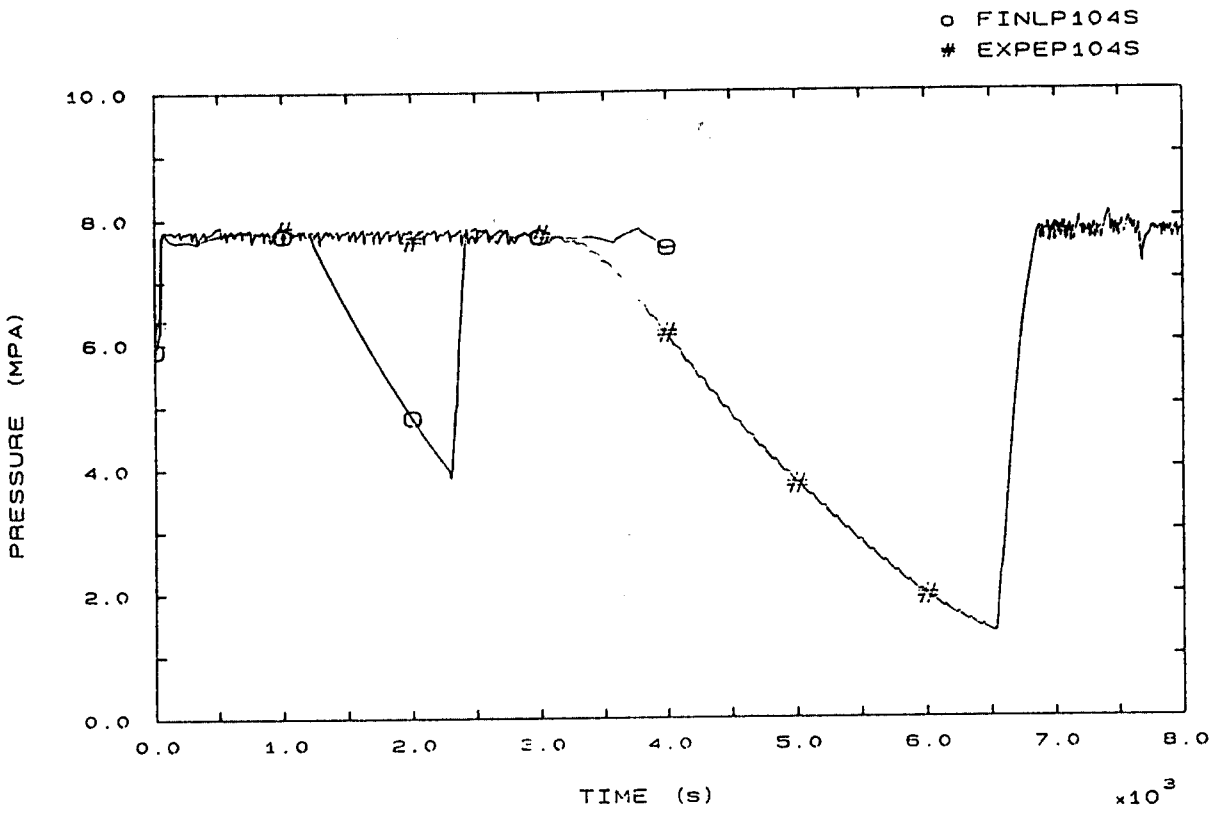

FIG. 3 SG1 STEAM DOME PRESSURE

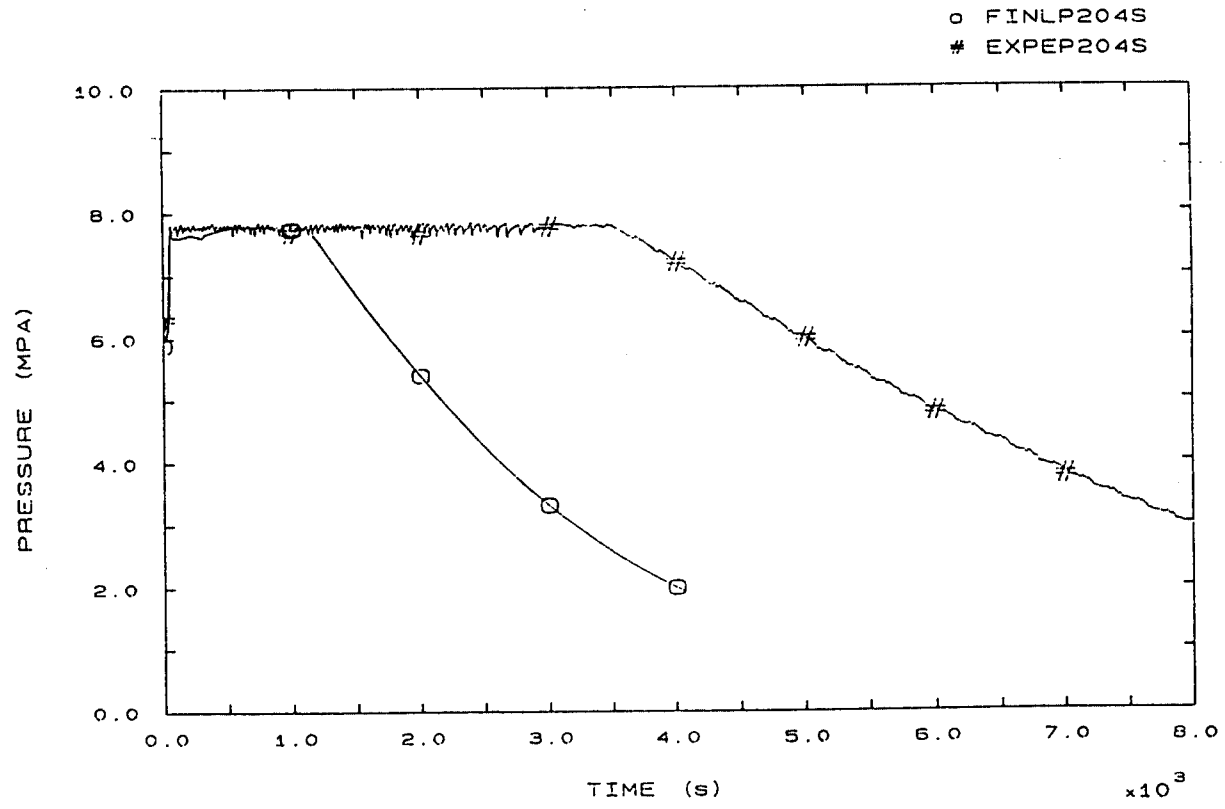

FIG. 4 SG2 STEAM DOME PRESSURE

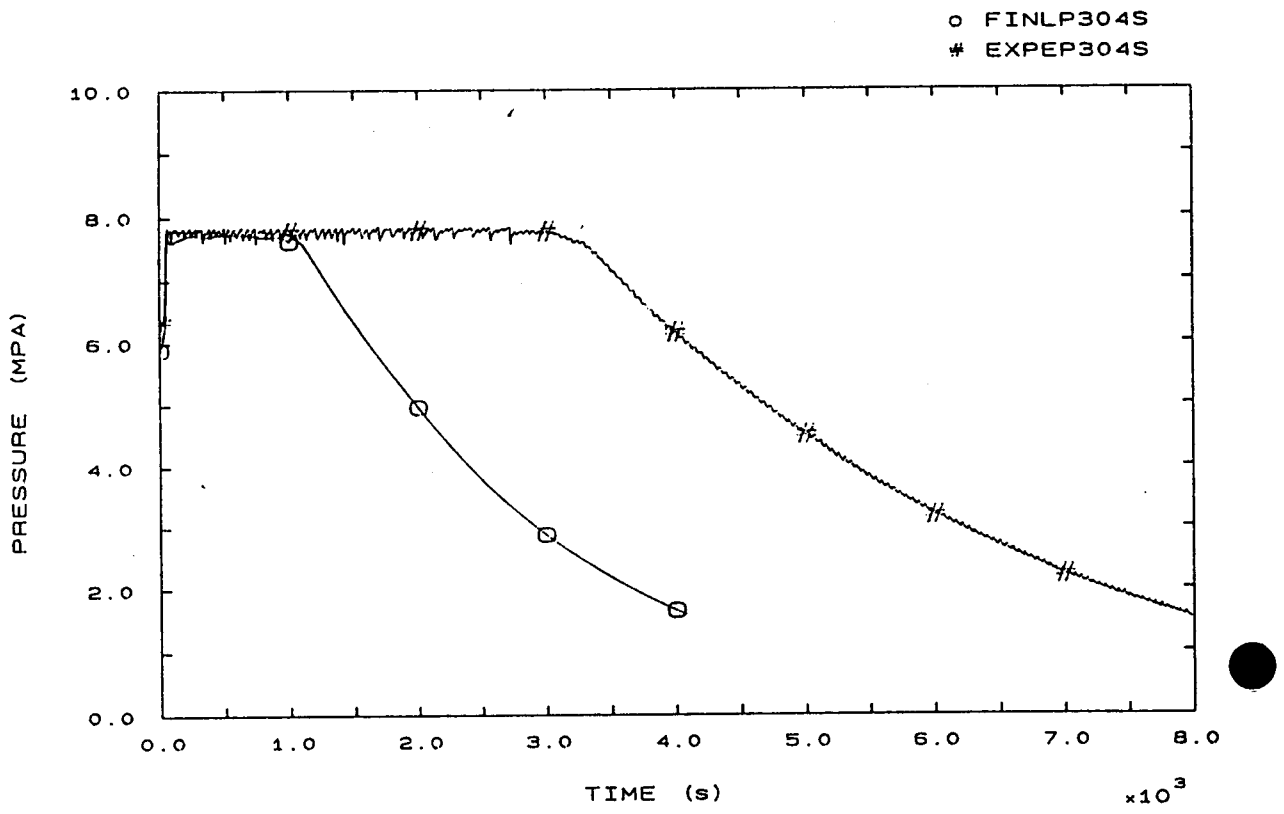

FIG. 5 SG3 STEAM DOME PRESSURE

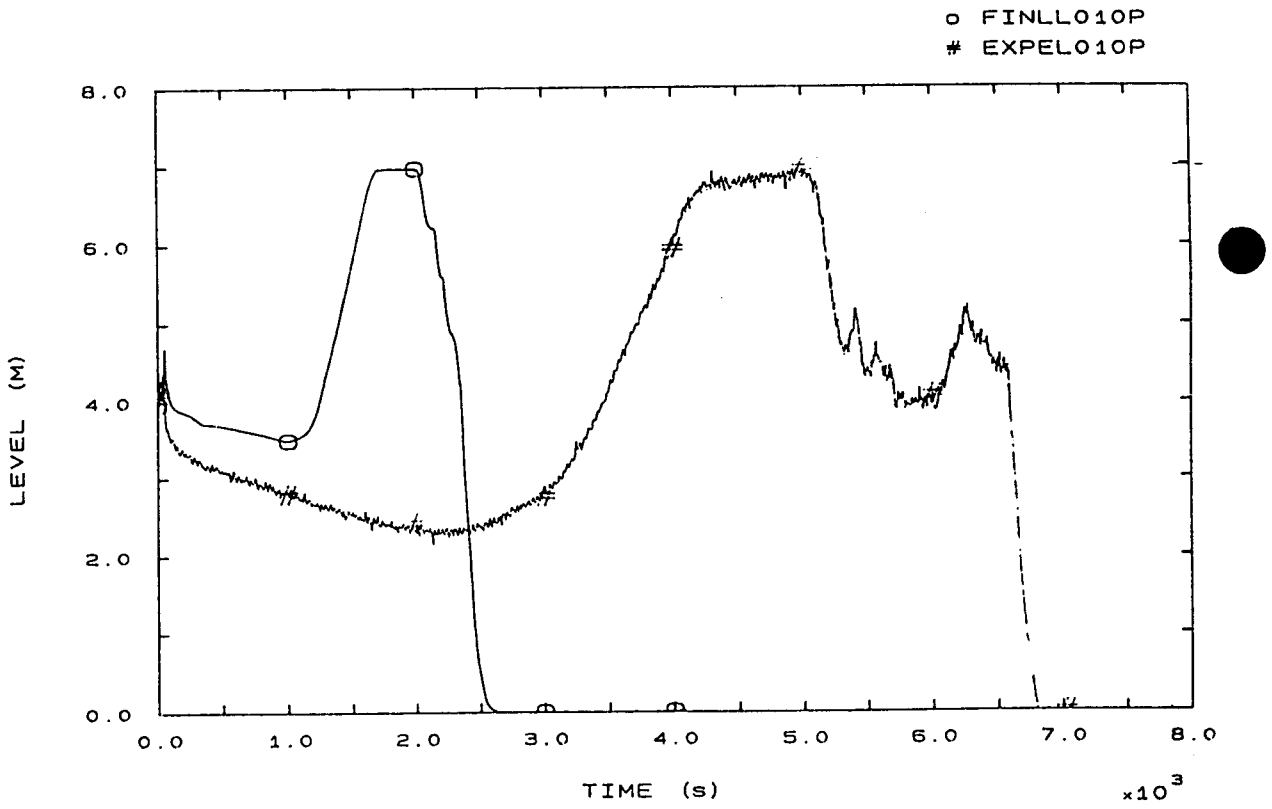

FIG. 6 PRESSURIZER LEVEL

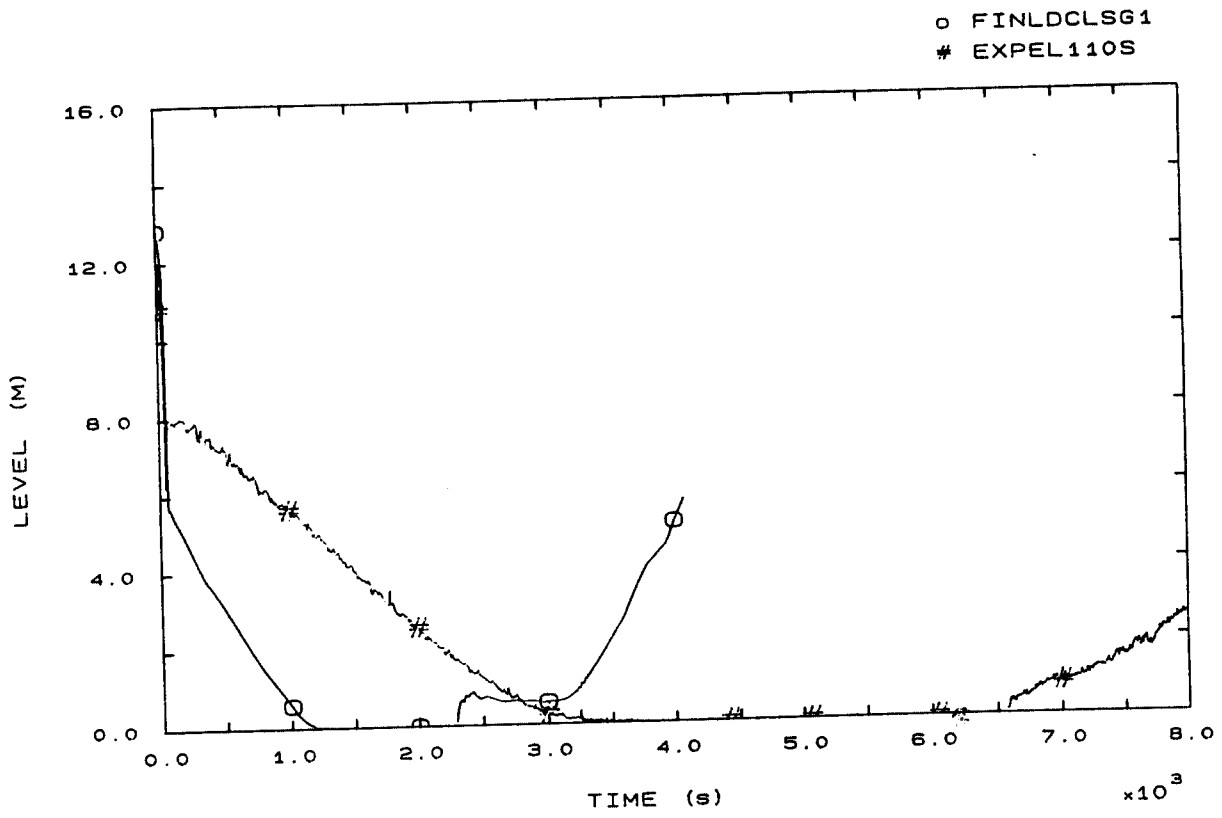

FIG. 7 SG1 DOWNCOMER LEVEL

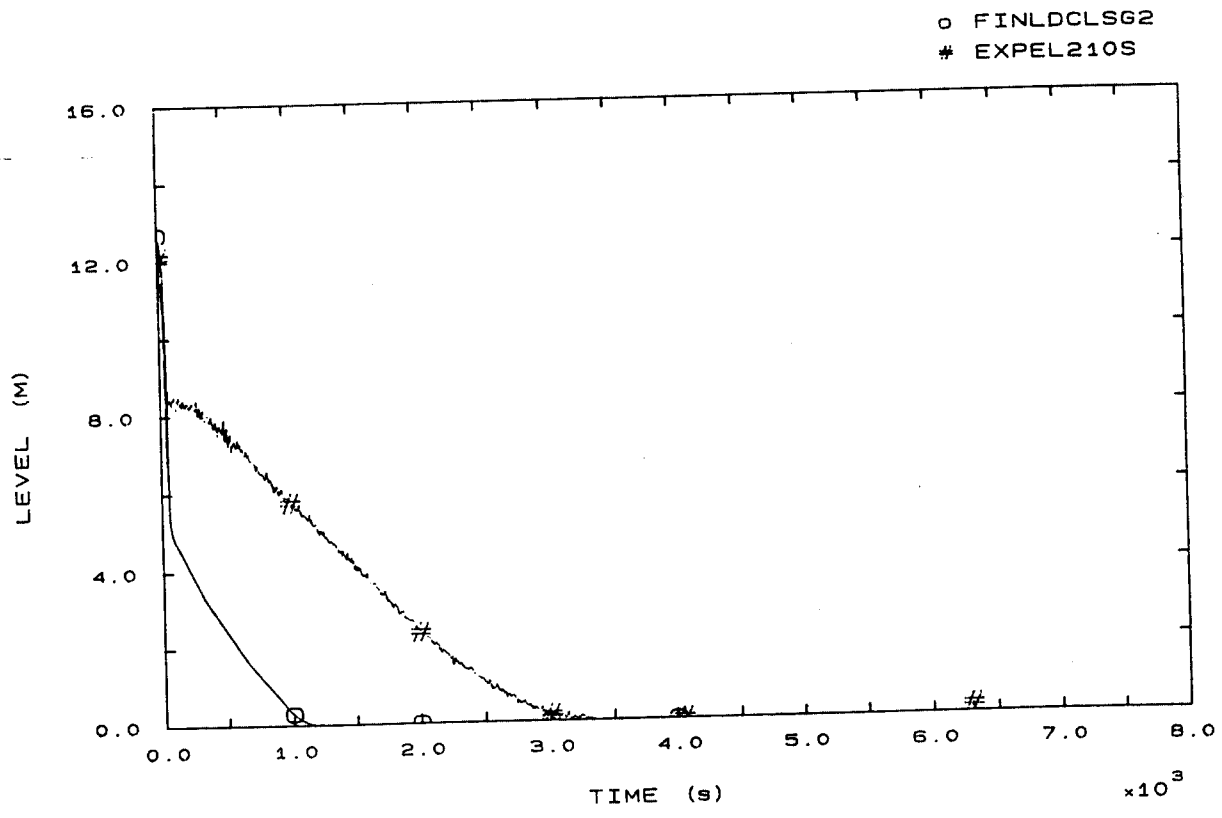

FIG. 8 SG2 DOWNCOMER LEVEL

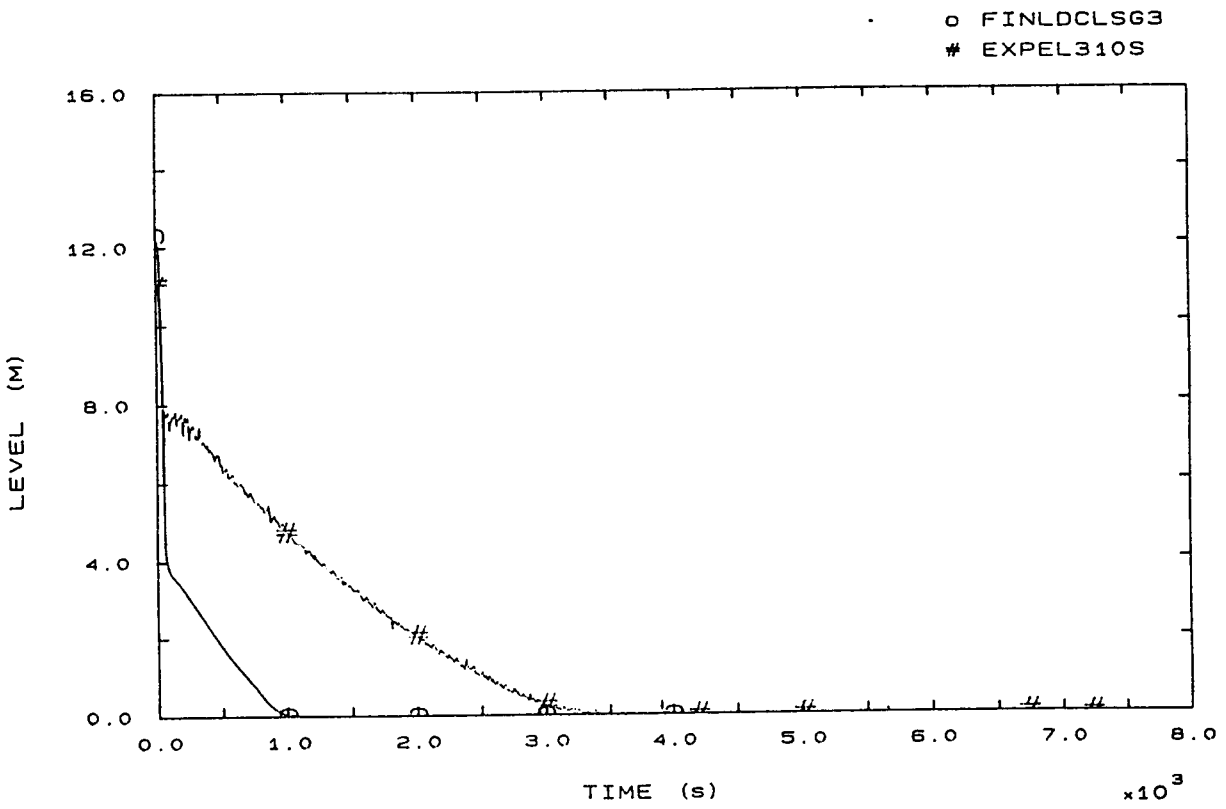

FIG. 9 SG3 DOWNCOMER LEVEL

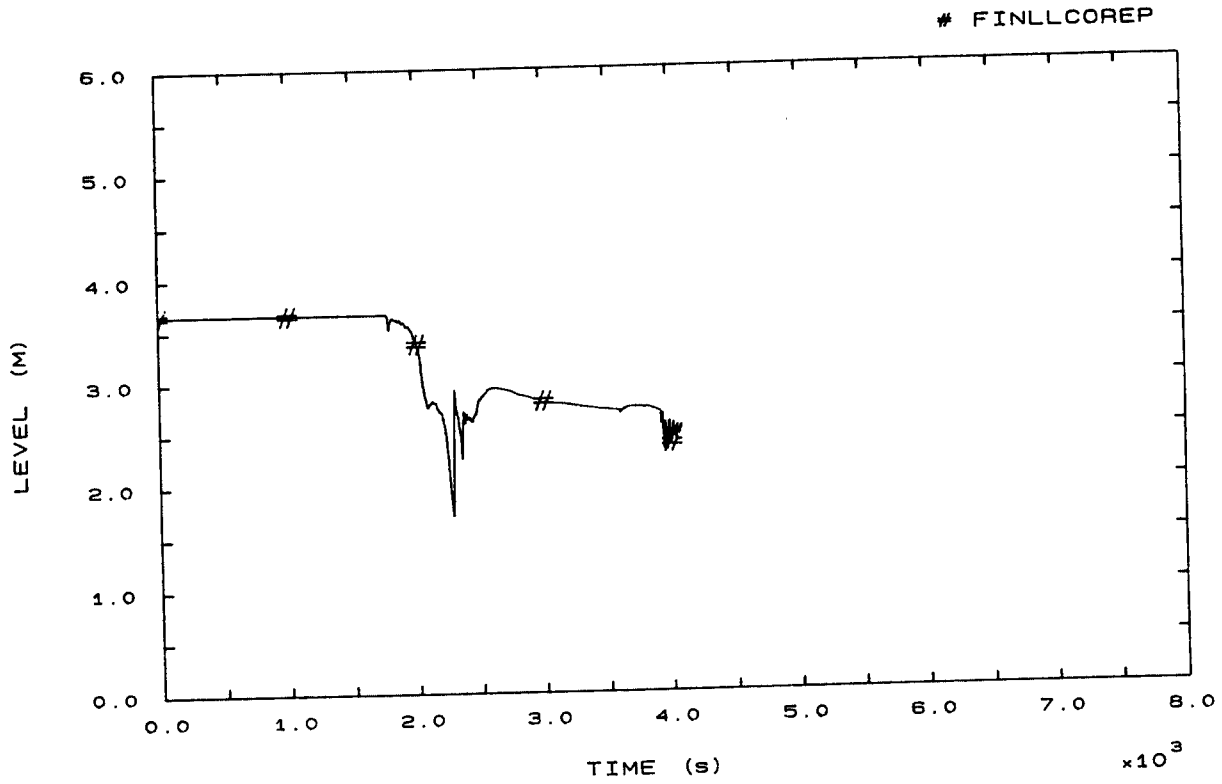

FIG. 11 CORE LEVEL

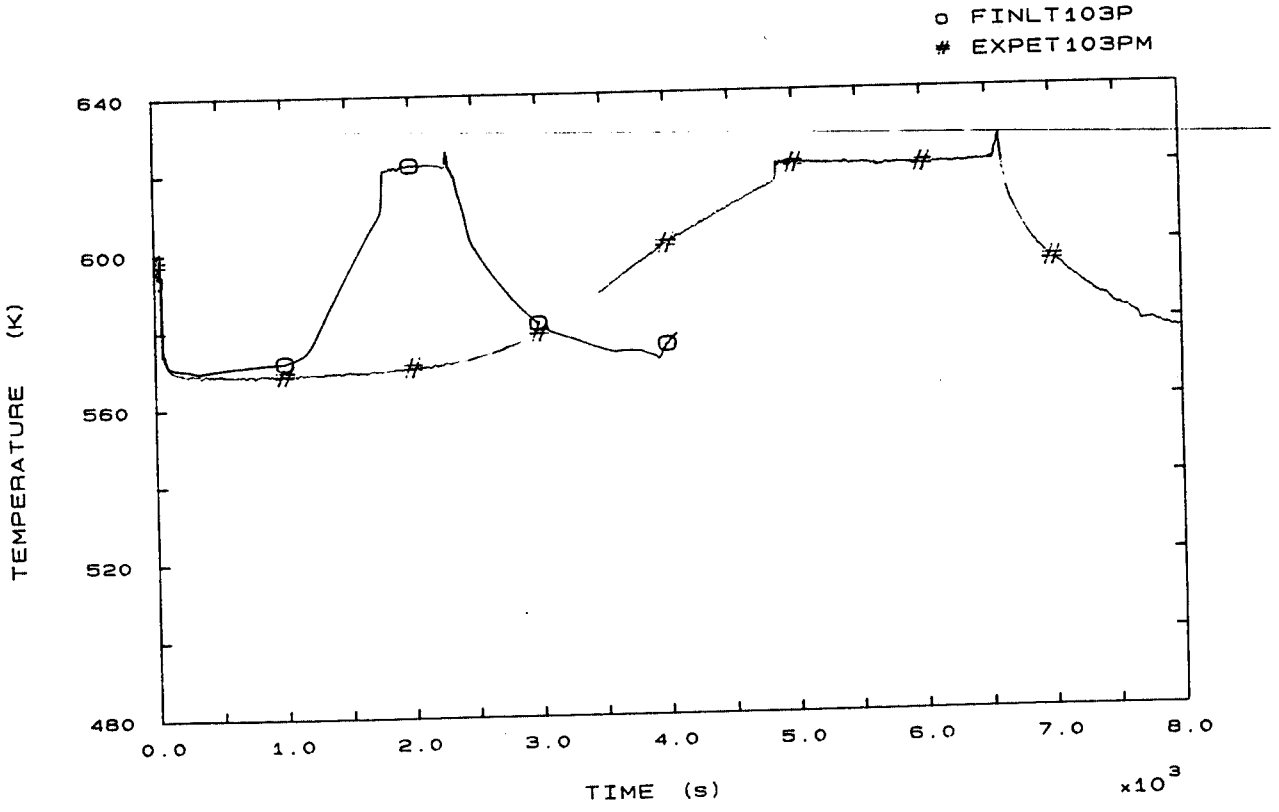

FIG. 12 LP1 HOT LEG OUTLET VESSEL TEMPERATURE

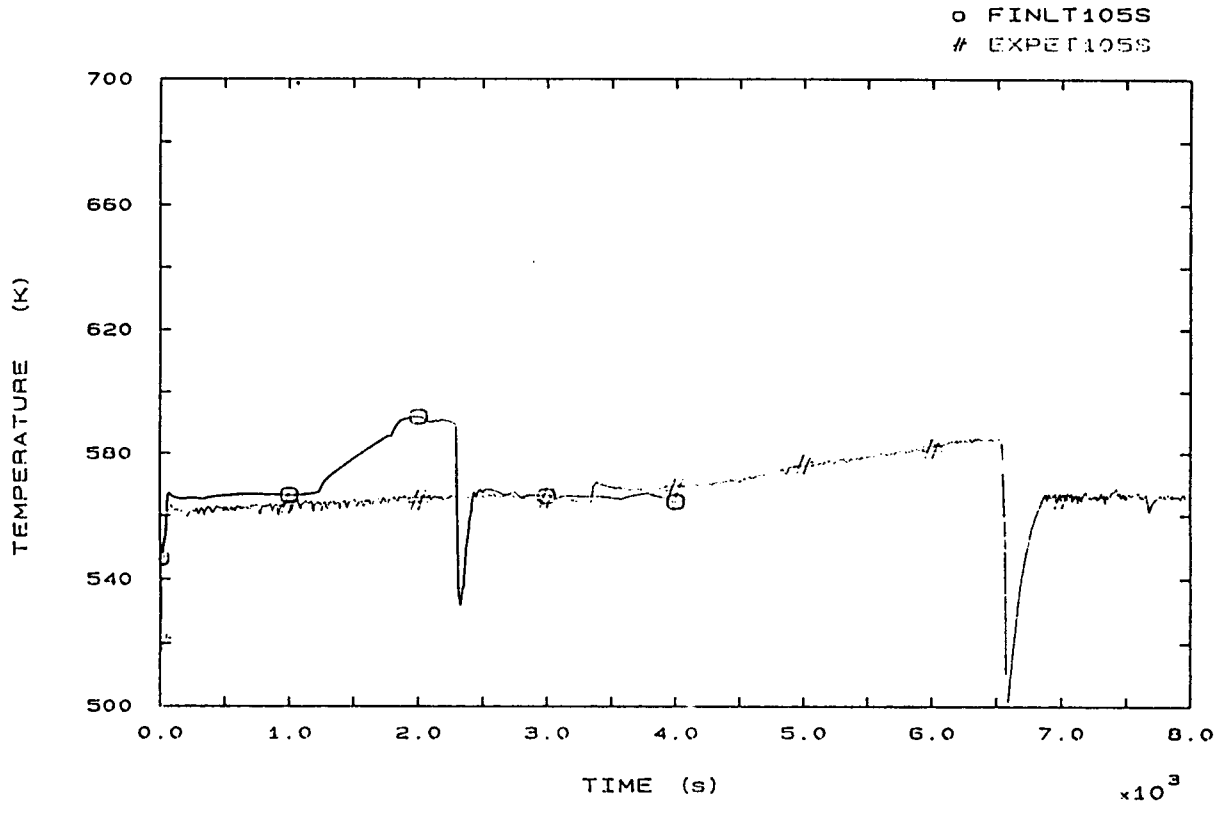

FIG. 15 FLUID TEMPERATURE SG1 RISER 185 MM A.T.S.

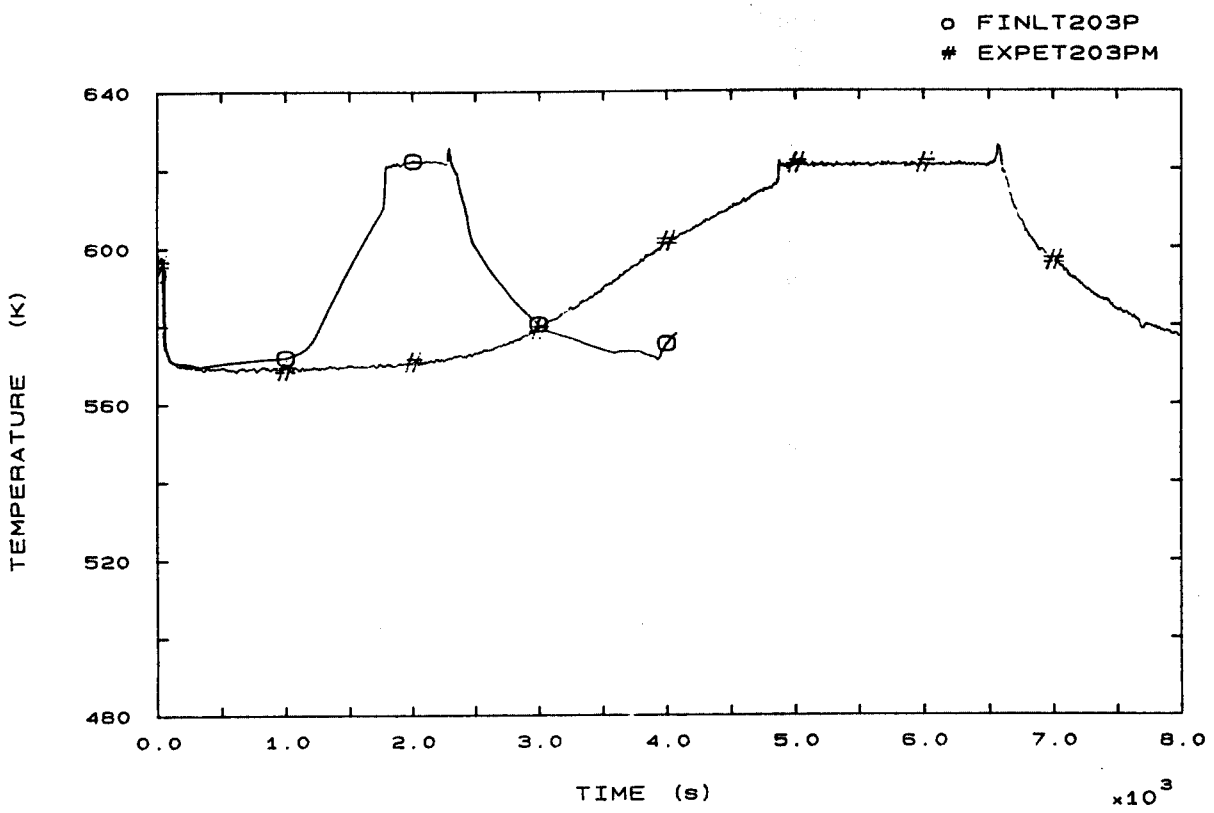

FIG. 22 LP2 HOT LEG OUTLET VESSEL TEMPERATURE

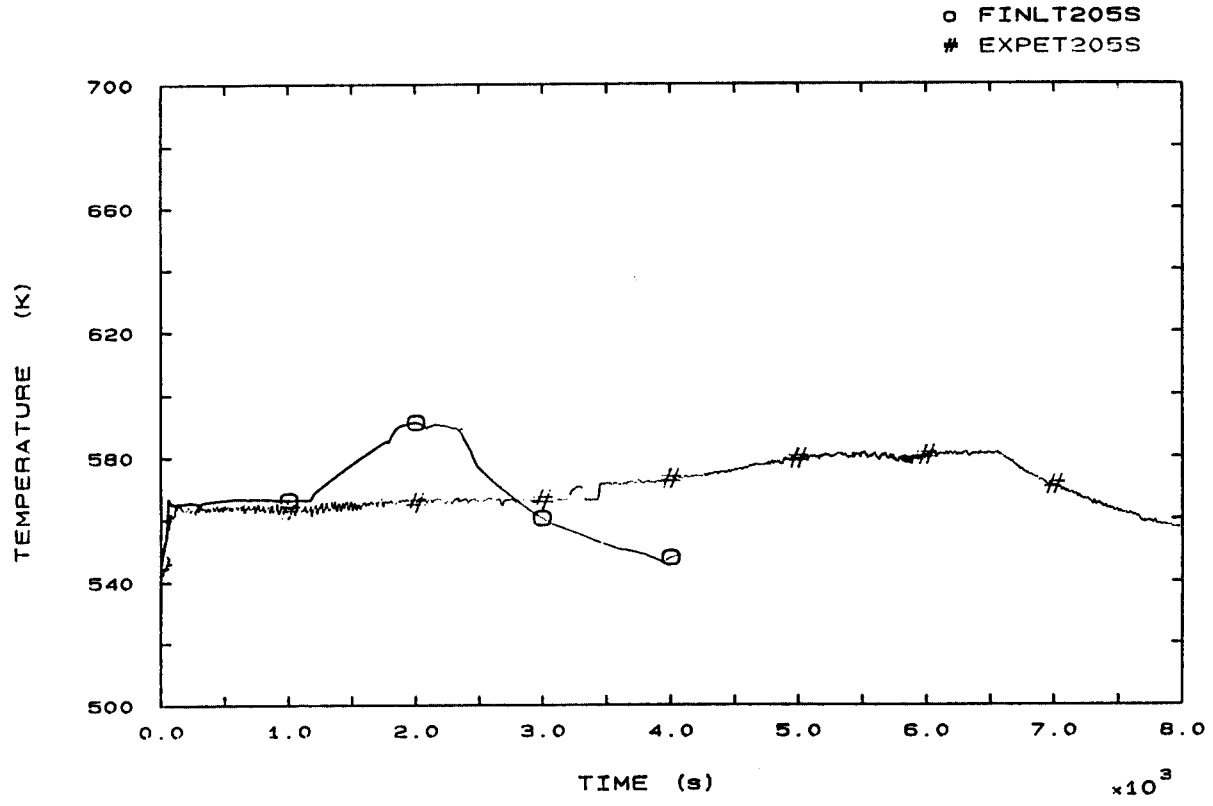

FIG. 25 FLUID TEMPERATURE SG2 RISER 185 MM A.T.S.

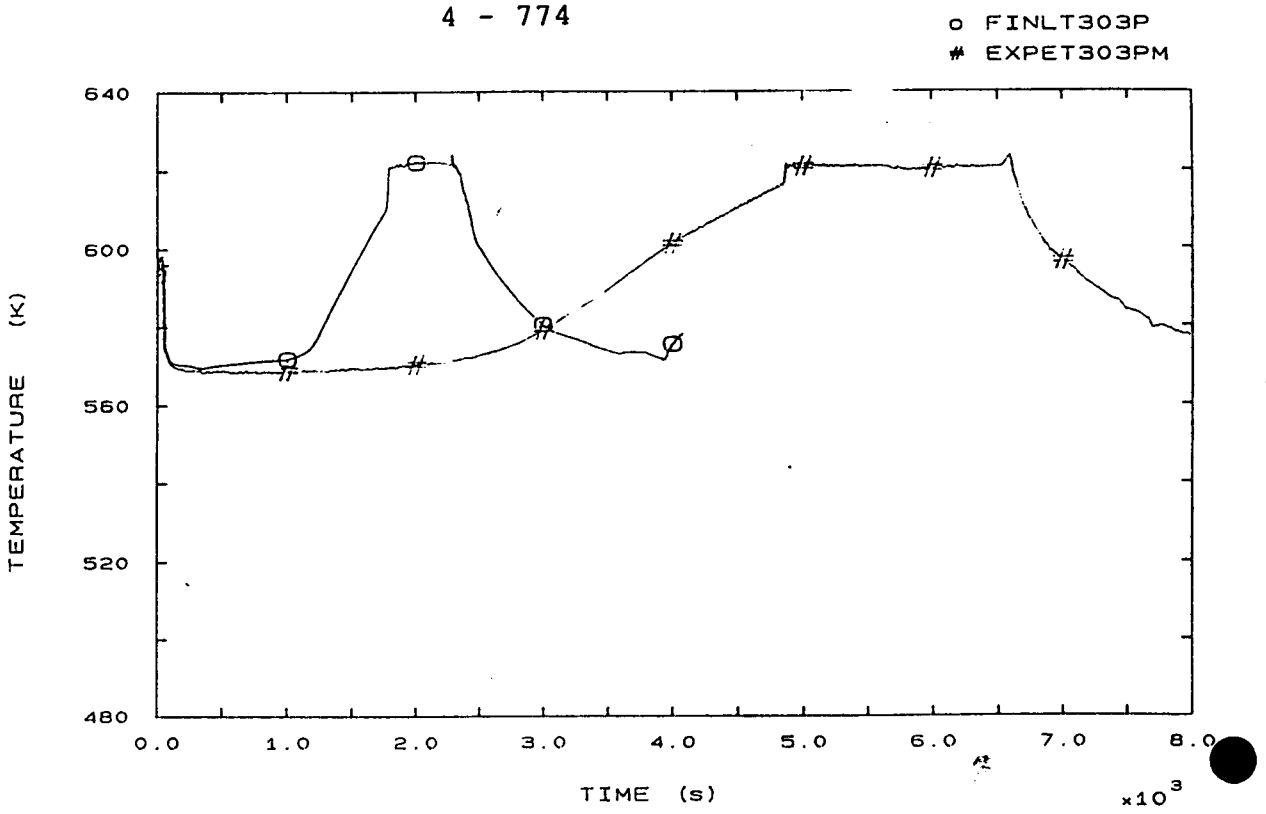

FIG. 32 LP3 HOT LEG OUTLET VESSEL TEMPERATURE

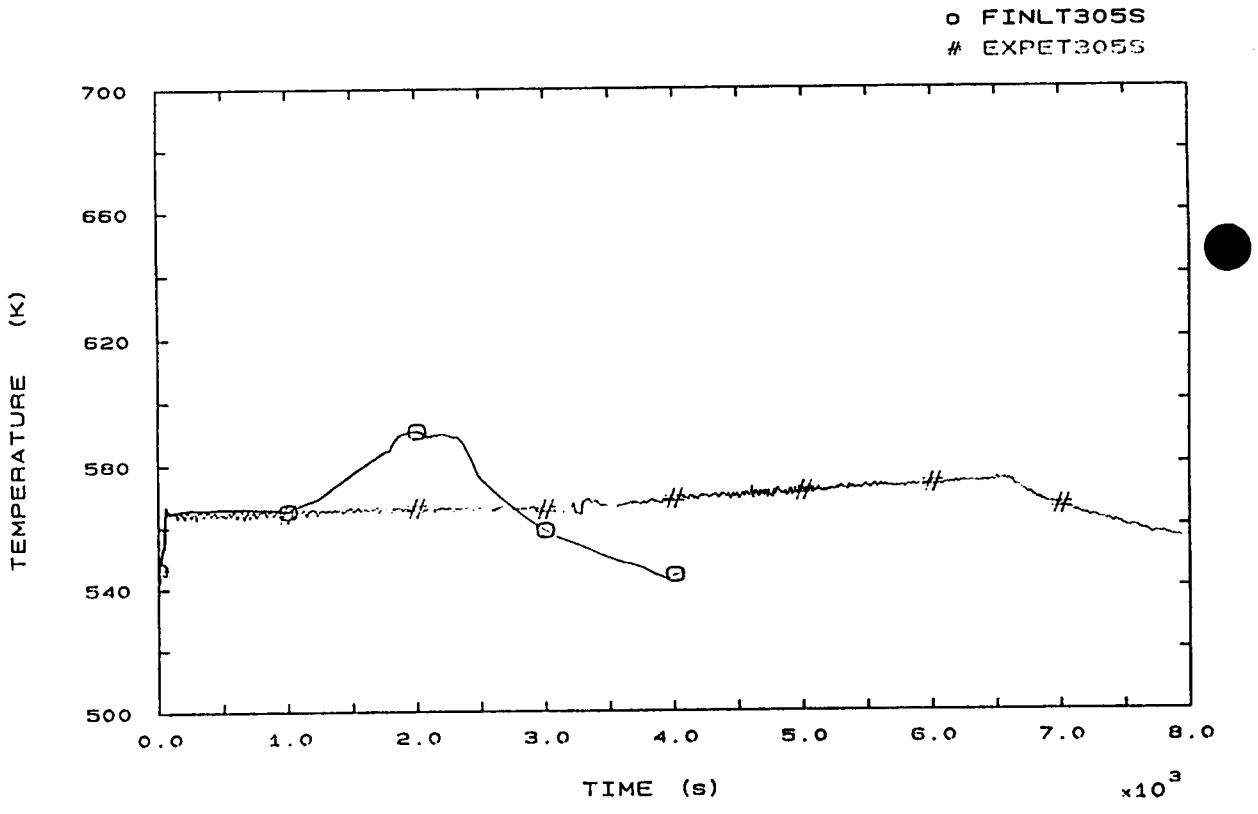

FIG. 35 FLUID TEMPERATURE SG3 RISER 185 MM A.T.S.

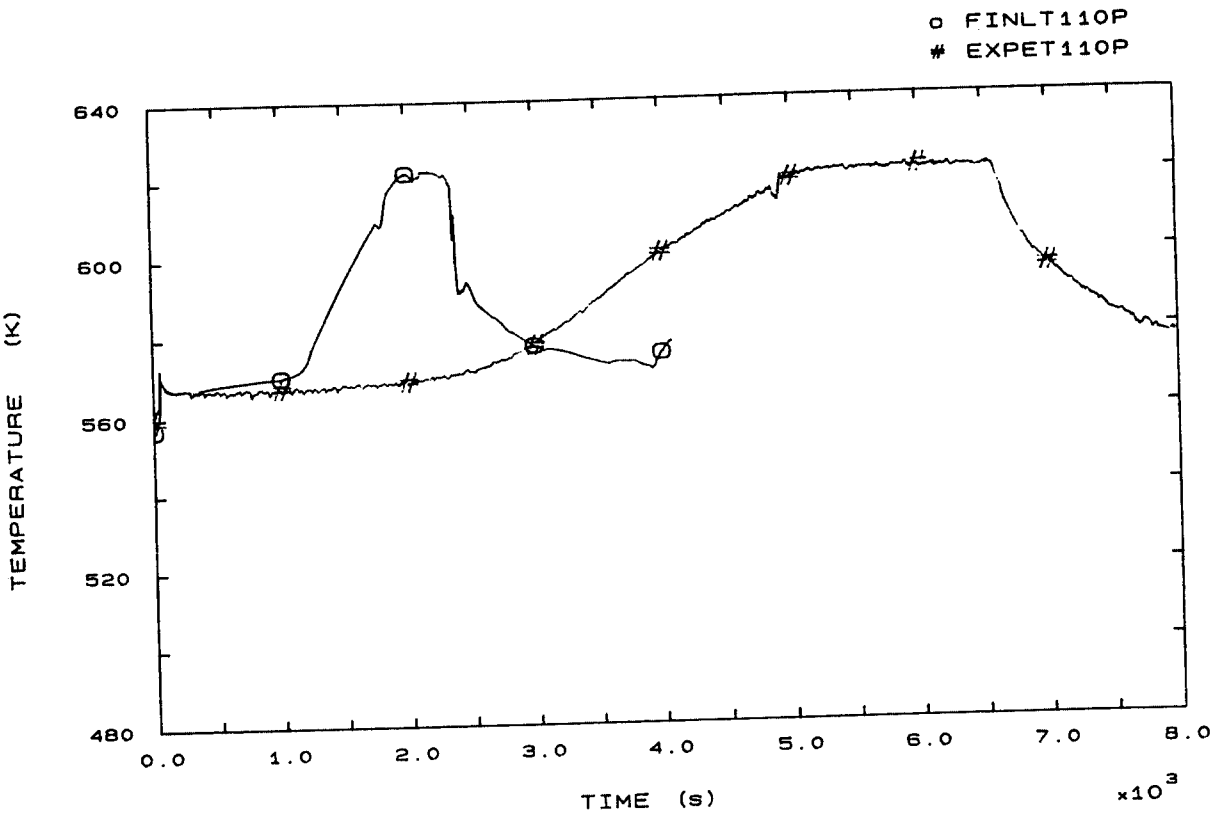

FIG. 42 SG1 OUTLET TEMPERATURE

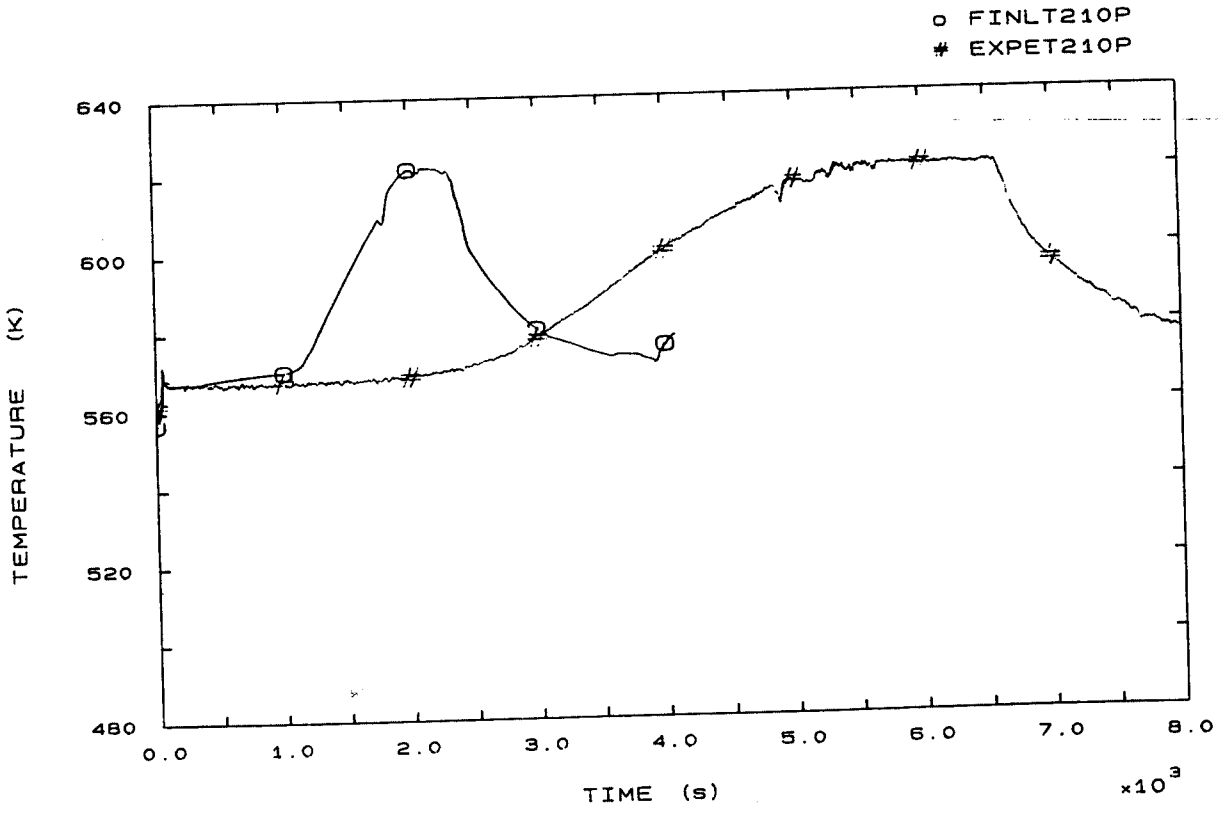

FIG. 44 SG2 OUTLET TEMPERATURE

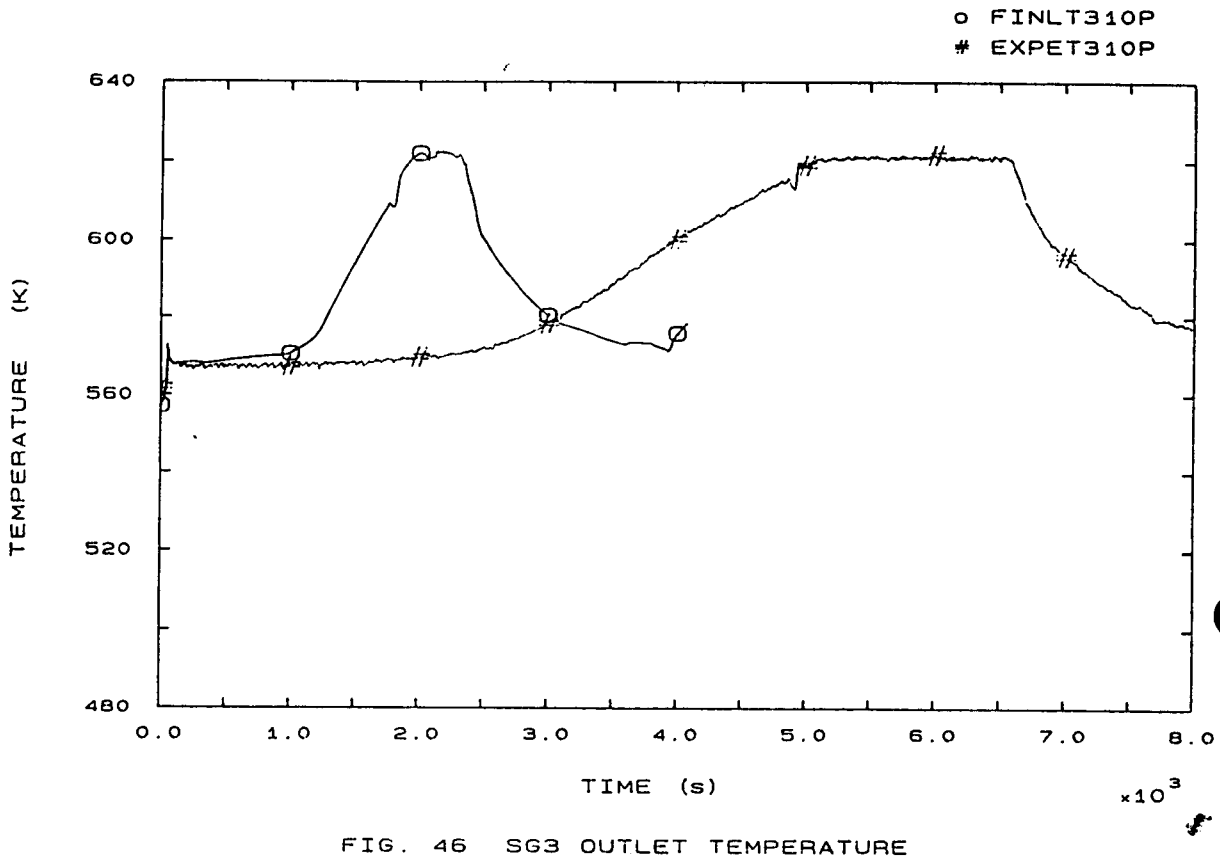

FIG. 46 SG3 OUTLET TEMPERATURE

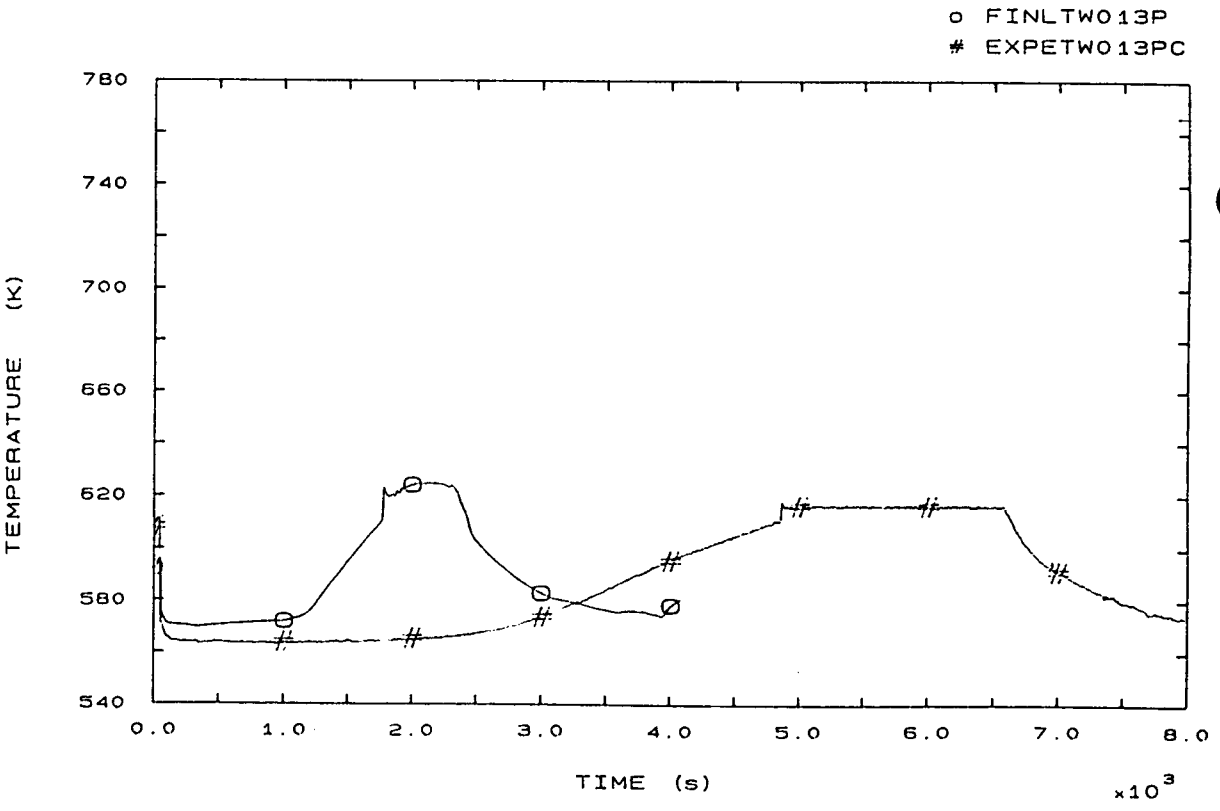

FIG. 49 CORE SURFACE TEMPERATURE AT ROD BUNDLE ELEVATION 1074 MM

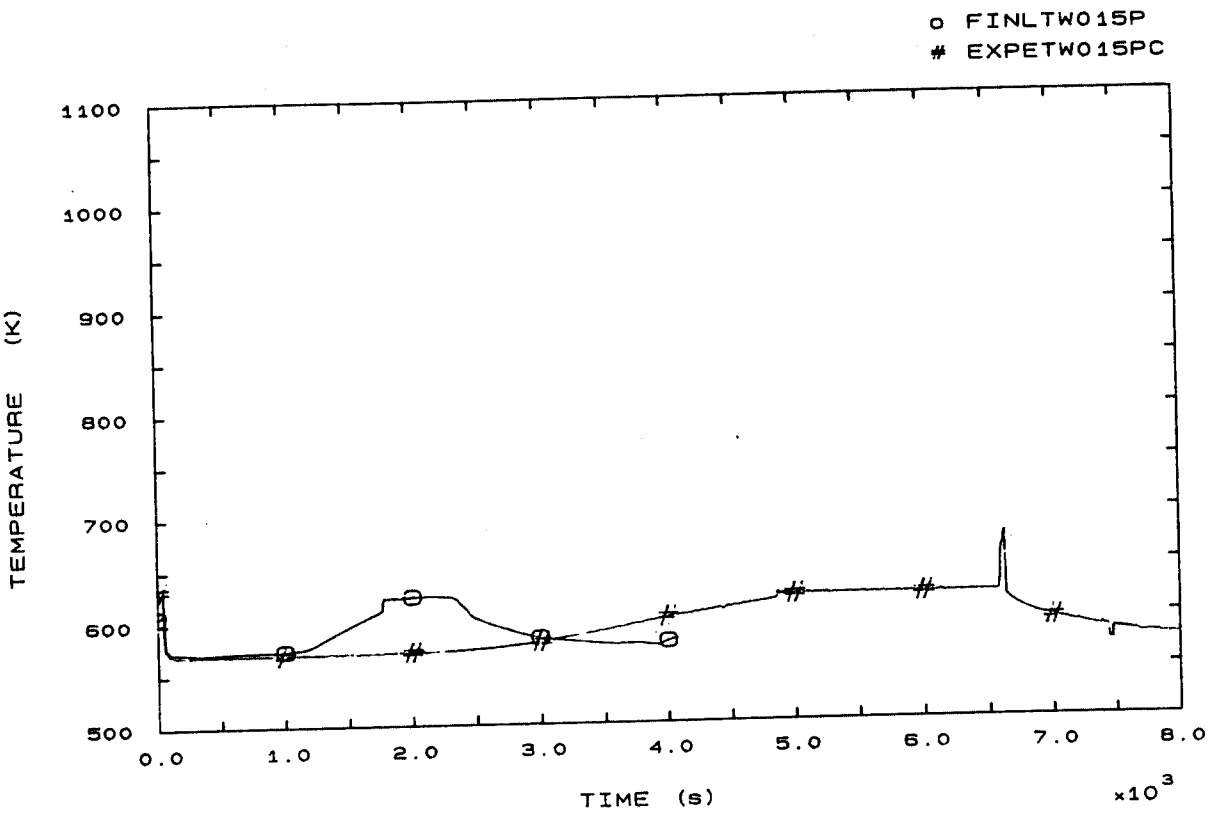

FIG. 50 SURFACE TEMPERATURE AT ROD BUNDLE ELEVATION 2294 MM

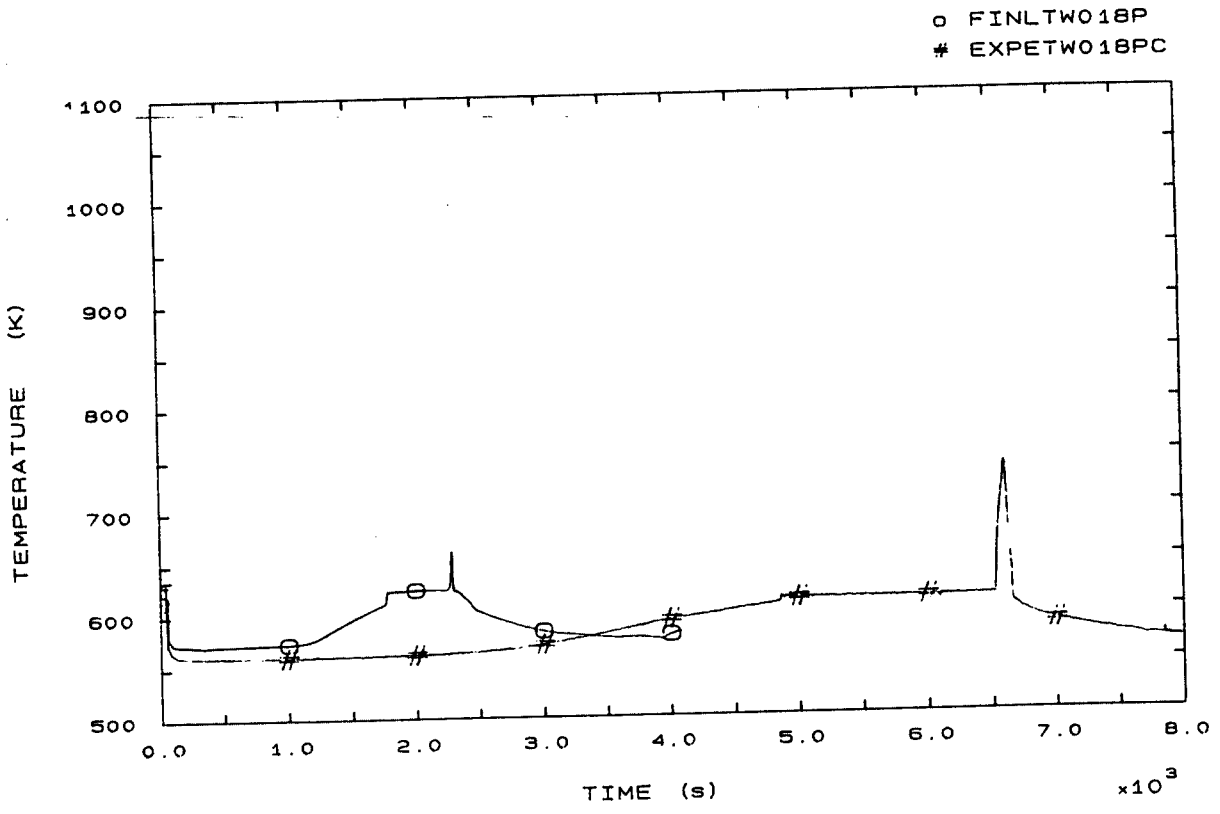

FIG. 51 SURFACE TEMPERATURE AT ROD BUNDLE ELEVATION 3294 MM

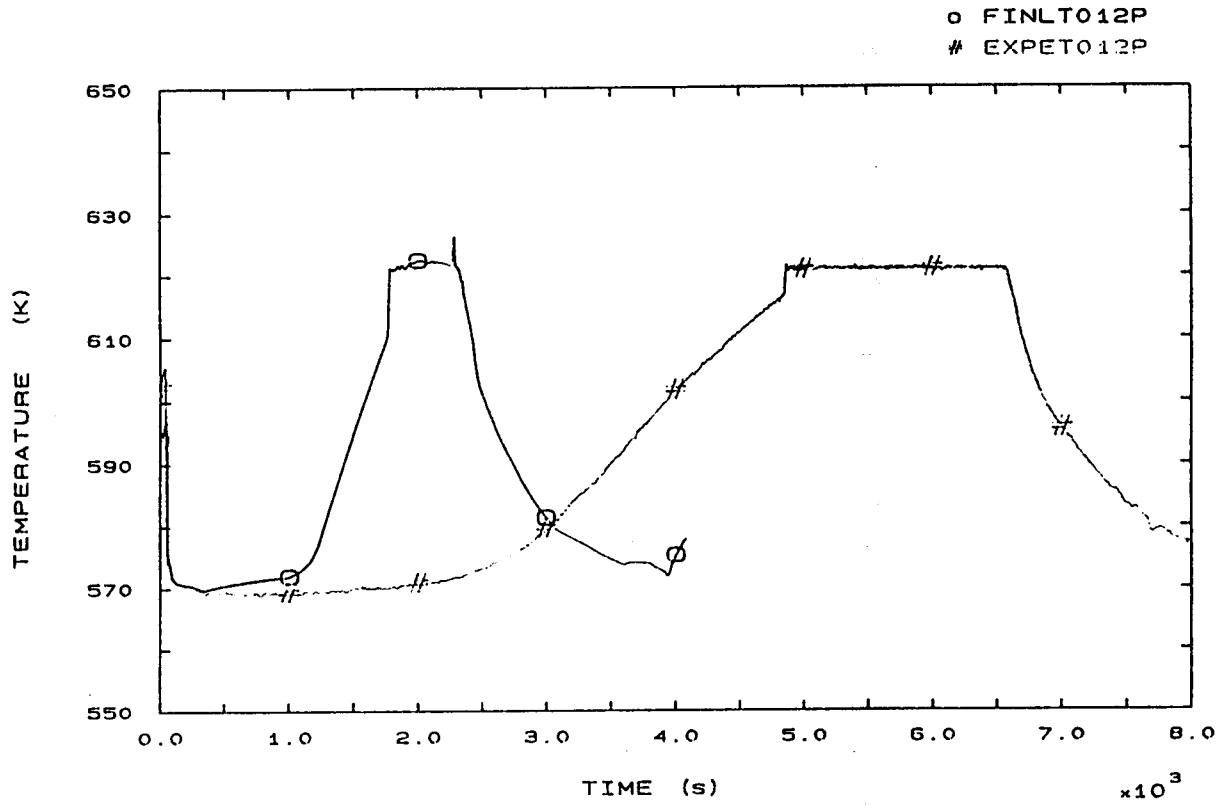

FIG. 53 CORE OUTLET TEMPERATURE

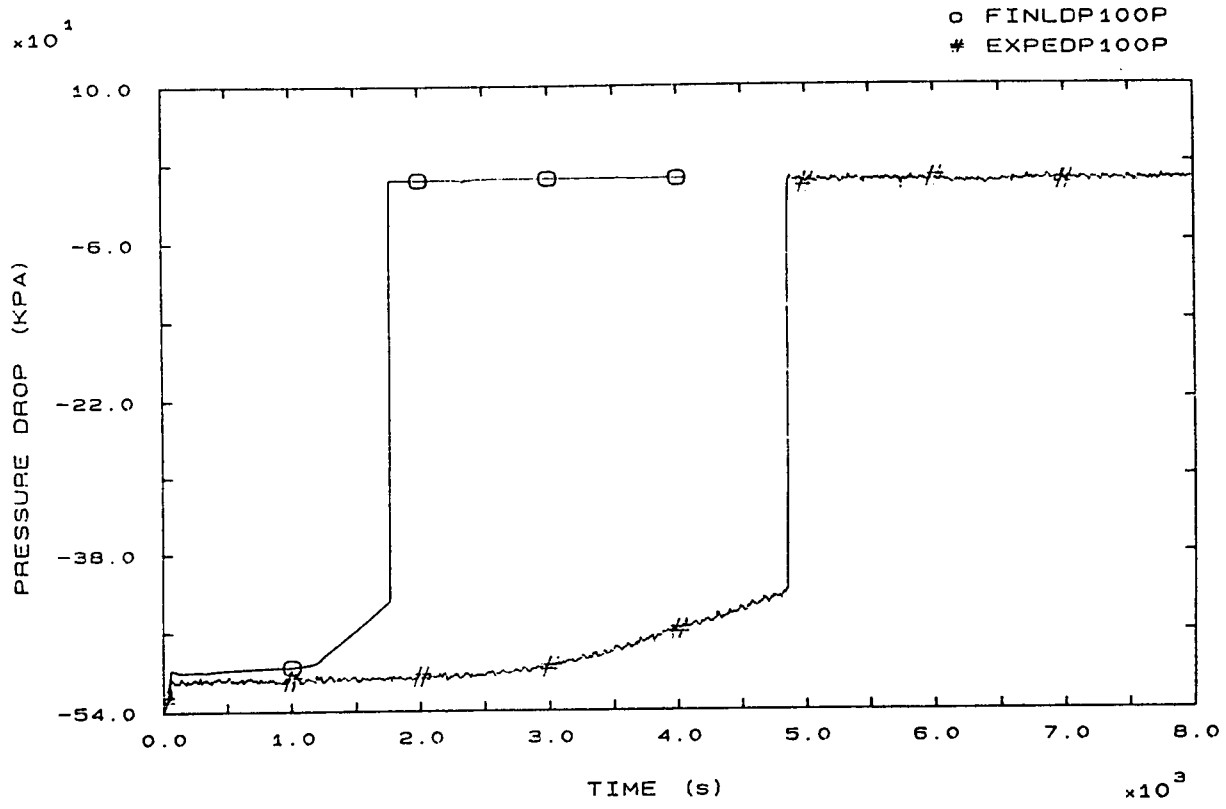

FIG. 54 PRIMARY PUMP 1 PRESSURE DROP

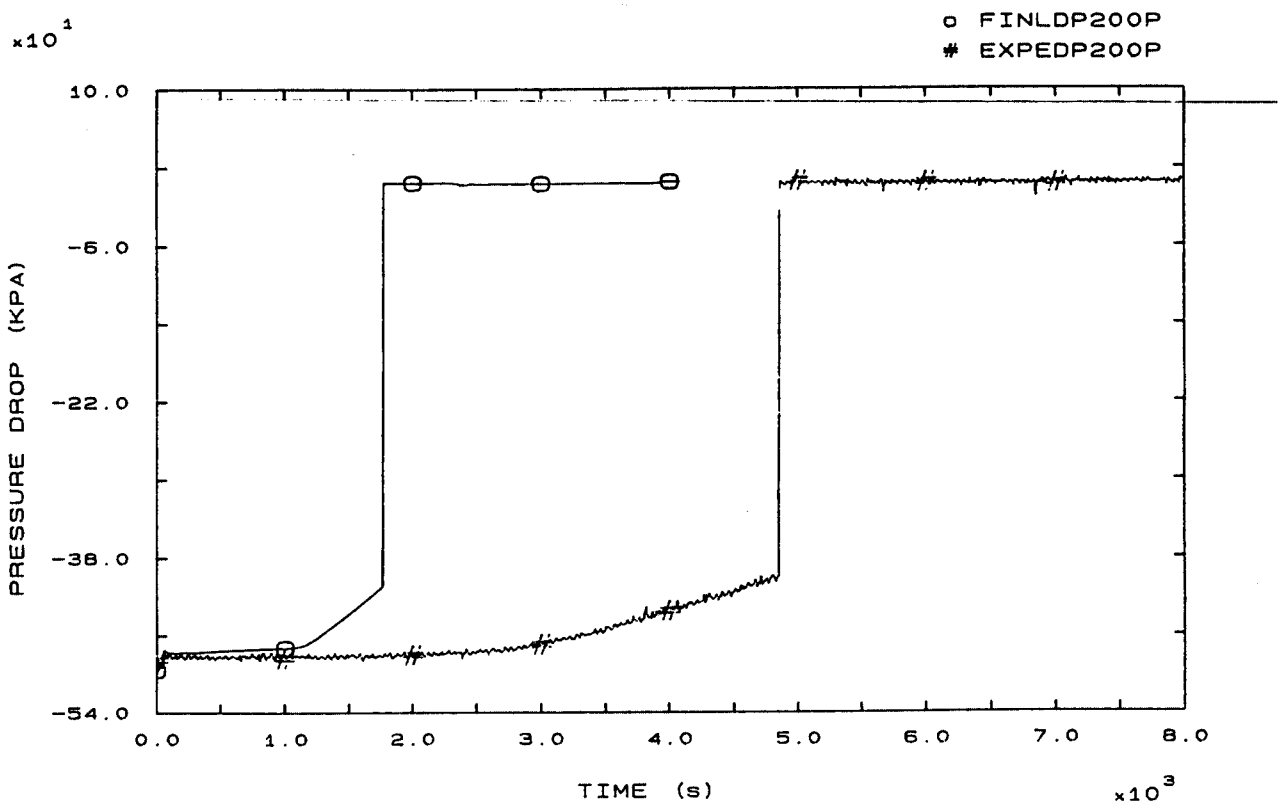

FIG. 55 PRIMARY PUMP 2 PRESSURE DROP

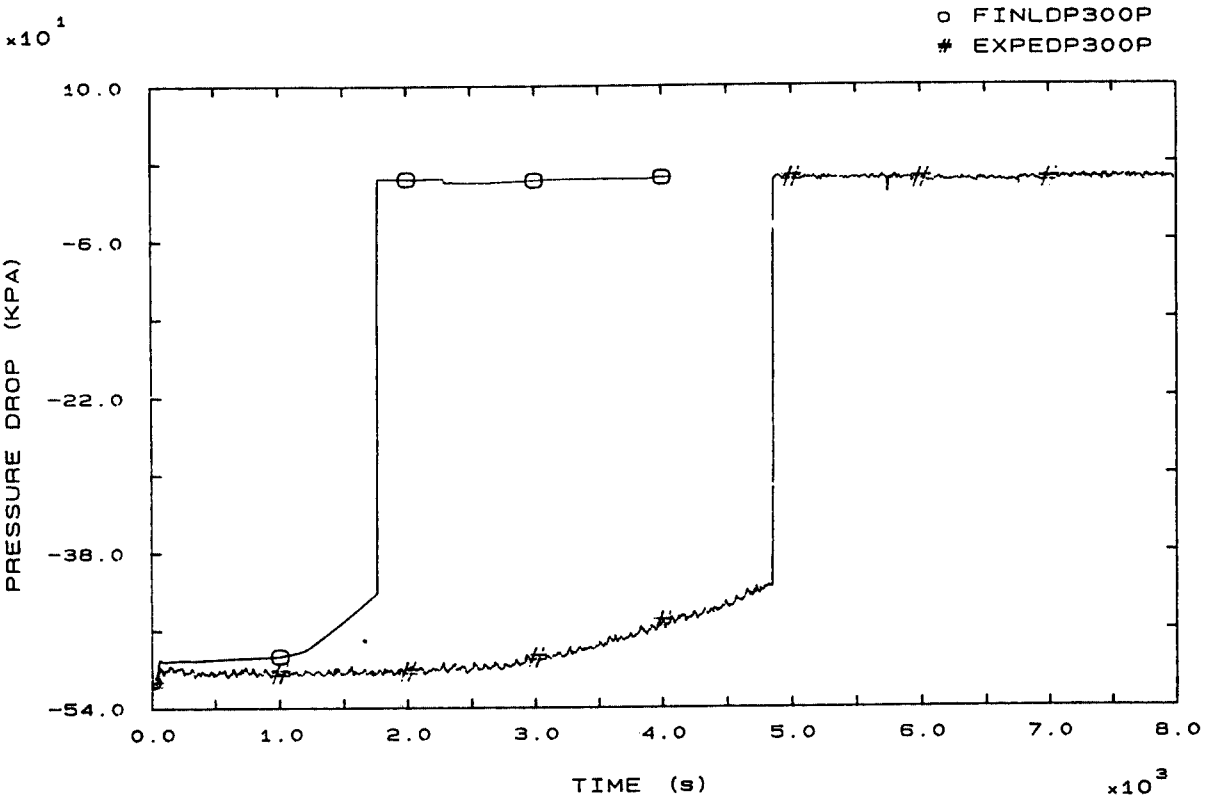

FIG. 56 PRIMARY PUMP 3 PRESSURE DROP

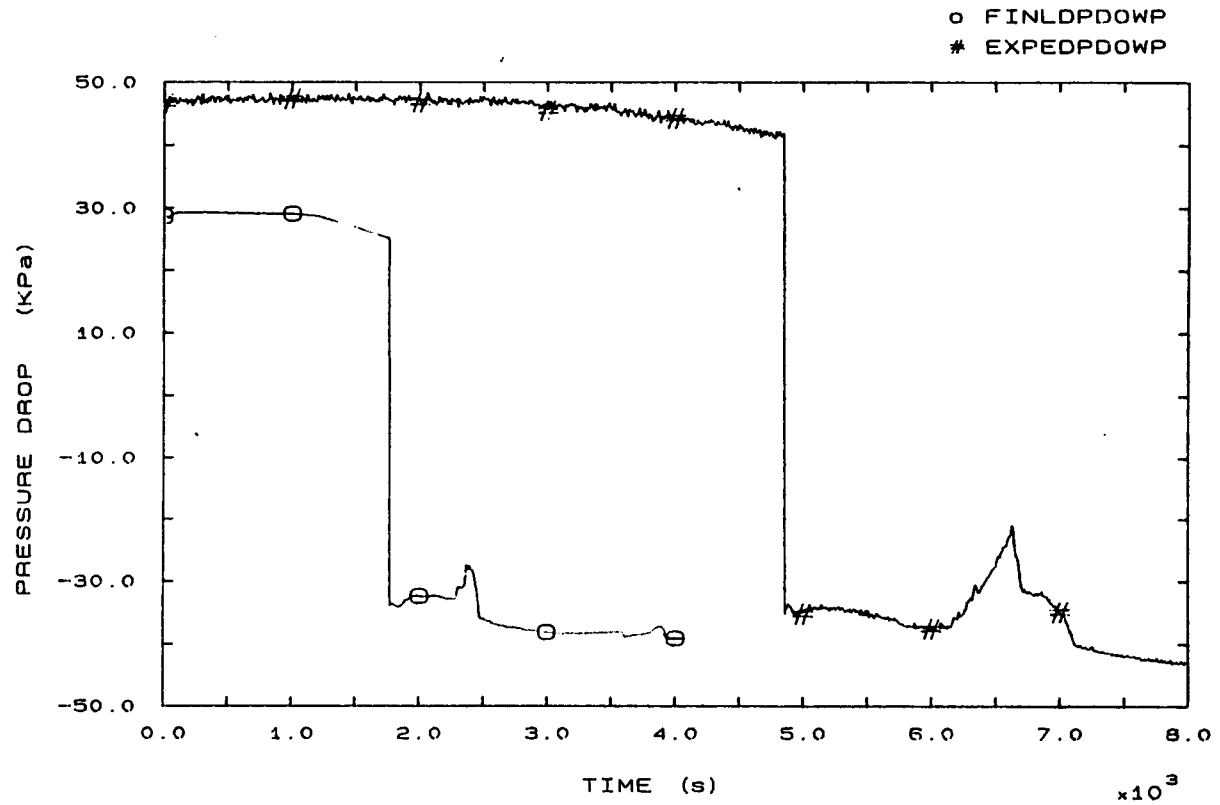

FIG. 57 VESSEL DOWNCOMER PRESSURE DROP

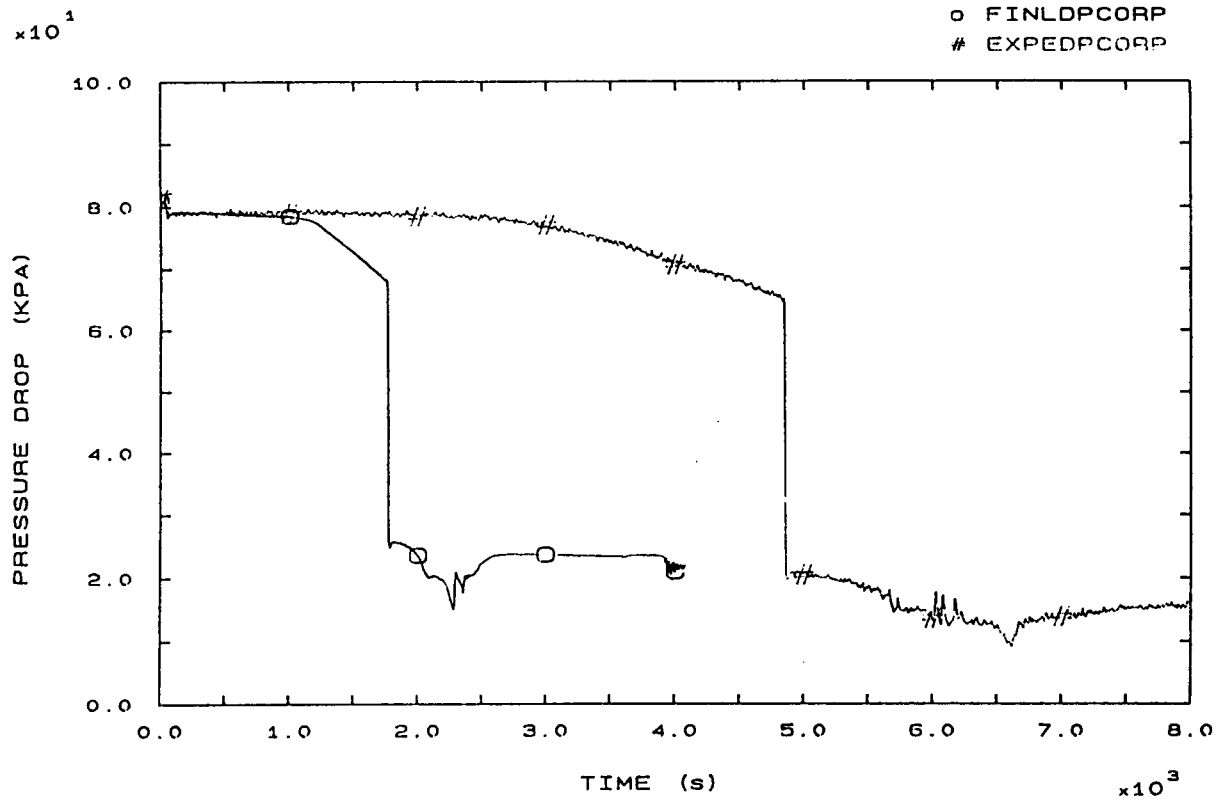

FIG. 58 CORE PRESSURE DROP

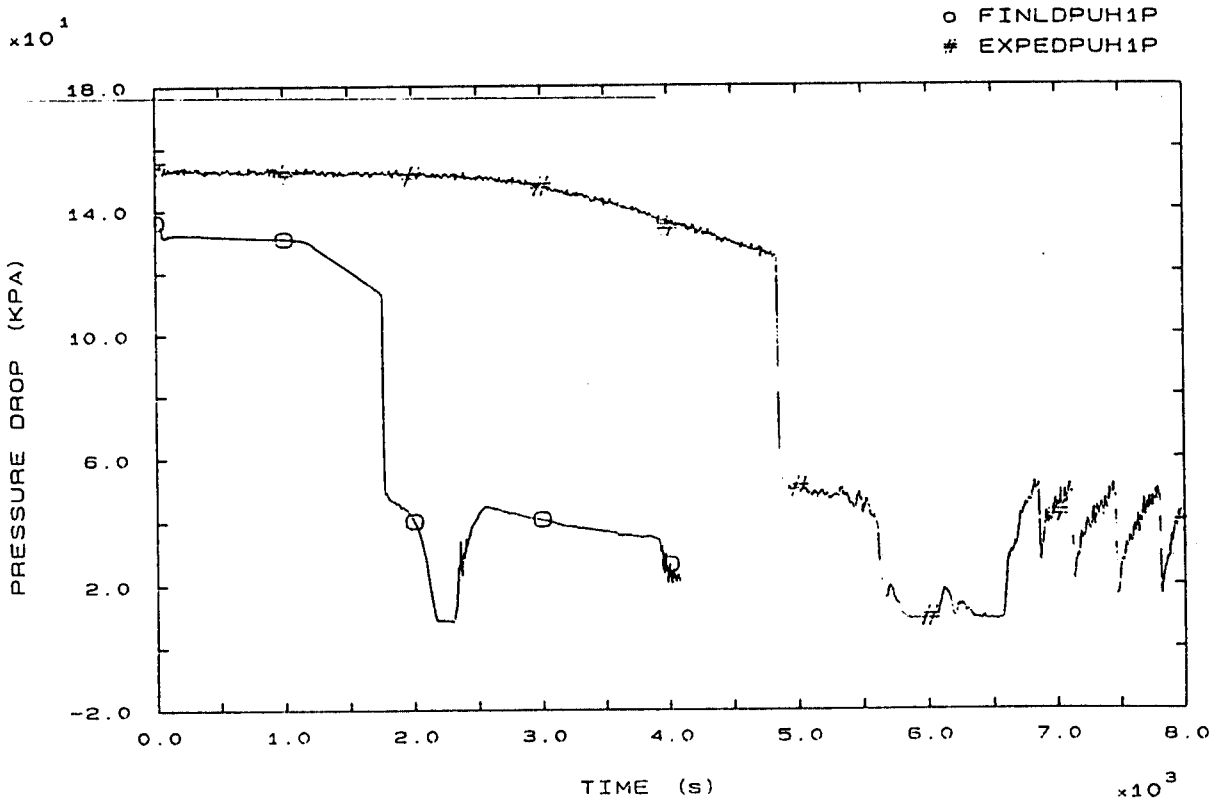

FIG. 62 SG1 INLET/U-BEND (UP-HILL) PRESSURE DROP

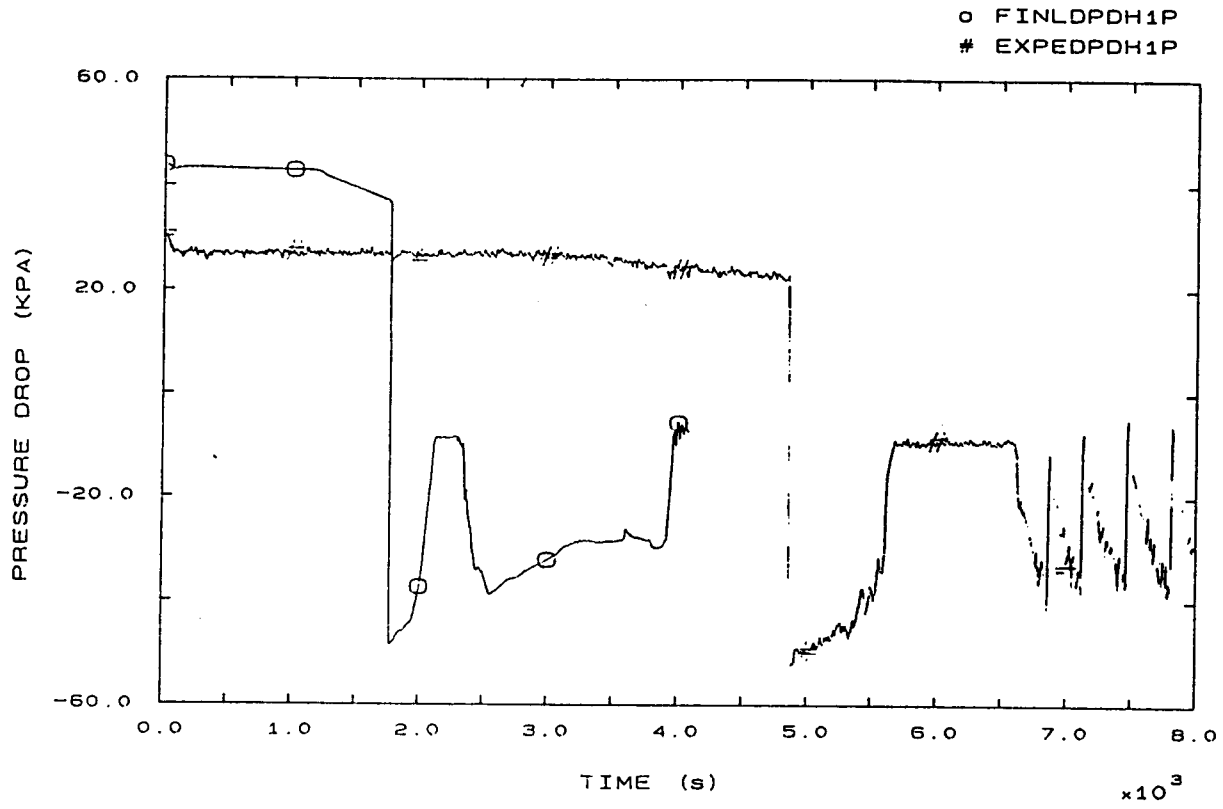

FIG. 63 SG1 U-BEND/OUTLET (DOWN-HILL) PRESSURE DROP

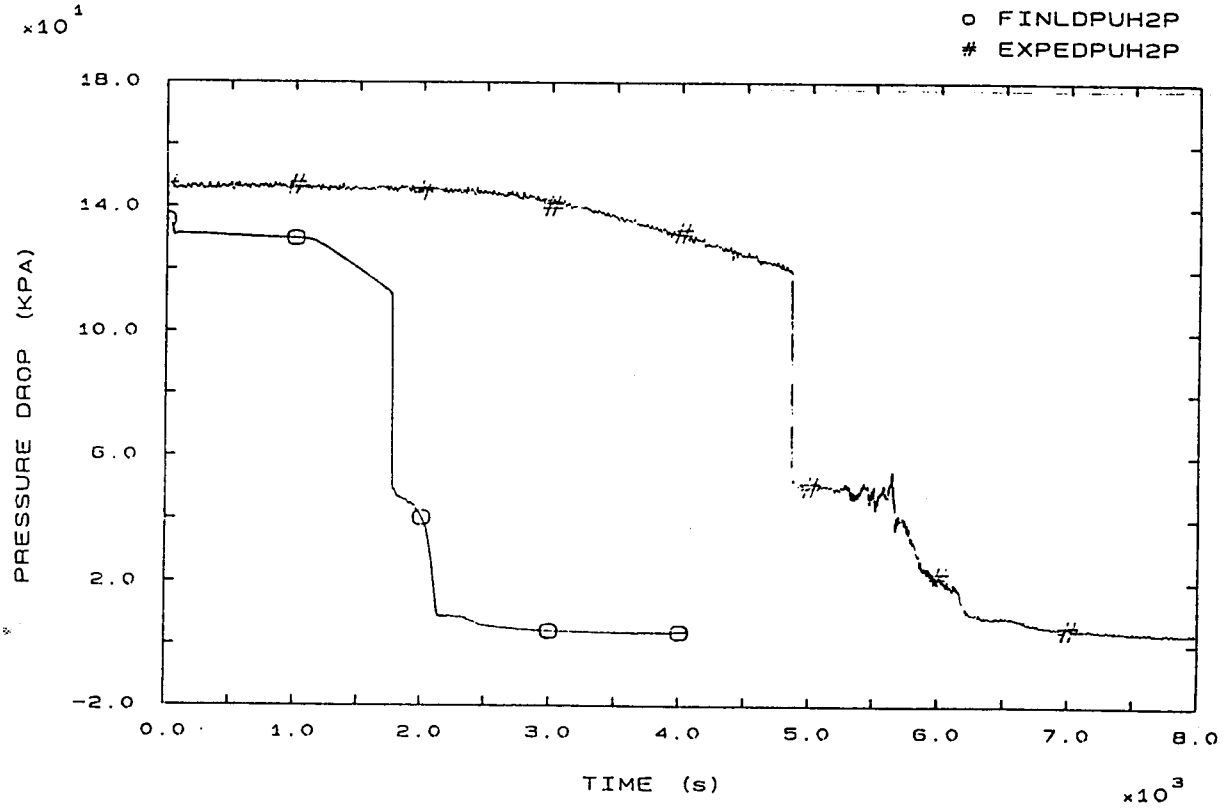

FIG. 64 SG2 INLET/U-BEND (UP-HILL) PRESSURE DROP

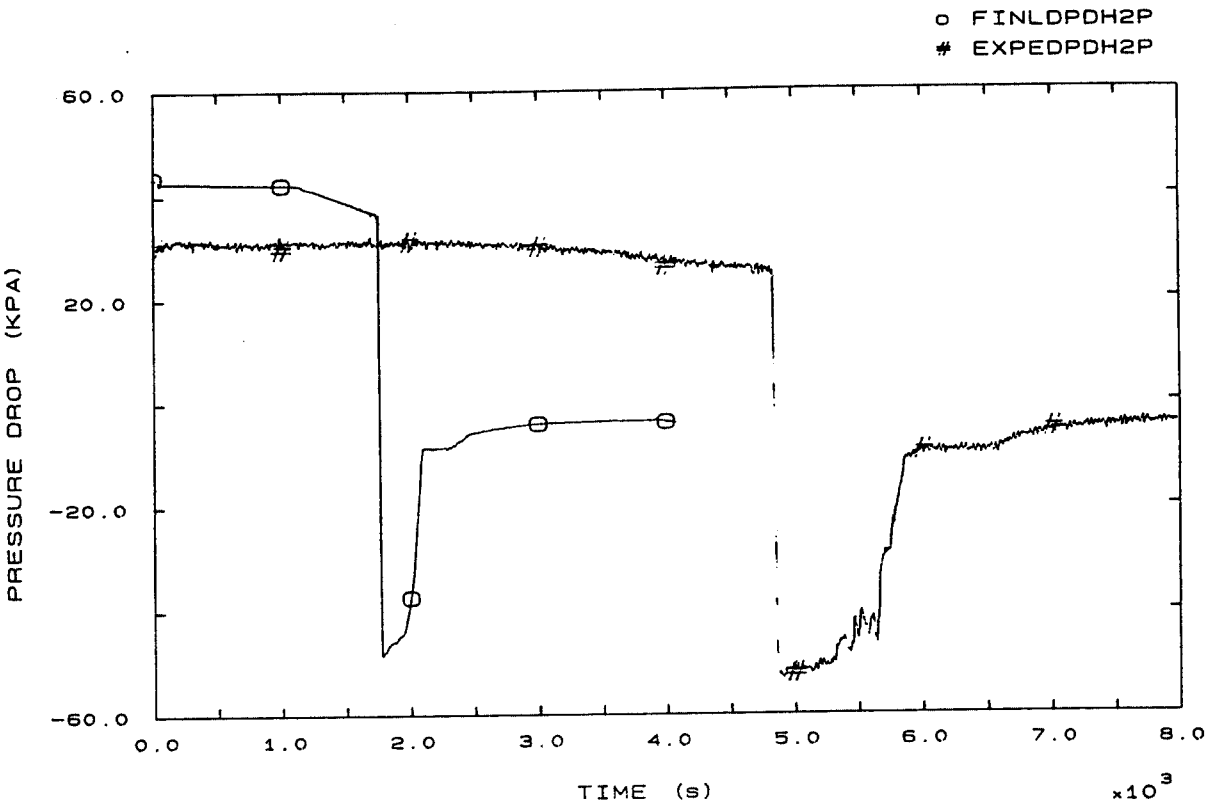

FIG. 65 SG2 U-BEND/OUTLET (DOWN-HILL) PRESSURE DROP

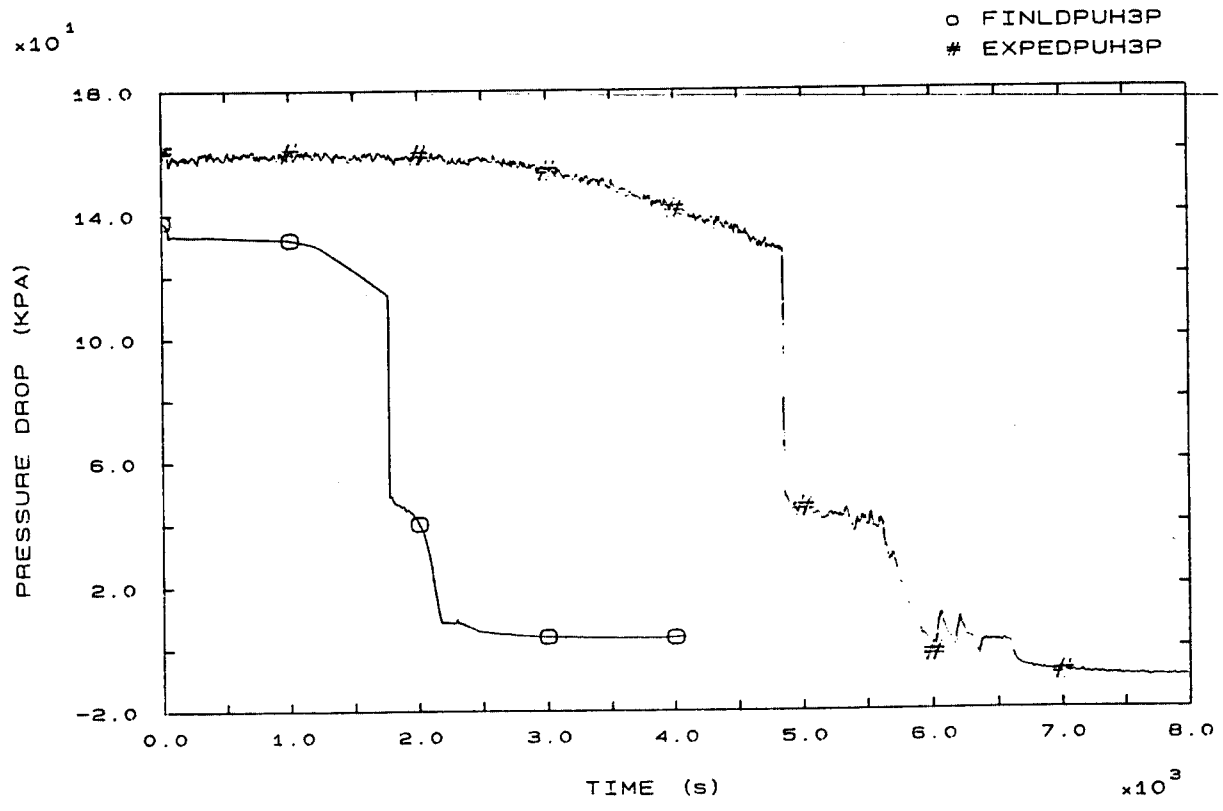

FIG. 66 SG3 INLET/U-BEND (UP-HILL) PRESSURE DROP

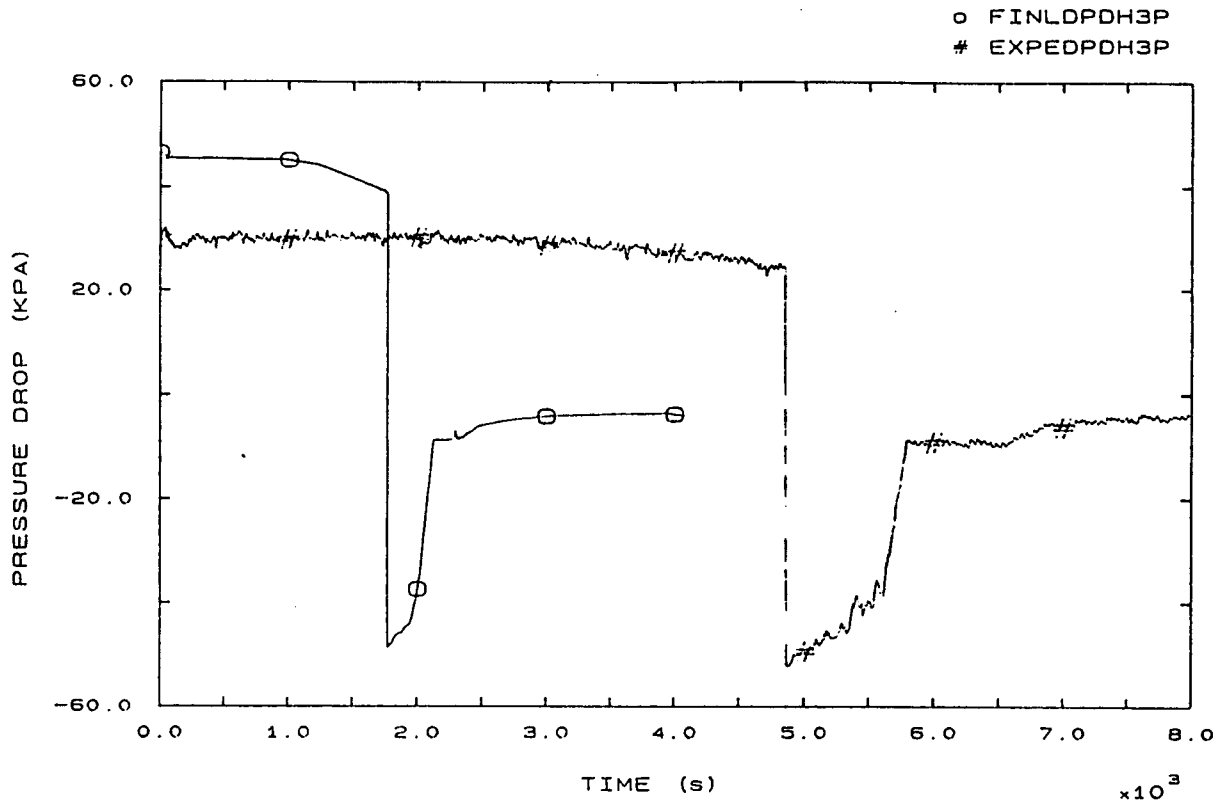

FIG. 67 SG3 U-BEND/OUTLET (DOWN-HILL) PRESSURE DROP

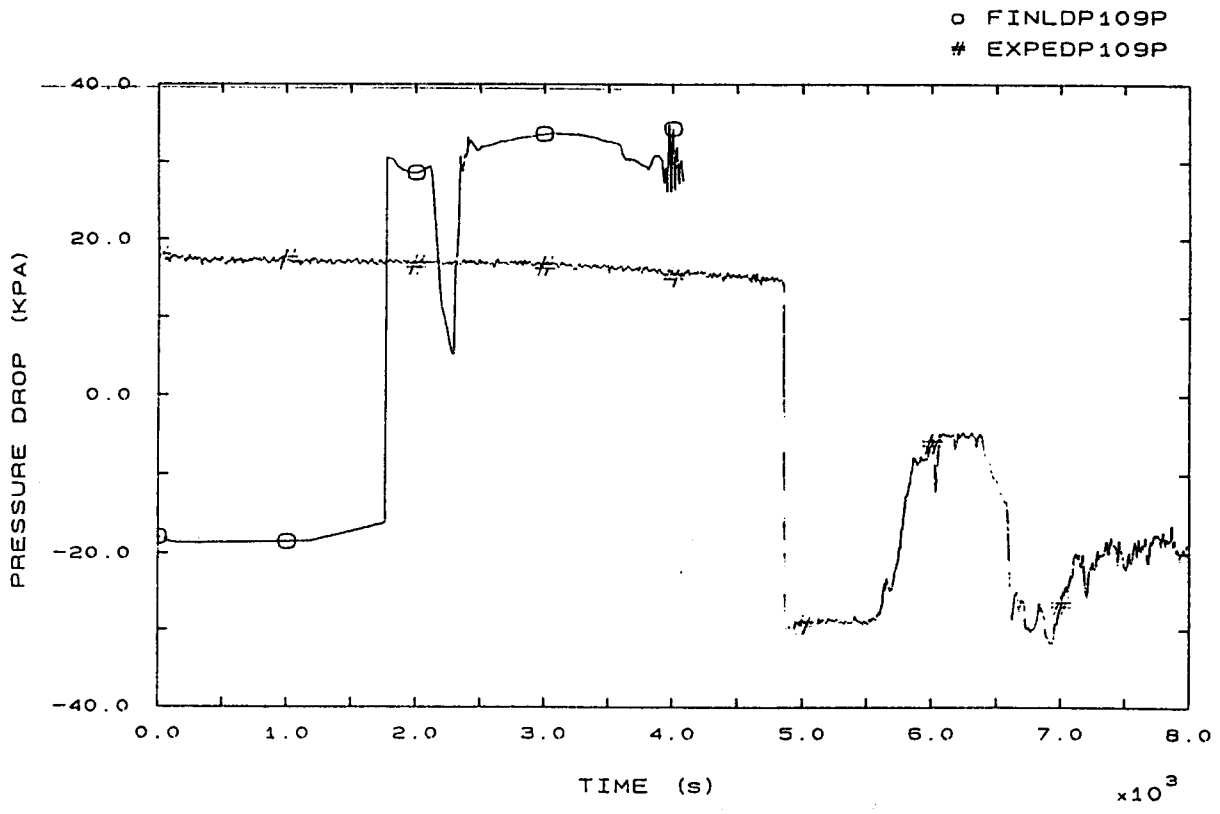

FIG. 68 SG1 OUTLET/LOOP SEAL BOTTOM PRESSURE DROP

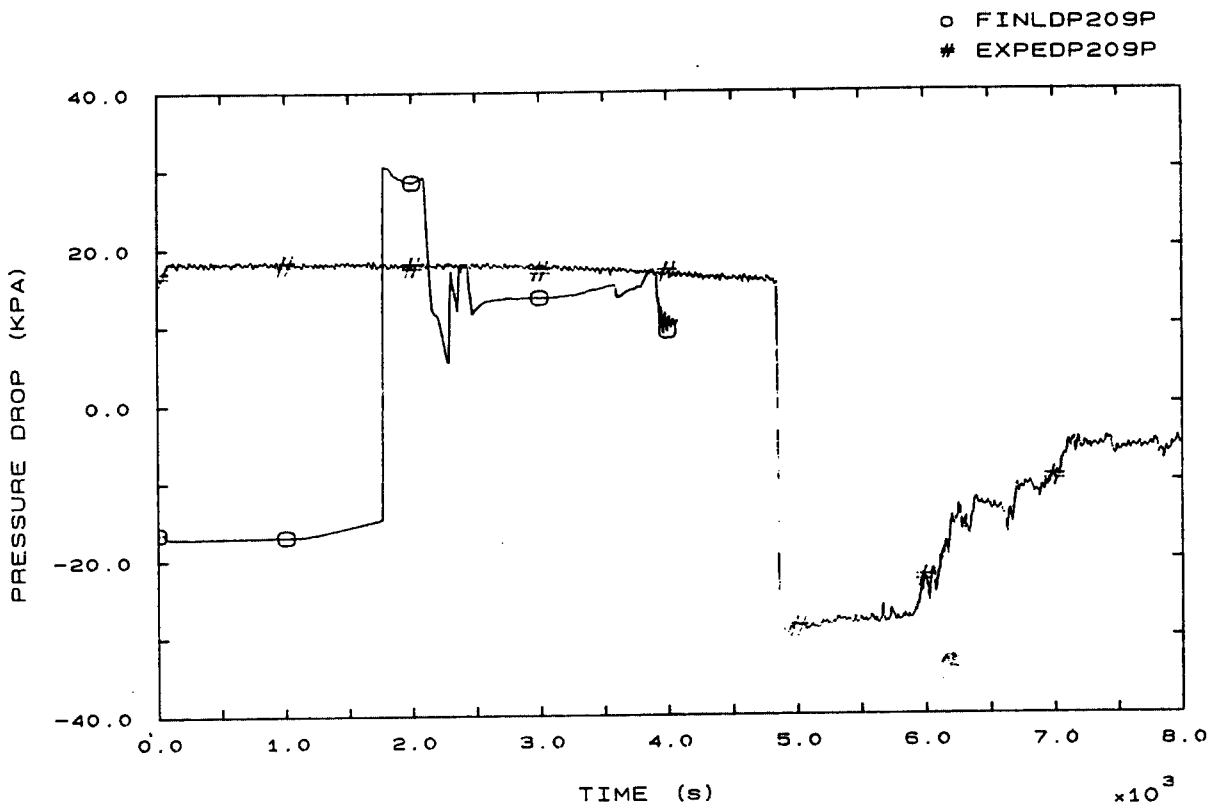

FIG. 69 SG2 OUTLET/LOOP SEAL BOTTOM PRESSURE DROP

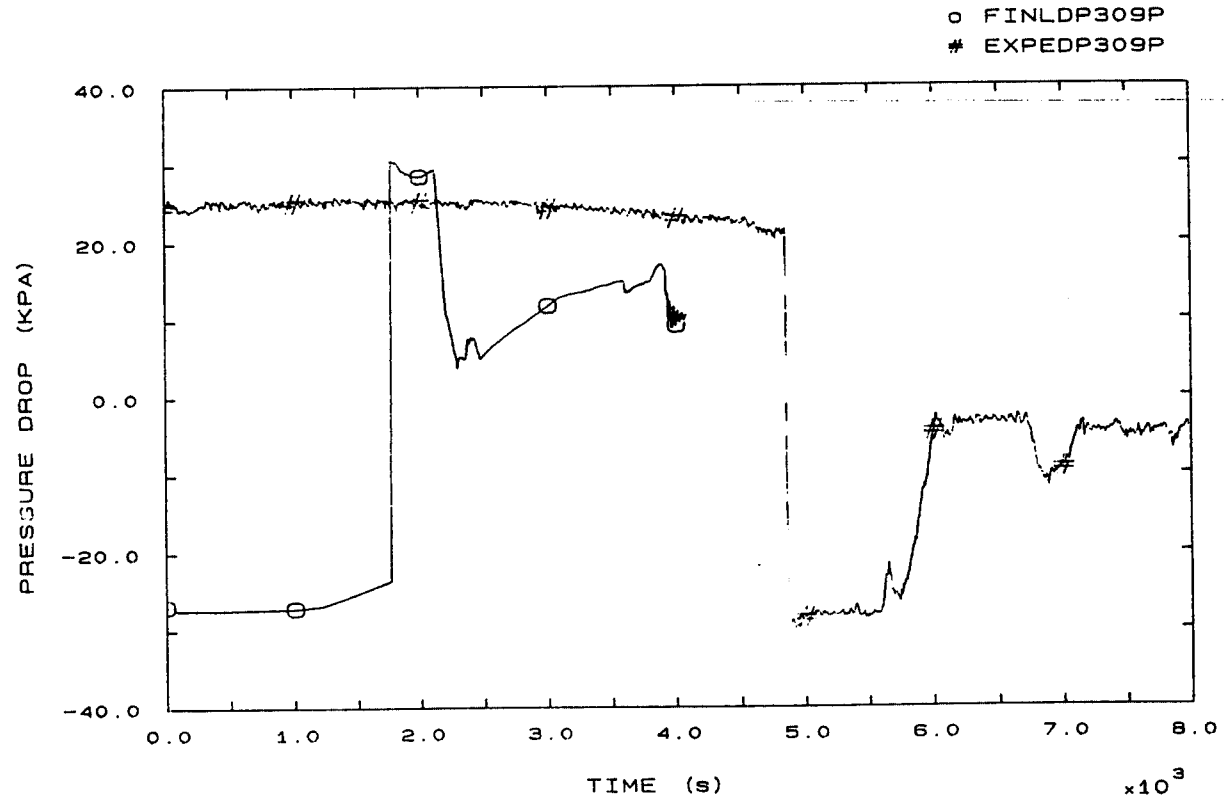

FIG. 70 SG3 OUTLET/LOOP SEAL BOTTOM PRESSURE DROP

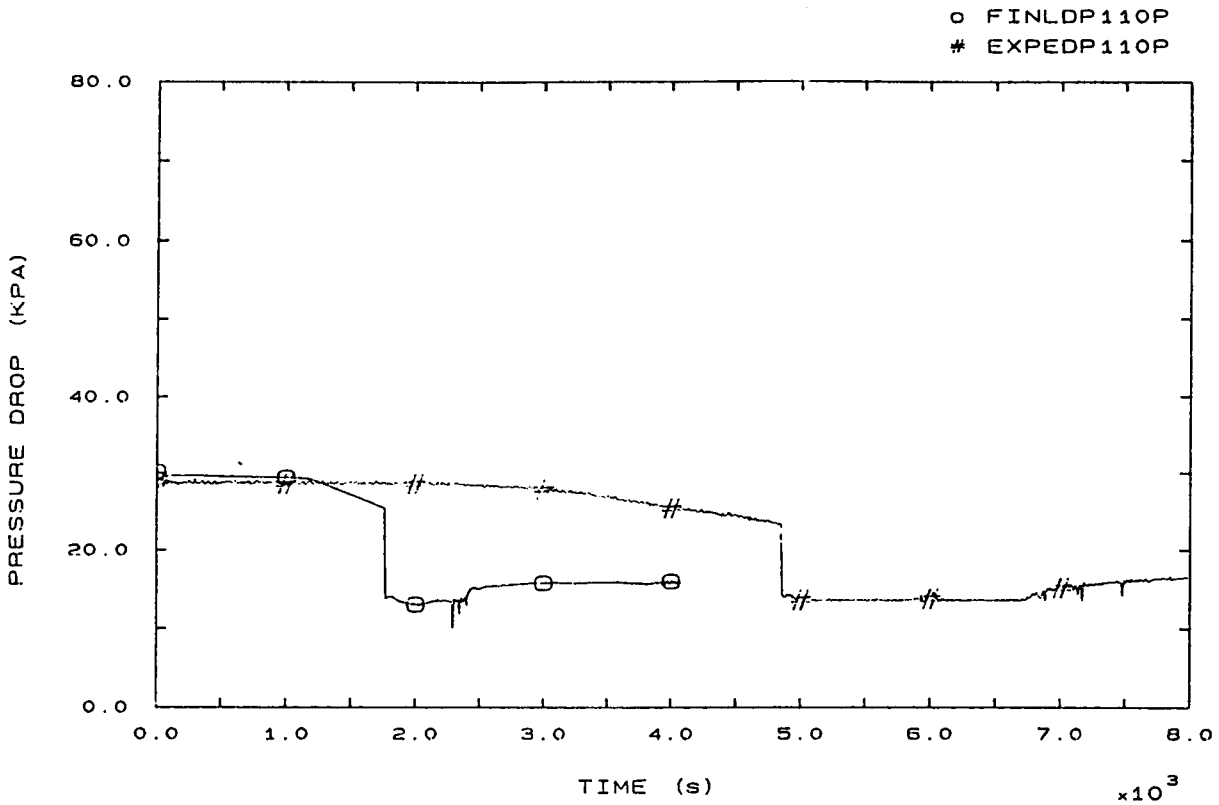

FIG. 71 LOOP SEAL BOTTOM/PUMP 1 INLET PRESSURE DROP

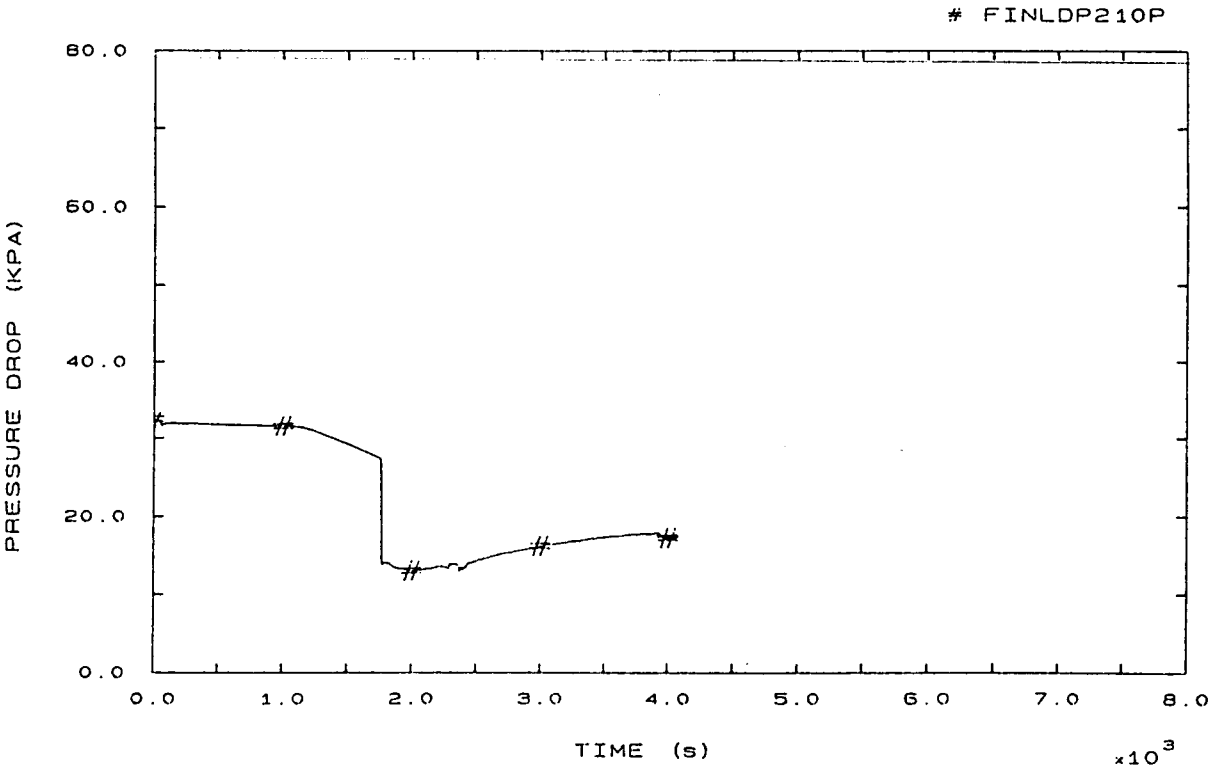

FIG. 72 LOOP SEAL BOTTOM/PUMP 2 INLET PRESSURE DROP

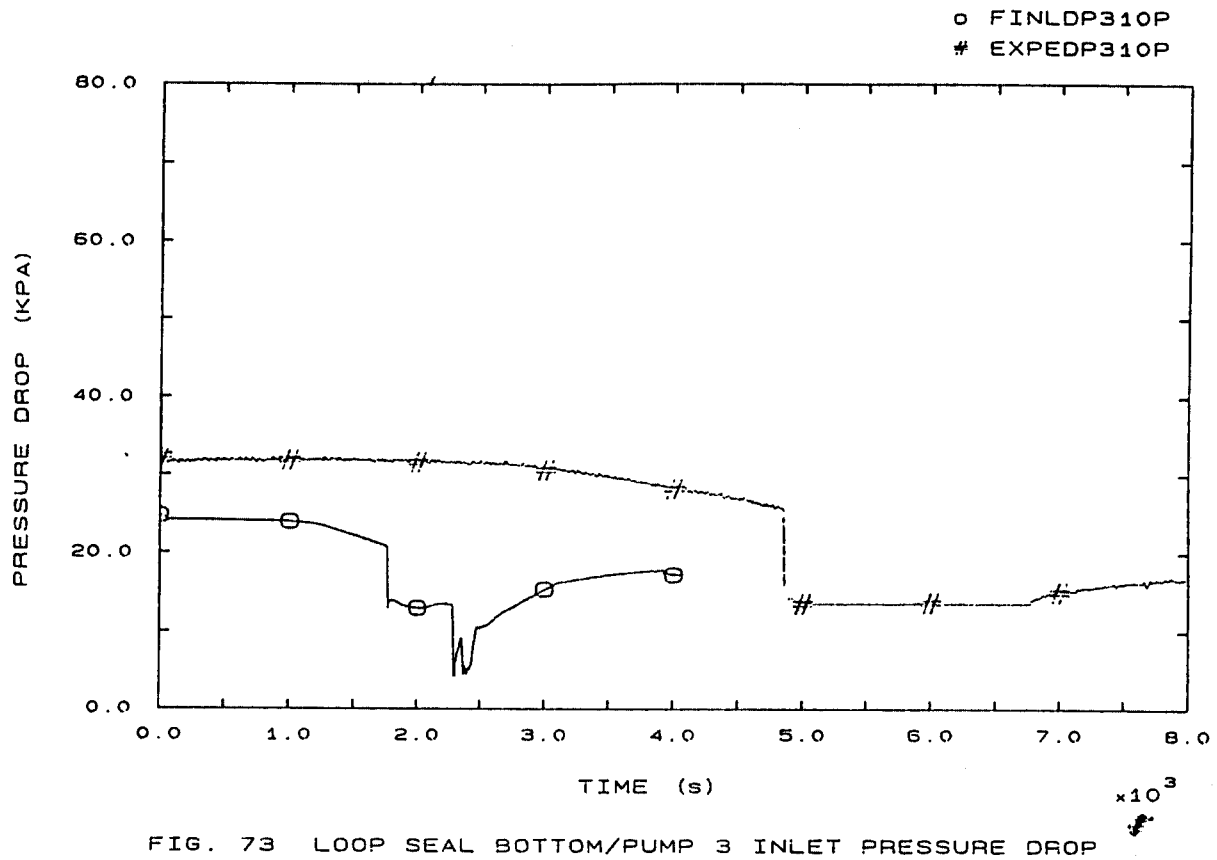

FIG. 73 LOOP SEAL BOTTOM/PUMP 3 INLET PRESSURE DROP

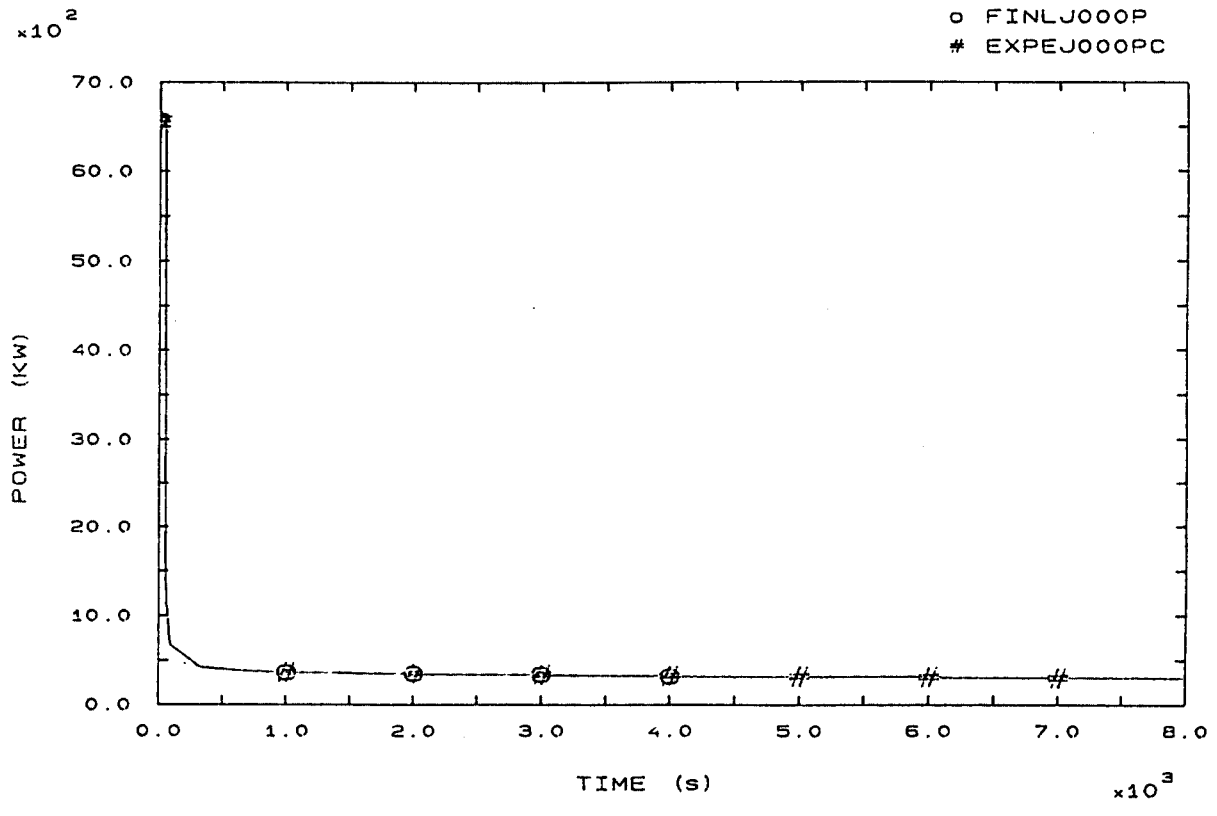

FIG. 81 HEATER RODS POWER

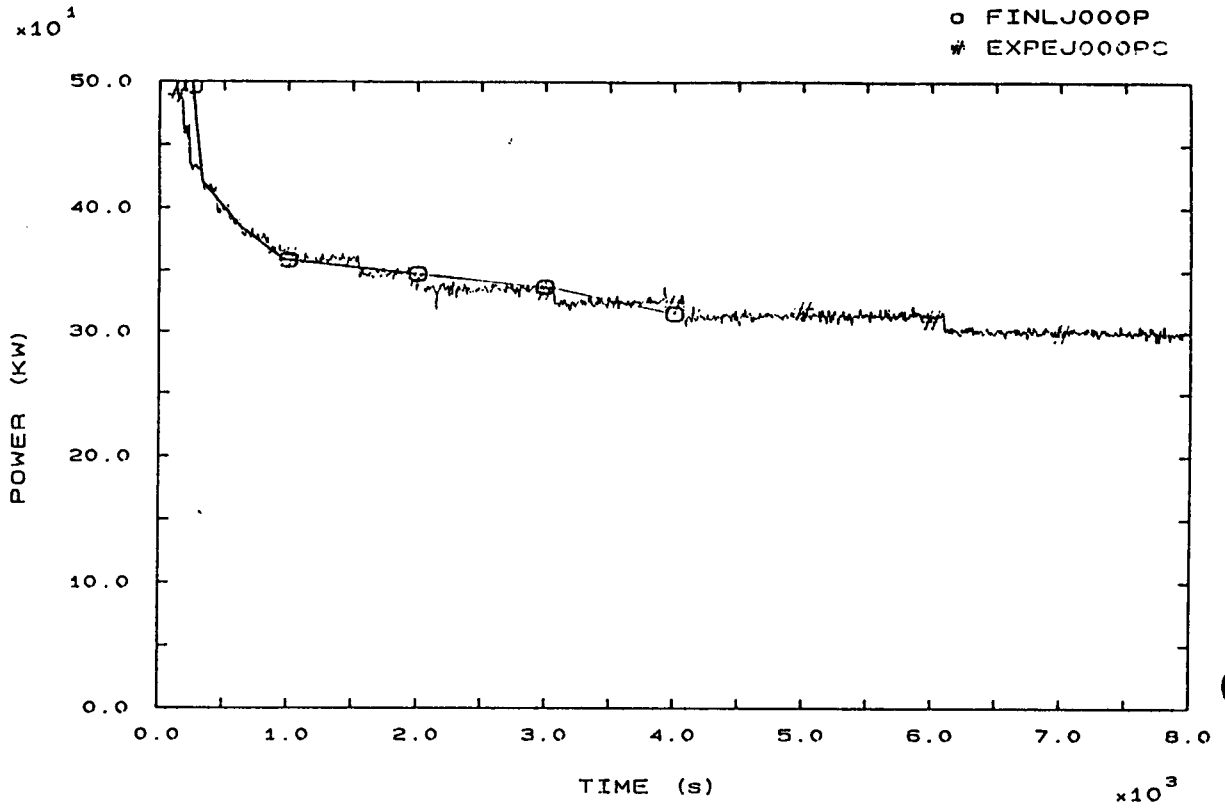

FIG. 81A HEATER RODS POWER

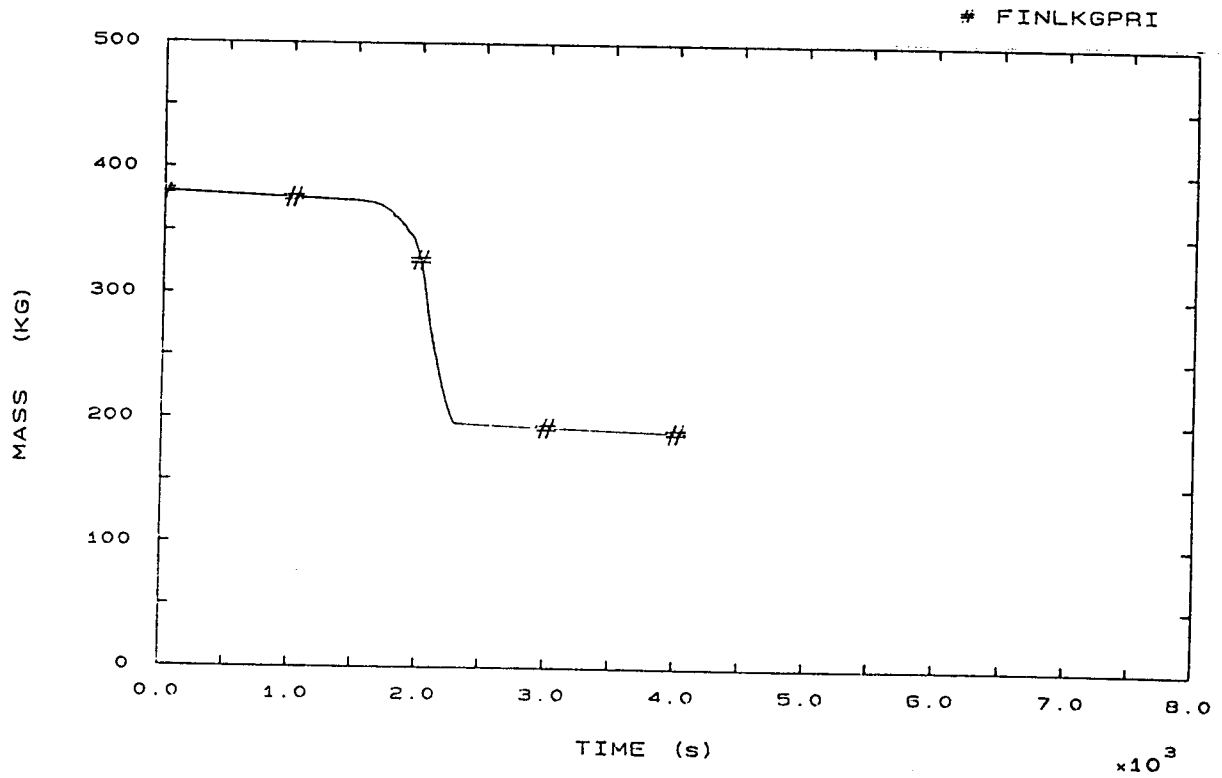

FIG. 85 PRIMARY COOLANT TOTAL MASS

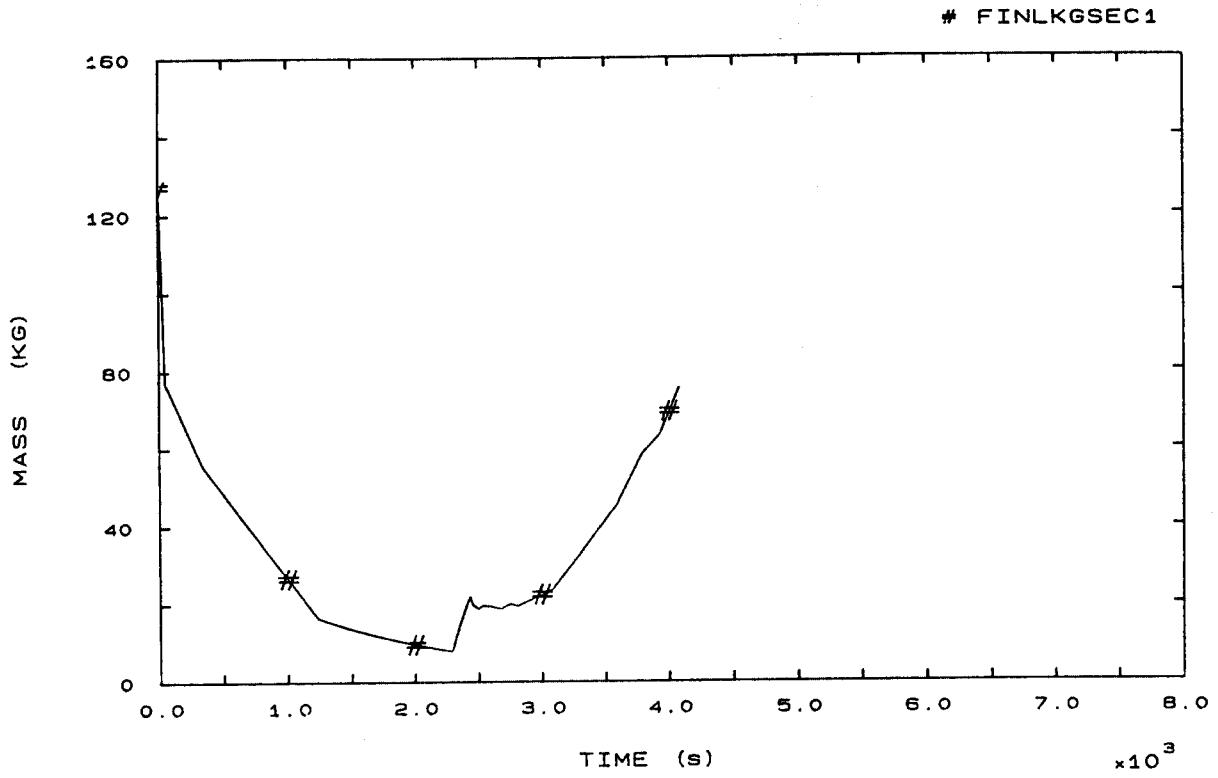

FIG. 86 SECONDARY COOLANT TOTAL MASS SG1

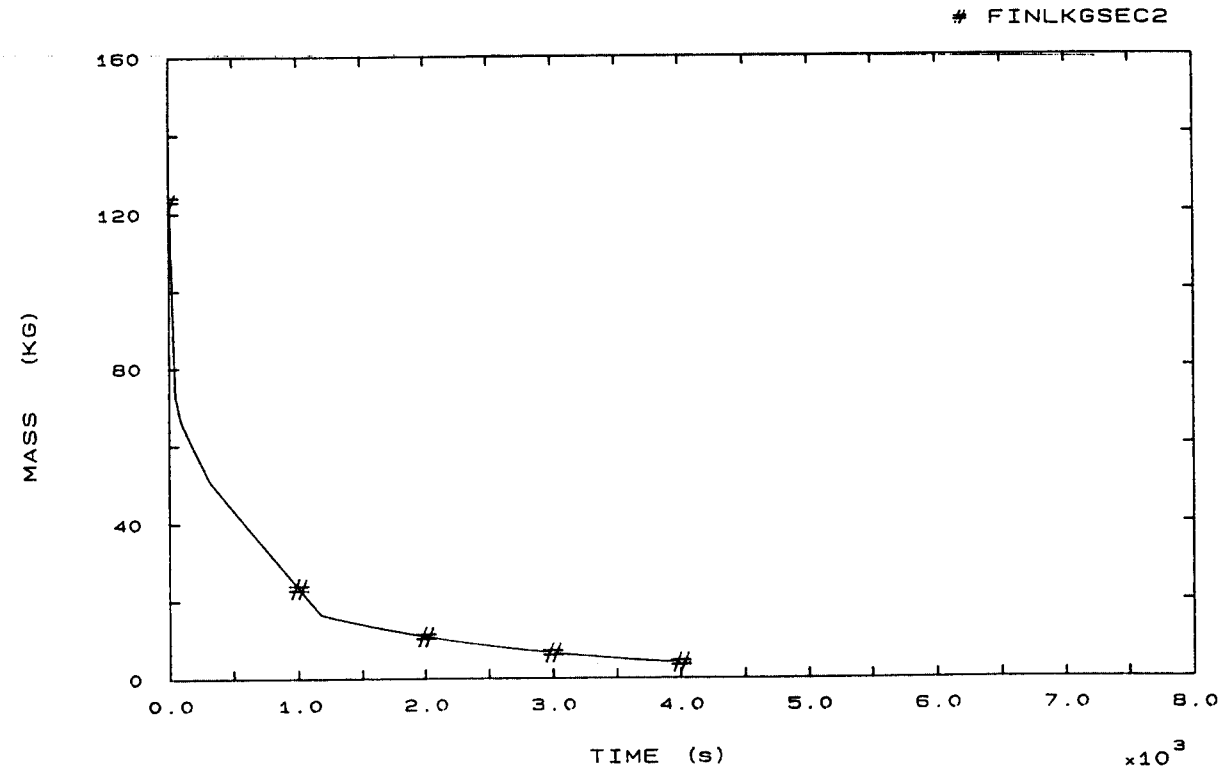

FIG. 87 SECONDARY COOLANT TOTAL MASS SG2

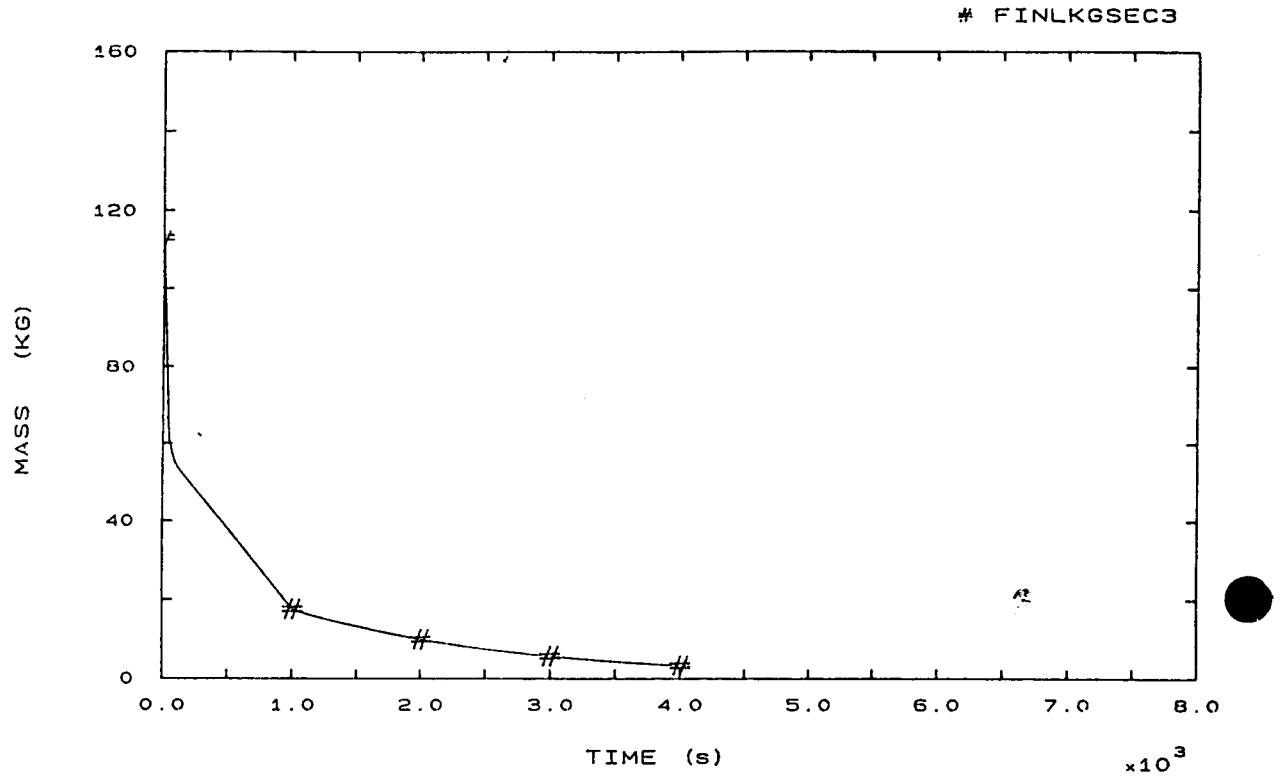

FIG. 88 SECONDARY COOLANT TOTAL MASS SG3

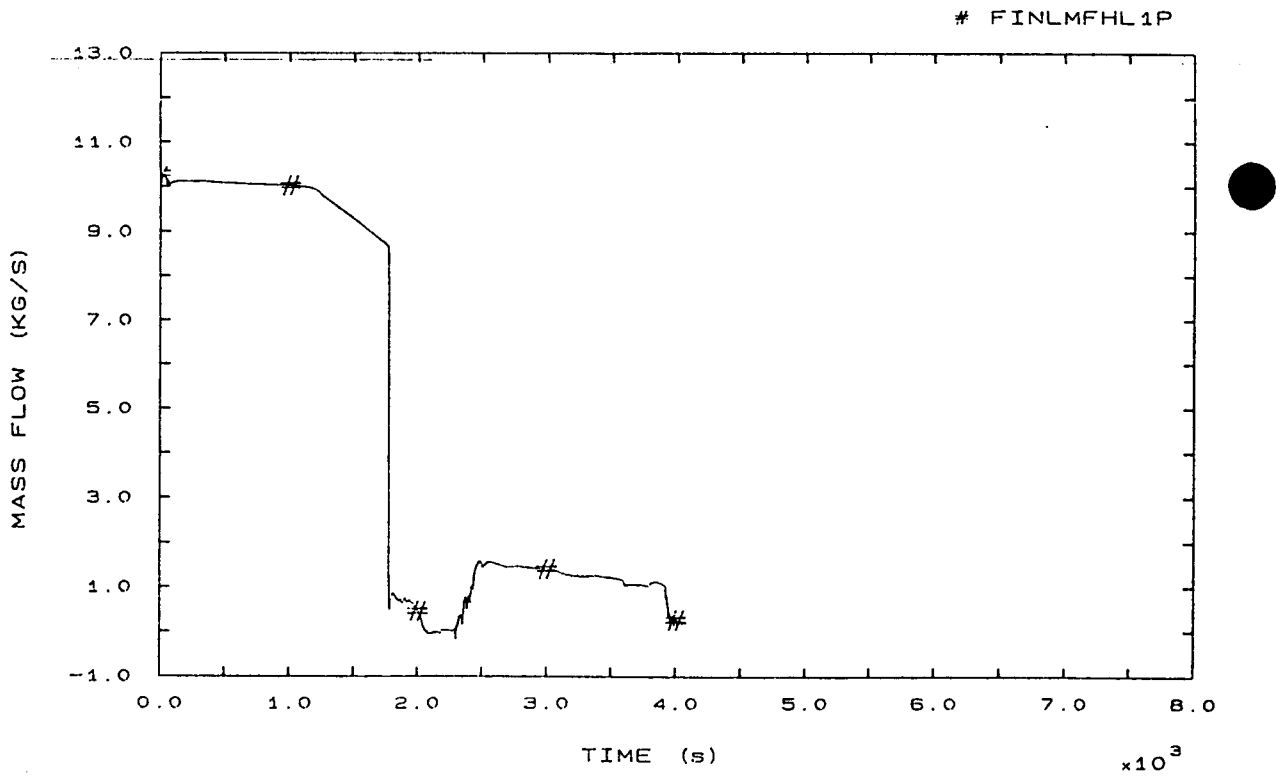

FIG. 89 HOT LEG 1 MASS FLOW

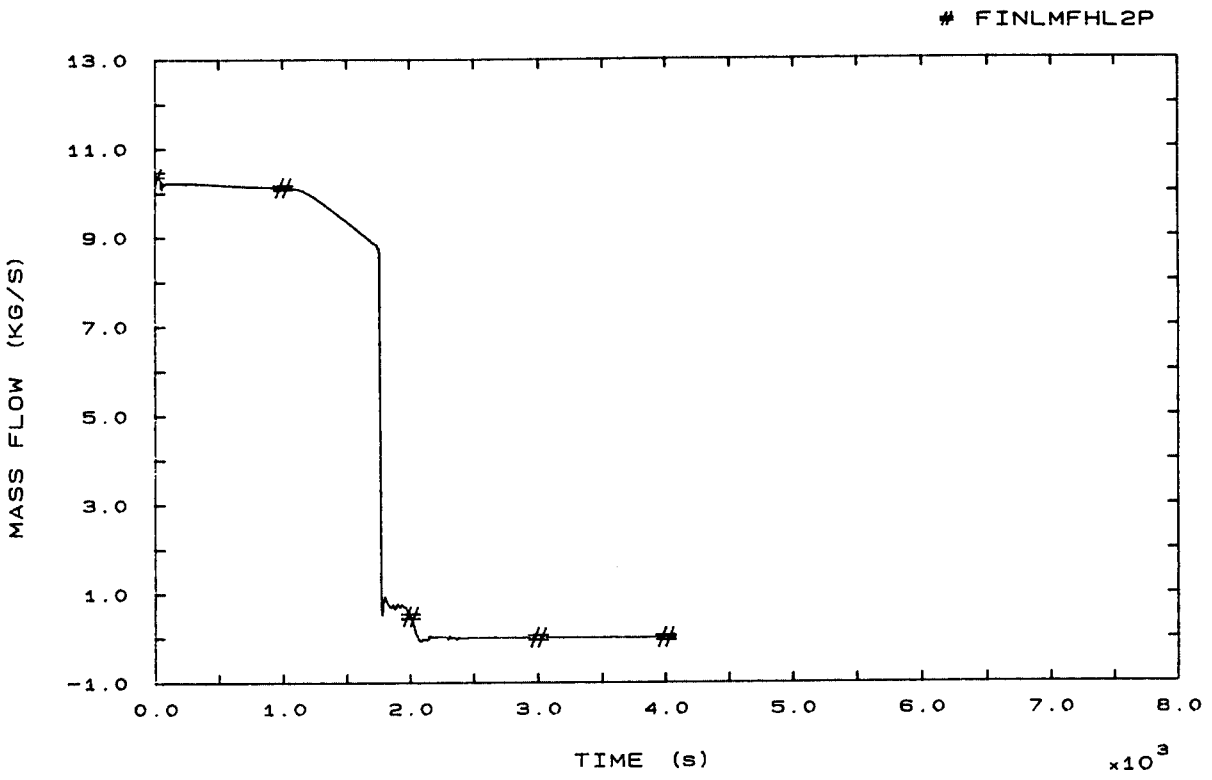

FIG. 90 HOT LEG 2 MASS FLOW

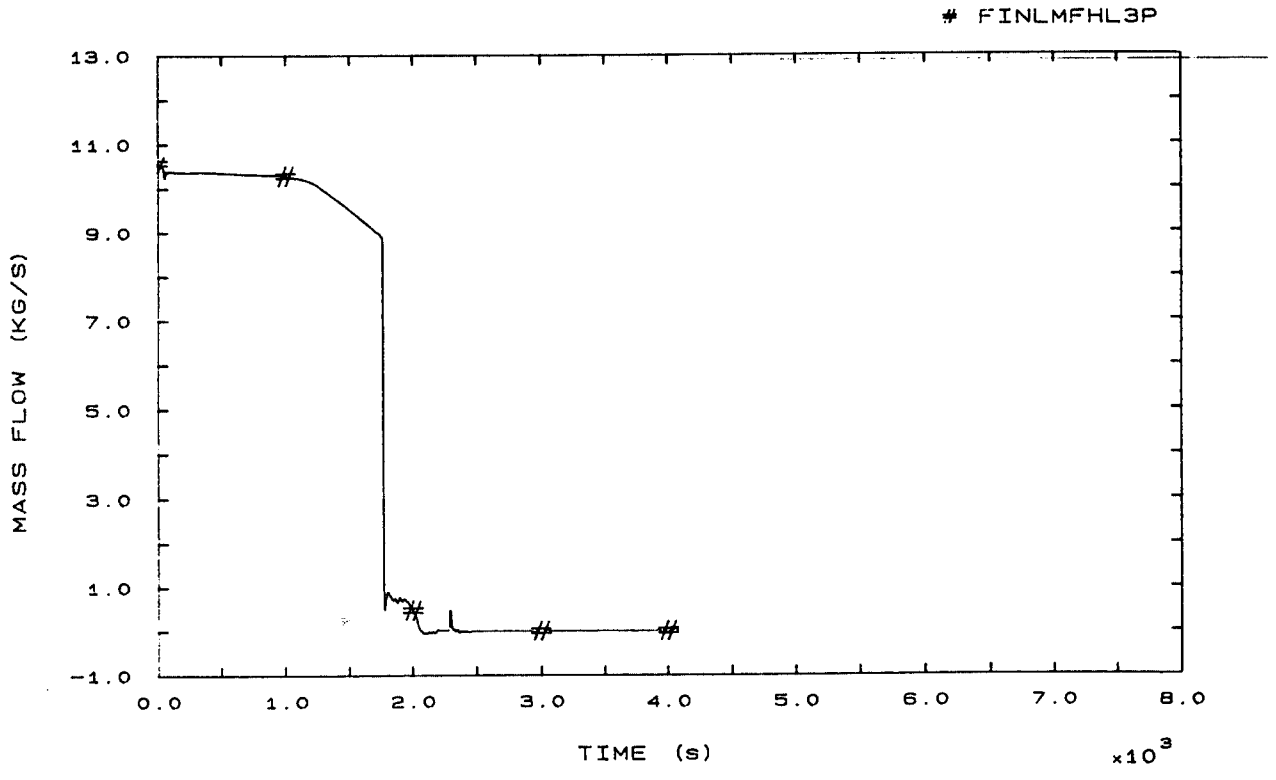

FIG. 91 HOT LEG 3 MASS FLOW

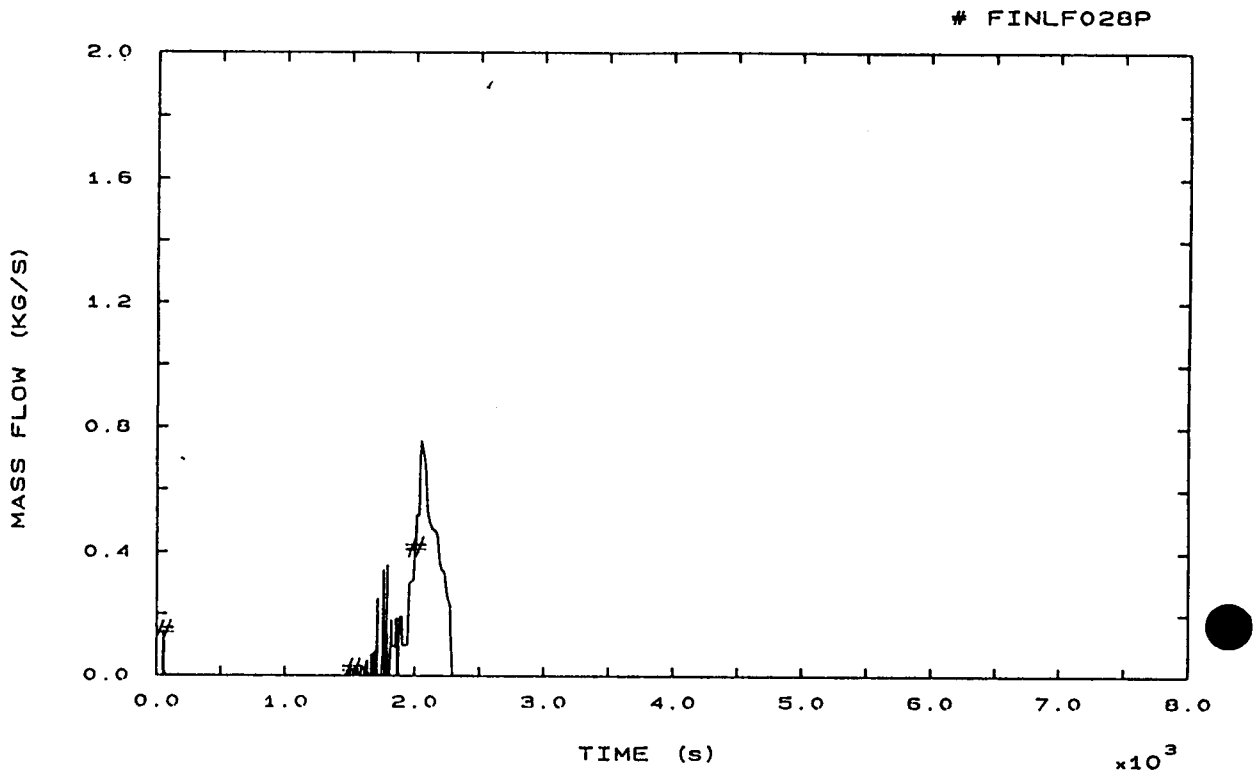

FIG. 92 PRZ PORV MASS FLOW

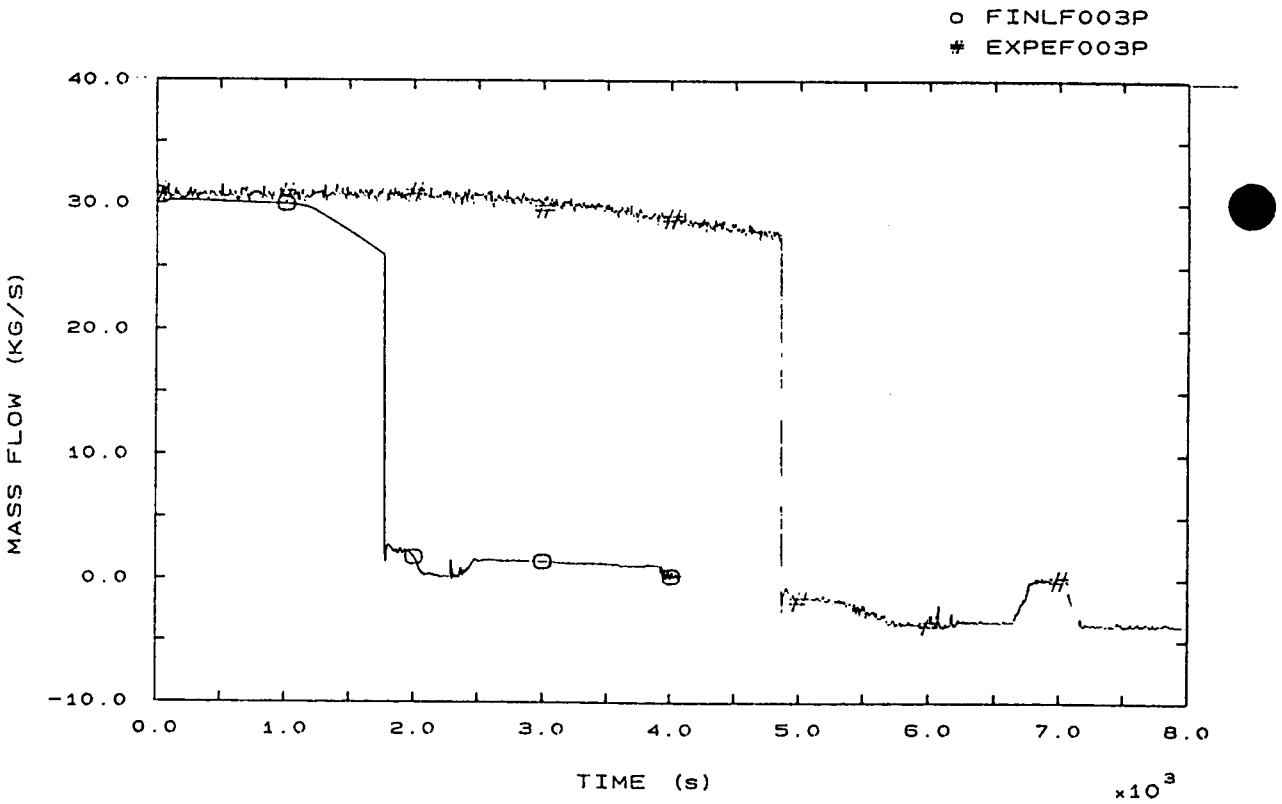

FIG. 94 VESSEL DOWNCOMER MASS FLOW

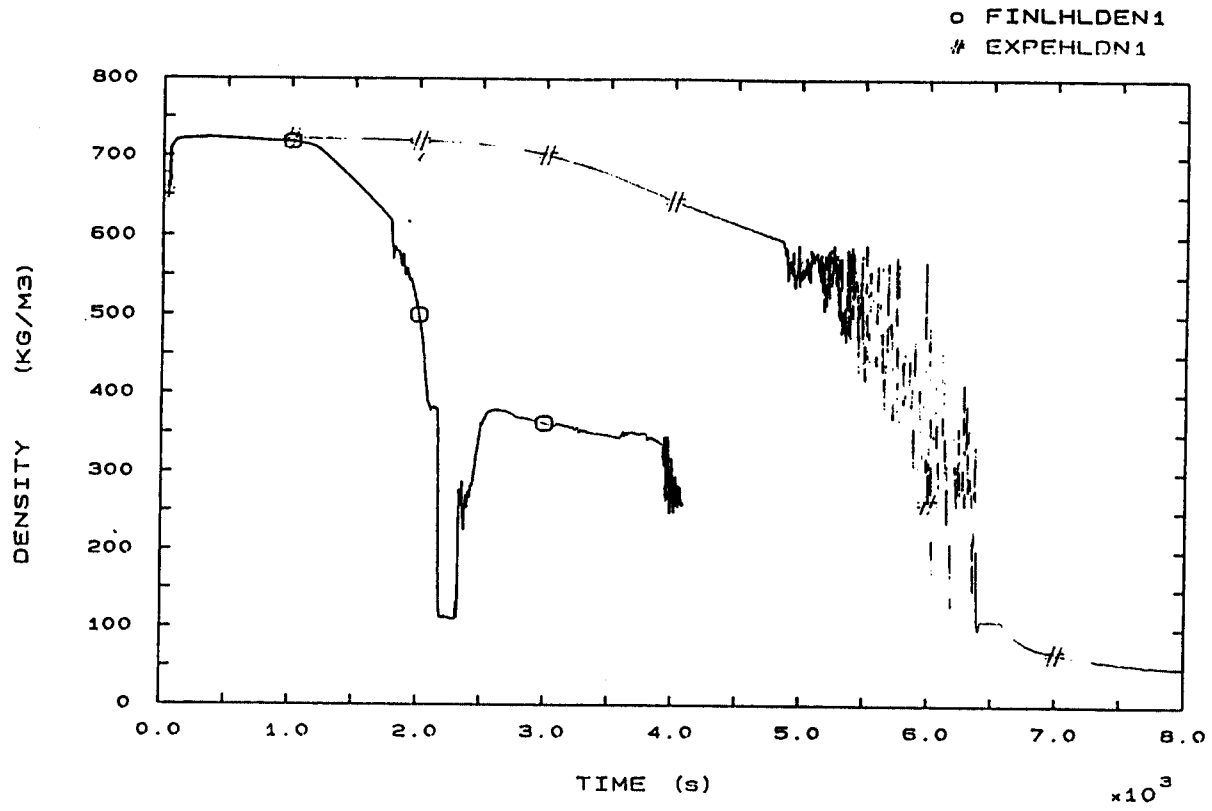

FIG. 100 HOT LEG 1 FLUID DENSITY

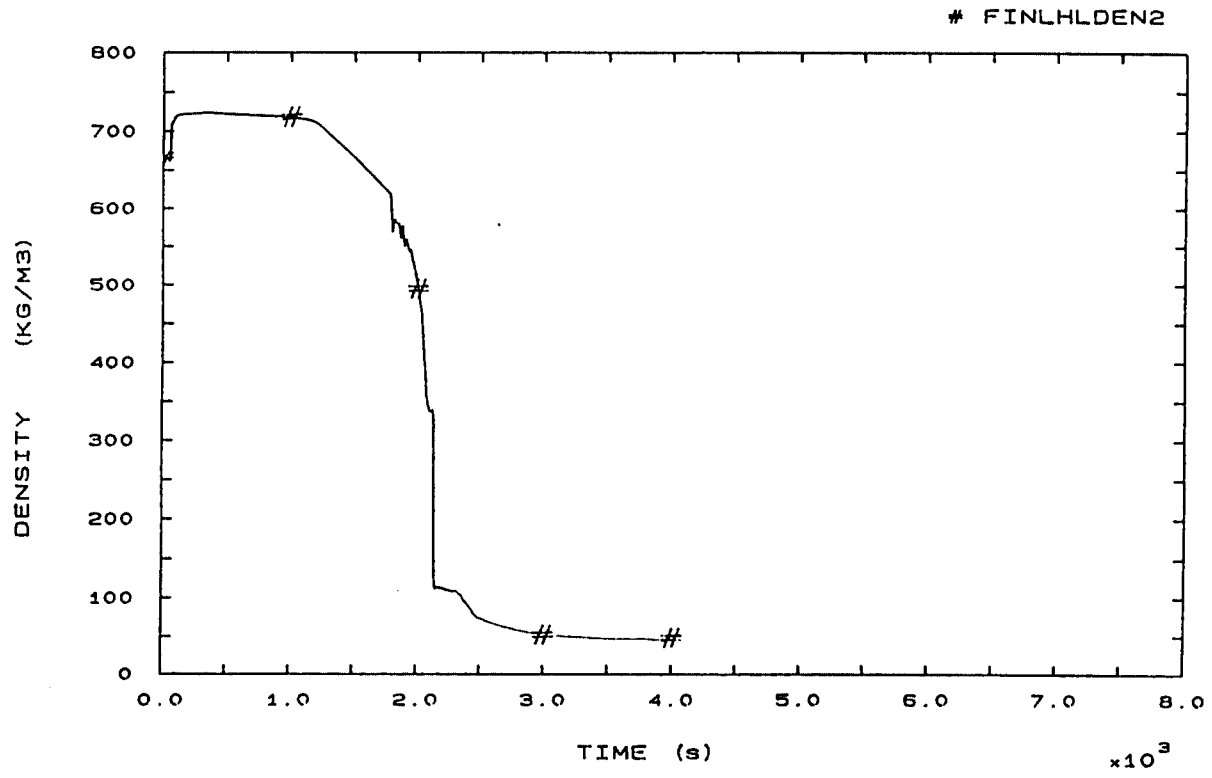

FIG. 101 HOT LEG 2 FLUID DENSITY

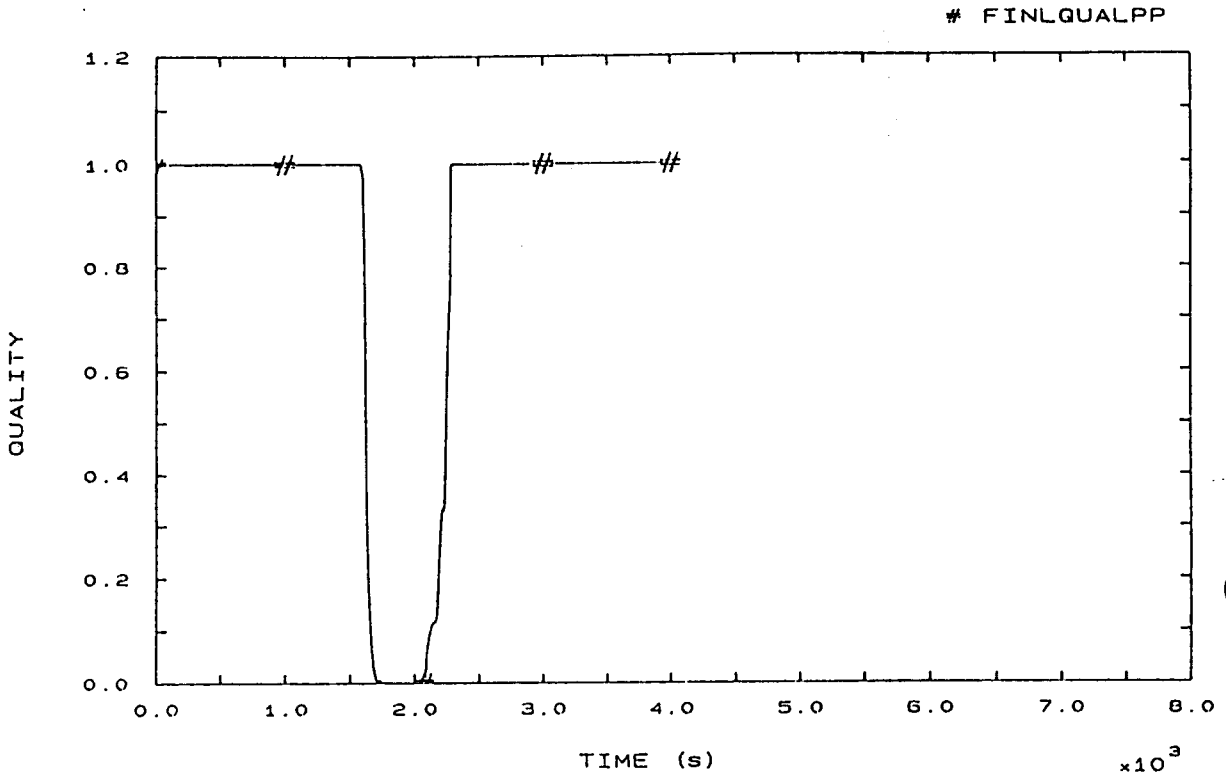

FIG. 103 PRZ PORV FLOW QUALITY

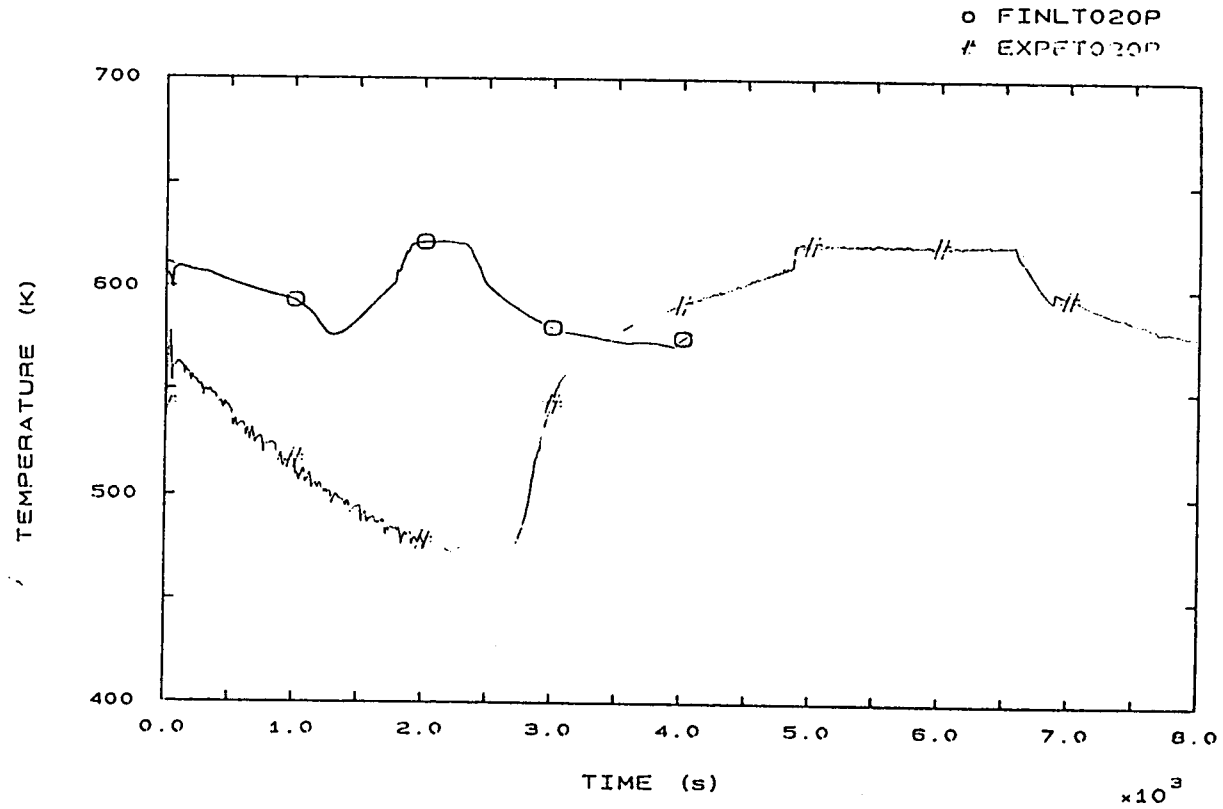

FIG. 112 FLUID TEMPERATURE SURGE LINE UPPER SIDE

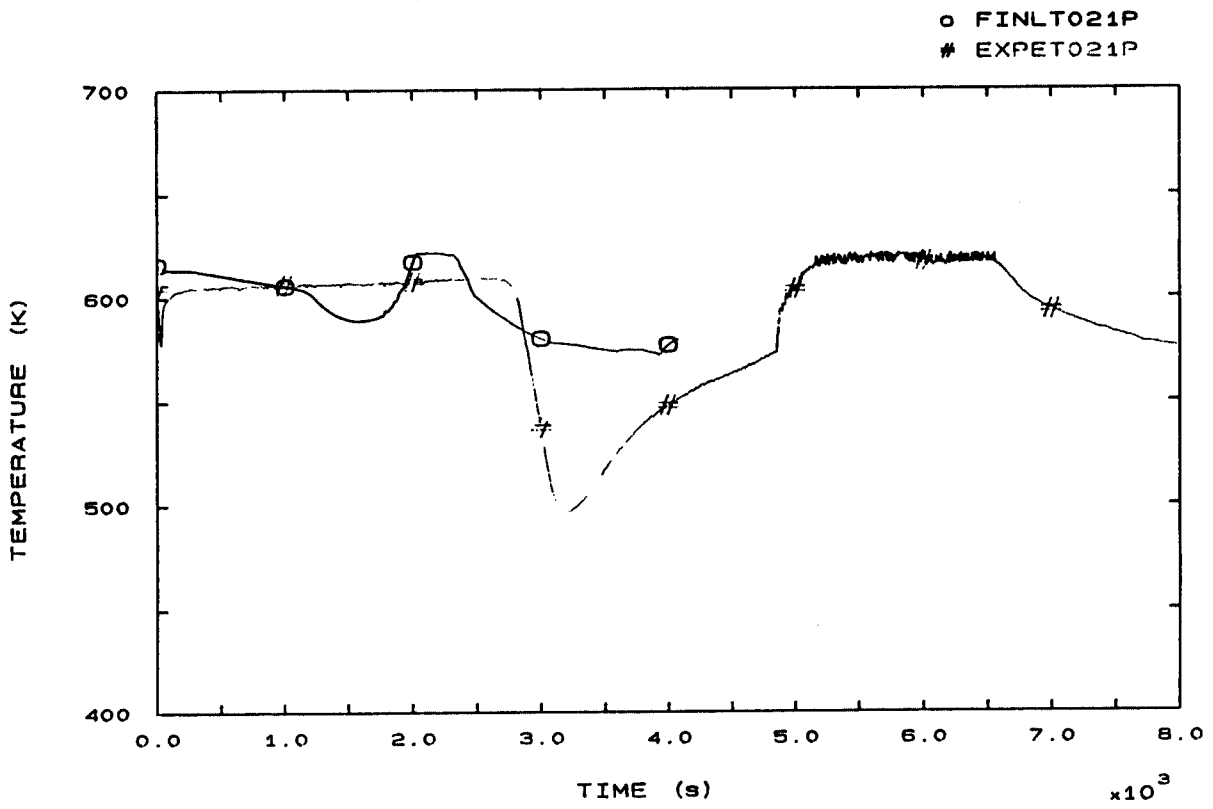

FIG. 113 PRZ FLUID TEMPERATURE

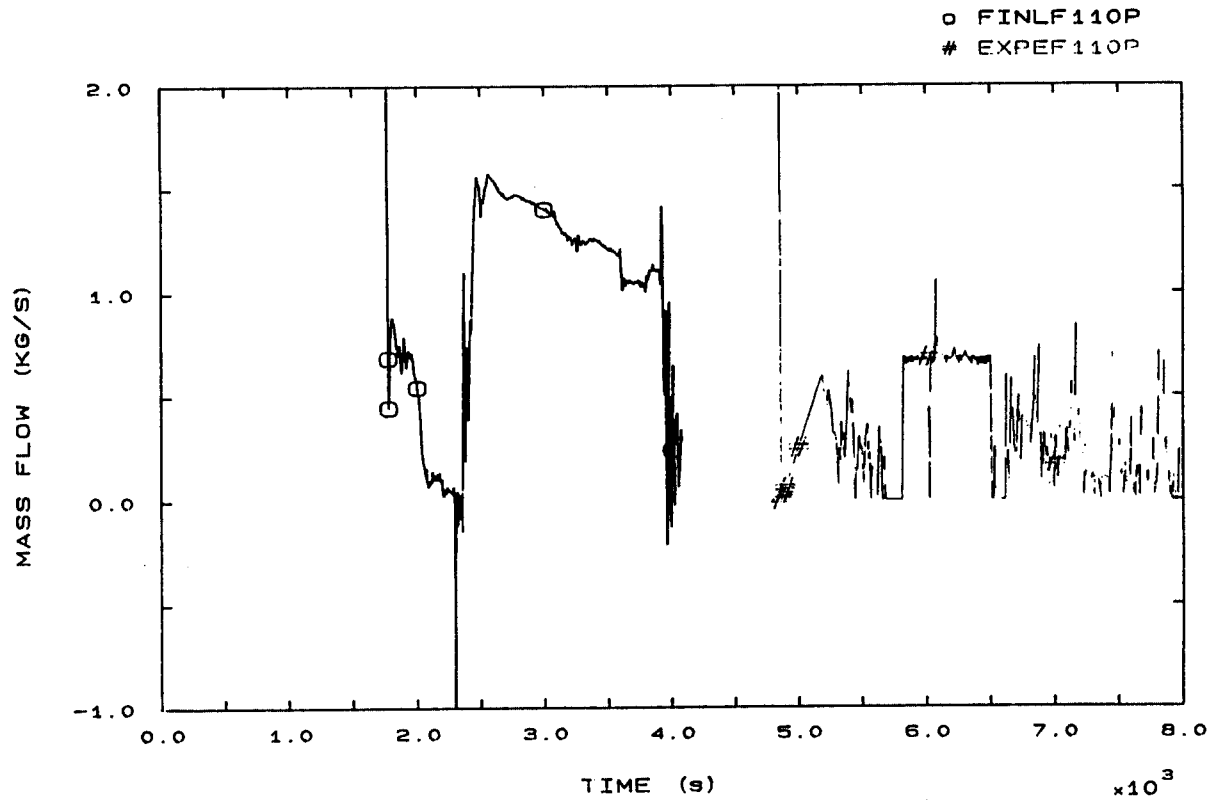

FIG. 125 LOOP SEAL 1 MASS FLOW

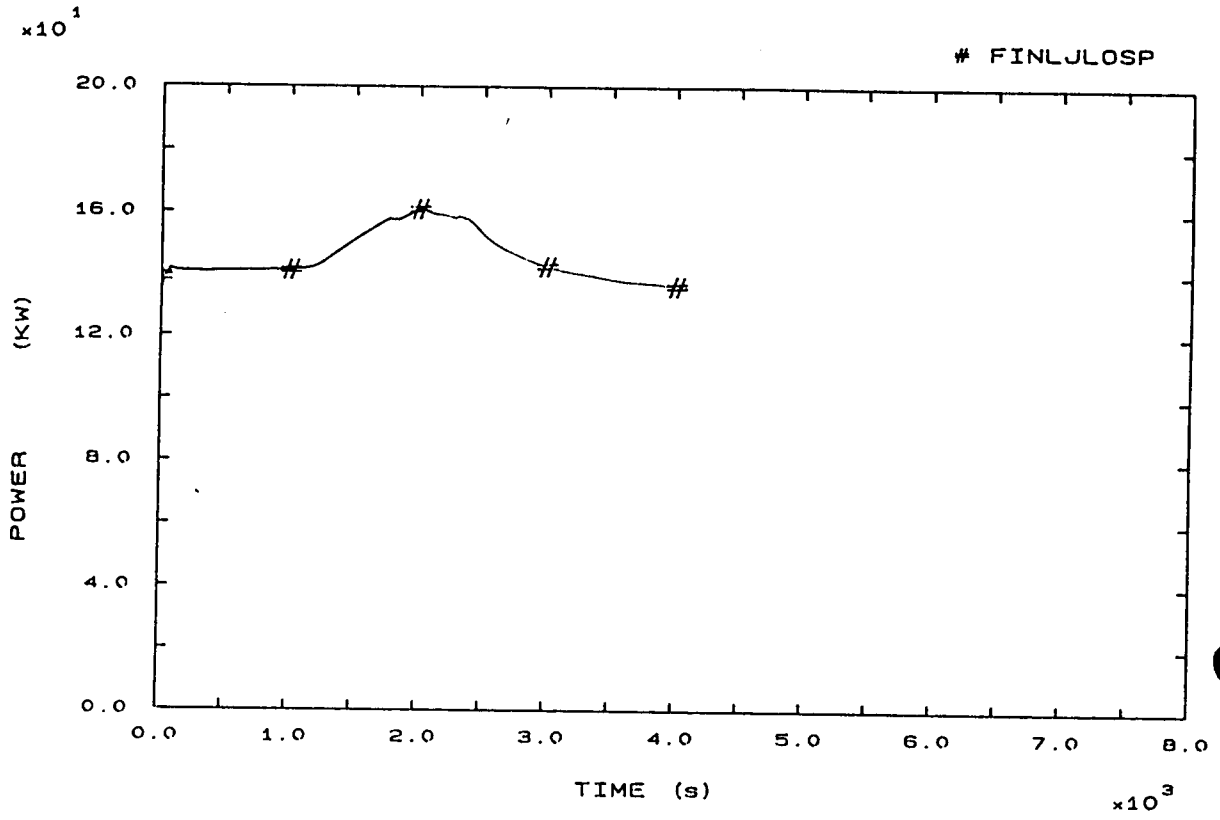

FIG. 131 PRIMARY HEAT LOSS

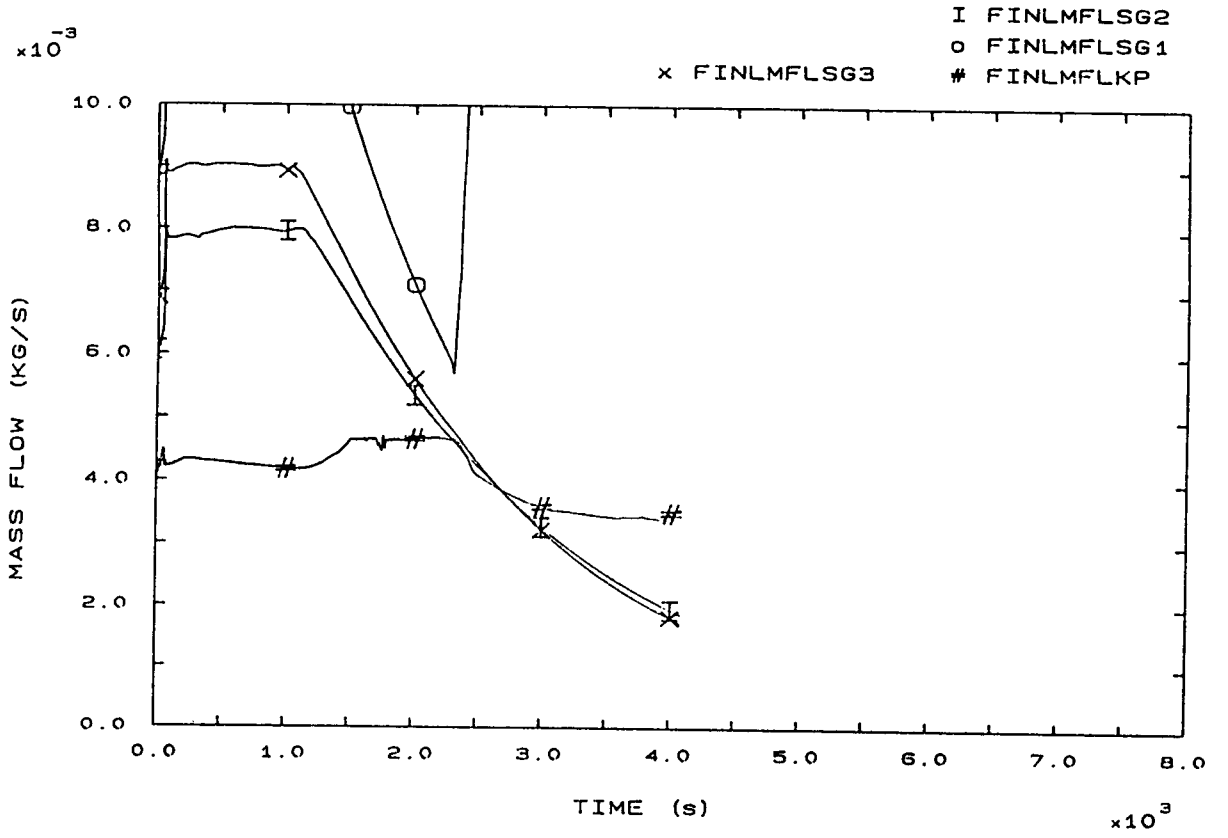

FIG. 137 PRIMARY AND SECONDARY LEAKS

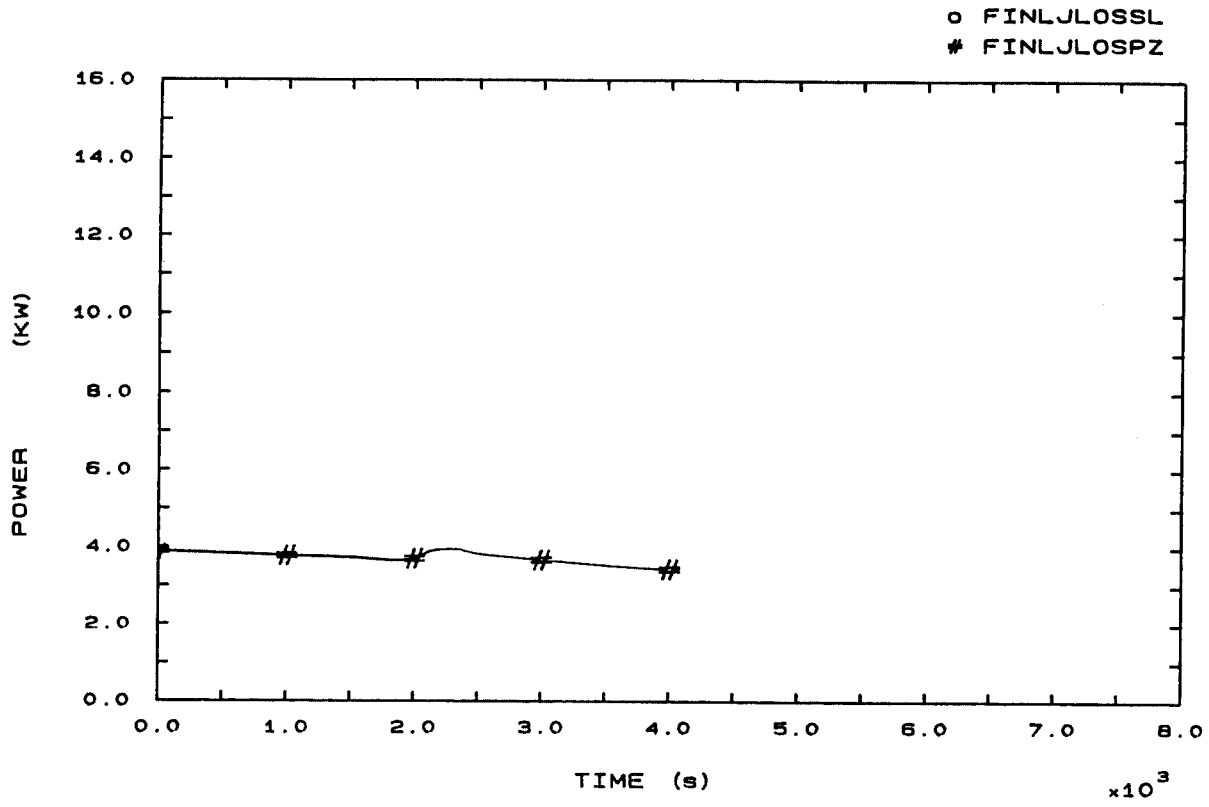

FIG. 138 PRZ AND SURGE LINE HEAT LOSSES

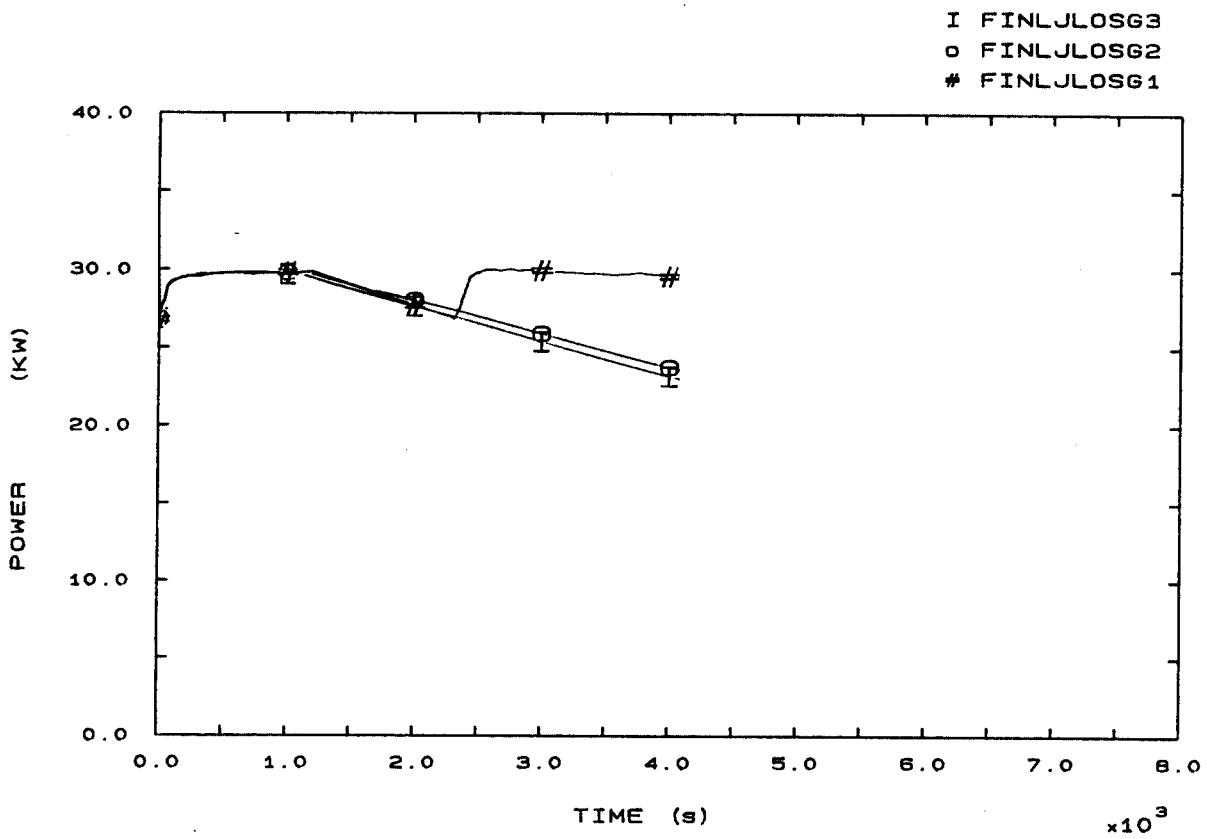

FIG. 139 SECONDARY HEAT LOSSES

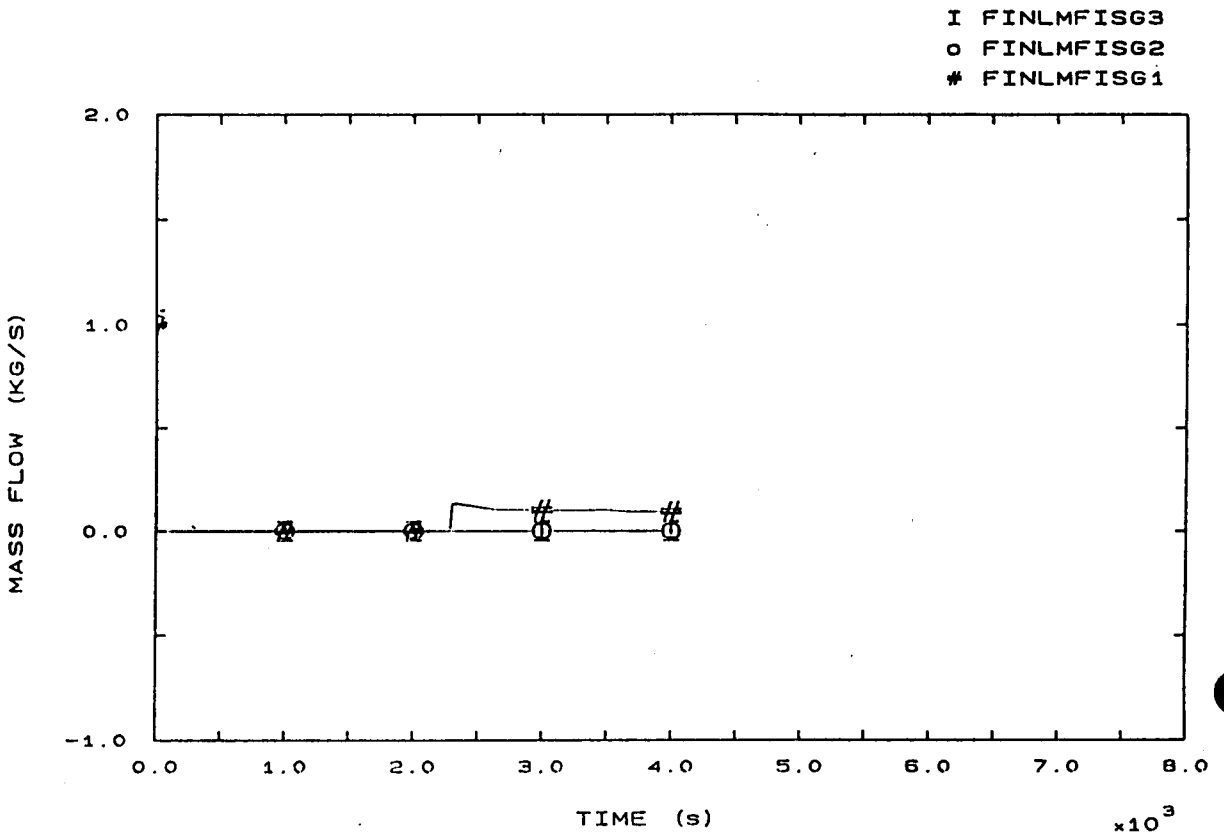

FIG. 140 SG INLET MASS FLOWS

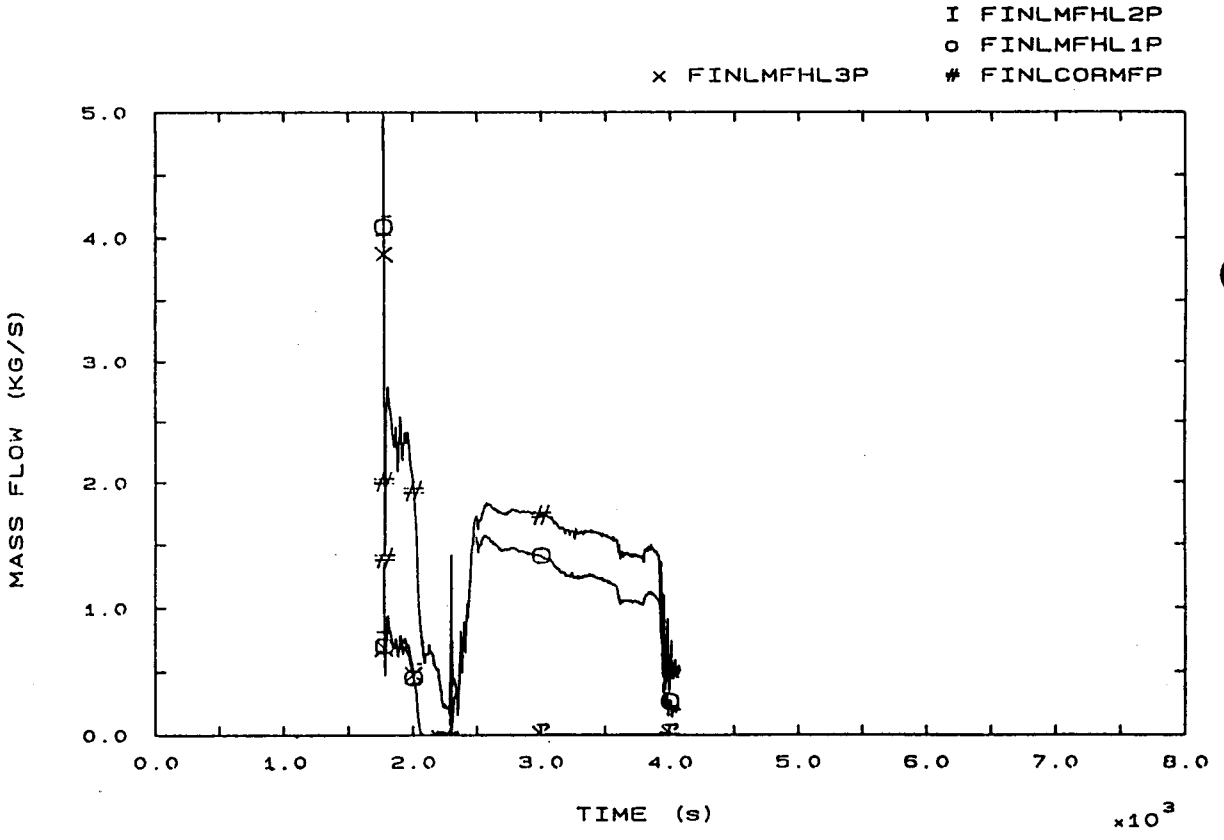

FIG. 141 BOTTOM CORE AND HOT LEG MASS FLOWS